The role of glutamate pyruvate transaminase 2 (GPT2) in neurometabolism and molecular mechanisms of GPT2 Deficiency

Ozan Baytaş

B.Sc. Boğaziçi University, 2014

A Dissertation Submitted in Partial Fulfillment of the Requirements for the Degree of Doctor of Philosophy in the Neuroscience Graduate Program at Brown University

Providence, RI, USA

Februrary 2022

This dissertation by Ozan Baytas is accepted in its present form
by the Department of Neuroscience as satisfying the
dissertation requirement for the degree of Doctor of Philosophy.

Date_____ _____
Eric M. Morrow, Advisor

Recommended to the Graduate Council

Date_____ _____
David M. Berson, Committee Chair

Date_____ _____
Judy S. Liu, Committee Member

Date_____ _____
Ted Abel, External Reader

Approved by the Graduate Council

Date_____ _____
Andrew G. Campbell, Dean of the Graduate School

OZAN BAYTAŞ
Brown University 185 Meeting St.
SFH318, Providence, RI 02912
E-mail: ozan_baytas@brown.edu, baytas.ozan@gmail.com

EDUCATION

Jan 2015 – cont'd	**PhD Candidate**, Brown University Neuroscience Graduate Program Thesis Advisor: Dr. Eric Morrow
Sept 2010 - June 2014	Bogazici University (BOUN), Istanbul, Turkey **BSc Molecular Biology and Genetics** (MBG) (Instruction in English) Rank: 1st. GPA: 3.93 High Honor List in all semesters.
June 2013 – Sept 2013	Julius-Maximillians-Universität Würzburg, Würzburg, Germany Erasmus Exchange Student – Student Mobility for Placement Scholarship
Sept 2005 – May 2010	American Robert College (High School), Istanbul, Turkey Math-Science Track (Instruction in English) GPA: 87/100 (in top 10%)

RESEARCH EXPERIENCE

Jan 2015 – cont'd	**Graduate Thesis Research** PhD Thesis: The role of GPT2 in neurometabolism and molecular mechanisms of GPT2 deficiency
Jan 2014 – Jul 2014	**Research Project Student** Prof. Dr. Aslıhan Tolun's Kommagene Lab, MBG, BOUN *Mutation Screening in gene LHX8 & Genetic Basis of Stuttering*
Sept 2013 – Jan 2014	**Research Project Student** Prof.Dr. Neş'e Bilgin's Biochemistry Lab, MBG, BOUN *Phosphorylation of Elongation factor Tu in E. coli*
Sept 2013 – June 2013	**Summer Research Student** Prof. Dr. Klaus Peter Lesch Laboratory of Translational Neuroscience, University of Würzburg Dept. Of Psychiatry, Psychosomatics and Psychotherapy

Gene Expression of Kir2.x channels in Tph2 knockout mice

Aug 2012 – June 2012 **Summer Intern**
Prof.Dr. Neş'e Bilgin's Biochemistry Lab, MBG, BOUN

Sept 2012 – Jun 2014 **Undergraduate Research Assistant**
Dr. Aysimi Elif Duman, Psychology Dept., BOUN
Glucocorticoid Receptor2 Methylation data processing

Sept 2011 – Jun 2014 **Undergraduate Research Assistant**
Prof.Dr. Reşit Canbeyli's Psychobiology Lab, Psychology Dept., BOUN *Animal models of Depression & Vision and Depression*

PEER-REVIEWED PUBLICATIONS

1. **Baytas O**, Davidson SM, DeBerardinis RJ, Morrow EM. Mitochondrial enzyme GPT2 regulates metabolic mechanisms required for neuron growth and motor function in vivo. Hum. Molec. Gen. 2021 doi: 10.1093/hmg/ddab269.
2. Ouyang Q, Kavanaugh BC, Joesch-Cohen L, Dubois B, Wu Q, Schmidt M, **Baytas O**, Pastore SF, Harripaul R, Mishra S, Hussain A, Kim KH, Holler-Managan YF, Ayub M, Mir A, Vincent JB, Liu JS, Morrow EM. GPT2 mutations in autosomal recessive developmental disability: extending the clinical phenotype and population prevalence estimates. Hum Genet. 2019 Oct;138(10):1183-1200. doi: 10.1007/s00439-019-02057-x.
3. Kavanaugh BC, Warren EB, **Baytas O**, Schmidt M, Merck D, Buch K, Liu JS, Phornphutkul C, Caruso P, Morrow EM. Longitudinal MRI findings in patient with SLC25A12 pathogenic variants inform disease progression and classification. Am J Med Genet A. 2019 Nov;179(11):2284-2291. doi: 10.1002/ajmg.a.61322.
4. **Baytaş O**, Morrow EM. The Role of Mitochondrial Glutamate Metabolism in Cognitive Development and Disease. Neuropsychopharmacology. 2018 Jan;43(1):229-230. doi: 10.1038/npp.2017.202.
5. Ouyang Q, Nakayama T, **Baytas O**, Davidson SM, Yang C, Schmidt M, Lizarraga SB, Mishra S, Ei-Quessny M, Niaz S, Gul Butt M, Imran Murtaza S, Javed A, Chaudhry HR, Vaughan DJ, Hill RS, Partlow JN, Yoo SY, Lam AT, Nasir R, Al-Saffar M, Barkovich AJ, Schwede M, Nagpal S, Rajab A, DeBerardinis RJ, Housman DE, Mochida GH, Morrow EM. Mutations in mitochondrial enzyme GPT2 cause metabolic dysfunction and neurological disease with developmental and progressive features. Proc Natl Acad Sci U S A. 2016 Sep 20;113(38): E5598-607. doi: 10.1073/pnas.1609221113.
6. Montalbano A, Waider J, Barbieri M, **Baytas O**, Lesch KP, Corradetti R, Mlinar B. Cellular resilience: 5-HT neurons in Tph2(-/-) mice retain normal firing behavior despite the lack of brain 5-HT. Eur Neuropsychopharmacol. 2015 Nov;25(11):2022-35. doi: 10.1016/j.euroneuro.2015.08.021.

ABSTRACTS AND PRESENTATIONS

March 26, 2019	Mind and Brain Research Day – Robert J. & Nancy D. Carney Institute for Brain Science. Awarded 1st Prize Graduate/Medical Student Poster Award.

WORKSHOPS

September 16-18, 2019	4th Suna Kıraç Workshop on Neurodegenerative Disease, Istanbul, From Genetics of Neurodegenerative Disease to Therapies
January 20-23, 2015	3rd Suna Kıraç Workshop on Neurodegenerative Disease, Istanbul, From Genetics of Neurodegenerative Disease to Therapies
Oct 5-6, 2012	Development and Function of the Nervous System
Apr 7-8, 2012	Molecular Biology and Genetic Weekend VII
Jan 21, 2012	Bogazici University (BOUN) Human Genome Project in Turkey

LANGUAGE SKILLS

- Python (Beginner)
- English (Advanced: TOEFL IBT: 115/120)
- German (Intermediate)
- Modern Greek (Beginner)

TEACHING EXPERIENCE

Fall 2015	Graduate Teaching Assistant Neur1650: Structure of the Nervous System taught by David Berson, Brown University

Acknowledgements

I am so much grateful to my graduate thesis advisor, Dr. Eric M. Morrow for all his guidance, inspiration and scientific excitement (that fiery gut feeling!). It was great fun working with him over the years and I admire his passion for science which resonated well with my own growing one. I will remember my days in his laboratory and his kindness very fondly. I cannot thank enough for all the work you have done to help me in my thesis project. I know your work will continue to inspire many and I will always stay up to date with the latest developments!

I want to thank my committee members, Drs. Judy Liu and David Berson. Dr. Liu as neighbor laboratory's principal investigator has been a great influence. She is ever so welcoming and encouraging with her smile and thoughtful science and I will not forget the days we spent in Philadelphia South Street (the Magic Gardens!!). Most of all though, I cannot thank her enough for recruiting Haruki Higashimori, who has been a great friend to me in my final years of graduate school. We had so much fun together; contemplating, dreaming, imagining and discussing. I will not forget you Haruki-kun! Thank you for calling me a genius now and then to cheer me up (lol).

I have always admired Dr. Berson's passion for science as well. My only regret is that I have not spent as much time as I think I should have as every moment with him has been a thoughtful experience. As a teaching assistant in his Neuroanatomy course, I had tremendous fun; I got to hold sheep brains, teach anatomy and even play Hercule Poirot in solving anatomical puzzles and medical conditions. Thank you so much for that opportunity. Brown Neuroscience Department has also been a tremendous help and I have to particularly mention, David Sheinberg, Gilad Barnea, Anne Hart and Carol Viveiros for all their support.

I have made so many good friends in Dr. Morrow's laboratory, Qing Ouyang (we cracked up in laughter every day), Li Ma and lovely "tickle" Bowen, to whom I give lots of hugs and wish him all the best in his future. Abbie Maguire has been such a great friend to me, a fellow lab companion, floor scavenger and donut tester. I am also very happy to have befriended Matthew Pescosolido, his calming manner was a great asset to have; of course I cannot forget Luke whom I loved to discuss Star Wars with. The hmm

invaders will get Michael Schmidt in the end too! He has helped me immensely and we had so much fun. Recently, Hasib A. Riaz has joined Dr. Morrow's laboratory, I wish we had more time together, as we are getting along very well and I wish him all the best for his future.

Julie Kauer is also one name I will not ever forget. I learned so much in my time at her laboratory; the beating action potentials, the living science, it was just mesmerizing. She was ever so kind to a cell patching newbie like me and I was always excited to show how good the cells were (and hid when they were not). Thank you for all your advice, I know you wanted the best for me.

I have to thank Ece, Alper and Kaan Ata Uzun, and in a famous Turkish expression, I have to say "Hakkınızı helal edin". They were my Turkish family abroad, and they helped me through so many ordeals. I wish you all the best in life; I know Kaan will grow into a person with all the goodness in his heart.

I am indebted to my family and friends in/from Turkey. So much happened, and so much more will. I could not be without their support. I have to thank Drs. Reşit Canbeyli and Aslı Tolun, with whom I began learning and enjoying science. Rosa L… Your voice echoed in my head whenever I felt down: "Sein sie ruhig… trotz alledem." and "Ich war, ich bin, ich werde sein." !! Another voice that echoed was that of the Lady of the Golden Wood: "Do we leave the Middle Earth to its fate? Do we let them stand alone?" Thank you, without your voice, my thesis work would have been much better.

I dedicate my work to my nephew, Arche Atlas, who has brought with him so much joy and laughter to my family. I hope his future will be full of love, trust, goodness, and happiness.

TABLE OF CONTENTS

LIST OF TABLES

LIST OF ILLUSTRATIONS

CHAPTER 1

CHAPTER 2

CHAPTER 3

CHAPTER 4

INTRODUCTION

My thesis work has focused on the contribution of the mitochondrial enzyme glutamate pyruvate transaminase 2 (GPT2) to neurometabolism. The Introduction will begin with the advent of my work on GPT2 in the context of its associated neurological disease, GPT2 Deficiency. The following sections will introduce metabolic pathways related to GPT2 as well as concepts that I think are crucial to understanding the function of GPT2 in the physiology of the nervous system. The last section of the Introduction will briefly outline each chapter in the thesis.

In 2016, Dr. Eric M. Morrow's laboratory discovered autosomal recessive loss-of-function mutations in *GPT2* that cause postnatal microcephaly, intellectual disability and progressive spastic paraplegia in humans (Ouyang et al., 2016). *GPT2* encodes for mitochondrial glutamate pyruvate transaminase, also known as alanine aminotransferase 2, that reversibly transfers an amino group from glutamate to pyruvate forming alanine and alpha-ketoglutarate (Figure 1.1). Following the clinical presentation of one of the pedigrees by Rajab and colleagues (Rajab et al., 2006), Ouyang and co-workers presented two large kindreds with recent shared ancestry from Pakistan and Sultanate of Oman. The LOD scores linked the disease to 16q11.2 and Sanger sequencing of *GPT2* confirmed the mutation in the two pedigrees. Since then, several more kindreds with *GPT2* mutations have been identified (Baytas and Morrow, 2018; Binaafar et al., 2020; Celis et al., 2015; Hengel et al., 2018; Kaymakcalan et al., 2018; Lobo-Prada et al., 2017; Ouyang et al., 2019; Ruaud et al., 2021). The full list of mutations along the *GPT2* gene sequence is given in Figure 1.2. For a full detailed clinical presentation, please refer to the Results of Chapter 2.

Conceptually, our investigations on GPT2 and its role in neurometabolism starts with the human neurological developmental disease as these monogenic disorders have been very useful in elucidating basic mechanisms of growth and maintenance of the nervous system. While this may be viewed as reductionist given the vast metabolic networks with hundreds of enzymes, the specific contribution of GPT2 may underlie critical metabolic mechanisms of cellular growth and energetics that have been left undiscovered in the nervous system. This perspective is relevant to why we care about this particular metabolic enzyme especially when the golden age of biochemistry has produced so prolifically a vast literature on metabolism for decades. The answer, as in any translational science, comes two-fold. On one hand, the questions that arise with the function of this protein are of great importance to the health and maintenance of neuronal cells. For example, the question of how synaptic glutamate release is regulated is fundamental to proper functioning of the nervous system as it not only forms the basis of neurotransmission but also that of energy homeostasis in the cell. Glutamate is an excellent carbon source for tricarboxylic acid cycle intermediates (Hertz et al., 2007; Kovacevic, 1971; McKenna, 2007; Westergaard et al., 1995) and has one of the highest P/O ratios, that is the amount of esterification of inorganic phosphate (i.e. formation of ATP) per oxygen atom consumed (Case and Mc, 1951; Milstein et al., 1968). This suggests that glutamate is a major endogenous energy substrate. Metabolic processes that handle glutamate availability have not been studied closely with modern genetic tools and further investigation will allow for a better understanding of neurometabolism. On the other hand, we care about the GPT2 function because dysregulation of metabolic pathways related to GPT2, such as macromolecule synthesis and energy balance, have

been implicated in neurodegenerative diseases including Alzheimer's and amyotrophic lateral sclerosis (ALS). Studying the role of GPT2 in neurometabolism may probe into pathophysiology of not only GPT2 Deficiency but that of other more common neurodegenerative diseases.

Importantly, the metabolic investigations have only recently focused on the GPT2 protein. However, the focus has been centered on cancer or liver metabolism (Caiola et al., 2020; DeBerardinis et al., 2008; Hao et al., 2016; Kim et al., 2019; Tan et al., 2017) and has abandoned the nervous system and the relevance of GPT2 to neuronal growth and maintenance. In the following chapters, you will find questions posed regarding the role of GPT2 in neurometabolism along with their putative answers. Figure 1.4 gives a summary of the overarching questions asked in this work and the associated chapters wherein results are presented. The same figure of questions is available with overall answers in the Conclusion chapter.

The following sections in the Introduction provide background information and literature on GPT2 and the related metabolic pathways, particularly in the context of the nervous system.

GPT2 and transamination

GPT2 and its paralog GPT1 are part of the class I pyridoxal 6-phosphate-dependent aminotransferases which also include glutamate oxaloacetate aminotransferase (aspartate aminotransferase) among other transaminases. Transamination, the collective process for the chemical reaction of transferring an amino group, has seen much attention

since Krebs (Krebs, 1953), and has been shown to be critical for a variety of metabolic processes including synthesis and degradation of amino acids, replenishment of the tricarboxylic acid (TCA) cycle intermediates, nitrogen balance and glucose-alanine cycle. Transamination usually involves glutamate and alpha-ketoglutarate along with an amino acid and its corresponding alpha-keto acid. Historically, GPT enzymes have been studied as biomarkers of liver toxicity as damaged hepatocytes release GPT enzymes into the bloodstream (Karmen et al., 1955; Yang et al., 2009). Studies regarding their role in cellular growth particularly in the cancer field had to wait for decades.

GPT2 **and** ***GPT1*****: where are they expressed?**

Humans and mice have two isozymes (isoforms of enzymes that carry out the same reaction), human *GPT2* on chromosome 16, mouse *Gpt2* on chr. 8 and human *GPT1* on chr. 8, mouse *Gpt1* on chr. 15 . Human *GPT2* is prominently expressed in muscle, fat, kidney, brain and liver and *GPT1* is expressed in kidney, liver and fat tissues (Yang et al., 2002). Murine expression patterns of *Gpt2* and *Gpt1* have been found to be similar to their human counterparts (Jadhao et al., 2004). GPT2 protein contains a mitochondrial localization sequence and is carried to the mitochondria whereas GPT1 lacks this signal and resides in the cytoplasm (Meton et al., 2004; Ouyang et al., 2016). Most important distinction between GPT2 and GPT1 in humans is that GPT2 is present in the brain tissue and GPT1 appears to be completely absent both at the level of protein (as determined by immunohistochemistry and western blotting) and mRNA (Hodge et al., 2019; Kang et al., 2011; Lindblom et al., 2007). However, expression patterns in different cell types either in the nervous system or other systems have not been studied.

Evolution of *GPT2* or *GPT1* genomic sequences have not been well studied; however the mutations in human *GPT2* that lead to GPT2 Deficiency disease were found to be in protein residues that have been well conserved in mammals (Celis et al., 2015; Ouyang et al., 2016). From E. coli to plants to humans, glutamate pyruvate transaminases have been shown to be important for alanine synthesis, nitrogen balance and regulation of glutamate, pyruvate and alpha-ketoglutarate (Escalera-Fanjul et al., 2017; Kim et al., 2010; Xu et al., 2017). Amusingly, recent evidence suggests that there is an upregulation of *Gpt2* in the evolution of venom glands of snakes (Barua and Mikheyev, 2021).

GPT2 in the tricarboxylic acid cycle metabolism

As can be seen immediately in the reaction, catalysis by GPT2 results in a net production of a tricarboxylic acid (TCA) cycle intermediate, alpha-ketoglutarate (Figure 1.1A). TCA cycle enzymes such as aconitase have the critical role of cycling TCA intermediates that produce reducing equivalents, NADH and $FADH_2$, which are used to make ATP via the electron transport chain. The same TCA cycle intermediates are also consumed to synthesize amino acids, fatty acids and nucleotides which in turn form macromolecules that help the cell grow. Therefore, there is always a need of external input toward the TCA cycle intermediates to ensure its continuity of the metabolic support for the cell. Hans Kornberg coined the term *anaplerotic reactions* to mean metabolic routes of carbon sources channeling into the TCA cycle (Kornberg, 1966). Kornberg used his term to mean pathways producing TCA cycle intermediates (e.g. pyruvate or acetate being a fuel source into the TCA cycle), and over time the term anaplerotic reaction came to mean a reaction resulting in the net synthesis or flux into the

TCA cycle (Owen et al., 2002). The following table lists of all known anaplerotic enzymes/processes (including preferred direction of the reaction, co-factors used, predominantly expressing cell types and any associated diseases) that I was able to curate (Table 1.1).

Deficiencies in almost all the anaplerotic reactions lead to neurological disorders with varying clinical features including psychomotor delay and intellectual disability. To date, much attention has been given to pyruvate carboxylase as the main anaplerotic enzyme in the mammalian brain. Pyruvate carboxylase is a biotin-dependent enzyme that fixes a CO_2 molecule to pyruvate yielding malate. In the mammalian brain, pyruvate carboxylase is expressed exclusively by glial cells (particularly astrocytes and oligodendrocytes) (Yu et al., 1983) and neither protein expression of this enzyme nor pyruvate carboxylation have been shown to occur in neurons. Astrocytes are known to give metabolic support for the neurons by releasing growth factors such as BDNF, GDNF and NGF as well as TCA cycle intermediates such as malate and citrate that are readily taken up by neurons (Westergaard et al., 1994). However, it is unlikely that neurons do not have indispensable intracellular mechanisms to replenish their own TCA cycle. Historically, the school of thought revolving around astrocytes as the main metabolic support for neurons may be responsible for downplaying the metabolic capabilities of neuronal cells. Only recently, metabolic flexibility in neurons has seen more attention and the role of anaplerotic processes in neurons have not been well studied (Divakaruni et al., 2017; Hohnholt et al., 2018).

The GPT2 reaction has indeed been studied in the context of the TCA cycle; however almost exclusively within the cancer field. GPT2 has been found to be critical

for tumorigenesis due to its anaplerotic ability of channeling glutamine into the TCA cycle. Yang and co-workers have shown that glutamine oxidation supports the TCA cycle and cell survival when mitochondrial pyruvate transport is blocked (Yang et al., 2014). While they do not look at GPT2 specifically, they attribute glutamine oxidation to transaminases. Hao and co-workers found that mutations in *PIK3CA* (phosphatidylinositol 3-kinase alpha) reprograms glutamine metabolism by upregulating GPT2 in colorectal cancer cells (Hao et al., 2016). These cells shift their metabolome to utilize glutamine more to resupply the TCA cycle intermediates due to upregulation of GPT2 protein with concomitant increases in alanine levels. Similarly, Smith and co-workers saw that in colon cancer cells, the GPT2 protein is upregulated to support glutamine oxidation into the TCA cycle and blocking *GPT2* translation by shRNAs makes the cancerous cells non-tumorigenic (Smith et al., 2016). Additionally, glutaminase, one of the major metabolic enzymes that convert glutamine into glutamate, allows for the first step for glutamine oxidation into the TCA cycle and when this enzyme is inhibited in HeLa cells, GPT2 protein is upregulated and increases cell viability (Kim et al., 2019). Overall, in the field of cancer, GPT2 has been found to be a major enzyme that replenishes TCA cycle intermediates and help the cells survive and grow.

There is other evidence that links GPT2 to the replenishment of the TCA cycle intermediates in several other biological entities. Strikingly, GPT2 forms 30% of all alpha-ketoglutarate in isolated rat liver mitochondria in State 4 respiration (in the absence of ADP) (Lenartowicz and Wojtczak, 1988). GPT2 has also been implicated in compensatory mechanisms to circumvent issues of TCA cycle metabolism. For example, the conditional knockout of pyruvate carboxylase in the mouse liver, alanine and alpha-

ketoglutarate levels increase and this has been attributed to GPT2 (Cappel et al., 2019). Interestingly, models of oxidative phosphorylation deficits induced by mitochondrial DNA mutations (Chen et al., 2018) and disrupted mitochondrial fusion dynamics (Motori et al., 2020) display increased levels of GPT2 and GPT1.

GPT2 and its role in replenishing the TCA have been not well studied in the context of the nervous system. More recently, McNair and co-workers find diminished entry of glutamate into the TCA cycle in synaptosomes (isolated nerve terminals) after deletion of glutamate transporter (GLT1) under the SynapsinI promoter (i.e. neuronal GLT1) and observe increased alanine levels. While they do not mention GPT2, they attribute this result to transaminases (McNair et al., 2019).

No other paper exists to this day that investigates the contributions of GPT2 to neurometabolism. To put GPT2 into the context of the nervous system, Figure 1.1B shows synaptosomes (isolated nerve terminals) and Figure 1.1C shows the metabolic interplay between glutamatergic, GABAergic neurons and astrocytes. (For a broader metabolic pathway map, refer to Figure 1.3). While currently the extent to which GPT2 is expressed in these cells is not known, GPT2 allows for glutamate oxidation into the TCA cycle along with other enzymes such as aspartate aminotransferase and glutamate dehydrogenase. Even though glutamate-glutamine cycle ensures that glutamine gets back into neurons to be made into glutamate again, glutamate itself can be used as a carbon source for all the three cell types shown in Figure 1.1C and one of the ways in which this may happen is via GPT2.

GPT2 in glutamate metabolism

Forty years ago (1980s), glutamate was finally accepted as the main excitatory neurotransmitter in the brain (Fonnum, 1984). To date, many enzymes and transporters have been identified and GPT2 has also seen attention with regard to glutamate metabolism. The role of GPT2 in glutamate metabolism in neuronal tissues has been the subject of study since Krebs's time (Haslam and Krebs, 1963). Haslam and Krebs found that in the presence of pyruvate, 90% of all amino nitrogen of glutamate is converted into alanine in guinea pig cerebral cortex slices *ex vivo* indicating that GPT2 reaction is a major route in glutamate oxidation into the TCA cycle.

However, since Krebs, many groups have given less role for GPT2 to play in synaptic glutamate availability. There are several lines of evidence that have led to this. Overall glutamate pyruvate transaminase activity (GPT1 and GPT2) doubles in the first three postnatal weeks in the developing rat brain, but it is still orders of magnitude lower compared to the activity of aspartate aminotransferase (Benuck et al., 1971; Wilbur and Patel, 1974). Glutaminase also shows higher activity than glutamate pyruvate transaminases in the rat brain (Salganicoff and Derobertis, 1965).

Since GPT2 is an equilibrium enzyme (i.e. the ratio of product to reactant concentrations is close to 1) (Krebs, 1953), alanine formation and glutamate formation are equally probable. However, due to relative concentrations and Michaelis constants of the substrates *in vivo*, the predicted direction of the GPT2 reaction is toward alanine formation (Erecinska and Silver, 1990; Miller et al., 1973; Ruscak et al., 1982). Furthermore, the velocity of ^{15}N-alanine (heavy nitrogen labeled) formation from the precursor ^{15}(amine)-N-glutamine was seven times higher than that of ^{15}N-glutamate

formation from ^{15}N-alanine; indicating alanine formation is more likely in synaptosomes (Erecinska et al., 1994). GPT2 may still influence glutamate levels available for synaptic release, even though it may not play a direct role in its synthesis.

Nevertheless, new evidence may point to different directions in different cell types. Alpha-ketoglutarate is a very good precursor for glutamate (Peng et al., 1993; Peng et al., 1991; Shank et al., 1989) and loss of isocitrate dehydrogenase (which converts isocitrate into alpha-ketoglutarate) has been linked to defects in the TCA cycle and synaptic transmission (Ugur et al., 2017). Excitatory synaptic transmission continues even when the glutamate-glutamine cycle is inhibited in rat hippocampal slices (Kam and Nicoll, 2007). These results could be about transaminases, most likely aspartate aminotransferase and particularly hexose-phosphate amidotransferase as glucose is an excellent source of glutamate (Issop et al., 2018; Peng et al., 1993). It is yet unclear whether GPT2 plays a role in glutamate homeostasis at the synaptic site.

GPT2 in alanine metabolism

Another prominent pathway that GPT2 influences is alanine, a non-essential amino acid in mammals. Alanine is the second most frequent amino acid in the primary structure of proteins (Fasman, 1989) and may have been one of the first amino acids that formed in the primordial soup in the famous Muller-Urey experiment (Miller, 1953; Miller and Urey, 1959). So, what have we learned since the times of abiogenesis?

One of the most prominent physiological pathways involving alanine is the glucose-alanine cycle (Felig, 1973). Alanine is released into the bloodstream from all

over the body and reaches the liver to be made into pyruvate and therefrom into glucose via gluconeogenesis. Direct roles of GPT2 and GPT1 have been studied in connection with the glucose-alanine cycle. For instance, hepatic GPT2 protein is upregulated in gluconeogenic conditions including diabetes and downregulated by insulin (Honma et al., 2017; Qian et al., 2015). Recently, loss of mitochondrial pyruvate carrier 2 in the liver has been found to cause gluconeogenesis defects and the TCA cycle is compensated by pyruvate-alanine cycling via GPT2 (Bowman et al., 2016; McCommis et al., 2015).

More recently, alanine has been shown to activate AMP kinase, an important nutrient sensor in hepatic cells *in vitro* or *in vivo* (Adachi et al., 2018). Interestingly, Ron-Harel and co-workers found that T-cell activation depends on extracellular alanine and preferentially used for protein synthesis *in vitro*, possibly in agreement with activating AMP kinase to increase macromolecule synthesis (Ron-Harel et al., 2019). Finally, Rossiter and colleagues found that alanine deprivation in *GPT2*-null cancerous cell lines leads to reduced cell division and growth (Rossiter et al., 2021). These results put alanine in the forefront of protein synthesis and cellular growth in multiple systems.

In the context of the nervous system, alanine metabolism and transport have been studied in neurons and astrocytes. One of the most prominent findings is that alanine is preferentially released from neurons and taken up by astrocytes (Rae et al., 2003; Waagepetersen et al., 2000). This is consistent with the view that the predicted reaction is toward alanine formation given much higher concentrations of glutamate compared to alanine in neurons. One timely piece of caution regarding metabolism: no metabolite is isolated in biological contexts; every metabolite is linked to each other as nodes in a vast network. This may be why opposite findings regarding preferential release of alanine are

obtained from the same group in two papers that are seven years apart (Waagepetersen et al., 2000; Westergaard et al., 1993). It is also imperative that medium conditions are absolutely controlled since the metabolite compositions would have large impacts on the metabolome. However, whether alanine formation within neurons is critical for survival and growth of neurons is yet unexplored.

Brief Outline of Chapters in the thesis

Chapter 2 presents the neurological disease and the mouse model for the human GPT2 Deficiency that has been described and published for the first time (Ouyang et al., 2016). The autosomal recessive mutations in *GPT2* are shown to be loss-of-function in HeLa cells transfected with the constructs of the *GPT2* coding sequence bearing the mutation. Expression patterns of GPT2 via lacZ staining in the mouse brain are presented in Chapter 2 and differential expression of GPT2 and GPT1 in neurons and astrocytes *in vitro* is studied in Chapter 3. Mitochondrial and cytosolic localization of GPT2 and GPT1, respectively are confirmed in a variety of different cells and in subcellular fractionation of brain tissues in Chapters 2, 3,4 and 6.

To address metabolic mechanisms of GPT2 Deficiency, the consequences of GPT2 loss on the entire mouse brain metabolome are presented. Chapter 2 contains targeted metabolomics (the omics study of the metabolome) on the whole mouse brain and Chapter 3 investigates the progression of the altered metabolome across developmental timepoints. Following metabolomics, Chapter 2 investigates the effects of GPT2 loss on glutamine-dependent anaplerosis, i.e. replenishment of the TCA cycle

intermediates, in mouse embryonic fibroblasts *in vitro* and Chapter 3 expands that line of inquiry to neurons and astrocytes.

Chapter 3 continues with addressing the extent to which GPT2 is needed for neuronal growth and survival particularly as it relates to motor function and behavior. Specifically, we asked whether GPT2 is redundant in neurons or astrocytes. We investigate if cell specific deletions of *Gpt2* are sufficient to cause the phenotype using Cre drivers *in vivo*. In addition, as alanine formation is a critical function of GPT2, we ask whether alanine is a non-essential amino acid because of GPT2 and we perform deprivation assays in *Gpt2*-null neurons and astrocytes *in vitro*. Conversely, we test alanine supplementation *in vivo* for possible therapeutic effects in alleviating the *Gpt2*-null phenotype.

Chapters 3 and 5 explore various brain and spinal cord regions that may have specific vulnerability to the loss of GPT2. Pathological screening in the nervous system via immunohistochemistry to visualize cell counts, neurodegeneration markers and stains, and axonal projections may identify different neuronal circuits for which GPT2 function is essential. This in turn may explain the behavioral and motor phenotypes observed in the *Gpt2*-null mice and may be suggestive of the human phenotype. Chapter 3 explores mainly the spinal cord and cortical motor areas. Chapter 5 focuses on locus coeruleus (LC), the main noradrenergic supplier in the central nervous system implicated in the pathophysiology of Alzheimer's and Parkinson's Disease. We present evidence for a novel mechanism of neurodegeneration in LC.

Chapter 4 delineates the contribution of GPT2 to synaptic glutamate availability in the context of electrophysiology in hippocampal slices and synaptosomes, isolated

nerve terminals. Among a multitude of enzymes and reactions (44 reactions as curated from KEGG – Kyoto Encyclopedia of Genes and Genomes), the role of GPT2 in synaptic glutamate levels is unexplored and this investigation may identify a novel mechanism of regulation of the glutamate pool via a mitochondria-localized metabolic enzyme. This chapter also contains evidence for rescuing of metabolic defects associated with glutamate and TCA cycle metabolism in *Gpt2*-null mice by supplementing the TCA cycle.

Chapter 6 involves a cancerous cell line, KBM-7 based leukemia near-haploid cell lines, HAP1 cells, that carry *GPT2* mutations introduced by CRISPR (clustered regularly interspaced short palindromic repeats). This line of inquiry was pursued to determine if there are findings in cancerous cell lines that correlate with any of the phenotype seen with GPT2 Deficiency in other cell types and tissues. While the differences between the biological contexts are vast and unavoidable, this study may attribute a ubiquitous mechanism to the role of GPT2 in cellular growth.

Chapter 7, the Conclusion chapter, will attempt to give a summary and a broader picture of the results shown in the prior chapters.

REFERENCES

Adachi, Y., De Sousa-Coelho, A.L., Harata, I., Aoun, C., Weimer, S., Shi, X., Gonzalez Herrera, K.N., Takahashi, H., Doherty, C., Noguchi, Y.*, et al.* (2018). l-Alanine activates hepatic AMP-activated protein kinase and modulates systemic glucose metabolism. Mol Metab *17*, 61-70.

Ballhausen, D., Mittaz, L., Boulat, O., Bonafe, L., and Braissant, O. (2009). Evidence for catabolic pathway of propionate metabolism in CNS: expression pattern of methylmalonyl-CoA mutase and propionyl-CoA carboxylase alpha-subunit in developing and adult rat brain. Neuroscience *164*, 578-587.

Barua, A., and Mikheyev, A.S. (2021). An ancient, conserved gene regulatory network led to the rise of oral venom systems. Proc Natl Acad Sci U S A *118*.
Baytas, O., and Morrow, E.M. (2018). The Role of Mitochondrial Glutamate Metabolism in Cognitive Development and Disease. Neuropsychopharmacology *43*, 229-230.
Benuck, M., Stern, F., and Lajtha, A. (1971). Transamination of amino acids in homogenates of rat brzain. J Neurochem *18*, 1555-1567.
Binaafar, S., Razmara, E., Mahdieh, N., Sahebjame, H., Tavasoli, A.R., and Garshasbi, M. (2020). A novel missense variant in GPT2 causes non-syndromic autosomal recessive intellectual disability in a consanguineous Iranian family. Eur J Med Genet *63*, 103853.
Bowman, C.E., Zhao, L., Hartung, T., and Wolfgang, M.J. (2016). Requirement for the Mitochondrial Pyruvate Carrier in Mammalian Development Revealed by a Hypomorphic Allelic Series. Mol Cell Biol *36*, 2089-2104.
Caiola, E., Colombo, M., Sestito, G., Lupi, M., Marabese, M., Pastorelli, R., Broggini, M., and Brunelli, L. (2020). Glutaminase Inhibition on NSCLC Depends on Extracellular Alanine Exploitation. Cells *9*.
Cappel, D.A., Deja, S., Duarte, J.A.G., Kucejova, B., Inigo, M., Fletcher, J.A., Fu, X., Berglund, E.D., Liu, T., Elmquist, J.K.*, et al.* (2019). Pyruvate-Carboxylase-Mediated Anaplerosis Promotes Antioxidant Capacity by Sustaining TCA Cycle and Redox Metabolism in Liver. Cell Metab *29*, 1291-1305 e1298.
Case, E.M., and Mc, I.H. (1951). Respiration and phosphorylation in preparations from Mammalian Brain. Biochem J *48*, 1-11.
Celis, K., Shuldiner, S., Haverfield, E.V., Cappell, J., Yang, R., Gong, D.W., and Chung, W.K. (2015). Loss of function mutation in glutamic pyruvate transaminase 2 (GPT2) causes developmental encephalopathy. J Inherit Metab Dis *38*, 941-948.
Chen, Q., Kirk, K., Shurubor, Y.I., Zhao, D., Arreguin, A.J., Shahi, I., Valsecchi, F., Primiano, G., Calder, E.L., Carelli, V.*, et al.* (2018). Rewiring of Glutamine Metabolism Is a Bioenergetic Adaptation of Human Cells with Mitochondrial DNA Mutations. Cell Metab *27*, 1007-1025 e1005.
Cruz, F., Scott, S.R., Barroso, I., Santisteban, P., and Cerdan, S. (1998). Ontogeny and cellular localization of the pyruvate recycling system in rat brain. J Neurochem *70*, 2613-2619.
DeBerardinis, R.J., Lum, J.J., Hatzivassiliou, G., and Thompson, C.B. (2008). The biology of cancer: metabolic reprogramming fuels cell growth and proliferation. Cell Metab *7*, 11-20.
Divakaruni, A.S., Wallace, M., Buren, C., Martyniuk, K., Andreyev, A.Y., Li, E., Fields, J.A., Cordes, T., Reynolds, I.J., Bloodgood, B.L.*, et al.* (2017). Inhibition of the mitochondrial pyruvate carrier protects from excitotoxic neuronal death. J Cell Biol *216*, 1091-1105.
Erecinska, M., Nelson, D., Nissim, I., Daikhin, Y., and Yudkoff, M. (1994). Cerebral alanine transport and alanine aminotransferase reaction: alanine as a source of neuronal glutamate. J Neurochem *62*, 1953-1964.
Erecinska, M., and Silver, I.A. (1990). Metabolism and role of glutamate in mammalian brain. Prog Neurobiol *35*, 245-296.
Escalera-Fanjul, X., Campero-Basaldua, C., Colon, M., Gonzalez, J., Marquez, D., and Gonzalez, A. (2017). Evolutionary Diversification of Alanine Transaminases in Yeast: Catabolic Specialization and Biosynthetic Redundancy. Front Microbiol *8*, 1150.

Fasman, G.D. (1989). Prediction of Protein Structure and the Principles of Protein Conformation.
Felig, P. (1973). The glucose-alanine cycle. Metabolism *22*, 179-207.
Fonnum, F. (1984). Glutamate: a neurotransmitter in mammalian brain. J Neurochem *42*, 1-11.
Hao, Y., Samuels, Y., Li, Q., Krokowski, D., Guan, B.J., Wang, C., Jin, Z., Dong, B., Cao, B., Feng, X.*, et al.* (2016). Oncogenic PIK3CA mutations reprogram glutamine metabolism in colorectal cancer. Nat Commun *7*, 11971.
Haslam, R.J., and Krebs, H.A. (1963). The Metabolism of Glutamate in Homogenates and Slices of Brain Cortex. Biochem J *88*, 566-578.
Hassel, B., and Bråthe, A. (2000). Neuronal Pyruvate Carboxylation Supports Formation of Transmitter Glutamate. The Journal of Neuroscience *20*, 1342-1347.
Hengel, H., Keimer, R., Deigendesch, W., Riess, A., Marzouqa, H., Zaidan, J., Bauer, P., and Schols, L. (2018). GPT2 mutations cause developmental encephalopathy with microcephaly and features of complicated hereditary spastic paraplegia. Clin Genet *94*, 356-361.
Hertz, L., Peng, L., and Dienel, G.A. (2007). Energy metabolism in astrocytes: high rate of oxidative metabolism and spatiotemporal dependence on glycolysis/glycogenolysis. J Cereb Blood Flow Metab *27*, 219-249.
Hodge, R.D., Bakken, T.E., Miller, J.A., Smith, K.A., Barkan, E.R., Graybuck, L.T., Close, J.L., Long, B., Johansen, N., Penn, O.*, et al.* (2019). Conserved cell types with divergent features in human versus mouse cortex. Nature *573*, 61-68.
Hohnholt, M.C., Andersen, V.H., Andersen, J.V., Christensen, S.K., Karaca, M., Maechler, P., and Waagepetersen, H.S. (2018). Glutamate dehydrogenase is essential to sustain neuronal oxidative energy metabolism during stimulation. J Cereb Blood Flow Metab *38*, 1754-1768.
Honma, K., Kamikubo, M., Mochizuki, K., and Goda, T. (2017). Insulin-induced inhibition of gluconeogenesis genes, including glutamic pyruvic transaminase 2, is associated with reduced histone acetylation in a human liver cell line. Metabolism *71*, 118-124.
Issop, Y., Hathazi, D., Khan, M.M., Rudolf, R., Weis, J., Spendiff, S., Slater, C.R., Roos, A., and Lochmuller, H. (2018). GFPT1 deficiency in muscle leads to myasthenia and myopathy in mice. Hum Mol Genet *27*, 3218-3232.
Jadhao, S.B., Yang, R.Z., Lin, Q., Hu, H., Anania, F.A., Shuldiner, A.R., and Gong, D.W. (2004). Murine alanine aminotransferase: cDNA cloning, functional expression, and differential gene regulation in mouse fatty liver. Hepatology *39*, 1297-1302.
Jitrapakdee, S., St Maurice, M., Rayment, I., Cleland, W.W., Wallace, J.C., and Attwood, P.V. (2008). Structure, mechanism and regulation of pyruvate carboxylase. Biochem J *413*, 369-387.
Kam, K., and Nicoll, R. (2007). Excitatory synaptic transmission persists independently of the glutamate-glutamine cycle. J Neurosci *27*, 9192-9200.
Kang, H.J., Kawasawa, Y.I., Cheng, F., Zhu, Y., Xu, X., Li, M., Sousa, A.M., Pletikos, M., Meyer, K.A., Sedmak, G.*, et al.* (2011). Spatio-temporal transcriptome of the human brain. Nature *478*, 483-489.
Karmen, A., Wroblewski, F., and Ladue, J.S. (1955). Transaminase activity in human blood. J Clin Invest *34*, 126-131.

Kaymakcalan, H., Yarman, Y., Goc, N., Toy, F., Meral, C., Ercan-Sencicek, A.G., and Gunel, M. (2018). Novel compound heterozygous mutations in GPT2 linked to microcephaly, and intellectual developmental disability with or without spastic paraplegia. Am J Med Genet A *176*, 421-425.
Kim, M., Gwak, J., Hwang, S., Yang, S., and Jeong, S.M. (2019). Mitochondrial GPT2 plays a pivotal role in metabolic adaptation to the perturbation of mitochondrial glutamine metabolism. Oncogene *38*, 4729-4738.
Kim, S.H., Schneider, B.L., and Reitzer, L. (2010). Genetics and regulation of the major enzymes of alanine synthesis in Escherichia coli. J Bacteriol *192*, 5304-5311.
Kornberg, H.L. (1966). The role and control of the glyoxylate cycle in Escherichia coli. Biochem J *99*, 1-11.
Kovacevic, Z. (1971). The pathway of glutamine and glutamate oxidation in isolated mitochondria from mammalian cells. Biochem J *125*, 757-763.
Krebs, H.A. (1953). Equilibria in transamination systems. Biochem J *54*, 82-86.
Labelle, Y., Puymirat, J., and Tanguay, R.M. (1993). Localization of cells in the rat brain expressing fumarylacetoacetate hydrolase, the deficient enzyme in hereditary tyrosinemia type 1. Biochimica et Biophysica Acta (BBA) - Molecular Basis of Disease *1180*, 250-256.
Lenartowicz, E., and Wojtczak, A.B. (1988). Significance of the alanine aminotransferase reaction in the formation of α-ketoglutarate in rat liver mitochondria. Archives of Biochemistry and Biophysics *260*, 309-319.
Lindblom, P., Rafter, I., Copley, C., Andersson, U., Hedberg, J.J., Berg, A.L., Samuelsson, A., Hellmold, H., Cotgreave, I., and Glinghammar, B. (2007). Isoforms of alanine aminotransferases in human tissues and serum--differential tissue expression using novel antibodies. Arch Biochem Biophys *466*, 66-77.
Lobo-Prada, T., Sticht, H., Bogantes-Ledezma, S., Ekici, A., Uebe, S., Reis, A., and Leal, A. (2017). A Homozygous Mutation in GPT2 Associated with Nonsyndromic Intellectual Disability in a Consanguineous Family from Costa Rica. JIMD Rep *36*, 59-66.
McCommis, K.S., Chen, Z., Fu, X., McDonald, W.G., Colca, J.R., Kletzien, R.F., Burgess, S.C., and Finck, B.N. (2015). Loss of Mitochondrial Pyruvate Carrier 2 in the Liver Leads to Defects in Gluconeogenesis and Compensation via Pyruvate-Alanine Cycling. Cell Metab *22*, 682-694.
McKenna, M.C. (2007). The glutamate-glutamine cycle is not stoichiometric: fates of glutamate in brain. J Neurosci Res *85*, 3347-3358.
McKenna, M.C., and Ferreira, G.C. (2016). Enzyme Complexes Important for the Glutamate-Glutamine Cycle. Adv Neurobiol *13*, 59-98.
McNair, L.F., Andersen, J.V., Aldana, B.I., Hohnholt, M.C., Nissen, J.D., Sun, Y., Fischer, K.D., Sonnewald, U., Nyberg, N., Webster, S.C.*, et al.* (2019). Deletion of Neuronal GLT-1 in Mice Reveals Its Role in Synaptic Glutamate Homeostasis and Mitochondrial Function. J Neurosci *39*, 4847-4863.
Meton, I., Egea, M., Fernandez, F., Eraso, M.C., and Baanante, I.V. (2004). The N-terminal sequence directs import of mitochondrial alanine aminotransferase into mitochondria. FEBS Lett *566*, 251-254.
Miller, A.L., Hawkins, R.A., and Veech, R.L. (1973). The mitochondrial redox state of rat brain. J Neurochem *20*, 1393-1400.

Miller, S.L. (1953). A production of amino acids under possible primitive earth conditions. Science *117*, 528-529.
Miller, S.L., and Urey, H.C. (1959). Organic compound synthesis on the primitive earth. Science *130*, 245-251.
Milstein, J.M., White, J.G., and Swaiman, K.F. (1968). Oxidative phosphorylation in mitochondria of developing rat brain. J Neurochem *15*, 411-415.
Motori, E., Atanassov, I., Kochan, S.M.V., Folz-Donahue, K., Sakthivelu, V., Giavalisco, P., Toni, N., Puyal, J., and Larsson, N.G. (2020). Neuronal metabolic rewiring promotes resilience to neurodegeneration caused by mitochondrial dysfunction. Sci Adv *6*, eaba8271.
Ouyang, Q., Kavanaugh, B.C., Joesch-Cohen, L., Dubois, B., Wu, Q., Schmidt, M., Baytas, O., Pastore, S.F., Harripaul, R., Mishra, S.*, et al.* (2019). GPT2 mutations in autosomal recessive developmental disability: extending the clinical phenotype and population prevalence estimates. Hum Genet *138*, 1183-1200.
Ouyang, Q., Nakayama, T., Baytas, O., Davidson, S.M., Yang, C., Schmidt, M., Lizarraga, S.B., Mishra, S., Ei-Quessny, M., Niaz, S.*, et al.* (2016). Mutations in mitochondrial enzyme GPT2 cause metabolic dysfunction and neurological disease with developmental and progressive features. Proc Natl Acad Sci U S A *113*, E5598-5607.
Owen, O.E., Kalhan, S.C., and Hanson, R.W. (2002). The key role of anaplerosis and cataplerosis for citric acid cycle function. J Biol Chem *277*, 30409-30412.
Peng, L., Hertz, L., Huang, R., Sonnewald, U., Petersen, S.B., Westergaard, N., Larsson, O., and Schousboe, A. (1993). Utilization of glutamine and of TCA cycle constituents as precursors for transmitter glutamate and GABA. Dev Neurosci *15*, 367-377.
Peng, L.A., Schousboe, A., and Hertz, L. (1991). Utilization of alpha-ketoglutarate as a precursor for transmitter glutamate in cultured cerebellar granule cells. Neurochem Res *16*, 29-34.
Qian, K., Zhong, S., Xie, K., Yu, D., Yang, R., and Gong, D.W. (2015). Hepatic ALT isoenzymes are elevated in gluconeogenic conditions including diabetes and suppressed by insulin at the protein level. Diabetes Metab Res Rev *31*, 562-571.
Rae, C., Hare, N., Bubb, W.A., McEwan, S.R., Broer, A., McQuillan, J.A., Balcar, V.J., Conigrave, A.D., and Broer, S. (2003). Inhibition of glutamine transport depletes glutamate and GABA neurotransmitter pools: further evidence for metabolic compartmentation. J Neurochem *85*, 503-514.
Rajab, A., Yoo, S.Y., Abdulgalil, A., Kathiri, S., Ahmed, R., Mochida, G.H., Bodell, A., Barkovich, A.J., and Walsh, C.A. (2006). An autosomal recessive form of spastic cerebral palsy (CP) with microcephaly and mental retardation. Am J Med Genet A *140*, 1504-1510.
Ron-Harel, N., Ghergurovich, J.M., Notarangelo, G., LaFleur, M.W., Tsubosaka, Y., Sharpe, A.H., Rabinowitz, J.D., and Haigis, M.C. (2019). T Cell Activation Depends on Extracellular Alanine. Cell Rep *28*, 3011-3021 e3014.
Rossiter, N.J., Huggler, K.S., Adelmann, C.H., Keys, H.R., Soens, R.W., Sabatini, D.M., and Cantor, J.R. (2021). CRISPR screens in physiologic medium reveal conditionally essential genes in human cells. Cell Metab *33*, 1248-1263 e1249.
Ruaud, L., Keren, B., Debs, R., Mignot, C., and Mochel, F. (2021). Demyelinating motor neuropathy associated with a homozygous GPT2 pathogenic variant. Muscle Nerve.

Ruscak, M., Orlicky, J., Zubor, V., and Hager, H. (1982). Alanine aminotransferase in bovine brain: purification and properties. J Neurochem *39*, 210-216.
Salganicoff, L., and Derobertis, E. (1965). Subcellular Distribution of the Enzymes of the Glutamic Acid, Glutamine and Gamma-Aminobutyric Acid Cycles in Rat Brain. J Neurochem *12*, 287-309.
Shank, R.P., Baldy, W.J., and Ash, C.W. (1989). Glutamine and 2-oxoglutarate as metabolic precursors of the transmitter pools of glutamate and GABA: correlation of regional uptake by rat brain synaptosomes. Neurochem Res *14*, 371-376.
Smith, B., Schafer, X.L., Ambeskovic, A., Spencer, C.M., Land, H., and Munger, J. (2016). Addiction to Coupling of the Warburg Effect with Glutamine Catabolism in Cancer Cells. Cell Rep *17*, 821-836.
Spiegel, E.K., Colman, R.F., and Patterson, D. (2006). Adenylosuccinate lyase deficiency. Mol Genet Metab *89*, 19-31.
Tan, H.W.S., Sim, A.Y.L., and Long, Y.C. (2017). Glutamine metabolism regulates autophagy-dependent mTORC1 reactivation during amino acid starvation. Nat Commun *8*, 338.
Ugur, B., Bao, H., Stawarski, M., Duraine, L.R., Zuo, Z., Lin, Y.Q., Neely, G.G., Macleod, G.T., Chapman, E.R., and Bellen, H.J. (2017). The Krebs Cycle Enzyme Isocitrate Dehydrogenase 3A Couples Mitochondrial Metabolism to Synaptic Transmission. Cell Rep *21*, 3794-3806.
Vogel, R., Jennemann, G., Seitz, J., Wiesinger, H., and Hamprecht, B. (1998). Mitochondrial malic enzyme: purification from bovine brain, generation of an antiserum, and immunocytochemical localization in neurons of rat brain. J Neurochem *71*, 844-852.
Waagepetersen, H.S., Sonnewald, U., Larsson, O.M., and Schousboe, A. (2000). A possible role of alanine for ammonia transfer between astrocytes and glutamatergic neurons. J Neurochem *75*, 471-479.
Westergaard, N., Sonnewald, U., and Schousboe, A. (1994). Release of α-ketoglutarate, malate and succinate from cultured astrocytes: possible role in amino acid neurotransmitter homeostasis. Neuroscience Letters *176*, 105-109.
Westergaard, N., Sonnewald, U., and Schousboe, A. (1995). Metabolic trafficking between neurons and astrocytes: the glutamate/glutamine cycle revisited. Dev Neurosci *17*, 203-211.
Westergaard, N., Varming, T., Peng, L., Sonnewald, U., Hertz, L., and Schousboe, A. (1993). Uptake, release, and metabolism of alanine in neurons and astrocytes in primary cultures. J Neurosci Res *35*, 540-545.
Wilbur, D.O., and Patel, M.S. (1974). Development of mitochondrial pyruvate metabolism in rat brain. J Neurochem *22*, 709-715.
Xu, Z., Ma, J., Qu, C., Hu, Y., Hao, B., Sun, Y., Liu, Z., Yang, H., Yang, C., Wang, H.*, et al.* (2017). Identification and expression analyses of the alanine aminotransferase (AlaAT) gene family in poplar seedlings. Sci Rep *7*, 45933.
Yang, C., Ko, B., Hensley, C.T., Jiang, L., Wasti, A.T., Kim, J., Sudderth, J., Calvaruso, M.A., Lumata, L., Mitsche, M.*, et al.* (2014). Glutamine oxidation maintains the TCA cycle and cell survival during impaired mitochondrial pyruvate transport. Mol Cell *56*, 414-424.

Yang, R.Z., Blaileanu, G., Hansen, B.C., Shuldiner, A.R., and Gong, D.W. (2002). cDNA cloning, genomic structure, chromosomal mapping, and functional expression of a novel human alanine aminotransferase. Genomics *79*, 445-450.
Yang, R.Z., Park, S., Reagan, W.J., Goldstein, R., Zhong, S., Lawton, M., Rajamohan, F., Qian, K., Liu, L., and Gong, D.W. (2009). Alanine aminotransferase isoenzymes: molecular cloning and quantitative analysis of tissue expression in rats and serum elevation in liver toxicity. Hepatology *49*, 598-607.
Yu, A.C., Drejer, J., Hertz, L., and Schousboe, A. (1983). Pyruvate carboxylase activity in primary cultures of astrocytes and neurons. J Neurochem *41*, 1484-1487.

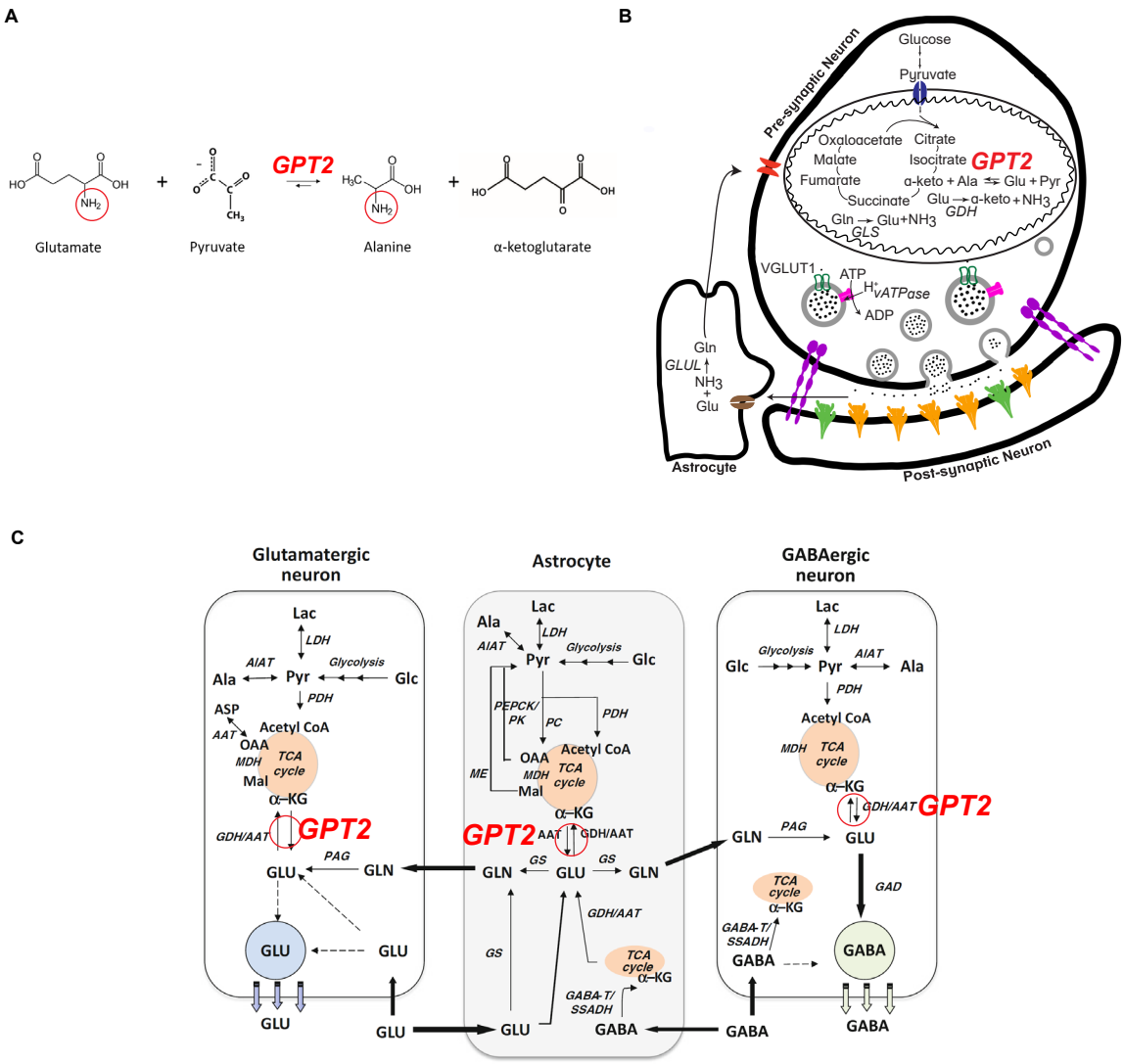

Figure 1.1 – Gpt2 and relevant metabolic pathways.
A. The reaction catalyzed by GPT2. It's a reversible reaction transferring an amino group (red circle) from glutamate to pyruvate yielding alanine and alpha-ketoglutarate. Note that the predicted direction of the reaction is toward alanine formation reflected in the arrow lengths.
B. Metabolic pathways relevant to Gpt2 and glutamate metabolism in synaptosomes (isolated nerve terminals) including pre-synaptic neuron, post-synaptic neuron and astrocytic components. GDH: glutamate dehydrogenase, GLS: glutaminase, GLUL: glutamine synthetase. **C.** Adapted from the first figure in (McKenna and Ferreira, 2016). GPT2 is added to the metabolic pathways along with GDH (glutamate dehydrogenase) and AAT (aspartate aminotransferase) noting the arrows in the reaction with a red circle. The authors omitted the mitochondrial isozyme of glutamate pyruvate transaminase but the cytosolic isozyme is denoted as A/AT. Abbreviations: Ala: alanine, a-KG: alpha-ketoglutarate, ASP: aspartate, GABA-T: GABA aminotransferase, Glc: glucose, Glu: glutamate, GAD: glutamate decarboxylase, Gln: glutamine, GS: glutamine synthetase, Lac: lactate, LDH: lactate dehydrogenase, Mal: malate, MDH: malate dehydrogenase, OAA: oxaloacetate, PAG: phosphate-activated glutaminase, PEPCK: phosphoenolpyruvate carboxykinase, Pyr: pyruvate, PDH: pyruvate dehydrogenase, PK: pyruvate kinase, SSADH: succinic semialdehyde dehydrogenase. Copyright permission for panel C is granted from Elsevier.

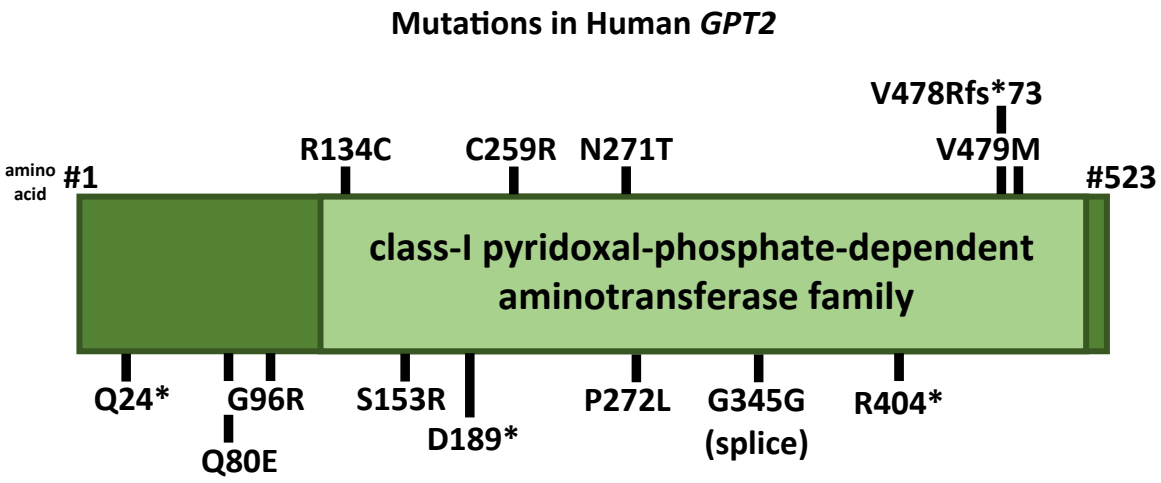

Figure 1.2 – Mutations in the human GPT2 gene.
Mutations in human GPT2 gene. Gpt2 belongs to the class-I pyridoxal-phosphate dependent aminotransferase enzyme family and the sequence that shows similarity within the members of the enzyme family is shown in lighter green. RefSeq number of Gpt2: NM_133443. Mutations are found in the following publications: S153R: (Celis et al. 2015); R404X, P272L: (Ouyang et al. 2016); R134C, V479M: (Kaymakcalan et al. 2018); Q24X: (Hengel et al. 2018); N271T, V478Rfs*73, C259R, G345G(splice), Q80E: (Ouyang et al. 2019); G96R: (Lobo-Prada et al. 2017), D189*: (Ruaud et al. 2021).

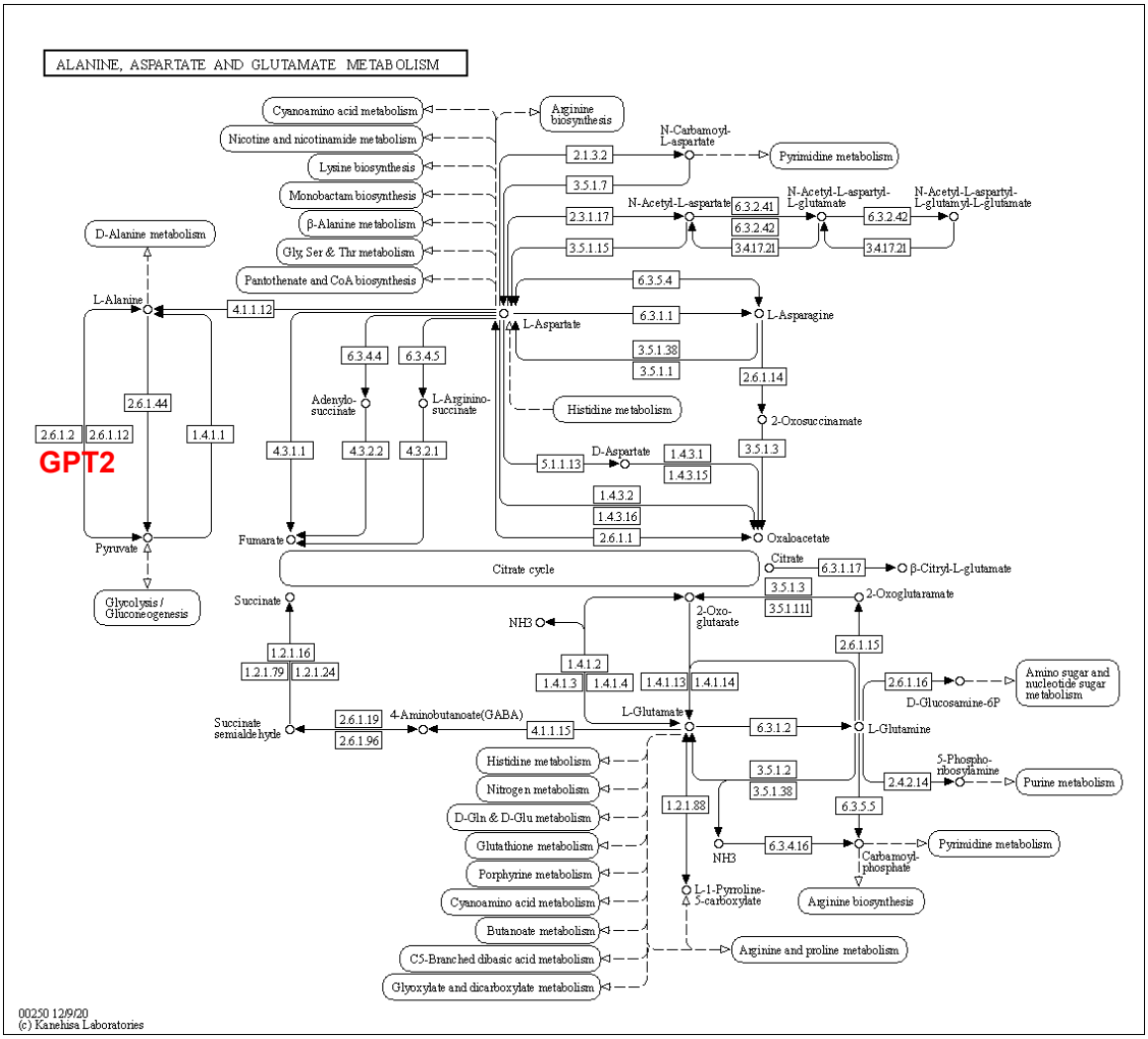

Figure 1.3 – KEGG: the Alanine, Aspartate and Glutamate Metabolism Pathway. **A**. Image taken from Kyoto Encyclopedia of Genes and Genomes (KEGG) (Kanehisa et al., 2020) showing Alanine, Aspartate and Glutamate metabolism and the related connections to other metabolic pathways (Pathway map no.: 00250). GPT2 is shown in red, the enzyme number: EC 2.6.1.2. Copyright permission granted from Kanehisa Laboratories.

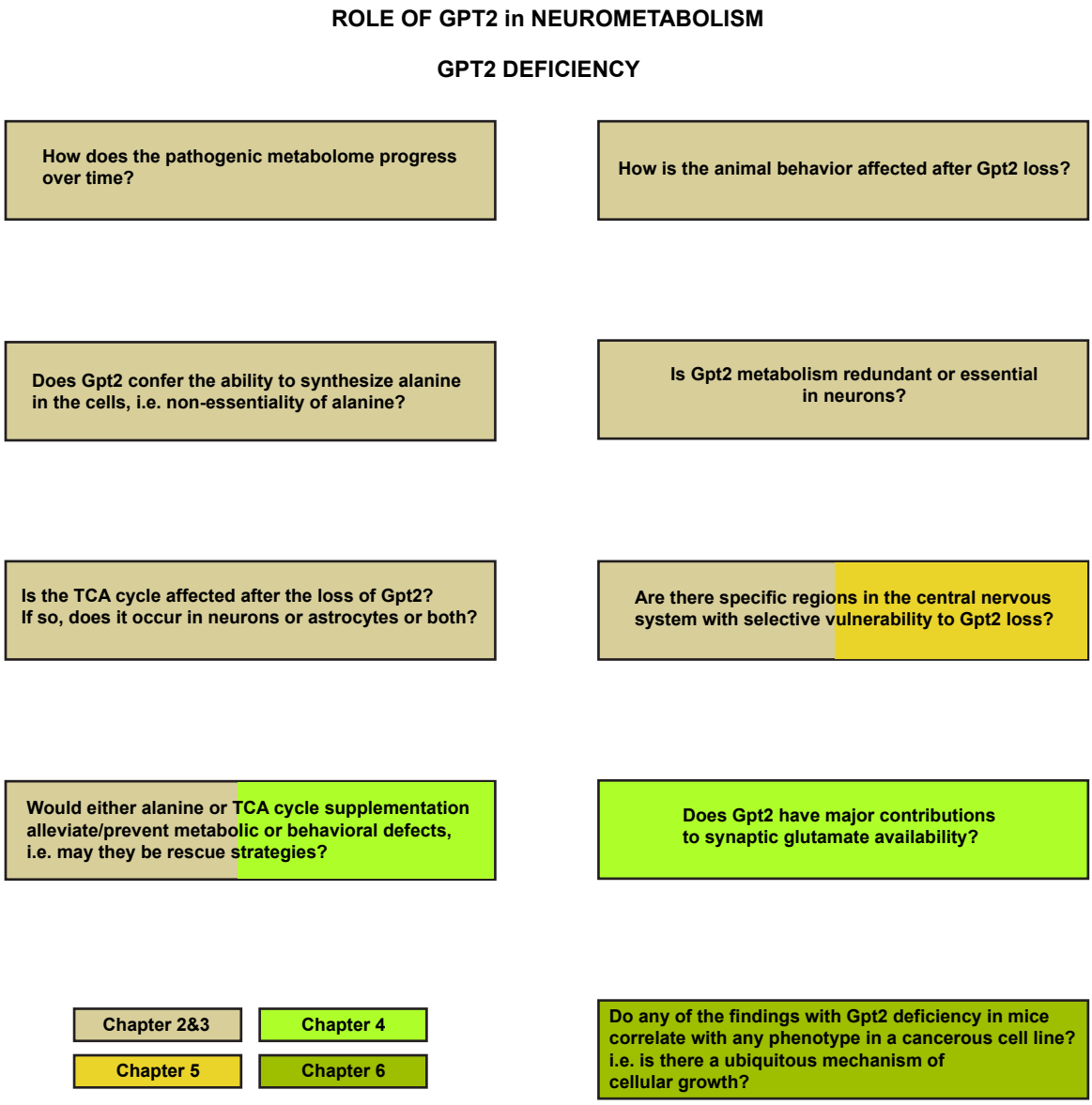

Figure 1.4 – Questions asked regarding the role of Gpt2 in neurometabolism through the study of Gpt2 deficiency.

Table 1.1. – Reactions that result in net production of a TCA cycle intermediate – a list of Anaplerotic pathways.

Enzyme/Process	Reaction	Predicted preferred reaction	Additional Co-factors	Predominantly expressing Cell Type	Any Associated Diseases
Pyruvate carboxylase[1]	pyruvate + $HCO3^-$ + ATP -> oxaloacetate + ADP + Pi	forward	biotin, acetyl CoA, $Mg2+$, $Mn2+$	glial	OMIM 266150: Pyruvate carboxylase deficiency (failure to thrive, intellectual disability, recurrent sezires, developmental delay, abnormal movements (spasticity, tremor, dyskenieska, hyperreflexia, Babinski sign)
Glutamate pyruvate transaminase 1/2[2,3]	glutamate + pyruvate <--> alanine + alpha-ketoglutarate	forward	pyridoxal 6-phosphate	???	OMIM 616281: GPT2 deficiency (postnatal microcephaly, intellectual disability, spastic paraplegia, hyperreflexia, hypertonia, wide-gait)
Glutamate dehydrogenase[3]	glutamate + H_2O + $NAD(P)^+$ -> alpha-ketoglutarate + NH_3 + NAD(P)H + H	forward		neuronal/glial	OMIM 606762: Hyperactivation of GLUD1 (hyperinsulinemic hypoglycemia, seizures)
Malic enzyme[4,5]	pyruvate + CO2 + NAD(P)H -> malate + $NAD(P)^+$	reverse		neuronal (mitochondrial), glial (cytosolic)	
Phosphoenolpyruvate carboxylase[1,6]	phosphoenolpyruvate + $HCO3^-$ -> oxaloacetate + Pi	reverse	$Co2+$, $Mg2+$, $Mn2+$	neuronal/glial	OMIM 261650: PCK deficiency (hypoglycemia, fatty liver, liver failure)
Adenylosuccinate lyase[7]	adenylosuccinate -> AMP + fumarate	forward		???	OMIM 103050: ADSL deficiency (failure to thrive, microcephaly, psychomotor delay, intellectual disability, autism, hyperreflexia, inability to walk, refractory seizures, spasticity, gait ataxia)
B-oxidation of fatty acids/cholesterol & Valine, isoleucine, threonine, methionine Degradation: methylmalonic acid mutase (final reaction)[8]	-->-->-->-->--> L-methylmalonyl CoA--> succinyl CoA	forward	cobamamide	neuronal	OMIM 251000: MMUT deficiency (failure to thrive, develpmental delay, hypotonia, lethargy)
Phenylalanine, Tyrosine Degradation: fumaryl acetoacetase (final reaction)[9]	-->--> fumarylacetoacetate --> fumarate + acetoacetate	forward	$Ca2+$, $Mg2+$	glial (oligodendrocytes)	OMIM 276700: FAH deficiency (failure to thrive, episodic paralysis, episodic peripheral neuropathy)

1 (Jitrapakdee et al., 2008), 2 (Ouyang et al., 2016), 3 (Erecinska and Silver, 1990), 4 (Vogel et al., 1998), 5 (Hassel and Bråthe, 2000), 6 (Cruz et al., 1998), 7 (Spiegel et al., 2006), 8 (Ballhausen et al., 2009), 9 (Labelle et al., 1993).

Chapter 2: Mutations in mitochondrial enzyme GPT2 cause metabolic dysfunction and neurological disease with developmental and progressive features.

This Chapter contains the paper published in Proceedings of the National Academy of Sciences of the United States of America (PNAS) in 2016 by Qing Ouyang and co-workers. doi.org/10.1073/pnas.1609221113. My contributions were Figure 5 and supplementary figure 7, involving metabolomics in *Gpt2*-null whole brain and lacZ staining for *Gpt2* expression pattern in *Gpt2*-heterozygous mouse brains. The rest were conducted by Dr. Qing Ouyang in Dr. Eric Morrow's laboratory and Dr. Toko Nakayama, and clinicians involved in human patients with GPT2 Deficiency. For funding sources please refer to the Chapter.

Mutations in mitochondrial enzyme GPT2 cause metabolic dysfunction and neurological disease with developmental and progressive features

Qing Ouyang[a,b,c,1], Tojo Nakayama[d,e,f,1], Ozan Baytas[a,b], Shawn M. Davidson[g], Chendong Yang[h], Michael Schmidt[a,b,c], Sofia B. Lizarraga[i], Sasmita Mishra[a,b], Malak El-Quessny[d,e], Saima Niaz[j,k], Mirrat Gul Butt[j,l], Syed Imran Murtaza[j], Afzal Javed[j], Haroon Rashid Chaudhry[j,l], Dylan J. Vaughan[d,e], R. Sean Hill[d,e], Jennifer N. Partlow[d,e,m], Seung-Yun Yoo[d,e,m,2], Anh-Thu N. Lam[d,e,m], Ramzi Nasir[f,n], Muna Al-Saffar[d,e,o], A. James Barkovich[p], Matthew Schwede[a,b], Shailender Nagpal[a,b,c], Anna Rajab[q], Ralph J. DeBerardinis[h], David E. Housman[g,3], Ganeshwaran H. Mochida[d,e,f,r,3], and Eric M. Morrow[a,b,c,3]

[a]Department of Molecular Biology, Cell Biology, and Biochemistry, Brown University, Providence, RI 02912; [b]Institute for Brain Science, Brown University, Providence, RI 02912; [c]Developmental Disorders Genetics Research Program, Emma Pendleton Bradley Hospital and Department of Psychiatry and Human Behavior, Alpert Medical School of Brown University, East Providence, RI 02915; [d]Division of Genetics and Genomics, Department of Medicine, Boston Children's Hospital, Boston, MA 02115; [e]Manton Center for Orphan Disease Research, Boston Children's Hospital, Boston, MA 02115; [f]Department of Pediatrics, Harvard Medical School, Boston, MA 02115; [g]Department of Biology, Massachusetts Institute of Technology, Cambridge, MA 02139; [h]Department of Pediatrics, Children's Medical Center Research Institute, University of Texas Southwestern Medical Center, Dallas, TX 75390; [i]Center for Childhood of Neurotherapeutics, Department of Biological Sciences, University of South Carolina, Columbia, SC 29208; [j]Pakistan Psychiatric Research Centre, Fountain House, Lahore, Pakistan; [k]North London Forensic Service, Chase Farm Hospital, Barnet, Enfield and Haringey Mental Health National Health Service Trust, Enfield EN2 8JL, United Kingdom; [l]Department of Psychiatry, Fatima Jinnah Medical College/Sir Ganga Ram Hospital, Lahore, Pakistan; [m]Howard Hughes Medical Institute, Boston Children's Hospital, Boston, MA 02115; [n]Division of Developmental Medicine, Department of Medicine, Boston Children's Hospital, Boston, MA 02115; [o]Department of Paediatrics, College of Medicine and Health Sciences, United Arab Emirates University, Al-Ain, United Arab Emirates; [p]Department of Radiology and Biomedical Imaging, University of California, San Francisco, CA 94143; [q]National Genetic Centre, Directorate General of Royal Hospital, Ministry of Health, Muscat, Sultanate of Oman; and [r]Pediatric Neurology Unit, Department of Neurology, Massachusetts General Hospital, Boston, MA 02114

Contributed by David E. Housman, June 22, 2016 (sent for review February 1, 2016; reviewed by Elizabeth M. C. Fisher and William C. Mobley)

Mutations that cause neurological phenotypes are highly informative with regard to mechanisms governing human brain function and disease. We report autosomal recessive mutations in the enzyme glutamate pyruvate transaminase 2 (GPT2) in large kindreds initially ascertained for intellectual and developmental disability (IDD). GPT2 [also known as alanine transaminase 2 (ALT2)] is one of two related transaminases that catalyze the reversible addition of an amino group from glutamate to pyruvate, yielding alanine and α-ketoglutarate. In addition to IDD, all affected individuals show postnatal microcephaly and ∼80% of those followed over time show progressive motor symptoms, a spastic paraplegia. Homozygous nonsense p.Arg404* and missense p.Pro272Leu mutations are shown biochemically to be loss of function. The *GPT2* gene demonstrates increasing expression in brain in the early postnatal period, and GPT2 protein localizes to mitochondria. Akin to the human phenotype, *Gpt2*-null mice exhibit reduced brain growth. Through metabolomics and direct isotope tracing experiments, we find a number of metabolic abnormalities associated with loss of Gpt2. These include defects in amino acid metabolism such as low alanine levels and elevated essential amino acids. Also, we find defects in anaplerosis, the metabolic process involved in replenishing TCA cycle intermediates. Finally, mutant brains demonstrate misregulated metabolites in pathways implicated in neuroprotective mechanisms previously associated with neurodegenerative disorders. Overall, our data reveal an important role for the GPT2 enzyme in mitochondrial metabolism with relevance to developmental as well as potentially to neurodegenerative mechanisms.

GPT2 | intellectual and developmental disability | mitochondria | metabolomics | spastic paraplegia

Intellectual and developmental disabilities (IDDs) occur in 2% of people worldwide and rank first in the United States as a cause of lifelong disability (1). IDD can be accompanied by various associated features, including motor disability. Hereditary spastic paraplegia (HSP) is a unique form of motor disability that is characterized by progressive spasticity and weakness of the lower extremities (2). In addition, postnatal microcephaly may occur with IDD and complicated forms of HSP, and likely reflects failures in processes driving postnatal brain growth such as neuronal arborization, synaptogenesis, and gliogenesis (3).

In this study, we present the discovery of loss-of-function mutations in the gene encoding the enzyme glutamate pyruvate transaminase 2 (GPT2) in autosomal recessive IDD with postnatal microcephaly and motor findings consistent with progressive spastic

Significance

We report autosomal recessive mutations in the enzyme glutamate pyruvate transaminase 2 (GPT2) in a neurological syndrome involving intellectual disability, reduced brain growth, and progressive motor symptoms. We show that the mutations inactivate the enzyme. GPT2 catalyzes the reversible addition of an amino group from glutamate to pyruvate, yielding alanine and α-ketoglutarate. The *GPT2* gene demonstrates expression in brain postnatally, and the protein localizes to mitochondria. As in humans, *Gpt2*-null mice exhibit reduced brain growth. Furthermore, mutant mouse brains show abnormal metabolite levels, including in pathways involving amino acid metabolism, the TCA cycle, and neuroprotective mechanisms. Our study identifies GPT2 as an important mitochondrial enzyme in disease that has general relevance to developmental and potentially to neurodegenerative mechanisms.

Author contributions: Q.O., T.N., O.B., S.M.D., C.Y., R.J.D., D.E.H., G.H.M., and E.M.M. designed research; Q.O., T.N., O.B., S.M.D., C.Y., M. Schmidt, S.B.L., S.M., M.E.-Q., S. Niaz, M.G.B., S.I.M., A.J., H.R.C., D.J.V., R.S.H., J.N.P., S.-Y.Y., A.-T.N.L., R.N., M.A.-S., A.J.B., M. Schwede, S. Nagpal, A.R., R.J.D., D.E.H., G.H.M., and E.M.M. performed research; Q.O., T.N., O.B., S.M.D., C.Y., R.J.D., D.E.H., G.H.M., and E.M.M. contributed new reagents/analytic tools; Q.O., T.N., O.B., S.M.D., C.Y., S.B.L., S. Niaz, M.G.B., S.I.M., A.J., H.R.C., R.S.H., J.N.P., A.J.B., M. Schwede, S. Nagpal, A.R., R.J.D., D.E.H., G.H.M., and E.M.M. analyzed data; and Q.O., T.N., O.B., S.M.D., S.B.L., R.S.H., J.N.P., R.J.D., D.E.H., G.H.M., and E.M.M. wrote the paper.

Reviewers: E.M.C.F., University College London; and W.C.M., University of California, San Diego.

The authors declare no conflict of interest.

Freely available online through the PNAS open access option.

[1]Q.O. and T.N. contributed equally to this work.

[2]Present address: Gilead Sciences, Inc., Foster City, CA 94404.

[3]To whom correspondence may be addressed. Email: dhousman@mit.edu, Ganesh.Mochida@childrens.harvard.edu, or Eric_Morrow@brown.edu.

This article contains supporting information online at www.pnas.org/lookup/suppl/doi:10.1073/pnas.1609221113/-/DCSupplemental.

paraplegia. GPT2 [also known as alanine transaminase 2 (ALT2) or alanine aminotransferase 2 (ALAT2)] is one of two related enzymes that catalyze the reversible addition of an amino group from glutamate to pyruvate, yielding alanine and α-ketoglutarate. GPT2 and highly related GPT are among several transaminases that regulate critical metabolic processes, including amino acid metabolism and the tricarboxylic acid (TCA) cycle. Glutamate is also a substrate in the synthesis of glutathione, an important antioxidant in cells (4). We show that GPT2 is localized to mitochondria and is expressed at increasing levels in brain during early postnatal development corresponding to periods of circuit development.

Mitochondria play an essential role in neurons given the high energy demands of these cells, and mitochondria are particularly abundant at synapses, where they mediate synaptic growth, energetics, signaling, and protection (5). Mitochondrial dysfunction is involved in both human neurodevelopmental as well as neurodegenerative disease (6–8). The TCA cycle in mitochondria functions in both energy production as well as in biosynthetic processes. TCA cycle intermediates may be extracted for biosynthetic metabolism through a process termed cataplerosis, and TCA intermediates are replenished via anaplerosis (9).

In addition to identification of mutations in GPT2 in human neurological disease, we have developed a mouse model of Gpt2 deficiency. Akin to the human phenotype, we see reduced brain growth in this mouse model. Metabolomics studies in *Gpt2*-null mouse brains reveal reduced TCA metabolites consistent with a defect in anaplerosis. We also identify metabolomic signatures reflecting abnormalities in amino acid metabolism, as well as in neuroprotective mechanisms previously implicated in neurodegenerative disease. Overall, our data support an important role for GPT2 in mitochondria-based metabolism and neurological disease with both developmental and progressive features.

Results

Clinical Analyses of Pedigrees with Intellectual Disability and Postnatal Microcephaly. As a contribution to understanding the genetic underpinnings of neurological disease, we have studied two large consanguineous kindreds with a neurodevelopmental condition. Affected members in families shown in Fig. 1*A* share a phenotype that includes intellectual disability with postnatal microcephaly and variable, progressive spasticity (see also ref. 10). In total, our studies included 14 affected individuals. All affected individuals

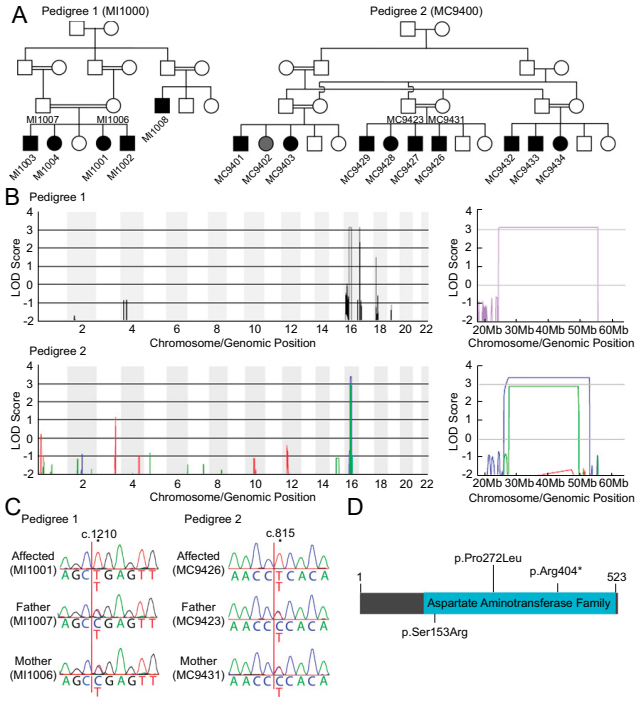

Fig. 1. Identification of *GPT2* mutations in large kindreds with recent shared ancestry affected by IDD with postnatal microcephaly. (*A*) Pedigree 1 (MI1000) is from Pakistan. Pedigree 2 (MC9400) is from the Sultanate of Oman. Filled symbols indicate affected individuals. Shaded symbol (MC9402) indicates a similarly affected individual, who was found not to have a homozygous *GPT2* mutation. We have described the clinical presentation of pedigree 2 (MC9400) in a prior publication (10). (*B*) Genome-wide LOD scores for pedigree 1 show a region of linkage on chromosome 16q11.2, with a maximum multipoint LOD score of 3.13. Linkage analysis of pedigree 2 was performed for each of the three branches. Branch 1 (red) did not show a region of statistically significant linkage given heterozygous individual MC9402 with phenocopy, whereas both branch 2 (blue) and branch 3 (green) indicate linkage to chromosome 16q11.2 with LOD scores of 3.38 and 2.90, respectively. Magnified LOD score graphs for chromosome 16q are shown on the *Right*. (*C*) Sanger sequencing of *GPT2* confirmed the identified mutations in pedigree 1 (c.1210C>T, p.Arg404*) and pedigree 2 (c.815C>T, p.Pro272Leu). Positions of mutations are according to NM_133443.3 (cDNA) and NP_597700.1 (protein). (*D*) Schematic diagram of conserved domains in GPT2. The positions of the mutations with a previously reported mutation (p.Ser153Arg) are shown (14).

were born after uneventful pregnancies without asphyxia. Head circumference was normal at birth for all seven individuals for whom data were available, but affected individuals subsequently developed microcephaly postnatally, ranging from 2.8 to 6.8 SDs below the mean (Table 1 and *SI Appendix*, Table S1). The majority (88%) of affected individuals were reported to be hypotonic during infancy. All 9 cases with data available (of 14 total cases) were able to walk by the age of 3 y. All had delayed speech and showed oral–motor dysfunction. Five (36%) had a history of seizures, with three (MC9426, MC9429, and MI1002) having been diagnosed with various types of epilepsy syndromes, including one with Lennox–Gastaut syndrome, and the other two individuals each reporting a single seizure episode. Full detailed clinical descriptions are provided in *SI Appendix*, Table S1.

The majority (83%) of the affected individuals showed subsequent difficulty in walking. Over time, motor examination was remarkable for hypertonia and hyperreflexia. In most cases (77%), lower extremities were more severely affected, thus presenting as spastic diplegia or spastic paraplegia. In some individuals, hand movements were clumsy, tremulous, and poorly coordinated. Results from brain imaging studies [computed tomography or magnetic resonance imaging (MRI)] were obtained for 10 individuals and showed no obvious structural malformation other than microcephaly, except for 1 individual who had reduced white matter volume and a thin corpus callosum (*SI Appendix*, Fig. S1).

Identifying *GPT2* Mutations by Linkage Mapping and Whole-Exome Sequencing. Pedigrees 1 and 2 showed strong linkage to a locus on chromosome 16q (Fig. 1*B*). In pedigree 1, genome-wide linkage analysis of the larger branch (affected individuals: MI1001, MI1002, MI1003, and MI1004) revealed a region of linkage on chromosome 16q with a maximum logarithm of odds (LOD) score of 3.13 (Fig. 1*B*). The region was delineated by SNP markers rs198188 to rs12917822 (chr16: 24,136,201–55,165,407). In pedigree 2, LOD scores were calculated for each of the three branches of the family separately due to complexity of the pedigree. Branches 2 and 3 showed evidence of linkage to the same region of chromosome 16q. The regions were delineated by SNP markers rs205162 to rs6498968 for branch 2 (chr16: 25,596,637–52,653,785) and rs17720179 to rs1567522 for branch 3 (chr16: 27,188,853–49,302,826), with maximum LOD scores of 3.38 and 2.91, respectively (Fig. 1*B*). In branch 1, two of the affected individuals (MC9401 and MC9403) showed linkage to this region.

Whole-exome sequencing (WES) of all affected individuals in pedigree 1 revealed a single shared homozygous, nonsense variant (c.1210C>T, p.Arg404*) in the *GPT2* gene (RefSeq NM_133443.3) in the linkage interval. There were no other rare, loss-of-function mutations shared by all affected members of the pedigree in the interval or elsewhere in the genome. The homozygous *GPT2* gene variant was confirmed by Sanger sequencing and segregated with the disease in pedigree 1 (Fig. 1*C*). All members unaffected for microcephaly in the pedigree were heterozygous. The candidate variant was not present in the National Heart, Lung, and Blood Institute (NHLBI) Exome Variant Server or in dbSNP. In pedigree 2, using WES of three affected individuals (MC9401, MC9428, and MC9432), we identified a homozygous missense variant in the *GPT2* gene (c.815C>T, p.Pro272Leu) as the only shared candidate variant in the linkage interval (Fig. 1*C*). All affected individuals were homozygous, and no unaffected individuals were found to be homozygous. Individual MC9402, who showed a microcephalic phenotype, was heterozygous, and thereby likely represents a phenocopy. This p.Pro272Leu variant was not found in the NHLBI Exome Variant Server or in dbSNP, and was predicted to be damaging by PolyPhen-2 (11), SIFT (12), and Provean (13), suggesting its pathogenicity (*SI Appendix*, Table S2). Since our discovery of the mutations above, a single homozygous missense change in *GPT2* (c.459C>G, p.Ser153Arg) was reported in two siblings with a similar phenotype, including microcephaly and developmental delay (14) (Fig. 1*D*).

Table 1. Phenotypic features of 14 affected individuals with *GPT2* mutations

Phenotype	No. of positive cases	Frequency, %
Microcephaly	14/14	100
Postnatal microcephaly	7/7	100*
Intellectual disability	14/14	100
Hypotonia during infancy	7/8	88*
Oral–motor dysfunction	12/12	100*
Hyperreflexia	11/13	85*
Hypertonia	12/13	92*
Joint contractures	3/14	21
Ability to walk by age 3	9/9	100*
Subsequent deterioration in walking ability	10/12	83*
Spastic diplegia/paraplegia	10/13	77*
Seizures	5/14	36

*Based on cases with data available.

Human Mutations in *GPT2* Lead to Reduced Protein Levels and Enzyme Activity. We studied the protein stability and enzymatic activity of the identified human mutations, and our results are consistent with a loss-of-function mechanism. We expressed each of the three mutated transcripts in HeLa cells and studied protein levels using Western blotting with an antibody raised to the full-length GPT2 (Fig. 2*A*). We detected a control, full-length protein at the predicted size of V5His-tagged GPT2 (62.8 kDa, arrow). For the truncating mutation p.Arg404*, we detected a scant quantity of the predicted truncated protein (44.4 kDa, arrowhead), consistent with nonsense-mediated decay of the mRNA and/or an unstable protein. Less than 4% of control protein was detected (quantified in Fig. 2*B*). The missense mutations p.Ser153Arg and p.Pro272Leu were expressed at 37.6 ± 6.3% and 10 ± 2.2% of control levels, respectively, reflecting protein instability (Fig. 2*B*). Structural predictions for the missense changes also suggest deleterious effects (*SI Appendix*, Fig. S2).

To substantiate further the interpretation that these mutations lead to loss of enzyme function, we tested the enzymatic activity of mutant proteins directly. We expressed constructs for full-length GPT2 protein, as well as for each of the three mutant alleles, in HeLa cells. We subsequently made protein extract from cells and tested GPT2 enzyme activity. In the cell lines expressing each of the mutant alleles, including the missense mutations, enzyme activity relative to control was substantially diminished (to background levels) (Fig. 2*C*). Thus, the mutations in *GPT2* are associated with reductions or loss of protein as well as loss of enzyme activity. Even in the case of the missense mutations, wherein there was a small level of intact protein, the enzyme activity of protein with these missense mutations was not detectable above background levels.

GPT2 Expression Increases in Postnatal Developing Brain. To evaluate the role of GPT2 in developing brain, we first measured protein and enzyme activity in developing mouse brains. In normal mice, we found highest levels of Gpt2 protein in the early postnatal period using Western blotting (*SI Appendix*, Fig. S3*A*). Total Gpt enzyme activity was detectable at postnatal day 1 (P1), yet enzyme activity was found to increase nearly 10-fold by P18 (*SI Appendix*, Fig. S3*B*), correlating with increases in Gpt2 protein levels. In published RNA-seq data from cell lineages purified from mouse brain, *Gpt2* mRNA expression was threefold higher than that for the related enzyme *Gpt* in neurons [8.9 vs. 3.0 fragments per kilobase of exons per million fragments mapped (FPKM), respectively] (*SI Appendix*, Fig. S3*C*) (15). *Gpt2* also has a

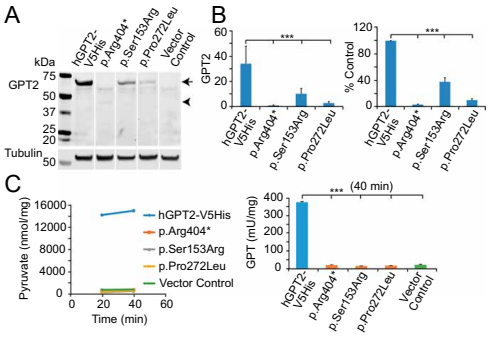

Fig. 2. Mutations in GPT2 lead to reduced protein levels and enzyme activity. (*A*) Western blot results of mutated GPT2 protein. Lysates of HeLa cells transfected with human control GPT2 (hGPT2-V5His), p.Arg404*, p.Ser153Arg, p.Pro272Leu, or vector-only constructs were probed with anti-GPT2 antibody. All of the three GPT2 mutants show reduced protein levels compared with control GPT2 (hGPT2-V5His). Arrow indicates the expected GPT2 protein band; arrowhead indicates the truncated GPT2 protein band. (*B*) Quantification of Western blots. (*Left*) Overexpressed GPT2 bands were normalized to tubulin. (*Right*) Overexpressed GPT2 level in each lane was normalized to the GPT2 control (hGPT2-V5His). $n = 6$ replicates. Data are presented as means ± SEMs. $***P < 0.001$. (*C*) GPT enzyme functional assay indicated that mutations in GPT2 lead to loss of the enzyme activity. HeLa cells were transfected with human control GPT2 (hGPT2-V5His), p.Arg404*, p.Ser153Arg, p.Pro272Leu, or vector-only constructs. Lysates were used to analyze the GPT activity. (*Left*) GPT activity was measured by pyruvate production after either a 20- or 40-min incubation with substrate at 37 °C. All three GPT2 mutants had similar pyruvate production as the vector control. (*Right*) GPT activity was measured in cell lysate after incubating with substrate at 37 °C for 40 min and is represented as enzyme activity (in milliunits) per milligram of tested sample. Only the overexpressed GPT2 control protein showed significant high enzyme activity. $n = 4$ replicates. Data are presented as means ± SEMs. $***P < 0.001$.

high level of expression (far exceeding *Gpt* expression) in oligodendrocyte precursor cells (137.7 vs. 4.8 FPKM, respectively) and newly formed oligodendrocytes (48.7 vs. 2.6 FPKM, respectively) (*SI Appendix*, Fig. S3*D*) (15).

In humans, through analyses of the Allen Institute's Developmental Transcriptome Dataset, we observed that *GPT2* mRNA is broadly expressed across all parts of the human brain throughout development and into adulthood, with highest levels in the early postnatal years (*SI Appendix*, Fig. S4*A*). Interestingly, although mRNA levels for *GPT2* and for *GPT* are correlated, *GPT2* mRNA levels are generally >20-fold higher than *GPT* levels in human brain (*SI Appendix*, Fig. S4*B*). Based on these data, peak levels of *GPT2* expression correlate with major periods of synaptogenesis and myelination in both mouse and human developing postnatal brain (16–19).

GPT2 Protein Is Localized to Mitochondria. GPT2 harbors a strong mitochondrial-localization sequence, which is not present in GPT (*SI Appendix*, Fig. S5*A*). None of the missense mutations appeared to interfere with the predicted mitochondrial localization using PSORT II predictions (20) (*SI Appendix*, Fig. S5*A*). Exogenously expressed GPT2 wild-type (WT) protein demonstrated a very high degree of costaining with mitochondrial markers, such as Mito-GFP (Fig. 3*A*, *Top*). By comparison, expression of the p.Arg404* mutant protein produced very little protein (Fig. 3*A*, *Bottom*); however, the small amount of protein that was discernible (by increasing the imaging parameters to maximal sensitivity) localized to mitochondria (*SI Appendix*, Fig. S5*B*). The exogenously expressed missense proteins, either the p.Ser153Arg or p.Pro272Leu, both demonstrated higher levels of protein than the truncating mutation but reduced levels of staining relative to the control (Fig. 3*B*). This reduced amount of staining did colocalize with the mitochondrial stains, yet we expect these enzymes to be inactive, as shown previously (Fig. 2*C*).

Next, we established two GPT2-mutant HEK293FT cell lines using CRISPR-Cas9 genome editing (Fig. 3*C* and *SI Appendix*, Table S3). We introduced homozygous nonsense mutations (c.265G>T, p.Glu89*; and c.1210C>T, p.Arg404*), the latter of which is the same variant as we identified in pedigree 1. We confirmed by quantitative reverse transcription–PCR (qRT-PCR) that cells containing either of these two *GPT2* mutations showed significant decreases in *GPT2* mRNA compared with WT cells (Fig. 3*D*). Western blot analysis of fractionated lysates from WT and mutant HEK293FT cells revealed that endogenous GPT2 localized to the mitochondrial fraction in WT cells and was absent from the cytoplasmic fraction, whereas GPT2 was undetectable in either fraction in mutant cells (Fig. 3*E*).

***Gpt2*-Null Mice Demonstrate Reduced Postnatal Brain Growth.** We generated mice with a germline disruption of the *Gpt2* gene (*SI Appendix*, Fig. S6) and observed decreases in postnatal brain growth akin to the human phenotype. Homozygous mutant mice were born in the expected Mendelian ratio (*SI Appendix*, Table S4). Western blotting of brain lysates demonstrated that Gpt2 protein was abolished in the mutant mice (*SI Appendix*, Fig. S6*C*). Also of note, postnatal brains of homozygous mutant mice at P18 showed significantly reduced total brain Gpt enzyme activity (*SI Appendix*, Fig. S6*D*). Homozygous mutant brain size was generally indistinguishable at birth, and, behaviorally, mutants were similar to control littermates for the first 2 wk postnatally. However, at approximately P18, homozygous mutant mice began to demonstrate reduced motor activity. Subsequent to the emergence of reduced motor behavior, homozygous mutant mice grew sickly and died generally between P18 and P26 (*SI Appendix*, Table S4). Given the expression of the β-galactosidase gene from the endogenous *Gpt2* promoter in the targeted allele, we were able to study the distribution of *Gpt2* expression in the heterozygous mouse brain. We found that, in P78 heterozygous mice, *Gpt2* expression was widely distributed throughout the brain (*SI Appendix*, Fig. S7). Staining was particularly apparent in the prefrontal cortex, striatum, hippocampus, and granular cell layer of the cerebellum.

We compared brain area between littermate homozygous mutant ($n = 12$) and WT animals ($n = 7$) at P18–P22 (Fig. 4). *Gpt2*-null brains showed a small but consistent and significant reduction in cortical area relative to control ($P < 0.03$) (Fig. 4*B*). Furthermore, analysis of areas and lengths of different brain regions showed a consistent and significant decrease in brain size in *Gpt2*-null animals compared with control animals (Fig. 4 *C* and *D*). For example, comparison of combined areas of cortex (CX), midbrain (MB), and cerebellum (CB) demonstrated a 13% decrease in area ($P < 0.0015$). We further observed that the number of SV2-positive puncta representing synapses were significantly reduced (30% less than WT, $P = 0.005$) at 10–14 d in vitro (Fig. 4 *E* and *F*). Based on these findings, we conclude that GPT2 has an important role in brain growth during postnatal development and potentially in synapse development.

Amino Acid Metabolism Is Defective in *Gpt2*-Null Mouse Brains. To identify metabolic defects in neural tissue in vivo, we investigated *Gpt2*-null mouse brains for derangements in metabolite levels. We analyzed 276 metabolites from P18 acute brain preparations from *Gpt2*-null and WT mice using targeted mass spectrometry (MS)-based metabolomics and metabolite set enrichment analysis (MSEA) (Fig. 5*A*). The top three pathways identified were as follows: protein biosynthesis [P value = 0.0000000644, false discovery rate (FDR) = 0.00000515] (largely reflecting changes in amino acid metabolism); citric acid cycle (P value = 0.00000733,

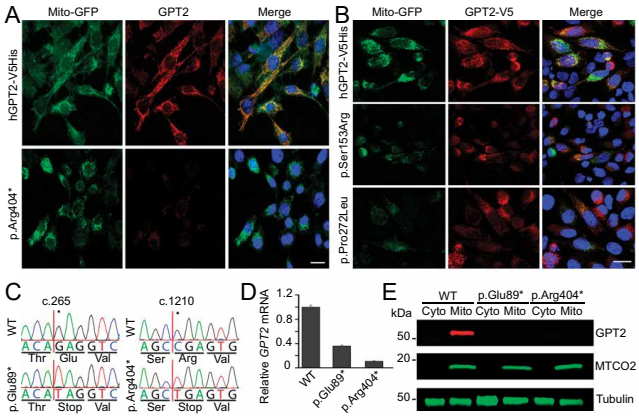

Fig. 3. GPT2 localizes to mitochondria. (*A*) HeLa cells coexpressing Mito-GFP (a mitochondrial marker, green) and either normal, human GPT2 (hGPT2-V5His) or human GPT2 with the p.Arg404* mutation were immunostained with anti-GPT2 antibody (red). Under the same imaging parameters, p.Arg404* showed a decrease in protein expression level. Immunostaining for GPT2 showed high colocalization with mitochondrial markers for control protein. (*B*) HeLa cells coexpressing Mito-GFP and C-terminal V5-tagged human GPT2 control (hGPT2-V5His) or mutations p.Ser153Arg or p.Pro272Leu were stained with anti-V5 antibody (red). Under the same imaging parameters as control, the images of cells expressing mutant GPT2 demonstrate reduced protein levels yet maintain mitochondrial localization in the residual signal. (Scale bar, 10 μm.) (*C*–*E*) *GPT2*-mutant HEK293FT cells were generated by CRISPR-Cas9 genome editing. (*C*) Sanger sequencing traces of WT HEK293FT cells and the *GPT2*-mutant HEK293FT cell lines are shown. The mutant cell lines harbor homozygous nonsense mutations in the *GPT2* gene (c.265G>T, p.Glu89*; c.1210C>T, p.Arg404*). Positions of the variants are according to NM_133443.3 (cDNA) and NP_597700.1 (protein). (*D*) Graphed are the results of qRT-PCR analysis of WT HEK293FT cells and the two lines of GPT2-mutant cells (p.Glu89*, p.Arg404*). For all samples, *GPT2* mRNA was normalized to 18S rRNA. (*E*) Immunoblot analysis of WT HEK293FT cells and the GPT2 mutant cells (p.Glu89*, p.Arg404*). In WT cells, GPT2 is absent from the cytosolic fraction (Cyto) and highly enriched in the mitochondrial fraction (Mito). In cells expressing either of the two mutants, GPT2 is absent from both fractions. Tubulin and MTCO2 (cytochrome *c* oxidase subunit II) are shown as a loading control marker and a mitochondrial marker, respectively.

FDR = 0.000293); and glutathione metabolism (*P* value = 0.0000142, FDR = 0.000379) (Fig. 5*A* and *SI Appendix*, Table S5).

At the level of primary metabolites in the GPT reversible reaction in *Gpt2*-null brains, alanine showed a strong decrease (fold change = 0.885, FDR = 0.008) (Fig. 5*B* and *SI Appendix*, Table S6). We corroborated these brain findings of alanine depletion by direct measure of alanine secretion and by isotope tracing experiments in *Gpt2*-null murine embryonic fibroblasts (MEFs) (Fig. 6). *Gpt2*-null MEFs exhibited near-complete loss of alanine secretion into the media (Fig. 6*A*). *Gpt2* deletion also substantially reduced transfer of ^{15}N from [α-^{15}N]glutamine to alanine (Fig. 6*B*), as would be expected if Gpt2 rather than Gpt1 were the major isoform exchanging amino groups between glutamate and α-ketoglutarate. When cultured in medium supplemented with uniformly labeled [U-^{13}C]glucose, the *Gpt2*-null MEFs also had reduced ^{13}C labeling in alanine, whereas lactate labeling was conserved (Fig. 6*C*, two left panels). Therefore, taken together, metabolomic and direct isotope tracing measures indicate that Gpt2 is the major Gpt isoform responsible for alanine production and secretion.

Although the alanine pool was depleted, several other amino acid pools were substantially elevated in P18 brain, particularly essential amino acids, including phenylalanine (fold change = 1.641, FDR = 0.024) (Fig. 5*C* and *SI Appendix*, Table S6). Notably urea was substantially decreased (fold change = 0.246, FDR = 0.017), which suggests a decrease in production of amine groups, consistent with dysregulation of total cellular aminotransferase activity and/or nitrogen disposal perhaps due to decreases in alanine secretion.

Additional Abnormal Metabolomics Signatures in *Gpt2*-Null Mouse Brains: Anaplerosis and Neuroprotective Mechanisms. In addition to defects in amino acid metabolism, P18 *Gpt2*-null mouse brains exhibit abnormal metabolomics signatures involving TCA cycle and neuroprotective mechanisms (Fig. 5*A* and *SI Appendix*, Table S5). With regard to the TCA cycle, five of eight TCA cycle intermediates were substantially decreased (Fig. 5*D* and *SI Appendix*, Table S6), including the following: citrate (fold change = 0.655, *P* = 0.015), isocitrate (fold change = 0.868, *P* = 0.0064), succinate (fold change = 0.759, *P* = 0.009), fumarate (fold change = 0.881, *P* = 0.002), and malate (fold change = 0.735, *P* = 0.001). Surprisingly, ATP and GTP levels were somewhat elevated, as was acetyl-CoA.

Depletion of TCA cycle intermediates in brain is consistent with a defect in anaplerosis, the metabolic process involved in replenishing TCA cycle intermediates used during cellular anabolism and biosynthesis. Because Gpt enzyme activity converts glutamate to α-ketoglutarate, this function has been proposed to promote glutamine-dependent anaplerosis (21). Overall, labeling of TCA cycle intermediates from [U-^{13}C]glucose was enhanced by *Gpt2* deletion (Fig. 6*C*). Altered label distributions included enhanced malate m+3 and citrate m+5 fractions, which is consistent with suppressed glutamine-dependent anaplerosis and increased carboxylation of pyruvate (22). These altered labeling patterns are expected if reduced entry of glutamine-derived carbon into the TCA cycle via α-ketoglutarate is offset by an increased contribution of 4-carbon intermediates from glucose. Culture in [U-^{13}C]glutamine confirmed a reduced contribution of glutamine-dependent anaplerosis to TCA cycle intermediates in *Gpt2*-deficient cells (Fig. 6*D*).

Finally, we found in P18 *Gpt2*-null brains that several metabolites related to neuroprotective mechanisms are misregulated (Fig. 5*E*): glutathione (fold change = 0.715, FDR = 0.038), folate (fold change = 0.383, FDR = 0.024), and cysteine (fold change = 0.609, FDR = 0.083) levels were reduced; whereas cystathionine levels were substantially elevated (fold change = 2.409, FDR = 0.00036). Elevations of cystathionine were also found in newborn P0 mouse brain (fold change = 1.701, FDR = 0.029) (*SI Appendix*, Table S8). We conducted metabolomics analysis on newborn (P0) brain from

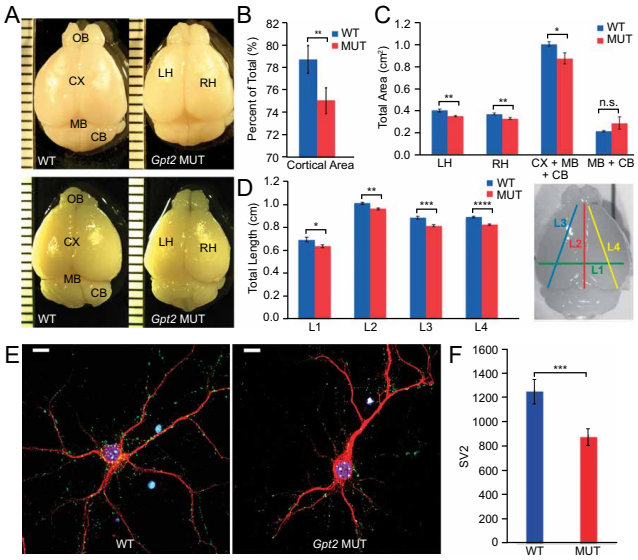

Fig. 4. *Gpt2* deficiency causes a reduction in brain size in mouse. (*A*) Panels depict two representative brain pairs from littermate animals for each genotype at P21 (*Top*) and P22 (*Bottom*). Left panels show WT perfused brains. Right panels show *Gpt2*-null brains (MUT). Measurements were taken of the cortex (CX), the midbrain (MB), the cerebellum (CB), the left hemisphere (LH), and the right hemisphere (RH). Ruler demarcations reflect 1-mm scale. (*B*) Cortical area presented as a percentage of total brain area is shown for WT animals and for *Gpt2*-null animals (MUT). $^{**}P < 0.03$. (*C*) Graphed is a comparison of area in square centimeters in four different brain regions: LH ($^{**}P < 0.0025$), RH ($^{**}P < 0.0015$), CX+MB+CB ($^{*}P < 0.0015$), and MB+CB (n.s., $P < 0.1$). (*D*) Graphed is a comparison of length measurements between WT and *Gpt2*-null (MUT) animals. Measurements are depicted in the brain image on the *Right*. We found significant differences in width across two hemispheres (L1, green line) ($^{*}P < 0.015$), in the midline anterior–posterior distance (L2, red line) ($^{**}P < 0.0015$), in the diagonal length of the left hemisphere (L3, blue line) ($^{***}P < 0.0002$), and in the right hemisphere (L4, yellow line) ($^{****}P < 0.000001$). $n = 7$ WT and 12 MUT animals for all brain size measurements. Data are presented as means ± SEMs. Statistical analysis was conducted using Student's *t* test. (*E*) *Gpt2*-null hippocampal neurons show reduced synapses compared with neurons from WT littermates at 10 DIV, as visualized by SV2 staining (green). Neurons were immunostained with antibodies against SV2 and MAP2 (red). (Scale bar, 10 μm.) (*F*) The graph depicts quantification of SV2 densities per 135-μm^2 region of field of view in WT and MUT neurons. Data are presented as means ± SEMs. $n = 4$ WT animals and 3 MUT animals across 3 litters. $^{***}P = 0.005$.

mutant animals compared with combined WT and heterozygous littermates. Although Gpt2 protein expression undergoes substantial up-regulation in the postnatal period (*SI Appendix*, Fig. S3*A*), we reasoned that analysis at this early time point could pinpoint the most proximal metabolic derangements resulting from loss of Gpt2. At P0, only four metabolites demonstrated misregulated levels adhering to a conservative FDR correction. Among these were two metabolites observed also at the P18 time point: alanine (fold change = 1.573, FDR = 0.000165), a primary metabolite in the Gpt2 reaction, and also interestingly, cystathionine (fold change = 1.701, FDR = 0.029). Of note, alanine was up-regulated at P0, whereas by contrast it was significantly down-regulated at P18. The other two misregulated metabolites that withstood FDR correction were hydroxyproline (fold change = 1.767, FDR = 0.000335) and sarcosine (fold change = 1.337, FDR = 0.0153). Both of these metabolites are involved in amino acid metabolism. Overall, our data support a role for Gpt2 in mitochondrial function and various metabolic pathways, including amino acid metabolism, anaplerotic processes involved in TCA cycle intermediates, and pathways implicated in neuroprotective mechanisms (e.g., pathways involving the metabolites cysteine, cystathionine, glutathione, and folate).

Discussion

In this study, we report rare, homozygous mutations in the gene encoding the enzyme GPT2 in large consanguineous pedigrees segregating with a neurological phenotype involving IDD, postnatal microcephaly, and spastic paraplegia with progressive features. We present one extended kindred with a LOD score greater than 3.1 (pedigree 1, MI1000) segregating a homozygous nonsense *GPT2* mutation (p.Arg404*). Another large extended kindred of three branches (pedigree 2, MC9400) segregates a deleterious, homozygous missense *GPT2* mutation (p.Pro272Leu) with LOD scores greater than 3.3 and 2.9 in branches 2 and 3, respectively. An individual of pedigree 2 (MC9402, branch 1), who similarly presented with microcephaly and IDD, was not homozygous for the *GPT2* variant. Because this family is highly consanguineous, it is likely that this individual has an additional genetic mutation. During the course of our work, a third homozygous, deleterious missense *GPT2* mutation (p.Ser153Arg) was reported in a large pedigree with recent shared ancestry and three affected individuals presenting with a similar phenotype (14).

In biochemical studies, we demonstrate that the human mutations are loss of function. For the p.Arg404* mutant protein, we demonstrate that the truncated GPT2 protein is not made or is unstable in expression studies in cell lines. We also show here that the p.Pro272Leu and p.Ser153Arg proteins are unstable and, through structural predictions, likely have deleterious effects on protein folding (*SI Appendix*, Fig. S2). All mutant GPT2 proteins, p.Arg404*, p.Pro272Leu, and p.Ser153Arg, are enzymatically inactive, consistent with loss-of-function, autosomal recessive mutations.

The clinical phenotype of the affected individuals associated with *GPT2* mutations presented herein is generally uniform. Postnatal microcephaly and IDD were noted in all affected

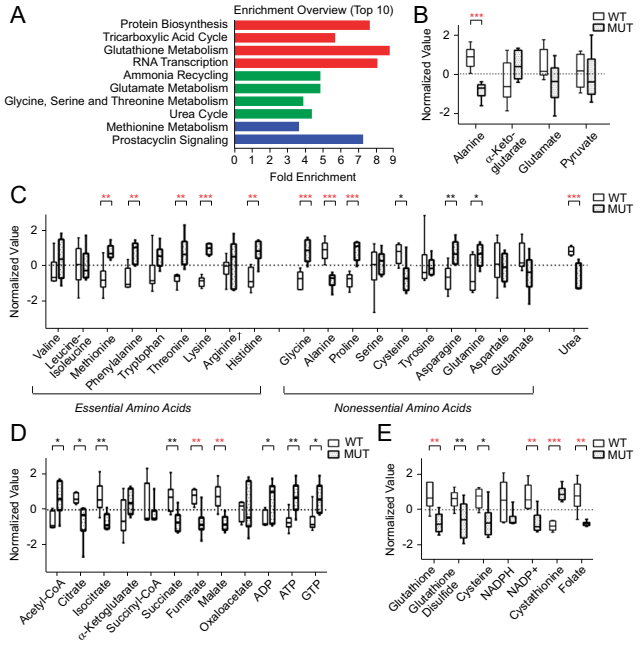

Fig. 5. Metabolomics profile of postnatal *Gpt2*-null mouse brain. (*A*) Overrepresentation analysis of metabolomics in brains from *Gpt2*-null (MUT) compared with WT *Gpt2* mice at P18. The reference library contained 88 metabolite sets for normal metabolic pathways. Metabolites showing significant increases or decreases (compared with control on Student's *t* test *P* value less than 0.05) were flagged. The hypergeometric test was used to determine whether flagged metabolites from specific pathways were significantly overrepresented. Red, FDR < 0.01; green, 0.01 < FDR < 0.03; blue, 0.03 < FDR < 0.05. (*B*–*E*) Box plots of metabolites, with whiskers representing minimum and maximum values. The peak intensity areas were normalized by a pooled reference sample from the WT *Gpt2* group (probabilistic quotient normalization), and auto (unit) scaling was performed whereby the data were mean-centered and divided by the SD of each group. Unpaired Student's *t* test was performed assuming equal group variance. The box plots in each of the panels show the following: (*B*) metabolites from the primary GPT enzyme reaction, (*C*) amino acids, (*D*) TCA cycle intermediates, and (*E*) metabolites involved in neuroprotective mechanisms. $n = 6$ WT animals and 6 MUT animals. * = 0.01 < raw $P < 0.05$, ** = 0.001 < $P < 0.01$, *** = $P < 0.001$. Red stars denote a corresponding FDR below 0.05. Also refer to *SI Appendix*, Table S5, for MSEA data; *SI Appendix*, Table S6, for full set of metabolite Student's *t* tests; and *SI Appendix*, Table S7, for raw data. †Arginine is a conditionally essential amino acid.

individuals, most had oral motor difficulties, and several had seizures. These clinical findings are highly consistent with those of the individuals reported in ref. 14. There is no clear difference in severity between individuals with truncating mutations and missense mutations, consistent with our biochemical data that all mutations lead to a severe or complete loss of GPT2 enzyme function.

An important aspect of our work is that we have had the opportunity to follow patients longitudinally. Thereby, we are able to extend the neurological phenotype, which appears to include progressive features in addition to developmental disease. With regard to motor findings, we find that hypotonia during infancy gives way to hypertonia more notably in the lower extremities (spastic diplegia or paraplegia). Among the 14 affected individuals studied herein, ∼80% showed slowly progressive spastic diplegia or paraplegia with hyperreflexia and hypertonia as one of the major features. Although rapid regression is not noted, motor difficulties seem to be slowly progressive in many of the cases, consistent with our metabolomics studies that suggest abnormalities in neuroprotective mechanisms. Defects in such mechanisms have been previously implicated in hereditary spastic diplegia (23).

The acquisition of neurological features during early postnatal life indicates the brain's requirement for GPT2 during this critical period of brain development. Postnatal brain development is characterized by the formation, refinement, and maintenance of circuitry involving neuronal arborization, synaptogenesis, oligodendrocyte expansion, and myelination (3). We find *GPT2* expression to increase in brain during the early postnatal period and to be expressed in both neurons and glia. Prior studies have indicated strong neuronal expression and weaker or absent glial expression in adult human brain (24); however, data presented here support a role for GPT2 in both neurons and glia, at least during early postnatal development (*SI Appendix*, Fig. S3). Our finding that GPT2 expression reaches highest levels in the early postnatal period both in human and in mouse brain, concurrent with peaks in synaptogenesis (17, 18, 25), suggests a role in this process. We also observe decreases in brain growth postnatally both in human and in mouse. Our initial findings support defects in synapse formation (Fig. 4 *E* and *F*), again consistent with failures in synaptogenesis perhaps arising from mitochondrial dysfunction. Importantly, we demonstrate here that GPT2 is localized to mitochondria. GPT2 has a strong mitochondrial localization signal, whereas GPT does not. The two isoforms of GPTs, GPT and GPT2, show different spatial expression patterns. GPT2 is highly expressed in the CNS. There is also a possibility that other defects in postnatal brain development are involved, including abnormal oligodendrocyte development. In humans, myelination increases rapidly between 6 and 24 mo

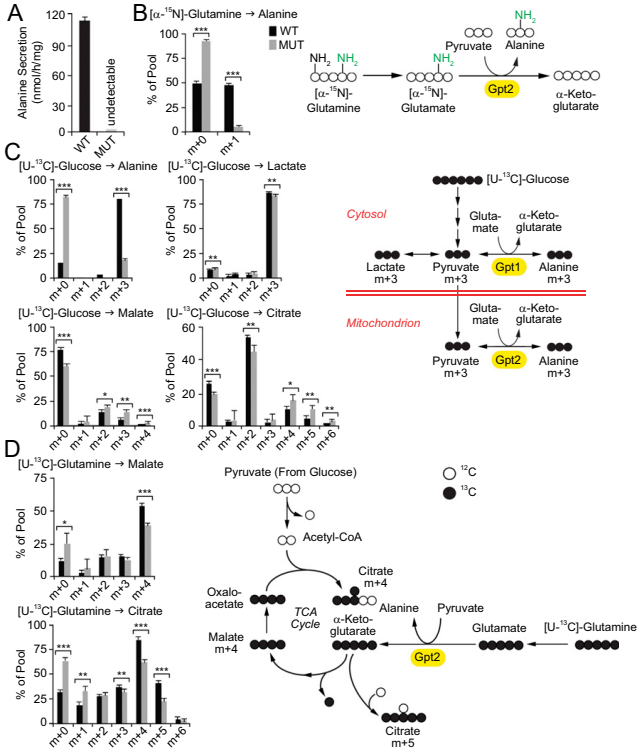

Fig. 6. Defective alanine production and glutamine-dependent anaplerosis in *Gpt2*-null cells. Immortalized MEF cell lines were prepared from WT and *Gpt2*-null mice (MUT) and investigated in culture. (*A*) Total alanine abundance in the medium was measured by HPLC. Alanine secretion in the MUT cells was scarcely detectable. (*B*) Graphed are fractional enrichments of extracellular alanine during culture with [α-^{15}N]glutamine. Levels of transfer of radioisotope from glutamine to alanine are substantially reduced in the *Gpt2*-null cells. (Schematic *Right*) ^{15}N (green) is transferred from [α-^{15}N]glutamine, via [α-^{15}N]glutamate, to [^{15}N]alanine. This pathway requires activity of a glutamate pyruvate transaminase, such as Gpt2. (*C*) Shown are mass isotopologue distributions for alanine, lactate, malate, and citrate after culture with [U-^{13}C]glucose and unlabeled glutamine. Altered label distributions, including reduced alanine m+3, and enhanced malate m+3 and citrate m+5 fractions, are consistent with suppressed glutamine-dependent anaplerosis (22). (Schematic *Right*) [U-^{13}C]Glucose gives rise to [U-^{13}C]pyruvate (pyruvate m+3) via the glycolytic pathway. This pyruvate can be converted to lactate m+3 or alanine m+3. Conversion of pyruvate to alanine involves the Gpt1 (cytosol)- or Gpt2 (mitochondrion)-dependent transfer of an amino group to pyruvate from glutamate. A large reduction of labeling of alanine from glucose in Gpt2-deficient cells implies that Gpt2 is required for alanine synthesis. (*D*) Shown are mass isotopologue distributions for malate and citrate after culture with unlabeled glucose and [U-^{13}C]glutamine. Reduced direct transfer of radioisotope from glutamine to malate and citrate demonstrates suppressed glutamine-dependent anaplerosis in *Gpt2*-null cells. (Schematic *Right*) [U-^{13}C]Glutamine generates fully labeled α-ketoglutarate via glutamate. The resulting α-ketoglutarate can proceed around the oxidative TCA cycle as shown, giving rise to malate m+4 and citrate m+4. In addition, α-ketoglutarate may become reductively carboxylated through the addition of one unlabeled carbon, resulting in citrate m+5 (49). Loss of Gpt2, which catalyzes the conversion of glutamate to α-ketoglutarate, is predicted to reduce labeling of metabolites downstream of α-ketoglutarate during culture with [U-^{13}C]glutamine. It would also increase the contribution of glucose carbon to TCA cycle metabolites, as described in ref. 22. Data are presented as the means ± SDs for three parallel cultures, with results shown for one representative experiment. $*P < 0.05$, $**P < 0.01$, $***P < 0.001$ by unpaired, two-sample Student's *t* test.

postnatally and may increase more gradually into adolescence (16, 26). A minority of patients have shown a reduced white matter volume on brain MRI [participant MI1003; *SI Appendix*, Table S1; and also an affected individual in the study by Celis et al. (14)]. Interestingly, in mouse, we observe strong *Gpt2* expression in oligodendrocyte precursor cells that undergo rapid expansion in the early postnatal period (19, 27–29).

It is appealing to speculate that disease progression in the postnatal period may be prevented by intervention, particularly in the setting of abnormalities of amino acid metabolism. GPTs serve an important role in a variety of metabolic functions, including amino acid metabolism, the urea cycle, and the TCA cycle, in addition to roles in neurotransmitter (both glutamate and GABA) synthesis. Glutamate, in turn, is also a substrate for the synthesis of glutathione, a key element in the cellular machinery to protect against oxidative damage and cell death (30, 31). Depletion of alanine levels is the strongest signal observed of the primary metabolites in the brain. Similarly, in patient cerebrospinal fluid, decreases in alanine were seen (14). Interestingly, we do not see strong changes in glutamate. Elevations of glutamate at the synapse would be predicted to be particularly excitotoxic (32); however, we do not see strong changes in total brain glutamate in newborn mice or at P18. Future studies

may examine specific cell types or tissue compartments (i.e., the synapse) more precisely for alterations in metabolites or damage. Given the lack of spatial resolution, our current experiments make it difficult to interpret a role for GPT2 in the glutamate–glutamine cycle at the synapse. Indeed, the GPT enzyme has been used experimentally and in therapeutic models to reduce excitotoxic glutamate levels through a proposed scavenging approach (33).

In the postnatal brain at P18, our experiments seem to indicate that Gpt2 serves to provide a source of alanine in the brain. Also, given the very low urea levels, Gpt2 activity may play an important role in nitrogen metabolism perhaps through generation of alanine. At P18, by contrast to decreases in alanine, *Gpt2*-null brains demonstrate elevations in several essential amino acids, including elevations in phenylalanine, which have been implicated in other encephalopathies, notably phenylketonuria, and may be modifiable by diet. We also observed elevations in glycine, which is also associated with progressive encephalopathy, intellectual disability, and seizures (34).

We also observe metabolic defects indicating abnormalities in glutamine-dependent anaplerosis of TCA cycle intermediates. GPT2 facilitates glutamine's ability to serve as an anaplerotic precursor by enabling the conversion of glutamate to α-ketoglutarate in the mitochondria. Our findings are similar to a previous study in which GPT activity was observed to be required for glutamine to stimulate both respiration and growth of KRAS-transformed cancer cells in culture (35). The importance of the role of GPT2 and anaplerosis in neurons and glia warrants further investigation.

Importantly, a metabolic signature previously associated with neurodegenerative disease was observed in *Gpt2*-null brain. Cystathionine elevation is among the strongest signals in the metabolomics dataset with statistically significant elevations at both P0 and P18. Recently, several studies have implicated the accumulation of this product, as well as decreases in cysteine, which are also observed in *Gpt2*-null brains, in neurodegenerative disease. More specifically, through deficiency in cystathionine γ-lyase and mechanisms involving both redox homeostasis and sulfhydration, this metabolic pathway has been pinpointed in both Huntington's disease (36, 37) and Parkinson's disease (38), as well as other neurological diseases with mitochondrial defects. Other statistically significant perturbations in P18 brain supporting abnormalities in neuroprotective mechanisms include reductions in glutathione and folate. In summary, we have identified mutations in the mitochondrial enzyme GPT2 in a human neurological disorder, wherein mutations lead to metabolic dysfunctions that have general relevance to developmental as well as potentially to neurodegenerative mechanisms and disease.

Subjects and Methods

Human Studies. Human subject research was conducted according to protocols approved by the institutional review boards of Boston Children's Hospital, Beth Israel Deaconess Medical Center, and Butler Hospital, and equivalent committees of the other participating institutions. Written informed consent was obtained from all participants or their legal guardians.

Genome-Wide SNP Genotyping, Linkage Analysis, and WES. DNA was genotyped using either Affymetrix Genome_Wide Human SNP Array 6.0 (MI1000) or Illumina HumanOmniExpress BeadChip array (MC9400). Affymetrix genotype calls were made using Birdsuite 1.5.5 (39) and Illumina calls by GenomeStudios version 2011.1 (Illumina). Genome-wide LOD scores were calculated using high-quality SNPs. PLINK, version 1.07 (40), was used to reduce linkage disequilibrium between markers. MERLIN, version 1.1.2 (41), was used to remove genotyping errors and to calculate LOD scores, assuming an autosomal recessive mode of inheritance with 100% penetrance and a disease allele prevalence of 0.0001. WES was performed using the Agilent Sure-Select Human All Exon or All Exon, version 5, capture array. Samples were sequenced on an Illumina HiSeq 2500. Sequence data were analyzed using GATK and variants annotated using ANNOVAR (42).

DNA Constructs and Antibodies. Human *GPT2* gene (GenBank: BC062555.1) was cloned into pcDNA3.1/V5-His-TOPO mammalian expression vector to generate C-terminal V5His-tagged phGPT2-V5His. GPT2 mutants p.Arg404*, p.Ser153Arg, and p.Pro272Leu were constructed using QuikChange site-directed mutagenesis (Agilent Technologies). The pTag GFP2-Mito vector was from Evrogen. Antibodies used were as follows: rabbit anti–C-terminal GPT2 antibody (SAB140991; Sigma-Aldrich), rabbit anti–full-length GPT2 antibody (16757-1-AP; Proteintech), mouse anti-V5 antibody (R960-25; Life Technologies), mouse anti-SV2 antibody (SV2-c; Developmental Studies Hybridoma Bank), chicken anti-MAP2 antibody (AB-15452; Millipore), mouse anti-Tubulin antibody (ab56676; Abcam), and rabbit anti-MTCO2 antibody (ab109739; Abcam).

GPT Enzyme Activity Assay. GPT activity was analyzed using the alanine aminotransferase (ALT) Assay Kit (Abcam). Mouse brains or cells were homogenized in ice-cold ALT Assay buffer and centrifuged. Protein concentrations of supernatants were determined by bicinchoninic acid assay. GPT activity was detected using 30 μg of brain extracts or 3.5 μg of cell extracts.

Genome Editing of *GPT2* in HEK293FT Cells. Genomic alterations in HEK293FT cells at the *GPT2* locus were made using the CRISPR-Cas9 system (43). Twenty nucleotide guide RNA (gRNA) sequences were designed to target double-stranded breaks at respective GPT2 target loci. For each transfection, a 180-nt single-stranded oligonucleotide was cotransfected with gRNA and the CRISPR-Cas9 construct [pSpCas9(BB)-2A-GFP; Addgene] to create single base substitutions via nonhomologous recombination. At 48 h posttransfection, single cells were sorted with GFP signal by FACS. The targeted genomic region was sequenced (see *SI Appendix*, Table S3, for sequences used). *GPT2* mRNA level was quantified by qRT-PCR using primers (Hs0037287_m1; Life Technologies).

Generation of *Gpt2*-Null Mice. Gpt2 cryopreserved mutant embryos were established through resources at the Knockout Mouse Project at University of California, Davis (Project ID CSD24977). The background of the embryos is C57BL/6N, and these mice were fully backcrossed into a C57BL/6J line. The targeting construct involved a gene trap (splice acceptor) and *LacZ*-Neo cassette (*SI Appendix*, Fig. S6*A*). Heterozygous males and heterozygous females were mated to produce offspring of both genders and all genotypes. Animals were genotyped by PCR with forward primer CSD-gene-F (5′-CTA ACT TGT CCT GCA TGG TGT CAG C-3′) and reverse primer CSD-gene-ttR (5′-CTA CAA ACA CTG GAC CCA AAC GTC C-3′) for a WT band of 504 bp. Forward primer CSD-loxF (5′-GAG ATG GCG CAA CGC AAT TAA TG-3′) and reverse primer CSD-gene-R (5′-GGC TTT CTA CCA GGA GGA ACA GAG G-3′) yields a 283-bp mutant band (*SI Appendix*, Fig. S6*B*, *Left*). WT and mutant mRNA were detected using RT-PCR, with the forward primer Unitrap-F (5′-CTG AGG TAA TCC GAG CCA AC-3′) and reverse primer Unitrap-wtR (5′-CGC TCG TTT CTT AGC GTC TT-3′) detecting a WT band (114 bp) and the Unitrap-F primer and Unitrap-lacZR primer (5′-TGG CGA AAG GGG GAT GTG-3′) detecting a 300-bp mutant band (*SI Appendix*, Fig. S6*B*, *Right*). LacZ staining was performed as described (44). All experiments involving mice were carried out in accordance with the National Institutes of Health *Guide for the Care and Use of Laboratory Animals* (45) under the protocols approved by the Brown University Institutional Animal Care and Use Committee.

Brain Size Measurement. Matched littermate pairs collected between P18 and P22 were transcardially perfused with 4% (wt/vol) paraformaldehyde and imaged using a Leica MZ16F. ImageJ analysis software was used to measure the area of the cortical hemispheres, midbrain, and cerebellum. Length measurements were done using four defined starting points.

Hippocampal Cultures. Hippocampal neurons were cultured as described (46). At 10–14 d in vitro (DIV), cells were immunostained with anti-SV2 and anti-MAP2 antibodies. MAP2-positive neurons were scored for SV2 puncta using ImageJ Particle Analysis.

Metabolomics. Craniotomies were performed on P0 and P18 litters from *Gpt2* heterozygous parents. Whole brains were used for metabolomics preparations performed as per Yuan et al. (47). Methanol extracts were dried and run by targeted tandem liquid chromatography (LC)-MS/MS. Briefly, samples were injected via hydrophilic interaction LC at high pH using HPLC coupled to a 5500 QTRAP mass spectrometer (AB/SCIEX). Metabolites were monitored using SRM mode for 300 transitions with positive/negative polarity switching. Peak areas for each detected metabolite were integrated using MultiQuant software (AB/SCIEX). The results were analyzed using MetaboAnalyst 3.0 (48).

Stable Isotope Tracing in MEFs. MEFs were maintained in DMEM with 10% (vol/vol) FCS and immortalized by SV40 T antigen. Experiments were performed between 5 and 15 passages. Stable isotope tracing experiments were performed as described previously (22). Briefly, cultures were overlaid with DMEM containing either 10 mM [U-^{13}C]glucose and 4 mM unlabeled glutamine,

or 10 mM unlabeled glucose and 4 mM [U-^{13}C]glutamine. After culturing for 6–8 h, the cells were rinsed in ice-cold normal saline and lysed with three freeze–thaw cycles in cold 50% (vol/vol) methanol. Lysates were centrifuged, and supernatants were evaporated and derivatized by *tert*-butyldimethylsilyl-methyltrifluoroacetamide (Sigma-Aldrich). One microliter of derivatized material was injected onto an Agilent 7890 gas chromatograph networked to an Agilent 5975 mass selective detector. For analysis of ^{15}N labeling in extracellular alanine, MEFs were incubated with medium containing 10 mM unlabeled glucose and 4 mM [α-^{15}N]glutamine for 8 h. An aliquot of medium was passed over an AG50 column (Bio-Rad), and then amino acids were eluted with 4 mL of 4 N ammonium hydroxide. These samples were evaporated and processed as above. Total alanine abundance in medium was measured by HPLC (Hitachi L8900).

ACKNOWLEDGMENTS. We thank the families who participated in this study. E.M.M. and G.H.M. kindly acknowledge Christopher A. Walsh for generous mentorship and support. The study was supported by the following: Burroughs Wellcome Fund Career Award for Medical Scientists 1006815.01 (to E.M.M.); Manton Center for Orphan Disease Research, National Institute of Neurological Disorders and Stroke Grant R01NS035129, National Institutes of Health/Fogarty International Center Grant R21TW008223, Dubai Harvard Foundation for Medical Research, F. Hoffmann-La Roche Ltd., Qatar National Research Fund, and Boston Children's Hospital Faculty Career Development Award (to G.H.M.); National Cancer Institute Grant R01CA157996 (to R.J.D.); the Suna and Inan Kirac Foundation (O.B.); and the Japan Foundation for Pediatric Research and the Japan Society for the Promotion of Science (T.N.).

1. Centers for Disease Control and Prevention (CDC) (1996) State-specific rates of mental retardation—United States, 1993. *MMWR Morb Mortal Wkly Rep* 45(3):61–65.
2. Fink JK (2014) Hereditary spastic paraplegia: Clinical principles and genetic advances. *Semin Neurol* 34(3):293–305.
3. Gilmore EC, Walsh CA (2013) Genetic causes of microcephaly and lessons for neuronal development. *Wiley Interdiscip Rev Dev Biol* 2(4):461–478.
4. Kelly A, Stanley CA (2001) Disorders of glutamate metabolism. *Ment Retard Dev Disabil Res Rev* 7(4):287–295.
5. Sheng ZH (2014) Mitochondrial trafficking and anchoring in neurons: New insight and implications. *J Cell Biol* 204(7):1087–1098.
6. Burté F, Carelli V, Chinnery PF, Yu-Wai-Man P (2015) Disturbed mitochondrial dynamics and neurodegenerative disorders. *Nat Rev Neurol* 11(1):11–24.
7. Kang HC, Lee YM, Kim HD (2013) Mitochondrial disease and epilepsy. *Brain Dev* 35(8): 757–761.
8. Sheng ZH, Cai Q (2012) Mitochondrial transport in neurons: Impact on synaptic homeostasis and neurodegeneration. *Nat Rev Neurosci* 13(2):77–93.
9. Owen OE, Kalhan SC, Hanson RW (2002) The key role of anaplerosis and cataplerosis for citric acid cycle function. *J Biol Chem* 277(34):30409–30412.
10. Rajab A, et al. (2006) An autosomal recessive form of spastic cerebral palsy (CP) with microcephaly and mental retardation. *Am J Med Genet A* 140(14):1504–1510.
11. Adzhubei IA, et al. (2010) A method and server for predicting damaging missense mutations. *Nat Methods* 7(4):248–249.
12. Kumar P, Henikoff S, Ng PC (2009) Predicting the effects of coding non-synonymous variants on protein function using the SIFT algorithm. *Nat Protoc* 4(7):1073–1081.
13. Choi Y, Sims GE, Murphy S, Miller JR, Chan AP (2012) Predicting the functional effect of amino acid substitutions and indels. *PLoS One* 7(10):e46688.
14. Celis K, et al. (2015) Loss of function mutation in glutamic pyruvate transaminase 2 (GPT2) causes developmental encephalopathy. *J Inherit Metab Dis* 38(5):941–948.
15. Zhang Y, et al. (2014) An RNA-sequencing transcriptome and splicing database of glia, neurons, and vascular cells of the cerebral cortex. *J Neurosci* 34(36):11929–11947.
16. Brody BA, Kinney HC, Kloman AS, Gilles FH (1987) Sequence of central nervous system myelination in human infancy. I. An autopsy study of myelination. *J Neuropathol Exp Neurol* 46(3):283–301.
17. Huttenlocher PR, Dabholkar AS (1997) Regional differences in synaptogenesis in human cerebral cortex. *J Comp Neurol* 387(2):167–178.
18. Li M, et al. (2010) Synaptogenesis in the developing mouse visual cortex. *Brain Res Bull* 81(1):107–113.
19. Mitew S, et al. (2014) Mechanisms regulating the development of oligodendrocytes and central nervous system myelin. *Neuroscience* 276:29–47.
20. Horton P, Nakai K (1997) Better prediction of protein cellular localization sites with the k nearest neighbors classifier. *Proc Int Conf Intell Syst Mol Biol* 5:147–152.
21. DeBerardinis RJ, et al. (2007) Beyond aerobic glycolysis: Transformed cells can engage in glutamine metabolism that exceeds the requirement for protein and nucleotide synthesis. *Proc Natl Acad Sci USA* 104(49):19345–19350.
22. Cheng T, et al. (2011) Pyruvate carboxylase is required for glutamine-independent growth of tumor cells. *Proc Natl Acad Sci USA* 108(21):8674–8679.
23. Lo Giudice T, Lombardi F, Santorelli FM, Kawarai T, Orlacchio A (2014) Hereditary spastic paraplegia: Clinical-genetic characteristics and evolving molecular mechanisms. *Exp Neurol* 261:518–539.
24. Lindblom P, et al. (2007) Isoforms of alanine aminotransferases in human tissues and serum—differential tissue expression using novel antibodies. *Arch Biochem Biophys* 466(1):66–77.
25. Glantz LA, Gilmore JH, Hamer RM, Lieberman JA, Jarskog LF (2007) Synaptophysin and postsynaptic density protein 95 in the human prefrontal cortex from mid-gestation into early adulthood. *Neuroscience* 149(3):582–591.
26. Barnea-Goraly N, et al. (2005) White matter development during childhood and adolescence: A cross-sectional diffusion tensor imaging study. *Cereb Cortex* 15(12): 1848–1854.
27. Kessaris N, et al. (2006) Competing waves of oligodendrocytes in the forebrain and postnatal elimination of an embryonic lineage. *Nat Neurosci* 9(2):173–179.
28. Rowitch DH, Kriegstein AR (2010) Developmental genetics of vertebrate glial-cell specification. *Nature* 468(7321):214–222.
29. Takebayashi H, Ikenaka K (2015) Oligodendrocyte generation during mouse development. *Glia* 63(8):1350–1356.
30. Franco R, Cidlowski JA (2009) Apoptosis and glutathione: Beyond an antioxidant. *Cell Death Differ* 16(10):1303–1314.
31. Snoke JE, Yanari S, Bloch K (1953) Synthesis of glutathione from gamma-glutamylcysteine. *J Biol Chem* 201(2):573–586.
32. Lau A, Tymianski M (2010) Glutamate receptors, neurotoxicity and neurodegeneration. *Pflugers Arch* 460(2):525–542.
33. Boyko M, Gruenbaum SE, Gruenbaum BF, Shapira Y, Zlotnik A (2014) Brain to blood glutamate scavenging as a novel therapeutic modality: A review. *J Neural Transm (Vienna)* 121(8):971–979.
34. Van Hove J, Coughlin CII, Scharer G (2013) Glycine encephalopathy. *GeneReviews*, eds Pagon RA, et al. (University of Washington, Seattle, WA). Available at www.ncbi.nlm.nih.gov/books/NBK1357/. Accessed January 14, 2016.
35. Weinberg F, et al. (2010) Mitochondrial metabolism and ROS generation are essential for Kras-mediated tumorigenicity. *Proc Natl Acad Sci USA* 107(19):8788–8793.
36. Paul BD, et al. (2014) Cystathionine γ-lyase deficiency mediates neurodegeneration in Huntington's disease. *Nature* 509(7498):96–100.
37. Paul BD, Snyder SH (2014) Neurodegeneration in Huntington's disease involves loss of cystathionine γ-lyase. *Cell Cycle* 13(16):2491–2493.
38. Vandiver MS, et al. (2013) Sulfhydration mediates neuroprotective actions of parkin. *Nat Commun* 4:1626.
39. Korn JM, et al. (2008) Integrated genotype calling and association analysis of SNPs, common copy number polymorphisms and rare CNVs. *Nat Genet* 40(10): 1253–1260.
40. Purcell S, et al. (2007) PLINK: A tool set for whole-genome association and population-based linkage analyses. *Am J Hum Genet* 81(3):559–575.
41. Abecasis GR, Cherny SS, Cookson WO, Cardon LR (2002) Merlin—rapid analysis of dense genetic maps using sparse gene flow trees. *Nat Genet* 30(1):97–101.
42. Wang K, Li M, Hakonarson H (2010) ANNOVAR: Functional annotation of genetic variants from high-throughput sequencing data. *Nucleic Acids Res* 38(16):e164.
43. Ran FA, et al. (2013) Genome engineering using the CRISPR-Cas9 system. *Nat Protoc* 8(11):2281–2308.
44. Cepko C, Ryder E, Fekete DM, Bruhn S (2006) *Detection of β-Galactosidase and Alkaline Phosphatase Activities in Tissue* (Department of Genetics, Harvard Medical School, Cambridge, MA). Available at genepath.med.harvard.edu/~cepko/protocol/xgalplap-stain.htm. Accessed February 22, 2015.
45. National Research Council (2011) *Guide for the Care and Use of Laboratory Animals* (National Academies Press, Washington, DC), 8th Ed.
46. Ouyang Q, et al. (2013) Christianson syndrome protein NHE6 modulates TrkB endosomal signaling required for neuronal circuit development. *Neuron* 80(1):97–112.
47. Yuan M, Breitkopf SB, Yang X, Asara JM (2012) A positive/negative ion-switching, targeted mass spectrometry-based metabolomics platform for bodily fluids, cells, and fresh and fixed tissue. *Nat Protoc* 7(5):872–881.
48. Xia J, Sinelnikov IV, Han B, Wishart DS (2015) MetaboAnalyst 3.0—making metabolomics more meaningful. *Nucleic Acids Res* 43(W1):W251–W257.
49. Mullen AR, et al. (2011) Reductive carboxylation supports growth in tumour cells with defective mitochondria. *Nature* 481(7381):385–388.

SI Appendix

Ouyang et al. (2016). Mutations in mitochondrial enzyme GPT2 cause metabolic dysfunction and neurological disease with developmental and progressive features.

Supplemental data include 7 figures and 9 tables. Also provided are a list of web resources and additional acknowledgments.

Supplemental Figures:

Supplemental Tables:

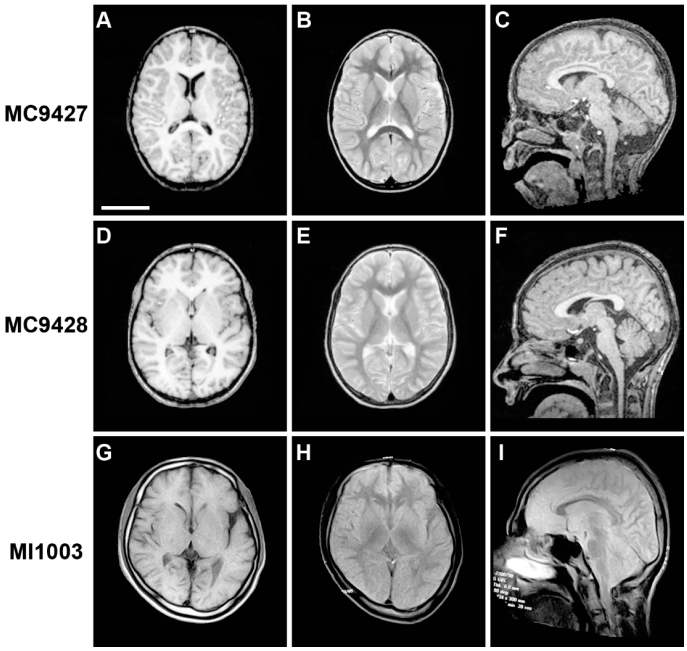

Fig. S1. Magnetic Resonance Imaging (MRI) findings in individuals with *GPT2* mutations. (*A-I*) Representative images of MRI scans from three affected individuals (MC9427, MC9428, and MI1003): T1-weighted axial images (*A, D,* and *G*), T2-weighted axial images (*B* and *E*), fluid-attenuated inversion recovery (FLAIR) axial image (*H*), T1-weighted sagittal images (*C* and *F*), and T2-weighted sagittal image (*I*). The ages at imaging were 13 years (MC9427), 10 years (MC9428), and 16 years (MI1003). Affected individuals MC9427 and MC9428 show microcephaly with normal brain architecture. Individual MI1003 shows reduced white matter volume and a thin corpus callosum. Scale bar, 10 cm.

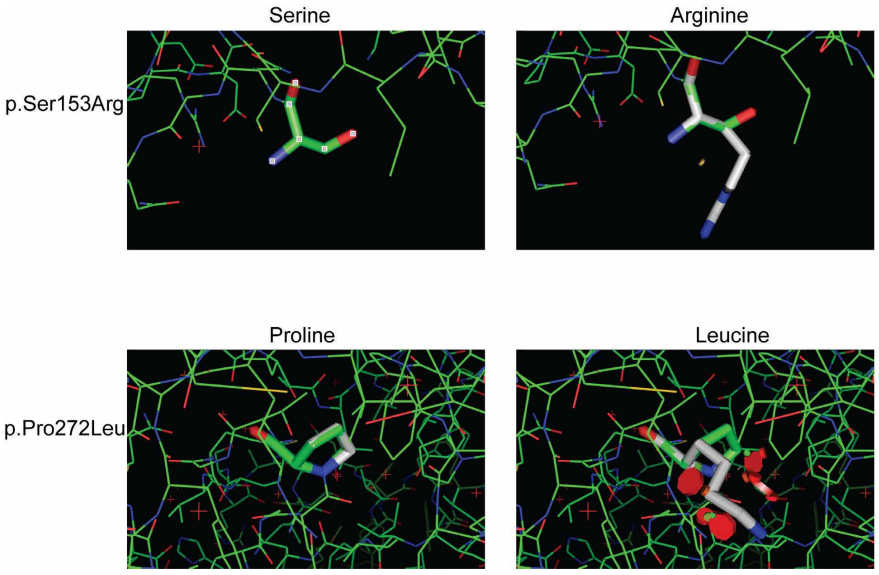

Fig. S2. Structural prediction of GPT2 missense mutations. Three-dimensional structural prediction of the two GPT2 missense mutations p.Ser153Arg and p.Pro272Leu as visualized by PyMOL software. Shown are predicted structures before (*Left*) and after (*Right*) the indicated amino acid substitutions. Both of the amino acid substitutions are non-conservative and are predicted to be deleterious to GPT2 protein structure.

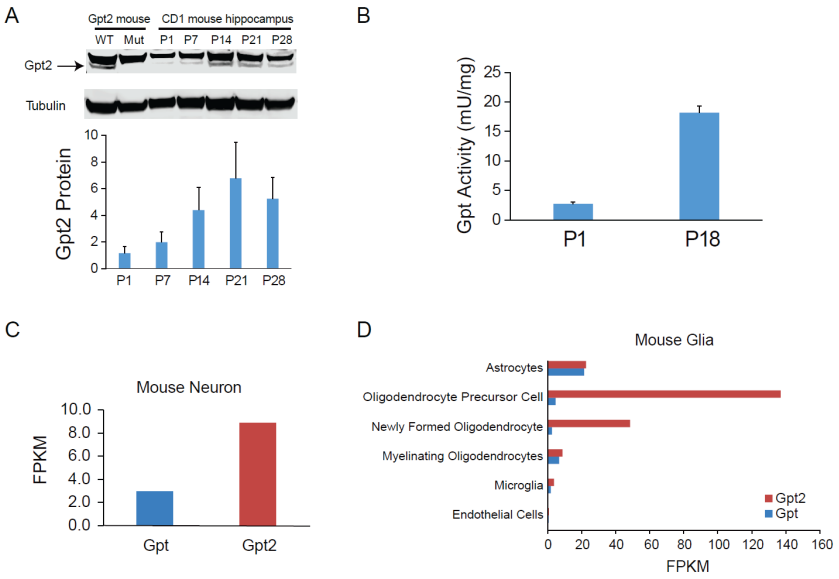

Fig. S3. *Gpt2* gene and protein expression in developing mouse brain. (*A*) Comparison of Gpt2 protein expression levels in wild-type (WT) mouse hippocampus throughout development. *Top*, western blot analysis showing the presence and absence of Gpt2 protein in WT and *Gpt2* null (Mut) mouse, respectively, and the developmental regulation of Gpt2 protein in mouse hippocampus. Arrow indicates the expected band for endogenous Gpt2 at 58 kDa. A nonspecific band is present at approximately 60 kDa. *Bottom*, quantification of western blots. Gpt2 expression was normalized to tubulin throughout WT CD1 mouse hippocampal development at stages of postnatal day 1 (P1), P7, P14, P21, and P28. *n* = 3. Data are presented as means ± SEMs (x 1000). (*B*) Gpt activity in brain lysate after incubating with substrate at 37 °C for 40 min and represented as enzyme activity (mU) per mg of tested sample. P1, *n* = 7; P18, *n* = 5. Data are presented as means ± SEMs. (*C*) *Gpt2* and *Gpt* gene expression in neurons of mouse cerebral cortex. (*D*) *Gpt2* and *Gpt* gene expression in major glia cell types of mouse cerebral cortex. Units are in fragments per kilobase of exon per million fragments mapped (FPKM, *x* axis) (1).

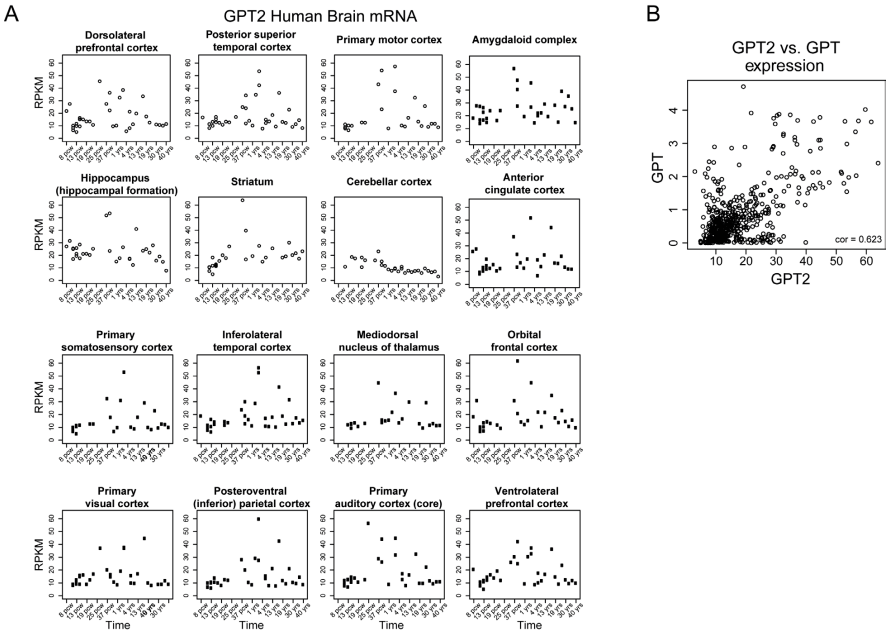

Fig. S4. *GPT2* gene expression in developing human brain. (*A*) *GPT2* gene expression in representative human brain regions across development. Gene expression data are from post-mortem human brain samples from the March 2014 version of the Allen Institute for Brain Science's BrainSpan (http://developinghumanbrain.org). BrainSpan's Developmental Transcriptome includes data generated by RNA sequencing, normalized to RPKM (reads per kilobase per million reads). Data were summarized to 21,392 unique Ensembl gene identifiers and consisted of 524 samples derived from 26 anatomic brain regions. Of those samples, 498 were derived from 16 brain regions. Donors were age 8 weeks post-conception to 40 years old. *GPT2* expression is generally highest in late fetal life and the first 5 years of life, except in cerebellar cortex. (*B*) *GPT2* and *GPT* expression in the BrainSpan transcriptome dataset plotted using all brain regions and time points. *GPT* and *GPT2* expression levels are correlated (r = 0.623), but *GPT2* expression is much higher overall, about 22-fold greater.

A

```
hGPT2  MQRAAALVRRGCGPRTPSSWGRS|QSSAAAE  30
hGPT   MASSTGDRSQAVRHGLRAKVLTLDGMNPRV  30
```

PSORT II Prediction

	Cytoplasmic	Nuclear	Mitochondrial	Vesicles of secretory system	Prediction
hGPT	34.8%	26.1%	26.1%	13.0%	Cytoplasmic
hGPT2		4.3%	95.7%		Mitochondrial
p.Arg404*		4.3%	95.7%		Mitochondrial
p.Ser153Arg		4.3%	95.7%		Mitochondrial
p.Pro272Leu		4.3%	95.7%		Mitochondrial

B

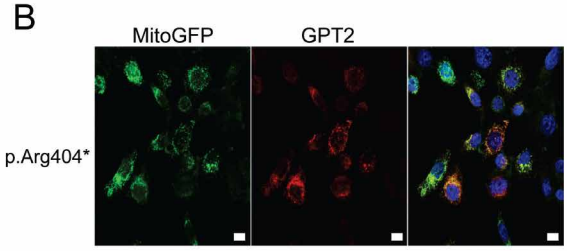

Fig. S5. Data related to the mitochondrial localization of GPT2. (*A*) N-terminal amino acid alignment of human GPT2 and GPT. On GPT2, the red line indicates the predicted cleavage site for the mitochondrial signal peptide sequence. GPT2 has a strong predicted mitochondrial localization signal, but GPT does not. None of the four mutations changes the PSORT II program's predicted mitochondrial localization for GPT2 (2). (*B*) Mitochondrial localization of the GPT2 truncation mutant p.Arg404* at increased imaging sensitivity parameters. The p.Arg404* GPT2 mutant shows little protein expression in studies involving transfection of cell lines (Main Text Fig. 3*A*). When microscopy parameters are altered to increase sensitivity substantially, the p.Arg404* protein becomes visible and, furthermore, shows a mitochondrial subcellular localization. This demonstrates that, although the protein expression level of this mutation is drastically reduced relative to control, the protein that is made continues to be localized to mitochondria. Scale bar, 10 μm.

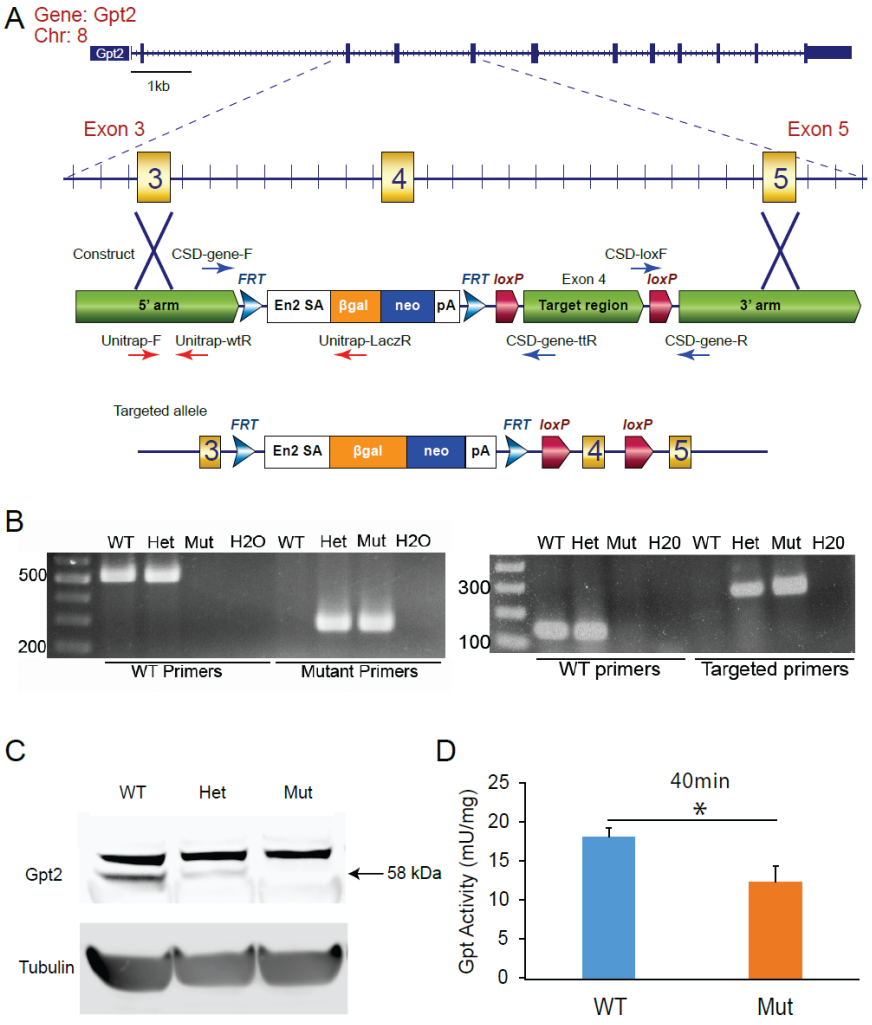

Fig. S6. *Gpt2* targeted gene disruption in mouse. (*A*) Diagrammatic representation of the *Gpt2* gene in the mouse genome. A mutant allele was generated by adding a gene trap (splice acceptor) and *LacZ*-Neo cassette before the targeted exon 4 of *Gpt2*. (*B*) PCR genotyping gels of wild-type (WT), heterozygous (Het), and homozygous mutant (Mut) mice. *Left*, representative PCR genotyping gel showing a 504 base pair (bp) band (primer pairs CSD-gene-F and CSD-gene-ttR) present in WT littermates and Het littermates, but not Mut littermates, and a 283 bp

band (primer pairs CSD-loxF and CSD-gene-R) present in Mut littermates and Het littermates, but not WT littermates. *Right*, RT-PCR gel showing that, when using primers specific for the WT *Gpt2* allele (Unitrap-F and Unitrap-wtR), the WT band (114 bp) cannot be amplified in Mut littermates; however, when using specific *LacZ*-targeted primers (Unitrap-F and Unitrap-LacZR), the *LacZ* band (300 bp) can be amplified in Mut littermates. (*C*) Western blot analysis of WT, Het, and Mut mouse brains. Gpt2 protein (58 kDa, *Arrow*) is not detected in brain lysates from *Gpt2* homozygous mutant (Mut) mice, but it is detected in WT and Het littermates. A nonspecific band is present at approximately 60 kDa. (*D*) Gpt activity in brain lysate after incubating with substrate at 37 °C for 40 min and represented as enzyme activity (mU) per mg of tested sample. WT, $n = 5$; Mut, $n = 3$. Data are presented as means ± SEMs. $^*P < 0.05$.

8

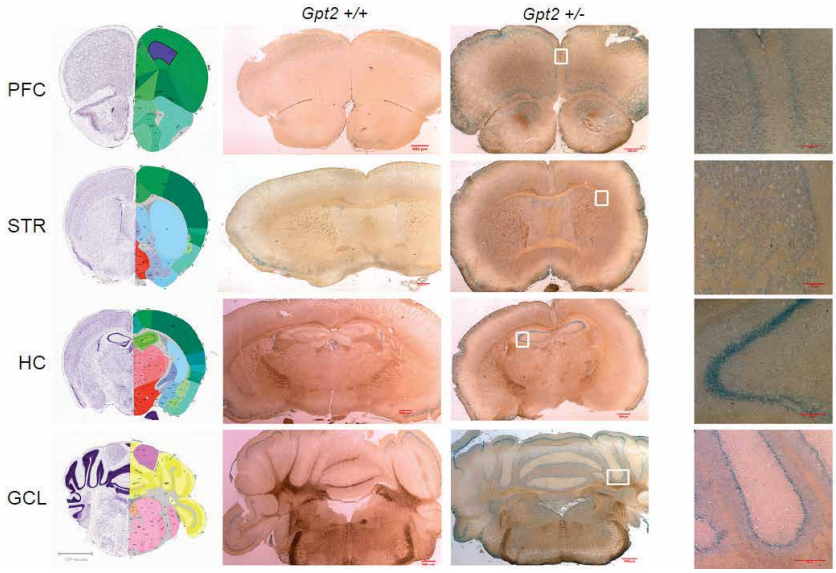

Fig. S7. LacZ staining of *Gpt2* wild-type and heterozygous brain sections. The coronal tissue sections from adult mouse brain were matched across genotypes with corresponding anatomical locations from Allen Brain Atlas images on the far left column. Lower magnification scale bar, 500 μm. The far right column shows higher magnification images of the *Gpt2* +/- tissue sections (within areas demarcated by the white boxes). Higher magnification scale bar, 200 μm. Regions of interest that showed considerable β-galactosidase activity were PFC, Prefrontal Cortex; Str, Striatum; HC, Hippocampus; and GCL, Granular Cell Layer.

Table S1. Detailed clinical summary of individuals with *GPT2* mutations.
(See attached.)

10

Table S2. *In silico* prediction of the pathogenicity of identified *GPT2* variants.

Amino acid change (Family)	p.Pro272Leu (Pedigree 2)
PolyPhen-2 score (prediction)	1.000 (probably damaging)
SIFT score (prediction)	0.001 (damaging)
PROVEAN score (prediction)	-9.48 (deleterious)

Table S3. Targeted guide RNA sequences and primer sequences for CRISPR-Cas9 editing.

Targeted sequences for CRISPR-Cas9 editing		
c.265G>T; p.Glu89*	GCTCGGATGACCTCTGTGAA	
c.1210C>T; p.Arg404*	CACTCGGCTGAATTGCTCAA	
Primers for verifying CRISPR-Cas9-engineered mutant cell lines		
c.265G>T; p.Glu89*	Forward	ACCCTTTAAGAGCCTTGATTTCC
	Reverse	TCAGAAAGGCAGGAAGGAGG
c.1210C>T; p.Arg404*	Forward	GCTTTCGATTCTGGCTGTCC
	Reverse	CACACACTCACAGTCCTCCT

Table S4. Comparison of numbers of littermate offspring and age at time of death across wild-type and *Gpt2* mutant mice resulting from Het X Het parental cross.

Postnatal (P) Age	Mut	Het	WT
P0	9	15	5
P1	7	6	7
P2	5	9	13
P3	0	2	1
P4	0	1	0
P5	1	2	0
P6	1	0	1
P7	0	0	0
P8	0	0	0
P9	0	0	0
P10	0	0	0
P11	0	1	0
P12	0	2	0
P13	0	0	0
P14	0	0	0
P15	0	1	0
P16	1	0	0
P17	0	0	0
P18	2	0	0
P19	2	1	2
P20	7	0	0
P21	9	0	0
P22	10	0	0
P23	4	2	0
P24	2	0	0
P25	4	0	0
Death after 1st postnatal week[1]	41	7	2
Animals surviving to P26[2]	1/65	222/264	92/121
Total pups born (genotyped at P0) across all experiments[3]	193	445	243

[1]"Death after 1st postnatal week" shows the total death number from P8–P25 in littermates of all genotypes resulting from matings from heterozygous parents. *Gpt2* null mice (Mut) had an unusually high occurrence of death in this period as compared to wild-type (WT) or heterozygous (Het) mice.

[2]"Animals born surviving to P26" is the number of animals alive at P26 as a proportion of the total number of animals born from heterozygous parents and allowed to grow to P26 (i.e., the total number is the sum of the number of animals that died from P0–P25 and the number of animals still surviving at P26). As shown, almost all *Gpt2* mutant mice (Mut) died before P26.

[3]"Total pups born (genotyped at P0) across all experiments" is the total number of littermates born of each indicated genotype from heterozygous matings. Genotypes reflect approximately the expected Mendelian ratio of Mut:Het:WT = 1:2:1 or a slight reduction in homozygous *Gpt2* null animals that was not statistically significant ($P = 0.25$).

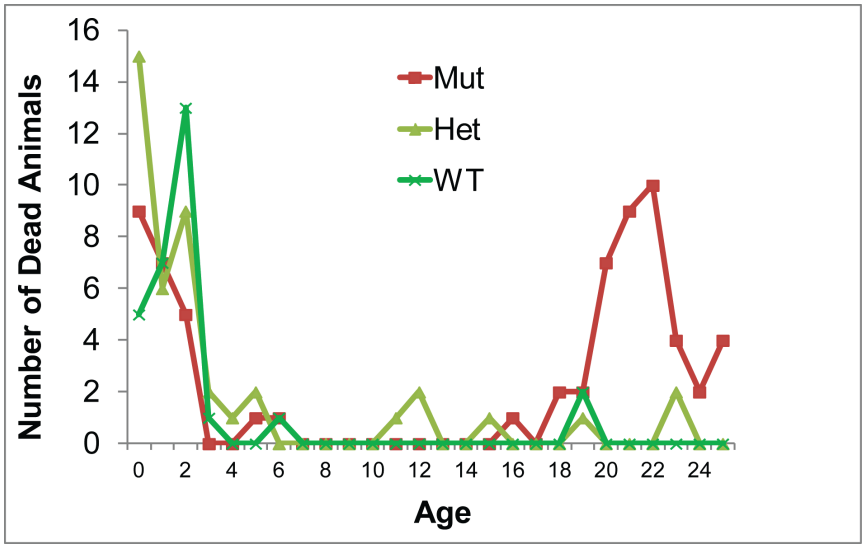
Number of Dead Animals
16
14
12
10
8
6
4
2
0
0
2
4
6
8
10
12
14
16
18
20
22
24
Age
Mut
Het
WT

14

Table S5. Metabolite set enrichment analysis of P18 *Gpt2* mutant mouse brain.
(See attached.)

Over-representation analysis of metabolites (hits) that were significantly increased or decreased in *Gpt2* mutant P18 mouse brains in comparison to controls as per Student's *t*-test results. A normal metabolic pathway-associated library containing 88 metabolite sets was referenced [Small Molecule Pathway Database (SMPDB)]. Hypergeometric test was used to determine whether a metabolite set is represented more than expected by chance. One-tailed *P* value was adjusted for multiple testing using the Holm-Bonferroni method. Fold enrichment refers to the ratio of observed number of hits to expected number of hits. FDR = False discovery rate. The results were compiled and analyzed in MetaboAnalyst 3.0 (3).

Table S6. Significantly changed metabolites in *Gpt2* mutant mouse brains (P18).
P values from two-sided Student's *t*-test (threshold *P* value = 0.05) and FDR values were calculated from the normalized data. The mean peak values are intensities; standard deviations and fold changes were calculated from the raw data. Negative and positive ion modes of mass spectrometry are denoted as "-nega" or "-posi", respectively. FDR = False Discovery Rate. The results were compiled and analyzed in MetaboAnalyst 3.0 (3).

	Mean Peak Area Intensity (WT)	Mean Peak Area Intensity (Mut)	Standard Deviation (WT)	Standard Deviation (Mut)	Fold Change (Mut/WT)	*P* value	(-log*P*)	FDR
lysine	803356.9333	1833545.117	152481.0854	270421.3016	2.282354257	8.12E-07	6.09	0.000199
cystathionine	547907.3	1320016.967	115697.8766	117903.0564	2.409197626	3.01E-06	5.521	0.000369
cholic acid	33105.94683	5314.160833	10497.15187	3375.28434	0.160519826	0.0001	3.904	0.0079908
proline	15475919	22428706.17	1329244.649	3164887.801	1.449264898	0.0001	3.848	0.0079908
alanine	17631392.5	15611829.17	762953.6881	1184463.913	0.885456391	0.0002	3.788	0.0079908
guanidoacetic acid	316621.8	445213.6833	66629.4731	45403.41862	1.406137175	0.0004	3.349	0.016581
glycine	2441.616167	6529.891833	1071.037025	1731.660534	2.674413744	0.0005	3.288	0.016581
2-keto-isovalerate	6931355.833	6067903.667	306813.5781	568595.4536	0.8754281	0.0006	3.211	0.016581
urea	1626969.735	400024.8083	226947.3301	524364.1094	0.245871082	0.0007	3.178	0.016581
deoxyribose-phosphate	156010.04	98624.67167	15201.34689	8289.089736	0.632168748	0.0007	3.17	0.016581
N-acetyl-glucosamine-1-phosphate	198716.0167	154847.1333	15196.24609	15077.2336	0.779238312	0.0008	3.071	0.018898
folate	98008.695	37548.31667	28771.46461	4640.057922	0.383112097	0.0012	2.925	0.023561
NADP+-nega	168018.315	67253.26667	51492.50621	23717.55948	0.400273427	0.0013	2.903	0.023561
malate	10470619.67	7700541.5	661844.1715	652751.5948	0.735442767	0.0014	2.867	0.023783
histidine	5510466.833	9870994.333	1564334.072	1396281.204	1.791317257	0.0015	2.833	0.023923
phenylalanine	2764123.167	4535573.333	852412.4465	820375.7523	1.640872371	0.0016	2.806	0.023923
fumarate	6453366.833	5686016.667	404988.2382	388485.7269	0.88109305	0.0022	2.654	0.031943
methionine	1285558.167	1879339.5	373058.3906	280172.5516	1.461886011	0.0025	2.606	0.033709
glutathione	14012643	10016342.33	2070523.752	1871473.958	0.714807502	0.0029	2.532	0.037849
threonine	4463144.5	6853462.167	568849.8393	1437858.811	1.535568066	0.0032	2.493	0.03898
dephospho-CoA-posi	49462.86167	124478.2683	19481.7889	45243.20567	2.51660062	0.0033	2.476	0.03898
hydroxyphenylpyruvate	41631.97333	30159.04167	3939.369415	7422.75454	0.724420181	0.0038	2.423	0.042066
NADP+-posi	199377.7683	94725.22	57191.16249	45194.65476	0.475104224	0.004	2.401	0.042295
dephospho-CoA-nega	27059.12	68188.84	13322.63876	25070.56369	2.519994737	0.0049	2.308	0.05023
methylmalonic acid	7567786.833	5705437.333	574682.4676	622323.7233	0.753910946	0.0055	2.257	0.052783
asparagine	799742.3667	1019191.617	85165.35657	91826.46778	1.274399931	0.0057	2.242	0.052783
pyroglutamic acid	132041.25	246045.8	29733.92463	81940.02195	1.863401021	0.0059	2.227	0.052783
UTP-nega	46838.85833	140972.6867	26117.64639	62769.55117	3.00973789	0.0061	2.214	0.052783
citrate-isocitrate	7921255.167	6877127.833	573904.6351	619933.245	0.868186631	0.0064	2.194	0.052783
glucosamine	137964.3183	81114.24667	32605.083	9449.288049	0.587936415	0.0065	2.19	0.052783
IMP	9235691.667	6869645.167	1615206.298	699879.7197	0.74381491	0.0076	2.122	0.058483
glutathione-nega	774181.5667	558013.2167	70706.01271	135519.4	0.720778227	0.0076	2.117	0.058483
ATP-nega	526053.2	1208106.35	254133.4215	463907.953	2.296547859	0.0084	2.076	0.062399
succinate	6104226.333	4632350.5	449631.9542	549639.4156	0.758875941	0.0095	2.024	0.065628

citraconic acid	327398.1333	725850.9	42156.96008	292604.0945	2.217028218	0.0095	2.022	0.065628
DL-pipecolic acid	68270150.83	76923811.67	7815936.201	6117821.015	1.126756141	0.0096	2.016	0.065628
trans, trans-farnesyl diphosphate	24560.80017	8587.927	9918.644297	4039.084121	0.349659903	0.0104	1.983	0.068792
homocysteine	81770.83833	63140.91167	10224.36149	8646.992739	0.772169064	0.0117	1.932	0.075475
cysteine	80887.08833	49257.67667	13389.49742	24897.01829	0.608968349	0.0133	1.877	0.083426
dGTP	572296.3833	1327639	240360.3648	572180.8785	2.319845169	0.0144	1.843	0.087925
maleic acid	6718346.5	6063339.167	280151.7174	633581.3479	0.902504681	0.0148	1.831	0.087925
acetyl-CoA-posi	16886.447	44016.03017	9332.737523	20092.08655	2.606589188	0.0153	1.816	0.087925
citrate	7099462.45	4653529.933	315287.6052	1887719.881	0.655476378	0.0154	1.812	0.087925
GTP-nega	23692.64933	73773.9435	25118.93136	34890.55861	3.113790377	0.0169	1.771	0.094309
O8P-O1P	15371.533	24820.4355	5174.16945	6048.999211	1.614701377	0.0181	1.742	0.098693
dCDP-nega	11139.37917	25371.15767	9161.169113	8006.167667	2.277609666	0.019	1.722	0.10095
ascorbic acid	27267959.67	23846210	1372067.637	2904782.378	0.874513909	0.0243	1.615	0.12661
GMP	12120754.83	9799956	1865185.158	1249335.112	0.808526873	0.0279	1.555	0.14234
ribose-phosphate	1460590.583	1018590.8	385200.6649	159073.9534	0.697382834	0.0297	1.527	0.14857
glutathione disulfide-nega	8982199.333	7006599	997146.645	1412732.04	0.780053831	0.0324	1.49	0.1568
cystine	32445.841	16897.46317	11347.30116	7284.471353	0.520789804	0.0328	1.485	0.1568
creatinine	5277095.667	4728426.5	588173.2638	608749.0511	0.896028194	0.0333	1.478	0.1568
N-carbamoyl-L-aspartate-nega	18208.46667	25464.065	3725.89318	6200.733923	1.398473878	0.0345	1.462	0.15947
guanine	99026.54633	233169.9418	73845.20487	101252.4476	2.354620558	0.0361	1.443	0.16357
OBP	46418.21	67602.865	15823.9628	14751.7061	1.456386728	0.0378	1.422	0.16846
dCMP	28319.545	19385.73167	5888.256613	5589.232082	0.684535421	0.0398	1.4	0.17417
glutamine	56321021	63188380.83	7868063.564	5154978.117	1.121932446	0.041	1.387	0.17642
pantothenate	1486.143833	4321.981167	969.7241714	2587.623957	2.908184975	0.0431	1.366	0.18139
fructose-6-phosphate	2526.723	7145.374167	1600.470659	4399.228125	2.827921449	0.0443	1.353	0.18139
hydroxyproline	379041.6	303953.5333	63605.58734	44461.86162	0.801900196	0.045	1.347	0.18139
4-aminobutyrate	9639418.5	8616305.833	1112532.086	849888.7394	0.893861578	0.0455	1.342	0.18139
UMP	678302.8833	511459.1667	138251.1972	94160.90048	0.754027705	0.0472	1.326	0.18139
ADP-nega	1659.808833	3923.48	872.1070656	2082.634948	2.363814387	0.048	1.319	0.18139
sarcosine	3824569.5	3510547.667	303820.4423	433722.8604	0.917893548	0.0488	1.311	0.18139
hexose-phosphate	668008.15	498977.5167	55006.01208	144936.0807	0.746963217	0.049	1.31	0.18139
carbamoyl phosphate	59255426.83	61509289	4426620.985	4602102.814	1.038036384	0.0499	1.302	0.18139

17

Table S7. Peak area intensities in *Gpt2* mutant mouse brains (P18).
(See attached.)

Columns contain different biological samples (*Gpt2* mutant and wild-type brains) and rows are analyzed metabolites.

18

Table S8. Significantly changed metabolites in *Gpt2* mutant mouse brains (P0).
Wild-type and heterozygote littermate brain samples were combined. *P* values from Student's *t*-test and FDR values were calculated from the normalized data. The mean peak values are intensities; standard deviations and fold changes were calculated from the raw data. Negative and positive ion modes of mass spectrometry are denoted as "-nega" or "-posi", respectively. FDR = False Discovery Rate. The results were compiled and analyzed in MetaboAnalyst 3.0 (3).

	Mean Peak Area Intensity (WT)	Mean Peak Area Intensity (Mut)	Standard Deviation (WT)	Standard Deviation (Mut)	Fold Change (Mut/WT)	*P* value	(-log*P*)	FDR
alanine	13573473	21346208	2074392	1988245	1.572642	6.25E-07	6.2043	0.000165
hydroxyproline	3623628	6403408	750493.7	1321084	1.767126	2.54E-06	5.5956	0.000335
sarcosine	2842840	3799557	573481.7	496537.2	1.336536	0.000173	3.7609	0.015259
cystathionine	616056.2	1047694	122304.9	314545.9	1.700647	0.000436	3.36	0.028808
anthranilate	13152.77	25941.14	7159.526	6575.875	1.972295	0.005587	2.2528	0.263
threonine	6499735	9971932	2547526	2754458	1.534206	0.00604	2.219	0.263
lysine	1288446	680140.4	441835.5	554968.2	0.527877	0.006974	2.1565	0.263
3-methylphenylacetic acid	10793.06	19526.2	5320.812	7036.357	1.809145	0.011704	1.9317	0.33095
citrulline	3736152	4712573	753161.1	529321.7	1.261344	0.012287	1.9106	0.33095
kynurenic acid	84407.48	129450.2	15280.7	34755.42	1.533634	0.012536	1.9018	0.33095
trans, trans-farnesyl diphosphate	45567.87	66091.31	17125.62	17798.62	1.450393	0.016342	1.7867	0.39222
N-carbamoyl-L-aspartate	21667.71	28648.35	5285.695	4586.656	1.322168	0.020742	1.6831	0.44767
histidine	2367147	3870416	1007695	1511573	1.635055	0.022044	1.6567	0.44767
myo-inositol	52450917	50668447	7628124	6402414	0.966016	0.027248	1.5647	0.51381
S-adenosyl-L-homocysteine-posi	168188.9	280300.7	66768.5	155909.4	1.666583	0.03479	1.4585	0.57404
hydroxyphenylacetic acid	39811.92	21733.41	12030.56	16485.57	0.545902	0.039253	1.4061	0.60957
allantoin	2477784	2917487	627221.1	494912.2	1.177458	0.048372	1.3154	0.70945

Table S9. Peak area intensities in *Gpt2* mutant mouse brains (P0).
(See attached.)

Columns contain different biological samples (*Gpt2* mutant and wild-type brains) and rows are analyzed metabolites. *Gpt2* heterozygote brain samples were labeled as wild-type to pool them with the wild-type brain samples in the analysis.

Web Resources

BrainSpan: Atlas of the Developing Human Brain, http://developinghumanbrain.org
1000 Genomes Project, http://www.1000genomes.org/
ANNOVAR, http://www.openbioinformatics.org/annovar/
Burrows-Wheeler Aligner, http://bio-bwa.sourceforge.net
Complete Genomics 69 Genomes Data, http://www.completegenomics.com/public-data/69-Genomes/
dbSNP, http://www.ncbi.nlm.nih.gov/SNP/
GATK, http://www.broadinstitute.org/gatk/
ImageJ, http://imagej.nih.gov/ij/
NHLBI Exome Sequencing Project (ESP) Exome Variant Server, http://evs.gs.washington.edu/EVS/
MetaboAnalyst 3.0, http://www.metaboanalyst.ca/
Online Mendelian Inheritance in Man (OMIM), http://www.omim.org
Picard, http://broadinstitute.github.io/picard/
PLINK, http://pngu.mgh.harvard.edu/purcell/plink/
Primer3, http://primer3.ut.ee/
PROVEAN, http://provean.jcvi.org
SAMtools, http://samtools.sourceforge.net/
SIFT, http://sift.jcvi.org
SMDPB, http://smpdb.ca/
PolyPhen-2, http://genetics.bwh.harvard.edu/pph2/
RefSeq, http://www.ncbi.nlm.nih.gov/RefSeq
Brain RNA-Seq, http://web.stanford.edu/group/barres_lab/brain_rnaseq.html

Additional Acknowledgments
Authors would like to thank: L. Benjamin Hills who helped with Sanger sequencing; M. Chiara Manzini for help with clinical data and sample collection; Xiaochang Zhang for technical assistance; the W.M. Keck Foundation Biotechnology Resource Laboratory at Yale University for microarray services; and John M. Asara at the Beth Israel Deaconess Medical Center Mass Spectrometry, Proteomics and Metabolomics Core. Exome sequencing of the individual MC9432 was funded by National Human Genome Research Institute (NHGRI) grant U54HG003067 to the Broad Institute. The *Gpt2* null mouse strain used for this research project was generated by the trans-NIH Knockout Mouse Project (KOMP) and obtained from the KOMP Repository (www.komp.org). NIH grants to the VelociGene division of Regeneron Pharmaceuticals, Inc. (U01HG004085) and the CSD Consortium (U01HG004080) funded the generation of gene-targeted embryonic stem cells for 8,500 genes in the KOMP Program and archived and distributed by the KOMP Repository at University of California (UC) Davis and Children's Hospital Oakland Research Institute (CHORI) (U42RR024244). For more information or to obtain KOMP products go to www.komp.org or email service@komp.org.

References

1. Zhang Y, *et al.* (2014) An RNA-sequencing transcriptome and splicing database of glia, neurons, and vascular cells of the cerebral cortex. *J Neurosci* 34(36):11929-11947.
2. Horton P & Nakai K (1997) Better prediction of protein cellular localization sites with the k nearest neighbors classifier. *Proc Int Conf Intell Syst Mol Biol* 5:147-152.
3. Xia J, Sinelnikov IV, Han B, & Wishart DS (2015) MetaboAnalyst 3.0--Making metabolomics more meaningful. *Nucleic Acids Res* 43(W1):W251-257.

Table S1. Detailed clinical summary of individuals with *GPT2* mutations.

	Pedigree 1 (MI1000)				
Individual code	**MI1001**	**MI1002**	**MI1003**	**MI1004**	**MI1008**
Consanguinity (Parental relatedness)	Yes (1st Cousins)				
Gender	Female	Male	Male	Female	Male
Age at examination	19y	18y	32y	28y	24y
Head circumference at birth	N/A	N/A	N/A	N/A	N/A
Length at birth	N/A	N/A	N/A	N/A	N/A
Weight at birth	N/A	N/A	N/A	N/A	N/A
Head circumference at examination	50.8 cm (-3.30 SDs)	49 cm (-4.10 SDs)	50 cm (-3.44 SDs)	49 cm (-5.01 SDs)	N/A
Height at examination	N/A	N/A	N/A	N/A	N/A
Weight at examination	46 kg (-1.69 SDs)	31 kg (-4.2 SDs)	48 kg (-2.5 SDs)	43 kg (-2.1 SDs)	N/A
Motor development	hypotonia during infancy, head control at 6m	hypotonia during infancy, head control at 7m, sat at 9m	head control at 4m, sat at 8m	hypotonia during infancy, head control at 6m, sat at 7m	hypotonia during infancy, delayed development
Age of being able to walk	N/A	2.5y	2y	N/A	N/A
Subsequent deterioration in walking	Yes	Yes	Yes	Yes	N/A
Speech and cognition	delayed speech, cognition at the level of 3-6y	delayed speech, limited to simple words, cognition at the level of 1y	delayed speech, one word speech at 1.5y, complete sentences at 8y	delayed speech	delayed speech
Oral-motor	dysarthria, drooling	drooling	dysarthria, drooling	N/A	N/A
Motor examination	N/A	hyperreflexia, hypertonia, spastic diplegia	hyperreflexia, hypertonia, spastic diplegia	hyperreflexia, hypertonia	N/A
Seizures/Epilepsy	No, EEG (19y): normal	febrile seizures at 8m, epilepsy with GTCs at 2.5y, EEG (18y): normal	febrile seizures at 3m, EEG (32y): normal	No	N/A
Imaging	CT (19y): normal	CT (18y): normal	MRI (16y): moderately diminished white matter	CT (28y): normal	N/A
Remarks	persistent diarrhea during infancy, fears and paranoia since 2y, progressive difficulty in walking	progressive difficulty in walking	progressive difficulty in walking	persistent diarrhea during infancy, progressive difficulty in walking	N/A
GPT2 mutation	p.Arg404*	p.Arg404*	p.Arg404*	p.Arg404*	p.Arg404*

	Pedigree 2 (MC9400)								
Individual code	**MC9401**	**MC9403**	**MC9429**	**MC9428**	**MC9427**	**MC9426**	**MC9432**	**MC9433**	**MC9434**
Consanguinity (Parental relatedness)	Yes (1st Cousins)								
Gender	Male	Female	Male	Female	Male	Male	Male	Male	Female
Age at examination	16y	11y	28y	19y	14y	11y	28y	17y	16y
Head circumference at birth	33 cm (-1.22 SDs)	33 cm (-1.16 SDs)	N/A	33 cm (-1.16 SDs)	33 cm (-1.22 SDs)	33 cm (-1.22 SDs)	N/A	N/A	33 cm (-1.16 SDs)
Length at birth	47 cm (-1.11 SDs)	49 cm (-0.13SD)	N/A	N/A	49 cm (-0.37 SD)	47 cm (-1.11 SDs)	N/A	N/A	49 cm (-0.13 SD)
Weight at birth	2.85 kg (-1.09 SDs)	2.5 kg (-1.72 SDs)	N/A	N/A	3.2 kg (-0.53 SD)	2.65 kg (-1.41 SDs)	N/A	N/A	2.7 kg (-1.34 SDs)
Head circumference at examination	45 cm (-6.79 SDs)	46 cm (-5.40 SDs)	51 cm (-2.77 SDs)	48 cm (-5.93 SDs)	49 cm (-3.57 SDs)	46.5 cm (-5.04 SDs)	50 cm (-3.44 SDs)	49 cm (-4.10 SDs)	49 cm (-4.99 SDs)
Height at examination	140 cm (-3.9 SDs)	115 cm (-4.1sSDs)	155 cm (-3.0 SDs) at 21y	138 cm (-1.76 SDs) at 12y	108 cm (-2.6 SDs) at 7y	102 cm (-0.05 SD) at 4y	175 cm (-0.22 SD)	179 cm (+0.79 SD)	153 cm (-1.42 SDs)
Weight at examination	27 kg (-4.0 SDs)	15 kg (-5.5 SDs)	48 kg (-2.5 SDs) at 21y	27 kg (-2.3 SDs) at 12y	15 kg (-3.1 SDs) at 7y	15 kg (-0.77 SD) at 4y	49 kg (-2.4 SDs)	39 kg (-2.9 SDs)	40 kg (-2.0 SDs)
Motor development	hypotonia during infancy	hypotonia during infancy	walked at 3y	better walking until 5y, afterwards unstable	unstable gait during development	hypotonia during infancy, walked at 2.5y	noted clumsy gait in preschool	clumsy gait at exam	delayed development, microcephaly noted at 6m
Age of being able to walk	3y	N/A	3y	N/A	1.5y	2.5y	3.5y	1.5y	1.5y
Subsequent deterioration in walking	Yes	N/A	Yes	Yes	No	Yes	Yes	No	Yes
Speech and cognition	delayed speech, limited to simple words, cognition at the level of 3y	delayed speech, limited to simple words, cognition at the level of 3y	delayed speech, limited to simple words, cognition at the level of 3y	delayed speech, can read name at exam	delayed speech, can speak 2-3 word sentences, cognition on the level of 3y	delayed speech, used to speak clearly, no speech at exam	delayed speech, cognition at the level of 3y, can speak short sentences	N/A	delayed speech, talking at 2y, speeks few words, cognition on the level of 1y
Oral-motor	dysarthria, drooling	dysarthria, reduced facial expression	dysarthria, drooling	dysarthria, mild drooling	dysarthria, drooling	dysarthria, drooling	dysarthria, drooling	dysarthria, drooling	drooling
Motor examination	hyperreflexia, hypertonia, spastic diplegia (R>L)	hyperreflexia, hypertonia, spastic diplegia	hyperreflexia, hypertonia, spastic diplegia, contracture on left ankle	hyperreflexia, hypertonia, spastic diplegia	mild hypertonia	hyperreflexia, mild hypertonia, spastic diplegia, pronounced tremor	hyperreflexia, hypertonia, tremors, spastic diplegia, contractures of the lower limbs	mild hypertonia, hyperreflexia	hyperreflexia, bilateral ankle joint contractures, spastic diplegia

Seizures/Epilepsy	No	No	epilepsy	No	No	Lennox-Gastaut syndrome, EEG showed bilateral slow waves with delta ranged slow waves	No	febrile seizures at the age of 2y for 9 days, no seizures afterwards	No
Imaging	MRI (16y): enlarged extracerebral fluid spaces	MRI (13y): normal	N/A	MRI (10y): normal	MRI (13y): normal	CT (4y): normal	N/A	N/A	CT (3y): normal
Remarks	N/A	N/A	Fell from the roof at 7y, became wheelchair-bound, progressive difficulty in walking	progressive difficulty in walking	mild kyphoscoliosis	past history of prolonged hyperpyrexia at 3y	N/A	N/A	Fell from the roof at 3y, no bladder or bowel control
GPT2 mutation	p.Pro272Leu	p.Pro272Leu	p.Pro272Leu	p.Pro272Leu	p.Pro272Leu	p.Pro272Leu	p.Pro272Leu	p.Pro272Leu	p.Pro272Leu

CT: compted tomography, EEG: electroencephalography, GTCs: generalized tonic clonic seizures, MRI: magnetic resonance imaging, N/A: not available

Table S5. Metabolite set enrichment analysis of P18 *Gpt2* mutant mouse brain.

Pathway-Associated Metabolite Set	Total	Expected	Hits	Raw *P*	Holm *P*	FDR	Fold Enrichment	Metabolite Hits	Whole Pathway Set
PROTEIN BIOSYNTHESIS	19	1.31	10	6.44E-08	5.15E-06	5.15E-06	7.633587786	L-Phenylalanine; L-Alanine; L-Proline; L-Threonine; L-Asparagine;L-Histidine; L-Lysine; L-Cysteine; L-Glutamine; L-Methionine;	L-Glutamic acid; L-Tyrosine; L-Phenylalanine; L-Alanine; L-Proline; L-Threonine; L-Asparagine; L-Isoleucine; L-Histidine; L-Lysine; L-Aspartic acid; L-Arginine; L-Cysteine; L-Glutamine; L-Leucine; L-Methionine; L-Valine; L-Tryptophan; D-Serine
CITRIC ACID CYCLE	23	1.59	9	7.33E-06	0.000579	0.000293	5.660377358	Citric acid; Fumaric acid; L-Malic acid; Isocitric acid;Succinic acid; Adenosine triphosphate;Acetyl-CoA;Guanosine triphosphate; ADP	cis-Aconitic acid; Citric acid; Fumaric acid; L-Malic acid; Isocitric acid; Oxoglutaric acid; Oxaloacetic acid; Pyruvic acid; Succinic acid; Adenosine triphosphate; Hydrogen carbonate; NAD; Succinyl-CoA; FADH; Guanosine diphosphate; Acetyl-CoA; FAD; Guanosine triphosphate; ADP; Coenzyme A; NADH; Carbon dioxide; Water
GLUTATHIONE METABOLISM	10	0.691	6	1.42E-05	0.00111	0.000379	8.683068017	Glycine; Glutathione; NADP;Pyroglutamic acid; L-Cysteine;Oxidized glutathione	Cysteinylglycine; Glycine; Glutathione; L-Glutamic acid; NADP; NADPH; Pyroglutamic acid; L-Cysteine; Gamma-Glutamylcysteine; Oxidized glutathione
RNA TRANSCRIPTION	9	0.622	5	0.000135	0.0104	0.0027	8.038585209	Uridine triphosphate; Uridine 5'-monophosphate; Adenosine triphosphate; Guanosine triphosphate; Guanosine monophosphate	Adenosine monophosphate; Cytidine triphosphate; Cytidine monophosphate; Pyrophosphate; Uridine triphosphate; Uridine 5'-monophosphate; Adenosine triphosphate; Guanosine triphosphate; Guanosine monophosphate
AMMONIA RECYCLING	18	1.24	6	0.000812	0.0617	0.0108	4.838709677	Glycine; L-Asparagine; L-Histidine;Adenosine triphosphate; L-Glutamine;ADP;	Ammonia; Glycine; L-Glutamic acid; L-Asparagine; L-Histidine; L-Serine; L-Aspartic acid; Oxoglutaric acid; Pyruvic acid; Urocanic acid; Adenosine triphosphate; L-Glutamine; NAD; Carbamoylphosphate; ADP; NADH; Carbon dioxide; Water
GLUTAMATE METABOLISM	18	1.24	6	0.000812	0.0617	0.0108	4.838709677	Gamma-Aminobutyric acid; Glutathione;Succinic acid; L-Glutamine;Guanosine monophosphate; Oxidized glutathione;	Ammonia; Gamma-Aminobutyric acid; Glutathione; L-Glutamic acid; Oxoglutaric acid; Succinic acid; L-Glutamine; NAD; Gamma-Glutamylcysteine; N-Acetyl-D-Glucosamine 6-Phosphate; Carbamoylphosphate; 5-Phosphoribosylamine; Glucosamine 6-phosphate; Succinic acid semialdehyde; 1-Pyrroline-5-carboxylic acid; Guanosine monophosphate; Oxidized glutathione; Chitin
GLYCINE, SERINE AND THREONINE METABOLISM	26	1.8	7	0.00122	0.0899	0.0139	3.888888889	L-Cystathionine; Glycine; Guanidoacetic acid; L-Threonine; Sarcosine;L-Cysteine; Homocysteine;	2-Ketobutyric acid; Betaine; Ammonia; Creatine; Dimethylglycine; L-Cystathionine; Glycine; Guanidoacetic acid; Glyceric acid; L-Threonine; L-Serine; Pyruvic acid; Sarcosine; Phosphoserine; L-Cysteine; Homocysteine; 3-Phosphoglyceric acid; Phosphohydroxypyruvic acid; 5-Aminolevulinic acid; Pyruvaldehyde; Hydroxypyruvic acid; 5,10-Methylene-THF; Tetrahydrofolic acid; Carbon dioxide; Aminoacetone; L-2-Amino-3-oxobutanoic acid
UREA CYCLE	20	1.38	6	0.00152	0.111	0.0152	4.347826087	Fumaric acid;L-Alanine;Urea;Adenosine triphosphate;L-Glutamine;ADP;	Adenosine monophosphate; Ammonia; Argininosuccinic acid; Fumaric acid; L-Glutamic acid; L-Alanine; L-Aspartic acid; Oxoglutaric acid; Ornithine; Oxaloacetic acid; Pyruvic acid; Urea; L-Arginine; Adenosine triphosphate; Hydrogen carbonate; L-Glutamine; Citrulline; Carbamoylphosphate; ADP; Water
METHIONINE METABOLISM	24	1.66	6	0.00424	0.305	0.0377	3.614457831	L-Cystathionine; Glycine;Adenosine triphosphate; L-Cysteine; L-Methionine;Homocysteine;	2-Ketobutyric acid; Betaine; Dimethylglycine; Choline; L-Cystathionine; Glycine; L-Serine; Adenosine triphosphate; L-Cysteine; L-Methionine; L-Homoserine; Homocysteine; S-Adenosylhomocysteine; 5-Methylthioribose 1-phosphate; S-Adenosylmethioninamine; 5'-Methylthioadenosine; S-Adenosylmethionine; Spermidine; 5-Methyltetrahydrofolic acid; Putrescine; 2-Oxo-4-methylthiobutanoic acid; Tetrahydrofolic acid; Carbon dioxide; Methionine sulfoxide
INTRACELLULAR SIGNALLING THROUGH PROSTACYCLIN RECEPTOR AND PROSTACYCLIN	6	0.415	3	0.0054	0.383	0.0432	7.228915663	Adenosine triphosphate;Guanosine triphosphate; ADP	Cyclic AMP; Adenosine triphosphate; Guanosine diphosphate; Guanosine triphosphate; Prostaglandin I2; ADP
PURINE METABOLISM	45	3.11	8	0.00903	0.632	0.0656	2.572347267	Guanine;Inosinic acid; Adenosine triphosphate; L-Glutamine;Guanosine triphosphate;ADP; Guanosine monophosphate;dGTP	Adenine; Adenosine monophosphate; Adenosine; Cyclic AMP; Deoxyinosine; Deoxyguanosine; Deoxyadenosine; Guanine; Guanosine; Hypoxanthine; Inosinic acid; Inosine triphosphate; Inosine; Phosphoribosyl pyrophosphate; Uric acid; Xanthine; Xanthosine; Adenylsuccinic acid; Adenosine triphosphate; L-Glutamine; SAICAR; Deoxyadenosine monophosphate; dGDP; 2'-Deoxyguanosine 5'-monophosphate; 5-Phosphoribosylamine; Adenosine diphosphate ribose; Guanosine diphosphate; 5-Aminoimidazole ribonucleotide; Guanosine triphosphate; 5'-Phosphoribosyl-N-formylglycinamide; Diguanosine tetraphosphate; ADP; Guanosine monophosphate; Phosphoribosyl formamidocarboxamide; dGTP; dADP; AICAR; dATP; D-Ribose 5-phosphate; Xanthylic acid; Glycineamideribotide; IDP; 2-[Formamido)-N1-(5-phospho-D-ribosyl)acetamidine; 5-amino- 1-(5-phospho-D-ribosyl)imidazole-4-carboxylate; Guanosine 2',3'-cyclic phosphate
MITOCHONDRIAL ELECTRON TRANSPORT CHAIN	15	1.04	4	0.0158	1	0.105	3.846153846	Fumaric acid; Succinic acid; Adenosine triphosphate;ADP	Glycerol 3-phosphate; Fumaric acid; Succinic acid; Adenosine triphosphate; NAD; Ubiquinol; Coenzyme Q10; D-Glyceraldehyde 3-phosphate; Glyceric acid 1,3-biphosphate; ADP; Hydrogen; Oxygen; Dihydroxyacetone phosphate; NADH; Water
INTRACELLULAR SIGNALLING THROUGH FSH RECEPTOR AND FOLLICLE STIMULATING HORMONE | INTRACELLULAR SIGNALLING THROUGH LHCGR RECEPTOR AND LUTEINIZING HORMONE/CHORIOGONADOTROPIN	4	0.276	2	0.0257	1	0.151	7.246376812	Adenosine triphosphate;Guanosine triphosphate	Cyclic AMP; Adenosine triphosphate; Guanosine diphosphate; Guanosine triphosphate
PANTOTHENATE AND COA BIOSYNTHESIS	10	0.691	3	0.0265	1	0.151	4.341534009	Pantothenic acid; L-Cysteine; Dephospho-CoA;	Pantothenic acid; L-Cysteine; D-4'-Phosphopantothenate; 4-Phosphopantothenoylcysteine; Dephospho-CoA; Pantetheine 4'-phosphate; Coenzyme A; Pantetheine; Pantothenol; D-Pantothenoyl-L-cysteine
PYRIMIDINE METABOLISM	36	2.49	6	0.0319	1	0.164	2.409638554	Uridine triphosphate; Uridine 5'-monophosphate; L-Glutamine; Ureidosuccinic acid;dCMP;dCDP	Deoxyuridine; Deoxycytidine; Ureidopropionic acid; Beta-Alanine; Dihydrouracil; Dihydrothymine; Cytidine triphosphate; Cytidine; Cytidine monophosphate; Orotidylic acid; Orotic acid; Thymine; Thymidine; Phosphoribosyl pyrophosphate; Uridine triphosphate; Uridine 5'-monophosphate; Uridine 5'-diphosphate; Uridine; Uracil; L-Glutamine; Ureidosuccinic acid; dCTP; dUDP; Carbamoylphosphate; Deoxyuridine triphosphate; dCMP; 5-Thymidylic acid; dCDP; dTDP; Thymidine 5'-triphosphate;Deoxyribose 1-phosphate; dUMP; CDP; Ureidoisobutyric acid; L-Dihydroorotic acid; 3-Aminoisobutanoic acid
EXCITATORY NEURAL SIGNALLING THROUGH 5-HTR 4 AND SEROTONIN | EXCITATORY NEURAL SIGNALLING THROUGH 5-HTR 7 AND SEROTONIN | EXCITATORY NEURAL SIGNALLING THROUGH 5-HTR 6 AND SEROTONIN	5	0.345	2	0.041	1	0.164	5.797101449	Adenosine triphosphate;Guanosine triphosphate	Cyclic AMP; Serotonin; Adenosine triphosphate; Guanosine diphosphate; Guanosine triphosphate
CORTICOTROPIN ACTIVATION OF CORTISOL PRODUCTION	5	0.345	2	0.041	1	0.164	5.797101449	Adenosine triphosphate;Guanosine triphosphate	Cyclic AMP; Cortisol; Adenosine triphosphate; Guanosine diphosphate; Guanosine triphosphate
VASOPRESSIN REGULATION OF WATER HOMEOSTASIS	5	0.345	2	0.041	1	0.164	5.797101449	Adenosine triphosphate;Guanosine triphosphate	Cyclic AMP; Adenosine triphosphate; Guanosine diphosphate; Guanosine triphosphate; Vasopressin
INTRACELLULAR SIGNALLING THROUGH HISTAMINE H2 RECEPTOR AND HISTAMINE	5	0.345	2	0.041	1	0.164	5.797101449	Adenosine triphosphate;Guanosine triphosphate	Cyclic AMP; Adenosine triphosphate; Histamine; Guanosine diphosphate; Guanosine triphosphate
INTRACELLULAR SIGNALLING THROUGH PGD2 RECEPTOR AND PROSTAGLANDIN D2	5	0.345	2	0.041	1	0.164	5.797101449	Adenosine triphosphate;Guanosine triphosphate	Cyclic AMP; Adenosine triphosphate; Guanosine diphosphate; Guanosine triphosphate; Prostaglandin D2
ASPARTATE METABOLISM	12	0.829	3	0.044	1	0.168	3.618817853	Fumaric acid; L-Asparagine;Ureidosuccinic acid	Argininosuccinic acid; Beta-Alanine; Fumaric acid; L-Asparagine; L-Aspartic acid; Oxaloacetic acid; Adenylsuccinic acid; Malonic acid; N-Acetyl-L-aspartic acid; Ureidosuccinic acid; Citrulline; D-Aspartic acid
PHENYLALANINE AND TYROSINE METABOLISM	13	0.898	3	0.0545	1	0.198	3.340757238	Fumaric acid; L-Phenylalanine; 4-Hydroxyphenylpyruvic acid;	Ammonia; Acetoacetic acid; Homogentisic acid;Fumaric acid; L-Tyrosine; L-Phenylalanine; Phenylpyruvic acid; 4-Hydroxyphenylpyruvic acid; 4-Fumarylacetoacetic acid; Oxygen; Maleylacetoacetic acid; Water; Hydrogen peroxide
AMINO SUGAR METABOLISM	15	1.04	3	0.0786	1	0.262	2.884615385	Fructose 6-phosphate; N-Acetyl-glucosamine 1-phosphate; Glucosamine;	Fructose 6-phosphate; N-Acetyl-D-glucosamine; N-Acetyleuraminic acid; Uridine diphosphate-N-acetylglucosamine; N-Acetyl-D-Glucosamine 6-Phosphate; N-Acetyl-D-mannosamine 6-phosphate; N-Acetylmannosamine; Cytidine monophosphate N-Acetyleuraminic acid; Glucosamine 6-phosphate; N-Acetyl-glucosamine 1-phosphate; Glucosamine; Chitin; Chitobiose; D-Glucosaminide; N-Acetyleuraminate 9-phosphate
INTRACELLULAR SIGNALLING THROUGH ADENOSINE RECEPTOR A2A AND ADENOSINE | INTRACELLULAR SIGNALLING THROUGH ADENOSINE RECEPTOR A2B AND ADENOSINE	7	0.484	2	0.0787	1	0.262	4.132231405	Adenosine triphosphate;Guanosine triphosphate	Adenosine; Cyclic AMP; Adenosine triphosphate; Guanosine diphosphate; Guanosine triphosphate; PIP2(16:0/16:0); PIP3(16:0/16:0)
ARGININE AND PROLINE METABOLISM	26	1.8	4	0.0978	1	0.313	2.222222222	Guanidoacetic acid; Fumaric acid; L-Proline;Urea	Ammonia; Argininosuccinic acid; Creatine; Guanidoacetic acid; Fumaric acid; L-Glutamic acid; L-Proline; L-Aspartic acid; Ornithine; Urea; L-Arginine; Citrulline; Carbamoylphosphate; 1-Pyroline-5-carboxylic acid; Pyroline hydroxycarboxylic acid; Phosphocreatine; 4-Hydroxy-2-oxoglutaric acid; L-Glutamic-gamma-semialdehyde; 1-Pyroline-4-hydroxy-2-carboxylate; 4-Hydroxy-L-glutamic acid; Nitric oxide; D-Proline; N-(ω)-Hydroxyarginine; 4-Hydroxy-L-proline; L-4-Hydroxyglutamate semialdehyde; 1-Pyrroline-2-carboxylic acid
GLUCONEOGENESIS	27	1.87	4	0.109	1	0.336	2.139037433	Fructose 6-phosphate;Adenosine triphosphate; Guanosine triphosphate;ADP	D-Glucose; Fructose 6-phosphate; L-Lactic acid; Oxoglutaric acid; Oxaloacetic acid; Pyruvic acid; Phosphoenolpyruvic acid; Beta-D-Glucose; Adenosine triphosphate; Malic acid; 3-Phosphoglyceric acid;NAD; Fructose 1,6-bisphosphate; D-Glyceraldehyde 3-phosphate; Guanosine diphosphate; Glyceric acid 1,3-biphosphate; Guanosine triphosphate; 2,3-Diphosphoglyceric acid; ADP; Glucose 6-phosphate; Dihydroxyacetone phosphate; NADH; Glucose 1-phosphate; Water; Alpha-D-Glucose; 2-Phospho-D-glyceric acid; Beta-D-Glucose 6-phosphate
BETAINE METABOLISM	10	0.691	2	0.148	1	0.438	2.894356006	L-Methionine; Homocysteine;	Betaine; Dimethylglycine; Choline; L-Methionine; Homocysteine; S-Adenosylhomocysteine; S-Adenosylmethionine; Betaine aldehyde; 5-Methyltetrahydrofolic acid; Tetrahydrofolic acid
GLYCOLYSIS	21	1.45	3	0.172	1	0.491	2.068965517	Fructose 6-phosphate;Adenosine triphosphate;ADP	D-Glucose; Fructose 6-phosphate; Pyruvic acid; Phosphoenolpyruvic acid; Beta-D-Glucose; Adenosine triphosphate; 3-Phosphoglyceric acid; NAD; Fructose 1,6-bisphosphate; D-Glyceraldehyde 3-phosphate; Glyceric acid 1,3-biphosphate; 2,3-Diphosphoglyceric acid; ADP; Glucose 6-phosphate; Dihydroxyacetone phosphate; NADH; Glucose 1-phosphate; Water; Alpha-D-Glucose; 2-Phospho-D-glyceric acid; Beta-D-Glucose 6-phosphate
GLUCOSE-ALANINE CYCLE	12	0.829	2	0.199	1	0.548	2.412545235	L-Alanine;NADP	Ammonia; D-Glucose; L-Glutamic acid; L-Alanine; Oxoglutaric acid; NADP; NADPH; Pyruvic acid; NAD; NADH; Pyridoxal 5'-phosphate; Water
BETA-ALANINE METABOLISM	13	0.898	2	0.225	1	0.58	2.227171492	Pantothenic acid;Acetyl-CoA	1,3-Diaminopropane; Ureidopropionic acid; Carnosine; Beta-Alanine; Dihydrouracil; L-Aspartic acid; Anserine; Pantothenic acid; Uracil; 3-Aminopropionaldehyde; Acetyl-CoA; Coenzyme A; Malonic semialdehyde
LYSINE DEGRADATION	13	0.898	2	0.225	1	0.58	2.227171492	L-Lysine;Acetyl-CoA	L-Lysine; Oxoadipic acid; Saccharopine; Aminoadipic acid; L-Pipecolic acid; D-1-Piperideine-2-carboxylic acid; 3-Hydroxybutyryl-CoA; Acetyl-CoA; Allysine; Glutaryl-CoA; Acetoacetyl-CoA; Crotonoyl-CoA; 3-Glutarylhydroxiproamate
BIOTIN METABOLISM	4	0.276	1	0.249	1	0.624	3.623188406	L-Lysine	Biotin; L-Lysine; Biocytin; Biotinyl-5'-AMP
FOLATE AND PTERINE BIOSYNTHESIS	17	1.17	2	0.331	1	0.802	1.709401709	Folic acid;Guanosine triphosphate	Tetrahydrobiopterin; Dihydrobiopterin; Folic acid; Neopterin; Dihydroneopterin triphosphate; Dihydrofolic acid; Dysropterin; Guanosine triphosphate; 7,8-Dihydropteroic acid; Tetrahydrofolic acid; 6-Lactoyltetrahydropterin; Molybdopterin; 7,8-Dihydroneopterin; 2,5-Diamino-6-(5'-triphosphoryl-3',4'-trihydroxy-2'-oxopentyl)-amino-4-oxopyrimidine; Dihydroneopterin phosphate; Tetrahydrolbyl-[Glu](2); Tetrahydrofolyl-[Glu](n)
ALANINE METABOLISM	6	0.415	1	0.35	1	0.816	2.409638554	L-Alanine	Glycolytic acid; L-Glutamic acid;L-Alanine; Oxoglutaric acid; Oxaloacetic acid; Pyruvic acid
PROPANOATE METABOLISM	18	1.24	2	0.357	1	0.816	1.612903226	Methylmalonic acid;Acetyl-CoA	Beta-Alanine; Methylmalonic acid; Propionic acid; Hydroxypropionic acid; L-Valine; Succinyl-CoA; Malonyl-CoA; Acetyl-CoA; Propionyl-CoA; Acetoacetyl-CoA; Malonyl-CoA semialdehyde; (S)-Methylmalonic acid semialdehyde; R-Methylmalonyl-CoA; Acrylyl-CoA; S-Methylmalonyl-CoA; Propinol adenylate; 3-Hydroxypropionyl-CoA; Malonic semialdehyde

INSULIN SIGNALLING	19	1.31	2	0.383	1	0.85	1.526717557	Acetyl-CoA; Guanosine triphosphate;	Adenosine monophosphate; Cyclic AMP; D-Glucose; Palmitic acid; Oxalacetic acid; Pyruvic acid; Uridine diphosphate glucose; CE(16:0); Guanosine diphosphate; AcetylCoA; Guanosine triphosphate; Coenzyme A; Carbon dioxide; Amylose; TG(16:0/16:0/16:0)[iso]; DG(16:0/16:0/0:0) ; PIP2(16:0/16:0); PIP3(16:0/16:0); MG(0:0/16:0/0:0)
TAURINE AND HYPOTAURINE METABOLISM	7	0.484	1	0.395	1	0.855	2.066115702	L-Cysteine	Taurine; L-Cysteine; Hypotaurine; 3-Sulfinoalanine; Cysteic acid; Cysteamine; 5-L-Glutamyl-taurine
PYRUVATE METABOLISM	20	1.38	2	0.408	1	0.859	1.449275362	L-Malic acid;Acetyl-CoA	Acetic acid; L-Malic acid; L-Lactic acid; Oxalacetic acid; Pyruvic acid; Phosphoenolpyruvic acid; Acetaldehyde; S-Lactoylglutathione; Pyruvaldehyde; Malonyl-CoA; Acetyl-CoA; D-Lactic acid; Acetoacetyl-CoA; Acetylphosphate; Propylene glycol; Lactaldehyde; 2-(a-Hydroxyethyl)thiamine diphosphate; D-Lactaldehyde; S-Acetyldihydrolipoamide-E; Acetyl adenylate
CYSTEINE METABOLISM	8	0.553	1	0.437	1	0.875	1.808318264	L-Cysteine	L-Glutamic acid; Pyruvic acid; L-Cysteine; 3-Sulfinoalanine; Gamma-Glutamylcysteine; 3-Mercaptopyruvic acid; 3-Sulfinylpyruvic acid; 3-Mercaptolactic acid
ONE CARBON POOL BY FOLATE	8	0.553	1	0.437	1	0.875	1.808318264	Folic acid	Folic acid; N10-Formyl-THF; Dihydrofolic acid; 5,10-Methenyltetrahydrofolic acid; 5-Methyltetrahydrofolic acid; 5,10-Methylene-THF; N5-Formyl-H4F; Tetrahydrofolic acid
VALINE, LEUCINE AND ISOLEUCINE DEGRADATION	36	2.49	3	0.46	1	0.897	1.204819277	Alpha-ketoisovaleric acid;Methylmalonic acid; Acetyl-CoA	Alpha-ketoisovaleric acid; (S)-3-Hydroxyisobutyric acid; Acetoacetic acid; L-Isoleucine; Methylmalonic acid; 3-Methyl-2-oxovaleric acid; L-Leucine; Ketoleucine; L-Valine; Lipoamide; Dihydrolipoamide; Methacrylyl-CoA; Succinyl-CoA; 2-Methylbutyryl-CoA; (S)-3-Hydroxyisobutyryl-CoA; 3-Methylglutaconyl-CoA; Isovaleryl-CoA; 2-Methylacetoacetyl-CoA; Acetyl-CoA; Isobutyryl-CoA; Methylmalonyl-CoA; Propionyl-CoA; 2-Methyl-3-hydroxybutyryl-CoA; Thiamine pyrophosphate; 3-Hydroxy-3-methylglutaryl-CoA; Acetoacetyl-CoA; 3-Methylcrotonyl-CoA; Tiglyl-CoA; (S)-b-aminoisobutyric acid; (S)-Methylmalonic acid semialdehyde; 3-Methyl-1-hydroxybutyl-ThPP; 2-Methyl-1-hydroxypropyl-ThPP; S-(3-Methylbutanoyl)-dihydrolipoamide-E; S-(2-Methylpropionyl)-dihydrolipoamide-E; S-(2-Methylbutenoyl)-dihydrolipoamide; 3-Hydroxyisovaleryl-CoA
BUTYRATE METABOLISM	9	0.622	1	0.477	1	0.908	1.607717042	Acetyl-CoA;	Butyric acid; Acetoacetic acid; Butyryl-CoA; 3-Hydroxybutyryl-CoA; Acetyl-CoA; 3-Hydroxy-3-methylglutaryl-CoA; Coenzyme A; Acetoacetyl-CoA; Crotonoyl-CoA
KETONE BODY METABOLISM	10	0.691	1	0.513	1	0.955	1.447178003	Acetyl-CoA;	(R)-3-Hydroxybutyric acid; Acetoacetic acid; NAD; Acetyl-CoA; 3-Hydroxy-3-methylglutaryl-CoA; Coenzyme A; Acetoacetyl-CoA; NADH; Acetone; Carbon dioxide
HISTIDINE METABOLISM	11	0.76	1	0.547	1	0.995	1.315789474	L-Histidine	1-Methylhistidine; Carnosine; L-Glutamic acid; L-Histidine; Urocanic acid; Formiminoglutamic acid; Histamine; 1-Methylhistamine; 4-Imidazolone-5-propionic acid; Methylimidazoleacetic acid; Methylimidazole acetaldehyde
NICOTINATE AND NICOTINAMIDE METABOLISM	13	0.898	1	0.609	1	1	1.113585746	NADP	NADP; Nicotinamide ribotide; Quinolinic acid; 1-Methylnicotinamide; Nicotinamide riboside; NAD; Nicotinic acid mononucleotide; Nicotinic acid adenine dinucleotide; Niacinamide; Nicotinic acid; N1-Methyl-2-pyridone-5-carboxamide; N1-Methyl-4-pyridone-3-carboxamide; Nicotinate D-ribonucleoside
OXIDATION OF BRANCHED CHAIN FATTY ACIDS	14	0.967	1	0.636	1	1	1.034126163	Acetyl-CoA;	L-Carnitine; L-Acetylcarnitine; Pristanic acid; Phytanic acid; Propionylcarnitine; Acetyl-CoA; Propionyl-CoA; 2-Hydroxyphytanoyl-CoA; Phytanoyl-CoA; Coenzyme A; Pristanal; Pristanoyl-CoA; 4,8 dimethylnonanoyl carnitine; 4,8-Dimethylnonanoyl-CoA
BETA OXIDATION OF VERY LONG CHAIN FATTY ACIDS	14	0.967	1	0.636	1	1	1.034126163	Acetyl-CoA;	L-Carnitine; L-Acetylcarnitine; Caprylic acid; Capric acid; Caproic acid; Dodecanoic acid; Acetyl-CoA; Coenzyme A; Tetradecanoyl-CoA; Tetracosanoyl-CoA; Hexacosanoic acid; Lauroyl-CoA; Hexacosanoyl-CoA; Tetracosanoyl-CoA
SELENOAMINO ACID METABOLISM	15	1.04	1	0.662	1	1	0.961538462	L-Alanine	L-Alanine; Selenocysteine; Selenomethionine; Adenylselenate; Se-Methylselenocysteine; Selenohomocysteine; Selenocystine; Selenocystathionine; Selenophosphate; Gamma-Glutamyl-Se-methylselenocysteine; 3-Phosphoadenylylselenate; Hydrogen selenide; Se-Adenosylselenohomocysteine; Se-Adenosylselenomethionine; Selenide
PENTOSE PHOSPHATE PATHWAY	18	1.24	1	0.728	1	1	0.806451613	Fructose 6-phosphate	Fructose 6-phosphate; Gluconolactone; Phosphoribosyl pyrophosphate; D-Ribose; D-Ribulose 5-phosphate; Xylulose 5-phosphate; Deoxyribose 5-phosphate; Fructose 1,6-bisphosphate; D-Sedoheptulose 7-phosphate; D-Glyceraldehyde 3-phosphate; 6-Phosphogluconic acid; D-Erythrose 4-phosphate; Deoxyribose 1-phosphate; Glucose 6-phosphate; Ribose 1-phosphate; D-Ribose 5-phosphate; Carbon dioxide; Beta-D-Glucose 6-phosphate
FRUCTOSE AND MANNOSE DEGRADATION	18	1.24	1	0.728	1	1	0.806451613	Fructose 6-phosphate	Fructose 6-phosphate; D-Mannose; L-Fucose; Sorbitol; D-Fructose; D-Fructose 2,6-bisphosphate; Fructose 1,6-bisphosphate; Fructose 1-phosphate; Mannose 6-phosphate; GDP-L-fucose; D-Glyceraldehyde 3-phosphate; Guanosine diphosphate mannose; Fucose 1-phosphate; GDP-4-Dehydro-6-deoxy-D-mannose; Dihydroxyacetone phosphate; Alpha-D-Glucose; D-Mannose 1-phosphate; Beta-D-Fructose 2-phosphate
TYROSINE METABOLISM	38	2.63	2	0.756	1	1	0.760456274	Fumaric acid;4-Hydroxyphenylpyruvic acid	p-Hydroxyphenylacetic acid; Iodotyrosine; 3-Methoxytyramine; Acetoacetic acid; Epinephrine; Dopamine; Homovanillic acid; Homogentisic acid; Fumaric acid; L-Tyrosine; L-Dopa; Norepinephrine; Thyroxine; Lidhyronine; Vanillylmandelic acid; Tyramine; 3,4-Dihydroxyphenylglycol; 4-Hydroxyphenylpyruvic acid; Normetanephrine; Dopaquinone; 5,6-Dihydroxyindole-2-carboxylic acid; 4-Fumarylacetoacetic acid; 3,4-Dihydroxybenzeneacetic acid; L-Dopachrome; Vanylglycol; 3,4-Dihydroxymandelic acid; Maleylacetoacetic acid; 3,5-Diiodo-L-tyrosine; 3,4-Dihydroxyphenylacetaldehyde; 5,6-Dihydroxyindole; 3-Methoxy-4-hydroxyphenylglycolaldehyde; Metanephrine; Leucodopachrome; Melanin; Homovanillin; 3,4-Dihydroxymandelaldehyde; Indole-5,6-quinone; 2-Hydroxy-3-(4-hydroxyphenyl)propenoic acid
PORPHYRIN METABOLISM	22	1.52	1	0.797	1	1	0.657894737	Glycine	Bilirubin; Glycine; Protoporphyrin IX; Porphobilinogen; Coproporphyrin III; Coproporphyrin I; Uroporphyrin III; Uroporphyrin I; Farnesyl pyrophosphate; Biliverdin; Uroporphyrinogen III; Protoporphyrinogen IX; Hydroxymethylbilane; 5-Aminolevulinic acid; Heme O ; Coproporphyrinogen III; Coproporphyrinogen I; Uroporphyrinogen I; Heme; Bilirubin diglucuronide; D-Urobilinogen; Heme A
BILE ACID BIOSYNTHESIS	49	3.39	2	0.869	1	1	0.589970501	Glycine; Cholic acid	Taurocholic acid; Cholesterol; Glycine; Glycocholic acid; Taurine; 3a,7a-Dihydroxycoprostanic acid; Chenodeoxycholic acid; Cholic acid; Deoxycholic acid; Deoxycholic acid glycine conjugate; Chenodeoxycholic acid glycine conjugate; Lithocholic acid glycine conjugate; Lithocholyltaurine; Lithocholic acid; Taurodeoxycholic acid; Taurochenodeoxycholic acid; 27-Deoxy-5b-cyprinol; Choloyl-CoA; 24-Hydroxycholesterol; Coenzyme A; 5-b-Cholestane-3a ,7a ,12a-triol; 7a-Hydroxycholesterol; 7a-Hydroxy-cholestene-3-one; 27-Hydroxycholesterol; 3a,7a-Dihydroxy-5b-cholestanoyl-CoA; 7a,12a-Dihydroxy-cholestene-3-one; 3a,7a,12a-Trihydroxy-5b-cholestan-26-al; 3a,7a,12a-Trihydroxy-5b-cholestanoic acid; 25-Hydroxycholesterol; 7-a,25-Dihydroxycholesterol; 7-a,27-dihydroxycholesterol; Chenodeoxycholoyl-CoA; 7a,12a-Dihydroxy-5b-cholestan-3-one; 5b-Cyprinol sulfate; 3a,7a,12a-Trihydroxy-5b-cholest-24-enoyl-CoA; 3a,7a,12a,24- Tetrahydroxy-5b-cholestanoyl-CoA; 3a,7a,12a-Trihydroxy-5b-24- oxocholestanoyl-CoA; 7a-Hydroxy-3b-cholestan-3-one; 3a,7a Dihydroxy-5b-cholestane; 3a,7a-Dihydroxy-5b-cholestan-26-al; 3a,7a-Dihydroxy-5b-cholest-24-enoyl-CoA; (24R)-Cholest-5-ene-3-beta,7-alpha,24-triol; 3 beta-hydroxy-5-cholestenoate; 3 beta,7 alpha-Dihydroxy-5-cholestenoate; 3 alpha,7 alpha,26-Trihydroxy-5beta-cholestane; 3 alpha,7 alpha,24-Trihydroxy-5beta-cholestanoyl-CoA; 7 alpha,24-Dihydroxy-4-cholesten-3-one; 7 alpha-Hydroxy-3-oxo-4-cholestenoate; 7 alpha,26-Dihydroxy-4-cholesten-3-one
FATTY ACID METABOLISM	29	2	1	0.879	1	1	0.5	Acetyl-CoA;	Palmitic acid; L-Palmitoylcarnitine; Octanoyl-CoA; Butyryl-CoA; 3-Hydroxybutyryl-CoA; Acetyl-CoA; Palmityl-CoA; Coenzyme A; Acetoacetyl-CoA; Tetradecanoyl-CoA; Crotonoyl-CoA; Hexanoyl-CoA; Lauroyl-CoA; (S)-3-Hydroxyhexadecanoyl-CoA; (S)-3-Hydroxytetradecanoyl-CoA; (S)-3-Hydroxydodecanoyl-CoA; 3-Oxododecanoyl-CoA; (S)-Hydroxydecanoyl-CoA; (S)-Hydroxyoctanoyl-CoA; 3-Oxooctanoyl-CoA; (S)-Hydroxyhexanoyl-CoA; 3-Oxohexanoyl-CoA; trans-2-Hexenoyl-CoA; (2E)-Hexadecenoyl-CoA; (2E)-Tetradecenoyl-CoA; (2E)-Decenoyl-CoA; (2E)-Octenoyl-CoA; 3-Oxohexadecanoyl-CoA; Decanoyl-CoA (n-C10:0CoA)
STEROID BIOSYNTHESIS	31	2.14	1	0.896	1	1	0.46728972	Acetyl-CoA;	7-Dehydrocholesterol; Cholesterol; Mevalonic acid; Squalene; Vitamin D3; Farnesyl pyrophosphate; 4,4-Dimethylcholesta-8,14,24-trienol; 5-Diphosphomevalonic acid; Dimethylallylpyrophosphate; Lathosterol; (S)-2,3-Epoxysqualene; Acetyl-CoA; 4a-Methylzymosterol; Lanosterin; Presqualene diphosphate; Geranyl-PP; 4,4-Dimethyl-5a-cholesta-8,24-dien-3-b-ol; Mevalonic acid-5P; Isopentenyl pyrophosphate; 3-Hydroxy-3-methylglutaryl-CoA; Acetoacetyl-CoA; 8-Dehydrocholesterol; Desmosterol; 7-Dehydrodesmosterol; Zymosterol intermediate 2; 3-Keto-4-methylzymosterol; 24,25-Dihydrolanosterol; 4,4-Dimethyl-5a-cholesta-8-en-3b-ol; 5a-Cholest-8-en-3b-ol; 5a-Cholesta-7,24-dien-3b-ol; 4a-Methylzymosterol-4-carboxylic acid

Table S7. Peak area intensities in *Gpt2* mutant mouse brains (P18).

Sample Name	062514QEMMut	062514QEMMut1	062514QEMMut2	062514QEMMut3	062514QEMMut5	062514QEMMut6	062514QEMWT	062514QEMWT1	062514QEMWT2	062514QEMWT3	062514QEMWT5	062514QEMWT6
Genotype	**MUT**	**MUT**	**MUT**	**MUT**	**MUT**	**MUT**	**WT**	**WT**	**WT**	**WT**	**WT**	**WT**
glyoxylate	45269.31666	42248.86498	35910.90083	37278.41361	6297.773306	32871.64636	54165.65025	45845.25203	67139.30448	27174.43426	43326.65929	26626.79474
glycolate	5236.477607	18600.40912	77018.88289	N/A	8005.476757	31364.89839	N/A	13177.14923	39715.54867	5683.406416	5244.417581	4280.914688
pyruvate	12719.2644	21406.96989	33822.53325	8321.779784	18855.96573	15887.95217	18643.47723	13870.68511	26391.63843	19365.96293	26541.44905	15849.04177
lactate	N/A	N/A	N/A	N/A	N/A	N/A	N/A	N/A	N/A	N/A	N/A	N/A
2-oxobutanoate	150054.4141	162637.3398	191061.8415	26602.7363	17677.23497	152461.8836	124682.7846	115479.9786	151357.2397	102237.5492	130906.4191	163509.1347
acetoacetate	165113.6886	172360.881	107304.7879	145319.3396	183083.6065	153273.8754	166333.3206	142324.4609	119024.6798	99485.21272	75906.88797	129031.0374
glycerate	4198.23994	95302.16103	122148.9343	59279.81051	105779.6046	97455.85995	40499.84022	54115.92012	43232.77636	36186.24092	48382.97482	92045.91365
uracil	65292.69557	52580.8607	36844.73178	66227.80214	63840.93948	72065.61002	62377.71017	68082.95443	85404.30001	12620.8372	27704.37055	22342.03268
fumarate	5077429.468	5631920.106	5849686.222	5596552.916	6382920.187	5577591.726	6303644.074	7231404.168	6323898.283	5873819.785	6508566.807	6478867.897
Maleic acid	5338482.666	5904483.599	6034273.947	5576525.22	7329103.43	6197165.615	6257986.546	7103796.362	7001268.249	6565956.496	6637652.1	6743419.956
2-keto-isovalerate	5572135.055	5819697.467	6348868.401	5615599.899	7207466.606	5843655.054	6502542.766	7190252.131	7286852.572	6562275.431	6891834.204	7154378.069
Guanidoacetic acid	397503.692	501585.8299	470223.1452	372221.753	474580.4374	455167.2685	282813.0937	445526.4295	281436.8535	245847.7072	286195.6664	357910.9939
succinate	4670153.511	5785264.254	4154522.406	4213502.254	4617614.734	4353046.054	6239017.763	5590479.201	6318396.186	6863326.911	6064169.39	5549969.105
Methylmalonic acid	5999525.717	6864639.689	5031419.52	5091553.081	5778709.982	5466775.12	8327055.073	6769103.278	7874800.753	8136321.797	7141784.967	7157654.724
3-S-methylthiopropionate	N/A	6429.648393	N/A	10729.16399	N/A	6491.383841	4464.862403	N/A	3842.631585	11635.20677	7149.047285	N/A
nicotinate	63038.51955	12234.84852	5611.001519	66835.71136	97366.11099	55053.78599	46655.64537	45572.32243	43853.81565	27158.23418	20797.47114	69942.68637
taurine	78690140.81	80623255.99	81780630.84	77593061.36	87271733.26	81180496.46	80782061.22	78027627.75	81749218.94	78105588.69	84357839.7	80202443.52
Pyroglutamic acid	235499.5074	309263.7674	290766.6702	142319.426	357374.829	141050.5836	116541.4076	186083.842	104542.5006	103713.4483	125922.1376	155444.3417
Citraconic acid	373735.0556	312003.2315	782504.4335	855900.7004	1139080.574	891881.3794	328191.7298	396912.3931	359918.0845	268189.2036	318155.3879	293022.029
2-ketohaxanoic acid	96055.80399	83176.38636	118544.3439	83910.65924	131697.0032	117934.6315	115653.3704	89064.65279	107780.0938	97369.00469	99218.39441	83787.5679
N-Acetyl-L-alanine	24371571.21	25842172.71	27823241.96	22990953.69	29230631.47	25924212.08	24570801.66	30248270.52	28385427.59	24789421.78	28034369.91	27688324.79
oxaloacetate	24079.38754	62227.43684	150776.9356	60308.21551	63437.27793	133812.6259	59062.31087	56834.62851	89595.39765	80764.01512	94940.06362	99154.66737
Hydroxyisocaproic acid	29623.07973	63106.42423	44915.22818	53397.45071	62694.42445	25551.08491	54051.42399	61792.99702	54022.42025	15679.469	68472.17301	48949.83546
malate	7949221.888	7223613.79	7116073.394	7888900.88	8933375.478	7092064.487	9688208.525	9490243.033	11051401.68	11225858.18	10851579.46	10516427.34
hypoxanthine	8997605.474	10249736.4	5876755.449	4613067.915	6097074.736	6586786.81	8974000.925	6749774.72	6657129.282	6570257.91	6278816.329	7295997.182
anthranilate	157798.8181	192499.0874	91803.72048	58852.85544	117845.1814	109250.9564	199473.2835	109498.6631	120373.62	91511.37899	116609.5283	114314.2832
p-aminobenzoate	36263.14253	66536.5482	21631.22057	14079.32456	28159.89172	65702.59216	8749.393463	16669.65366	312555.0609	22943.33224	13327.41481	29796.08213
p-hydroxybenzoate	115427.3042	129818.2294	165795.7537	143584.7699	161056.1826	81490.85568	179663.4433	215190.1548	293953.6927	260068.2144	980964.1427	110391.427
acetylphosphate	23966.38956	676851.2295	513237.901	45299.3532	35555.6184	11804.76104	674307.8151	579641.9192	378288.3827	368268.9087	414855.6491	538883.3087
Carbamoyl phosphate	61689123.99	59927494.33	62920168.53	52775743.04	67898511.76	63844691.87	57283991.57	68041935.17	60932044.02	54605065.29	55807388.43	58862137.07
a-ketoglutarate	1399447.039	1797223.992	2010065.476	1319207.492	2134932.479	1514805.743	1015369.767	2087516.857	1440856.933	1216934.789	1631002.675	1338459.111
Phenylpropiolic acid	4775935.416	5285742.817	6298498.607	3940632.015	6386152.516	5083801.138	3613655.35	6595039.636	4279913.279	3566161.959	5410546.481	3818913.125
2-oxo-4-methylthiobutanoate	26682.15247	45238.28691	N/A	15448.47411	3970.848591	N/A	33836.44689	N/A	19698.79268	8156.932986	14726.80871	32214.44069
2-Hydroxy-2-methylbutanedioic acid	141034.7547	288259.9168	182310.0113	399471.7999	228718.1682	219441.645	260153.4884	224605.0438	236759.156	175897.4811	194621.6747	276344.6406
3-methylphenylacetic acid	10368.50574	6208.457468	3607.54466	N/A	6349.146496	5610.978094	6059.175814	N/A	8931.604449	9779.789197	11323.96437	4847.89131
xanthine	1536357.338	1990296.494	1242271.056	1013936.512	1391405.287	1428984.052	1634492.124	1880477.096	1322552.041	1778266.058	1641711.269	1416762.797
Hydroxyphenylacetic acid	46918.56577	49574.30064	21860.85272	78450.16053	21642.65623	57297.39062	37435.04276	48074.28641	39891.59367	77026.82142	48443.85048	39838.86329
2,3-dihydroxybenzoic acid	7991.31075	N/A	7541.106237	3526.007098	16878.5102	6626.122868	16791.48127	4937.703605	5907.894248	N/A	N/A	10967.52631
orotate	150959.5589	105028.4115	121761.724	153932.9327	129066.2403	112177.1874	12033.39936	9919.396829	6265.241021	177467.3091	163024.4439	127027.097
dihydroorotate	135385.6961	188457.4538	149776.9341	129754.0929	135436.5181	132669.0823	149201.1284	124657.0407	132953.3746	169200.885	107029.7647	172104.9211
allantoin	180363.4838	231487.4376	175088.5513	143686.3185	253257.0689	274316.129	212028.5711	281009.8844	251318.5259	191935.9286	314983.0817	202560.842
Aminoadipic acid	144953.6583	213777.5444	153006.7786	177109.589	180259.66	205641.297	117582.5455	178564.5808	149270.2329	130293.9518	159738.2637	173656.3318
Indole-3-carboxylic acid	87160.68504	142145.8204	118387.0986	127798.3064	191391.9344	143536.5113	131572.1162	103805.7575	110918.5757	66812.32735	139581.5832	121433.3168
phenylpyruvate	N/A	N/A	N/A	N/A	N/A	N/A	N/A	N/A	N/A	N/A	3667.477329	N/A
Atrolactic acid	9053.97583	7610.289486	11326.99508	12000.63802	12702.6167	N/A	8709.95342	8775.01295	N/A	6705.587224	6138.525174	16383.36692
Phenyllactic acid	63246.87679	62497.75508	70592.81919	41814.8539	59735.76632	32952.16773	34676.23342	97423.91986	35285.92801	29881.53337	38686.55901	47217.45177

quinolinate	56429.96536	79733.85522	8625.17063	61401.0438	37094.60011	55279.04712	33789.75198	38608.28052	34882.73241	36935.63789	39366.82918	61678.14955
phosphoenolpyruvate	4703.922595	6257.335138	21989.22788	5300.360256	5752.745264	5588.125473	N/A	12384.96612	15059.54701	N/A	7832.654806	13591.29444
Uric acid	19562.29165	33550.55148	22080.9182	29007.00186	19649.1605	26778.72558	19393.25317	13199.17949	25952.92083	12905.95589	26276.28138	5209.002344
dihydroxy-acetone-phosphate	383395.2217	179192.4722	309885.5816	252203.7427	437708.4993	296260.281	212674.4156	325596.288	257489.2286	215602.2907	312950.5308	284378.4676
D-glyceraldehdye-3-phosphate	165376.2866	82970.78878	85094.59171	63531.13425	126948.8237	109303.1277	74110.02693	141132.3085	45110.84172	45785.63541	57058.48838	79419.58787
sn-glycerol-3-phosphate	6110934.932	6104421.196	7620495.283	3516501.344	10879415.55	5582640.365	7164501.165	8174337.818	6720410.691	6658957.86	6385410.89	5968552.09
shikimate	44960.27651	345513.9339	101907.2795	148193.7752	45467.7401	42333.43601	49626.47469	96049.8745	67428.51547	50179.2254	140620.0012	11024.69372
aconitate	118481.7072	141308.0967	172450.5995	63661.87774	120133.0325	115084.6024	59822.72977	58519.41683	108045.2108	129986.8825	141391.6237	109106.3565
allantoate	49157.88747	44905.05427	46524.77737	39119.9905	45454.23449	45519.48949	52814.85019	46087.88664	39173.62606	51204.84226	50184.17937	59593.00965
Ascorbic acid	20414743.4	21694213.74	25597761.45	21103214.83	28137121.77	26130205.13	25867383.54	25751006.94	29469854.83	26684017.29	28624458.42	27211037.12
2-Isopropylmalic acid	52328665.79	57755722.24	56555468.99	55019902.57	65083438.4	65095941.26	59513422.93	62121934.25	68305118.53	65700090.26	69436240.71	70755249.53
N-carbamoyl-L-aspartate-nega	25614.16717	17531.34371	29751.17321	28737.38044	33900.58833	17249.74111	22480.49045	19335.31982	16207.54737	10977.28512	19866.86653	20383.28379
Pyrophosphate	82583.9024	123884.6791	142175.4943	75793.47138	134847.4399	99312.17184	127542.3583	144260.9115	182423.1563	108722.9176	103497.1847	130716.8207
glucono-delta-lactone	5044.23354	3653.121815	10846.4855	6686.461956	11980.00222	6274.229954	9932.047308	3143.896773	5226.622246	5740.114012	8896.768276	10977.23272
myo-inositol	8068988.845	9036925.951	8873337.797	6899097.176	9994698.976	7303514.824	8471179.119	8232863.122	10877680.21	6586956.978	10096833.48	10343033.16
hydroxyphenylpyruvate	27183.02844	28763.21719	36592.9367	18379.23773	41815.06616	28220.74811	43387.3857	47583.48599	37114.13835	44388.27381	36546.46812	40772.08018
homocysteic acid	40770.75752	26368.3369	35014.90721	18304.69057	35940.37383	13256.75039	32052.3713	22349.70904	23811.2951	32394.78114	28134.53416	37471.80945
4-Pyridoxic acid	28360.20786	6401.096259	11973.65751	27011.02586	28840.2178	18304.1908	18767.59678	15648.88515	24238.96227	27090.94528	30326.34036	20692.68128
3-phosphoglycerate	4941.57402	23879.2848	4517.673931	11356.87586	34933.39298	23526.34261	12218.31928	15152.54433	16373.47372	14762.60219	6264.209027	10854.33657
Indoleacrylic acid	11866.31806	N/A	6932.019916	10718.07072	10144.97567	7411.442883	N/A	15306.43864	N/A	11537.97548	8769.921313	N/A
Kynurenic acid	74485.60438	37009.14384	67433.35282	61278.0044	61386.85325	41443.93779	53756.4719	55014.11294	57601.55388	78624.97039	8505.666004	64963.90666
citrate-isocitrate	6620385.005	6574110.023	7747078.189	5847153.323	7426044.056	7047997.203	8099287.292	7738533.155	8162370.658	6863432.563	8777287.544	7886618.653
isocitrate	N/A	N/A	N/A	N/A	N/A	N/A	N/A	N/A	N/A	N/A	N/A	N/A
citrate	4432890.82	5971634.912	906401.6021	4136797.678	6606744.192	5866710.371	6936545.348	7283449.712	7200039.307	6867772.936	7637284.92	6671682.55
2-dehydro-D-gluconate	2612.997529	N/A	N/A	N/A	N/A	N/A	N/A	N/A	N/A	N/A	N/A	N/A
D-gluconate	4704.570484	6274.213374	8885.228845	11502.4606	3658.571461	7840.971042	10454.68749	N/A	10992.24996	6272.356375	12546.99861	8365.997321
D-erythrose-4-phosphate	41812.97886	29313.09346	32925.94287	27990.30292	25592.89622	15641.93181	12544.75196	21953.67387	38684.1641	15677.61452	24568.52555	19331.19043
Xanthurenic acid	N/A	12675.35338	5878.162368	N/A	6321.419546	7855.268521	N/A	N/A	31832.50997	7256.446672	N/A	17758.53676
lipoate	N/A	N/A	N/A	N/A	N/A	N/A	N/A	N/A	N/A	N/A	N/A	N/A
D-glucarate	N/A	N/A	N/A	N/A	N/A	N/A	N/A	N/A	3660.120997	N/A	N/A	N/A
deoxyribose-phosphate	108418.9421	91063.09164	110587.3295	98369.4396	94721.78796	88587.43539	159306.4193	150876.3673	160053.974	179787.5378	157680.074	128355.8665
pantothenate	N/A	5058.756835	7798.75786	N/A	4169.295826	6800.13592	N/A	N/A	3654.513227	N/A	N/A	N/A
prephenate	N/A	N/A	N/A	N/A	N/A	N/A	N/A	N/A	N/A	N/A	N/A	N/A
deoxyuridine	N/A	4698.321884	N/A	N/A	N/A	5235.939033	N/A	N/A	N/A	N/A	N/A	N/A
ribose-phosphate	932204.3438	1101986.169	1116454.228	777220.8726	1263365.48	920313.6507	2192023.249	1705318.333	1366143.325	1263516.316	1036820.852	1199721.48
thymidine	10976.93323	7318.920573	N/A	8360.979423	6794.99002	5750.323691	7318.769687	13591.41807	6835.486491	5216.029911	9513.80663	9944.51844
uridine	N/A	7673.280243	N/A	N/A	N/A	N/A	N/A	N/A	9238.491788	8682.768037	N/A	6703.846724
deoxyinosine	3658.593528	6794.648983	4710.740222	4204.101773	5746.432755	N/A	N/A	N/A	N/A	N/A	N/A	6272.73709
shikimate-3-phosphate	16241.66087	20386.28509	38158.30233	23014.42871	32578.06243	33432.69038	24614.85565	36093.29096	14845.04424	14713.07446	10941.58183	21424.63683
D-glucono-delta-lactone-6-phosphate	58176.97151	54093.86776	15942.27685	16665.16989	50863.52301	49853.51139	31744.33434	65497.92541	20860.23564	35175.50896	N/A	22734.75417
hexose-phosphate	616946.2912	207616.9669	624641.6216	587155.0727	516477.7195	441027.4342	691288.3957	722999.9144	742102.3373	596813.4781	608253.6643	646591.1373
glucose-1-phosphate	N/A	5751.103845	9252.780864	N/A	9499.582933	5230.23031	N/A	10270.16026	4943.022061	5733.918519	9946.298248	5786.869034
glucose-6-phosphate	38679.84031	31357.40199	44406.83087	49941.00671	7320.464029	16205.25208	14622.14246	50133.60345	47139.65192	19335.088	35036.46554	7219.960461
fructose-6-phosphate	4182.273677	8887.077684	4704.963161	N/A	14635.14948	9410.311314	3656.995112	N/A	N/A	3135.898393	N/A	5210.0345
1,3-diphopshateglycerate	19865.22746	41260.38491	59629.99214	28759.61471	35996.23014	22800.28106	29598.28759	39295.21976	62537.9056	52790.12112	45220.03478	52731.87395
2,3-Diphosphoglyceric acid	N/A	N/A	N/A	N/A	N/A	N/A	N/A	N/A	N/A	N/A	N/A	N/A
S-ribosyl-L-homocysteine-nega	N/A	N/A	N/A	N/A	5282.852434	N/A	N/A	6800.712	N/A	N/A	N/A	4704.58954
inosine	N/A	N/A	N/A	N/A	N/A	N/A	N/A	N/A	N/A	N/A	N/A	N/A

6-phospho-D-gluconate	N/A	N/A	8884.996811	8366.004695	8365.205699	N/A	N/A	10453.03073	6274.205581	N/A	N/A	7316.826152
xanthosine	N/A	N/A	N/A	N/A	N/A	N/A	6268.898199	N/A	2104.940149	N/A	N/A	N/A
D-sedoheptulose-1-7-phosphate	43420.846	57060.89765	51747.38452	27182.71738	29947.1452	41309.77035	71068.51648	61737.11694	53320.10813	41770.14273	34497.36899	57474.52899
N-acetyl-glucosamine-1-phosphate	132850.5735	170302.0043	150374.5261	138841.9151	168494.557	168219.2022	225772.7547	197148.9956	189666.0607	181418.6263	187535.3342	210754.3278
glutathione-nega	554062.6948	609953.0991	786675.9492	487430.5204	575350.596	334606.5243	772763.8742	822304.4878	880232.6996	772270.4052	648506.7146	749011.1899
dUMP-nega	6795.538814	7324.06721	6796.315543	7318.612229	7320.308868	5750.401422	4708.299514	4704.540462	15681.40401	6794.872682	7318.442991	10977.06223
Geranyl-PP	30289.12553	51231.61098	86766.59182	69518.41273	91998.17689	61733.17337	37770.84534	40009.378	66908.92905	57505.13009	49636.91503	49636.00951
O8P-O1P	20987.91059	17837.88491	30856.6094	24062.48304	34791.63427	20386.09147	12356.20206	13427.25618	16654.32474	15252.42003	25603.02777	8935.967291
dTMP-nega	22999.93929	41296.45243	30317.19113	36607.25526	40249.7891	31361.43523	31363.25822	21432.01678	29781.72546	26664.6789	36066.06414	40250.14818
cyclic-AMP	9909.670172	N/A	13061.08286	9432.62327	15207.50614	14217.09417	6387.332891	15133.57195	14113.74769	14114.59879	18529.67938	5352.812954
fructose-1,6-bisphosphate	60627.11876	49699.08887	50752.21301	61863.55277	77361.05362	32377.0253	54147.7604	73451.62697	71782.76057	26728.48097	35993.26803	40542.04727
trehalose-sucrose	N/A	N/A	N/A	N/A	3135.838754	N/A	N/A	N/A	6248.276562	N/A	N/A	5742.565077
Cellobiose	N/A	N/A	N/A	N/A	N/A	N/A	N/A	N/A	N/A	N/A	N/A	N/A
orotidine-5-phosphate	N/A	N/A	N/A	N/A	N/A	N/A	N/A	N/A	N/A	N/A	N/A	N/A
SBP	14638.3724	6236.317999	12019.7131	10981.18901	10454.71145	7236.531125	10978.52723	7743.613865	N/A	9410.058429	12024.22673	12114.22944
trans, trans-farnesyl diphosphate	5292.998861	4810.510412	7623.552608	17057.62587	8381.908095	8360.966036	17241.46238	18820.48597	40345.6674	26119.37956	33441.30043	11396.5056
S-adenosyl-L-homocysteine-nega	147948.0287	246696.3625	202717.2264	126496.5951	194989.4893	101920.3353	223746.0335	119199.0882	155273.7737	249853.8592	155771.5558	176668.4617
dCDP-nega	20909.18234	14732.287	31361.91585	28203.10746	38202.5146	18817.93923	N/A	8176.142469	5831.958891	5772.996789	17773.73587	28228.97108
5-phosphoribosyl-1-pyrophosphate	N/A	N/A	N/A	N/A	N/A	N/A	N/A	N/A	N/A	N/A	N/A	N/A
Deoxycholic acid	N/A	N/A	N/A	N/A	N/A	N/A	N/A	N/A	N/A	N/A	N/A	N/A
OBP	48606.17667	73703.63786	61673.60875	52279.87091	79452.72701	89901.1561	25602.83431	39734.81335	48608.53146	32409.06196	61054.66635	71099.35885
dTDP-nega	N/A	N/A	N/A	N/A	N/A	N/A	N/A	N/A	N/A	N/A	N/A	N/A
CDP-nega	N/A	N/A	N/A	N/A	N/A	N/A	N/A	N/A	N/A	N/A	N/A	N/A
UDP-nega	113945.1804	116043.9284	300559.6481	214839.1278	299510.1636	201732.289	81571.7087	154715.4649	149891.5153	129618.2103	125458.8208	188167.6393
Cholic acid	9931.114991	N/A	N/A	7304.027863	7840.690001	4704.19181	42341.43527	44431.33611	42341.59404	23521.36444	28751.48874	17248.46289
trehalose-6-Phosphate	27705.91186	26494.74489	66763.17093	48095.23159	38996.85567	41821.53266	34518.54776	62979.95376	55471.72111	40396.54354	56839.33584	65088.61337
Thiamine pyrophosphate	N/A	N/A	N/A	N/A	N/A	N/A	N/A	N/A	N/A	N/A	N/A	N/A
adenosine 5-phosphosulfate	N/A	N/A	N/A	N/A	N/A	N/A	N/A	N/A	N/A	N/A	N/A	N/A
ADP-nega	6272.37349	5226.573501	4704.543781	N/A	N/A	5232.449299	N/A	N/A	N/A	N/A	2612.667219	3136.306336
dGDP-nega	N/A	N/A	N/A	N/A	N/A	N/A	4712.946281	N/A	N/A	2602.211346	N/A	N/A
IDP-nega	3414960.219	3275329.146	6225416.332	5169152.977	7857112.066	5876528.691	3482171.55	6195061.304	5497298.882	4193954.764	4346606.155	6273551.319
GDP-nega	N/A	N/A	N/A	N/A	4181.994366	N/A	N/A	N/A	N/A	N/A	N/A	N/A
CDP-ethanolamine	N/A	N/A	3136.454696	N/A	N/A	N/A	N/A	N/A	N/A	N/A	N/A	N/A
FMN	N/A	N/A	N/A	N/A	N/A	N/A	N/A	N/A	N/A	N/A	N/A	N/A
cholesteryl sulfate	N/A	N/A	N/A	N/A	N/A	4165.975048	N/A	N/A	N/A	N/A	N/A	N/A
dCTP-nega	N/A	N/A	N/A	N/A	7318.782791	N/A	N/A	N/A	N/A	5155.647319	N/A	N/A
dUTP-nega	N/A	4705.998353	N/A	6272.500101	N/A	N/A	N/A	N/A	N/A	N/A	N/A	N/A
dTTP-nega	N/A	N/A	N/A	N/A	N/A	N/A	N/A	N/A	N/A	N/A	N/A	N/A
CTP-nega	N/A	N/A	N/A	N/A	N/A	N/A	N/A	N/A	N/A	N/A	N/A	N/A
UTP-nega	84118.14786	90428.65775	191763.4277	148939.0819	249039.4567	81547.33721	18816.51961	39729.32003	52273.36804	35541.12985	33724.49797	100948.3056
CDP-choline	N/A	N/A	N/A	N/A	N/A	N/A	N/A	N/A	N/A	N/A	N/A	N/A
dATP-nega	N/A	N/A	N/A	N/A	4207.5516	6794.648993	N/A	N/A	N/A	N/A	N/A	N/A
Taurodeoxycholic acid	N/A	N/A	N/A	N/A	N/A	N/A	N/A	N/A	N/A	N/A	N/A	N/A
ATP-nega	566906.7704	938754.889	1501758.242	1194363.901	2034456.446	1012397.859	195462.8482	534492.7603	513292.188	449059.3835	426050.5499	1037961.503
dGTP	545005.9455	1005130.539	1459577.669	1631269.018	2338464.119	986386.8368	304227.881	564247.2592	599034.2944	453627.4275	446332.0437	1066309.375
GTP-nega	36588.33501	56451.2186	97182.97401	73178.31305	137426.4219	41816.3976	11463.39562	3647.003247	14637.31295	15122.88814	18361.16112	78924.13515
UDP-D-glucose	1546749.703	1551420.479	2356397.789	2008819.337	2342386.63	2118077.213	1637193.018	1773608.197	2005176.184	1767784.79	1795612.612	2426349.974
UDP-D-glucuronate	106636.7162	108722.9927	129108.9701	133818.2033	190275.0097	140614.2532	148973.7321	157342.079	153154.7992	132768.9112	148449.1912	177721.64

ADP-D-glucose	8885.239886	5744.541797	18283.4041	9401.596569	13606.16938	9932.040548	18824.50612	10978.64339	22997.12047	13590.97491	11500.82081	19339.88474
guanosine 5-diphosphate,3-diphosphate	N/A	9407.431153	13435.49053	N/A	N/A	N/A	N/A	N/A	N/A	N/A	N/A	10983.73926
UDP-N-acetyl-glucosamine	674835.0167	654200.0794	808653.6529	669607.526	866163.346	711397.8832	596962.7773	727624.4422	1004147.502	655985.3895	594344.6727	917848.6509
glutathione disulfide-nega	6203309.855	9226521.072	8561979.598	6847751.978	5608596.964	5591433.633	8475817.188	10169389.86	10329306.08	8377246.28	7526779.991	9014657.494
NAD+-nega	239392.3938	621719.7571	908856.7591	920533.0609	831668.8753	1027584.771	591270.4461	1730154.308	1517379.559	1238701.62	815950.1015	1435316.653
NADH-nega	10973.64741	224773.6396	128592.4359	138523.6336	183479.1206	88339.39126	98830.11313	294279.0162	189760.2307	212194.1775	220064.9557	223730.1064
dephospho-CoA-nega	58195.2194	26057.5063	83824.25705	54070.35299	102763.5961	84222.0992	26739.40855	16253.52237	17030.70926	14573.04056	35947.94817	51810.08952
cyclic bis(3->5) dimeric GMP	N/A	N/A	N/A	N/A	N/A	N/A	N/A	N/A	N/A	N/A	N/A	N/A
NADP+-nega	20907.75903	59069.36143	88319.54673	77362.69518	91998.53005	65861.70051	93039.87261	260874.4871	192887.053	159689.8838	136939.988	164678.6132
NADPH-nega	N/A	N/A	N/A	N/A	N/A	N/A	N/A	N/A	3136.21559	N/A	N/A	N/A
coenzyme A-nega	40667.88085	42339.0758	53956.65361	75997.72121	144798.2729	105080.1885	59608.56432	65868.67021	60635.33952	47112.36744	49134.60018	114014.3903
acetyl-CoA-nega	N/A	N/A	N/A	N/A	5959.017916	6590.011352	N/A	N/A	N/A	N/A	N/A	N/A
propionyl-CoA-nega	N/A	N/A	N/A	N/A	N/A	N/A	N/A	N/A	N/A	N/A	N/A	N/A
butyryl-CoA	N/A	N/A	N/A	N/A	N/A	N/A	N/A	N/A	N/A	N/A	N/A	N/A
acetoacetyl-CoA-nega	N/A	N/A	N/A	N/A	N/A	N/A	N/A	N/A	N/A	N/A	N/A	N/A
malonyl-CoA-nega	N/A	N/A	N/A	N/A	N/A	N/A	N/A	N/A	N/A	N/A	N/A	N/A
3-hydroxybutyryl-CoA	N/A	N/A	N/A	N/A	N/A	N/A	N/A	N/A	N/A	N/A	N/A	N/A
succinyl-CoA-methylmalonyl-CoA-nega	N/A	N/A	N/A	N/A	N/A	3658.383397	N/A	N/A	N/A	N/A	N/A	N/A
3-hydroxy-3-methylglutaryl-CoA-nega	N/A	N/A	N/A	N/A	N/A	N/A	N/A	N/A	N/A	N/A	N/A	N/A
2-hydroxygluterate	796688.8583	812878.9117	817971.6843	693211.8709	1092327.366	777670.7896	858656.1598	1088314.802	1042494.228	819067.9829	865806.2535	875139.4176
2-deoxyglucose-6-phosphate	N/A	N/A	N/A	N/A	N/A	N/A	N/A	7180.026061	N/A	N/A	N/A	N/A
4-phosphopantothenate	13065.60042	N/A	3623.883719	12545.39072	14935.10433	12021.71593	4430.361228	18292.93294	N/A	7840.895944	7809.723428	7824.785071
Urea	26598.03081	55445.43136	11872.14585	1099306.514	1181880.143	25046.58609	1449391.521	2028366.594	1715474.956	1373423.531	1743407.561	1451754.25
ethanolamine	N/A	N/A	N/A	N/A	N/A	N/A	N/A	N/A	N/A	N/A	N/A	N/A
Imidazole	9731.364576	N/A	N/A	21004.33401	N/A	9866.414889	8936.532513	N/A	9990.949486	N/A	N/A	11396.55833
glycine	4160.755615	5228.308364	6794.91616	5747.331643	9408.743991	7839.294959	2614.190639	3659.919923	N/A	3658.182111	N/A	2612.463842
alanine	15671829.05	15612101.28	16512724.2	13853991.73	17458470.74	14561858.4	17719105.36	18231286.93	17928062.83	15973456.15	18143361.71	17793082.31
betaine aldehyde	297101.2877	231442.3263	248604.0205	232174.6897	259133.0158	258661.9973	318510.8151	256093.7742	274731.1108	270899.4271	245518.0234	292143.7855
choline	109902.0666	71282.23858	26721.38616	N/A	31564.3187	43041.15517	N/A	49289.03127	64402.74489	54905.44431	69585.33693	N/A
4-aminobutyrate	8714626.294	8120577.612	8115663.606	7925225.104	10432524.45	8389217.675	10711425.65	11168775.8	8826641.168	8016318.746	8995658.399	10117690.58
dimethylglycine	N/A	15956.61186	N/A	N/A	13225.49775	15916.00404	21489.20368	6659.258424	N/A	13536.22685	19975.5905	11482.01101
serine	2749332.676	2434459.925	3330419.481	2199098.749	3300387.933	2804177.561	3222319.741	2879542.451	2855278.579	2435967.894	1539294.98	3087478.01
cytosine	100862.7543	62343.86762	169131.5825	74602.00523	50749.62231	66293.45454	44322.22304	96745.96196	59491.08431	63870.07009	60980.43273	60345.14861
Creatinine	4713066.138	4944040.61	4621007.038	3851688.794	5858371.193	4382384.676	5284788.163	6102834.058	5828145.365	4312072.523	5255631.663	4879101.678
proline	19957964.29	23431326.3	25082534.82	20193108.76	27447949.75	18459353.18	16297284.89	15716474.44	13108530.82	14537931	17256412.63	15938880.03
indole	115637.5956	104848.8702	88451.05506	69069.98631	112653.3053	112447.297	54655.91406	183222.8248	41961.2015	47978.19033	55816.8231	79965.90453
betaine	6171498.405	7634578.259	7031479.514	6663044.229	6577884.806	6787086.654	5603426.045	9383230.773	6307022.387	7910265.254	7085883.414	5453515.525
valine	170364.9951	163492.7763	122808.0273	122877.4789	118010.1678	139132.8213	160666.0074	140374.7004	120810.5569	102646.858	109160.2733	114737.5536
threonine	5701872.058	7062709.005	7597306.731	4624190.885	6934939.227	9199754.604	3345026.096	4850881.323	4887092.54	4190889.805	4507828.321	4997149.445
homoserine	21422.8686	23499.26351	28226.82956	32355.6663	29252.45533	33973.41729	31362.48852	31361.31692	19747.81378	22955.41501	13497.56233	12021.52126
purine	46218.08105	77992.96516	109318.764	49603.01788	98835.99286	108471.3544	45409.79661	84689.14102	55486.66462	53398.91458	32147.14547	63604.98378
cysteine	25265.31919	46894.69542	46265.02047	26810.73987	100490.6252	49819.65258	94430.35506	101242.2214	71275.68493	81707.70605	74235.46368	62431.10339
creatine	126722436.2	116783735.3	124647832.2	116175701.5	130642679.3	135190201	127795816.1	103006097.6	117667675.8	119990959.1	113596431.1	114251995
nicotinamide	100841663.1	84980345.94	85840974.92	77625767.88	113571109.2	85791569.49	100338977.3	33721490.6	79403034.67	60996361.28	83243564.11	18008660.74
Imidazoleacetic acid	53755.34208	67973.38743	47632.41228	30839.47767	54287.59292	64444.20394	26183.35376	86305.02109	56562.56416	56932.45416	88118.54852	32170.25248
thymine	N/A	N/A	4637.560506	6482.477678	8570.947109	N/A	5209.349009	N/A	3889.417068	N/A	6030.893694	14073.98738
DL-Pipecolic acid	67804919.28	77106245.43	83963789	72030219.76	85052655.26	75585042.15	65071590.82	81081445.15	66101211.9	56142713.77	74447714.35	66776228.53

N-Acetylputrescine	4611.067357	4239.85446	17464.68113	15283.95822	8456.929984	5912.92092	N/A	N/A	N/A	6791.638184	15745.02206	12823.04601
hydroxyproline	324103.6998	278816.2647	322346.1019	216670.3827	349188.4194	332596.3183	353093.3808	356276.7246	431175.401	404654.6964	266323.2603	462726.081
leucine-isoleucine	3094908.994	3339654.398	3736218.363	2882205.304	3558145.653	3170441.89	3222088.199	3918232.146	3321436.481	3015975.338	2927857.357	3556303.69
ornithine	N/A	N/A	N/A	N/A	N/A	N/A	N/A	N/A	N/A	N/A	N/A	N/A
asparagine	1068070.8	921086.2113	947683.7811	930019.4567	1082410.907	1165878.469	845213.7989	877393.5388	660009.6512	873317.1157	704699.8143	837820.2625
aspartate	11632090.25	10022644.83	12702130.5	9175179.668	12297224.26	11408971.4	13007132.38	13717451.88	11380301.65	10018015.74	9269863.411	12058530.93
adenine	1800867.414	1465244.986	2888413.102	2419476.996	3275451.001	3415147.551	1804252.023	3869226.671	2956559.58	2039275.265	2548468.789	3006719.364
Methylcysteine	305011.6743	210661.7673	255493.7877	216466.6392	303362.6967	379396.7383	270754.4124	420914.1322	299364.7596	238616.6631	202524.3387	273111.1861
homocysteine	76940.49963	57910.26721	57704.6191	51266.14136	64190.91438	70833.03454	95968.18336	90602.66449	71229.57058	76861.66347	68397.04074	87565.91838
methylnicotinamide	1517311.177	2519486.977	1096088.207	760473.5954	1566456.253	1513711.02	1856202.899	1643958.792	1324244.971	1143879.476	1404720.803	1076064.566
histidinol	12023.8886	13576.58832	17279.28834	12525.60885	20094.01615	14121.82537	18994.76516	30842.35617	18295.75895	9410.015526	14604.53591	20821.3828
lysine	1730867.036	1991900.912	1999925.858	1452298.706	2242870.006	1583408.182	787449.7427	735458.9064	902452.1502	761437.7266	568974.1281	1064369.023
glutamine	55807379.2	66462312.05	69202153.67	59665298.35	68706191.59	59286949.66	50243450.96	70780805.53	55251749.46	48106503.13	62081621.8	51461994.83
O-acetyl-L-serine	14947.99137	10052.66054	12134.171	8363.614614	10895.94709	10264.34393	8464.827144	14181.28061	3818.752494	5124.898786	4715.82346	17563.08706
glutamate	80385538.86	76905192.02	73245278.08	76450296.37	90178728.78	79195439.52	87356131.28	90284478.86	86105794.87	82165096.65	79148979.62	85468267.37
methionine	1779303.23	1953858.859	1833641.283	1478767.365	2416548.325	1813918.837	1257675.211	2030685.368	1343729.736	1067464.26	816120.9751	1197673.921
guanine	312730.1923	336610.3349	293452.0284	114062.8734	268427.8342	73736.3895	7097.305189	134438.7771	96539.17435	154197.8727	N/A	200833.6789
histidine	9466532.61	10292692.38	12292547.28	10128331.24	7576489.524	9469372.73	4914173.52	7935584.448	4626526.1	7040472.047	3209705.812	5336338.713
2-Aminooctanoic acid	5119021.288	7758904.04	6203801.352	5574006.209	5542331.318	5455902.59	5579015.632	7922328.639	6881452.644	5820618.842	6188234.901	4695600.973
carnitine	34363587.13	33335841.53	33742046.28	32206338.6	37435006.78	33770850.48	32980918.86	36372102.65	36787905.84	31307612.23	32840415.87	35201057.51
Methionine sulfoxide	31153.50542	24600.78373	51339.10653	20401.9511	52182.06653	57678.14603	41864.47829	42891.83653	31414.99499	26124.67785	47568.03706	24568.26959
phenylalanine	3596692.558	5249570.043	5042535.657	4146735.824	5645576.255	3532329.357	2280633.016	4385905.818	2488808.978	1955798.539	2118322.226	3355269.738
Pyridoxamine	N/A	N/A	N/A	N/A	N/A	N/A	N/A	N/A	N/A	N/A	N/A	N/A
pyridoxine	24306.85885	7722.060084	12240.48946	9733.925232	20661.87149	9484.407531	6397.423022	21197.1011	10649.58249	N/A	N/A	3571.553992
1-Methyl-Histidine	812691.2388	890264.7642	1030219.856	728774.0203	894085.815	749583.3595	684515.7437	1154327.311	767952.748	671436.9207	689983.1859	902643.6493
N-acetyl-L-ornithine	5627.371333	5384.014138	N/A	N/A	N/A	6091.854517	4443.766408	9062.063885	7581.093734	3220.270787	N/A	6460.977084
arginine	2363218.384	2538713.451	6499904.142	5691786.218	8780801.601	4921758.354	4753200.408	6496246.182	4847481.304	2261789.321	4655230.552	4581679.573
citrulline	N/A	N/A	3841.109661	N/A	N/A	5717.199263	N/A	N/A	5811.888945	N/A	N/A	8833.664085
N-carbamoyl-L-aspartate	52274.6342	65339.52813	57497.57702	47058.64202	54359.50963	47566.14994	59070.01152	59064.18751	38679.53066	53850.15111	55481.70986	48087.36563
glucosamine	85220.57232	81796.17695	75107.51953	99381.73205	71306.93251	73872.54505	165580.0024	182541.6038	102316.4481	142566.1308	144688.3692	90093.35785
tyrosine	683064.2238	571247.3968	607895.9029	519867.4026	928518.5088	691972.88	565895.3458	1301773.732	566023.2484	585114.4356	515465.9313	663503.7465
Phosphorylcholine	57955218.81	57903235.27	62917783.88	47167461.15	70165910.01	54579053.09	47365765.71	62177583.64	53095455	48502044.11	57546720.41	58167183.21
3-phospho-serine	7321.569684	4197.842549	9409.412948	13071.59974	23000.00422	16726.91248	22479.56717	14215.32762	29232.70353	15032.60677	8494.574491	9914.176661
N6-Acetyl-L-lysine	5638214.274	6688771.238	6139783.329	4371114.827	6361328.085	4604195.721	4088333.355	3251523.03	5087698.149	3613527.342	4795255.559	6922885.02
Acetyllysine	2508706.734	4984249.26	5743862.193	3561596.795	3328573.637	4313590.536	3191186.511	3757916.407	2665069.295	3097000.236	3678196.227	2445274.657
N-acetyl-glutamine	269004.2577	406905.7236	96771.34794	205367.8282	182576.6525	227882.3916	130838.2199	134936.9377	113190.3909	124994.3408	178218.5191	351337.6884
N-acetyl-glutamate	212951.3534	270797.5474	179914.4094	187988.0003	249611.3013	236762.5775	235076.1236	269402.2916	191088.3146	146296.3209	232446.2781	222112.7131
Ng,NG-dimethyl-L-arginine	671455.2534	837377.2054	667161.2765	226355.3516	747492.0284	600926.4344	533199.1612	877115.2422	570130.4547	339994.4265	450463.7667	716749.1894
Acetylcarnitine DL	58087724.19	57958743.58	59294105.18	49854974.76	59916324.18	58102838.89	60644485.12	61171388.75	63602805.47	56857433.52	59735200.98	62172032.74
tryptophan	766240.361	941890.5499	1198187.26	605697.9181	1000622.471	908944.9059	544024.5536	1312617.224	571726.5178	497980.5708	399733.3228	654196.5761
Kynurenine	N/A	12668.28972	8407.708407	6794.420629	7881.656053	9880.42819	N/A	7306.634983	N/A	4620.669126	N/A	12001.90031
N-acetyl-glucosamine	21937.37973	5001.546705	36877.8931	18135.46179	20382.09525	31810.34696	25293.93152	26687.52786	34485.87975	25592.07168	37607.62327	3150.300642
Flavone	8410.829388	16915.24668	7315.655415	6634.869726	9713.479949	10307.003	N/A	16015.1057	4392.542067	13063.71052	8165.358618	6857.708929
cystathionine	1574662.603	1320672.604	1244843.686	1222607.503	1279417.223	1277898.169	452377.3167	547823.6563	682672.9246	518426.4254	381652.4581	704491.0267
5-methoxytryptophan	N/A	N/A	N/A	4371.784659	N/A	N/A	6648.956825	N/A	4844.820335	5101.294906	4162.778179	N/A
Cystine	18849.84625	28749.94035	17572.64445	20384.17928	8105.014857	7723.154819	50705.05587	35350.20859	41822.03842	22685.79073	26034.85381	18077.09817
cytidine	1446855.771	1827885.275	1502291.323	1194383.904	1163583.868	1602159.122	1544064.644	1102944.187	933988.3295	1136931.59	1037078.649	1125979.132
biotin	29370.01862	41315.69859	20540.9368	45318.10317	37857.36833	33926.70523	56474.0135	31204.92974	27060.92476	34692.51553	56856.91584	13528.71308
deoxyadenosine	15171.27453	11103.15631	16751.50908	10435.56565	23465.25471	15950.81389	32472.25329	19780.05382	19744.71237	20134.22319	20904.60666	14373.43445
Glycerophosphocholine	29644360.66	27489019.22	36192078.43	36125515.34	48204919.5	39715576.74	40215754.43	43520146.99	47447708.49	41564862.59	33568489.22	40530372.97
acadesine	9388.689568	N/A	N/A	N/A	4712.9595	N/A	N/A	4198.689979	N/A	4178.422368	N/A	N/A

D-glucosamine-6-phosphate	29779.20532	33977.55586	24021.889	24545.29128	N/A	20386.7879	21405.08756	29784.74469	19327.73506	12506.70594	22763.20315	17761.43921
D-glucosamine-1-phosphate	47047.6609	12550.44514	21417.21069	25613.25782	38920.15136	46527.18094	43904.39382	24044.65976	55149.42976	30358.7207	45809.41429	49102.16985
thiamine	5721.655069	N/A	N/A	N/A	6706.145131	3882.372987	22767.56167	12061.33728	N/A	N/A	N/A	N/A
S-ribosyl-L-homocysteine-posi	27178.93109	19861.5487	27179.01307	24077.71241	31887.32733	47566.8433	21428.1792	26658.21798	37635.45	23510.92545	27702.41591	27705.21008
deoxyguanosine	6795.164806	N/A	N/A	N/A	N/A	5802.914581	N/A	4181.047506	9447.534714	7302.138102	10971.1178	4715.678506
adenosine	599880.1909	475396.1935	425615.5399	245092.1742	656485.8382	279109.7477	500628.8975	383653.06	284153.3524	171871.5452	303422.4618	210985.0779
1-Methyladenosine	N/A	N/A	3641.770421	N/A	N/A	N/A	N/A	N/A	N/A	N/A	N/A	N/A
guanosine	650874.1218	700991.7244	415152.9282	219023.7308	591109.2452	149106.7172	508146.8082	293112.5702	211154.1997	371276.3541	209606.7119	246682.119
L-arginino-succinate	278157.0285	175004.6214	350057.8828	215185.4344	288156.5862	243066.5152	224242.6265	203870.5229	242294.2981	230524.1285	241044.5147	142453.2839
S-methyl-5-thioadenosine	5790.159098	9869.392531	5718.809917	8903.223384	15103.34566	14158.63963	14253.93036	N/A	12491.35185	N/A	5071.750416	10255.72564
7-methylguanosine	24044.10086	31880.84865	31885.00843	26135.62787	43382.86439	36065.15607	20386.69122	49136.45538	35548.05314	28749.32892	25091.07578	37639.12614
dCMP	23287.17407	15678.39477	29271.41463	19852.38951	15679.90836	12545.11655	36067.09381	34001.1072	22479.07547	29271.20722	19346.22134	28752.56448
glutathione	8604912.073	9125381.871	8524767.514	9163665.809	13836502.12	10842824.22	10904427.9	14667263.84	14461517.59	11657385.19	15757055.29	16628208.25
dTMP	10450.02016	9930.946125	5228.146832	8362.708844	9914.487219	9410.370174	11502.79745	13060.67243	8886.671458	6229.49838	13589.63364	8363.933136
CMP	1994124.134	1765768.923	2637189.747	1861099.921	2060848.93	1783728.908	1952488.02	2733453.297	2518386.892	2040195.271	2098336.523	1823028.863
UMP	423628.0991	379965.0026	592372.984	568860.4087	465161.7043	638766.7592	634062.6202	899139.8371	805908.7711	493645.9162	675218.6129	561841.6141
dAMP	31153.3868	15159.1654	30317.71164	25577.83374	31885.29823	20908.32348	25091.06453	27704.8937	34499.6643	21957.39711	26136.68268	34497.61576
Nicotinamide ribotide	40244.97902	97633.2821	90903.25777	44918.56088	90256.63554	52156.67957	76574.73067	91258.76841	78846.96613	107183.5357	68477.49957	89956.7471
aminoimidazole carboxamide ribonucleotide	10964.39185	13591.21799	14629.89277	19339.71011	20366.94001	13556.25603	10989.49616	29796.29301	28749.57133	18815.19711	18282.69795	15159.15598
thiamine-phosphate	151002.2208	123640.8291	165745.0041	101731.8486	131051.9838	108080.4042	203343.6856	136038.2557	132570.6472	136716.9831	167793.6772	116962.7889
dGMP	12938.21024	13546.36922	16725.71109	15678.53187	8877.858015	12018.23905	14109.64044	15159.69339	12019.86015	10977.16314	9929.687639	10468.75773
AMP	55325277.24	46849706.14	63153859.16	65955127.99	60214937.07	77006071.59	63824257.32	85543038.18	76407943.71	60509028.25	75816373.68	73315596.42
IMP	6636944.692	6340074.497	7776427.722	6034201.922	6564926.23	7865295.968	10161672.57	11822861.21	9583225.28	7933099.785	9184044.79	6729246.407
S-adenosyl-L-methioninamine	N/A	N/A	N/A	N/A	N/A	N/A	N/A	N/A	N/A	N/A	N/A	N/A
GMP	11501050.17	9492436.504	10797391.33	7508249.402	9500291.852	10000317.27	13845315.4	15337825.5	11596684.96	11130106.36	9947979.378	10866618.94
xanthosine-5-phosphate	47045.99325	96434.91309	118011.8312	70550.50557	13591.04386	63255.40917	100883.2709	102453.5572	114984.2409	106890.0754	137490.419	76314.50475
riboflavin	N/A	N/A	N/A	N/A	N/A	N/A	N/A	4185.205628	N/A	N/A	N/A	6266.458444
S-adenosyl-L-homocysteine-posi	213801.2314	70019.40414	40773.02737	139053.8941	168818.1965	140865.1741	218020.892	107074.2144	123886.3494	140109.9388	128075.0174	90909.15094
S-adenosyl-L-methionine	397783.3095	706498.0938	771095.8253	255659.6063	1401216.541	432454.0214	280176.5349	199577.7029	370724.725	144894.12	282233.6585	712373.4003
folate	45998.54808	37111.2612	38679.71111	33453.21691	38683.14717	31364.01015	141652.644	117093.8449	87808.8769	105071.7421	87811.02104	48614.04903
7,8-dihydrofolate	N/A	N/A	N/A	N/A	N/A	N/A	N/A	N/A	N/A	N/A	N/A	N/A
5-methyl-THF	32393.51338	10978.44571	14547.45903	9918.881029	11495.58828	11480.73521	28751.208	20479.24048	17819.0281	7320.331657	10427.27634	17665.06275
Diiodothyronine	N/A	N/A	N/A	N/A	N/A	N/A	N/A	N/A	N/A	N/A	N/A	N/A
glutathione disulfide-posi	1717061.885	2853493.906	2510256.188	1283511.445	1502459.311	1327139.005	3205125.072	3258309.282	2092720.597	2360379.883	1874847.301	2363808.959
NAD+-posi	634960.0721	1393381.605	2586031.858	1734879.425	2007568.979	1778798.589	1157557.868	3909655.083	3024760.876	2422348.497	1788303.622	2457687.796
NADH	51752.89135	980637.664	603744.7755	488215.4189	623621.8596	228945.1824	452674.4955	1139967.15	656019.4427	599536.2058	636173.9292	670094.0605
dephospho-CoA-posi	146723.128	53548.73504	137349.622	78580.04929	189262.5554	141405.5064	64863.09759	44153.60104	32387.72997	24341.07017	48577.35022	82454.3192
NADP+-posi	55406.12382	77362.56239	185566.6566	67446.47715	117627.8419	64941.65757	150526.5561	307875.9	238235.1763	158903.2883	188179.6203	152546.0614
NADPH	3152.977453	N/A	N/A	N/A	N/A	N/A	2594.587365	4713.407236	N/A	N/A	6272.650783	5225.960079
coenzyme A-posi	335842.6231	112501.1181	244609.1297	135260.9578	368938.8591	307304.5109	215410.0299	168223.9998	152111.5997	134307.2563	176497.0321	242733.6711
FAD	55931.91313	17776.93252	23519.54383	19340.18873	47564.74266	47042.47474	25088.87947	23520.24473	19862.36648	15680.97485	27184.64061	39203.79048
acetyl-CoA-posi	34184.36068	38576.5317	47038.9705	10035.06238	72764.81784	61496.43654	11935.66838	11917.55479	9722.450476	8154.041206	27285.7761	32303.19155
propionyl-CoA-posi	4180.810762	5277.397696	3659.879331	N/A	N/A	N/A	4704.500546	N/A	4182.360815	4709.530406	6838.428034	N/A
acetoacetyl-CoA-posi	N/A	N/A	N/A	N/A	N/A	N/A	N/A	N/A	N/A	N/A	N/A	N/A
malonyl-CoA-posi	N/A	N/A	N/A	N/A	N/A	N/A	N/A	N/A	N/A	N/A	N/A	N/A
succinyl-CoA-posi	N/A	N/A	N/A	N/A	5226.76965	N/A	4704.561007	N/A	7318.395123	N/A	N/A	N/A

sarcosine	3339855.944	3852798.28	3803528.714	2697400.786	3980328.449	3389374.482	3840177.27	4108509.789	4070676.961	3207886.874	3981710.558	3738455.078
putrescine	N/A	N/A	N/A	N/A	N/A	N/A	N/A	N/A	N/A	9307.600983	N/A	N/A
spermidine	N/A	N/A	N/A	N/A	N/A	N/A	N/A	N/A	N/A	N/A	186759.8494	N/A
spermine	N/A	N/A	N/A	N/A	N/A	N/A	N/A	2613.763684	N/A	N/A	N/A	N/A
N-acetyl spermine	N/A	N/A	N/A	N/A	13726.43797	N/A	N/A	N/A	20460.14331	N/A	N/A	N/A
N-acetyl spermidine	5442.3976	N/A	3918.256752	4231.248549	N/A	6389.922329	4708.464401	N/A	N/A	N/A	6246.323053	N/A

Table S9. Peak area intensities in *Gpt2* mutant mouse brains (P0).

Sample	030614QEM1	030614QEM2	030614QEM3	030614QEM4	030614QEM5	030614QEM6	030614QEM7	030614QEM8	030614QEM9	030614QEM10	030614QEM11	030614QEM12	030614QEM13	030614QEM14	030614QEM15	030614QEM16	030614QEM17	030614QEM18
Genotype	WT	HET	MUT	WT	HET	MUT	WT	HET	MUT	WT	HET	MUT	WT	HET	MUT	WT	HET	MUT
glyoxylate	9315.704377	23509.75536	21503.05475	10130.1163	6007.241602	8758.01536	16016.41557	18311.34748	25394.22157	16216.98688	32551.13372	14547.65896	11883.20299	12744.51518	18193.50625	38048.89471	14287.73658	19407.1185
glycolate	18466.78952	28206.06453	19077.64356	28409.84914	10593.23776	17685.60039	20276.07437	14109.66124	23243.06902	25354.4649	24515.79107	35826.69505	11886.74692	11259.94005	16993.1275	23767.32815	33357.35176	78183.98487
pyruvate	17319.58075	12466.6369	21166.76482	8746.775293	19025.49679	14780.26967	23777.97765	4486.745311	10668.20329	28901.39161	14932.87871	23438.03563	22292.28311	13701.3059	15802.49101	31039.32424	16048.36772	20651.02951
lactate	9457660.72	8746183.431	11753358.13	28906921.35	20141359.54	22840153.77	10880584.26	5683024.315	6970272.324	10155950.98	9724582.922	12682830.18	8940745.691	5462430.539	8447105.413	11624105.56	10616010.74	11626906.82
2-oxobutanoate	207336.1069	199882.0495	184370.7338	204547.219	171395.5753	131786.1517	147564.9032	185835.5536	201414.3965	224591.3754	167492.8727	208269.0615	213217.4065	153840.2166	192065.5051	245413.1147	351567.7445	270777.6216
acetoacetate	294696.5281	236013.7764	224166.8721	185902.3385	164896.4954	225233.9545	160829.4481	142349.0625	218611.7111	195841.2705	211375.6726	219018.1446	201843.0245	160554.6661	208136.7016	283376.09	345530.5031	291438.5028
glycerate	9150.543626	30720.69214	15569.54229	20113.78822	8208.538077	16585.11521	15266.7362	11413.57274	29135.86484	11789.45941	22027.56381	17369.9807	8175.727896	27678.48887	45532.95198	67827.25295	88587.69406	126553.6268
uracil	256598.9256	165349.843	208276.9778	1929286.903	754764.3967	695630.8111	435216.7828	132964.7032	161068.7515	183153.527	109181.094	1889664.325	646283.9892	1231150.396	1335409.48	712433.61	536253.0151	812350.2292
fumarate	4326140.391	4537357.578	4902007.038	4888251.546	3536214.779	3646921.083	4449925.821	4075894.178	3837168.391	5918360.777	5083568.27	5452519.079	5801148.149	3336544.998	5995544.52	5839936.313	4447983.858	5382203.99
Maleic acid	4207101.094	5214155.772	4461779.484	4767099.368	3025929.901	4004504.385	4654602.361	3793471.536	4539723.13	6079675.702	5056667.733	5895940.191	5534952.673	3810339.084	5609478.147	5379189.009	5403996.78	5612084.516
2-keto-isovalerate	4264245.456	4685741.621	4188558.176	4779362.316	3180264.719	4155911.877	4466075.168	3866153.503	4784093.49	5751180.869	5113088.661	5354532.49	5711807.147	4256279.224	6190394.89	5890398.164	4410838.927	5027835.656
Guanidoacetic acid	131779.0548	182566.7641	83527.4331	147609.7649	106643.9632	118520.7781	128483.285	119203.2653	132397.0831	178910.667	130284.7789	143640.061	134406.9548	131822.727	148944.7555	304989.5804	222515.1525	315237.8723
succinate	2812266.655	2463898.919	2334613.918	5709552.987	4706995.137	5217229.745	2617576.438	2143027.747	2397972.218	2987517.451	2537289.999	3298932.053	3005643.179	2569291.308	2907972.289	2708706.705	3081158.176	2901181.808
Methylmalonic acid	3386966.759	3140074.817	3396888.883	7487545.117	6174260.481	6392608.35	3207958.783	2645725.147	3209398.023	3562513.553	3459439.652	3488791.221	3794344.589	3366837.299	3298090.902	3480645.24	3605325.873	3454346.367
3-S-methylthiopropionate	24475.80243	12560.47713	29663.41335	20443.35189	15025.62707	14272.39168	12257.84371	18161.68603	25989.84613	18652.33244	21877.75101	22392.11679	17658.95286	14597.48061	21358.40574	45325.82907	42105.53058	36972.6405
nicotinate	330085.0142	130029.2556	301960.5904	191214.3352	75015.54233	88626.06846	146886.0404	130447.2451	120838.1613	319272.6209	189485.8686	150888.3365	141628.8024	122337.8954	143457.5561	277483.5203	134252.3508	230033.8296
taurine	8216771.095	7314999.918	8229383.284	8053087.386	8387734.071	8107048.57	8639554.89	8147543.673	8005190.763	8698278.574	7767578.811	8130899.229	8083259.535	7863302.535	9072778.349	8885381.989	8999596.196	8556820.283
Pyroglutamic acid	287405.4277	222589.2709	209072.5068	133704.018	147376.6882	142871.1129	159994.409	209579.5601	147101.4073	263571.0981	293890.3858	231233.2148	250935.5848	149881.5978	254299.1662	260632.3826	247627.0052	268376.0447
Citraconic acid	613547.9319	509182.874	562682.8427	608196.9432	369223.4764	593248.2703	565947.1534	690854.7329	732058.7998	919443.4841	762914.0883	667698.9868	707415.5439	650601.29	622135.4606	588760.4131	1959048.449	2034122.686
2-ketohexanoic acid	36328.73714	12762.99903	22048.80656	14130.67328	17026.86741	5109.727267	25987.16269	19244.62722	31493.11544	36732.54016	46290.5	43251.47514	44598.18603	29047.96095	27895.82743	35763.66626	22375.88569	43249.27934
N-Acetyl-L-alanine	3664426.51	34117207.83	36246065.27	41973182.72	35143499.88	36872997.38	33054800.83	32356773.96	32719105.18	47553013.44	40972959.29	42842123.72	37218385.74	30977099.82	41607668.69	41122323.35	38954947.99	39936338.68
oxaloacetate	193356.2739	166624.3396	119740.1436	171658.9488	112626.4931	124916.6299	146425.4324	184322.4754	141806.5244	139813.7379	182433.7025	149049.575	135143.3839	81573.81416	148534.5263	173658.558	221224.6681	148323.9812
Hydroxyisocaproic acid	773018.9363	643032.875	683839.0745	759082.7319	400129.3555	534629.5082	785321.4117	997904.7265	1459050.296	1674483.763	1203691.703	1287442.976	994032.0592	641643.6322	1012946.773	1556743.947	1260356.87	1197359.381
malate	11227089.6	14120161.55	15318092.14	17271985.33	10814570.22	15209987.41	17142789.59	13784094.96	14097878.57	23241762.32	15109364	20642469.37	19861104.8	13923128.19	17037287.72	19934248.33	18445599	19779792.31
hypoxanthine	74252.2941	48032.84065	27512.52544	1567877.421	600526.8431	1083778.563	69456.58405	21910.92506	62528.31195	147995.5546	93409.76426	103436.1837	71549.71889	37693.03555	41732.84479	76115.22723	183316.7692	69035.43612
anthranilate	9193.482008	21247.32307	35126.08	N/A	10842.88029	16142.65074	10371.83501	13544.14415	19583.77453	9427.580712	20750.89644	27454.06271	24537.71744	14743.27922	25392.97855	N/A	20068.04973	31947.28687
p-aminobenzoate	60901.73803	283741.8211	29593.46624	64627.62157	37299.61562	43995.01324	22244.47898	39239.74989	52349.53691	85581.03512	65771.69479	59061.38708	29385.42807	15400.67496	27526.50898	81398.28205	50957.93842	49963.22651
p-hydroxybenzoate	331306.5999	330549.345	207860.6425	266304.4861	171082.8796	250713.8549	240646.972	241152.5192	303339.2937	606993.0207	377443.6662	408006.2622	329945.1019	186593.3632	370453.6259	432056.617	451287.019	380591.281
acetylphosphate	155050.6147	197953.1754	114556.1721	180966.5649	133130.702	156258.9736	193476.6932	86999.20663	93015.63064	206786.4709	119013.4536	169844.1777	99319.87529	108623.1703	103587.9685	284607.1552	201591.9239	254378.5979
Carbamoylphosphate	155377422.6	153224339.1	157397513.6	154316449.5	126019434.1	132679279.9	128461559.9	132051226.4	135323528.7	180721930.6	160263928.9	172441037.3	149662376.2	130258422.1	174366026	175129331.7	165746980.6	163645044.8
a-ketoglutarate	2730144.096	2782632.019	2551794.64	2852046.239	1983735.675	1883511.766	2168125.993	2725543.122	3210749.205	3606301.804	3590126.028	2945006.749	2609804.312	2067255.686	2613885.531	3774842.898	3225702.259	2922647.428
Phenylpropiolic acid	9422539.961	10264504.33	9384002.463	9293657.467	6850375.11	6561742.984	8133197.696	9312837.49	8635064.886	10716489.12	10931135.76	11047582.52	10579506.56	6085841.367	8146390.873	13156031.92	11211784.24	10837505.46
2-oxo-4-methylthiobutanoate	45511.27458	56359.01386	61856.48674	9278.431028	10713.92405	15524.13339	14939.63815	32364.44161	25533.62449	48225.8664	37811.75031	40879.36063	57195.93579	29850.88442	36193.65912	37224.03105	33026.30094	43406.5508
2-Hydroxy-2-methylbutanedioic acid	404029.2542	457217.389	502774.6982	461339.1434	439040.6804	418209.7442	552812.6652	511484.2087	538687.768	593560.6556	548749.2924	632832.4548	461960.357	500381.4556	676773.7902	621387.9157	588137.6284	1017055.708
3-methylphenylacetic acid	18586.3012	19962.34952	28295.99909	8280.030188	5616.712724	13265.89209	7848.351789	4558.312835	18290.1033	17685.40048	5846.152763	20221.93802	8049.916395	11094.14023	9133.921659	15153.58421	6835.430606	27949.36251
xanthine	1283834.799	1123460.104	966832.676	2796961.395	1495866.047	1737803.521	924246.0321	579055.9809	678098.5682	3006385.178	1236931.554	2919175.763	1400793.698	1608953.022	2827723.16	2219346.209	1706480.002	1993616.211
Hydroxyphenylacetic acid	29142.62674	26365.91946	N/A	50824.82833	58071.45679	33896.38523	44359.45383	35809.14718	16000.17346	29772.3342	49561.95482	N/A	43431.12046	55386.49826	44161.50072	37421.79145	17595.88996	33236.4009
2,3-dihydroxybenzoic acid	N/A	N/A	N/A	3603.695712	7410.935222	6585.012732	10679.00037	N/A	3750.25877	8300.588906	N/A	16400.42296	8392.842294	16808.80216	N/A	N/A	25081.99421	N/A
orotate	48108.51858	22795.58947	36324.68566	48534.18429	42023.18547	38690.3024	41601.05733	49152.62496	27824.08435	494341.5452	51938.58061	502227.1394	292729.66	277089.8731	405475.3247	525498.7534	338309.6681	302049.9731
dihydroorotate	204763.258	430126.473	179746.3452	136980.745	172576.3057	126447.8508	130068.992	424209.9092	270643.289	153695.1433	125627.0522	596153.9235	172963.3371	N/A	136012.115	131667.6407	87493.81688	109203.9885
allantoin	2991542.722	2260708.046	3223633.829	2966862.698	1711658.047	2326940.343	1652117.748	2201285.804	2237633.629	3492218.59	2119436.792	3286566.667	2516097.039	1575798.788	2860372.596	3224705.492	3020973.927	3569771.333
Aminoadipic acid	171398.6611	207197.039	192800.3971	135466.5289	90895.63706	144621.0371	169840.2318	167309.0198	240353.6199	166231.5991	57978.62035	144997.2277	117160.226	164968.151	178359.9916	220841.7332	258831.2698	298577.2854
Indole-3-carboxylic acid	149585.3368	121481.9095	136313.9358	103701.359	139147.4857	124462.32	161189.4055	132725.3649	96341.53593	138760.1887	169106.1937	167187.6419	110173.6881	48992.10194	159006.6891	201526.7734	190686.7683	192120.0452
phenylpyruvate	15111.02436	16179.95284	10435.30041	N/A	14067.89131	4665.047977	4002.876036	6185.088326	9377.544138	9880.133939	13026.3386	30180.9657	5211.152868	N/A	17107.87047	16666.24031	20310.23546	3440.215402
Atrolactic acid	14165.87964	13482.94003	17064.97224	20737.3211	9391.362378	4981.696589	8047.984353	7265.072125	11229.46767	28898.13542	N/A	16391.51036	15831.39028	5951.744826	10840.27039	24775.08916	10532.51829	11828.62509
Phenyllactic acid	80355.25724	79327.08107	98981.731	93135.22683	79702.97622	61829.33734	55348.69015	89094.12499	40018.64337	129221.7844	69792.86173	105106.5271	61475.53778	50547.39454	112592.739	90655.4751	54728.27562	88098.61832
quinolinate	7077.066322	12418.00486	5722.522658	9813.13215	11433.86618	4613.544028	8624.696958	N/A	7004.331645	30850.33071	39005.38859	13227.53227	5128.058146	9994.854503	8125.080879	22428.22806	11951.19895	6370.427435
phosphoenolpyruvate	129623.8909	269742.3368	142663.2362	147222.7676	100204.0908	147406.7673	122784.7239	60833.75743	80623.92683	142230.1582	258279.2243	124835.7931	192306.691	155940.9596	188056.3895	158780.7874	139315.9642	86566.53504
Uric acid	61073.45715	32140.42052	38933.1999	89611.33588	73474.81889	32047.34477	44371.70218	40230.07192	48822.96839	107010.0682	28630.48696	162382.5304	68627.98896	70722.69225	92142.06147	73341.31392	71317.20292	96892.4573
dihydroxy-acetone-phosphate	403429.1831	404098.3946	223706.9163	488563.1997	380381.0327	374278.7355	266501.122	148893.9666	340782.2694	282777.8307	366215.3987	318162.2702	216484.5025	228972.5272	499306.6445	401386.6553	417288.8748	270820.2778
D-glyceraldehdye-3-phosphate	312322.4545	247237.5434	173400.6272	349663.671	291939.4766	327356.572	216720.8814	147858.3941	291214.6797	231232.2036	290924.1393	242310.4266	202301.5587	195833.4995	427949.0456	243541.8387	300433.546	231933.3616
sn-glycerol-3-phosphate	1036542.421	1163995.207	1286029.691	3377536.498	2084455.337	2310543.963	1921716.4705	886106.2365	782983.0692	1188024.542	1174484.788	1554092.717	1162821.186	759550.8094	1171969.608	1253266.139	1405523.853	1335303.52
shikimate	815877.8555	342782.7646	316222.0424	335547.7795	329505.6989	271247.5805	85279.95356	219353.5536	184568.2641	144814.6082	194866.8573	218843.9867	100033.5519	69821.85693	60442.17593	156234.8746	158390.2026	168128.9247
aconitate	336986.0633	185038.6463	244148.4399	272728.4012	212787.6134	103025.0816	259243.431	261133.6378	298316.2274	343564.7331	387276.2085	450748.6272	330166.9689	258270.0722	236470.2623	399900.2294	308137.2502	309948.808
allantoate	38930.50546	45702.60977	39947.70859	34045.92204	33021.22023	19751.01343	42739.19818	39463.48334	34529.25395	41471.82596	47150.02761	38214.60241	56045.75586	30862.53209	31503.25543	34403.51459	35842.23575	52974.54073
Ascorbic acid	7556963.002	78246490.87	78831664.78	81921978.38	68512719.61	69308162.13	67762047.02	76382747.15	76206577.46	81856255.79	80024967.53	86757387.67	75253117.76	71054212.65	85272235.75	81095077.4	85186265.31	81080096.37
2-Isopropylmalic acid	1068868029	1125185672	1069761707	1032768921	1052872032	1046795281	1123961676	1109716166	1147040598	1067355788	1028295495	1141909821	1124155225	1054254192	1142987191	1062096887	1116896924	1180712256

N-carbamoyl-L-aspartate-nega	50856.79922	36111.20301	54457.13528	30358.26176	31096.29264	30392.91613	31716.1617	40986.40004	46835.88854	38185.79179	29049.1941	49515.56908	42696.2016	22419.26651	36410.31498	44241.98879	49602.84799	48857.90034
Pyrophosphate	115140.1695	75832.20584	48057.94842	372404.6275	185934.4437	216615.6304	59112.81186	40424.02369	41851.69884	111947.6053	83448.43013	124790.5499	81653.4499	47638.24806	103019.9997	130080.1562	96458.39066	97766.44629
glucono-delta-lactone	25011.99653	23435.27286	22877.03281	25531.02337	25454.46599	22406.23927	38037.9324	33824.93904	22925.35266	37510.3624	25532.65797	31764.46352	24488.01714	16691.92328	35442.77685	36811.59462	30221.16827	24474.44288
myo-inositol	50272084.82	49418851.7	50749473.78	50893561.4	43718786.89	41712456.14	46013019.72	50341432.84	42789676.63	63600764.57	55899374.97	55037472.35	51074568.71	40657886.11	58845137.41	67418204.17	60102460.92	54876465.74
hydroxyphenylpyruvate	62007.75254	42461.10457	17452.83378	6827.109446	5727.326738	N/A	21872.01259	16025.21544	28575.44534	53442.98353	60104.14061	21914.78863	18227.53825	31322.12768	47235.23975	38596.20851	47133.2945	31453.52163
homocysteic acid	30012.47919	44949.95311	44157.71928	64373.32453	28636.69663	35453.45356	17091.09229	30316.809	24103.14227	50850.34094	48770.91906	64784.69633	36088.90485	25228.78283	53758.07126	70529.91568	57535.70545	39838.41518
4-Pyridoxic acid	383082.5105	198993.6759	209118.3129	240479.3943	288118.6676	187127.8877	254151.7956	368976.0736	819384.9602	336314.9188	221039.2784	381761.3936	389006.3727	249384.888	241770.2131	370908.5035	439557.0027	474168.6701
3-phosphoglycerate	732990.716	682994.4363	603474.1164	1318236.403	758250.7733	1003403.282	615210.7186	388072.0786	539333.9502	1322132.445	1031855.572	1115612.517	700603.7391	430097.8508	704334.3964	731276.6382	837220.2802	867602.0849
Indoleacrylic acid	109603.9065	120257.6566	154379.6654	125758.8916	77606.06234	95964.01011	89559.74696	120628.4517	91278.2045	142753.9102	109029.2635	125984.167	122097.9124	68736.18831	151666.8448	149431.6893	126918.6212	74212.30642
Kynurenic acid	70189.72539	77308.33519	116639.3801	87462.85764	90047.75798	161125.0106	79728.28329	63479.47087	179708.1392	691333.3886	114406.2688	80869.34458	79937.33769	73399.33103	141352.6111	106566.9305	101230.0899	97006.45306
citrate-isocitrate	202680.1436	31179029.96	268386.4176	42659767.18	17650072.35	32503162.28	26491622.98	21957759.52	34131910.28	64767787.99	51292294.79	46448327.63	42118007.6	28961738.11	41362156.18	41720179.58	44952040.62	53150028.59
isocitrate	44785.18386	55664.73043	74066.14749	99137.85764	52911.40091	54620.21656	116459.402	76124.95737	74118.77813	202075.2801	113398.9961	146755.915	111001.9858	68587.08947	91987.50357	89728.3752	95725.47173	95991.65813
citrate	1729699.377	1061977.669	1020447.316	1003738.345	822052.3747	865570.9843	956829.897	1025638.459	1092518.442	1426044.317	888836.8136	1823007.869	1274419.652	1821250.22	23044929.89	24405672.36	24166798.72	24335672.12
2-dehydro-D-gluconate	32404.55041	14616.1487	23928.01556	20307.46636	12477.70769	14588.19661	20336.05365	20828.72509	9920.004722	18212.28065	28489.6163	27613.71373	28184.30749	19361.37994	41273.51061	27954.09956	32821.04543	51065.63896
D-gluconate	512120.9396	425103.3813	633856.2178	396544.9502	419614.8448	403068.9717	505511.2514	461468.0422	438694.8376	605343.1485	494403.0378	631914.9706	557116.3453	456939.953	465518.5458	566871.7989	661418.3746	525217.1249
D-erythrose-4-phosphate	149937.1083	128903.1814	102543.1273	107582.0036	81780.35877	93198.98214	160889.4102	150901.3547	142100.5189	185087.5109	190890.4772	126607.8721	122358.248	106925.8127	162569.9199	180069.0189	263601.1502	211738.2216
Xanthurenic acid	307032.9133	366019.9668	336101.5597	312371.9411	382495.6213	461838.3226	365061.9437	357539.1461	308354.8627	265788.0395	334329.5554	475876.1755	342693.1775	216037.3269	386214.4906	258325.4907	298354.1084	184352.7408
lipoate	N/A	N/A	N/A	N/A	N/A	N/A	N/A	N/A	N/A	N/A	N/A	N/A	N/A	N/A	N/A	N/A	N/A	N/A
D-glucarate	13296.17642	21415.93675	14098.87984	7499.314867	16106.05349	15126.52285	8324.837321	10154.18376	N/A	12467.32084	9769.659904	26054.28511	12981.29626	17194.85131	15798.82782	11558.17429	21959.59715	29702.80681
deoxyribose-phosphate	308467.1135	284076.15	286835.3615	472914.5417	538280.8244	613780.6987	323141.7999	336831.1219	285426.2259	513557.1461	519754.871	583754.0183	501023.6291	489324.0493	432777.4977	318304.9275	283774.9201	169252.6345
pantothenate	1195002.942	1035739.762	1042679.307	999745.025	627690.5672	829447.6263	837710.1065	524178.9327	645741.8398	991304.1939	956046.6412	965729.4941	664860.3164	392992.3824	972022.7056	1165112.636	1407859.788	1137745.362
prephenate	N/A	N/A	N/A	N/A	N/A	N/A	N/A	N/A	N/A	N/A	N/A	N/A	N/A	N/A	N/A	N/A	N/A	N/A
deoxyuridine	N/A	6252.360547	N/A	5209.304291	N/A	N/A	N/A	N/A	5207.281746	N/A	3632.226427	N/A	N/A	N/A	N/A	3120.220968	4164.710897	4685.07077
ribose-phosphate	212679.2993	133798.6907	98833.37025	449187.8768	334216.6976	375790.2085	105239.368	84054.78674	124184.0638	174077.8429	147224.7479	154513.3742	123467.6574	157534.171	210051.5657	159975.8406	146846.7531	120724.9493
thymidine	N/A	4689.467827	6254.272433	7294.280029	N/A	9925.08052	9899.474057	8856.77013	N/A	7815.022073	6773.232715	9899.633214	6252.461557	N/A	N/A	N/A	6252.611745	6252.545183
uridine	6802.858308	10415.11701	N/A	65414.45119	66692.42405	69754.76735	12929.07156	14483.31484	11449.71436	27624.27496	11534.18272	25823.07104	10338.00136	15943.67005	24292.06895	5693.562078	26040.4994	7275.152534
deoxyinosine	5212.511487	N/A	N/A	N/A	N/A	N/A	N/A	N/A	N/A	N/A	N/A	N/A	N/A	N/A	N/A	N/A	N/A	N/A
shikimate-3-phosphate	N/A	N/A	N/A	7913.729779	7789.39069	N/A	N/A	N/A	N/A	N/A	N/A	7300.200803	N/A	N/A	N/A	5239.446004	N/A	N/A
D-glucono-delta-lactone-6-phosphate	N/A	5199.550173	15275.70783	7624.648683	N/A	7565.265491	13238.99491	8986.958875	7324.826821	4689.292772	10568.67395	10134.03716	15587.77267	4677.918771	11274.99191	16598.29096	10875.90797	6759.045528
hexose-phosphate	812628.2255	821582.627	838795.6677	1219907.267	954130.6317	850150.4026	872996.0788	931798.7727	998487.0038	1503055.703	1194855.7	1248037.832	1016193.963	790780.1516	907331.9147	1465881.272	1161422.32	1436501.98
glucose-1-phosphate	16994.12562	16555.57126	14149.79058	133027.0413	22361.22071	27535.0904	29365.79878	20013.51933	19906.36085	31273.75199	38320.6889	26074.2991	16515.07193	22846.25417	27561.59664	17599.85218	13623.6797	24594.94056
glucose-6-phosphate	112264.3402	91037.66205	102154.2029	152066.6367	95038.16013	112383.4736	110895.9163	100859.5683	115745.5612	164334.3246	156553.2727	166165.6238	134108.3923	82997.15459	66795.21781	187259.7672	143411.8064	221373.5262
fructose-6-phosphate	39081.95559	40293.40885	34901.08451	52929.23839	25723.31957	28544.57141	33857.70402	42812.27128	30344.04438	58749.94221	63560.82085	32560.88061	35016.24491	21141.86694	65753.44992	63041.01268	36434.27214	80756.60785
1,3-diphosphateglycerate	12662.73088	195893.256	11373.7738	25526.16142	25901.80103	4145.612241	141617.1223	11967.08361	13651.57551	165393.7676	110898.4305	143449.6952	127115.1811	68360.89335	82362.30748	100168.1337	85081.67151	85937.46904
2,3-Diphosphoglyceric acid	N/A	N/A	N/A	N/A	N/A	N/A	N/A	N/A	N/A	N/A	N/A	N/A	N/A	9105.663609	111904.111	65549.66096	68608.42083	81017.98087
S-ribosyl-L-homocysteine-nega	20331.3532	10939.38319	15111.36528	N/A	N/A	6768.918526	6743.637472	18236.52275	6766.642408	16152.85376	14003.42926	11991.98229	4696.028002	N/A	N/A	11982.91284	4687.533765	N/A
inosine	15631.33491	20842.84883	10421.34372	94834.3361	46385.29962	76102.87647	8333.903148	7795.320235	9399.867382	9380.071283	7292.701189	26572.61125	7778.912624	16157.11179	19777.71267	13765.89446	8858.155118	17236.83622
6-phospho-D-gluconate	17704.20935	13027.21036	11462.03433	14908.99295	15112.60392	13067.32839	16674.01954	14068.16758	6247.241982	17231.27012	8869.30845	13547.50397	6290.332747	5776.856895	13529.32446	17193.31933	17163.42811	25449.9473
xanthosine	N/A	N/A	N/A	N/A	N/A	N/A	N/A	N/A	4689.381146	N/A	N/A	N/A	N/A	N/A	N/A	N/A	4708.292013	N/A
D-sedoheptulose-1-7-phosphate	45393.59297	48326.39175	54100.20316	26775.56454	17956.82171	37529.03318	65607.52823	82484.9185	50935.36364	120058.7119	68295.25735	178616.2945	74583.76756	47870.00499	58309.19294	145895.3762	67008.23557	103877.8602
N-acetyl-glucosamine-1-phosphate	44188.99063	64311.74256	37315.41446	51471.72008	62106.73444	65457.13277	29995.37752	52504.13514	40486.98637	87782.45129	61567.12536	44878.24896	41817.91235	N/A	38322.30497	110032.5147	64472.66122	66256.53761
glutathione-nega	1097237.764	624007.2833	831154.2356	799312.2218	533025.4678	717449.9281	766020.6101	1170835.042	668321.7753	1460625.308	901619.6959	1619855.805	999361.2057	936097.9213	1629454.733	1652607.406	2250283.665	1867403.359
dUMP-nega	5731.53292	N/A	6166.426267	22886.29085	10531.87906	29345.36801	5731.446542	5726.782176	3646.752933	8858.731463	N/A	6252.368951	N/A	11464.03618	4705.920562	8339.566543	N/A	N/A
Geranyl-PP	138576.3723	200855.1792	178945.4634	90569.74914	56732.03414	88404.02378	132804.8476	122683.4615	144783.5825	363633.2136	174560.3295	198830.4113	129087.0289	67376.92246	106545.8927	112906.6585	66685.55565	62638.8297
O8P-O1P	18209.07618	12499.07157	16108.89062	16066.4482	10444.48454	14851.58829	10626.68294	21723.01376	9378.013004	42870.58339	27571.72429	43229.25892	14252.80779	7827.634782	16046.05498	27787.68833	10648.71942	24588.634
dTMP-nega	45852.94304	24746.58629	41666.0381	44283.28374	38556.82293	17714.30183	28095.54554	12505.18813	43240.06697	52625.78199	38038.28571	36472.48745	41779.56064	27089.53686	20295.62922	22928.26489	30737.90437	15087.62767
cyclic-AMP	7446.256913	23995.05399	9287.160842	15634.07037	26572.99853	30245.04096	5350.867285	24528.76266	6544.480181	10521.99107	29214.16701	23444.6618	17659.99733	13545.71377	15117.77409	14592.77298	14063.72019	9902.695073
fructose-1,6-bisphosphate	N/A	81823.49428	66819.66677	183299.8175	144990.5037	157025.6633	145210.1573	84176.38291	134559.5032	85882.88172	113369.908	149291.3205	123816.5342	78149.72801	71616.33381	85635.56004	84596.2071	105160.5743
trehalose-sucrose	N/A	4008.14041	N/A	5679.904856	N/A	N/A	N/A	N/A	4689.227473	N/A	N/A	9167.269317	N/A	N/A	7296.008951	8318.660589	4165.063499	N/A
Cellobiose	N/A	N/A	N/A	N/A	N/A	N/A	N/A	N/A	N/A	N/A	N/A	N/A	N/A	N/A	N/A	N/A	N/A	N/A
orotidine-5-phosphate	N/A	N/A	N/A	N/A	N/A	N/A	N/A	N/A	N/A	N/A	N/A	N/A	N/A	N/A	N/A	N/A	N/A	N/A
SBP	10470.78957	21066.8676	12505.26122	19156.84011	30276.38179	34902.37535	21892.06232	10471.30994	20313.5886	21195.78014	16914.93464	44433.29415	23571.44642	17661.03026	22181.06578	21875.61613	14582.15653	30181.17432
trans, trans-farnesyl diphosphate	47978.51387	45626.53542	39706.28492	25449.57217	30378.25145	75027.56715	29845.03663	28844.2851	52134.6117	50429.30786	49242.00694	56561.02053	58861.91732	28429.02785	85772.98137	77844.61114	73885.31691	87345.37712
S-adenosyl-L-homocysteine-nega	162237.7622	214966.1674	212338.5798	292939.4637	169974.6528	153074.9489	151903.8059	155039.193	177053.5717	239619.9434	165277.1949	232662.8079	191866.3643	139670.0735	195882.7889	255854.921	177158.9373	182358.8497
dCDP-nega	183230.1676	22870.28882	5225.37081	14122.99557	9667.555541	16547.60496	116668.958	10137.89522	104056.7328	224063.3924	147778.0779	173515.9271	105243.5654	80251.38954	143255.3423	169852.0546	156599.7201	132838.2352
5-phosphoribosyl-1-pyrophosphate	N/A	N/A	N/A	N/A	N/A	N/A	N/A	N/A	N/A	N/A	N/A	N/A	N/A	N/A	N/A	N/A	N/A	N/A
Deoxycholic acid	N/A	N/A	N/A	N/A	N/A	N/A	N/A	N/A	N/A	N/A	N/A	N/A	N/A	N/A	N/A	N/A	N/A	N/A

OBP	101473.5331	110495.8898	75571.24883	8316.44944	N/A	207744.537	84402.2647	91752.01549	80769.35052	111114.2661	62132.97797	66593.46354	51207.23888	28824.24626	66722.66374	61221.74458	35459.08306	30604.87133
dTDP-nega	N/A	N/A	N/A	N/A	N/A	N/A	N/A	N/A	N/A	N/A	N/A	N/A	N/A	N/A	N/A	N/A	N/A	3646.449002
CDP-nega	N/A	N/A	N/A	N/A	N/A	N/A	N/A	N/A	N/A	N/A	N/A	N/A	N/A	N/A	N/A	N/A	N/A	N/A
UDP-nega	N/A	N/A	N/A	N/A	785848.6696	946272.6907	1435648.642	5644.211044	1307255.715	2179408.466	1360425.418	2133567.862	1509964.473	831006.6674	1132015.796	1422646.169	1251668.864	1237100.399
Cholic acid	25533.31039	33367.80682	20995.02159	39081.24261	42208.43398	34388.43074	25526.30814	45854.41958	20886.03633	34829.63734	39071.54102	55811.07482	42203.5004	17699.68984	25530.67532	14589.75504	20842.15399	13550.77918
trehalose-6-Phosphate	16797.73663	8438.15285	11597.49626	9126.480636	12208.42439	18213.23377	21634.9101	18855.34245	24671.23417	15359.92804	12877.99587	15418.2045	19865.55274	14566.75513	15098.04999	10923.06636	14237.30494	25356.62537
Thiamine pyrophosphate	7032.942056	14879.36307	16633.53245	9546.076373	16167.56933	4141.862843	13756.33035	27969.56844	48131.21818	5911.442549	18868.62694	5654.427637	24431.85668	7345.758072	34199.77453	40061.5438	22732.67544	22720.43093
adenosine 5-phosphosulfate	19285.38477	27046.81292	27056.07824	14071.18902	N/A	6855.102256	18179.98831	20331.63909	10868.69541	23891.27233	13039.60989	14588.05462	4183.6035	N/A	N/A	N/A	N/A	N/A
ADP-nega	N/A	N/A	N/A	3677.171093	N/A	N/A	4254.726687	N/A	N/A	9378.578915	N/A	N/A	N/A	3648.818213	N/A	N/A	N/A	N/A
dGDP-nega	8338.723105	8338.089714	N/A	5207.803587	4165.464316	N/A	N/A	N/A	N/A	9897.661064	N/A	N/A	4565.325811	N/A	N/A	N/A	3669.161834	N/A
IDP-nega	20663378.14	19556473.36	20370314.15	16622911.04	13177999.17	12864192.78	17702957.63	15874927.82	16417299.56	23856375.98	19214872.36	21557320.54	14100509.35	9865771.643	13917408.06	18004182.37	18597211.9	14780456.1
GDP-nega	N/A	N/A	N/A	N/A	N/A	N/A	6769.418474	3646.663427	N/A	N/A	4167.506367	N/A	N/A	N/A	N/A	N/A	N/A	N/A
CDP-ethanolamine	N/A	N/A	N/A	N/A	N/A	N/A	N/A	N/A	N/A	N/A	N/A	N/A	N/A	N/A	N/A	N/A	N/A	N/A
FMN	N/A	N/A	N/A	N/A	N/A	N/A	N/A	N/A	N/A	N/A	N/A	N/A	N/A	N/A	N/A	N/A	N/A	N/A
cholesteryl sulfate	124971.90117	6246.981775	7815.711149	10943.13303	N/A	14068.18858	4528.216	8339.291708	12503.18982	14007.26294	14068.5614	18225.41222	10942.28387	11461.111	N/A	9363.816433	25550.37559	17717.34638
dCTP-nega	52625.12722	38555.27829	41166.88318	7813.975261	9915.460534	N/A	23960.90754	34420.01149	24053.88538	41697.52637	52137.12478	28658.56782	22401.92542	16661.01836	36473.79232	30222.85483	31261.99071	29182.54669
dUTP-nega	26563.94869	26055.88075	33347.35812	4688.686745	7814.984699	3133.508954	22405.3391	25008.98613	34901.70683	24489.71914	20323.19211	17717.49948	18251.50951	15633.47953	24487.11437	32815.61942	35985.55752	28137.45027
dTTP-nega	N/A	N/A	N/A	N/A	N/A	N/A	N/A	N/A	N/A	N/A	N/A	N/A	N/A	N/A	4689.447079	N/A	8333.662455	N/A
CTP-nega	20320.24081	55245.58015	28657.42091	N/A	N/A	N/A	22920.36321	34912.98869	15631.57247	23969.85964	41161.08099	24488.29764	22402.87508	11982.73975	40643.22508	45915.55766	42203.13355	33346.81697
UTP-nega	1137342.001	1133614.567	946819.8493	148161.0884	154459.552	189188.4447	509497.0313	735705.5485	654031.0085	684736.1896	876107.1554	506898.1782	575117.9293	514239.4048	992129.3923	1250945.473	1363920.065	867636.6326
CDP-choline	N/A	N/A	N/A	4689.39733	N/A	N/A	N/A	N/A	N/A	6252.465531	N/A	N/A	N/A	N/A	N/A	N/A	N/A	N/A
dATP-nega	5730.231012	N/A	5208.454704	N/A	N/A	N/A	N/A	N/A	4689.320509	3646.85415	3126.454696	N/A	N/A	3648.57263	N/A	N/A	N/A	N/A
Taurodeoxycholic acid	3644.553035	N/A	N/A	N/A	N/A	N/A	N/A	N/A	N/A	N/A	5724.178815	N/A	5730.747249	N/A	9378.983359	N/A	N/A	N/A
ATP-nega	9364832.097	9191156.638	9917163.129	1418298.372	1167365.046	1091788.998	6141870.553	6171728.253	6233502.555	11499670.13	6902729.448	7964396.255	4902717.218	3151382.885	6456337.887	8505982.349	5982295.943	8341263.238
dGTP	8749640.31	8489761.3	10504000.33	1318288.428	1188383.616	1425711.701	6144391.851	6446025.839	6099675.145	10419078.26	7080452.315	8672996.961	5094548.06	3395425.277	6367357.194	9099771.551	6045334.888	7860788.531
GTP-nega	371307.8624	317310.707	319419.8953	75549.23901	47456.6667	67211.38728	124930.5455	140545.414	139121.4955	163089.6945	162040.1018	152117.4163	127093.9744	102381.2726	220922.8939	419996.6383	277826.0504	339711.8018
UDP-D-glucose	472136.226	4231599.936	4474817.68	4026474.852	2516815.988	3520499.572	2823104.243	3320773.326	3418025.571	4332413.229	4662326.796	3384551.666	3812545.506	2579561.732	4739606.627	5344380.019	4354080.858	4469152.862
UDP-D-glucuronate	422007.546	423596.6168	399116.2007	431930.2638	255831.2952	310022.5217	322008.6504	361590.535	350135.5503	438759.1709	444981.2529	381393.2623	377754.9076	221048.9167	461220.3136	681953.9159	552291.198	519046.3138
ADP-D-glucose	18207.91404	20350.70899	10144.91618	28134.683	15918.22271	25531.83776	6780.610214	17185.96946	24994.92835	23401.72959	20962.75479	28678.0475	27614.4657	22405.98416	11985.1051	16154.0831	28655.39181	20316.36278
guanosine 5-diphosphate,3-diphosphate	87470.00317	83886.26555	82320.47868	45852.30526	34911.06605	23443.53188	79197.56002	51061.32305	53663.61394	91707.10386	83793.3468	60962.57916	44270.70157	47438.65987	55749.86777	84411.14003	101074.3077	62005.5949
UDP-N-acetyl-glucosamine	1572152.846	1392989.733	1604510.548	182368.31	1118182.6	1290540.249	1680926.264	1228940.552	1418794.695	2042022.2	2242760.856	2442410.57	1737594.877	1273461.791	2714731.405	2524193.038	2062608.28	2344363.347
glutathione disulfide-nega	12283194.84	9078837.685	8585122.456	10242369.54	6302320.705	7642872.731	8939144.822	8938756.944	10412508.35	17787202.43	12932302.68	19013951.03	13299394.43	9768321.104	18390217.06	18789497.66	18361526.93	17316384.06
NAD+-nega	2656509.09	2814538.862	2744524.196	1253783.703	1388481.762	1389530.717	2262502.452	2407757.701	2178590.151	2915997.285	2967569.175	2571232.583	2854532.519	2630799.687	3691300.777	3700541.952	3091051.715	4455878.534
NADH-nega	21368.42285	20835.58142	23968.08316	23448.1719	19797.91248	16152.89559	25009.25041	19827.44005	38037.93899	23446.22088	27580.27802	23967.80649	25531.25051	21357.35902	8856.993476	28137.04245	22944.59351	25006.99768
dephospho-CoA-nega	16197.14586	11359.83338	11462.69478	14997.33572	16701.58695	11185.87606	12040.61952	3944.595321	22910.54381	6250.386022	30220.76761	18236.93733	30741.40956	30741.35027	30768.11741	10905.91614	51574.72759	45851.6652
cyclic bis(3->5) dimeric GMP	N/A	N/A	N/A	N/A	N/A	N/A	N/A	N/A	N/A	N/A	N/A	N/A	N/A	N/A	N/A	N/A	N/A	N/A
NADP+-nega	198678.6646	277769.9796	275502.5912	154184.2986	141433.1695	173976.5979	155896.6908	238733.8174	318226.0353	204867.9794	224984.1797	232132.8138	217770.5935	170361.9078	197067.9219	293877.838	302149.7622	300627.0876
NADPH-nega	17714.14101	11982.6834	10941.75014	5195.262821	N/A	10941.73425	9377.846098	N/A	N/A	13546.83148	10942.17768	8858.066743	9900.65129	9899.576398	8338.191379	11462.77836	12504.68194	4169.060657
coenzyme A-nega	23966.87384	32155.2204	33554.25816	36536.28354	30748.92271	29697.2127	41676.44007	27111.51811	29228.9493	25256.5765	36470.49378	17022.29256	24488.20637	15435.80464	26581.26585	27616.97934	20321.21996	16675.73076
acetyl-CoA-nega	N/A	N/A	N/A	N/A	N/A	N/A	N/A	N/A	N/A	N/A	N/A	N/A	N/A	N/A	6877.771023	N/A	N/A	N/A
propionyl-CoA-nega	N/A	N/A	N/A	N/A	N/A	N/A	N/A	N/A	N/A	N/A	N/A	N/A	N/A	N/A	N/A	N/A	N/A	N/A
butyryl-CoA	N/A	N/A	N/A	N/A	N/A	N/A	N/A	N/A	N/A	N/A	N/A	N/A	N/A	N/A	N/A	N/A	N/A	N/A
acetoacetyl-CoA-nega	N/A	N/A	N/A	N/A	N/A	N/A	N/A	N/A	N/A	N/A	N/A	N/A	N/A	N/A	N/A	N/A	N/A	N/A
malonyl-CoA-nega	N/A	N/A	3669.488844	N/A	N/A	N/A	3648.176805	N/A	N/A	N/A	N/A	N/A	N/A	N/A	N/A	N/A	N/A	N/A
3-hydroxybutyryl-CoA	N/A	N/A	N/A	N/A	N/A	N/A	N/A	N/A	N/A	N/A	N/A	N/A	N/A	N/A	N/A	N/A	N/A	N/A
succinyl-CoA-methylmalonyl-CoA-nega	N/A	N/A	N/A	N/A	N/A	N/A	N/A	N/A	N/A	N/A	N/A	N/A	N/A	N/A	8316.91604	N/A	N/A	N/A
3-hydroxy-3-methylglutaryl-CoA-nega	N/A	N/A	N/A	N/A	N/A	N/A	N/A	N/A	N/A	3706.649181	3661.641912	N/A	9899.727518	N/A	N/A	N/A	4689.526441	4152.003074
2-hydroxygluterate	1069049.743	1378285.462	912800.5256	750953.9596	822978.1429	704444.2544	1096000.088	856971.8785	1095566.41	928300.8669	1245034.948	1546715.11	1285290.493	809310.7347	1111313.349	1201439.806	1051602.655	1318718.135
2-deoxyglucose-6-phosphate	3314100.051	3477864.393	2386254.169	5843181.979	3264705.767	3075263.45	1938288.051	1945842.009	1859091.36	3378373.15	2886022.355	2162455.615	2134669.496	1147369.536	1501121.599	2187779.087	2378567.938	1675277.676
Urea	1976644.735	1546229.682	1782375.017	1823102.148	1391423.87	2009148.789	1534130.852	1670628.736	2007084.785	3667868.421	3111821.869	3312160.868	2686608.933	2125462.155	2588086.065	2926225.219	2654559.134	2806501.396
ethanolamine	272685.554	635685.3283	396065.0823	868174.8142	464128.3393	233032.3401	546346.9865	478437.6704	159096.045	1162509.5	806977.8681	1031587.153	973249.3446	312945.7726	342822.6839	325082.0874	512818.6718	N/A
Imidazole	N/A	N/A	N/A	N/A	N/A	N/A	N/A	N/A	N/A	N/A	N/A	N/A	N/A	N/A	N/A	N/A	N/A	N/A
glycine	N/A	N/A	N/A	N/A	N/A	N/A	N/A	N/A	N/A	N/A	N/A	N/A	N/A	N/A	N/A	N/A	N/A	N/A
alanine	1241348.862	1194671.602	2180043.503	1602121.867	1279554.83	1806438.153	1208947.204	1079124.359	2293236.391	1711772.913	1550443.771	2382877.34	1475143.448	1024785.813	1944252.662	1495852.034	1424400.884	2200876.799
betaine aldehyde	471270.1042	415986.3078	376395.6481	457272.7662	330401.4938	329811.0174	392929.7172	338629.8515	389612.1025	435056.7247	363819.4521	371483.5052	456137.5851	420212.1682	373521.8136	417730.1614	479351.6832	425811.6823
choline	462599.2878	409974.3854	536145.0125	386331.169	342608.0876	449347.5095	450120.4312	678970.3928	402681.0071	734605.3599	509463.5371	696755.3437	485432.0859	364193.3178	253457.4021	833963.628	515725.6709	622162.7487
4-aminobutyrate	6403287.239	6044064.93	6624118.826	5748925.748	4772392.027	5392073.886	4643959.385	4782945.22	5256417.821	7818872.37	6493638.997	6316684.739	5301574.976	4609164.513	6023783.177	7650965.188	6808622.848	7523801.042

dimethylglycine	1695849.488	1422262.156	1352632.926	1757032.04	1029240.171	1387969.332	739087.1081	1212886.022	1544290.156	1881107.79	1393655.908	1909497.252	1468133.21	939311.0948	2039117.363	2031231.108	1743867.482	1602813.545	
serine	2725083.118	2532814.29	2627156.604	2867346.724	2655012.93	3068525.441	2796688.471	2386727.96	1843327.691	3689925.28	4333326.096	4394279.492	3795217.129	2566319.388	3511518.758	4034992.79	3013540.926	3436732.001	
cytosine	90015.39014	59229.21942	100542.6069	40930.87145	48152.88797	40783.57778	51151.0083	50292.85116	76798.52432	130161.9175	362017.7018	45049.95077	53564.79721	31073.28125	62641.1746	75508.39861	75807.33036	73050.88697	
Creatinine	3415446.369	3642148.008	3561344.207	4797316.695	3164255.039	3466996.845	2663592.44	2775335.627	2938519.395	4844877.678	3876576.664	4729233.617	3744525.6	2516239.221	3707164.023	4009052.757	3620762.765	3708918.258	
proline	34622701.63	25320769.69	37217569.82	30866937.15	23749430.68	28309932.68	23525869.62	24207822.06	33901472.74	30912522.81	36130923.74	32051358.55	24694384.85	17935445.38	25392025.34	36826768.47	32656246.94	32034699.95	
indole	457533.9168	392745.4302	370286.6072	415470.7811	240634.3674	252611.4568	173432.2611	374398.003	370604.1927	421710.5453	365621.3716	465345.1911	311509.4916	206367.6365	450982.0125	601424.8522	428941.617	420249.309	
betaine	55999470.75	63145941.97	67160413.9	76341212.38	58637507.95	53835307.79	63352131.24	69230285.68	73634776.2	83886479.35	74867292.7	76232809.61	78278838.02	82133758.21	70889461.48	76938965.27	66443277.74	75217377.05	
valine	3089643256	3372273751	308414.584	276520.641	314281.4049	342827.9018	196568.8995	232231.3682	330770.8243	321510.6031	350251.3501	355036.3236	269500.3967	197060.6587	239956.8372	470913.6426	444554.3351	392925.4031	
threonine	5301581.189	5160690.946	7394487.135	4680458.831	3077870.859	6479733.755	3839782.309	8586422.836	9187539.354	8169541.653	8371591.334	14678244.71	7682258.102	3320678.71	10147863.4	11805687.7	8000251.329	11943721.91	
homoserine	15854.45136	40049.3782	42508.91328	8630.513142	7466.495251	7909.743182	21332.15081	8153.147912	5588.225362	11634.97363	37425.41606	8191.497128	38708.45166	11874.91807	9707.770474	15912.014	11275.54828	12117.53776	
purine	125704.6569	107714.8348	91157.86747	119821.045	81784.79118	87803.62213	58530.33528	60298.83338	62718.61007	117195.7967	86897.70311	140021.9377	82464.29365	83603.70887	145378.0665	130233.6423	105538.4891	142490.7619	
cysteine	32256.81464	163077.3381	141523.3421	120484.4716	90523.0618	92750.97732	75115.10266	19214.53274	7637.566299	14144.70422	8583.533327	46582.70902	42378.53746	30098.47241	12786.93735	42094.09188	9406.777521	9424.157318	
creatine	9970306625	102053329	101705662.4	101131862.5	104989706.6	101589589.2	93578116.28	102288036.3	104423599	110622949.1	108521626.3	119594142.2	99591758.51	104815141	107995970	106743898.5	106514331.3	100363153.3	
nicotinamide	15449600.27	13857278.69	16757262.78	39505069.82	14975015.22	29072639.04	9806872.172	12275592.15	13378125.87	17402887.49	14785895.22	16685884.29	7982879.822	4267274.066	10373962.86	10360459.88	14757135.27	7971897.844	
Imidazoleacetic acid	55551.92214	39506.873	47973.81585	16300.09683	19829.45617	N/A	30315.48697	25555.0579	49845.66409	44122.8192	68793.21113	42113.63553	29799.50294	35732.94269	19283.52368	67608.66092	43364.56178	76694.08372	
thymine	213298.8141	171837.2028	130527.0516	199858.5612	128409.8514	163391.1079	120870.4938	135142.2355	139937.2454	174497.0986	157475.711	154459.0091	179143.2501	114027.0656	145551.5018	206429.6534	155346.0709	117818.4074	
DL-Pipecolic acid	867573.17.16	82402867.42	76504031.86	87850045.26	79365995.27	73127126.35	71789612.27	79868912.17	85869881.56	98255862.13	85423291.4	94031442.11	81548017.77	75080625.53	91722808.19	100006801.8	90183180.13	92386520.17	
N-Acetylputrescine	4477.778199	13129.76985	1119.16639	11382.94224	20595.71129	N/A	4773.374832	6257.169253	58120.74335	7482.541997	9214.38171	N/A	15887.42236	3869.20122	4663.207837	13904.41602	5517.736004	12651.09776	
hydroxyproline	3047203.953	3021052.381	5255320.98	3568858.134	3815702.864	4325936.851	2786659.172	3444198.328	6181871.718	4845929.112	2800773.451	7942000.496	4705435.016	2722265.559	6809909.875	4511909.507	4213550.341	7905404.783	
leucine-isoleucine	8556251.986	7131759.28	5970524.366	6462468.033	4987139.327	3829855.221	6122731.266	5860531.544	5984749.25	8491323.045	9868870.091	10967533.33	6887016.124	4361194.698	7783320.827	8947730.716	7834212.785	8933715.566	
ornithine	351831.0273	354453.1075	247894.5177	157014.5363	136672.3639	170857.7489	134289.6612	124053.8375	198576.9234	200960.0439	370088.4534	518221.7923	224438.6817	129422.9414	233565.2933	374619.5917	291825.0698	196149.4597	
asparagine	1149429.042	990045.411	985067.1389	1315029.554	918047.5305	1076760.276	1348504.517	1157197.482	1390845.165	1792880.308	1660948.899	1801644.305	1708078.455	1778550.701	1938846.161	1914777.662	1700919.855	2183581.416	
aspartate	5520677.694	5640131.193	4991948.034	5206735.621	3113657.07	2868943.378	5917673.486	5829156.168	3676286.487	11189440.69	5458481.217	6932420.993	4077388.341	4558413.031	10005813.37	7639832.095	7437036.597	10572132.8	
adenine	2145399.583	1972702.168	2343844.433	2403818.733	1892850.347	2039732.411	1384165.132	1178036.183	1921269.736	2267574.207	896756.818	2296115.233	2075062.908	1316898.707	2403262.967	3293408.966	2685728.602	2044041.836	
Methylcysteine	620427.9978	644418.3138	831242.6671	740618.8504	649086.8322	643318.1888	489013.2508	397325.4695	636188.4457	614822.6538	545882.8368	838743.9425	920825.2696	492907.5695	692115.2344	630232.6159	671580.1293	788286.8019	
homocysteine	51098.88592	43479.95023	57711.1068	37016.25616	33733.71548	36990.92181	34732.69627	28110.77406	38736.81759	81694.90447	69121.24135	45067.47894	37770.99132	24009.47353	56267.29551	44230.85446	35323.534	40592.21059	
methylnicotinamide	48688.2588	87162.26385	49917.49146	508055.0266	243217.74	220916.9691	25314.58325	46965.37713	72283.75334	68440.80562	40737.83899	89409.52116	44657.21011	32925.57109	587.55.58784	49828.03212	64426.9074	101909.3774	
histidinol	60886.80154	33870.52527	32764.23415	52087.09036	18210.68333	17143.22842	15673.54811	29180.89232	20829.90541	27613.89891	34896.5172	40136.04883	22389.55636	21892.13896	47542.67963	68778.72117	39078.45075	54751.77168	
lysine	929136.276	1243016.581	1260842.059	1344211.43	925861.9255	651695.9437	767532.0159	881181.5554	718588.9398	1595093.366	1385342.535	1446609.222	1416168.205	904937.7064	N/A	2394887.556	1673980.48	N/A	
glutamine	64315960.75	62579917.15	57101798.29	59002319.49	56624185.62	51315458.36	50102972.78	58923141.8	56231760.23	68399381.34	64495413.57	59991758.92	47970783.48	48086188.34	54614566.17	58879327.91	69831166.26	62385859.98	
O-acetyl-L-serine	N/A	7677.867072	N/A	8132.680197	8625.793509	6772.751996	8008.744606	N/A	15613.7196	13815.36709	N/A	14078.59432	9770.823788	5809.230405	11427.26881	9149.844445	9797.347814	16651.74014	
glutamate	27907230.28	28770289.84	35553020.84	27922807.69	28865055.15	34630689.97	25711794.61	32733591.85	25588639.76	45884197.81	37693131.51	43894995.48	36870383.81	31792237.68	39399275.1	35454663.87	35272227.1	40814259.13	
methionine	2431046.483	3405247.315	3100590.022	2381501.482	2941972.406	2658276.057	1810895.695	2547928.846	2069206.35	3289532.269	2425698.479	3452780.705	2337300.116	1964433.43	2935632.414	3321101.264	3375471.968	3691289.62	
guanine	31860.79695	32131.91352	26420.34912	278957.9056	132475.3338	133547.0141	26615.65835	24710.47648	27991.43082	19725.11739	39108.10365	32335.42933	N/A	6156.127945	30733.79502	37833.3934	6435.09887	18473.87176	
histidine	1801465.842	1339742.231	548818.1	2328059.345	1123592.573	2520194.399	2720825.409	980880.6006	1923799.497	2930522.132	3736588.538	4384734.88	3894456.83	1402415.823	2946694.861	3690347.09	2456869.646	5958913.429	
2-Aminooctanoic acid	8141831.31	8167586.737	6273468.287	8450865.426	7279388.689	6977557.256	5473750.855	5908593.163	4792367.052	6531098.503	6787330.136	6882820.188	5854723.624	4113361.715	5618523.429	5386278.476	6556774.96	5363972.903	
carnitine	645964.22.64	62155517.82	65928442.12	57676692.62	48188382.69	52396593.57	59411552.57	58333347.43	55080830.78	66745857.09	61409721.96	58879359.64	59172383.75	53592169.02	62873399.91	74276221.67	64033896.75	61788038.08	
Methionine sulfoxide	90124.27125	47447.15	41186.36325	68778.18352	77134.73431	54713.69048	94828.60052	76077.06022	66170.56396	94255.112	61481.7323	138066.8896	92753.21161	48978.47268	81281.70143	81833.64417	105914.7133	158387.8152	
phenylalanine	5105923.072	5648900.148	5232437.941	6554605.242	5345584.151	4004192.382	2333777.103	3554859.441	2636615.397	6303400.508	4492470.994	6555887.021	3607212.62	3375454.673	6760557.411	9015599.066	4994588.861	5618124.151	
Pyridoxamine	3444.890341	N/A	8182.560305	N/A	N/A	N/A	N/A	N/A	N/A	5726.337536	5730.466845	4792.954925	N/A	N/A	N/A	N/A	N/A	N/A	
pyridoxine	N/A	3733.346008	1055.39313	9885.613397	16834.21234	10989.73779	7083.264895	13851.9911	81047.68385	5381.006169	10736.75587	9923.765385	3106.002673	10500.9845	8430.635485	22785.7998	8547.426092	N/A	
1-Methyl-Histidine	471694.8.049	2411722.719	386648.2.012	4662466.205	281119.4.351	3667917.496	1300998.506	1822644.404	3819789.729	2576801.97	1601209.168	2896685.464	2402859.906	1158024.531	2789709.264	4363931.127	2365539.66	4975057.445	
N-acetyl-L-ornithine	N/A	N/A	4478.585697	9840.667985	5494.992705	10453.56435	7575.413.19	8485.501792	N/A	15328.05489	9323.418974	4027.252439	5680.799636	N/A	7661.591779	9000.832617	11786.99188	13068.78269	
arginine	2049595.346	746407.3077	2450107.164	2724397.564	1343234.765	962094.4695	1120206.309	1196947.573	900079.0896	2378328.255	1651150.082	2386147.141	770684.2756	N/A	821390.2146	3039234.679	4170494.036	2926115.661	
citrulline	4401589.302	3532636.272	5209939.896	4124758.903	3395556.032	4367180.3	2325267.054	3710745.82	5057343.622	4768874.268	3028806.928	4148238.761	3835655.746	2645401.443	4085007.646	4408877.409	4655653.063	5407727.554	
N-carbamoyl-L-aspartate	15055.81249	20845.52753	33082.65541	21381.13191	197.92.69434	26627.70544	17313.85578	23470.8893	21847.091	17741.44428	23415.22467	29357.70745	27125.3423	18933.60422	25540.07858	35895.70845	19041.31728	35434.86312	
glucosamine	N/A	208365.5617	272283.9252	333448.4532	296337.995	278661.4766	N/A	N/A	283658.9701	429677.4653	332383.5144	1083171.644	314218.3692	187206.6712	687933.3753	1070789.828	593360.3587	617736.437	
tyrosine	2001116.915	1877103.054	2096943.191	1394971.876	1522385.556	1739783.778	1262500.507	1226609.239	2191230.725	1545500.437	1599712.072	1926269.117	1667438.04	1446219.575	1262838.741	2095155.47	1725363.013	2126545.19	
Phosphorylcholine	241285825.9	215502863	233678123.1	232738598	173545306.1	174771985	153537158.4	169506256.5	181746622.1	283502359	219343522	216921623	160208148.9	139117423.3	240440094	247111251.9	244007613.1	224724714.8	
3-phospho-serine	48965.24354	24452.00449	59295.35666	12494.13788	13009.59528	14700.78916	29507.82421	18958.33386	43928.74081	34328.635	31660.20145	57312.26262	40639.05882	30776.72839	32801.34507	26248.99186	38502.50296	25141.66432	
N6-Acetyl-L-lysine	4695199.696	1809263.083	462771.8.931	5753755.457	3908890.797	4152129.148	2560806.399	3541236.987	2009805.48	7649569.208	4022850.52	6473942.852	3234288.86	2079029.204	5936136.005	7455403.59	3560594.258	9587123.979	
Acetyllysine	3962637.756	2528609.582	178210.3.43	1564232.06	885802.4642	1123369.602	2402028.135	2532693.69	2687930.07	5017939.151	3839417.11	3009422.181	4819360.737	2823406.058	4865355	3329440.264	5664202.247	4955397.375	
N-acetyl-glutamine	230238.7948	154909.6443	143622.3802	183597.0291	138967.1827	114403.5381	76394.46238	100321.0421	128311.5325	120603.0258	136223.894	839641.67367	124008.2898	90927.41152	80635.11005	227659.0694	190570.993	133531.5715	
N-acetyl-glutamate	61494.61588	50474.92279	46299.66195	47212.06105	23377.27359	28425.04894	37382.83841	40029.72162	50890418.74	55225.30437	30690.73878	88220.26308	39922.71696	28087.31744	39844.29091	88383.92795	43362.65454	66203.7125	
Ng,NG-dimethyl-L-arginine	292296.2218	659875.2502	953275.2304	1064586.872	810608.9906	208826.4384	333385.4557	318698.5274	N/A	1109538.255	109729.2615	772646.6428	N/A	279406.2471	485006.1765	1250053.167	446006.4559	N/A	
Acetylcarnitine DL	49404007.13	55242607.41	41352291.34	74474479.77	62698140.76	70981277.93	34805249.08	37492235.64	40377019.81	62156690.25	48944996.69	68952430.05	56557548.13	40832593.97	51403016.26	65236067.03	59911661.25	57299181.1	
tryptophan	3634553.459	2722244.895	2666566.01	3653688.6	1965021.98	1780551.366	1719619.346	3413108.841	3078566.5	3667032.277	2875679.115	2821806.884	2519815.254	1847699.003	3405556.635	3930849.421	3316772.852	3762903.034	
Kynurenine	185998.3974	104755.5714	98995.1675	130763.2761	83896.62369	80439.37995	45998.9613	72967.735	83762.39114	120364.2287	84890.87871	81992.78244	65508.49017	60411.40911	99716.79112	180604.6364	125122.5342	99983.91835	
N-acetyl-glucosamine	N/A	N/A	N/A	N/A	N/A	N/A	N/A	N/A	N/A	N/A	N/A	N/A	N/A	N/A	3649.724067	N/A	7288.131103	4649.948433	
Flavone	18839.98277	25784.62575	28394.44759	52125.2687	51532.25296	12132.35478	40288.38231	29066.9097	46500.12239	51157.50275	40846.79223	32513.1071	36520.4485	34814.50722	30380.70778	22268.4734	19017.22865	19248.15701	
cystathionine	730394.3445	674245.0087	1016090.324	489773.7038	334624.9153	796067.0191	568424.5443	533537.659	579810.9517	651361.0448	537771.8518	1551261.53	762278.2846	671670.9495	1057042.845	666153.9344	772438.2765	1285890.758	
5-methoxytryptophan	N/A	N/A	4037.799625	N/A	8070.158462	5207.662105	N/A	5700.254521	9438.461176	7007.670012	N/A	4528.785412	5833.636216	4483.469241	5497.71296	5437.068287	N/A	N/A	
Cystine	127647.9703	68967.32341	64924.58526	69268.82117	38777.65386	17734.78366	21802.13276	15998.75635	17844.83801	6124.648177	10391.83421	8084.830761	10483.05943	6425.591672	12358.51482	41579.97384	38061.52068	3991.19664	

cytidine	180782.3947	175070.3539	163612.1622	1519227.13	940450.6377	1126698.015	146917.6994	141208.6662	116207.0958	306897.2628	158928.4644	319938.7445	221148.561	213117.1009	381413.0853	288964.6723	198522.928	174553.6287	
biotin	665306.3754	356806.4074	576459.4029	459796.2612	773574.7543	394191.349	744003.8823	N/A	121790.0017	58994.44559	318510.3721	641902.2626	248756.2867	294273.8848	43228.28971	71786.27848	76111.90146	49887.5718	
deoxyadenosine	N/A	8858.366766	5606.218718	10413.45845	8779.579694	6220.500531	4691.267931	4686.925179	13335.58494	8143.926183	11483.28914	12663.69757	16717.21876	5446.198617	9427.956271	8941.739687	12489.27263	17705.04727	
Glycerophosphocholine	20370783.3	16093903.45	10979796.28	18228378.67	11925331.77	11119006.92	22457756.18	16837566.14	9562000.542	34876400.86	26763392.85	24810470.54	32979170	23743653.34	25471744.2	31204600.34	24400797.18	26133108.29	
acadesine	N/A	N/A	N/A	N/A	N/A	4689.630214	N/A	N/A	5732.052748	5740.603739	N/A	N/A	N/A	N/A	N/A	5459.087977	4675.258427	4689.614926	
D-glucosamine-6-phosphate	51660.35836	48942.4088	80143.89277	75034.48878	45876.37917	69816.02143	58999.97139	73446.72608	60378.77021	131091.1529	90410.73407	114998.0961	86492.23787	54109.07778	48014.45814	116164.2144	70863.0119	102587.1567	
D-glucosamine-1-phosphate	17194.81368	7819.756078	N/A	21475.48255	5730.480095	N/A	5697.423168	15111.09257	10943.62865	7206.177698	8829.985346	8898.068164	N/A	6880.250936	7893.418757	18198.12019	14038.2763	13028.68028	
thiamine	25788.92866	N/A	N/A	N/A	N/A	17208.41607	29217.64898	N/A	27156.74633	48945.33724	N/A	33004.73249	35252.40275	10724.47555	20094.02164	84055.17004	16508.41516	83737.0759	
S-ribosyl-L-homocysteine-posi	26574.3266	22921.58961	23441.01923	18757.93249	8335.96107	8866.926165	12572.72757	20317.22672	24789.82238	28135.04453	19788.46968	16106.55696	21871.7256	20319.25079	20840.2312	30220.93642	27614.85869	14738.22996	
deoxyguanosine	23967.43245	14588.87703	24470.2517	11984.23628	N/A	16153.64841	10290.53047	12002.10688	4816.09453	23484.15634	7571.226432	18745.56084	16645.21213	12011.65658	9324.503237	25516.71387	18019.92781	17875.43082	
adenosine	5339.363439	N/A	N/A	15030.59498	11332.88825	13178.90072	N/A	7698.888816	19111.29409	N/A	3406.067804	16720.93939	7418.346128	6732.014148	6238.557208	9076.478329	8036.461324	16559.2403	
1-Methyladenosine	N/A	3139.87952	4167.867323	10941.74607	N/A	4186.50394	4688.167603	5731.982605	N/A	11459.59774	7308.085045	19277.05919	13024.0283	N/A	9368.317977	6771.375775	7293.114587	14067.83518	
guanosine	6229.32672	8900.96781	8368.047033	27173.4194	12542.68493	11985.31509	17707.44812	9375.53221	N/A	17119.91191	4681.203858	20714.16272	7322.851574	8863.608762	11028.29874	18224.29573	5234.746083	7306.467002	
L-arginino-succinate	105621.0061	123854.1597	12556.87128	152662.7627	67206.93278	106813.1274	115641.5133	94816.81423	130747.7499	165463.6697	94462.69756	84903.41166	151625.9551	76846.95644	69352.46729	157404.9962	94223.59585	122962.945	
S-methyl-5-thioadenosine	N/A	N/A	5349.907981	10785.38575	N/A	N/A	N/A	N/A	N/A	N/A	N/A	3600.186156	N/A	N/A	N/A	N/A	N/A	N/A	
7-methylguanosine	228213.3228	198519.1766	225090.6809	159430.9481	132760.1336	141198.1399	130762.0063	130811.7033	126089.559	241924.7473	222518.0913	317165.2787	186008.6091	111938.7705	196944.6891	237074.1678	321951.1792	419430.0601	
dCMP	18767.40883	21366.51992	35947.89166	33852.77703	34781.96626	40638.98606	22406.49876	19278.77526	14068.23882	33866.92865	16151.50725	19792.88224	30740.24741	30216.24477	16673.89036	39596.86543	32305.49719	19277.50416	
glutathione	6435981.349	10770549.23	11656932.45	12302783.22	8106676.114	9260587.57	8331183.115	7426243.677	8135741.145	5881359.967	7325212.968	4541748.618	5374078.91	7155610.084	6602596.932	6573918.412	5767744.482	4299102.496	
dTMP	13032.18327	5842.070654	8032.031519	28125.42653	12682.40466	26568.83383	18243.55497	N/A	16153.43111	16068.95147	13988.52047	17190.97474	11464.09721	15621.9687	13922.31273	17713.02751	25534.22538	11935.49171	
CMP	13919.28516	1240220.163	1011676.529	5123367.335	3130249.493	2948538.164	1237837.468	1156924.399	1320092.742	1449808.044	1620167.915	1578407.954	1546217.946	1128833.856	1412940.585	1626863.635	1539841.309	1236997.061	
UMP	501898.1541	853105.1925	434680.741	2639038.722	2343251.431	2538077.637	537331.983	499011.2812	579051.2654	614635.8369	580618.19	620841.509	614872.7016	549534.6154	505888.6474	630409.1158	901620.5127	486137.2027	
dAMP	24489.77486	21721.20483	30739.10268	56695.53381	38558.40116	30203.29104	28140.96867	25008.36364	34410.4726	23447.64288	16816.36995	37505.56661	19278.43137	11463.88204	29173.70097	17105.73169	11754.47581	33349.09634	
Nicotinamide ribotide	82518.27543	64136.46137	91316.11411	58380.3385	19020.17362	41448.30974	32810.20597	75337.14761	63735.98361	63357.01152	66544.95019	42545.81986	58302.43121	63760.58545	105871.6185	96496.4929	90564.40126	55684.00556	
aminoimidazole carboxamide ribonucleotide	6774.403029	6250.328715	5219.121384	5235.738819	14606.00568	9917.565865	N/A	N/A	5731.982532	N/A	7295.399683	N/A	N/A	3639.723472	N/A	5732.309367	5741.699561	N/A	
thiamine-phosphate	N/A	N/A	N/A	N/A	N/A	N/A	N/A	N/A	N/A	N/A	N/A	N/A	N/A	N/A	N/A	N/A	N/A	N/A	
dGMP	5209.384893	6252.382715	5731.968554	9897.255684	5238.277202	8331.863075	N/A	7295.08675	N/A	N/A	N/A	N/A	10941.70852	3646.635906	6255.925073	5211.626258	8335.487701	4690.861256	
AMP	41645215.97	35415147.15	24400802.22	57366090.45	44669159.98	49898357	29825165.56	28375185.79	28226067.13	31184937.16	36501949.97	29476075.29	31430826.56	29718335.6	32221879.7	33214998.92	45346859.14	27419248.52	
IMP	3929213.345	3086489.715	2190382.171	22500513.23	17390240.24	14857935.63	2976422.64	2725226.035	3390307.5	3381734.351	3621195.79	2935032.252	3625321.922	2341322.197	2593556.617	3511056.863	4709152.737	2836330.038	
S-adenosyl-L-methioninamine	N/A	N/A	N/A	N/A	N/A	N/A	N/A	N/A	N/A	N/A	N/A	N/A	N/A	N/A	N/A	N/A	N/A	N/A	
GMP	970510.5931	1161932.207	836218.3661	8176078.14	5136653.041	5600560.851	895097.2319	951339.1683	1207180.433	899244.5789	944918.6237	1053226.364	1034757.207	809533.7838	669046.5143	1034770.804	1139605.611	1024074.713	
xanthosine-5-phosphate	5211.626209	4162.720121	N/A	N/A	N/A	5213.125183	4156.400764	N/A	12504.84039	N/A	N/A	N/A	N/A	N/A	N/A	N/A	N/A	N/A	
riboflavin	8958.036142	18764.1656	14590.71182	17227.94496	N/A	10415.73144	21363.85512	8058.422239	11461.3942	15648.82743	24483.58559	19731.51699	29724.03422	6276.453128	13870.63996	15038.65195	9369.75294	53169.27329	
S-adenosyl-L-homoCysteine-posi	138080.7729	85462.70958	258431.505	212180.2735	170341.3113	282376.3254	127123.3731	133425.6951	132983.3218	259440.7787	133929.5426	593770.5604	174536.4678	65144.02393	121425.0177	304850.9103	213750.7386	292817.4876	
S-adenosyl-L-methionine	840969.845	458660.8132	507066.6586	372301.3015	191537.3456	230552.7628	208791.9413	228640.1301	214089.0268	446132.8228	416921.1852	231251.9124	261610.1865	296959.685	506119.7792	661798.707	588310.1948	699632.1136	
folate	N/A	N/A	3646.645714	3647.910881	3126.320092	N/A	N/A	N/A	3652.237985	N/A	3646.920524	N/A	4171.634035	N/A	N/A	N/A	N/A	3646.615197	
7,8-dihydrofolate	N/A	N/A	N/A	N/A	N/A	N/A	N/A	N/A	N/A	N/A	N/A	N/A	N/A	N/A	N/A	N/A	4167.236493	N/A	
5-methyl-THF	150310.4896	22930.7335	101329.5791	44134.58435	38743.47013	31273.08043	29713.74595	17832.09429	N/A	31071.08726	17676.27348	26109.38962	31085.47397	24415.18309	15905.65442	33474.47984	14154.29353	23831.88653	
Diiodothyronine	N/A	N/A	N/A	N/A	N/A	N/A	N/A	N/A	N/A	N/A	N/A	N/A	N/A	N/A	N/A	N/A	N/A	N/A	
glutathione disulfide-posi	2804215.373	1472005.524	1066558.194	1102973.59	683234.455	1326396.47	1108049.942	1495009.279	1171183.751	3753129.681	1357226.22	3160537.81	1988868.701	1183329.537	2833194.669	2613493.637	2725665.446	3303865.3	
NAD+-posi	2252809.697	2031103.566	3671513.627	1097241.068	897355.8855	983389.3096	1839488.493	2552986.162	2750961.519	2719797.699	2835635.002	2778958.599	1993688.802	1943903.683	2966611.117	3481127.544	2874470.763	2486538.699	
NADH	17193.81609	36990.66354	19799.51752	27612.50671	27093.0778	17715.12654	29707.42478	39595.86823	38556.83168	33867.61669	16144.57695	28649.35241	13030.43464	27095.89996	6745.885108	34387.40947	84930.77692	25531.64948	
dephospho-CoA-posi	N/A	6272.510923	N/A	N/A	N/A	N/A	N/A	N/A	N/A	5730.646126	4689.299987	6302.604059	7301.497763	11982.66317	7299.47203	7292.866158	10381.37964	5731.595443	
NADP+-posi	92739.96538	80684.94719	184347.9917	58877.36518	49355.71286	69892.63831	144333.0015	120289.3703	145813.6214	152640.3914	94826.47077	117413.1247	76684.28014	80629.41398	96311.59265	155791.5377	141910.1196	121292.6318	
NADPH	25145.32345	17186.07755	33380.70844	21379.84724	20089.92517	15881.63271	12505.11798	5735.387544	9379.689757	40527.71606	26009.69988	14588.01769	17193.90145	22962.13998	31830.50795	20854.47886	20840.67386	18780.62157	
coenzyme A-posi	25014.31141	35948.3579	41290.31313	27662.81237	37509.33379	20839.82978	41695.28278	16657.61831	24213.62679	18759.73917	28105.6566	9898.953242	22404.14867	40643.1505	44810.50326	24489.65371	16675.56498	15633.86525	
FAD	15109.50037	8856.255079	19801.04215	16672.35385	7807.368537	10419.46573	9900.606004	7293.20921	11975.9525	10422.314	7814.241628	22925.89686	11479.13717	6252.65158	9902.716871	24065.95005	18760.57211	18234.49198	
acetyl-CoA-posi	N/A	9378.416721	9691.941602	3751.532797	N/A	N/A	N/A	N/A	N/A	N/A	5314.364536	N/A	N/A	6877.39193	14692.9982	4376.677274	5940.11365	N/A	
propionyl-CoA-posi	N/A	N/A	N/A	N/A	N/A	N/A	N/A	N/A	N/A	N/A	N/A	N/A	N/A	N/A	N/A	N/A	N/A	N/A	
acetoacetyl-CoA-posi	N/A	N/A	3126.356167	N/A	N/A	N/A	3126.066791	N/A	N/A	N/A	N/A	N/A	N/A	N/A	7294.707693	4169.088334	N/A	N/A	
malonyl-CoA-posi	N/A	N/A	N/A	N/A	N/A	N/A	N/A	N/A	N/A	N/A	N/A	N/A	N/A	N/A	N/A	N/A	N/A	N/A	
succinyl-CoA-posi	N/A	9900.37683	9379.000669	N/A	N/A	N/A	N/A	N/A	N/A	N/A	N/A	N/A	N/A	N/A	6772.660553	3648.41101	N/A	N/A	
sarcosine	2881222.619	2741027.354	3211898.62	3158205.025	2474415.678	3913753.722	1961529.11	2341351.194	3047157.76	4002768.58	3388178.053	4378731.613	2594847.085	2081021.486	4051264.002	3423043.761	3066467.633	4194534.947	
putrescine	55798.97646	41322.43056	92651.20579	24154.07105	17995.00793	41412.25017	24965.04626	57566.68942	23696.99517	39513.56112	123088.193	149726.7873	135372.5961	73746.51427	78060.99471	97821.46438	53551.36285	54941.80825	
spermidine	210286.9822	200057.1511	N/A	289792.2043	134841.0583	203327.8109	240275.3582	257763.8813	387687.5858	177353.2086	237169.6667	307883.0641	241383.9006	225437.965	218001.1916	285645.9337	389900.22	328209.2987	
spermine	N/A	N/A	N/A	N/A	N/A	N/A	N/A	N/A	N/A	N/A	3124.61756	N/A	N/A	N/A	N/A	N/A	N/A	N/A	
N-acetyl spermine	38836.96581	21322.7741	33790.55768	13957.25198	14698.3788	8557.815279	9609.58484	15600.43073	17352.88708	N/A	17711.42171	9816.654611	8157.385799	13254.53484	10361.03941	22952.8452	32131.98258	39188.67247	
N-acetyl spermidine	7317.720232	4977.250635	11248.36212	10647.38502	13057.35	N/A	8220.869723	17258.43469	12356.20199	N/A	5607.618434	N/A	N/A	10160.86249	4719.102783	8116.045105	N/A	8388.332393	

Chapter 3: Mitochondrial enzyme GPT2 regulates metabolic mechanisms required for neuron growth and motor function *in vivo*.

This Chapter contains the paper published in Human Molecular Genetics in 2021, doi.10.1093/hmg/ddab269. I conducted all the experiments, Shawn M. Davidson ran LC-MS at Princeton. Ralph DeBerardinis contributed intellectually, and the project was performed under the supervision of Eric M. Morrow. For funding sources please refer to the Chapter.

Human Molecular Genetics, 2021, Vol. 00, No. 00 1–17

https://doi.org/10.1093/hmg/ddab269
General Article

GENERAL ARTICLE

Mitochondrial enzyme GPT2 regulates metabolic mechanisms required for neuron growth and motor function *in vivo*

Ozan Baytas[1,2,3], Shawn M. Davidson[4], Ralph J. DeBerardinis[5,6] and Eric M. Morrow[1,2,*,†]

[1]Department of Molecular Biology, Cell Biology and Biochemistry, Brown University, Providence, RI 02912, USA, [2]Center for Translational Neuroscience, Carney Institute for Brain Science and Brown Institute for Translational Science, Brown University, Providence, RI 02912, USA, [3]Neuroscience Graduate Program, Brown University, Providence, RI 02912, USA, [4] Lewis-Sigler Institute for Integrative Genomics, Princeton University, Princeton, NJ 08540, USA, [5]Department of Pediatrics, Children's Medical Center Research Institute, University of Texas Southwestern Medical Center, Dallas, TX 75390, USA and [6] Howard Hughes Medical Institute, UT Southwestern Medical Center, Dallas, TX 75390, USA

*To whom correspondence should be addressed. Tel: +1 4018639778; Fax: +1 4014321607; Email: eric_morrow@brown.edu

Abstract

The metabolic needs for postnatal growth of the human nervous system are vast. Recessive loss-of-function mutations in the mitochondrial enzyme glutamate pyruvate transaminase 2 (GPT2) in humans cause postnatal undergrowth of brain, and cognitive and motor disability. We demonstrate that GPT2 governs critical metabolic mechanisms in neurons required for neuronal growth and survival. These metabolic processes include neuronal alanine synthesis and anaplerosis, the replenishment of tricarboxylic acid (TCA) cycle intermediates. We performed metabolomics across postnatal development in *Gpt2*-null mouse brain to identify the trajectory of dysregulated metabolic pathways: alterations in alanine occur earliest; followed by reduced TCA cycle intermediates and reduced pyruvate; followed by elevations in glycolytic intermediates and amino acids. Neuron-specific deletion of GPT2 in mice is sufficient to cause motor abnormalities and death pre-weaning, a phenotype identical to the germline *Gpt2*-null mouse. Alanine biosynthesis is profoundly impeded in *Gpt2*-null neurons. Exogenous alanine is necessary for *Gpt2*-null neuronal survival *in vitro* but is not needed for *Gpt2*-null astrocytes. Dietary alanine supplementation in *Gpt2*-null mice enhances animal survival and improves the metabolic profile of *Gpt2*-null brain but does not alone appear to correct motor function. In surviving *Gpt2*-null animals, we observe smaller upper and lower motor neurons *in vivo*. We also observe selective death of lower motor neurons *in vivo* with worsening motor behavior with age. In conclusion, these studies of the pathophysiology of GPT2 Deficiency have identified metabolic mechanisms required for neuronal growth and that potentially underlie selective neuronal vulnerabilities in motor neurons.

[†]Eric M. Morrow, http://orcid.org/0000-0003-3430-3520
Received: June 8, 2021. **Revised:** September 6, 2021. **Accepted:** September 6, 2021

Introduction

After birth, the human brain and spinal cord continue to increase dramatically in size, reaching near adult proportions by age 6 (1–5). Postnatal growth of the nervous system is largely driven by axonal, dendritic, and synaptic growth, as well as glial development, as processes such as neurogenesis are completed prior to birth. The biosynthetic needs for postnatal nervous system growth are vast, particularly for long-projecting neurons such as in the motor system. The metabolic mechanisms governing this growth have broad significance to nervous system development and disease.

Genetic diseases offer a powerful lens to investigate metabolism in the human brain. Childhood metabolic diseases may also be amenable to treatments via dietary restrictions or supplements (6). We have identified a new childhood neurometabolic disease caused by autosomal recessive, loss-of-function mutations in the mitochondrial enzyme glutamate pyruvate transaminase 2 (*GPT2*) (7). GPT2 Deficiency is associated with undergrowth of the brain in the postnatal period (i.e. postnatal microcephaly), as well as cognitive and motor disability. Motor disability in GPT2 Deficiency has been diagnosed as progressive spastic paraplegia, a condition preferentially affecting lower limbs and construed to be caused by selective vulnerabilities in long-projecting motor neurons (7,8). Spastic paraplegia has been linked to over 70 genetic loci; however, there are only a limited number of genes reflecting a mitochondrial process (8). Knowledge of GPT2 function, therefore, may contribute uniquely to an understanding of metabolic mechanisms governing neuronal growth, as well as to selective neuronal vulnerabilities in large and long-projecting neurons, such as motor neurons.

GPT2 is one of two transaminases that catalyze the reversible addition of an amino group from glutamate, the major excitatory neurotransmitter in brain, to pyruvate, yielding alanine and α-ketoglutarate, a tricarboxylic acid (TCA) cycle intermediate (9). GPT2-mediated metabolism has been studied in the context of cancer, particularly the role of GPT2 in supporting the TCA cycle (10–14). The TCA cycle enables fuel oxidation, as well as cataplerosis, the process wherein TCA cycle intermediates are consumed for synthesis of macromolecules for cell growth (15). Anaplerosis is the process whereby TCA cycle intermediates are replenished. Homeostatic regulation of anaplerosis and cataplerosis is crucial for times of high biosynthetic need, such as postnatal brain development during which there is a strong upregulation in *GPT2* expression (7).

In the current study, we discover GPT2-mediated metabolic processes critical for neuronal growth and motor function. Both germline and conditional pan-neuronal deletion of GPT2 in mice result in motor abnormalities and premature death pre-weaning. Motor abnormalities include wide hind-limb gait, reminiscent of spastic paraplegia in humans. We demonstrate that GPT2-mediated metabolic fluxes into alanine and the TCA cycle are required preferentially for neurons, despite expression in both neurons and glia. We also find metabolic impairments in the *Gpt2*-null brain starting in the first postnatal week, including reduced levels of alanine and TCA cycle intermediates, followed by abnormalities in amino acid and glucose metabolism. Alanine, a non-essential amino acid, becomes essential for survival and growth of *Gpt2*-null neurons *in vitro*, but not for *Gpt2*-null astrocytes. Treatment of *Gpt2*-null animals with supplemental dietary alanine extends survival of mutant animals but does not ameliorate motor function. Lifespan extension of *Gpt2*-null animals on the high-alanine diet permitted us to study the progression of neuropathology and to identify selective death of lower motor neurons in *Gpt2*-null spinal cords. Overall, our data point to alanine as a potential therapeutic supplement for human patients with GPT2 Deficiency and identify a central role for GPT2-mediated mechanisms in neuronal growth, particularly in long-projecting neurons in motor circuitry.

Results

GPT2 activity is required in neurons *in vivo* for motor function and animal survival

We observed a motor phenotype in germline *Gpt2*-null mice, potentially akin to spastic paraplegia that is observed in patients with GPT2 Deficiency. In order to study the neuronal requirements of GPT2 as it may relate to this motor phenotype, we generated a neuron-specific deletion of GPT2. We mated mice carrying a conditional *Gpt2* allele, with loxP sites flanking exon 4 (Fig. 1A), to mice expressing Cre-recombinase driven by the rat Synapsin-I promoter, allowing for cell-specific deletion of GPT2 in neurons starting at as early as embryonic day 12 (16). Of the tissues examined, excision of exon 4 by Synapsin-I-Cre–mediated recombination was observed only in the nervous tissue, brain and spinal cord (Fig. 1B). The excised allele was not present in the liver, kidney or hind-limb or fore-limb muscle. The neuronal specificity of the Synapsin-I-Cre line was further confirmed by an Ai14-tdTomato Cre reporter line (Supplementary Material, Fig. S1). We previously reported that *Gpt2*-null mice demonstrated premature death between postnatal day 18 (P18) and P28 (7). The pan-neuronal deletion of GPT2 (the mice hence named SynI-cKO) resulted in a similar premature death phenotype as observed for *Gpt2*-null mice (Fig. 1C). All *Gpt2*-null mice ($n = 56$) and SynI-cKO mice ($n = 34$) died by P28. SynI-cKO mice also started showing weight loss at the same time as *Gpt2*-null mice, at approximately P18 (Fig. 1D).

Gpt2-null and SynI-cKO mice demonstrated a similar motor phenotype, involving motor weakness particularly of hind-limbs, beginning at approximately P18. To measure overall limb grip strength, we performed the wire hang test on *Gpt2*-null and SynI-cKO mice (Fig. 1E). Both groups displayed average and maximum hanging times less than 50% of their wild-type (WT) littermates' performances, indicating poor grip strength and weakness (average hanging time WT: 28.1 ± 2.3, *Gpt2*-null: 12.52 ± 1.5, SynI-cKO: 10.6 ± 0.9 seconds). Both *Gpt2*-null and SynI-cKO mice had hind-limb clasping reflex (Fig. 1F and Supplementary Material, Videos S1–S3). Furthermore, gait with a wide hind-limb stance was also present in both *Gpt2*-null and SynI-cKO mice as quantified by DigiGait, a ventral plane videography of rodent gait on a treadmill (Fig. 1G). Further, in the open field arena, animals could be seen dragging their hind-limbs, again reflecting weakness of the hind-limbs (Supplementary Material, Videos S4–S6). Overall, these data indicate the importance of the GPT2 enzyme in motor function and mouse survival. Deletion of GPT2 specifically in neuronal cells was sufficient to cause a similar behavioral phenotype as the germline *Gpt2*-null, emphasizing the requirement for GPT2 enzyme activity in neurons.

Metabolomics across postnatal development in *Gpt2*-null brain identifies the trajectory of dysregulated metabolic pathways

In order to investigate the role of GPT2 in postnatal brain growth and to observe the progression of metabolic perturbations

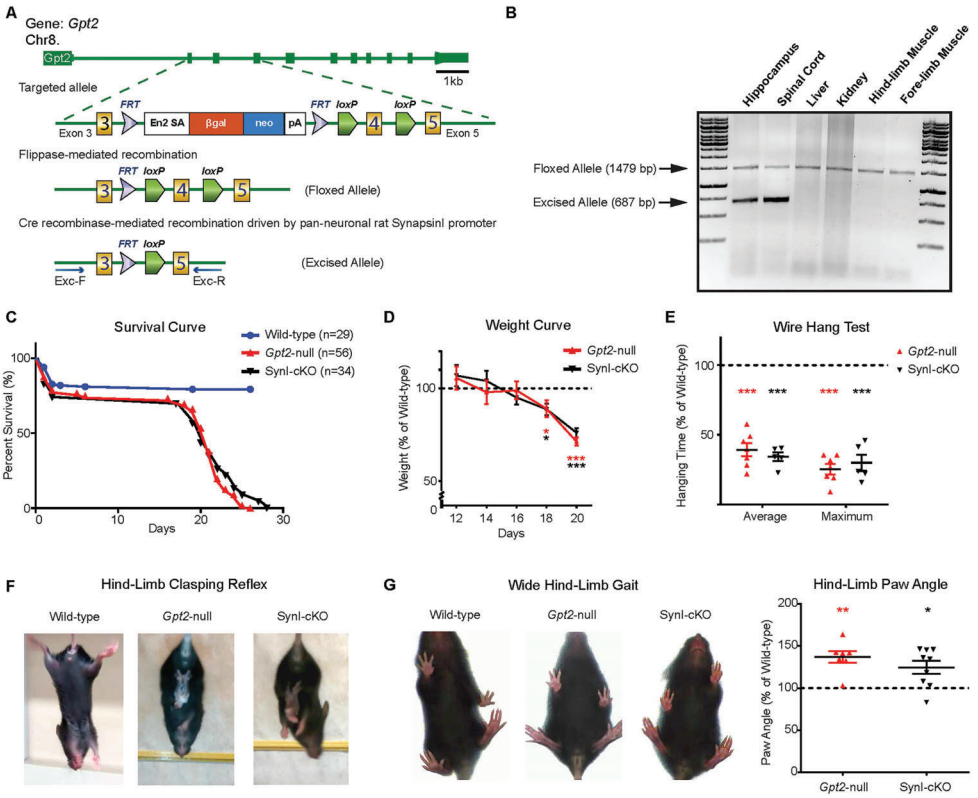

Figure 1. GPT2 activity is required in neurons *in vivo* for motor function and animal survival. (**A**) Schematic depicting disruption of the *Gpt2* gene at the mouse genomic locus, leading to the germline-null and conditional alleles. The targeted allele consists of flippase recognition sites (FRT) flanking a cassette containing a strong splicing acceptor site (Engrailed 2-SA), β-galactosidase gene, neomycin resistance gene and polyadenylation site between exon 3 and exon 4. After flippase-mediated recombination, the floxed *Gpt2*-allele is converted to a conditional construct with two loxP sites flanking exon 4 (the floxed allele). Prior to Cre recombinase-mediated excision by a tissue-specific promoter, the floxed allele produces a normal GPT2 protein. The excised allele is detected with primers Exc-F & Exc-R (see Materials and Methods). (**B**) Validation of the conditional allele *in vivo*. Cre recombinase driven by the rat Synapsin-I promoter excises exon 4 only in neuronal cells. In PCR genotyping, the floxed allele appears at 1479 bp and the excised allele at 687 bp. The excision of exon 4 is absent in non-neuronal tissues such as liver, kidney and muscle. (**C**) Similar timelines of postnatal death in germline *Gpt2*-null and Synapsin-I-Cre conditional mutant (Synl-cKO) animals. Survival curves of wild-type (blue), germline *Gpt2*-null (red) and Synl-cKO (black) mice. Wild-type $n = 29$ mice, *Gpt2*-null $n = 56$, Synl-cKO $n = 34$. Log-rank (Mantel-Cox) test was used to determine differences between the curves. $P < 0.0001$ (wild-type versus *Gpt2*-null), $P < 0.0001$ (wild-type versus Synl-cKO), $P = 0.5777$ (*Gpt2*-null versus Synl-cKO). (**D**) Reduction in weight gain in germline *Gpt2*-null and Synl-cKO animals compared to wild-type. Weight curves of *Gpt2*-null (red) and Synl-cKO (black) animals expressed as a percentage of their wild-type littermates ($n = 7$–11). $^{*}0.01 < P < 0.05$, $^{**}0.001 < P < 0.01$, $^{***}P < 0.001$. (**E**) Reduced performance on wire hang test by *Gpt2*-null (red) and Synl-cKO (black) animals. Average and maximum hanging times are expressed as a percentage of their wild-type littermates. $^{***}P < 0.001$. (**F**) *Gpt2*-null and Synl-cKO mice demonstrate hind-limb clasping reflex. When suspended by the tail, the wild-type mice extend their hind-limbs but the *Gpt2*-null and Synl-cKO mice bend their hind-limbs toward the body midline and clasp their hind paws. (**G**) *Gpt2*-null and Synl-cKO mice stand in a wide stance with hind paws spread further apart. Representative images of wide hind-limb gait in *Gpt2*-null and Synl-cKO mice and quantification of the absolute paw angle with respect to the midline, expressed as a percentage of their wild-type littermates; *Gpt2*-null: $136.9 \pm 6.8\%$ $P = 0.0017$, Synl-cKO: $124.7 \pm 7.5\%$ $P = 0.011$. Data were collected and analyzed with DigiGait software.

during postnatal brain development in *Gpt2*-null mice, we conducted targeted polar metabolic profiling on acutely dissected hippocampus at P0, P7, P14 and P18 (Fig. 2 and Supplementary Material, Tables S1–S4). We chose hippocampus as the target tissue to monitor metabolic changes, given the high *Gpt2* gene expression (7). Notably, alanine was among the first metabolites in the entire metabolome in *Gpt2*-null hippocampus to show a significant fold change with respect to the WT littermate controls, evident as early as P0 (Fig. 2C and E). Alanine levels were increased at P0, $134 \pm 7.9\%$ of WT ($P = 0.0035$), then gradually reduced to $89 \pm 1.7\%$ ($P = 0.0024$) at P7, then to $74 \pm 2.6\%$ ($P = 1.16 \times 10^{-6}$) at P14 and finally to $72 \pm 2.6\%$ of WT at P18 ($P = 3.20 \times 10^{-7}$). With regard to the other metabolites in the GPT2 reaction (Fig. 2C), pyruvate remained within the range of the WT levels at P0, P7 and P14 but reduced to $60.8 \pm 4.9\%$ of the WT at P18 ($P = 0.008$). Glutamate levels were slightly elevated in the *Gpt2*-null tissue at P7 ($112.3 \pm 2.1\%$, $P = 0.0103$) but then gradually decreased at P14 ($91.2 \pm 2.9\%$, $P = 0.0423$) and at P18 ($69.5 \pm 4.4\%$,

$P = 0.0001$) in comparison to WT. Alpha-ketoglutarate levels in *Gpt2*-null tissue remained similar to WT levels at P0, P7 and P14 but increased at P18 ($134.7 \pm 10.6\%$, $P = 0.011$).

To investigate how the global metabolic profile changes in the hippocampus during postnatal development, we plotted the 2-D scores of the principal component analysis (PCA) of the metabolomics data (Fig. 2D). The two groups, WT and *Gpt2*-null, did not separate well at ages P0 and P7. However, consistent with upregulation of the GPT2 protein in the brain postnatally (7), at P14 and P18, the metabolic profile of *Gpt2*-null hippocampus was distinctly different from WT. The indistinct metabolic profiles seen at P0 and P7 point out that any significant changes happening early during the first postnatal week, such as changes in alanine, likely reflect primary effects of GPT2 Deficiency.

For a more comprehensive view of the metabolome, volcano plots were graphed (Fig. 2E). At P0, alanine and kynurenic acid were elevated, whereas tryptophan and xanthurenic acid were decreased. At P7, the early decrease of alanine was accompanied by reductions in malate ($80.7 \pm 5.4\%$, $P = 0.0126$) and fumarate ($86.5 \pm 5.4\%$, $P = 0.0286$) levels, key metabolites of the TCA cycle, as well as a reduction in serine ($74.4 \pm 3.5\%$, $P = 2.7 \times 10^{-4}$), a major interconvertible precursor of alanine (17).

Subsequent to decreases in alanine and TCA cycle intermediates, we noted elevations in several amino acids. At P14, alanine dropped to 74% of the WT value, along with reductions in TCA cycle intermediates including malate ($73.1 \pm 3.2\%$, $P = 1.87 \times 10^{-6}$), fumarate ($78.7 \pm 2.2\%$, $P = 1.55 \times 10^{-5}$) and succinate ($75.5 \pm 2\%$, $P = 7.18 \times 10^{-6}$). At P14, although glutamate levels were at 91% of the WT, some of the other amino acids were elevated, such as valine, threonine, proline, arginine and leucine–isoleucine. Serine levels were still low in *Gpt2*-null hippocampus at P14 ($70.3 \pm 2.7\%$, $P = 8.58 \times 10^{-4}$) (Fig. 2E).

At P18, 7 out of 10 essential amino acids had increased levels in the *Gpt2*-null hippocampus, including valine, leucine–isoleucine, phenylalanine, threonine, lysine and arginine (Fig. 2E). Methionine, tryptophan and histidine remained unchanged. On the other hand, from the non-essential amino acids, only proline showed an increase ($181.8 \pm 6.6\%$, $P = 2.3 \times 10^{-5}$), whereas alanine ($72 \pm 2.6\%$, $P = 3.2 \times 10^{-7}$), glutamate ($69.5 \pm 4.4\%$, $P = 0.0332$), serine ($69.8 \pm 2.3\%$, $P = 0.0003$) and cysteine ($67.3 \pm 9.9\%$, $P = 0.0478$) showed a decrease. The *GPT2* gene has been shown to be a target of the stress-induced transcription factor ATF4, which promotes transcription of metabolic enzymes and amino acid transporters at times of metabolic stress such as amino acid limitation (14,18,19). However, we found no increases of ATF4 protein levels in cortex, hippocampus or liver tissue of *Gpt2*-null mice at P18, suggesting the elevation of amino acids in the *Gpt2*-null metabolome was not caused by a compensatory increase of ATF4 (Supplementary Material, Fig. S2A).

The overall decline of TCA cycle intermediates at P18 was accompanied by dramatic increases in levels of almost all glycolytic intermediates except pyruvate, including glucose 6-phosphate ($380.3 \pm 25.8\%$, $P = 7.64 \times 10^{-6}$), fructose 1,6-bisphosphate ($453.8 \pm 65\%$, $P = 9.15 \times 10^{-5}$) and phosphoenolpyruvate ($244.1 \pm 29.6\%$, $P = 0.0075$). We searched for protein level increases in glycolytic enzymes such as hexokinase I and pyruvate dehydrogenase, but these proteins were not increased in hippocampus (Supplementary Material, Fig. S2B). These data suggest that the increases in glycolytic intermediate metabolites may be due to regulation of enzyme activities at a substrate level, given that pyruvate levels are particularly reduced in *Gpt2*-null hippocampus at P18, which would directly promote glycolysis. Overall, the metabolomics data indicate that alanine synthesis is one of the first metabolic pathways that was altered as a result of loss of GPT2 in postnatal brain development. The early decline in alanine levels was followed by reductions in TCA cycle intermediates and subsequent increases in amino acids and glycolytic intermediates in *Gpt2*-null hippocampus.

GPT2 is enriched in neurons as compared to astrocytes

Brain metabolomics studies indicated that alanine biosynthesis was altered early in postnatal development in the *Gpt2*-null brain (Fig. 2). One intriguing possibility of a mechanism for pathogenesis is that alanine, normally a non-essential amino acid, has become an essential amino acid in GPT2 Deficiency. Before investigating the role of GPT2 in alanine biosynthesis in neurons and astrocytes, we characterized GPT2 expression in these cells.

We initially confirmed mitochondrial localization of GPT2 in the mouse brain. After subcellular fractionation of the whole mouse brain at P18, GPT2 was enriched in the mitochondrial fraction, whereas the paralog of GPT2, GPT1, remained in the cytosolic fraction (Fig. 3A). Enzyme activity in the mitochondrial fractions of *Gpt2*-null whole mouse brains revealed almost zero alanine transaminase activity (Fig. 3B), confirming the localization of GPT2 to the mitochondria at the activity level and the absence of GPT1 in mitochondria based on enzyme activity.

GPT2 expression was more enriched in neurons than astrocytes. We separately cultured cortical neurons and astrocytes from brains of newborn mouse pups and examined GPT2 expression by western blotting. We observed both GPT2 and GPT1 in both cortical neuronal and astrocyte-enriched cultures; however, GPT1 appeared far less abundant in the neuronal culture (Fig. 3C). The ratio of GPT2 to GPT1 band intensities was significantly greater in cortical neuronal cultures (36.15 ± 7.7) than astrocyte cultures (5.98 ± 1.88). Notably, the *Gpt2*-null cortical neuronal cultures had significantly more reduction in total alanine aminotransferase activity ($35 \pm 1\%$ of WT) than *Gpt2*-null astrocytes ($52.3 \pm 3.1\%$ of WT) as compared to the corresponding WT cultures, confirming the enrichment of GPT2 in neurons (Fig. 3D). Confocal microscopy images of cortical neurons (days *in vitro*—DIV14) and astrocytes in culture revealed the presence of GPT2 in both cell types co-localizing with the mitochondrial marker MitoTracker Red (Fig. 3E). In addition, we analyzed *Gpt1* and *Gpt2* gene expression in the adult mouse hippocampus *in silico*. We curated the number of transcripts from the single-cell RNA sequencing data that are publicly available in DropViz (www.dropviz.org) (20) (Supplementary Material, Fig. S3). We found that mouse neurons preferentially express the *Gpt2* isozyme. *Gpt1* expression was virtually absent, whereas the astrocytes expressed both isozymes. Overall, these data suggest the enrichment of GPT2 in neuronal cells.

Alanine biosynthesis and glutamine-fueled anaplerosis are diminished in *Gpt2*-null neurons *in vitro*

To study alanine biosynthesis in *Gpt2*-null cells, we investigated the conversion of glutamine or glucose into alanine via isotope tracing experiments with [α-^{15}N]-glutamine and [U-^{13}C]-glucose in cortical neuronal and astrocyte-enriched cultures (Fig. 3F and G). After 24 h in Tyrode medium (artificial cerebrospinal fluid-like, see Materials and Methods), fractional enrichment of labeled alanine in the WT cortical neuronal culture was $28.3 \pm 1.9\%$ and $29.6 \pm 4.8\%$ with the [α-^{15}N]-glutamine and [U-^{13}C]-glucose precursor, respectively (Fig. 3G, top). In contrast, in *Gpt2*-null cortical neurons, neither [α-^{15}N]-glutamine nor [U-^{13}C]-glucose precursors resulted in labeling of

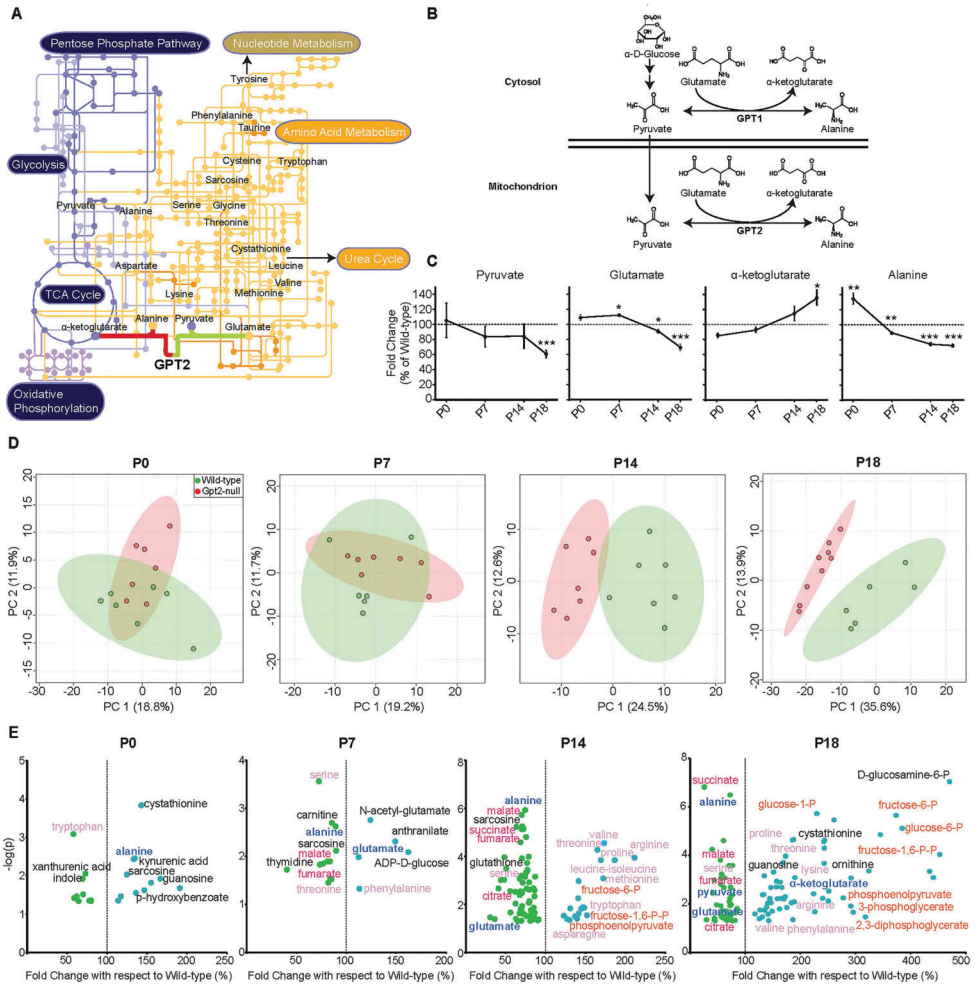

Figure 2. Metabolomics in *Gpt2*-null hippocampus across postnatal development reveals the trajectories of defective metabolic pathways. (**A**) GPT2 and the relevant metabolic pathways. The metabolic pathway map was modified from KEGG (Kyoto Encyclopedia of Genes and Genomes) (https://www.kegg.jp/) (48). GPT2 links amino acid metabolism (orange pathways and nodes) to the TCA cycle metabolism and glycolysis (dark purple pathways and nodes). The metabolic network illustrates the interconnection of pathways that GPT2 has an immediate influence on as well as more remote connections such as, nucleotide metabolism, pentose phosphate pathway and the urea cycle. (**B**) In the mitochondrion, the primary reaction of GPT2 involves a reversible transfer of an amino group from glutamate to pyruvate yielding alanine and α-ketoglutarate. The cytosolic paralog, GPT1, catalyzes the same transaminase reaction. (**C**) Fold changes of the metabolites in the GPT2 reaction in *Gpt2*-null hippocampus across postnatal development. The peak intensities obtained from targeted tandem liquid chromatography–mass spectrometry (LC–MS/MS) were normalized to the sample median. At each time point, *Gpt2*-null (P0: $n = 7$, P7: $n = 6$, P14: $n = 7$, P18: $n = 9$) was compared to the average of the wild-type (P0: $n = 7$, P7: $n = 7$, P14: $n = 7$, P18: $n = 6$). One sample t-test was run for each metabolite ($^{*}0.01 < P < 0.05$, $^{**}0.001 < P < 0.01$, $^{***}P < 0.001$). (**D**) 2-D Score Plots of PCA in the *Gpt2*-null hippocampus. The peak intensities obtained from LC–MS/MS were normalized to the sample median and auto-scaled (mean-centered and divided by the standard deviation of each group). Analyses were performed in MetaboAnalyst 4.0 (https://www.metaboanalyst.ca). (**E**) Volcano plots of significantly changed metabolites in *Gpt2*-null hippocampus across postnatal development. The fold changes are expressed as a percentage of the wild-type average. Note the greater $-\log(P)$ value on the y-axis, the stronger the raw *P*-value is. The dashed line is positioned at 100% of wild-type, so that any metabolite (green dots) left of the line had a reduced level and any metabolite (blue dots) right of the line had an increased level in *Gpt2*-null hippocampus. Dark blue metabolites are the GPT2 primary reaction metabolites (alanine, α-ketoglutarate, pyruvate, glutamate), magenta metabolites are TCA cycle intermediates, pale pink metabolites are proteinogenic amino acids and orange metabolites are glycolysis intermediates. The entire metabolomics data sets along with false discovery rates for each metabolite can be found in Supplementary Material, Tables S1–S4.

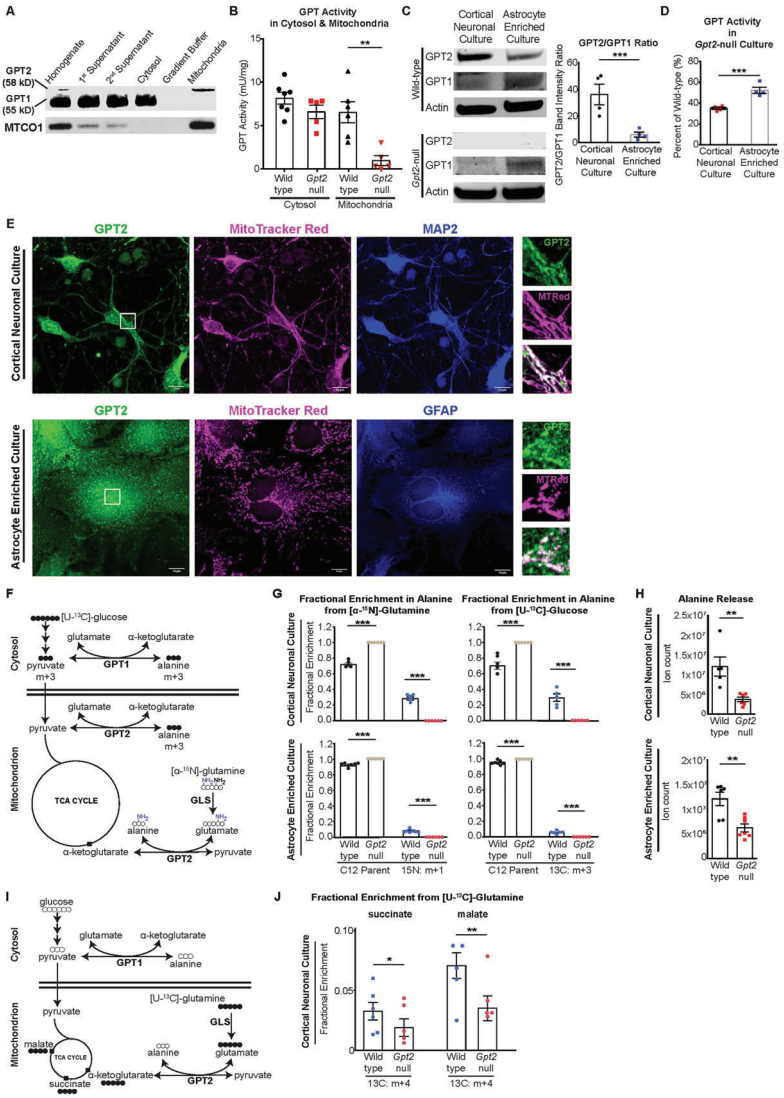

Figure 3. GPT2 is enriched in neurons and sustains alanine biosynthesis and the TCA cycle in neurons *in vitro*. (**A**) Western blotting of GPT2 and GPT1 in subcellular fractions of the mouse brain at P18. GPT2 (58 kDa) was present only in the total homogenate and mitochondrial fractions. GPT1 (55 kDa) was present in the homogenate and other intermediate fractions containing cytosol but not in the mitochondrial fraction. MTCO1: Mitochondrially encoded cytochrome c oxidase subunit 1. (**B**) GPT enzyme activity assay in the cytosolic and mitochondrial fractions extracted from wild-type and *Gpt2*-null mouse brain. Wild-type cytosol: 8.15 ± 0.68 mU/mg; *Gpt2*-null cytosol: 6.57 ± 0.77 mU/mg; wild-type mitochondria: 6.53 ± 1.21 mU/mg; *Gpt2*-null: 0.95 ± 0.58 mU/mg. $^{**}P = 0.0038$. (**C**) GPT2 is enriched in neuronal cultures as compared to GPT1, which is more abundant in astrocytes. Representative images of western blotting of GPT2 and GPT1 in wild-type and *Gpt2*-null cortical neuronal and astrocyte-enriched cultures. Quantification of the ratio of GPT2 to GPT1 band intensity (right). $^{***}P = 0.009$. (**D**) GPT enzyme activity assay in *Gpt2*-null cortical neuronal and astrocyte-enriched cultures expressed as percentage of their wild-type littermate cultures. $^{***}P = 0.0006$. (**E**) Primary cortical neurons (top) and astrocyte-enriched cultures (bottom) from wild-type mice demonstrate localization of GPT2 to mitochondria. Confocal microscopy images of GPT2 (green), MitoTracker Red CMXRos (magenta) and MAP2 or GFAP (blue). Scale bar: 10 μm. Regions boxed in white in the images on the left (GPT2) were magnified and are depicted in images on the right to demonstrate co-localization of GPT2 and MitoTracker Red. (**F**) Metabolic pathways that convert [U-^{13}C]-glucose and [α-^{15}N]-glutamine into alanine. GLS: Glutaminase. The filled circles refer to heavy isotope 13-carbon atoms. The heavy nitrogen isotope is highlighted blue. Molecules with heavy isotopes are designated as 'm + #' and the number refers to the number of heavy isotope atoms. (**G**) GPT2 is required for alanine synthesis from glucose or glutamine in both primary neurons and

alanine. In astrocyte-enriched WT cultures (Fig. 3G, bottom), fractional enrichment of labeled alanine was 8.3 ± 0.9% and 5.1 ± 0.8% with the [α-^{15}N]-glutamine and [U-^{13}C]-glucose precursor, respectively, a far lower level of labeling than in WT neurons. As in *Gpt2*-null neurons, *Gpt2*-null astrocytes showed no labeling of alanine from either [α-^{15}N]-glutamine or [U-^{13}C]-glucose. Alanine release into the Tyrode medium was also substantially reduced in *Gpt2*-null cortical neurons and astrocytes (Fig. 3H). Importantly, the reduction in alanine release was more pronounced in cortical neuronal cultures (31.2 ± 5.1% of WT) than in astrocyte cultures (51.2 ± 6.5% of WT). Thus, in the medium conditions tested, *Gpt2*-null cortical neurons and astrocytes lacked the ability to produce alanine from either glutamine or glucose. The lack of labeling of alanine in *Gpt2*-null cells, despite the expression of GPT1, indicates that GPT2 is mainly responsible for alanine synthesis. In addition, the greater enrichment of labeled alanine in cortical neuronal cultures compared to astrocyte cultures suggests that the GPT2 reaction is more engaged to synthesize alanine in neurons compared to astrocytes.

Our data indicate that GPT2 supports the TCA cycle in cortical neuronal cultures (Fig. 3I and J). In *Gpt2*-null neurons, fractional enrichment of TCA cycle intermediates from ^{13}C-glutamine was reduced by approximately 40–50%. Fractional enrichments in labeled succinate from [U-^{13}C]-glutamine precursor were 3.27 ± 0.74% and 1.89 ± 0.72% for the WT and *Gpt2*-null cortical neuronal cultures, respectively. Similarly, fractional enrichments in labeled malate from [U-^{13}C]-glutamine precursor were 7.91 ± 1.2% and 3.93 ± 1.16% for the WT and *Gpt2*-null cortical neuronal cultures, respectively. These data indicate that glutamine-fueled anaplerosis in *Gpt2*-null neurons is significantly diminished.

Exogenous alanine is required for survival of *Gpt2*-null neurons *in vitro* and extends lifespan of *Gpt2*-null animals *in vivo*

Given the profound decrease in alanine biosynthesis, particularly in neurons, we tested the hypothesis that exogenous alanine may be essential for growth and survival of *Gpt2*-null cells. To test this hypothesis in neurons, we continuously monitored cell death in these cultures (Fig. 4A). *Gpt2*-null hippocampal cultures deprived of alanine showed significantly greater apoptotic cell death than *Gpt2*-null neurons with alanine or WT neurons, as measured by fluorescence of Annexin V Orange Reagent. We also measured neurite length (neurite phase confluence) in hippocampal neuronal cultures with alanine deprivation (Fig. 4B). Growth of neurites as measured by increases in neurite length using the IncuCyte S3 Live-Cell Analysis System came to a halt in *Gpt2*-null neuronal cultures without alanine. As expected, WT cultures grown in medium with or without alanine showed a similar growth pattern, confirming that alanine is a non-essential amino acid in WT cultures. In a complementary experiment using Opera Phenix High Content Screening Confocal Microscopy, neurons (NeuN+) and apoptotic cells (cleaved Caspase3+, Cas3+) were counted at DIV14 after alanine deprivation in hippocampal neuronal cultures (Fig. 4C). NeuN+ counts for *Gpt2*-null cultures deprived of alanine were greatly reduced. *Gpt2*-null cultures with alanine had slightly reduced NeuN+ counts compared to WT cultures, albeit without statistical significance (with alanine, WT: 470 ± 78.5 versus *Gpt2*-null: 331 ± 59.7, $P = 0.2093$). Cas3+ to NeuN+ count ratio was greater in *Gpt2*-null cultures deprived of alanine compared to WT cultures. Therefore, both live-cell analysis (IncuCyte) and high-content imaging (Opera Phenix) experiments showed independently that exogenous alanine needs to be supplied for the survival of *Gpt2*-null neurons *in vitro*. To test the reliance of synapse development on exogenous alanine *in vitro*, we stained *Gpt2*-null cultures for synaptic vesicle glycoprotein 2 (SV2) and imaged cells using Opera Phenix High Content Screening Confocal Microscopy (Supplementary Material, Fig. S4). Synapse counts (SV2 puncta) per nuclei were greatly reduced in *Gpt2*-null cultures deprived of alanine. Interestingly, *Gpt2*-null cultures grown with alanine also had modestly fewer SV2+ puncta compared to WT cultures, indicating loss of GPT2 leads to decreased synaptogenesis that is specifically enhanced by alanine deprivation.

In contrast to *Gpt2*-null neurons, which required exogenous alanine, *Gpt2*-null astrocytes deprived of alanine grew comparably to controls *in vitro* (Fig. 4D). The cell growth of *Gpt2*-null astrocytes over time, as determined by IncuCyte Live-Cell Analysis, was not impacted by alanine deprivation. It is important to note that WT and *Gpt2*-null astrocytes grew much better in astrocyte-plating medium (APM), which has regular fetal bovine serum, compared to the cultures that had custom-made media with dialyzed fetal bovine serum. We repeated the alanine deprivation experiment in astrocyte cultures using Opera Phenix High Content Screening Confocal Microscopy (Fig. 4E). Astrocytes were examined 14 days after alanine deprivation. GFAP+ cell count and Cas3+ count to GFAP+ count ratio were similar between WT and *Gpt2*-null astrocytes. Thus, unlike neurons, *Gpt2*-null astrocytes were able to grow in alanine-deficient media. To address the role of GPT2 in astrocytes *in vivo*, we used the GFAP-Cre 77.6 line (21) to delete GPT2 specifically in astrocytes in living animals. Unlike SynI-cKO and conventional germline *Gpt2*-null mice, GFAP-Cre conditional *Gpt2*-null mice survived past P30 and into adulthood, indicating that GPT2 expression in astrocytes is dispensable for animal survival (Supplementary Material, Fig. S5). Overall, the need for GPT2 was more apparent in neurons compared to astrocytes both *in vitro* and *in vivo*, and there is a requirement for exogenous alanine in *Gpt2*-null neurons *in vitro*.

Given the observation that exogenously supplied alanine is required for *Gpt2*-null neurons *in vitro*, we set out to test the hypothesis that supplemental dietary alanine would ameliorate the phenotype seen in *Gpt2*-null animals *in vivo* (Fig. 5). We increased the alanine content from 1.19% alanine (regular alanine diet, RA) to 5% alanine (high-alanine diet, HA) by weight in the rodent diet given *ad libitum*. We first investigated the extent to which alanine levels were affected in the serum of *Gpt2*-null mice. *Gpt2*-null mice fed RA diet showed substantial reductions in the serum alanine concentration at P18 [WT (RA) 0.776 ± 0.006 mM versus *Gpt2*-null (RA) 0.652 ± 0.025 mM, $P = 0.0007$] (Fig. 5A). Importantly, in the *Gpt2*-null animals, the

astrocytes. Fractional enrichment in alanine from [α-^{15}N]-glutamine (left) or [U-^{13}C]-glucose (right) in wild-type and *Gpt2*-null cortical neuronal cultures (top) at DIV15 and astrocytes (bottom). The culture medium was replaced with Tyrode medium at DIV14 and samples were collected at DIV15. ***$P < 0.0001$. (**H**) Prominent decreases in alanine release from *Gpt2*-null neurons and astrocytes. Medium samples were collected at same time as the cell pellets in G. Neuronal culture: **$P = 0.0057$; astrocyte culture: **$P = 0.0031$. (**I**) Metabolic pathways that convert [U-^{13}C]-glutamine into alanine and the TCA cycle intermediates. (**J**) GPT2 sustains TCA cycle intermediates in cortical neuronal cultures. Fractional enrichment in succinate or malate from [U-^{13}C]-glutamine in cortical neuronal cultures as processed in G. Mixed model analysis was done to assess statistical significance with genotype as fixed factor and litters used for culture as random factor. *$P = 0.0139$ **$P = 0.0044$.

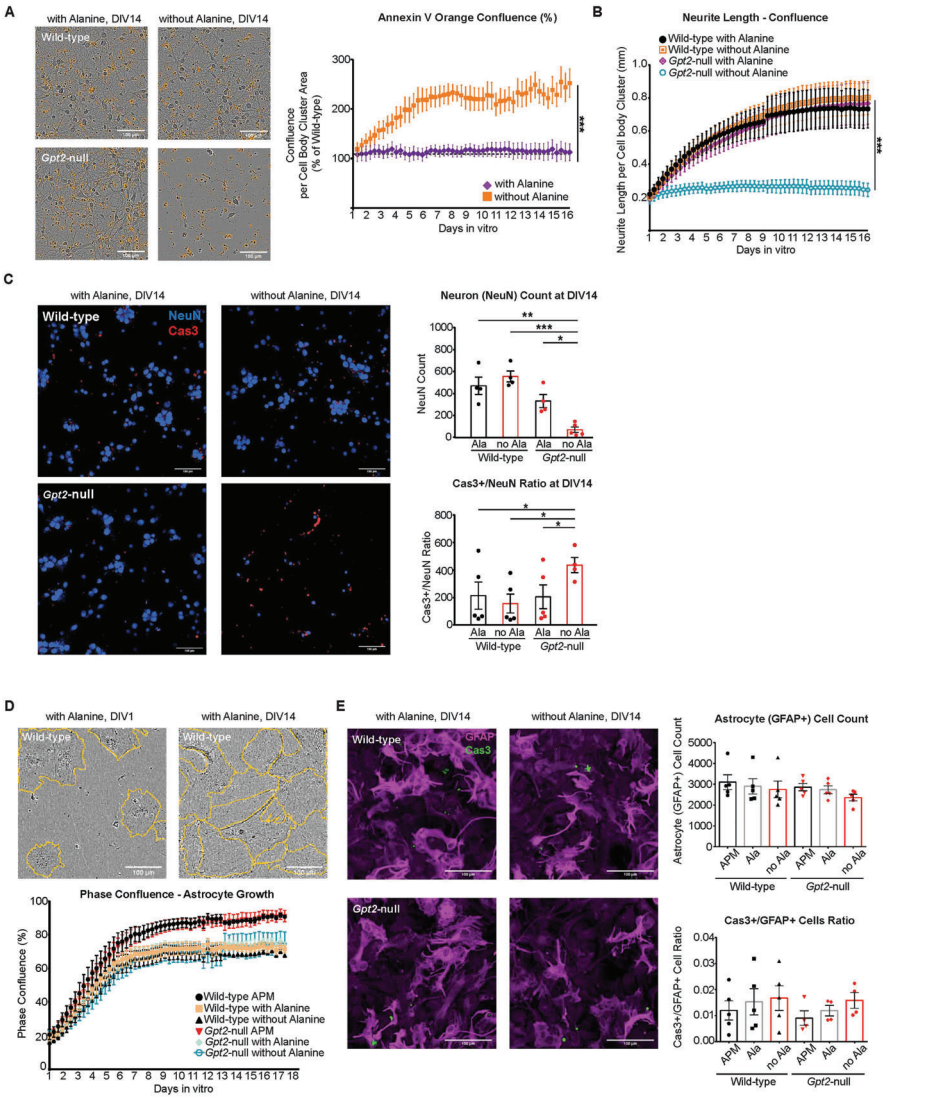

Figure 4. Exogenous alanine is required in *Gpt2*-null neurons for survival *in vitro*. (**A**) *Gpt2*-null culture deprived of alanine undergoes apoptosis. Representative images of Annexin V Orange Reagent staining in IncuCyte (left). Scale bar: 100 µm. The orange confluence per Cell Body Cluster Area values for *Gpt2*-null cultures were expressed as a percentage of their wild-type littermate cultures (right). The curves were fit by non-linear regression (one-phase exponential association) and best-fit values were compared (***$P < 0.0001$). $n = 5$ cultures. (**B**) *Gpt2*-null neurons fail to arborize without exogenous alanine. Graphs based on IncuCyte S3 NeuroTrack continuous analysis of neurite length as detected by phase confluence. The curves were fit by non-linear regression (one-phase exponential association) and best-fit values were compared ($P < 0.0001$). $n = 5$–7 cultures. (**C**) Neuronal cell count is decreased and Cas3+ cell count is increased in *Gpt2*-null cultures deprived of alanine. Images from Opera Phenix High Content Screening Confocal Microscopy (left) and quantification of NeuN+ cell counts (top) and Cas3+/NeuN+ ratio (bottom). Scale bar: 100 µm. The cells were fixed at DIV14 and the quantification represents the time point DIV14 only. *$P < 0.05$, **$P < 0.005$, ***$P < 0.0005$. (**D**) *Gpt2*-null astrocytes do not need exogenous alanine to survive *in vitro*. IncuCyte S3 phase contrast images from a wild-type astrocyte-enriched culture grown with alanine, at DIV1 (left) and DIV14 (right). Orange lines delineate the cell perimeter. Scale bar: 100 µm. Quantification of phase confluence over time (bottom). Refer to Materials and Methods for composition of Astrocyte Plating Medium (APM). Other media are similar to APM except they have dialyzed fetal bovine serum and 200 mM glutamine (instead of GlutaMAX) with or without 0.02 mM alanine. (**E**) Opera Phenix High Content Screening Confocal Microscopy (20× water objective) images of GFAP (magenta) and Caspase3 (Cas3, green) in wild-type and *Gpt2*-null astrocyte-enriched cultures and quantification of GFAP+ cell count (right, top), Cas3+/GFAP+ cell count ratio (right, bottom). Scale bar: 100 µm. GFAP+ cell count for no alanine condition, wild-type: 2750 ± 398.6 versus *Gpt2*-null: 2362 ± 161.4, $P = 0.3936$. Cas3+/GFAP+ cell count ratio for no alanine condition, wild-type: 0.0167 ± 0.0047 versus *Gpt2*-null: 0.0158 ± 0.003, $P = 0.8855$.

HA diet normalized serum alanine (Fig. 5A). Overall, there was no statistically significant difference between *Gpt2*-null (HA) and WT (HA) serum alanine levels, albeit with a trend toward a decrease [WT (HA): 0.775 ± 0.004 mM versus *Gpt2*-null (HA): 0.687 ± 0.044 mM, $P = 0.0703$]. Interestingly, in WT mice given HA diet [WT (HA)], alanine levels did not change compared to alanine levels in WT (RA) mice, which is suggestive of normalizing effects due to hepatic metabolism [WT (RA): 0.775 ± 0.006 mM versus WT (HA) 0.775 ± 0.004 mM, $P = 0.8980$]. The alanine levels in *Gpt2*-null brain at P18 were also normalized by the HA diet as per targeted metabolomics (Fig. 5B). Importantly, we discovered that *Gpt2*-null mice fed the HA diet *ad libitum* have increased survival past P30 (Fig. 5C). Out of a total of 38 *Gpt2*-null animals fed HA diet, 13 (34%) were able to survive past P30, whereas none of the *Gpt2*-null mice fed the RA survived (Fig. 5C). WT mice showed no negative effect of HA diet on survival, suggesting good tolerability of high levels of alanine in the diet. However, despite encouraging improvements in survival, *Gpt2*-null mice on HA diet failed to thrive and stagnated in weight gain (Fig. 5D). Motor defects such as wide gait and clasping reflex in the hindlimbs were present in *Gpt2*-null (HA) mice at P18, similar to the *Gpt2*-null (RA) mice (Fig. 5E and Supplementary Material, Videos S7–S10). As *Gpt2*-null mice aged on HA diet, their walking progressively worsened as evidenced by Open Field Tests performed at P18, P30, P60 and P90 (Fig. 5E, Supplementary Material, Videos S11–S18). At around age P90, they tended to lose the ability to stand on their paws completely and displayed crawling behavior. To determine the extent to which the altered metabolome in the neural tissue was corrected by the HA diet, we performed targeted metabolomics on acutely dissected hippocampal tissue from WT (HA) and *Gpt2*-null (HA) mice at P18 (Supplementary Material, Fig. S6A–D, Supplementary Material, Tables S5 and S6). The HA diet resulted in marked improvements in the metabolic profile of *Gpt2*-null hippocampus, particularly for GPT2 reaction metabolites, TCA cycle intermediates and glucose metabolism (Supplementary Material, Fig. S6A–D, Supplementary Material, Tables S5 and S6). In summary, the supplemental dietary alanine improved survival of *Gpt2*-null mice and the metabolic profile of the *Gpt2*-null brain but failed to correct growth and motor abnormalities.

Surviving adult *Gpt2*-null mice on high-alanine diet reveal worsening hypoplasia of the central nervous system and death of lower motor neurons in the spinal cord

Rescue of survival on the HA diet permitted us to examine the progression of neuropathology in surviving *Gpt2*-null animals. Initially at P18, we examined gross anatomy abnormalities in *Gpt2*-null mice fed RA diet. From the two representative WT and *Gpt2*-null images (Fig. 6A), the overall decreased size of the *Gpt2*-null central nervous system was apparent. Thicknesses of the cervical and lumbar enlargements of the spinal cord in the *Gpt2*-null mice (RA) were decreased as well. Also at P18, we examined the spinal cord by immunohistochemistry in *Gpt2*-null (RA) mice. Neuronal numbers were similar; however, motor neurons in the ventral horn, stained for choline acetyltransferase (ChAT), were notably smaller in soma size in the *Gpt2*-null animals in both cervical and lumbar spinal cords (Fig. 6B and C). Reductions in soma size in *Gpt2*-null spinal cord appeared relatively selective for ChAT+ cells, as staining for NeuN, a pan-neuronal marker, in the dorsal horn of cervical and lumbar spinal cord yielded similar densities of NeuN+ soma (Fig. 6B and C) and similar soma size across both genotypes (Supplementary Material, Fig. S7A). Calbindin+ interneuron counts in the dorsal horn were also similar between the two genotypes (Supplementary Material, Fig. S7C).

We subsequently investigated progressive neuropathology in surviving *Gpt2*-null animals on the HA diet at P90. Surviving adult *Gpt2*-null (HA) mice displayed progressive dysfunction in motor behavior (Fig. 5). The gross anatomy showed worsening on several measurements in the brain and spinal cord of *Gpt2*-null (HA) mice (Fig. 6D and Supplementary Material, Fig. S8A–G). At P90, there was pronounced difference in size of the enlargements in *Gpt2*-null (HA) and WT (HA) spinal cords. It is noteworthy that whereas the WT spinal cord had apparently grown from P18 to P90, the *Gpt2*-null mice stagnated in growth in the spinal cord.

Spinal cords from surviving *Gpt2*-null mice on the HA diet demonstrated reduced motor neuron count, as well as smaller soma sizes in both the cervical and lumbar spinal cord (Fig. 6E and F). This is in contrast to the spinal cords at P18, which only demonstrated reduced soma size, but not reduced soma count at this earlier time point. Loss of neurons at P90 was selective to ChAT+ motor neurons in the ventral horn, as the NeuN+ soma densities in the dorsal horn of both cervical and lumbar spinal cord were comparable (Fig. 6E and F), as was the soma size between the two genotypes (Supplementary Material, Fig. S7B). Also, Calbindin+ interneuron counts in the dorsal horn were similar between WT (HA) and *Gpt2*-null (HA) mice (Supplementary Material, Fig. S7D). We did not detect any microgliosis or positive Fluoro-Jade C staining in either *Gpt2*-null (RA) or *Gpt2*-null (HA) spinal cord (Supplementary Material, Fig. S9). However, in agreement with motor neuron death, in the *Gpt2*-null (HA) spinal cord, we observed astrogliosis with enhanced GFAP staining in the gray matter (Fig. 6G). We also examined for any pathology in the primary motor cortex, as dysfunction in upper motor neurons has been implicated in the etiology of hereditary spastic paraplegia (8). As in the lower motor neurons of the spinal cord, reduced soma size was also present in layer 5 neurons of the primary motor cortex of both *Gpt2*-null (RA) mice at P18 and *Gpt2*-null (HA) mice at P90 (Supplementary Material, Fig. S10). We did not detect any reduction in NeuN+ count, astrogliosis, microgliosis or positive Fluoro-Jade C staining in layer 5 of the primary motor cortex in either *Gpt2*-null (RA) mice at P18 or *Gpt2*-null (HA) mice at P90. Overall, these results indicate that GPT2 regulates processes involved in neuronal growth of both upper and lower motor neurons and that the ventral horn motor neurons in the spinal cord demonstrate selective vulnerability to the loss of GPT2, likely conferring progressive worsening of motor function with age in *Gpt2*-null animals.

Discussion

In this study, we identify metabolic mechanisms wherein the mitochondrial enzyme GPT2 governs neuronal growth. Evidence from both patients with progressive spastic paraplegia and from mouse here indicates that motor function is vulnerable to defects in GPT2-mediated metabolism. Metabolomics on developing postnatal *Gpt2*-null brain demonstrated an early defect in alanine synthesis and impairments in anaplerosis of the TCA cycle. Notably, through conditional deletion of GPT2 in neurons, corroborated by studies in primary cultures, our data support a prominent role for GPT2-mediated mechanisms within neurons, as opposed to in astrocytes. Therefore, these studies pinpoint fundamental metabolic processes required for neuronal growth, and that potentially underlie selective vulnerabilities in motor neuron disease.

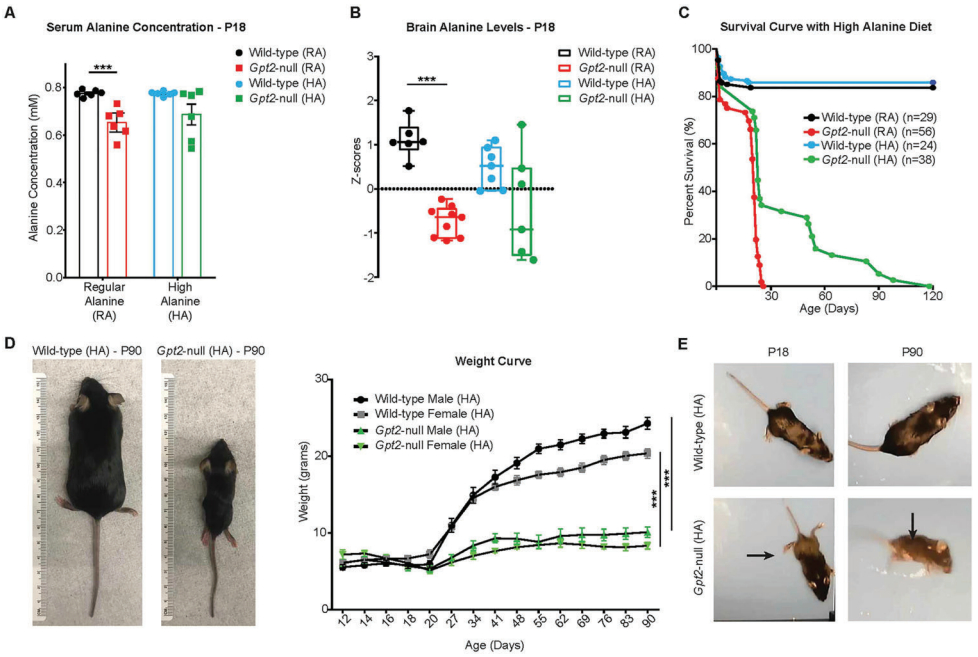

Figure 5. High-alanine diet improves survival and metabolomic profile in the hippocampus of *Gpt2*-null mice but does not alleviate body weight or motor deficits. (**A**) Serum alanine levels are normalized by the high-alanine (HA) diet in *Gpt2*-null mice at P18. Serum alanine concentrations of wild-type and *Gpt2*-null mice fed either RA or HA diet measured at P18. ***P (wild-type (RA) versus *Gpt2*-null (RA) < 0.0001); P (wild-type (HA) versus *Gpt2*-null (HA) $= 0.07$). (**B**) Alanine levels are normalized by the HA diet in *Gpt2*-null hippocampus. Z-scores of alanine levels are shown in the box-and-whisker plot. The peak intensities obtained from targeted tandem liquid chromatography–mass spectrometry (LC–MS/MS) were normalized to the sample median as in Figure 2. ***$P < 0.001$. (**C**) *Gpt2*-null mice on HA diet can survive up to P120. Survival curves of germline *Gpt2*-null mice and their wild-type littermates given RA diet (1.19% w/w) or HA diet (5% w/w). Log-rank (Mantel-Cox) test was used to determine significant differences between the curves, P (*Gpt2*-null (RA) versus *Gpt2*-null (HA)) < 0.0001, P (wild-type (HA) versus *Gpt2*-null (HA)) < 0.0001. (**D**) *Gpt2*-null mice that survive on HA diet do not gain body weight in a manner similar to wild-type mice. Representative images of wild-type (left) and *Gpt2*-null (right) mice at P90 fed HA diet. Weight curves of wild-type and *Gpt2*-null mice fed HA diet at ages from P12 to P90. The curves were fit to the Gompertz equation; P (wild-type male (HA) versus *Gpt2*-null male (HA)) < 0.0001, P (wild-type female (HA) versus *Gpt2*-null female (HA)) < 0.0001. $n = 5$–13 mice. (**E**) Adult *Gpt2*-null mice that survive on HA diet display worsening motor dysfunction. Pictures of wild-type (HA) (top) and *Gpt2*-null (HA) (bottom) mice at ages P18 (left) and P90 (right). Note the wide hind-limb gait (horizontal arrow) in the *Gpt2*-null (HA) mouse at P18 and the crawling behavior at P90 (vertical arrow). Also see Supplementary Material, Videos S11–S18.

Our experiments indicate that GPT2 is required particularly for neurons. While we do not know the exact cause of animal death, the neuron-specific deletion of GPT2 *in vivo* was sufficient to cause motor abnormalities and premature death similar to that seen in the germline *Gpt2*-null mice. This phenotype was not observed after astrocyte-specific deletion of GPT2. In further support of a role for GPT2 in neurons, our data demonstrated that GPT2 is enriched in neuronal cultures compared to GPT1, which is more abundant in astrocyte cultures. At the mRNA level, *Gpt2* is more abundant than *Gpt1* in mouse neurons, whereas in astrocytes, expression levels of *Gpt1* and *Gpt2* are comparable (22). In contrast to the mouse brain, *GPT1* mRNA is virtually absent in the human cortex (23,24) wherein there is an abundance of GPT2 mRNA.

During the early postnatal period in which GPT2 expression is upregulated (7), dysregulation of alanine occurs earliest (at P0) shortly preceding reductions in TCA cycle intermediates (at P7). There is also reduced conversion of glutamine into TCA cycle intermediates via pyruvate transamination in *Gpt2*-null neuronal cultures. In the brain, studies have focused on pyruvate carboxylase as the major anaplerotic enzyme, particularly in astrocytes (25,26). Human patients with deficiencies in mitochondrial pyruvate carboxylase and pyruvate dehydrogenase, enzymes that support the TCA cycle directly, have hyperalaninemia, most likely due to channeling of pyruvate with glutamate to alanine and α-ketoglutarate via GPT2 (27,28). Our study pinpoints the non-redundant function of GPT2 for neuronal TCA cycle maintenance and alanine synthesis.

Subsequent to reductions in TCA cycle intermediates in *Gpt2*-null brain, we observed prominent increases in almost all glycolytic intermediates, although pyruvate was decreased. Reduced pyruvate may cause decreased substrate inhibition of glycolytic enzymes. Flux analysis *in vivo* may also address the possibility of pyruvate being consumed more by pyruvate carboxylase to make oxaloacetate, which is one of the few TCA cycle intermediates that did not change in *Gpt2*-null brain. Surprisingly, α-ketoglutarate too is unchanged or increased in *Gpt2*-null brain. Metabolites including the TCA cycle intermediates can be efficiently managed by complexes of multiple enzymes (29). To date, the only enzyme that GPT2 is known to form

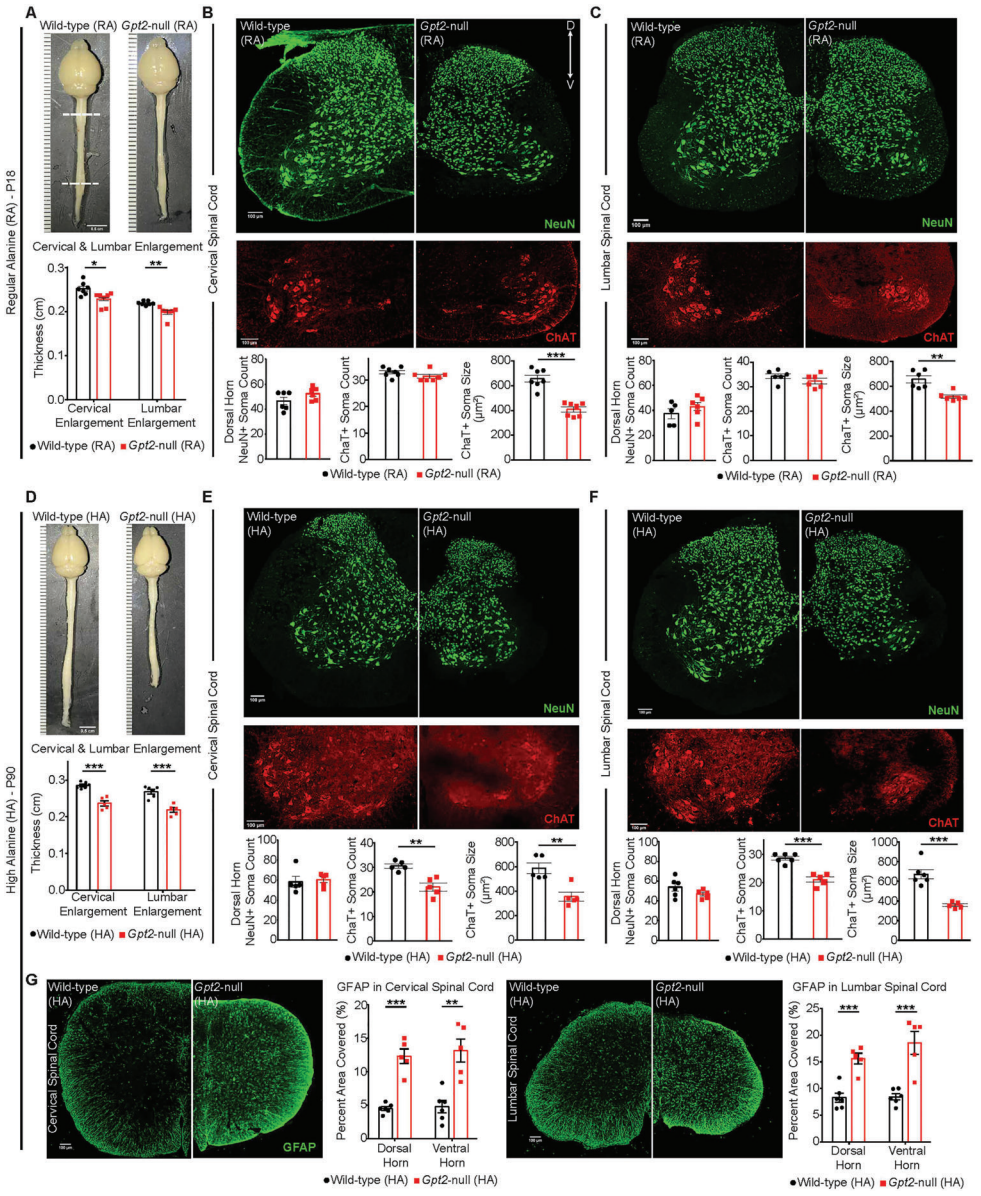

Figure 6. Surviving adult *Gpt2*-null mice fed high-alanine diet exhibit worsening hypoplasia in the central nervous system and selective death of lower motor neurons in the spinal cord. (**A**) Images of the gross anatomy of the central nervous system of P18 wild-type and *Gpt2*-null mice fed RA diet. Top and bottom dashed lines denote cervical and lumbar enlargement, respectively. Quantification of thickness is shown below the images. Scale bar: 0.5 cm. (**B**) Images of cervical spinal cord sections from wild-type (RA) and *Gpt2*-null (RA) mice at P18 stained for neurons (top, NeuN, green) and motor neurons (bottom, ChAT, red). Quantification of dorsal horn NeuN+ soma count, ChAT+ soma count and ChAT+ soma size is shown below the images. (**C**) Images of lumbar spinal cord sections from wild-type (RA) and *Gpt2*-null (RA) mice at P18 stained for neurons (top, NeuN, green) and motor neurons (bottom, ChAT, red). Quantification of dorsal horn NeuN+ soma count, ChAT+ soma count and ChAT+ soma size is shown below the images. (**D**) Images of the gross anatomy of the central nervous system of P90 wild-type and *Gpt2*-null mice fed HA diet. Cervical and lumbar enlargements were identified as in A. Quantification of thickness is shown below the images. Scale bar: 0.5 cm. (**E**) Images of cervical spinal cord sections

complexes with is glutamate dehydrogenase (30). Glutamate dehydrogenase is another major anaplerotic enzyme in the brain and may be acting in part to upregulate α-ketoglutarate levels in neurons (31).

Following defects in TCA cycle and alanine levels, we saw prominent increases in essential amino acids in the *Gpt2*-null brain. GPT2 links alanine synthesis and the TCA cycle, thereby supporting both energetics and biosynthesis of macromolecules, particularly proteins. Of note, alanine is the second most frequent amino acid in the primary structure of proteins overall across the domains of Bacteria and Eukarya (32). More studies *in vivo* are warranted to determine the possibilities of changes in specific transporter levels or increased protein breakdown in a compensatory attempt to support both alanine supply and also the TCA cycle. By removing alanine from medium at DIV1, we observed decline of neuronal arborization, as well as cell death in neurons but not in astrocytes. This indicates that alanine has become an essential amino acid and must be supplied exogenously to *Gpt2*-null neurons, whereas GPT2 is not required for astrocytes *in vitro* even without exogenous alanine.

Improvement of animal survival in *Gpt2*-null mice with HA diet re-asserts the conversion of alanine from being a non-essential amino acid to an essential amino acid and allowed us to observe progression of the motor dysfunction in *Gpt2*-null mice as they age. The phenotype of premature death in *Gpt2*-null mice was not completely abolished with HA diet. The variability of the rescue is most likely due to the *ad libitum* nature of the diet regimen and the *Gpt2*-null pup may survive better if alanine is continuously force-fed. Surviving *Gpt2*-null animals on HA diet almost completely lost their ability to walk at around P60 to P90. Neuropathology demonstrated reduced number and soma size of lower motor neurons in the spinal cord, but not of dorsal horn neurons; therefore, we conclude that *Gpt2*-null animals demonstrate selective loss of lower motor neurons. Smaller soma sizes and loss of spinal cord motor neurons have been observed in other neurological diseases, including amyotrophic lateral sclerosis (ALS) (33). Genetic mutations in *SPG11*, or spatacsin, a spastic paraplegia gene, also cause spinal cord motor neuron death (34).

Hereditary spastic paraplegia has been attributed to upper motor neuron degeneration due to requirements for long-range axonal projections (8). Although we did not observe any degeneration or cell loss in the primary motor cortex of *Gpt2*-null mice, the soma sizes of the layer 5 neurons were reduced, suggesting that GPT2 acts on similar mechanisms of neuronal growth in both upper and lower motor neurons. Importantly, a majority of mouse models of spastic paraplegia show motor disability without death of upper motor neurons (8,35). Whether the loss of lower motor neurons in *Gpt2*-null mice occurs cell autonomously or due to diminished connectivity from other circuits remains to be explored. Interestingly, one recent case report of a patient with GPT2 Deficiency has demonstrated motor neuropathy consistent with our findings of loss of lower motor neurons in the mouse model (36).

Our data suggest that dietary modifications may involve alanine as a potential therapeutic supplement for human patients with GPT2 Deficiency. Supplemental alanine has been shown to be well tolerated in humans (37–39). To date, the only biochemical finding in human patients with GPT2 Deficiency is decreased alanine levels in the plasma (40), a result which is supported by our data here in the *Gpt2*-null mouse. In our experiments, high alanine supplementation rescued survival and improved metabolic derangements in *Gpt2*-null brain; however, this dietary supplementation did not prevent progression of motor disability or improve weight gain. Alternative procedures to enhance alanine delivery may be warranted, or alanine supplementation in combination with additional dietary modifications may be needed.

In summary, these studies of GPT2 Deficiency have identified broadly significant metabolic mechanisms critical for neuronal growth and for motor circuitry, which contain some of the largest and longest projecting neurons in the nervous system. We present evidence that GPT2-mediated mechanisms are essential for neuronal alanine synthesis and anaplerotic support of the TCA cycle. We find that the loss of GPT2 *in vivo* causes selective vulnerability in lower motor neurons. Finally, our data permit evaluation of high alanine supplementation as a potential treatment for GPT2 Deficiency that may be rapidly implemented and has a favorable risk benefit profile in children.

Materials and Methods

Ethics statement

All experiments involving mice were done in accordance with the National Institutes of Health *Guide for the Care and Use of Laboratory Animals* (41) and approved by the Brown University Institutional Animal Care and Use Committee.

Animals

Gpt2-null animals were obtained as described previously [Knockout Mouse Project at University of California, Davis (MMRRC_047980-UCD)] (7). For generation of the conditional-null ready mouse, the sequence flanked by two FRT sites was excised by mating the *Gpt2*-heterozygous mouse with a mouse containing the flippase transgene (IMSR_JAX:003946). To obtain a pan-neuronal conditional-null mouse, the animal with *Gpt2*-flox allele was mated with a mouse having the Cre recombinase transgene driven by the rat Synapsin-I promoter (IMSR_JAX:003966). The excision of exon 4 by Cre recombinase was tested by PCR with the following primers: Exc-F (5′-CTAACTTGTCCTGCATGGTGTCAGC-3′) and Exc-R (5′-GGCTTTCTACCAGGAGGAACAGAGG-3′); the primers detect the floxed allele (1479 bp), the WT allele (1347 bp) and the excised allele (687 bp). To obtain an astrocyte-specific conditional-null mouse, the animal with *Gpt2*-flox allele was mated with the GFAP-Cre line 77.6 (IMSR_JAX:024098). For both Synapsin-I-Cre

from wild-type (HA) and *Gpt2*-null (HA) mice at P90 stained for neurons (top, NeuN, green) and motor neurons (bottom, ChAT, red). Quantification of dorsal horn NeuN+ soma count, ChAT+ soma count and ChAT+ soma size is shown below the images. (**F**) Images of lumbar spinal cord sections from wild-type (HA) and *Gpt2*-null (HA) mice at P90 stained for neurons (top, NeuN, green) and motor neurons (bottom, ChAT, red). Quantification of dorsal horn NeuN+ soma count, ChAT+ soma count and ChAT+ soma size is shown below the images. (**G**) Images of GFAP staining in cervical (left) and lumbar (right) spinal cord sections from wild-type (HA) and *Gpt2*-null (HA) mice at P90. Quantification is shown to the right of corresponding images and is represented as percent total area of the dorsal horn or ventral horn covered by GFAP staining. For B, C, E and F, dorsal horn NeuN+ soma were counted in a $100 \times 100\ \mu m^2$ window. ChAT staining belongs to the same section as NeuN but images of the ventral horn were cropped and magnified to better visualize motor neurons. Soma size was measured by the surface area of the cell in the maximum intensity projection image. Scale bar: 100 μm. For all figures: $^*0.01 < P < 0.05$; $^{**}0.001 < P < 0.01$; $^{***}P < 0.001$.

and GFAP-Cre lines, only females possessing the Cre transgene were used to mate with male *Gpt2* flox/flox due to germline recombination observed in males. Every animal was checked for germline recombination by PCR genotyping in the tail. The Synapsin-I-Cre line was confirmed using a Cre reporter line, Ai14-R26-tdTomato (IMSR_JAX:007914). The background of all mice was C57BL6/J (IMSR_JAX:000664); the mice with a different strain of origin were backcrossed to C57BL6/J at least for six generations.

The mice were maintained under a 12-h light/dark cycle (lights on at 7 a.m./off at 7 p.m.) throughout the year. Feed and water were given *ad libitum*. Formulations for the RA diet (1.19% by weight, LabDiet) and HA diet (5% by weight, Envigo) can be found in Supplementary Material Table S7. The breeding pairs were set up when the *Gpt2*-heterozygous mice were two months old. As soon as they were set up for breeding, their diet was switched from RA diet to the HA diet and they were fed with the HA diet for the entire duration of collecting samples from their progeny.

Behavioral tests

Open field test. The mice were placed at the center of an empty solid mouse cage (31 cm × 31 cm) and the movement was recorded from an overhead camera.

Wire hang test. The mouse was allowed to grab onto a cage topper. The cage topper was inverted approximately 30 cm above the floor of the cage. The time elapsed before the mouse fell off into the cage was recorded. The inter-trial interval was 1 min with five trials in total. The trial was terminated if the hanging time exceeded 2 min.

Hind-limb clasping reflex. The mouse was suspended from the tail for 10 s and the clasping reflex was noted. Three trials were performed.

DigiGait. DigiGait (MouseSpecifics), a ventral plane videography high-throughput instrument with a treadmill, was used for capturing a variety of motor deficits. The lane length was adjusted to an appropriate length depending on the age (P18) and size of the animal to be tested (approximately 8 cm). The animal was placed on the DigiGait treadmill and allowed to walk or run freely as the belt moved at 8 cm/s. Five seconds of video was captured and analyzed by the DigiGait Analyzer software.

Metabolomics and isotope tracing

Metabolomics. Craniotomies on pups after decapitation or cervical dislocation at designated postnatal ages were performed. Hippocampi were dissected immediately on ice. Wet weight of the tissue was measured, and the tissue was flash frozen in liquid nitrogen to quench metabolism. The tissue was processed as previously described with minor modifications (42). The tissue was immersed in 500 µl of 80% (vol/vol) high-performance liquid chromatography (HPLC)-grade methanol (cooled to −80°C). The tissue was ground with a Kimble pestle, vortexed for 1 min and incubated at −80°C for 4 h. To pellet debris, the sample was centrifuged at 14 000 × *g* for 10 min at 4°C. While the supernatant was kept at −80°C, 400 µl of 80% (vol/vol) methanol (cooled to −80°C) was added to the pellet, which was then vortexed for 1 min, incubated at −80°C for 30 min and then centrifuged at 14 000 × *g* for 10 min at 4°C. The supernatants were combined and re-spun at 14 000 × *g* for 10 min at 4°C. The supernatants were divided equally in 1.5-ml Eppendorf tubes and concentrated using a Savant SpeedVac vacuum concentrator (Thermo Scientific) at ambient temperature. Tandem mass spectrometry (MS) was done at Beth Israel Deaconess Medical Center Mass Spectrometry Facility. The samples were re-suspended in liquid chromatography (LC)/mass spectrometry (MS)-grade water and run in tandem LC–MS/MS. Samples were injected into hydrophilic interaction liquid chromatography (HILIC) at high pH using HPLC coupled to a 5500 QTRAP mass spectrometer (AB/SCIEX). Selected Reaction Monitoring (SRM) mode for 300 transitions with positive/negative polarity switching fragmented precursor ions and selected for product ions. Peak areas for each detected metabolite were integrated using MultiQuant software (AB/SCIEX). The statistical analyses and data visualization were done using MetaboAnalyst 4.0 (43) (RRID:SCR_015539). If half of data for a metabolite was not available, then that metabolite was omitted from analysis. All data were normalized by median normalization and auto-scaled (mean-centered and divided by standard deviation of each variable). Unpaired Student's *t*-test assuming equal variance was used to generate a *P*-value.

Isotope tracing. The cortical neuronal cultures at 14 days *in vitro* (DIV14) were incubated with Tyrode medium (140 mM NaCl, 4 mM KCl, 2 mM $CaCl_2$, 2 mM $MgCl_2$, 10 mM HEPES) with either 0.5 mM [α-^{15}N]-glutamine (Sigma-Aldrich, 486 809), 0.5 mM [U-^{13}C]-glutamine (Sigma-Aldrich, 605 166) or 4 mM [U-^{13}C]-glucose (Cambridge Isotope Laboratories, CLM-1396-PK) for 24 h. LC–MS analysis for soluble metabolites was achieved on the Q Exactive PLUS Hybrid Quadrupole-Orbitrap Mass Spectrometer (Thermo Scientific) coupled with hydrophilic interaction chromatography (HILIC). To perform the LC separation of cultured cell samples, an XBridge BEH Amide column (150 mm × 2.1 mm, 2.5 µM particle size, Waters, Milford, MA) was used with a gradient of solvent A (95%:5% H_2O: acetonitrile with 20 mM ammonium acetate, 20 mM ammonium hydroxide, pH 9.4), and solvent B (100% acetonitrile). The gradient was 0 min, 85% B; 2 min, 85% B; 3 min, 80% B; 5 min, 80% B; 6 min, 75% B; 7 min, 75% B; 8 min, 70% B; 9 min, 70% B; 10 min, 50% B; 12 min, 50% B; 13 min, 25% B; 16 min, 25% B; 18 min, 0% B; 23 min, 0% B; 24 min, 85% B; 30 min, 85% B. The flow rate was 150 µl/min; the injection volume was 10 µl; and the column temperature was 25°C. MS full scans were in negative ion mode with a resolution of 140 000 at m/z 200 and scan range of 75–1000 m/z. The automatic gain control (AGC) target was 1×10^6.

Cell culture

Mouse primary hippocampal neuron culture. Hippocampal neurons were cultured as described previously (44). Hippocampi from pups aged P0-P1 were dissected in Hank's Balanced Salt Solution (HBSS) (Gibco, 14 170–112) and placed in 500 µl of 20 U/ml papain (Worthington, LK003176) in Earle's Balanced Salt Solution (EBSS) (Worthington, LK003188). The tube with hippocampi/papain was incubated at 37°C for 15 min. The tissue was triturated with a 1-ml pipette tip for 12 strokes. The tissue was further incubated at 37°C for 15 min and triturated. The remaining bits of tissue were allowed to settle and the overlying solution with dissociated cells was spun in a separate tube at 300 *g* for 5 min at room temperature. The cell pellet was dissolved gently in Inhibitor Solution (540 µl EBSS, 60 µl Ovomucoid Protease Inhibitor (Worthington Biochemical, LK003182), 30 µl DNase (Worthington Biochemical, LK003170) per hippocampi) and filtered through a 70-µm nylon mesh (Fisher Scientific, 22 363 548). The filtered cell suspension was layered on top of 1 ml Ovomucoid Protease Inhibitor and spun at 70 *g* for 10 min

at room temperature. The supernatant was discarded, and the cell pellet was re-suspended in Neurobasal A+ (NeuroBasal-A (Thermo Fisher Scientific, 10 888 022), 1× B27 Supplement (Thermo Fisher Scientific, 17 504 044), 2 mM GlutaMAX (Thermo Fisher Scientific, 35 050 061)). The full media was changed the next day followed by half media changes every 3 days.

Mouse primary astrocyte-enriched cultures. The culturing protocol was adapted from (45,46). Cortices from pups aged P0-P1 were dissected in HBSS, diced into 6 pieces and transferred to a 15-ml conical tube. The tissue was incubated in 0.25% Trypsin–EDTA in HBSS at 37°C for 30 min. The solution was removed carefully to leave the tissue pieces at the bottom, and 6 ml of Astrocyte Plating Medium (APM) (DMEM (Thermo Fisher Scientific, 10 569–010), 10% fetal bovine serum (Invitrogen, 16 000 044), 1% Penicillin/Streptomycin (Invitrogen, 15 140 122)) was added. The tissue was triturated for 15 strokes with a 10-ml pipette and then 5 strokes more with a 1-ml pipette. The cell suspension was filtered through 70-µm nylon mesh and seeded in a 25-cm^2 flask (Corning, 3289). After 2 days, the full medium was changed, and then half medium was changed every 3 days. When the astrocyte layer was confluent (∼7 days), the flask was shaken at 225 rpm overnight at 37°C. The full medium was changed to APM with 20 µM cytosine arabinoside (Ara-C) to remove any other contaminating proliferative cell types. After two days, the full medium was changed to APM. The Ara-C treatment was repeated the next day. Mild trypsin (0.0675%) treatment was used to lift off the astrocyte layer as a whole and leave the remaining microglia at the bottom of the flask. The layer was incubated in 1 ml of Accutase (StemCellTechnologies, 07920) in a fresh tube at 37°C for 10 min. The layer was dissociated with a 1-ml pipette tip with five strokes. About 2 ml APM was added; the solution was mixed and filtered through a 70-µm nylon mesh. Cells were seeded to plates/dishes coated with 5 µg/ml laminin.

Alanine deprivation in vitro and custom-made cell culture medium. For neuronal cultures, the Neurobasal A+ composition can be found in Supplementary Material Table S7. The cells were incubated with custom-made Neurobasal A+ without alanine, along with 1× B27, 1% Penicillin/Streptomycin and 2 mM glutamine. Neurons were seeded in a 96-well plate (Corning 3596, coated with 100 µg/ml poly D-lysine) at a density of 25 000 cells per well. For alanine deprivation in astrocytes, instead of regular fetal bovine serum, dialyzed fetal bovine serum (Invitrogen, 26 400 044) was used to avoid extra alanine coming from the fetal bovine serum. The rest of the medium composition was the same as APM. Astrocytes were seeded in a 96-well plate (Corning, 3596) at a density of 2000 cells per well.

Continuous analysis of cellular growth and death *in vitro*

Mouse primary hippocampal neurons were seeded in a 96-well plate (Corning, 3596, coated with 100 µg/ml poly D-lysine) at a density of 25 000 cells per well. The plate was imaged continuously using an IncuCyte S3 Live-Cell Analysis System (Essen BioScience) with the 10× objective. The imaging was interrupted only at media changes every 3 days. The neurites were identified with the NeuroTrack module using phase contrast images. The neurites and cell bodies were segmented in the Brightness mode with an adjustment of 0.3. Any cell body cluster smaller than 100 μm^2 was excluded. Neurite sensitivity and width were set at 0.75 and 1 µm, respectively. Every data point for Neurite length and Neurite Branch Point was normalized to the cell body cluster of the first time point in order to account for cell density variability. IncuCyte Annexin V Orange Reagent (Essen BioScience, 4759), a specific phosphatidylserine (PS) cyanine dye, was used to detect apoptotic cells over time. The orange fluorescence confluence was normalized to the cell body cluster area at each time point and expressed as a percentage of its paired WT culture. The orange fluorescence was segmented in adaptive mode with a threshold adjustment of 2. Edge Sensitivity was set at −15. Any orange dot with eccentricity greater than 0.95 was excluded or with a mean intensity lower than 4 was excluded. The acquisition time was 400 ms.

Astrocyte-enriched cultures were seeded in a 96-well plate (Corning, 3596) at a density of 2000 cells per well. The plate was imaged continuously using an IncuCyte S3 Live-Cell Analysis System (Essen BioScience) with the 10× objective. The imaging was interrupted only at media changes every 3 days. The phase confluence was determined using the BasicAnalyzer module with segmentation adjustment set at 2 and area filter at minimum 1 μm^2.

Immunofluorescence

Cultured cells. The cells were washed with 1× phosphate-buffered saline (PBS) (Fisher Scientific, BP3994) and fixed with 4% paraformaldehyde (PFA) at room temperature for 10 min. The following steps were performed in order: 3 × 5-min 1× PBS washes, 10-min permeabilization in PBS with 0.25% Triton X-100 (T8787, Sigma), 1-h blocking with 10% normal goat serum (NGS) (Jackson ImmunoResearch, 005-000-121) in PBS with 0.1% Triton X-100 (PBST), overnight incubation at 4°C with primary antibody in 2% NGS-PBST, 3 washes with PBST, 1-h incubation with secondary antibody in 2% NGS-PBST, 3 washes with PBST and counterstaining with 300 nM DAPI (Invitrogen, D1306). To visualize mitochondria *in vitro*, the cells were incubated with 100 nM MitoTracker Red CMXRos (Invitrogen, M7512) for 25 min at 37°C, 5% CO_2, prior to performing the immunofluorescence protocol. Coverslips were mounted onto slides with Fluoromount G (SouthernBiotech, 0100-01).

Tissue. The tissues from mice were dissected out after transcardial perfusion with 1× PBS and then with 4% PFA. The tissues were cryoprotected by serially incubating in sucrose solutions of 10%, 20% and 30% overnight at 4°C. The final solution was then changed to half by volume sucrose/OCT (Optimal Cutting Temperature, Fisher Scientific, 23-730-571) and gently shaken for 1 h at 4°C. The tissues were frozen in dry ice/methanol bath and stored at −80°C until the day of sectioning at the cryostat. The sections were cut at 30-µm thickness. The immunofluorescence protocol was as follows, in order: 3-min fixing with 4% PFA, 3 × 5-min 1× PBS washes, 2-h blocking in NGS or normal donkey serum (NDS, Jackson ImmunoResearch, 017-000-121) with 1% (w/v) bovine serum albumin (Fisher Scientific, BP1600) and 0.4% Triton X-100 (Sigma-Aldrich, T8787) (Note: if a mouse-raised antibody was used, a 1-h incubation with 20 µg/ml AffiniPure Fab Fragment Goat Anti-Mouse IgG (H + L) (AB_2338476) or AffiniPure Fab Fragment Donkey Anti-Mouse IgG (H + L) (AB_2307338) in blocking solution was performed), overnight incubation at 4°C with primary antibody in blocking solution, 2 × 4-min washes with blocking solution, 3 × 4-min washes with 0.4% Triton X-100 in PBS, 2-h incubation with secondary antibody in blocking solution, 2 × 4-min washes with blocking solution, 3 × 4-min washes with 0.4% Triton X-100 in PBS, 5-min incubation in DAPI (Invitrogen, D1306) and 3 × 5-min washes with PBS. Coverslips

were then mounted onto slides with Fluoromount G (Southern-Biotech, 0100-01). The list of antibodies can be found in the Key Resources Table.

Confocal microscopy. Imaging and quantification of cell death, cell count, synapse count and arborization were done using an Opera Phenix High Content Screening System and Harmony software (PerkinElmer, RRID:SCR_018809). Hippocampal neuronal cultures, astrocyte-enriched cultures or co-cultures were seeded on an Opera Phenix Ultra CellCarrier 96-well plate (PerkinElmer, 6 055 302), and at indicated times, different media conditions were tested. Immunofluorescence as described above was done at DIV14 for all plates. The wells were filled with 1× PBS and imaged immediately after. For confocal microscopy on tissues, Olympus FV3000 confocal laser scanning microscope and FluoView software were used (RRID:SCR_017015). Images were processed and analyzed with ImageJ (RRID:SCR_003070).

Fluoro-Jade C staining

The tissue cryostat sections were mounted on Superfrost Plus microscope slides (Fisher Scientific, 22-230-892) and dried at 50°C for 30 min. The slides were immersed in the following solutions at room temperature in order: 0.2% NaOH in 80% ethanol for 5 min, 70% ethanol for 2 min, distilled water for 2 min, 0.06% potassium permanganate for 10 min, distilled water for 2 min, 0.0001% Fluoro-Jade C (Sigma-Aldrich, AG325) in 0.1% acetic acid for 10 min and 3 times distilled water for 1 min. The slides were dried at 50°C for 10 min, immersed in xylene for 1 min and coverslipped with DPX (Millipore Sigma 06522).

Subcellular fractionation of mouse brain

The protocol was adapted from (47). The brain was immediately removed after cervical dislocation and rinsed in ice-cold 1× brain homogenization buffer (0.320 M sucrose, 1 mM EDTA, 5 mM Tris base, pH 7.4). After decanting, fresh 10 ml/g 1× brain homogenization buffer was added, and the brain was cut into small chunks with surgical scissors. A Kimble pestle was used to homogenize the tissue with 12 strokes each lasting 4 s. The tube was spun at 1300 × g for 3 min at 4°C. The first supernatant was put aside on ice and the pellet was re-suspended in half starting volume with 1× brain homogenization buffer. The pellet was homogenized with a Kimble pestle with eight strokes each lasting 4 s. The tubes were spun at 1300 × *g* for 3 min at 4°C. The second supernatant was combined with the first and the sample was spun at 10 000 × *g* for 10 min at 4°C with a Sorvall RC6Plus centrifuge using the SS34 rotor. The pellet was re-suspended in 10 ml/g original tissue of 15% Percoll (Percoll, Cytiva 17 089 102 prepared in 1× brain homogenization buffer). The suspension was carefully layered onto a Percoll gradient (23–40%) and the tube was spun at 22 000 × *g* for 10 min at 4°C. The bottom layer was considered the mitochondrial fraction. After carefully removing the upper layers, the mitochondria were aspirated and re-spun with 4 volumes of 1× brain homogenization buffer, at 11 600 rpm for 10 min at 4°C. The supernatant was removed, and 4 volumes of Tyrode-like buffer (118 mM NaCl, 5 mM KCl, 1 mM $MgCl_2$, 1.2 mM $CaCl_2$, 0.1 mM $Na_2HPO_4.H_2O$, 20 mM HEPES, 10 mM glucose, pH 7.4) was added. The tube was spun at 18 000 × *g* for 10 min at 4°C. After carefully removing the supernatant, the mitochondria were re-suspended in 0.5 ml/g (of original tissue) fatty-acid free bovine serum albumin (10 mg/ml in 1× brain homogenization buffer). The final volume was brought to 3 ml/g (of original tissue) and tube was spun at 6900 × *g* for 10 min at 4°C with a tabletop centrifuge. The final pellet was re-suspended in the appropriate buffer for the subsequent assay.

Western blotting

Cells were homogenized in NP40 Cell Lysis Buffer (Invitrogen, FNN0021), 1× PhosStop (Roche, 04906837001), 1× Protease inhibitor Cocktail (PIC, Roche 05892970001) and 0.1 mM PMSF (Sigma-Aldrich, 93 482). Tissues were homogenized in RIPA buffer (50 mM Tris, 0.15 M NaCl, 1 mM EDTA, 1% Triton X-100, 0.5 g sodium deoxycholate, 0.1% SDS) with 1× PhosStop and 1× PIC. Twenty-µg protein samples were incubated in NuPage Sample buffer (Invitrogen, NP0007) and NuPage reducing agent (Invitrogen, NP0004) at 70°C for 10 min and immediately placed on ice. The samples were run in NuPage 4–12% Bis-Tris gel (Invitrogen, NP0321) at 175 V until the dye front was at the end of the gel. The gel was transferred to a nitrocellulose membrane (Invitrogen, LC2000) in NuPage Transfer Buffer with 20% methanol at 30 V for 1 h. The blot was blocked with Li-Cor Blocking Buffer (Li-Cor, 927–50 000) for 30 min and then permeabilized for 5 min in TBST (Fisher Scientific, BP2411) with 0.05% Tween20 (Sigma-Aldrich, P7949). The blot was incubated in primary antibodies at 4°C overnight. The blot was washed 3 × 5 min with TBST, incubated with secondary antibodies for 1 h, washed with TBST and finally placed in TBS. The blot was imaged using the Li-Cor Odyssey CLx Imaging System (resolution: 84 µm, background subtraction: median) and analyzed using Image Studio Lite software (RRID:SCR_013715). Protein amount in each sample was determined using the bicinchoninic acid (BCA) assay (Thermo Scientific Pierce, PI23227).

GPT enzyme activity assay

GPT activity assay was performed using the Alanine Aminotransferase (ALT) Assay Kit (Sigma-Aldrich, MAK052) according to the manufacturer's manual. Five-µg protein sample of cytosolic or mitochondrial fractions were used. Protein amount in each sample was determined using the BCA assay (Thermo Scientific Pierce, PI23227). BioTek Cytation5 plate reader was used to detect fluorescence; Gen5 software was used to analyze the data (RRID:SCR_017317).

Serum alanine concentration

Blood samples were collected from mice by cardiac puncture, clotted in SST-Mini Gold Top tubes for 15 min, and spun at 2500 rpm with a tabletop minicentrifuge for 10 min. The serum samples were deproteinized with a 10-kDa molecular weight cutoff spin filter (Corning, 431 481). Alanine concentration was determined using the Alanine Assay Kit according to the manufacturer's manual (Sigma-Aldrich, MAK001). BioTek Cytation5 plate reader was used to detect fluorescence; Gen5 software was used to analyze the data (RRID:SCR_017317).

In silico analysis of *Gpt1* and *Gpt2* gene expression

Gene expression profiles of the mouse hippocampus were extracted from DropViz (www.dropviz.org) (20). Data were visualized using JMP Pro 14 (RRID:SCR_014242).

Statistical analysis

All data presented in the figures and the Results section are presented as average ± standard error of the mean, unless otherwise noted. The statistical test for comparisons of two groups was unpaired two-tailed Student *t*-test unless otherwise noted

or when the data are presented as percentage of the WT average value, in which case one-sample *t*-test was performed with a hypothetical value of 100. All statistical analyses were compiled using GraphPad Prism software (RRID:SCR_002798). Mixed model analysis was done using JMP Pro 14 (RRID:SCR_014242).

Supplementary Material

Supplementary Data are available at *HMGJ* online.

Acknowledgements

The authors wish to thank John M. Asara at the Beth Israel Deaconess Medical Center Mass Spectrometry, Proteomics and Metabolomics Core.
Conflict of Interest statement. The authors declare no competing interests.

Funding

AQ8
Brain & Behavior Research Foundation NARSAD Independent Investigator (25701, to E.M.M.); a Dr Ralph and Marian Falk Medical Research Trust Catalyst Award (to E.M.M.); a Brown University Research Seed Award (to E.M.M.); National Institute for Neurological Disorders and Stroke (NINDS) (R01NS113141 to E.M.M); National Cancer Institute (R35CA22044901 to R.J.D.); the Carney Institute for Brain Science and Suna KıraçFellowship Graduate Award in Brain Science (to O.B.); the Hassenfeld Child Health Innovation Institute at Brown University; The Opera Phenix High Content Screening System in the Center to Advance Predictive Biology at Brown University is supported by National Institutes of Health/National Institute of Environmental Health Sciences (U01 ES028184; National Science Foundation EPSCoR Award (1655221); a generous gift by Donna McGraw Weiss (1989) and Jason Weiss; the Howard Hughes Medical Institute Investigator Program (to R.J.D.).

Author contributions

Conceptualization O.B. and E.M.M.; O.B. conducted all experiments; S.M.D. contributed to studies involving mass spectrometry for isotope tracing; Data Curation and Visualization O.B.; Experimental Design and Data Analysis O.B., S.M.D., R.J.D. and E.M.M.; Formal Analysis and Writing—Original Draft, O.B. and E.M.M.; Writing—Review & Editing, O.B., S.M.D. R.J.D. and E.M.M; Supervision, Project Administration, and Funding Acquisition, E.M.M.

References

1. Dekaban, A.S. (1978) Changes in brain weights during the span of human life: relation of brain weights to body heights and body weights. *Ann. Neurol.*, **4**, 345–356.
2. Holland, D., Chang, L., Ernst, T.M., Curran, M., Buchthal, S.D., Alicata, D., Skranes, J., Johansen, H., Hernandez, A., Yamakawa, R. *et al.* (2014) Structural growth trajectories and rates of change in the first 3 months of infant brain development. *JAMA Neurol.*, **71**, 1266–1274.
3. Iwasaki, N., Hamano, K., Okada, Y., Horigome, Y., Nakayama, J., Takeya, T., Takita, H. and Nose, T. (1997) Volumetric quantification of brain development using MRI. *Neuroradiology*, **39**, 841–846.
4. van Dyck, L.I. and Morrow, E.M. (2017) Genetic control of postnatal human brain growth. *Curr. Opin. Neurol.*, **30**, 114–124.
5. Ashwell, K.W.S. (2009) Development of the spinal cord. *The Spinal Cord*, 8–16.
6. van Karnebeek, C.D. and Stockler, S. (2012) Treatable inborn errors of metabolism causing intellectual disability: a systematic literature review. *Mol. Genet. Metab.*, **105**, 368–381.
7. Ouyang, Q., Nakayama, T., Baytas, O., Davidson, S.M., Yang, C., Schmidt, M., Lizarraga, S.B., Mishra, S., Ei-Quessny, M., Niaz, S. *et al.* (2016) Mutations in mitochondrial enzyme GPT2 cause metabolic dysfunction and neurological disease with developmental and progressive features. *Proc. Natl. Acad. Sci. USA.*, **113**, E5598–E5607.
8. Blackstone, C. (2018) Hereditary spastic paraplegia. *Handb. Clin. Neurol.*, **148**, 633–652.
9. Krebs, H.A. (1953) Equilibria in transamination systems. *Biochem. J.*, **54**, 82–86.
10. Kim, M., Gwak, J., Hwang, S., Yang, S. and Jeong, S.M. (2019) Mitochondrial GPT2 plays a pivotal role in metabolic adaptation to the perturbation of mitochondrial glutamine metabolism. *Oncogene*, **38**, 4729–4738.
11. DeBerardinis, R.J., Lum, J.J., Hatzivassiliou, G. and Thompson, C.B. (2008) The biology of cancer: metabolic reprogramming fuels cell growth and proliferation. *Cell Metab.*, **7**, 11–20.
12. Tan, H.W.S., Sim, A.Y.L. and Long, Y.C. (2017) Glutamine metabolism regulates autophagy-dependent mTORC1 reactivation during amino acid starvation. *Nat. Commun.*, **8**, 338.
13. Caiola, E., Colombo, M., Sestito, G., Lupi, M., Marabese, M., Pastorelli, R., Broggini, M. and Brunelli, L. (2020) Glutaminase inhibition on NSCLC depends on extracellular alanine exploitation. *Cell*, **9**.
14. Hao, Y., Samuels, Y., Li, Q., Krokowski, D., Guan, B.J., Wang, C., Jin, Z., Dong, B., Cao, B., Feng, X. *et al.* (2016) Oncogenic PIK3CA mutations reprogram glutamine metabolism in colorectal cancer. *Nat. Commun.*, **7**, 11971.
15. Owen, O.E., Kalhan, S.C. and Hanson, R.W. (2002) The key role of anaplerosis and cataplerosis for citric acid cycle function. *J. Biol. Chem.*, **277**, 30409–30412.
16. Zhu, Y., Romero, M.I., Ghosh, P., Ye, Z., Charnay, P., Rushing, E.J., Marth, J.D. and Parada, L.F. (2001) Ablation of NF1 function in neurons induces abnormal development of cerebral cortex and reactive gliosis in the brain. *Genes Dev.*, **15**, 859–876.
17. Sallach, H.J. (1956) Formation of serine hydroxypyruvate and L-alanine. *J. Biol. Chem.*, **223**, 1101–1108.
18. Salgado, M.C., Meton, I., Anemaet, I.G. and Baanante, I.V. (2014) Activating transcription factor 4 mediates up-regulation of alanine aminotransferase 2 gene expression under metabolic stress. *Biochim. Biophys. Acta*, **1839**, 288–296.
19. Wortel, I.M.N., van der Meer, L.T., Kilberg, M.S. and van Leeuwen, F.N. (2017) Surviving stress: modulation of ATF4-mediated stress responses in normal and malignant cells. *Trends Endocrinol. Metab.*, **28**, 794–806.
20. Macosko, E.Z., Basu, A., Satija, R., Nemesh, J., Shekhar, K., Goldman, M., Tirosh, I., Bialas, A.R., Kamitaki, N., Martersteck, E.M. *et al.* (2015) Highly parallel genome-wide expression profiling of individual cells using nanoliter droplets. *Cell*, **161**, 1202–1214.
21. Gregorian, C., Nakashima, J., Le Belle, J., Ohab, J., Kim, R., Liu, A., Smith, K.B., Groszer, M., Garcia, A.D., Sofroniew, M.V. *et al.* (2009) Pten deletion in adult neural stem/progenitor cells enhances constitutive neurogenesis. *J. Neurosci.*, **29**, 1874–1886.

22. Zhang, Y., Chen, K., Sloan, S.A., Bennett, M.L., Scholze, A.R., O'Keeffe, S., Phatnani, H.P., Guarnieri, P., Caneda, C., Ruderisch, N. *et al.* (2014) An RNA-sequencing transcriptome and splicing database of glia, neurons, and vascular cells of the cerebral cortex. *J. Neurosci.*, **34**, 11929–11947.
23. Zhang, Y., Sloan, S.A., Clarke, L.E., Caneda, C., Plaza, C.A., Blumenthal, P.D., Vogel, H., Steinberg, G.K., Edwards, M.S., Li, G. *et al.* (2016) Purification and characterization of progenitor and mature human astrocytes reveals transcriptional and functional differences with mouse. *Neuron*, **89**, 37–53.
24. Hodge, R.D., Bakken, T.E., Miller, J.A., Smith, K.A., Barkan, E.R., Graybuck, L.T., Close, J.L., Long, B., Johansen, N., Penn, O. *et al.* (2019) Conserved cell types with divergent features in human versus mouse cortex. *Nature*, **573**, 61–68.
25. Schousboe, A., Scafidi, S., Bak, L.K., Waagepetersen, H.S. and McKenna, M.C. (2014) Glutamate metabolism in the brain focusing on astrocytes. *Adv Neurobiol.*, **11**, 13–30.
26. Cooper, A.J. and Jeitner, T.M. (2016) Central role of glutamate metabolism in the maintenance of nitrogen homeostasis in normal and Hyperammonemic brain. *Biomol. Ther.*, **6**.
27. De Meirleir, L. (2014) Pyruvate carboxylase and pyruvate dehydrogenase deficiency, in Physician's guide to the diagnosis, treatment, and follow-up of inherited metabolic diseases. 303–311.
28. Shin, H.K., Grahame, G., McCandless, S.E., Kerr, D.S. and Bedoyan, J.K. (2017) Enzymatic testing sensitivity, variability and practical diagnostic algorithm for pyruvate dehydrogenase complex (PDC) deficiency. *Mol. Genet. Metab.*, **122**, 61–66.
29. McKenna, M.C. and Ferreira, G.C. (2016) Enzyme complexes important for the glutamate-glutamine cycle. *Adv Neurobiol.*, **13**, 59–98.
30. Fahien, L.A., Hsu, S.L. and Kmiotek, E. (1977) Effect of aspartate on complexes between glutamate dehydrogenase and various aminotransferases. *J. Biol. Chem.*, **252**, 1250–1256.
31. Hohnholt, M.C., Andersen, V.H., Andersen, J.V., Christensen, S.K., Karaca, M., Maechler, P. and Waagepetersen, H.S. (2018) Glutamate dehydrogenase is essential to sustain neuronal oxidative energy metabolism during stimulation. *J. Cereb. Blood Flow Metab.*, **38**, 1754–1768.
32. Fasman, G.D. (1989) *Prediction of Protein Structure and the Principles of Protein Conformation*.
33. Taylor, J.P., Brown, R.H., Jr. and Cleveland, D.W. (2016) Decoding ALS: from genes to mechanism. *Nature*, **539**, 197–206.
34. Stevanin, G., Azzedine, H., Denora, P., Boukhris, A., Tazir, M., Lossos, A., Rosa, A.L., Lerer, I., Hamri, A., Alegria, P. *et al.* (2008) Mutations in SPG11 are frequent in autosomal recessive spastic paraplegia with thin corpus callosum, cognitive decline and lower motor neuron degeneration. *Brain*, **131**, 772–784.
35. Salinas, S., Proukakis, C., Crosby, A. and Warner, T.T. (2008) Hereditary spastic paraplegia: clinical features and pathogenetic mechanisms. *The Lancet Neurology.*, **7**, 1127–1138.
36. Ruaud, L., Keren, B., Debs, R., Mignot, C. and Mochel, F. (2021) Demyelinating motor neuropathy associated with a homozygous GPT2 pathogenic variant. *Muscle Nerve*.
37. Bodamer, O.A., Halliday, D. and Leonard, J.V. (2000) The effects of l-alanine supplementation in late-onset glycogen storage disease type II. *Neurology*, **55**, 710–712.
38. Carlin, J.I., Olson, E.B., Jr., Peters, H.A. and Reddan, W.G. (1987) The effects of post-exercise glucose and alanine ingestion on plasma carnitine and ketosis in humans. *J. Physiol.*, **390**, 295–303.
39. Genuth, S.M. and Castro, J. (1974) Effect of oral alanine on blood beta-hydroxybutyrate and plasma glucose, insulin, free fatty acids, and growth hormone in normal and diabetic subjects. *Metabolism*, **23**, 375–386.
40. Celis, K., Shuldiner, S., Haverfield, E.V., Cappell, J., Yang, R., Gong, D.W. and Chung, W.K. (2015) Loss of function mutation in glutamic pyruvate transaminase 2 (GPT2) causes developmental encephalopathy. *J. Inherit. Metab. Dis.*, **38**, 941–948.
41. Council, N.R. (2011) *Guide for the Care and Use of Laboratory Animals*, 8th edn. The National Academies Press, Washington, DC, p. 246.
42. Yuan, M., Breitkopf, S.B., Yang, X. and Asara, J.M. (2012) A positive/negative ion-switching, targeted mass spectrometry-based metabolomics platform for bodily fluids, cells, and fresh and fixed tissue. *Nat. Protoc.*, **7**, 872–881.
43. Chong, J., Wishart, D.S. and Xia, J. (2019) Using MetaboAnalyst 4.0 for comprehensive and integrative metabolomics data analysis. *Curr. Protoc. Bioinformatics*, **68**, e86.
44. Ouyang, Q., Lizarraga, S.B., Schmidt, M., Yang, U., Gong, J., Ellisor, D., Kauer, J.A. and Morrow, E.M. (2013) Christianson syndrome protein NHE6 modulates TrkB endosomal signaling required for neuronal circuit development. *Neuron*, **80**, 97–112.
45. Schildge, S., Bohrer, C., Beck, K. and Schachtrup, C. (2013) Isolation and culture of mouse cortical astrocytes. *J. Vis. Exp.*.
46. Albuquerque, C., Joseph, D.J., Choudhury, P. and MacDermott, A.B. (2009, 2009) Dissection, plating, and maintenance of cortical astrocyte cultures. *Cold Spring Harb Protoc*, pdb prot5273.
47. Sims, N.R. and Anderson, M.F. (2008) Isolation of mitochondria from rat brain using Percoll density gradient centrifugation. *Nat. Protoc.*, **3**, 1228–1239.
48. Kanehisa, M., Furumichi, M., Sato, Y., Ishiguro-Watanabe, M. and Tanabe, M. (2020) KEGG: integrating viruses and cellular organisms. *Nucleic Acids Res.*.

SUPPLEMENTARY FIGURE 1.

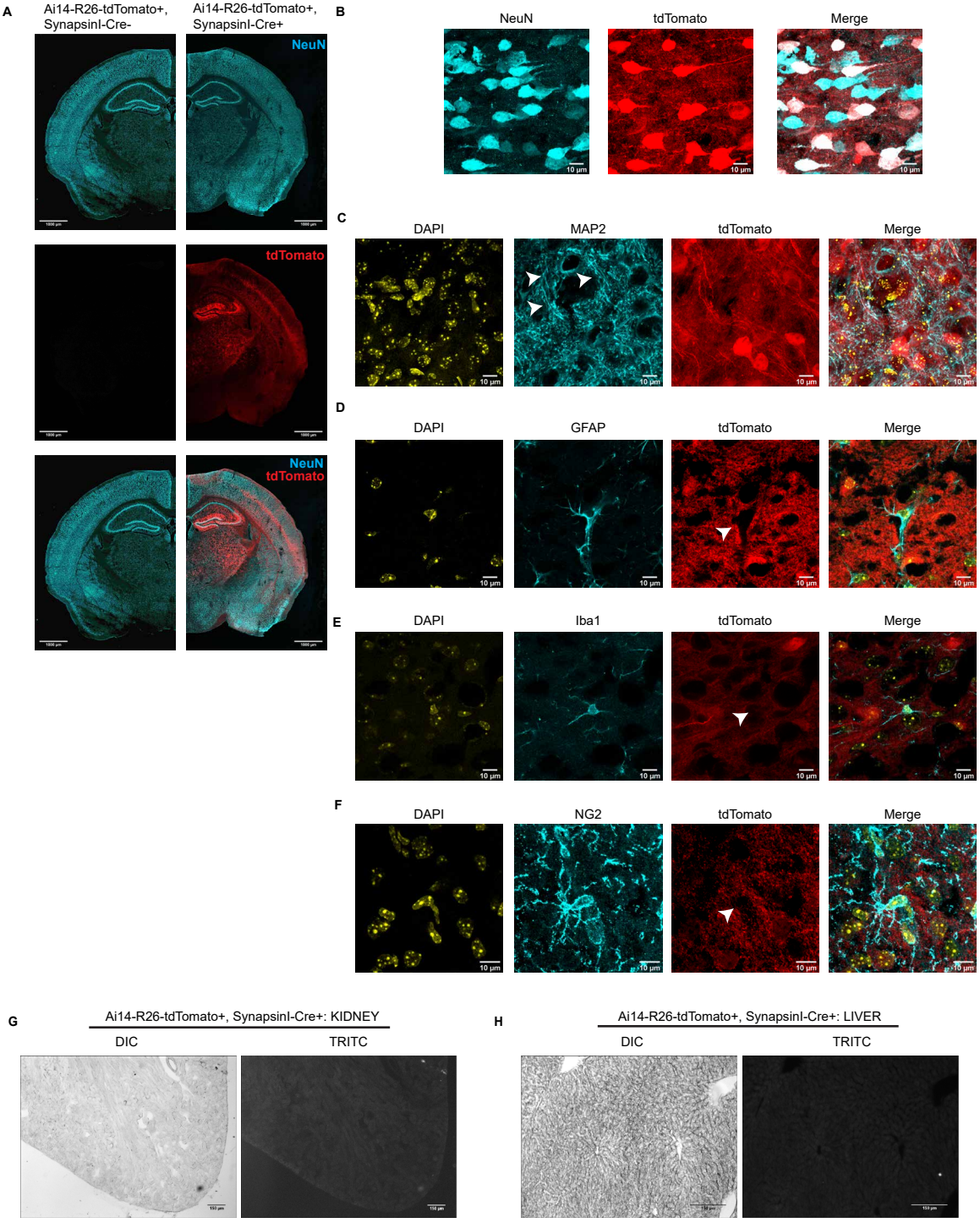

SUPPLEMENTARY FIGURE 2

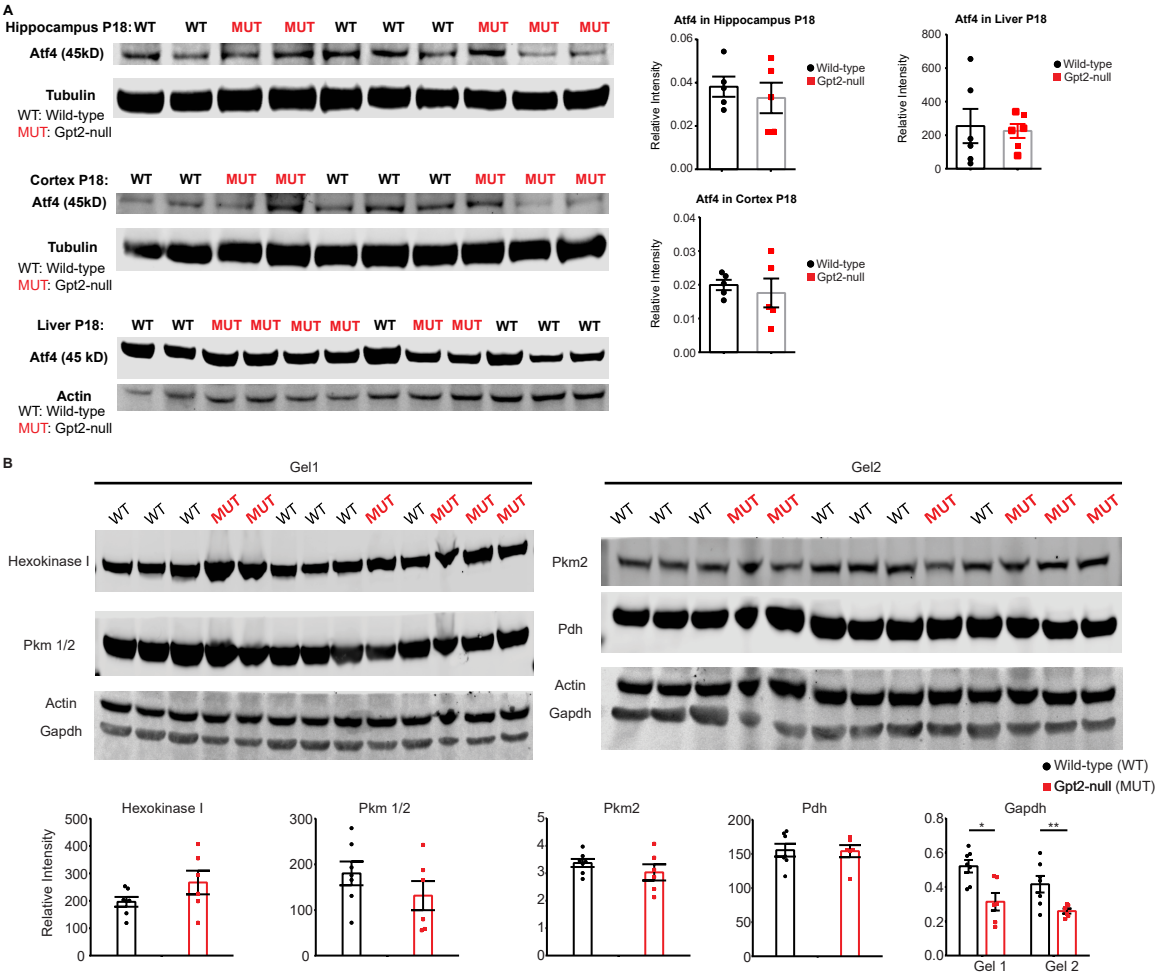

SUPPLEMENTARY FIGURE 3

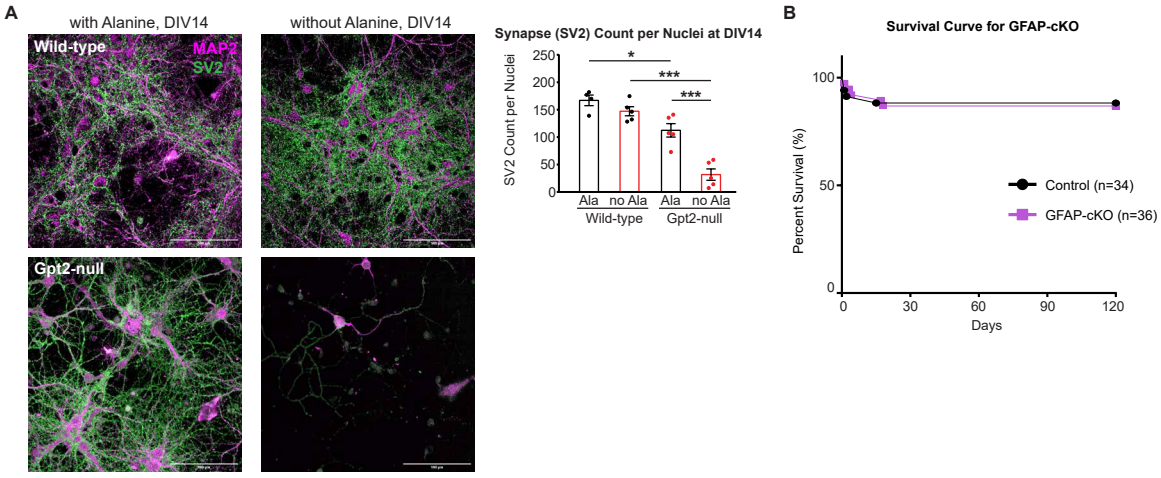

SUPPLEMENTARY FIGURE 4

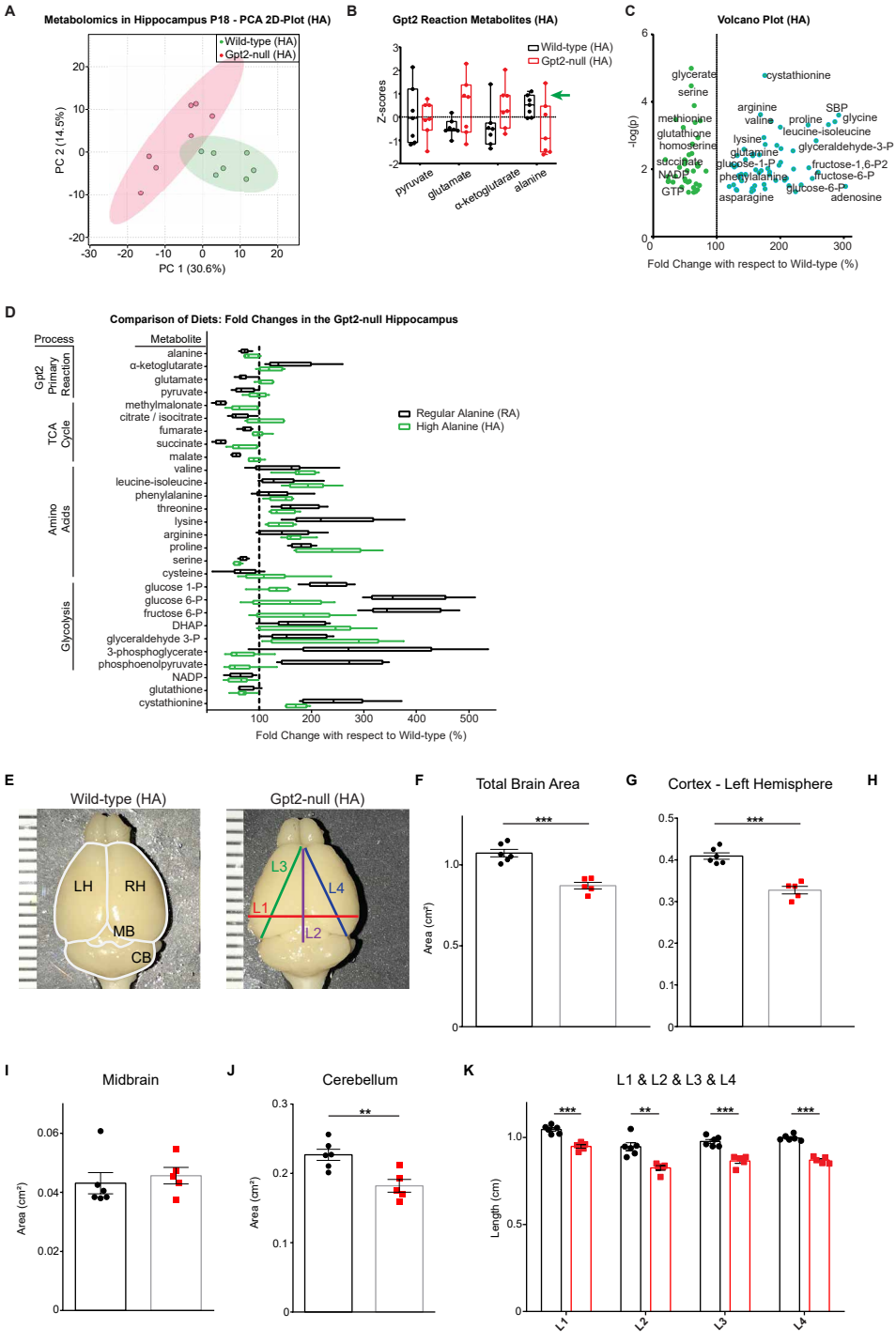

SUPPLEMENTARY FIGURE 5

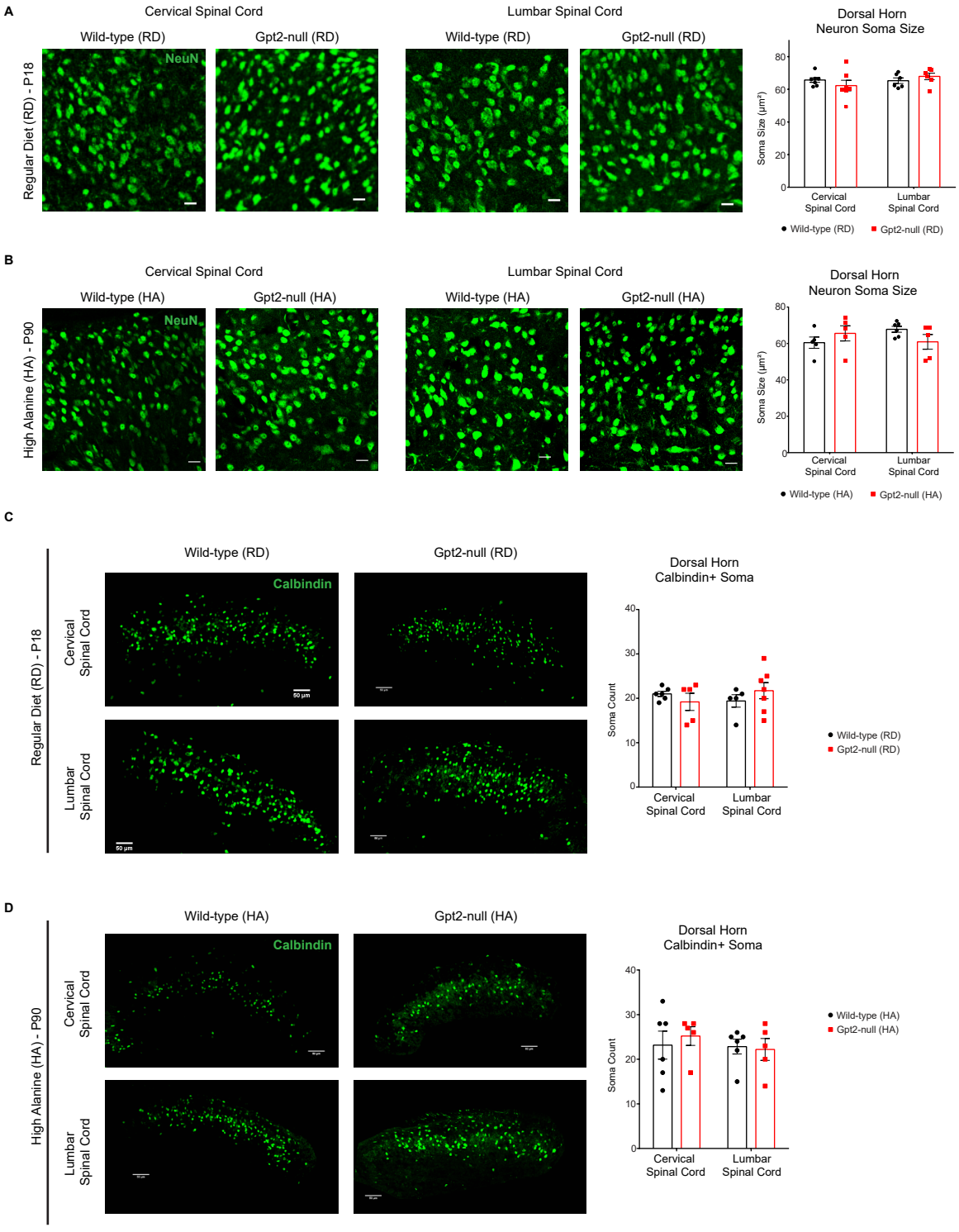

SUPPLEMENTARY FIGURE 6

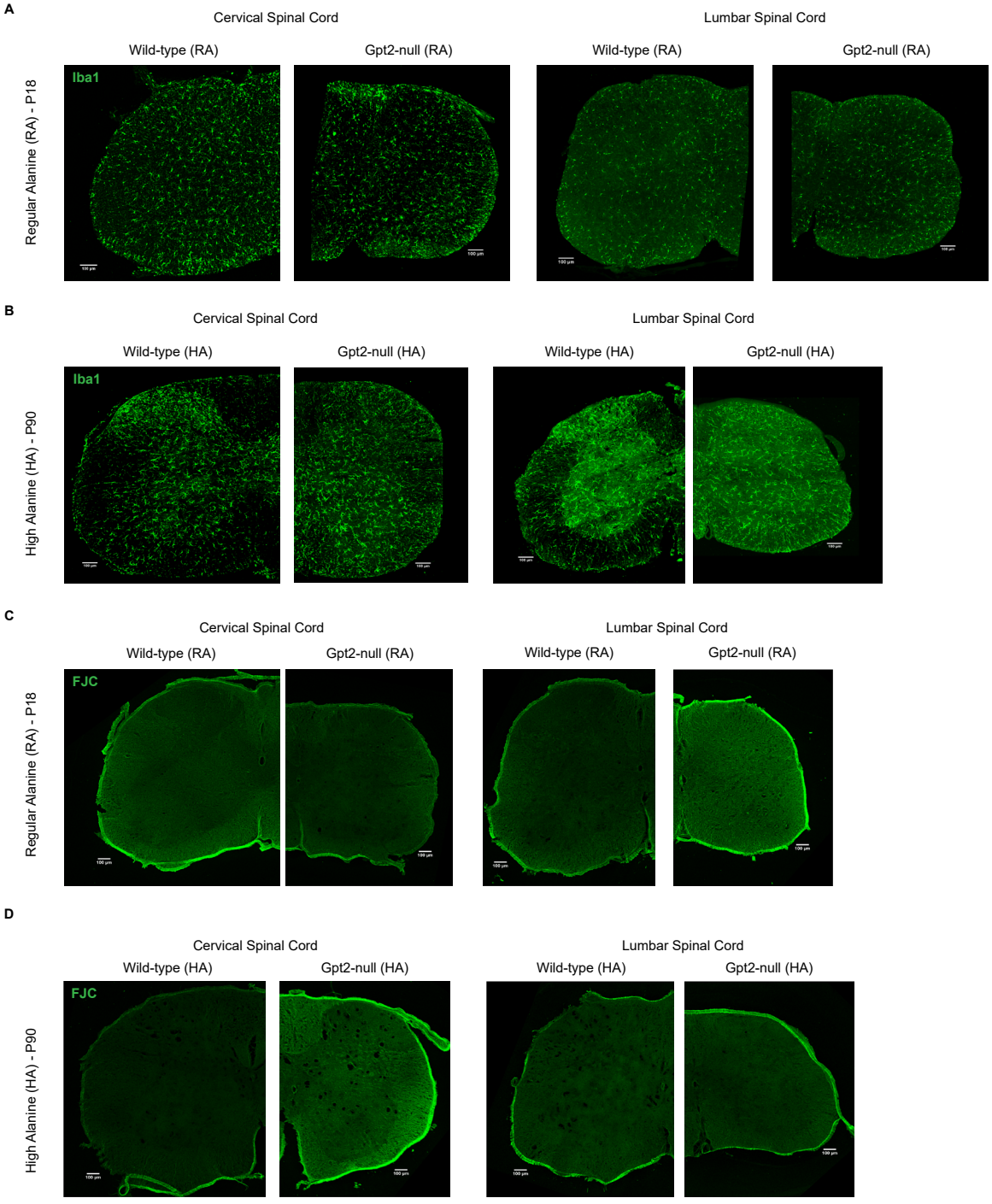

SUPPLEMENTARY FIGURE 7

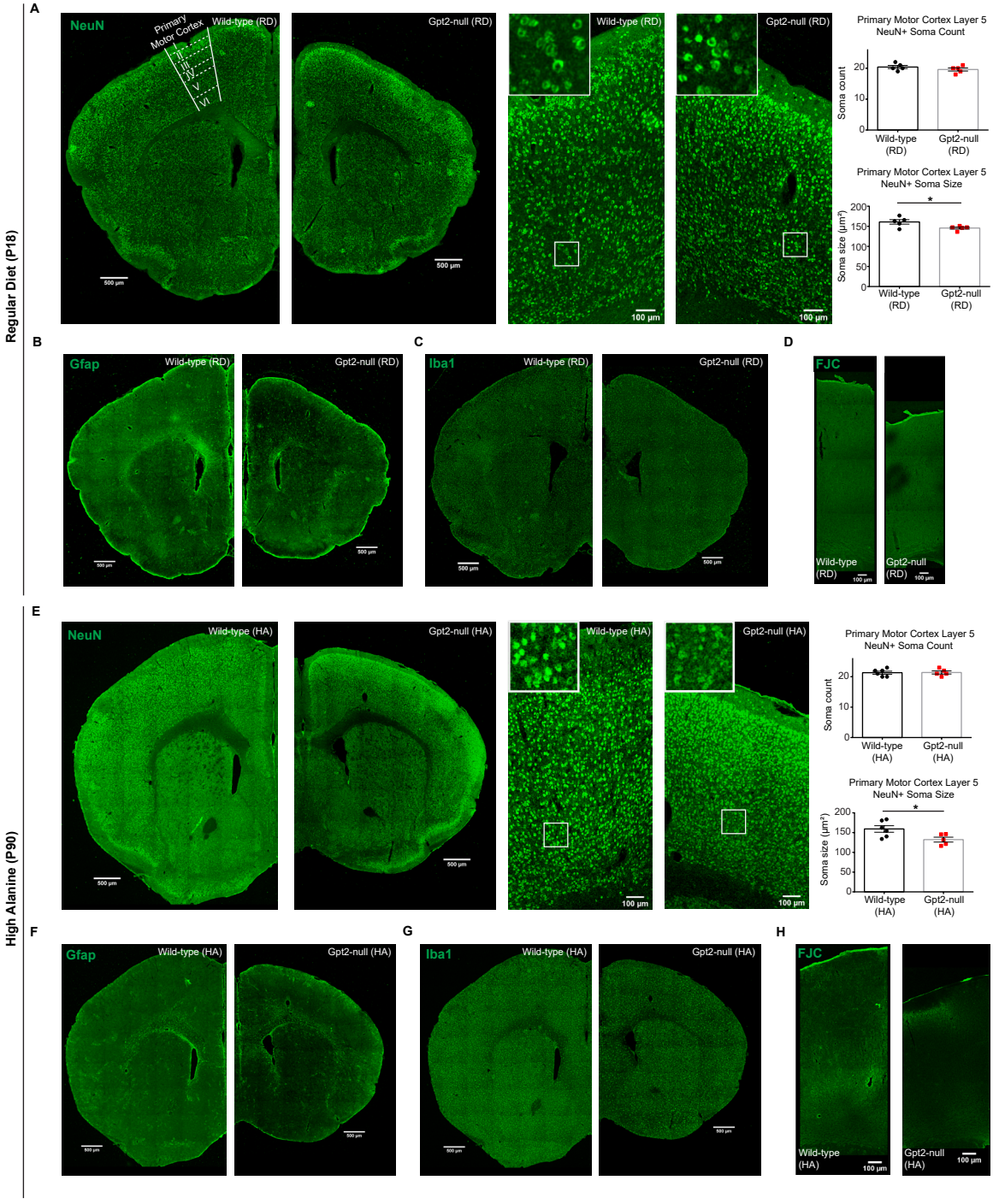

SUPPLEMENTARY Data

Supplementary Figure Legends

Supplementary Figure S1. Confirmation of the SynapsinI-Cre mouse line with the Ai14-R26-tdTomato Cre reporter line.

A. Coronal brain section images of Ai14-R26-tdTomato Cre+/SynapsinI-Cre- (left) and Ai14-R26-tdTomato Cre+/SynapsinI-Cre+ (right) animals at P50. Note the tdTomato (middle) is absent in the animal without the SynapsinI-Cre transgene. Overall tdTomato signal appears abundant near the neuronal soma (NeuN, cyan, top). Scale bar: 1000 μm.

B. NeuN (cyan) and tdTomato (red) signals in images of somatosensory cortex (layer 3) from an Ai14-R26-tdTomato Cre+/SynapsinI-Cre+ animal, taken with a 63X objective. White color indicates co-localization of NeuN and tdTomato. Scale bar: 10 μm.

C. MAP2 (cyan) and tdTomato (red) signals in images of somatosensory cortex (layer 3) from an Ai14-R26-tdTomato Cre+/SynapsinI-Cre+ animal, taken with a 63X objective. White color indicates co-localization of MAP2 and tdTomato. Arrow heads point toward example areas where co-localization of MAP2 and tdTomato is observed. Scale bar: 10 μm.

D. GFAP (cyan) and tdTomato (red) signals in images of somatosensory cortex (layer 3) from an Ai14-R26-tdTomato Cre+/SynapsinI-Cre+ animal, taken with a 63X objective. Note that the GFAP signal is not present in cells positive for tdTomato signal (arrowhead). Scale bar: 10 μm.

E. Iba1 (cyan) and tdTomato (red) signals in images of somatosensory cortex (layer 3) from an Ai14-R26-tdTomato Cre+/SynapsinI-Cre+ animal, taken with a 63X objective. Note that the Iba1 signal is not present in cells positive for tdTomato signal (arrowhead). Scale bar: 10 μm.

F. NG2 (cyan) and tdTomato (red) signals in images of somatosensory cortex (layer 3) from an Ai14-R26-tdTomato Cre+/SynapsinI-Cre+ animal, taken with a 63X objective. Note that the NG2 signal is not present in cells positive for tdTomato signal (arrowhead). Scale bar: 10 μm.

G. Differential interference contrast (DIC, left) microscopy image and the TRITC signal (tdTomato, right) in a corresponding fluorescence microscopy image of the kidney from an Ai14-R26-tdTomato Cre+/SynapsinI-Cre+ animal, taken with a 10X objective. Note the absence of fluorescence in the kidney tissue. Scale bar: 150 μm.

H. Differential interference contrast (DIC, left) microscopy image and the TRITC signal (tdTomato, right) in a corresponding fluorescence microscopy image of the liver from an Ai14-R26-tdTomato Cre+/SynapsinI-Cre+ animal, taken with a 10X objective. Note the absence of fluorescence in the liver tissue. Scale bar: 150 μm.

Supplementary Figure 2. Quantification of protein levels of the transcription factor Atf4 and enzymes involved in glycolysis in wild-type and Gpt2-null mice at P18 by Western blotting.

A. Western blotting for Atf4 (Entrez gene: 468) in hippocampus, cortex and liver protein lysates from wild-type and Gpt2-null mice at P18. There were no statistically significant changes in normalized band intensities (Hippocampus: WT: 0.038 ± 0.0047 vs. MUT:

0.033 ± 0.0070, $P = 0.5560$; Cortex: WT: 0.0199 ± 0.0015 vs. MUT: 0.0176 ± 0.0043, $P = 0.6172$; Liver: WT: 254.7 ± 102.1 vs. MUT: 225.2 ± 41.68, $P = 0.7947$). Each Atf4 band was normalized to its corresponding tubulin band. Each lane represents a protein lysate sample from a different animal.

B. Western blotting for hexokinase I, pyruvate kinase (Pkm1/2), pyruvate kinase (Pkm2), pyruvate dehydrogenase (Pdh) and glyceraldehyde 3-phosphate dehydrogenase (Gapdh) in hippocampus protein lysates from wild-type and Gpt2-null animals at P18. There were no statistically significant changes in normalized band intensities of hexokinase I (WT: 196.3 ± 17.8 vs. MUT: 266.8 ± 43.1, $P = 0.138$), Pkm 1/2 (WT: 180.3 ± 25.95 vs. MUT: 131.7 ± 31.84, $P = 0.2567$) or Pkm2 (WT: 3.37 ± 0.15 vs. MUT: 3.03 ± 0.29, $P = 0.3013$) between the wild-type and Gpt2-null samples. Gapdh was significantly reduced in the Gpt2-null hippocampus (Gel1: WT: 0.521 ± 0.036 vs. MUT: 0.314 ± 0.051, $P = 0.0063$; Gel2: WT: 0.416 ± 0.048 vs. MUT: 0.2594 ± 0.015, $P = 0.0148$). Each band was normalized to its corresponding actin band. Each lane represents a protein lysate sample from a different animal.

Supplementary Figure 3. Synaptogenesis in Gpt2-null hippocampal neurons in vitro and survival curve of GFAP-cKO animals *in vivo*.

A. Synapse count per neuron is decreased in Gpt2-null cultures and this phenotype is worsened by alanine deprivation. Images from Opera Phenix High Content Screening Confocal Microscopy of SV2 (green) and MAP2 (magenta) (left) and quantification of SV2 count per nuclei (right). The cells were processed as in panel C. Scale bar: 100 μm. $*P < 0.05$, $**P < 0.005$, $***P < 0.0005$.

B. Survival curve of GFAP-Cre conditional-null (GFAP-cKO) and control mice. Control (black) n=34, GFAP-cKO (magenta) n=36 animals. Log-rank (Mantel-Cox) test was used to determine significant differences between the curves. *P* (Control vs. GFAP-cKO) = 0.8937.

Supplementary Figure 4. Metabolic profile and gross anatomy measurements of wild-type and Gpt2-null brain at P90 on High Alanine diet.

A. 2-D Score Plots of PCA of the polar metabolic profile in the wild-type (HA) (green) and Gpt2-null (HA) (red) hippocampus at P18. Note that the confidence regions (95%) of the two groups intersect.

B. Z-scores of normalized peak intensities of metabolites in the Gpt2 reaction from wild-type (HA) (black) and Gpt2-null (HA) (red) hippocampus at P18. The green arrow points to the three Gpt2-null (HA) samples that were closest to the wild-type (HA) samples. All comparisons were statistically insignificant.

C. Volcano plots of significantly changed metabolites in the Gpt2-null (HA) hippocampus with respect to wild-type (HA) levels. The peak intensities were processed as in (Figure 2D). Wild-type (HA) n=7 mice, Gpt2-null (HA) n=7.

D. Comparison of fold changes of metabolites in hippocampal samples obtained at P18 from mice fed RA diet (black) or HA diet (green). Metabolites of interest were sorted according to processes, including Gpt2 reaction metabolites, TCA cycle metabolites, amino acids and glycolysis. In the box-and-whisker plots, the whiskers are minimum and maximum with the vertical line denoting the average. The entire metabolomics data sets along with false discovery rates for each metabolite can be found in Table S5.

E. Images of brains from a wild-type (HA, left) and Gpt2-null (HA, right) littermate pair at age P90 marked with the area and length measurements. Ruler demarcations are at 1-mm scale. LH: Left Hemisphere, RH: Right Hemisphere, MB: Midbrain, CB: Cerebellum.

F. Total brain area measurements of wild-type (HA, black) and Gpt2-null (HA, red) mice at P90. There was a statistically significant reduction in total brain area in Gpt2-null (HA) mice compared to wild-type (HA) mice at P90. Wild-type (HA): 1.072 ± 0.023 cm^2 vs. Gpt2-null (HA): 0.8709 ± 0.02 cm^2, ***P = 0.0001. The measurements excluded the olfactory bulb.

G. Cortex - Left Hemisphere area measurements of wild-type (HA, black) and Gpt2-null (HA, red) mice at P90. There was a statistically significant reduction in the measured area in Gpt2-null (HA) mice compared to wild-type (HA) mice at P90. Wild-type (HA): 0.3834 ± 0.01 cm^2 vs. Gpt2-null (HA): 0.3102 ± 0.005 cm^2, ***P = 0.0003.

H. Cortex - Right Hemisphere area measurements of wild-type (HA, black) and Gpt2-null (HA, red) mice at P90. There was a statistically significant reduction in the measured area in Gpt2-null (HA) mice compared to wild-type (HA) mice at P90. Wild-type (HA): 0.4091 ± 0.0076 cm^2 vs. Gpt2-null (HA): 0.3274 ± 0.009 cm^2, ***P < 0.0001.

I. Midbrain area measurements of wild-type (HA, black) and Gpt2-null (HA, red) mice at P90. The Gpt2-null (HA) mice at P90 had similar midbrain area as their wild-type (HA) littermates. Wild-type (HA): 0.0431 ± 0.0036 cm^2 vs. Gpt2-null (HA): 0.0456 ± 0.0028 cm^2, P = 0.6017.

J. Cerebellum area measurements of wild-type (HA, black) and Gpt2-null (HA, red) mice at P90. There was a statistically significant reduction in the measured area in Gpt2-null

(HA) mice compared to wild-type (HA) mice at P90. Wild-type (HA): 0.2268 ± 0.008 cm^2 vs. Gpt2-null (HA): 0.1821 ± 0.009 cm^2, $^{**}P = 0.0051$.

K. L1, L2, L3 and L4 length measurements of wild-type (HA, black) and Gpt2-null (HA, red) mice at P90. There were statistically significant reductions in all four measured areas in Gpt2-null (HA) mice compared to wild-type (HA) mice at P90. L1, Wild-type (HA): 1.046 ± 0.0096 cm vs. Gpt2-null (HA): 0.949 ± 0.01 cm, $^{***}P < 0.0001$; L2, Wild-type (HA): 0.947 ± 0.023 cm vs. Gpt2-null (HA): 0.825 ± 0.013 cm, $^{**}P = 0.0018$; L3, Wild-type (HA): 0.977 ± 0.012 cm vs. Gpt2-null (HA): 0.865 ± 0.014 cm, $^{***}P = 0.00016$; L4, Wild-type (HA): 0.998 ± 0.0069 cm vs. Gpt2-null (HA): 0.8702 ± 0.008 cm, $^{***}P < 0.0001$.

Supplementary Figure S5. NeuN+ and Calbindin+ cell analyses in the spinal cord in wild-type and Gpt2-null mice on regular alanine diet at P18 or high alanine diet at P90.

A. Images of NeuN+ soma in cervical and lumbar spinal cord sections (100 μm x 100 μm) from wild-type and Gpt2-null mice on RA diet at P18. (Cervical spinal cord NeuN+ count, Wild-type (RA): 46.5 ± 2.99 vs. Gpt2-null (RA): 52.3 ± 2.12, $P = 0.1425$; Lumbar spinal cord NeuN+ count, Wild-type (RA): 37.4 ± 4 vs. Gpt2-null (RA): 43 ± 3.36, $P = 0.3073$.) Quantification of soma size for neurons of the dorsal horn is shown to the right. (Cervical spinal cord NeuN+ soma size, Wild-type (RA): 65.68 ± 1.41 μm^2 vs. Gpt2-null (RA): 62.26 ± 3.25 μm^2, $P = 0.3541$; Lumbar spinal cord NeuN+ soma size, Wild-type (RA): 65.26 ± 1.72 μm^2 vs. Gpt2-null (RA): 67.89 ± 2.03 μm^2, $P = 0.3457$.) Scale bar: 10 μm.

B. Images of NeuN+ soma in cervical and lumbar spinal cord sections (100 μm x 100 μm) from wild-type and Gpt2-null mice on HA diet at P90. (Cervical spinal cord NeuN+ count, Wild-type (HA): 58.2 ± 5.36 vs. Gpt2-null (HA): 60.4 ± 2.94, $P = 0.7283$; Lumbar spinal cord NeuN+ count, Wild-type (HA): 53.8 ± 3.86 vs. Gpt2-null: 46.6 ± 2.01, $P = 0.1533$.) Quantification of soma size for neurons of the dorsal horn is shown to the right. (Cervical spinal cord NeuN+ soma size, Wild-type (HA): 60.45 ± 3.1 μm^2 vs. Gpt2-null: 65.54 ± 4.18 μm^2, $P = 0.3566$; Lumbar spinal cord NeuN+ soma Size, Wild-type (HA): 67.79 ± 1.62 μm^2 vs. Gpt2-null: 60.89 ± 4.05 μm^2, $P = 0.1245$.) Scale bar: 10 μm.

C. Images of Calbindin+ soma in cervical and lumbar spinal cord sections from wild-type and Gpt2-null mice on RA diet at P18 (stitched images taken with 20X objective). Quantification of Calbindin+ soma in the dorsal horn is shown to the right. (Cervical spinal cord Calbindin+ count, Wild-type (RA): 21 ± 0.58 vs. Gpt2-null (RA): 19.2 ± 1.93, $P = 0.3581$; Lumbar spinal cord Calbindin+ count, Wild-type (RA): 19.4 ± 1.4 vs. Gpt2-null (RA): 21.7 ± 1.82, $P = 0.3717$.) Scale bar: 50 μm.

D. Images of Calbindin+ soma in cervical and lumbar spinal cord sections from wild-type and Gpt2-null mice on HA diet at P90 (stitched images taken with 20X objective). Quantification of Calbindin+ soma in the dorsal horn is shown to the right. (Cervical spinal cord Calbindin+ count, Wild-type (HA): 23.17 ± 3.13 vs. Gpt2-null (HA): 25.2 ± 2.08 $P = 0.6185$; Lumbar spinal cord Calbindin+ count, Wild-type (HA): 22.83 ± 1.66 vs. Gpt2-null (HA): 22.2 ± 2.46, $P = 0.8309$.) Scale bar: 50 μm.

Supplementary Figure S6. Iba1 and Fluoro-Jade C staining in spinal cord in wild-type and Gpt2-null mice on regular alanine diet at P18 or high alanine diet at P90.

A. Images of Iba1 staining in cervical and lumbar spinal cord sections from wild-type and Gpt2-null mice on RA diet at P18 (stitched images taken with 20X objective). Scale bar: 100 μm.

B. Images of Iba1 staining in cervical and lumbar spinal cord sections from wild-type and Gpt2-null mice on HA diet at P90 (stitched images taken with 20X objective). Scale bar: 100 μm.

C. Images of Fluoro-Jade C (FJC) fluorescence in cervical and lumbar spinal cord sections from wild-type and Gpt2-null mice on RA diet at P18 (stitched images taken with 20X objective). Scale bar: 100 μm.

D. Images of Fluoro-Jade C (FJC) fluorescence in cervical and lumbar spinal cord sections from wild-type and Gpt2-null mice on HA diet at P90 (stitched images taken with 20X objective). Scale bar: 100 μm.

Supplementary Figure S7. NeuN, Iba1, Gfap and Fluoro-Jade C staining in the primary motor cortex of Gpt2-null mice on regular alanine diet at P18 and high alanine diet at P90.

A. Images of NeuN staining in coronal sections containing primary motor cortex from wild-type (left) and Gpt2-null (right) mice on RA diet at P18 (stitched images taken with 20X objective). Cortical layers are demarcated, and the primary motor cortex is denoted. Scale bar: 500 μm. The primary motor cortex was cropped, and layer 5 neurons boxed in white were magnified and are shown in the inset in the upper left corner. Scale bar: 100 μm. Quantification of NeuN+ soma count and soma size are shown on the right. *$0.01 < P < 0.05$.

B. Images of Gfap staining in coronal sections containing the primary motor cortex from wild-type (left) and Gpt2-null (right) mice on RA diet at P18. Scale bar: 500 μm.

C. Images of Iba1 staining in coronal sections containing the primary motor cortex from wild-type (left) and Gpt2-null (right) mice on RA diet at P18. Scale bar: 500 μm.

D. Images of Fluoro-Jade C (FJC) staining in coronal sections containing the primary motor cortex from wild-type (left) and Gpt2-null (right) mice on RA diet at P18. Scale bar: 100 μm.

E. Images of NeuN staining in coronal sections containing primary motor cortex from wild-type (left) and Gpt2-null (right) mice on HA diet at P90 (stitched images taken with 20X objective). Scale bar: 500 μm. The primary motor cortex was cropped, and the layer 5 neurons boxed in white were magnified and are shown in the inset in the upper left corner. Scale bar: 100 μm. Quantification of NeuN+ soma count and soma size are shown on the right. *$0.01 < P < 0.05$.

F. Images of Gfap staining in coronal sections containing the primary motor cortex from wild-type (left) and Gpt2-null (right) mice on HA diet at P90. Scale bar: 500 μm.

G. Images of Iba1 staining in coronal sections containing the primary motor cortex from wild-type (left) and Gpt2-null (right) mice on HA diet at P90. Scale bar: 500 μm.

H. Images of Fluoro-Jade C (FJC) staining in coronal sections containing the primary motor cortex from wild-type (left) and Gpt2-null (right) mice on HA diet at P90. Scale bar: 100 μm.

For supplementary videos, refer to the Brown Thesis Repository.

Supplementary Video S1. Hind-limb clasping reflex of wild-type mouse at P18 raised on regular alanine diet.

Supplementary Video S2. Hind-limb clasping reflex of Gpt2-null mouse at P18 raised on regular alanine diet.

Supplementary Video S3. Hind-limb clasping reflex of SynapsinI-Cre Gpt2-cKO mouse at P18 raised on regular alanine diet.

Supplementary Video S4. Open Field Test of wild-type mouse at P18 raised on regular alanine diet.

Supplementary Video S5. Open Field Test of Gpt2-null mouse at P18 raised on regular alanine diet.

Supplementary Video S6. Open Field Test of SynapsinI-Cre Gpt2-cKO mouse at P18 raised on regular alanine diet.

Supplementary Video S7. Hind-limb clasping reflex of wild-type mouse at P18 raised on high alanine diet.

Supplementary Video S8. - Hind-limb clasping reflex of Gpt2-null mouse at P18 raised on high alanine diet.

Supplementary Video S9. Hind-limb clasping reflex of wild-type mouse at P90 raised on high alanine diet.

Supplementary Video S10. Hind-limb clasping reflex of Gpt2-null mouse at P90 raised on high alanine diet.

Supplementary Video S11. Open Field Test of wild-type mouse at P18 raised on high alanine diet.

Supplementary Video S12. Open Field Test of Gpt2-null mouse at P18 raised on high alanine diet.

Supplementary Video S13. Open Field Test of wild-type mouse at P30 raised on high alanine diet.

Supplementary Video S14. Open Field Test of Gpt2-null mouse at P30 raised on high alanine diet.

Supplementary Video S15. Open Field Test of wild-type mouse at P60 raised on high alanine diet.

Supplementary Video S16. Open Field Test of Gpt2-null mouse at P60 raised on high alanine diet.

Supplementary Video S17. Open Field Test of wild-type mouse at P90 raised on high alanine diet.

Supplementary Video S18. Open Field Test of Gpt2-null mouse at P90 raised on high alanine diet.

Supplementary Tables

Supplementary Table S1. Targeted polar metabolomics in hippocampal tissue from wild-type and Gpt2-null littermates at age P18 raised on regular alanine diet.

This dataset includes Original Data of Liquid Chromatography-Mass Spectrometry (LC-MS) Peak Intensities, Normalized Data (Original Data was normalized to the sample median and auto-scaled (z-score)) and T-test Results (t.stat, raw p-value, -log(raw p-value), False Discovery Rate (FDR) and Fold Change of Gpt2-null average with respect to the wild-type average).

Supplementary Table S2. Targeted polar metabolomics in hippocampal tissue from wild-type and Gpt2-null littermates at age P14 raised on regular alanine diet.

This dataset includes Original Data of Liquid Chromatography-Mass Spectrometry (LC-MS) Peak Intensities, Normalized Data (Original Data was normalized to the sample median and auto-scaled (z-score)) and T-test Results (t.stat, raw p-value, -log(raw p-value), False Discovery Rate (FDR) and Fold Change of Gpt2-null average with respect to the wild-type average).

Supplementary Table S3. Targeted polar metabolomics in hippocampal tissue from wild-type and Gpt2-null littermates at age P7 raised on regular alanine diet.

This dataset includes Original Data of Liquid Chromatography-Mass Spectrometry (LC-MS) Peak Intensities, Normalized Data (Original Data was normalized to the sample median and auto-scaled (z-score)) and T-test Results (t.stat, raw p-value, -log(raw p-

value), False Discovery Rate (FDR) and Fold Change of Gpt2-null average with respect to the wild-type average).

Supplementary Table S4. Targeted polar metabolomics in hippocampal tissue from wild-type and Gpt2-null littermates at age P0 raised on regular alanine diet.

This dataset includes Original Data of Liquid Chromatography-Mass Spectrometry (LC-MS) Peak Intensities, Normalized Data (Original Data was normalized to the sample median and auto-scaled (z-score)) and T-test Results (t.stat, raw p-value, -log(raw p-value), False Discovery Rate (FDR) and Fold Change of Gpt2-null average with respect to the wild-type average).

Supplementary Table S5. Targeted polar metabolomics in hippocampal tissue from wild-type and Gpt2-null littermates at age P18 raised on high alanine diet.

This dataset includes Original Data of Liquid Chromatography-Mass Spectrometry (LC-MS) Peak Intensities, Normalized Data (Original Data was normalized to the sample median and auto-scaled (z-score)) and T-test Results (t.stat, raw p-value, -log(raw p-value), False Discovery Rate (FDR) and Fold Change of Gpt2-null average with respect to the wild-type average).

Supplementary Table S6. Comparison of fold changes of Gpt2-null liquid chromatography-mass spectrometry average peak intensities between regular alanine diet and high alanine diet at P18.

The table involves metabolites in the main Figure 6H and includes RA diet raw p-values and False Discovery Rates (FDR) from wild-type vs. Gpt2-null comparison, HA diet raw p-values and FDR from wild-type vs. Gpt2-null comparison, fold changes of Gpt2-null average peak intensities with respect to wild-type average peak intensities in the RA diet, fold changes of Gpt2-null average peak intensities with respect to wild-type average peak intensities in the HA diet, and raw p-values for the comparison of fold changes between RA diet and HA diet. The raw LC-MS peak intensity data can be found in Supplementary Tables 1 and 5.

Supplementary Table S7. Composition of regular alanine diet (1.19% w/w), high alanine diet (5% w/w) and Neurobasal-A culture medium.

In the "Diet" sheet, all of the components of the two different diets are given side by side; N/A indicates non-applicable for components with no available information in the respective diet product sheet.

SUPPLEMENTARY TABLE 1. ORIGINAL DATA.

Label	MUT	MUT	MUT	MUT	MUT	MUT	MUT	MUT	MUT	WT	WT	WT	WT	WT	WT
glyoxylate	39267.82	54094.13	37731.21	29402.29	49846.21	41141.63	33029.45	40658.45	30924.01	32849.41	39281.14	46944.07	41549.47	52418.46	57115.11
glycolate	15236.08	9007.836	12586.13	17879.73	43291.8	8655.577	13107.35	45297.41	20534.13	4247.501	10308.67	9246.831	12130.06	14946.21	23716.06
pyruvate	33377.25	74054.83	35580.61	31841.01	69958.27	64689.47	57147.76	53189.09	26268.37	31280	26006.58	43202.87	57281.12	49098.88	67861.09
lactate	42843169	53009566	39601581	33061722	54234715	50428009	47659951	60446561	45216498	19170573	19142849	32794816	43450115	45441380	42322028
2-oxobutanoate	376575.1	323155.6	237507.4	271823.9	282640.8	364480.7	356543	285242.7	285129.2	193187.5	195661.9	348947.2	288978.8	345846	344516.1
acetoacetate	284552.3	254719.6	337804.1	328989.7	250576.8	321629.3	388331.2	235174.3	318639.2	171029	284849	310276.3	265090.6	308025.7	399374
glycerate	82043.69	148797	82487.56	61066.7	188209.2	129191	114042.4	219629.2	102352.7	31118.61	31107.64	61961.83	144660.4	123072	120719.5
uracil	15046898	36421044	6801377	6283759	43936271	17437371	16404508	52034260	15531311	935782	945976.2	3267742	8052119	16722711	15440460
fumarate	6189334	8415431	6004407	4574900	8463659	6548164	5342453	8487050	4900041	4142529	4151932	5850976	6872247	7096646	6547351
Maleic acid	6064453	8438828	5396539	4234883	8520426	6191221	5715685	8432516	5214969	3597019	4328955	5522321	6329187	6417668	6657515
2-keto-isovalerate	5740515	8113367	5743452	4542200	7807647	6363512	5721346	9250987	5263641	3409316	3839485	5535804	7042614	6797507	7129786
Guanidoacetic acid	5067.529	562314.4	245727	169788.2	10193.3	348832.6	5801.69	542703.9	192986.8	28905.49	25344.96	39785.36	88178.12	85280.43	83028.4
succinate	1149355	2786181	2141852	1865914	2240202	1336156	1374956	1017963	2132357	3668450	2734744	5065805	6135828	5705623	5965096
Methylmalonic acid	1499605	3439240	2611233	2214037	2692660	1691408	1546786	1167422	2674086	4452560	3410255	6172128	7422525	7000590	7028340
3-S-methylthiopropionate	13345.88	22977.74	17632.59	14964.46	35271.79	21908.99	8014.312	39546.5	13361.47	6947.12	9084.023	6948.289	20841.87	24579.84	16032.18
nicotinate	28238.05	59700.29	29176.79	27958.57	58446.1	74801.07	12399.55	122232	16754.15	8380.195	N/A	22065.23	N/A	14190.2	11586.85
taurine	32630712	38724134	35943576	32798792	41894617	33893118	32821219	44047171	32601362	31736356	32773489	33558516	35551581	35265004	33391807
Pyroglutamic acid	269680.9	389063.9	186851.9	99973.42	584895.3	180450.5	153478.5	603559.3	177426.3	42463.07	51286.28	86492.16	157476.9	143630.3	123601.4
Citraconic acid	1407046	1776094	1297043	1255143	2138782	1562213	1913545	1770134	1068707	889760.9	610150.6	1285243	1471114	1241388	1294188
2-ketohaxanoic acid	104108	103787	79992.97	68833.26	89653.67	103407.9	89680.82	122946.5	88379.75	40830.69	53373.16	77048.67	82878.84	108233	76065.46
N-Acetyl-L-alanine	40793910	50382737	37825055	29920317	48884179	43898264	37443497	53596427	37701283	20160394	19994067	29352942	41303529	42466157	38916884
oxaloacetate	210181.6	227845.1	224823.9	202068.1	120155.8	212416.6	326003	253389.5	199368.9	163224.5	176678.8	210136.4	204422	227722	256339.8
Hydroxyisocaproic acid	N/A	N/A	N/A	N/A	N/A	N/A	N/A	N/A	36358.01	15884.48	20745.55	19596.68	N/A	N/A	N/A
malate	21470005	25095958	19191630	16807276	20875738	18277915	18846510	25816485	17131135	17428759	18963440	26055347	28634134	24874839	29823672
hypoxanthine	29446787	42570180	24434066	18843300	43453156	31809763	26506049	44790519	26454470	8954622	7189520	18221787	28305442	26838169	26189907
anthranilate	N/A	N/A	N/A	42827.78	80815.42	1122034	41944.48	N/A	N/A	264303	33443.73	881123.8	44969.43	N/A	14683.28
p-aminobenzoate	N/A	N/A	N/A	N/A	40888.44	1036142	39572.55	N/A	N/A	225398.2	350801.8	18186.35	52114.81	N/A	N/A
p-hydroxybenzoate	354639.9	807208.9	403295.7	334773.6	699630.6	490952.6	387994.7	768146.4	397144.7	226272.7	151586.1	253383.2	729287.7	597548.5	350015.9
acetylphosphate	1170805	1989787	1099389	855276.1	2220517	1693480	1591624	2128984	1304897	8054.273	21932.74	463407.3	755515.6	66925.14	820945.8
Carbamoyl phosphate	61419311	85944689	55839673	45131863	92513393	67621490	56958470	97058497	57561823	22348342	5183.988	42439198	65995111	65396536	58628627
a-ketoglutarate	2799486	4727127	2152684	1544101	5751075	2732137	2326287	4698671	2031344	568892.3	857679.6	1420901	1613799	1849897	1652058
Phenylpropiolic acid	8513243	13731000	6522430	4413771	16088618	7860042	7609889	13446304	6032584	1877193	2603697	4735504	5965794	5305611	4585430
2-oxo-4-methylthiobutanoate	N/A	29879.98	15895.91	6703.648	17645.37	N/A	11259.76	42320.93	16725.41	8631.87	N/A	6014.291	8665.714	33106.34	12988.73
2-Hydroxy-2-methylbutanedioic acid	510466.9	724668.9	519432.8	557341.4	685064.8	618220	818072.2	788216.1	587268.2	449277.3	340452.4	633489.9	784536.8	715224.4	726307.3
3-methylphenylacetic acid	20071.96	39592.69	21713.57	15874.64	N/A	97812.52	20556.24	27293.69	20110.46	7576.56	14593.26	16743.91	21250.35	21130.11	43498.45
xanthine	8105829	10540726	5305026	4750339	13300824	7895328	7283431	14653456	8196020	2324648	1900587	3772918	7855057	6311225	5497384
Hydroxyphenylacetic acid	732175.3	894687.3	677504.8	613471.1	765208.6	636971.6	723194.1	521515.1	697818.6	323337.6	281339.4	617630.2	710138	767439.9	698019.5
2,3-dihydroxybenzoic acid	24852.15	72278.36	14488.5	19945.62	30214.99	44555.21	18415.97	99505.3	17376.13	19745.74	21934.95	52612.94	55046.07	16560.8	28138.45
orotate	304486.7	347172.8	173024.5	207224.6	422374.2	224395.4	350856.1	282587.5	233588.5	76479.03	126698.8	168102.5	218558.9	212075.2	208972.9
dihydroorotate	296683.8	255931.3	202084.5	220594.3	247010.7	287353	260500.6	304811.9	261800.9	458202.9	469822.2	141195.1	195678.6	258536.1	207535.7
allantoin	322260.5	657566.9	227697.6	163810.8	390602.2	262933.1	206513.7	557850.1	185419.7	97106.05	64110.15	107927.7	246327.7	266066.6	191787.4
Aminoadipic acid	167476	200453.3	111992	183809.9	169517.4	369372.1	326361.2	469391.8	367532.2	43788.07	52472	50233.85	290514.1	277400.8	158240.1
Indole-3-carboxylic acid	152172.1	214510.4	112514.3	173463.4	231607.7	315415.2	341810.7	535168.6	329140.9	45257.52	64006.78	46963.29	298939	300241.3	169866.9
phenylpyruvate	15517.17	21386.38	5217.637	2689.788	27784.95	11689.31	12822.46	31219.36	14959.2	N/A	4270.82	4233.909	6166.449	3355.728	4799.008
Atrolactic acid	N/A	5440.51	5656.95	9101.959	5523.545	9424.305	3492.925	6427.65	6367.682	8842.317	N/A	5002.235	7204.256	N/A	8015.935
Phenyllactic acid	N/A	10021.44	N/A	N/A	15458.4	N/A	N/A	5427.615	N/A	N/A	N/A	N/A	N/A	3347.811	N/A
quinolinate	16690.44	5361.567	7713.128	8172.776	22001.12	12368.37	13098.94	22137.04	10026.12	13819.92	7110.099	8903.06	21678.02	10870.59	3382.301
phosphoenolpyruvate	73879.23	63369.25	107316.7	92358.65	59652.63	112142.2	142692.5	73719.48	87757.5	14634.72	18776.44	35729.84	24004.14	31195.87	29393.44
Uric acid	33946.36	70136.73	29881.8	30477.79	71881.37	37628.05	41285.95	69885.92	27216.26	22664.31	19874.96	14089.5	66656.69	58855.57	37314.25
dihydroxy-acetone-phosphate	4977531	5345391	4946688	5981046	9189287	3555556	5540073	6746101	6631211	951063.5	1448763	2189944	3465122	3615105	3254020
D-glyceraldehdye-3-phosphate	4393070	3903321	3641451	4909194	8143819	3213216	4457562	5235703	5409241	932518	1153317	1895905	2405345	3133122	2654618
sn-glycerol-3-phosphate	1308932	3917228	1917285	2327991	6600757	1671695	1461234	2918452	3505617	2867433	1620170	4236161	8010850	6746910	6376458
shikimate	36679.55	101049.7	25636.3	72670.32	78569.63	81477.34	195528	78100.45	51307.08	24909.3	41143.16	N/A	17641.03	19751.17	15833.3
aconitate	538292.1	811567.6	651632.5	796254.5	1017908	613638.1	1300414	645787.6	511617.7	542212.2	416556.7	623893.1	656760.9	536946	538931.2
allantoate	58778.1	89139.64	59686.45	41988.57	91368.85	62653.65	56536.77	91889.86	58993.27	18495.8	35243.77	31845.07	50511.98	55035.67	63177.95
Ascorbic acid	41121363	35510916	40348179	39439175	36388174	41102321	40185522	35444728	43211728	19823326	22927536	35888554	39692541	41980280	44544334
2-Isopropylmalic acid	35368057	31807269	36804192	40590770	32569501	36061242	39348140	29225455	44168603	38793713	36828473	45474330	35826809	36776674	36983611
N-carbamoyl-L-aspartate-nega	61174.7	61862.58	50722.49	33005.14	94308.55	63076.25	45426.44	87668.26	53016.95	29258.29	26097.78	27276.45	37524.48	54050.62	48629.06
Pyrophosphate	1978085	3969402	1588614	719139	4091476	2233103	1795379	4720115	1471898	190440.5	241425.7	723870.6	1697234	1762256	1629424
glucono--lactone	16033.5	39024.54	19244.65	17598.65	27792.9	22444.96	23204.56	25164.63	13893.44	8549.816	9083.606	10154.12	22978.98	24592.66	13369.84
myo-inositol	23423853	34739872	19194415	15215670	32759272	29254049	19360290	41502016	22274720	8780316	9454800	14613368	30010450	29758605	26244376
hydroxyphenylpyruvate	60795.38	130918.2	60374.88	46418.59	103199.2	92449.86	54531.41	184367.2	51320.29	24050.71	24011.39	39021.07	112130.3	113650.6	104209.5
homocysteic acid	41762.35	64085.19	32364.9	29309.84	69016.58	66046.84	44412.12	132676.2	22926.91	10798.37	7555.091	18402.82	31001.75	44135.41	29104.46
4-Pyridoxic acid	74523.2	36976.16	64595.51	108938	22226.56	50001.78	61845.88	21946.78	46292.67	60928.29	111457.4	68731.13	50728.25	50296.05	54796.08
3-phosphoglycerate	84393.6	103744.1	150968.8	63134.57	31548.97	138569.2	174868.8	53991.58	73667.8	29950.15	17212.91	14615.92	15755.49	28968.05	18800.4
Indoleacrylic acid	71612.65	141774.2	74580.21	61676.72	145757	58962.18	91745.51	168187.6	91433.37	19817.69	32433.4	37628.08	43998.29	78623.27	40716.93
Kynurenic acid	669703.9	794733.9	579532.9	589921.2	912174.6	753863	693994.5	836524.4	633502.7	232888.1	316118.4	495495.4	716461.4	782033	745086.8
citrate-isocitrate	54297960	35394352	39956200	34426350	34027290	32549944	39807165	34362129	27909706	37704108	32816514	50986549	38325694	33825418	39097209
isocitrate	171360	107377.8	93864.9	90157.86	78869.86	74244.21	34771.67	67272.94	58850.9	35439.59	21380.04	16373.23	22803.65	53491.36	9938.133
citrate	20454342	23276910	30349725	20071083	26304950	21332833	29922789	20375556	23077679	15154700	11101412	23596867	23025152	19742205	19411268
2-dehydro-D-gluconate	3809.237	10247.8	9510.166	14771.16	21792.03	6385.197	10687.17	12860.79	8568.481	N/A	6946.936	11125.71	16770.09	5010.56	4311.062
D-gluconate	98327.19	149993.5	95134.16	86040.57	146151.8	135784	56653.77	163014.3	92523.57	45951.09	51838.86	74276.63	103211	136881.6	106300
D-erythrose-4-phosphate	1739157	2210872	1810406	2082048	3302499	2582762	2257118	2516203	2028318	353057.6	377586.7	502538.1	761393.1	882647.6	754084.9
Xanthurenic acid	23220.12	17151.29	32839.33	32620.78	12619.47	34705.31	12396.68	21551.5	20407.3	17787.23	51876.44	43371.32	21001.52	39019.54	30447.06
lipoate	N/A	N/A	N/A	N/A	N/A	N/A	N/A	N/A	N/A	N/A	N/A	N/A	N/A	N/A	N/A
D-glucarate	29793.37	N/A	6782.376	6173.779	7976.816	6539.747	5144.6	7926.568	4551.573	4860.431	10582.66	4070.84	21970.84	31175.61	15518.58
deoxyribose-phosphate	103288	175639	67973.7	65068.86	322250.6	94225.3	101905.1	258864.5	133708.8	59508.87	38807.35	73035.06	82897.77	124029.5	105243.9
pantothenate	N/A	N/A	21343.89	7959.244	N/A	14021.84	76308.23	N/A	14019.19	N/A	16074.51	9740.187	N/A	79559.68	53148.72
prephenate	N/A	N/A	N/A	N/A	N/A	N/A	N/A	N/A	N/A	N/A	N/A	N/A	N/A	N/A	N/A
deoxyuridine	43291.04	50561.14	22920.27	26329.48	71805.06	24017.95	27349.18	73771.22	11619.97	24961.42	13445.07	33007	37272.81	27179.05	15445.14
ribose-phosphate	19456628	26707492	14730255	10561645	32423152	20829700	21636628	29301334	18024730	3465482	3383917	8376144	15719052	17809190	17326365
thymidine	9076.983	4018.057	6671.667	3819.555	9898.061	6975.191	16037.72	17764.08	4807.393	7030.097	7052.768	4841.459	5767.279	3699.634	14432.87
uridine	1205687	1105331	2197932	1124018	1037800	725344.3	319828	909931.5	146965.5	1159469	1111051	1813266	2458384	531816.4	181376.4
deoxyinosine	13356.4	15291.82	14501.41	12807.02	13675.51	21917.67	15923.45	17203.96	11785.27	11719.63	4012.048	6832.341	16498.7	24889.05	18578.49
shikimate-3-phosphate	49618.76	55561.01	18163.44	36004.59	12335.22	47908.32	32172.71	52239.21	45148.32	19072.91	28554.65	10885.49	17603.49	28022.95	22928.69
D-glucono--lactone-6-phosphate	37450.47	19923.31	18560.63	27150.64	53545.53	70054.04	14094.48	103309.9	36004.58	6579.071	7002.364	9913.535	32195.1	19313.95	18709.37
hexose-phosphate	35349038	40515028	33661665	40085554	44874338	48388412	40016354	40931797	35304067	6447031	7033313	9731235	14159037	18695305	14282282
glucose-1-phosphate	821119.5	1143502	818534.3	816408.5	1418506	1271204	810008.2	1224400	687867.8	142852.8	197793.9	214940.6	408943.1	441912.5	408505.9
glucose-6-phosphate	3240735	4317586	3424738	4139278	5821708	6475464	4467261	4905987	3528135	461076.5	589807.7	588150.5	815365.9	1372076	962195
fructose-6-phosphate	3950527	5381507	3990770	4910628	7160763	6846421	5000824	5676702	3824484	490332.5	662966.8	729800.4	1090759	1584011	1250330
1,3-diphopshateglycerate	28325.03	27389.37	7962.12	23807.32	37082.15	15016.65	17073.59	45616.71	8742.86	6109.411	N/A	19640.17	27106.31	30156.33	14210.24
2,3-Diphosphoglyceric acid	3573.909	10244.52	3840.117	N/A	12946.42	8608.627	14320.01	23085.19	N/A	N/A	N/A	N/A	N/A	N/A	4257.867
S-ribosyl-L-homocysteine-nega	55050.97	112719.7	61931.61	34756.3	80078.65	85984.31	59869.29	134295.1	39545.24	35793.16	33052.4	82329.87	127091.4	96860.48	106259.9
inosine	41602736	25007944	40200903	41016980	24703728	40439241	38490114	24224670	40407363	43103946	41381993	45139596	41364981	39089017	40265248
6-phospho-D-gluconate	75143.42	178526.9	75773.67	50765.74	132729.4	163466.9	59311.5	281648.7	57676.68	N/A	10139.67	12833.04	40531.64	33019.66	19773.76
xanthosine	299707.5	355801.8	266946.1	242812.1	441850.3	238374.1	268585.9	385978.5	287800.5	25750.1	23778.2	142359.5	248248.8	221048.2	236164.6
D-sedoheptulose-1-7-phosphate	7151408	9386490	7788937	5964069	12149630	9742786	6425205	9819379	5738780	1440766	1697483	2293580	5092735	4389450	3745387
N-acetyl-glucosamine-1-phosphate	337740.7	654830	368504.9	383217.2	1053885	493907.5	473175.4	930946.1	490338.1	202648.5	209660.3	411932.3	705204.9	721684	519631.9
glutathione-nega	6784109	9143000	6853986	5712156	8537316	7293698	6551974	10315126	7075972	3059401	3253885	6907745	11167278	10478951	10410240
dUMP-nega	N/A	N/A	N/A	N/A	5014.368	4843.03	6367.439	10873.98	3909.338	N/A	N/A	N/A	N/A	8273.535	N/A
Geranyl-PP	17643.6	30489.82	8592.742	20359.66	16673.15	31188.49	22543.34	37703.3	18372.33	9168.166	9068.369	12196.9	12896.96	24788.81	16166.36
O8P-O1P	666387.4	1134213	629630.4	443634.3	1002053	716160.5	487639.8	902810.8	469943.4	205741	196578.8	336543.1	522077.4	507319	550931.3
dTMP-nega	5382.973	13072.03	5168.778	N/A	10266.07	20531.49	6416.959	7957.474	4292.033	N/A	N/A	5860.978	6329.68	5342.775	N/A
cyclic-AMP	203629.9	288203.4	145897.2	80682.03	340888.8	179574.6	155627.6	443521.6	122089.4	43825.65	53964.15	81195.41	175800.2	161379.3	152250.7

fructose-1,6-bisphosphate	3903521	8926311	2826099	2136110	12301016	7567674	5707871	10116125	3345505	375957.1	456317.9	662821.1	1432068	1716357	926888.8		
trehalose-sucrose	72808.05	63921.55	209524	62497.77	147156.2	60951.63	72593.25	107954.6	53353.92	24974	13865.37	16095.07	46704.3	31024.87	123623.6		
Cellobiose	10701.22	8532.079	4226.493	6703.262	9568.942	7950.542	5881.082	14530.82	5252.643	5321.988	7553.62	N/A	4794.921	3843.595	6966.205		
orotidine-5-phosphate	30265.59	28610.26	28203.77	29367.52	21842.75	31296.54	22936.74	26730.77	25549.92	26712.05	18249.66	37792.55	19665.99	24273.05	26924.74		
SBP	1351324	2118409	1449753	1043571	3768331	1642128	1199312	2966722	1444663	212978.2	231921	440848.8	783702.4	916948.7	650738.2		
trans, trans-farnesyl diphosphate	4665.438	14427.12	N/A		7415.671	15919.34	9109.81	7930.051	4557.226	4438.841	N/A	N/A	N/A	8546.889	4479.477	N/A	
S-adenosyl-L-homocysteine-nega	935580.1	1329704	589819.5	538660.3	1714173	1112735	870654.4	2704536	760527.6	276894.1	298673.3	606883	989979.2	924288.1	921872.9		
dCDP-nega	N/A	4809.41	N/A	N/A	4275.774	N/A	N/A	N/A	N/A	N/A	N/A	N/A	N/A	N/A	N/A		
5-phosphoribosyl-1-pyrophosphate	16560.92	7489.554	7576.822	16561.71	20748.65	6590.672	4124.004	50987.85	20770.19	6412.818	6618.742	24047.93	34722.75	26186.6	27634.24		
Deoxycholic acid	N/A	N/A	N/A	N/A	N/A	N/A	N/A	N/A	N/A	N/A	N/A	N/A	N/A	N/A	N/A		
OBP	702956.2	1021932	577310.3	485196.4	1623591	816856.7	663226.9	1509715	754399.5	126616.7	182838.5	367533.9	702799.1	740125.8	679744.2		
dTDP-nega	6375.484	4275.739	N/A	N/A	4273.871	3195.957	N/A	6405.576	N/A	N/A	N/A	N/A	N/A	N/A	N/A		
CDP-nega	22667.44	18035.91	14911.13	28722.56	44359.83	34868.51	25922.41	46625.4	27061.45	21429.51	23070.85	25155.38	34127.8	45318.37	16757.9		
UDP-nega	120746.9	239924.2	118146.7	134134.3	441358.9	158358	242506.4	457611	206290.1	30513.87	66797.92	240537	220696.5	248497.6	210512.7		
Cholic acid	N/A	N/A	N/A	N/A	N/A	N/A	N/A	N/A	N/A	N/A	N/A	N/A	N/A	N/A	N/A		
trehalose-6-Phosphate	16391.47	91467.81	15333.04	7118.777	105818	17274.26	15452.65	102388.3	35203.25	14029.75	4886.636	9290.319	22359.18	12524.3	48223.76		
Thiamine pyrophosphate	125823	258696.1	109768.7	76146.86	213127.5	152021.9	149867.7	274115.5	139264.1	40104.78	37891.66	49485.45	124242	159309.2	106559.1		
adenosine 5-phosphosulfate	4274.241	6412.956	5877.454	4266.675	6946.491	6411.362	4271.108	6399.907	8014.36	N/A	2670.998	N/A	N/A	5879.062	10156.33		
ADP-nega	948800.5	1431482	733222.3	597289.1	1932751	934405.3	760146.2	1874135	769609.4	295950	404570.2	799196.3	1266103	1114138	1297594		
dGDP-nega	948046.3	1309024	692641.5	543076.6	1956750	872390.9	809692.8	2048049	748515.3	353105	396454	831519.1	1213470	1271721	1284694		
IDP-nega	146017.4	154265.6	72724.4	59282.44	259175.3	116508.4	90532.54	294688	102483.3	41685.63	46492.83	110211.4	135203.6	176567.4	174321.4		
GDP-nega	133062	178549.8	128882.5	125055.6	320002.4	136265.7	211746.3	340661.6	135352.8	44474.73	61991.73	128787.1	153865.8	187566.9	173556.5		
CDP-ethanolamine	222846.2	353925.9	202537	179797.3	293924.2	260793	208946.3	360711	213223.6	83908.87	107950.2	173685.2	301643.2	238031.2	290702.8		
FMN	N/A	N/A	N/A	N/A	N/A	N/A	N/A	2782.005	N/A	N/A	N/A	N/A	N/A	N/A	2679.408		
cholesteryl sulfate	49698.27	51948.23	42212.95	30460.62	68977.43	46985.37	6149.449	89230.22	9603.293	6412.776	4809.726	6403.872	20828.89	12827.02	11758.37		
dCTP-nega	N/A	N/A	N/A	N/A	N/A	N/A	N/A	N/A	N/A	N/A	N/A	N/A	N/A	N/A	N/A		
dUTP-nega	N/A	4274.375	N/A	N/A	N/A	N/A	N/A	2672.518	N/A	N/A	N/A	N/A	N/A	3165.274	N/A		
dTTP-nega	N/A	N/A	N/A	N/A	N/A	N/A	N/A	2671.116	N/A	N/A	N/A	N/A	N/A	N/A	N/A		
CTP-nega	110622.9	214890.8	68721.32	26518.07	280836.3	129113.4	82188.9	224247.2	54568.78	6296.949	8081.623	18354.47	25999.5	32521.26	27538.82		
UTP-nega	33148.48	23614	21371.04	23920.35	51069.58	27788.83	39493.79	51833.28	35301.8	26184.14	32615.09	48091.71	48949.68	47838.28	29592.45		
CDP-choline	216431.3	178411.3	184361.7	262922.5	218038.1	229260.5	297653.2	216965.9	305687.6	160853	214830.1	278425.1	283229.7	276280.4	275550.1		
dATP-nega	N/A	N/A	N/A	N/A	N/A	N/A	N/A	N/A	N/A	N/A	N/A	N/A	N/A	N/A	N/A		
Taurodeoxycholic acid	13371.79	22981.38	11220.67	9620.607	9912.77	7285.056	13878.07	30429.69	9091.111	12288.52	7492.112	N/A	8016.034	10161.95	11220.88		
ATP-nega	232898.7	283708.8	210516.8	228565.7	639716.2	193440.9	317800.5	441818.6	310225.7	168450.6	163333.4	301545.1	262325.3	295952.1	425622		
dGTP	198883.2	290719.8	210329.4	203626	580387.7	193682	350066.9	457768	333250.3	177789.6	161505.1	278526.3	308126.5	310893.4	396008.7		
GTP-nega	105383.3	223785.7	65200.58	70541.04	372925	82833.85	146521.8	366688.5	110622.5	34564.55	31044.99	124574	201820.4	231823.9	234702.2		
UDP-D-glucose	2480240	2919768	1824329	1160738	3625938	2546132	2154898	4033370	2525842	738025	688860.6	1775862	2501948	2309533	2527572		
UDP-D-glucuronate	111690	95123.35	57715.53	48629.79	160322.4	87642.94	101116.4	188111.1	99367.07	21375.89	28358.82	96725.3	96849.33	120763.8	109548.1		
ADP-D-glucose	11756.27	14962.79	6412.946	8016.282	14428.89	16566.18	17100.19	19765.64	12289.73	6412.869	5877.484	8549.901	13893.65	12825.57	18168.78		
guanosine 5-diphosphate,3-diphosphate	9619.251	10687	5425.195	10153.35	15498.55	14962.5	7716.578	12289.99	6945.246	4275.666	N/A	N/A	3737.132	3307.452	N/A		
UDP-N-acetyl-glucosamine	981688.4	1029767	510913.9	378658.2	1015545	679538.5	571288.1	1060222	591043.2	188646.4	188648.8	460289.8	813291.7	604958.1	604642.9		
glutathione disulfide-nega	3617065	7902284	3100831	1372872	7038317	5698820	2743042	10124315	3356130	1203072	1079208	1776146	4611331	3778933	3164135		
NAD_nega	26721.08	54529.82	31548.29	31529.55	55042.49	34732.6	48103.1	29931.72	34200.47	16029.96	11764.75	26607.36	24581.6	38476.25	27788.54		
NADH-nega	N/A	N/A	N/A	N/A	N/A	N/A	N/A	N/A	N/A	N/A	N/A	N/A	N/A	N/A	N/A		
dephospho-CoA-nega	33735.99	68407.75	22229.2	17053.48	63854.89	68891.85	52859.35	71843.22	23282.12	N/A	3744.577	9105.161	17665.38	18175.88	14249.34		
cyclic bis3-5 dimeric GMP	N/A	N/A	N/A	N/A	N/A	N/A	N/A	N/A	N/A	N/A	N/A	N/A	N/A	N/A	N/A		
NADP_nega	22475.86	22979.34	11756.31	14427.64	28324.87	9619.342	9085.519	21909.72	13892.94	11222.6	5864.874	28322.56	19212.71	25114.61	17633.66		
NADPH-nega	N/A	N/A	N/A	N/A	N/A	N/A	N/A	N/A	N/A	N/A	N/A	N/A	N/A	N/A	N/A		
coenzyme A-nega	10075.3	124247	54862	57214.23	15692.7	14372.37	66318.22	24710.9	70592.09	13354.25	19234.93	63059.09	84898.38	11366.8	11641.91		
acetyl-CoA-nega	N/A	N/A	3527.076	N/A	N/A	N/A	N/A	N/A	N/A	N/A	N/A	N/A	N/A	N/A	N/A		
propionyl-CoA-nega	N/A	N/A	N/A	N/A	N/A	N/A	N/A	N/A	N/A	N/A	N/A	N/A	N/A	N/A	N/A		
butyryl-CoA	N/A	N/A	N/A	N/A	N/A	N/A	N/A	N/A	N/A	N/A	N/A	N/A	N/A	N/A	N/A		
acetoacetyl-CoA-nega	N/A	N/A	N/A	N/A	N/A	N/A	N/A	N/A	N/A	N/A	N/A	N/A	N/A	N/A	N/A		
malonyl-CoA-nega	N/A	N/A	N/A	N/A	N/A	N/A	N/A	N/A	N/A	N/A	N/A	N/A	N/A	N/A	N/A		
3-hydroxybutyryl-CoA	N/A	N/A	N/A	N/A	N/A	N/A	N/A	N/A	N/A	N/A	N/A	N/A	N/A	N/A	N/A		
succinyl-CoA-methylmalonyl-CoA-nega	N/A	N/A	N/A	N/A	N/A	N/A	N/A	N/A	N/A	N/A	N/A	N/A	N/A	N/A	N/A		
3-hydroxy-3-methylglutaryl-CoA-nega	N/A	N/A	N/A	N/A	N/A	N/A	N/A	N/A	N/A	N/A	N/A	N/A	N/A	N/A	N/A		
2-hydroxygluterate	1122760	1909895	1011511	800367.3	2022468	1704118	1473599	2445032	1347246	631192.4	662668.7	965156.5	1796147	1674509	1617216		
2-deoxyglucose-6-phosphate	6854454	10871056	4336882	3658727	10292688	5729074	4730343	13156945	3796723	1083605	1171606	2721068	4644954	3840321	3925876		
3-hydroxybutyric acid	124323.7	2332640	1006924	126452.8	116113	558262.6	145383.5	85640.64	147571.8	154918.6	114331.9	644274.3	891104.6	122067.2	148286.1		
4-phosphopantothenate	27141.38	19318.13	12220.23	8994.09	71067.21	18890.15	10922.2	52539.59	8553.491	2672.892	10153.23	N/A	9558.728	14419.77	36314.65		
gamma-hydroxybuterate	N/A	N/A	N/A	N/A	N/A	N/A	N/A	N/A	N/A	N/A	N/A	N/A	N/A	N/A	N/A		
Urea	1809642	2277597	1382358	758104.2	1199439	1400579	731476.4	1863408	1025670	502966.2	307710.2	507573.1	1311874	1288709	1005744		
ethanolamine	N/A	N/A	N/A	N/A	N/A	N/A	N/A	N/A	N/A	N/A	N/A	N/A	N/A	N/A	N/A		
Imidazole	N/A	N/A	N/A	N/A	N/A	N/A	N/A	N/A	N/A	N/A	N/A	N/A	N/A	N/A	N/A		
glycine	N/A	4275.394	3206.502	N/A	N/A	N/A	N/A	5335.461	N/A	N/A	N/A	N/A	N/A	N/A	N/A		
alanine	11865706	17312752	10667153	8225019	16691128	13509459	11798704	18881582	10223569	6686738	6449467	11465268	18117793	17469817	15271155		
betaine aldehyde	102233	5074.393	123713.7	80440.51	119462.7	121907	91162.93	146063.7	102792.8	5557.059	5748.296	5013.377	125713.7	109686.5	9331.723		
choline	317319.6	414570	1937135	1034668	421130.3	2459281	1426725	121225.6	2679169	21378.94	142690.1	102774	277495.4	474920.4	665489.9		
4-aminobutyrate	11143988	17771785	8514047	7839955	19306798	13357066	11136888	22335231	11008614	3591694	3921322	7561860	14539246	12806847	11245584		
dimethylglycine	643067.3	1372837	805867.2	635329.2	1500049	902286.9	1168784	1346824	845347.4	197867.3	152243.9	405854.4	608317.5	633585.5	600763.4		
serine	5054199	6716978	5243421	4681574	8630823	6830643	6204866	9521625	6018196	3222072	2952453	5100879	9430449	9319073	9618432		
cytosine	836482.9	1002323	692949.3	493287.6	725026.9	762718.1	682692.7	742122.1	514294.6	231878.3	222938.4	509248	664979.2	492789.2	536945.4		
Creatinine	2531831	4103816	1832595	1416533	6141268	3282271	2323450	7648229	2148301	742498.8	784105.8	1271329	3340829	3217822	2469108		
proline	29514476	33655335	25719875	17977236	32250310	28711482	25578939	35338141	25082132	4526277	4496233	9618260	16534351	15578589	16293164		
indole	13379.87	29992.6	23679.9	30510.66	67626.11	48483.66	30328.47	68754.73	30278.18	24476.63	17943.24	21547.25	40772.38	38158.87	20014.14		
betaine	15595598	11863676	36268836	26974680	27898523	29817067	26771815	34113085	36398372	22059960	15305853	24669583	16477153	47475812	16430903		
valine	527282.8	1003707	475588.5	188730.9	764428.8	394587.2	321807.6	842525.9	337846	144740.5	104008.5	239886.7	354503.9	338796.6	326198.1		
threonine	10465177	17832929	9141835	6212912	16855107	10847696	10438236	21256295	8327464	1589959	2055230	3872456	7549719	7897216	7611483		
homoserine	18435.19	38956.67	23354.74	42749.99	49356.05	37909.75	38496.1	66160.42	31000.3	7470.142	17098.83	24480.66	43249.72	45890.6	39131.41		
purine	59136.39	89877.66	53602.29	29575.81	156927	96185.06	64192.35	170579	51091.95	15319.31	29882.69	59865.76	69028.22	71983.95	58486.59		
cysteine	23528.49	40460.33	41450.75	42737.44	45426.36	40553.88	39809.28	8677.485	53859.4	28819.37	30083.35	36830.28	47532.61	48612.17	42341.42		
nicotinamide	1.13E+08	1.53E+08	99827104	68967575	1.6E+08	1.31E+08	1.13E+08	1.14E+08	1.03E+08	30803427	37774105	74848107	1.16E+08	1.05E+08			
Imidazoleacetic acid	109327.9	141024.7	168706.9	140515.9	140438.2	173034.7	164446.8	131377.1	130978.9	50293.04	40728.96	37860.26	57202.1	68942.38	58010.29		
thymine	143285.5	161317.5	99229.23	97512.91	130905	104389.1	110690.7	149861.7	145146.2	61261.18	75370.52	117786.3	119261	120891	126485.6		
DL-Pipecolic acid	33371870	34048320	34495533	35078179	36135109	35794082	34147960	36850203	32893473	29135905	31753590	30683814	33817660	33914998	31728249		
N-Acetylputrescine	16250.55	16990.69	3656.873	5178.047	19269.1	5273.95	10711.88	10997.47	12994.21	9474.485	11912.39	3184.894	4398.649	7824.374	6705.334		
hydroxyproline	145041.2	179189.6	151528	198259.5	238202.1	270393.4	364949.1	387911.3	313151.5	92426.82	94043.27	238350.8	445353.4	410871.6	435939.5		
leucine-isoleucine	20797871	38909575	16037561	11163068	31711267	21426143	16801202	34257661	14471707	5070878	4304813	9486457	17873673	16898736	14129668		
ornithine	621765.9	1534941	554611.9	336224.5	1663570	656194.8	691995.1	1353547	361788.3	90387.91	7414.596	241490.9	300611.3	262519.7	329430.7		
asparagine	1687036	3316579	887428.3	1388352	3685120	2798356	1777795	4831155	2263778	598620.3	537042.7	1162619	2013001	1689888	1677612		
aspartate	16674262	24640862	12554259	11207472	26065722	22047840	18900018	30617647	18840736	5542294	6879317	7763129	19036981	17451808	16199949		
adenine	672471.2	1309224	561588.6	549957.8	1259975	1180856	967418.2	1699044	748951.1	299599.7	471715	736124.4	1156458	996581.2	885375.3		
Methylcysteine	221906.1	343838	199483.4	291274.7	667792.2	468854	490966	658705.4	366754.9	85498.84	305702.4	478759	433951.3	365542.4	430716.7		
homocysteine	100968.3	125078.1	82844.25	53671.01	197667.8	123967.1	84565.16	171933.6	86564.24	15155.16	38557.67	50472.78	106526.7	78634.37	72135.72		
methylnicotinamide	5723752	10491180	5121809	3469656	11891596	6071717	5155642	13276066	4796851	1403343	1330283	2832693	6022338	4828113	4818693		
histidinol	17100.27	34208.78	21913.44	9085.562	47560.67	16013.47	19235.09	35865.43	28858.28	5877.35	3735.753	10687.23	15498.12	29409.41	21912.35		
lysine	1919748	4064215	1500624	1140622	3898702	2919349	2074881	5823862	1998980	188429.1	290821.4	507299.5	1400399	1409466	1174938		
glutamine	32995231	34938706	32552842	35423717	34205490	34382115	30781019	31478485	35048130	25733528	31475709	32688872	33280709	32008239	29671847		
O-acetyl-L-serine	6733.544	46467.53	22154.71	2604.553	5617.949	33111.23	24041.75	62467.75	24599.51	10012.11	13898.26	14705.57	3760.129	36421.08	5366.917		
glutamate	22643295	27510751	23642008	27421574	28817064	27637630	24617681	28087262	23459254	21794782	22172590	23161705	28106386	27888497	23425615		
methionine	1890079	2200824	1610916	1731910	3231347	2579713	2636843	3380335	2803216	724441.3	1287455	1946234	1758829	2037613	2154784		
guanine	7610.198	6864.338	19688.71	6139.524	23559.94	21927.17	12338.08	23010.28	12898.73	3921.821	9874.812	6007.151	13795.26	9834.149	11299.53		
histidine	7459559	11016029	6729297	9238602	17958909	11137150	11011681	15623803	11720865	3540753	3968220	8646213	8447603	7950586	7528475		
2-Aminooctanoic acid	4310162	6665102	3225459	6007717	11302844	9990062	5574295	13991846	2786519	1512108	3129352	3660994	4002822	3970782	3651647		
carnitine	34715636	35430782	33070053	31568571	35289278	35797118	33824818	36156342	36411399	30187706	28717426	30452996	33454258	36665031	33985441		
Methionine sulfoxide	38944.97	24573.37	24620.89	28856.9	74989.85	53445.95	54507.1	105810.9	29441.79	6943.282	20595.66	29800.9	45959.04	33796.74	28290.39		

phenylalanine	7343663	10869925	6412059	4539554	17474459	9647778	6760880	17925357	7226667	1945839	2835605	5188895	6932462	7700164	6578312	
Pyridoxamine	N/A	N/A	N/A	N/A	N/A	N/A	N/A	N/A	N/A	5340.906	N/A	N/A	3120.541	N/A	N/A	
pyridoxine	N/A	N/A	N/A	N/A	N/A	N/A	N/A	5343.538	N/A	N/A	N/A	N/A	N/A	2483.25	N/A	
1-Methyl-Histidine	631394.2	1626959	667721.7	1166166	3393746	2718680	825917.7	3797531	921488.7	287131.6	563559.4	912859.1	1026477	1076596	752297.4	
N-acetyl-L-ornithine	4588.068	4813.342	4284.307	3032.963	4004.526	5446.657	N/A	5389.325	N/A	N/A	N/A	N/A	N/A	5750.974	N/A	
arginine	11088480	18277740	8696955	5821514	22689529	13391266	9383344	22988612	6921076	3187669	2374754	4490037	10047683	9585502	6736370	
citrulline	926954.2	1196785	876242.9	943187.7	1811403	1240722	1176007	1809765	1092336	285415.6	355285.7	711992.1	873431.2	737628.6	788070	
N-carbamoyl-L-aspartate	142137.4	271428.5	140544.1	96727.69	312092.6	142129.7	159009.8	353785.3	151235.1	60413.64	55578.04	116995.5	125124.8	167811.8	102602.1	
glucosamine	68861.33	63703.36	72898.74	232910.6	50142.63	64600.84	57785.68	54973.68	184330.1	61584.13	67642.73	46229.82	183605.3	80972.63	56020.34	
tyrosine	898106.4	1338185	991781.4	1221071	2700119	1901738	2193934	2652369	1607717	428571.9	1126114	1809731	1825561	1569111	1241718	
Phosphorylcholine	1.02E+08	1.24E+08	79576251	62620579	1.29E+08	1.03E+08	88158398	22769407	73756808	20840750	25979888	58955018	78052616	87649143	83652228	
3-phospho-serine	7501.145	10786.78	7063.823	9556.048	5998.884	9640.518	7498.946	12716.97	8693.661	6874.532	4818.125	9626.659	13378.72	9895.372	16504.04	
N6-Acetyl-L-lysine	10941263	25191040	11577180	7011166	29653945	15639886	12775583	35642812	8923899	2022934	3602116	6079630	14044185	13383638	13137593	
Acetyllysine	11023517	18981609	9051640	8431309	22064022	15274780	7232772	29474872	8343137	2313447	3022373	5003849	10326317	10663081	10956536	
N-acetyl-glutamine	688016.3	1339658	627917.2	21073.07	1869554	600080.6	631452.1	62344.3	25998.94	173702.3	21622.85	420930.9	32881.52	33571.52	8408.203	
N-acetyl-glutamate	510005.3	1005719	423710.2	323602.4	1112567	609014.1	555394.7	1026499	530369.9	148837.1	201123.5	333516.6	553558	695773.8	470478	
Ng,NG-dimethyl-L-arginine	3410527	4943519	1860776	1044655	4455920	3058147	1852483	7616213	1692226	452158.3	224415.4	663571.7	1653606	1547631	1589875	
Acetylcarnitine DL	40399425	44340681	40009706	37248004	41584064	39072179	31972836	41544365	38059218	37066524	34769780	35822058	41810842	37612467	39782792	
tryptophan	2882678	4184010	2282640	2445426	2324821	3324939	3042693	3429397	2954900	1225947	1259674	2023319	2857269	2474823	2614916	
Kynurenine	10084.14	14469.06	9620.904	10160.03	54196.04	14961.92	N/A	37959.71	3738.899	N/A	N/A	9087.329	9617.71	6863.192	3200.372	
N-acetyl-glucosamine	60958.22	140015.9	58029.27	44633.41	139522.6	102335.4	108854.6	142483	88575.92	31645.9	50321.99	75750.81	117624.7	116403.1	98231.11	
Flavone	9914.762	31053.12	9878.449	14945.79	21374.81	15406.1	17135.59	22913.35	17200.48	30035.55	18235.48	18443.74	5882.264	5775.881	9439.38	
cystathionine	3242180	4923995	2379260	1530277	4077265	2397496	2546464	4021051	1774927	355421.6	420558.7	839383.7	1138522	1184875	1123624	
5-methoxytryptophan	N/A	11416.64	16976.57	6614.141	9220.323	6599.778	5890.039	8195.447	10998.87	5552.644	12555.19	26367.77	5991.229	N/A	3504.038	
Cystine	18190.38	16565.75	10688.92	18726.46	16851.52	14416.07	18717.3	24051.96	13908.85	6424.842	9631.027	12283.66	20281.89	16558.16	12235.47	
cytidine	5738512	7437007	4351209	3720133	4506408	6077016	4723782	4214041	3799261	1615587	1440867	2830737	4166579	3541597	3161483	
biotin	121550.7	124136.1	121459.5	111083.4	80883.58	106673	110353.9	88750.48	118804.5	109185.6	130605.1	140174.3	131843.1	130039.7	125691.3	
deoxyadenosine	13817.54	24676.01	6149.599	5978.314	33192.37	17593.77	7236.005	17462.77	11755.36	N/A	N/A	6737.579	5775.901	13950.37	12710.51	
Glycerophosphocholine	8916582	13829887	10606395	9624638	14187486	27048373	19294846	27232284	13951261	4231517	6640184	11895907	21279380	21278691	18697767	
acadesine	9185.578	14970.73	10150.39	9078.462	21336.02	15515.86	13933.31	18738.61	7973.525	N/A	N/A	6445.825	9609.551	8222.236	5676.577	
D-glucosamine-6-phosphate	403455.5	509175.4	378898.3	378969.3	608726.3	606394.8	380771.4	575314.9	346000.1	27793.99	69449.23	30459.41	79433.99	123313.3	68782.5	
D-glucosamine-1-phosphate	45955.78	51841.4	27811.52	29298.02	79629.76	47178.32	51194.19	72046.53	56017.27	30994.83	28857.44	63064.72	79626.48	81332.76	62037.45	
thiamine	N/A	N/A	N/A	N/A	2670.709	N/A	N/A	N/A	N/A	N/A	4245.807	N/A	N/A	N/A	6626.711	
S-ribosyl-L-homocysteine-posi	5330.242	18670.5	8016.502	4772.941	20842	N/A	5861.829	24594.22	N/A	N/A	N/A	6974.761	5172.977	8087.641	7072.475	
deoxyguanosine	17359.73	22834.66	5369.448	18518.82	44281.91	23627.99	17537.62	46655.51	17027.41	6957.145	4809.582	10688.44	12284.79	17378.13	17602.45	
adenosine	23263.72	42437.07	29924.35	5749.674	36887.49	21071.76	17202.31	31035.83	18739.82	18950.51	10047.95	12851.73	13886.43	24165.48	32269.55	
1-Methyladenosine	N/A	10107.96	2596.072	3739.986	3767.186	2133.918	3899.604	N/A	N/A	N/A	N/A	4114.861	4278.267	4809.635	3893.923	
guanosine	715570.3	1008729	652075.4	502544.9	1325780	579291.9	589999.2	1282012	784587.4	213413.4	160436.5	296053.6	536356.3	580436.3	470703.6	
L-arginino-succinate	457909.5	811244	271483.7	286209.9	751396.4	417249.1	417772.3	677803	358160.5	162986.4	107910	287988.9	456458.1	398343	440301.7	
S-methyl-5-thioadenosine	13511.74	36989.78	20969.63	5296.374	23989.49	14346.71	28076.67	46780.17	12316.7	5568.05	4286.444	12251	19277.11	15181.79	16960.55	
7-methylguanosine	92154.58	117570.9	53552.6	79050.53	148012	91917.14	122355.7	189596.7	79022.03	16085.24	29708.3	75875.29	106868.3	100461.2	116485.4	
dCMP	44898.34	91249.31	70627.27	39009.95	90848.34	74281.93	63594.13	108475.7	60655.34	37375.68	26719.1	43821.38	69468.86	81230.91	60920.49	
glutathione	10557588	13156336	13189358	12742192	15401881	12555908	12331601	16521845	16364630	7271564	8234397	11369339	16305315	16563447	18156466	
dTMP	19770.34	31082.7	19126.03	22444.17	33422.32	26372.77	25619.1	44329.62	21909.53	6946.707	11224.06	6907.394	10847.66	16042.26	10167.83	
CMP	4053123	5553257	3411183	2618789	5407721	5002009	2959455	6203646	3073293	1722561	1995733	2477672	3958098	3514241	3054078	
UMP	959485.8	1349794	993182.3	860317	1087166	927910.4	1021960	1130749	795119.1	718888.9	699799.8	943445.4	967905.7	1078845	960843.3	
dAMP	36329.59	60778.24	47560.75	30979.93	56092.39	61482.8	45952.93	77974.33	41196.17	28324.22	24596.74	44339.49	47055.79	43752.4	51834.68	
Nicotinamide ribotide	22688.6	26101.77	11370.39	9789.32	19920.12	21644.55	14125.79	27622.35	10783.17	4037.014	19238.37	6263.554	36445.72	16333.74	19234.17	
aminoimidazole carboxamide ribonucleotide	16036.12	14421.39	12825.67	18698.68	27160.52	17114.93	9617.483	22978.44	15429.54	5879.071	11756.58	22982.45	12261.58	9084.562	15481.64	
thiamine-phosphate	462098.3	891820.9	383960.4	260058.1	N/A	587487.4	411262.4	1239098	367272.6	132813.6	113497.9	276414.2	530343	583069.3	455094.9	
dGMP	12861.81	21408.56	17216.4	8551.638	16054.36	9085.181	5852.794	17618.91	8551.407	N/A	5343.754	10861.27	11227.49	15494.75	14432	
AMP	41164798	51475603	36469035	30452867	43378470	46853375	40861774	55976485	37463295	30512119	30231727	34924903	45189048	44116883	42356324	
IMP	22577759	27727440	20323511	17885442	30967591	22061294	14746252	29010120	14767860	10453955	11680942	17813449	13471293	17448096	15045409	
S-adenosyl-L-methioninamine	N/A	N/A	N/A	N/A	N/A	N/A	N/A	N/A	N/A	N/A	N/A	N/A	N/A	N/A	N/A	
GMP	18442690	22477560	17566060	14784369	22318282	20816215	18792363	23605912	16287430	10588292	10673216	16953815	19551250	19851734	17263457	
xanthosine-5-phosphate	27763.6	56632.3	24629.8	17641.66	214095.7	9366.382	21841.73	76167.34	40159.37	24176.44	32588.59	36334.06	71039.9	48237.26	37416.32	
riboflavin	N/A	N/A	N/A	N/A	N/A	N/A	N/A	N/A	N/A	N/A	N/A	N/A	N/A	N/A	N/A	
S-adenosyl-L-homoCysteine-posi	683350.3	1292086	529424.8	346827.9	2066101	1024959	821848.3	1859209	672292.6	249035.7	256856.1	458443.5	1052532	1083582	895647.5	
S-adenosyl-L-methionine	895475.4	1723641	859975.7	911995.7	2153452	1910729	1448986	3890760	1049706	256795.7	521005	930234.2	1798896	1809375	1307598	
folate	N/A	4263.197	N/A	6418.844	4260.734	4751.867	N/A	8549.893	3740.505	4818.287	N/A	5862.077	2671.967	4814.743	N/A	
7,8-dihydrofolate	N/A	N/A	N/A	N/A	N/A	N/A	N/A	N/A	N/A	N/A	N/A	N/A	N/A	N/A	N/A	
5-methyl-THF	53271.2	51485.91	21008.71	39048.03	67306.01	47523.23	47722.55	74794.49	46249.74	44456.79	N/A	33054.49	39129.85	42348.18	57292.12	
Diiodothyronine	N/A	N/A	N/A	N/A	N/A	N/A	N/A	N/A	N/A	N/A	N/A	N/A	N/A	N/A	N/A	
glutathione disulfide-posi	1601059	3959158	1039632	620373.2	3293100	1679053	1238783	4996851	1235339	591979.4	564981.6	663664	1858227	1540231	1379605	
NAD_posi	130923.2	262588.3	111251.9	95632.96	280017.4	169854.1	130931	181703.4	149641.2	57714.21	52905	99966.07	106332.4	98319.67	113292	
NADH	6946.779	3206.351	2672.627	8017.797	11220.59	N/A	4275.482	5879.062	9619.381	4809.649	N/A	N/A	4809.504	7480.617	N/A	
dephospho-CoA-posi	26532.83	27660.73	21682.92	10399.21	21534.57	33988.46	36254.92	5510.25	14439.81	N/A	N/A	8076.243	18039.07	22102.89	16977.88	
NADP_posi	75350.19	92332.91	39237.6	56113.79	139466.4	42660.25	43282.15	88132.94	60304.73	57727.54	44334.59	93537.49	108223.3	85898.72	86053.09	
NADPH	N/A	N/A	N/A	N/A	3721.727	N/A	N/A	N/A	N/A	N/A	N/A	N/A	N/A	N/A	3744.511	
coenzyme A-posi	654186.9	706561	570744.2	466400.3	976143.8	714162.3	737715.1	828940.1	674208.5	158436.8	179701.4	550363.8	814480.2	795150.5	846155.3	
FAD	182260.1	346635	103912.8	129328.3	431262.9	200012	172083.4	436298.8	197197.1	43819.48	39011.7	80179.09	181155.4	134671.5	200486.9	
acetyl-CoA-posi	33027.96	41369.41	45210.73	30457.18	46214.15	35266.52	28855.49	47437.4	39763.87	8978.016	8973.513	32704.3	38518.11	45531.91	51320.48	
propionyl-CoA-posi	N/A	N/A	N/A	N/A	N/A	N/A	N/A	N/A	N/A	N/A	N/A	N/A	N/A	3206.515	3206.221	
acetoacetyl-CoA-posi	N/A	N/A	N/A	N/A	N/A	N/A	N/A	N/A	N/A	N/A	N/A	N/A	2672.419	N/A	N/A	
malonyl-CoA-posi	N/A	N/A	N/A	N/A	N/A	N/A	N/A	N/A	N/A	N/A	N/A	N/A	N/A	N/A	N/A	
succinyl-CoA-posi	N/A	3740.194	N/A	N/A	5883.269	N/A	3740.277	5878.858	N/A	N/A	N/A	3206.528	N/A	4273.185	N/A	
sarcosine	3791533	6156546	2971815	2142875	5478340	4348668	3450169	6709584	2984977	1359943	1585045	2494991	4639854	4712898	3620748	
putrescine	56320.45	67602.32	37983.52	22374.44	79390.94	50619.29	45766.59	56696.6	37187.4	69030.88	75034.17	32020	90496.41	66199.76	100828.9	
spermidine	149158.1	160241	101934.4	152748.7	169590.2	133135.5	157214	143086.7	160468.3	141974.2	125592.1	143389.3	161023.9	143458.2	126387.4	
spermine	5050.678	5401.663	22400.99	19671.74	10655.79	4762.688	18572.5	6190.369	16404.41	16275.33	7048.281	16034.24	12288.47	20837.2	24451.77	
creatine	71080218	72753865	664153.4	55309831	80305878	67653557	61031685	10038547	590209	52522732	51078988	59390151	65118912	72681926	66285718	
N-acetyl spermine	115282.2	43199.92	121028.6	172118.1	51612.63	127897.1	122883.5	39300.01	159266.1	262595.1	252431.6	157260.2	83972.87	96518.94	106249.8	
N-acetyl spermidine	14545.94	5653.476	8108.831	7806.155	14076.9	13251.04	17991.34	8662.944	15455.12	21463.21	20138.92	5153.608	23434.13	13733.94	11959.08	
N1-Methyl-2_2-pyridone-3_5-carboximide	235828.3	406778.9	169827.6	139840	534495.8	274054.8	263467.4	645777.9	227417.8	52121.09	51664.87	109872	196573.6	174280.4	247909.6	
N1-Methyl-2_4-pyridone-3_5-carboximide	N/A	N/A	N/A	N/A	N/A	6927.208	N/A	N/A	N/A	5359.566	3739.204	N/A	3206.277	N/A	N/A	
Nicotinamide Riboside	N/A	5264.199	N/A	3108.128	8156.349	N/A	N/A	N/A	N/A	3203.899	2964.521	N/A	N/A	N/A	6237.392	
Adenylosuccinate	482569.9	1383590	236210.5	74275.35	1407603	371398.5	309416.3	2385133	164063.5	20831.74	13892.71	101005.5	455856.9	366594.4	329135	
cholesterol	284285.2	309772.8	211101	207291.6	359620.9	299383.6	213229.2	433930.8	190243.2	82295.28	60924.61	147493.3	226535.7	147492.5	210549.4	
3-hydroxypropanoate	N/A	N/A	N/A	N/A	N/A	N/A	N/A	N/A	N/A	N/A	N/A	N/A	N/A	N/A	N/A	
succinic acid semialdehyde	N/A	N/A	N/A	N/A	N/A	N/A	N/A	N/A	N/A	N/A	N/A	N/A	N/A	N/A	N/A	

SUPPLEMENTARY TABLE 1. NORMALIZED DATA.

Label	MUT	MUT	MUT	MUT	MUT	MUT	MUT	MUT	MUT	WT	WT	WT	WT	WT	WT
glyoxylate	-0.360701	-0.432099	-0.081629	-0.467885	-0.831283	-0.560817	-0.745322	-1.290751	-0.682093	1.711308	2.29276	0.993686	-0.348299	0.128876	0.674248
glycolate	-0.191691	-1.50741	-0.26028	0.911537	1.509866	-1.33325	-0.545457	1.26893	0.84241	-0.980789	0.927918	-0.591424	-0.739055	-0.417754	1.106449
pyruvate	-1.188593	0.21033	-0.559024	-0.658156	-0.447509	0.517371	0.509413	-1.479376	-1.558693	1.776143	0.628383	0.701271	0.393734	-0.313934	1.468641
lactate	0.156142	-1.112379	0.976564	-0.036588	-1.947332	0.354843	1.024095	-1.945546	1.539521	0.563005	0.050142	0.515416	-0.192818	-0.109148	0.164084
2-oxobutanoate	0.592759	-1.035018	-0.471293	0.251758	-1.602901	-0.065865	0.295824	-1.782083	-0.144302	1.390384	1.207639	1.639389	-0.515753	-0.053854	0.293317
acetoacetate	-0.357561	-1.182177	0.515574	0.682284	-1.369234	-0.401913	0.390394	-1.559836	0.11488	0.529963	2.341835	0.702399	-0.611893	-0.37399	0.579274
glycerate	-0.970181	0.115043	-0.256085	-1.187177	0.688225	0.479168	0.464808	0.954145	0.423015	-1.433096	-1.60781	-0.877787	1.711228	0.519651	0.976853
uracil	0.137802	1.363579	-0.684732	-0.684942	1.547954	0.1462	0.256938	1.74671	0.344394	-1.360388	-1.370325	-1.098619	-0.723063	0.171233	0.207257
fumarate	-0.218459	-0.413212	0.378014	-0.482097	-0.884497	-0.574374	-0.88317	-1.248608	-0.83208	2.186498	1.868734	0.990508	0.019664	0.002695	0.090384
Maleic acid	-0.174174	-0.281325	0.033705	-0.704078	-0.790346	-0.712063	-0.53356	-1.245218	-0.495773	1.612062	2.543105	0.921067	-0.211927	-0.312991	0.351516
2-keto-isovalerate	-0.541211	-0.58159	0.391038	-0.514922	-1.393451	-0.749104	-0.667776	-1.10849	-0.578216	1.508668	2.029715	1.09933	0.34716	-0.082163	0.841011
Guanidoacetic acid	-1.071463	1.946333	1.122091	0.558784	-1.061915	1.230946	-1.066695	1.220141	0.507528	-0.589519	-0.676346	-0.693345	-0.461837	-0.505273	-0.45943
succinate	-0.933701	-0.620412	-0.404084	-0.459978	-0.842333	-0.930147	-0.857009	-1.160643	-0.483386	1.936398	0.96992	1.284476	0.883871	0.650979	0.966049
Methylmalonic acid	-0.902473	-0.609948	-0.402364	-0.483131	-0.849808	-0.913042	-0.897472	-1.174728	-0.456195	1.931888	1.030541	1.290682	0.872678	0.669607	0.893765
3-S-methylthiopropionate	-0.870526	-0.246302	0.774133	0.396117	1.022186	0.39407	-2.10036	1.05249	-0.618663	-0.236459	0.642896	-1.750422	0.576034	1.186939	-0.222131
nicotinate	0.023466	0.707878	0.323818	0.387101	0.418069	1.855015	-0.781381	2.002605	-0.481332	-0.412773	-1.270807	0.106441	-1.338214	-0.738115	-0.801771
taurine	-0.410118	-0.768861	0.220075	0.18516	-0.854326	-0.624081	-0.441681	-0.950739	-0.233451	2.312693	2.222713	0.436752	-0.33365	-0.429522	-0.330963
Pyroglutamic acid	0.966807	1.008484	0.370101	-0.723334	2.054716	-0.374082	-0.446432	1.738223	0.048754	-1.055865	-0.882558	-0.839132	-0.454439	-0.667269	-0.743975
Citraconic acid	-0.084508	-0.636327	0.313155	0.561007	-0.377888	-0.265828	1.529076	-1.551708	-0.945936	2.211081	-0.279348	1.069609	-0.114967	-1.012094	-0.415323
2-ketohaxanoic acid	0.972698	-0.976463	0.334487	-0.068875	-2.066316	0.070897	-0.041872	-1.268306	0.449169	0.409789	1.848751	0.990673	-0.608639	0.669181	-0.715173
N-Acetyl-L-alanine	0.413615	-0.73639	1.177912	-0.179788	-1.83259	-0.166572	-0.459979	-1.935543	0.421825	1.721133	1.149215	0.196459	0.087217	0.019846	0.123639
oxaloacetate	-0.303621	-0.888229	0.321651	0.237441	-1.886711	-0.606545	0.968077	-1.114523	-0.236692	1.675935	1.803579	0.564626	-0.488694	-0.319579	0.273285
Hydroxyisocaproic acid	-0.562939	-0.581629	-0.552042	-0.545992	-0.586905	-0.571283	-0.564218	-0.590883	1.690498	1.550217	2.075385	0.936103	-0.566049	-0.568151	-0.562114
malate	-0.284452	-0.704213	-0.169465	-0.298011	-1.218967	-0.897804	-0.612572	-1.064328	-0.602577	1.801361	1.952696	1.224693	0.342333	-0.138353	0.66966
hypoxanthine	1.042989	1.166805	0.829174	-0.488389	0.32466	0.524813	0.076441	-0.234187	0.82221	-1.342867	-2.714457	-0.277969	0.336652	-0.300145	0.234268
anthranilate	-0.520049	-0.520862	-0.519575	-0.383623	-0.394977	1.966133	-0.417657	-0.521264	-0.519822	1.051955	-0.333386	2.531552	-0.413431	-0.520275	-0.48472
p-aminobenzoate	-0.505198	-0.506232	-0.504596	-0.504261	-0.426476	2.412863	-0.382602	-0.506743	-0.50491	1.19837	2.016548	-0.428535	-0.347589	-0.505486	-0.505153
p-hydroxybenzoate	-0.934948	1.196087	0.257042	-0.226561	-0.153333	-0.221466	-0.679381	-0.217034	-0.176768	0.795735	-1.12675	-1.04866	2.464888	1.006329	-0.935179
acetylphosphate	0.408078	0.82594	0.628579	0.251984	0.780438	0.957162	1.124833	0.426948	0.855562	-1.718048	-1.663066	-0.593887	-0.427435	-1.63941	-0.217678
Carbamoyl phosphate	0.415739	0.347161	0.679778	0.152703	0.144147	0.236882	0.055119	-0.07031	0.474967	-0.185504	-3.523335	0.164483	0.499498	0.322509	0.286163
a-ketoglutarate	0.870565	1.686152	0.442273	-0.44473	2.055646	0.195072	0.053847	0.567873	-0.069788	-1.442734	-0.542838	-0.500925	-1.114925	-0.860093	-0.895396
Phenylpropiolic acid	1.029434	1.691009	0.526339	-0.674927	1.868605	0.033994	0.408991	0.411577	-0.130958	-1.398191	-0.582438	-0.199727	-0.637075	-1.109038	-1.237595
2-oxo-4-methylthiobutanoate	-1.379823	0.909638	0.642275	-0.523707	-0.248563	-1.396131	-0.234411	1.196516	0.580023	0.808562	-1.230968	-0.565651	-0.555608	1.987472	0.010372
2-Hydroxy-2-methylbutanedioic acid	-0.909	-0.918479	-0.323596	0.256227	-1.422665	-0.758106	0.808562	-1.341227	-0.167632	2.254435	0.526423	1.144725	0.479527	-0.050814	0.421621
3-methylphenylacetic acid	-0.326225	0.088331	-0.035986	-0.321437	-1.36731	3.145559	-0.322725	-0.590679	-0.234584	-0.456393	0.329714	-0.185986	-0.319498	-0.36358	0.960797
xanthine	1.039526	0.518107	-0.352349	-0.495348	1.125288	0.106349	0.320608	1.056565	1.610385	-0.953915	-1.847517	-1.177348	0.565617	-0.677461	-0.838507
Hydroxyphenylacetic acid	0.458371	-0.277797	0.904414	0.790942	-1.377502	-0.815882	0.290332	-2.678697	0.625546	0.605952	-0.31669	1.199826	0.053021	0.25674	0.281423
2,3-dihydroxybenzoic acid	-0.590688	0.877003	-1.035383	-0.563526	-0.940609	0.190105	-0.97666	1.128914	-0.932534	0.606796	0.752355	2.04051	0.96567	-1.138437	-0.383514
orotate	1.379864	0.175748	-0.631911	0.560512	0.51888	-0.80065	2.157799	-1.550449	0.358342	-1.126998	0.903132	-0.141952	-0.539448	-0.80258	-0.46029
dihydroorotate	-0.132278	-0.529125	-0.33418	-0.188336	-0.62083	-0.293553	-0.273054	-0.565169	-0.176855	2.481529	2.389515	-0.489784	-0.507859	-0.334543	-0.425479
allantoin	1.023865	2.800226	0.323085	-0.430725	-0.005378	-0.176893	-0.503828	0.860858	-0.522732	-0.20018	-1.272965	-1.217892	-0.098612	0.026829	-0.605658
Aminoadipic acid	-0.366993	-0.638772	-0.733577	0.304041	-1.004706	1.187181	1.181543	0.57814	1.978519	-1.033263	-0.889097	-1.378231	0.738142	0.516855	-0.439783
Indole-3-carboxylic acid	-0.604991	-0.622078	-0.827762	0.14932	-0.704727	0.73806	1.417441	0.997118	1.656966	-1.12284	-0.721133	-1.585255	0.855934	0.758308	-0.384363
phenylpyruvate	1.057887	0.967594	-0.639509	-1.128749	1.357402	0.085374	0.52373	1.383398	1.181569	-1.297033	-0.037778	-0.709428	-0.68698	-1.190014	-0.867463
Atrolactic acid	-1.056426	-0.498704	0.072292	1.068999	-0.580953	0.382638	-0.579443	-0.550286	0.12442	2.898694	-0.79415	0.100346	0.114441	-1.074373	0.372506
Phenyllactic acid	-0.58244	1.803994	-0.508384	-0.467273	2.810627	-0.639144	-0.591133	0.194619	-0.547017	-0.015681	-0.064865	-0.43106	-0.603573	0.218162	-0.576833
quinolinate	0.54268	-1.329842	-0.563839	-0.371562	0.094905	-0.321682	-0.016301	-0.09622	-0.302142	2.787336	0.404776	-0.127685	1.109618	-0.431216	-1.378825
phosphoenolpyruvate	0.221206	-0.520304	1.535358	1.316983	-0.712731	0.810584	1.884466	-0.611228	0.755405	-0.783164	-0.594383	-0.421529	-1.067527	-0.921388	-0.891747
Uric acid	-0.635327	0.760028	-0.53284	-0.201199	0.320744	-0.755779	-0.042845	-0.195658	-1.042864	1.082092	0.280814	-1.989876	2.046007	1.190227	-0.283525
dihydroxy-acetone-phosphate	0.372061	-0.37683	0.878713	1.974192	0.801965	-0.787181	0.647151	-0.383683	1.720813	-1.318215	-0.711272	-0.857911	-0.658335	-0.645195	-0.656274
D-glyceraldehdye-3-phosphate	0.607551	-0.630471	0.518135	1.987632	1.087778	-0.596672	0.587792	-0.507924	1.705652	-1.056988	-0.771335	-0.759413	-0.971226	-0.531531	-0.668981
sn-glycerol-3-phosphate	-1.177459	-0.512155	-0.743103	-0.41712	0.101337	-1.112621	-1.120923	-1.034385	-0.029419	1.300089	-0.126536	0.867174	1.732037	1.073405	1.19968
shikimate	-0.417792	0.320599	-0.559791	0.780221	-0.161732	0.313874	2.91821	-0.274631	-0.010895	0.041711	0.753916	-1.176788	-0.846743	-0.817789	-0.862371
aconitate	-0.680173	-0.567091	0.130598	1.012954	-0.354746	-0.702506	1.953146	-1.324702	-0.623548	1.913168	0.693646	0.418964	-0.372578	-0.844609	-0.652525
allantoate	0.200766	0.594955	1.365286	-0.362419	-0.036869	-0.259417	-0.149841	-0.605384	0.72918	-1.421593	2.187984	-1.413971	-0.911772	-0.658014	0.741109
Ascorbic acid	0.148226	-1.453545	0.765034	1.03567	-1.695317	-0.394455	-0.02545	-1.975388	0.710265	0.647442	1.10121	0.890969	-0.187809	-0.111768	0.544917
2-Isopropylmalic acid	-0.361785	-0.978692	0.008684	0.404238	-1.082959	-0.555914	-0.211357	-1.268495	0.228421	2.24051	1.822841	0.880577	-0.424099	-0.439668	-0.262303
N-carbamoyl-L-aspartate-nega	1.063578	-0.814413	0.889396	-0.975618	0.758639	0.376908	-0.702095	-0.264496	0.666014	1.801005	0.702899	-1.500805	-1.63769	-0.166101	-0.197221
Pyrophosphate	0.459258	1.607989	0.297956	-1.052219	1.241403	0.399809	0.147947	1.36826	-0.085761	-1.719146	-1.590115	-0.95644	-0.058805	-0.05486	-0.005278
glucono--lactone	-0.770464	1.969067	0.808453	0.751717	-0.494296	0.055373	0.84347	-1.270135	-1.008079	0.16393	0.211059	-1.318715	0.628732	0.799827	-1.369938
myo-inositol	0.139996	0.45923	-0.154942	-1.208591	-0.904244	0.778444	-1.326581	0.008056	0.370565	-0.838887	-0.680839	-1.052057	1.817565	1.410957	1.181328
hydroxyphenylpyruvate	-0.626611	0.806291	-0.1635	-0.711405	-0.488767	0.264514	-0.966048	1.282391	-0.866509	-0.846804	-0.978454	-0.991306	1.480224	1.371549	1.434435
homocysteic acid	0.262565	0.488816	-0.001382	-0.054507	0.325372	1.345788	0.384453	2.487105	-0.920421	-0.898282	-1.486897	-0.913187	-0.596607	0.172292	-0.59511
4-Pyridoxic acid	-0.009155	-0.804639	0.011953	1.036523	-1.004919	-0.519768	-0.237486	-1.030543	-0.40864	1.094506	2.811695	0.295599	-0.44014	-0.474464	-0.320523
3-phosphoglycerate	0.302909	0.086482	2.042415	0.223967	-0.91362	0.973156	1.932216	-0.717717	0.216536	0.028384	-0.564924	-0.907953	-0.998479	-0.781246	-0.922128
Indoleacrylic acid	-0.032612	1.287423	0.719388	0.284796	0.840649	-1.000619	0.830189	0.991986	1.262563	-1.235433	-0.024101	-1.007204	-1.440214	-0.009858	-1.466955
Kynurenic acid	0.222458	-1.13463	0.349576	1.188981	-1.064345	0.027131	0.345771	-2.277357	0.421987	-1.325419	0.587591	0.242642	0.359293	0.798485	1.257837
citrate-isocitrate	0.564034	-0.896405	0.196799	0.039484	-1.085905	-0.729326	-0.194961	-1.183683	-0.629857	2.226135	1.473847	1.297402	-0.322389	-0.590735	-0.164438
isocitrate	2.528834	0.279001	1.094039	1.195785	-0.345793	0.02046	-0.690186	-0.613847	0.005585	0.446252	-0.379231	-0.968678	-0.980658	-0.338819	-1.252743
citrate	-0.396155	-0.964649	1.701833	0.300604	-0.976424	-0.666996	0.829349	-1.662156	0.231925	1.656691	0.173694	1.197253	-0.198338	-0.721475	-0.505157
2-dehydro-D-gluconate	-1.133921	-0.475707	0.294987	1.771717	0.743708	-0.798273	0.160467	-0.487681	-0.070652	-1.391325	1.114341	1.055504	1.223524	-0.98131	-1.025378
D-gluconate	-0.238008	0.195802	0.588064	0.440586	-0.733082	0.964851	-2.892947	-0.727537	-0.121408	0.300486	0.779902	-0.094633	-0.252285	1.447359	0.342853
D-erythrose-4-phosphate	0.316527	0.048441	0.870262	1.616277	0.75052	1.034855	0.994263	-0.176492	0.973685	-1.000212	-0.980709	-1.203147	-1.141744	-1.018698	-1.083827
Xanthurenic acid	-0.38289	-0.803442	0.193626	0.302291	-0.963104	-0.124345	-0.799665	-0.80676	-0.424954	0.302093	3.064264	0.954616	-0.505528	0.08969	-0.095892
D-glucarate	1.895855	-1.161668	-0.402572	-0.415118	-0.721475	-0.643621	-0.709998	-0.777642	-0.721592	-0.04894	1.225468	-0.65989	0.957761	1.768831	0.414601
deoxyribose-phosphate	-0.263009	0.338615	-0.968661	-0.882739	2.615389	-0.910996	-0.366858	0.946941	0.983312	0.796458	-0.784821	-0.392971	-0.998262	0.050384	-0.162784
pantothenate	-0.773751	-0.785906	0.143715	-0.42787	-0.789337	-0.349481	2.045085	-0.791925	-0.233724	-0.719511	0.546601	-0.309706	-0.775773	1.976231	1.245352
deoxyuridine	0.850349	0.21409	-0.488905	0.045384	0.939724	-0.985305	-0.49776	0.656924	-1.65854	2.06294	-0.255126	0.967297	0.207716	-0.650524	-1.408264
ribose-phosphate	0.824895	0.658106	0.310134	-0.609507	0.963779	0.493466	1.237663	0.064844	0.840359	-1.87773	-2.015446	-1.099533	-0.247149	0.082813	0.373308
thymidine	0.093251	-1.23309	-0.171119	-0.802787	-0.534074	-0.549015	1.499805	0.25809	-0.727362	1.640029	1.478774	-0.440448	-0.669089	-1.112036	1.269072
uridine	-0.053012	-0.493289	1.355266	0.174388	-0.631326	-0.644228	-0.967727	-0.771469	-1.125722	1.47896	1.232041	1.229477	1.106179	-0.789019	-1.100518
deoxyinosine	-0.306768	-0.785775	0.363309	0.225357	-1.203707	0.726292	0.10345	-1.004229	-0.415118	2.242752	-1.125486	-1.056606	0.11851	1.424828	0.69319
shikimate-3-phosphate	1.037667	0.355683	-0.782525	0.787361	-1.66315	0.518008	-0.126542	-0.28976	0.991319	0.703199	1.911586	-1.204951	-1.077473	-0.500918	-0.659504
D-glucono--lactone-6-phosphate	0.595602	-0.916836	-0.414417	0.404236	0.315016	2.097038	-0.928629	1.875903	0.695171	-0.830986	-0.819493	-0.952803	0.153957	-0.677017	-0.596741
hexose-phosphate	0.621772	0.073407	0.952212	1.858533	0.016866	1.146815	0.927898	-0.383055	0.851247	-0.994426	-0.950372	-1.1398	-1.118161	-0.82525	-1.037683
glucose-1-phosphate	0.546243	0.479508	1.059206	1.339317	0.751006	1.57948	0.444702	0.024622	0.26642	-1.249257	-0.862756	-1.401644	-1.043417	-0.982633	-0.950797
glucose-6-phosphate	0.269803	0.144458	0.736947	1.479419	0.484482	1.693914	0.951003	-0.041677	0.61802	-1.030213	-0.891162	-1.196321	-1.209485	-0.919616	-1.089572
fructose-6-phosphate	0.382653	0.290591	0.775907	1.608832	0.637831	1.447675	0.891317	-0.047209	0.48542	-1.123774	-0.949141	-1.205883	-1.180203	-0.957205	-1.056811
1,3-diphopshateglycerate	1.102711	0.022946	-1.151335	1.329647	0.461019	-0.714845	-0.274802	0.744105	-1.136567	-0.571404	-1.980598	0.899179	0.798477	1.022796	-0.55133
2,3-Diphosphoglyceric acid	-0.300479	0.554782	-0.080036	-0.824735	0.745903	0.618672	2.169586	1.88089	-0.871871	-0.557807	-0.586879	-0.803331	-0.9053	-0.913743	-0.125653
S-ribosyl-L-homocysteine-nega	-0.861969	0.141175	-0.127975	-1.316055	-1.093057	-0.050255	-0.71221	-0.052495	-1.370657	0.316236	-0.10809	1.489767	1.874461	0.54348	1.327643
inosine	-0.13196	-1.108453	0.094617	0.294099	-1.20148	-0.397587	-0.290248	-1.275879	-0.044203	2.25546	1.898755	0.662424	-0.224864	-0.365896	-0.164786
6-phospho-D-gluconate	0.201174	1.272102	0.495198	-0.02636	0.348334	1.62125	-0.162235	1.930639	-0.069158	-1.348317	-0.922662	-1.030498	-0.579773	-0.755617	-0.974076
xanthosine	0.885048	0.267673	1.053312	0.992401	0.555877	-0.26672	0.431942	-0.17466	1.033575	-2.0832	-2.174008	-0.437503	0.095632	-0.316117	0.136748
D-sedoheptulose-1-7-phosphate	0.687662	0.398983	1.71307	0.905693	0.872468	1.355498	0.245973	-0.1905	0.205357	-1.268395	-1.061197	-1.39603	-0.503174	-0.923363	-1.042046
N-acetyl-glucosamine-1-phosphate	-1.845521	-0.5427	-0.834357	-0.255882	1.502222	-0.879711	-0.50311	0.061447	0.217593	-0.413351	-0.497111	0.506571	1.703106	1.612311	0.168494
glutathione-nega	-0.499606	-0.715985	0.249574	-0.219855	-1.395621	-0.773195	-0.717042	-1.131012	0.023375	-0.296953	-0.250762	1.031737	1.777591	1.179917	1.737838
dUMP-nega	-0.847193	-0.990402	-0.763693	-0.71734	0.068903	0.564503	1.483275	1.390686	0.580229	-0.208159	-0.263615	-0.676509	-0.871021	2.091207	-0.840872
Geranyl-PP	-0.259031	0.476152	-1.734521	1.344296	-1.6913	1.575523	0.607703	0.379641	0.181078	0.464739	0.215236	-0.477185	-1.310321	0.733898	-0.505908
O8P-O1P	0.989357	2.185995	1.657077	0.042027	0.557021	0.571243	-0.746757	-0.533992	-0.458998	-0.733477	-1.138387	-0.946471	-0.576459	-0.861857	-0.006322
dTMP-nega	-0.090834	0.846298	0.077846	-1.085169	0.146843	2.974889	0.132127	-0.329958	-0.272145	-0.80628	-0.836655	0.540705	0.065447	-0.210283	-1.152829
cyclic-AMP	1.054044	1.02475	0.297113	-1.309331	1.219541	-0.065721	-0.141516	2.044813	-0.614039	-1.318778	-0.912552	-1.133036	0.200369	-0.246116	-0.099541
fructose-1,6-bisphosphate	0.189031	1.189419	-0.059194	-0.314691	1.754484	1.31359	0.903196	0.911777	0.070503	-1.092049	-1.035133	-1.082518	-0.886619	-0.796621	-1.065175
trehalose-sucrose	0.009498	-0.500175	3.16907	0.129346	0.340861	-0.354837	-0.021432	-0.226359	-0.264716	-0.257855	-0.759261	-0.921419	-0.50922	-0.800205	0.966705

Cellobiose	0.926459	-0.324265	-0.598001	0.345474	-0.344542	-0.084667	-0.385343	0.225308	-0.404542	1.376023	2.524798	-1.531319	-0.705026	-0.979313	-0.041043
orotidine-5-phosphate	0.027721	-0.730097	0.238887	0.551427	-1.220767	-0.205385	-0.552912	-1.121945	-0.165438	2.406681	0.782213	1.587287	-0.834253	-0.568689	-0.194729
SBP	0.301545	0.556771	0.95762	0.252905	2.133962	0.437344	-0.029075	0.853204	0.701241	-1.301034	-1.268489	-1.111189	-0.834736	-0.65499	-0.995078
trans, trans-farnesyl diphosphate	-0.157952	1.474546	-1.177495	1.261693	1.387781	0.807819	0.768919	-0.796394	-0.115514	-0.809317	-0.84607	-1.119714	0.874954	-0.324613	-1.228644
S-adenosyl-L-homocysteine-nega	0.232933	0.224084	-0.922207	-0.960754	0.821559	0.371608	-0.159507	2.913652	-0.298183	-1.147139	-1.069871	-0.304857	0.258308	-0.185015	0.225389
dCDP-nega	-0.563989	2.321383	-0.3326	-0.204149	1.404422	-0.741161	-0.591152	-1.157344	-0.453309	1.206858	1.053181	-0.091001	-0.630019	-0.67465	-0.546471
5-phosphoribosyl-1-pyrophosphate	-0.162121	-1.313362	-0.943261	0.293508	-0.542638	-1.266986	-1.437555	1.032133	0.442374	-0.327784	-0.356684	1.469991	1.512655	0.596878	1.002852
OBP	0.226413	0.312004	0.077924	-0.280623	1.983704	0.257378	-0.084837	1.012842	0.893359	-2.158941	-1.51685	-0.9717	0.021941	0.084423	0.142962
dTDP-nega	2.909483	0.577078	-0.633145	-0.562029	0.327726	0.41709	-0.776289	0.958085	-0.699974	0.21916	0.134079	-0.499386	-0.797808	-0.822517	-0.751552
CDP-nega	-0.674575	-1.565938	-1.135036	0.55616	-0.251048	-0.00042	-0.431603	-0.389641	-0.082725	1.752763	1.856303	0.342776	0.195995	1.008549	-1.18156
UDP-nega	-1.111364	-0.393106	-0.841766	-0.364814	1.177167	-0.862195	0.646623	0.891792	0.433833	-1.859068	-0.703332	1.9762	0.228223	0.500627	0.28118
trehalose-6-Phosphate	-0.618575	1.718698	-0.540207	-0.977709	1.776388	-0.687655	-0.679834	1.355686	0.443405	0.176945	-0.890948	-0.804419	-0.381129	-0.858336	0.967692
Thiamine pyrophosphate	0.054259	1.89979	0.15361	-0.908098	0.249864	0.252165	0.748069	0.921591	0.880876	-1.017508	-1.332311	-1.888462	-0.201488	0.723842	-0.536197
adenosine 5-phosphosulfate	-0.264122	-0.171435	0.79817	0.19928	-0.256187	0.256026	-0.300639	-0.557236	1.519653	-0.988617	0.399116	-1.40934	-1.584071	0.187966	2.171435
ADP-nega	-0.061165	0.242833	-0.538155	-1.088679	1.266033	-0.810079	-1.163849	0.428948	-0.683975	-1.463096	-0.349195	0.662221	1.312874	0.331562	1.913723
dGDP-nega	-0.103681	-0.251912	-0.797961	-1.43085	1.239706	-1.088265	-0.899282	0.862632	-0.809399	-0.749542	-0.465768	0.813942	0.951054	1.016676	1.712649
IDP-nega	0.671494	-0.46332	-1.154975	-1.457905	1.09862	-0.683306	-1.054564	1.197091	-0.382932	-0.801871	-0.626233	0.771209	0.144223	1.149826	1.592642
GDP-nega	-0.755119	-1.01044	-0.150453	0.100818	1.395884	-1.250607	1.715735	1.102673	-0.305507	-1.734793	-0.616923	0.621585	-0.317228	0.538282	0.666092
CDP-ethanolamine	-0.233601	0.603923	0.251	-0.054176	-1.57607	-0.126831	-0.825833	-0.975428	0.030139	-1.128315	0.291694	0.173619	1.848811	-0.38302	2.104088
FMN	-0.496283	-0.994557	-0.205757	-0.044478	-1.135218	-0.718736	-0.530388	0.250679	-0.357317	1.727144	1.534191	0.097587	-0.579188	-0.635226	2.087548
cholesteryl sulfate	1.329859	0.563328	1.320838	0.691344	0.92044	0.810362	-1.202427	1.318331	-0.948655	-0.685791	-0.934412	-1.048619	-0.403867	-0.869746	-0.860985
dUTP-nega	-0.639741	1.928201	-0.393813	-0.257292	-1.180594	-0.828045	-0.668611	-0.088069	-0.522107	1.242371	1.079038	-0.137035	-0.70992	1.796737	-0.621123
CTP-nega	0.754822	1.522365	0.183657	-0.71162	1.954946	0.780065	0.180983	1.017365	-0.227109	-1.073997	-1.012547	-0.879517	-0.882526	-0.785149	-0.821738
UTP-nega	-0.364931	-1.395341	-0.866654	-0.537154	-0.463254	-0.928082	-0.02034	-0.638261	-0.048638	1.366076	2.063659	1.626175	0.467005	0.301652	-0.561912
CDP-choline	-0.491095	-1.384935	-0.49166	0.661003	-1.291817	-0.664188	0.24588	-1.433188	0.63313	1.059976	2.049718	1.085894	0.026319	-0.129187	0.12415
Taurodeoxycholic acid	0.1905	0.630509	0.158236	0.007008	-0.962048	-0.931963	0.226041	0.748723	-0.370407	2.616145	0.701567	-1.706887	-0.724765	-0.454424	-0.128233
ATP-nega	-0.854603	-1.267391	-0.680907	-0.151244	1.137452	-1.653441	0.106606	-0.705132	0.408964	1.0991	0.722171	1.298579	-0.653247	-0.383006	1.5761
dGTP	-1.313317	-1.245938	-0.698843	-0.548191	0.734689	-1.709817	0.531978	-0.608004	0.762528	1.443006	0.718591	0.973342	-0.109463	-0.20916	1.2786
GTP-nega	-0.630827	0.217728	-1.103996	-0.889765	1.42066	-1.181065	-0.005348	0.97637	-0.394305	-1.038838	-1.231911	0.408687	0.786259	1.126486	1.539865
UDP-D-glucose	0.89524	-0.303059	-0.04989	-1.908523	0.229358	0.135483	-0.133849	0.218666	1.606961	-1.226883	-1.767357	0.688843	0.610247	-0.114976	1.119741
UDP-D-glucuronate	0.897702	-0.968921	-0.929769	-1.178234	0.37424	-0.586606	0.372375	0.592622	0.728479	-1.676322	-1.136145	1.702921	0.081129	0.85801	0.868519
ADP-D-glucose	-0.252125	-0.688079	-1.728008	-0.801809	-1.242141	0.657664	1.490882	-0.528301	0.290173	0.856915	0.185361	-0.312036	0.25345	-0.250643	2.068699
guanosine 5-diphosphate,3-diphosphate	7.26E-01	1.78E-01	-1.17E-01	1.57E+00	7.16E-01	1.60E+00	1.92E-01	-5.06E-05	1.82E-01	8.14E-01	-1.15E+00	-1.39E+00	-8.46E-01	-9.81E-01	-1.49E+00
UDP-N-acetyl-glucosamine	2.656489	0.787877	-0.104369	-0.962274	0.098774	-0.179778	-0.393305	-0.187338	0.188328	-1.2627	-1.419866	0.069317	1.14841	-0.428871	-0.010693
glutathione disulfide-nega	-0.010002	1.656633	0.009137	-1.626234	0.622809	1.13227	-0.812249	1.714759	0.005361	-0.713329	-1.06955	-1.05429	0.650624	-0.14108	-0.364859
NAD_nega	-0.802387	0.704739	0.540018	0.93305	0.148857	-0.360302	1.855221	-2.120255	0.54194	0.579798	-0.890875	0.413011	-1.239753	0.312689	-0.615751
dephospho-CoA-nega	0.350538	1.191001	-0.098909	-0.359316	0.687589	1.878467	1.411174	0.710132	-0.15023	-1.486232	-1.145106	-0.907181	-0.645449	-0.65271	-0.783769
NADP_nega	0.600858	-0.241837	-0.552662	0.048921	-0.059415	-1.278041	-1.203619	-0.771115	-0.38662	1.08736	-0.661056	2.714224	0.040576	0.674389	-0.011962
coenzyme A-nega	-1.092942	1.328101	0.610988	0.870615	-1.104712	-1.01808	0.629132	-0.978972	0.989562	-0.433336	-0.073269	1.271472	1.122473	-1.082038	-1.038993
2-hydroxygluterate	-1.399635	-0.235618	-1.056415	-1.966125	-0.720576	0.491616	0.310432	-0.154441	0.393484	0.451164	0.434556	-0.413661	1.715506	0.80028	1.349433
2-deoxyglucose-6-phosphate	1.280279	1.770883	0.169264	-0.109818	0.970352	0.092103	-0.117854	1.559971	-0.446438	-1.446613	-1.402645	-0.714154	-0.255824	-0.818332	-0.531174
3-hydroxybutyric acid	-0.660363	2.501931	1.54882	-0.584578	-0.770151	0.09115	-0.622557	-0.820845	-0.586188	-0.166353	-0.391371	0.903654	0.849335	-0.686255	-0.606229
4-phosphopantothenate	0.796921	-0.346046	-0.280635	-0.526413	2.210236	-0.10918	-0.587297	0.965666	-0.708164	-0.964022	0.404033	-1.366373	-0.723217	-0.374908	1.609397
Urea	1.969374	1.368852	1.434702	-0.448589	-1.080766	0.269679	-1.151703	-0.246174	-0.025877	0.146822	-1.252884	-1.234043	0.362485	0.176379	-0.28826
glycine	-0.644027	1.367495	2.158601	-0.344558	-1.067532	-0.791476	-0.666633	1.323435	-0.551916	0.829725	0.701831	-0.250393	-0.698979	-0.736123	-0.629449
alanine	-0.517018	-0.393123	-0.238985	-1.120884	-1.175631	-0.581826	-0.647813	-1.108831	-0.854325	1.059664	0.508272	1.043579	1.760441	1.249614	1.016864
betaine aldehyde	0.626158	-1.401011	1.508814	0.624695	0.042898	0.697371	0.360547	0.190485	0.813062	-1.208331	-1.212801	-1.334659	0.980592	0.592157	-1.279977
choline	-0.583113	-0.611507	1.536107	0.496702	-0.64487	1.383159	0.587255	-0.854027	2.21666	-0.872942	-0.584704	-0.776022	-0.641152	-0.455101	-0.196446
4-aminobutyrate	0.027588	0.944337	-0.763012	-0.787343	0.57004	0.327756	-0.133136	0.883164	0.562362	-1.880571	-1.664005	-0.589025	1.863954	0.439067	0.198823
dimethylglycine	-0.406535	1.046958	0.964495	0.335385	0.880393	0.224153	1.866492	0.064779	0.827551	-1.231978	-1.792692	-0.828452	-0.700425	-0.687762	-0.562361
serine	-1.051412	-1.278942	-0.310161	-0.450462	-0.862151	-0.466127	-0.361042	-0.897851	-0.06469	0.59976	-0.052996	0.200436	1.583488	1.301749	2.110401
cytosine	1.802329	0.768474	1.621424	0.165706	-1.224124	0.43711	0.495284	-1.508417	-0.375796	-0.508258	-0.870892	0.660676	0.208886	-1.195241	-0.47716
Creatinine	-0.060599	0.401412	-0.563769	-1.028293	1.608942	0.354125	-0.398319	2.198784	-0.331448	-1.120542	-1.111994	-1.129273	0.789124	0.492419	-0.100568
proline	1.403208	0.518063	1.504236	0.397502	-0.038422	0.707906	0.732485	-0.088305	1.049686	-1.452096	-1.540656	-1.077221	-0.673463	-0.888688	-0.554236
indole	-1.89332	-1.177423	-0.550074	0.471246	0.755742	0.777726	-0.371246	0.414532	-0.083926	2.172555	0.56154	-0.419258	0.4715	0.12086	-1.250453
betaine	-0.991609	-1.563329	1.130884	0.477091	-0.861813	-0.184409	-0.155033	-0.72969	0.883385	1.824054	0.447312	0.411545	-0.986484	1.206973	-0.908876
valine	1.052045	2.421443	1.290301	-1.166449	0.629574	-0.376276	-0.583614	0.589962	-0.192833	-0.415189	-1.239471	-0.508146	-0.416293	-0.618987	-0.466067
threonine	0.73112	1.512203	0.831371	-0.246471	0.713456	0.328743	0.640101	1.234803	0.182038	-1.836589	-1.515152	-1.250276	-0.517937	-0.492958	-0.314452
homoserine	-1.6714	-0.713973	-0.708104	2.177417	-0.375533	-0.122111	0.397583	0.289212	-0.046388	-1.782838	0.412354	-0.089892	0.762012	0.866454	0.605207
purine	-0.391954	-0.164421	-0.175999	-1.626715	1.775172	0.996556	-0.177474	1.639268	-0.609496	-1.734629	0.009267	0.865906	-0.021571	0.001231	-0.385142
cysteine	-1.128013	-0.836686	0.370761	0.706654	-0.85648	-0.433887	-0.205029	-2.244637	0.948595	1.472681	1.44132	0.445613	0.163676	0.127755	0.027676
nicotinamide	0.777589	0.441328	1.042902	-0.770638	-0.0766	0.835346	0.637532	-2.273711	0.696865	-1.742951	-1.014493	0.077168	0.645271	0.332371	0.392022
Imidazoleacetic acid	0.010539	-0.206709	1.880729	1.468581	-0.464403	0.868969	1.10235	-0.758181	0.696616	0.175003	-0.393826	-1.21336	-1.148621	-0.961975	-1.055713
thymine	0.765341	-0.343202	-0.225647	0.047161	-1.538628	-1.18422	-0.522088	-1.456704	1.279407	0.742571	1.635319	1.367752	-0.340442	-0.43278	0.20616
DL-Pipecolic acid	-0.274136	-0.925607	0.215567	0.495414	-1.03386	-0.435001	-0.268627	-1.164246	-0.118994	2.099676	2.267265	0.29056	-0.358804	-0.430631	-0.358575
N-Acetylputrescine	0.849958	0.214443	-0.909402	-0.573318	0.211499	-0.868072	0.002988	-0.64328	0.529664	1.705349	2.338522	-0.905947	-0.925753	-0.485288	-0.541362
hydroxyproline	-1.160849	-1.346056	-0.844715	-0.131857	-1.139655	-0.299104	0.887119	-0.484697	0.710248	-0.484116	-0.552366	0.553998	1.521129	1.072592	1.698328
leucine-isoleucine	0.943572	2.468848	0.481715	-0.604169	0.663929	0.424486	-0.070838	0.524209	-0.254374	-1.157766	-1.690905	-0.913665	0.052903	-0.296038	-0.571908
ornithine	0.382353	1.905932	0.479725	-0.268251	1.740468	0.205918	0.569845	0.813632	-0.385769	-0.991554	-1.639944	-0.601685	-0.740285	-0.890604	-0.579782
asparagine	-0.329769	0.985819	-1.652852	-0.173565	0.881263	1.185477	-0.21802	1.705516	1.237722	-0.930172	-1.351043	-0.558843	0.133905	-0.611552	-0.303886
aspartate	0.183414	0.435014	-0.59324	-0.793533	-0.041661	1.161082	0.920191	0.307722	1.677098	-1.324565	-0.395673	-2.2808	0.751633	-0.085469	0.078786
adenine	-1.388944	0.316558	-1.481312	-1.209383	-0.654154	1.038673	0.512514	0.476773	-0.43082	-1.214456	1.178951	0.855892	1.558878	0.278481	0.162347
Methylcysteine	-1.191981	-1.052826	-1.104976	-0.137651	0.167603	0.122985	0.653208	-0.16983	0.056722	-1.354316	2.047345	1.847916	0.165227	-0.385098	0.335672
homocysteine	0.714417	0.083669	0.53491	-0.860434	1.732944	1.027281	-0.1558	0.446055	0.368074	-2.438393	-0.035412	-0.849695	0.72786	-0.67125	-0.624227
methylnicotinamide	0.336653	1.515571	0.542853	-0.608404	1.503853	0.007126	-0.146354	1.514034	-0.042532	-1.425156	-1.657302	-1.016252	0.336782	-0.593611	-0.267261
histidinol	-0.342643	0.659741	0.90553	-1.148096	1.438546	-0.808393	-0.090241	0.062256	1.707411	-0.836907	-1.621643	-0.722063	-0.685902	1.086391	0.396011
lysine	0.23031	1.358831	0.038755	-0.338853	0.822465	0.969015	0.36663	1.814083	0.526603	-1.558776	-1.311214	-1.258527	-0.480939	-0.527556	-0.650829
glutamine	-0.225208	-0.829992	0.147182	0.632068	-1.072328	-0.45281	-0.428318	-1.33544	0.129587	1.699981	2.39637	0.582192	-0.322672	-0.48574	-0.434873
O-acetyl-L-serine	-1.105687	1.029887	0.483305	-1.388196	-1.374608	0.706579	0.281267	1.196789	0.53617	0.261901	0.876084	-0.01781	-1.366263	1.093155	-1.212572
glutamate	-0.518226	-0.845404	-0.016055	0.680456	-0.993511	-0.388366	-0.373337	-1.213082	-0.246237	2.247915	2.082904	0.341643	-0.117734	-0.23001	-0.410955
methionine	-0.563333	-1.329723	-0.562104	0.124859	-0.324708	0.207484	0.977647	-0.596412	1.984806	-1.014614	1.570779	1.097561	-1.048963	-0.611524	0.088245
guanine	-0.92877	-1.452012	1.977536	-0.893668	0.375162	1.209475	-0.089279	0.037891	0.263938	-0.643113	1.743289	-0.829543	0.102969	-0.664847	-0.209027
histidine	-1.002895	-0.852146	-0.763452	1.332396	0.986869	0.197545	0.81544	-0.343044	1.857547	-0.573193	-0.279272	1.322438	-0.691721	-1.095352	-0.911161
2-Aminooctanoic acid	-0.511267	-0.311357	-0.794683	1.282116	0.934581	1.839549	0.110246	1.353341	-1.209327	-0.937309	0.902346	-0.159998	-0.784439	-0.87273	-0.841071
carnitine	-0.186424	-0.905964	0.113253	0.206941	-1.130253	-0.455466	-0.302026	-1.258713	0.158849	2.416882	1.924142	0.292447	-0.399958	-0.26655	-0.207159
Methionine sulfoxide	0.111366	-1.67496	-0.716255	-0.077722	0.721523	0.720425	1.301537	1.738147	-0.469913	-1.764353	0.658593	0.229413	0.501483	-0.543778	-0.735505
phenylalanine	0.007505	0.194801	0.125232	-1.014728	2.247069	0.669056	-0.459209	1.691615	0.320473	-1.81381	-0.68352	-0.195248	-0.481301	-0.175745	-0.432191
Pyridoxamine	-0.317448	-0.425002	-0.254737	-0.219925	-0.455365	-0.365465	-0.32481	-0.478259	-0.287452	3.531684	0.120837	-0.189259	0.325341	-0.34744	-0.312701
pyridoxine	-0.54832	-0.996343	-0.287094	-0.14208	-1.122818	-0.748338	-0.578986	2.126925	-0.423368	1.450874	1.277381	-0.014342	-0.622864	1.157916	-0.528544
1-Methyl-Histidine	-1.059382	-0.138048	-0.78487	0.472412	1.584231	2.051964	-0.739043	1.600202	-0.398419	-0.992143	0.051276	0.032168	-0.438817	-0.417943	-0.823588
N-acetyl-L-ornithine	1.116249	0.33593	1.400536	0.640803	-0.248335	1.203082	-1.172015	0.083872	-1.100732	-0.242208	-0.32168	-0.913372	-1.192114	1.558894	-1.148909
arginine	0.644837	1.299498	0.314375	-0.740504	1.745841	0.84069	-0.066169	1.268781	-0.702104	-0.729193	-1.541664	-1.23157	0.067957	-0.217103	-0.953673
citrulline	-0.129085	-0.615571	0.440922	1.393304	0.953922	0.707131	1.13572	0.303558	1.310057	-1.602804	-0.918674	0.08304	-0.673043	-1.53717	-0.851308
N-carbamoyl-L-aspartate	-0.276842	1.408098	0.516282	-0.94758	1.488671	-0.934148	0.197118	1.604956	0.47623	-0.326987	-0.941404	0.292832	-1.08395	0.131327	-1.604602
glucosamine	-0.439244	-0.759063	-0.217955	2.568767	-0.94115	-0.609556	-0.601659	-0.947759	1.294165	0.549014	0.632638	-0.521726	0.961052	-0.367839	-0.599685
tyrosine	-1.350898	-1.2678	-0.819327	-0.046012	0.190363	0.150121	1.150379	-0.204798	0.334749	-1.151013	1.8371	1.755863	0.32247	-0.269898	-0.6313
Phosphorylcholine	1.215417	0.516385	0.812959	0.177072	0.183659	0.622486	0.490412	-2.891363	0.193254	-1.24455	-0.833018	0.193142	-0.068075	0.215634	0.416586
3-phospho-serine	-0.695208	-0.6746	-0.473358	0.607779	-1.761437	-0.454124	-0.738794	-0.820734	-0.157021	1.696598	0.194192	0.862752	0.770637	-0.253177	1.896496
N6-Acetyl-L-lysine	-0.333444	1.297062	0.305954	-0.825624	1.451925	0.299457	0.046865	1.800467	-0.641814	-1.838851	-1.050569	-0.986762	0.248177	-0.011835	0.238992
Acetyllysine	0.236374	0.995754	0.104556	0.132442	1.097733	0.967789	-1.060865	1.991202	-0.418291	-1.620066	-1.191038	-1.16148	-0.161828	-0.174032	0.261752
N-acetyl-glutamine	0.768836	1.419711	0.894872	-0.934414	1.973307	0.33683	0.589985	-0.914268	-0.930821	0.038633	-0.880065	0.465712	-0.922851	-0.924058	-0.981408
N-acetyl-glutamate	-0.177201	1.808866	-0.305988	-1.179514	1.621578	0.005391	0.167647	0.424398	0.474816	-1.831006	-0.833216	-0.765421	-0.013991	1.118344	-0.514704
Ng,NG-dimethyl-L-arginine	1.288444	1.345946	0.128414	-0.682169	0.667896	0.570697	-0.22069	2.05869	-0.203619	-0.941027	-1.467079	-1.086587	-0.450542	-0.594813	-0.413562
Acetylcarnitine DL	-0.158103	-0.689595	0.21813	0.238162	-1.001232	-0.532303	-0.678971	-1.153741	-0.11101	2.476759	1.939815	0.308766	-0.195989	-0.49721	-0.163479
tryptophan	0.458367	0.576789	0.022395	0.935854	-2.635886	0.458799	0.668114	-1.63979	1.13825	0.399266	0.256455	0.156118	0.100946	-0.854493	-0.041182
Kynurenine	-0.012998	-0.003954	0.130656	0.322471	2.773207	0.330702	-1.088512	1.292713	-0.731049	-0.917219	-0.931859	0.252176	-0.125201	-0.464063	-0.82707
N-acetyl-glucosamine	-1.575809	0.468127	-1.184805	-1.809551	-0.192517	-0.056485	0.923122	-0.586545	0.337574	-0.878781	1.183218	0.704384	1.205454	0.928651	0.533963

Flavone	-0.583109	0.139012	-0.481147	-0.032482	-0.382843	-0.374013	-0.165801	-0.413299	-0.053889	3.062757	1.266137	0.332415	-0.845704	-0.863592	-0.604444
cystathionine	1.521805	1.770843	1.001869	0.020593	0.687329	0.176933	0.657593	0.352509	-0.003856	-1.269172	-1.149883	-0.911312	-0.975123	-0.970068	-0.91006
5-methoxytryptophan	-0.94572	-0.250096	0.941767	-0.211721	-0.48205	-0.479752	-0.474981	-0.59746	0.139829	0.241822	1.729211	2.523464	-0.48255	-0.954588	-0.697175
Cystine	0.647519	-1.061733	-0.823906	2.105205	-1.37867	-0.835765	0.685415	-0.616012	-0.167323	-0.193766	1.462883	0.244361	0.930715	-0.136283	-0.862641
cytidine	1.641332	1.131962	1.017989	0.641018	-1.272239	1.178144	0.545135	-1.714122	0.03929	-0.308333	-0.873751	-0.236327	-0.113331	-0.816452	-0.860316
biotin	-0.204627	-0.725051	0.113215	0.09096	-1.287691	-0.64449	-0.408153	-1.299244	-0.09684	1.804382	2.331452	0.830339	-0.147721	-0.239587	-0.116945
deoxyadenosine	0.646708	1.315712	-0.611308	-0.539788	1.923695	0.920624	-0.635875	-0.140539	0.439743	-1.513361	-1.536813	-0.246951	-0.940614	0.451217	0.467548
Glycerophosphocholine	-1.309151	-1.136211	-0.540682	-0.589534	-1.34111	1.853886	0.863634	0.037875	0.038569	-1.105025	-0.051007	0.257959	1.151622	0.996401	0.872774
acadesine	-0.012813	0.360598	0.754724	0.646946	1.113707	1.188158	1.243405	0.327561	-0.167545	-1.8986	-1.933227	-0.13999	-0.027498	-0.47608	-0.979345
D-glucosamine-6-phosphate	0.730788	0.462781	0.971478	1.185194	0.572113	1.444783	0.55307	0.238674	0.563153	-1.246438	-0.726922	-1.383367	-1.183573	-0.964239	-1.217496
D-glucosamine-1-phosphate	-0.550648	-1.120729	-1.34525	-1.072608	-0.355757	-0.852012	-0.300312	-0.908039	0.327434	1.01449	0.518843	1.806149	1.22325	1.157472	0.457716
thiamine	-0.421734	-0.548769	-0.347665	-0.306546	-0.188293	-0.478448	-0.430429	-0.611672	-0.386305	0.145129	2.909176	-0.270327	-0.442871	-0.457158	1.835912
S-ribosyl-L-homocysteine-posi	-0.348639	1.492255	0.616326	-0.17555	1.438468	-1.390957	-0.25113	1.618363	-1.336424	-1.02191	-1.051023	0.626237	-0.446499	0.144888	0.085595
deoxyguanosine	0.012474	-0.225276	-1.971304	1.117513	1.80866	0.573428	-0.019743	1.541287	0.206565	-0.195174	-1.191918	-0.503759	-1.007163	-0.243116	0.097527
adenosine	0.044437	0.747605	1.32011	-1.672885	-0.005318	-0.492823	-0.645447	-0.606164	-0.274838	2.289818	-0.065537	-0.585023	-1.038512	-0.07445	1.059027
1-Methyladenosine	-1.200658	2.136495	-0.10509	0.837285	-0.502524	-0.767248	0.322798	-1.46354	-1.151622	-0.416095	-0.48418	1.294066	0.459012	0.649339	0.391962
guanosine	0.732591	0.685028	1.059187	0.224771	1.415175	-0.668218	-0.171069	0.70377	1.613814	-0.702778	-1.634548	-1.332446	-0.61892	-0.471442	-0.834915
L-arginino-succinate	0.812193	2.315279	-1.061354	-0.457787	0.900318	-0.480922	0.157759	-0.28953	-0.129407	-0.241511	-2.134207	-0.098486	0.488441	-0.433988	0.653202
S-methyl-5-thioadenosine	-0.529868	1.424153	1.210379	-1.593738	-0.323387	-0.698022	1.664079	1.420484	-0.556847	-0.61524	-1.160724	-0.045758	0.224336	-0.465687	0.045839
7-methylguanosine	0.137802	-0.30485	-1.213858	0.517969	0.107182	-0.436847	1.415837	0.738464	-0.165221	-2.385056	-1.07966	0.629121	0.57224	0.136148	1.33073
dCMP	-1.717046	0.019284	1.722919	-1.296437	-0.697728	0.04924	-0.141636	-0.333788	0.16578	2.09887	-0.427202	-0.406267	0.195986	0.961863	-0.193839
glutathione	-1.016488	-1.402435	0.423448	0.629237	-1.319931	-0.920243	-0.571029	-1.423807	1.080022	0.849108	1.227297	0.401565	0.428675	0.338159	1.276424
dTMP	0.014917	0.353218	0.455372	1.452185	0.161207	0.524389	0.891416	0.808228	0.666364	-0.57622	0.849959	-1.698285	-1.541781	-0.817761	-1.543208
CMP	0.901837	0.572006	0.795286	-0.659325	-0.623384	1.511235	-1.575614	-0.411437	-0.653723	0.812721	1.684413	-0.59245	0.276786	-0.881574	-1.156777
UMP	-0.259418	-0.299807	0.454516	0.201673	-1.254997	-0.796015	-0.115203	-1.40994	-0.599945	2.215751	1.782308	0.84472	-0.396351	-0.156318	-0.210976
dAMP	-1.235797	-0.535047	0.915362	-0.902927	-1.418708	0.638257	-0.277005	-0.471361	-0.32099	2.035036	0.763808	1.38535	-0.30924	-0.817525	0.550789
Nicotinamide ribotide	0.512563	0.047226	-0.484703	-0.582041	-0.594792	0.093998	-0.432071	-0.273542	-0.662509	-0.905542	2.636092	-1.003194	1.78811	-0.310452	0.170859
aminoimidazole carboxamide ribonucleotide	-0.015263	-0.946044	-0.170162	1.19939	0.103281	-0.203747	-1.057124	-0.53332	0.091041	-0.384548	1.557857	2.363669	-0.705477	-1.229009	-0.070545
thiamine-phosphate	0.256648	1.260737	0.186493	-0.54973	-2.566153	0.545885	-0.105618	1.634755	-0.136834	-0.678048	-1.033299	-0.279082	0.513371	0.700476	0.250401
dGMP	0.356133	0.863409	2.071935	-0.111363	-0.330308	-0.808416	-1.309276	-0.365306	-0.484983	-2.068277	0.114751	0.78941	-0.155672	0.670657	0.767305
AMP	-0.184368	-0.617755	-0.043039	-0.399286	-1.423657	-0.231059	-0.28246	-1.057622	-0.235315	2.39709	2.039639	0.347245	-0.030214	-0.245805	-0.033395
IMP	0.740774	0.003942	1.043006	0.773318	-0.073865	-0.077142	-1.187398	-0.796797	-0.820182	1.160002	1.518135	1.110261	-1.576698	-0.819051	-0.998303
GMP	-0.071493	-0.88634	0.594574	0.030823	-1.495593	-0.192248	-0.081724	-1.710261	-0.317421	1.833409	1.516825	1.316309	-0.028652	-0.144881	-0.363327
xanthosine-5-phosphate	-0.629771	-0.220891	-0.590842	-0.81229	2.932428	-1.298862	-0.846656	-0.136214	-0.093912	0.342402	0.881715	0.101458	0.724464	-0.068816	-0.284213
S-adenosyl-L-homoCysteine-posi	-0.536445	0.462624	-0.813024	-1.619914	2.112433	0.379591	0.006678	1.016136	-0.336677	-0.997633	-1.048527	-0.813877	0.877858	0.847616	0.463161
S-adenosyl-L-methionine	-1.104105	-0.269651	-0.802446	-0.407667	0.050434	0.913288	0.284544	2.242805	-0.464304	-1.892368	-0.420898	-0.136954	1.053932	0.919726	0.033664
folate	-0.966298	-0.326015	-0.904729	1.388307	-0.445627	0.048349	-0.973525	0.255344	0.025444	2.408237	-0.535997	1.318725	-0.476906	0.146328	-0.961637
5-methyl-THF	0.411577	-0.404461	-0.952529	0.236188	-0.144623	-0.163644	0.100691	-0.149986	0.259973	2.807687	-2.015363	0.007107	-0.354995	-0.276787	0.639163
glutathione disulfide-posi	0.081087	2.109014	-0.574059	-1.317528	0.828421	-0.16872	-0.585444	2.094966	-0.371466	-0.301463	-0.521667	-1.126044	0.36504	-0.243524	-0.268613
NAD_posi	-0.0199	1.989509	-0.033198	-0.375685	1.564754	0.594521	-0.119912	-1.152099	1.150677	0.111094	-0.539132	0.15014	-1.142113	-1.55209	-0.626565
NADH	0.540709	-0.798549	-0.54606	1.463744	0.537574	-1.176882	-0.246096	-0.510506	1.530914	1.754169	-0.767097	-1.028401	-0.13689	0.51579	-1.13242
dephospho-CoA-posi	0.986538	0.26587	0.87656	-0.364229	-0.353698	1.28423	1.897124	-1.393156	-0.117722	-1.451132	-1.463604	-0.593773	0.034949	0.351435	0.040607
NADP_posi	-0.080301	-0.440341	-1.083612	-0.220154	0.291521	-1.393933	-1.208627	-0.986359	-0.423995	1.943118	0.69998	1.679362	0.861753	0.036652	0.324936
NADPH	-0.503027	-0.870978	-0.288487	-0.169391	0.925453	-0.667297	-0.528212	-1.053174	-0.400407	1.138867	0.996381	-0.064482	-0.564248	-0.60563	2.654632
coenzyme A-posi	0.182334	-0.9204	0.2916	-0.249193	-0.172143	-0.0617	0.66023	-1.17369	0.712752	-1.807716	-1.606771	0.82092	1.019189	0.70518	1.599406
FAD	0.195075	1.299412	-0.89405	-0.130186	1.717877	0.035416	-0.052071	1.274583	0.760644	-1.253566	-1.537036	-1.134587	0.013008	-0.866377	0.571858
acetyl-CoA-posi	-0.198819	-0.586133	1.75147	0.351572	-0.63317	-0.437356	-0.662284	-0.852314	0.778467	-1.378682	-1.480448	0.899745	0.149862	0.650388	1.647701
propionyl-CoA-posi	-0.49379	-0.867873	-0.275676	-0.154595	-0.973475	-0.660798	-0.519395	-1.053104	-0.38946	1.175462	1.030602	-0.047938	-0.556032	1.711655	2.074416
succinyl-CoA-posi	-0.979299	0.28324	-0.829303	-0.746037	1.101187	-1.094149	1.123378	0.797252	-0.907552	0.168634	0.069015	1.674415	-1.022102	1.329265	-0.967944
sarcosine	0.372338	1.513666	-0.279715	-1.925033	-0.497649	0.327183	-0.511575	0.22319	-0.827075	-0.968288	-0.235198	-0.510051	1.7001	1.510262	0.107846
putrescine	-0.24557	-0.448543	-0.514854	-0.885535	-0.411763	-0.530669	-0.50901	-0.815915	-0.613538	2.149762	2.271953	-0.542234	0.435393	-0.145072	0.805597
spermidine	-0.179844	-0.726051	-0.620006	0.488612	-0.84073	-0.68261	-0.107517	-1.2202	0.187472	2.525776	1.741061	0.492909	-0.121893	-0.442427	-0.494554
spermine	-1.075626	-1.198411	0.998056	0.870454	-0.925665	-1.165564	0.207565	-1.23346	0.165872	2.131791	-0.045518	0.552344	-0.428439	0.296694	0.849907
creatine	0.351941	-0.211956	-1.630914	0.328385	-0.252801	0.001592	0.03343	-1.49583	-1.634869	1.79713	1.536153	0.616778	0.092792	0.226881	0.241287
N-acetyl spermine	-0.336551	-0.816313	-0.185408	0.246936	-0.807455	-0.361341	-0.307767	-0.86451	-0.013432	2.466249	2.168159	0.215775	-0.536878	-0.487789	-0.379676
N-acetyl spermidine	-0.136704	-0.921147	-0.50972	-0.480259	-0.570205	-0.36342	0.091646	-0.859154	0.02594	2.49186	2.090849	-0.697672	0.436422	-0.281522	-0.316915
N1-Methyl-2_2-pyridone-3_5-carboximide	0.209826	0.903622	-0.298737	-0.601197	1.526905	0.234761	0.519996	1.914811	0.355765	-1.384226	-1.482012	-1.00138	-0.4726	-0.849025	0.42349
N1-Methyl-2_4-pyridone-3_5-carboximide	-0.483216	-0.574649	-0.429904	-0.40031	-0.60046	0.938104	-0.489474	-0.619923	-0.457716	2.80149	1.591514	-0.374241	0.086677	-0.508712	-0.47918
Nicotinamide Riboside	-0.724186	0.353743	-0.648241	0.456594	0.905169	-0.782337	-0.733102	-0.918934	-0.68786	1.8971	1.528431	-0.568946	-0.745858	-0.760507	1.428934
Adenylosuccinate	0.197764	1.519052	-0.357098	-0.851296	1.244863	-0.236058	-0.287157	2.469032	-0.626053	-0.975099	-1.023094	-0.736391	0.064549	-0.197873	-0.205142
cholesterol	1.628954	0.035408	0.757053	1.12726	0.149277	1.039271	-0.170795	0.58907	-0.238556	-0.582007	-1.937631	-0.386542	-0.017368	-1.928439	-0.064955

SUPPLEMENTARY TABLE 1. T-TEST RESULTS.

	t.stat	p.value	#NAME?	FDR	Fold Change with respect to Wild-type
D-glucosamine-6-phosphate	10.614	8.97E-08	7.047	1.38E-05	4.7053
succinate	-10.176	1.47E-07	6.8332	1.38E-05	0.25503
Methylmalonic acid	-10.142	1.53E-07	6.816	1.38E-05	0.25573
alanine	-9.5125	3.20E-07	6.4944	2.18E-05	0.72356
glucose-1-phosphate	8.136	1.86E-06	5.7308	0.000101	2.2966
fructose-6-phosphate	8.0051	2.22E-06	5.6535	0.000101	3.735
D-erythrose-4-phosphate	7.6933	3.42E-06	5.4658	0.000133	2.6093
glucose-6-phosphate	7.1358	7.64E-06	5.1171	0.00026	3.8465
acetylphosphate	6.7383	1.39E-05	4.8579	0.000419	3.451
D-sedoheptulose-1-7-phosphate	6.4386	2.21E-05	4.6565	0.000515	1.8756
proline	6.4046	2.33E-05	4.6333	0.000515	1.8561
cystathionine	6.4015	2.34E-05	4.6312	0.000515	2.4378
D-glucosamine-1-phosphate	-6.3686	2.46E-05	4.6087	0.000515	0.60301
SBP	6.3164	2.67E-05	4.5728	0.00052	2.4239
hexose-phosphate	5.9288	4.99E-05	4.3015	0.000906	2.4318
sn-glycerol-3-phosphate	-5.8579	5.61E-05	4.2509	0.000954	0.39787
fructose-1,6-bisphosphate	5.5651	9.15E-05	4.0387	0.001464	4.5254
threonine	5.4697	0.000108	3.9684	0.001625	1.7303
malate	-5.2508	0.000157	3.8051	0.002243	0.54869
dimethylglycine	5.1179	0.000197	3.7045	0.002686	1.6855
lysine	5.0761	0.000212	3.6727	0.002752	2.43
2-keto-isovalerate	-4.9633	0.000259	3.5863	0.003078	0.76705
serine	-4.9611	0.00026	3.5846	0.003078	0.70543
dephospho-CoA-nega	4.6724	0.000436	3.3601	0.004933	3.2447
6-phospho-D-gluconate	4.6513	0.000453	3.3435	0.004933	4.3435
guanosine	4.6165	0.000483	3.316	0.005053	1.5122
NADP_posi	-4.5115	0.000585	3.2329	0.005892	0.57027
citrulline	4.4176	0.000695	3.1582	0.006749	1.3455
CTP-nega	4.3298	0.000817	3.0878	0.007027	4.4112
acadesine	4.3284	0.000819	3.0867	0.007027	1.8972
glyoxylate	-4.3242	0.000825	3.0833	0.007027	0.56157
ornithine	4.3074	0.000851	3.0698	0.007027	2.9203
S-ribosyl-L-homocysteine-nega	-4.3067	0.000853	3.0693	0.007027	0.62762
propionyl-CoA-posi	-4.2028	0.001034	2.9854	0.008274	0.43477
a-ketoglutarate	4.1459	0.00115	2.9393	0.008937	1.5662
dTMP	4.0933	0.001269	2.8965	0.009588	1.6296
UTP-nega	-3.9822	0.001564	2.8058	0.011495	0.55752
Indoleacrylic acid	3.8532	0.001996	2.7	0.013616	1.5643
glutathione-nega	-3.8462	0.002022	2.6942	0.013616	0.73341
2-deoxyglucose-6-phosphate	3.8294	0.002088	2.6804	0.013616	1.6604
3-phospho-serine	-3.8274	0.002095	2.6787	0.013616	0.60835
Phenylpropiolic acid	3.822	0.002117	2.6743	0.013616	1.4627
fumarate	-3.8133	0.002153	2.6671	0.013616	0.73379
guanosine 5-diphosphate,3-diphosphate	3.6447	0.002967	2.5277	0.018341	2.5147
putrescine	-3.5424	0.003609	2.4426	0.021813	0.41599
Ng,NG-dimethyl-L-arginine	3.5121	0.003824	2.4174	0.022614	2.2382
xanthine	3.4785	0.004079	2.3895	0.023605	1.3306
cholesterol	3.4619	0.004211	2.3757	0.023859	1.3149
Maleic acid	-3.4429	0.004367	2.3598	0.024241	0.76004
dihydroxy-acetone-phosphate	3.3694	0.00503	2.2984	0.027362	1.7218
cholesteryl sulfate	3.313	0.005606	2.2514	0.029638	2.7763
phenylpyruvate	3.2944	0.00581	2.2358	0.029638	2.4033
ribose-phosphate	3.2881	0.005881	2.2306	0.029638	1.4435
xanthosine	3.2815	0.005956	2.225	0.029638	1.6541
2-Hydroxy-2-methylbutanedioic acid	-3.2783	0.005993	2.2224	0.029638	0.71885
N1-Methyl-2_2-pyridone-3_5-carboximide	3.2656	0.006141	2.2117	0.02975	1.5805
D-glyceraldehdye-3-phosphate	3.2578	0.006234	2.2052	0.02975	1.6991
phosphoenolpyruvate	3.1606	0.007517	2.124	0.03525	2.5057

pyruvate	-3.1303	0.007968	2.0987	0.036732	0.71086
Pyroglutamic acid	3.1174	0.008169	2.0879	0.037031	1.8876
methylnicotinamide	3.0935	0.008553	2.0679	0.038136	1.4281
arginine	3.0732	0.008893	2.0509	0.038975	1.466
Imidazoleacetic acid	3.0655	0.009027	2.0444	0.038975	1.8355
leucine-isoleucine	3.0413	0.009456	2.0243	0.04019	1.4029
glutathione	-2.9783	0.010675	1.9716	0.044672	0.74152
creatine	-2.967	0.010909	1.9622	0.044959	0.47892
AMP	-2.9271	0.011778	1.9289	0.047817	0.72286
biotin	-2.9134	0.012092	1.9175	0.04833	0.55546
nicotinate	2.9062	0.01226	1.9115	0.04833	2.9146
OBP	2.8456	0.013773	1.861	0.05352	1.3879
Pyrophosphate	2.8314	0.014152	1.8492	0.054217	1.7528
2-hydroxygluterate	-2.7825	0.015543	1.8085	0.058718	0.8514
homocysteic acid	2.7626	0.016145	1.792	0.060156	1.6196
O8P-O1P	2.7075	0.017934	1.7463	0.065921	1.2672
Thiamine pyrophosphate	2.6968	0.018306	1.7374	0.06639	1.3478
FMN	-2.677	0.019009	1.721	0.068032	0.59108
CDP-choline	-2.6622	0.019554	1.7088	0.069075	0.64678
FAD	2.6523	0.019926	1.7006	0.069486	1.4878
uracil	2.6206	0.021163	1.6744	0.072863	2.2623
3-phosphoglycerate	2.5943	0.022246	1.6527	0.075637	2.9583
GMP	-2.5785	0.022921	1.6398	0.07697	0.82108
dGTP	-2.5459	0.024381	1.613	0.080872	0.74965
UMP	-2.5312	0.025066	1.6009	0.082144	0.73415
hypoxanthine	2.5177	0.025714	1.5898	0.082774	1.1749
inosine	-2.5146	0.025867	1.5873	0.082774	0.5485
Acetyllysine	2.5014	0.02652	1.5764	0.083878	1.4132
CDP-nega	-2.4364	0.029969	1.5233	0.093697	0.6711
2-oxobutanoate	-2.4242	0.030664	1.5134	0.094779	0.73572
citrate-isocitrate	-2.3877	0.03283	1.4837	0.10021	0.60868
glutamate	-2.3824	0.033157	1.4794	0.10021	0.6801
5-phosphoribosyl-1-pyrophosphate	-2.3686	0.034024	1.4682	0.10061	0.56668
2,3-Diphosphoglyceric acid	2.3641	0.034312	1.4645	0.10061	3.1795
homocysteine	2.3627	0.034401	1.4634	0.10061	1.3102
taurine	-2.3514	0.035137	1.4542	0.10167	0.66429
Acetylcarnitine DL	-2.3433	0.035669	1.4477	0.10213	0.65566
NADP_nega	-2.3217	0.03713	1.4303	0.1052	0.64732
2-Isopropylmalic acid	-2.2999	0.038668	1.4127	0.10768	0.60313
hydroxyproline	-2.2929	0.039174	1.407	0.10768	0.66867
Xanthurenic acid	-2.2926	0.039194	1.4068	0.10768	0.44059
phenylalanine	2.2695	0.040906	1.3882	0.11126	1.2551
carnitine	-2.2511	0.042319	1.3735	0.11397	0.68848
D-glucono--lactone-6-phosphate	2.2207	0.044758	1.3491	0.11763	1.8631
N-acetyl spermidine	-2.2207	0.044762	1.3491	0.11763	0.43676
thiamine	-2.2181	0.044976	1.347	0.11763	0.29626
spermidine	-2.2025	0.046282	1.3346	0.11989	0.65964
cysteine	-2.1845	0.04784	1.3202	0.12194	0.67508
N-acetyl-glucosamine	-2.183	0.047971	1.319	0.12194	0.81509
valine	2.1727	0.048886	1.3108	0.12202	1.4232
ATP-nega	-2.1691	0.049209	1.308	0.12202	0.76463
D-glucarate	-2.1676	0.049345	1.3068	0.12202	0.45083

SUPPLEMENTARY TABLE 2. ORIGINAL DATA.

Label	MUT	MUT	MUT	MUT	MUT	MUT	MUT	WT	WT	WT	WT	WT	WT	WT
glyoxylate	119035	80264.45	77641.08	92245.72	58246.93	74646.64	78210.51	108960.4	100897.3	78069.37	72080.94	98815.02	111500.5	91878.49
glycolate	272544.9	169907	242858.6	68040.34	55383.94	171697.6	70788.01	57563.05	224162.3	84820.04	186285.4	287603.3	277290.1	35435.59
pyruvate	19468.4	24382.37	43315.93	35640.96	38923.29	40116.13	73009.04	45678.01	33553.66	36797.94	44209.72	34974.32	54764.17	37561.1
lactate	57251351	63683682	68006748	62928972	56457970	56711516	61103747	59045028	56115292	57771916	49464989	59369250	58364688	46773345
2-oxobutanoate	639439.9	635164.2	600812.7	649710.4	605700.3	793086	562666.7	515495.4	538281.7	558128.7	554856.5	540420.9	548334.7	490989.4
acetoacetate	620474.3	681780.2	634793.9	551250.6	558467.7	653392.5	596762.6	506247.4	459590.8	586768.5	391234.2	565570	541890.6	555912.4
glycerate	389177	254719.5	233716.8	329454.9	324268.5	240491.4	230641.2	412264.3	391411.7	373869.3	330588.1	346646.4	453258.3	250612.7
uracil	541829.1	599485.3	733342.3	671453.4	591034.9	469209.6	610392.2	306757	468013.8	429875.3	476262	316564.3	433842.3	366534.7
fumarate	7259592	7466704	7245278	6919799	6978921	6951783	6706929	7107820	8115434	8103464	8121352	8688543	8370911	8405213
Maleic acid	6946223	6931403	7856592	6914395	6485134	7348242	6488165	7626877	8343229	7764344	7730685	8587693	7091001	7886364
2-keto-isovalerate	6789768	7581922	7941130	6633488	6893442	6838389	6759958	7739500	7784259	7607435	7096167	7745077	8411784	8063759
Guanidoacetic acid	18384.85	N/A	N/A	N/A	N/A	7321.485	10900.96	N/A	4201.209	N/A	N/A	N/A	6398.429	7069.308
succinate	8526298	8646430	8835118	8438479	9441728	8038577	8083296	9332330	9071454	10281068	11044511	9843521	11592116	10879175
Methylmalonic acid	9640383	9583414	11186539	10270596	10415077	8217116	9235525	11974760	11738669	11322659	12655001	11118111	13270568	12659081
3-S-methylthiopropionate	2475.059	6950.589	4949.552	9089.346	3280.311	4246.491	N/A	7423.083	6527.041	6264.857	4808.895	7452.622	N/A	4130.068
nicotinate	763883.8	856052	497607.5	687983.9	587825.9	35442.78	513032.3	24292.18	1119458	514764	774646.8	729273.1	755556.6	430075.6
taurine	1.8E+08	1.8E+08	1.84E+08	1.82E+08	1.85E+08	1.77E+08	1.8E+08	1.77E+08	1.78E+08	1.84E+08	1.77E+08	1.84E+08	1.88E+08	1.82E+08
Pyroglutamic acid	340366.4	369240.5	327941	394008.7	280885.7	261513.4	297222.7	253607.6	706662	286688.7	835915.2	323975.6	981845	264123.7
Citraconic acid/itaconic acid	2413012	2242816	1585361	1780745	1552720	2350601	1642633	1724236	2619726	2226416	2248741	1672228	2023735	1644710
2-ketohaxanoic acid	196638.2	205736.5	174000.4	172700.4	164572	141950.6	146643.7	178975.2	164273.8	146429.3	172042.5	182880.8	162072.2	201498.9
N-Acetyl-L-alanine	1.09E+08	1.02E+08	1.06E+08	1.01E+08	97328128	97451048	89899548	1.03E+08	95235192	1.08E+08	87855904	1.08E+08	1.03E+08	1.02E+08
oxaloacetate	289200	265099.4	301104.3	761476.5	284342	618957.3	814819.5	115985.6	77370.32	119987.4	84152.57	87693.77	80788.11	859324.8
Hydroxyisocaproic acid	N/A	139992.5	N/A	28913.23	20627.44	46242.28	32202.48	60674.23	N/A	18337.5	N/A	17774.31	41368.31	N/A
malate	28647820	34200065	30025270	26537905	27057573	30109487	26407520	32714370	37100412	37380656	32333535	35868541	35124166	41080716
hypoxanthine	2170707	1278340	2245757	1954778	2743293	1468912	2152595	1509181	2421726	2038658	1802252	1412474	1611310	1506594
anthranilate	21147.62	21466.47	8488.885	56413.2	11513.26	3922.193	15117.19	39304.88	3358.991	22754.01	14611.36	17832.63	55182.34	19666.36
p-aminobenzoate	43778.46	36560.38	63217.11	4409.741	17663.48	9503.135	17549.59	21859.49	33318.35	24527.46	37721.93	5396.297	22674.44	6449.536
p-hydroxybenzoate	258844.8	393048.5	288852.7	412837.2	1321065	367524.6	356297.9	814265.7	312160	372993.6	369997.1	522215.8	341111.3	455585.5
acetylphosphate	145624.5	104543.6	114112.3	230472.8	126213.4	80886.1	168646.2	85832.8	99864.27	115406.9	162304.8	93059.28	92098.15	95204.53
Carbamoyl phosphate	1.61E+08	1.63E+08	1.6E+08	1.82E+08	1.38E+08	1.44E+08	1.5E+08	1.45E+08	1.52E+08	1.58E+08	1.21E+08	1.63E+08	1.36E+08	1.43E+08
a-ketoglutarate	5413332	5611739	4551503	5136688	5008744	3764780	6970041	3607990	3940080	3654828	4029749	5019823	3643013	3673606
Phenylpropiolic acid	407605	586710.3	372898.9	360302.6	285584.4	245461.6	291875.3	451959.6	301851.1	401091.8	326875.5	443811.3	353026.7	434688.7
2-oxo-4-methylthiobutanoate	40876.38	64449.91	46073.76	30659.46	48326.09	15481.68	43664.22	61436.79	59855.66	61225.83	73514.4	45845.52	44897.73	57135.37
2-Hydroxy-2-methylbutanedioic acid	1561083	1191908	1464770	1141068	1396129	1263649	1202337	1125531	1287986	1369590	1335052	1040305	1368145	1688449
3-methylphenylacetic acid	36772.8	18768.05	27891.2	32119.26	28734.51	37408.51	19928.82	7739.572	38252.23	38637.47	18703.54	30416.98	25171.14	20226.98
xanthine	4392.154	1301225	1371742	1493903	1578929	1510081	1543956	1505816	1977470	1620718	1701617	1620123	2120570	1656247
Hydroxyphenylacetic acid	78954.83	430593.9	34655.2	32232.01	349211.7	725537.5	22189.45	490904.1	468048.6	67115.49	469095.7	49674.44	65273.21	39825.5
2,3-dihydroxybenzoic acid	194558.8	112836.4	71827.14	73108.58	74403.17	57022.97	70461.59	58469.41	73374.81	110058.8	73769.97	78685.34	121051.4	65968.75
orotate	243670.2	294016.7	216049.7	223528.8	122854.4	176533.2	213671.4	211372.1	219014.3	312890.9	228052.2	195790.7	202839.4	206278.7
dihydroorotate	495145.3	487504.8	424387	462385.7	434672.4	328028.4	519728.6	514697.5	472314.8	462232	545327.9	574867.2	483088.8	539375.7
allantoin	790331.5	712047.7	594253.5	697876	503730	680807.7	541736.2	838571.4	763106.2	713027.8	765297.8	728324.7	642406	1074151
Aminoadipic acid	313677.3	202837.2	314464.7	272050	269775.6	305100.2	240201.1	198045.8	173930.6	274290.6	146216.1	208652.3	215586.1	278137.8
Indole-3-carboxylic acid	204281.8	176270.8	339998.4	277823.1	198940.4	341377.9	173413.6	182516.5	151000.3	199871	167556.6	158367.1	210616.1	288084.4
phenylpyruvate	4904.066	7412.044	N/A	N/A	10690.44	5782.308	5779.389	6345.47	4117.828	N/A	N/A	8058.213	6581.569	N/A
Atrolactic acid	14862.21	22299.06	28826.29	28361.86	24051.56	8721.379	20187.95	20605.29	7220.513	9941.19	17326.14	42052.56	14111.69	9330.241
Phenyllactic acid	113876.2	175857.5	147797.7	84357.07	111410.3	80932.91	178405.9	92497.76	78331.12	43845.91	78450.74	117140.5	68618.58	81736.26
quinolinate	70984.02	50535.96	74106.01	86291.65	119034.8	86400.99	73205.15	57625.51	66912.97	31898.82	17473.18	83973.94	47222.23	68035.12
phosphoenolpyruvate	258412.4	364354.2	288105.3	511147.6	508647.7	315448.9	432542.3	237944.8	249147.4	218932.2	153529.2	240241.6	195060.6	309391.4
Uric acid	50323.68	93755.18	55033.33	56016.99	42664.22	36846.81	78129.32	49054.24	37227.78	53643.41	34767.81	60269.68	52695.5	61286.51
dihydroxy-acetone-phosphate	1242429	908065.6	999485	1027941	938731.7	1004479	787459.1	1155583	772225.4	553944.7	574032.3	875046.6	698446.6	684223.6
D-glyceraldehdye-3-phosphate	272342.6	350431.1	430640.3	410045.6	352867.3	451684.5	404872.6	303451.4	222062.2	267621.6	175251.3	239776.9	204603.1	244250.2
sn-glycerol-3-phosphate	11611829	10772640	13273058	13250404	13208011	11848762	12795323	11584570	9197907	11045577	11878188	12272446	11787969	10253893
shikimate	17347.23	37160.54	26410.78	50380.21	94975.81	241997.9	44597.17	35512.15	25566.8	317957.7	954673.1	199650.5	61987.2	186598
aconitate	662729.9	708817.6	576885.7	617072.5	590546.7	462189.2	497098.6	516578	597275.2	656147.9	505213.6	595353.7	509992.5	610338.7
allantoate	149446.8	124529.2	143670.4	158495.6	146982.9	130395.6	159170.9	146958.7	162529.1	181677.2	158560.3	147815.9	160167.4	107204.4
Ascorbic acid	6123658	8949676	9012124	7589803	6694338	2313227	7962040	24793630	19085936	12052990	12809135	13252151	8916036	11896363
2-Isopropylmalic acid	17838392	24781545	23321907	22097262	18823992	10349246	20330247	53582044	43710897	31955420	31694723	33077799	25436900	27467216
N-carbamoyl-L-aspartate-nega	127180.8	137124.7	155244.8	171802.4	116432	126708.5	147819.9	108466.3	123068.1	122066.4	96632.7	140374.7	124706.1	100768.8
Pyrophosphate	864102.7	844189.5	966058	1098173	837504.1	896744.2	729721.1	1589941	1330691	962713.3	1346721	716020.1	980522.6	936948.4
glucono-?-lactone	6605.657	4056.417	9085.336	6608.316	4951.874	2421.176	3303.956	13203.59	6605.283	6110.881	2429.494	6471.21	8260.297	6605.25
myo-inositol	38939755	28222476	35629544	38003053	29058294	36964373	28081495	44620391	34191733	45015809	42107244	36557643	43585859	45768254
hydroxyphenylpyruvate	N/A	10991.04	11549.4	10766.94	9072.073	12357.82	5767.95	4019.645	N/A	N/A	9355.023	N/A	9900.561	11538.38
homocysteic acid	290903.5	217920.8	222064.1	213098.3	199821.7	232799.5	199143.4	144204.5	236155.5	239878.8	220922.6	216310.6	248020.3	199852.1
4-Pyridoxic acid	168632.9	36911.78	29054.53	19340.7	8918.276	49039.2	41206.19	10675.36	48435.45	17620.41	15584.95	44720.65	240325.8	30934.01
3-phosphoglycerate	3229192	2784200	3483493	4127267	2981502	4214612	3857934	2403089	2339576	2248682	1629628	3214390	1806712	2924951
Indoleacrylic acid	112473.2	157277.5	123100.1	73957.09	90216.15	72132.72	146406	87596.92	80666.28	80839.23	63740.51	76692.7	80731.26	64426.65
Kynurenic acid	972183.5	835481.4	1006785	844775.7	837831.5	767010.3	889682	823087.2	768930.5	727049.3	902681.3	871893.1	894623.7	705575.9
citrate-isocitrate	62652268	51009572	60226884	62987541	55767768	64060516	55514117	56625510	48672345	76375801	72285228	51879917	55846827	64133544
isocitrate	83614.26	194763.7	134007.3	124170	143328.5	148979.6	104308.4	141751.9	159473.4	99848.57	109622.7	112728.1	126624.2	124712.3
citrate	35316460	25409848	27658697	30516582	27998195	26621458	25474624	30606279	32043899	39792965	29588711	27464739	27922530	29605840
2-dehydro-D-gluconate	23906.27	29736.65	18100.15	22437.08	20465.14	27462.19	16365.44	32061.31	17482.2	17465.49	6591.549	36303.01	25568.26	19856.27
D-gluconate	191733	215577.8	207410	187454.5	170089.6	209003.7	202336.4	249392.5	208936.9	203596.9	231091.2	219660.8	227603.2	228688.4
D-erythrose-4-phosphate	145496.8	194165.1	164018.9	170706.8	160870.7	129926.3	179308.4	127244.9	124275.8	150159.4	115591.9	165259.6	133651.4	196197.1
Xanthurenic acid	220113.2	278778.4	186624	216617.8	169335.6	190029.4	243724.4	457328.7	165102.7	200137.6	165318.3	197360.2	164055.6	164691
lipoate	N/A	N/A	N/A	N/A	N/A	4130.192	N/A	5782.708	N/A	N/A	N/A	N/A	N/A	N/A
D-glucarate	79128.9	103173.7	72732.11	87232.08	76700.94	59783.23	79156.6	105586.8	110634.5	98580.02	62870.31	66503.07	60021.55	75557.45
deoxyribose-phosphate	66285.13	57802.24	71034.59	44550.79	91698.19	95582.36	53176.59	58299.02	49645.35	81949.49	59330.88	51904.18	55662.99	44014.6
pantothenate	17423976	15057966	17351081	15646882	11205771	13016135	15297174	14114441	15260395	16758285	10691751	16833749	15355400	16028818
prephenate	N/A	N/A	N/A	N/A	N/A	N/A	N/A	N/A	N/A	N/A	N/A	N/A	N/A	N/A
deoxyuridine	4896.574	9083.328	N/A	N/A	5732.851	N/A	N/A	N/A	N/A	4102.671	N/A	N/A	N/A	N/A
ribose-phosphate	813773.2	752326.8	843096.3	821533.4	854810.7	664198.7	879942.3	806156.9	937529.7	873632.3	888138.4	683719.7	728435.9	512103.9
thymidine	40776.17	5064.082	40439.18	24718.05	20933.06	37754.55	19852.25	N/A	N/A	3247.828	N/A	22406.67	27191.34	48860.28
uridine	543460.9	843999.6	720153.2	915064.4	1058421	558665.9	765555.5	699661	973937	811059.3	767680	648299.8	820929.3	475171.2
deoxyinosine	15735.43	21515.28	15693.31	18874.83	31387.62	13278.18	18304.45	14843.57	16132.33	14053.99	26250.19	12377.76	14761.48	7444.63
shikimate-3-phosphate	N/A	N/A	N/A	N/A	N/A	N/A	N/A	N/A	N/A	N/A	N/A	N/A	N/A	N/A
D-glucono-?-lactone-6-phosphate	25767.44	14916.12	20499.74	18369.82	30752.61	27863.74	9399.841	17266.17	19066.34	25947.67	15875.18	34739.81	29908.91	18582.53
hexose-phosphate	16572710	16937409	18950981	17629709	18482447	16464248	20776290	15750348	18552656	17335694	18692106	19539826	16115209	15062597
glucose-1-phosphate	1039315	1235461	1147191	1178075	868763.6	904932.2	1082413	739410.8	681760.8	866222.9	655986.3	1111620	883266.3	880692.8
glucose-6-phosphate	462318.4	470612.4	492250.4	410777.8	342213.3	426033	557187.4	214256	234987.2	257514.9	278423.5	287242.2	264562.4	496300.1
fructose-6-phosphate	429900.4	495415.2	423744.1	439145.9	482158.8	521791.6	554142	286350.9	263128	255376	276241.3	357870.5	262376.4	361399.1
1,3-diphopshateglycerate	N/A	700632.1	361868.6	538890.3	515163.5	548243.3	495221.6	436160.2	N/A	371172.6	561272.3	337023.6	236602.2	590219.1
2,3-Diphosphoglyceric acid	1006715	1002627	422082.6	918912	507856.7	799148	568346.1	598296.7	576717.6	528050.2	717357.4	504270.5	632712.4	677530.8
S-ribosyl-L-homocysteine-nega	17339.91	7027.724	30779.88	45420.25	19783.72	31173.1	26379.78	30476.2	29721.61	10433.17	24353.88	21336.35	24236.95	19000.23
inosine	15422866	20100374	12110821	25722787	22641492	14889826	20139440	13758485	25984607	19373205	19220658	11600927	14922029	14372779
6-phospho-D-gluconate	113617.9	86724.75	82568.84	97547.01	110672.9	107276.7	72209.34	109032.6	61431.58	98508.84	96050.22	105523.5	114804.1	138370.4
xanthosine	54389.15	67620.64	67512.61	78202.75	53369.39	60559.91	72617.89	59224.37	74058.45	27548.34	98822.68	29291.94	87320.11	79766.98

D-sedoheptulose-1-7-phosphate	1442115	1385121	1761912	1479952	1316866	1175715	1631158	965135.5	752061	994873.8	857088.6	1175204	903724.9	1606281	
N-acetyl-glucosamine-1-phosphate	614091.6	557711	705135.1	582944.5	523903.3	553206.2	559064.3	634711.4	547852	666131	588663.2	779938.3	673745.6	615508.5	
glutathione-nega	882517.5	762310.2	801127.7	871549	710673.8	781470.5	809406	2130924	1275801	1533977	1134198	1253418	1155197	1174483	
dUMP-nega	11371.24	6567.706	5542.988	4131.321	N/A	3263.98	6901.994	N/A	N/A	14066.01	3981.994	3281.211	6601.933	5730.672	
Geranyl-PP	40525.86	51542.84	55568.36	28522.21	22405.09	51625.14	32673.76	29963.17	26682.42	31592.68	47088.38	54755.77	48405.32	37472.55	
O8P-O1P	658957.4	684392.6	729663.8	654560.8	625388.4	522652.5	705673.2	650237.3	552132.8	587028.2	563314.8	576602.4	610149.8	664251.8	
dTMP-nega	17349.06	13190.25	17387.99	9085.534	9911.864	10823.31	18966.9	12355.6	11572.5	16321.36	2451.485	22283.61	2477.686	8250.246	
cyclic-AMP	3915252	4335782	5847622	4326262	4524093	3225457	3714351	3594826	3132844	3296735	3790499	3203125	4843630	2832521	
fructose-1,6-bisphosphate	12782656	14731676	14556219	9086655	16588323	11405479	15026527	10100775	9602990	4196875	7676712	5683706	8465435	12415217	
trehalose-sucrose	34693.67	49448.73	36858.44	32038.58	23774.09	40667.79	36376.55	75637.5	51197.2	37194.54	35466.59	43774.48	32956.13	39394.52	
Cellobiose	N/A	9899.675	N/A	N/A	N/A	N/A	N/A	N/A	N/A	N/A	N/A	N/A	N/A	N/A	
orotidine-5-phosphate	68737.32	47874.19	67687.14	52669.9	55659.47	78711.94	55762.58	7968.486	45646.28	55542.27	26361.15	55414.07	38043.51	43584.59	
SBP	667736.5	556278.3	624476.3	810123.2	801571.9	673860.7	750342.6	375036.5	745339.9	324057	262299.8	335427.2	254789.9	702875.2	
trans, trans-farnesyl diphosphate	9898.826	17382.63	13237.08	10681.62	21403.41	24418.03	23702.44	16424.01	12485.38	8132.918	27949.77	4610.199	16841.07	16734.84	
S-adenosyl-L-homocysteine-nega	3598429	4704223	5817032	4511111	4343302	4302163	3991080	5830836	5100693	5510683	5091883	6383358	6295451	4121257	
dCDP-nega	28897.83	22402.12	30426.14	33834.46	46249.08	39641.29	28078.77	39438.09	49553.08	52063.14	34672.71	33861.23	39637.61	42116.44	
5-phosphoribosyl-1-pyrophosphate	30566.19	57260.76	20669.58	38769.97	22950.61	17552.66	40424.64	59746.59	55000.96	17802.61	24035.32	16381.91	54596.63	14537.68	
Deoxycholic acid	N/A	N/A	N/A	N/A	N/A	N/A	N/A	N/A	N/A	N/A	N/A	N/A	N/A	N/A	
OBP	41298.42	27741.28	35607.67	35947.47	53462.28	30763.96	39496.87	61600.76	23027.83	16292.29	34668.55	32167.42	41765.38	15811.35	
dTDP-nega	36389.63	30611.99	37176.78	34685.52	38814.3	37163.96	39664.54	46278.58	58761.97	47924.08	38804.37	24604.66	49852.5	37707.45	
CDP-nega	549741.6	519868.1	428737.3	501131.9	580259.6	676116.2	633289.9	619254.4	551694.2	438916.1	462721	374211	471140.5	445276.3	
UDP-nega	6272473	6018011	4593586	4612817	6141346	5362472	4997868	6474884	5486770	5961023	4531244	5189418	4521146	4863144	
Cholic acid	N/A	5760.434	N/A	N/A	3304.418	2478.611	N/A	3326.722	2481.564	N/A	2625.778	4130.103	N/A	N/A	
trehalose-6-Phosphate	210222.3	145053.6	204406.5	136290.1	106120.9	144087.1	162175.2	216309.4	138498.4	160611.8	115346	320868.8	227439.8	318053.2	
Thiamine pyrophosphate	8692.747	36264.7	16481.36	30556.24	23119.83	29709.86	14010.68	35751.92	35477.79	20309.84	30556.31	10456.32	11535.7	22475.4	
adenosine 5-phosphosulfate	327673.3	283965.6	241627.9	276617.9	296615.4	287439.1	292211.9	347501.3	267879.7	246081.8	225473.2	293015.8	291471.1	289735.2	
ADP-nega	30177664	29438242	23452001	25347979	30757791	29228226	28333717	29930530	30245889	28380564	23907084	25714198	32797135	24167505	
dGDP-nega	31932294	30562879	23535954	25203024	27097154	27912664	30917747	34695893	27726435	26687250	23814201	26633234	27345677	24609673	
IDP-nega	3995032	3834214	2891834	3262733	3848624	3941392	3706544	4501334	3650831	3853680	2948646	3269420	3508037	2944465	
GDP-nega	717578	910009.9	599460.4	721861.4	784639.9	510740.4	666734.6	1978135	974175	403291.3	853693.6	591649.3	696917.1	571471.6	
CDP-ethanolamine	253544.8	374088.3	429447.9	332795.1	296613.4	289046.3	298871.4	370819.4	319590.7	363373.8	270886.5	275021.4	348514.7	249394.5	
FMN	N/A	9083.452	8256.037	7432.692	5782.189	5782.829	4130.142	4957.132	7467.354	N/A	14839.99	7426.44	N/A	N/A	
cholesteryl sulfate	71069.58	33100.76	75102.86	232920.2	459180.2	227934.2	23975.16	86117.36	103231.9	81915.96	407144.3	61092.91	75159.76	859687.3	
dCTP-nega	22298.38	50376.75	28886.14	27240.52	37170.82	47044	42948.9	52028.18	25594.49	17339.41	33849.48	35512.15	33084.52	27251.44	
dUTP-nega	3302.669	15690.62	N/A	6605.369	5782.759	2475.589	N/A	6607.976	N/A	N/A	3302.705	N/A	4103.591	N/A	
dTTP-nega	58644.28	45889.51	31315.74	46915.89	33059.59	23516.11	32811.82	23982.16	24745	14139.73	19503.85	13352	28111.79	31763.56	
CTP-nega	354773.2	502122.4	323713.5	441320.9	705408.1	377720.5	362553.2	546749.7	378126.7	166242	383656.4	267807.9	367265.5	432333.7	
UTP-nega	4529963	6712557	3864449	4419630	6454977	4808278	4681047	6568241	4358026	2456664	4279998	4064354	4297532	5409540	
CDP-choline	665648.7	701151.3	734186.8	777914.1	664824.4	607834.8	687118	610331	607026	655737.7	659844.4	657373	671388.1	466627.2	
dATP-nega	14038.69	23085.46	17343.13	21470.83	12387.93	11561.47	23948.58	14040.82	18993.52	9082.934	18995.94	7433.105	9966.253	8256.36	
Taurodeoxycholic acid	24818.36	19282.35	19670.84	31594.6	23854.58	8234.043	25769.26	17977.38	16418.19	27422.92	21176.43	28679.75	18285.96	24072.79	
ATP-nega	35283629	43157074	26898655	34674417	44041938	35847793	34202990	40015333	31452426	21087720	27523066	25677256	30395336	36132580	
dGTP	35206507	43957353	27689842	32420483	44388805	36758175	36861205	38074408	30024591	20015130	27776119	27892501	28786042	35792206	
GTP-nega	1022070	2298184	710108.3	953095.3	1911797	1072715	976460	2002052	1696178	578907.6	1278569	706878.9	971404.5	1068033	
UDP-D-glucose	3297148	2865064	2271968	2205075	2723726	2267843	2048070	3315103	3000641	1596391	2523927	1867471	2312905	2079555	
UDP-D-glucuronate	109837.8	146178.8	61943.22	79284.61	139569.1	128012.4	84236.48	190773.3	206472.4	48723.98	133794.4	61939.52	105708.2	134615.2	
ADP-D-glucose	156060.7	102406.7	152758.2	165176.7	115605.1	125533.4	124721.9	113130.1	131310.9	105701.5	138713.1	121274.7	149482.9	90866.95	
guanosine 5-diphosphate,3-diphosphate	11581.9	9899.739	17345.64	14874.94	5985.802	22298.72	10735.4	30550.04	8255.303	2486.924	16742.58	12413.9	21349.9	13291.26	
UDP-N-acetyl-glucosamine	2298378	2309811	2224890	2082054	2068799	2389253	1927557	1969715	2047136	2406534	1866481	2178155	2206711	2057220	
glutathione disulfide-nega	29141734	27534912	29520433	29348008	26746097	28930496	25938788	30116857	28877813	39196729	28647818	35274846	38131089	30619895	
NAD+_nega	6381818	7736175	6422969	6474289	7338524	6767407	6976875	8306392	7343074	8282746	7540299	6857419	8101547	6110701	
NADH-nega	326214.9	343554	382185.2	335306	355136.6	323737.5	285754.5	324558.9	275016.1	267477.5	355913.4	336955.9	440188.7	341070.4	
dephospho-CoA-nega	265979.4	238536.4	221012.7	233428.1	237024.5	216048.5	228767.5	155882.3	205648.2	202874.3	206469.5	180138.3	175726.1	185772.4	
cyclic bis(3->5) dimeric GMP	N/A	N/A	N/A	N/A	N/A	N/A	N/A	N/A	N/A	N/A	N/A	N/A	N/A	N/A	
NADP+_nega	355206.2	378920.6	184602	268304.8	386379.1	278788.9	274882.2	423083	406991.5	266165.4	385680.9	274668.1	317404.6	273063.4	
NADPH-nega	56158.99	47899.67	43771.97	47077.84	45434.4	37151.69	42116.43	53679.53	47072.37	33904.29	35546.85	28903.59	53677.92	50377.37	
2-hydroxygluterate	6513959	5692584	6957528	6744832	6997579	6348039	5330285	6315283	6205677	6760688	6119729	6327397	7194319	6875593	
2-deoxyglucose-6-phosphate	29516.34	37900.63	26876.62	N/A	19712.4	22102.45	34053.97	23298.88	32964.4	38100.41	N/A	23335.52	30465.03	22434.73	
4-phosphopantothenate	15719.28	12343.51	8246.133	14023.61	15685.06	8262.319	4127.544	11560.14	9961.017	19820.75	13184.28	15652.51	24773.47	11388.93	
dehydroascorbic acid	N/A	6774.51	N/A	N/A	N/A	61957.49	N/A	N/A	N/A	N/A	6565.249	N/A	9936.897	N/A	
3-hydroxybuterate	1855700	1548822	178697.7	244054.7	188579.8	207654.3	1548872	130098.7	169050.5	200804.9	154767.1	216472.9	183509.6	233672.7	
itaconic acid	2413012	2242816	1585361	1780745	1552720	2350601	1642633	1724236	2619726	2226416	2248741	1672228	2023735	1644710	
Urea	9112829	7167421	6095490	7781555	8672373	7101836	6382251	6076805	5425114	6517226	7188222	9496258	7843994	5414531	
ethanolamine	6863.492	15382.04	7646.642	9283.844	8286.183	18735.19	N/A	9091.868	N/A	N/A	N/A	9510.162	9024.828	9089.661	
glycine	N/A	N/A	N/A	5780.274	4130.542	N/A	N/A	N/A	N/A	N/A	N/A	N/A	N/A	N/A	
alanine	20808131	19248466	22216484	20957839	20036504	19807336	18217238	23434890	23552782	23073371	23353465	22462103	23755067	25641781	
betaine aldehyde	122878.9	160897.1	110747.3	149166.2	125993.6	157420.9	134303.2	149946.2	156915.7	145425.7	135536	139569.6	173222.5	117250.7	
choline	4276066	3524904	6116561	6938000	6714295	7163590	4529426	755616.2	5736529	5183183	2838227	4997177	5350629	8985785	
4-aminobutyrate	8854638	8044110	7890275	8852711	10124475	8552609	8392577	9368116	8509878	8764849	9514647	7359954	8932608	8801822	
dimethylglycine	2137564	1880805	2000277	2119135	1694939	1556959	1394695	1613610	1559761	1890302	1464016	1004133	1682624	1910804	
serine	7547890	6727767	7074497	8826373	7257698	7254069	6043748	10582347	10430984	9148213	10077701	7110053	10388095	7201461	
cytosine	112635.6	101768.5	57846.27	87017.39	48442.91	56863.11	112026.4	59282.97	58189.4	73623.67	45618.68	90336.71	44794.28	38339.27	
Creatinine	3758734	3313460	4039445	4113978	2904701	3425666	2689233	3890770	3503403	3800337	3642394	3863993	3856437	3858966	
proline	28174272	37953801	23861325	35903177	33366033	22355361	38156610	13720263	15357942	14776561	14981286	16364540	15099509	11278951	
indole	31500.51	99482.14	68118.26	51261.88	34099.36	75225.1	65751.15	53997.63	21988.23	37715.83	22926.61	50254.24	37368.55	40836.35	
betaine	49416615	51892001	61099786	44354163	39152503	53110531	56858655	49984034	50519554	59778263	43786585	60147535	52538643	54895546	
valine	465785.6	475751.9	367498.6	404162.4	395971.8	325946.1	458001.2	214874.1	161491.6	253848.2	217393.1	214852.7	202276.3	181919.3	
threonine	12748839	14390432	13610919	15733597	13602232	11338747	16789877	7558807	6407151	8168996	7227747	6887309	8213455	7466207	
homoserine	55333.16	47905.14	57812.72	36217.67	75978.68	42962.94	60169.19	85068.52	62780.77	70198.49	62765.36	63593.32	56982.23	66066.88	
purine	71414.56	72720.8	77289.05	61617.25	74941.75	51748.8	108186.3	47198.21	28572.84	36914.94	39236.95	75326.56	48215.95	75147.62	
cysteine	7365.536	11490.92	7054.239	6752.825	13510.82	16941.62	6273.405	11143.17	10582.92	12949.41	12401.3	N/A	8768.99	9982.822	
creatine	2.37E+08	2.15E+08	2.32E+08	2.33E+08	2.28E+08	2.16E+08	2.17E+08	2.21E+08	2.28E+08	2.2E+08	2.31E+08	2.27E+08	2.44E+08	2.22E+08	
nicotinamide	41872198	27026854	37204290	30555233	28906787	28990940	29924291	24092731	24780673	33271071	27677189	22335931	27808713	20766143	
Imidazoleacetic acid	33417.28	27895.13	45624.65	25251.97	25437.2	53119.43	31087.47	44386.6	25041.78	26021.71	11467.54	46752.56	N/A	57428.25	
thymine	205361.4	177554.1	152664.6	195827.9	200655.4	198915.3	148249.3	157329.3	182607.8	191057.7	201060.4	243761.8	218865.5	168775.2	
DL-Pipecolic acid	58688489	48204223	59783135	55524864	46955867	57902593	46880693	57417156	46325352	54641404	46374823	50893076	51435047	47178998	
N-Acetylputrescine	16144.66	N/A	N/A	29279.08	21878.66	13089.02	11408.49	20716.82	7867.24	10912.72	16053.81	15030.31	8100.218	21634.05	
hydroxyproline	1309832	944010.5	1091525	879576.7	1059138	912933.2	965334.6	2229144	1957350	1537874	1458426	748280.4	1361094	1971689	
leucine-isoleucine	13824538	12358583	10924476	10185309	9763525	9618804	10269163	4007108	3878180	6561618	5461332	5866784	6804037	7079129	
ornithine	46293.4	380950.6	64746.02	64385.9	502148.1	6638.501	202756.6	17661.3	8901.644	119315.1	251350.8	47163.79	24828.52	156600.9	
asparagine	2344138	2466239	2569165	1831280	2046827	2093166	2191214	1756694	1414630	2115000	1440196	1595158	1327210	1375172	
aspartate	22074158	16550116	20677588	19595727	21941518	21124257	18896530	19035295	16403443	19768646	20312634	23236764	19032840	13711708	
adenine	861985.4	1283303	863152	889301.9	660568.5	754285.1	1107498	581741.9	502386.2	737223.7	607081.2	741714.5	683113.1	357669.5	
Methylcysteine	861985.4	1283303	863152	889301.9	660568.5	754285.1	1107498	581741.9	502386.2	737223.7	607081.2	741714.5	683113.1	357669.5	
homocysteine	123987.8	113596.2	121004.4	83596.96	108393.8	86236.12	146611.6	75970.08	92566.22	79468.06	56917.73	89035.81	97639.24	42284.02	
methylnicotinamide	22410.53	38109.75	56730.38	22354.13	37641.94	126484.6	27950.97	8930.099	32193.76	18096.49	30041.43	36309.88	17373.34	43970.92	
histidinol	N/A	N/A	N/A	N/A	N/A	N/A	N/A	N/A	N/A	N/A	N/A	5782.717	N/A	N/A	
lysine	2066001	1377384	1434641	1332990	1393719	1070710	1261985	368219.2	789353.2	1091580	951826.2	755801	1201614	1063996	
glutamine	91890043	96856905	90409982	88397378	93641436	87605526	1.02E+08	76633333	60996721	59299780	70616987	98652973	67251209	75135466	

O-acetyl-L-serine	N/A	4092.218	N/A	N/A	3352.605	10070.01	N/A	5031.643	6607.728	N/A	N/A	4974.955	5847.754	N/A	
glutamate	1.03E+08	1.01E+08	97041279	1.14E+08	1E+08	1.14E+08	96044145	1.05E+08	99608497	97205637	96281295	95993736	1.02E+08	93048954	
methionine	3129815	3780892	3100862	4367304	2828376	2409896	3480548	1998020	1517187	1301621	1706207	2248485	1761935	1005237	
guanine	147143.7	155769.3	148046	187425.7	223094	149856.1	180687.8	195040.7	228008.5	136288.3	194541.1	137961.9	139976	154227.9	
histidine	11343716	14664514	12790150	11114699	11247971	10732916	16379596	8919111	8494613	8056335	8255870	10680661	8058130	8119208	
2-Aminooctanoic acid	9151564	7054035	16672492	15015368	12161820	11624026	19993082	15035740	13004439	8696065	8832657	11669442	16634514	27939382	
carnitine	35108609	35958089	34533730	36115638	35570240	38783714	31375509	36887144	40903014	40215800	41135441	42565754	41673440	33941176	
Methionine sulfoxide	324543.6	371645.1	381199.4	421244	257667.4	344393	455885.4	291862	220505.5	240293.9	245230.1	355097.3	227094.9	151962.3	
phenylalanine	5953143	9991067	4857161	5642119	6487540	5613355	9530074	6382784	3139712	3311197	4130620	6742390	3155634	5348413	
Pyridoxamine	N/A	6624.168	N/A	N/A	2475.762	N/A	4152.321	N/A	N/A	N/A	N/A	9085.379	N/A	N/A	
pyridoxine	3303.477	N/A	N/A	N/A	N/A	N/A	5782.768	53361.05	10147.55	6079.19	5916.277	3366.554	3245.535	N/A	
1-Methyl-Histidine	1063008	862856.9	1303679	1114857	854316.7	788921.6	1233661	863744.6	712771.7	872504.7	754787	535015.1	673275	1622911	
N-acetyl-L-ornithine	N/A	6598.09	N/A	2861.195	N/A	5763.458	N/A	12047.22	N/A	N/A	4762.087	4128.196	N/A	N/A	
arginine	6291444	4245531	8065877	5961983	5802386	5574017	5485482	2273659	1624288	2555710	2998924	2116687	2902193	2712057	
citrulline	77229.97	27801.89	N/A	25051.78	13743.18	13237.19	22360.87	21941.01	6702.46	19149.87	30037.58	11019.34	18873.54	65144.19	
N-carbamoyl-L-aspartate	200622.5	119751.7	138608.6	112316.1	113965.1	87540.22	102409.9	96666.43	96619.31	113095.9	125532.6	105712	110660.5	118101.7	
glucosamine	153209.7	116557.1	126846.6	187198.3	161598.6	188064.6	129613.3	344152.7	327042.3	335393.4	202049.6	210202.9	237555.8	249098.2	
tyrosine	3351752	4894155	3088324	3292540	2290957	3117601	5432997	2241667	1988185	2257131	2403150	3285999	2321670	1201043	
Phosphorylcholine	1.09E+08	1.02E+08	1.09E+08	91480721	98952402	95098044	91519754	81492421	82902463	1.13E+08	60176202	89376923	98762760	95468014	
3-phospho-serine	56129.03	69392.65	45112.88	49092.46	54512.01	10835.94	63538.94	17828.23	63638.14	85065.91	64734.74	63705.73	12306.08	49516.83	
N6-Acetyl-L-lysine	552424.3	426955.5	1447039	466150.6	1225710	1433797	193034	1408236	403800.2	1478178	926267.4	498031.8	1866660	852402.9	
Acetyllysine	2239236	1651519	649206.3	1330415	743979	2087540	965290	907930.5	1093484	1616824	790094.2	N/A	1172474	424113.2	
N-acetyl-glutamine	21006.73	5808.615	44579.68	5335.391	10400.54	9497.271	6792.543	N/A	3941.881	4871.139	28005.48	5308.429	11208.88	3247.934	
N-acetyl-glutamate	683006.2	492223.2	519362.1	548382.5	548299.6	487243.2	497887.8	460648.8	445127.3	433770.5	590492.1	444367.3	436041.5	722651.2	
Ng,NG-dimethyl-L-arginine	49245.26	323827.3	43051.11	229560.5	79252.74	78349.58	31988.89	241980.5	97018.82	114776.6	131677.6	95709.83	N/A	51058.57	
Acetylcarnitine DL	1.16E+08	1.09E+08	1.23E+08	1.1E+08	1.02E+08	1.06E+08	1.03E+08	1.07E+08	1.21E+08	90360462	93095332	1.07E+08	1.1E+08	1.25E+08	
tryptophan	2123462	2653343	2094811	1546127	2129417	1215414	2141219	1015249	881293.1	1052546	995901.8	1571922	987913.9	1719192	
Kynurenine	21084.41	44560.34	16645.82	10575.42	14943.85	12467.08	39618.23	7606.536	9889.474	N/A	4123.684	14213.63	N/A	31440.44	
N-acetyl-glucosamine	41294.68	30551.1	38767.22	47838.58	33754.44	39679.96	30450.56	31518.38	43724.89	25601.97	26368.16	44597.21	42938.06	33861.29	
Flavone	20763.63	5630.028	12733.18	9842.363	7427.166	23536.46	5106.563	25099.33	13765.76	11861.07	6139.604	18116.48	15793.72	31184.81	
cystathionine	4046901	5320708	4400960	3927203	4432358	3658523	6212066	3109534	1921574	2440508	3332745	2333402	3667841	1948784	
5-methoxytryptophan	36086.75	19698.03	21550.84	16351.06	34025.54	28758.36	25964.42	27855.4	36718.47	35768.55	37216.1	31364.22	29815.62	26167.47	
Cystine	52896.64	68627.39	67755.23	75953.72	68549.59	62699.08	63784.13	77629.61	40396.97	67659.78	51235.57	42947.79	43769.09	51972.23	
cytidine	856411	1032326	1099376	1215142	1372196	852385	1103356	928289.8	1265198	821729.3	1311461	877916.5	1023259	942285.4	
biotin	685515.4	591283.3	713871.1	719821.2	591190.2	680968.4	549927.4	842554.9	712141.1	886823.3	956317.6	952729.3	921039.2	951067.8	
deoxyadenosine	2065.462	3298.812	1648.791	2477.816	1652.656	2477.532	N/A	2566.731	9086.622	1655.538	9917.974	10831.79	N/A	4935.752	
Glycerophosphocholine	33409191	28950688	30284394	33201872	33316709	32116994	25315706	36939900	30103082	43103803	39380734	42056305	42289014	40501816	
acadesine	N/A	N/A	4103.654	N/A	3326.883	10688.99	9101.892	N/A	9800.107	4172.782	7424.705	9634.243	7435.281	2479.811	
D-glucosamine-6-phosphate	318741.9	232790.9	295381.8	297995.7	268964.6	288833.1	315729.1	199578.7	213816.4	256375.5	136698.5	215088.7	193981	265221.4	
D-glucosamine-1-phosphate	559451.7	338182	684434.3	400689.4	437493.7	512931.6	414599.1	506230	448389.8	619678.2	456113.8	673811.1	822666.9	430087.3	
thiamine	N/A	N/A	N/A	N/A	N/A	N/A	N/A	N/A	N/A	N/A	9089.45	N/A	N/A	4955.119	
S-ribosyl-L-homocysteine-posi	14040.23	15696.21	4501.755	13180.26	11556.41	6643.613	18623.99	10729.92	11565.42	17245.11	13130.83	14849.49	13213.14	8231.478	
deoxyguanosine	4954.664	18064.3	7469.284	14050.02	13013.58	8662.249	5779.723	11519.34	9886.217	3302.603	6599.86	12381.7	8203.958	7431.122	
adenosine	155358.9	9963.311	11755972	13406.92	12911.42	8142.841	20469.76	3257623	111304.7	2067205	177578.7	5456623	2058339	28946.47	
1-Methyladenosine	147314.5	63569.57	160935.4	119745.5	130508	97464.49	95163.83	84031.27	101561.3	91274.78	93474.25	75071.33	101589.3	81787.79	
guanosine	50381.78	56159.6	74424.31	7426.59	63452.36	63593.14	145339.8	8169.912	4163.189	66920.57	62811.77	52811.87	58635.59	55355.9	
L-arginino-succinate	472726.8	391417.5	405498	371625.7	433215.2	374940.6	441565.4	232021.9	288941.1	337724.3	362257.2	279110	305127.3	402519.9	
S-methyl-5-thioadenosine	N/A	N/A	N/A	N/A	64643.13	4184.853	N/A	N/A	6916.482	N/A	N/A	N/A	N/A	N/A	
7-methylguanosine	147877.6	128695.3	195724.6	213899.1	143729.2	149419.9	137873.3	145348.5	180037.4	128852.2	147835	165945.1	155668.9	164362.5	
dCMP	122210.1	94150.78	89192.31	100634.9	93419.83	96632.42	119649.5	103237.4	70172.41	118916.6	95790.48	123737.5	102526.9	101730.4	
glutathione	763564.3	684628.7	561163.9	710148.7	737598.2	665276.8	682074.8	2581173	2042756	1805392	1521591	1252585	1180866	857968.9	
dTMP	52222.65	52159.52	34682.37	20253.08	17134.4	56013.9	27849.74	27254.13	28912.8	27257.62	24272.06	45370.75	13276.92	16720.4	
CMP	6718967	5837199	6991019	7435019	6283768	5625664	6072991	5865442	6814930	6507160	6991561	6615132	6807022	6274288	
UMP	3961515	3544088	3688906	4341554	3438345	3378205	4006955	3871124	3994614	3818088	4223138	3586599	3842565	3248520	
dAMP	187315	175069.5	138997.4	147823.8	151139.2	143378	121275.9	138593	223868.7	72081.59	165960.5	97656.18	188168.4	151101.3	
Nicotinamide ribotide	12827.97	27689.56	4116.869	20764.81	21996.41	28649.72	10591.93	13316.44	12993.39	13622.8	17828.4	9834.098	13888.99	17431.22	
aminoimidazole carboxamide ribonucleotide	14012.86	12387.03	13263.66	13169.13	17363.8	19822.46	18934.53	21338.87	15688.06	22510.41	18154.82	30429.17	13207.7	19703.51	
thiamine-phosphate	N/A	N/A	N/A	N/A	N/A	4130.141	N/A	9085.405	N/A	N/A	N/A	N/A	N/A	N/A	
dGMP	14042.91	9910.351	26429.34	10826.77	23951.4	21467.32	19793.8	14885.81	18830.97	24795.72	23952.14	12388.37	29181.14	11584.41	
AMP	1.17E+08	1.07E+08	1.06E+08	1.23E+08	1.08E+08	82342053	1.02E+08	1.02E+08	1.12E+08	1.15E+08	1.28E+08	1E+08	1.13E+08	84222136	
IMP	12684140	13629629	13555959	17240702	14522710	10477657	11905397	11327795	18625848	12768628	17452861	12069960	14695340	12147580	
S-adenosyl-L-methioninamine	N/A	N/A	N/A	N/A	N/A	N/A	N/A	N/A	N/A	N/A	N/A	N/A	N/A	N/A	
GMP	11646764	12985734	9964298	11550846	13123386	11500837	12081048	11709081	16288882	13199362	14912234	8550909	12525544	9599024	
xanthosine-5-phosphate	N/A	4130.102	4077.994	2477.702	9910.549	4999.581	7430.141	4130.205	N/A	5780.451	4152.371	4512.91	N/A	N/A	
riboflavin	6774.651	21474.04	34592.15	28770.32	19820.61	3329.273	28020.7	16416.81	12390.67	29733.88	17342.65	34625.5	25571.48	28087.01	
S-adenosyl-L-homoCysteine-posi	2864775	2625475	3366896	3693625	2516012	2882249	1729406	3102793	2709995	2507000	2972513	3000575	3739938	2862248	
S-adenosyl-L-methionine	33858.23	24778.41	33858.83	11363.12	14458.26	33858.49	14106.98	38789.68	54500.71	39642.37	46344.4	37164.01	21469.3	19829.03	
folate	9916.847	12381.92	14064.29	8750.605	7501.172	10314.17	16523.05	N/A	7882.897	N/A	N/A	13211.82	14863.24	18993.43	
7,8-dihydrofolate	N/A	3302.638	7432.989	5780.345	14041.78	4903.01	4130.102	3305.182	3300.64	11560.52	N/A	8258.001	N/A	5782.821	
5-methyl-THF	12848.33	15548.08	28688.34	19121.13	10232.62	14865.48	28227.36	5780.445	N/A	19363.66	11278.27	15902.75	10745.96	15652.98	
Diiodothyronine	N/A	N/A	N/A	N/A	N/A	N/A	N/A	N/A	N/A	N/A	N/A	N/A	N/A	N/A	
glutathione disulfide-posi	10261637	7134327	8905498	9836062	7673528	8112451	7302976	12641925	10316376	11658628	8761159	11273178	9327639	10029237	
NAD+_posi	6765579	6731148	8592362	8600850	7651310	7133454	6739160	6769549	7988326	4951358	8695501	6750812	8407584	5813959	
NADH	420373	436078.8	639237.3	550022.1	571517	393114.2	683815.3	415424.6	369163.2	341112.3	542617.1	363347.7	431140.6	481546.4	
dephospho-CoA-posi	178337.8	157741.9	185820.4	194063.3	206388.6	180868.5	169296.6	133023.6	175231.6	177557.1	171775.9	157742	175746.5	142853.7	
NADP+_posi	564905.5	512763.9	253575.8	447926.5	595440.9	516384.6	355076.2	641845.4	680015.9	425635.7	710053.6	349262.1	485030	479379.5	
NADPH	48726.77	39641.08	30619.5	66090.26	53674.5	30555.49	37208.57	44548.88	62768.18	42908.85	42941.99	31381.36	57860.54	60340.83	
coenzyme A-posi	14850.96	6605.354	16517.75	12508.51	13268.22	9089.395	9064.474	31584.89	25245.74	25580.47	29636.03	13172.54	23793.5	13988.69	
FAD	312197.4	353454.2	296412.7	286823.5	293134.6	288225.1	278568.1	308051.9	256907.8	240504.7	333000.7	297292.1	294147.3	210598.5	
acetyl-CoA-posi	N/A	2477.624	2477.668	N/A	N/A	N/A	N/A	1983.127	N/A	N/A	N/A	1982.219	N/A	N/A	
propionyl-CoA-posi	4127.625	11560.75	7435.332	7433.072	14869.33	8258.108	N/A	8257.616	13215.75	14835.32	2484.812	4955.326	24773.57	7432.953	
acetoacetyl-CoA-posi	4127.564	4130.224	3302.677	N/A	N/A	4999.636	2477.529	N/A	N/A	N/A	7430.142	N/A	7426.686	8253.588	
malonyl-CoA-posi	N/A	N/A	N/A	N/A	N/A	N/A	N/A	4130.255	N/A	N/A	3302.66	N/A	N/A	3278.705	
succinyl-CoA-posi	N/A	N/A	N/A	N/A	N/A	N/A	N/A	N/A	N/A	N/A	N/A	3300.124	N/A	N/A	
sarcosine	20939081	18510825	20155653	20776476	21484544	20725758	16964418	24014744	23836162	23844461	25041126	24754996	26785116	22890286	
putrescine	72297.9	80278.41	12743.42	N/A	51862.18	23437.29	71552.8	61305.02	55972.71	44004.19	48764.47	69735.4	25491.14	52412.13	
spermidine	721271.4	538985.6	836847	907169.5	1088971	294646.9	424760.6	385548.1	757379.3	337459.8	798704	1011173	822757.1	1101452	
N-acetyl spermine	144222.2	177815.5	14860.04	7419.652	214319.6	22674.82	170704	120242.5	137875.8	137701.5	138120.8	131434.7	125239.2	141532.5	
N-acetyl spermidine	15110.63	23129.55	10031.76	9027.358	12280.18	11631.98	30558.07	N/A	18164.42	22457.24	28860.09	18933.64	16313.6	10484.9	
Nicotinamide Riboside	4095.608	N/A	8252.421	35774.38	7924.55	5801.852	4917.029	6756.796	14653.71	14917.69	15689.63	11023.54	18112.46	9888.227	
Adenylosuccinate	60290.28	55332.97	62764.57	91670.71	66255.87	76807.49	33888.39	26426.14	52031.61	56152.05	75152.88	47900.1	69375.21	57809.54	
cholesterol	129683.5	88322.22	282370.4	354299.6	291529.5	411239.7	193282.9	183344.1	130490	142891.5	477358.4	183347.9	149492.2	1310612	
arginosuccinic acid	512598.4	374433.6	438456.1	361631.3	463542.3	397444.3	402551.2	294064.1	193781	342925.2	360565.4	224001.1	259614.2	440072.5	
phosphocreatine	1223606	1221164	1309831	1053007	1156881	1093309	941178.4	1475728	1048981	1030797	1040076	1774127	1472393	2152602	
retinoic acid	N/A	3711.258	N/A	2477.675	N/A	N/A	3727.01	3131.836	N/A	N/A	3041.248	N/A	N/A	N/A	
spermine	36974.28	213080.6	120978.4	146874.8	10318.64	169464.9	154669.8	174601.5	156134.4	126313.3	85095.52	24354.2	158211.5	127295.3	
HMG-CoA_pos	N/A	6605.412	5780.219	N/A	N/A	N/A	6607.684	N/A	N/A	N/A	4122.56	N/A	3302.632	N/A	
N-acetyl-L-aspartic acid	9208711	7251369	9064880	8080206	7188756	10332370	6482613	8252027	8054180	6766554	8669300	7476662	9225501	7486704	
N-acetyl-L-aspartylglutamic acid	21291955	17044470	19963633	19821614	15947224	17947306	19170448	23076624	21622937	19975056	21099833	21406915	19263598	26091891	

SUPPLEMENTARY TABLE 2. NORMALIZED DATA.

Label	MUT	MUT	MUT	MUT	MUT	MUT	MUT	WT	WT	WT	WT	WT	WT	WT
glyoxylate	1.108911	-1.00353	-0.62833	-0.31982	-1.77383	-0.86282	-0.40882	1.219036	1.082943	-0.4201	-0.51657	0.995675	1.45223	0.075013
glycolate	0.984751	-0.17324	0.752706	-0.98232	-1.10712	0.018529	-0.86354	-0.97715	0.896157	-0.72222	0.409285	1.609713	1.390017	-1.23556
pyruvate	-1.52064	-1.38876	0.11345	-0.60397	-0.46649	-0.18429	2.388838	0.558668	-0.20537	-0.19108	0.507196	-0.08482	1.309262	-0.23199
lactate	-0.51425	-0.69038	1.293128	-0.2715	-1.38403	-0.68038	0.762374	0.766012	0.76618	0.217416	-0.67873	1.373326	0.848118	-1.80728
2-oxobutanoate	0.436781	-0.8491	0.017919	-0.0675	-0.974	2.768825	-0.09355	-0.59424	0.315543	-0.18407	0.281941	0.394861	0.190193	-1.64359
acetoacetate	0.50749	0.197336	0.928784	-1.09504	-1.20902	0.909502	0.853705	-0.34555	-0.73258	0.676547	-2.19418	1.211711	0.449922	-0.15863
glycerate	0.458259	-1.23476	-1.08772	-0.37209	-0.50652	-1.09322	-0.98537	1.184491	1.179793	0.593783	0.315045	0.656435	1.758522	-0.86664
uracil	0.213704	0.088846	2.050034	0.981826	0.180017	-0.47382	1.243464	-1.5592	0.280836	-0.4895	0.202511	-1.2855	-0.21335	-1.21987
fumarate	-0.57139	-1.09833	-0.46676	-1.17383	-1.26759	-0.86228	-0.59603	-0.05686	1.169638	0.551329	0.932674	1.716457	1.169874	0.5531
Maleic acid	-0.68481	-1.34437	0.154197	-1.05686	-1.49959	-0.42924	-0.64923	0.536135	1.540553	0.41723	0.743955	1.795106	0.193497	0.283423
2-keto-isovalerate	-0.89606	-0.99799	0.272384	-1.4131	-1.35272	-0.91484	-0.45679	0.741131	1.188037	0.344651	0.226392	1.178244	1.574669	0.505993
Guanidoacetic acid	2.574079	-0.71208	-0.69054	-0.70359	-0.70749	0.501404	1.338859	-0.676	0.070589	-0.68203	-0.67302	-0.66636	0.507946	0.518229
succinate	-0.76818	-1.26746	-0.49926	-1.11225	-0.73061	-1.07934	-0.66747	0.261234	0.390949	0.618338	1.421551	0.910183	1.780351	0.741958
Methylmalonic acid	-0.82463	-1.34418	-0.05674	-0.83745	-0.89338	-1.47531	-0.68994	0.780889	0.962466	0.274452	1.214627	0.669631	1.533788	0.685764
3-S-methylthiopropionate	-1.00479	0.353859	-0.04386	1.243538	-0.81423	-0.36049	-1.59637	1.15998	0.929068	0.586315	0.107446	1.346706	-1.57778	-0.32939
nicotinate	0.418872	0.388273	-0.3461	0.059892	-0.2649	-1.75945	-0.21188	-1.78331	2.063414	-0.2084	0.76367	0.704253	0.705809	-0.53014
taurine	-0.5471	-1.76786	-0.0974	-1.13266	-1.22436	-0.83656	0.25147	0.425684	1.068624	0.46271	0.608129	1.517104	1.344223	-0.07199
Pyroglutamic acid	-0.3956	-0.44917	-0.41525	-0.29642	-0.69208	-0.68106	-0.4659	-0.59674	1.317243	-0.50701	1.734823	-0.25063	2.325313	-0.62753
Citraconic acid/itaconic acid	0.739597	-0.23228	-1.0218	-0.91536	-1.47576	0.548105	-0.68529	-0.34521	2.207318	0.702324	1.048484	-0.24113	0.496152	-0.82514
2-ketohaxanoic acid	0.718081	0.049177	-0.10214	-0.79255	-1.30089	-1.70244	-0.94684	0.848618	0.554139	-0.96539	0.659191	1.531545	0.192595	1.256899
N-Acetyl-L-alanine	0.290008	-1.32713	0.226043	-0.95783	-1.46822	-0.78747	-0.75102	0.85883	0.54154	0.92765	-0.50481	1.932183	0.982497	0.037729
oxaloacetate	-0.18565	-0.37275	-0.12476	1.233584	-0.28741	0.898651	1.788445	-0.72138	-0.85068	-0.72224	-0.83495	-0.80873	-0.84692	1.834789
Hydroxyisocaproic acid	-0.83033	2.746328	-0.82983	-0.06396	-0.3058	0.482812	0.159437	1.123169	-0.82614	-0.27781	-0.82707	-0.24249	0.521088	-0.82941
malate	-0.82145	-0.6058	-0.52605	-1.38454	-1.41428	-0.65106	-0.84958	0.336974	1.378239	0.888231	0.36694	1.188702	0.850292	1.243383
hypoxanthine	0.448628	-1.83637	0.714694	-0.29795	1.162559	-1.11826	0.774268	-0.61608	1.917803	0.499808	0.175144	-0.65808	-0.28785	-0.87832
anthranilate	-0.11714	-0.24354	-0.81867	1.661151	-0.71663	-1.08749	-0.39012	1.158713	-1.08407	0.070663	-0.37361	-0.12467	2.223925	-0.15851
p-aminobenzoate	1.033042	0.368599	2.222577	-1.23985	-0.55468	-0.93721	-0.39234	-0.07852	0.765523	0.03677	0.977833	-1.11188	0.002808	-1.09268
p-hydroxybenzoate	-0.87088	-0.53716	-0.73304	-0.38296	2.741654	-0.46923	-0.39199	1.615491	-0.45905	-0.32507	-0.25418	0.493833	-0.37569	-0.05171
acetylphosphate	0.459596	-0.8792	-0.26845	2.209444	-0.30812	-1.17842	1.36179	-0.78631	-0.24986	-0.07548	1.423846	-0.43894	-0.55997	-0.70994
Carbamoyl phosphate	0.169894	-0.80562	0.316674	0.686946	-1.84442	-0.90435	0.218389	0.249782	1.192187	0.678589	-1.19774	1.944317	-0.15852	-0.54612
a-ketoglutarate	0.652766	0.18052	-0.11343	0.046921	-0.19978	-1.03187	2.747566	-0.73355	-0.13433	-0.82498	-0.18554	1.15402	-0.61277	-0.94554
Phenylpropiolic acid	0.169868	1.40373	-0.13551	-0.62823	-1.5025	-1.69529	-0.8845	1.264209	-0.4336	0.442568	-0.24467	1.476859	0.103801	0.663272
2-oxo-4-methylthiobutanoate	-0.65204	0.25306	-0.30088	-1.34735	-0.47424	-2.10994	-0.29961	0.926256	1.024594	0.775376	1.776452	0.098075	-0.06889	0.39914
2-Hydroxy-2-methylbutanedioic acid	0.899498	-1.60601	0.576976	-1.51579	-0.52103	-0.61984	-0.39999	-0.59587	0.658842	0.4733	0.675429	-0.74162	0.8798	1.836311
3-methylphenylacetic acid	0.819695	-1.17494	0.001933	0.158038	-0.22589	0.844713	-0.68709	-1.95198	1.620546	1.293589	-0.71139	0.728099	0.019274	-0.73459
xanthine	-2.7566	-0.77286	-0.33015	-0.33419	-0.26565	-0.166	0.12799	0.155982	1.270942	0.267952	0.593137	0.554462	1.43102	0.22397
Hydroxyphenylacetic acid	-0.67124	0.526868	-0.84521	-0.86602	0.282614	1.880346	-0.89097	1.1998	1.206878	-0.69807	1.139042	-0.75275	-0.68988	-0.82142
2,3-dihydroxybenzoic acid	2.774521	0.198107	-0.50589	-0.63869	-0.65709	-0.96258	-0.43524	-0.7248	-0.15921	0.715261	-0.22419	0.019077	1.237868	-0.63715
orotate	0.286185	0.592972	-0.18146	-0.41137	-2.37908	-1.10755	0.014989	0.12723	0.557582	2.168005	0.592972	0.024303	0.026951	-0.31173
dihydroorotate	-0.12764	-0.81802	-0.77596	-0.78149	-1.16857	-1.91186	0.551901	0.699806	0.492951	-0.1032	1.168315	1.780144	0.444362	0.549243
allantoin	0.208899	-0.74712	-0.86566	-0.59408	-1.73148	-0.47229	-0.9991	1.058009	0.825664	0.074788	0.666841	0.606102	-0.13746	2.106885
Aminoadipic acid	1.255285	-1.53455	1.406472	0.03476	-0.15079	1.013882	0.123025	-0.65967	-1.00594	0.873884	-1.79502	-0.14484	-0.15554	0.73905
Indole-3-carboxylic acid	-0.37807	-1.18039	1.955154	0.531983	-0.75687	1.805324	-0.66255	-0.38895	-0.81973	-0.20109	-0.6085	-0.66673	0.200674	1.169755
phenylpyruvate	0.050816	0.540814	-1.17698	-1.19817	1.50988	0.298409	0.450931	0.708145	0.029579	-1.16316	-1.14852	1.438509	0.832455	-1.17272
Atrolactic acid	-0.47462	-0.03322	0.873176	0.606108	0.176244	-1.05118	0.163292	0.277357	-1.06566	-0.85989	-0.03007	2.736071	-0.36374	-0.95387
Phenyllactic acid	0.165347	1.222622	1.12058	-0.73686	-0.1563	-0.70665	2.189223	-0.11057	-0.40082	-1.55666	-0.47589	0.789223	-0.75864	-0.5846
quinolinate	0.085337	-1.01242	0.278499	0.489877	1.634044	0.687607	0.412802	-0.19214	0.398715	-1.43337	-2.03413	1.244255	-0.62906	0.069972
phosphoenolpyruvate	-0.58714	0.079218	-0.20586	1.762716	1.599549	-0.01202	1.632443	-0.5119	-0.22322	-0.83063	-1.48642	-0.32335	-0.97631	0.082927
Uric acid	-0.41121	1.729131	-0.02234	-0.27208	-1.17426	-1.33156	1.839006	-0.11879	-0.85123	0.081114	-1.13281	0.963851	0.229778	0.471418
dihydroxy-acetone-phosphate	1.662802	-0.53459	0.56073	0.27125	-0.26119	0.43164	-0.29083	1.894674	-0.00356	-1.54279	-1.26822	0.614739	-0.55716	-0.97749
D-glyceraldehdye-3-phosphate	-0.58061	-0.12901	1.507659	0.809817	0.029751	1.601141	1.46657	0.245845	-0.72633	-0.38474	-1.49745	-0.45317	-1.07366	-0.81581
sn-glycerol-3-phosphate	-0.49134	-2.01148	0.892472	0.071051	-0.19714	-0.40845	1.063643	0.445938	-1.07334	-0.29413	0.844733	1.544575	0.797318	-1.18386
shikimate	-0.57408	-0.51919	-0.53975	-0.46766	-0.32724	0.219478	-0.46439	-0.49454	-0.52885	0.586203	3.234148	0.204251	-0.38407	0.055683
aconitate	0.812665	0.276917	-0.20965	-0.36811	-0.91947	-2.02847	-0.94591	-0.38372	1.344103	1.414143	-0.42341	1.350082	-0.32676	0.407604
allantoate	-0.23973	-1.65894	-0.33922	-0.28018	-0.79737	-0.96625	0.547267	0.277168	1.233902	1.402975	0.848279	0.642037	0.930748	-1.60068
Ascorbic acid	-0.81198	-0.55357	-0.35921	-0.66794	-0.81634	-1.37639	-0.45039	2.358333	1.58468	0.196166	0.426778	0.585388	-0.21969	0.104167
2-Isopropylmalic acid	-0.84317	-0.5525	-0.40716	-0.63576	-0.89448	-1.39801	-0.54584	2.22066	1.602205	0.366191	0.481769	0.701236	-0.03145	-0.06369
N-carbamoyl-L-aspartate-nega	-0.32307	-0.62817	1.154802	1.263116	-1.32387	-0.40644	1.193658	-0.61473	0.493344	-0.12498	-1.14964	1.482814	0.373357	-1.3902
Pyrophosphate	-0.6128	-0.98422	-0.23791	-0.11047	-0.92523	-0.54063	-0.85164	2.181755	1.531422	-0.08432	1.428511	-0.67534	0.160801	-0.27993
glucono-?-lactone	0.014852	-0.91344	0.831171	-0.11422	-0.6269	-1.2728	-0.91674	2.500203	0.366068	0.006047	-1.16234	0.326858	0.869951	0.091296
myo-inositol	-0.08581	-1.74507	-0.38837	-0.48357	-1.55596	-0.36279	-1.10757	1.190293	0.055104	1.033688	0.956477	0.401508	1.169748	0.922312
hydroxyphenylpyruvate	-1.36669	0.542719	0.998541	0.628767	0.236919	1.093955	-0.20376	-0.57721	-1.33577	-1.35313	0.745903	-1.33496	0.885996	1.038711
homocysteic acid	1.51119	-0.968	-0.09632	-0.77891	-1.217	-0.00257	-0.39862	-1.74332	1.168598	0.691924	0.50624	0.609974	1.295027	-0.57821
4-Pyridoxic acid	1.501053	-0.34804	-0.38659	-0.5436	-0.67915	-0.13014	-0.18629	-0.62766	-0.01716	-0.53184	-0.54916	-0.07364	2.925562	-0.35334
3-phosphoglycerate	0.234179	-0.79009	0.664241	1.067347	-0.44385	1.474814	1.456082	-0.48762	-0.40144	-0.83087	-1.58189	0.969539	-1.31002	-0.02043
Indoleacrylic acid	0.56322	1.509147	1.043091	-1.01156	-0.54128	-0.9318	2.21183	0.026391	-0.08396	-0.36377	-0.89721	-0.24112	-0.18634	-1.09663
Kynurenic acid	0.71141	-1.25564	1.172915	-0.7988	-1.02983	-1.05909	0.599637	0.263025	0.133224	-0.86534	1.146816	1.170588	1.093526	-1.28244
citrate-isocitrate	-0.00468	-1.78797	-0.12266	-0.3777	-1.19911	0.071147	-0.28902	0.04752	-0.55915	1.959799	1.944275	-0.15722	0.086361	0.388411
isocitrate	-1.90418	1.387815	0.088521	-0.68342	-0.14815	0.48826	-0.82534	0.888461	1.977487	-1.01052	-0.37492	-0.05968	0.3627	-0.18705
citrate	0.767869	-1.64734	-0.55352	-0.49337	-1.06577	-0.90492	-0.69932	0.549237	1.196747	2.169092	0.44465	0.217072	0.107765	-0.08819
2-dehydro-D-gluconate	0.055094	0.319626	-0.57682	-0.28365	-0.55893	0.436298	-0.67464	1.435465	-0.33877	-0.53945	-1.85632	2.25138	0.659364	-0.32866
D-gluconate	-0.83113	-0.88444	-0.28299	-1.27878	-1.84299	-0.41597	-0.10962	1.540887	0.636989	-0.07997	1.104021	1.009423	1.014525	0.420037
D-erythrose-4-phosphate	-0.62589	0.456058	0.306745	-0.02022	-0.58555	-1.34444	1.403901	-0.77651	-0.60943	0.059366	-1.23391	1.468265	-0.34481	1.846432
Xanthurenic acid	-0.06518	0.226154	-0.40594	-0.26557	-0.82426	-0.4337	0.42423	3.273074	-0.36788	-0.11943	-0.43887	0.078127	-0.4496	-0.63115
lipoate	-0.40071	-0.45985	-0.39044	-0.43248	-0.44504	1.556279	-0.36235	2.973317	-0.31476	-0.36302	-0.33397	-0.31253	-0.33246	-0.38198
D-glucarate	-0.29539	0.290937	-0.54016	-0.17021	-0.76163	-1.29521	0.013824	1.641776	2.246884	1.055795	-0.68466	-0.3336	-0.83747	-0.33088
deoxyribose-phosphate	0.056766	-0.94768	0.462879	-1.54779	1.178168	1.90432	-0.52911	-0.02455	-0.46563	1.486279	0.125709	-0.27737	-0.13477	-1.28723
pantothenate	0.615635	-0.90933	0.720892	-0.40255	-2.02752	-1.04595	0.271848	0.001659	0.794851	0.839675	-1.31964	1.498506	0.634558	0.327362
deoxyuridine	1.126181	2.443006	-0.59624	-0.62602	1.263043	-0.60709	-0.57634	-0.56304	-0.54264	0.921852	-0.55624	-0.54105	-0.55517	-0.59025
ribose-phosphate	-0.10067	-1.11281	0.212387	-0.40158	-0.33869	-1.14561	0.798015	0.471283	1.815859	0.744628	1.197793	-0.15473	0.001224	-1.98711
thymidine	1.113382	-0.99089	1.142542	0.09095	-0.14509	0.915986	-0.00968	-1.19591	-1.19313	-1.04667	-1.19499	0.280635	0.543815	1.689052
uridine	-1.4029	-0.2734	-0.31822	0.367456	0.974392	-1.34911	0.190344	-0.06111	1.991777	0.461619	0.452719	-0.15506	0.808979	-1.68749
deoxyinosine	-0.36621	0.199957	-0.31607	-0.02598	1.900822	-0.82407	0.338351	-0.22068	0.199208	-0.47389	2.116538	-0.56924	-0.17826	-1.78049
D-glucono-?-lactone-6-phosphate	0.314951	-1.2252	-0.2752	-0.7306	0.586466	0.53581	-1.59115	-0.47796	-0.09777	0.578099	-0.62953	2.163932	1.323132	-0.47498
hexose-phosphate	-0.72668	-1.35177	0.316258	-0.75518	-0.63172	-0.8307	1.461563	-0.35103	1.231882	0.057747	1.020281	1.701051	-0.06161	-1.08009
glucose-1-phosphate	0.323444	0.609358	1.102274	0.696362	-1.14569	-0.52578	1.075063	-0.94447	-1.08988	-0.30947	-1.41946	1.923526	0.121886	-0.41717
glucose-6-phosphate	0.74113	0.293461	1.115657	0.014336	-0.66512	0.362196	2.029175	-1.34126	-0.99789	-0.98569	-0.62324	-0.41375	-0.76242	1.233421
fructose-6-phosphate	0.350571	0.419602	0.379822	0.141062	0.45022	1.30662	2.197722	-0.8692	-0.98601	-1.36182	-0.93452	0.260104	-1.09946	-0.25472
1,3-diphopshateglycerate	-2.03834	0.977812	-0.23371	0.426708	0.253878	0.614647	0.570631	0.340124	-2.03764	-0.08638	1.076911	-0.09781	-0.72391	0.95708
2,3-Diphosphoglyceric acid	1.896757	1.131469	-1.65648	0.990684	-1.46234	0.565689	-0.53592	-0.19653	-0.13773	-0.80829	0.708994	-0.64843	0.128121	0.024008
S-ribosyl-L-homocysteine-nega	-0.81291	-1.9443	0.615371	1.739618	-0.74496	0.558111	0.311838	0.877091	0.967367	-1.43284	0.232198	-0.02139	0.22625	-0.57144
inosine	-0.64817	-0.18747	-1.26847	1.104482	0.403426	-0.78701	0.624635	-0.66314	2.408251	0.451934	0.647601	-1.00338	-0.33206	-0.75062
6-phospho-D-gluconate	0.436332	-1.2758	-0.91129	-0.58993	-0.15489	0.094716	-1.20855	0.804757	-1.47048	0.087312	0.225068	0.929256	1.219103	1.814387
xanthosine	-0.59622	-0.37365	0.032513	0.217012	-0.84749	-0.35588	0.436721	-0.0906	0.812443	-1.66703	1.904507	-1.45633	1.350977	0.63302
D-sedoheptulose-1-7-phosphate	0.521359	-0.23789	1.736505	0.326162	-0.30827	-0.42782	1.597541	-0.72446	-1.38551	-0.74482	-1.07868	0.326091	-0.88879	1.288593
N-acetyl-glucosamine-1-phosphate	-0.28034	-1.32839	0.619557	-0.86442	-1.44818	-0.84678	-0.37939	0.519947	-0.0333	0.595216	0.179894	2.316233	1.019632	-0.06969

glutathione-nega	-0.58437	-1.02241	-0.71853	-0.72313	-1.07249	-0.81027	-0.60569	2.51289	0.690186	1.007897	0.254463	0.647466	0.311166	0.112827
dUMP-nega	1.457816	0.07054	0.039793	-0.40506	-1.17833	-0.56273	0.481487	-1.13632	-1.1244	2.392906	-0.24279	-0.4049	0.500307	0.111689
Geranyl-PP	-0.10801	0.270889	1.157061	-1.18867	-1.68023	0.717751	-0.52321	-0.66245	-0.82689	-0.61756	0.901148	1.766301	1.029452	-0.23558
O8P-O1P	0.054551	-0.78187	1.327183	-0.63392	-1.27411	-2.04464	1.558687	1.039405	-0.10589	-0.34805	-0.23566	0.358405	0.579837	0.506068
dTMP-nega	0.673151	-0.19686	0.733849	-0.6686	-0.58954	-0.33327	1.14177	0.132481	0.102246	0.706046	-1.53597	2.024352	-1.53031	-0.65933
cyclic-AMP	-0.17907	-0.30116	2.376133	-0.01355	0.073685	-1.07818	-0.07034	-0.06069	-0.47478	-0.63579	0.302465	-0.35416	1.807976	-1.39254
fructose-1,6-bisphosphate	0.479878	0.536206	1.106107	-0.81113	1.179153	0.029347	1.508555	0.023129	0.024392	-2.01347	-0.74765	-1.35567	-0.4698	0.510952
trehalose-sucrose	-0.55694	0.037449	-0.35988	-0.87388	-1.43452	-0.18314	-0.25393	2.784099	1.151318	-0.19806	-0.18296	0.578718	-0.36779	-0.14048
orotidine-5-phosphate	0.95632	-0.53705	0.976329	-0.13613	-0.05847	1.471409	0.470704	-2.40487	0.105204	0.453127	-1.22373	0.763219	-0.4725	-0.36357
SBP	0.441282	-0.4488	0.28985	0.892988	0.751092	0.437521	1.145558	-0.80552	1.477332	-1.15367	-1.40895	-0.92118	-1.44767	0.750167
trans, trans-farnesyl diphosphate	-0.93974	-0.18928	-0.438	-0.92635	0.391289	1.041815	1.232514	0.230009	-0.27913	-1.09884	2.090887	-1.55993	0.34718	0.097573
S-adenosyl-L-homocysteine-nega	-1.28301	-0.86258	0.528203	-0.80081	-1.00786	-0.77217	-0.73919	0.967179	0.566641	0.522789	0.405499	1.754644	1.47801	-0.75733
dCDP-nega	-0.9889	-1.86713	-0.78211	-0.72447	0.274919	0.000687	-0.8587	0.456341	1.812762	1.608355	0.011942	0.064315	0.562916	0.429065
5-phosphoribosyl-1-pyrophosphate	-0.25232	0.802725	-0.75564	0.051399	-0.76661	-0.95371	0.438618	1.666267	1.555173	-0.85872	-0.42699	-0.85106	1.426056	-1.07519
OBP	0.347012	-0.88949	-0.01574	-0.21429	0.887009	-0.44786	0.439633	2.356376	-0.69833	-1.39418	0.204223	0.098415	0.803781	-1.47655
dTDP-nega	-0.49426	-1.30821	-0.35978	-0.83337	-0.5853	-0.46019	0.053589	0.819755	2.315822	0.815442	0.165746	-1.13199	1.260164	-0.25742
CDP-nega	0.096753	-0.8841	-1.09753	-0.76419	-0.13246	1.369654	1.510579	1.600066	1.139532	-0.7274	-0.16472	-1.06217	-0.04756	-0.83646
UDP-nega	0.85034	-0.38058	-1.15001	-1.62071	-0.01101	-0.36839	-0.26981	2.051661	1.062932	1.031141	-0.57643	0.651569	-0.57345	-0.69726
Cholic acid	-0.8851	1.817857	-0.8742	-0.91881	0.50472	0.151626	-0.84437	0.95227	0.44421	-0.84509	0.487035	1.68771	-0.81265	-0.86522
trehalose-6-Phosphate	0.15841	-0.85671	0.139116	-0.85878	-1.23924	-0.67323	-0.27779	0.540905	-0.42767	-0.3012	-0.81711	2.223642	0.756536	1.633141
Thiamine pyrophosphate	-1.47921	0.740735	-0.7023	0.422219	-0.29882	0.499969	-0.86719	1.501159	1.669447	-0.22124	1.004032	-1.13249	-1.05538	-0.08093
adenosine 5-phosphosulfate	0.735126	-1.1059	-1.18523	-0.89617	-0.63136	-0.28798	0.43221	2.157206	0.421864	-0.75391	-0.96555	1.152545	0.830983	0.096172
ADP-nega	0.20807	-0.82747	-1.30803	-1.36149	-0.32123	-0.09516	0.294402	0.988919	1.502704	0.297288	-0.53136	0.238094	1.94527	-1.03001
dGDP-nega	0.66506	-0.50656	-1.17841	-1.28129	-1.02866	-0.33846	0.987998	2.244462	0.808424	-0.08329	-0.47791	0.537276	0.476056	-0.82469
IDP-nega	0.43181	-0.6527	-1.39432	-1.21719	-0.42867	0.267493	0.430414	2.229174	0.940497	0.698814	-0.70305	0.182518	0.427254	-1.21204
GDP-nega	-0.25202	-0.05995	-0.49487	-0.34878	-0.2596	-0.73938	-0.24994	3.170734	0.727011	-0.90367	0.325742	-0.29888	-0.07834	-0.53805
CDP-ethanolamine	-1.35313	-0.08045	1.750396	-0.38144	-1.07656	-0.80654	-0.2025	1.335925	0.688944	0.956359	-0.44777	-0.16872	1.049627	-1.26414
FMN	-1.14741	0.482873	0.580782	0.246094	-0.13837	-0.03378	-0.32316	-0.07779	0.657635	-1.13312	2.493764	0.654339	-1.12154	-1.14031
cholesteryl sulfate	-0.56242	-0.73742	-0.53908	0.050607	0.885527	0.08255	-0.75121	-0.45807	-0.35328	-0.49109	1.069637	-0.55858	-0.50204	2.864867
dCTP-nega	-1.23448	0.781111	-0.57749	-0.94273	-0.17977	0.983432	0.957705	2.032627	-0.52646	-1.56688	0.239062	0.552293	0.168946	-0.68737
dUTP-nega	-0.1167	2.756251	-0.7894	0.670026	0.419451	-0.34967	-0.77659	0.995541	-0.7549	-0.7769	0.005204	-0.75388	0.257095	-0.78554
dTTP-nega	2.405583	0.803514	0.062951	1.110989	-0.10137	-0.70016	0.360821	-0.39471	-0.19337	-1.40776	-0.80016	-1.36247	0.065326	0.150828
CTP-nega	-0.51668	0.243441	-0.72859	-0.0099	1.986042	-0.3504	-0.20386	1.705648	0.259256	-2.04815	0.185995	-0.858	0.033753	0.301446
UTP-nega	-0.39834	0.879631	-0.94045	-0.7636	0.848683	-0.18598	0.078178	2.193174	0.144301	-2.14537	-0.09456	-0.15804	-0.06396	0.606326
CDP-choline	-0.22648	-0.8171	0.796617	0.533982	-0.96443	-1.00811	0.686825	-0.04041	0.346413	0.263049	0.790478	1.104251	0.975511	-2.44059
dATP-nega	-0.27847	0.829737	0.367714	0.788732	-0.7654	-0.73606	1.796602	0.008109	1.177455	-1.03015	1.047847	-1.20938	-0.75388	-1.24285
Taurodeoxycholic acid	0.290586	-0.94063	-0.45335	1.035698	-0.19653	-2.32617	0.75387	-0.45711	-0.58001	1.027769	0.167728	1.699947	-0.33854	0.316745
ATP-nega	0.137001	0.63184	-1.29162	-0.3809	1.014873	0.173211	0.424347	1.845214	0.43591	-2.16086	-0.60127	-0.78047	0.010811	0.541913
dGTP	0.13373	0.768364	-1.12763	-0.75107	1.07901	0.347534	0.954323	1.454726	0.14072	-2.34946	-0.53498	-0.2912	-0.31069	0.486622
GTP-nega	-0.48746	1.435404	-1.05826	-0.73754	0.892078	-0.41122	-0.4295	1.839179	1.37362	-1.2538	0.336731	-0.85063	-0.32715	-0.32146
UDP-D-glucose	1.256452	-0.07557	-0.42482	-0.86455	-0.14923	-0.55286	-0.61761	1.946171	1.643629	-1.45812	0.513043	-0.62868	0.113436	-0.7013
UDP-D-glucuronate	-0.23112	0.116963	-1.09158	-0.88923	0.086718	0.080298	-0.58306	1.670254	2.21569	-1.29079	0.544682	-0.91142	-0.03789	0.320488
ADP-D-glucose	0.847023	-1.71242	0.842041	0.788892	-1.12669	-0.38827	0.005912	-0.31231	0.772506	-0.79568	0.900696	0.336237	1.393169	-1.5511
guanosine 5-diphosphate,3-diphosphate	-0.41289	-0.76513	0.339695	-0.12566	-1.16653	0.876111	-0.41451	2.35206	-0.6453	-1.50724	0.4991	-0.03852	1.149748	-0.14094
UDP-N-acetyl-glucosamine	0.247032	-0.92991	0.125917	-1.30857	-1.59735	0.542491	-0.73588	-0.20154	0.712221	1.543022	-0.55222	1.439294	1.19363	-0.47814
glutathione disulfide-nega	-0.48904	-1.27165	-0.3306	-0.75722	-1.25461	-0.56991	-0.67902	0.222687	0.270641	1.594018	0.04981	1.49526	1.787331	-0.06769
NAD+_nega	-0.99028	-0.62684	-0.84232	-1.26441	-0.73722	-0.72207	-0.02719	1.454198	0.906096	1.15568	0.854075	0.449252	1.414848	-1.02381
NADH-nega	-0.43598	-0.8551	0.691479	-0.65566	-0.48755	-0.53796	-0.75847	0.196707	-0.49563	-1.11234	0.935697	0.813855	2.64686	0.054082
dephospho-CoA-nega	2.01607	-0.39802	0.274903	-0.03453	-0.14923	-0.23231	1.177035	-1.95478	0.956255	-0.0382	0.651941	-0.30009	-0.82974	-1.13932
NADP+_nega	0.239349	-0.02079	-1.7678	-1.01404	0.197537	-0.71461	-0.47061	1.64495	1.714293	-0.58802	1.232896	-0.14027	0.311874	-0.62475
NADPH-nega	1.088675	-0.47645	-0.19542	-0.26574	-0.567	-1.08027	-0.11667	1.50556	0.987745	-1.11192	-0.68042	-1.38381	1.640336	0.655403
2-hydroxygluterate	-0.31296	-2.20814	0.428955	-0.5684	-0.49444	-0.60398	-1.28424	0.357387	0.659254	0.648628	0.232096	0.875528	1.798437	0.47189
2-deoxyglucose-6-phosphate	0.308334	0.618797	0.140518	-2.00941	-0.6247	-0.30765	0.887333	0.024189	1.048497	1.234748	-1.99616	0.145609	0.724016	-0.19412
4-phosphopantothenate	0.309554	-0.5089	-0.92204	-0.12843	0.066548	-0.96244	-1.59159	-0.16656	-0.36957	1.25629	0.182242	0.769247	2.413706	-0.34806
dehydroascorbic acid	-0.37035	-0.05	-0.36928	-0.37365	-0.37495	3.400547	-0.36636	-0.36441	-0.36141	-0.36643	0.042721	-0.36118	0.283137	-0.3684
3-hydroxybuterate	2.187262	1.388252	-0.5293	-0.45468	-0.54674	-0.49176	1.884304	-0.58981	-0.50328	-0.47458	-0.54026	-0.41131	-0.48638	-0.43171
itaconic acid	0.739597	-0.23228	-1.0218	-0.91536	-1.47576	0.548105	-0.68529	-0.34521	2.207318	0.702324	1.048484	-0.24113	0.496152	-0.82514
Urea	1.107017	-0.79873	-0.85847	-0.13812	0.278774	-0.30961	-0.41279	-0.47963	-0.75904	-0.31992	0.45834	2.51953	0.980732	-1.26809
ethanolamine	-0.15674	1.103295	0.020999	0.187372	-0.0285	2.047036	-1.28406	0.461999	-1.26909	-1.28428	-1.27514	0.662687	0.486158	0.328262
glycine	-0.42292	-0.49414	-0.41055	2.887645	1.697058	-0.429	-0.37671	-0.3541	-0.31941	-0.37752	-0.34254	-0.31673	-0.34072	-0.40036
alanine	-0.59231	-1.61051	-0.09933	-0.90784	-1.26939	-0.90943	-0.90258	0.814387	1.210835	0.468716	0.909995	0.900041	1.049305	0.938119
betaine aldehyde	-1.00926	-0.2668	-1.39809	-0.34858	-1.33294	0.293473	-0.14507	0.747004	1.416175	0.321192	0.215239	0.635694	1.928099	-1.05614
choline	-0.55351	-1.12101	0.398539	0.518813	0.334941	0.808294	-0.26081	-2.21467	0.635772	0.076661	-1.0638	0.226737	0.323924	1.890121
4-aminobutyrate	-0.26064	-2.01706	-1.05366	-0.82609	0.09798	-0.64635	-0.07305	1.321083	0.863723	0.3126	1.666101	-0.44075	1.038629	0.017477
dimethylglycine	1.358194	-0.43372	1.002142	0.783196	-0.85352	-0.86051	-1.00232	0.103162	0.217742	0.974652	-0.41185	-2.19144	0.530206	0.784061
serine	-0.52893	-1.25419	-0.67461	-0.21142	-0.94893	-0.69311	-0.9909	1.371482	1.567377	0.496716	1.20755	-0.15826	1.378967	-0.56175
cytosine	1.513857	0.626632	-0.54958	0.312116	-1.12521	-0.65606	1.825216	-0.27664	-0.19307	0.227849	-0.82951	1.275728	-0.86027	-1.29106
Creatinine	-0.06907	-1.46182	0.534347	0.081378	-1.91334	-0.67807	-1.49347	0.893741	0.516409	0.479338	0.552262	1.245725	0.973789	0.338775
proline	0.551209	1.155903	0.110653	1.176999	0.8051	-0.14671	2.045138	-0.93394	-0.6198	-0.86504	-0.738	-0.4749	-0.71718	-1.34944
indole	-0.97118	1.866291	0.953144	-0.13798	-0.99439	1.202268	1.019976	0.482924	-1.25903	-0.51119	-1.24835	0.431254	-0.41321	-0.42053
betaine	-0.54867	-0.93941	0.80738	-1.37703	-1.99081	-0.21869	0.69248	0.115686	0.486397	1.013351	-0.51913	1.698055	0.537678	0.242706
valine	1.490242	1.019546	0.581343	0.612018	0.434254	0.05481	1.768618	-0.77643	-1.2792	-0.44064	-0.70593	-0.60008	-0.87176	-1.28679
threonine	0.548379	0.523441	0.905847	1.164668	0.434001	0.071985	2.216987	-0.79925	-1.08384	-0.68707	-0.87074	-0.89815	-0.51359	-1.01266
homoserine	-0.51661	-1.33687	-0.28717	-1.85325	0.345639	-1.31505	0.07596	1.949987	0.628074	0.743714	0.474961	0.705425	0.076648	0.308535
purine	0.32664	-0.01247	0.669762	-0.30435	0.180185	-0.59963	2.398491	-0.53386	-1.41059	-1.1267	-0.9063	1.122426	-0.43208	0.628488
cysteine	-0.66491	0.010861	-0.70538	-0.92202	0.547147	1.645138	-0.81359	0.579594	0.57753	0.949448	0.983568	-2.23572	-0.02267	0.070999
creatine	-0.03292	-1.89561	-0.03148	-0.76342	-1.18988	-0.94336	-0.12197	0.338242	1.210742	-0.0084	0.982948	1.174962	1.576732	-0.29657
nicotinamide	2.114574	-1.14867	1.411536	-0.28256	-0.69363	-0.26395	0.377168	-0.59195	-0.1928	1.019997	0.226872	-0.69261	0.269161	-1.55313
Imidazoleacetic acid	-0.02162	-0.54329	0.753027	-0.59797	-0.62584	1.10661	-0.01673	0.926456	-0.25842	-0.34026	-1.22294	1.254711	-1.93413	1.520392
thymine	0.189838	-1.11652	-1.12924	-0.39921	-0.41474	-0.03592	-1.02485	-0.60505	0.429456	0.196916	0.798362	2.370788	1.354447	-0.61428
DL-Pipecolic acid	0.646225	-1.82067	1.000965	-0.37558	-1.77398	0.43723	-0.59385	1.460853	-0.00782	0.664393	-0.27247	0.841003	0.623265	-0.82955
N-Acetylputrescine	0.218097	-1.73931	-1.72462	1.646677	0.696963	-0.18677	-0.27074	1.102566	-0.65906	-0.34045	0.481746	0.417003	-0.66114	1.01904
hydroxyproline	-0.15456	-1.00313	-0.5013	-1.01734	-0.76724	-0.87456	-0.63237	1.931663	1.596366	0.457502	0.457861	-0.9133	0.269421	1.150993
leucine-isoleucine	1.981535	0.883582	0.984747	0.380429	0.140704	0.376612	0.952958	-1.50665	-1.47602	-0.54023	-0.86213	-0.59566	-0.28607	-0.4338
ornithine	-0.6279	1.434272	-0.48667	-0.52835	2.302702	-0.91126	0.600479	-0.81758	-0.88359	-0.0421	1.076959	-0.56168	-0.75656	0.2013
asparagine	1.062912	0.579333	1.841483	-0.70032	-0.28178	0.301343	1.110876	-0.01194	-0.84861	0.873157	-0.92113	-0.23585	-1.26841	-1.50105
aspartate	0.513463	-1.77151	0.219031	-0.62462	-0.12605	0.158573	-0.00753	0.2582	-0.34483	0.270461	0.812236	2.129683	0.387627	-1.87474
adenine	0.363302	1.627456	0.453472	0.222526	-0.86709	-0.18143	1.928016	-0.64212	-0.92184	0.039744	-0.45303	0.420133	-0.0358	-1.95333
Methylcysteine	0.363302	1.627456	0.453472	0.222526	-0.86709	-0.18143	1.928016	-0.64212	-0.92184	0.039744	-0.45303	0.420133	-0.0358	-1.95333
homocysteine	0.930223	0.073656	0.91347	-0.70436	0.026038	-0.44967	2.144795	-0.47122	0.382754	-0.44353	-1.19095	0.249081	0.470645	-1.93093
methylnicotinamide	-0.56172	-0.16376	0.706366	-0.61504	-0.1382	3.109918	-0.28631	-1.00639	-0.01229	-0.66653	-0.14423	0.16617	-0.65596	0.267982
lysine	2.416399	0.06738	0.760583	0.162975	0.221879	-0.3533	0.472898	-2.13972	-0.7199	-0.03665	-0.2967	-0.81893	0.493809	-0.23072
glutamine	0.413691	-0.06509	0.442516	-0.24971	-0.06695	0.039152	1.753946	-0.04901	-1.05364	-1.61637	-0.43527	2.175626	-0.69671	-0.59218
O-acetyl-L-serine	-0.83826	0.043617	-0.83282	-0.85507	-0.13119	2.06384	-0.81795	0.681829	1.362145	-0.8183	-0.80293	0.760892	1.012543	-0.82834
glutamate	-0.23894	-1.84225	-0.71082	0.10791	-1.53673	0.751018	-0.22891	1.199136	1.228251	-0.10744	0.39859	0.814829	1.145596	-0.98024
methionine	0.67618	0.901529	0.7164	1.760927	0.046948	-0.16781	1.380029	-0.345	-0.85289	-1.28379	-0.67649	0.131774	-0.59868	-1.68911
guanine	-0.8179	-1.08343	-0.71234	-0.06865	0.666425	-0.7865	0.444178	1.051119	2.379401	-0.83017	1.136565	-0.40855	-0.49526	-0.47488
histidine	0.131183	0.778993	0.839223	-0.25884	-0.3255	-0.16669	2.739389	-0.44507	-0.43624	-0.97419	-0.68475	0.644869	-0.76738	-1.07501
2-Aminooctanoic acid	-0.91019	-1.40639	0.417016	-0.08373	-0.58634	-0.5131	1.180536	0.375689	0.121221	-0.87516	-0.7628	-0.13426	0.73965	2.437876

carnitine	-0.66696	-1.1969	-0.64505	-0.86859	-1.08575	-0.16352	-0.8662	0.260732	1.314376	0.587884	1.110949	1.643515	1.224248	-0.64873
Methionine sulfoxide	0.071183	0.101866	0.820805	0.879522	-0.97335	0.260804	2.006584	0.083477	-0.69147	-0.6941	-0.46514	1.161169	-0.69602	-1.86534
phenylalanine	0.017163	1.440953	-0.48121	-0.32018	-0.00655	-0.18171	2.179154	0.601919	-1.11853	-1.1796	-0.61631	1.014852	-1.16574	-0.18421
Pyridoxamine	-0.50715	1.228633	-0.50121	-0.52551	-0.01167	-0.51007	0.758186	-0.47411	-0.45746	-0.48536	-0.46856	2.918301	-0.46769	-0.49632
pyridoxine	-0.28198	-0.45043	-0.44287	-0.44745	-0.44882	-0.44454	-0.09062	3.392463	0.28059	-0.07029	-0.05902	-0.23861	-0.25648	-0.44195
1-Methyl-Histidine	0.276771	-0.77247	1.202849	0.208353	-0.70997	-0.69903	1.198166	-0.06705	-0.50593	-0.15199	-0.43676	-1.21927	-0.74963	2.425954
N-acetyl-L-ornithine	-0.65929	0.721763	-0.65455	-0.14588	-0.67977	0.692907	-0.64156	2.83617	-0.61958	-0.64187	0.609906	0.460151	-0.62775	-0.65064
arginine	1.088162	-0.28567	2.132899	0.704851	0.545165	0.671616	0.883632	-0.93185	-1.27066	-0.81667	-0.46525	-0.95457	-0.51954	-0.78212
citrulline	2.388799	-0.07389	-1.17722	-0.12216	-0.63246	-0.60486	-0.09161	-0.07383	-0.84921	-0.25436	0.375068	-0.61033	-0.21378	1.93984
N-carbamoyl-L-aspartate	2.889618	-0.6217	0.708467	-0.63375	-0.68368	-1.31438	-0.43977	-0.53261	-0.3269	-0.0207	0.745124	0.084395	0.134974	0.010905
glucosamine	-0.76297	-1.29115	-1.01067	-0.53371	-0.82667	-0.41914	-0.90428	1.64568	1.645332	1.405899	0.031687	0.223442	0.459975	0.336578
tyrosine	0.274776	1.140521	0.094507	0.029815	-0.87079	0.034156	2.539197	-0.49507	-0.64611	-0.55981	-0.28987	0.745599	-0.36712	-1.62981
Phosphorylcholine	0.823519	-0.62775	0.957335	-0.9293	-0.59554	-0.29368	0.041529	-0.53334	-0.05589	1.746811	-2.21935	0.540884	1.068762	0.076003
3-phospho-serine	0.140024	0.344015	-0.27428	-0.27889	-0.12738	-1.72637	0.647347	-1.34968	0.903536	1.596177	0.85308	0.918618	-1.59155	-0.05465
N6-Acetyl-L-lysine	-0.75714	-1.06222	0.84079	-0.95798	0.216423	0.740664	-1.3523	1.003106	-0.89264	1.037432	0.105024	-0.69761	1.959384	-0.18293
Acetyllysine	1.773589	0.495474	-0.79237	0.155274	-0.76866	1.492018	-0.17793	-0.22239	0.218221	0.96123	-0.41138	-1.86939	0.30084	-1.15453
N-acetyl-glutamine	0.717215	-0.54602	2.664512	-0.55565	-0.19993	-0.2053	-0.37068	-0.87938	-0.58469	-0.53578	1.574066	-0.45528	0.061464	-0.68454
N-acetyl-glutamate	1.528357	-1.22376	-0.15657	-0.34402	-0.49852	-0.68439	-0.08625	-0.33571	-0.2407	-0.8544	1.387443	-0.22842	-0.53029	2.267227
Ng,NG-dimethyl-L-arginine	-0.7418	1.945691	-0.80219	1.144854	-0.48084	-0.41926	-0.91015	1.773229	-0.00519	0.104678	0.400134	-0.01778	-1.29227	-0.69909
Acetylcarnitine DL	0.132801	-1.21702	0.787037	-0.74212	-1.44802	-0.5851	-0.20189	0.395938	1.934272	-1.13078	-0.55957	0.862736	0.731797	1.039913
tryptophan	1.014611	1.443089	1.044612	-0.34999	0.641552	-0.84159	1.385573	-0.98355	-1.18137	-0.98316	-0.98808	0.467836	-1.00027	0.330725
Kynurenine	0.342697	1.716679	0.032794	-0.5045	-0.22374	-0.31945	1.978937	-0.61127	-0.37479	-1.18665	-0.89942	0.014426	-1.18279	1.217075
N-acetyl-glucosamine	0.35101	-1.32391	0.150702	0.754691	-0.87823	0.11607	-0.63553	-0.36239	1.518089	-1.24738	-0.97119	1.660627	1.23188	-0.36444
Flavone	0.58822	-1.22935	-0.30473	-0.74027	-1.02185	0.879434	-1.16652	1.420397	0.058783	-0.33143	-0.99799	0.655433	0.267516	1.922369
cystathionine	0.26252	0.803811	0.640902	-0.05345	0.252332	-0.09905	2.510976	-0.2283	-1.25882	-0.94377	0.038166	-0.83928	0.370724	-1.45675
5-methoxytryptophan	0.621535	-1.57964	-1.03278	-1.81933	0.021214	-0.27347	-0.33045	0.033097	1.445395	0.904461	1.344228	0.723972	0.368579	-0.42682
Cystine	-0.81941	-0.13222	0.666813	0.841368	0.049134	0.017756	0.627687	2.260339	-1.31972	1.000869	-0.33909	-1.02842	-1.10117	-0.72393
cytidine	-1.15869	-0.90765	0.114226	0.185326	0.722073	-1.21962	0.433999	-0.30056	1.852369	-1.02469	1.86847	-0.30574	0.316941	-0.57646
biotin	-0.61367	-1.40556	-0.40635	-0.67101	-1.32094	-0.66886	-1.05964	0.607739	0.108518	0.6773	1.306115	1.484868	1.127415	0.834066
deoxyadenosine	-0.52425	-0.32105	-0.6169	-0.46292	-0.66017	-0.43054	-0.80943	-0.33091	1.559589	-0.59298	1.702684	2.067765	-0.79735	0.216468
Glycerophosphocholine	-0.43865	-1.4134	-0.74572	-0.72665	-0.81764	-0.63798	-1.19275	0.521253	-0.20143	1.158685	0.950408	1.548463	1.372485	0.622916
acadesine	-1.10517	-1.12824	-0.31781	-1.11756	-0.58935	1.177787	0.997229	-1.08286	1.39405	-0.24712	0.674021	1.358664	0.682148	-0.69578
D-glucosamine-6-phosphate	1.230076	-1.12214	0.87409	0.405493	-0.29734	0.550941	1.674339	-0.75612	-0.1703	0.345071	-2.15123	-0.11936	-0.79508	0.331545
D-glucosamine-1-phosphate	0.039923	-1.47735	0.846919	-1.0297	-0.89452	-0.26011	-0.61326	0.070655	-0.15197	0.663013	-0.20212	1.399696	2.224366	-0.61555
thiamine	-0.37694	-0.41353	-0.37058	-0.39659	-0.40437	-0.38006	-0.35319	-0.34157	-0.32375	-0.35361	3.145624	-0.32236	-0.33469	1.225631
S-ribosyl-L-homocysteine-posi	0.236313	0.185802	-1.91568	-0.15258	-0.56573	-1.46443	1.610066	-0.2353	0.130609	1.266163	0.433075	1.024245	0.463564	-1.01612
deoxyguanosine	-1.2704	1.677595	-0.55154	0.93551	0.585302	-0.29592	-0.92746	0.855743	0.520276	-1.64742	-0.58748	1.324077	-0.0905	-0.52778
adenosine	-0.51596	-0.55825	2.901341	-0.55716	-0.55739	-0.55846	-0.55442	0.487705	-0.52309	0.081093	-0.50263	1.294299	0.115054	-0.55212
1-Methyladenosine	1.507241	-1.94288	2.147981	0.175418	0.43049	-0.41308	-0.18344	-0.51597	0.446149	-0.34641	-0.04953	-0.71549	0.310071	-0.85055
guanosine	-0.18651	-0.21145	0.492094	-1.33831	0.009222	0.146637	2.630887	-1.2809	-1.39301	0.387421	0.36804	0.127768	0.247088	0.001027
L-arginino-succinate	1.631983	-0.5671	0.622774	-0.51297	0.287154	-0.11194	1.685388	-2.03878	-0.66003	-0.243	0.575524	-0.83647	-0.52136	0.688831
S-methyl-5-thioadenosine	-0.32028	-0.32668	-0.31917	-0.32372	3.443438	-0.10507	-0.31613	-0.3141	0.152899	-0.31621	-0.31306	-0.31074	-0.3129	-0.31826
7-methylguanosine	-0.58987	-1.77266	1.185951	1.198409	-1.17264	-0.58927	-0.56602	-0.1016	1.581005	-0.90456	0.091491	1.040761	0.411923	0.187079
dCMP	0.756875	-1.23991	-0.82566	-0.66706	-1.13049	-0.59204	1.098434	0.399488	-1.26604	1.050112	0.072075	1.955296	0.476253	-0.08734
glutathione	-0.6337	-0.8487	-0.88868	-0.7661	-0.75683	-0.77416	-0.67186	2.19492	1.551077	0.943025	0.654252	0.3187	0.142104	-0.46404
dTMP	1.368609	0.922013	0.176814	-0.98888	-1.22653	1.596746	-0.20523	-0.17734	0.073138	-0.25307	-0.37968	1.456581	-1.26108	-1.1021
CMP	-0.09998	-1.86169	0.365322	0.165768	-1.21347	-1.38299	-0.29466	-0.2956	1.328169	0.217131	1.25653	1.09996	1.046189	-0.33069
UMP	-0.01587	-1.54928	-0.373	0.168364	-1.53124	-1.14176	0.633754	0.634998	1.310251	0.253364	1.500164	0.466868	0.734331	-1.09094
dAMP	0.668643	-0.06903	-0.34111	-0.42023	-0.43667	-0.34046	-0.58998	-0.05817	2.346285	-1.77047	0.692077	-0.937	1.265122	-0.00901
Nicotinamide ribotide	-0.61683	1.318469	-2.06222	0.489577	0.589002	1.98543	-0.85376	-0.27701	-0.21055	-0.30957	0.624476	-0.82456	-0.11767	0.265218
aminoimidazole carboxamide ribonucleotide	-0.76802	-1.25352	-0.84201	-1.03202	-0.48776	0.107994	0.230474	0.761892	-0.08017	0.827698	0.26203	2.644658	-0.60889	0.237655
thiamine-phosphate	-0.36362	-0.40212	-0.35694	-0.3843	-0.39248	0.910445	-0.33864	3.271401	-0.30767	-0.33908	-0.32017	-0.30621	-0.31918	-0.35143
dGMP	-0.78275	-1.51055	0.98752	-1.31809	0.279326	0.203319	0.214524	-0.43189	0.320582	0.947565	1.015951	-0.70675	1.840383	-1.05913
AMP	0.242061	-1.01174	-0.21885	0.154775	-0.79234	-1.75079	-0.14315	0.077589	1.099574	0.667673	1.890772	0.307784	0.892616	-1.41597
IMP	-0.56883	-0.7861	-0.20293	0.525157	-0.39871	-1.30265	-0.52273	-0.58367	2.343174	-0.23317	1.691348	-0.08068	0.712791	-0.59301
GMP	-0.3988	-0.47882	-0.94934	-0.71152	-0.28692	-0.49704	0.113142	0.129548	2.390163	0.556121	1.57101	-0.98482	0.574472	-1.02717
xanthosine-5-phosphate	-1.21333	-0.15197	0.046857	-0.64932	1.881135	0.343502	1.497976	0.214821	-1.15923	0.823929	0.254595	0.482939	-1.17036	-1.20154
riboflavin	-1.52308	-0.38961	1.143332	0.359455	-0.47015	-1.84819	0.665357	-0.44479	-0.79702	0.834081	-0.31681	1.656428	0.563211	0.567781
S-adenosyl-L-homoCysteine-posi	-0.28101	-1.17071	0.638761	0.670029	-1.20447	-0.30021	-1.89061	0.678369	0.227697	-0.54886	0.537502	0.79789	1.956318	-0.1107
S-adenosyl-L-methionine	0.090498	-0.67458	0.135228	-1.38486	-1.22422	0.068567	-1.09462	0.688623	2.003746	0.649962	1.281178	0.721624	-0.50818	-0.75296
folate	-0.04043	0.115872	0.664881	-0.31503	-0.53106	0.005968	1.212809	-1.46977	-0.14582	-1.47493	-1.46723	0.857439	1.071427	1.515867
7,8-dihydrofolate	-1.17748	-0.64822	0.540769	-0.01271	1.860687	-0.15396	-0.25617	-0.45012	-0.40255	1.774163	-1.1492	1.085397	-1.14856	0.137953
5-methyl-THF	-0.32916	-0.2233	1.742714	0.306696	-0.77455	-0.09401	1.885642	-1.13588	-1.82679	0.678272	-0.33511	0.413463	-0.40714	0.099151
glutathione disulfide-posi	0.088858	-1.60328	-0.40895	-0.36069	-1.30378	-0.8599	-0.92785	1.721907	0.874594	1.060604	-0.04611	1.373657	0.239323	0.151617
NAD+_posi	-0.59659	-1.1926	0.826862	0.313886	-0.45488	-0.38713	-0.24404	-0.03826	1.257275	-1.61637	1.60676	0.247742	1.393033	-1.1157
NADH	-0.67719	-1.01247	1.457603	0.190069	0.241439	-0.96474	2.23347	-0.28106	-0.55785	-1.16685	1.120702	-0.60555	-0.03072	0.053155
dephospho-CoA-posi	-0.05456	-2.00851	0.507074	0.106682	0.417955	-0.02064	0.148391	-1.53669	1.300107	0.577154	0.768895	0.318892	1.018619	-1.54337
NADP+_posi	0.245954	-0.47884	-1.70883	-0.685	0.09996	-0.0976	-0.91818	1.211275	1.736307	-0.43625	1.785344	-0.73342	0.163549	-0.18427
NADPH	0.013256	-1.01767	-1.28929	0.991199	0.023298	-1.36475	-0.63017	0.085738	1.873768	-0.17655	0.014258	-0.86257	1.289875	1.049611
coenzyme A-posi	-0.40416	-1.32833	-0.19858	-0.72594	-0.68773	-1.00293	-0.92404	1.680824	1.107955	0.892754	1.517315	-0.3355	0.8465	-0.43814
FAD	0.237227	0.21262	0.006223	-0.81399	-0.85109	-0.40867	-0.05094	0.992401	-0.01766	-1.04318	1.815554	1.152233	0.778788	-2.00952
acetyl-CoA-posi	-0.66027	1.314188	1.820468	-0.73735	-0.76784	-0.67251	-0.56715	1.359516	-0.45168	-0.56879	-0.49829	1.539128	-0.49462	-0.61481
propionyl-CoA-posi	-0.81669	0.059802	-0.31512	-0.40701	0.546306	-0.23051	-1.28596	-0.08008	0.832801	0.898433	-1.00608	-0.56872	2.669867	-0.29704
acetoacetyl-CoA-posi	0.196225	0.033818	-0.05371	-0.91293	-0.91985	0.46757	-0.28553	-0.86392	-0.84805	-0.87464	1.619233	-0.84682	1.625438	1.663171
malonyl-CoA-posi	-0.51542	-0.58954	-0.50254	-0.55523	-0.57098	-0.52174	-0.46732	2.328211	-0.40768	-0.46816	1.682469	-0.40488	-0.42986	1.42267
sarcosine	-0.53844	-1.54623	-0.61759	-0.86352	-0.83824	-0.63066	-1.11541	0.731843	0.990071	0.486939	1.085957	1.248461	1.533419	0.073396
putrescine	0.86417	0.799905	-1.48372	-1.9683	-0.12925	-1.0802	1.054593	0.709503	0.603077	-0.12339	0.192982	1.25531	-0.85001	0.155335
spermidine	-0.0973	-0.93383	0.353452	0.335305	0.818177	-1.55376	-0.99071	-1.08431	0.471525	-1.31119	0.530794	1.496954	0.631869	1.333012
N-acetyl spermine	0.284729	0.481624	-1.77744	-1.90888	1.097736	-1.6612	0.919603	0.123674	0.566378	0.348324	0.485239	0.455041	0.257725	0.327448
N-acetyl spermidine	-0.22687	0.345136	-0.75731	-0.95257	-0.65506	-0.61866	1.713842	-1.77241	0.449691	0.759769	1.695001	0.557342	0.149481	-0.68739
Nicotinamide Riboside	-0.92203	-1.31709	-0.4146	2.522356	-0.55645	-0.72894	-0.78099	-0.51847	0.614445	0.480061	0.685555	0.120702	1.014438	-0.199
Adenylosuccinate	-0.08392	-0.78719	0.145619	1.464613	-0.08244	0.871878	-1.52803	-1.95556	-0.03605	-0.07519	1.43543	-0.31754	1.049929	-0.10155
cholesterol	-0.59618	-0.75718	-0.10461	0.029627	-0.17545	0.263728	-0.35249	-0.3641	-0.52334	-0.52145	0.681562	-0.3284	-0.47077	3.219078
arginosuccinic acid	1.731071	-0.54393	0.922423	-0.43508	0.604211	0.248736	0.75119	-0.56361	-1.81436	-0.05359	0.445974	-1.36067	-0.96895	1.036593
phosphocreatine	-0.31968	-0.6873	-0.0389	-0.90939	-0.7416	-0.6698	-0.83791	0.726609	-0.30047	-0.60235	-0.42635	1.826242	0.799309	2.181588
retinoic acid	-0.72836	1.208838	-0.71478	0.456435	-0.78699	-0.73503	1.802785	1.388528	-0.6147	-0.67851	1.35522	-0.61175	-0.63809	-0.70359
spermine	-1.45143	0.971537	-0.05962	0.164728	-1.89512	0.652128	0.635063	1.087292	0.902214	0.14072	-0.49246	-1.58456	0.850349	0.079162
HMG-CoA_pos	-0.70148	1.384527	1.420091	-0.72362	-0.73238	-0.705	1.930108	-0.66165	-0.64157	-0.67521	0.909703	-0.64002	0.524945	-0.68843
N-acetyl-L-aspartic acid	0.511284	-1.53214	0.543494	-0.68062	-1.41624	1.247855	-1.09676	0.509326	0.68913	-0.88208	0.967855	0.223137	1.444929	-0.52917
N-acetyl-L-aspartylglutamic acid	-0.01604	-1.62034	-0.24917	-0.71629	-1.74495	-0.91633	-0.17773	1.12022	1.027868	0.036613	0.661989	0.987815	0.145135	1.461216

SUPPLEMENTARY TABLE 2. T-TEST RESULTS.

	t.stat	p.value	#NAME?	FDR	Fold Change with respect to Wild-type
alanine	-8.9586	1.16E-06	5.9359	0.000266	0.74235
malate	-8.5599	1.87E-06	5.7285	0.000266	0.6994
sarcosine	-7.6894	5.63E-06	5.2498	0.00035	0.70529
biotin	-7.6594	5.85E-06	5.2326	0.00035	0.63282
succinate	-7.5058	7.18E-06	5.144	0.00035	0.72223
Methylmalonic acid	-7.4854	7.38E-06	5.1321	0.00035	0.7016
fumarate	-6.9453	1.55E-05	4.81	0.000631	0.75395
Glycerophosphocholine	-6.6006	2.54E-05	4.5959	0.000877	0.68414
valine	6.5401	2.77E-05	4.5576	0.000877	1.7315
threonine	6.099	5.34E-05	4.2721	0.001523	1.646
2-keto-isovalerate	-5.6809	0.000102	3.9907	0.002464	0.78756
glucosamine	-5.6429	0.000108	3.9646	0.002464	0.48409
arginine	5.6146	0.000113	3.9451	0.002464	2.111
myo-inositol	-5.574	0.000121	3.9171	0.002464	0.70177
leucine-isoleucine	5.4762	0.000142	3.849	0.002553	1.6904
proline	5.4685	0.000143	3.8437	0.002553	1.863
D-gluconate	-5.2988	0.000189	3.7242	0.003164	0.76608
glutathione-nega	-4.9785	0.000321	3.494	0.005077	0.50625
Maleic acid	-4.9052	0.000363	3.4404	0.005441	0.77185
carnitine	-4.8603	0.000391	3.4075	0.005577	0.7706
N-acetyl-L-aspartylglutamic acid	-4.7271	0.000491	3.309	0.006663	0.75036
glutathione disulfide-posi	-4.5701	0.000643	3.1915	0.008335	0.69533
taurine	-4.5214	0.0007	3.1548	0.008394	0.86689
glutathione disulfide-nega	-4.5159	0.000707	3.1507	0.008394	0.74114
glutathione	-4.4886	0.000741	3.1301	0.008449	0.36882
methionine	4.4312	0.000819	3.0865	0.008982	1.7187
serine	-4.4047	0.000858	3.0663	0.00906	0.67459
2-Isopropylmalic acid	-4.3506	0.000944	3.0251	0.009458	0.48015
coenzyme A-posi	-4.3396	0.000962	3.0167	0.009458	0.43719
fructose-6-phosphate	4.285	0.00106	2.9749	0.010066	1.4109
NAD_nega	-4.2132	0.001203	2.9196	0.011063	0.79157
allantoin	-4.1942	0.001245	2.9049	0.011085	0.71182
2-hydroxygluterate	-3.9	0.00211	2.6757	0.017822	0.84424
Ascorbic acid	-3.8871	0.00216	2.6656	0.017822	0.40859
dihydroorotate	-3.8798	0.002189	2.6598	0.017822	0.76155
Creatinine	-3.8255	0.002415	2.6171	0.01912	0.79601
creatine	-3.7895	0.002579	2.5886	0.019862	0.85906
hydroxyproline	-3.7429	0.002807	2.5517	0.020676	0.55569
dCDP-nega	-3.735	0.002848	2.5455	0.020676	0.68327
S-adenosyl-L-homocysteine-nega	-3.7216	0.002919	2.5348	0.020676	0.70452
2-oxo-4-methylthiobutanoate	-3.7112	0.002975	2.5266	0.020676	0.61806
homoserine	-3.6416	0.003378	2.4714	0.022921	0.70061
glycerate	-3.5405	0.004067	2.3907	0.026957	0.67399
4-aminobutyrate	-3.4775	0.004568	2.3403	0.029183	0.85947
N-Acetyl-L-alanine	-3.4727	0.004608	2.3365	0.029183	0.86117
D-glyceraldehdye-3-phosphate	3.3724	0.005545	2.2561	0.034356	1.4063
citrate	-3.2251	0.007285	2.1376	0.044174	0.79725
N-acetyl-glucosamine-1-phosphate	-3.1372	0.008577	2.0667	0.050925	0.78983
xanthine	-3.0991	0.009206	2.0359	0.053544	0.62281
5-methoxytryptophan	-2.9729	0.011639	1.9341	0.066344	0.70423
tryptophan	2.909	0.013105	1.8826	0.073231	1.4681
CMP	-2.8906	0.013561	1.8677	0.073483	0.84958
cystathionine	2.8865	0.013665	1.8644	0.073483	1.4823
uracil	2.8483	0.014668	1.8336	0.077417	1.307
phosphoenolpyruvate	2.8315	0.015134	1.82	0.077976	1.4453
Pyrophosphate	-2.8248	0.015322	1.8147	0.077976	0.6858
betaine aldehyde	-2.7642	0.017144	1.7659	0.084692	0.81423
phosphocreatine	-2.7614	0.017236	1.7636	0.084692	0.69579
S-adenosyl-L-methionine	-2.6352	0.021764	1.6623	0.10463	0.55863
2-ketohaxanoic acid	-2.6287	0.022027	1.657	0.10463	0.86036
aminoimidazole carboxamide ribonucleotide	-2.5957	0.02341	1.6306	0.10938	0.67308
fructose-1,6-bisphosphate	2.579	0.024142	1.6172	0.11098	1.411
dTDP-nega	-2.5389	0.02599	1.5852	0.11757	0.72885

dTTP-nega	2.4951	0.028168	1.5502	0.12544	1.5165
thymine	-2.4839	0.028753	1.5413	0.12607	0.80775
asparagine	2.4679	0.029609	1.5286	0.12786	1.2267
glucose-6-phosphate	2.4461	0.030813	1.5113	0.12972	1.3688
glyoxylate	-2.4436	0.030951	1.5093	0.12972	0.76083
deoxyadenosine	-2.3851	0.034443	1.4629	0.14227	0.30437
UMP	-2.3702	0.035388	1.4511	0.14408	0.86011
lysine	2.3158	0.039064	1.4082	0.15399	1.3916
histidine	2.3059	0.039768	1.4005	0.15399	1.2653
4-phosphopantothenate	-2.3055	0.039798	1.4001	0.15399	0.62868
allantoate	-2.303	0.039982	1.3981	0.15399	0.82509
malonyl-CoA-posi	-2.2926	0.040738	1.39	0.15481	0.36189
citrate-isocitrate	-2.2813	0.041578	1.3811	0.15592	0.84483
glutamate	-2.2714	0.04233	1.3734	0.15668	0.91185
3-phosphoglycerate	2.24	0.044797	1.3488	0.16324	1.2995
UDP-N-acetyl-glucosamine	-2.2344	0.04525	1.3444	0.16324	0.90039
trehalose-sucrose	-2.2074	0.047505	1.3233	0.16924	0.69607
6-phospho-D-gluconate	-2.1942	0.048643	1.313	0.16936	0.80539
trehalose-6-Phosphate	-2.1932	0.04873	1.3122	0.16936	0.64971
betaine	-2.1648	0.051268	1.2902	0.17535	0.83613
NADP_nega	-2.1449	0.053127	1.2747	0.17535	0.77668
adenine	2.1409	0.053502	1.2716	0.17535	1.3167
Methylcysteine	2.1409	0.053502	1.2716	0.17535	1.3167
NADP_posi	-2.1378	0.053798	1.2692	0.17535	0.73833
S-adenosyl-L-homoCysteine-posi	-2.1342	0.054145	1.2664	0.17535	0.81253
AMP	-2.1192	0.055618	1.2548	0.1781	0.8536
SBP	2.1104	0.056487	1.2481	0.17887	1.4184
3-hydroxybuterate	2.0516	0.062693	1.2028	0.19635	3.9369
ADP-nega	-2.0304	0.065083	1.1865	0.20162	0.87199
Pyroglutamic acid	-2.0181	0.066509	1.1771	0.2033	0.5319
D-glucosamine-1-phosphate	-2.0122	0.067198	1.1726	0.2033	0.73747
aconitate	-2.0074	0.067768	1.169	0.2033	0.89074
D-glucosamine-6-phosphate	1.9551	0.07426	1.1292	0.22046	1.1939
arginosuccinic acid	1.9266	0.078036	1.1077	0.22424	1.2244
Acetylcarnitine DL	-1.9233	0.078487	1.1052	0.22424	0.88592
NADPH	-1.9232	0.078506	1.1051	0.22424	0.77113
Phenylpropiolic acid	-1.9219	0.078682	1.1041	0.22424	0.80977
IMP	-1.9099	0.080336	1.0951	0.22669	0.81602
tyrosine	1.8987	0.081901	1.0867	0.22884	1.4037
GMP	-1.8738	0.085503	1.068	0.23484	0.82377
D-sedoheptulose-1-7-phosphate	1.8725	0.085694	1.067	0.23484	1.2328
2-Hydroxy-2-methylbutanedioic acid	-1.8564	0.088102	1.055	0.23715	0.87354
orotate	-1.8558	0.088202	1.0545	0.23715	0.82138
Methionine sulfoxide	1.8424	0.090252	1.0445	0.24039	1.279
orotidine-5-phosphate	1.8243	0.093089	1.0311	0.24565	1.3658
Phenyllactic acid	1.791	0.098525	1.0065	0.25761	1.3795
Citraconic acid/itaconic acid	-1.7509	0.10546	0.97691	0.26843	
itaconic acid	-1.7509	0.10546	0.97691	0.26843	
NADH-nega	-1.7483	0.10592	0.97503	0.26843	
L-arginino-succinate	1.7455	0.10643	0.97294	0.26843	
Kynurenine	1.7369	0.10797	0.96668	0.26993	
glucono--lactone	-1.7188	0.11132	0.95342	0.27449	
Flavone	-1.7166	0.11172	0.95185	0.27449	
UDP-nega	-1.6847	0.11785	0.92869	0.28284	
oxaloacetate	1.6847	0.11785	0.92866	0.28284	
adenosine 5-phosphosulfate	-1.6771	0.11936	0.92314	0.28284	
indole	1.6763	0.11952	0.92254	0.28284	
homocysteine	1.6735	0.12008	0.92052	0.28284	

SUPPLEMENTARY TABLE 3. ORIGINAL DATA.

Label	MUT	MUT	MUT	MUT	MUT	MUT	MUT	WT	WT	WT	WT	WT	WT
glyoxylate	110519.6	118579.8	64140.53	65916.99	86173.52	89454.91	109677	115481.7	141668.7	126471.8	95805.72	141646	53783.19
glycolate	122709.5	177948.8	306795.2	68915.74	88347.58	249835.7	74169.25	83574.93	95331.01	104235.6	94233.64	107074.8	272053.6
pyruvate	41053.91	89883.33	63223.61	50215.43	32525.23	33091.1	21191.51	60959.7	61948.49	57912.08	54480.94	79111.44	27377.27
lactate	73940559	79239926	75572408	60157055	42101591	68981567	31677503	62826530	75530701	64520553	63713691	69092833	40759416
2-oxobutanoate	914669.4	857791.6	1063067	874038.3	759053.9	1178298	689192	947478.1	865085.2	1015468	984749.7	1239195	814608.8
acetoacetate	866609.6	857339.8	1089616	933466.5	664476.8	1045218	705682	907274.3	942174.4	1087453	1000508	1072303	685818.1
glycerate	494344.2	551918.8	533586.5	565144.2	482455.8	363959	446790.2	516655	680403.2	589010.2	868314.1	743339.7	535533.7
uracil	1405315	1499141	1492567	2664384	1271736	1099435	485349.7	1064053	2553976	1350500	628862.9	1624644	992040.4
fumarate	7939062	7650847	7769203	6354674	5688577	5619491	5004767	7345421	9105933	9100840	7601744	8500357	6399759
Maleic acid	7657831	7764346	6841429	6388641	5182692	5941178	5174389	7687631	8695052	8846048	7083170	8388911	6323157
2-keto-isovalerate	7130882	7939743	7358669	6126655	5487875	5616532	4843312	7584016	9077497	8117664	6911841	8090670	6141624
Guanidoacetic acid	N/A	N/A	N/A	N/A	8560.767	22155.52	12264.91	N/A	N/A	N/A	N/A	N/A	N/A
succinate	8624330	10612581	9443969	9214724	8932213	9196706	7642812	9033999	9640380	9539365	9188645	10224546	9608864
Methylmalonic acid	10253989	12080209	11370588	10110591	9718883	9958617	8062998	10475924	10645447	10826440	10065108	11621831	10694164
3-S-methylthiopropionate	5846.957	10072.96	5743.835	3979.531	N/A	N/A	7283.04	13871.68	N/A	9237.282	N/A	17136.15	5396.04
nicotinate	1307222	981563.3	1514228	953289.7	872980.6	836438.4	992779.2	90444.78	258094.9	1070077	1554917	1147266	661570.6
taurine	1.76E+08	1.79E+08	1.61E+08	1.61E+08	1.64E+08	1.58E+08	1.66E+08	1.78E+08	1.66E+08	1.66E+08	1.69E+08	1.63E+08	1.56E+08
Pyroglutamic acid	1552092	1314402	1533236	1266681	1127075	1520829	1150497	1626061	1283925	1431061	1453142	1572879	844623.8
Citraconic acid/itaconic acid	2590823	2968266	3069414	2195686	2500311	2581583	1780787	3179233	2246591	2811487	2534515	3124636	2536118
2-ketohaxanoic acid	289099.2	213884.8	304704.8	214338.8	180654	216666.3	195922.9	231834	238153.4	263955.6	232171.6	223605	163539
N-Acetyl-L-alanine	88808859	97346257	88398787	93730541	80020998	72233348	73596942	88575670	94620871	88440094	90280640	92205960	78684590
oxaloacetate	1863624	1880070	1822985	1431691	1200908	709970.7	263233.1	2440974	1896939	375516.2	2095783	1787431	1153278
Hydroxyisocaproic acid	78025.13	100362.6	111445.7	57736.4	56033.34	77466.11	75696.05	71069.85	42265.49	71618.89	104706.7	67076.69	80837.22
malate	34431877	37153583	34050019	25791956	23204971	27339234	24159802	39875731	43336085	39858267	33855848	37087841	29445730
hypoxanthine	1501386	2094637	2310570	2454573	2169496	1514995	906080	2317640	2157036	1876569	1776986	1606678	1958798
anthranilate	42134.85	44956.34	38389.91	51840.4	51587.05	42702.51	54882.77	19347.15	30056.01	38959.73	43729.47	29998.12	30738.43
p-aminobenzoate	66329.08	43555.37	19351.06	58621.67	60004.19	20704.98	18550.98	41138.43	52183.35	19344.94	34824.91	58974.68	51692.3
p-hydroxybenzoate	1220799	1212835	1203965	1135847	475141.9	12637473	560422.1	1116586	1717141	1037113	964803.7	796085.4	2092993
acetylphosphate	301073.6	273068.2	296501.1	274200.6	238232.7	259053.3	213976.9	289682.5	291095.9	241108.3	322240.2	356475	194668.7
Carbamoyl phosphate	2.8E+08	2.83E+08	2.53E+08	2.66E+08	2.23E+08	2.21E+08	2.34E+08	2.79E+08	2.47E+08	2.82E+08	2.5E+08	2.78E+08	1.93E+08
a-ketoglutarate	7852477	8307419	8640708	7551673	5448269	7104182	7300443	9591657	7850520	9337046	8310185	8130124	6179894
Phenylpropiolic acid	1002411	727908.2	1000288	811533.8	447874.1	928976.2	638262.8	907077.4	1308779	1059432	870638.4	887310.7	890670
2-oxo-4-methylthiobutanoate	72119.24	238153	132901.9	119563.5	148164	119257.1	79917.58	262749.3	127121.6	106844.2	166473.3	107633.6	130282.4
2-Hydroxy-2-methylbutanedioic acid	2102777	2279909	2331449	1728754	1456014	1657283	1779805	2059299	2089905	2265518	2176028	1935602	1445732
3-methylphenylacetic acid	18211.82	25377.74	27478.7	34749.03	20656.9	38280.17	22638.42	26985.88	19287.55	51058.27	21167.81	12921.74	32166.36
xanthine	1873083	2459779	2674687	3418.546	8879.833	2560609	1887806	2031522	4163.603	5718.568	9350.184	2877758	12788.65
Hydroxyphenylacetic acid	1036776	1033197	1628141	1546827	1305029	986261.1	1332134	817376.3	402456.3	1047517	966141.6	952943.2	1872106
2,3-dihydroxybenzoic acid	118925.4	162930.3	144104.1	62481.45	162491.3	25682.34	44972.04	137111	45877.68	202538.5	124053.2	112141.8	136911
orotate	389378.6	287146	332468.5	180510.4	236859.5	253010.3	162895.3	388257.5	316006.7	292090.4	320395.5	228473.8	156777.9
dihydroorotate	247847.7	239155.7	203273.6	268524.4	185436.2	278351.4	233407.3	172527.2	160425.6	306838	269440	235508.7	230219.4
allantoin	5079359	4107942	3964132	4035522	4465979	3506101	4842488	4092497	5225855	5193387	5122880	5293914	2657871
Aminoadipic acid	263457.7	170012.5	234654.1	176454.3	143167.8	242128.4	161545.2	208355.3	212330.6	204947.4	204682.2	36643.35	171916.3
Indole-3-carboxylic acid	180939.3	158590.1	197121.2	183661.7	126905.9	151186.7	148224.8	242786.7	217655.9	153989.6	198646.1	182139.1	169040.4
phenylpyruvate	10209.44	9763.226	12185.65	9060.302	9234.424	N/A	14960.67	13081.88	8112.407	3484.091	13402.18	6537.655	8507.119
Atrolactic acid	31397.78	19561.28	42894.62	33684.84	41731.34	23966.64	29815.85	36741.46	38268.25	17591.22	30167.15	35513.24	21493.62
Phenyllactic acid	431694.6	297997.7	337760.7	357596.2	267214.9	225386.1	259363	237567.8	264311.7	339972.2	311334.9	308248.5	268116.2
quinolinate	243720.3	428824.8	230119.3	322676.2	317995.1	400536.4	244112.6	45292.24	686405.8	264834.2	362799.2	221662	345569
phosphoenolpyruvate	1239206	1546180	1337445	1325008	1219133	998577	1164340	1355066	1615964	1452818	1494051	1712754	934398.9
Uric acid	92146.67	37640.59	68536.87	61415.42	127169.6	80781.02	51283.53	45810.24	107873.8	129709.4	71558.55	132384.7	71425.8
dihydroxy-acetone-phosphate	1739187	2099038	1958027	1373513	1199225	1868013	1349382	1662235	1945235	1769498	1751369	1928263	1757063
D-glyceraldehdye-3-phosphate	763954.2	797580.8	758450.8	686845.3	577998.1	623077.3	589977.3	616750.1	635916.1	706831.8	696516.4	798860.4	811911.8
sn-glycerol-3-phosphate	8876306	12446266	11660939	13409882	13643035	8299841	7893673	9272372	13838510	8995785	8439976	14625658	12263648
shikimate	289386.9	345072.1	695257.5	270916.7	702643.9	166664.4	811134.7	521708.5	573988.5	615680	146016.3	777120.1	114350.4
aconitate	1113324	1097988	1319509	786660.2	853733.1	836992.8	845956	1223179	1220288	1052950	1031482	1040040	949976.3
allantoate	175066.7	201289.2	231105.6	189967	256839.5	178996.3	145298.1	180127.5	238481.3	231988.6	207320.9	203402.7	191724.6
Ascorbic acid	1.44E+08	1.58E+08	1.43E+08	1.45E+08	1.27E+08	1.08E+08	1.21E+08	1.54E+08	1.66E+08	1.44E+08	1.52E+08	1.45E+08	84071684
2-Isopropylmalic acid	1.99E+08	2.04E+08	1.96E+08	1.94E+08	1.81E+08	1.64E+08	1.77E+08	1.98E+08	2.07E+08	1.98E+08	2.03E+08	1.99E+08	1.38E+08
N-carbamoyl-L-aspartate-nega	168387	204487.5	174196.1	174376.5	181506.5	140281.8	161617.9	162815.8	256000.7	183581.8	199000.9	182438.4	180643.2
Pyrophosphate	1625487	2562059	1557020	1702071	1716491	1411582	1025527	1314910	1640250	1656977	1321508	1431641	1408126
glucono-?-lactone	4137.569	89943.15	61116.12	60264.8	66893.33	40432.2	65174.8	57795.95	96627.4	76185.36	66894.74	77570.89	20409.64
myo-inositol	66224805	61493337	68069487	71193652	63695303	59314506	61854167	61347668	67382851	67071366	68821940	66634503	54534017
hydroxyphenylpyruvate	46821.51	32231.88	27897.92	41217.03	10324.36	28780.2	48512.68	48401.12	16744.74	4162.475	44210.38	8077.645	30779.44
homocysteic acid	412644.8	239401.9	328380.7	364837.4	356178.2	237675.3	345623	382711.6	376995.7	446993.4	459428.6	425669.3	310080.8
4-Pyridoxic acid	136353.8	14958.35	196774.2	170031	180987.4	140185.5	160713.3	171756.5	30300.87	152369	167949.5	156836	143736.1
3-phosphoglycerate	9516769	10365138	8108719	9977905	9589778	7413126	9434714	8262074	9257827	11200281	12587774	11967294	7882653
Indoleacrylic acid	59972.65	50367.11	72529.98	65434.38	58513.87	43278.29	30215.03	105388	48299.15	72463.16	51053.38	34560.41	67413.12
Kynurenic acid	751688.9	685592.9	991957.9	670787.4	687201.6	685127.4	611998.8	571152.6	635619.6	612166.6	513664.4	684201.4	744506
citrate-isocitrate	86355413	90207420	90335872	88508477	84791124	85375299	67417395	1.23E+08	87975070	91275643	94372594	94359292	91011207
isocitrate	300830.7	442461.3	320244.3	372311.5	240246.8	273216.3	499606.2	328813.9	410841.1	341514.2	433660.1	442245	292590.7
citrate	52323326	48350018	56998277	43340640	52860251	46478339	35787962	63603954	51474965	50539910	50245443	51203256	44793589
2-dehydro-D-gluconate	72191.91	69113.21	78274.98	74539.67	93207.42	68740.29	71659.82	67691.43	53821.62	67579.81	89306.01	66293.82	56237.6
D-gluconate	728106.9	518241.3	728362.3	638948	919526	631733.3	829920.9	768690.6	663781.4	869820.6	991777.9	858482.8	584193.6
D-erythrose-4-phosphate	316635.5	320818.1	268194.2	346546	250120	265133	289117.3	214858.7	376071	261615.2	408791	317383.2	222263.6
Xanthurenic acid	459155.1	498300.3	474640.9	482231.3	380031	462791.2	436043.6	627385.3	445827.5	507283.5	573769.4	520508.6	354025.6
lipoate	N/A	N/A	N/A	N/A	N/A	N/A	N/A	N/A	N/A	5782.827	N/A	N/A	N/A
D-glucarate	154489	201629.1	233112.5	273732.1	132291.8	311602	173462.9	243798.4	251670.8	242558.2	234341.2	245717.3	243898.9
deoxyribose-phosphate	928374.4	124344.8	912388.6	825039	576010.6	715511	565862.3	849350.3	133092.7	919901.6	895438.3	966301	572873.4
pantothenate	36144331	37798487	39072760	33844241	29126723	30103213	38366676	40433777	32934857	39881409	38129644	36649795	33368001
prephenate	N/A	4955.244	4883.031	N/A	N/A	6615.224	N/A	N/A	3302.722	N/A	8257.82	N/A	N/A
deoxyuridine	N/A	N/A	N/A	4558.882	N/A	8198.894	N/A	5769.871	5737.718	N/A	6177.417	9444.467	5022.331
ribose-phosphate	539011.7	717591.9	684065.4	666080.4	473731.7	530310.7	252440.8	768244	619067	658235.4	655553.3	635121.3	538708.9
thymidine	37308.14	51092.85	30616	30740.52	27187.35	50207.14	25669.36	47421.75	51044.33	55310.44	49515.85	46179.38	51461.05
uridine	522140.6	566102.3	518537.8	534925.8	369080.9	374138.1	230468.6	789893.2	537783.1	477406.8	485578.9	479852	313019.2
deoxyinosine	59639.75	45030.14	63073.73	61241.96	36993.8	59504.71	47943.14	64365.21	31388.5	96651.32	89794.63	49229.63	21898.16
shikimate-3-phosphate	N/A	N/A	N/A	N/A	N/A	N/A	N/A	N/A	N/A	N/A	N/A	N/A	N/A
D-glucono-?-lactone-6-phosphate	79848.88	81122.12	66894.2	41207.32	79793.94	59091.92	43408.84	42500.43	53654.07	67402.92	60674.22	107205.6	38200.23
hexose-phosphate	24712065	27130861	17222788	17863663	15891284	15167501	12826909	25837170	21395905	21300172	18743646	16762879	13177107
glucose-1-phosphate	1431679	1517340	1441870	1491476	1241428	1190171	1033049	1276028	1364101	1477918	1395377	1487245	1017886
glucose-6-phosphate	926843	746400.2	455881.3	451107.8	532650.7	545638.6	429096.5	848410.6	648324.2	719616.1	827061.4	556294.8	552221.9

fructose-6-phosphate	768795.4	715383.9	430654.2	465065.8	348189.9	471353.8	484554.9	746038.2	522400.5	678476.7	717350.4	501620.5	408219
1,3-diphopshateglycerate	1152302	1827287	1985233	1727416	1697798	1769264	1346061	1026043	1337506	1404491	1985401	1702905	1189302
2,3-Diphosphoglyceric acid	1002848	1648573	1945528	1455500	1472127	1456509	1250619	824343.5	1241153	1248326	1764400	1656863	1118418
S-ribosyl-L-homocysteine-nega	19401.83	15883.15	28637.56	33037.94	35944	18978.9	11563.64	21149.78	31031.71	19966.42	9876.768	30396.03	19089.69
inosine	18085473	30373536	30809491	34475414	29617792	25554330	16857689	31131273	29599042	18568076	25275349	26787274	27787325
6-phospho-D-gluconate	150087	207222.4	198996.9	176677	146179.7	202959.2	130498	143526.9	172245.4	154431.2	183239.2	208854.4	185829
xanthosine	221563.3	231309.1	206400.4	191828.2	231736.7	176388.8	164540.8	186941.5	312384.5	236935.5	179856.2	226975.8	208691
D-sedoheptulose-1-7-phosphate	2772428	2401595	1978064	1533040	1258524	1827229	2023037	3252608	1784616	2426518	3044907	2234191	1363279
N-acetyl-glucosamine-1-phosphate	1182072	1396118	1774515	1457304	1655057	1475325	1878155	1341440	1494085	1583654	1837103	1661042	1403685
glutathione-nega	803185.6	1484919	718636.4	654020.2	575382.4	835791.5	550272	1411822	1867171	877084.7	861843.8	793041.8	547046.8
dUMP-nega	6719.259	35136.29	8113.226	8042.615	8150.914	14078.51	12491.45	28079.24	16752.59	18650.14	24656.36	5465.403	13912.03
Geranyl-PP	112045	121475.3	591645.6	576738.6	398868.9	449430.8	344208.9	91803.24	154104.2	168328.7	181473.7	524549	473101
O8P-O1P	916765	826648	814666.2	696269.2	547494.3	664408.2	501258.2	884014.1	831800.5	822744.2	892590.7	801635.6	636164.6
dTMP-nega	9840.095	13922.07	17311.33	23210.71	25199.08	25627.7	5778.793	22196.95	18166.33	22279.8	23133.11	18022.14	9902.496
cyclic-AMP	2449873	3335943	3870010	3506287	3202030	2230366	1710500	2600393	4409367	2500209	2206457	2793092	1973704
fructose-1,6-bisphosphate	19752836	21865179	20221701	17716907	15065574	19085259	14920806	18450178	21204150	21489426	22251140	21725868	14995291
trehalose-sucrose	33673.36	23809.59	55995.27	48147.88	37283.2	33447.31	33608.22	36028.83	40074.8	20169.5	28038.47	58331.34	33081.41
Cellobiose	N/A	N/A	N/A	N/A	N/A	3335.997	N/A	N/A	N/A	N/A	N/A	N/A	N/A
orotidine-5-phosphate	42586.82	47517.99	29664.62	28596.02	35104.98	49406.84	24655	30289.88	19615.33	24313.67	27851.5	31754.64	44184.8
SBP	590221.2	832568.6	753565.4	721467.4	606104.5	557634.6	572242.6	719570	662949	636023.2	733747.5	759257.2	522877.9
trans, trans-farnesyl diphosphate	53078.01	84637.99	77089.71	69028.71	45020.96	78888.45	68906.78	91323.33	N/A	81754.72	47099.74	57497.4	68351.39
S-adenosyl-L-homocysteine-nega	12504935	9146624	9656027	10550453	9629386	8170036	9841698	9122974	12449584	10174942	9316844	9092804	8740350
dCDP-nega	60187.7	89960	66060.27	85862.38	58640.68	78485.49	8060.71	72399.54	85029.49	62814.19	98456.04	101604	81681.9
5-phosphoribosyl-1-pyrophosphate	131949.8	280913.4	178188.4	179864.7	179827.7	205249.3	220983.1	163813	119823.8	148654.1	239757.5	178759.2	127775.8
Deoxycholic acid	N/A	N/A	N/A	N/A	N/A	N/A	N/A	N/A	N/A	N/A	N/A	N/A	N/A
OBP	83317.64	85749.26	85271.5	121828.2	125251.1	80057.14	118140	147611.4	98007.88	115641.6	116620.1	177688.1	89300.01
dTDP-nega	66680.78	85851.74	91769.19	134544.5	102977.6	71048.7	60283.8	38865.42	68439.54	103250.7	77570.27	94139.3	66158.87
CDP-nega	835709.5	839527.1	1078200	1048422	786930	1208410	750589.2	819837.4	1078513	1204264	1128441	1138407	751218.2
UDP-nega	12593589	15613105	15998754	16853927	13877826	13031754	12997505	16887590	12668536	11225089	16050883	16259976	10017877
Cholic acid	4107.924	4969.624	13201.8	7430.243	N/A	N/A	N/A	4127.016	9769.82	3418.916	6627.838	N/A	8903.668
trehalose-6-Phosphate	2916841	1319249	2964293	2274447	2767250	1456643	6026008	1754920	2932267	3302081	5446527	4526677	1781179
Thiamine pyrophosphate	123505.8	161650.4	112313.6	98311.85	97911.46	115666	122234.1	63366.45	158625.8	147132.9	116128.1	221033.3	97832.85
adenosine 5-phosphosulfate	588133	479322.8	365360.6	378637.1	291969.6	382239.3	322149	540513.3	505957.4	392611.4	436216.2	405960.8	304335.6
ADP-nega	46312385	55701030	37752547	32990480	30629340	37994380	30671066	49403575	43247465	39624961	41881420	38145941	28880981
dGDP-nega	45259297	52570917	39390651	32433147	31617474	36818219	27462482	48073158	43184138	40921720	40752594	37729837	27505061
IDP-nega	6080104	7329367	5174156	4064350	4193457	5322566	3747867	6656441	6484732	6299993	6713617	4570027	3645550
GDP-nega	1966949	2709129	3804984	3108810	2973864	3106847	2783089	2290290	4162856	3491986	3537844	3717565	2776292
CDP-ethanolamine	925419.7	856345.2	454186.3	421554.6	393934.1	472307.8	365037.5	773032.4	792039.8	772985.5	585543.6	522068.2	308878.4
FMN	9910.393	9065.087	6603.482	12304.99	N/A	8924.122	N/A	4897.227	8960.704	N/A	5758.64	5759.243	N/A
cholesteryl sulfate	101540	222754.4	139714.4	1146151	2408519	266599.4	2281617	112291.5	1079925	173498.6	101155.6	95208.83	3189755
dCTP-nega	111488.8	159351.9	148646.7	142692.4	94984.01	112406.3	126366	141229.2	236221.8	191465.7	196240.9	183887.7	84411.42
dUTP-nega	23126.27	30576.27	19444.91	7402.434	8252.856	14112.91	7356.551	14847.66	22299.24	17411.74	18167.52	29729.65	17340.8
dTTP-nega	70770.22	79773.86	140660.3	91576.48	74520.98	89012.02	64015.76	74381.93	124476.4	113146.7	118068.2	137089.3	46225.85
CTP-nega	2695516	4027296	3817269	3119791	2725538	3578160	3313493	3242621	5296471	5008151	4200226	3840357	3113833
UTP-nega	31559336	35543937	33279015	27391469	25029637	25175644	31647172	28539246	44911562	39169904	40158137	37749219	25873674
CDP-choline	440971.3	337782.6	303626.1	256790.4	312248.7	175026.7	167196.3	262576.7	436880.1	360889.8	206453.8	336120.5	195731.8
dATP-nega	39630.28	31207.71	51202.99	45423.97	24778.33	46202.86	40467.39	17341.14	51205.65	58638.62	52851.98	62764.58	33036.46
Taurodeoxycholic acid	84663.99	90019.59	98048.26	74950.07	74126.24	78453.8	76794.86	105754.5	96695.83	79311.86	120567.2	79451.61	52020.81
ATP-nega	62928106	62975174	63715383	58965348	53180188	58664647	66176895	53843677	75492365	69209601	78721300	67778350	55850719
dGTP	61835368	62523982	62880113	58604818	54842114	56460985	63313896	55296519	74735013	69649702	77015308	67275007	56648091
GTP-nega	7732544	12378756	8669494	8543916	8361756	9143246	12482312	7928218	11392692	10705000	12294837	11548456	8416512
UDP-D-glucose	4891697	8500171	6043099	4299456	4133096	4755606	3791518	5039760	6677647	5515092	4956781	6464472	5961146
UDP-D-glucuronate	417899.3	680501	469104.2	334477.4	433555.5	445976.3	331164.3	553338.2	527730.2	476522.9	619404.4	441850.6	412929.8
ADP-D-glucose	33854.86	93323.45	64238.64	75980.99	71937.09	52021.17	60621.46	37999.36	42085.69	37990.17	27696.38	48910.36	48787.38
guanosine 5-diphosphate,3-diphosphate	214716.8	309685.2	453408.9	425338.7	411191.2	477359.5	394730.3	317148.9	402200.3	420246.6	472391.8	425323.5	417881.1
UDP-N-acetyl-glucosamine	4549756	4851991	4001770	4469817	4126520	3564997	3899296	4387198	4947577	5047108	4705594	4498096	3540454
glutathione disulfide-nega	26221857	25031888	26179196	24972937	20318677	25955702	18960429	25772590	26543132	26565564	24777477	28273523	21114078
NAD+_nega	5132541	6219603	4867526	4353170	3333146	4451286	3579251	6219431	5095163	5189159	4492664	5266679	3812742
NADH-nega	469089.7	521944	433589.3	480653.6	486432.3	381544.4	495555	360898.8	773810.3	366718.8	390639.7	491388.7	368349.7
dephospho-CoA-nega	64441.99	99926.94	50280.73	65163.28	71784.94	56155.2	32093.83	48171.54	37704.82	75981.14	49555.82	71028.75	13749.85
cyclic bis(3->5) dimeric GMP	N/A	N/A	3302.934	N/A	N/A	N/A	N/A	N/A	3306.054	N/A	N/A	N/A	N/A
NADP+_nega	260401.9	285837	279315	280153.8	175466.9	312293.1	199588.7	289672.5	311535.2	251369.8	269649.1	311818.8	200714
NADPH-nega	128005.6	126435.1	144528.4	99905.27	70197.49	96626.86	103234.7	131314	108184.3	92496.56	106535.9	111493	101581.9
2-hydroxygluterate	10386240	11332732	11274180	10067224	8169173	8420134	7395182	9522857	10804878	10659601	8421510	10527575	7611353
2-deoxyglucose-6-phosphate	5718179	7721880	7247795	7195684	5764839	6238785	4227630	7399209	8093138	7404509	6677967	6665936	4947802
4-phosphopantothenate	56790.56	33628.51	36350.74	33059.08	22736.11	20789.79	20286.07	53703.94	32348.43	36826.08	39643.97	27145.06	29596.48
dehydroascorbic acid	73871.25	501449.1	N/A	51156.95	16238.89	43867.94	18314.25	685242	N/A	27899.99	51659.29	N/A	N/A
3-hydroxybuterate	117502	63597.28	299473.7	49926.62	272506.3	290329	311451.6	80208.39	76877.56	61721.53	282219.5	84619.41	56714.14
itaconic acid	2590823	2968266	3069414	2195686	2500311	2581583	1780787	3179233	2246591	2811487	2534515	3124636	2536118
Urea	18524497	16008173	18656714	17745174	14700521	20602540	11484332	26020177	18924989	18797152	15550814	17631127	12138643
ethanolamine	15006.72	13057.25	14005.99	6929.086	26728.45	6104.05	4150.255	17731.3	N/A	12611.15	17482.99	N/A	N/A
glycine	N/A	3320.494	N/A	N/A	N/A	N/A	N/A	3302.719	N/A	N/A	N/A	N/A	N/A
alanine	21898031	22329492	20995418	23750070	22196217	19819510	21293398	22651993	27882498	25185510	24643540	24569740	24868899
betaine aldehyde	155397.9	176169	162856	185716.7	144735.4	134986.7	166874.9	151321.9	200367	235597.5	243810.5	203236.4	115918.8
choline	341649.6	995884.1	1344569	1235411	402206	908944.8	501869.1	1093995	325700.3	988670.8	1368308	328413.5	262894.8
4-aminobutyrate	12812577	17173209	16361116	18647501	17071721	14012983	19053943	13657331	18481329	15778487	15040561	15635994	13958847
dimethylglycine	203303.9	289146.6	242104.4	314205.3	192047.1	220795.3	230360.9	221693.3	385074	254223.2	227857.6	285200.1	217908.9
serine	6685857	6915322	7060039	8521734	8244270	6622974	6955001	8567356	11566140	10879954	10969637	11213722	8747210
cytosine	109369.6	136841.7	113881.3	112920.4	138202.7	128085.4	156731.8	147520.1	140008	121607.4	173360.2	122895.8	146278.5
Creatinine	3766666	3953413	4057312	5069139	4801660	4125766	4535936	4264005	4468295	4391650	3803010	3907783	4498324
proline	57762445	62206581	61334142	64552628	65808827	53338655	60845065	74848244	68631293	76846770	54342861	59692663	63429818
indole	201372.2	202374.8	126856.3	163504.7	142694.3	142552.2	187497.8	189211.8	168886.3	123099.1	143513.9	137547.3	102517.9
betaine	25932046	29384421	27746811	34460153	32221610	34646114	36826519	34599022	35912325	44903498	35838174	33032896	38378139
valine	494078.2	425332.4	392408.5	387945.8	398119.6	462586.1	335066.9	695397.8	512567.4	403080	406318.8	350002.8	290120.3
threonine	15236323	17793890	17784836	22605330	18449466	11634873	19067970	25031200	23146896	24612042	18851572	21369891	18191714
homoserine	28899.62	80919.34	66901.42	81815.78	66895.88	38807.28	90018.73	36334.18	100007.1	87549.53	118469.2	62768.37	76796.24
purine	270135.1	143597.1	174223.7	177106.1	182517.8	127192	202351.8	194879.2	182184.8	151997.5	200696.1	208941.7	155238
cysteine	9449.428	12172.78	6223.588	8501.997	10169.2	5042.74	23116.3	23230.13	34251.99	28885.85	7838.555	8947.409	5386.39
creatine	1.56E+08	1.59E+08	1.58E+08	1.65E+08	1.56E+08	1.52E+08	1.56E+08	1.52E+08	1.56E+08	1.58E+08	1.56E+08	1.49E+08	1.55E+08
nicotinamide	37331199	35171150	35090617	36036850	12362205	29187784	13024422	34526158	35185295	33955970	29928764	26873732	7491992
Imidazoleacetic acid	104230.9	124966.4	108527.6	104484	66508.5	86752.54	22286.67	93474.71	136693.3	58907.88	80954.45	85766.49	60773.4
thymine	118609.5	145984	118423.1	150027.8	195503	114233.8	151423.5	111243.6	157114.9	134594.5	137104.9	128367	117573
DL-Pipecolic acid	1.07E+08	1.12E+08	1.05E+08	1.14E+08	1.09E+08	1.08E+08	1.13E+08	1.19E+08	1.12E+08	1.17E+08	1.11E+08	1.11E+08	1.08E+08

N-Acetylputrescine	9008.977	11485.06	9932.931	20548.71	N/A	11414.93	28831.65	22659.36	50480.53	33328.88	12508.08	10248.38	10248.8	
hydroxyproline	1807753	3400305	2294326	3858002	3083931	1411528	3128987	1913542	3952821	4027646	4985593	3235194	2674170	
leucine-isoleucine	41802414	48137735	33998518	39061863	39355258	41411249	48052410	55517574	45008456	46868600	32726446	33857254	29112233	
ornithine	1278960	1212610	1108677	1077699	1515096	1799900	2506515	1558604	1470908	2675662	1620552	1373503	1155311	
asparagine	3307952	3252850	3477497	4257192	4280672	2843150	3692480	3299934	3769500	4925210	3353278	3574124	3167569	
aspartate	18875040	18712262	16851426	19587460	16895431	16618004	15628774	15236799	19750707	18704481	15996780	19959114	18033566	
adenine	471001.2	469047.3	609036.3	511600	556866.7	476849.6	549886.7	742379.9	576099.8	525365.2	500912.1	487186.6	501297.6	
Methylcysteine	471001.2	469047.3	609036.3	511600	556866.7	476849.6	549886.7	742379.9	576099.8	525365.2	500912.1	487186.6	501297.6	
homocysteine	114599.8	242221.1	126799.7	244485	291425	232564.9	268496.9	220496.5	253580.1	242555.7	276054.3	120318.4	127741.9	
methylnicotinamide	N/A	12155.72	9131.936	N/A	3300.04	11296.08	3209.404	8949.577	8052.374	N/A	7191.16	6812.94	N/A	
histidinol	N/A	N/A	N/A	3299.096	N/A	N/A	N/A	N/A	N/A	N/A	N/A	N/A	N/A	
lysine	2846622	2868531	3792653	2924615	3166221	2539211	3256898	2498201	4211573	2739413	2694830	4185336	2385040	
glutamine	74399060	80756570	86691794	87676378	85798251	81416271	89298741	97773366	87021172	92071889	86092175	86715052	84015204	
O-acetyl-L-serine	97393.56	73506.95	40473.2	71023.19	90020.11	6597.863	90568.34	7098.278	111318.9	95854.38	72677.23	66103.39	6226.779	
glutamate	1.05E+08	1.09E+08	99291727	1.18E+08	1.04E+08	93143388	94963799	77718042	1.08E+08	94798291	93562697	99058292	92027869	
methionine	2787541	4443348	3406134	4424043	4190751	3013957	3815062	3610690	3494740	2963680	4293713	3209407	3107743	
guanine	18757.4	70085.22	22435.19	77644.11	85664.95	54993.66	83594.43	39484.1	71701.12	39643.31	27785.66	60219.91	78656.9	
histidine	18202724	21858379	19435369	23200671	22342076	18642182	22682073	20772152	18492162	21986764	26407341	19546266	18384126	
2-Aminooctanoic acid	34248925	15587941	28950297	19980025	17621464	11814411	27324849	21158750	18953966	21497263	23973624	27493367	19504589	
carnitine	32756612	38909406	34851244	39474529	34913861	36659996	34759041	45157213	44119287	47389320	43653236	39693037	39058210	
Methionine sulfoxide	323791.5	371638.4	399695.1	347702.3	406355.8	263450.4	489711.2	237788	356763.2	433576.9	350061.6	375765.4	637260.3	
phenylalanine	18987288	16981692	15651800	18303951	15232576	13798478	17666672	14590364	14435402	16127355	16576030	16995163	11657816	
Pyridoxamine	3298.827	N/A	6609.739	5780.125	N/A	3301.881	N/A	2477.614	N/A	N/A	N/A	3300.691	N/A	
pyridoxine	2477.648	N/A	N/A	N/A	3302.663	3833.511	N/A	N/A	N/A	3169.143	4178.611	N/A	N/A	
1-Methyl-Histidine	42632.64	18786.89	44807.45	64831.38	78975.93	52330.86	113507.4	50779.28	9017.096	44675.53	46235.66	46403.13	50964.54	
N-acetyl-L-ornithine	N/A	8982.257	12597.13	6572.217	N/A	4979.149	N/A	N/A	4862.534	N/A	3308.854	9063.535	26272.63	
arginine	9106568	8121419	9062811	11599349	10280649	8279902	9625279	7419679	10106472	8613577	5313072	9741328	8046683	
citrulline	155244.1	232114.6	180424.1	303123	284373.9	183310.4	194280.8	170907.7	201907.4	266212	155332	272654.5	209913.7	
N-carbamoyl-L-aspartate	109014.4	104881.3	173430.4	127194.1	150292	98281.22	116446.6	147007	206473.1	128102.3	128831.9	108237.7	143670.4	
glucosamine	1253092	869646	943477	1277743	1269173	1231936	2055679	1784325	803261.2	1035464	1622369	1130506	703041.6	
tyrosine	1447113	1344418	1588367	1620245	1821671	1718731	1367834	2468557	1482339	1393409	1310549	1585343	1598218	
Phosphorylcholine	2.31E+08	2.75E+08	2.67E+08	3.05E+08	2.84E+08	2.55E+08	2.68E+08	2.96E+08	2.95E+08	2.98E+08	2.83E+08	2.76E+08	2.57E+08	
3-phospho-serine	81570.6	64189.65	60092.2	81989.62	137288.3	47737.63	82904.09	90267.15	167563.9	114154.7	128546.8	61831.52	75512.47	
N6-Acetyl-L-lysine	13542003	18960390	14009128	15326564	17847545	10892493	24421206	8781471	17945734	14343448	15395822	12005511	14480919	
Acetyllysine	11360834	17864675	13241443	12438551	14489971	11060529	12367402	11087156	14860191	12742781	14480780	11660464	11527274	
N-acetyl-glutamine	34474.63	55052.11	38397.32	44810.03	29650.61	25238.71	43402.02	33134.34	35751.48	29070.69	37164.76	34431.85	38395.52	
N-acetyl-glutamate	537304.3	498389.9	474244.7	486873.3	519992.4	452383.6	527483.2	409010.1	450748.6	442187.1	325078.2	445595.3	403861.8	
Ng,NG-dimethyl-L-arginine	2092913	2565160	1456291	1795170	2020229	1703795	2442931	1339574	2429613	2216529	5673524	2154712	1589772	
Acetylcarnitine DL	62761578	70152897	53110802	68565389	57714308	53277923	42613687	76007936	81276687	74812954	56843515	47151516	53769398	
tryptophan	5041863	6077852	4701816	5379601	5389946	5102621	6056499	7119933	5584990	4733893	5366610	4704561	4923621	
Kynurenine	35282.82	68505.85	24522.86	59851.32	43825.56	30404.45	57904.82	74984.07	47978.61	145602.2	75783.82	37906.4	43881.49	
N-acetyl-glucosamine	30045.31	21471.36	38685.88	46319	52173.59	40978.85	42484.47	53569.71	30574.89	20565.93	32060.07	30347.48	36345.5	
Flavone	17239.32	17519.99	41585.86	56084.55	54204.23	26474.56	57352.98	6577.482	13645.07	20994.33	26348.39	55052.69	41375.62	
cystathionine	3903984	5702959	4888264	4729729	6248365	5952605	6785426	4384170	4331423	5069158	5300269	4428640	4337306	
5-methoxytryptophan	14504.7	6537.03	52333.6	16307.25	27252.02	11068.4	5099.848	11504.02	17592.4	N/A	4912.368	31323.53	37135.66	
Cystine	64420.15	57843.3	55115.95	68281.65	92561.99	54560.96	109841.3	45008.98	47943.35	98473.38	83116.39	81056.16	89299.28	
cytidine	712852	1235517	1160336	1542913	1845050	811847.5	859597.2	1374433	1254531	846763.6	695374.5	831624.7	1785282	
biotin	696774.1	643367.1	786388	789358.3	923486.9	658746.5	884989.2	534588.8	528720.2	825270	431973.4	839500.9	942224.8	
deoxyadenosine	4259.732	10964.01	23956.53	9169.46	4239.469	2481.375	3301.552	22297.42	4126.894	8261.452	3218.168	2477.958	18441.18	
Glycerophosphocholine	43847064	36507527	47489841	55509421	44749586	35990880	41124562	41571727	61307112	55715812	40944480	56718331	57517551	
acadesine	4125.169	N/A	N/A	4959.913	5787.291	N/A	6597.781	N/A	6611.065	N/A	N/A	5783.408	12383.98	
D-glucosamine-6-phosphate	585914.7	574583.4	463167.1	430854.2	410382.5	416461.3	567149.6	649026	476080.2	545866.9	525867.9	453489.4	437038.4	
D-glucosamine-1-phosphate	362492	253794.4	334312.7	139489.9	397781.9	127769.7	188643	341873.3	268305.5	347920.6	190293.3	340689.2	421979.8	
thiamine	N/A	N/A	N/A	N/A	N/A	N/A	N/A	N/A	N/A	N/A	N/A	N/A	N/A	
S-ribosyl-L-homocysteine-posi	29216.73	22337.68	36192.94	19976.94	16529.99	26434.9	46707.5	42749.29	19630.02	31984.87	62639.83	28162.93	23126.4	
deoxyguanosine	42847.15	48441.27	57712.64	39505.44	47460	52498.95	43671.59	45707.57	74337.57	70288.02	59124.73	33784.95	47312.93	
adenosine	13122649	8011708	8610926	12377274	15244634	4473356	7506051	29142187	17039914	10688760	9554594	7475368	15799659	
1-Methyladenosine	95850.77	100631.3	111402.7	154913.5	125511	122215.8	126107.9	151799.8	124843.5	111843.4	110782.3	136191.8	95578.91	
guanosine	34686.73	61061.76	52849.61	77298.66	79209.81	48652.2	36056.28	96493.72	60968.44	60245.86	56241.07	56961.03	85059.98	
L-arginino-succinate	601825.6	372477.4	514148.2	677747.5	654145.1	516786.8	515248.2	535934.6	844272.9	667285.9	511075.9	579101	606162.9	
S-methyl-5-thioadenosine	14269.1	8281.639	2510.943	9564.746	78794.21	8367.02	57547.43	76384.83	152059.1	190182.2	13471.21	20259.67	12551.22	
7-methylguanosine	580570.9	483137.1	403937	512031	564408.9	401361.4	606173.1	470731.3	593790.3	536852.9	530083.1	549977.4	480657.8	
dCMP	112318.7	71024.04	103241.3	117238.2	113970.9	79955.31	68548.8	93343.11	72675.5	102230.6	95800.18	112848	83490.42	
glutathione	608612.7	1053382	360457.4	533785.7	431305.8	484752.4	463493.4	1448705	2436987	609073.6	564700.1	706039.8	438809.8	
dTMP	41276.08	58598.25	45968.04	43130.63	17792.39	40438.14	33803.32	64938.49	40674.58	56166.66	50394.2	59801.87	35544.8	
CMP	4221245	3607439	2764545	3406587	3590153	3086793	2679291	3962368	3792106	3752145	3035735	2868870	2777632	
UMP	2327456	2335055	2335740	2714354	2322675	2941589	1597512	2897164	2643967	2277203	2146677	2127337	2519152	
dAMP	145877.8	118407.7	107452.3	190237	135518	116450.9	104867.2	115887.8	169946	115183.5	93080.06	116500.9	78855.35	
Nicotinamide ribotide	4804.464	2409.952	6332.266	17974.54	48173.66	6588.606	4911.317	31597.87	N/A	33595.52	4712.664	N/A	32491.64	
aminoimidazole carboxamide ribonucleotide	18243.01	17757.17	37132.28	18224.59	31363.72	15828.85	15763.54	18219.03	19818.54	15879.89	23126.6	42120.28	32227.71	
thiamine-phosphate	20742.13	52033.46	39633.48	45422	29717.49	33031.41	50380.21	32520.21	47139.11	66068.13	23123.33	36055.07	40533.08	
dGMP	14869.62	19513.71	4121.871	12390.38	10733.01	9930.57	7271.22	13193.62	9931.944	4965.647	4951.964	N/A	7424.747	
AMP	50646759	56267979	53865057	71485467	63882427	48888522	43050614	51167376	49188073	57003849	44895306	45326413	58776386	
IMP	4849543	8751442	6173199	9085063	8137840	5525314	3525127	6405736	5226066	5935435	4810495	4774226	6767109	
S-adenosyl-L-methioninamine	N/A	N/A	N/A	N/A	N/A	N/A	N/A	N/A	N/A	N/A	N/A	N/A	N/A	
GMP	4272521	5577784	3923176	6228813	5997996	3313362	3079238	4892463	3895068	3854979	3767337	3165072	4243917	
xanthosine-5-phosphate	8260.489	16519.66	N/A	4130.194	5422.951	8260.489	4955.207	5792.934	N/A	2477.529	4955.172	6612.932	12407	
riboflavin	82616.64	66865.7	4593.259	4274.537	9400.091	72650.93	116448.1	6184.189	75358.51	5928.335	87306.08	66917.83	71858.38	
S-adenosyl-L-homoCysteine-posi	6416475	4644401	4710542	5692652	5768206	4394536	5266255	4332864	6578289	6137039	4732316	4022300	6703074	
S-adenosyl-L-methionine	63140.64	534773.4	281028.8	198205.3	195142.6	242799	291486.4	118928	323709.4	382901.1	457289.5	386726	608643.9	
folate	23126.17	26394.61	50392.34	56855.62	52854.11	81784.46	6451.508	20652.97	14044.11	32219.55	39640.71	23980.56	6836.3	
7,8-dihydrofolate	2477.702	4130.041	5025.223	4127.833	3346.646	4130.275	4130.293	2477.704	N/A	4130.042	4051.975	N/A	3215.771	
5-methyl-THF	27137.67	18130.07	27146.69	12549.56	24621.12	25909.84	23928.2	22727.41	25231.93	29338.18	20192.02	12056.41	20914.23	
Diiodothyronine	N/A	N/A	N/A	N/A	N/A	N/A	N/A	N/A	N/A	N/A	N/A	N/A	N/A	
glutathione disulfide-posi	6312526	3947142	5010234	5891969	5664565	5774161	5791230	6793447	6907400	6936257	5953600	5747582	6978570	
NAD+_posi	6868498	5789690	4250964	4817539	5430047	4636918	4854005	6359617	6932656	5360127	4924837	5442973	4706796	
NADH	581411.8	552434.6	625998.6	697872.7	734211.4	356783.5	768026	314662.7	687979.7	410467.8	645819.2	725035.8	467471.3	
dephospho-CoA-posi	56071.73	60780.64	32998.38	42937.43	45857.58	43775.33	38817.24	61249.15	11333.71	52843.65	34691.64	15411.32	31870.65	
NADP+_posi	304678.2	259314.6	395778.2	495578.1	377237.8	442662.7	368954.1	343613.8	411501.6	446084	365383.7	385913.9	361477.4	
NADPH	70563.07	63536.93	65999.29	98182.28	83426.72	62581.64	117940.7	39642.71	62912.95	69367.81	79210.4	75115.92	61917.47	
coenzyme A-posi	39063.72	102982.6	26254.83	28422.3	26579.14	49845.84	17377.29	145706.8	197332.6	43330.13	21746.21	37844.5	28998.99	
FAD	399732.1	545919.9	379833.9	513705	359838.9	388989.9	414560.7	403030	540949.8	515372.6	450063.9	412105.4	423409.3	
acetyl-CoA-posi	1982.081	N/A	N/A	5450.824	7437.967	1982.023	3484.794	2472.938	2594.049	2968.376	6633.314	N/A	2911.208	

propionyl-CoA-posi	4923.62	9900.36	3306.524	2499.853	2477.648	2425.483	N/A	3302.719	8208.132	4906.727	N/A	2475.671	5005.93	
acetoacetyl-CoA-posi	N/A	8233.963	7432.759	N/A	8287.981	4955.181	7432.771	7432.932	13215.56	5785.416	2425.623	8882.309	12387.76	
malonyl-CoA-posi	N/A	8260.328	N/A	N/A	4130.261	5781.467	N/A	14038.13	8283.584	4130.114	7435.255	7398.504	6607.485	
succinyl-CoA-posi	3331.685	10735.49	N/A	4955.232	4939.016	N/A	N/A	N/A	4127.033	N/A	N/A	4955.173	N/A	
sarcosine	23622314	25076195	23261222	26965524	25695411	21504143	23855299	25864395	29684073	29629634	27212762	26936577	26900435	
putrescine	11553.23	3880.415	20926.51	89357.55	51825.15	64498.7	95639.79	15279.43	18450.95	9560.998	57247.86	116323.5	97490.88	
spermidine	60874.55	73592.36	190276.2	87650.25	165993.7	27243.6	125173.2	92912.24	129217.2	175754.9	130334.3	197297.5	60115.48	
N-acetyl spermine	56871.88	19580.61	59763.52	58292.12	14783.7	52179.06	68566.39	61642.52	13226.93	19525.98	51720.19	67634.57	59198.16	
N-acetyl spermidine	25581.39	38296.49	59313.18	50573.86	60028.07	63213.01	71620.67	9927.56	46467.83	51654.34	60544.32	4614.731	63300.32	
Nicotinamide Riboside	N/A	9673.623	13937.68	5230.753	13105.31	16330.28	N/A	2475.125	7163.776	10436.56	4795.692	9798.261	15861.02	
Adenylosuccinate	209770	203989.6	120576.7	92463.9	85062.68	88366.47	66070.28	246107	183343.3	104884.4	97452.09	71026.28	71852.96	
cholesterol	184815.2	229592.8	237157.5	1818610	3845339	359627.2	3617547	196552.3	979483.7	254456.5	187467.7	199033.4	4022461	
arginosuccinic acid	460061.7	359647.7	284373.5	593620.5	551415.9	367334.1	341900.7	457036.8	527858.3	592892.3	373842.2	411179.3	448498.7	
phosphocreatine	4201208	3887395	5230796	3783003	3915016	2872636	6175433	3063237	5837287	5482801	6376827	4712822	3141131	
retinoic acid	11113.45	3667.718	7397.434	8249.712	8095.305	6135.332	15591.85	3115.25	9280.8	5038.955	5084.168	N/A	6679.403	
spermine	505398.2	648295.1	685354.3	524428.8	609125.7	670619.9	569115.8	652518.9	817302.4	697410.9	706445.7	627550.3	601115.5	
HMG-CoA_pos	8258.033	3157.876	6859.825	8953.726	10587.59	3983.183	8724.883	6605.463	9238.367	4684.802	7360.329	13178.98	13960.43	
N-acetyl-L-aspartic acid	9206557	7796160	9290669	7435841	8441058	7144562	8971049	7367402	10446932	9376917	6936283	6752714	8383097	
N-acetyl-L-aspartylglutamic acid	35584665	37537107	41909591	40442547	36780592	35879567	29940807	39221282	43962993	39659002	35153655	39576045	34170060	

SUPPLEMENTARY TABLE 3. NORMALIZED DATA.

Label	MUT	MUT	MUT	MUT	MUT	MUT	MUT	WT	WT	WT	WT	WT	WT
glyoxylate	0.190685	0.309902	-1.320821	-1.482224	-0.309863	-0.121305	0.609944	0.538242	1.180288	0.902535	-0.225457	1.422582	-1.694509
glycolate	-0.296717	0.225597	1.966814	-0.894748	-0.55156	1.466082	-0.733985	-0.686473	-0.62427	-0.466057	-0.570707	-0.445605	1.611628
pyruvate	-0.641351	1.729224	0.782009	-0.20691	-0.877771	-0.815887	-1.558488	0.528663	0.361077	0.327473	0.162363	1.43025	-1.220652
lactate	0.671377	0.819196	1.205929	-0.376886	-1.210287	1.003737	-2.063355	0.060827	0.629981	0.132653	0.105376	0.417393	-1.39594
2-oxobutanoate	-0.372023	-0.888691	0.935919	-0.687567	-0.720395	2.046104	-1.207541	0.023351	-0.792302	0.3559	0.216449	1.585289	-0.494495
acetoacetate	-0.533671	-0.812683	1.424361	-0.213176	-1.294959	1.528809	-1.05224	-0.049081	-0.226416	1.059667	0.536774	0.894949	-1.262332
glycerate	-0.756787	-0.474424	-0.106569	-0.268762	-0.374017	-1.393053	-0.736001	-0.415085	0.577091	0.133111	2.481949	1.346519	-0.013972
uracil	-0.050542	0.005149	0.292937	1.986267	-0.010779	-0.305674	-1.504547	-0.553514	1.755571	-0.079515	-1.318227	0.367415	-0.584542
fumarate	0.374796	-0.148021	0.75974	-1.108023	-0.978087	-0.965202	-1.699914	0.10844	1.165768	1.612115	0.31099	1.000409	-0.433013
Maleic acid	0.307149	0.105217	0.035763	-1.035352	-1.475908	-0.552528	-1.542355	0.630178	1.071881	1.701376	-0.012019	1.165665	-0.399068
2-keto-isovalerate	-0.083778	0.388541	0.696737	-1.160682	-1.018168	-0.788671	-1.773392	0.644374	1.548804	1.091041	-0.063122	0.988236	-0.46992
Guanidoacetic acid	-0.473697	-0.479095	-0.463223	-0.476033	0.687612	2.792634	1.228979	-0.468448	-0.47754	-0.469986	-0.469058	-0.471278	-0.460868
succinate	-1.562484	0.705457	0.709087	-0.938297	0.492466	1.144822	-1.742444	-0.449171	-0.488247	0.155009	-0.276476	1.035585	1.214691
Methylmalonic acid	-0.70804	0.773637	1.518384	-1.063134	0.03055	0.510366	-2.132887	-0.005399	-0.614131	0.259912	-0.529507	1.040975	0.919274
3-S-methylthiopropionate	-0.13511	0.59292	-0.068775	-0.504458	-1.037619	-1.034513	0.294567	1.499024	-1.066426	0.560311	-1.054412	2.076621	-0.122131
nicotinate	0.723652	-0.0968	1.455461	-0.108574	-0.009032	-0.070361	0.2678	-2.000553	-1.648794	0.258	1.401253	0.411191	-0.583242
taurine	0.249629	-0.217316	-0.052381	-1.80353	1.236883	0.793211	1.296839	1.296824	-1.421719	-0.290747	0.140246	-0.955277	-0.272663
Pyroglutamic acid	0.573325	-0.667659	1.006511	-0.73894	-0.645337	1.348836	-0.589046	1.161865	-0.728531	0.226821	0.366772	0.783677	-2.098293
Citraconic acid/itaconic acid	-0.346032	0.257081	1.340702	-1.362356	0.166466	0.479974	-1.776213	1.326409	-1.304606	0.354516	-0.271424	1.038	0.097484
2-ketohaxanoic acid	1.284827	-0.818268	2.276108	-0.683952	-0.874349	0.229623	-0.500179	0.07764	-0.164704	0.838467	0.059802	-0.255792	-1.469224
N-Acetyl-L-alanine	-0.317453	0.756849	1.208752	0.448987	-0.058872	-1.826234	-1.941807	0.442532	0.403652	0.171279	0.760093	0.867047	-0.914826
oxaloacetate	0.538619	0.45008	0.690778	-0.139754	-0.224683	-1.0262	-1.793096	1.538197	0.506946	-1.654777	0.99141	0.473628	-0.351148
Hydroxyisocaproic acid	-0.094773	0.765569	1.890519	-1.097502	-0.803903	0.389773	0.195551	-0.290547	-1.835534	-0.302564	1.332717	-0.552929	0.403623
malate	0.023957	0.23668	0.424244	-1.563951	-1.43575	-0.545916	-1.296499	1.248811	1.361059	1.16536	0.12898	0.605288	-0.352263
hypoxanthine	-1.0849	0.086153	1.196572	1.011348	1.07162	-0.564785	-2.221717	1.005038	0.281986	-0.100597	-0.307853	-0.77531	0.402446
anthranilate	0.024122	0.110854	-0.039108	0.785682	1.39452	0.591089	1.660894	-1.882594	-1.096444	-0.156914	0.293799	-0.97941	-0.70649
p-aminobenzoate	1.281566	-0.090369	-1.260196	0.793203	1.342765	-1.10728	-1.273471	-0.036427	0.40656	-1.31541	-0.412241	0.930144	0.741155
p-hydroxybenzoate	-0.259639	-0.275055	-0.238641	-0.28797	-0.445254	3.303746	-0.421088	-0.275926	-0.138885	-0.301478	-0.319747	-0.370504	0.030442
acetylphosphate	0.412715	-0.54295	0.870513	-0.362334	-0.404129	0.272486	-1.130733	0.412912	-0.036627	-0.890412	1.204814	1.926442	-1.732698
Carbamoyl phosphate	0.74912	0.390849	0.454964	-0.091449	-0.577514	-0.52753	-0.121742	1.223061	-1.049238	1.212091	-0.194928	0.888361	-2.356044
a-ketoglutarate	-0.26154	-0.151336	1.100097	-0.663584	-1.868084	-0.032342	-0.013326	1.703419	-0.473328	1.357789	0.431655	0.133069	-1.262489
Phenylpropiolic acid	0.418493	-1.086686	0.796929	-0.597086	-2.053256	0.699265	-1.029964	0.12317	1.748862	0.846794	-0.084096	-0.071793	0.289367
2-oxo-4-methylthiobutanoate	-1.313523	1.50874	-0.02833	-0.495147	0.389363	-0.161411	-1.010926	2.313122	-0.387056	-0.633247	0.493636	-0.63742	-0.037802
2-Hydroxy-2-methylbutanedioic acid	0.286387	0.595537	1.786488	-1.186601	-1.41404	-0.490852	-0.162485	0.423214	0.020121	1.108906	0.828952	-0.194812	-1.600815
3-methylphenylacetic acid	-0.928001	-0.363519	0.12253	0.536685	-0.468301	1.410447	-0.287311	-0.02355	-0.88018	2.222948	-0.588499	-1.392896	0.639646
xanthine	0.418792	0.791037	1.191824	-1.009947	-1.004889	1.21826	0.591956	0.60095	-1.009423	-1.008022	-1.00512	1.226382	-1.001801
Hydroxyphenylacetic acid	-0.397621	-0.5025	1.263948	0.718137	0.594908	-0.195139	0.630163	-0.830185	-1.889854	-0.305485	-0.483186	-0.551378	1.94819
2,3-dihydroxybenzoic acid	0.005772	0.670473	0.654195	-1.016557	1.136827	-1.587028	-1.218529	0.424753	-1.315609	1.5915	0.17353	-0.078628	0.559301
orotate	1.37321	-0.101056	0.974346	-1.372299	-0.222481	0.066357	-1.322704	1.556526	0.305252	0.218671	0.624242	-0.656651	-1.443414
dihydroorotate	0.089871	-0.301226	-0.519233	0.429917	-0.750645	1.569323	0.340165	-1.369042	-1.869582	1.527382	0.748999	-0.081897	0.185968
allantoin	0.606541	-0.864589	-0.433041	-0.834641	0.527443	-0.792729	1.003072	-0.461322	0.601287	0.940807	0.893182	1.008107	-2.194116
Aminoadipic acid	1.12939	-0.53624	0.957098	-0.366364	-0.573782	1.338395	-0.261547	0.350692	0.17901	0.252648	0.271762	-2.625183	-0.115879
Indole-3-carboxylic acid	-0.134699	-1.102276	0.930174	-0.151331	-1.42428	-0.423066	-0.675455	2.266807	0.889315	-0.897042	0.693195	0.016735	0.011922
phenylpyruvate	0.145435	-0.052196	0.834394	-0.161766	0.184616	-1.987301	1.655897	0.941069	-0.402043	-1.411536	1.004863	-0.689197	-0.062236
Atrolactic acid	-0.112036	-1.516111	1.540746	0.076652	1.610624	-0.564983	0.084164	0.642856	0.529275	-1.592717	-0.132223	0.41714	-0.983388
Phenyllactic acid	2.304283	-0.512401	1.001594	0.751339	-0.235697	-1.072374	-0.463367	-1.266447	-1.077444	0.714564	0.187626	0.026771	-0.358447
quinolinate	-0.584323	0.570602	-0.553556	-0.079634	0.197758	0.881636	-0.392982	-1.938203	2.327354	-0.388234	0.322381	-0.70852	0.345721
phosphoenolpyruvate	-0.780653	0.493955	0.279429	-0.454201	-0.099152	-1.30607	-0.48953	0.1017	0.941471	0.544197	0.819433	1.851052	-1.90163
Uric acid	0.158367	-1.477143	-0.373712	-0.770083	1.639685	0.156922	-0.866413	-1.14158	0.526725	1.360156	-0.369965	1.402991	-0.245951
dihydroxy-acetone-phosphate	-0.213436	0.845605	1.221985	-1.714893	-1.722399	1.290995	-1.131688	-0.257903	0.364461	0.092976	0.06813	0.649684	0.506483
D-glyceraldehdye-3-phosphate	0.460233	0.476862	1.128264	-0.641422	-0.954699	-0.20212	-0.87152	-1.059091	-1.348591	-0.00272	-0.073869	1.070652	2.018021
sn-glycerol-3-phosphate	-1.06842	0.17899	0.436949	0.680393	1.557087	-0.829935	-1.107737	-0.758851	0.788126	-0.918006	-1.126526	1.378445	0.789486
shikimate	-0.718541	-0.566098	0.964021	-0.803371	1.108987	-1.081664	1.520624	0.20539	0.260981	0.536334	-1.223869	1.11515	-1.317945
aconitate	0.262065	-0.108464	2.182394	-1.848216	-0.692701	-0.724025	-0.806688	1.241377	0.707173	0.069394	-0.0229	-0.075299	-0.18411
allantoate	-1.064038	-0.533821	1.112086	-0.724564	2.26618	-0.213252	-1.45887	-0.707669	0.594578	0.79497	0.093564	-0.124663	-0.034503
Ascorbic acid	0.056104	0.462481	0.607075	-0.047461	-0.016994	-1.086149	-0.43475	0.909293	0.975066	0.256271	0.796024	0.261286	-2.738246
2-Isopropylmalic acid	0.128258	-0.079828	0.931965	-0.38129	0.440798	-0.662537	-0.001407	0.580802	0.306898	0.429055	0.858491	0.416	-2.967206
N-carbamoyl-L-aspartate-nega	-0.924498	0.29317	-0.07166	-0.796042	0.631823	-1.294467	-0.426866	-0.887922	2.586966	-0.036031	0.718109	-0.164796	0.372214
Pyrophosphate	-0.003424	2.628611	0.16658	0.144382	0.954884	-0.054509	-1.535649	-0.821387	-0.10611	0.241756	-0.818824	-0.533977	-0.262333
glucono-?-lactone	-2.304352	0.941507	0.136114	-0.128799	0.501501	-0.64682	0.395848	-0.094785	1.239396	0.62555	0.266708	0.652125	-1.583994
myo-inositol	-0.224164	-1.889206	1.433827	0.634114	1.008719	0.098389	0.368931	-0.792158	-0.404793	0.401325	0.926654	0.148942	-1.71058
hydroxyphenylpyruvate	0.944258	-0.014881	-0.065496	0.562489	-1.181138	0.098841	1.374898	1.154515	-0.899846	-1.623028	0.879465	-1.384914	0.154837
homocysteic acid	0.536667	-2.112408	-0.310169	-0.248179	0.356727	-1.514951	0.127881	0.321286	-0.136859	1.214144	1.445513	0.83705	-0.516702
4-Pyridoxic acid	-0.200012	-2.247806	1.073504	0.315275	0.924797	0.193926	0.511644	0.507673	-1.994772	0.139951	0.428358	0.191517	0.155946
3-phosphoglycerate	-0.362538	-0.07191	-0.885254	-0.16847	0.490512	-1.084398	0.299496	-0.992501	-0.718774	0.989507	2.015295	1.445207	-0.95617
Indoleacrylic acid	-0.047799	-0.617481	0.845203	0.16334	0.234806	-0.567953	-1.337757	2.37702	-0.686999	0.661916	-0.39731	-1.260422	0.633437
Kynurenic acid	0.293873	-0.402023	2.653171	-0.39317	0.44577	0.511991	-0.232614	-0.878215	-0.702624	-0.614462	-1.338717	-0.114578	0.771598
citrate-isocitrate	-0.645684	-0.629202	0.262477	-0.596249	0.085831	0.254739	-1.578207	2.715028	-0.720717	-0.03395	0.280932	0.151017	0.453986
isocitrate	-0.961467	0.625579	-0.389871	-0.128201	-1.357551	-0.82474	2.307632	-0.436538	0.297855	-0.317735	0.935842	0.955382	-0.706185
citrate	0.042287	-0.778861	1.309367	-1.306648	1.021674	0.134492	-1.691131	1.950866	-0.280536	-0.009981	-0.003489	0.015752	-0.403792
2-dehydro-D-gluconate	-0.193853	-0.62793	0.709584	-0.116864	2.210022	0.262524	0.361015	-0.329541	-1.665479	-0.395684	1.29985	-0.540764	-0.972878
D-gluconate	-0.346006	-1.772039	0.008889	-0.965927	1.538871	-0.394671	0.858401	0.091564	-0.86152	0.678918	1.495897	0.555561	-0.887938
D-erythrose-4-phosphate	0.163779	-0.006676	-0.366476	0.62546	-0.525405	-0.114338	0.259299	-1.643431	1.104948	-0.760772	2.223694	0.289705	-1.249788
Xanthurenic acid	-0.55888	-0.289479	0.190054	-0.351195	-1.015057	0.413068	-0.19219	2.179808	-0.930422	0.32469	1.351451	0.446085	-1.567932
D-glucarate	-1.509863	-0.790738	0.278351	0.601579	-1.617595	2.193986	-0.800626	0.314782	0.149259	0.239397	0.11366	0.255389	0.572417
deoxyribose-phosphate	0.685591	-2.047561	0.873614	0.287688	-0.264153	0.305102	-0.324481	0.531541	-2.013962	0.743417	0.67952	0.872904	-0.32922
pantothenate	-0.326834	-0.293822	1.265634	-1.095078	-1.234036	-0.811256	1.406933	1.234821	-1.431136	0.960223	0.55252	-0.016121	-0.211849
prephenate	-0.694499	0.678064	0.864702	-0.700829	-0.649812	1.694528	-0.653934	-0.680277	0.11385	-0.684445	2.060337	-0.687946	-0.659739
deoxyuridine	-0.951222	-0.963538	-0.927326	0.119831	-0.913595	1.61475	-0.917066	0.585922	0.45557	-0.942756	0.707311	1.697132	0.434986
ribose-phosphate	-0.625411	0.564147	0.955791	0.292608	-0.678741	-0.103668	-2.679677	1.438611	-0.130455	0.468674	0.483023	0.23075	-0.215651
thymidine	-0.646707	0.432626	-1.041716	-1.301305	-1.269346	1.189419	-1.453447	0.456843	0.483179	1.153375	0.63647	0.247633	1.112977
uridine	0.218198	0.378709	0.501215	0.244245	-0.600956	-0.510733	-1.808681	2.496956	0.219332	-0.021647	0.068163	-0.037924	-1.146877
deoxyinosine	0.062754	-0.69142	0.447675	0.087057	-0.766671	0.439131	-0.227101	0.395881	-1.275377	1.884846	1.590066	-0.374062	-1.572778
D-glucono-?-lactone-6-phosphate	0.687698	0.58952	0.311514	-1.234925	1.166919	0.078181	-0.854168	-1.054827	-0.667237	0.171383	-0.145793	2.11883	-1.167094
hexose-phosphate	1.211218	1.533441	-0.28604	-0.535973	-0.461453	-0.599052	-1.337234	1.733772	0.251757	0.52336	-0.085912	-0.654044	-1.293839
glucose-1-phosphate	0.319986	0.500436	1.238378	0.570571	0.046492	-0.236534	-1.783634	-0.464662	-0.475374	0.970036	0.410938	0.934175	-2.030805
glucose-6-phosphate	1.715019	0.371067	-1.061307	-1.370558	-0.379717	-0.229392	-1.153307	1.427623	-0.181085	0.52064	1.261913	-0.584706	-0.336191
fructose-6-phosphate	1.401373	0.793765	-0.843612	-0.899314	-1.383809	-0.305742	-0.294245	1.45006	-0.527295	0.874331	1.205892	-0.502462	-0.968942
1,3-diphopshateglycerate	-1.319058	0.374149	1.466629	0.215908	0.809118	1.117266	-0.347575	-1.561007	-0.90586	-0.498523	1.222445	0.319082	-0.892572

2,3-Diphosphoglyceric acid	-1.314221	0.372266	1.876554	-0.070014	0.582867	0.601481	-0.183661	-1.739676	-0.724252	-0.498054	1.082711	0.67827	-0.664272
S-ribosyl-L-homocysteine-nega	-0.487898	-0.964466	0.827272	1.007405	1.91543	-0.23187	-1.236873	-0.192419	0.741542	-0.359635	-1.539351	0.834247	-0.313385
inosine	-1.693173	0.262653	0.985041	1.098725	0.994098	0.260864	-1.57568	0.83074	0.192277	-1.516467	-0.266135	-0.068286	0.495344
6-phospho-D-gluconate	-1.095279	0.606277	1.157338	-0.275175	-0.600763	1.742612	-1.267772	-1.127121	-0.495056	-0.793692	0.284313	1.088175	0.776143
xanthosine	-0.013449	-0.002141	0.017319	-0.988429	1.130397	-0.616354	-1.149259	-0.816691	2.397002	0.633591	-1.057881	0.267247	0.198648
D-sedoheptulose-1-7-phosphate	0.880518	0.120594	-0.157056	-1.175409	-1.324865	-0.238554	0.032447	1.867976	-0.806822	0.428482	1.494852	0.072388	-1.194551
N-acetyl-glucosamine-1-phosphate	-1.663923	-1.069705	1.096255	-0.722067	0.891992	0.221709	1.756722	-0.863708	-0.649417	0.01695	1.04772	0.256281	-0.31881
glutathione-nega	-0.383133	1.249193	-0.456971	-0.804903	-0.794497	0.009925	-0.88507	1.36095	2.269497	-0.125015	-0.150405	-0.37201	-0.917561
dUMP-nega	-1.03391	1.995022	-0.806019	-0.901231	-0.760189	0.013111	-0.228934	1.486737	0.037711	0.362993	1.074907	-1.163478	-0.076719
Geranyl-PP	-1.120251	-1.098183	1.451704	1.102295	0.523188	0.837071	0.203709	-1.201553	-0.936326	-0.82218	-0.749953	0.943025	0.867455
O8P-O1P	1.109905	0.064549	0.787367	-0.858504	-1.441204	-0.237526	-1.929063	1.127125	0.18844	0.508166	1.167985	0.258951	-0.746191
dTMP-nega	-1.273513	-0.777618	-0.028937	0.553634	1.330313	1.457557	-1.754495	0.591159	-0.173784	0.567082	0.713374	-0.074284	-1.130486
cyclic-AMP	-0.645182	0.353171	1.646516	0.677444	0.880932	-0.521649	-1.372805	-0.309078	1.790653	-0.485817	-0.866753	-0.121628	-1.025803
fructose-1,6-bisphosphate	-0.061459	0.459038	0.810751	-1.056437	-1.259222	0.789215	-1.400386	-0.305992	0.294936	0.928492	1.326144	0.942309	-1.467388
trehalose-sucrose	-0.425952	-1.339466	1.828327	0.724115	0.267558	-0.049712	-0.113186	-0.107603	0.016727	-1.517938	-0.819105	1.743686	-0.20745
orotidine-5-phosphate	0.703574	0.987042	-0.294693	-0.66212	0.40755	1.998537	-0.72553	-0.342961	-1.514515	-0.954746	-0.593806	-0.262988	1.254656
SBP	-1.304878	1.332618	1.507904	0.194434	-0.156757	-0.729356	-0.720241	0.688117	-0.626981	-0.502252	0.831946	1.005891	-1.520444
trans, trans-farnesyl diphosphate	-0.539119	0.590739	0.668275	0.052895	-0.639128	0.941213	0.407152	1.141106	-2.632046	0.703853	-0.713426	-0.319771	0.338257
S-adenosyl-L-homocysteine-nega	2.002953	-1.35502	0.120042	0.076275	0.485503	-0.870394	0.599246	-0.719593	1.630069	0.159435	-0.576511	-0.921594	-0.630411
dCDP-nega	-0.640729	0.440737	-0.183006	0.359599	-0.404673	0.571561	-2.760607	-0.017424	0.285986	-0.459712	1.084738	1.149569	0.57396
5-phosphoribosyl-1-pyrophosphate	-1.184613	1.653992	0.057962	-0.261107	0.261846	0.920744	1.163871	-0.394278	-1.505994	-0.754683	1.211499	-0.15205	-1.017188
OBP	-1.095421	-1.130277	-0.805238	0.124957	0.830944	-0.828569	0.517665	1.256398	-0.697317	0.096918	0.157878	2.178643	-0.606581
dTDP-nega	-0.753938	-0.109587	0.571793	1.935219	1.2588	-0.166054	-0.738777	-1.833013	-0.762683	0.865216	-0.196173	0.443345	-0.514149
CDP-nega	-0.948836	-1.106865	0.765282	0.069449	-0.694602	1.890849	-0.953414	-0.862967	0.160524	1.157722	0.79053	0.745294	-1.012965
UDP-nega	-0.966202	0.100378	1.116147	0.805092	0.374042	0.045036	-0.134073	1.248863	-1.095767	-1.43804	0.827577	0.803344	-1.686398
Cholic acid	-0.287402	-0.125848	2.190223	0.493309	-1.019736	-1.015753	-1.022501	-0.243014	1.028489	-0.432651	0.385264	-1.04531	1.094932
trehalose-6-Phosphate	-0.164402	-1.192888	0.010162	-0.5894	-0.044437	-0.94692	2.193804	-0.845204	-0.207419	0.132808	1.529462	0.889581	-0.765145
Thiamine pyrophosphate	-0.187912	0.649451	-0.250788	-0.901108	-0.5453	0.033688	0.141923	-1.715363	0.621574	0.546591	-0.276395	2.502485	-0.618847
adenosine 5-phosphosulfate	1.9604	0.369964	-0.447181	-0.720648	-1.265645	0.070535	-0.890568	1.633529	0.760193	-0.329543	0.264062	-0.208117	-1.19698
ADP-nega	0.782591	1.828208	-0.037487	-1.254607	-0.960899	0.343546	-1.005307	1.520577	0.15077	-0.035984	0.346633	-0.312938	-1.365102
dGDP-nega	0.756619	1.534212	0.340281	-1.252544	-0.703259	0.264098	-1.450574	1.462465	0.258715	0.276733	0.293184	-0.270195	-1.509735
IDP-nega	0.405124	1.225097	-0.024958	-1.391232	-0.77251	0.394854	-1.240281	1.126674	0.592597	0.745249	1.151385	-0.823362	-1.388636
GDP-nega	-1.992021	-1.007334	1.334445	-0.29921	0.147916	0.460027	-0.235216	-1.348363	1.239726	0.533287	0.644977	0.838169	-0.316402
CDP-ethanolamine	1.651249	1.114549	-0.602303	-0.993856	-0.846545	-0.350753	-1.036082	1.02021	0.843105	0.973838	-0.001855	-0.386639	-1.384918
FMN	1.001872	0.691723	0.288449	1.5594	-1.248849	1.069382	-1.251742	-0.231468	0.692837	-1.273147	-0.00914	-0.033504	-1.255814
cholesteryl sulfate	-0.698318	-0.604546	-0.657244	0.157958	1.478686	-0.529153	1.337757	-0.685639	0.093383	-0.634143	-0.695699	-0.702166	2.139124
dCTP-nega	-1.030783	-0.015866	0.165895	-0.32733	-1.147441	-0.622404	-0.318598	-0.165741	1.859254	1.059737	1.213474	0.825207	-1.495404
dUTP-nega	0.674292	1.534256	0.376058	-1.520236	-1.243312	-0.29972	-1.394341	-0.390802	0.470878	-0.049696	0.075329	1.66299	0.104305
dTTP-nega	-0.898237	-0.706833	1.784293	-0.261795	-0.468519	0.119652	-0.883962	-0.681518	0.762946	0.610617	0.805497	1.38224	-1.564381
CTP-nega	-1.524347	0.034403	0.371444	-1.031386	-1.034855	0.321283	-0.20418	-0.624523	1.740923	1.745716	0.677217	0.095347	-0.567043
UTP-nega	-0.437358	0.013411	0.329775	-1.26022	-1.045493	-0.943185	0.20709	-0.77323	1.697558	1.103011	1.332306	0.779745	-1.003411
CDP-choline	1.638798	0.265498	0.304945	-0.578491	0.579813	-1.198361	-1.357981	-0.336211	1.442805	0.815687	-1.032803	0.478249	-1.021946
dATP-nega	-0.353889	-1.065812	0.792266	0.013483	-1.220351	0.604945	0.041497	-1.942044	0.388497	1.163177	0.753036	1.430198	-0.605003
Taurodeoxycholic acid	-0.253071	-0.152418	0.986355	-0.901296	-0.333737	0.027927	-0.208959	1.231415	0.290471	-0.438002	2.104046	-0.474799	-1.87793
ATP-nega	-0.459136	-0.796314	0.321277	-1.132417	-0.886683	0.073839	0.979802	-1.397936	0.941089	0.646943	2.038361	0.360198	-0.689022
dGTP	-0.601443	-0.87998	0.303191	-1.245182	-0.63352	-0.21812	0.696749	-1.261189	1.023618	0.873215	2.099028	0.405592	-0.561959
GTP-nega	-1.426479	0.798493	-0.558158	-1.071294	-0.533781	0.018221	1.875012	-1.153991	0.361958	0.328858	1.251867	0.734144	-0.62485
UDP-D-glucose	-0.683859	2.18451	0.744797	-1.270414	-0.901376	-0.21808	-1.276625	-0.379504	0.716359	-0.001293	-0.475213	0.801087	0.759612
UDP-D-glucuronate	-0.781081	1.71155	0.152526	-1.727834	-0.046581	0.179148	-1.30668	0.886049	0.222366	-0.018849	1.584148	-0.442135	-0.412627
ADP-D-glucose	-1.139301	1.743363	0.694502	0.972318	1.292298	0.178214	0.598368	-0.847377	-0.776023	-0.870549	-1.408218	-0.314103	-0.123492
guanosine 5-diphosphate,3-diphosphate	-2.254643	-1.327077	0.831784	0.031488	0.528221	1.453105	0.269431	-0.961629	-0.275428	0.189565	0.829613	0.201924	0.483645
UDP-N-acetyl-glucosamine	0.070773	0.381357	-0.615061	-0.393477	0.326034	-1.353282	-0.553588	0.100349	0.819766	1.941957	1.008121	0.158503	-1.891451
glutathione disulfide-nega	0.212502	-0.666749	1.015896	-0.460508	-1.140762	1.557392	-1.836182	0.437953	0.035525	0.644614	-0.020066	1.235921	-1.015535
NAD+_nega	0.232389	1.302487	0.382529	-0.863699	-1.544754	0.158471	-1.242804	1.938267	-0.003545	0.489844	-0.387182	0.526562	-0.988566
NADH-nega	-0.12036	0.197479	-0.134918	-0.088856	0.655863	-0.461915	0.701918	-1.061868	2.708761	-1.043637	-0.770129	0.192267	-0.774605
dephospho-CoA-nega	0.268629	1.725903	-0.204748	0.249158	1.020383	0.249146	-1.06375	-0.397649	-1.020994	0.90144	-0.341472	0.633622	-2.019666
cyclic bis(3->5) dimeric GMP	-0.461858	-0.507122	2.439813	-0.481447	-0.323577	-0.305195	-0.336334	-0.417851	2.043162	-0.430748	-0.422967	-0.44158	-0.354296
NADP+_nega	-0.316402	0.001085	0.618823	0.023491	-1.764346	1.873375	-1.195881	0.614781	0.648861	-0.363097	0.110026	0.990317	-1.241035
NADPH-nega	0.73804	0.391439	2.182526	-0.808981	-1.808091	-0.186685	0.054776	1.177302	-0.450755	-0.968901	-0.182647	-0.012967	-0.125054
2-hydroxygluterate	0.376291	0.803729	1.930052	-0.057748	-0.681289	-0.312934	-1.517261	-0.051881	0.47035	0.875651	-1.088654	0.667397	-1.413702
2-deoxyglucose-6-phosphate	-1.108922	0.601727	1.013993	0.258115	-0.340701	0.301703	-2.136662	0.88599	1.057542	0.805188	0.096826	-0.027986	-1.406814
4-phosphopantothenate	1.97096	-0.27686	0.359058	-0.257373	-0.892828	-1.061968	-1.166382	1.881743	-0.354862	0.234893	0.525649	-0.701267	-0.260763
dehydroascorbic acid	-0.185787	1.663046	-0.516269	-0.292965	-0.438291	-0.294089	-0.428653	2.711898	-0.516752	-0.390947	-0.278462	-0.516541	-0.51619
3-hydroxybuterate	-0.408929	-0.858081	1.225225	-0.953282	1.091715	1.288926	1.411471	-0.680409	-0.749612	-0.838873	0.979047	-0.658228	-0.84897
itaconic acid	-0.346032	0.257081	1.340702	-1.362356	0.166466	0.479974	-1.776213	1.326409	-1.304606	0.354516	-0.271424	1.038	0.097484
Urea	0.089314	-0.726214	0.500969	-0.19165	-0.427772	1.368736	-1.392949	2.285096	0.052009	0.294358	-0.537725	-0.058541	-1.255632
ethanolamine	0.462434	0.173124	0.474	-0.494828	2.216845	-0.47715	-0.750709	0.862001	-1.177281	0.223703	0.82253	-1.17185	-1.162819
glycine	-0.46987	2.100451	-0.378749	-0.490195	-0.326386	-0.307314	-0.339624	2.389183	-0.503302	-0.437589	-0.429516	-0.448828	-0.358261
alanine	-1.226764	-1.47673	-0.831926	-0.466729	0.383606	-0.857408	-0.281857	-0.355962	1.515393	0.883962	0.679876	0.423041	1.611499
betaine aldehyde	-0.748666	-0.363633	-0.177189	0.01531	-0.544481	-0.791056	0.103976	-0.69564	0.357714	1.700087	1.986238	0.70567	-1.548328
choline	-1.063788	0.333977	1.459999	0.921826	-0.812687	0.517704	-0.570756	0.747135	-1.121465	0.471943	1.382003	-1.080365	-1.185525
4-aminobutyrate	-1.764205	-0.089221	0.444364	0.752819	1.146585	-0.318686	2.065039	-1.132617	0.582829	-0.208359	-0.507123	-0.344489	-0.626935
dimethylglycine	-1.31893	0.349187	-0.018196	1.052482	-1.037921	-0.22947	-0.128413	-0.708893	2.521213	-0.014145	-0.5882	0.640056	-0.518768
serine	-1.315251	-1.343409	-0.79672	-0.373404	0.124256	-0.832275	-0.72903	-0.076315	1.223935	1.195849	1.289938	1.326764	0.305661
cytosine	-1.378714	-0.413825	-0.786853	-1.30952	0.64144	0.233946	1.478699	0.554949	-0.208337	-0.691538	1.70153	-0.685649	0.863872
Creatinine	-1.369048	-1.317456	-0.193505	0.972779	1.773578	0.439016	1.097621	-0.085667	-0.263635	0.072598	-1.043741	-0.960039	0.8775
proline	-1.133847	-0.872171	0.005533	-0.365078	1.064465	-0.719802	0.212551	1.58711	0.073949	1.748886	-1.341649	-0.724627	0.464679
indole	1.285063	1.047408	-0.849206	-0.061575	-0.071581	0.000603	1.522129	1.129183	0.050164	-1.189539	-0.462815	-0.742623	-1.657211
betaine	-1.722114	-1.323915	-1.019431	-0.327758	0.085592	0.66514	0.922115	0.042442	-0.148089	1.835795	0.240204	-0.367296	1.117315
valine	0.480325	-0.359194	-0.211681	-0.622561	0.023927	0.80563	-0.705338	2.713726	0.516674	-0.298882	-0.238765	-0.864781	-1.239078
threonine	-1.401215	-0.892802	-0.3096	0.528269	0.119111	-1.946764	0.251227	1.581633	0.603155	1.382548	-0.219457	0.403196	-0.0993
homoserine	-1.748451	0.102859	-0.105629	0.206867	0.008791	-1.165691	0.956579	-1.411785	0.842766	0.57156	1.809851	-0.418896	0.35118
purine	2.221221	-1.451798	-0.060873	-0.446642	0.415951	-1.251304	0.97039	0.345515	-0.365273	-0.940028	0.487816	0.628103	-0.553079
cysteine	-0.519286	-0.292714	-0.797299	-0.630643	-0.318462	-0.895126	1.132406	0.973281	1.8997	1.536508	-0.655216	-0.553797	-0.879352
creatine	-0.770918	-1.205369	0.901264	-0.129817	1.387665	1.178371	1.203609	-0.602161	-1.260737	-0.063523	-0.168771	-1.299221	0.829607
nicotinamide	0.823891	0.467914	0.875036	0.632614	-1.504597	0.421115	-1.44544	0.68021	0.510027	0.582442	0.191947	-0.166511	-2.068649
Imidazoleacetic acid	0.494468	1.040481	0.940912	0.439544	-0.532902	0.308986	-2.272329	0.247961	1.487895	-1.026949	-0.218148	-0.094441	-0.815478
thymine	-0.905978	-0.111476	-0.568699	0.15962	2.834729	-0.47565	0.937589	-1.016585	0.351651	-0.175759	-0.044956	-0.458681	-0.525804
DL-Pipecolic acid	-1.339649	-1.405639	-0.527741	-0.608071	1.025635	1.092407	1.39156	1.137139	-1.120344	0.703061	-0.254214	-0.426503	0.33236
N-Acetylputrescine	-0.709619	-0.556856	-0.580198	0.139541	-1.309315	-0.40542	1.041804	0.394919	2.329878	1.208017	-0.410807	-0.601366	-0.540578
hydroxyproline	-1.35549	0.089635	-0.693251	0.613824	0.290841	-1.552644	0.305673	-1.175622	0.662007	0.960732	1.973141	0.120598	-0.239445
leucine-isoleucine	-0.141832	0.423021	-0.802891	-0.582787	0.169635	0.554724	1.357327	1.905362	0.104005	0.678343	-1.163883	-1.085773	-1.415251
ornithine	-0.644658	-0.848174	-0.791395	-1.032791	0.101989	0.718387	2.015722	-0.043468	-0.380943	1.949159	0.05698	-0.434054	-0.666753

asparagine	-0.806279	-1.11942	-0.06414	0.66031	1.712195	-0.917817	0.533383	-0.601992	-0.214483	2.135154	-0.534754	-0.251317	-0.53084
aspartate	0.296785	-0.42358	-0.251535	0.585937	0.382497	0.35228	-0.871356	-2.082163	0.536852	0.57062	-1.521068	1.428834	0.995896
adenine	-1.036449	-1.27686	1.097602	-0.673179	0.740074	-0.202303	0.577993	2.414975	-0.020273	-0.244427	-0.492999	-0.749174	-0.134979
Methylcysteine	-1.036449	-1.27686	1.097602	-0.673179	0.740074	-0.202303	0.577993	2.414975	-0.020273	-0.244427	-0.492999	-0.749174	-0.134979
homocysteine	-1.519253	0.144806	-1.206312	0.254765	1.487176	0.60703	1.080036	0.098983	0.34052	0.3833	0.896722	-1.40767	-1.160103
methylnicotinamide	-1.151454	1.331001	0.908901	-1.155492	-0.519468	1.613551	-0.551672	0.781609	0.437045	-1.145042	0.348856	0.23145	-1.129284
lysine	-0.598522	-0.751253	1.418387	-0.555119	0.554529	-0.520215	0.659501	-1.004087	1.418013	-0.648793	-0.692696	1.695277	-0.975021
glutamine	-1.96632	-1.57759	0.437303	-0.488712	0.803242	0.352012	1.170031	1.459361	-0.693414	0.580014	-0.118058	-0.218562	0.260692
O-acetyl-L-serine	0.836254	0.127482	-0.581786	0.107623	0.935396	-1.535089	0.924389	-1.538903	1.119063	0.866	0.250777	0.04226	-1.553466
glutamate	0.160479	0.156462	0.412435	1.42008	1.529926	0.313772	0.251232	-2.481109	0.146551	-0.649108	-0.717187	-0.273119	-0.270414
methionine	-1.616756	0.858686	-0.130695	0.997967	1.605729	-0.528906	0.824736	0.002098	-0.599532	-1.183067	1.15977	-0.811614	-0.578417
guanine	-1.538393	0.318437	-1.330104	0.664426	1.429239	0.144162	1.303635	-0.685229	0.409831	-0.696399	-1.155682	0.091106	1.044971
histidine	-1.327664	-0.318872	-0.323307	0.343936	1.185031	-0.216947	1.229916	-0.094663	-1.41625	0.272618	1.993615	-0.709507	-0.617905
2-Aminooctanoic acid	1.762555	-1.289346	1.283957	-0.550091	-0.523157	-1.524681	1.152374	-0.176544	-0.743434	-0.160103	0.268929	0.772716	-0.273175
carnitine	-1.899102	-0.844804	-0.78647	-0.511214	-0.408091	0.182527	-0.539471	1.365956	0.424963	1.774375	0.959966	-0.135909	0.417275
Methionine sulfoxide	-0.674006	-0.394408	0.240413	-0.522122	0.45792	-0.873748	1.208584	-1.327257	-0.480593	0.364486	-0.346353	-0.172964	2.520048
phenylalanine	1.279331	-0.156276	0.156368	0.744125	0.281765	-0.45639	1.632408	-0.75862	-1.369023	-0.006146	0.301175	0.3816	-2.030317
Pyridoxamine	0.37189	-0.784194	2.257692	1.543794	-0.704109	0.601142	-0.709675	0.015542	-0.778502	-0.75087	-0.747475	0.402277	-0.717512
pyridoxine	0.324144	-0.768952	-0.68452	-0.752662	1.207202	1.679376	-0.660597	-0.712314	-0.760676	0.88235	1.646011	-0.727369	-0.671992
1-Methyl-Histidine	-0.399607	-1.243264	-0.204405	0.322575	1.181291	0.184256	2.467254	-0.051776	-1.561073	-0.286952	-0.220944	-0.241481	0.054128
N-acetyl-L-ornithine	-0.723268	0.260742	0.901584	-0.018116	-0.70746	-0.118798	-0.708918	-0.718237	-0.241895	-0.719711	-0.409411	0.339327	2.864161
arginine	-0.094088	-0.898277	0.314716	1.307348	1.402619	0.109869	0.88467	-0.947896	0.339715	-0.249174	-2.302936	0.402553	-0.269119
citrulline	-1.344073	-0.052134	-0.590698	1.385656	1.801571	-0.315033	-0.179134	-0.915399	-0.562003	0.922383	-1.238964	0.998601	0.089227
N-carbamoyl-L-aspartate	-0.983067	-1.250142	1.504495	-0.474557	0.925165	-0.886336	-0.329504	0.412459	1.934072	-0.260989	-0.208512	-0.945264	0.562179
glucosamine	-0.084086	-1.024402	-0.613109	-0.078986	0.304515	0.256016	2.236852	1.266826	-1.146431	-0.508202	0.87207	-0.313384	-1.167678
tyrosine	-0.641055	-1.089897	0.118824	-0.227508	1.072535	0.822786	-0.428934	2.554639	-0.662425	-0.68374	-0.901002	-0.164016	0.229793
Phosphorylcholine	-2.579038	-1.112386	0.008421	0.534967	1.384183	0.132105	0.442615	0.873835	-0.080891	0.831936	0.190846	-0.330603	-0.29599
3-phospho-serine	-0.391438	-0.95116	-0.860972	-0.419931	1.645106	-1.151941	-0.093388	-0.048285	1.88247	0.610392	1.049867	-0.91303	-0.35769
N6-Acetyl-L-lysine	-0.539792	0.51926	-0.182939	-0.194566	0.943102	-0.79565	2.561603	-1.545102	0.345229	-0.266442	0.004243	-0.840089	-0.008857
Acetyllysine	-1.213509	1.985708	0.402692	-0.737649	1.509767	-0.522229	0.111767	-1.123517	0.486176	-0.252529	0.791826	-0.930676	-0.507826
N-acetyl-glutamine	-0.53632	2.044492	0.439473	0.806953	-0.69916	-1.338072	1.404475	-0.541443	-0.501603	-1.182636	0.023821	-0.454525	0.534546
N-acetyl-glutamate	0.836551	-0.028569	0.4585	-0.026705	1.524478	0.521038	1.559616	-0.806237	-0.620912	-0.376018	-2.105277	-0.387923	-0.548543
Ng,NG-dimethyl-L-arginine	-0.236834	0.092171	-0.703221	-0.530799	-0.078672	-0.371181	0.32059	-0.862495	0.001331	-0.071382	3.136848	-0.146758	-0.549597
Acetylcarnitine DL	-0.092483	0.348702	-0.623645	0.353634	0.109986	-0.28829	-1.581676	1.481266	1.475079	1.277269	-0.474482	-1.522572	-0.462789
tryptophan	-0.790419	0.260255	-0.751642	-0.466555	0.558894	0.241048	1.463119	2.345986	-0.282076	-1.024867	-0.110307	-1.125569	-0.317867
Kynurenine	-0.766	0.196002	-1.045098	-0.022939	-0.324916	-0.785562	0.154013	0.581479	-0.408579	2.847225	0.596786	-0.6614	-0.361011
N-acetyl-glucosamine	-0.700169	-1.479349	0.263459	0.575698	1.658041	0.675675	0.719706	1.414868	-0.729156	-1.435145	-0.441928	-0.62983	0.10813
Flavone	-0.91134	-0.932929	0.480057	0.996607	1.28909	-0.259083	1.43441	-1.435557	-1.112267	-0.692691	-0.406153	1.044414	0.505442
cystathionine	-1.267485	0.120269	-0.05675	-0.610047	1.490915	1.283398	1.956459	-0.689867	-0.999653	-0.111559	0.131285	-0.732121	-0.514843
5-methoxytryptophan	-0.291051	-0.798875	2.296004	-0.197477	0.703159	-0.40738	-0.835899	-0.44823	-0.131846	-1.122971	-0.872237	0.781491	1.325314
Cystine	-0.504776	-0.874348	-0.710999	-0.394313	1.135757	-0.596612	1.888446	-1.2358	-1.244836	1.019956	0.389801	0.245549	0.882175
cytidine	-1.116943	-0.043563	0.106181	0.706704	1.972298	-0.633863	-0.564589	0.508291	0.031098	-0.759344	-1.101718	-0.812973	1.70842
biotin	-0.358929	-0.76871	0.4218	0.047303	1.399419	-0.079098	1.124225	-1.086969	-1.304313	0.422262	-1.647276	0.455765	1.374522
deoxyadenosine	-0.627298	0.131791	1.989028	-0.051467	-0.566195	-0.800777	-0.698545	1.666157	-0.657821	-0.114224	-0.740018	-0.83789	1.307258
Glycerophosphocholine	-0.680519	-1.722559	0.190714	0.582874	0.080079	-1.013138	-0.456756	-0.756092	1.174227	0.90535	-0.85528	0.962199	1.588902
acadesine	-0.026869	-0.866994	-0.835782	0.171067	0.602432	-0.819635	0.823546	-0.846057	0.580655	-0.849081	-0.847257	0.439767	2.474207
D-glucosamine-6-phosphate	0.829413	0.367382	-0.324474	-1.342788	-0.837594	-0.65491	1.429109	2.013664	-0.821048	0.497284	0.271564	-0.829756	-0.597847
D-glucosamine-1-phosphate	0.592761	-0.516489	0.574788	-1.509248	1.380389	-1.428863	-0.830757	0.525949	-0.357489	0.547142	-0.951087	0.447075	1.525829
S-ribosyl-L-homocysteine-posi	-0.249276	-0.805196	0.452002	-0.934231	-1.009453	-0.183472	1.374474	0.837457	-0.974413	0.011995	2.293598	-0.288071	-0.525413
deoxyguanosine	-0.87406	-0.567129	0.764475	-1.214794	0.01131	0.562482	-0.390357	-0.4805	1.605094	1.609103	0.674626	-1.587818	-0.112432
adenosine	0.060043	-0.768961	-0.524975	-0.086712	0.671203	-1.16361	-0.668128	2.678329	0.582644	-0.265833	-0.433496	-0.780633	0.70013
1-Methyladenosine	-1.475177	-1.440505	-0.284485	1.285959	0.738629	0.655628	0.701003	1.559045	-0.230769	-0.539077	-0.554752	0.622552	-1.038051
guanosine	-1.533252	-0.313843	-0.394995	0.571466	1.237663	-0.473145	-1.256936	1.813447	-0.282135	-0.143894	-0.333916	-0.344272	1.453811
L-arginino-succinate	-0.068034	-2.253473	-0.490993	0.504658	1.122963	-0.181096	-0.325054	-0.468613	1.88225	0.683234	-0.720534	-0.177331	0.492022
S-methyl-5-thioadenosine	-0.603373	-0.706314	-0.791601	-0.682694	0.605801	-0.680384	0.206416	0.456887	1.568694	2.346851	-0.608737	-0.499858	-0.611688
7-methylguanosine	0.603065	-1.078342	-1.479723	-0.510919	1.373806	-1.164533	1.948895	-0.709369	0.547186	0.189375	0.14237	0.30669	-0.168502
dCMP	0.744878	-1.638413	0.69251	0.899524	1.594422	-0.397034	-1.201713	-0.080816	-1.507174	0.353996	0.033329	0.883849	-0.377356
glutathione	-0.339993	0.383673	-0.735627	-0.491473	-0.563096	-0.440686	-0.507526	1.274392	2.823927	-0.308673	-0.383677	-0.141629	-0.569614
dTMP	-0.45527	0.752197	0.2152	-0.366502	-2.174236	-0.065436	-0.752375	1.662194	-0.598494	0.873551	0.422686	1.128532	-0.642046
CMP	1.586803	-0.051505	-1.086063	-0.29842	1.183213	0.073061	-1.089536	1.364811	0.425923	0.800391	-0.741767	-1.217025	-0.949886
UMP	-0.441349	-0.657627	0.035693	0.40315	0.26145	2.112403	-1.811637	1.260103	0.156742	-0.40876	-0.705454	-0.843361	0.638647
dAMP	0.630373	-0.533341	-0.451298	2.110233	0.861107	0.157352	-0.424327	-0.286882	1.321912	-0.361199	-1.157296	-0.353061	-1.513573
Nicotinamide ribotide	-0.646746	-0.790169	-0.530201	0.0931	2.192056	-0.490946	-0.608871	0.966831	-0.867861	1.064027	-0.642597	-0.865184	1.126561
aminoimidazole carboxamide ribonucleotide	-0.651887	-0.774073	1.559971	-0.686136	1.072433	-0.671849	-0.723924	-0.581596	-0.549988	-0.846786	-0.074926	1.847646	1.081114
thiamine-phosphate	-1.630004	0.677309	0.109534	0.258222	-0.62994	-0.292635	1.160147	-0.597692	0.349501	2.098646	-1.378181	-0.367721	0.242815
dGMP	1.080551	1.866482	-1.045023	0.530757	0.507668	0.357092	-0.302422	0.844663	0.015363	-0.910799	-0.906643	-1.745771	-0.291918
AMP	-0.592454	-0.205376	0.269712	1.674857	1.854051	-0.003213	-0.912423	-0.299112	-0.925353	0.326997	-1.077504	-1.113188	1.003007
IMP	-0.926856	1.185009	0.149644	1.499729	1.62958	-0.063834	-1.479722	0.149564	-0.792348	-0.182159	-0.850518	-0.920158	0.602069
GMP	-0.217325	0.806908	-0.256492	1.535281	2.123461	-0.686986	-1.021586	0.553537	-0.681922	-0.511737	-0.572338	-1.213614	0.142813
xanthosine-5-phosphate	0.385182	2.102303	-1.241699	-0.565529	-0.105032	0.646954	-0.236714	-0.121455	-1.265762	-0.907435	-0.323558	0.039601	1.593143
riboflavin	0.679794	0.241586	-1.164058	-1.181965	-1.030903	0.684817	1.793323	-1.129072	0.455927	-1.137008	0.863212	0.335885	0.588461
S-adenosyl-L-homoCysteine-posi	0.860315	-1.136315	-0.500662	0.021414	0.926487	-0.572265	0.290748	-1.088498	0.83209	0.749575	-0.687636	-1.504247	1.808994
S-adenosyl-L-methionine	-1.610118	1.128574	-0.149715	-0.809225	-0.659883	-0.309689	-0.021256	-1.242106	-0.081021	0.400816	0.88551	0.401945	2.066167
folate	-0.49408	-0.405189	0.767408	0.828433	0.971039	2.338727	-1.138518	-0.561168	-0.877363	-0.090474	0.228841	-0.441993	-1.125663
7,8-dihydrofolate	-0.745702	0.338569	1.402222	0.406209	0.190783	0.883178	0.799234	-0.67452	-1.851919	0.544483	0.506483	-1.817956	0.018934
5-methyl-THF	0.608305	-0.981584	0.957684	-1.808489	0.694449	1.000291	0.522823	0.034474	0.178626	1.100653	-0.41069	-1.817421	-0.079122
glutathione disulfide-posi	0.066162	-2.580359	-0.886395	-0.482771	0.121136	0.34967	0.201066	0.850379	0.48106	0.922107	-0.093027	-0.41671	1.467682
NAD+_posi	1.67949	-0.099873	-1.415074	-1.213995	0.640121	-0.464222	-0.31199	1.329041	1.49578	-0.16237	-0.722192	-0.118426	-0.636291
NADH	-0.160137	-0.478292	0.420829	0.48587	1.349463	-1.242515	1.530642	-1.736567	0.377474	-1.14879	0.378211	0.811444	-0.587634
dephospho-CoA-posi	0.856879	0.998692	-0.434708	-0.018782	0.570342	0.468172	0.043568	1.335347	-1.984847	0.746018	-0.415254	-1.689505	-0.475923
NADP+_posi	-1.362799	-2.16876	0.400043	1.266353	0.357139	1.522818	0.162112	-0.605923	0.007443	0.85652	-0.303578	-0.089727	-0.041642
NADPH	-0.277109	-0.720161	-0.248547	0.91847	0.792895	-0.240859	2.521034	-1.63245	-0.713927	-0.243205	0.249228	-0.004065	-0.401304
coenzyme A-posi	-0.3877	0.716396	-0.586291	-0.593535	-0.557666	-0.059437	-0.752388	1.688835	2.431791	-0.28659	-0.693725	-0.397549	-0.522141
FAD	-1.229673	1.334252	-1.024551	0.939264	-1.134627	-0.325754	0.038095	-0.833856	1.366077	1.455845	0.133628	-0.819631	0.100933
acetyl-CoA-posi	-0.582169	-1.033589	-0.981964	0.894548	2.20887	-0.460648	0.246901	-0.324686	-0.346985	-0.114249	1.554986	-1.008164	-0.05285
propionyl-CoA-posi	0.350546	2.175145	-0.190711	-0.633339	-0.502581	-0.510057	-1.173148	-0.243934	1.565885	0.398236	-1.203758	-0.607624	0.57534
acetoacetyl-CoA-posi	-1.559995	0.194525	0.223905	-1.564402	0.553081	-0.377149	0.287544	0.150018	1.447401	-0.301725	-1.174297	0.484672	1.636421
malonyl-CoA-posi	-1.154732	0.58729	-1.135185	-1.159092	-0.23789	0.252037	-1.126792	2.261377	0.617164	-0.337351	0.528967	0.488485	0.415722
succinyl-CoA-posi	0.075244	2.557263	-0.73064	0.622537	0.865165	-0.708913	-0.71874	-0.744466	0.316151	-0.748536	-0.746081	0.685425	-0.724409
sarcosine	-1.531773	-1.330059	-0.858342	-0.2125	0.88091	-1.120849	-0.194292	-0.033757	0.86081	1.607564	0.553029	0.21569	1.16357
putrescine	-0.989744	-1.175704	-0.728102	0.820938	0.118907	0.482299	1.262262	-0.886967	-0.838548	-1.030743	0.142786	1.548646	1.273972
spermidine	-1.04368	-0.876962	1.427206	-0.611609	1.107114	-1.554051	0.297497	-0.432667	0.062493	1.006557	0.22293	1.352871	-0.957699
N-acetyl spermine	0.355817	-1.316656	0.688895	0.373349	-1.412235	0.470728	1.207361	0.671848	-1.577614	-1.260398	0.208563	0.882325	0.708017

N-acetyl spermidine	-0.992891	-0.524807	0.616535	0.017752	0.762419	0.956012	1.274267	-1.632782	-0.173377	0.160429	0.561157	-1.868385	0.843671
Nicotinamide Riboside	-1.329821	0.040627	0.991059	-0.64417	0.94042	1.583758	-1.311435	-1.06841	-0.343629	0.279439	-0.673372	0.155312	1.380222
Adenylosuccinate	1.334724	1.099912	0.001036	-0.654733	-0.575503	-0.489105	-0.945113	2.104598	0.80428	-0.371052	-0.487503	-0.964716	-0.856824
cholesterol	-0.671412	-0.650795	-0.63018	0.259346	1.731677	-0.540572	1.558984	-0.660099	-0.226091	-0.626836	-0.666083	-0.661054	1.783116
arginosuccinic acid	-0.020967	-1.176799	-1.562724	1.21721	1.582895	-0.435867	-0.823079	0.129428	0.507724	1.480232	-0.757061	-0.437443	0.29645
phosphocreatine	-0.398294	-0.771034	0.741189	-0.781568	-0.241737	-1.131005	1.711925	-1.20321	0.763004	0.736274	1.498333	0.074063	-0.997941
retinoic acid	0.924907	-0.927109	0.160331	0.191279	0.432972	-0.079522	2.443857	-0.995743	0.412765	-0.522313	-0.502355	-1.539301	0.000232
spermine	-1.865333	-0.525476	0.819628	-1.752261	0.191058	1.111267	-0.399854	0.119309	1.446552	0.562827	0.725926	-0.331682	-0.101962
HMG-CoA_pos	-0.071514	-1.561865	-0.316548	0.082102	0.965778	-1.131092	0.34074	-0.468518	0.132077	-1.052993	-0.254458	1.399436	1.936854
N-acetyl-L-aspartic acid	0.46509	-0.948708	1.13159	-1.092076	0.692995	-0.404153	1.096987	-0.803969	1.234593	0.818316	-1.197013	-1.444671	0.451018
N-acetyl-L-aspartylglutamic acid	-1.113392	-0.982284	1.797009	0.142533	0.625066	0.497123	-1.804469	0.454428	1.039102	0.453699	-0.87384	0.311868	-0.546842

SUPPLEMENTARY TABLE 3. T-TEST RESULTS.

	t.stat	p.value	#NAME?	FDR	Fold Change with respect to Wild-type
serine	-5.2562	0.00027	3.5687	0.077215	0.72498
N-acetyl-glutamate	4.1086	0.001734	2.761	0.16854	1.241
carnitine	-4.0278	0.00199	2.7012	0.16854	0.85477
alanine	-3.9287	0.002357	2.6276	0.16854	0.89179
anthranilate	3.5139	0.00485	2.3142	0.27744	1.4886
sarcosine	-3.2632	0.007556	2.1217	0.3312	0.89694
ADP-D-glucose	3.2236	0.008106	2.0912	0.3312	1.6195
glutamate	3.09	0.010286	1.9877	0.35051	1.1233
Maleic acid	-2.9755	0.01262	1.8989	0.35051	0.83563
malate	-2.9745	0.012643	1.8982	0.35051	0.80745
glycerate	-2.9139	0.014091	1.8511	0.35051	0.76458
thymidine	-2.89	0.014707	1.8325	0.35051	0.7343
malonyl-CoA-posi	-2.7501	0.018887	1.7238	0.41552	0.40459
fumarate	-2.5176	0.028595	1.5437	0.57153	0.83805
2-keto-isovalerate	-2.4911	0.029975	1.5232	0.57153	0.84802
threonine	-2.4016	0.035135	1.4543	0.62804	0.81845
phenylalanine	2.2366	0.046977	1.3281	0.79031	1.1304

SUPPLEMENTARY TABLE 4. ORIGINAL DATA.

Label	MUT	MUT	MUT	MUT	MUT	MUT	MUT	WT	WT	WT	WT	WT	WT	WT
glyoxylate	79153.87157	136384.6993	137067.2464	91055.22444	125418.5364	83964.80401	45738.42724	116185.935	65145.85722	108532.2753	55958.86559	95671.278	88495.7862	88857.04122
glycolate	340443.8773	285080.9157	243951.3286	265650.7414	328315.8335	316351.8141	242351.2522	343319.3732	274890.3579	292501.9817	269739.339	266100.63	288007.7715	367998.6861
pyruvate	77952.54505	62065.49229	49829.7944	87307.66617	31422.64541	16241.66087	12448.15857	67384.84632	63612.59568	34269.77819	51687.02149	42565	52640.54161	26561.47888
lactate	31246759.46	21609233.48	41272562.24	22261462.11	27051093.88	38390163.36	25639434.91	27663764.95	22278209.94	19797325.94	28468176.32	37242837	24640975.22	31353018.02
2-oxobutanoate	576614.7545	583711.845	609815.9375	656867.2169	553405.8641	420988.8303	526787.4186	662589.2009	579283.6348	542644.6158	646512.227	688383.18	568829.7908	595068.0698
acetoacetate	591027.617	521283.8249	656844.6967	593505.8342	633257.6123	453371.5992	525269.9474	482022.7296	601370.636	531655.436	635911.2301	572314.25	679912.4534	526880.6746
glycerate	313429.8726	253953.7946	356313.0531	331279.0789	253162.4568	244996.927	166107.8146	312175.2623	364281.7604	269702.6796	279361.1014	364889.09	260744.6436	294299.2185
uracil	336911.2279	241235.2584	451364.1491	201105.4372	505551.7875	224302.0579	326991.0389	465338.6303	376876.0654	258905.1214	344733.61	377878.12	338584.7244	704620.018
fumarate	6042850.804	5923156.869	7524366.996	5986651.856	6490013.493	6485762.039	4981867.487	6390982.384	4537389.453	4652254.337	4470228.148	8121080.2	6616397.894	7574437.975
Maleic acid	6349446.72	5664772.405	6857082.322	5707569.677	5948084.963	6056037.595	5076846.109	6294806.058	4426936.217	4662946.382	5388646.902	7466811.2	6900007.175	7218440.888
2-keto-isovalerate	6734231.921	5147033.67	6879442.212	5621717.644	5470231.818	6256577.005	5165246.57	6381358.066	4240371.287	4475246.68	5192047.86	7073653.3	5909962.257	7395414.586
Guanidoacetic acid	N/A	N/A	11158.74053	N/A	N/A	10204.4462	N/A	30698.33561	4668.054901	N/A	N/A	N/A	12983.81119	N/A
succinate	8270795.377	5992130.817	7955985.192	6429203.459	8135861.721	8106360.52	6379861.919	7793055.862	6399449.685	6391777.669	6437831.468	7948625.5	7608523.247	6942158.499
Methylmalonic acid	9065600.432	7178275.674	8847885.49	6761564.682	9304218.511	9510767.739	6966565.095	8837295.413	7150990.737	6897960.201	7742337.229	8831860.4	8611373.787	8099874.071
3-5-methylthiopropionate	9077.363102	N/A	9142.737041	5071.9246	N/A	N/A	6585.814234	12074.40695	9894.448696	N/A	9103.570817	N/A	N/A	N/A
nicotinate	93755.94328	809106.5018	3866035.524	371726.7115	1068827.336	1669489.828	824755.5986	1545169.387	2374524.967	2199200.426	895940.5494	2460283.2	1900180.146	838831.87359
taurine	156746730.9	159550507.5	166502406.2	160637546.3	162754814.2	142275934.4	138368761.6	175871253.3	166327133.8	159587056	165027622.3	165064139	164789944.6	156713006
Pyroglutamic acid	140411.6768	97768.69445	197144.8444	151753.8795	128749.8443	129112.7442	124556.3269	206320.1328	373706.1581	116837.7113	511790.1085	129783.02	133674.0871	174321.393
Citraconic acid/itaconic acid	10155760.16	6620579.201	8201255.136	3763520.655	4965986.805	8006414.917	6559671.448	5862307.32	4282749.992	6028347.404	3768425.225	6506879.5	8265980.945	5642249.096
2-ketohexanoic acid	130636.3523	95165.79237	118395.8634	99205.36781	113682.4734	112324.4684	77598.78653	120229.8516	103048.6138	77743.34737	99067.92442	103114.54	100486.1893	116791.9388
N-Acetyl-L-alanine	51019292.27	44859529.74	58679389.77	47718625.85	52488729.91	45157565.71	41241475.98	60576262.74	48844951.19	46298340.84	53426490.58	55399463	45484086.46	49593288.08
oxaloacetate	1727504.126	1543374.345	1569384.314	285762.7713	319401.4064	299910.9066	1096914.071	1730852.733	1631086.893	356412.1721	366952.1252	1631324.9	368415.853	466006.5442
Hydroxyisocaproic acid	80883.16007	43680.50832	82706.31168	65786.86921	49009.48203	78907.61832	56452.17182	73499.63953	60356.85594	81441.89543	66471.11587	74186.241	65914.42938	106409.186
malate	31345444.54	32532047.93	32124620.11	26694171.09	33195573.43	37097096.3	27892173.31	32293565.19	20205286.62	20883642.36	25418696.29	47261738	32383217.43	40153467.85
hypoxanthine	2282530.382	1083570.002	2731895.186	1217710.281	2153448.507	1999769.764	2206196.402	1720882.55	1567546.265	1329566.997	2259214.672	1673239	1489376.955	1945720.478
anthranilate	64212.61407	36993.71537	68991.13172	52663.61271	58706.24103	18160.99401	26842.82464	39148.4918	64355.16755	38192.99462	44803.85768	99398.273	29727.04608	33856.1649
p-aminobenzoate	62880.9639	27699.46787	79960.64039	86405.91964	88604.25727	58581.90225	38218.57123	58675.54685	60402.57981	36268.69956	40797.71135	43367.207	44843.28202	24501.46303
p-hydroxybenzoate	837498.0853	835283.153	461416.421	612568.7083	836960.9389	532974.1137	726388.7047	497563.5691	594763.9329	422511.2559	595608.9939	595526.64	364116.2029	566560.5224
acetylphosphate	154825.2592	119027.1006	170665.557	241813.578	119203.5565	156532.1183	152971.4498	179281.4366	235456.1087	144378.8283	188369.8964	180801.9	197048.307	200080.8775
Carbamoyl phosphate	166458949.8	143172348	189607445	170575462.2	177651346.9	148146779.7	124750882.2	181013528.7	190603817	162102286.2	187054554.5	180406116	154329688.1	149563159.2
a-ketoglutarate	3956524.953	3004613.499	3726789.096	3540845.814	3124594.833	2965299.589	1890559.962	3981546.817	4586220.836	4011785.446	5042075.043	3469806	2780527.907	4069813.865
Phenylpropiolic acid	859760.0212	673270.5499	1067745.64	847609.2501	904417.6291	858797.6942	567507.8793	820710.3397	647237.0514	699395.5049	744499.2386	1070505.9	1123511.413	698458.0678
2-oxo-4-methylthiobutanoate	139807.6962	191338.1086	361933.6421	188047.2943	169981.3821	144177.8057	200328.8814	170154.5879	235022.9569	167702.982	247414.5317	232158.65	216893.9605	264716.6198
2-Hydroxy-2-methylbutanedioic acid	2156930.496	1747166.933	1756765.58	1602844.289	1457637.015	1752596.033	1541879.711	1527511.26	1575056.122	1322284.909	1591295.258	1930019.3	2000056.602	1657516.667
3-methylphenylacetic acid	11377.11272	10606.66591	39856.93759	6487.521569	27580.39513	26655.03427	19184.01758	31746.61017	15212.74661	23342.05118	31121.73764	15016.152	19997.81982	13387.12044
xanthine	N/A	N/A	5145.889878	5094.295857	4141.016652	6296.146856	N/A	834500.3159	6406.853475	6639.870078	9335.395232	18198.216	6592.289375	11965.71056
Hydroxyphenylacetic acid	1515659.256	131209.1408	889019.1127	155262.246	1156027.051	1005333.794	872391.6822	1356782.869	1298843.126	1128493.594	1231276.85	893155.95	73114.74853	870833.0339
2,3-dihydroxybenzoic acid	271462.2378	179133.5715	170903.297	122674.9392	167579.4058	156228.8743	164750.1665	144672.3282	187356.8061	128561.8328	157342.7438	140189.71	162481.8322	176034.642
orotate	500766.4126	444004.1649	382459.6782	344252.7494	366130.0813	347855.5461	504605.4813	439644.8788	453932.1343	339157.8389	305451.2507	509037.51	260923.9632	311871.9093
dihydroorotate	211714.3018	195679.6235	228799.4316	248817.3066	401472.7669	330208.2935	310447.0393	209161.5146	210080.4478	308915.8467	265030.0967	250376.51	321804.4878	216994.0454
allantoin	2935155.398	3009256.651	3509686.175	4345805.891	4510508.196	3855793.25	2927605.174	3852489.727	4793894.774	4096176.769	5591322.104	4330815.4	4339912.75	4568898.896
Aminoadipic acid	15752.76087	21330?.9523	299418.4897	209617.0958	320160.8761	294024.9728	247069.7886	9445.357485	220973.8422	201996.8243	209806.4287	263612.47	260688.9835	376348.4524
Indole-3-carboxylic acid	187001.5372	230871.2803	329042.9062	213607.252	263647.0563	231045.397	244253.9364	173535.7831	216934.1497	187332.7612	263802.1538	243801.59	337664.3617	392250.1287
phenylpyruvate	15185.74401	7877.844757	4124.498607	8648.169795	7335.677005	N/A	15570.58627	22166.31335	5455.540552	N/A	11872.05367	12387.363	8557.65112	7316.250707
Atrolactic acid	15738.332	29751.78063	31165.73052	8613.263443	15231.17127	7874.224825	7685.979321	19892.3103	69103.2391	17392.54701	40550.06134	24783.628	4749.766432	47473.88633
Phenyllactic acid	120697.4948	112406.9012	207204.8902	133961.3378	173292.4806	128178.7841	89300.47051	142036.2322	231827.6878	147003.262	184354.3765	178052.41	148476.5034	155400.4123
quinolinate	221631.2988	294526.8344	213488.2784	167563.4879	166715.9215	172245.8229	213711.8014	205482.9528	228148.8375	30407.61116	28952.91782	22132.842	168810.7077	166369.751
phosphoenolpyruvate	395698.5049	233902.501	493132.4176	311274.6274	348370.0427	401425.5628	127008.2554	399817.5773	496265.8548	88273.01322	574945.232	495549.29	424142.5663	312366.3547
Uric acid	23335.41154	30035.35562	20157.96576	23154.77652	44513.9038	38917.77008	18496.68598	27260.06599	38684.65705	34144.36181	44438.12277	54758.347	47328.32435	65063.80102
dihydroxy-acetone-phosphate	531212.3796	472100.5934	644965.9349	686689.5701	464482.8294	476768.3976	354143.8393	599196.0926	539962.7962	414025.7107	655765.3311	605907.91	430575.4555	346846.9704
D-glyceraldehdye-3-phosphate	214361.487	218810.2113	294504.1452	312980.8804	235296.699	192310.1143	204454.4501	227887.0338	328749.9206	215858.307	315548.5186	250742.66	192065.8035	222415.7537
sn-glycerol-3-phosphate	3320416.022	2176518.693	4368673.728	2783785.348	2312246.904	2518523.287	2328038.007	3091117.906	2710751.614	2639675.98	3959192.696	3367245	1869428.086	2866265.81
shikimate	611902.4405	715214.5819	249456.8611	127165.5948	19472.6354	20592.50964	14917.74303	706911.3819	763914.8947	317137.0482	749051.2976	34677.363	10732.35542	148702.7222
aconitate	1160279.478	1254555.303	1433126.993	984948.1637	1169368.175	1359097.317	996633.2013	1177732.355	1101727.992	1103224.496	987030.3473	1135445.6	1290713.338	1057394.946
allantoate	162292.2476	138633.1362	199062.7051	142789.4652	97529.17193	148593.7539	94360.16767	148463.828	157495.991	158767.2263	165761.9989	190579.05	130521.6811	134570.7556
Ascorbic acid	74684394.61	65304338.66	96891127.67	88299193.3	70239937.89	65418998.84	46809410.73	90728401.82	91178697.42	67607504.18	76411132.78	86510277	54023347.12	37778145.99
2-isopropylmalic acid	118332348.5	107411127.1	150880383	143297285.5	111482686.8	105907254.1	81280293.57	145073223.2	141996254.9	117426910.9	125006003.7	146269362	94272911.24	66983581.38
N-carbamoyl-L-aspartate-nega	164408.3721	137798.0563	172555.7488	112646.6099	165216.2998	142781.5113	101162.8826	138689.798	174328.521	124693.4516	180432.3059	157800.33	117394.9673	114529.8239
Pyrophosphate	412472.4478	240308.1683	433138.2041	163719.9458	211806.7665	187105.5051	216394.207	365901.1108	313642.0363	218689.8557	326808.502	377516.11	142467.3599	208941.1035
glucono-?-lactone	19898.20599	15733.99772	48776.30508	11200.57273	11920.72218	37192.23677	4966.755229	42114.98924	46152.97889	39513.99973	52845.10902	14722.414	13950.5978	12507.06299
myo-inositol	4786392.29	3971286.67	4882882.883	3864008.45	4168519.16	3895?000.97	2781094?.47	3551?98.14	4926936.85	3446953.25	46866804.59	47919098	39257788.03	40869693.42
hydroxyphenylpyruvate	16901.28719	14698.92928	26053.17005	30157.81525	20946.73582	30419.66965	12178.51669	11863.58793	8167.334572	23192.12514	36099.52853	21189.097	20736.01634	8636.838476
homocysteic acid	173782.1805	203260.1764	128746.429	175591.2751	212925.6308	173368.3652	119598.8883	157229.9575	216070.3866	330616.1198	188135.4658	196675.56	184831.6724	171439.315
4-Pyridoxic acid	13075.6335	7714.6504	144759.7062	108457.5507	8825.761868	5868.357425	78309.30765	8540.954555	17156.91692	68317.17147	126185.1676	54474.722	93282.48781	14240.94025
3-phosphoglycerate	3175642.673	2419437.016	3703564.455	2552207.064	2036161.913	2485167.71	2371921.638	3252319.079	3202409.617	2405443.101	3580298.296	3577778.4	2167920.341	2680668.33
Indoleacrylic acid	N/A	110636.0747	N/A	34673.08719	N/A	31643.49866	40239.88566	38898.49279	61026.96311	N/A	N/A	47784.273	36412.62198	N/A
Kynurenic acid	169181.1471	164894.649	217475.3753	136977.5014	165966.4722	180114.0874	117019.3257	156082.0182	156088.6924	91914.20491	130519.397	156379.01	122919.0658	119620.6287
citrate-isocitrate	132125067	114983456.8	127192811.1	96012292.2	87543544.9	111207714.6	103750769.2	101034736.6	109156071.3	103264579.7	81172768.84	115880712	101365140.3	101224361.2
isocitrate	289309.4458	304599.8491	430876.2247	358870.8292	285396.8683	284810.4869	166312.0283	368642.9151	373142.8973	267636.2226	334349.0266	348089.87	449907.1029	339496.6941
citrate	55895652.05	62922065.29	73735318.84	56135788.1	51891695.59	56003434.74	59052362.06	52520068.12	61937315.85	54187517.01	39160458.6	58815915	57151805	52332665.26
2-dehydro-D-gluconate	62002.54396	98733.0521	91124.18065	95585.32668	81209.66549	78322.41391	52678.29172	70289.86289	99636.53882	80171.06406	95128.72772	80077.71	62523.40782	114991.2391
D-gluconate	889116.9665	1020861.939	1077209.291	752516.6335	789520.649	917899.065	517301.971	1062627.665	918955.2202	666128.7737	953069.9058	900581.44	722254.1708	776608.819
D-erythrose-4-phosphate	206995.7524	179779.1332	244824.9217	167134.9198	192608.3429	169967.0339	102243.0888	204558.3962	234827.7322	167392.9679	215372.8538	174535.8	163546.9801	133477.9631
Xanthurenic acid	414255.8338	230426.6093	341084.5568	377955.845	393364.675	247166.3957	343478.2352	433789.8771	545646.9425	613220.5517	492219.9801	497697.39	441817.0178	444733.7682
lipoate	N/A	N/A	N/A	N/A	N/A	N/A	N/A	N/A	N/A	N/A	N/A	N/A	N/A	4127.770618
D-glucarate	221004.4132	238512.3878	330006.8823	284949.4293	324857.9554	243822.4204	195497.3838	216246.7634	358293.9407	269608.9517	322372.5598	263936.48	334971.7422	252875.0246
deoxyribose-phosphate	282466.1745	336112.2639	103587.8507	300844.7496	42099.08978	48625.00056	198108.5186	410949.0142	409727.8245	330253.516	73460.90113	71440.251	304240.2355	55951.20052
pantothenate	20382828.21	19037389.94	16686313.82	33963061.98	18377995.61	14182035.11	11332824.32	24140691.16	25884000.97	14795755.9	18225956.3	15669407	11645662.95	14049816.22
prephenate	N/A	9088.307397	4126.525437	7414.992554	7925.148146	N/A	N/A	4006.75646	8258.005772	3330.627957	4952.972772	4086.1061	6659.194196	N/A
deoxyuridine	5880.949022	5817.497998	7171.030526	N/A	N/A	4124.665958	N/A	N/A	5801.482411	N/A	5647.79574	N/A	N/A	N/A
ribose-phosphate	782132.5636	461766.4261	731888.6301	504022.6086	695530.365	441069.5161	586833.3118	626945.0026	813475.4933	513230.0885	581099.1288	668226.2	495528.1359	476793.4975
thymidine	87142.75923	106542.617	72652.74157	74633.51156	91913.08036	51213.83213	45462.67124	109923.0294	78558.95273	68698.86855	99742.23004	74061.213	75919.6204	67708.89975
uridine	421198.207	334558.725	591635.2312	412909.7033	379070.5122	338650.7451	361478.2845	397380.9419	477280.1074	390430.3555	473754.4976	530119.58	273599.3776	431856.4616
deoxyinosine	70256.34436	61996.78617	187511.7281	122398.3656	173951.1907	112850.8852	151987.1173	217293.1939	262535.4259	128692.0128	161345.4952	304883.09	162951.5519	134590.8208
shikimate-3-phosphate	N/A	N/A	N/A	N/A	N/A	N/A	N/A	N/A	N/A	N/A	N/A	N/A	N/A	N/A
D-glucono-?-lactone-6-phosphate	29949.22208	27462.63411	50542.05136	31330.70834	37302.70903	63384.70896	14668.59067	29212.38932	40810.94407	21669.69829	34664.89261	40386.711	37620.87151	20474.08347
hexose-phosphate	14093214.45	10373679.69	16343871.39	11822279.04	10354938.71	11851584.81	9937344.724	16002327.53	12019654.29	9397470.211	12466028.33	12967123	9467096.276	8716589.992
glucose-1-phosphate	873309.4041	589502.6927	962781.416	741680.0808	721893.3666	660117.9849	549722.0563	1136301.571	917206.4264	733205.9653	656795.8233	810267.17	632895.4366	514492.0603
glucose-6-phosphate	393247.7797	279651.756	357664.4089	397702.0427	315780.6682	250435.5235	250968.5828	343109.9731	438465.9141	390820.8477	228622.865	290346.84	374235.8616	233863.4333
fructose-6-phosphate	397362.933	284074.0924	410098.6117	467959.8909	357324.787	316077.4928	266721.4468	415849.4252	374213.4097	312374.5407	332427.0921	360142.17	335565.7626	239039.798
1,3-diphosphateglycerate	461307.5402	741195.951	1059859.327	422169.6022	697213.047	622433.7843	350772.6835	962726.1322	958081.0039	314304.8222	852685.4086	1006433.7	681144.3881	682413.5439
2,3-Diphosphoglyceric acid	577429.5281	685554.6089	932788.2009	636447.5654	677221.1185	432484.7878	371775.6384	900681.749	861329.9203	431917.7591	720627.8406	876426.78	527475.2031	528078.3685
S-ribosyl-L-homocysteine-nega	9331.32207	6589.432485	13882.767	13239.82902	13102.22609	11062.12949	21475.08155	5659.698226	25091.91125	19758.70967	4969.220029	13478.958	5549.996938	22903.20662
inosine	18810309.38	13806423.75	27856580.56	16778193.17	16821203.03	15211935.39	16937054.41	16303914.68	16386086.5	14523824.88	22289936.82	18410194	14133632.73	14281816.84
6-phospho-D-gluconate	64408.90212	11708.40846	85064.33083	29117.23455	9344.218675	20743.82396	52778.03784	89175.33649	88366.60584	71028.98064	64343.61336	21986.844	87961.00032	76713.34632
xanthosine	168291.6497	94448.63825	206898.9116	189510.6055	134602.4398	104910.5616	42004.99589	168718.8408	59401.42878	75021.50989	79160.85179	178738.1	149430.2135	148304.4009
D-sedoheptulose-1-7-phosphate	1377619.942	1303670.121	1444636.396	2092112.963	1803082.097	1256466.711	1005041.404	2207278.862	2135588.374	1556247.548	1500041.605	1840232.1	2067653.559	1139196.979
N-acetyl-glucosamine-1-phospha	1079361.3	1116575.922	1274833.984	971874.1621	1238497.633	797672.3432	785847.3967	1321739.863	1160543.795	1167202.202	1109161.68	1174111.1	1174115.851	1151630.14
glutathione-nega	1450400.329	1068093.803	977593.6385	970631.1645	776859.929	476655.5421	645843.2611	1255792.349	1042799.097	1161550.202	896366.8809	1054928.6	792514.0751	809100.2602
dUMP-nega	11588.73789	8257.604724	15668.98374	21495.70095	12385.73542	15841.14414	4955.52441	8953.353879	11678.73528	10734.8853	14883.56229	10819.817	14291.2158	18168.82538
Geranyl-PP	87968.39898	71227.63627	70306.49478	36877.90789	80245.09743	61080.70364	51167.0839	109909.8328	87806.37283	68292.1288	71682.36627	68884.916	70125.66296	51811.14184
O8P-O1P	521727.3937	514782.9931	602648.3099	498691.0834	454264.8743	419050.0238	340918.2077	634912.4927	586807.3247	466824.4537	526300.8088	566830.4	514506.5612	380072.0181
dTMP-nega	24775.81737	8282.371683	32748.12124	22276.93379	22268.88457	18170.61738	9083.243957	22276.54121	22431.87015	23916.47734	22296.50802	23950.516	12322.72994	24843.95679
cyclic-AMP	574514.3133	413300.5608	768986.7893	616470.4043	481985.7643	494629.1559	291922.8663	572897.4813	579088.6813	436302.8725	653441.5917	412098.78	427288.5376	527800.0436
fructose-1,6-bisphosphate	8419430.389	7957920.652	11931238.01	6593923.898	7939357.255	7133957.859	7516188.259	10389970	9238577.332	7345288.921	9976851.81	9194142.6	6873760.962	6614030.298
trehalose-sucrose	26208.61213	19413.11619	28601.98332	20097.1902	18392.1985	23478.07439	18160.91433	24510.71202	35238.4795	7833.902291	17452.44873	33749.323	35135.65312	27444.10208
Cellobiose	8240.422091	N/A	N/A	N/A	N/A	N/A	N/A	4775.259429	N/A	N/A	N/A	N/A	N/A	N/A
orotidine-5-phosphate	49531.08983	26633.87629	50883.89406	33840.93006	45529.33001	31553.45449	23918.0662	26576.59562	43042.79048	46242.9221	33034.49627	23621.558	39399.86755	43841.01272
SBP	184422.1443	262639.3886	348541.0936	158604.6074	255385.1651	199576.1054	260634.6781	301627.9079	249294.0782	278501.6674	307016.8474	320048.89	213277.2036	216559.6276
trans, trans-farnesyl diphosphate	14185.74553	N/A	58061.42287	23738.08363	39644.95554	8668.147429	8595.263685	41595.12327	29847.22149	29876.13352	50047.6667	25354.437	17205.98603	31292.60459
S-adenosyl-L-homocysteine-nega	4282543.288	3460188.935	4598455.27	3401548.219	2963208.992	2139226.654	2599837.494	4631798.428	3753733.129	3120195.12	4576940.272	3902144.2	2859305.212	2989532.35
dCDP-nega	61118.60445	56157.02737	49546.94796	50377.43901	56956.00413	42119.4012	44597.2852	56984.96687	42921.15376	37992.61342	45422.20015	68525.742	28082.67514	29068.67945
5-phosphoribosyl-1-pyrophospate	299116.3849	361173.4585	348085.4861	317886.028	220790.4739	232022.109	229074.3657	478652.6125	545265.5403	385903.2241	438874.8467	325255.19	263614.4141	172976.3713
Deoxycholic acid	N/A	N/A	N/A	N/A	N/A	N/A	N/A	N/A	N/A	N/A	N/A	N/A	N/A	N/A
OBP	30819.07096	42599.96595	24665.28403	21727.2534	33122.09284	20035.94764	12875.57084	86980.05027	39262.73005	39553.12567	28381.4911	44498.81	31899.43817	44992.48583
dTDP-nega	55435.18122	30434.62895	39584.47334	39642.29642	24776.47092	19793.95021	48706.69234	36337.70466	43720.4732	47081.9395	25604.07117	60291.157	33032.80999	42944.13285
CDP-nega	452736.649	517894.2463	525545.8767	494213.8581	481614.2519	469765.1004	426893.826	620172.3728	551301.2075	473554.8849	473509.2366	583889.89	435892.0583	445913.2181
UDP-nega	10308894.21	12205196.2	11597414.6	8812384.959	8986264.819	7434638.27	7793617.864	11390619	11187456.8	8841008.703	13110351.37	9647052.1	7900904.439	7215435.447
Cholic acid	N/A	9890.383396	10737.79584	N/A	4127.670437	14104.09526	4081.993763	N/A	4100.324695	N/A	2547.710068	N/A	N/A	N/A
trehalose-6-Phosphate	1655190.647	2220487.374	2179756.631	2744083.146	3165227.186	2204722.258	1607259.203	2992805.95	3507909.591	3435267.493	3989382.068	2478587.8	3214129.866	2376109.821
Thiamine pyrophosphate	131299.883	127998.5698	173406.889	165767.8415	160117.1156	68638.20699	94904.09301	141234.9617	139769.9884	97747.07353	150088.4283	177718.87	111350.9048	122399.171
adenosine 5-phosphosulfate	158807.4177	137341.4103	151053.4568	128861.8706	134848.77	103233.3954	112578.6057	190718.816	157739.8781	104906.661	129616.4407	164346.5	148131.1932	138736.0873
ADP-nega	21873661.86	20988853.44	19839262.76	17092792.43	15558728.49	14544680.5	16249565.05	21012683.42	18587324.19	16566979.39	19207873.59	18935132	16237716.96	17137589.52
dGDP-nega	21243448.13	19219209.79	19937850.28	15863323.27	16082477.11	13973497.9	15509100.92	20666884.11	19318899.3	16325071.38	20312838.22	21082125	17382954.71	17809390.51
IDP-nega	2752591.013	2591233.222	2619353.145	2319959.566	2041229.281	1699300.371	1963169.77	3022863.293	2237431.587	2041914.285	2659331.382	2438348	2324875.094	2171504.571
GDP-nega	1746179.45	1555994.991	1820411.689	1428951.517	1487312.124	1132975.778	1280102.82	1870190.764	1679993.507	1295752.977	1605553.084	1771643.8	1348369.363	1337175.485
CDP-ethanolamine	300729.1901	281541.6278	324577.5177	308421.4113	267590.2623	185821.8961	298975.4198	357593.0699	339434.1842	340258.8366	381584.3846	297317.75	241160.9486	213066.6582
FMN	N/A	4154.739404	4130.176166	4130.245037	N/A	4955.146452	N/A	5780.036477	3294.538229	4127.691438	N/A	N/A	N/A	N/A
cholesteryl sulfate	1073213.878	749405.9844	103534.3024	3101937.684	60278.64598	52033.57881	60902.43918	1466076.497	1452852.963	54389.05871	88893.93316	47012.606	205675.3535	33150.12196
dCTP-nega	123861.6707	101564.2021	105736.5998	138745.4154	169286.6074	126397.8497	77644.04945	132889.9023	141199.1844	108189.1731	125536.9815	136265.17	139533.3712	82357.76555
dUTP-nega	11610.52129	7395.294503	9083.017979	17339.22696	21473.97128	9085.490416	N/A	23948.99677	9836.393587	12376.38863	13215.31723	14037.73	11560.7046	11586.90375
dTTP-nega	99796.9053	81623.99905	98278.80834	113960.6852	99932.87569	83461.32234	75875.31932	81744.75866	107303.6663	122213.6017	91496.7455	101577.28	91673.65492	103077.4615

CTP-nega	2430436.757	2419347.461	2903840.743	2877166.043	2693687.088	2105982.534	1404754.22	3601999.954	2532943.252	2282674.234	2735215.71	3210905.2	2669582.875	2281243.066		
UTP-nega	32245967.19	30224633.59	32356142.51	34836475.18	35963480.32	29269313.83	20761837.19	42913727.33	39354027.97	34302464.89	40660719.29	35139042	33192664.33	29257150.62		
CDP-choline	80106.52309	38817.40245	85064.4729	51206.08544	36339.76806	39639.79077	58641.80569	52857.98298	39646.88663	37162.28149	56157.06226	76798.518	78461.30603	41288.99326		
dATP-nega	52866.14207	65254.35515	40466.26517	49554.27884	51280.7535	34677.33486	43772.64136	40440.01332	28900.9636	17358.634	36323.39898	62768.826	35512.41871	53682.38334		
Taurodeoxycholic acid	69394.80789	46616.93893	75154.83117	59463.87742	67154.10565	42606.90627	35052.07051	70033.27856	73784.81264	69543.40092	82767.52855	81061.183	50168.30611	61142.33627		
ATP-nega	49602334.33	50272464.36	49456649.04	55711550.53	50292609.27	47367041.98	40313951.67	53700646.72	58632103.65	49851242.26	53466074.24	62229393	54357512.67	49933233.95		
dGTP	49061593.8	49105879.86	51789298.03	55644171.77	52548015.56	47401222.86	39043908.99	58847765.72	57822848.24	50000785.86	51294164.25	60341960	53025802.2	51257663.9		
GTP-nega	6262532.509	6231278.997	7301986.412	7459130.025	6357270.44	5450006.397	3820146.035	8182705.617	7730061.521	6693217.267	7548307.394	8041430.5	5792073.127	6122521.903		
UDP-D-glucose	3938094.857	3095554.696	4092947.898	2733293.155	4056853.065	2755295.092	1938096.277	4443539.232	3242132.259	2807196.746	3713299.289	3526103.7	2519857.004	2980116.454		
UDP-D-glucuronate	422861.3362	395580.2908	570675.1177	403035.0763	512864.2998	405488.409	260157.6938	588037.9817	352647.3589	313829.624	432765.524	470793.89	387343.7428	492226.2335		
ADP-D-glucose	10745.50763	5780.205507	9907.656747	9886.900671	N/A	6651.938803	8255.294312	14866.1463	18171.85653	4955.245948	N/A	10733.988	9088.0817	N/A		
guanosine 5-diphosphate,3-diphosphate	119771.3506	90020.18066	117278.522	95787.67024	90020.77054	3858.110648	88370.93831	147003.751	119756.9127	102413.781	124789.9403	112324.38	67721.99234	114799.0603		
UDP-N-acetyl-glucosamine	1602223.276	1356907.075	1632745.546	1490724.078	1636852.25	1278426.088	1008448.448	1556799.498	1677350.615	1290833.681	1483290.775	1542724.8	1149620.801	1189276.647		
glutathione disulfide-nega	12028352.3	13540276.72	14757656.34	11752784.49	12878912.94	10220226.2	9701926.768	17264349.19	12882809.49	13901717.73	18929560.35	16851365	13583710.68	13360515.16		
NAD+_nega	953791.279	902067.5176	1101367.12	983145.3323	916681.9887	824070.3531	824163.6384	1074036.753	805301.753	763874.7272	913584.5398	1001339.4	873651.5449	885134.6948		
NADH-nega	64419.26823	52032.52333	60290.49677	47075.48479	48726.61299	47074.11128	25732.33105	68581.76082	52855.67357	59464.45424	42120.20463	33033.54	38817.58399	61116.34821		
dephospho-CoA-nega	18212.52409	3278.68269	11563.23688	4150.148749	N/A	12388.0585	4955.293038	11582.78507	2631.500426	7433.051231	10735.47254	13213.485	4127.535709	7432.285014		
cyclic bis(3->5) dimeric GMP	N/A	N/A	N/A	N/A	N/A	N/A	N/A	N/A	N/A	N/A	N/A	N/A	N/A	N/A		
NADP+_nega	130602.839	148625.2507	179195.0884	132047.0108	132961.8251	98273.87884	99969.03051	165356.8398	148238.9282	112193.6807	146983.5021	141161.12	107365.0386	166160.3604		
NADPH-nega	23949.12523	18186.06022	29733.90969	17344.55205	13212.98286	24775.93884	20646.37776	18179.81597	31381.50737	17342.03805	23126.2159	44598.663	16518.59684	19821.1914		
2-hydroxygluterate	4286602.541	3518609.905	4832833.646	4313239.129	3981892.321	3823534.364	3301728.153	4296963.164	3373195.965	3003500.215	3394510.561	3932884.5	3774923.234	3814805.771		
2-deoxyglucose-6-phosphate	2906092.452	2068968.318	3519573.552	2410479.765	2088332.107	2342405.604	1969082.803	3554891.858	3337890.95	2471411.498	3485381.583	2885875.6	1916239.846	2883931.474		
4-phosphopantothenate	11560.7929	4190.593549	18172.67615	14009.61588	23953.09335	10755.54622	6387.385498	31377.36116	5756.075974	12508.4541	21426.38154	12386.835	2481.245074	9471.895758		
dehydroascorbic acid	19758.84852	27276.64707	N/A	N/A	N/A	15056.43574	18766.94476	N/A	N/A	N/A	N/A	N/A	N/A	N/A		
3-hydroxybuterate	70760.34269	186024.1644	266000.5788	273971.8376	3846975.775	246755.0406	153163.4239	1990402.007	2824969.14	3464309.04	3721467.95	321062.28	185237.2758	302381.2805		
itaconic acid	10155760.16	6620579.201	8201255.136	3763520.655	4965986.805	8006414.917	6559671.448	5862307.32	4282749.992	6028347.404	3768425.225	6506879.5	8265980.945	5642249.096		
Urea	9034362.223	9418190.094	5582255.927	4267380.428	9180474.782	6067835.884	8309845.689	9915995.438	9186406.278	10607221.86	13821379.73	5641940.8	7779350.062	9470154.104		
ethanolamine	20165.58022	16484.60897	25899.37691	32234.21473	7357.060173	16831.81362	16730.14142	34909.95186	N/A	N/A	14469.30081	28403.611	28068.14598	19207.02019		
glycine	N/A	N/A	N/A	N/A	N/A	N/A	N/A	N/A	3304.570658	N/A	N/A	N/A	N/A	N/A		
alanine	23769637.1	18130941.98	19208287.31	15851479.37	16224728.13	17586105.84	12050452.16	17447026.2	13091125.19	11671180.25	13620788.2	15896530	13435977.17	12747618.9		
betaine aldehyde	195269.1221	231107.8751	270882.4275	296598.3423	210604.7152	285710.1044	159052.9796	238188.8324	222764.2808	219834.7296	226196.7029	217501.12	207975.41	206963.8563		
choline	387292.3441	14669.97202	441986.1852	556329.0506	508931.9435	497867.6902	10139.06778	576008.1187	407873.0361	470849.4596	504049.3908	541519.96	456271.811	677412.7276		
4-aminobutyrate	3879580.366	3754212.287	5424901.74	4013361.759	3328718.023	2917271.875	2415192.467	5337720.077	5610562.594	3631946.753	3547810.003	4540144.3	2801017.708	2671029.871		
dimethylglycine	79742.708	2050825.086	110178.6578	84168.73577	64397.4341	56778.48051	83136.59784	116841.743	106072.0786	86258.04673	82042.77321	84463.846	103757.8563	63171.40194		
serine	6082065.51	4874501.914	5564738.13	5868645.731	4944111.714	5170817.285	3608600.608	6018694.47	6560045.411	4741208.857	5598136.247	5537553.6	5711971.164	4818932.865		
cytosine	101364.9853	69328.16508	108627.6091	95968.22103	60409.88796	N/A	57317.06178	81862.39142	76182.42811	61354.19218	113980.3661	72237.389	61720.93277	64103.64592		
Creatinine	1733640.453	1681438.497	2368381.499	1958561.157	2051838.578	1494354.523	1382199.478	2528428.005	2174264.444	1820403.321	2135656.692	2130690.3	1691811.09	1701333.408		
proline	45427966.75	43958583.61	50294336.34	44964854.5	28576450.01	43431403.6	25280009.14	47790210.05	43337781.01	36433999.68	44951043.75	42550927	33404766.69	41041992.13		
indole	135279.0624	119598.9398	175731.571	134694.1518	190223.5673	110619.05	171627.688	188051.2557	267266.8764	246265.456	234475.781	234380.99	187818.9036	257791.0244		
betaine	7261823.196	6438417.82	8520148.84	5973127.25	6873923.94	8044903.99	9039746.48	6458223.53	6871046.63	8297039.01	6235815.15	92055163	69489017.41	69844193.22		
valine	450844.7389	311829.2818	316146.944	264792.6692	261710.5137	249784.484	168576.7758	315762.8161	368736.9872	389834.4494	401288.8274	219294.86	179183.5152	441808.844		
threonine	14696709.08	11980965.96	17516144.57	12523011.47	9913679.021	11274793.71	9006374.555	18135087.86	13591147.34	12535106.41	19078878.22	14267734	10310618.1	10871027.19		
homoserine	54356.78321	43771.44452	82913.24491	51145.19405	47072.9787	23881.67546	42089.44864	48721.74886	42119.60077	36335.63411	42103.39969	65156.57	57006.91353	41322.86705		
purine	72976.00947	66818.35295	129023.5223	100819.9401	108874.7802	62386.19039	68071.43022	98240.6146	141804.1175	97232.67451	138362.4756	166421.05	65750.57291	105148.1993		
cysteine	9426.730823	9995.768176	13166.02174	11458.74213	5552.106976	4754.283771	5799.706952	11087.87573	14164.5025	N/A	15724.51386	12700.615	6658.080107	5982.382013		
creatine	128656625	121376669.8	132723481.7	119200778.3	121968353.3	104978529	95131516.15	139022096.3	123668110.2	121028079.9	125958522.9	131992799	115905434	116705386.9		
nicotinamide	10460345.29	9158830.104	11460415.58	3222351.294	9518921.033	7012880.415	8224025.214	9754019.609	12056227.73	11125105.49	14454045.98	9049085.2	7150540.184	10087474.95		
Imidazoleacetic acid	26400.25617	40060.49811	45272.51639	45735.6093	56744.41068	31378.38788	18039.04524	75737.56636	42885.46174	69500.21434	55484.65532	28863.599	31225.73017	33504.08628		
thymine	104178.2175	144434.1926	103611.9435	114307.0788	114592.4145	112661.8593	126134.0038	144372.6653	129426.0023	132954.125	146487.7309	111349.43	96566.80367	96971.56512		
DL-Pipecolic acid	83869994.87	82707311.08	97171220.78	95322710.31	81198907.4	78183588.27	64078469.8	107632225.9	104509920.5	98191204	109602830.8	87396636	82403744.35	99555342.94		
N-Acetylputrescine	5836.636693	N/A	N/A	32110.43141	39608.80383	11746.81814	6918.846388	80913.369425	8057.324621	21840.73349	18554.87945	25824.073	6761.431429	15277.36208		
hydroxyproline	2871032.915	2205690.674	4321208.17	3790407.327	3663582.964	2593220.602	2427015.577	3018665.595	3364741.695	2394632.817	3154165.367	4742721.4	2817404.455	2646115.674		
leucine-isoleucine	24325696.08	24361872.82	26395874.24	22146559.21	22035012.23	16652373.69	12000900.52	29452250.45	30355591.44	31679087.49	31679191.07	17785254	14857554.82	23280772.62		
ornithine	1179167.94	1052129.608	1052106.019	883788.3226	657249.9643	455282.5414	455889.8986	1147736.14	1338652.037	1189007.689	1380521.517	621323.54	487201.4491	649560.7843		
asparagine	2077532.972	2051059.834	2741392.467	2522990.358	2213770.125	1655018.445	1482478.788	2822579.106	2257191.017	2073846.795	2159311.827	2488978	2001014.062	2848853.558		
aspartate	9468655.895	9189001.356	11517329.86	10405316.17	12343729.37	7278970.354	9044644.213	11330398.51	9817486.906	8545963.993	8937342.723	9181264.5	8957497.834	9193123.17		
adenine	547593.7545	401203.1359	557922.9332	470592.1559	274289.7081	301421.0927	303301.0648	406564.2744	546047.9783	362327.9578	382892.218	375461.66	403859.631	514728.2709		
Methylcysteine	547593.7545	401203.1359	557922.9332	470592.1559	274289.7081	301421.0927	303301.0648	406564.2744	546047.9783	362327.9578	382892.218	375461.66	403859.631	514728.2709		
homocysteine	104454.5919	133559.1713	135537.8595	105596.1024	124806.5506	75792.35131	78735.64902	143007.4923	100204.3278	75315.27282	106215.6376	107897.64	102258.8823	69081.99516		
methylnicotinamide	9323.175168	16134.74668	N/A	N/A	9746.50979	N/A	N/A	20320.85075	9633.094852	10551.77511	12698.44764	N/A	N/A	N/A		
histidinol	4064.89377	N/A	N/A	N/A	N/A	N/A	N/A	N/A	N/A	N/A	N/A	N/A	N/A	N/A		
lysine	1265607.709	967718.302	1568961.386	1309996.02	1154404.955	1269343.965	840180.0566	1659125.969	1956662.479	1103259.614	1342893.304	1598292.8	1225698.904	1799638.512		
glutamine	5941944281	55341967.13	71161330.95	63217543.83	59329097.53	51614613.95	40511111.6	70360646.71	71725041.32	59428992.65	75062612.85	57618536	52392386.59	61016844.39		
O-acetyl-L-serine	N/A	N/A	N/A	N/A	N/A	N/A	N/A	N/A	N/A	N/A	N/A	N/A	4130.024128	N/A		
glutamate	50125799.3	41709738.58	56703855.01	41448005.46	35348129	36961854.04	34127925.43	49410919.29	36557074.93	37901609.89	38400082.13	42900175	39438246.02	44260419.64		
methionine	1718203.974	1462373.924	3171611.89	1868587.237	975690.7576	1152599.471	817502.7362	2554829.98	2135708.941	1821277.92	1287485.096	1899180.9	1531957.64	1733787.577		
guanine	17997.94142	106195.8289	105116.8966	25265.40367	32210.85535	23590.4034	25645.81973	37988.10648	72784.92529	45275.72024	52614.84977	49159.041	10494.83886	47648.70841		
histidine	17961018.57	12547403.08	20162557.43	14256048.12	7673051.058	5381548.509	5841414.857	17508075.93	17010986.21	14565745.73	20447919.98	11287316	6437060.792	9436457.942		
2-Aminooctanoic acid	24565807.01	21946917.62	21121046.75	22075440.02	9541012.044	10563472.99	7997588.796	25565851.87	19334639.87	18909069.78	17605731.29	11409566	10103983.01	27145903.05		
carnitine	51809549.14	52555424.42	55880182.71	57103921.89	54824005.28	47653327.66	47938632.83	58432603.37	59523269.29	56566065.78	55849983.5	60198033	54580860.64	55944277.3		
Methionine sulfoxide	277211.2379	232982.4623	301556.7955	285300.1769	179318.9008	167867.9537	142991.127	268355.3689	222980.4558	116664.7826	218862.0508	266986.65	139571.648	260982.31		
phenylalanine	7818444.171	6651312.741	11675533.53	12883594.8	7823709.442	7014634.39	6590213.589	8700375.522	14208959.24	8267182.449	11199312.31	9926321.2	7540892.024	8653034.924		
Pyridoxamine	2477.688002	5633.991947	N/A	N/A	N/A	N/A	N/A	3446.851809	4029.823775	4106.75668	4907.320321	N/A	N/A	N/A		
pyridoxine	6572.99227	N/A	3036.17857	14077.50669	N/A	N/A	N/A	N/A	N/A	3174.146339	2419.144853	N/A	4831.400706	2474.699055		
1-Methyl-Histidine	1096237.13	927120.7701	2029991.359	1468610.683	1257755.349	978126.8093	1116159.449	1849009.4136	2163009.643	1084052.087	1956869.811	1837378.2	1568217.01	1127004.922		
N-acetyl-L-ornithine	4632.907251	8422.850639	N/A	7117.52864	3251.785147	10752.16544	8205.073412	N/A	8488.58089	4708.065458	N/A	4726.9406	N/A	16354.67398		
arginine	3990890.74	2926339.949	5433375.634	4540908.864	3547618.428	2216887.652	2319475.271	6636925.84	5557557.297	4347949.526	4621047.54	3708291.6	3040480.957	5690394.799		
citrulline	68635.16531	111066.2617	164421.84	111638.8801	131882.1748	60678.93735	52901.66502	156421.3475	126337.9144	119802.568	106768.6963	99082.286	87324.28351	135531.8849		
N-carbamoyl-L-aspartate	33036.85866	30556.91014	46235.2134	29730.97428	27257.39453	16518.26116	32217.93791	27253.70554	37163.96081	25601.55714	36338.02017	30557.986	23878.70954	31014.32549		
glucosamine	507993.1192	458814.4874	773437.1805	609169.2043	653630.1321	455773.3619	451887.8645	589854.9579	775444.9597	500683.5037	797075.6189	537727.37	652012.1319	220909.0188		
tyrosine	1248590.29	1113529.651	1997834.896	1472807.809	1094329.973	999324.2028	938113.5699	1283089.198	1469684.007	928901.8303	1218129.35	1582951.6	975525.7157	1466553.1		
Phosphorylcholine	296717176.2	288625697.4	321463436.4	304203368.5	306881973.1	266765646.4	219643603.5	373893076.5	360207718.8	296560281.9	346565552.4	312367976	289900848.8	317008754.2		
3-phospho-serine	111550.0232	110635.2683	142720.6564	68426.64462	98467.20622	99188.71889	106945.4033	58258.13432	61698.16194	61329.65886	125280.705	151165.02	84136.19073	129639.0635		
N6-Acetyl-L-lysine	8320503.257	6533372.198	9474331.85	8505084.589	9644916.908	5528570.901	5355240.909	12649573.6	8294413.878	8125516.998	9508220.36	11396786	9987825.416	10650115.23		
Acetyllysine	6479212.234	7167790.923	10263219.21	8054061.089	8462354.507	5605354.169	3942860.553	13357263.01	7873438.433	8733359.026	9322422.696	10336647	7213276.816	9311847.219		
N-acetyl-glutamine	71963.43421	36941.06794	41857.36791	52335.17681	42234.77692	48915.06967	37729.6055	64878.96146	69745.37033	54143.14434	67520.92388	49520.874	48373.55956	68852.93716		
N-acetyl-glutamate	126742.9668	49698.97023	115546.8457	91667.65966	45847.60527	60263.1267	42119.55816	93800.49232	93387.74573	59177.09119	100753.5613	95003.812	73723.3155	60043.41731		
Ng,NG-dimethyl-L-arginine	1332821.561	1327237.738	3413684.718	2071738.685	2959961.92	1639144.734	1095620.163	2085341.072	2151856.37	1500156.676	2090954.769	2550227.6	2232667.453	1585032.512		
Acetylcarnitine DL	88367755.94	65866739.62	85648386.93	71148465.75	78809477.92	82643200.06	76033214.67	80695258.94	79102336.1	80562326	83320766.64	75013407	91064717.62	79750483.64		
tryptophan	3558789.218	2864027.797	2817484.457	2520911.209	3792107.207	2068769.496	3432379.323	5170245.649	6049913.564	5838925.13	4644766.563	6163621.3	6666445.667	4977931.352		
Kynurenine	56951.50673	67679.65373	45835.16697	48346.17259	152291.2506	85177.66677	110696.7251	111542.6366	115671.792	184988.1658	133765.009	145385.05	234703.1927	103160.3336		
N-acetyl-glucosamine	26409.47294	22195.0177	15778.13833	32996.22697	17225.38777	17951.40371	12363.18609	20520.9907	27254.17819	18999.96365	32154.81333	26000.789	14022.49741	13178.80337		
Flavone	13727.00812	22651.80364	24263.108	24023.57907	27963.60608	26638.12449	16708.462	14233.77553	30711.40351	29156.27917	15437.32673	11645.696	13971.54994	42041.05604		
cystathionine	5318061.334	5269201.611	5688506.494	5027492.811	4345280.051	3387385.458	3534180.616	4187013.331	4377264.295	3472289.494	3039272.847	4135657.7	2910957.512	2620887.161		
5-methoxytryptophan	14959.72976	14502.41335	12314.34454	7749.49433	20741.14604	19959.41123	27200.12573	22852.82845	16781.2083	12642.68046	21440.33786	21470.862	12362.60637	17954.51304		
Cystine	69353.00243	46149.68004	76748.03238	69374.44811	59425.47691	68546.52229	56141.17453	54946.20821	47030.71636	57796.14664	56858.98188	70201.2	74264.15112	68540.82643		
cytidine	676397.6562	294833.8578	519467.9627	464136.2172	447666.3616	426191.0781	489902.5789	433085.2841	477344.9631	322922.3555	630138.4428	501601.98	417017.1373	525243.5346		
biotin	445194.3827	465012.9584	377513.7574	315559.4761	407750.3267	384690.4353	302079.0625	460548.4372	332304.6701	408005.9275	399261.7071	330515.34	373607.9533	644929.6069		
deoxyadenosine	14046.9252	15687.02722	25503.47142	13476.45788	12801.91065	7526.19317	4933.385038	26446.05409	14046.70685	22124.81672	12570.87467	37152.436	18172.25406	14034.73485		
Glycerophosphocholine	23819846.55	19971117.04	33922222.8	28653366.53	24172767.52	20871556.95	15047556.89	31135751.98	25777728.92	16390717.52	20782070.21	33928239	28840360.12	43090977.56		
acadesine	N/A	N/A	N/A	2477.621132	N/A	2477.696882	N/A	N/A	N/A	N/A	5727.898424	N/A	N/A	5798.588331		
D-glucosamine-6-phosphate	246915.7323	214664.1063	223264.9127	274507.7004	236916.0798	168501.5127	131352.4521	279348.1588	243048.1929	220249.0162	213438.2057	220554.2	240289.3491	125883.7022		
D-glucosamine-1-phosphate	259722.2225	244045.5662	163372.8375	193174.5596	317314.1617	265523.3275	188932.8162	217036.0785	260928.7866	287665.4725	138507.3233	257779.78	255720.3889	215529.1749		
thiamine	N/A	N/A	N/A	N/A	N/A	N/A	N/A	N/A	N/A	N/A	3304.469998	N/A	N/A	N/A		
S-ribosyl-L-homocysteine-posi	13886.61679	11588.26335	16392.04214	13181.71024	16435.70897	4121.809267	4925.052748	10638.01669	13148.23152	11397.77748	14789.7136	19807.982	22313.35229	9077.446589		
deoxyguanosine	44543.38481	43698.73715	97639.61529	81714.76986	95822.78813	60267.88226	63585.78943	116451.0173	127095.6496	118710.8714	87734.33992	152798.02	64759.12283	87540.73372		
adenosine	5031277.063	2870556.622	8680027.184	7222438.544	4535074.926	5658238.398	4263560.272	4356249.062	8042867.024	4180172.379	6600183.797	5693410.8	6299604.033	3151155.179		
1-Methyladenosine	17345.10019	28067.9928	29210.17721	30227.19545	16502.64831	20683.90264	10735.56284	30559.11743	24724.85311	9861.617271	26431.97482	29698.567	17365.24593	36981.71271		
guanosine	32189.48001	35515.56502	62736.21431	28906.31422	44575.96928	47096.06045	34522.2873	25589.91101	16358.93146	26427.68662	23936.36245	48732.971	19867.84073	21536.73076		
L-arginino-succinate	215668.2655	157741.8144	352924.8976	226255.7262	209775.8622	169159.6542	142031.3656	220328.4281	179928.2833	156877.2824	143412.9462	246940.87	247752.5571	284078.5716		
S-methyl-5-thioadenosine	21340.70246	N/A	N/A	13445.70438	7825.383326	13299.7659	46721.83309	N/A	7531.822933	2812.771806	23250.75191	N/A	13781.578	9945.816754		
7-methylguanosine	311482.3674	185410.274	436452.4901	358308.9169	340255.631	213926.6909	191601.2601	296473.1047	319775.0832	185740.5313	254369.9664	345227.94	240252.4691	360886.6469		
dCMP	28847.28983	33960.65117	33138.1151	27252.64148	34692.96725	23125.57717	29731.8475	41268.5679	26408.86769	28052.44412	37976.10141	30556.52	37990.26222	25600.83982		
glutathione	1509425.812	918518.0654	629428.0416	626858.908	510239.3809	354822.7519	377591.3535	1217327.943	992814.4077	916907.6983	642712.2	683640.59	474421.0989	404951.2328		
dTMP	23009.85575	27069.15905	22664.84887	23916.20828	25603.81827	17066.7082	16701.63575	28862.74202	26390.50898	22257.6085	29633.63368	23201.642	4074.439163	23954.92896		
CMP	2344055.944	1779905.89	1870078.659	1598192.696	1951549.234	1599803.288	1768246.237	1788481.206	1968536.635	1875406.448	2105532.657	2250651.8	1738188.283	1892221.42		
UMP	1487804.502	1080995.694	1168655.219	930295.379	1139216.62	1037043.84	1197110.871	1099657.485	1263003.672	1156511.124	1269954.883	1220914.9	938164.8365	1273269.129		
dAMP	38820.75622	55322.0041	53684.13192	47883.53612	40492.13958	23934.34305	45399.45098	47905.36198	31158.1486	53685.64021	41305.83855	51945.702	52833.66332	35503.76171		
Nicotinamide ribotide	10558.70636	13544.40023	4957.173585	2475.921244	86308.42991	10888.76785	17046.65442	15590.7691	28174.78931	3238.596889	20504.23777	24266.921	21366.47646	12270.90261		
aminoimidazole carboxamide ribonucleotide	10240.62681	4130.138164	4955.331801	4153.761634	N/A	9914.643888	7480.801802	N/A	16515.62742	4957.845516	10733.10774	12412.593	8175.687265	4955.18094		
thiamine-phosphate	26446.48385	14042.97355	56093.36851	33859.02807	22395.71591	14865.7103	12212.55854	63592.0531	24048.80158	9908.101632	22296.12261	23966.124	12385.08194	14390.19994		
dGMP	4130.248167	N/A	8348.87001	5007.236096	N/A	8401.840059	5780.198195	8260.24999	4955.364498	3282.424357	7388.87942	N/A	8205.805961	3301.340268		
AMP	30643721.12	25292782.52	37328214.96	21639301.07	18242324.88	18044851.93	27033791.58	27929510.11	38583269.07	25177568.22	27890111.48	32382445	22621359.4	25104593.69		
IMP	3313935.752	2242748.428	3499789.542	2062705.976	1881142.58	1993564.804	3303401.004	2641744.747	3021037.951	2300871.001	3161315.22	2716238.7	2064911.534	2760511.783		
S-adenosyl-L-methioninamine	N/A	N/A	N/A	N/A	N/A	N/A	N/A	N/A	N/A	N/A	N/A	N/A	N/A	N/A		
GMP	1969609.679	1716878.738	2549589.9	1722060.347	1186933.64	1501309.448	2419196.924	1865624.964	2017140.225	1589699.555	1688130.564	2118840.5	1292851.895	1766793.503		
xanthosine-5-phosphate	7430.519266	N/A	N/A	4124.578488	N/A	N/A	3302.546457	2477.621132	N/A	N/A	2477.529225	N/A	N/A	N/A		
riboflavin	29761.06862	2477.731874	3365.796646	5388.827097	3301.397921	34685.58859	14092.28294	35511.66768	2479.766356	12390.61286	18996.29013	43772.165	27250.2263	33005.87038		
S-adenosyl-L-homoCysteine-posi	1919093.457	1821105.937	2139880.173	1793669.033	1677338.887	1394800.209	1373166.092	2313885.177	2185672.193	1615304.949	2138966.837	2976580.6	1820336.18	1513929.862		
S-adenosyl-L-methionine	580486.1553	474287.5918	627582.0617	809245.7808	518924.8375	401358.6882	332760.2066	994987.8262	504430.4167	371850.821	543603.97	542487.03	463328.2549	413884.3356		
folate	12384.05732	N/A	10740.59129	3302.20743	13208.84593	4127.575576	4117.951019	5780.27366	3302.68613	14015.4892	9928.451047	4134.7644	4958.766628	3301.444376		
7,8-dihydrofolate	N/A	N/A	N/A	N/A	4127.743636	N/A	2477.529225	N/A	5780.082632	N/A	N/A	4127.7794	N/A	N/A		
S-methyl-THF	11329.33234	13461.84225	14999.64682	12658.92356	13290.53711	10576.18413	12100.30354	7874.674793	13252.59124	9413.919976	18969.59222	9558.6157	9956.19933	20020.29223		
Diiodothyronine	N/A	N/A	N/A	N/A	N/A	N/A	N/A	N/A	N/A	N/A	N/A	N/A	N/A	N/A		
glutathione disulfide-posi	5136718.614	4805020.357	5625834.442	5646163.957	5187874.278	4479857.515	4322846.267	7373889.051	6493037.42	4750977.92	5462229.299	4628302.7	5367167.457	5292852.818		

NAD+_posi	2173499.801	2236996.905	2390609.287	2484417.748	1857078.773	1857480.913	1735626.37	2625957.241	2095622.206	1991614.282	1912899.078	2707030.4	1837546.12	2876606.255
NADH	95801.17033	72676.07123	175908.341	104883.1938	104061.0127	121407.1952	49551.34074	92538.51859	132136.8302	88368.25141	107360.7475	90023.291	92498.72184	86814.07553
dephospho-CoA-posi	12388.12217	N/A	8822.77704	N/A	N/A	3305.109935	9082.906912	9087.930042	6851.74831	10714.97056	3355.77124	9092.8183	8258.055333	N/A
NADP+_posi	176241.8383	178926.8495	239504.5072	266422.737	176445.9699	188306.9057	148682.7505	269130.0819	246160.784	188906.0868	226796.3553	184112.79	194910.7258	182566.854
NADPH	30557.36003	25601.83956	28906.56319	38836.17969	28079.09509	26426.12835	17342.89639	42942.93762	14810.6119	28080.91946	26428.43626	21471.392	23949.13102	28926.40816
coenzyme A-posi	35158.39825	29739.05167	32163.32008	39638.65623	5763.645034	14038.4441	10742.44462	28940.43722	44595.89659	22376.78683	14040.2669	17339.746	17318.93179	8259.838292
FAD	182519.3475	107363.4692	147021.1505	170949.0464	187470.9165	31378.83817	58636.81859	175927.191	180088.6073	131293.7431	173423.979	146176.57	112320.1297	143700.9715
acetyl-CoA-posi	24806.06706	20315.79252	21307.13281	28244.92814	19820.52564	20812.27537	6937.433586	12883.90385	22322.64671	18830.10944	23814.94492	28736.182	21803.34763	10901.75322
propionyl-CoA-posi	4133.84853	N/A	N/A	2477.559808	N/A	N/A	N/A	N/A	3280.311086	N/A	N/A	N/A	N/A	N/A
acetoacetyl-CoA-posi	3302.815685	N/A	N/A	4127.793599	N/A	N/A	4130.234365	3274.774318	3302.776368	N/A	3305.182424	N/A	N/A	3302.577063
malonyl-CoA-posi	N/A	4952.724177	N/A	4127.78683	N/A	N/A	N/A	N/A	N/A	N/A	N/A	N/A	N/A	N/A
succinyl-CoA-posi	N/A	N/A	N/A	N/A	3319.094957	N/A	N/A	N/A	N/A	4127.767869	N/A	N/A	N/A	5780.274518
sarcosine	18059366.27	15543373.66	17936790.12	12985413.11	14743476.19	13675661.61	11247031.62	16967909.67	12215084.66	9711514.846	13869700.56	15084913	11198265.92	11171291.45
putrescine	29451.80706	49422.48926	26128.98725	120098.7434	123654.2587	137670.854	161626.0075	42164.82882	13712.43472	N/A	35011.44774	213363.92	196639.419	186009.8832
spermidine	542650.1992	654370.0883	628926.2975	603417.378	770781.1689	1002578.568	1060505.864	788009.6742	847730.4069	624054.1929	751494.1012	978066.2	1312095.4	998763.4812
N-acetyl spermine	138807.2599	199267.4575	230195.6224	190611.4313	151337.3481	157045.374	226877.1064	154959.4878	163588.5621	253145.0973	203814.1224	172428.34	123564.0024	131311.0489
N-acetyl spermidine	36156.30144	29977.45415	11726.20409	5583.138484	8210.883169	13919.59311	26484.63821	30749.88949	23282.26053	70011.15026	15153.60388	10172.661	26429.06485	7141.40285
Nicotinamide Riboside	5491.194196	6450.737678	2461.851037	3496.822163	4878.6159	N/A	6256.751424	14509.62431	4513.526443	8065.931562	7376.101931	7034.4119	6969.132456	8847.816542
Adenylosuccinate	79283.5059	37163.95484	105710.5625	32209.57234	38814.38439	36339.6824	33862.10483	81761.9456	61112.25187	22298.44158	51205.55186	96623.951	21475.49203	33861.16902
cholesterol	373325.6755	270887.8624	81734.73779	875437.0153	64195.2144	84217.12993	67970.30108	592119.3629	447618.5329	72675.15361	60287.31427	68993.57	110715.2886	69557.45225
arginosuccinic acid	165207.4475	166615.1791	253995.2821	217769.3251	168985.6266	141515.3004	129779.5564	178487.7044	134348.7401	112930.5028	140741.3268	228403.02	336995.4948	231126.4076
phosphocreatine	1700467.391	2817446.101	2913102.331	2933919.845	3251974.979	2537982.893	1990425.121	3129745.615	3778327.828	2738212.122	2977436.986	2733366.8	3037965.223	2571091.163
retinoic acid	7435.177383	6266.155978	3111.653254	4953.496715	N/A	N/A	N/A	N/A	4368.794763	4914.644343	N/A	4952.4315	3644.148464	N/A
spermine	680404.9321	815302.5903	733881.6556	578374.9849	725345.5902	733916.0955	840593.8718	800977.3302	510597.4353	563555.9776	677947.3028	564930.11	582716.5568	465411.6383
HMG-CoA_pos	4921.434224	6605.427453	10813.88772	7432.587675	13213.0361	9083.058999	2477.529225	5780.460184	5825.028855	7432.943982	N/A	14865.861	4127.78027	N/A
N-acetyl-L-aspartic acid	1276049.903	1615719.847	1597639.681	1088276.736	1156243.976	843194.7243	635602.7009	1585680.626	1471341.123	1127462.551	1114084.081	1478418.5	988376.1339	975872.8529
N-acetyl-L-aspartylglutamic acid	14056283.32	14240186.19	17856543.11	13508034.17	14260639.55	9203192.734	10233937.72	22499383.33	15384690.54	11007030.38	11869540.92	15372696	10368522.95	12750540.76

SUPPLEMENTARY TABLE 4. NORMALIZED DATA.

Label	MUT	MUT	MUT	MUT	MUT	MUT	MUT	WT	WT	WT	WT	WT	WT	WT
glyoxylate	-0.687459	2.059388	0.701178	-0.216529	1.249347	0.135589	-1.170605	-0.018732	-1.538801	0.458241	-1.444387	0.060925	0.055586	0.35626
glycolate	0.404806	0.29018	-1.61639	-0.696166	0.641414	1.172825	0.470846	-0.3699	-1.363419	-0.180779	-0.63489	-0.538931	0.2115	2.208904
pyruvate	1.35919	1.102223	-0.27712	1.888577	-0.729451	-1.397137	-1.504684	0.374686	0.173187	-0.655603	0.158075	-0.209692	0.505804	-0.788056
lactate	0.100248	-0.628263	0.684804	-0.937547	-0.139172	2.039322	0.734126	-0.8423	-1.442925	-1.201659	-0.171064	1.083049	-0.284367	1.005749
2-oxobutanoate	-0.526106	0.705664	-1.038275	0.565739	-0.265418	-1.215838	1.484011	-0.686746	-1.621514	-0.683226	0.433869	1.225538	0.309984	1.312317
acetoacetate	-0.178544	0.016166	-0.362449	-0.023112	0.826519	-0.538268	1.481335	-2.112208	-1.136771	-0.597018	0.429885	-0.037002	1.780091	0.451376
glycerate	0.255002	-0.173722	0.198468	0.890983	-0.763595	-0.062795	-1.740778	-0.991851	-0.001292	-0.611723	-0.486274	2.111944	-0.164622	1.540254
uracil	-0.339508	-0.677232	0.013088	-1.149096	0.953078	-0.71582	0.447612	0.0193	-0.48032	-0.758927	-0.250602	0.042224	-0.038299	2.9345
fumarate	-0.327626	0.234505	0.010559	-0.285475	0.299029	0.90381	0.336938	-0.719637	-1.771945	-1.103229	-1.276618	1.28904	0.628925	1.781723
Maleic acid	-0.0527	0.144715	-0.313872	-0.434109	0.011516	0.74167	0.578521	-0.78041	-1.984628	-1.149275	-0.674891	1.061664	1.047212	1.804587
2-keto-isovalerate	0.336607	-0.175576	-0.180537	-0.375093	-0.243699	1.018435	0.771979	-0.600404	-1.946883	-1.154206	-0.692112	0.860883	0.337889	2.042718
Guanidoacetic acid	-0.591479	-0.564315	0.543957	-0.588195	-0.578232	0.915703	-0.523607	2.71562	-0.235096	-0.585404	-0.58838	-0.582483	1.215747	-0.553835
succinate	0.457641	-0.510136	-0.55169	-0.848982	0.866388	1.750953	1.06948	-0.803661	-1.787573	-0.793454	-0.84793	0.551094	0.76415	0.683719
Methylmalonic acid	0.251328	-0.179271	-0.601326	-1.130097	0.892169	1.925047	0.787267	-0.742836	-1.730611	-0.965018	-0.497507	0.417245	0.729299	0.844311
3-S-methylthiopropionate	1.076432	-0.9118	0.793352	0.064124	-0.938951	-0.892891	1.150933	1.382366	0.860179	-0.952942	1.128726	-0.947244	-0.920929	-0.891356
nicotinate	-1.405729	-0.533306	1.956296	-1.113317	-0.317136	0.599504	-0.300859	-0.157704	0.524131	0.835269	-0.566626	1.158459	0.71682	-1.395802
taurine	-0.729678	0.928824	-1.36002	-0.329895	0.352549	0.281021	1.500668	-1.139666	-1.742556	-0.235318	-0.090748	0.2487	1.002989	1.313131
Pyroglutamic acid	-0.485622	-0.730626	-0.187529	-0.350239	-0.495555	-0.314209	-0.141571	-0.15893	1.117091	-0.665269	3.088562	-0.517226	-0.373618	0.214741
Citraconic acid/itaconic acid	1.458461	0.404746	0.15421	-1.29459	-0.625632	1.321187	1.097335	-0.797913	-1.413192	-0.241551	-1.294304	0.026439	1.138317	0.066486
2-ketohaxanoic acid	1.080108	0.008528	-0.423219	-0.544122	0.66074	1.49018	-0.040996	-0.494515	-1.393258	-1.6793	-0.558183	-0.121568	0.190559	1.825046
N-Acetyl-L-alanine	-0.358009	-0.088084	-0.312706	-0.801635	0.746422	0.497205	1.095603	-0.274673	-2.326459	-0.924854	0.297261	1.068001	-0.201196	1.583124
oxaloacetate	1.185658	1.307441	0.617879	-1.100367	-1.014227	-0.977732	0.918551	0.776127	0.598959	-0.975751	-0.969145	1.177772	-0.896085	-0.649083
Hydroxyisocaproic acid	0.274705	-1.141751	-0.135541	-0.378431	-1.047311	1.039478	0.245618	-0.601442	-1.178258	0.447293	-0.348915	0.153685	0.001376	2.669494
malate	-0.248557	0.411219	-0.57294	-0.654118	0.204159	1.158999	0.572692	-0.635106	-1.681739	-1.20394	-0.785561	1.584466	0.300992	1.549433
hypoxanthine	0.551731	-1.178393	0.728492	-1.219225	0.633896	0.850472	2.006886	-0.845901	-1.111137	-0.98558	0.586133	-0.326497	-0.444429	0.753554
anthranilate	0.715152	-0.331077	0.518179	0.192643	0.681626	-1.374651	-0.58412	-0.829259	0.186679	-0.510944	-0.210043	2.747764	-0.797951	-0.403999
p-aminobenzoate	0.35479	-1.186845	0.706804	1.632868	2.023564	0.815872	-0.076664	-0.304196	-0.279721	-0.920944	-0.721555	-0.508848	-0.240037	-1.29509
p-hydroxybenzoate	0.861903	1.510627	-1.168083	-0.130658	1.181436	0.009589	1.774788	-1.076485	-0.735902	-1.0026	-0.214733	-0.113117	-1.112199	0.215434
acetylphosphate	-0.748563	-1.146084	-0.894107	1.5792	-1.40202	0.202842	0.838855	-0.81276	0.298551	-0.875031	0.192747	0.165252	1.018064	1.583054
Carbamoyl phosphate	-0.690602	-0.617164	-0.759508	-0.063881	1.43901	0.598588	0.210611	-1.737823	-1.321711	-0.545058	1.305163	1.291718	0.088135	0.802521
a-ketoglutarate	0.317411	-0.345801	-0.728654	-0.194901	-0.539892	-0.14779	-1.574796	-0.539573	0.115417	0.625876	2.081876	-0.119253	-0.857258	1.907339
Phenylpropiolic acid	-0.091343	-0.474468	0.29245	-0.064217	0.535656	0.939179	-0.369266	-0.947153	-1.778104	-0.796335	-0.62248	1.332864	2.123258	-0.080041
2-oxo-4-methylthiobutanoate	-1.376578	0.03359	1.589447	-0.500636	-0.633637	-0.747454	1.063007	-1.297029	-0.434548	-0.800876	0.513479	0.395084	0.429886	1.766263
2-Hydroxy-2-methylbutanedioic acid	0.985561	0.664899	-0.754025	-0.471668	-0.633495	0.9778	1.084797	-1.416471	-1.375214	-1.207743	-0.509739	0.653001	1.328469	0.673828
3-methylphenylacetic acid	-1.143237	-1.031788	1.416053	-1.662684	0.874047	1.191875	0.593052	0.559077	-1.001527	0.2595	1.078198	-0.654188	0.103301	-0.58168
xanthine	-0.297402	-0.296314	-0.279897	-0.276149	-0.279966	-0.262613	-0.294683	3.473153	-0.275405	-0.267132	-0.253148	-0.20146	-0.263812	-0.225171
Hydroxyphenylacetic acid	1.243875	-1.674879	-0.339657	-1.664025	0.677314	0.644006	0.654283	0.465828	0.315104	0.505665	0.685392	0.013082	-1.824924	0.298937
2,3-dihydroxybenzoic acid	2.140303	0.72494	-0.645258	-1.194741	0.086465	0.329166	1.292162	-1.247021	-0.489854	-1.007052	-0.392452	-0.673894	0.173411	0.903825
orotate	0.709777	0.870019	-0.756575	-0.605266	-0.209403	0.065742	2.616502	-0.410199	-0.368405	-0.599246	-0.956677	1.032958	-1.079312	-0.309916
dihydroorotate	-0.816345	-0.631977	-0.94486	-0.359109	1.598868	1.288136	1.673645	-1.185346	-1.213933	0.363703	-0.1831	-0.245506	0.864519	-0.208696
allantoin	-1.552131	-0.886868	-1.402937	0.160971	0.672155	0.509114	-0.149459	-1.166717	-0.342168	-0.048882	1.605711	0.319178	0.745947	1.536088
Aminoadipic acid	-1.849037	0.020201	0.117959	-0.26335	0.798038	0.917014	0.836362	-1.910893	-0.501721	-0.297537	-0.263741	0.252482	0.402716	1.741509
Indole-3-carboxylic acid	-0.940535	-0.014902	0.18131	-0.594588	0.158258	0.142898	0.850364	-1.38284	-1.010435	-0.857805	-0.025785	-0.153681	1.269868	2.377873
phenylpyruvate	0.877682	-0.093627	-1.004452	-0.155929	-0.29973	-1.348295	2.007719	1.469697	-0.851279	-1.385906	0.376394	0.535529	-0.004963	-0.122841
Atrolactic acid	-0.52441	0.573514	0.137957	-0.925183	-0.481324	-0.873897	-0.801779	-0.457562	1.888389	-0.391131	0.951567	0.077175	-1.11985	1.946535
Phenyllactic acid	-1.391744	-1.016659	0.723704	-0.830449	0.954125	-0.098922	-1.171387	-1.393332	1.150269	-0.274089	0.966149	0.969792	0.310942	1.101603
quinolinate	0.483241	1.78637	0.109747	-0.054952	0.045575	0.377825	1.357268	-0.017097	0.148054	-1.536576	-1.558309	-1.623556	0.172684	0.309727
phosphoenolpyruvate	0.133295	-0.785622	0.396699	-0.453297	-0.006769	0.867408	-1.482936	-0.288038	0.266881	-2.151584	1.563327	1.09177	0.792468	0.0564
Uric acid	-0.920576	-0.24165	-1.250887	-0.903729	0.512267	0.492378	-0.749548	-0.930924	-0.407528	-0.222825	0.345856	1.068294	0.844704	2.364167
dihydroxy-acetone-phosphate	-0.09903	0.143232	0.27911	1.893308	-0.4338	0.545042	-0.424005	-0.360297	-1.054991	-1.292716	1.513496	1.17725	-0.574533	-1.312065
D-glyceraldehdye-3-phosphate	-1.128566	-0.036059	0.003302	1.64263	-0.064748	-0.547695	0.886498	-1.677045	0.442838	-0.873951	1.702165	0.20157	-1.008482	0.457542
sn-glycerol-3-phosphate	0.505019	-0.81011	1.344641	-0.307745	-0.880248	0.124137	0.487868	-0.671746	-1.293781	-0.479282	1.71628	0.903322	-1.510285	0.87193
shikimate	0.960735	1.68849	-0.31883	-0.605078	-0.958048	-0.944296	-0.957608	0.923651	1.040542	0.04234	1.453002	-0.907579	-0.986769	-0.430552
aconitate	-0.340859	1.067652	0.080446	-1.055045	0.144016	2.006671	0.84095	-1.076376	-1.4559	-0.41169	-1.050509	-0.162976	1.089347	0.324274
allantoate	0.281061	0.271148	0.743233	-0.380373	-1.981133	1.092425	-0.840205	-1.161631	-0.957872	0.37957	0.546739	1.833971	-0.258327	0.431392
Ascorbic acid	-0.023544	0.119941	0.842999	1.319071	0.093118	0.47488	-0.731099	0.184112	0.088237	-0.417498	0.255001	1.427587	-1.165204	-2.467601
2-Isopropylmalic acid	-0.285427	0.144811	0.517155	1.377268	-0.146482	0.420448	-0.449846	0.006665	-0.286877	-0.075052	0.255971	1.867664	-0.934183	-2.412113
N-carbamoyl-L-aspartate-nega	0.629336	0.477826	0.008944	-1.613828	1.28299	1.132167	-0.303201	-1.483979	-0.239679	-0.95824	1.513663	0.729849	-0.758618	-0.417232
Pyrophosphate	1.644435	-0.021969	1.212294	-1.463477	-0.675942	-0.666737	0.317529	0.35701	-0.269792	-0.705075	0.639295	1.469097	-1.522767	-0.313902
glucono-?-lactone	-0.443454	-0.541536	1.034243	-0.994556	-0.898695	1.236447	-1.278724	0.589663	0.764004	0.930106	1.766744	-0.726685	-0.703594	-0.733961
myo-inositol	0.723505	0.396845	-0.69655	-1.159288	0.107175	0.722726	-1.13345	0.492437	-0.79884	-1.978799	0.697498	1.327339	0.02418	1.275224
hydroxyphenylpyruvate	-0.48569	-0.455387	0.148555	1.016681	0.139244	1.733192	-0.440677	-1.224711	-1.579141	0.29046	1.668798	0.10701	0.24351	-1.161843
homocysteic acid	-0.479174	0.703155	-1.615533	-0.379216	0.57113	0.249264	-0.548142	-1.224569	-0.363489	2.658516	-0.146034	0.148882	0.20434	0.220871
4-Pyridoxic acid	1.195243	0.400345	1.107351	0.794121	-1.213482	-1.259932	0.807582	-1.259095	-1.119331	0.004439	1.150377	-0.261125	0.707742	-1.054235
3-phosphoglycerate	0.434384	-0.306984	0.561159	-0.784007	-1.638048	0.176197	0.8546	-0.446298	-0.64782	-1.014397	1.444406	1.718629	-1.068429	0.716609
Indoleacrylic acid	-0.853522	2.729173	-0.8578	0.102114	-0.850736	0.20035	0.712807	0.036708	0.534615	-0.852244	-0.85287	0.523712	0.273299	-0.845606
Kynurenic acid	0.364507	1.090588	1.005107	-0.54182	0.686648	1.973343	0.278561	-0.763437	-0.841531	-1.909889	-0.749564	0.239463	-0.531771	-0.300205
citrate-isocitrate	0.918559	1.028679	-0.098841	-0.734381	-0.890221	1.13939	1.663927	-1.32237	-1.074438	-0.289519	-1.471791	0.445986	0.115548	0.569472
isocitrate	-0.824325	0.169447	0.472325	0.320775	-0.532581	0.080537	-1.611074	-0.469377	-0.502864	-0.996587	-0.057631	0.340998	2.50403	1.106329
citrate	-0.389199	1.168319	0.36192	-0.266885	-0.365444	0.752512	2.087768	-1.384726	-0.767808	-0.359364	-1.799276	0.158683	0.426498	0.377003
2-dehydro-D-gluconate	-1.222171	1.273202	-0.400005	0.438239	-0.012195	0.378941	-0.619301	-1.329411	-0.240327	-0.231746	0.411339	-0.168327	-0.789475	2.511238
D-gluconate	-0.062725	2.067451	0.300317	-0.911875	-0.304932	1.611894	-1.138221	0.032031	-0.927478	-1.448362	0.513788	0.370308	-0.524359	0.422163
D-erythrose-4-phosphate	0.589807	0.639702	0.829384	-0.719686	0.642745	0.658586	-1.614048	0.973585	0.182297	-0.587264	1.039819	-0.225729	-0.149895	-2.259303
Xanthurenic acid	-0.219719	-1.592739	-1.321752	-0.490533	-0.110747	-1.266252	0.482755	-0.653407	0.162715	1.884764	0.608781	0.834537	0.626505	1.055091
D-glucarate	-1.431132	-0.246311	-0.052052	-0.000717	1.246795	0.182187	-0.262855	-2.196225	0.158297	-0.225789	0.774647	-0.248219	1.865672	0.4357
deoxyribose-phosphate	0.465616	1.269382	-0.932049	0.644132	-1.259067	-1.155687	0.460003	0.950574	0.894491	0.904311	-1.045684	-1.041612	0.933729	-1.088137
pantothenate	0.231835	0.590957	-0.883798	2.973963	0.137423	-0.33516	-0.588178	0.255542	0.459127	-0.734168	-0.11508	-0.50533	-1.13396	-0.353174
prephenate	-1.187792	1.940457	-0.3919	0.924683	1.260785	-1.095693	-1.018195	-0.458703	0.696715	-0.441132	0.087909	-0.155936	0.932528	-1.093727
deoxyuridine	1.13771	1.532933	1.302434	-0.860781	-0.828562	0.788807	-0.651907	-0.949723	0.687283	-0.851757	1.084223	-0.84231	-0.798687	-0.749662
ribose-phosphate	1.461322	-0.844073	0.102918	-1.085946	1.182392	-0.821392	1.958749	-0.912429	0.468708	-0.91191	-0.344272	0.733356	-0.605845	-0.381578
thymidine	0.247065	2.348143	-1.083555	-0.370228	0.940422	-1.112474	-1.017151	0.597195	-0.971687	-0.643551	1.063008	-0.255285	0.212706	0.045394
uridine	-0.215204	-0.624425	1.082628	-0.213282	-0.363342	-0.282475	1.044572	-1.350734	-0.534767	-0.432744	0.622173	1.665934	-1.699796	1.301462
deoxyinosine	-1.434827	-1.406396	-0.231319	-0.731777	0.083696	-0.554085	0.441884	0.036132	0.475652	2.050099	-0.222819	1.803421	0.050917	-0.360577
D-glucono-?-lactone-6-phosphate	-0.426842	-0.276414	0.56622	-0.285491	0.302259	2.927159	-1.06267	-0.785951	-0.143355	-0.948648	-0.050349	0.46106	0.477436	-0.754414
hexose-phosphate	0.998314	-0.170194	1.107147	-0.206894	-0.715208	1.279683	1.020242	0.701349	-1.423727	-1.579402	0.174643	0.760217	-0.963001	-0.983169
glucose-1-phosphate	1.048927	-1.02837	0.712702	-0.251803	0.029128	0.373175	0.032828	2.136202	-0.16732	-0.205152	-1.252988	0.879787	-0.658164	-1.648953
glucose-6-phosphate	0.964541	-0.240849	-0.503335	1.192896	0.029913	-0.586997	0.303665	-0.88415	0.457338	1.188494	-1.945247	-0.609378	1.569251	-0.936141
fructose-6-phosphate	0.719604	-0.718207	-0.141937	2.483919	0.485982	0.524459	0.321059	-0.251604	-1.16415	-0.891536	-0.568838	0.343606	0.391765	-1.534122
1,3-diphopshateglycerate	-1.248583	0.646142	0.924166	-1.391342	0.123489	0.172229	-1.073335	0.418923	0.32755	-1.880703	0.65901	1.564641	0.22511	0.532702
2,3-Diphosphoglyceric acid	-0.756153	0.945499	1.047915	-0.208841	0.426146	-1.104652	-1.126996	0.670059	0.309493	-1.738125	0.437699	1.888817	-0.598855	-0.192006
S-ribosyl-L-homocysteine-nega	-0.620971	-0.82201	-0.276021	-0.105304	-0.022499	-0.094622	1.995683	-1.179199	0.807349	0.757846	-1.147445	-0.016137	-0.99186	1.715191
inosine	0.155308	-0.620555	1.758633	-0.335208	-0.020021	0.122504	1.686131	-1.28497	-1.342104	-0.929917	1.290164	0.338036	-0.628889	-0.189111
6-phospho-D-gluconate	0.24113	-1.435143	0.568147	-0.905522	-1.553184	-1.044817	0.592669	0.615914	0.545699	0.548547	0.279932	-1.120175	1.425775	1.241028
xanthosine	0.673537	-0.474506	0.920145	1.171036	0.225277	-0.106657	-1.479299	0.178299	-1.68228	-1.119845	-1.063703	1.078898	0.713697	0.965399
D-sedoheptulose-1-7-phosphate	-0.992796	-0.535169	-1.355023	1.377422	0.803767	-0.470894	-0.831678	0.564005	0.264622	-0.249697	-0.519144	0.777404	2.071811	-0.904631
N-acetyl-glucosamine-1-phosphate	-0.615957	0.944446	-0.379476	-1.221722	1.188818	-1.299684	-0.352949	-0.316089	-1.392975	0.295798	-0.262324	0.492709	1.173217	1.746187
glutathione-nega	2.14074	1.187189	-0.675726	-0.031123	-0.737594	-1.941521	-0.371612	0.329071	-0.605363	0.983929	-0.393837	0.551911	-0.442685	0.006623
dUMP-nega	-0.410507	-0.803484	0.015246	1.68877	-0.041832	1.188825	-1.332201	-1.218769	-0.787573	-0.501508	0.31622	-0.443757	0.54318	1.787391
Geranyl-PP	1.037639	0.694555	-0.895539	-2.626864	0.956448	0.099063	-0.069826	1.430326	-0.040518	-0.207026	-0.047442	-0.071182	0.452273	-0.711906
O8P-O1P	-0.080714	1.7587	0.027146	-0.376338	-0.771881	-0.233964	-0.93086	0.323962	-0.835311	-0.937911	0.257598	1.685466	1.407057	-1.292949
dTMP-nega	0.556467	-1.969018	1.19724	0.214477	0.443845	0.147914	-1.427829	-0.4228	-0.461786	0.563796	0.213515	0.64247	-1.23886	1.54057
cyclic-AMP	0.37847	-0.633468	1.454389	0.982196	-0.206394	0.748673	-1.386174	-0.594144	-0.640219	-0.969019	1.391439	-1.16422	-0.590082	1.228553
fructose-1,6-bisphosphate	-0.311477	0.447662	1.411536	-1.7663	-0.162013	-0.011139	1.639903	0.038097	-0.932731	-0.997007	1.193864	0.797447	-0.81471	-0.533132
trehalose-sucrose	0.108071	-0.324828	-0.042648	-0.593612	-0.667551	0.43408	0.060663	-0.555083	0.495925	-2.117046	-0.928247	1.268454	1.811244	1.05058
Cellobiose	3.205022	-0.30755	-0.491375	-0.399942	-0.361397	-0.270049	-0.150053	1.052129	-0.516475	-0.389146	-0.40066	-0.377845	-0.325656	-0.267003
orotidine-5-phosphate	1.163417	-0.470058	-0.986194	-0.168181	1.140999	0.209231	-0.214538	-1.229643	-1.529416	1.026529	-0.244619	-1.019498	0.752901	1.569073
SBP	-1.452296	0.655588	0.611953	-1.840609	0.129773	-0.405284	1.749565	-0.217597	-1.051867	0.346515	0.757747	1.187957	-0.443381	-0.028064
trans, trans-farnesyl diphosphate	-0.872251	-1.715575	1.539894	-0.209514	1.024373	-1.105437	-1.001929	0.524082	-0.166906	0.238272	1.559349	-0.041168	-0.514027	0.740836
S-adenosyl-L-homocysteine-nega	1.120086	0.684715	0.634024	-0.3642	-0.846627	-1.903495	0.048732	0.483469	-0.992392	-0.790298	1.819771	0.823454	-0.751993	0.034753
dCDP-nega	0.830952	1.188146	-0.578319	0.063658	0.872632	0.092406	1.01228	-0.173361	-1.172292	-0.882649	-0.339936	1.718841	-1.468776	-1.163582
5-phosphoribosyl-1-pyrophosphate	-0.548582	1.086343	-0.482961	-0.212958	-1.347717	-0.733709	-0.195018	0.879416	1.513374	0.798179	1.420709	0.040395	-0.530714	-1.686757

OBP	-0.404912	0.830224	-1.00858	-0.967861	-0.077452	-0.808004	-1.219304	2.398422	-0.281641	0.26085	-0.527998	0.647541	-0.044348	1.203063
dTDP-nega	0.970198	-0.426892	-0.497003	-0.083787	-1.042903	-1.217887	1.942477	-0.758001	-0.366899	0.507672	-1.093514	1.548946	-0.280864	0.798456
CDP-nega	-1.257857	1.396068	-1.147754	-0.361107	-0.065994	0.910004	1.424952	0.03016	-1.143173	-0.584851	-0.738011	1.590703	-0.491268	0.438127
UDP-nega	0.143037	2.890169	0.019147	-0.770921	-0.261415	-0.669727	0.679664	-0.296499	-0.542651	-0.644186	0.989471	0.058091	-0.761928	-0.832251
Cholic acid	-0.671421	1.420932	0.980063	-0.666429	-0.012845	2.588317	0.257358	-0.708231	-0.225352	-0.662188	-0.391008	-0.657748	-0.637245	-0.614203
trehalose-6-Phosphate	-1.755294	-0.355953	-1.384956	-0.051379	0.879919	-0.185671	-0.81739	-0.435164	0.131084	1.086956	1.832916	-0.323599	1.23339	0.145139
Thiamine pyrophosphate	-0.281871	0.361029	0.426287	1.046953	1.192649	-1.929553	-0.15386	-0.679556	-0.803073	-1.330178	0.479202	1.696578	-0.435804	0.411198
adenosine 5-phosphosulfate	0.566039	0.651749	-0.767534	-0.79005	-0.072129	-1.018741	0.629127	0.724814	-0.793401	-1.913289	-0.759249	1.297315	1.063941	1.181409
ADP-nega	1.02047	2.034364	-0.711826	-0.669118	-0.898547	-0.503122	1.490139	-0.513806	-1.414517	-0.764111	0.145235	0.303883	-0.262881	0.743837
dGDP-nega	0.811095	1.304352	-0.734856	-1.231109	-0.7385	-0.832085	1.13797	-0.678487	-1.267915	-0.926428	0.593259	1.222106	0.233205	1.107393
IDP-nega	0.83781	1.680556	-0.579608	-0.337658	-0.819736	-1.187917	0.956452	0.273886	-1.872786	-1.09524	0.70956	0.295065	0.524296	0.615319
GDP-nega	0.842891	1.274623	-0.085384	-0.870766	0.031494	-1.260789	1.283293	-0.094397	-1.218152	-1.545637	0.190279	1.58377	-0.402498	0.271271
CDP-ethanolamine	-0.197919	0.357983	-0.535285	0.076333	-0.415599	-1.61596	2.240737	-0.138573	-0.549244	0.828953	1.531328	0.061157	-0.704896	-0.939015
FMN	-0.968504	1.145193	0.421494	0.773219	-0.910772	1.860512	-0.672703	1.1762	-0.078595	0.813208	-0.955	-0.929299	-0.870511	-0.804442
cholesteryl sulfate	0.541838	0.317715	-0.574783	2.91881	-0.60341	-0.604872	-0.579145	0.737422	0.697803	-0.613407	-0.574591	-0.621135	-0.411187	-0.631058
dCTP-nega	-0.190375	-0.39587	-1.448102	0.517003	2.179956	1.06722	-0.727715	-0.628733	-0.438636	-0.653019	-0.026932	0.609125	1.214088	-1.078011
dUTP-nega	-0.217838	-0.762356	-0.89269	0.898711	1.917307	-0.29922	-2.03337	1.38518	-0.844712	0.008535	0.123467	0.3718	0.069634	0.275553
dTTP-nega	-0.167972	-0.449299	-1.062055	0.888957	0.368185	0.01067	0.350672	-2.113792	-0.834157	1.564591	-0.586997	0.31021	0.132656	1.58833
CTP-nega	-0.70176	0.330931	-0.426115	0.611573	0.558568	-0.291051	-1.826756	0.933237	-1.533317	-0.861715	0.227022	1.792618	0.889111	0.297654
UTP-nega	-0.844585	0.029753	-1.974207	0.091908	1.04983	0.213259	-1.617274	0.348663	-0.690597	0.10612	1.764294	0.533346	0.739867	0.249622
CDP-choline	1.129539	-0.684383	0.826536	-0.325133	-0.999815	-0.509449	1.300706	-0.709049	-1.328789	-1.039852	-0.064684	1.181065	1.616348	-0.393039
dATP-nega	0.328063	1.7022	-0.700365	0.193032	0.482896	-0.273281	0.878434	-0.758831	-1.36185	-1.717923	-0.602004	1.11546	-0.39929	1.113459
Taurodeoxycholic acid	0.321214	-1.000887	-0.011091	-0.451949	0.612965	-1.188917	-1.413118	-0.557352	-0.381176	0.567324	1.648744	1.758053	-0.762149	0.858339
ATP-nega	-0.815297	0.598698	-1.803569	0.303403	-0.069393	0.515034	0.376635	-1.430712	-0.931296	-0.486259	-0.059844	1.671224	1.091701	1.039675
dGTP	-1.035322	0.438047	-1.711024	0.328822	0.345615	0.590681	0.105648	-0.871585	-1.191718	-0.535633	-0.466129	1.554675	0.975189	1.472732
GTP-nega	-0.904481	0.449188	-0.750944	0.883903	-0.084796	-0.326172	-2.00568	0.008006	-0.668514	0.001637	0.993002	2.050229	-0.454855	0.809476
UDP-D-glucose	0.980961	0.373706	0.29192	-1.200798	1.840814	-0.066251	-1.263976	0.670417	-1.367566	-0.965139	0.689929	0.573077	-1.043244	0.486148
UDP-D-glucuronate	-0.339856	0.125019	0.549767	-0.476284	1.215669	0.548659	-0.962566	0.561744	-1.857825	-1.483014	-0.125291	0.53368	-0.120784	1.831083
ADP-D-glucose	0.572014	-0.324359	0.102146	0.424442	-1.548319	-0.005342	0.795115	0.995008	1.559535	-0.687005	-1.565465	0.704302	0.485025	-1.507097
guanosine 5-diphosphate,3-diphosphate	0.496718	0.053343	-0.03131	-0.174543	-0.183974	-3.008568	0.676062	0.652146	-0.112518	0.085632	0.722899	0.461197	-0.800929	1.163844
UDP-N-acetyl-glucosamine	0.831269	0.709022	-0.498579	0.21878	2.111341	0.597937	-0.440239	-1.282824	-0.71531	-1.153167	0.148539	1.033552	-1.374315	-0.186006
glutathione disulfide-nega	-1.002274	0.58772	-0.64121	-1.017184	-0.202296	-0.778934	-0.262602	0.101469	-1.544222	0.001649	2.039152	1.411064	0.443556	0.864113
NAD+_nega	-0.143719	0.666308	-0.077207	0.254237	0.165279	0.332057	1.612368	-0.477488	-2.420949	-1.440583	-0.325755	0.689969	0.194245	0.971238
NADH-nega	1.045344	0.730344	0.016826	-0.388068	0.023385	0.47142	-1.389647	0.506134	-0.737915	0.808293	-0.834738	-1.53914	-0.719962	2.007725
dephospho-CoA-nega	1.939057	-0.920892	0.325741	-0.840835	-1.422703	1.345179	-0.281747	0.273712	-1.247025	-0.148955	0.493138	1.091798	-0.747444	0.140976
NADP+_nega	-0.545023	1.275846	0.549745	-0.370197	0.016948	-0.959373	-0.057485	-0.1287	-0.844568	-1.143492	0.266252	0.23417	-0.892591	2.598468
NADPH-nega	-0.010694	-0.336086	0.233908	-0.766198	-1.176873	0.775396	0.643032	-1.038869	0.254888	-0.730147	-0.056317	2.786702	-0.629755	0.051012
2-hydroxygluterate	0.373133	0.078885	0.262948	0.567299	0.412391	1.072262	1.064163	-0.704478	-2.125759	-1.60698	-1.026367	0.146651	0.400154	1.085699
2-deoxyglucose-6-phosphate	0.199176	-0.954054	0.59706	-0.856299	-1.327741	0.135358	-0.051943	0.467771	-0.096467	-0.607927	1.727594	0.532948	-1.507955	1.742479
4-phosphopantothenate	-0.2627	-1.174611	0.327648	0.111621	1.703424	-0.03562	-0.601924	1.803042	-1.188628	-0.068341	1.144104	-0.05483	-1.457959	-0.245227
dehydroascorbic acid	1.069745	2.15364	-0.602264	-0.586378	-0.579681	0.957756	1.688966	-0.604866	-0.606625	-0.584502	-0.586503	-0.582538	-0.573471	-0.56328
3-hydroxybuterate	-0.780234	-0.68515	-0.675481	-0.644876	1.87307	-0.629495	-0.684924	0.269923	0.699689	1.50445	1.632818	-0.606336	-0.68924	-0.584214
itaconic acid	1.458461	0.404746	0.15421	-1.29459	-0.625632	1.321187	1.097335	-0.797913	-1.413192	-0.241551	-1.294304	0.026439	1.138317	0.066486
Urea	0.007994	0.711581	-1.473922	-1.659824	0.329489	-0.553755	0.999308	-0.209845	-0.483977	0.711285	1.808883	-1.088564	-0.051754	0.953101
ethanolamine	0.017598	-0.068147	0.25246	1.233784	-1.148509	0.067554	0.363855	0.92434	-1.81315	-1.789502	-0.500113	0.956623	1.147689	0.355519
alanine	1.98793	1.263449	0.022494	-0.147163	0.242405	1.382315	0.122647	-0.528041	-1.628151	-1.28947	-0.791511	0.024436	-0.389252	-0.272088
betaine aldehyde	-1.061596	0.663704	-0.108699	1.413129	-0.308507	2.531264	-0.349676	-0.898904	-1.284377	-0.304159	-0.248446	-0.26895	-0.098848	0.324063
choline	-0.284655	-1.975101	-0.2902	0.539205	0.462271	0.741307	-1.98757	0.181159	-0.501412	0.178152	0.292914	0.557999	0.321635	1.764298
4-aminobutyrate	-0.164147	0.744026	1.369929	0.221053	-0.658327	-0.688949	-0.959411	1.004617	1.255471	-0.36143	-0.634545	1.468754	-1.390982	-1.206061
dimethylglycine	-0.283281	3.473395	-0.256535	-0.273321	-0.29956	-0.299419	-0.220917	-0.251657	-0.269285	-0.267439	-0.276991	-0.267971	-0.220841	-0.28618
serine	0.848961	0.108829	-1.50228	0.668744	-0.558088	1.37553	-0.98184	-1.017636	-0.337774	-1.387897	0.12486	0.396811	1.673568	0.588212
cytosine	0.957985	0.194103	0.714575	0.828823	-0.393976	-2.794926	0.211578	-0.237919	-0.465784	-0.458358	1.514503	0.015307	-0.207474	0.121563
Creatinine	-1.709915	-0.258134	0.389774	-0.050331	1.342051	-1.063997	-0.258108	0.884484	-1.221846	-0.735705	1.066346	1.523967	-0.490514	0.581927
proline	0.543502	-0.388595	0.300437	0.617437	-1.812914	1.836352	-0.997568	-0.241963	-0.971269	-0.694676	0.606717	0.462636	-0.651754	1.391659
indole	-1.134576	-1.056148	-0.818102	-1.096978	0.091623	-1.122677	0.754194	-0.709795	0.383243	0.954315	0.666513	0.814046	0.233733	2.04061
betaine	-0.275992	-0.145571	-0.90265	-0.852706	-0.187933	1.022226	2.481894	-1.153798	-1.035722	0.39057	-0.723728	0.9392	0.049428	0.394781
valine	1.296578	0.400898	-0.515239	-0.577032	-0.441546	-0.195179	-0.893323	-0.597517	-0.193025	0.81648	0.862769	-0.977803	-1.261253	2.27519
threonine	0.398789	0.080906	0.675919	-0.481584	-1.421906	0.013865	-0.468874	0.7238	-1.14936	-0.376115	2.578888	0.568111	-0.952929	-0.189512
homoserine	0.273306	0.023092	1.688867	0.103504	0.006354	-1.685552	0.703508	-0.742834	-1.235888	-1.031044	-0.623135	1.404861	1.105185	0.009776
purine	-1.114705	-0.940909	0.2323	-0.100821	0.406493	-0.989108	-0.307174	-0.759562	0.416921	-0.167748	1.192694	2.369247	-1.048083	0.810456
cysteine	0.013178	0.620032	0.570799	0.622442	-0.905688	-0.950246	-0.304095	0.010982	0.65171	-2.183948	1.78795	1.084417	-0.481023	-0.53651
creatine	0.040008	1.23949	-1.114567	-0.597303	0.344546	0.074019	0.640188	-0.918809	-2.285094	-0.237545	0.015336	1.012676	0.353073	1.433981
nicotinamide	0.181298	0.275526	0.00846	-2.575952	0.120726	-0.526318	0.655533	-0.654781	0.021614	0.598362	1.823653	-0.166702	-0.706877	0.945458
Imidazoleacetic acid	-1.260766	0.158053	-0.347614	0.147215	1.171664	-0.415551	-1.312872	1.374351	-0.612598	1.915456	0.833805	-0.977529	-0.622384	-0.051231
thymine	-0.944982	1.657955	-1.495495	-0.443184	-0.145708	0.435963	2.081881	-0.201754	-0.797753	0.415818	0.872199	-0.40552	-0.707977	-0.321443
DL-Pipecolic acid	-1.102297	0.096788	-1.007732	0.152512	-0.726246	0.042782	-0.423829	-0.394499	-0.802121	0.586143	1.505312	-0.314325	-0.160945	2.548457
N-Acetylputrescine	-0.779161	-1.135213	-1.163974	1.388753	2.202203	-0.086698	-0.457031	-0.695578	-0.708596	0.575625	0.273478	0.946158	-0.628629	0.268663
hydroxyproline	-0.630333	-1.05732	0.687004	0.822863	0.964978	-0.169119	0.215256	-1.077676	-0.728898	-1.193049	-0.12897	2.485105	-0.134385	-0.055457
leucine-isoleucine	0.011351	0.832184	-0.239583	-0.330224	-0.082824	-0.751692	-1.424846	0.148304	0.202391	1.702365	1.586469	-1.085549	-1.450576	0.88223
ornithine	0.928979	1.111131	-0.006927	-0.068771	-0.753969	-1.3	-0.981096	0.194248	0.699329	1.125912	1.749041	-0.952933	-1.31546	-0.429484
asparagine	-0.717561	0.095445	0.088355	0.54552	0.092024	-0.827647	-0.6402	0.095993	-1.217981	-0.52789	-0.404001	0.681912	-0.201181	2.937213
aspartate	-0.506873	0.350942	-0.107783	0.26802	2.117396	-0.858827	1.780613	-0.401732	-1.376077	-0.911466	-0.749072	-0.354446	-0.007262	0.756569
adenine	1.255944	0.349247	0.561353	0.478919	-1.634724	-0.786072	-0.085214	-1.075793	0.187851	-0.722345	-0.557965	-0.486593	0.249587	2.265804
Methylcysteine	1.255944	0.349247	0.561353	0.478919	-1.634724	-0.786072	-0.085214	-1.075793	0.187851	-0.722345	-0.557965	-0.486593	0.249587	2.265804
homocysteine	-0.245123	2.228577	0.422344	-0.087225	1.221597	-0.786068	0.114091	0.570022	-1.249128	-1.504291	-0.062821	0.208682	0.334179	-1.164837
methylnicotinamide	0.366228	1.849389	-0.919474	-0.891837	0.556898	-0.852575	-0.816304	1.60087	0.16449	0.619284	0.929226	-0.885158	-0.869383	-0.851654
lysine	-0.564683	-1.037477	-0.195898	-0.314586	-0.621429	0.470991	-0.814085	-0.05934	0.717342	-0.989001	-0.20201	0.91924	-0.102649	2.793586
glutamine	-0.829327	0.102352	-0.344648	0.070663	0.018758	-0.118145	-1.150457	-0.430417	-0.769157	0.63378	2.193015	-0.577978	-0.776959	1.978517
glutamate	0.959795	0.737753	0.863618	-0.307033	-0.95977	0.200308	0.701223	-0.359162	-2.221563	-0.786057	-0.817295	0.17905	0.122683	1.686449
methionine	-0.116123	-0.135963	2.233865	0.304938	-1.594979	-0.789523	-1.357373	0.893329	0.020603	0.26768	-1.022685	0.525256	-0.053849	0.824825
guanine	-1.119516	1.977426	1.034653	-0.892397	-0.627376	-0.798603	-0.580599	-0.703084	0.124877	-0.273649	-0.079806	-0.130004	1.996998	0.071082
histidine	1.11912	0.354801	1.038187	0.327164	-1.120893	-1.513014	-1.12063	0.402575	0.240418	0.459086	1.787399	-0.282613	-1.345473	-0.346126
2-Aminooctanoic acid	0.911203	1.073251	-0.000444	0.607192	-1.211124	-0.815086	-1.055328	0.486566	-0.34925	0.174501	-0.075643	-0.954624	-1.033819	2.242604
carnitine	-0.994893	0.482041	-1.455104	-0.003148	0.160941	0.043208	1.515934	-1.328661	-1.335103	0.063228	-0.209471	0.809657	0.601726	1.649645
Methionine sulfoxide	0.824514	0.738042	0.580287	1.070767	-0.646698	-0.429984	-0.483217	-0.047278	-0.793654	-1.938965	-0.133573	0.907797	-1.266241	1.618204
phenylalanine	-1.028774	-1.054175	0.346992	2.050916	-0.653345	-0.564412	-0.131525	-1.276122	1.294863	-0.588958	1.050056	0.510421	-0.57997	0.624032
Pyridoxamine	-0.03702	2.382945	-0.874242	-0.769555	-0.725423	-0.620833	-0.483443	0.228224	0.481337	1.014075	1.450036	-0.744255	-0.684501	-0.617346
pyridoxine	0.894359	-0.545328	-0.199777	3.06873	-0.574532	-0.52499	-0.459913	-0.653144	-0.658636	-0.020656	-0.251787	-0.583452	0.596808	-0.087683
1-Methyl-Histidine	-0.808262	-1.415234	0.853492	0.178706	-0.158579	-1.153531	0.396164	-1.523004	0.924647	-0.73931	1.397392	1.26363	0.888391	-0.104503
N-acetyl-L-ornithine	-0.348295	0.589224	-0.99156	0.124744	-0.548549	1.195472	0.916905	-0.996795	0.090506	-0.302798	-0.95985	-0.283836	-0.933631	2.448461
arginine	-0.308473	-0.835401	0.389185	0.28528	-0.448091	-1.47807	-0.948461	1.21287	0.282335	0.173058	0.355898	-0.377968	-0.793864	2.491704
citrulline	-1.56452	0.561612	1.04121	0.00899	1.010587	-1.357885	-1.335635	0.667593	-0.291802	0.370668	-0.167977	-0.313998	-0.490972	1.862129
N-carbamoyl-L-aspartate	0.123754	0.512498	1.18985	-0.267715	-0.388973	-1.723278	1.976686	-1.310235	-0.176887	-0.814494	0.70411	0.012062	-0.720499	0.883122
glucosamine	-0.652385	-0.437438	0.620667	0.210543	0.862595	-0.255849	0.369618	-0.705117	0.396453	-0.564298	1.659907	-0.198149	1.133688	-2.440234
tyrosine	-0.329746	-0.122072	1.616681	0.667067	-0.581195	-0.40932	0.004772	-0.951754	-0.424153	-1.44543	-0.357174	1.327966	-0.865655	1.870012
Phosphorylcholine	-0.987261	0.515799	-1.575818	-0.480783	0.323075	0.165342	-0.41044	-0.214978	-0.86155	-0.578954	1.102866	0.237394	0.259058	2.506249
3-phospho-serine	0.071439	0.53836	0.416154	-1.025087	-0.059279	0.34382	1.136215	-1.559509	-1.509098	-1.187439	0.495684	1.334626	-0.339923	1.344037
N6-Acetyl-L-lysine	-0.491645	-0.837398	-0.514198	-0.310531	0.579523	-1.262779	-0.848471	0.734226	-1.204419	-0.435093	0.201451	1.385914	1.057164	1.946254
Acetyllysine	-1.173383	-0.136507	0.183897	-0.223705	0.289943	-0.94927	-1.649928	1.484122	-1.129288	0.237493	0.477108	1.248461	-0.222056	1.563114
N-acetyl-glutamine	1.190879	-1.133753	-1.668103	-0.308018	-0.929143	0.234604	-0.288237	-0.170114	0.543126	-0.083176	0.937138	-0.397947	-0.168196	2.240941
N-acetyl-glutamate	2.110065	-1.10148	0.90257	0.556777	-1.497636	-0.353965	-1.017308	-0.091629	-0.179108	-0.946156	0.985059	0.873825	0.111841	-0.352855
Ng,NG-dimethyl-L-arginine	-1.316686	-0.934572	1.566631	0.04924	1.954494	-0.124431	-0.923165	-0.549871	-0.512294	-0.925056	0.079306	1.061257	0.802309	-0.227162
Acetylcarnitine DL	0.239217	-0.607838	-0.769752	-0.934531	0.010785	1.22269	1.709176	-1.236383	-1.432922	-0.115377	-0.017024	-0.44266	1.387568	0.987051
tryptophan	-0.630391	-0.762348	-1.31648	-1.246923	-0.289382	-1.26543	0.195764	-0.109706	0.295811	0.932569	0.104295	1.213131	1.89438	0.98471
Kynurenine	-1.061337	-0.704572	-1.333684	-1.184005	0.675727	-0.292605	0.556093	-0.452724	-0.42655	1.112755	0.216981	0.493504	2.329	0.071417
N-acetyl-glucosamine	0.67594	0.601514	-1.3388	1.834384	-0.563111	-0.017333	-0.732936	-0.756552	0.085277	-0.391813	1.69147	0.842726	-0.987748	-0.943018
Flavone	-0.970155	0.230164	-0.267188	0.045372	0.586912	0.81993	-0.025791	-1.124189	0.14648	0.586059	-0.781146	-1.104786	-0.763283	2.621621
cystathionine	1.08252	1.982505	0.708895	0.881397	0.42438	-0.153107	0.769237	-0.802586	-0.705847	-0.752535	-1.293634	0.064597	-1.058163	-1.14766
5-methoxytryptophan	-0.506457	-0.245347	-1.057487	-1.430991	0.475418	0.748557	2.602857	0.077278	-0.634677	-0.747636	0.397307	0.504576	-0.620403	0.437005
Cystine	0.1715	-0.908079	0.009457	0.272228	-0.18116	1.215269	0.90537	-1.417313	-1.941962	-0.48523	-0.627056	0.505944	1.242761	1.238272
cytidine	1.407229	-1.293651	-0.405199	-0.243581	-0.154696	0.165313	1.571722	-1.104288	-0.861452	-1.371026	1.129459	0.212622	-0.229793	1.177341
biotin	0.579589	1.470444	-0.466073	-0.536358	0.544563	0.829941	0.437722	0.090581	-0.945203	0.382284	0.233172	-0.291812	0.404168	-2.733018
deoxyadenosine	-0.437866	0.097855	0.590147	-0.474753	-0.461698	-1.036937	-1.316182	0.613511	-0.730578	0.675436	-0.591983	2.707563	0.394653	-0.029168
Glycerophosphocholine	-0.432404	-0.486036	0.222017	0.177768	-0.168506	-0.225898	-0.705296	-0.136432	-0.696182	-1.199288	-0.729405	0.919541	0.586894	2.873227

acadesine	-0.532545	-0.425967	-0.612378	0.155494	-0.480572	0.425352	-0.266255	-0.627564	-0.637832	-0.508711	1.882604	-0.497251	-0.444328	2.569953
D-glucosamine-6-phosphate	0.571049	0.684346	-0.899504	1.511787	0.840546	-0.557022	-1.133308	0.298309	-0.687569	0.051048	-0.261148	0.173518	1.43196	-2.024013
D-glucosamine-1-phosphate	0.159206	0.560672	-1.680556	-0.82508	1.475524	1.206924	0.299541	-1.025664	-0.506206	0.769336	-1.704644	0.355311	0.658261	0.257376
S-ribosyl-L-homocysteine-posi	0.066012	0.001731	0.147323	-0.016021	0.800632	-1.594357	-1.229762	-0.846995	-0.485877	-0.32147	0.28964	1.389172	2.239373	-0.439401
deoxyguanosine	-1.634958	-1.411548	-0.241918	-0.307076	0.388	-0.625255	-0.066693	0.224077	0.462518	1.054001	-0.100533	2.358269	-0.634339	0.535455
adenosine	-0.455507	-1.595708	1.279844	1.135499	-0.539015	0.85301	0.246024	-1.360927	0.680528	-0.927139	0.698343	0.211557	1.006401	-1.232912
1-Methyladenosine	-0.822964	0.910844	0.093151	0.690688	-0.765049	0.082805	-1.056187	0.142829	-0.457976	-1.620322	0.253026	0.748437	-0.548542	2.349259
guanosine	-0.251934	0.400045	1.329227	-0.440253	0.870927	1.545045	0.92976	-0.982844	-1.549782	-0.585062	-0.796822	1.095501	-0.919376	-0.644433
L-arginino-succinate	-0.114724	-0.635436	1.426559	0.138347	0.074699	-0.243707	-0.342894	-0.589203	-1.209036	-0.994533	-1.271222	0.635527	0.995529	2.130093
S-methyl-5-thioadenosine	-0.058893	-0.533535	-0.542045	-0.240407	-0.365468	-0.177839	1.015212	-0.542738	-0.417738	-0.497683	-0.00273	-0.536789	3.175524	-0.274872
7-methylguanosine	0.127122	-1.190195	1.096901	0.879761	0.91661	-0.547651	-0.415584	-0.702008	-0.499173	-1.523344	-0.598699	0.864599	-0.39624	1.987902
dCMP	-0.701345	1.024399	-0.685582	-0.866512	0.683071	-0.768659	1.434977	0.286258	-1.790102	-0.65927	0.867248	-0.157607	1.597869	-0.264743
glutathione	2.535414	1.076612	-0.67681	-0.376056	-0.66862	-1.057375	-0.720005	0.944156	0.251694	0.667918	-0.324387	-0.100853	-0.707193	-0.844496
dTMP	-0.084402	1.246241	-0.579625	0.130624	0.640617	-0.397821	0.029474	0.148027	-0.241958	-0.070795	1.024869	0.145212	-2.916081	0.92562
CMP	1.033234	0.202671	-1.205675	-1.2142	0.302819	-0.156926	1.569714	-1.565863	-1.184839	-0.220345	0.409435	1.135501	-0.110318	1.004789
UMP	1.085912	0.108208	-0.949916	-1.261803	-0.024809	0.156657	2.020591	-1.328016	-0.812689	-0.167999	0.242821	0.220032	-0.738613	1.449626
dAMP	-0.70218	1.471125	-0.023301	0.142171	-0.281213	-1.492891	1.461915	-0.544728	-1.783693	0.718377	-0.426285	0.645855	1.097274	-0.282426
Nicotinamide ribotide	-0.455014	-0.2194	-0.733332	-0.813927	3.247372	-0.328786	0.156278	-0.335046	0.122119	-0.776642	0.00704	0.218162	0.161369	-0.250193
aminoimidazole carboxamide ribonucleotide	0.601264	-0.657862	-0.773949	-0.794872	-1.476276	1.053847	0.693494	-1.541805	1.420007	-0.584012	0.763911	1.267945	0.386756	-0.35845
thiamine-phosphate	0.131922	-0.645134	1.873666	0.756823	-0.048561	-0.501551	-0.571622	2.261734	-0.365101	-1.119162	-0.157258	0.04224	-0.822787	-0.835209
dGMP	-0.398857	-1.303641	0.654524	-0.0727	-1.338498	1.665117	0.963023	0.562543	-0.399374	-0.639964	0.733934	-1.349145	1.340661	-0.417625
AMP	0.435472	0.232096	0.805137	-1.177222	-1.617291	-1.158722	1.903828	-0.867676	0.718544	-0.41496	0.018037	1.104006	-0.479951	0.498701
IMP	0.720982	-0.261386	0.356607	-0.994345	-1.091904	-0.504177	2.683342	-0.796863	-0.409515	-0.592951	0.590854	0.088541	-0.641501	0.852316
GMP	0.071195	0.142894	0.567548	-0.338246	-1.249201	-0.168461	2.9056	-0.670727	-0.485881	-0.545458	-0.408746	0.587295	-0.885073	0.477259
xanthosine-5-phosphate	2.738619	-0.492958	-0.684842	1.00822	-0.549166	-0.453812	1.269886	-0.121939	-0.711043	-0.578131	0.10399	-0.566334	-0.511857	-0.450633
riboflavin	0.561918	-1.104114	-1.101391	-0.942707	-1.062122	1.36016	-0.04105	0.586985	-1.15559	-0.486296	-0.082969	1.582618	0.642418	1.24214
S-adenosyl-L-homoCysteine-posi	-0.216416	0.365302	-0.354928	-0.462956	-0.504112	-0.784746	-0.12357	-0.087519	-0.488599	-0.890453	0.508383	3.181501	0.215787	-0.357675
S-adenosyl-L-methionine	0.150442	-0.051158	-0.098892	2.044514	0.005044	-0.522668	-0.678338	2.194489	-1.086677	-1.352214	-0.053505	0.091271	-0.254162	-0.388146
folate	1.240354	-1.293399	0.546976	-0.841676	1.682079	-0.448186	-0.267543	-0.485893	-0.984391	1.739401	0.717363	-0.611551	-0.314552	-0.678982
7,8-dihydrofolate	-0.644435	-0.502884	-0.750467	-0.627321	1.613441	-0.452376	0.958688	-0.770635	1.85473	-0.612781	-0.628289	1.537872	-0.52727	-0.448274
5-methyl-THF	-0.505098	0.467119	-0.113859	-0.154667	0.16919	-0.136562	0.791636	-1.52905	-0.568557	-0.849324	1.261503	-0.777886	-0.501016	2.446572
glutathione disulfide-posi	-0.88232	0.030686	-1.305816	0.306674	0.028129	-0.178935	1.040031	1.262655	-0.362484	-1.275021	-0.062542	-1.357363	0.984092	1.772213
NAD+_posi	-0.349893	0.615313	-0.536449	0.441169	-0.707526	-0.110216	0.294147	-0.224966	-1.284965	-0.583242	-0.839338	1.1483	-0.522941	2.660607
NADH	-0.397606	-0.862385	2.08018	0.083053	0.323127	1.890329	-1.482963	-1.133996	0.214483	-0.573021	0.18602	-0.429455	0.014669	0.087564
dephospho-CoA-posi	1.396072	-1.159564	0.305901	-1.201379	-1.183934	-0.542783	1.518815	0.308918	-0.159392	1.100665	-0.692281	0.747092	0.703085	-1.141213
NADP+_posi	-1.632	-0.22874	-0.225871	2.446446	-1.003554	0.722858	-0.131755	0.601708	-0.401317	-0.787572	0.710612	-0.857141	0.326289	0.460036
NADPH	0.258535	0.164552	-0.530424	1.607103	0.233857	0.544486	-0.618105	1.138638	-2.449612	0.048033	-0.279578	-0.913659	-0.226193	1.022369
coenzyme A-posi	1.126956	1.089516	0.461514	1.625274	-1.597563	-0.559699	-0.746233	0.130699	1.315173	0.002427	-0.837071	-0.460361	-0.325616	-1.225017
FAD	0.911325	-0.417956	-0.349647	0.722975	1.386606	-2.444199	-1.399701	0.140258	0.154358	-0.167182	0.77718	0.254714	-0.359072	0.79034
acetyl-CoA-posi	0.595863	0.42716	-0.390316	1.23518	0.061968	0.719212	-1.78301	-1.61111	-0.39242	-0.242369	0.5111	1.47743	0.603003	-1.211691
propionyl-CoA-posi	2.817682	-0.354141	-0.770742	0.945263	-0.476175	-0.269152	0.002792	-0.804678	1.184242	-0.539062	-0.565156	-0.513449	-0.395174	-0.262251
acetoacetyl-CoA-posi	0.517644	-0.762175	-1.004224	1.133677	-0.833078	-0.712796	2.258902	0.164611	0.14432	-0.869616	0.562382	-0.854734	-0.786016	1.041101
malonyl-CoA-posi	-0.43576	2.842979	-0.545304	1.7139	-0.364447	-0.23734	-0.070373	-0.56614	-0.58023	-0.403058	-0.419079	-0.387332	-0.314714	-0.233103
succinyl-CoA-posi	-0.492098	-0.375991	-0.57907	-0.47806	0.8624	-0.334562	-0.201998	-0.595613	-0.6068	1.255319	-0.478854	-0.453648	-0.395993	2.874968
sarcosine	1.352232	1.395451	0.401971	-0.558597	0.517068	0.85541	0.530914	-0.096545	-1.779756	-1.819127	-0.206404	0.505508	-0.752118	-0.346007
putrescine	-0.872492	-0.562639	-0.945018	0.14624	0.269739	0.656854	1.320029	-0.802843	-1.069751	-1.181032	-0.804276	1.270522	1.257711	1.316956
spermidine	-1.055212	-0.398645	-1.035353	-0.839273	-0.193651	0.982378	1.796855	-0.680803	-0.57167	-0.745072	-0.3954	0.392853	1.760029	0.982962
N-acetyl spermine	-0.959759	0.780203	0.191533	0.069979	-0.497684	0.042706	2.438351	-1.09246	-1.006148	1.330931	0.314714	-0.159877	-0.922266	-0.530222
N-acetyl spermidine	0.686684	0.624307	-0.760841	-1.01477	-0.836581	-0.377308	0.770632	0.126077	-0.249423	2.725502	-0.470224	-0.732989	0.349674	-0.840739
Nicotinamide Riboside	-0.356606	0.290765	-1.412173	-0.964205	-0.423223	-1.621891	0.719396	1.802699	-0.903428	0.553166	0.283855	0.255292	0.418161	1.358191
Adenylosuccinate	1.083226	-0.413316	1.628313	-0.854738	-0.472981	-0.362121	-0.216682	0.672761	-0.101112	-1.260844	-0.047897	2.032819	-1.205033	-0.482396
cholesterol	0.593662	0.358602	-0.658176	2.749582	-0.666113	-0.525014	-0.553475	1.1312	0.592086	-0.641494	-0.699419	-0.65214	-0.430991	-0.59831
arginosuccinic acid	-0.466971	-0.053566	0.325868	0.330747	-0.21938	-0.344782	-0.196496	-0.65716	-1.2124	-1.138814	-0.771393	0.596059	2.596004	1.212284
phosphocreatine	-2.741353	0.771834	-0.879386	0.111438	1.271542	0.388633	-0.249393	-0.628072	0.451555	-0.224287	0.201807	-0.125898	1.145438	0.506142
retinoic acid	1.743069	1.694025	-0.343484	0.690068	-0.966679	-0.888149	-0.784993	-1.091289	0.064318	0.710241	-1.000432	0.767365	0.291471	-0.885531
spermine	-0.161439	1.245027	-0.364503	-0.626976	0.378657	0.982346	2.495173	-0.161528	-1.477152	-0.654561	-0.106738	-0.59427	-0.245231	-0.708805
HMG-CoA_pos	-0.496814	0.144418	0.539576	0.113144	1.651674	0.933138	-0.81717	-0.499389	-0.512425	0.142761	-1.341709	1.971456	-0.546449	-1.282209
N-acetyl-L-aspartic acid	0.068716	2.607112	0.563952	-0.617383	-0.033198	-0.924498	-1.474068	0.362549	-0.139169	-0.370622	-0.513575	1.250005	-0.550945	-0.228876
N-acetyl-L-aspartylglutamic acid	-0.119404	1.010699	0.553583	-0.238355	0.48249	-1.317544	0.096956	2.087783	-0.659927	-1.269155	-0.974255	0.830603	-1.096665	0.61319

SUPPLEMENTARY TABLE 4. T-TEST RESULTS.

	t.stat	p.value	#NAME?	FDR	Fold Change with respect to Wild-type
cystathionine	5.4603	0.000145	3.8379	0.041247	1.4288
tryptophan	-4.4333	0.000816	3.0881	0.11592	0.5798
alanine	3.6209	0.003509	2.4549	0.26152	1.3483
Kynurenic acid	3.5944	0.003683	2.4338	0.26152	1.3339
Xanthurenic acid	-3.1259	0.008758	2.0576	0.42252	0.73046
sarcosine	3.0953	0.00927	2.0329	0.42252	1.2478
guanosine	2.961	0.011898	1.9245	0.42252	1.6672
indole	-2.9608	0.011902	1.9244	0.42252	0.69533
p-aminobenzoate	2.8331	0.015088	1.8214	0.47611	1.5513
quinolinate	2.6568	0.020914	1.6796	0.54334	1.9124
dehydroascorbic acid	2.6534	0.021045	1.6769	0.54334	11.581
p-hydroxybenzoate	2.5904	0.023638	1.6264	0.55908	1.4665
spermine	2.5008	0.027873	1.5548	0.55908	1.3629
deoxyguanosine	-2.4542	0.030358	1.5177	0.55908	0.70009
Cholic acid	2.4509	0.030541	1.5151	0.55908	4.0976
deoxyinosine	-2.392	0.034009	1.4684	0.55908	0.6206
2-hydroxygluterate	2.3904	0.034109	1.4671	0.55908	1.1728
Nicotinamide Riboside	-2.3329	0.037868	1.4217	0.55908	0.59065
N6-Acetyl-L-lysine	-2.2598	0.043224	1.3643	0.55908	0.79847
fructose-6-phosphate	2.2506	0.043953	1.357	0.55908	1.14
trehalose-6-Phosphate	-2.2469	0.04424	1.3542	0.55908	0.77888
Acetyllysine	-2.2367	0.045062	1.3462	0.55908	0.80026
OBP	-2.2341	0.045277	1.3441	0.55908	0.64391

SUPPLEMENTARY TABLE 5. ORIGINAL DATA.

Label	MUT	MUT	MUT	MUT	MUT	MUT	MUT	WT	WT	WT	WT	WT	WT	WT
glyoxylate	132352.3	114778.1	96634.91	92219.5	49536.26	71085.55	75587.23	121391.3	123904.6	137873.1	137159.4	128639.6	98941.87	83565.1
glycolate	84256.09	114634.9	49686.51	73037.76	34777.97	104340.7	144985.4	83414.53	125114.8	92380.09	123833.1	126863.8	125578.1	128294.3
pyruvate	109911.1	204796.6	160713.3	102984.9	116593.6	186847.3	189832.1	173495	201217.5	160422	135408.4	134219.7	237165.1	282693.9
lactate	1.29E+08	1.39E+08	1.36E+08	1.31E+08	87310947	1.44E+08	1.45E+08	1.16E+08	1.28E+08	1.19E+08	1.32E+08	1.33E+08	1.18E+08	1.23E+08
2-oxobutanoate	647573.4	712230.1	449416.1	529270	642936.4	1063016	779781.8	729823.6	795397.1	791043.5	866688.2	911148.7	632263.4	743291.8
acetoacetate	699191.7	715972.7	522262.5	705208.5	632249.1	1222959	985177.6	743918.3	743734.1	698349.3	661690.8	1015170	689399.1	770681.6
glycerate	290128.8	331052.5	212999.9	169317.7	205558.7	410707.5	363425.6	538232.1	713024.4	518083.3	511268.6	500520.3	541125.2	574084.3
uracil	58429.85	54662.89	594158.5	53152.48	107464	724939.3	113753.6	460448.2	60468.6	543089.1	665586.4	152171.2	505709	550831.6
fumarate	14703589	14140638	15201568	11924825	12105319	15532231	13237200	16475021	17209894	16014826	18445750	15899922	15499359	16596447
Maleic acid	13907076	12932406	14791760	11381345	12207172	14373107	13403564	15145514	17477859	15999610	16509447	16494246	15829936	16879340
2-keto-isovalerate	13977588	12729577	13489931	11499311	12240622	13780621	13850935	15020964	15999238	15252361	16538231	16133051	15941024	16010127
Guanidoacetic acid	1401970	1556486	1028554	628120.3	1256871	2013191	1174149	1271552	1467303	1262108	2222224	1395902	1335983	1697597
succinate	17985633	19783705	5662127	7159647	9635141	18628535	11711098	19994116	20590232	22095799	22482955	17656434	23098451	23034725
Methylmalonic acid	20300298	22754618	6096167	7874775	9518945	20681685	13485495	22567208	23179359	25401725	25364263	20723755	25945173	24766929
3-S-methylthiopropionate	80956.03	75979.86	59432.27	66920.19	104080.5	85067.92	56161	50379.23	47896.63	54507.39	62758.01	42119.27	53680.32	77654.64
nicotinate	212106.8	337572	203238.1	712328.7	537073.7	239716.3	242546	368785.1	469196.6	341737.6	345487.6	297047	315058.7	1253627
taurine	1.89E+08	1.87E+08	1.87E+08	1.82E+08	1.88E+08	1.96E+08	1.93E+08	1.92E+08	2.03E+08	2.12E+08	2.06E+08	1.83E+08	1.97E+08	2.11E+08
Pyroglutamic acid	583194.5	821450	945090.3	739916.9	1146450	742149.9	642935.3	682777.2	564900.1	595603.3	631853.7	982734.8	848180.6	714229.2
Citraconic acid/itaconic acid	1897260	2317385	2731848	3009591	2008964	2802077	2294030	2141651	2788685	2627639	2432966	2969474	2349415	2224467
2-ketohaxanoic acid	300134.1	451987.1	232788.3	187019.3	200190	425007.4	430456.8	495405.6	389681	491849.9	430690.9	465625	409841.1	376734.9
N-Acetyl-L-alanine	1.43E+08	1.46E+08	1.42E+08	1.06E+08	1.4E+08	1.38E+08	1.35E+08	1.63E+08	1.59E+08	1.46E+08	1.61E+08	1.58E+08	1.64E+08	1.65E+08
oxaloacetate	1651379	1813832	1237712	1007081	1978850	2115715	2067300	1517828	1768758	1740781	1625132	1964147	1270870	1487847
Hydroxyisocaproic acid	N/A	N/A	125863.8	23111.08	N/A	30013.44	23224.69	33612.55	71223.35	27306.07	60009.27	56579.38	N/A	N/A
malate	53005858	52813013	48345311	49352827	39058379	53864960	53173257	55875365	67631212	64943935	75866622	67899701	64608265	59619756
hypoxanthine	15963677	10627439	22880517	27086666	21799187	19223933	21290364	16858400	20766156	6053228	9719625	19215580	5164449	6136891
anthranilate	262665.7	207567.5	407129.1	353290.8	391295.5	235356.7	331849.4	283874.7	404358.7	78888.44	158843.2	242320.1	88544.89	89013.92
p-aminobenzoate	338777.4	41699.36	416604.1	404392.2	445591.6	303625.4	359603.9	282076	314473.6	52490.93	193173.3	295227.2	103185	149906.9
p-hydroxybenzoate	319711.7	540219.7	386672.9	305323.9	332113.2	243318.2	497327.4	295379	679507.4	437396.6	433225.4	291179.3	438198.3	565734.5
acetylphosphate	669493.9	708545.1	1002839	630413.2	852109.5	601517.8	750275.7	789126.7	891163.9	460956.3	684670.1	747531.4	431704.7	405509.3
Carbamoyl phosphate	1.44E+08	1.46E+08	1.44E+08	1.1E+08	1.64E+08	1.63E+08	1.44E+08	1.7E+08	1.75E+08	1.24E+08	1.75E+08	1.71E+08	1.6E+08	1.7E+08
a-ketoglutarate	9186938	8827032	9321812	7831728	9935041	10857109	7591889	8268945	7244648	6820408	8893979	13202079	9057920	8537466
Phenylpropiolic acid	364195.3	279791.6	369779.5	493980.2	325107.4	294689.5	384720.7	270855.5	371402.3	433860.4	384865.2	403415.6	410748.9	395751.7
2-oxo-4-methylthiobutanoate	357004.2	426757.2	294563.4	212933.6	572339.4	535556.1	366254.7	703997.5	473252.4	398602.5	283297.3	729589.5	609603.2	344964.4
2-Hydroxy-2-methylbutanedioic acid	1498574	1640543	1270308	1440819	1242294	2237873	1627430	1837296	1754216	2097772	1863610	1684737	1822412	2066606
3-methylphenylacetic acid	21517.68	46914.98	53727.37	25088.2	41086.88	54302.15	41042.66	104346.7	60062.22	65334.34	39795.39	56986.08	49255.7	85717.45
xanthine	2732191	3004627	3974177	5738430	3950311	5398945	3433905	3714999	4387675	3328278	3526973	4322016	3425198	5213079
Hydroxyphenylacetic acid	74263.99	71518.9	63612.65	45039.13	61620.26	73311.26	74630.66	94505.76	88574.22	68422.84	86668.43	105368.6	48870.8	66688.95
2,3-dihydroxybenzoic acid	N/A	5528.012	36092.23	18182.42	N/A	32077.52	N/A	30616.88	44014.63	49260.11	N/A	31108.77	31110.89	79066.54
orotate	184724.5	144076.9	307145.1	239967.3	348312.1	263212.9	148613.7	262589.9	337467.4	150982	330593.2	251403.8	131060.5	311799.9
dihydroorotate	578916.3	419337.1	423765.2	441136.8	504458.8	395500.3	436227.1	471123.9	501549.9	516562.2	418873.3	492103.3	460458.3	591805.8
allantoin	449453.3	486020	780702.5	870827.1	1711980	1182363	478231.9	474044.8	919231.2	545086.8	595483.3	632869.4	416448.5	502486.1
Aminoadipic acid	784126.9	1026007	982492.2	667599.6	1080899	855429.8	946963.1	861617.5	990674.9	1030454	929721.5	1101706	840111.6	1264382
Indole-3-carboxylic acid	521189.2	565013	487962.2	414934.2	504757.6	496814.7	596693.9	625237.4	577640	327812.5	400324.3	563681.9	467764.9	678386.2
phenylpyruvate	N/A	7309.182	N/A	7961.057	6370.33	5032.774	9645.449	N/A	N/A	5774.149	N/A	10727.11	N/A	8126.401
Atrolactic acid	17278.56	15606.06	24568.01	20892.45	24196.96	27583.73	16543.16	25124.99	16638	12885.91	28629.47	45140.32	24640.07	28743.02
Phenyllactic acid	155264.8	146228.6	139225.8	88007.61	164448.2	219739.5	123728.4	115618.7	123011.8	112322.4	126513.8	225533.6	138771.3	76670.71
quinolinate	195188	218640.8	179299.1	156896.3	138323.4	83575.12	612458.1	109722.5	116307.7	263305.3	184062.1	177394.5	120917.9	279342.2
phosphoenolpyruvate	2550787	4716018	1237184	808604	1173074	2901785	1736487	4323190	2305033	4973515	4229998	2193682	3629278	3525027
Uric acid	125732.7	88131.79	181823.1	156501.9	197393.6	122251.9	103500.4	69611.65	109974.7	84892.79	69627.14	96003.34	72448.51	68663.39
dihydroxy-acetone-phosphate	6706151	7181191	5114713	2042143	2142150	8443591	8797709	3500823	2937742	2660122	4082140	3092707	2270557	2220013
D-glyceraldehdye-3-phosphate	5795157	7363546	4491591	1931709	1816420	6896333	7855881	3010978	2355898	1970557	2950926	2857659	1608492	1101357
sn-glycerol-3-phosphate	5512141	10169178	2947986	2818359	3421888	6550408	4546207	6197407	5621442	13011411	11507195	4625314	25882268	27009632
shikimate	89193.85	68547.21	95796.47	74621.77	76759.84	9199.56	57809.65	29731.91	210637.1	20596.2	103256.5	1709519	1025711	1796302
aconitate	1620560	1248600	1849496	1515572	1529067	1428372	1324877	1324640	1942539	1219056	1200024	1475466	1533389	2089491
allantoate	238422.8	260479.3	240616.4	198220.8	193993.2	243398.8	228938.5	247402	241002.9	241542.5	275563.3	242996.5	279671.3	276465.8
Ascorbic acid	82404487	78034800	92720086	47845170	74913328	85233340	70555007	1.05E+08	1.06E+08	98131032	1.15E+08	1.1E+08	1.07E+08	1.3E+08
2-Isopropylmalic acid	1.31E+08	1.33E+08	1.47E+08	86167269	1.22E+08	1.36E+08	1.21E+08	1.58E+08	1.63E+08	1.54E+08	1.69E+08	1.63E+08	1.52E+08	1.82E+08
N-carbamoyl-L-aspartate-nega	203125.7	236796.9	175948.4	161725.2	197340.3	244008.3	197131.2	268135.1	220470.5	198093	219241.3	211970.7	229325.3	249620.6
Pyrophosphate	3149528	3286649	3573507	2435257	2752627	4086791	3203059	4609462	4675785	2929364	3331459	4266332	2916917	3772692
glucono-?-lactone	30554.52	32207.14	22292.72	23115.34	30502.92	46250.12	23953.88	58638.75	31298.67	36321.22	45442	7182.337	32042.27	54510.88
myo-inositol	67408650	64438963	63742041	47628542	52545973	60386269	50892101	84249460	79740116	65335978	90388532	71624606	81852283	94500808
hydroxyphenylpyruvate	11460.4	23943.03	35426.35	8582.405	N/A	32128.97	19824.65	5727.801	5753.983	3275.07	N/A	3301.11	2477.63	N/A
homocysteic acid	184246.7	129711.4	242301.8	179207.1	186106.2	196872.7	250571.9	166937.1	194818.2	111471	117611.9	209370.4	102653	147478.8
4-Pyridoxic acid	109111.8	71698.6	151452.2	243890.6	199729.8	130984.6	206829.4	224067.1	152549.8	95472.13	101781.3	261181.1	94526.35	204851.3
3-phosphoglycerate	5009491	8192629	2291161	1511069	2275728	5971001	3301350	6401959	4814508	8017968	8490433	4543102	6707856	6053581
Indoleacrylic acid	65426.97	70885.93	63484.22	125674.6	65983.02	100726.8	108676.9	100213.3	89101.08	39240.05	50990.63	121363.1	39509.52	61272.28
Kynurenic acid	1159246	1175783	842189.6	909873.9	890460.9	1573944	1544677	1571426	1328193	1469843	1251996	1604813	1365515	1442279
citrate-isocitrate	52468120	56137022	83023107	77971725	86814744	80033127	62521587	71079630	97455584	69129014	75780663	76458889	67637873	95455327
isocitrate	132216.6	181318	160577.7	227448.4	178945.1	64956.65	7830.715	200007.2	180185.4	84218.85	99519.71	41896.9	100993.5	282951.2
citrate	40750981	41397667	52577092	40497870	59428060	47311948	42709477	45385503	53613158	37686916	51592291	48371155	29168235	60712507
2-dehydro-D-gluconate	34380.32	21196.3	8997.843	29669.1	24464.61	28162.91	23961.02	37460.61	31337.54	28350.71	31669.24	31017.83	21672.53	45473.61
D-gluconate	237927.2	227950.1	202340.2	121866	232888.6	261739.9	233665.1	335295.9	265614.2	254309.5	253149.8	305570.2	255999.9	295873.2
D-erythrose-4-phosphate	864749.2	814568.9	879671.8	558895.8	677605.8	742571.5	1181607	958853.1	777941.8	708071.4	779590	793512.8	723235.4	940325.2
Xanthurenic acid	181607.9	313551.3	164058.6	133565.5	169339	356473.9	306100.8	219274.7	313089.8	217195.5	226444	450427.9	193305.1	220941.8
lipoate	21471.09	32205.42	6204.522	18170.81	4110.903	4795.548	6696.159	5905.239	23126.42	8922.354	5040.903	7993.288	15823.69	7500.889
D-glucarate	253759.8	300087.3	414385.3	279104.5	204918	385094.8	232193.9	419606.2	459105.3	124357.7	265934.7	433807.8	359265.6	284233.2
deoxyribose-phosphate	292133.1	224100.7	333202.8	238362.7	240132.4	172788.5	301671.3	312688	360765	299519.8	358199.7	205812.2	286083.5	215994.2
pantothenate	17227732	16518489	20955706	12932430	19730040	21073273	15656240	14406113	20340926	20309038	17572564	17733999	15741592	21345220
prephenate	N/A	N/A	6565.5	N/A	N/A	N/A	4952.841	N/A	N/A	N/A	7433.438	N/A	N/A	N/A
deoxyuridine	5696.816	5611.608	5732.883	4857.796	5776.093	N/A	7295.209	N/A	N/A	4046.267	N/A	3687.072	13068.96	5622.341
ribose-phosphate	8678038	6467936	7725741	10960105	8212550	8347116	8917153	8442451	10214622	2276215	4237432	9044684	1854269	2123816
thymidine	24865.05	23191.48	23919.45	13127.74	10479.22	27211.89	20175.69	10740.62	26367.36	20632.44	27006.39	12660.64	25319.72	17769.74
uridine	1622777	1698157	1955373	1831090	1863975	2251873	1627559	2281100	2192260	1557023	1844867	1925383	1475564	2098886
deoxyinosine	42655.5	44465.82	78954.29	54672.04	51059.23	48172.84	38293.98	33059.88	29902.33	31226.98	23202.82	75062.73	41084.44	22352.42
shikimate-3-phosphate	N/A	N/A	N/A	N/A	N/A	N/A	N/A	N/A	N/A	N/A	N/A	N/A	N/A	N/A
D-glucono-?-lactone-6-phosphate	53041.21	56790.6	71228.83	21935.39	36125	52945.44	68612.94	29070.77	24450.18	32224.16	9385.34	19450.86	21834.26	11033.75
hexose-phosphate	23463145	22126168	19707564	13254223	14031448	23338987	27183837	20436787	17683819	19194416	21143612	16742557	20437516	22137523
glucose-1-phosphate	1516614	1427063	1104334	553187.4	976177.2	1443815	1546021	1064071	1037343	1164188	1068525	1098797	1074539	1183794
glucose-6-phosphate	1638315	1142598	1313573	377226.9	573548.3	1419667	1919813	861058	733271.6	859443.3	938891.5	711654.8	882265.4	1120540
fructose-6-phosphate	1540801	1264550	1156845	415712.2	543739.1	1445989	1958515	836299.8	595535.6	660921.9	791291.5	675572.3	805526.9	970088.5
1,3-diphopshateglycerate	101314.7	386447.7	77732.21	78783.21	40873.45	70430.64	69969.16	98022.02	71858.23	420877.4	159484.8	60836.91	410708.2	524934.8
2,3-Diphosphoglyceric acid	88665.3	421952.8	44435.45	83604.84	37316.78	84125.05	32503.8	117501.8	50625.24	600685.9	166919.4	34432.74	631865.5	626999.2
S-ribosyl-L-homocysteine-nega	345033	190222.8	251657.5	224065.7	154653.7	288457	264766.4	347219.8	332477.5	116861.9	215280.6	331078.2	132122.8	181094.3
inosine	1.04E+08	1.04E+08	1.07E+08	1.21E+08	1.03E+08	1.16E+08	96361812	1E+08	1.1E+08	95129528	95334702	98011586	80095204	95301784
6-phospho-D-gluconate	473929.6	321276.7	345430.9	210459.9	346897.6	403102.7	433288.4	307782.7	331165.2	160484.8	271346.5	374352.9	165603.4	207517
xanthosine	153296.7	300270.1	177467.6	150133.2	345672.4	306859.7	204504.2	443455.6	493921.7	399647.3	243487.6	368866.5	368039.5	414604.6

D-sedoheptulose-1-7-phosphate	1814930	1467011	2373716	2320891	1981888	1893952	1975375	1498469	1608722	1028742	1061490	1503564	990337.7	953118.9	
N-acetyl-glucosamine-1-phosphate	913904	945095.7	883638.4	737107.8	1105583	1063867	849146.8	1264677	1163242	1103306	1100495	1216301	1115866	1261016	
glutathione-nega	24882796	22504091	18928375	9163645	18287991	20991731	21266015	38973136	30981300	32509493	33069748	39058998	36675705	34849509	
dUMP-nega	33861.72	21076.49	26425.4	4950.759	7555.312	10738.15	3184.603	24782.2	18030.61	14866.61	43677.37	22336.74	28435.15	36676.97	
Geranyl-PP	26931.78	61227.15	71873.38	33824.89	20885.84	22152.41	35023.25	38386.81	55256.94	37327.82	45642.83	34987.95	69349.11	88349.65	
O8P-O1P	582576.6	576446.5	507272	450680.8	419898.4	1031110	731519.3	618657.5	529687.5	494927.4	575117.3	607442.6	346479.3	587117.5	
dTMP-nega	31384.05	37992.46	33859.52	44576.87	55270.28	61083.7	42142.42	46226.41	39594.58	18227.53	33836.57	34839.17	22696.98	9681.908	
cyclic-AMP	156095	87499.38	189800.8	94187.7	42062.78	55328.6	92560.31	66949.06	112330	288765.8	154368.8	56104.03	902666.6	828236.2	
fructose-1,6-bisphosphate	3463757	6843898	4634642	1159041	1565546	6378680	8622405	1967130	2093487	2025868	2502236	2105630	2258154	2058720	
trehalose-sucrose	4877.691	11565.13	8336.842	10637.34	N/A	11676.58	8266.359	N/A	4178.312	4944.644	7646.325	4902.492	N/A	3245.734	
Cellobiose	N/A	N/A	6543.808	N/A	N/A	5705.541	N/A	4129.143	N/A	N/A	N/A	N/A	N/A	N/A	
orotidine-5-phosphate	47651.44	51270.28	46096.22	34450.36	30816.2	42845.22	38617.07	38637.14	29969.05	18981.2	43883.86	43598.62	45349.48	39059.5	
SBP	724535.7	814764.2	1323513	877615.4	1250681	1382732	962415.5	409713.9	620078.2	371187.3	595102.1	651650.8	315931.7	324026.2	
trans, trans-farnesyl diphosphate	9078.622	16475.9	22075.14	6401.783	10707.73	29050.11	18122.25	6012.707	10784.45	16491.59	21151.59	17507.6	7563.802	33347.68	
S-adenosyl-L-homocysteine-nega	3144196	3244980	3070099	1833258	2258725	2698076	2451439	4946685	4701161	5394714	4699911	4146720	4733533	6621893	
dCDP-nega	10735.51	13215.87	14865.97	8257.099	14865.86	14803.28	4130.239	22270.86	17343.67	32212.2	33034	22230.31	42946.72	18160	
5-phosphoribosyl-1-pyrophosphate	28245.29	47100.38	14275.9	43769.81	22304.95	27452.93	58775.53	46229.94	61060.86	68454.15	46209.25	55170.01	73247.58	72701.05	
Deoxycholic acid	N/A	N/A	N/A	N/A	N/A	N/A	N/A	3302.535	N/A	N/A	N/A	N/A	N/A	N/A	
OBP	68386.15	127360.7	206168.7	172700.9	115119	114820.5	186159.2	158418.1	132279.8	122571.7	115624.9	194831.3	109614.3	113104.8	
dTDP-nega	60291.2	48613.98	31384.46	17372.86	10010.86	84950.07	39663.36	50285.67	49471.59	45362.89	60069.14	52854.41	63445.39	56981.27	
CDP-nega	244463.1	267676.9	195209.7	109592.8	174475.2	224915.8	236224.2	309147	283004.4	469675.2	357799	349013.2	571593.5	480375.8	
UDP-nega	2140631	2516990	1486987	924106.9	1844896	2630506	2091434	3273693	2592745	5343999	3606271	2759206	5732882	5592984	
Cholic acid	N/A	N/A	N/A	4148.663	N/A	N/A	N/A	N/A	2451.095	N/A	N/A	2597.642	6603.82	8287.639	
trehalose-6-Phosphate	277828.9	249220.3	201975.5	131198.2	223099.2	338480.4	284158.5	468887.9	377465.5	238725	292314.6	382450.4	273697.3	334532.5	
Thiamine pyrophosphate	190786.1	329367.8	109591.2	128643.7	213732.1	394579.5	274010.6	353105.4	278900.3	286126.8	341697.5	377312.5	257204.6	386668.9	
adenosine 5-phosphosulfate	190945.9	195615.4	88369.75	57774.01	71832.57	175089.8	136261.6	203983.7	137905.5	330302.4	270134.7	136279.5	422027.5	371367.9	
ADP-nega	14041138	16866289	7577173	5766104	7008811	14250102	11665726	19446600	13118898	33908769	25844673	13945086	35139380	35994869	
dGDP-nega	13952143	16471073	7671568	6013149	6383992	12913370	11132929	20654166	12914624	32652296	24626968	13406077	34486059	38263355	
IDP-nega	1821618	2203399	1027535	768625.1	856434.7	1747647	1410558	2858622	1644009	4082155	3074315	1727186	4777801	5269336	
GDP-nega	899747.1	752852.6	690311.5	504690.5	489395	834819.6	699441.8	914551.9	926889.2	1553531	1131564	878857.9	1367858	1665715	
CDP-ethanolamine	462486.3	563270	458293.2	375770	576286	638418.7	526913.7	753218.8	668966.5	570691.3	683740.1	754015.8	590516.1	685469.8	
FMN	19001.86	25520.08	41292.66	20643.8	55329.62	19831.65	21473.93	22295.89	42117.06	55333.72	28941.9	27251.23	64425.61	49494.79	
cholesteryl sulfate	7156001	5071360	10024580	3782789	599498.4	3085606	2808010	1880504	1270839	5603146	1938237	317015.5	2991974	7279203	
dCTP-nega	7433.016	13952.51	9133.555	N/A	12388.29	4952.718	4127.777	11560.55	4952.854	32282.18	13215.65	10733.03	28907.09	32208.26	
dUTP-nega	4042.352	30558.99	10737.99	9907.828	10733.86	9910.985	9047.627	3180.725	N/A	5349.864	8328.083	4105.677	16228.14	7432.052	
dTTP-nega	4942.393	11611.61	9084.593	N/A	N/A	15693.45	11560.7	11407.27	16490.31	41295.07	11561.59	13213.43	43623.53	35605.11	
CTP-nega	380697.8	380854.9	272773.3	242300	259326.1	349386.1	509566.8	349069	265486.7	814026.1	390518.3	320681.9	681986.5	673146.8	
UTP-nega	614502.9	871466.2	442207.8	200734.6	406665.6	634608	571268.9	1011084	805390.3	4401948	1927721	793649.6	5445861	4885983	
CDP-choline	387334.2	393110.5	235393.4	431955.4	150311.7	531229.9	376598.1	350985.2	390628.6	346256.1	308056	308871.9	370823	387460.7	
dATP-nega	N/A	10735.73	N/A	N/A	N/A	N/A	N/A	9082.951	8257.145	20646.38	6605.346	4130.114	18169.02	23123.34	
Taurodeoxycholic acid	90825.11	82595.62	74322.45	46347.08	82586.46	103665.6	99093.18	91602.5	53174.75	80936.22	91670.42	90841.67	95801.92	85039.01	
ATP-nega	6116186	8272377	3523994	2108139	2162668	5869687	4162713	8254347	5515964	35514590	15471772	5671287	45678864	45130960	
dGTP	6320400	8906933	3575161	1958013	2096990	5946151	4195002	8108913	6220631	34471020	16127032	5965357	46977108	41650654	
GTP-nega	588142.4	676297.1	459933.9	344682.1	251911.4	557500.1	467985.4	736077.3	555178.5	2983192	1292202	584636.7	3523834	3304428	
UDP-D-glucose	6870196	6707750	4455716	3323486	2792244	8616515	6978398	8314870	7908507	6754650	8517994	8592311	6722593	8132719	
UDP-D-glucuronate	372472.5	293187.5	256026.8	133795.2	196552.5	448435	355132.7	403017.1	449280	392283.5	370809	473227.1	320455.4	381545.9	
ADP-D-glucose	63510.09	61939.16	37823.3	33043.61	33036.11	49531.2	45440.28	73502.61	62765.66	70617.73	88200.91	59557.25	61933.86	50365.45	
guanosine 5-diphosphate,3-diphosphate	9908.042	19819.03	17340.81	14040.84	9562.973	10184.94	18995.79	17323.25	24776.29	26409.74	15905.58	6660.879	34170.53	37989.53	
UDP-N-acetyl-glucosamine	1578270	1936690	1384180	1065395	1455987	1912620	1835971	2013465	2217293	1924335	2297532	2740251	1877297	1870613	
glutathione disulfide-nega	9032244	8989996	12625691	7779692	12033139	8388175	9237887	12517422	10111880	9610044	11166221	10379591	11869026	11741020	
NAD+_nega	1171111	1516514	372957.9	380348.1	468439.5	1452311	682033.4	1694279	1094947	1994441	1805137	883017.9	3137470	3295852	
NADH-nega	517014.2	917434.1	128015	80936.65	274206.7	678044.1	279997.3	1186791	806093.4	1427049	1478327	872136.5	1769773	1489067	
dephospho-CoA-nega	293582.1	259041.6	133627.1	103829.7	80532.91	216486.5	394747	244931	142946.9	72121.78	143270.1	231515.8	139685.1	78785	
cyclic bis(3->5) dimeric GMP	N/A	N/A	N/A	N/A	N/A	N/A	N/A	N/A	N/A	N/A	N/A	N/A	N/A	N/A	
NADP+_nega	371975.2	562869	175862.3	126354.9	224369.8	459601.2	349050.8	506785.9	435625.2	689421.6	741670.3	372111	669297.5	709625.8	
NADPH-nega	5780.388	6607.936	4130.255	5749.217	3302.66	9908.029	N/A	10732.98	4127.752	7432.933	4954.674	5777.48	9085.815	9906.385	
2-hydroxygluterate	14086373	13598431	10162803	9438780	10675497	13775860	13232923	14663880	15194430	12912372	15240337	13896527	15209049	17071037	
2-deoxyglucose-6-phosphate	56903.36	38311.92	41567.52	35490.7	52892.13	31087.19	43761.22	108731.8	105642	51987.35	44931.11	71762.89	124826.1	85147.87	
4-phosphopantothenate	36346.56	37997.42	18862.03	16395.01	10729.15	22380.42	24774.07	23414.46	11560.82	12406.62	16520.55	22279.08	4954.724	14810.57	
dehydroascorbic acid	N/A	898282.9	N/A	407140.9	1339798	1092401	810082.2	1401416	N/A	N/A	1383114	N/A	1054559	66230.42	
3-hydroxybuterate	2365597	2471169	178807.8	268799.9	211426.1	176338.1	185104.5	177879.5	1892093	734041.1	608618.1	980715	172948.7	673839.6	
itaconic acid	1897260	2317385	2731848	3009591	2008964	2802077	2294030	2141651	2794306	2627639	2432966	2969474	2349415	2224467	
Urea	12761387	10169981	27827942	26875983	60991301	9423095	8904603	14435509	12559290	9801519	18845740	11377649	16052482	13980075	
ethanolamine	4122132	4275373	4118742	3918964	4221291	6468371	4357484	4995026	4668805	5144795	4820787	5155817	4370421	4580670	
glycine	49549.94	86715.86	38850.4	30556.78	71023.88	50561.11	59386.54	22298.43	19852.16	21471.22	19821.14	19825.09	23954.17	37162.27	
alanine	24552046	26110464	26617860	21308759	26313188	26438961	23362342	36766715	35426570	34505723	35975696	35535308	33847772	37891843	
betaine aldehyde	164324.3	145752	147966.1	104363.6	152993.3	143713.8	133053.7	153374.4	184660.5	179839.1	125481.4	149071.5	196333.6	159185.6	
choline	144257.6	254748.8	202412.3	174080.1	36634.36	55828.89	133157.4	347326.3	112282	264854.4	499869.5	272275	413665	494411.9	
4-aminobutyrate	16676874	18308149	17483693	12675799	14542553	19124358	16613724	18187181	19076255	18214011	18030932	17505816	17751598	22533879	
dimethylglycine	215190.3	227565.8	207447.7	111897.5	206155.2	257363	251421.5	345941.1	238165	228306.6	307228.6	236101.7	259785.7	267968.4	
serine	7374145	8460685	4964173	4761674	5362193	8559934	8395430	14945056	16818949	13848622	13259737	9820693	12377115	14060283	
cytosine	97939.37	45030.19	90029.97	48797.6	63146.46	72195.84	39808.75	107026.7	33439.31	76211.24	97890.31	85389.54	52103.92	44915.93	
Creatinine	6962135	6595769	6125831	4452720	5970979	7043401	5898336	7721246	7321483	6911749	7337355	7128417	7067951	8260824	
proline	40632172	40354965	44745206	39287071	60895485	73220917	36748246	20711975	23579915	24358284	23170366	28210713	21613722	28594346	
indole	97379.72	101009.7	68134.39	33394.07	65136.57	99086.82	82976.81	72511.89	87197.83	57018.36	80202.68	156563.7	65851.48	56829.47	
betaine	94181582	58220146	66096865	61853976	48768478	54973938	86891436	48005476	58364352	69315506	46855179	50012910	51057528	45235642	
valine	618362.5	486939.6	598119.4	589916	629302.5	736119.9	625254.1	542022.4	288736.4	386932.5	404621.9	398802	341522.3	483918.8	
threonine	15364796	17838486	18153629	12667283	19884504	22798179	17988992	15076575	17626739	12645679	14832929	10279724	15828197	18954163	
homoserine	40088.12	86423.12	58063.54	45466.8	37153.23	121290.1	99552.48	125548.9	178355.4	98651.43	110111.3	104919.8	158730.7	158559.4	
purine	126930.2	133705	113128.6	64418.47	97015.13	135486.2	109580.5	67265.37	70697.85	70881.79	100938.2	196132.8	32488.95	64385.76	
cysteine	10558.71	18371.16	12784.32	9029.605	28801.8	9888.816	21849.7	20977.02	14678.15	13059.75	4942.512	25639.59	14543.57	19104.18	
creatine	2.66E+08	2.69E+08	2.61E+08	2.36E+08	2.56E+08	2.57E+08	2.54E+08	2.61E+08	2.63E+08	2.65E+08	2.62E+08	2.63E+08	2.63E+08	2.81E+08	
nicotinamide	1.88E+08	2.03E+08	1.95E+08	2.02E+08	2.46E+08	2.24E+08	2.91E+08	2.39E+08	2.64E+08	82039894	1.8E+08	2.76E+08	79849816	73278902	
Imidazoleacetic acid	147207.8	82763.62	86225.61	74900.45	162450.9	90101	87725.27	101176.6	122991.9	107916.4	113622.1	102810.9	125915.8	148443.2	
thymine	185187	186046.7	185943.7	163536.1	198876.6	187885.7	231889.9	217208.4	211434.9	213959.8	210038	204536.6	207573.6	215472.7	
DL-Pipecolic acid	84193564	83517563	67362563	56615629	66176348	74813967	78941703	84784392	78790430	82847522	78374733	82718739	86456610	91529755	
N-Acetylputrescine	3974.954	6401.25	N/A	17535.53	6241.646	24455.92	17806.53	13563.87	11484.23	12420.2	12474.82	10607.23	10304.35	9448.079	
hydroxyproline	238702.5	391794.5	194915.5	151028.6	269253	937306.9	643279	590463.4	1023916	967116.8	609377.5	476516.3	626881.3	745603.2	
leucine-isoleucine	27063639	19640838	19341527	19165820	27284370	27969890	20234320	15718376	11651269	10323469	13038568	13292318	14514142	20785061	
ornithine	337855.1	871680.9	780445.6	761114.1	937731.9	1435225	655784.3	352738.7	688782.3	489631.6	624735.5	524628.5	300641.2	535182	
asparagine	2850161	2650035	2126461	1595772	1147621	3699058	2816529	2294967	2099516	2158405	2371912	2097407	2048794	2542270	
aspartate	38137595	37225092	26611884	21633062	37545605	38734544	35642528	41972062	37076296	35074868	41966175	49873901	37238234	39163497	
adenine	325242.1	455303.9	307819.7	318494	198315.9	447402	365021.7	420190.9	483176.7	423321	316387.3	744723	493966.7	341018	
Methylcysteine	325242.1	455303.9	307819.7	318494	198315.9	447402	365021.7	420190.9	483176.7	423321	316387.3	744723	493966.7	341018	
homocysteine	151896.8	149483.8	108445.2	99048.88	118114.7	174574	134285.7	243190.6	195053	226586.2	210510.8	231532.1	190110	216923.4	
methylnicotinamide	3708.094	11535.08	N/A	6958.994	2344.236	4343.405	5699.52	11166.1	N/A	4990.244	5287.536	2460.848	3711.423	2981.647	
histidinol	N/A	N/A	N/A	N/A	N/A	N/A	N/A	N/A	N/A	N/A	N/A	N/A	N/A	N/A	
lysine	2398080	3176341	2825208	1981282	1979885	4150693	3514841	2673239	2085355	2139014	2651413	1387497	2798066	2907767	
glutamine	1.26E+08	1.29E+08	1.28E+08	1.11E+08	1.17E+08	1.41E+08	1.22E+08	1.11E+08	1.06E+08	1.03E+08	1.12E+08	1.44E+08	1.13E+08	1.18E+08	

O-acetyl-L-serine	16227.03	N/A	6985.101	N/A	N/A	N/A	N/A	N/A	N/A	N/A	19601.24	N/A	N/A	N/A
glutamate	1.52E+08	1.48E+08	1.4E+08	1.29E+08	1.15E+08	1.41E+08	1.41E+08	1.42E+08	1.53E+08	1.46E+08	1.55E+08	1.51E+08	1.53E+08	1.59E+08
methionine	1662881	2720645	2526666	1462042	844353.6	1604642	2288866	4791208	4143508	4873697	3640059	3614463	4609335	7756599
guanine	349941.6	337369.9	393353	371448.5	279720.6	347333.8	415790.8	384371.8	335800	370063.1	382271	364372.9	205732.1	302644.2
histidine	7360176	9672030	7925109	4285806	4509626	17265198	16115479	7565140	4660787	8150298	12128998	9947887	2682579	6156924
2-Aminooctanoic acid	4308745	7525460	10766491	7496626	7776518	6468009	5707702	20550724	12869439	12011384	12688704	12196159	4079850	5257931
carnitine	67795794	56627111	63205712	42764032	46795904	45393340	50657861	65903178	66379691	73763995	70607092	59784037	72500431	70714004
Methionine sulfoxide	61250.96	72886.66	123579	40365.9	21266.1	34788.25	99575.91	187993.8	88850.16	89169.67	157629.9	67006.61	166399.5	228471.9
phenylalanine	10608035	13590796	10948822	6655572	10338543	15339083	10031737	9697612	6449329	8251594	9917073	14705337	6308883	7961552
Pyridoxamine	N/A	N/A	N/A	4983.016	N/A	N/A	N/A	4125.693	13202.06	N/A	N/A	4061.643	N/A	N/A
pyridoxine	N/A	N/A	N/A	N/A	N/A	N/A	N/A	2473.781	N/A	N/A	2477.489	N/A	3302.638	N/A
1-Methyl-Histidine	1857428	2227099	811511.4	776042	1198638	3744677	1013599	436238	1807223	1240102	899524.6	1825363	298754.4	531029.8
N-acetyl-L-ornithine	4352.141	6870.328	10060.88	13513.56	2419.524	N/A	N/A	8942.048	6005.414	3302.627	4955.117	7288.221	11534.83	3172.255
arginine	9676554	11987599	7058238	7444752	7924362	14869715	9805969	4012085	7649254	8637708	8640035	5102208	5678833	8993664
citrulline	144953	271848.5	189906.8	145339.8	126326.2	295306.4	333281.1	85526.07	96892.76	191660.6	213340.4	87423.42	112960.2	119276.8
N-carbamoyl-L-aspartate	238679.8	246937	213901.5	189955.1	224641.2	208915.8	247716.2	263430.8	227941.8	245290.6	202337.8	207296	166006.8	321261.8
glucosamine	46230.24	179812.5	364569.6	125119.2	70437.31	217684	208042.7	76490.2	43110.82	186936.4	121585.6	47086.16	89309.66	133427.2
tyrosine	904057.9	1544099	1009195	1128649	581372.4	1038755	1114837	998685.2	1564867	1239586	856982.2	1780791	1582182	1062479
Phosphorylcholine	88091944	87103389	99466759	66777439	1.06E+08	1.04E+08	77467289	1.11E+08	92073043	1.16E+08	1.17E+08	99693216	95057571	1.25E+08
3-phospho-serine	19782.19	48880.91	22338.84	16543.16	53771.05	35787.2	15846.51	109191.9	48806.43	87760.08	48810.59	46937.52	67817.97	38880.92
N6-Acetyl-L-lysine	11794711	10972071	7705525	6188844	7267682	10273393	10435814	11725935	3906256	4670946	9535782	10031577	11414183	12066430
Acetyllysine	11303914	9684086	7547469	6183250	6122039	8890381	6465603	7716775	8580602	9590728	8261057	7306548	7889859	10871120
N-acetyl-glutamine	63513.8	56444.07	49664.13	21075.7	51888.51	59626.31	67161.23	77032.04	50090.3	42323.91	38438.5	44445.5	68060.97	72181.94
N-acetyl-glutamate	1043223	920978.5	687923.8	522394.8	626035.9	1034741	981724	1185602	1021570	1262496	1133817	1105834	1142691	1487844
Ng,NG-dimethyl-L-arginine	1389142	1267063	1390304	885429.9	1116022	2442297	1191316	1233537	1115602	1060536	1028901	911684.3	714495.4	1285629
Acetylcarnitine DL	1.67E+08	1.59E+08	1.75E+08	1.58E+08	1.45E+08	1.56E+08	1.48E+08	1.51E+08	1.47E+08	1.66E+08	1.82E+08	1.33E+08	1.69E+08	2E+08
tryptophan	2166639	3084131	1482698	1002484	1095510	3804680	1982014	2435776	3314720	1813802	2157105	3689892	1364026	2403127
Kynurenine	37809.41	39024.65	38659.55	39787.87	43913.05	59685.6	22273.32	12566.06	24172.53	46778.03	29754.46	49783.22	35361.48	25033.42
N-acetyl-glucosamine	43035.99	28051.46	51857.61	34684.63	28066.17	84206.76	49380.82	66805.75	59134.42	54522.18	64016.85	61088.62	48678.29	57873.24
Flavone	22554.43	20068.53	N/A	4144.243	17272.75	19246.39	16914.22	7091.537	6309.074	5717.715	N/A	17365.27	21733.22	25951.17
cystathionine	2744033	3666652	2281765	2277253	3085415	4095323	3217965	1920271	2007298	2257823	1941284	1691855	2386432	2513001
5-methoxytryptophan	12036.04	7778.041	4106.036	9755.733	5589.116	16059.66	4901.659	17932.18	11588.36	8706.743	7266.172	16204.28	10928.2	11450.31
Cystine	39654.28	35517.66	37864.43	28945.99	44567.46	61070.7	56337.84	41143	49640.6	29547.98	39648.17	72675.33	42048.6	30547.98
cytidine	2396664	2020053	2565166	3721354	2379380	3564470	2885201	2600257	3060990	1993914	2671081	3157346	1963321	2284652
biotin	57750.25	52490.82	52891.87	22765.82	53046.12	73986.22	28933.49	83151.51	44484.03	60878.36	67354.14	55350.18	52071.82	69272.28
deoxyadenosine	10641.42	19630.91	5016.136	21590.76	31404.99	6134.536	29047.56	29332.86	19867.26	8183.96	37187.54	39456.22	3583.335	12988.38
Glycerophosphocholine	67100509	66184334	65473590	20558725	30659437	43243441	66020075	1.07E+08	67823530	74321652	1.05E+08	58004722	1.05E+08	1.11E+08
acadesine	4954.527	9960.061	10878.4	N/A	N/A	8340.484	N/A	8383.661	7599.036	3204.762	4146.173	N/A	4099.777	12729.36
D-glucosamine-6-phosphate	84020.57	53709	72432.29	13313.12	61278.55	47937.84	54517.2	55359.25	59435.51	91728.57	84254.62	42166.77	91480.46	91467.7
D-glucosamine-1-phosphate	50272.84	65331.68	39708.3	23675.05	24913.69	66895.42	51233.37	93179.53	63161.76	58678.41	71793.16	68475.04	38814.06	73642.23
thiamine	N/A	N/A	N/A	N/A	N/A	N/A	N/A	N/A	N/A	N/A	N/A	N/A	N/A	N/A
S-ribosyl-L-homocysteine-posi	40468.7	46247.85	19797.1	24657.65	17343.62	66067.82	51206.24	46257.59	24682.37	63591.31	61113.96	49543.49	52852.88	61961.54
deoxyguanosine	24777.81	10063.76	5062.29	14503	7976.255	7202.823	3461.458	3372.18	22277.67	19827.75	8075.361	3282.465	5605.946	2464.366
adenosine	9008.955	N/A	18874.09	28814.12	18544.67	16932.63	19522	16285.88	2859.961	7067.043	N/A	9162.66	11406.53	N/A
1-Methyladenosine	6619.589	9911.759	4084.194	12386.82	9085.28	14866.58	7339.027	17376.96	14773.37	18995.35	23094.71	15729.22	39343.18	16507.82
guanosine	129421.1	128739.1	162696.1	201121.2	148660.5	180141.8	122301.4	124730.6	128993.8	100731.2	114777.9	93506.02	108191.4	141533
L-arginino-succinate	514519.3	502114.4	327832.3	349340.2	337779.2	870878.4	575569.6	210614	456752.9	415415.2	347016.9	345251.8	239272.5	337777.3
S-methyl-5-thioadenosine	N/A	129316.4	N/A	37896.22	4941.937	140274.3	93076.87	484349.6	29653.26	N/A	N/A	227353.2	N/A	51094.99
7-methylguanosine	73449.24	1620.883	80749.07	44601.88	67723.13	1640.785	98275.32	92497.85	137919.5	2689.848	101581	107341.7	87515.78	175908.8
dCMP	82583.38	76874.16	70221.98	72637.1	78457.68	72679.81	80531.66	87519.32	89163.93	85860.82	78449.35	86718.95	50376.41	54529.36
glutathione	25583153	27480963	27953330	11502784	18229103	27086841	26501731	42072071	37288622	44284591	44453975	36775080	37795932	35647665
dTMP	22623.72	36935.97	40633.87	40467.42	28900.34	32032.54	41089.44	37164.83	23974.33	33047.55	35512.04	28832.84	28903.41	31933.29
CMP	6726256	6312156	5005765	3670112	5165854	7493040	6531595	8946581	7106457	6762832	6888040	7221041	4369748	5916785
UMP	2708857	2672333	3005402	2396159	2958531	2590482	3080145	3174202	2991692	2314189	2386931	3235184	1805505	2260259
dAMP	81768.95	90022.61	56976.57	57433.35	100767.5	96628.13	56989.99	93325.21	113117.8	132712.3	136266.5	140877.7	87449.22	121375.9
Nicotinamide ribotide	6359.529	N/A	4960.851	N/A	22349.65	N/A	N/A	N/A	N/A	N/A	N/A	N/A	N/A	2333.519
aminoimidazole carboxamide ribonucleotide	19762.53	15694.39	23989.37	18996.22	18171.11	14034.76	9089.084	37164.59	27278.04	25602.51	40371.49	28904.88	26425.55	23176.79
thiamine-phosphate	202863.9	188669.7	312429.2	279382.4	230725.5	216755.5	150214.5	251606.7	305020.1	119697.6	144432.4	366276	80994.88	60488.33
dGMP	57804.32	45237.02	15868.84	21780.34	15913.38	34350.18	19266.84	33515.66	30995.17	36027.12	51104.82	30155.55	20944.25	41888.07
AMP	1.66E+08	1.65E+08	1.3E+08	1.08E+08	1.14E+08	1.64E+08	1.43E+08	1.57E+08	1.59E+08	1.54E+08	1.64E+08	1.58E+08	1.39E+08	1.58E+08
IMP	44250550	31226901	66681287	45629569	58147124	45757403	46791267	41918950	52109590	23453317	30909126	55564085	17079067	22691563
S-adenosyl-L-methioninamine	N/A	N/A	N/A	N/A	N/A	N/A	N/A	N/A	2477.655	N/A	N/A	N/A	N/A	N/A
GMP	31786327	26673890	29795959	21065456	19260838	26703832	22766692	26687749	30121674	21028425	20774888	26957460	12617144	17033583
xanthosine-5-phosphate	530929.6	378233	494615.8	175413.3	529500.7	768689.9	582217.9	680909.7	783052	546513	487709.3	493249.3	385291.2	652480.4
riboflavin	N/A	4955.134	N/A	N/A	N/A	4130.329	N/A	2473.931	N/A	2473.847	N/A	N/A	2451.604	N/A
S-adenosyl-L-homoCysteine-posi	1888685	1232497	1879364	758960.1	609574.9	1151951	1584625	1983770	2362862	3030211	2065878	1283464	2054583	3659220
S-adenosyl-L-methionine	249602.7	365934.3	156959	135226.2	83426.42	410893	241538.9	199872.6	222375.4	255499.9	224071	294313.2	192581.2	395319.6
folate	19824.09	19827.83	16344.28	9069.872	5799.37	22298.98	19821.14	12389.2	8257.806	18171.47	12371.57	9910.318	13183.67	25602.07
7,8-dihydrofolate	N/A	2700.151	3304.464	N/A	N/A	N/A	N/A	N/A	N/A	N/A	N/A	N/A	N/A	N/A
5-methyl-THF	27983.8	19822.27	23831.51	21960.28	9221.25	11662.48	17341.19	14405.33	23623.53	38402.55	28132.63	12064.74	31558.16	16636.67
Diiodothyronine	N/A	N/A	N/A	N/A	N/A	N/A	N/A	N/A	N/A	N/A	N/A	N/A	N/A	N/A
glutathione disulfide-posi	2317128	2600719	3842231	2499549	2650466	2688025	2264117	2438711	2387345	3340872	2704317	1899962	3097604	3675359
NAD+_posi	1855524	1913936	643332.3	456689.9	457277.4	2141247	762372.5	2096121	1446957	3707255	2455798	935158.2	4293325	6036164
NADH	548388	848943.9	138746.9	40465.24	158569	576458.3	237847.7	966192.4	445973.1	1217409	1004269	444325.2	1152273	1570833
dephospho-CoA-posi	137067.8	75188.07	59948.37	55740.03	9145.526	128065.5	178850.1	61424.79	37409.48	44606.4	33976.38	85861.91	20634.81	28011.26
NADP+_posi	443400.4	527257.6	265090.1	125068.4	147784	493766.4	298988	409676.1	406185.9	824407.3	557249.8	288254.8	623327.9	978503.2
NADPH	N/A	N/A	N/A	N/A	N/A	N/A	N/A	N/A	N/A	1652.591	N/A	N/A	N/A	N/A
coenzyme A-posi	1219859	1079872	1063287	402679	469088.6	1342240	1152022	1540128	1594332	1539960	1485236	1119459	1274343	2241372
FAD	241957.6	187473.4	177562.4	100560.5	71835.47	189866.2	187491.8	208593.2	112930.5	151120.9	132930.8	128886.3	90010.48	206368.4
acetyl-CoA-posi	6444.237	10901.74	9415.057	13871.13	9910.162	32719.43	25270.06	2973.221	15858.06	8424.916	3468.541	8921.7	3468.633	6441.799
propionyl-CoA-posi	3302.669	7432.939	3327.245	12387.88	8257.956	8262.493	N/A	18170.85	18995.43	6607.868	14040.71	4130.16	11562.57	6607.829
acetoacetyl-CoA-posi	N/A	N/A	1652.629	5780.196	N/A	3302.927	2477.761	1626.496	N/A	4130.125	1652.479	4130.222	4955.149	10738.3
malonyl-CoA-posi	N/A	N/A	N/A	N/A	N/A	N/A	N/A	2477.614	N/A	N/A	N/A	N/A	N/A	3305.2
succinyl-CoA-posi	N/A	N/A	4195.83	N/A	N/A	2474.031	N/A	N/A	3301.225	N/A	N/A	3290.498	2477.655	4130.141
sarcosine	30457093	28524807	30556606	25234558	25514769	29477081	26750552	37444676	37298440	39674465	40898339	36699716	40776628	44257044
putrescine	26027.86	7256.665	43932.38	12335.29	15147.02	11861.73	10826.03	26744.82	29504.28	10194.56	8763.876	9107.452	11977.08	27114.49
spermidine	369143.2	400272.2	317245.8	436453.6	260773.1	287766.7	317568.8	540785.3	454404.2	446673.4	480349.3	283665.7	406314.6	424128
N-acetyl spermine	396563.8	432171.6	312246.5	432240.7	280317.4	302042.7	315551.6	194163.3	338016.9	283040	401717	521715.9	392318.2	307628
N-acetyl spermidine	12733.86	10374.68	13534.39	15353.45	3222.527	9763.345	7350.506	33777.45	5787.418	23953.26	15550.79	19590.01	21191.54	8344.017
Nicotinamide Riboside	N/A	7203.332	5760.006	5500.512	12766.54	N/A	5777.416	5778.357	7323.687	5644.527	2477.58	N/A	3176.866	N/A
Adenylosuccinate	2883937	3433654	3906961	2512293	3406662	3187932	3780256	3808164	3594256	3655215	3978324	3815467	3174159	3605721
cholesterol	934036.4	688770.9	1077759	602553.7	269228.3	910060.2	393124.5	365866.6	465713.9	1123201	532988.4	233479.8	696216	1088505
arginosuccinic acid	396430.8	441393.7	312949.1	294577.9	321311.3	810625.8	486442.3	173428.1	394772.9	339820.2	360764.8	266522.4	217198	294838.5
phosphocreatine	151765.6	139253.4	205912.5	173592.3	273867.9	120429.5	100332.9	118487	120244.1	512574.9	230168.3	83864.36	1048530	849903.3
retinoic acid	5589.91	9943.498	10070.26	11732.44	9324.24	16107.43	5493.493	6500.945	8689.873	6066.268	9298.026	8011.206	5556.599	10457.79
spermine	223581.4	204046.2	186121.9	241748.7	144751.9	137095.5	150399.5	197001.7	177437.1	204559.2	167282.9	177718.1	196700.6	203457.4
HMG-CoA_pos	N/A	N/A	N/A	N/A	N/A	N/A	2477.529	N/A	N/A	N/A	N/A	N/A	N/A	N/A
N-acetyl-L-aspartic acid	17503616	17779223	22165455	11695591	13118655	17832546	14535596	19944195	16502189	21406122	21693518	18472264	19725817	23078834
N-acetyl-L-aspartylglutamic acid	16711150	15991469	14504315	10732684	10521892	16552673	11923737	18417768	17439436	13992382	19357152	25263610	16728231	19672185

cysteine sulfinate	N/A	1652.513	1652.512	1652.591	N/A	1652.591	N/A	N/A	N/A	N/A	N/A	N/A	N/A	N/A

SUPPLEMENTARY TABLE 5. NORMALIZED DATA.

Label	MUT	MUT	MUT	MUT	MUT	MUT	MUT	WT	WT	WT	WT	WT	WT	WT
glyoxylate	1.374571	-0.00082	0.502513	1.0937	-1.33065	-1.58069	-1.15522	0.46328	0.198766	0.607693	1.040507	0.653344	-0.63156	-1.23544
glycolate	-0.35442	0.243036	-1.52079	0.289653	-1.99062	-0.23493	1.768771	-0.73003	0.502261	-0.70816	0.833077	0.871823	0.534307	0.496022
pyruvate	-1.4756	0.508425	0.773759	-0.56387	-0.1377	-0.08477	0.504186	-0.05207	0.27378	-0.80911	-1.09444	-1.18573	1.201083	2.142059
lactate	0.346628	-0.09429	1.538038	2.499289	-0.25935	-0.04483	0.543668	-0.73218	-0.62684	-1.02397	-0.08497	-0.11404	-0.99171	-0.95544
2-oxobutanoate	-0.37137	-0.70197	-1.5457	0.269406	1.425239	1.752899	0.274375	-0.25838	-0.23388	-0.34438	0.840896	1.08095	-1.42482	-0.76328
acetoacetate	-0.18745	-0.72224	-0.81423	1.434826	0.665721	1.817565	1.12909	-0.35064	-0.68193	-0.96676	-0.8151	1.089994	-0.95228	-0.64656
glycerate	-0.8271	-0.88578	-1.2454	-1.37259	-0.99455	-0.34856	-0.41181	0.966194	1.944987	0.411798	0.743981	0.589403	0.653691	0.775734
uracil	-1.03057	-1.07953	1.601259	-0.97203	-0.67713	1.278335	-0.83344	0.482915	-1.06446	0.610069	1.267228	-0.70499	0.510161	0.61219
fumarate	0.189623	-1.34069	1.802676	1.084983	0.958726	-0.84299	-1.27545	0.30919	-0.02165	-0.71682	1.364392	-0.13475	-0.8389	-0.53833
Maleic acid	-0.05478	-1.80625	1.837809	0.918938	1.328374	-1.24243	-1.00068	-0.18144	0.35621	-0.51841	0.583752	0.42726	-0.46711	-0.18125
2-keto-isovalerate	0.190086	-1.80658	1.158994	1.270241	1.624245	-1.4235	-0.57943	-0.06199	-0.22642	-0.74207	0.831129	0.440799	-0.22797	-0.44754
Guanidoacetic acid	0.300408	0.074975	-0.43594	-1.51103	1.158931	1.218522	-0.74905	-0.5314	-0.29083	-0.90301	2.312921	-0.22611	-0.64004	0.221649
succinate	0.59466	0.34204	-2.21773	-1.42383	-0.68946	-0.00331	-1.15918	0.62008	0.393736	0.640568	1.171116	0.040092	0.921723	0.769504
Methylmalonic acid	0.606937	0.439125	-2.18096	-1.40195	-1.0092	-0.03094	-1.0358	0.631485	0.402214	0.730929	1.161567	0.219398	0.900856	0.566332
3-S-methylthiopropionate	0.636528	0.036021	0.150964	1.01734	2.782848	0.2582	-0.46537	-0.70403	-0.91823	-0.73242	-0.2796	-1.0103	-0.72963	-0.04232
nicotinate	-0.70005	-0.4232	-0.62501	2.01429	1.086231	-0.7435	-0.6572	-0.26399	-0.05778	-0.45264	-0.33959	-0.51224	-0.51549	2.190175
taurine	0.0924	-0.85571	0.948878	2.077651	2.101191	-0.75953	-0.26315	-0.40989	-0.56494	-0.39788	0.002971	-0.76451	-0.70889	-0.49857
Pyroglutamic acid	-0.56018	-0.14037	1.17988	0.910798	2.682118	-0.43506	-0.52293	-0.44007	-0.95062	-0.88471	-0.60026	0.454207	-0.12092	-0.57189
Citraconic acid/itaconic acid	-0.78071	-0.63619	1.234284	2.80153	0.457041	-0.06195	-0.41876	-0.71482	-0.08327	-0.35011	-0.28474	0.437155	-0.66965	-0.92981
2-ketohaxanoic acid	-0.75069	0.650035	-1.28454	-1.4866	-1.32074	0.124104	0.815682	1.628342	-0.35366	0.926588	0.687751	1.087304	-0.0646	-0.65897
N-Acetyl-L-alanine	0.177644	-0.79532	1.257718	0.221853	2.52431	-1.38413	-0.81866	0.446113	-0.39268	-1.08813	0.299132	0.020757	-0.16452	-0.30409
oxaloacetate	0.203585	-0.05624	-0.41822	-0.55092	2.786059	0.508147	0.894999	-0.541	-0.26999	-0.38438	-0.28106	0.463976	-1.37126	-0.98371
Hydroxyisocaproic acid	-0.79993	-0.80291	2.922217	-0.00557	-0.79323	-0.17128	-0.2643	-0.03198	0.719221	-0.23824	0.587463	0.485742	-0.80334	-0.80385
malate	-0.16249	-1.24366	0.17584	1.806149	-0.35371	-1.28794	-0.70489	-0.50476	0.308149	-0.10543	2.018956	0.876162	-0.01736	-0.80501
hypoxanthine	-0.01427	-0.72833	1.055265	2.159305	1.324446	-0.00647	0.371377	-0.08833	0.126058	-1.15825	-0.76093	0.10483	-1.22682	-1.15789
anthranilate	0.049301	-0.50933	1.394125	1.484023	1.726806	-0.38753	0.338369	0.010877	0.539563	-1.25369	-0.73436	-0.25989	-1.19318	-1.20507
p-aminobenzoate	0.389174	-1.33065	1.177357	1.587529	1.809647	-0.09584	0.351741	-0.08511	-0.04568	-1.28843	-0.54157	-0.04181	-1.04358	-0.84278
p-hydroxybenzoate	-0.68171	0.7768	0.577329	0.29085	0.533666	-1.87028	0.740878	-1.21606	1.831067	-0.27399	0.054069	-1.29763	-0.20461	0.739609
acetylphosphate	-0.01244	-0.26176	1.909043	0.738876	1.815754	-0.6831	0.081837	0.165424	0.281193	-1.17405	-0.21262	-0.02836	-1.24604	-1.37376
Carbamoyl phosphate	-0.09327	-0.83006	0.711978	0.107927	2.750195	-0.42206	-0.52701	0.281018	-0.04886	-1.75068	0.442451	0.228221	-0.49234	-0.35751
a-ketoglutarate	0.253608	-0.47724	0.929624	0.912701	2.031283	0.195591	-0.72547	-0.51456	-1.16396	-1.35747	-0.25984	1.409523	-0.47139	-0.7624
Phenylpropiolic acid	0.055784	-1.09761	0.609875	2.906702	0.663822	-1.04108	-0.0259	-1.04855	-0.45018	-0.0124	-0.09241	0.009055	-0.13513	-0.34199
2-oxo-4-methylthiobutanoate	-0.43578	-0.37987	-0.55969	-0.86937	2.133746	0.141682	-0.55589	1.364109	-0.1946	-0.6233	-1.0832	1.445156	0.547581	-0.93057
2-Hydroxy-2-methylbutanedioic acid	-0.69682	-1.26546	-0.9549	2.128445	0.184496	1.562438	-0.66768	0.306877	-0.91888	0.693671	0.452954	-0.68873	-0.53799	0.401574
3-methylphenylacetic acid	-1.56303	-0.5132	0.689098	-0.8551	0.279816	-0.22656	-0.64186	2.53228	0.041152	0.247163	-0.74906	0.078486	-0.45699	1.137801
xanthine	-0.83785	-0.9518	0.482532	2.832545	0.964321	0.444704	-0.51952	-0.38269	-0.16806	-0.83407	-0.50578	-0.03045	-0.74156	0.247675
Hydroxyphenylacetic acid	0.385051	-0.5411	0.290246	-0.54378	0.898768	-0.54986	0.005063	1.187163	0.354616	-0.89868	0.68118	1.77983	-1.99735	-1.05114
2,3-dihydroxybenzoic acid	-1.15004	-0.94733	0.940547	0.082488	-1.13673	0.187378	-1.15319	0.235703	0.698916	0.895902	-1.15398	0.235457	0.149381	2.115496
orotate	-0.52878	-1.13618	1.131317	0.875252	2.205207	-0.183	-0.99918	-0.00476	0.428957	-1.12909	0.605285	-0.14115	-1.27329	0.149422
dihydroorotate	1.262633	-0.98218	0.31139	1.47721	2.162102	-1.28249	-0.53624	-0.29819	-0.38143	-0.31236	-0.78145	-0.17688	-0.71801	0.255895
allantoin	-0.53764	-0.60215	0.334475	0.900252	3.011722	0.513193	-0.55269	-0.57788	0.082376	-0.53985	-0.36287	-0.31459	-0.73545	-0.61889
Aminoadipic acid	-0.6563	-0.1546	1.150032	-0.00339	2.745907	-1.02795	-0.17816	-0.68049	-0.43616	-0.32181	-0.35534	0.381539	-1.08556	0.622278
Indole-3-carboxylic acid	0.28701	-0.07426	0.660719	0.707521	1.713055	-0.7544	0.57985	0.721251	-0.10005	-2.16847	-1.26487	0.098117	-0.98084	0.575358
phenylpyruvate	-0.98068	0.439421	-0.9501	1.625926	1.00062	-0.09745	1.127597	-1.00055	-1.01539	0.045635	-1.00055	1.294085	-1.01478	0.526214
Atrolactic acid	-0.63797	-1.11675	0.69714	0.72695	1.16545	0.065088	-0.88279	0.030572	-1.05587	-1.45695	0.419323	2.170655	-0.22931	0.104461
Phenyllactic acid	0.497305	-0.185	0.596735	-0.31312	1.912525	1.1365	-0.43586	-0.65652	-0.70343	-0.9349	-0.43198	1.534158	-0.39506	-1.62135
quinolinate	0.028521	-0.03712	0.115629	0.180927	-0.07481	-1.02346	3.135668	-0.77574	-0.79514	0.20774	-0.21177	-0.28387	-0.75998	0.293392
phosphoenolpyruvate	-0.03906	1.375394	-1.11358	-1.41618	-0.98802	-0.16226	-0.93748	1.252104	-0.63622	1.422181	1.172129	-0.60635	0.421352	0.255994
Uric acid	0.204699	-0.55321	1.453608	1.51938	2.245851	-0.15362	-0.25003	-0.74253	-0.30936	-0.63926	-0.74231	-0.40305	-0.7784	-0.85178
dihydroxy-acetone-phosphate	1.19421	0.940697	0.807852	-0.609	-0.58385	1.349499	1.846221	-0.42991	-0.75961	-0.87943	-0.18852	-0.6199	-1.01185	-1.05641
D-glyceraldehdye-3-phosphate	1.098266	1.345074	0.788945	-0.42043	-0.52858	1.078359	1.798915	-0.37383	-0.73824	-0.90276	-0.39986	-0.46013	-1.03468	-1.25107
sn-glycerol-3-phosphate	-0.43128	0.083483	-0.77403	-0.70126	-0.59017	-0.43886	-0.6423	-0.41602	-0.56406	0.402957	0.356272	-0.65543	2.163161	2.207551
shikimate	-0.45803	-0.51506	-0.41937	-0.43502	-0.43503	-0.61069	-0.52506	-0.57469	-0.29623	-0.59334	-0.45011	2.225066	0.981742	2.10583
aconitate	0.400016	-1.01443	1.684463	1.531567	1.429832	-0.70171	-0.61911	-0.68433	0.396897	-1.18736	-0.97394	-0.38859	-0.4679	0.594593
allantoate	0.323069	-0.28908	1.830571	1.576268	1.048982	-1.09978	-0.76124	-0.26402	-1.18682	-1.27708	0.761486	-0.56583	0.143066	-0.23959
Ascorbic acid	-0.29239	-1.31682	1.284019	-1.43587	0.804382	-1.0372	-1.42864	0.535181	0.075895	-0.40411	1.110881	0.702221	0.181522	1.220925
2-Isopropylmalic acid	-0.24999	-1.18281	1.818427	-0.98932	1.427471	-1.1891	-1.26027	0.392834	0.045881	-0.47544	0.945164	0.520821	-0.4705	0.666845
N-carbamoyl-L-aspartate-nega	-0.00397	-0.01235	-0.06014	0.674823	2.328989	0.014249	-0.85328	1.590166	-0.78498	-1.62765	-0.1965	-0.58608	-0.46002	-0.02325
Pyrophosphate	-0.26255	-0.85073	1.410856	0.023842	0.601709	0.196707	-0.59933	1.540007	1.058786	-1.56956	-0.50161	0.882916	-1.51531	-0.41575
glucono-?-lactone	-0.10086	-0.36155	-0.54144	-0.02321	0.761021	0.607671	-0.84425	1.88378	-0.49457	-0.16095	0.830595	-2.23208	-0.4317	1.107547
myo-inositol	0.200345	-0.97	0.745265	-0.05297	0.397888	-1.43464	-1.75814	1.046766	0.110528	-1.11234	1.580151	-0.14939	0.302339	1.094213
hydroxyphenylpyruvate	0.065181	0.820789	2.497752	0.082774	-0.80244	1.345364	0.636865	-0.45859	-0.49076	-0.6662	-0.83037	-0.64574	-0.71802	-0.83659
homocysteic acid	0.248346	-0.92139	1.745722	1.199879	1.237139	-0.07164	1.003981	-0.28315	-0.10119	-1.233	-0.99731	0.28279	-1.32599	-0.78418
4-Pyridoxic acid	-0.62044	-1.21961	0.19071	2.176825	1.326865	-0.61832	0.409512	0.556138	-0.39348	-1.0049	-0.83442	0.930714	-0.99799	0.098391
3-phosphoglycerate	0.156074	1.334438	-1.23999	-1.57518	-1.01641	0.139744	-0.99234	0.614662	-0.42754	1.084869	1.721893	-0.40928	0.508675	0.100386
Indoleacrylic acid	-0.31814	-0.44871	-0.11288	2.622941	0.289796	0.200758	0.656727	0.385639	-0.07138	-1.24255	-0.85609	0.870256	-1.2209	-0.75547
Kynurenic acid	-0.32729	-1.36457	-1.65139	0.206774	-0.20456	0.725139	1.502925	1.467719	-0.68312	0.01233	-0.50851	1.515603	-0.44333	-0.24774
citrate-isocitrate	-0.98242	-1.19699	1.118763	1.652067	2.081683	-0.27894	-0.72246	-0.40008	0.432698	-0.76657	-0.19086	-0.21509	-0.78018	0.248356
isocitrate	-0.05811	0.211301	0.545563	2.001922	1.155744	-0.96572	-1.51198	0.508842	0.151162	-0.79036	-0.54872	-1.16223	-0.61337	1.075954
citrate	-0.31594	-0.71323	1.154818	0.762549	2.531433	-0.41221	-0.41371	-0.2925	-0.01909	-1.05045	0.130389	-0.14176	-1.5472	0.326907
2-dehydro-D-gluconate	0.9081	-1.04616	-1.99182	1.627167	0.662503	-0.40352	-0.56772	0.849276	-0.0869	-0.42505	0.217878	0.092771	-1.05029	1.213752
D-gluconate	0.125793	-0.96872	-0.02666	-1.72967	1.923488	-0.37679	-0.44165	1.807237	-0.29836	-0.6134	-0.10265	1.00255	-0.48529	0.184138
D-erythrose-4-phosphate	0.598599	-0.48476	1.53331	-0.08176	0.800357	-0.99485	2.072037	0.61657	-0.80653	-1.2363	-0.43728	-0.43003	-1.08926	-0.0601
Xanthurenic acid	-0.71906	0.596174	-0.62097	-0.71863	-0.08081	1.029875	0.808634	-0.46564	0.479997	-0.76392	-0.36764	2.594583	-1.01968	-0.75292
lipoate	1.21904	1.959989	-0.5173	1.610822	-0.72038	-0.89377	-0.62957	-0.7315	0.953899	-0.49014	-0.82607	-0.51701	0.223198	-0.6412
D-glucarate	-0.48238	-0.44671	1.844833	0.840165	-0.30215	0.227542	-0.89527	0.840998	0.873437	-2.07494	-0.62069	0.910138	0.009353	-0.72432
deoxyribose-phosphate	0.422717	-1.03181	1.729147	0.887987	0.7907	-1.72759	0.227029	0.288576	0.547819	-0.24261	0.88698	-1.15979	-0.34482	-1.27432
pantothenate	0.022766	-0.8026	1.849204	0.119248	2.401575	0.117794	-0.72009	-1.10383	-0.05005	-0.11801	-0.33422	-0.36391	-1.06775	0.049862
prephenate	-0.47095	-0.51825	2.300759	-0.35195	-0.36448	-0.52573	1.083936	-0.50244	-0.52596	-0.52964	1.970109	-0.50722	-0.525	-0.53317
deoxyuridine	0.383617	0.099695	0.663767	0.674339	1.003599	-1.22371	0.716779	-1.20564	-1.22388	-0.37373	-1.20564	-0.38825	2.057485	0.021562
ribose-phosphate	0.459559	-0.37184	0.507279	2.110619	1.037338	0.005072	0.342655	0.183847	0.416367	-1.34509	-0.82493	0.293646	-1.4302	-1.38432
thymidine	1.12266	0.176532	1.607889	-0.20653	-0.9645	0.712847	-0.0578	-1.74846	0.575901	-0.37386	1.040972	-1.4539	0.424258	-0.85601
uridine	-0.43719	-0.85911	1.121721	1.746533	1.681255	0.207267	-0.73764	0.67321	0.078296	-1.29867	-0.32045	-0.20717	-1.41519	-0.23287
deoxyinosine	-0.03963	-0.24365	2.106167	1.381038	1.074059	-0.15012	-0.36604	-0.61092	-0.8343	-0.80041	-1.01067	1.04387	-0.41113	-1.13827
D-glucono-?-lactone-6-phosphate	0.817064	0.615109	2.138294	-0.25421	0.573198	0.407742	1.29427	-0.41707	-0.69027	-0.40775	-1.23907	-0.83175	-0.788	-1.21756
hexose-phosphate	1.499391	0.026847	1.215751	-0.27928	-0.10754	0.19404	2.038269	-0.12704	-1.35292	-1.01106	0.082172	-1.29929	-0.58283	-0.29651
glucose-1-phosphate	1.864963	0.578557	0.768159	-1.48254	0.87471	0.498355	1.477415	-0.56095	-0.98996	-0.5837	-0.54325	-0.49293	-0.84054	-0.56828
glucose-6-phosphate	1.663185	0.022617	1.334101	-1.13748	-0.52713	0.533577	1.999413	-0.47536	-0.89288	-0.65496	-0.30008	-0.83738	-0.57741	-0.15021
fructose-6-phosphate	1.523656	0.408534	1.00067	-0.85569	-0.48128	0.707975	2.178239	-0.38906	-1.02369	-0.90871	-0.48837	-0.76758	-0.59102	-0.31367
1,3-diphopshateglycerate	-0.4502	1.252741	-0.54052	-0.40706	-0.80051	-0.76549	-0.72198	-0.54378	-0.75703	1.363902	-0.13176	-0.79956	1.344664	1.956591
2,3-Diphosphoglyceric acid	-0.50999	0.897009	-0.70444	-0.38096	-0.71277	-0.60526	-0.81231	-0.41903	-0.74953	1.579924	-0.18853	-0.80906	1.757876	1.657074
S-ribosyl-L-homocysteine-nega	1.447636	-0.85088	0.734274	0.938443	-0.32753	0.129681	0.179125	1.057593	0.590589	-1.69554	-0.44973	0.812735	-1.51362	-1.05279
inosine	0.200538	-0.35847	0.917995	2.529991	1.446136	-0.06389	-0.36977	-0.3037	-0.25948	-0.78584	-0.47635	-0.43758	-1.22001	-0.81957
6-phospho-D-gluconate	1.601242	-0.22651	0.884625	-0.12626	1.460176	0.334814	0.923188	-0.1975	-0.21956	-1.54536	-0.50084	0.306935	-1.48522	-1.20973
xanthosine	-1.47303	-0.34929	-0.93089	-0.92343	1.807915	-0.36329	-1.08828	1.205412	1.319194	0.421996	-0.74918	0.418707	0.19697	0.507201
D-sedoheptulose-1-7-phosphate	0.283367	-0.4567	1.486285	2.062875	1.351571	-0.02815	0.296379	-0.32587	-0.34532	-1.002	-0.85039	-0.3486	-1.02545	-1.09798

N-acetyl-glucosamine-1-phosphate	-0.48885	-1.11594	0.109395	0.044624	2.812754	-0.64749	-1.26958	0.899488	-0.15245	-0.5278	0.004092	0.529625	-0.37106	0.173192
glutathione-nega	-0.0305	-0.8851	-0.51598	-1.92659	-0.13827	-1.15544	-0.83016	1.553679	0.113589	0.252734	0.738414	1.479326	0.854425	0.489872
dUMP-nega	1.303742	-0.13411	0.979468	-1.16499	-0.86874	-0.9624	-1.50996	0.262689	-0.40987	-0.66497	1.818385	0.031962	0.386904	0.931881
Geranyl-PP	-0.87703	0.52971	2.17907	0.173358	-0.8396	-1.34253	-0.57841	-0.44742	0.176926	-0.66937	-0.08574	-0.64469	0.835152	1.59058
O8P-O1P	0.30172	-0.36905	0.294452	0.531163	0.093766	2.403917	1.006984	0.128725	-0.76585	-1.02699	-0.16946	-0.01458	-1.91449	-0.5003
dTMP-nega	-0.27008	-0.20213	0.160837	1.423739	2.144869	0.864194	0.167028	0.334706	-0.17605	-1.21977	-0.31471	-0.29136	-0.98833	-1.63295
cyclic-AMP	-0.18483	-0.54207	0.086129	-0.30818	-0.6274	-0.669	-0.49574	-0.60553	-0.45989	0.173708	-0.25719	-0.65232	2.453299	2.089012
fructose-1,6-bisphosphate	0.138709	1.296294	1.030713	-0.77135	-0.53343	1.034505	2.308842	-0.67321	-0.68987	-0.72794	-0.43978	-0.62747	-0.62054	-0.72548
trehalose-sucrose	-0.20444	1.013417	0.928282	2.115728	-1.12811	0.972596	0.463023	-1.20912	-0.5419	-0.40065	0.289288	-0.3286	-1.22236	-0.74714
Cellobiose	-0.45204	-0.50691	2.75062	-0.31403	-0.32856	1.439692	-0.48128	0.950091	-0.51584	-0.52012	-0.48857	-0.49412	-0.51473	-0.5242
orotidine-5-phosphate	1.055286	0.66298	1.604248	0.970611	0.325635	-0.20145	-0.20923	-0.28476	-1.33758	-2.32681	0.216363	0.122533	0.029699	-0.62753
SBP	-0.08187	-0.13937	1.649119	0.941816	1.945833	0.854806	0.277207	-0.85431	-0.53511	-0.99706	-0.48815	-0.39705	-1.08659	-1.08927
trans, trans-farnesyl diphosphate	-0.82916	-0.11008	1.486679	-0.88235	-0.10481	1.33347	0.263951	-1.34831	-0.84178	-0.18923	0.605888	0.099366	-1.22171	1.738081
S-adenosyl-L-homocysteine-nega	-0.42334	-0.81278	-0.02066	-1.12097	-0.59279	-1.3803	-1.36585	1.00299	0.40678	0.961788	0.763829	0.163311	0.450372	1.967625
dCDP-nega	-0.81548	-0.7463	-0.07522	-0.75759	0.230782	-0.626	-1.62743	0.289053	-0.37871	1.033436	1.431634	0.247036	2.140088	-0.34531
5-phosphoribosyl-1-pyrophosphate	-1.05415	-0.22629	-1.86566	1.082905	-0.96929	-1.41909	0.725604	-0.12623	0.493864	0.862828	-0.12748	0.371915	1.202478	1.048586
OBP	-1.24926	-0.48063	1.919315	1.890512	0.331308	-0.7323	0.704284	0.164194	-0.45927	-0.63768	-0.56601	0.732422	-0.80965	-0.80725
dTDP-nega	1.168994	-0.11772	-0.5096	-1.36306	-2.08064	1.899822	-0.46439	0.147241	-0.14659	-0.41805	0.758546	0.254959	0.670536	0.199952
CDP-nega	-0.36748	-0.53429	-0.59578	-1.4228	-0.52016	-0.9958	-0.65781	0.02218	-0.46197	1.20104	0.509006	0.365253	2.216824	1.241794
UDP-nega	-0.54348	-0.52881	-0.93676	-1.34132	-0.27421	-0.49473	-0.73184	0.197748	-0.52476	1.491586	0.469368	-0.2584	1.852942	1.622661
Cholic acid	-0.59083	-0.64355	-0.53683	1.631816	-0.47218	-0.65189	-0.61893	-0.62593	-0.02087	-0.65624	-0.62593	0.102829	1.577814	2.130733
trehalose-6-Phosphate	0.121793	-0.89596	-0.6107	-1.45257	0.392751	0.194107	-0.12114	2.44021	0.705146	-1.16865	-0.08974	1.114134	-0.65225	0.022863
Thiamine pyrophosphate	-1.03144	0.390295	-2.04395	-1.27772	0.395116	1.120201	-0.06253	0.968957	-0.38303	-0.33897	0.808563	1.224605	-0.6526	0.882501
adenosine 5-phosphosulfate	0.149027	-0.1267	-0.91079	-1.17986	-0.98598	-0.38154	-0.62049	0.073427	-0.7495	1.103542	0.781183	-0.67422	2.065724	1.45617
ADP-nega	-0.28316	-0.23082	-0.96309	-1.07057	-0.88968	-0.55651	-0.69784	0.168106	-0.6775	1.475647	0.903336	-0.48968	1.66687	1.644877
dGDP-nega	-0.26367	-0.24345	-0.90576	-0.98279	-0.95012	-0.65948	-0.72046	0.325908	-0.66044	1.34317	0.773532	-0.51483	1.591289	1.867112
IDP-nega	-0.27654	-0.21566	-0.86526	-0.98682	-0.90726	-0.60915	-0.75102	0.423071	-0.68927	1.128589	0.601634	-0.5363	1.713422	1.970565
GDP-nega	0.121	-0.94763	-0.33341	-0.77474	-0.9399	-0.7321	-0.94359	-0.18251	-0.41234	1.707509	0.641609	-0.37139	1.147172	2.020324
CDP-ethanolamine	-1.04266	-0.82215	-0.35509	-0.51283	2.225968	-0.27675	-0.77793	1.348295	-0.00344	-0.96739	0.662029	1.237131	-0.69882	-0.01637
FMN	-0.88829	-0.71446	0.830206	-0.33824	2.394641	-1.03723	-0.83769	-0.81734	0.08838	0.719017	-0.45274	-0.5694	1.227279	0.395874
cholesteryl sulfate	1.136114	0.210039	2.565577	0.473159	-0.9609	-0.37373	-0.36729	-0.6614	-0.87296	0.296595	-0.64418	-1.12906	-0.39729	0.725324
dCTP-nega	-0.5448	-0.00736	-0.1837	-1.29832	0.517931	-0.937	-0.97491	-0.18522	-0.93739	1.726749	-0.00729	-0.29262	1.445157	1.678771
dUTP-nega	-0.7459	2.606269	0.505895	0.681794	0.790255	-0.10612	-0.09266	-0.92219	-1.25657	-0.69174	-0.21721	-0.8045	0.697145	-0.44448
dTTP-nega	-0.81834	-0.36902	-0.32724	-1.16389	-1.16662	-0.08704	-0.30363	-0.33579	-0.0284	1.785554	-0.32326	-0.20632	2.012345	1.331647
CTP-nega	-0.04851	-0.47248	-0.57873	-0.44798	-0.344	-0.7446	0.653885	-0.55479	-1.29223	2.205266	-0.26213	-0.79139	1.432553	1.245145
UTP-nega	-0.54855	-0.45875	-0.62152	-0.7804	-0.60075	-0.60629	-0.60748	-0.34471	-0.50993	1.492133	0.218306	-0.48605	2.126924	1.727072
CDP-choline	0.573649	0.029579	-0.69247	2.730722	-1.45984	1.175996	0.148298	-0.17867	-0.09149	-0.53189	-0.59736	-0.63758	-0.25792	-0.21102
dATP-nega	-0.8716	0.426164	-0.85342	-0.82697	-0.83167	-0.89214	-0.88105	0.2744	0.068182	1.628712	-0.07201	-0.42734	1.353252	1.905493
Taurodeoxycholic acid	0.773854	-0.52093	0.411502	-1.02155	1.959355	0.493755	0.819808	0.260472	-2.22936	-0.79288	0.264497	0.131175	0.083717	-0.63342
ATP-nega	-0.45411	-0.37801	-0.61651	-0.70833	-0.70894	-0.54949	-0.63178	-0.34835	-0.57287	1.352672	0.162548	-0.5376	2.056909	1.933864
dGTP	-0.44654	-0.341	-0.62521	-0.74074	-0.73194	-0.55589	-0.64323	-0.36482	-0.53781	1.325513	0.218692	-0.52774	2.205914	1.764804
GTP-nega	-0.46456	-0.47379	-0.52979	-0.59266	-0.73825	-0.59654	-0.63175	-0.38108	-0.59902	1.536693	0.158708	-0.53714	2.066814	1.782382
UDP-D-glucose	0.550152	-0.37357	-0.89986	-1.3848	-2.06662	0.812407	0.201161	1.087377	0.321735	-0.53206	1.238726	1.191737	-0.47605	0.329666
UDP-D-glucuronate	0.854135	-1.06098	-0.39262	-2.15559	-0.92508	0.880325	0.152406	0.730191	0.886641	0.066981	0.269918	1.625563	-0.79518	-0.13672
ADP-D-glucose	0.971891	0.055207	-0.79806	-0.66014	-0.77105	-0.97753	-0.92032	1.234685	-0.01109	0.494884	2.403227	0.050406	-0.05627	-1.01584
guanosine 5-diphosphate,3-diphosphate	-1.05033	-0.04642	0.364872	0.253066	-0.66238	-1.25049	0.033565	-0.23235	0.474388	0.62582	-0.41432	-1.61475	1.599573	1.919757
UDP-N-acetyl-glucosamine	-0.60444	-0.29915	-0.57151	-1.09024	0.696298	-0.539	-0.16268	0.309119	0.409413	-0.58774	1.273843	2.628439	-0.634	-0.82835
glutathione disulfide-nega	-0.37647	-0.90521	1.790235	0.239418	2.360099	-1.18601	-0.575	0.536088	-0.61637	-0.82551	0.049568	-0.29347	-0.01969	-0.17769
NAD+_nega	-0.12864	0.051153	-1.16949	-1.04403	-0.90117	-0.07187	-0.88613	0.377817	-0.4903	0.5283	0.518252	-0.66759	1.906078	1.977624
NADH-nega	-0.51269	0.08518	-1.33506	-1.41661	-0.85589	-0.40456	-1.08658	0.723922	-0.16848	0.945984	1.309833	0.063573	1.627307	1.02406
dephospho-CoA-nega	1.442336	0.607473	-0.19436	-0.33442	-0.73941	0.125166	2.27091	0.603033	-0.59134	-1.28913	-0.46938	0.422483	-0.61833	-1.23501
NADP+_nega	-0.26672	0.483116	-1.42405	-1.62656	-0.77872	-0.18878	-0.60333	0.321222	-0.3267	1.058549	1.76512	-0.54319	1.00995	1.120106
NADPH-nega	-0.03007	-0.08075	-0.47932	0.846247	-0.63818	1.038835	-2.19689	1.659858	-1.03598	0.113124	-0.58803	-0.30388	0.752531	0.942503
2-hydroxygluterate	1.316647	-0.94242	-0.94302	0.155766	1.341421	-1.09063	-0.41241	0.556031	-0.00152	-1.90117	1.040329	-0.27499	0.050664	1.105299
2-deoxyglucose-6-phosphate	-0.09577	-1.08651	-0.47621	-0.45133	0.440096	-1.37026	-0.77399	1.611013	1.18675	-0.67793	-0.76463	0.191744	1.859805	0.407235
4-phosphopantothenate	2.027197	1.594526	0.344717	0.421214	-0.50593	0.007041	0.488557	0.294157	-1.0256	-0.96082	-0.41872	0.139929	-1.6534	-0.75286
dehydroascorbic acid	-0.98887	0.309047	-0.98868	-0.05569	1.999391	0.5481	0.27283	1.149876	-0.9891	-0.98911	1.12195	-0.98902	0.498754	-0.89947
3-hydroxybuterate	2.185815	1.856014	-0.68764	-0.47415	-0.58857	-0.76464	-0.73289	-0.74626	1.137415	-0.15737	-0.22797	0.200895	-0.76789	-0.23276
itaconic acid	-0.78129	-0.63677	1.233796	2.801116	0.456516	-0.0625	-0.41933	-0.7154	-0.07617	-0.35067	-0.2853	0.436629	-0.67023	-0.9304
Urea	-0.33154	-0.53672	0.639219	0.87462	3.109832	-0.57998	-0.56153	-0.31638	-0.44774	-0.56985	-0.11405	-0.465	-0.29773	-0.40314
ethanolamine	-0.45149	-1.1584	0.474071	1.410131	1.797386	1.513678	-0.60097	0.160794	-0.80631	-0.2829	-0.08221	0.27016	-1.17036	-1.07357
glycine	0.459461	1.502905	0.248503	0.122501	2.328267	0.149004	0.683156	-0.77853	-0.9313	-0.88451	-0.87298	-0.88491	-0.78427	-0.35731
alanine	-0.92082	-1.42602	0.463702	0.106138	1.453857	-1.49951	-1.61026	1.100752	0.234799	-0.03258	0.934771	0.723018	-0.04785	0.520008
betaine aldehyde	0.806373	-0.81596	1.025594	-0.11536	2.367328	-1.02163	-0.89792	-0.24541	0.378954	0.131067	-1.28381	-0.4943	0.802764	-0.6377
choline	-0.62723	-0.03481	0.075409	0.112655	-1.39393	-1.40876	-0.79729	0.732791	-1.03253	-0.03853	1.837056	0.158014	0.987201	1.429957
4-aminobutyrate	0.041752	-0.58637	2.183528	0.398397	1.661791	-0.41682	-0.80376	-0.09948	-0.45057	-1.03658	-0.18923	-0.65226	-1.11988	1.069486
dimethylglycine	-0.22545	-0.7178	0.327339	-1.7628	1.173522	-0.23696	0.190683	2.160263	-0.63163	-0.8942	1.305922	-0.34725	-0.17361	-0.16804
serine	-0.70017	-0.7452	-1.31144	-1.02669	-0.80382	-0.78467	-0.56171	1.533297	1.714686	0.758951	0.979352	-0.20276	0.382374	0.767798
cytosine	1.246059	-1.04194	1.449802	0.028688	0.688651	-0.20751	-1.11189	1.203354	-1.45488	-0.11311	0.884734	0.401105	-0.84926	-1.12381
Creatinine	0.851604	-1.05761	0.941209	-0.47002	2.209194	-0.73083	-1.35427	0.886001	-0.39996	-1.01004	0.379923	-0.04589	-0.67816	0.478828
proline	0.25053	-0.06358	0.80446	0.914708	2.320318	1.31243	-0.09656	-0.88596	-0.83832	-0.81874	-0.77049	-0.55495	-0.92016	-0.65368
indole	0.900265	0.463188	0.122377	-1.19865	0.445123	0.306083	0.062972	-0.38311	-0.09693	-1.13873	-0.10205	2.596873	-0.80795	-1.16945
betaine	1.958847	-0.42972	0.96668	1.416003	0.356653	-0.64682	1.20836	-0.77799	-0.49641	-0.04576	-0.83409	-0.71904	-0.81693	-1.1398
valine	0.622123	-0.43248	0.975679	1.586403	1.742216	0.600014	0.40821	-0.04902	-1.35851	-0.95183	-0.70094	-0.75881	-1.12255	-0.56052
threonine	-0.09047	-0.10873	1.177154	0.342554	2.450325	0.75993	0.200861	-0.49159	-0.2465	-1.24519	-0.54284	-1.53571	-0.5846	-0.08519
homoserine	-1.60745	-0.54793	-0.78139	-0.92931	-1.32585	0.298378	0.010442	0.685028	1.779531	-0.32711	0.249434	0.055587	1.28361	1.157027
purine	0.80906	0.499608	0.878649	-0.17599	0.842231	0.461057	0.165187	-0.84589	-0.89405	-0.91	-0.08279	2.003416	-1.6895	-1.061
cysteine	-0.60769	0.032835	-0.1012	-0.39509	2.792288	-0.89292	0.58152	0.432669	-0.40045	-0.58513	-1.35978	0.908081	-0.40911	0.003983
creatine	0.407869	-0.46924	1.212706	1.764303	2.177906	-0.86846	-0.36487	-0.34252	-0.76123	-0.79546	-0.30538	-0.38635	-0.73906	-0.53021
nicotinamide	-0.03976	-0.21497	0.392187	1.025614	1.644095	-0.0554	0.957035	0.311407	0.349856	-1.52793	-0.34649	0.667085	-1.53632	-1.62641
Imidazoleacetic acid	1.110978	-0.97762	-0.21265	-0.13065	2.960499	-0.86129	-0.70074	-0.41317	-0.11228	-0.48929	-0.10486	-0.41339	-0.03556	0.380025
thymine	-0.22849	-1.13488	0.757067	1.080754	2.506653	-1.22901	0.792658	0.170213	-0.54272	-0.55259	-0.058	-0.33728	-0.63484	-0.58955
DL-Pipecolic acid	1.555735	-0.35137	0.504597	0.467877	2.053003	-1.73372	-0.14695	0.424981	-1.24066	-0.86928	-0.4509	-0.038	-0.23748	0.06217
N-Acetylputrescine	-1.07629	-0.83107	-1.57226	2.149772	-0.38202	1.590812	0.948744	0.270656	-0.16739	-0.0632	0.110716	-0.17984	-0.32223	-0.47639
hydroxyproline	-1.22308	-0.77182	-1.29386	-1.37802	-0.67782	1.303423	0.430215	0.151163	1.636212	1.365887	0.230768	-0.36029	0.105498	0.481721
leucine-isoleucine	1.121029	-0.17842	0.500379	0.994052	2.26474	0.64758	0.057841	-0.50983	-1.08233	-1.2375	-0.8177	-0.81297	-0.77393	-0.17295
ornithine	-0.95215	0.302376	0.755774	1.185747	1.813272	1.683639	-0.13058	-1.00955	-0.22746	-0.75328	-0.25492	-0.55593	-1.20108	-0.65587
asparagine	1.51519	0.231882	0.602338	0.008593	-1.43792	2.03796	0.964859	-0.19909	-0.92164	-0.86619	-0.04482	-0.66226	-1.00217	-0.22673
aspartate	0.54011	-0.48453	-0.71237	-0.89192	2.42862	-0.41603	-0.31613	0.513222	-0.6474	-0.98566	0.512413	1.569011	-0.60752	-0.50183
adenine	-0.50513	0.159139	-0.2218	0.598696	-1.15043	-0.01372	-0.38292	0.056834	0.288312	-0.27052	-0.90408	2.950944	0.394976	-1.0003
Methylcysteine	-0.50513	0.159139	-0.2218	0.598696	-1.15043	-0.01372	-0.38292	0.056834	0.288312	-0.27052	-0.90408	2.950944	0.394976	-1.0003
homocysteine	-0.32573	-1.10638	-1.22966	-0.88989	-0.18628	-0.53071	-1.23928	1.908933	0.02537	0.804749	0.939182	1.453141	-0.09174	0.46829
methylnicotinamide	-0.25981	1.706394	-1.14738	1.572328	-0.45367	-0.28667	0.235765	1.775695	-1.2273	-0.13367	0.082654	-0.74279	-0.45189	-0.66966
lysine	-0.12295	0.403256	1.243988	0.358505	0.233474	1.607456	1.256248	-0.08962	-1.19495	-1.16101	-0.12167	-2.01256	-0.21631	-0.18386
glutamine	0.451897	-0.21658	1.365501	1.528028	1.704238	0.118559	-0.11847	-0.63964	-1.16374	-1.30252	-0.59514	0.579653	-0.88437	-0.82742
O-acetyl-L-serine	2.106146	-0.48449	0.736067	-0.41722	-0.42229	-0.48752	-0.47555	-0.47809	-0.48761	-0.4891	2.35742	-0.48003	-0.48722	-0.49052
glutamate	0.859695	-0.64889	1.37549	2.291873	0.919733	-1.16738	-0.41146	-0.53693	-0.58956	-1.02193	0.182039	-0.19461	-0.58493	-0.47315
methionine	-0.95763	-0.47654	-0.06953	-0.72349	-1.35101	-1.19088	-0.63275	0.965188	0.331417	0.730362	0.215717	0.161417	0.620471	2.377259
guanine	0.207155	-0.5273	1.427154	2.080652	0.446789	-0.5191	0.619319	0.180788	-0.63801	-0.34301	0.157887	-0.10124	-1.93976	-1.05132

histidine	-0.1436	0.112708	0.333189	-0.56665	-0.5298	1.801804	1.93496	-0.28601	-1.10324	-0.32497	0.854358	0.269626	-1.55652	-0.79586
2-Aminooctanoic acid	-1.07654	-0.56574	0.841467	0.328365	0.348864	-0.81696	-0.84651	2.332948	0.455717	0.253025	0.635176	0.486691	-1.29037	-1.08614
carnitine	1.169328	-1.00822	1.697399	0.079931	0.499084	-2.21208	-1.20378	0.246073	-0.23867	0.364009	0.727057	-0.4772	0.361619	-0.00455
Methionine sulfoxide	-0.62816	-0.60488	0.922001	-0.75066	-1.26674	-1.2492	-0.03593	1.469211	-0.38117	-0.39519	0.939836	-0.65891	0.873933	1.765859
phenylalanine	0.35034	0.709489	1.023259	-0.18825	1.408641	1.107651	-0.11361	-0.28411	-1.45931	-0.97144	-0.21539	1.20951	-1.49349	-1.08329
Pyridoxamine	-0.49796	-0.5352	-0.45981	1.44029	-0.41414	-0.54109	-0.51781	0.452779	2.812379	-0.54417	-0.52275	0.414925	-0.54051	-0.54694
pyridoxine	-0.46593	-0.62604	-0.30192	-0.06316	-0.10557	-0.65136	-0.55126	1.536906	-0.65212	-0.66459	1.541618	-0.58871	2.268634	-0.67651
1-Methyl-Histidine	0.80463	0.871746	-0.4144	-0.25015	0.445856	2.470492	-0.40669	-1.11895	0.343199	-0.29669	-0.56773	0.499093	-1.30933	-1.07106
N-acetyl-L-ornithine	-0.34294	-0.02022	1.167032	2.605232	-0.58542	-1.11709	-1.10201	0.442838	-0.20544	-0.6868	-0.3154	0.106155	0.770519	-0.71644
arginine	0.667153	0.900607	0.046712	0.842495	0.980334	1.73628	0.424926	-1.70146	-0.62552	-0.34046	-0.06124	-1.34401	-1.26252	-0.26329
citrulline	-0.25856	0.951914	0.742621	0.466275	0.044753	1.13651	1.982326	-1.18805	-1.14137	-0.0841	0.402609	-1.18182	-0.95264	-0.92047
N-carbamoyl-L-aspartate	0.492791	-0.1509	0.649016	0.959796	1.87889	-1.03796	0.258501	0.484638	-0.66423	-0.38538	-0.82953	-0.79418	-1.8804	1.018936
glucosamine	-0.87636	0.224548	2.918366	0.388516	-0.39776	0.50553	0.613355	-0.64186	-0.98141	0.22112	-0.2254	-0.92036	-0.58567	-0.2426
tyrosine	-0.7015	0.821978	0.218286	1.591395	-1.19395	-0.83752	-0.24435	-0.70333	0.754104	-0.28177	-1.16931	1.775139	0.823217	-0.85238
Phosphorylcholine	-0.31688	-1.05339	1.10419	-0.16799	2.566026	-0.41033	-1.22213	0.338701	-0.9377	0.096385	0.64235	-0.28057	-0.7864	0.42775
3-phospho-serine	-1.00672	-0.07479	-0.76091	-0.89226	1.156151	-0.58196	-1.22358	2.324144	-0.12544	1.202311	0.021073	-0.079	0.550983	-0.50999
N6-Acetyl-L-lysine	1.355396	0.329446	0.086103	-0.0934	0.417626	-0.02698	0.431389	0.846902	-2.30613	-2.05509	-0.0028	0.12732	0.392007	0.498215
Acetyllysine	2.6396	0.358133	0.627655	0.441693	0.202354	-0.3109	-1.40763	-0.64156	-0.51152	0.046558	-0.26767	-1.00351	-0.93131	0.75811
N-acetyl-glutamine	0.937738	-0.19725	0.445303	-1.67415	1.318665	-0.094	0.827267	1.400894	-0.69277	-1.21331	-1.21579	-0.85669	0.444661	0.569432
N-acetyl-glutamate	0.801744	-1.05078	-1.0542	-1.62552	-0.77066	-0.51055	-0.19277	1.016464	-0.59575	0.766365	0.674844	0.373513	0.164752	2.002543
Ng,NG-dimethyl-L-arginine	0.632234	-0.19163	1.18876	0.129704	0.866457	2.393354	-0.15174	-0.10947	-0.61472	-0.7715	-0.61226	-0.9361	-1.51719	-0.3059
Acetylcarnitine DL	0.43213	-0.60605	1.534461	2.01063	1.226665	-0.78104	-0.58778	-0.58934	-1.05412	-0.58652	0.350285	-1.18487	-0.43291	0.268438
tryptophan	0.129989	0.840779	-0.56647	-1.06902	-0.94218	1.633855	-0.37115	0.185376	1.020398	-0.8772	-0.19089	1.799215	-1.40073	-0.19197
Kynurenine	0.202122	-0.10623	0.662099	1.352657	1.631175	1.048268	-1.0145	-1.66436	-1.04444	0.249021	-0.56655	0.661799	-0.37877	-1.03229
N-acetyl-glucosamine	-0.49137	-2.15075	0.942997	-0.13047	-1.00954	1.885996	-0.26609	1.028966	0.055399	-0.33352	0.808626	0.500017	-0.69364	-0.14662
Flavone	1.274471	0.606634	-1.42257	-0.83466	1.309406	0.464519	0.410549	-0.7374	-0.88159	-0.95099	-1.44675	0.390057	0.72917	1.089147
cystathionine	0.342842	0.847931	0.180593	0.790564	2.036808	1.196493	0.632853	-0.93462	-1.01586	-0.78278	-0.91047	-1.22791	-0.60603	-0.55041
5-methoxytryptophan	0.654047	-0.79111	-1.3178	0.985239	-0.5964	1.020684	-1.36622	1.780925	0.014801	-0.65768	-0.81563	1.297233	-0.12477	-0.08332
Cystine	-0.13853	-0.91329	0.177447	-0.16294	1.480577	0.810972	0.902603	-0.3428	0.006647	-1.42881	-0.45644	1.966642	-0.51505	-1.38703
cytidine	-0.21479	-0.97593	0.407785	2.831527	0.641562	0.445217	0.092261	-0.26522	-0.03749	-1.0801	-0.19192	0.258924	-1.07734	-0.83448
biotin	0.419891	-0.48242	0.62434	-1.4732	1.294473	0.700888	-1.77227	1.655092	-1.0405	-0.12274	0.645198	-0.17882	-0.58289	0.312963
deoxyadenosine	-0.66465	-0.1822	-1.04635	0.796554	1.745409	-1.09578	0.599155	0.576223	-0.20253	-0.96987	1.13095	1.246606	-1.2613	-0.67223
Glycerophosphocholine	0.114284	-0.35527	0.474576	-1.65548	-1.08697	-1.28834	-0.16219	1.472056	-0.36322	-0.15577	1.389982	-0.58471	1.037697	1.163348
acadesine	-0.02332	0.92331	1.964353	-1.04476	-1.0528	0.506492	-1.13727	0.672144	0.341582	-0.63634	-0.34144	-1.14437	-0.4265	1.398923
D-glucosamine-6-phosphate	1.141354	-0.67588	1.094829	-2.01123	0.997393	-0.96428	-0.46855	-0.48165	-0.50743	0.731183	0.768729	-1.08167	0.782864	0.674333
D-glucosamine-1-phosphate	-0.09912	0.304803	-0.43468	-1.3775	-1.32516	0.292528	-0.30749	2.307475	0.069205	-0.24136	0.939177	0.65681	-1.35821	0.573538
S-ribosyl-L-homocysteine-posi	-0.02276	-0.09366	-1.52709	-0.60997	-1.50764	1.2176	0.555667	0.09428	-1.70679	0.979019	1.232195	0.285307	0.294167	0.809682
deoxyguanosine	2.072427	-0.12427	-0.50771	1.385008	0.136921	-0.47982	-0.86219	-0.88211	1.228415	0.920632	-0.30346	-0.89961	-0.6593	-1.02494
adenosine	-0.27901	-1.03352	0.866288	2.457052	1.12705	0.185048	0.539243	0.240138	-0.87969	-0.56884	-1.03004	-0.35622	-0.2307	-1.0368
1-Methyladenosine	-1.00928	-0.74456	-1.28287	0.435096	-0.24775	-0.19231	-0.98671	0.27643	-0.20472	0.262523	1.007184	0.033726	2.704542	-0.05131
guanosine	-0.05821	-0.41674	1.013944	2.646327	1.201452	0.33356	-0.36691	-0.36928	-0.46907	-0.93239	-0.53828	-0.92492	-0.7887	-0.33078
L-arginino-succinate	0.847187	0.257369	-0.12349	0.570988	0.371278	2.33188	0.967323	-1.42104	-0.08932	-0.36301	-0.55698	-0.60313	-1.3538	-0.83527
S-methyl-5-thioadenosine	-0.6368	0.278744	-0.63583	-0.21459	-0.58911	0.330477	0.072055	3.003405	-0.43776	-0.63799	-0.63744	1.041006	-0.6379	-0.29827
7-methylguanosine	0.023562	-1.65331	0.468824	-0.27418	0.397775	-1.65378	0.426882	0.261792	0.989837	-1.63415	0.453049	0.538193	0.01796	1.637554
dCMP	0.546586	-0.42978	0.425629	1.493068	1.781856	-0.73592	0.067811	0.34784	0.064223	-0.15262	-0.13166	0.232249	-1.8168	-1.69247
glutathione	-0.51324	-0.81194	0.43647	-1.97306	-0.73121	-0.95154	-0.67514	1.319705	0.294689	1.078656	1.636245	0.537819	0.372862	-0.02031
dTMP	-0.95562	-0.03183	1.496686	2.360617	0.638913	-0.53596	0.613297	0.170069	-1.22557	-0.4893	0.01709	-0.64396	-0.79655	-0.61788
CMP	0.781229	-0.47288	-0.15837	-0.87091	0.879324	0.329175	0.121663	2.0838	0.017498	-0.32702	0.310611	0.497991	-2.14258	-1.04954
UMP	0.17566	-0.44908	1.274937	0.995551	1.968987	-0.64112	0.379113	0.418746	-0.14489	-1.02576	-0.64361	0.431268	-1.61198	-1.12782
dAMP	-0.39489	-0.58814	-1.08175	-0.54799	1.75429	-0.443	-1.61158	-0.2835	0.128503	0.749073	1.339556	1.428689	-0.75482	0.305565
Nicotinamide ribotide	0.354383	-0.38248	0.267131	-0.33005	3.366605	-0.38483	-0.37551	-0.37749	-0.38491	-0.38607	-0.37749	-0.379	-0.3846	-0.22569
aminoimidazole carboxamide ribonucleotide	-0.31726	-1.12763	0.676551	0.461929	0.229505	-1.35093	-1.7762	1.461975	0.064867	-0.15105	1.834435	0.449149	-0.01653	-0.43881
thiamine-phosphate	-0.02753	-0.41284	1.425802	1.628953	0.928138	-0.23357	-0.62723	0.204241	0.453388	-1.00433	-0.70285	1.125238	-1.29148	-1.46593
dGMP	2.42935	0.756018	-1.05187	-0.04778	-0.802	-0.13222	-1.08675	0.01408	-0.38007	-0.0467	1.412739	-0.29142	-1.11113	0.337752
AMP	2.109415	0.138995	0.740195	0.529834	0.868921	-0.2376	-0.60777	0.178033	-0.57192	-1.05437	0.696019	0.083555	-1.90126	-0.97203
IMP	0.146681	-0.73098	1.762549	1.039902	1.783465	-0.15815	0.095126	-0.17067	0.105999	-1.10577	-0.67047	0.408465	-1.3568	-1.14934
S-adenosyl-L-methioninamine	-0.18258	-0.4903	0.132633	0.591504	0.509985	-0.53897	-0.3466	-0.38746	3.203717	-0.5644	-0.38744	-0.41856	-0.5342	-0.58731
GMP	1.386085	0.000562	1.754855	0.898945	0.404843	-0.08921	-0.28295	0.200415	0.350098	-0.86257	-0.62969	0.177796	-1.9086	-1.40058
xanthosine-5-phosphate	0.230165	-1.27594	0.493618	-1.89913	1.461445	1.034087	0.28034	0.850041	1.117475	-0.3629	-0.42289	-0.43836	-1.28917	0.221213
riboflavin	-0.63759	2.388382	-0.53427	-0.38388	-0.4106	1.685247	-0.69134	0.624132	-0.75487	0.445248	-0.70473	-0.71493	0.459423	-0.77023
S-adenosyl-L-homoCysteine-posi	0.354159	-0.96836	0.7769	-1.00656	-1.36598	-1.11941	-0.32082	0.205017	0.482915	1.313001	0.323057	-0.83097	0.08412	2.072932
S-adenosyl-L-methionine	0.39336	1.350638	-0.64866	-0.58982	-1.69115	1.787994	-0.0029	-0.63563	-0.56764	-0.19708	-0.30801	0.579189	-0.93093	1.46063
folate	1.199076	0.606077	0.972089	-0.36867	-1.34562	0.943714	0.882079	-0.60418	-1.50949	0.177936	-0.60749	-1.10361	-0.64199	1.400086
7,8-dihydrofolate	-0.32517	1.372981	3.029976	-0.00077	-0.03493	-0.47451	-0.3939	-0.41102	-0.47512	-0.48517	-0.41101	-0.42406	-0.47252	-0.49477
5-methyl-THF	1.021131	-0.39188	0.936382	1.262699	-1.00806	-1.32419	-0.51619	-0.8998	-0.04409	1.483848	0.695968	-1.1943	0.817505	-0.83903
glutathione disulfide-posi	-0.43356	-0.55547	2.443201	1.057061	1.201402	-0.53619	-0.74444	-0.58609	-0.88401	0.159724	-0.25501	-1.29543	-0.05599	0.484795
NAD+_posi	0.018528	-0.15088	-0.86061	-0.95228	-0.96528	-0.0358	-0.88686	0.050712	-0.4921	0.957195	0.306642	-0.78595	1.383682	2.412998
NADH	-0.09768	0.379396	-1.13472	-1.41189	-1.00007	-0.27735	-0.97321	0.770097	-0.56815	1.108755	0.861888	-0.50474	1.009153	1.838512
dephospho-CoA-posi	1.58654	0.001901	0.095785	0.249957	-1.13995	0.927211	2.200517	-0.19133	-0.72338	-0.60334	-0.73309	0.263923	-1.02714	-0.90761
NADP+_posi	0.198269	0.245886	-0.59023	-1.34708	-1.20409	0.020452	-0.74715	-0.21306	-0.39424	1.525006	0.541877	-0.85774	0.639421	2.182677
coenzyme A-posi	0.255973	-0.66423	0.253664	-1.84467	-1.61802	-0.05658	-0.23052	0.798306	0.59724	0.401963	0.643164	-0.44155	-0.22477	2.130039
FAD	2.036883	0.297385	1.215935	-0.21391	-1.1079	0.249345	0.56573	0.897962	-1.12555	-0.48048	-0.56656	-0.68475	-1.52876	0.444661
acetyl-CoA-posi	-0.56712	-0.19007	-0.00102	1.048863	0.29909	2.146354	1.631747	-1.05563	0.314492	-0.50401	-0.99731	-0.37213	-1.0281	-0.72517
propionyl-CoA-posi	-0.96085	-0.38607	-0.86486	1.577503	0.466234	-0.28788	-1.44094	1.501331	1.387961	-0.56125	0.801022	-0.8907	0.23294	-0.57444
acetoacetyl-CoA-posi	-0.83469	-0.87986	-0.40468	1.943314	-0.73301	-0.06588	-0.24961	-0.57127	-0.88722	0.186519	-0.56201	0.296777	0.480976	2.280653
malonyl-CoA-posi	-0.35101	-0.53269	-0.16489	0.106044	0.057912	-0.56143	-0.44785	1.927246	-0.56229	-0.57645	-0.47196	-0.49034	-0.55861	2.626312
succinyl-CoA-posi	-0.73093	-0.81961	2.366218	-0.50783	-0.53132	0.244006	-0.7782	-0.78998	0.775502	-0.84097	-0.78997	0.912644	0.250584	1.239846
sarcosine	-0.30626	-1.72257	0.771941	0.60277	0.464753	-1.68746	-1.65971	0.499404	-0.15652	0.205818	1.235442	0.215678	0.55419	0.982525
putrescine	0.720264	-0.94669	2.768728	-0.05837	0.215078	-0.6372	-0.62843	0.566212	0.599728	-0.76439	-0.80274	-0.78767	-0.62687	0.382351
spermidine	0.010663	-0.27621	-0.04863	2.473397	-0.25713	-1.40577	-0.82115	1.329079	0.116668	-0.00871	0.729022	-1.26904	-0.3104	-0.26179
N-acetyl spermine	0.564586	0.31456	0.196985	2.38798	0.316856	-0.81379	-0.43725	-1.54153	-0.52982	-0.99687	0.248905	1.212078	-0.0874	-0.83529
N-acetyl spermidine	-0.09615	-0.6115	0.277142	0.995993	-1.23231	-0.71136	-0.89312	2.293984	-1.15665	0.838006	0.082946	0.53494	0.573347	-0.89527
Nicotinamide Riboside	-0.91658	0.337519	0.438267	0.642831	2.837258	-0.94762	0.142322	0.116887	0.321746	-0.01982	-0.58048	-0.93714	-0.48335	-0.95184
Adenylosuccinate	-0.73593	-0.63603	1.990733	0.174109	2.031862	-1.11912	0.303125	0.223532	-0.544	-0.52679	0.486675	0.140548	-1.12674	-0.66197
cholesterol	1.008742	-0.14194	2.018417	0.625125	-0.92614	0.423806	-0.90196	-1.0095	-0.818	0.974499	-0.50342	-1.42167	-0.16815	0.840194
arginosuccinic acid	0.389444	0.250809	0.102716	0.421212	0.605495	2.522764	0.792794	-1.43629	-0.12384	-0.50189	-0.14434	-0.82366	-1.24739	-0.80783
phosphocreatine	-0.48417	-0.6172	-0.13833	-0.13842	0.378279	-0.69453	-0.72649	-0.66695	-0.6955	0.622409	-0.25254	-0.80039	2.490677	1.723161
retinoic acid	-0.83055	0.000864	0.859026	2.109676	1.080443	1.395815	-0.97673	-0.74778	-0.36132	-1.0009	-0.0299	-0.39304	-1.09768	-0.00792
spermine	0.850961	-0.09885	0.652495	2.901015	0.222953	-1.27761	-0.79906	-0.03292	-0.62391	-0.22766	-0.55698	-0.42308	-0.2998	-0.28756
HMG-CoA_pos	-0.18304	-0.4494	0.089797	0.486982	0.416421	-0.49152	3.265885	-0.36038	-0.49278	-0.51354	-0.36037	-0.3873	-0.48739	-0.53336
N-acetyl-L-aspartic acid	0.111252	-0.65206	2.773429	-0.42678	0.057173	-0.77247	-1.26066	0.293233	-1.14978	0.145712	0.825946	-0.24484	-0.22617	0.526
N-acetyl-L-aspartylglutamic acid	0.525801	-0.53337	0.497236	-0.21927	-0.46066	-0.4959	-1.48036	0.508961	-0.23953	-1.30642	0.80833	2.561523	-0.43127	0.264931
cysteine sulfinate	-0.43277	0.756875	1.684503	2.368032	0.067934	0.684533	-0.55134	-0.58089	-0.69148	-0.70881	-0.58087	-0.60337	-0.68697	-0.72537

SUPPLEMENTARY TABLE 5. T-TEST RESULTS.

	t.stat	p.value	#NAME?	FDR	Fold Change with respect to Wild-type
glycerate	-7.2467	1.02E-05	4.9917	0.002382	0.59934
cystathionine	6.8987	1.65E-05	4.7815	0.002382	1.756
serine	-6.4074	3.37E-05	4.473	0.003231	0.59893
S-adenosyl-L-homocysteine-nega	-5.531	0.00013	3.8872	0.009335	0.6456
arginine	5.1544	0.000239	3.6212	0.010754	1.6884
D-glucono--lactone-6-phosphate	5.1337	0.000248	3.6063	0.010754	2.9197
NADH-nega	-4.9492	0.000337	3.4726	0.010754	0.35569
homocysteine	-4.8999	0.000366	3.4365	0.010754	0.7418
valine	4.8846	0.000376	3.4253	0.010754	1.8568
glycine	4.8625	0.00039	3.409	0.010754	2.86
glutathione-nega	-4.8318	0.000411	3.3864	0.010754	0.66039
SBP	4.7438	0.000477	3.3214	0.010809	2.7581
proline	4.7308	0.000488	3.3117	0.010809	2.4381
leucine-isoleucine	4.6449	0.000565	3.2476	0.0111	2.0011
methionine	-4.632	0.000578	3.238	0.0111	0.47253
L-arginino-succinate	4.2378	0.001152	2.9385	0.019719	1.7427
glutathione	-4.2319	0.001164	2.9341	0.019719	0.70268
D-glyceraldehdye-3-phosphate	4.1154	0.001432	2.844	0.022917	2.5645
CDP-nega	-3.9911	0.00179	2.7471	0.026541	0.61685
arginosuccinic acid	3.9749	0.001843	2.7344	0.026541	1.7624
citrulline	3.94	0.001963	2.7071	0.026918	1.9468
D-sedoheptulose-1-7-phosphate	3.818	0.002448	2.6112	0.032049	2.0116
lysine	3.7917	0.002568	2.5904	0.03216	1.4301
dihydroxy-acetone-phosphate	3.7349	0.002848	2.5454	0.034179	2.2005
homoserine	-3.635	0.003419	2.4661	0.038128	0.60759
Ng,NG-dimethyl-L-arginine	3.6102	0.003579	2.4463	0.038128	1.5687
6-phospho-D-gluconate	3.5857	0.003743	2.4268	0.038128	1.6706
UDP-nega	-3.5855	0.003744	2.4267	0.038128	0.56257
glutamine	3.5582	0.003937	2.4048	0.038128	1.3233
betaine	3.5534	0.003972	2.401	0.038128	1.5678
threonine	3.4095	0.005179	2.2858	0.045896	1.4523
dATP-nega	-3.4081	0.005191	2.2847	0.045896	0.19132
dGDP-nega	-3.4011	0.005259	2.2791	0.045896	0.49547
ADP-nega	-3.3534	0.005744	2.2408	0.048651	0.51019
ornithine	3.3074	0.006254	2.2038	0.051465	2.0062
hydroxyphenylpyruvate	3.2915	0.006442	2.191	0.051536	6.8436
Methylmalonic acid	-3.2467	0.006999	2.155	0.053183	0.69378
IDP-nega	-3.2453	0.007017	2.1538	0.053183	0.49359
hexose-phosphate	3.2135	0.007443	2.1282	0.053525	1.2375
glucose-1-phosphate	3.2033	0.007586	2.12	0.053525	1.3174
cysteine sulfinate	3.2009	0.00762	2.118	0.053525	1.9806
succinate	-3.1739	0.008011	2.0963	0.054486	0.7079
GDP-nega	-3.1656	0.008135	2.0896	0.054486	0.69803
lactate	3.1387	0.008552	2.0679	0.055979	1.2755
NADH	-3.1216	0.008829	2.0541	0.056505	0.41451
fructose-1,6-bisphosphate	3.1075	0.009062	2.0428	0.056736	2.4496
fructose-6-phosphate	3.0801	0.009536	2.0206	0.058435	1.8032
Uric acid	3.0612	0.009877	2.0054	0.059263	2.2095
homocysteic acid	3.0313	0.010441	1.9812	0.061369	1.6144
dCDP-nega	-3.0016	0.011034	1.9573	0.061903	0.53362
3-S-methylthiopropionate	3.0008	0.011051	1.9566	0.061903	1.7009
NADP_nega	-2.9872	0.011334	1.9456	0.061903	0.63235
N-acetyl-glutamate	-2.9844	0.011392	1.9434	0.061903	0.83082
4-phosphopantothenate	2.9546	0.012041	1.9193	0.064218	1.8328
acetyl-CoA-posi	2.9436	0.01229	1.9105	0.064354	2.5965

guanosine	2.9269	0.012677	1.897	0.065196	1.6667
inosine	2.869	0.014117	1.8503	0.070832	1.385
phenylalanine	2.8633	0.014265	1.8457	0.070832	1.4539
dTMP-nega	2.8532	0.014536	1.8376	0.070954	1.8303
O8P-O1P	2.8249	0.01532	1.8147	0.073536	1.348
dTTP-nega	-2.7951	0.01619	1.7907	0.07644	0.35175
UTP-nega	-2.782	0.016588	1.7802	0.077053	0.23091
orotidine-5-phosphate	2.7651	0.017116	1.7666	0.078244	1.3564
hypoxanthine	2.7154	0.018768	1.7266	0.083295	2.0986
trehalose-sucrose	2.7145	0.018799	1.7259	0.083295	2.5039
NAD_nega	-2.7036	0.01918	1.7172	0.083693	0.49777
anthranilate	2.6473	0.021286	1.6719	0.090101	2.0677
ribose-phosphate	2.6421	0.021492	1.6677	0.090101	1.9297
dGTP	-2.6358	0.021741	1.6627	0.090101	0.24142
choline	-2.625	0.022178	1.6541	0.090101	0.5075
GMP	2.6242	0.022212	1.6534	0.090101	1.3926
adenosine 5-phosphosulfate	-2.6072	0.022918	1.6398	0.091673	0.56891
ATP-nega	-2.598	0.02331	1.6325	0.091964	0.23462
1-Methyladenosine	-2.5793	0.024131	1.6174	0.092837	0.54323
GTP-nega	-2.5782	0.024176	1.6166	0.092837	0.31133
Glycerophosphocholine	-2.5115	0.02733	1.5634	0.10357	0.67541
IMP	2.4915	0.028354	1.5474	0.10605	1.7447
asparagine	2.4765	0.029145	1.5354	0.10642	1.2644
dephospho-CoA-posi	2.4756	0.029193	1.5347	0.10642	2.3286
coenzyme A-posi	-2.4589	0.030099	1.5214	0.10836	0.72882
p-aminobenzoate	2.4443	0.030912	1.5099	0.1087	2.1363
glucose-6-phosphate	2.4437	0.030948	1.5094	0.1087	1.5977
adenosine	2.4192	0.032364	1.4899	0.11133	3.028
creatine	2.4174	0.032471	1.4885	0.11133	1.1964
NAD_posi	-2.3924	0.033989	1.4687	0.11516	0.44918
2-deoxyglucose-6-phosphate	-2.3747	0.035098	1.4547	0.11754	0.63464
Kynurenine	2.3398	0.037397	1.4272	0.1238	1.5596
deoxyinosine	2.3275	0.038247	1.4174	0.12517	1.76
guanine	2.3032	0.039967	1.3983	0.12933	1.3063
5-phosphoribosyl-1-pyrophosphate	-2.2955	0.04053	1.3922	0.1297	0.69725
nicotinamide	2.2803	0.041657	1.3803	0.1314	1.579
UMP	2.2761	0.041974	1.377	0.1314	1.3173
S-adenosyl-L-homoCysteine-posi	-2.229	0.045689	1.3402	0.14101	0.67077
dUTP-nega	2.22	0.046441	1.3331	0.14101	2.2411
retinoic acid	2.2191	0.046512	1.3324	0.14101	1.5482
Methionine sulfoxide	-2.1977	0.048334	1.3157	0.14408	0.55589
hydroxyproline	-2.1955	0.048528	1.314	0.14408	0.63787

SUPPLEMENTARY TABLE 6.

Process	Metabolite	Regular Alanine diet raw p-value Wild-type vs. Gpt2-null	Regular Alanine diet FDR Wild-type vs. Gpt2-null	HighAlanine Diet raw p-value Wild-type vs. Gpt2-null	HighAlanine Diet FDR Wild-type vs. Gpt2-null	Regular Alanine diet Average Fold Change of Gpt2-null with respect to Wild-type	HighAlanine Diet Average Fold Change of Gpt2-null with respect to Wild-type	T-test raw p-value Regular Alanine diet Fold Change vs. HighAlanine Diet Fold Change
Gpt2 Primary Reaction	alanine	3.20E-07	2.18E-05	0.063088	0.16917	0.72356	0.840525514	0.0395784
	alpha-ketoglutarate	0.00115	0.0089368	0.095833	0.20905	1.5662	1.220052429	0.0858246
	glutamate	0.033157	0.10021	0.084423	0.20094	0.6801	1.093886	< 0.0001
	pyruvate	0.0079676	0.036732	0.81071	0.87777	0.71086	0.963193571	0.0228856
TCA Cycle	methylmalonate	1.5274E-07	0.000013849	0.0069988	0.053183	0.25573	0.69378	0.000371539
	citrate / isocitrate	0.03283	0.10021	0.39294	0.54147	0.60868	1.112621429	0.0025491
	fumarate	0.0021525	0.013616	0.77129	0.85861	0.73379	0.998334714	0.000732427
	succinate	1.4684E-07	0.000013849	0.0080114	0.054486	0.25503	0.7079	0.000181595
	malate	0.00015665	0.0022425	0.36458	0.5097	0.54869	0.914192571	< 0.0001
Amino Acids	valine	0.048886	0.12202	0.00037558	0.010754	1.4232	1.8568	0.156672
	leucine-isoleucine	0.0094564	0.04019	0.00056542	0.0111	1.4029	2.0011	0.0156494
	phenylalanine	0.040906	0.11126	0.014265	0.070832	1.2551	1.4539	0.387461
	threonine	0.00010754	0.0016251	0.0051785	0.045896	1.7303	1.4523	0.109879
	lysine	0.00021246	0.0027518	0.0025683	0.03216	2.43	1.4301	0.00902864
	arginine	0.0088934	0.038975	0.00023922	0.010754	1.466	1.6884	0.367231
	proline	0.000023263	0.0005152	0.0004879	0.010809	1.8561	2.4381	0.0285752
	serine	0.00026027	0.003078	0.000033653	0.0032307	0.70543	0.59893	0.00766536
	cysteine	0.04784	0.12194	0.47334	0.60858	0.67508	1.183571571	0.0431325
Glycolysis	glucose 1-phosphate	1.8585E-06	0.00010066	0.0075861	0.053525	2.2966	1.3174	< 0.0001
	glucose 6-phosphate	7.6364E-06	0.00025964	0.030948	0.1087	3.8465	1.5977	< 0.0001
	fructose 6-phosphate	2.2205E-06	0.00010066	0.0095363	0.058435	3.735	1.8032	0.000121749
	DHAP	0.0050298	0.027362	0.0028482	0.034179	1.7218	2.2005	0.173065
	Glyceraldehyde 3-phosphate	0.0062344	0.02975	0.0014323	0.022917	1.6991	2.5645	0.044075
	3-phosphoglycerate	0.022246	0.075637	0.087256	0.20266	2.9583	0.711067857	0.00194799
	phosphoenolpyruvate	0.0075166	0.03525	0.077768	0.19143	2.5057	0.673756	0.000213552
	NADP	0.03713	0.1052	0.011334	0.061903	0.64732	0.63235	0.783583
	glutathione	0.0020221	0.013616	0.00041074	0.010754	0.73341	0.66039	0.585811
	cystathionine	0.00002338	0.0005152	0.00001654	0.0023817	2.4378	1.756	0.014917

SUPPLEMENTARY TABLE 7. DIET COMPOSITION

Nutrient	Regular Diet (RA) - PicoLab Rodent Diet 20 (5053)	High Alanine Diet (HA) - Envigo Teklad (TD. 190381)
Protein, % (w/w)	21	19.9
Arginine, %	1.29	1.21
Cystine, %	0.36	0.35
Glycine, %	0.97	2.33
Histidine, %	0.53	0.45
Isoleucine, %	0.8	0.82
Leucine, %	1.57	1.11
Lysine, %	1.18	1.8
Methionine, %	0.62	0.82
Phenylalanine, %	0.91	0.75
Tyrosine, %	0.6	0.5
Threonine, %	0.78	0.82
Tryptophan, %	0.24	0.18
Valine, %	0.97	0.82
Serine, %	0.98	0.35
Aspartic acid, %	2.19	0.35
Glutamic acid, %	4.18	4
Alanine, %	1.19	5
Proline, %	1.31	3.5
Fat, % (w/w)	6.3	8
Soybean Oil %	N/A	8
Cholesterol, ppm	142	N/A
Linoleic Acid, %	2.12	N/A
Linolenic Acid, %	0.27	N/A
Arachidonic Acid, %	0.01	N/A
Omega-3 Fatty Acids, %	0.45	N/A
Total Saturated Fatty Acids, %	0.78	N/A
Total Monounsaturated Fatty Acids, %	0.96	N/A
Carbohydrates, % (w/w)	65.9	60.2
Fiber (Crude), %	4.6	N/A
Neutral Detergent Fiber, %	16	N/A
Acid Detergent Fiber, %	5.8	N/A
Nitrogen-Free Extract (by difference), %	53.4	N/A
Cellulose	N/A	30
Maltodextrin	N/A	15
Starch, %	28.2	15
Glucose, %	0.1	N/A
Fructose, %	0.24	N/A
Sucrose, %	3.25	N/A
Lactose, %	1.34	N/A
Sucrose, %	N/A	29.838
Total Digestible Nutrients, %	75.1	N/A
Gross Energy, kcal/gm	4.11	N/A
Physiological Fuel Value, kcal/gm	3.43	N/A
Metabolizable Energy, kcal/gm	3.03	N/A
Minerals	N/A	3.5 (AIN-93M-MX (94049)
Ash, %	5.9	N/A
Calcium, %	0.81	0.82
Phosphorus, %	0.64	N/A
Phosphorus (non-phytate), %	0.34	N/A
Potassium, %	1.1	N/A
Magnesium, %	0.22	N/A
Sulfur, %	0.33	N/A
Sodium, %	0.3	N/A
Chloride, %	0.52	N/A
Fluorine, ppm	9.3	N/A
Iron, ppm	185	N/A
Zinc, ppm	89	N/A
Manganese, ppm	84	N/A
Copper, ppm	14	N/A
Cobalt, ppm	0.71	N/A
Iodine, ppm	0.97	N/A
Chromium (added), ppm	0.01	N/A
Selenium, ppm	0.37	N/A
Vitamins	N/A	1.95 (AIN-93-VX (94047)
Carotene, ppm	1.5	N/A
Vitamin K, ppm	3.3	N/A
Thiamin, ppm	17	N/A
riboflavin, ppm	8	N/A
Niacin, ppm	85	N/A
Pantothenic Acid, ppm	17	N/A
Choline Chloride	2000 (ppm)	0.27 (%)
Folic Acid, ppm	3	N/A
Pyridozine, ppm	9.6	N/A
Biotin, ppm	0.3	N/A
B12, mcg/kg	51	N/A
Vitamin A, IU/gm	15	N/A
Vitamin D3 (added), IU/gm	2.3	N/A
Vitamine E, IU/kg	99	N/A
Ascorbic Acid, mg/gm	0	N/A
TBHQ, antioxidant	N/A	0.002
Food Color	N/A	0.01
Calories provided by:		
Protein, %	24.517	20.3

Fat (ether extract), %	13.134	18.3
Carbohydrates, %	62.349	61.4
Gross Energy, kcal/gm	4.07	3.9

SUPPLEMENTARY TABLE 7. MEDIUM COMPOSITION

NEUROBASAL MEDIUM

Components	Molecular Weight	Concentration (mg/L)	mM
Amino Acids			
Glycine	75	30	0.4
L-Alanine	89	2	0.02247191
L-Arginine hydrochloride	211	84	0.39810428
L-Asparagine-H2O	150	0.83	0.005533333
L-Cysteine	121	31.5	0.2603306
L-Histidine hydrochloride-H2O	210	42	0.2
L-Isoleucine	131	105	0.8015267
L-Leucine	131	105	0.8015267
L-Lysine hydrochloride	183	146	0.7978142
L-Methionine	149	30	0.20134228
L-Phenylalanine	165	66	0.4
L-Proline	115	7.76	0.06747826
L-Serine	105	42	0.4
L-Threonine	119	95	0.79831934
L-Tryptophan	204	16	0.078431375
L-Tyrosine Sodium dihydrate	265.47	72	0.39779004
L-Valine	117	94	0.8034188
Vitamins			
Choline chloride	140	4	0.028571429
D-Calcium pantothenate	238.27	4	0.008385744
Folic Acid	441	4	0.009070295
Niacinamide	122	4	0.032786883
Pyridoxal hydrochloride	204	4	0.019607844
Riboflavin	376	0.4	0.00106383
Thiamine hydrochloride	337	4	0.011869436
Vitamin B12	1355	0.0068	5.02E-06
i-Inositol	180	7.2	0.04
Inorganic Salts			
Calcium Chloride (CaCl2) (anhyd.)	147	200	1.8018018
Ferric Nitrate (Fe(NO3)3"9H2O)	404	0.1	2.48E-04
Magnesium Chloride (anhydrous)	203.3	77.3	0.8136842
Potassium Chloride (KCl)	75	400	5.3333335
Sodium Bicarbonate (NaHCO3)	84	2200	26.190475
Sodium Chloride (NaCl)	58	4000	68.965515
Sodium Phosphate monobasic (NaH2PO4-H2O)	138	125	0.9057971
Zinc sulfate (ZnSO4-7H2O)	288	0.194	6.74E-04
Other Components			
D-Glucose (Dextrose)	180	4500	25
HEPES	238	2600	10.92437
Phenol Red	376.4	8.1	0.021519661
Sodium Pyruvate	110	25	0.22727273
Glutamine / Glutamax	146.14 / 203	292.28 / 406	2

Additional Components: 1% P/S and 1X B27 Supplement.

Chapter 4 : Loss of mitochondrial enzyme GPT2 causes degeneration in locus coeruleus.

I conducted all experiments. Erin Fingleton contributed to Figure 6. Electrophysiology was investigated in Julie A. Kauer's laboratory and the project was performed under Eric M. Morrow's supervision. For funding sources please refer to the Chapter.

Loss of mitochondrial enzyme GPT2 causes early neurodegeneration in locus coeruleus

Short/running title: Loss of GPT2 causes degeneration in locus coeruleus

Ozan Baytas[1,2,3], Julie A. Kauer[4] and Eric M. Morrow[1,2#]

[1]Department of Molecular Biology, Cell Biology and Biochemistry, Brown University, Providence, RI 02912, USA;
[2]Center for Translational Neuroscience, Carney Institute for Brain Science and Brown Institute for Translational Science, Brown University, Providence, RI 02912, USA;
[3]Neuroscience Graduate Program, Brown University, Providence, RI 02912, USA;
[4]Department of Psychiatry and Behavioral Sciences, Stanford University School of Medicine, Stanford, CA 94035, USA

[#]To whom correspondence should be addressed:
Eric M. Morrow MD PhD
Brown University, Laboratories for Molecular Medicine,
70 Ship Street, Providence, RI 02912, USA
Tel: 401-863-9778
Fax: 401-432-1607
E-mail: eric_morrow@brown.edu

Keywords: locus coeruleus, GPT2, neurodegeneration, neurometabolism, neurogenetics, selective vulnerability

Abstract

Background

Locus coeruleus (LC) is among the first brain areas to degenerate in Alzheimer's disease and Parkinson's disease; however, the underlying causes for the vulnerability of LC neurons are not well defined. Here we report a novel mechanism of degeneration of LC neurons caused by loss of the mitochondrial enzyme glutamate pyruvate transaminase 2 (GPT2). GPT2 Deficiency is a newly-recognized childhood neurometabolic disorder. The GPT2 enzyme regulates cell growth through replenishment of tricarboxylic acid (TCA) cycle intermediates.

Methods

We investigated neuropathology in GPT2-null mice. We examined projections of LC noradrenergic neurons via immunohistochemical staining for norepinephrine transporter (NET) and ELISA measurements of norepinephrine. Electrophysiological properties of GPT2-null LC neurons were studied using whole cell recordings.

Results

In GPT2-null mice, we observe an early and striking loss of tyrosine hydroxylase (TH) positive neurons in LC and reduced soma size at postnatal day 18. GPT2-null LC shows positive Fluoro-Jade C staining. Neuron loss is accompanied by selective, prominent microgliosis and astrogliosis in LC. We observe reduced noradrenergic projections to and norepinephrine levels in hippocampus and spinal cord. Whole cell recordings in GPT2-null LC slices show reduced soma size and abnormal firing and action potentials.

Conclusions

As compared to the few genetic animal models with selective LC degeneration, loss of LC neurons in GPT2-null mice is the earliest developmentally. Early neuron loss in LC in a model of human neurometabolic disease provides important clues regarding the metabolic vulnerability of LC and may lead to new therapeutic targets.

Introduction

Locus coeruleus (LC) is the main source of norepinephrine for virtually the entire central nervous system, serving a multitude of functions including modulation of arousal, sleep-wake states, motor function, inflammatory response, and metabolism (1-8). LC dysfunction has been noted in psychiatric disorders, including anxiety, depression, attention-deficit hyperactivity disorder and addiction (9-15). LC is also a particularly vulnerable brain area implicated in neurodegenerative diseases, including Alzheimer's disease (AD) and Parkinson's disease (PD), wherein LC is among the first brain regions to degenerate (16-21). In these degenerative diseases, the underlying causes for LC vulnerability are not clear and pinpointing these mechanisms may pave the way for therapeutic interventions.

Genetic mutations offer a powerful and unbiased approach to identify disease mechanisms; however, there are very few known genetic mutations in animal models that lead to selective neurodegeneration in LC. Such mutations may reveal mechanisms of selective vulnerability of LC neurons. Previously reported mouse mutations with LC neurodegeneration include models of Parkinson's Disease: the PARKIN null (22); the PINK1 null (23); and the LRRK1/2 double knockout (24). LC neuron loss is also seen in transgenic mouse models of Alzheimer's Disease (Tg2576) (25) and Down Syndrome (Ts65Dn) (26). In all of these models, neuron loss generally occurs after six months of age. The only model reported to date that has early dysfunction of LC neurons, at two months of age, is the MECP2-null mouse (27).

Here we report a novel mechanism of degeneration, gliosis, and neuron loss in LC in an animal model of Glutamate Pyruvate Transaminase 2 (GPT2) Deficiency. GPT2 is a

metabolic enzyme in the mitochondria, catalyzing a reversible transfer of an amino group from glutamate to pyruvate producing alanine and alpha-ketoglutarate (28). GPT2 is a major metabolic enzyme that links amino acid metabolism with the tricarboxylic acid (TCA) cycle. GPT2 supports cellular growth and energetics through replenishment of tricarboxylic acid (TCA) cycle intermediates (29-31). GPT2 also modulates levels of glutamate, the main excitatory neurotransmitter in the central nervous system (29-31). Importantly, human patients with recessive, loss-of-function mutations in GPT2 display postnatal microcephaly, intellectual disability, and motor abnormalities including spasticity and weakness in the lower limbs (spastic paraplegia) (28, 32). GPT2-null mice recapitulate the phenotype of postnatal microcephaly and motor dysfunction and prematurely die pre-weaning (28); however, LC neurodegeneration in the GPT2-null mouse has not been previously described. The degeneration and neuron loss in LC in a model of neurometabolic disease may provide important new clues regarding the underlying pathophysiology GPT2 Deficiency. These findings may also pinpoint novel metabolic mechanisms involved in neuronal vulnerability of LC in more common neurodegenerative diseases.

Methods and Materials

Ethics Statement

All experiments involving mice were done in accordance with the National Institutes of Health *Guide for the Care and Use of Laboratory Animals* (33) and approved by the Brown University Institutional Animal Care and Use Committee.

Animals

GPT2-null animals were obtained from Knockout Mouse Project at University of California, Davis as described previously (28). The background of all mice was C57BL/6J. The mice were maintained under a 12-hour light/dark cycle (lights on at 7am / off at 7pm) throughout the year. Feed and water were given ad libitum.

Immunofluorescence

The brains and spinal cord from mice were dissected out after transcardial perfusion with 1X PBS then with 4% PFA. The tissues were cryoprotected by serially incubating in sucrose solutions of 10%, 20% and 30% overnight at 4ºC. The final solution was then changed to half by volume sucrose/OCT (Optimal Cutting Temperature, FisherScientific, 23-730-571) and gently shaken for 1 hr at 4ºC. The tissues were frozen in dry ice/methanol bath and stored at -80ºC until day of sectioning at the cryostat. The sections were cut at 30 µm thickness. The immunofluorescence protocol was as follows, in order: 3-min fixing with 4% PFA, 3 x 5-min 1X PBS washes, 2-hr blocking in normal goat serum (NGS, Jackson ImmunoResearch, 005-000-121) with 1% (w/v) bovine serum albumin (FisherScientific, BP1600) and 0.4% TritonX-100 (Sigma-Aldrich, T8787)

(Note: if a mouse-raised antibody was used, a 1-hr incubation with 20 µg/mL AffiniPure Fab Fragment Goat Anti-Mouse IgG (H+L) (Jackson ImmunoResearch, 115-007-003) in blocking solution was performed), overnight incubation at 4ºC with primary antibody in blocking solution, 2 x 4-min washes with blocking solution, 3 x 4-min washes with 0.4% TritonX-100 in PBS, 2-hr incubation with secondary antibody in blocking solution, 2 x 4-min washes with blocking solution, 3 x 4-min washes with 0.4% TritonX-100 in PBS, 5-min incubation in DAPI (Invitrogen, D1306) and 3 x 5-min washes with PBS. Coverslips were then mounted onto slides with Fluoromount G (SouthernBiotech, 0100-01). Primary antibodies used in this study: mouse anti-tyrosine hydroxylase (TH) (Millipore-Sigma MAB318, 1:300), rabbit anti-Iba1 (Wako Chemicals 019-19741, 1:500), mouse anti-norepinephrine transporter (NET, abcam, ab211463, 1:400), rat anti-CD68 (Abd Serotec (Bio-rad), MCA1957, 1:100), chicken anti-Gfap (Aves, Gfap, 1:400), chicken anti-beta-galactosidase (abcam, ab9361, 1:500). Secondary antibodies used in this study: Goat anti-mouse IgG (H+L) AlexaFluor 594 (Invitrogen, A-11032, 1:600), goat anti-rabbit IgG (H+L) AlexaFluor 488 (Invitrogen, A-11034, 1:600), goat anti-chicken IgY (H+L) AlexaFluor 647 (Invitrogen, A-32933, 1:600), goat anti-rat IgG (H+L) AlexaFluor 647 (Invitrogen, A-21247, 1:600).

For confocal microscopy on tissues, Olympus FV3000 confocal laser scanning microscope and FluoView software were used. Images were processed and analyzed with ImageJ.

Quantification of LC TH+ neurons. Every serial coronal section (30 µm) starting approximately from the section where cerebral aqueduct first appears were stained with tyrosine hydroxylase (TH) to prevent loss of sections containing LC. The sections with

LC proper, identified by the canonical “boomerang” shaped cluster of TH+ neurons were selected for counting, at least two sections 60 µm apart were blindly counted for each animal.

Fluoro-Jade C Staining

The tissue cryostat sections were mounted on Superfrost Plus microscope slides (FisherScientific, 22-230-892) and dried at 50ºC for 30 min. The slides were immersed in the following solutions at room temperature in order: 0.2% NaOH in 80% ethanol for 5 min, 70% ethanol for 2 min, distilled water for 2 min, 0.06% potassium permanganate for 10 min, distilled water for 2 min, 0.0001% Fluoro-Jade C (Sigma-Aldrich, AG325) in 0.1% acetic acid for 10 min and 3 times distilled water for 1 min. The slides were dried at 50ºC for 10 min, immersed in xylene for 1 min and coverslipped with DPX Mounting medium (Millipore Sigma 06522).

Hematoxylin & Eosin (H&E) Staining

10 µm sections obtained from paraffin embedded tissue were processed in the following steps in order: 2 x 10-min deparaffinization with xylene; 2 x 5-min rehydration in 100% ethanol; 2 min 95% ethanol and 2 min with 70% ethanol; wash in distilled water; 8 min stain in Mayer hematoxylin solution (Sigma-Aldrich MHS1); 10 min rinse in warm running tap water; wash in distilled water for 30 seconds; dip slides in 95% ethanol 10 times; stain in Eosin Y solution (Sigma-Aldrich HT110116) for 30 seconds; 95% ethanol 5 min; 100% ethanol 5 min each 2 times; clear in xylene 5 min each 2 times; mount with DPX Mounting medium (Millipore Sigma 06522).

Norepinephrine Enzyme-Linked immunosorbent Assay (ELISA)

Tissues were acutely dissected after cervical dislocation and weighed immediately before flash freezing in liquid nitrogen. The spinal cord and hippocampus tissues were homogenized in 300 µl ddH_2O and cortex tissues in 500 µl ddH_2O using a Kimble pestle and motor. The homogenate was spun at 5000 x *g* for 5 min and 200 µl was extracted from each sample. The norepinephrine in tissues was detected using Norepinephrine ELISA Kit (Abnova, KA1891) according to the manufacturer's manual.

Brain Slice Preparation

Coronal slices (250 µm) were prepared from anesthetized mice. The brain was immediately extracted and placed in a vibratome (Leica, VT1000). Slices were cut in ice-cold oxygenated artificial cerebrospinal fluid (ACSF, in mM): 119 NaCl, 2.5 KCl, 2.5 $CaCl_2.2H_2O$, 1.0 $NaH_2PO_4.H_2O$, 1.3 $MgSO_4.7H_2O$, 26.0 $NaHCO_3$, 11 glucose. Slices were recovered in the same oxygenated ACSF solution at room temperature for 1 hr and then transferred to a recording chamber where they were continuously submerged in ACSF at 28ºC with a flow rate of 1-2 ml/min.

Electrophysiological Recordings

Locus coeruleus was recognized by its proximity to the fourth ventricle bordering lateral pons and all LC neurons had a characteristic pacemaking activity. Whole cell recordings were performed at current-clamp mode using a MultiClamp 700B Amplifier (Molecular Devices). Signals were low-pass filtered at 3kHz and digitized at 10kHz through Digidata

1550 digitizer (Molecular Devices). Patch electrodes were fabricated from borosilicate glass capillaries (Sutter Instruments) using a P-97 micropipette puller (Sutter Instruments). Patch pipettes had a resistance of 3-8 MOhm filled with patch pipette internal solution consisting of (in mM): 125.0 KCl, 2.8 NaCl, 10.0 HEPES, 2.0 $MgCl_2$, 2.37 ATP-Mg, 0.32 GTP-Na, 0.6 EGTA, (pH 7.23-7.28, 270-278 mOsm). Capacitance and membrane resistance were calculated from voltage response to an injection of -100 pA. For constructing averaged action potential, action potentials within pacemaking activity in each cell were detected and averaged. All electrophysiological recordings were analyzed using Clampfit software.

Statistical Analysis

All data presented in the Figures and the Results section are presented as average ± standard error of the mean, unless otherwise noted. The statistical test for comparisons of two groups was unpaired two-tailed Student t-test unless otherwise noted. All statistical analyses were compiled using GraphPad Prism software. Mixed model analysis was done using JMP Pro 14.

Results

We observed prominent microgliosis in the LC of GPT2-null mice at postnatal day 18 (P18) (Fig.1). Screening in sagittal sections of GPT2-null mouse brains revealed selective microglial activation in a pontine region, later confirmed to be LC (Fig.1, Fig.S1A). The microgliosis in GPT2-null LC was already visible in images taken with a 2X objective, indicating the severity of microglial activation (Fig.1B, left). The zoomed-in images of the LC showed clustered microglia with increased fluorescence intensity for Ionized calcium binding adaptor molecule 1 (Iba1), a marker for microglia (Fig.1B, right). The microglia appeared more amoeboid in shape and clustered particularly around the ventral LC. Microglia were evenly distributed throughout the rest of the sagittal section of GPT2-null mouse brain indicating that there was a selective microgliosis in LC after loss of GPT2. The microglial response in the ventral LC was visible in the coronal sections (Fig.2B) and astrogliosis was also apparent (Fig.S2A). CD68, a lysosomal glycoprotein that is expressed in high levels in activated, phagocytic microglia (34), was also elevated in GPT2-null LC, detected as enlarged immunofluorescent puncta (Fig.S3). Absence of microgliosis was observed in coronal sections of other areas of the GPT2-null brain, including various regions of cortex, hippocampus, thalamus, hypothalamus, midbrain, cerebellum and medulla, confirming selective vulnerability of LC (Fig.S1B-E). Microgliosis and astrogliosis were absent with no apparent cell loss in LC of GPT2-null mice at P10 (Fig.S2B), suggesting that the damage in LC occurred later in postnatal development.

There was significant degeneration and neuron loss in GPT2-null LC. Given the strong microgliosis phenotype, we tested for loss of neurons in GPT2-null LC. We

quantified the tyrosine hydroxylase (TH)+ cell count in the LC proper and there was a significant loss in TH+ cells in GPT2-null LC (Fig.3C). The soma size of the remaining GPT2-null TH+ cells in LC was also greatly reduced. Consistent with microglial activation, average Iba1 relative fluorescence intensity in GPT2-null LC was increased. Interestingly, the average TH relative fluorescence intensity was also increased in the GPT2-null LC. To further investigate the pathology, we stained the LC with Fluoro-Jade C (FJC), a fluorescein derivative that is selectively taken up by degenerating neurons (35). There were FJC+ cells in GPT2-null LC, particularly on the ventral side (Fig.4B). We also did H&E stains on GPT2-null LC and observed hypereosinophilic and necrotic neurons, consistent with neurodegeneration (Fig.4D).

In order to characterize the selective degeneration of LC in GPT2-null mice further, we quantified noradrenergic projections by staining coronal mouse brain sections for norepinephrine transporter (NET) (Fig.5). Coronal sections that contained hippocampus proper and surrounding cortical and subcortical areas showed overall reductions of NET staining in GPT2-null mice (Fig.5B). We quantified the noradrenergic innervation in the hippocampus CA1 region and the retrospenial cortex (RSC) (Fig.5C&D). The RSC was chosen due to the easy identification of its anatomical location with respect to the hippocampus proper. A trend toward a decrease of NET staining in GPT2-null RSC was observed but it did not reach statistical significance (Fig.5C). In the GPT2-null hippocampus CA1 area, there was a significant reduction in NET staining (Fig.5D).

We found severe denervation of noradrenergic projections in GPT2-null spinal cord. The degeneration of the ventral LC may be exacerbated due to its long-range

projections to the spinal cord (1, 36). We hypothesized that NET staining in the cervical and lumbar enlargements of GPT2-null mice would be reduced. We examined the spinal cord in four anatomical areas for quantification: dorsolateral (DL), dorsomedial (DM), ventrolateral (VL) and ventromedial (VM) areas corresponding to approximately lateral spinal nucleus, laminae 3-4 of the dorsal horn, lamina 9 of the ventral horn and laminae 7-8 of the ventral horn, respectively (Fig.6). There were significant reductions of NET staining in both cervical and lumbar spinal cord of GPT2-null mice (Fig.6C&D). There were no significant differences of NET staining in the dorsolateral area of either cervical or lumbar enlargements albeit with trend toward a decrease in GPT2-null mice.

Norepinephrine levels were profoundly decreased in GPT2-null mice. We tested for alterations of norepinephrine levels in acutely dissected cortex, hippocampus, cervical and lumbar spinal cord of GPT2-null mice by an enzyme-linked immunosorbent assay (ELISA) (Fig.7). Consistent with the NET staining results from above (Fig.6), there was a significant reduction in norepinephrine levels of GPT2-null hippocampus, cervical and lumbar spinal cord but not of cortex (Fig.7A). Decreased norepinephrine levels were also observed at P14 but not at P7 (Fig.7B&C), suggesting that the denervation occurs after P7 in postnatal development. Reduction in norepinephrine levels was particularly profound in the spinal cord, consistent with the observation of selective degeneration in ventral LC, which preferentially projects to the spinal cord (36, 37). Overall, these data suggest a dramatic decrease in noradrenergic inputs into various regions of the central nervous system of GPT2-null mice.

Given the selective vulnerability of LC and decreased noradrenergic innervation in central nervous system, we hypothesized that performing whole-cell recordings in

GPT2-null LC neurons at P18 may capture alterations in electrophysiological properties associated with the decay in noradrenergic inputs (Fig.8). GPT2-null LC neurons had lower capacitance, consistent with a decreased soma size (Fig.8B), which corroborates our findings of decreased cell area as quantified by immunohistochemistry (Fig.3C). This finding also fits with a proposed function of GPT2 in cell growth (28). We also observe an increased membrane resistance (Fig.8C). Interestingly, there was a slightly increased pacemaking frequency in the GPT2-null LC neurons (Fig.8D), as apparent in the representative recordings (Fig.8A). This may be due to decreased autoinhibition caused by reduced norepinephrine levels and innervation (Fig.7) (38). Averaged action potential was plotted to visualize abnormalities in the overall shape of the spikes (Fig.8E). Several parameters were significantly changed. Peak amplitude of GPT2-null LC neuron spikes was increased (Fig.8F). Time to decay to half of the peak amplitude in GPT2-null spikes was reduced, indicating faster action potential kinetics (Fig.8G). Hyperpolarization peak amplitude of GPT2-null LC neurons was also increased (Fig.8H). Overall, the electrophysiological characterization of GPT2-null LC neurons indicated intrinsic cell properties consistent with reduced neuron size and altered action potential parameters that may in part underlie the deficiencies in norepinephrine supply in GPT2-null mice.

Discussion

LC has been shown to be one of the first brain areas that degenerate in AD and PD (18, 20, 21, 39, 40). The underlying causes for the vulnerability of LC have not been clearly defined, particularly in sporadic forms of AD and PD. One intriguing possibility is the distinct metabolic enzyme and metabolome profile of LC. To our knowledge, our study is the first to provide a strong phenotype of early microgliosis and degeneration in LC in an animal model of a neurometabolic disease.

One of the major clinical features of GPT2 Deficiency is postnatal microcephaly along with intellectual disability (ID), general in the range of moderate ID (28). LC has been shown to consolidate memory (41, 42) and synchronous LC neuron firing has been correlated with improved performance at cognitive tasks (43). Furthermore, stimulating the LC restores reversal learning in a rat model of Alzheimer's Disease (44). Reductions in norepinephrine levels in the GPT2-null mouse hippocampus (Fig.7), may suggest involvement of norepinephrine dysregulation in the etiology of ID seen in patients with GPT2 Deficiency. Interestingly, the GPT2-null mouse cortex did not show decreased norepinephrine levels, however different cortical areas may have been affected locally.

Among the diseases with LC dysfunction, the neurodevelopmental disorder Rett Syndrome has clinical features that are the most similar to GPT2 Deficiency. In Rett Syndrome, females with *MECP2* mutations display cognitive and motor abnormalities, including ID, loss of speech, spasticity, ataxia as well as postnatal microcephaly and seizures (45, 46). The Rett Syndrome mouse model (MECP2-null) displays reduced cell size and hyperexcitability of LC neurons, similar to our data in GPT2-null mice (Fig.8) as well as decreased norepinephrine levels in the pons and cingulate cortex (47, 48). While

the MECP2-null mouse has early dysfunction of LC neurons, no clear evidence of neurodegeneration or gliosis has been demonstrated in the MECP2-null LC. Rett Syndrome and GPT2 Deficiency may have commonalities regarding the role of LC dysfunction in their pathophysiology.

Human patients with GPT2 Deficiency display cognitive as well as motor abnormalities including spastic paraplegia (28). Motor deficits in the lower limbs seen in spastic paraplegia have been attributed to high energetic and biosynthetic costs of maintaining long-range projecting neurons (49). Locus coeruleus projects to virtually the entire central nervous system and descending noradrenergic tracts have been shown to influence motor function (1, 5, 50-53). LC neurons that project to the cortex are spread out along the dorsal-ventral axis of LC and those that project to the hippocampus remain dorsally whereas the spinal cord-projecting LC neurons reside at the ventral most region of LC (3, 37, 50, 54). Given the strong gliosis phenotype seen in the ventral LC and greatest reduction of norepinephrine levels in the spinal cord, it is possible that the LC neurons projecting to the spinal cord are particularly affected in GPT2-null mice.

An intriguing connection between GPT2 Deficiency in human patients and LC metabolism has recently emerged, where Ruaud and co-workers found reduced amount of pterins and homovanilic acid in the cerebrospinal fluid of patients with GPT2 Deficiency (55). A decreased level of homovanilic acid, a metabolite of tyrosine metabolism in dopaminergic and noradrenergic neurons, may reflect a secondary consequence of LC dysfunction in human patients with GPT2 Deficiency. A pterin derivative, tetrahydrobiopterin (BH4) is used as a co-enzyme for nitric oxide synthase, the activity of which has been shown to modulate oxidative stress in LC (56). Increased pacemaking

activity (Fig.8) may also lead to increases in Ca^{2+} levels leading to more oxidative stress and possibly apoptosis.

GPT2 catalyzes a reaction that results in a net production of a tricarboxylic acid cycle intermediate and the replenishment of the TCA cycle is collectively named anaplerosis. Our data suggest that this reaction may have particular importance in maintaining the health of LC neurons and that the underlying pathophysiology may be influenced by dysregulation in metabolic pathways related to the TCA cycle. These pathways have not seen much attention in the context of LC (56, 57), but recently, dysfunction of oxidative phosphorylation which relies on the continuity of the TCA cycle, has been proposed to explain selective neuron loss seen in Alzheimer's Disease (58). Empirical data in favor of this proposal is not extensive, however LC dysfunction in the GPT2-null animal model may provide novel insights as to the significance of dysregulated pathways of energetics in the degenerating brain.

Two isoforms of glutamate pyruvate transaminase exist, a cytosolic, GPT1, and a mitochondrial isoform, GPT2 (59, 60). In a recent study of transcriptomic profiling by translating ribosome affinity purification (TRAP) in LC neurons (61), GPT2 expression turned out to be almost 4 times the expression of GPT1, suggesting GPT2 is the primary glutamate pyruvate transaminase in LC neurons. GPT2 expression was confirmed by β-galactosidase staining (a marker for GPT2 promoter activity in the GPT2-null allele) that co-localized with tyrosine hydroxylase in LC neurons of GPT2-het mice (Fig.S4). Other cells including astrocytes also express GPT2 (62). However, whether the degeneration of LC in GPT2-null mice occur cell or non-cell autonomously needs to be clarified by future experiments.

In summary, our results identify a novel metabolic mechanism of neurodegeneration in LC. The neuronal death in LC is caused by loss of GPT2, an enzyme that replenishes the TCA cycle. This process is critical for both energetics and biosynthetic pathways, and LC degeneration in GPT2-null mice may be a consequence of defects in these pathways. Studies of GPT2-mediated metabolism in LC may allow us to deepen our understanding of metabolic mechanisms involved in selective vulnerability in LC. This knowledge may lead to new therapeutic targets with benefit to a wide range of neurological and psychiatric diseases.

Acknowledgements

This work was supported by a Brain & Behavior Research Foundation NARSAD Independent Investigator grant (25701, to E.M.M.), a Dr. Ralph and Marian Falk Medical Research Trust Catalyst Award (to E.M.M.), a Brown University Research Seed Award (to E.M.M.), an NIH NINDS grant (R01NS113141) to E.M.M., an NIH NIDA grant (R01DA011289) to J.A.K., the Carney Institute for Brain Science and Suna Kıraç Fellowship Graduate Award in Brain Science (O.B.). This study was also supported by the Hassenfeld Child Health Innovation Institute at Brown University.

Author contributions

Conceptualization O.B. and E.M.M.; O.B. conducted all experiments; Data curation and Visualization O.B.; Experimental Design and Data Analysis O.B, J.A.K. and E.M.M.; Formal analysis and Writing – Original Draft, O.B. and E.M.M.; Writing – Review & Editing, O.B., J.A.K. and E.M.M.; Supervision, Project Administration and Funding Acquisition, E.M.M.

Disclosures

The authors declare no competing interests.

REFERENCES

1. Amaral, D. and H. Sinnamon, *The locus coeruleus: neurobiology of a central noradrenergic nucleus.* Progress in Neurobiology, 1977. **9**(3): p. 147-196.
2. Dienel, G.A. and N.F. Cruz, *Aerobic glycolysis during brain activation: adrenergic regulation and influence of norepinephrine on astrocytic metabolism.* J Neurochem, 2016. **138**(1): p. 14-52.
3. O'Donnell, J., D. Zeppenfeld, E. McConnell, S. Pena, and M. Nedergaard, *Norepinephrine: a neuromodulator that boosts the function of multiple cell types to optimize CNS performance.* Neurochem Res, 2012. **37**(11): p. 2496-512.
4. Fallon, J.H. and R.Y. Moore, *Catecholamine innervation of the basal forebrain. III. Olfactory bulb, anterior olfactory nuclei, olfactory tubercle and piriform cortex.* J Comp Neurol, 1978. **180**(3): p. 533-44.
5. Foote, S.L., F.E. Bloom, and G. Aston-Jones, *Nucleus locus ceruleus: new evidence of anatomical and physiological specificity.* Physiol Rev, 1983. **63**(3): p. 844-914.
6. Nestler, E.J., M. Alreja, and G.K. Aghajanian, *Molecular control of locus coeruleus neurotransmission.* Biological Psychiatry, 1999. **46**(9): p. 1131-1139.
7. Zhang, J., Y. Zhu, G. Zhan, P. Fenik, L. Panossian, M.M. Wang, et al., *Extended wakefulness: compromised metabolics in and degeneration of locus ceruleus neurons.* J Neurosci, 2014. **34**(12): p. 4418-31.
8. Chandler, D.J., P. Jensen, J.G. McCall, A.E. Pickering, L.A. Schwarz, and N.K. Totah, *Redefining Noradrenergic Neuromodulation of Behavior: Impacts of a Modular Locus Coeruleus Architecture.* J Neurosci, 2019. **39**(42): p. 8239-8249.
9. Nestler, E.J. and G.K. Aghajanian, *Molecular and cellular basis of addiction.* Science, 1997. **278**(5335): p. 58-63.
10. Aston-Jones, G., J. Rajkowski, and J. Cohen, *Role of locus coeruleus in attention and behavioral flexibility.* Biological Psychiatry, 1999. **46**(9): p. 1309-1320.
11. Morris, L.S., J.G. McCall, D.S. Charney, and J.W. Murrough, *The role of the locus coeruleus in the generation of pathological anxiety.* Brain Neurosci Adv, 2020. **4**: p. 2398212820930321.
12. Grueschow, M., N. Stenz, H. Thorn, U. Ehlert, J. Breckwoldt, M. Brodmann Maeder, et al., *Real-world stress resilience is associated with the responsivity of the locus coeruleus.* Nat Commun, 2021. **12**(1): p. 2275.
13. Klimek, V., C. Stockmeier, J. Overholser, H.Y. Meltzer, S. Kalka, G. Dilley, et al., *Reduced Levels of Norepinephrine Transporters in the Locus Coeruleus in Major Depression.* The Journal of Neuroscience, 1997. **17**(21): p. 8451-8458.
14. Yamamoto, K., T. Shinba, and M. Yoshii, *Psychiatric symptoms of noradrenergic dysfunction: a pathophysiological view.* Psychiatry Clin Neurosci, 2014. **68**(1): p. 1-20.
15. Guitart, X., M.A. Thompson, C.K. Mirante, M.E. Greenberg, and E.J. Nestler, *Regulation of cyclic AMP response element-binding protein (CREB) phosphorylation by acute and chronic morphine in the rat locus coeruleus.* J Neurochem, 1992. **58**(3): p. 1168-71.

16. Szot, P., *Common factors among Alzheimer's disease, Parkinson's disease, and epilepsy: possible role of the noradrenergic nervous system.* Epilepsia, 2012. **53 Suppl 1**: p. 61-6.
17. Weinshenker, D., *Long Road to Ruin: Noradrenergic Dysfunction in Neurodegenerative Disease.* Trends Neurosci, 2018. **41**(4): p. 211-223.
18. Oertel, W.H., M.T. Henrich, A. Janzen, and F.F. Geibl, *The locus coeruleus: Another vulnerability target in Parkinson's disease.* Mov Disord, 2019. **34**(10): p. 1423-1429.
19. Olivieri, P., J. Lagarde, S. Lehericy, R. Valabregue, A. Michel, P. Mace, et al., *Early alteration of the locus coeruleus in phenotypic variants of Alzheimer's disease.* Ann Clin Transl Neurol, 2019. **6**(7): p. 1345-1351.
20. Braak, H. and K. Del Tredici, *The pathological process underlying Alzheimer's disease in individuals under thirty.* Acta Neuropathol, 2011. **121**(2): p. 171-81.
21. Grudzien, A., P. Shaw, S. Weintraub, E. Bigio, D.C. Mash, and M.M. Mesulam, *Locus coeruleus neurofibrillary degeneration in aging, mild cognitive impairment and early Alzheimer's disease.* Neurobiol Aging, 2007. **28**(3): p. 327-35.
22. Von Coelln, R., B. Thomas, J.M. Savitt, K.L. Lim, M. Sasaki, E.J. Hess, et al., *Loss of locus coeruleus neurons and reduced startle in parkin null mice.* Proc Natl Acad Sci U S A, 2004. **101**(29): p. 10744-9.
23. Grant, L.M., C.A. Kelm-Nelson, B.L. Hilby, K.V. Blue, E.S. Paul Rajamanickam, J.D. Pultorak, et al., *Evidence for early and progressive ultrasonic vocalization and oromotor deficits in a PINK1 gene knockout rat model of Parkinson's disease.* J Neurosci Res, 2015. **93**(11): p. 1713-27.
24. Giaime, E., Y. Tong, L.K. Wagner, Y. Yuan, G. Huang, and J. Shen, *Age-Dependent Dopaminergic Neurodegeneration and Impairment of the Autophagy-Lysosomal Pathway in LRRK-Deficient Mice.* Neuron, 2017. **96**(4): p. 796-807 e6.
25. Guerin, D., J. Sacquet, N. Mandairon, F. Jourdan, and A. Didier, *Early locus coeruleus degeneration and olfactory dysfunctions in Tg2576 mice.* Neurobiol Aging, 2009. **30**(2): p. 272-83.
26. Lockrow, J., H. Boger, H. Bimonte-Nelson, and A.C. Granholm, *Effects of long-term memantine on memory and neuropathology in Ts65Dn mice, a model for Down syndrome.* Behav Brain Res, 2011. **221**(2): p. 610-22.
27. Roux, J.C., N. Panayotis, E. Dura, and L. Villard, *Progressive noradrenergic deficits in the locus coeruleus of Mecp2 deficient mice.* J Neurosci Res, 2010. **88**(7): p. 1500-9.
28. Ouyang, Q., T. Nakayama, O. Baytas, S.M. Davidson, C. Yang, M. Schmidt, et al., *Mutations in mitochondrial enzyme GPT2 cause metabolic dysfunction and neurological disease with developmental and progressive features.* Proc Natl Acad Sci U S A, 2016. **113**(38): p. E5598-607.
29. Kim, M., J. Gwak, S. Hwang, S. Yang, and S.M. Jeong, *Mitochondrial GPT2 plays a pivotal role in metabolic adaptation to the perturbation of mitochondrial glutamine metabolism.* Oncogene, 2019. **38**(24): p. 4729-4738.
30. Hao, Y., Y. Samuels, Q. Li, D. Krokowski, B.J. Guan, C. Wang, et al., *Oncogenic PIK3CA mutations reprogram glutamine metabolism in colorectal cancer.* Nat Commun, 2016. **7**: p. 11971.

31. Schousboe, A., S. Scafidi, L.K. Bak, H.S. Waagepetersen, and M.C. McKenna, *Glutamate metabolism in the brain focusing on astrocytes.* Adv Neurobiol, 2014. **11**: p. 13-30.
32. Ouyang, Q., B.C. Kavanaugh, L. Joesch-Cohen, B. Dubois, Q. Wu, M. Schmidt, et al., *GPT2 mutations in autosomal recessive developmental disability: extending the clinical phenotype and population prevalence estimates.* Hum Genet, 2019. **138**(10): p. 1183-1200.
33. Council, N.R., *Guide for the Care and Use of Laboratory Animals: Eighth Edition*. 2011, Washington, DC: The National Academies Press. 246.
34. Neher, J.J., J.V. Emmrich, M. Fricker, P.K. Mander, C. Thery, and G.C. Brown, *Phagocytosis executes delayed neuronal death after focal brain ischemia.* Proc Natl Acad Sci U S A, 2013. **110**(43): p. E4098-107.
35. Schmued, L.C., C. Albertson, and W. Slikker, *Fluoro-Jade: a novel fluorochrome for the sensitive and reliable histochemical localization of neuronal degeneration.* Brain Research, 1997. **751**(1): p. 37-46.
36. Bruinstroop, E., G. Cano, V.G. Vanderhorst, J.C. Cavalcante, J. Wirth, M. Sena-Esteves, et al., *Spinal projections of the A5, A6 (locus coeruleus), and A7 noradrenergic cell groups in rats.* J Comp Neurol, 2012. **520**(9): p. 1985-2001.
37. Schwarz, L.A. and L. Luo, *Organization of the locus coeruleus-norepinephrine system.* Curr Biol, 2015. **25**(21): p. R1051-R1056.
38. Hein, L., J.D. Altman, and B.K. Kobilka, *Two functionally distinct alpha2-adrenergic receptors regulate sympathetic neurotransmission.* Nature, 1999. **402**(6758): p. 181-4.
39. Zarow, C., S.A. Lyness, J.A. Mortimer, and H.C. Chui, *Neuronal loss is greater in the locus coeruleus than nucleus basalis and substantia nigra in Alzheimer and Parkinson diseases.* Arch Neurol, 2003. **60**(3): p. 337-41.
40. German, D.C., K.F. Manaye, C.L. White, 3rd, D.J. Woodward, D.D. McIntire, W.K. Smith, et al., *Disease-specific patterns of locus coeruleus cell loss.* Ann Neurol, 1992. **32**(5): p. 667-76.
41. Takeuchi, T., A.J. Duszkiewicz, A. Sonneborn, P.A. Spooner, M. Yamasaki, M. Watanabe, et al., *Locus coeruleus and dopaminergic consolidation of everyday memory.* Nature, 2016. **537**(7620): p. 357-362.
42. Murchison, C.F., X.-Y. Zhang, W.-P. Zhang, M. Ouyang, A. Lee, and S.A. Thomas, *A Distinct Role for Norepinephrine in Memory Retrieval.* Cell, 2004. **117**(1): p. 131-143.
43. Usher, M., J.D. Cohen, D. Servan-Schreiber, J. Rajkowski, and G. Aston-Jones, *The role of locus coeruleus in the regulation of cognitive performance.* Science, 1999. **283**(5401): p. 549-54.
44. Rorabaugh, J.M., T. Chalermpalanupap, C.A. Botz-Zapp, V.M. Fu, N.A. Lembeck, R.M. Cohen, et al., *Chemogenetic locus coeruleus activation restores reversal learning in a rat model of Alzheimer's disease.* Brain, 2017. **140**(11): p. 3023-3038.
45. Chahrour, M. and H.Y. Zoghbi, *The story of Rett syndrome: from clinic to neurobiology.* Neuron, 2007. **56**(3): p. 422-37.

46. Hagberg, B., J. Aicardi, K. Dias, and O. Ramos, *A progressive syndrome of autism, dementia, ataxia, and loss of purposeful hand use in girls: Rett's syndrome: report of 35 cases.* Ann Neurol, 1983. **14**(4): p. 471-9.
47. Zhang, X., N. Cui, Z. Wu, J. Su, J.S. Tadepalli, S. Sekizar, et al., *Intrinsic membrane properties of locus coeruleus neurons in Mecp2-null mice.* Am J Physiol Cell Physiol, 2010. **298**(3): p. C635-46.
48. Taneja, P., M. Ogier, G. Brooks-Harris, D.A. Schmid, D.M. Katz, and S.B. Nelson, *Pathophysiology of locus ceruleus neurons in a mouse model of Rett syndrome.* J Neurosci, 2009. **29**(39): p. 12187-95.
49. Blackstone, C., *Hereditary spastic paraplegia.* Handb Clin Neurol, 2018. **148**: p. 633-652.
50. Loughlin, S.E., S.L. Foote, and R. Grzanna, *Efferent projections of nucleus locus coeruleus: Morphologic subpopulations have different efferent targets.* Neuroscience, 1986. **18**(2): p. 307-319.
51. Kwasniewska, A., K. Miazga, H. Majczynski, L.M. Jordan, M. Zawadzka, and U. Slawinska, *Noradrenergic Components of Locomotor Recovery Induced by Intraspinal Grafting of the Embryonic Brainstem in Adult Paraplegic Rats.* Int J Mol Sci, 2020. **21**(15).
52. Harro, J., A. Meriküla, M. Lepiku, A.-R. Modiri, A. Rinken, and L. Oreland, *Lesioning of Locus coeruleus Projections by DSP-4 Neurotoxin Treatment: Effect on Amphetamine-Induced Hyperlocomotion and Dopamine D2 Receptor Binding in Rats.* Pharmacology & Toxicology, 2008. **86**(5): p. 197-202.
53. Rekling, J.C., G.D. Funk, D.A. Bayliss, X.W. Dong, and J.L. Feldman, *Synaptic control of motoneuronal excitability.* Physiol Rev, 2000. **80**(2): p. 767-852.
54. Mason, S.T. and H.C. Fibiger, *Regional topography within noradrenergic locus coeruleus as revealed by retrograde transport of horseradish peroxidase.* J Comp Neurol, 1979. **187**(4): p. 703-24.
55. Ruaud, L., B. Keren, R. Debs, C. Mignot, and F. Mochel, *Demyelinating motor neuropathy associated with a homozygous GPT2 pathogenic variant.* Muscle Nerve, 2021.
56. Sanchez-Padilla, J., J.N. Guzman, E. Ilijic, J. Kondapalli, D.J. Galtieri, B. Yang, et al., *Mitochondrial oxidant stress in locus coeruleus is regulated by activity and nitric oxide synthase.* Nat Neurosci, 2014. **17**(6): p. 832-40.
57. Wang, Q., E.A. Oyarzabal, S. Song, B. Wilson, J.H. Santos, and J.S. Hong, *Locus coeruleus neurons are most sensitive to chronic neuroinflammation-induced neurodegeneration.* Brain Behav Immun, 2020. **87**: p. 359-368.
58. Demetrius, L.A., P.J. Magistretti, and L. Pellerin, *Alzheimer's disease: the amyloid hypothesis and the Inverse Warburg effect.* Front Physiol, 2014. **5**: p. 522.
59. Yang, R.Z., S. Park, W.J. Reagan, R. Goldstein, S. Zhong, M. Lawton, et al., *Alanine aminotransferase isoenzymes: molecular cloning and quantitative analysis of tissue expression in rats and serum elevation in liver toxicity.* Hepatology, 2009. **49**(2): p. 598-607.
60. Glinghammar, B., I. Rafter, A.K. Lindstrom, J.J. Hedberg, H.B. Andersson, P. Lindblom, et al., *Detection of the mitochondrial and catalytically active alanine*

aminotransferase in human tissues and plasma. Int J Mol Med, 2009. **23**(5): p. 621-31.
61. Mulvey, B., D.L. Bhatti, S. Gyawali, A.M. Lake, S. Kriaucionis, C.P. Ford, et al., *Molecular and Functional Sex Differences of Noradrenergic Neurons in the Mouse Locus Coeruleus.* Cell Rep, 2018. **23**(8): p. 2225-2235.
62. Zhang, Y., K. Chen, S.A. Sloan, M.L. Bennett, A.R. Scholze, S. O'Keeffe, et al., *An RNA-sequencing transcriptome and splicing database of glia, neurons, and vascular cells of the cerebral cortex.* J Neurosci, 2014. **34**(36): p. 11929-47.

Figure Legends

Figure 1. GPT2 Deficiency leads to selective gliosis and neuron loss in locus coeruleus.

Selective microgliosis in GPT2-null LC in sagittal brain sections at P18. Images of tyrosine hydroxylase (TH, magenta), Iba1 (green) staining in wild-type (a) and GPT2-null (b) sagittal sections. D: Dorsal V: Ventral. Low magnification images taken with a 2X objective (are shown on the left, (scale bar: 500 μm), high magnification images taken with a 60X objective are on the right (scale bar: 100 μm).

Figure 2. Selective microgliosis in GPT2-null LC in coronal brain sections at P18.

Images of tyrosine hydroxylase (TH, magenta), Iba1 (green) staining in wild-type (a) and GPT2-null (b) coronal sections containing LC. D: Dorsal, V: Ventral, M: Medial, L: Lateral. Scale bar: 200 μm.

Figure 3. Smaller TH+ neurons and loss of TH+ in GPT2-null LC at P18.

High magnification images of microgliosis in GPT2-null LC at P18. Tyrosine hydroxylase (TH, magenta) and Iba1 (green) staining in wild-type (a) and GPT2-null (b) LC. (c) Quantification of TH+ cell count, TH+ soma area, TH average relative fluorescence intensity and Iba1 average relative fluorescence intensity are given below (wild-type: black, GPT2-null: red). Scale bar: 50 μm. **$0.001 < P < 0.01$.

Figure 4. Degeneration of LC neurons in GPT2-null LC.

Fluoro-Jade C staining at P18, wildtype (a), GPT2-null (b). Arrows point to degenerating cells and arrowheads point to normal cells. The asterisk denotes the 4th ventricle. Scale bar: 100 μm. Eosinophilic and necrotic neurons are present in GPT2-null LC at P18. Images of H&E staining in wild-type (c) and GPT2-null (d) LC (Scale bar: 100 μm). The top arrow points to a necrotic neuron and the bottom arrow points to a hypereosinophilic neuron in GPT2-null LC, both visualized with higher magnification on the right (Scale bar: 5 μm). The arrowhead points to a healthy neuron of the motor nucleus of the trigeminal nerve bordering the LC laterally. The asterisk denotes the LC.

Figure 5. Noradrenergic innervation in hippocampus is reduced in GPT2-null mice.

Noradrenergic innervation in hippocampus of GPT2-null mice at P18 is reduced. Images of

norepinephrine transporter (NET, green) staining in coronal sections containing hippocampus of

wild-type (a) and GPT2-null (b) mice (scale bar: 500 μm). The white boxes indicate example areas of CA1 of hippocampus and retrospenial cortex (RSC) where the staining was quantified.

Representative images of higher magnification are shown on the right for RSC (c) and hippocampus (d) (scale bar: 100 μm). Quantification of NET staining as a fraction of the total

field of view is shown for cortex (c, right) and hippocampus (d, right) (wild-type: black, GPT2-null: red). SR: stratum radiatum, SP: stratum pyramidale, SO: stratum oriens. **$0.001 < P < 0.01$.

Figure 6. Noradrenergic innervation in spinal cord of GPT2-null mice at P18 is reduced.

Images of norepinephrine transporter (NET, green) staining in coronal sections of cervical and

lumbar spinal cord of wild-type (a) and GPT2-null (b) mice (scale bar: 200 μm). The white boxes

indicate example areas where the staining was quantified for cervical spinal cord (c) and lumbar spinal cord (d) (DL: dorsolateral, DM: dorsomedial, VL: ventrolateral, VM: ventromedial).

Quantification of NET staining as a fraction of the total field of view is shown (wild-type: black,

GPT2-null: red). *$0.01 < P < 0.05$; **$0.001 < P < 0.01$; ***$P < 0.001$.

Figure 7. Norepinephrine levels in hippocampus and spinal cord of GPT2-null mice are reduced at postnatal day 18 (P18) and P14 but not at P7.

Norepinephrine levels in hippocampus and spinal cord of GPT2-null mice at P18 (a) and P14 (b)

are reduced but not at P7 (c). Quantification of norepinephrine levels per wet weight of tissue

(pmol/g) in cortex, hippocampus, cervical and lumbar spinal cord of wild-type (black) and GPT2-

null (red) mice as detected by enzyme-linked immunosorbent assay (ELISA) is shown. *0.01 <

$P < 0.05$; **0.001 < $P < 0.01$.

Figure 8. Electrophysiological characterization of LC in GPT2-null mice reveals changes in intrinsic cell properties and action potential parameters.

(a) Representative image of LC with a patch pipette (left) and representative traces of recordings in LC neurons of wild-type (black) and GPT2-null (red) mice at P18. (b) Capacitance of GPT2-null LC neurons at P18 is reduced. Wild-type: black, GPT2-null: red. Each dot represents a different cell. *0.01 < $P < 0.05$. (c) Membrane resistance of GPT2-null LC neurons at P18 is increased. Wild-type: black, GPT2-null: red. Each dot represents a different cell. ***0.001 < $P < 0.01$. (d) Pacemaking frequency of GPT2-null LC neurons at P18 is slightly increased. Wild-type: black, GPT2-null: red. Each dot represents a different cell. *$P = 0.0318$. Mixed model analysis was employed here with fixed effects: genotype, presence of hyperpolarization in resting membrane potential toward the end of recording and whether the pacemaking activity was retained throughout the recording, random effects: day of recording. (e) Shape of the averaged action potential from the pacemaking activity of wild-type (black, n=11 cells) and GPT2-null (red, n=11 cells) LC neurons at P18. (f) Peak amplitude of GPT2-null LC neuron action potential at P18 is increased. Wildtype: black, GPT2-null: red. Each dot represents a different cell. *0.01 < $P < 0.05$. (g) Time to decay to half amplitude of GPT2-null LC

neuron action potential at P18 is decreased. Wild-type: black, GPT2-null: red. Each dot represents a different cell. **$0.001 < P < 0.01$. (h) Hyperpolarization peak amplitude of GPT2-null LC neuron action potential at P18 is increased. Wild-type: black, GPT2-null: red. Each dot represents a different cell. *$0.01 < P < 0.05$.

SUPPLEMENTAL INFORMATION

Supplemental Figure Legends

Supplemental Figure 1. Selective microgliosis is observed in a pontine region in GPT2-null mice at P18.

a. Images of Iba1 (green) staining in GPT2-null sagittal sections at P18. Each section is separated by approximately 500 μm and succeeded medially from top to bottom. The arrowhead notes the pontine nucleus where clustered activated microglia are present. Note the absence of gliosis in other brain regions. The tile images taken with a 20X objective were stitched. Scale bar: 500 μm.

b. Images of Iba1 (green) staining in wild-type (left) and GPT2-null (right) coronal sections containing various brain regions including motor cortex and somatosensory areas, caudoputamen, nucleus accumbens. Note the absence of microgliosis throughout the brain section. Scale bar: 500 μm.

c. Images of Iba1 (green) staining in wild-type (left) and GPT2-null (right) coronal sections containing various brain regions including hippocampus, thalamus, hypothalamus, amygdala. Note the absence of microgliosis throughout the brain section. Scale bar: 500 μm.

d. Images of Iba1 (green) staining in wild-type (left) and GPT2-null (right) coronal sections containing various brain regions including cortical visual and entorhinal areas, midbrain. Note the absence of microgliosis throughout the brain section. Scale bar: 500 μm.

e. Images of Iba1 (green) staining in wild-type (left) and GPT2-null (right) coronal sections containing various brain regions including cerebellum and medulla oblongata. Note the absence of microgliosis throughout the brain section. Scale bar: 500 μm.

Supplemental Figure 2. Microgliosis and astrogliosis is present in GPT2-null mice at P18 but not at P10.

a. Images of Gfap (cyan), Iba1 (yellow), tyrosine hydroxylase (TH, magenta) staining in wild-type and GPT2-null coronal sections at P18. Note the increase in Gfap staining in GPT2-null LC and clustering of microglia particularly around the ventral LC. Scale bar: 100 μm.

b. Images of Gfap (cyan), Iba1 (yellow), tyrosine hydroxylase (TH, magenta) staining in wild-type and GPT2-null coronal sections at P10. Note the absence of either microgliosis or astrogliosis in GPT2-null LC at P10. Scale bar: 100 μm.

Supplemental Figure 3. CD68 staining in reactive microglia in GPT2-null LC at P18.

a. Images of CD68 (cyan), Iba1 (yellow), tyrosine hydroxylase (TH, magenta) staining in wild-type and GPT2-null coronal sections at P18, taken with a 20X objective. Arrowheads point to the increased size of CD68 puncta within the reactive microglia in GPT2-null LC. Scale bar: 100 μm.

b. Images of CD68 (cyan), Iba1 (yellow), tyrosine hydroxylase (TH, magenta) staining in wild-type and GPT2-null coronal sections at P18, taken with a 60X objective. Note the

enlarged CD68 puncta within the reactive microglia in GPT2-null LC. Scale bar: 100 μm.

Supplemental Figure 4. GPT2 is expressed in LC neurons.

a. Target allele construct that results in a GPT2-null allele. The targeted allele consists of flippase recognition sites (FRT) flanking a strong splicing acceptor site (Engrailed 2-SA), β-galactosidase (β-gal, an enzymatic reporter), neomycin (a selective marker for embryonic cells) and a polyadenylation site.

b. Immunofluorescence of β-galactosidase in CA3 area of hippocampus of a GPT2-heterozygous (GPT2-het) mouse at P18. Note the pattern of the β-gal (cyan) puncta aligning with the nuclei (DAPI, yellow) the stratum pyramidale of CA3, indicating strong expression in neurons and validity of the β-gal reporter. Scale bar: 100 μm.

c. Images of β-gal (cyan) and tyrosine hydroxylase (TH, magenta) staining in LC of GPT2-het mouse at P5 (top) and P18 (bottom). Note the stronger staining at P18 indicating increased expression of GPT2 at this timepoint compared to P5. Scale bar: 50 μm.

d. High magnification images of β-gal (cyan) and tyrosine hydroxylase (TH, magenta) staining in representative neurons in LC of GPT2-het mouse at P5 (top) and P18 (bottom). Note the larger puncta of β-gal at P18 indicating increased expression of GPT2 at this timepoint compared to P5. Scale bar: 5 μm.

FIGURE 1

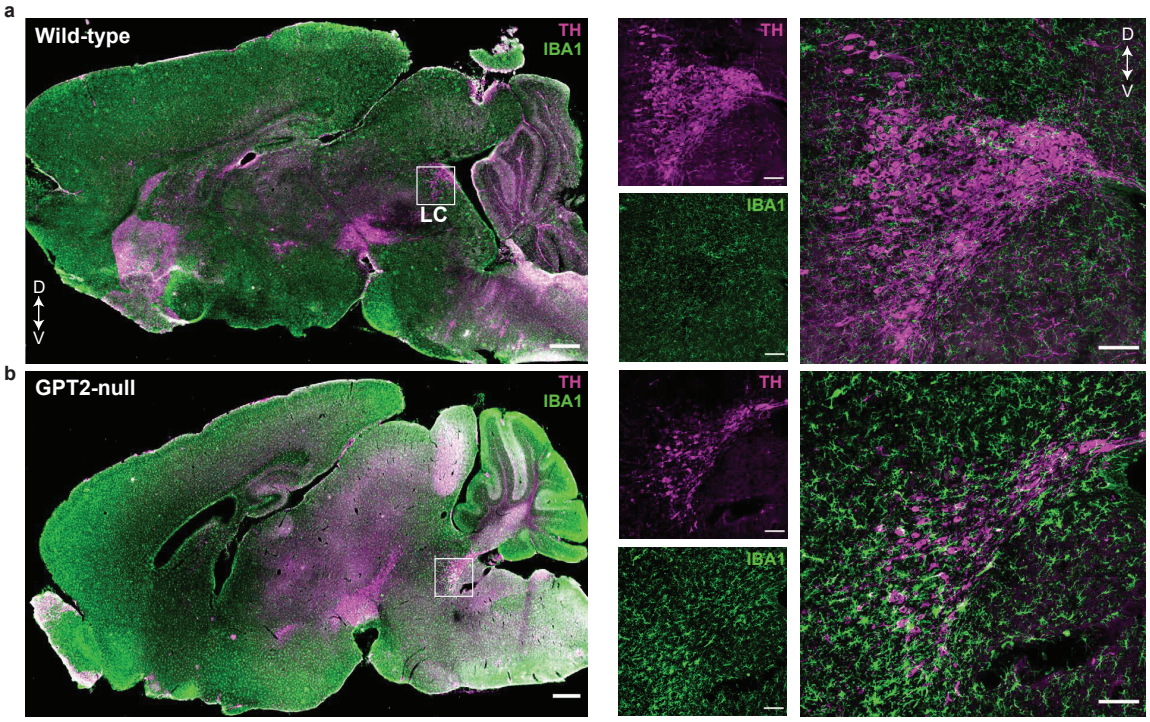

FIGURE 2

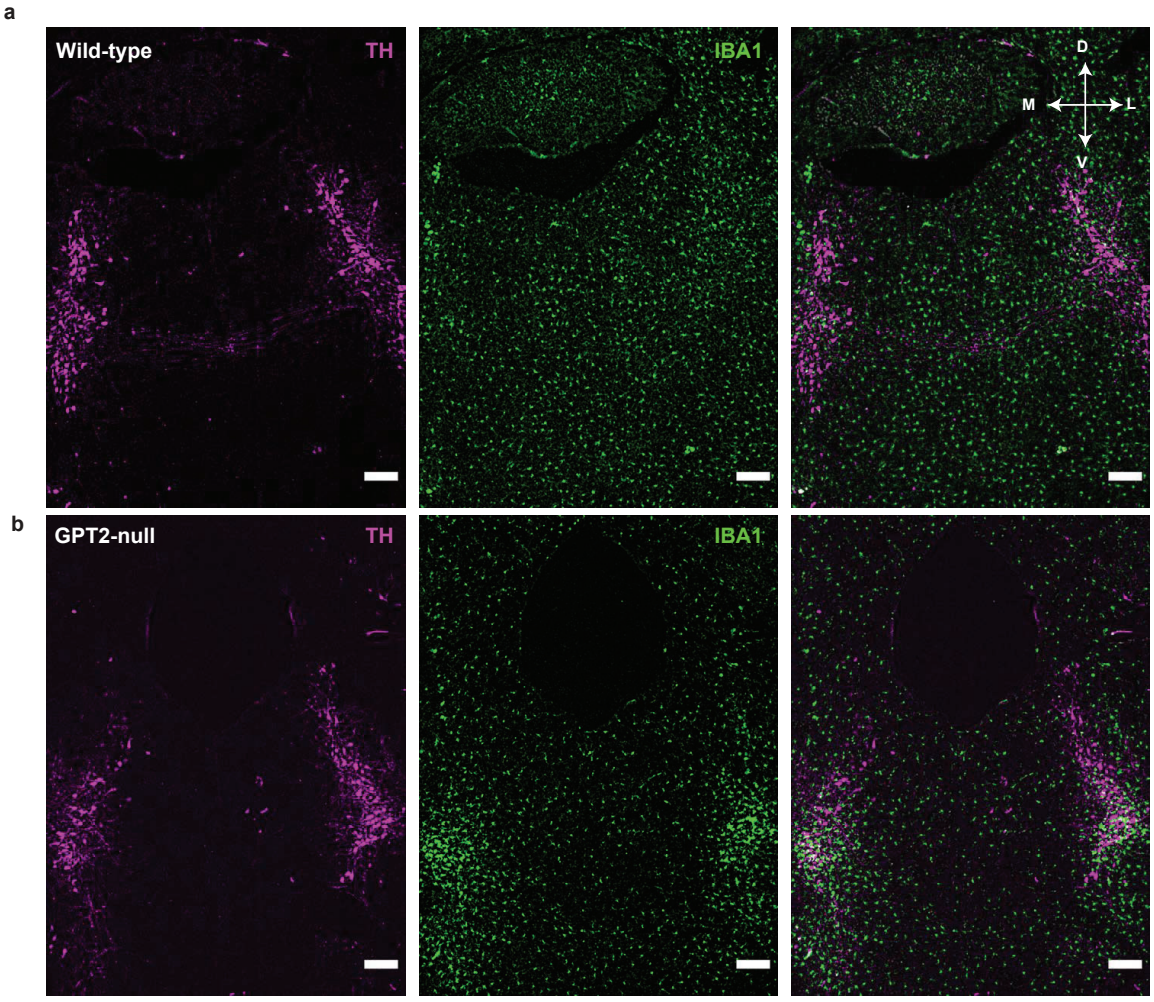

FIGURE 3

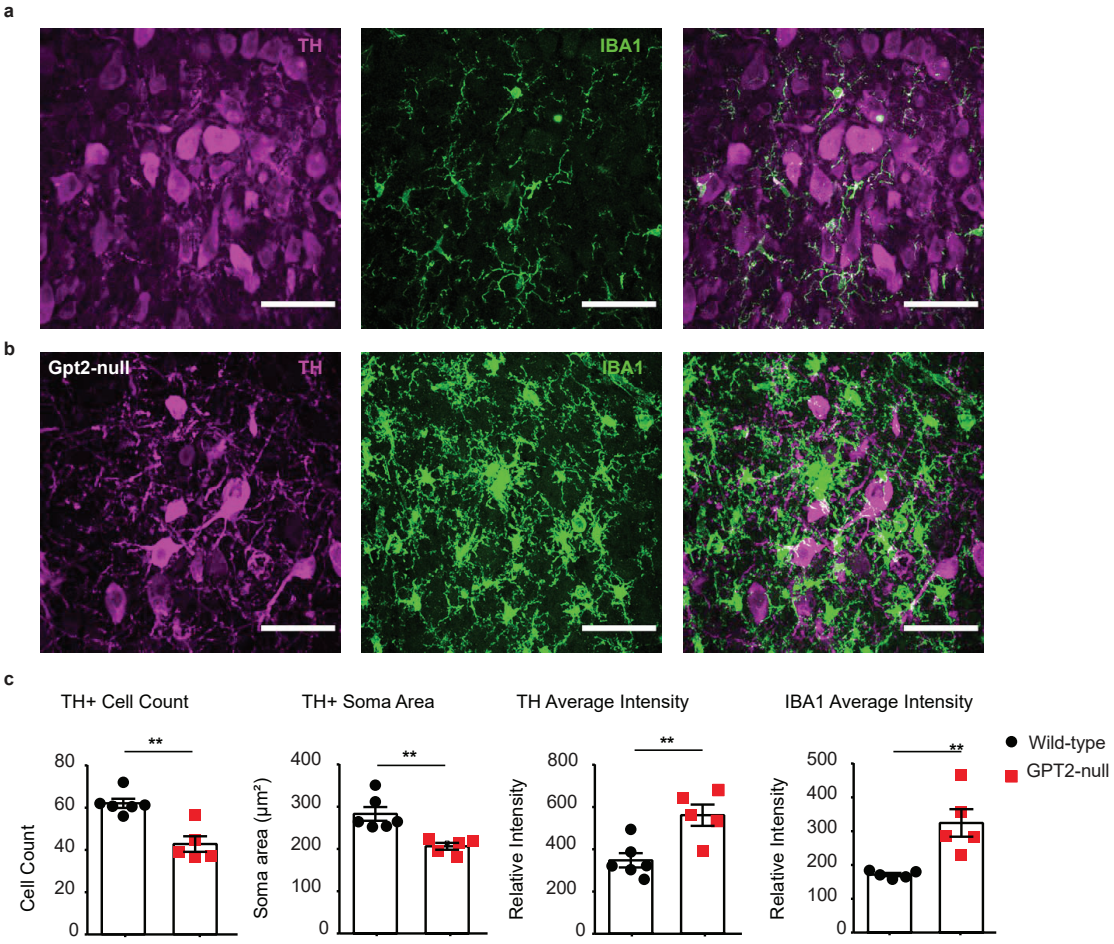
a
TH
IBA1
b
Gpt2-null
TH
IBA1
c
TH+ Cell Count
TH+ Soma Area
TH Average Intensity
IBA1 Average Intensity
Cell Count
Soma area (µm²)
Relative Intensity
Relative Intensity
**
Wild-type
GPT2-null

FIGURE 4

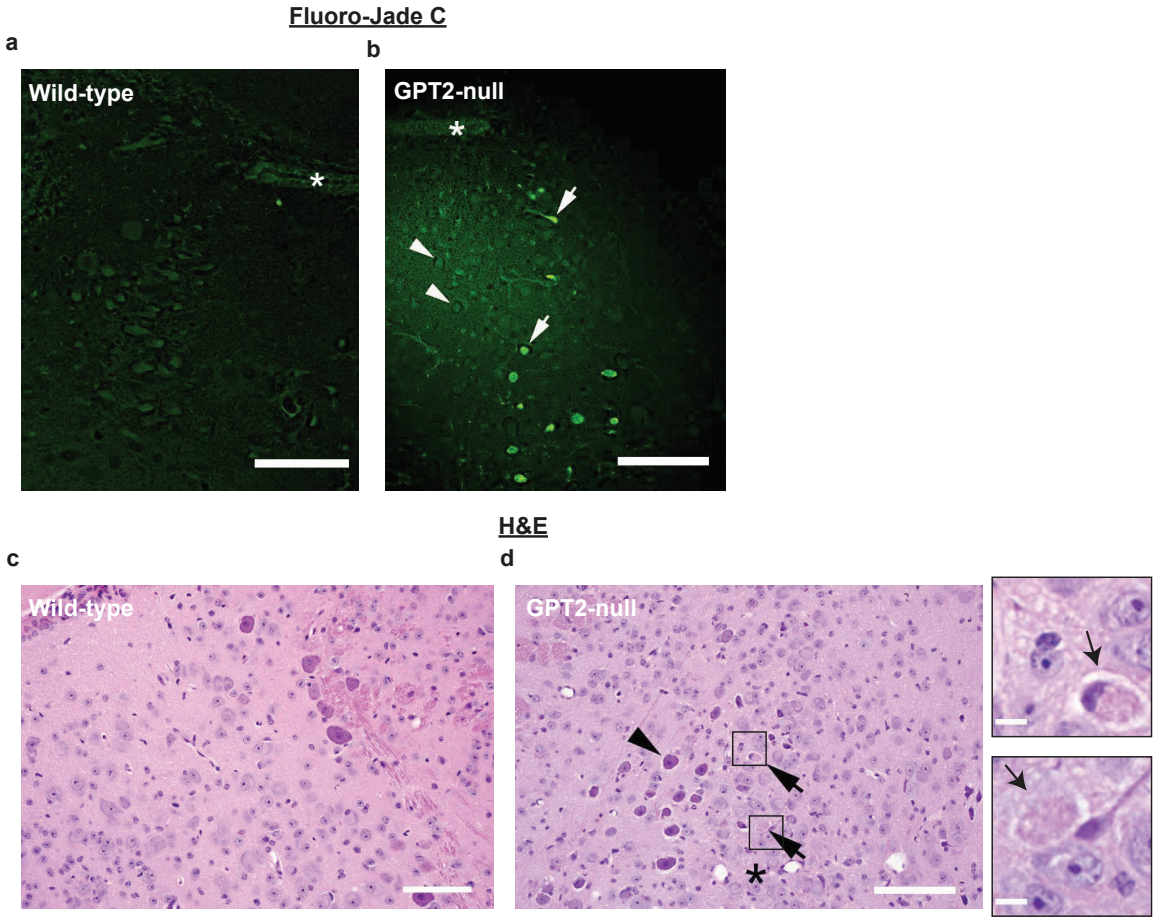

FIGURE 5

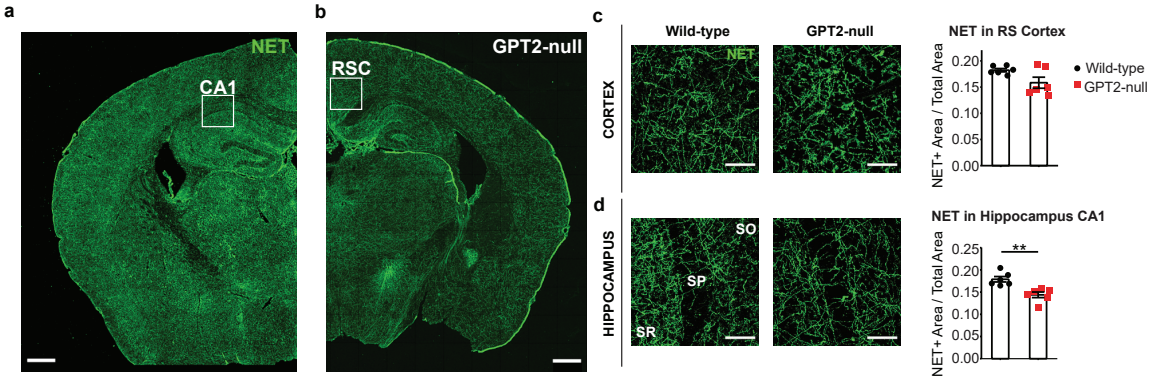
a
NET
CA1
b
GPT2-null
RSC
c
Wild-type
GPT2-null
CORTEX
NET
d
HIPPOCAMPUS
SO
SP
SR
NET in RS Cortex
NET+ Area / Total Area
0.20
0.15
0.10
0.05
0.00
Wild-type
GPT2-null
NET in Hippocampus CA1
**
0.25

FIGURE 6

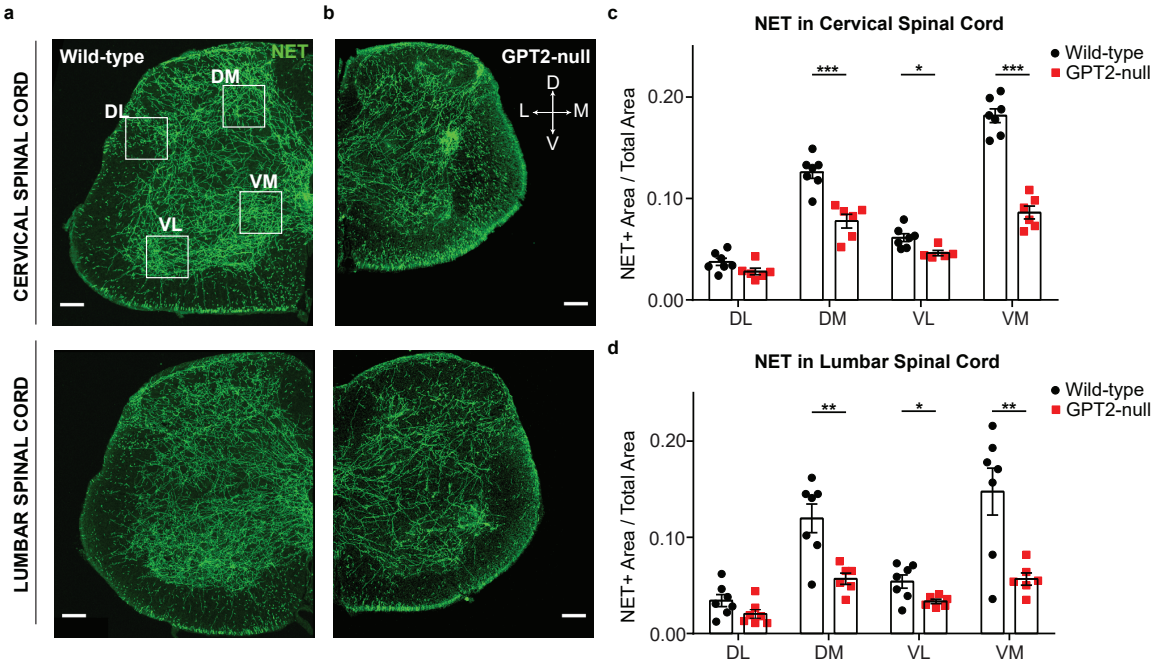
a
b
c
CERVICAL SPINAL CORD
LUMBAR SPINAL CORD
Wild-type
NET
DM
DL
VM
VL
GPT2-null
D
L
M
V
NET in Cervical Spinal Cord
Wild-type
GPT2-null
NET+ Area / Total Area
0.20
0.10
0.00
***
*
***
DL
DM
VL
VM
d
NET in Lumbar Spinal Cord
Wild-type
GPT2-null
NET+ Area / Total Area
0.20
0.10
0.00
**
*
**
DL
DM
VL
VM

FIGURE 7

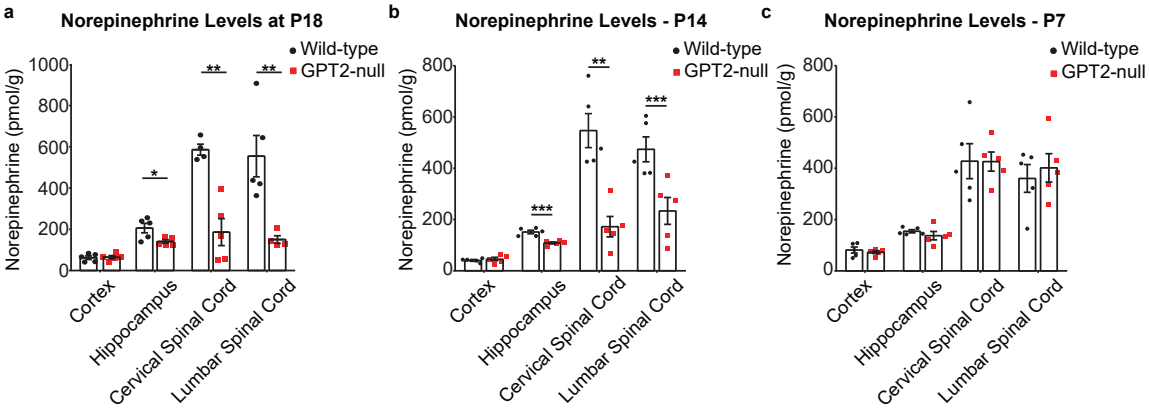
a
Norepinephrine Levels at P18
Wild-type
GPT2-null
Norepinephrine (pmol/g)
1000
800
600
400
200
0
*
**
**
Cortex
Hippocampus
Cervical Spinal Cord
Lumbar Spinal Cord
b
Norepinephrine Levels - P14
Wild-type
GPT2-null
Norepinephrine (pmol/g)
800
600
400
200
0
***
**
***
Cortex
Hippocampus
Cervical Spinal Cord
Lumbar Spinal Cord
c
Norepinephrine Levels - P7
Wild-type
GPT2-null
Norepinephrine (pmol/g)
800
600
400
200
0
Cortex
Hippocampus
Cervical Spinal Cord
Lumbar Spinal Cord

FIGURE 8

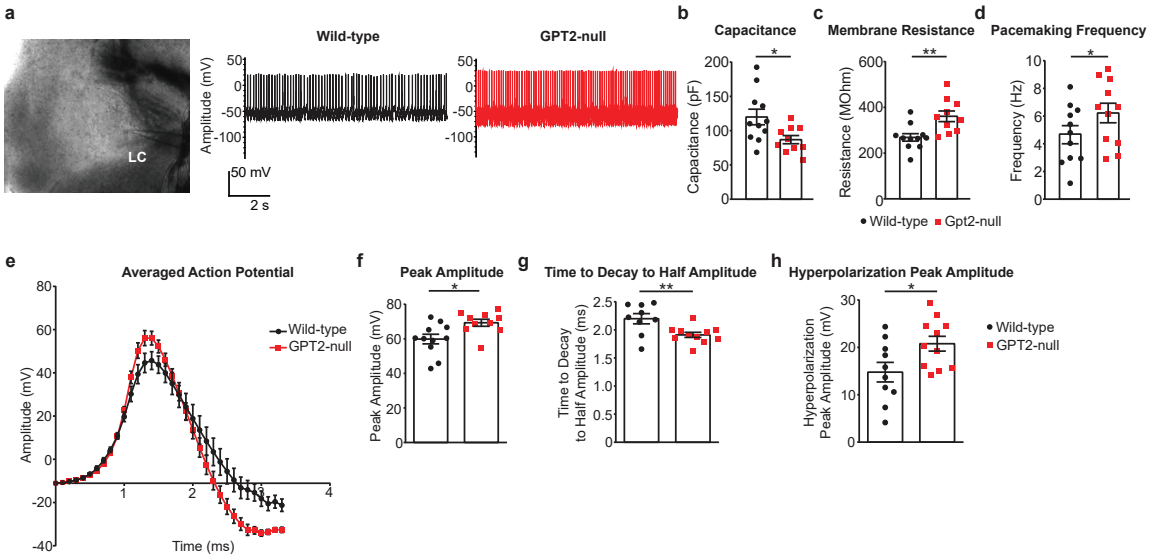
a
LC
Wild-type
GPT2-null
Amplitude (mV)
50
0
-50
-100
50 mV
2 s
b
Capacitance
Capacitance (pF)
200
150
100
50
0
*
c
Membrane Resistance
Resistance (MOhm)
600
400
200
0
**
Wild-type
Gpt2-null
d
Pacemaking Frequency
Frequency (Hz)
10
8
6
4
2
0
*
e
Averaged Action Potential
Amplitude (mV)
80
60
40
20
0
-20
-40
1
2
3
4
Time (ms)
Wild-type
GPT2-null
f
Peak Amplitude
Peak Amplitude (mV)
80
60
40
20
0
*
g
Time to Decay to Half Amplitude
Time to Decay to Half Amplitude (ms)
2.5
2.0
1.5
1.0
0.5
0
**
h
Hyperpolarization Peak Amplitude
Hyperpolarization Peak Amplitude (mV)
30
20
10
0
*
Wild-type
GPT2-null

FIGURE S1

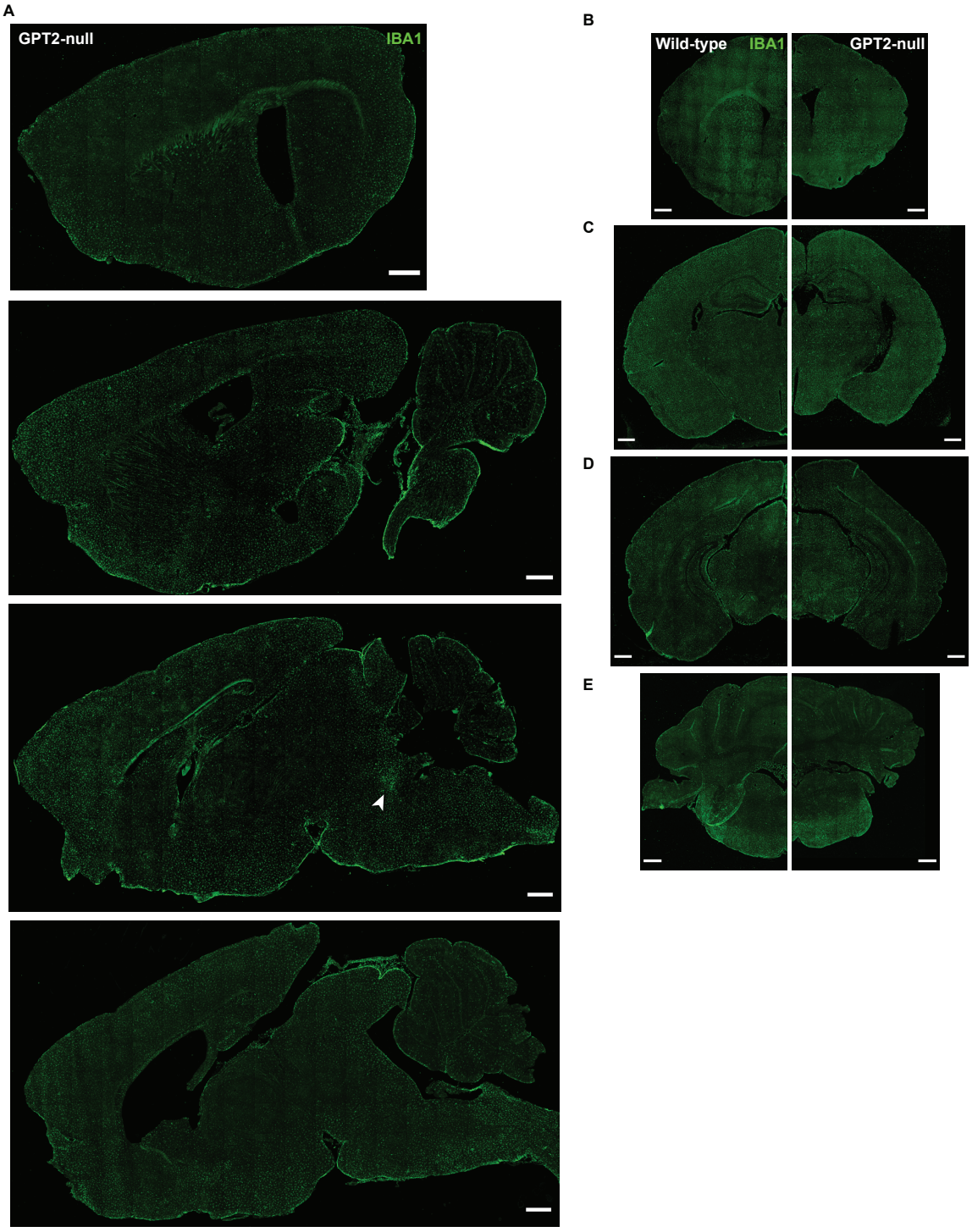

FIGURE S2

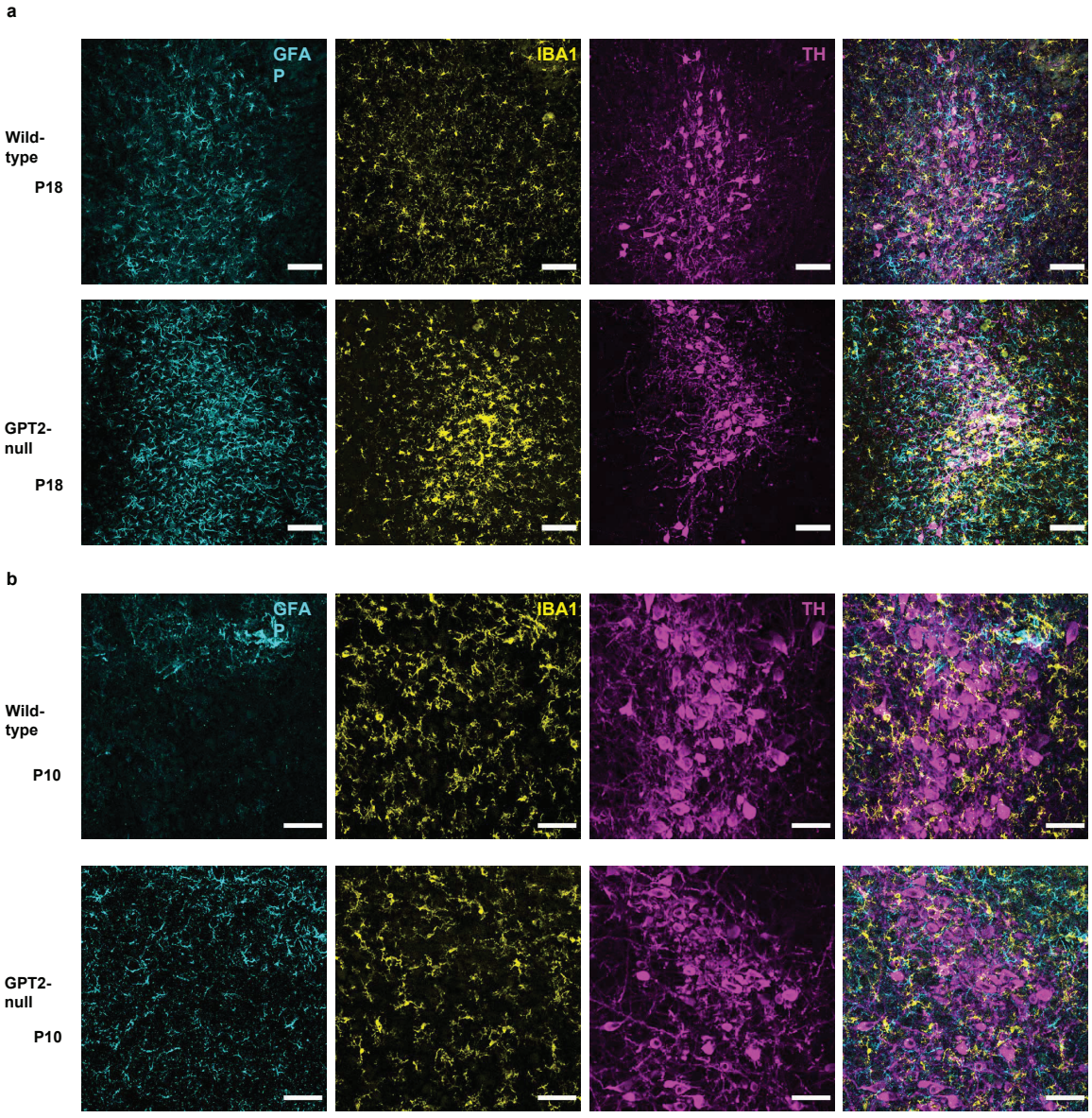
a
GFA
P
IBA1
TH
Wild-
type
P18
GPT2-
null
P18
b
GFA
P
IBA1
TH
Wild-
type
P10
GPT2-
null
P10

FIGURE S3

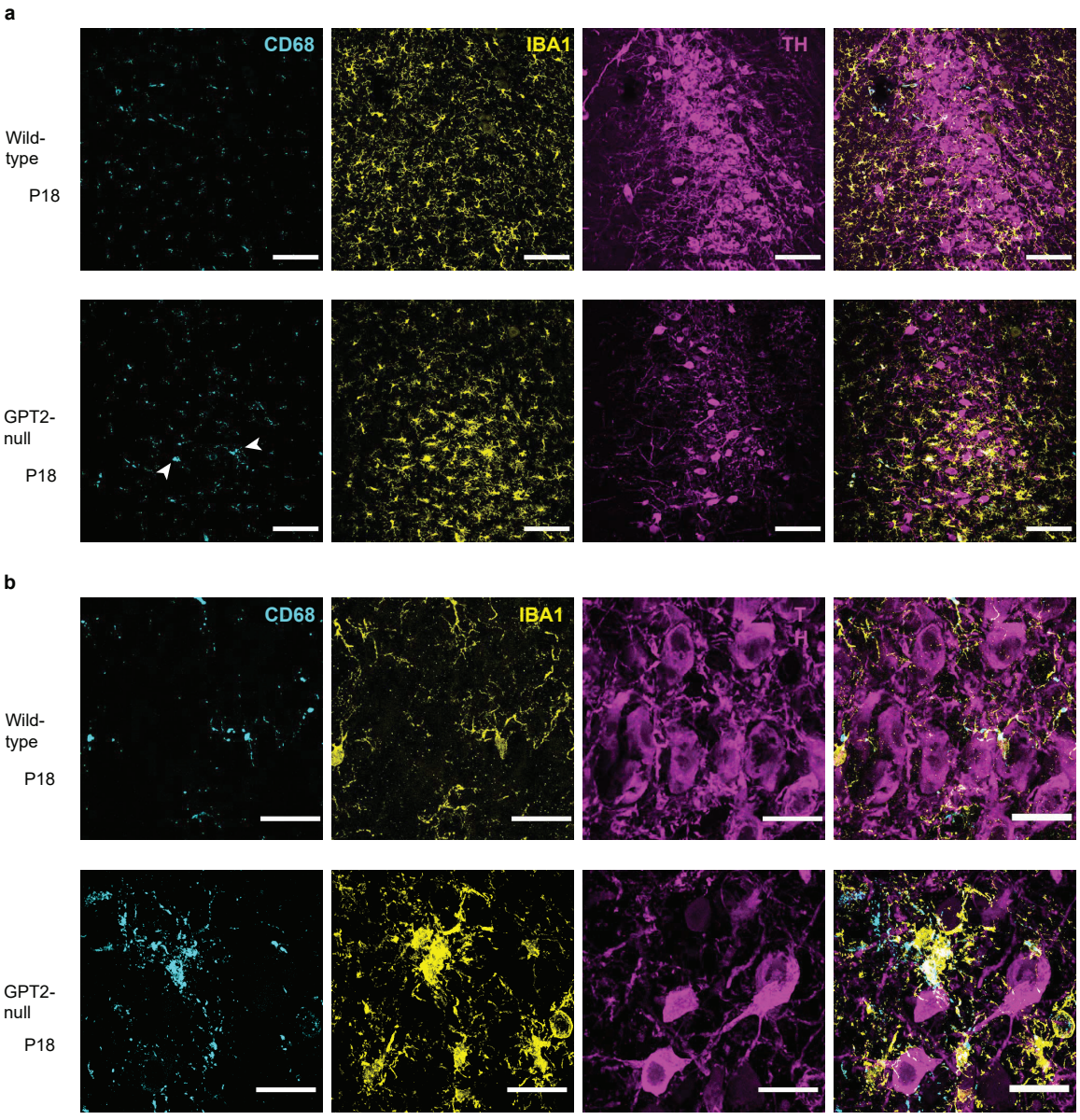
a
CD68
IBA1
TH
Wild-type
P18
GPT2-null
P18
b
CD68
IBA1
TH
Wild-type
P18
GPT2-null
P18

FIGURE S4

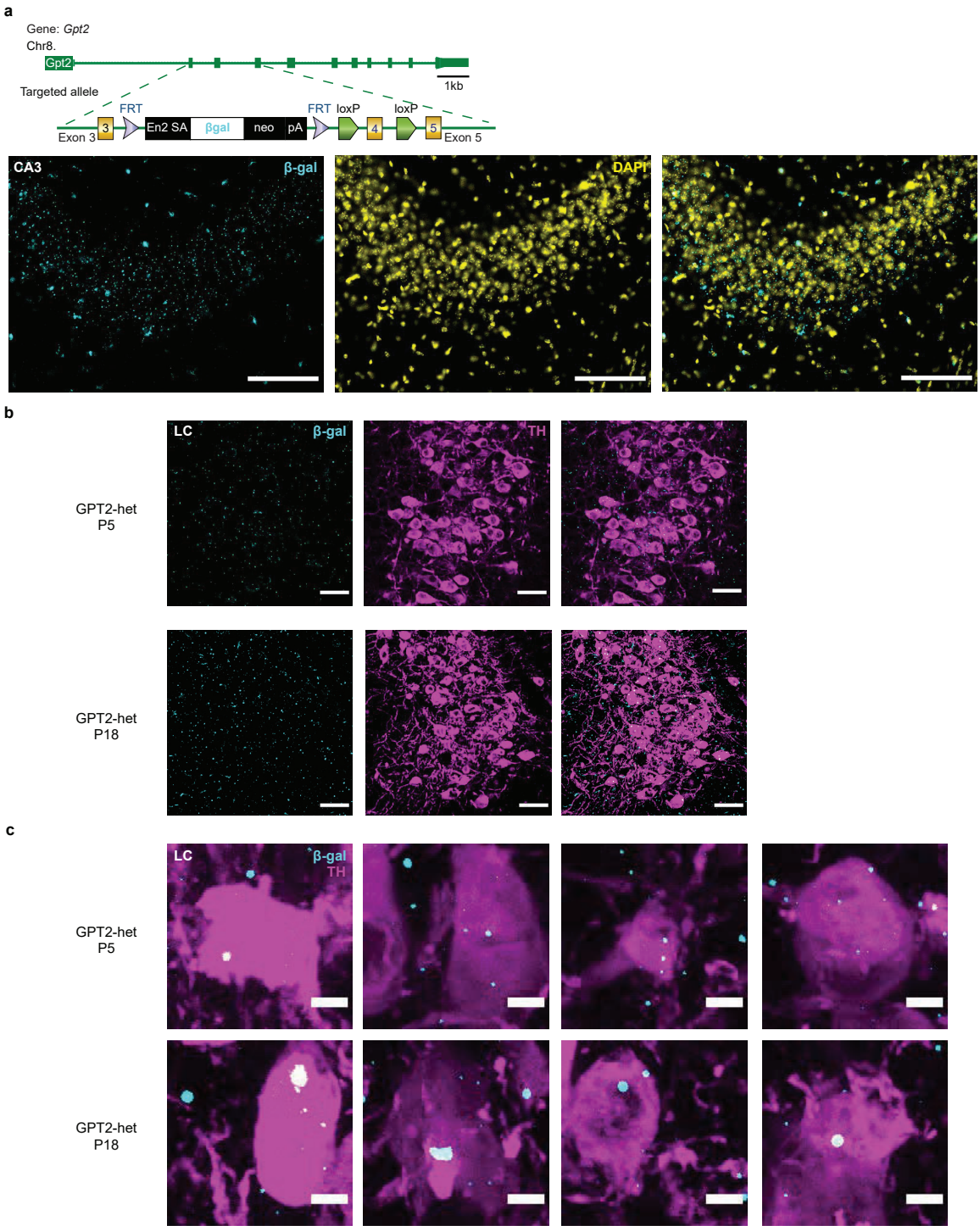
a
Gene: Gpt2
Chr8.
Gpt2
1kb
Targeted allele
FRT
FRT
loxP
loxP
Exon 3
3
En2 SA
βgal
neo
pA
4
5
Exon 5
CA3
β-gal
DAPI
b
LC
β-gal
TH
GPT2-het
P5
GPT2-het
P18
c
LC
β-gal
TH
GPT2-het
P5
GPT2-het
P18

Chapter 5: Loss of mitochondrial enzyme GPT2 leads to reprogramming of synaptic glutamate metabolism.

I conducted all experiments. Shawn M. Davidson ran LC-MS at Princeton. The project was performed under the supervision of Julie A. Kauer and Eric M. Morrow. For funding sources please refer to the Chapter.

Loss of mitochondrial enzyme GPT2 leads to reprogramming of synaptic glutamate metabolism

Abbreviated Title: Loss of GPT2 rewires synaptic glutamate metabolism

Ozan Baytas[1,2,3], Shanequia R. Jackson[4], Shawn M. Davidson[4], Julie A. Kauer[5] and Eric M. Morrow[1,2#]

[1]Department of Molecular Biology, Cell Biology and Biochemistry, Brown University, Providence, RI 02912, USA; [2]Center for Translational Neuroscience, Carney Institute for Brain Science and Brown Institute for Translational Science, Brown University, Providence, RI 02912, USA; [3]Neuroscience Graduate Program, Brown University, Providence, RI 02912, USA; [4]Lewis-Sigler Institute for Integrative Genomics, Princeton University, Princeton, NJ 08540, USA; [5]Department of Psychiatry and Behavioral Sciences, Stanford University School of Medicine, Stanford, CA 94035, USA

[#]To whom correspondence should be addressed:
Eric M. Morrow MD PhD
Brown University, Laboratories for Molecular Medicine,
70 Ship Street, Providence, RI 02912, USA
Tel: 401-863-9778
Fax: 401-432-1607
E-mail: eric_morrow@brown.edu

Number of pages: 46
Number of figures: 6
Number of words for Abstract: 222
Number of words for Introduction: 388
Number of words for Discussion: 1442

Competing interests: The authors declare no competing interests.

Acknowledgments: This work was supported by a Brain & Behavior Research Foundation NARSAD Independent Investigator grant (25701, to E.M.M.), a Dr. Ralph and Marian Falk Medical Research Trust Catalyst Award (to E.M.M.), a Brown University Research Seed Award (to E.M.M.), an NIH NIDA grant (R01DA011289) to J.A.K., the Carney Institute for Brain Science and Suna Kıraç Fellowship Graduate Award in Brain Science (O.B.). This study was also supported by the Hassenfeld Child Health Innovation Institute at Brown University.

Author contributions: Conceptualization O.B., J.A.K. and E.M.M.; O.B. conducted all experiments; S.R.J. and S.M.D. contributed to studies involving mass spectrometry for isotope tracing; Data Curation and Visualization O.B.; Experimental Design and Data Analysis O.B., S.R.J., S.M.D., J.A.K. and E.M.M.; Formal Analysis and Writing – Original Draft, O.B. and E.M.M.; Writing – Review & Editing, O.B., S.M.D., J.A.K. and E.M.M; Supervision, Project Administration, and Funding Acquisition, J.A.K. and E.M.M.

Abstract

Glutamate metabolism is tightly regulated by a multitude of metabolic enzymes to sustain both excitatory neurotransmission and energetics. Previously, we reported loss-of-function mutations in mitochondrial enzyme glutamate pyruvate transaminase 2 (*GPT2*) in humans that cause postnatal microcephaly, intellectual disability and motor abnormalities. Here we report that Gpt2 is enriched in isolated synaptic terminals and the loss of Gpt2 leads to a reprogramming of glutamate metabolism in male and female mice. Gpt2 governs a reversible reaction that may synthesize glutamate using alanine and alpha-ketoglutarate and mediate conversion of glutamine into alanine. Glutamatergic synaptic transmission in Gpt2-null CA1 hippocampal slices is impaired in a fashion consistent with decreased pre-synaptic glutamate levels. Glutamate levels released from Gpt2-null synaptosomes are reduced but restored to wild-type levels by alpha-ketoglutarate. Through isotope labeling studies, we observe that fractional enrichment of double heavy nitrogen labeled glutamine in Gpt2-null synaptosomes is increased but rescued by alpha-ketoglutarate. Gpt2 loss results in changes in levels of synaptic proteins involved in glutamate metabolism, particularly increases in glutamate dehydrogenase and glutamine synthetase. We find deficits in the tricarboxylic acid (TCA) cycle in Gpt2-null synaptosomes, but glutamine entry into the TCA cycle was intact. In conclusion, Gpt2 is a mitochondrial enzyme in synaptic terminals that links glutamate metabolism to alanine and TCA cycle metabolism, and in the absence of Gpt2, regulatory enzymatic mechanisms appear to be reprogramed to partly maintain functioning of the glutamatergic synaptic transmission.

Significance Statement

Investigation of neurometabolism have recently implemented genetic approaches, furthering our understanding of metabolic pathways that sustain glutamatergic neurotransmission. Here we investigate the contributions of glutamate pyruvate transaminase 2 (Gpt2) to glutamate metabolism and the consequences of Gpt2 deficiency on synaptic transmission. Gpt2 deficiency in humans causes microcephaly and intellectual disability and understanding the function of Gpt2 may help delineate the metabolic mechanisms that support brain and cognitive development. In the absence of Gpt2, glutamate transmission is impaired but rescued by alpha-ketoglutarate supplementation. Gpt2 deficiency leads to compensatory upregulation of enzymes and transporters involved in glutamate metabolism. Our results emphasize the use of glutamate for replenishing the tricarboxylic acid cycle and the role of Gpt2 in sustaining energetics and neurotransmitter availability.

Introduction

Glutamate, the main excitatory neurotransmitter in the central nervous system (Fonnum, 1984; Villa and Nedivi, 2016), is crucial for neurotransmission as well as the tricarboxylic acid (TCA) cycle (Kovacevic, 1971; Westergaard et al., 1995), nitrogen balance (Cooper and Jeitner, 2016; Kurmi and Haigis, 2020), synthesis of proteins (Young and Ajami, 2000), glutathione (Sedlak et al., 2019), and gamma-aminobutyric acid synthesis (Sonnewald and McKenna, 2002). Glutamate metabolism has been studied widely using measurement of enzyme activities, concentrations, and labeling patterns of metabolites with heavy isotope or radioisotope labeled precursors (Erecinska and Silver, 1990b). Genetic approaches have since followed, furthering our understanding of the intricate metabolic pathways of glutamate metabolism that sustain neurotransmission.

Previously, we reported recessive loss-of-function mutations in the gene glutamate pyruvate transaminase 2 (*GPT2*) (also known as alanine aminotransferase) that lead to a neurodevelopmental disorder involving microcephaly, intellectual disability, and motor abnormalities (Ouyang et al., 2016). Gpt2 is an alanine aminotransferase that catalyzes a reversible transamination, transferring an amino group from glutamate to pyruvate synthesizing alanine and alpha-ketoglutarate. Gpt2 resides in the mitochondria while its paralog, Gpt1 catalyzes the same reaction in the cytoplasm (Lindblom et al., 2007; Ouyang et al., 2016). Gpt2 has been widely studied in the context of cancer and liver metabolism (Jin et al., 2015; Kim et al., 2019; McCommis et al., 2015; Smith et al., 2016); however, its role as a metabolic enzyme modulating glutamate levels in the

nervous system remains unknown. Genetic ablation of Gpt2 in mice has allowed us to study the extent to which Gpt2 regulates glutamate availability.

In this study, we report that Gpt2 is enriched in the mitochondria of isolated synaptic terminals (synaptosomes) and the loss of Gpt2 leads to a reprogramming of glutamate metabolism. Gpt2 may produce glutamate with alanine and alpha-ketoglutarate as precursors and mediate conversion of glutamine into alanine. Glutamatergic transmission in mouse brain slices is impaired evidenced by decreased miniature postsynaptic excitatory currents and faster decline of postsynaptic response in CA1 pyramidal neurons to repeated CA3 Schaffer collateral stimulation. Glutamate levels released upon membrane depolarization are reduced in Gpt2-null synaptosomes. Through isotope labeling studies, we observe that fractional enrichment of double heavy nitrogen labeled glutamine is increased. Alpha-ketoglutarate was able to raise glutamate and decrease fractional enrichment of double-labeled glutamine in Gpt2-null synaptosomes back to wild-type levels. We find increased protein levels of glutamate dehydrogenase and glutamine synthetase in Gpt2-null synaptosomes, two metabolic enzymes that mediate glutamate oxidation and ammonia fixation, respectively. We also find deficits in the TCA cycle in Gpt2-null synaptosomes although glutamine entry into the TCA cycle remains intact. Our results indicate that Gpt2 plays a role in sustaining energetics and neurotransmitter availability, and in the absence of Gpt2, these processes appear to be partly compensated by upregulation of metabolic enzymes and transporters involved in glutamate metabolism.

Results

Gpt2 is the primary glutamate-pyruvate transaminase in isolated nerve terminals.

To understand the contribution of Gpt2 to glutamate metabolism at the synapse, we first investigated Gpt2 protein expression in synaptosomes. Synaptosomes are isolated nerve terminals that form during homogenization and medium-speed centrifugation of mouse nervous tissues in a sucrose-based solution (Figure 1A) (Dunkley et al., 2008). Gpt2 was enriched both in synaptosomes and mitochondria (Figure 1C). Gpt1, the cytosolic paralog of Gpt2, was enriched in the cytosolic fraction but virtually absent in both synaptosomal and mitochondrial fractions. In Western blotting of the different subcellular fractions, we also confirmed the presence of some of the proteins involved in glutamate/glutamine metabolism at synaptic terminals (Figure 1B,C). We fractionated synaptosomes further into synaptic membranes, cytosol and vesicles and Gpt2 was not enriched in any of these fractions indicating that Gpt2 is enriched in the mitochondria situated in synaptic terminals (Figure 1D).

In agreement with the exclusive expression of Gpt2 in synaptosomes, we found only residual Gpt enzyme activity in Gpt2-null synaptosomes compared to the wild-type controls (Figure 1E). To further confirm absence of Gpt activity in Gpt2-null synaptosomes and assess the function of metabolic pathways that utilize Gpt2, we conducted isotope labeling experiments with heavy isotope labeled tracers (Figure 1F). From amine nitrogen-labeled glutamine ([α-^{15}N]-glutamine), alanine was not labeled at all in Gpt2-null synaptosome pellets or medium indicating that glutamine could not act as a precursor for alanine in the absence of Gpt2. Interestingly, the alanine pool that was released from wild-

type synaptosomes into the medium originated from [α-^{15}N]-glutamine more than the alanine pool that remained in the pellet (Figure 1F, left).

Akin to a Gpt enzyme activity assay, an excess supply of heavy nitrogen labeled alanine (1.6 mM) and unlabeled alpha-ketoglutarate (1.6 mM) resulted in 41.7 ± 2.4 % labeling in glutamate of wild-type synaptosomal pellets as well as in 47.2 ± 2.3 % of the glutamate pool released into the medium, suggesting that alanine along with alpha-ketoglutarate can be used as substrates for glutamate in our wild-type synaptosome preparations (Figure 1F, right). On the other hand, Gpt2-null synaptosomal pellet or medium showed residual heavy nitrogen labeling in glutamate (5.1 ± 0.4 % in pellet; 4.9 ± 0.4 % in medium). Thus, we conclude that Gpt2 is the main alanine aminotransferase in synaptic terminals.

Electrophysiological recordings suggest decreased glutamatergic transmission in Gpt2-null hippocampus.

To assess the role of Gpt2 in synaptic transmission and modulation of glutamate, we conducted whole-cell patch-clamp recording experiments in pyramidal neurons of CA1 hippocampal slices (Figure 2A). We first characterized the electrophysiological properties of the Gpt2-null pyramidal neurons. The resting membrane potential of Gpt2-null pyramidal neurons was slightly depolarized (Wild-type: -63.8 ± 1.9 mV vs Gpt2-null: -59.8 ± 1.0 mV) (Figure 2B). The capacitance was reduced, and the membrane resistance was increased in Gpt2-null pyramidal neurons suggesting that Gpt2-null CA1 pyramidal neurons are smaller in soma size (Wild-type: 121.7 ± 6.7 pF vs Gpt2-null: 92.7 ± 4.8 pF; Wild-type: 122.7 ± 7.3 MOhm vs Gpt2-null: 160.5 ± 9.5 MOhm, respectively) (Figure 2C).

Slight depolarization and increased membrane resistance in Gpt2-null pyramidal neurons are visible in the representative traces in Figure 2A. Overall, the electrophysiological properties of Gpt2-null neurons were significantly altered.

Miniature post-synaptic currents are indirect measures of neurotransmitter levels in synaptic quanta, individual synaptic vesicles (Fatt and Katz, 1952; Ropert et al., 1990). To test whether absence of Gpt2 affected glutamate pools in synaptic vesicles, we recorded miniature post-synaptic excitatory currents (mEPSCs) from Gpt2-null CA1 pyramidal neurons voltage-clamped at -80mV. The mEPSC frequency was unchanged (Figure 2F, Wild-type: 0.12 ± 0.01 Hz vs Gpt2-null: 0.13 ± 0.01 Hz); however, the mEPSC peak amplitude was slightly decreased in Gpt2-null pyramidal neurons (Figure 2E&G, Wild-type: 13.7 ± 0.5 pA vs Gpt2-null: 11.6 ± 0.3 pA). The cumulative probability histogram of mEPSC peak amplitudes of all miniature excitatory events was shifted to the left in a representative Gpt2-null pyramidal neuron compared to its wild-type control (Figure 2H, Kolmogorov-Smirnov D value: 0.2386). Overall, these results suggest that glutamate levels were reduced in synaptic vesicles of excitatory afferents on Gpt2-null CA1 pyramidal neurons.

To test whether the GABAergic input onto Gpt2 pyramidal neurons was similarly affected, we recorded miniature post-synaptic inhibitory currents (mIPSCs) from Gpt2-null CA1 pyramidal neurons voltage-clamped at -80mV (Figure 2I-K). Both mIPSC frequency (Figure 2J) and peak amplitude (Figure 2K) were unchanged in Gpt2-null CA1 pyramidal neurons (Wild-type: 4.04 ± 1.03 Hz vs Gpt2-null: 3.3 ± 0.65 Hz; Wild-type: 35.5 ± 3.0 pA vs Gpt2-null: 33.1 ± 1.9 pA, respectively). The cumulative probability histogram of mIPSC peak amplitudes had a distribution similar to the wild-type control (Figure 2L). Overall,

these results suggest that GABA levels remained the same in synaptic vesicles at inhibitory synapses on Gpt2-null CA1 pyramidal neurons.

Protein levels of AMPAR, NMDAR and SV2 are reduced in Gpt2-null hippocampus.

The decreased glutamatergic transmission could be explained by alterations in cell properties and receptor protein levels of the post-synaptic neuron as well as in glutamate levels in the pre-synaptic neuron. To investigate levels of proteins involved in glutamatergic transmission, we did Western blotting in acutely dissected hippocampus tissues of wild-type and Gpt2-null mice at P18 (Figure 3A). There were significant decreases in AMPA receptor subunit 1 (AMPAR, Gria1), synaptic vesicle protein 2 (SV2), and NMDA receptor (NMDAR, GluN1) in Gpt2-null hippocampus. Interestingly, there was also a modest increase in Psd95 protein levels in Gpt2-null hippocampus. There were no differences in the neuronal or astrocytic alanine/glutamine transporters, Snat1 and Asct1, respectively. The levels of astrocytic glutamate transporter, Glt1, essential for glutamate clearing from the synaptic cleft (Genda et al., 2011), remained unchanged in Gpt2-null hippocampus. Two metabolic enzymes, glutamine synthetase and glutamate dehydrogenase, crucial for glutamine/glutamate cycle (Hertz, 2013) and glutamate oxidation (McKenna et al., 2000), respectively, were unaltered in expression. There were no differences in vesicular glutamate (Vglut1, 2) or GABA (Vgat) transporters, suggesting that the decreased glutamate transmission was not due to a deficiency in vesicular transporter levels. The Gpt2-null cortex tissue was spared of any changes but Glt1 was significantly increased (Figure 3B).

We qualitatively assessed AMPAR and SV2 staining in Gpt2-null hippocampus by immunohistochemistry. Puncta patterns of AMPAR and SV2 in CA1 areas of wild-type and Gpt2-null hippocampus appeared to be similar (Figure 4A&B). There may be reductions of AMPAR particularly in dentate gyrus granular layer and reductions of SV2 particularly in CA3 stratum oriens, as assessed qualitatively in the images. AMPAR and SV2 puncta appeared to be morphologically intact in Gpt2-null CA1 hippocampus suggesting that decreases in AMPAR is unlikely to explain decreased glutamatergic transmission in Gpt2-null CA1.

Spines and synaptic vesicles were morphologically intact in Gpt2-null CA1 stratum radiatum.

We examined the ultrastructural properties of Gpt2-null CA1 stratum radiatum by electron microscopy (Figure 5&6). Spine counts as well as mitochondria counts per image taken at 21000X magnification were unchanged in Gpt2-null CA1 stratum radiatum (Figure 5B&C). Number of synaptic vesicles per spine and post-synaptic density length were also similar to the wild-type controls. Interestingly, we observed an increase in synaptic vesicle area suggesting increased vesicular size in Gpt2-null CA1 spines. Overall, the electron micrographs indicate that the ultrastructural morphology in Gpt2-null CA1 stratum radiatum was intact.

More rapid decline of glutamatergic synaptic transmission with electrical stimulation of Schaffer collaterals to CA1 in Gpt2-null hippocampus.

We reasoned that if overall glutamate levels in synaptic vesicles were reduced, the vesicular pool of glutamate would be depleted faster during a high frequency stimulus train of excitatory inputs to the CA1 pyramidal neurons. To test this, we stimulated the Schaffer collaterals (Figure 7A). The paired pulse facilitation remained the same in Gpt2 pyramidal neurons (Figure 7B, Wild-type: 1.41 ± 0.05 vs Gpt2-null: 1.51 ± 0.05) suggesting that the synaptic release probability is unchanged. The train response at 10 Hz yielded modest reductions in half-life of the fit curve in the Gpt2-null pyramidal neurons, as can be seen in the representative wild-type (black) and Gpt2-null (red) examples (the averaged peak amplitudes are normalized to the first peak amplitude) (Figure 7C, nonlinear regression with one-phase decay fit F = 8.126 (3,2594); Wild-type half-life 39.79 with 95% confidence interval of 31.07 to 55.31 vs Gpt2-null half-life 31.63 with 95% confidence interval of 25.45 to 41.78). The train response at 20 Hz for 10 seconds (200 pulses) resulted in greater reduction in half-life of the fit curve suggesting a more rapid depletion of glutamate levels in the Gpt2-null pyramidal neurons. (Figure 7D, nonlinear regression with one-phase decay fit F = 95.48 (3,5387); Wild-type half-life 45.34 with 95% confidence interval of 40.51 to 51.47 vs Gpt2-null half-life 31.70 with 95% confidence interval of 28.87 to 35.15). Overall, these data indicate that decreases in glutamatergic synaptic transmission in Gpt2-null hippocampus can be explained partly by decreases in vesicular glutamate levels in pre-synaptic neuron.

Released glutamate levels are reduced in Gpt2-null synaptosomes but rescued by alpha-ketoglutarate.

To determine whether vesicular glutamate levels were decreased, we detected glutamate release from synaptosomes upon depolarization by liquid chromatography/mass spectrometry (LC/MS). We initially confirmed the viability of our synaptosome preparations by observing increased levels of glutamate released after depolarization with 50 mM KCl in Krebs-like buffer compared to the release at baseline (Figure 8A). Overall glutamate levels in the cytosolic fraction of the Gpt2-null forebrain obtained during synaptosome preparation were significantly reduced as determined by enzymatic detection (Figure 8B), in agreement with the reduced glutamatergic transmission in Gpt2-null hippocampal slices (Figure 2). We then tested glutamate release and discovered that levels of glutamate released from Gpt2-null synaptosomes were reduced (Figure 8C). In contrast, released GABA levels were unchanged (Figure 8D) which agrees with the unchanged mIPSC amplitudes in CA1 hippocampal slices (Figure 2K).

Gpt2 catalyzes a reaction that results in a net production of a TCA intermediate (i.e. anaplerosis). TCA cycle intermediates, particularly, alpha-ketoglutarate have been shown to be precursors for synaptic glutamate (Peng et al., 1993; Peng et al., 1991; Shank et al., 1989; Shank and Bennett, 1993). We hypothesized that with the absence of the Gpt2 reaction, deficits of the TCA cycle may reduce the availability of synaptic glutamate. Therefore, we sought to rescue the decreases in synaptic glutamate levels by supplementing the synaptosomes with alpha-ketoglutarate.

When supplemented with alpha-ketoglutarate, released glutamate levels of Gpt2-null synaptosomes were restored to the wild-type levels (Figure 9A). However, alanine, another major product of the Gpt2 reaction, failed to correct the synaptic glutamate levels (Figure

9B). Alpha-ketoglutarate combined with alanine also corrected the glutamate levels in Gpt2-null synaptosomes (Figure 9C). In contrast, released GABA levels in Gpt2-null synaptosomes were unchanged with or without alpha-ketoglutarate or alanine supplementation (Figure 9D-F). We also demonstrated that alanine and alpha-ketoglutarate readily enter synaptosomes (Figure 9G-J). Notably, baseline alpha-ketoglutarate levels were unchanged but alanine levels were reduced in Gpt2-null synaptosomes (Figure 9G-J) in corroboration of our previous finding that alanine levels in the whole Gpt2-null brain were reduced (Ouyang et al., 2016). Overall, these results indicate that alpha-ketoglutarate was able to rescue glutamate levels and that a metabolic intervention was sufficient to correct glutamatergic deficiencies in Gpt2-null synaptosomes.

Glutamine metabolism is altered in Gpt2-null synaptosomes but rescued by alpha-ketoglutarate.

Glutamate is replenished in neurons primarily by glutamate-glutamine cycle at the tripartite synapse, formed by pre-synaptic neuron, post-synaptic neuron and astrocyte compartments (Ventura and Harris, 1999) (Figure 10A). We investigated changes in glutamine metabolism in Gpt2-null synaptosomes and discovered an increased fraction of double heavy nitrogen labeled glutamine, that is glutamine with a heavy nitrogen in both amine and amide groups (Figure 10B, left). This increase was reduced by supplementing the synaptosomes with alpha-ketoglutarate but not by alanine.

Glutamine levels at baseline without supplement are increased in Gpt2-null synaptosomes (Figure 10C). Glutamine entry into synaptosomes was not affected by alpha-ketoglutarate as evident in unchanged glutamine levels (Figure 10D) as well as in

unchanged fractional enrichments of single heavy nitrogen labeled glutamine (Figure 10E) and glutamate (Figure 10F) compared to the no supplement condition. This suggests that the action of alpha-ketoglutarate in decreasing the fractional enrichment of double-labeled glutamine was not caused by decreases in glutamine entry but by changes in glutamine metabolism.

In contrast, alanine decreased overall glutamine levels approximately by 50% in both wild-type and Gpt2-null synaptosomes (Figure 10D). While glutamine entry may be affected by alanine, as they compete for the same neutral amino acid transporters (Leke and Schousboe, 2016), this led to only modest decreases in the fractional enrichment of single heavy nitrogen labeled glutamine (Figure 10E) and glutamate (Figure 10F). This is also reflected by the observation that glutamate levels were unchanged with alanine supplementation (Figure 9B). Furthermore, alanine supplement did not result in any changes in fractional enrichment of double labeled glutamine in Gpt2-null synaptosomes (Figure 10B). Overall, these results suggest the reductions in double-labeled glutamine are feasible by alpha-ketoglutarate and not alanine.

Double-labeled glutamine can be formed by the concerted actions of glutamate dehydrogenase and glutamine synthetase (Figure 10A). We hypothesized that expression of these metabolic enzymes could be up-regulated in Gpt2-null synaptosomes and that this upregulation can explain the increases in fractional enrichment of double-labeled glutamine in Gpt2-null synaptosomes. We performed Western blotting in synaptosomes (Figure 11) for these metabolic enzymes and the synaptic proteins tested for earlier (Figure 3). We find increases of glutamate dehydrogenase and glutamine synthetase in Gpt2-null synaptosomes as well as increases in astrocytic glutamate transporter, Glt1, neuronal and

astrocytic neutral amino acid transporter (Snat1 and Asct1), vesicular glutamate (Vglut1) and GABA transporters. We also observed decreases in AMPA receptor (Gria1) and modest decreases in Psd95. These results suggest that increased levels of glutamate dehydrogenase and glutamine synthetase may lead to increases in double-labeled glutamine and that there is an up-regulation of proteins related to glutamate metabolism and transport in Gpt2-null synaptosomes.

TCA cycle has deficits but glutamine entry into the TCA cycle is intact in Gpt2-null synaptosomes.

Gpt2 and glutamate dehydrogenase not only modulate glutamate levels but also replenish the tricarboxylic acid (TCA) cycle by augmenting alpha-ketoglutarate (Erecinska and Silver, 1990b). Loss of Gpt2 leads to major deficits in the TCA cycle intermediates in the mouse brain and the process of replenishment of these intermediates, collectively called anaplerosis (Ouyang et al., 2016; Owen et al., 2002). We investigated whether the same TCA cycle deficits were present in Gpt2-null synaptosomes (Figure 12). We observed decreases in baseline levels of malate and fumarate but not succinate/methylmalonate (Figure 10A, left). In a separate experiment, we tested whether alpha-ketoglutarate along with glutamine would be able to rescue these deficits (Figure 10A, right). Malate levels were still decreased with glutamine but corrected by alpha-ketoglutarate in Gpt2-null synaptosomes. Fumarate levels remained the same as wild-type suggesting that glutamine alone had sufficient increases in overall fumarate levels. Succinate/methylmalonate levels remained the same as wild-type but augmented by alpha-ketoglutarate in Gpt2-null synaptosomes.

We also tested for glutamine as a precursor for the TCA cycle intermediates in Gpt2-null synaptosomes (Figure 10B). Given the loss of Gpt2, a decreased fractional enrichment of labeled TCA cycle intermediates using [U-^{13}C]-glutamine as precursor was expected (Figure 6B, left). However, the fractional enrichments for all the TCA cycle intermediate measured were unchanged in Gpt2-null synaptosomes. This does not agree with the finding that glutamine cannot be used as a precursor to make alanine in Gpt2-null synaptosomes (Figure1). This is also in stark contrast to decreased labeling of TCA cycle intermediates from 13C-glutamine in Gpt2-null fibroblasts as we reported previously (Ouyang et al., 2016). These results indicate that glutamine can be used by Gpt2-null synaptosomes to supplement the TCA cycle. We also tested for other metrics of energetics such as ATP levels, energy charge, as well as NAD to NADH and NADP to NADPH ratios. All remained unchanged in Gpt2-null synaptosomes albeit with a trending decrease in the energy charge. These results suggest that in the measures tested, the TCA cycle had deficits but was being supported by up-regulation of metabolic enzymes and of substrate transporters related to glutamate metabolism in isolated Gpt2-null synaptic terminals.

FIGURE 1

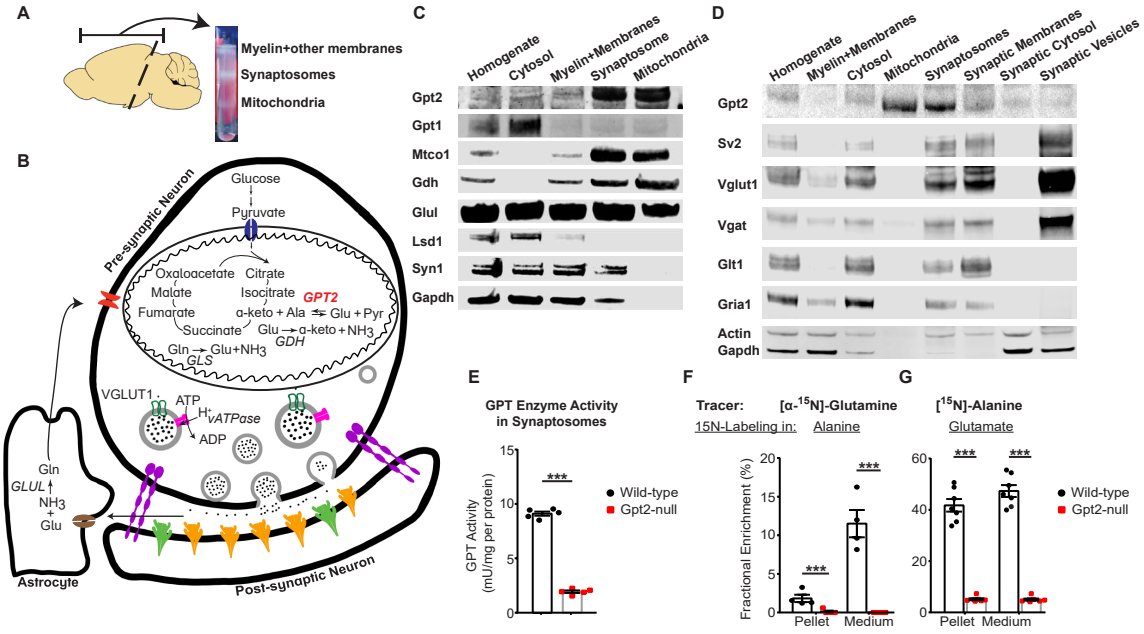
A
Myelin+other membranes
Synaptosomes
Mitochondria
B
Pre-synaptic Neuron
Glucose
Pyruvate
Oxaloacetate
Citrate
Malate
Isocitrate
GPT2
Fumarate
α-keto + Ala ⇌ Glu + Pyr
Succinate
Glu → α-keto + NH3
GDH
Gln → Glu + NH3
GLS
VGLUT1
ATP
H+
vATPase
ADP
Gln
GLUL
NH3
+
Glu
Astrocyte
Post-synaptic Neuron
C
Homogenate
Cytosol
Myelin+Membranes
Synaptosome
Mitochondria
Gpt2
Gpt1
Mtco1
Gdh
Glul
Lsd1
Syn1
Gapdh
D
Homogenate
Myelin+Membranes
Cytosol
Mitochondria
Synaptosomes
Synaptic Membranes
Synaptic Cytosol
Synaptic Vesicles
Gpt2
Sv2
Vglut1
Vgat
Glt1
Gria1
Actin
Gapdh
E
GPT Enzyme Activity in Synaptosomes
GPT Activity (mU/mg per protein)
***
Wild-type
Gpt2-null
F
Tracer: [α-15N]-Glutamine
15N-Labeling in: Alanine
Fractional Enrichment (%)
***
***
Pellet
Medium
G
[15N]-Alanine
Glutamate
***
***
Pellet
Medium
Wild-type
Gpt2-null

FIGURE 2

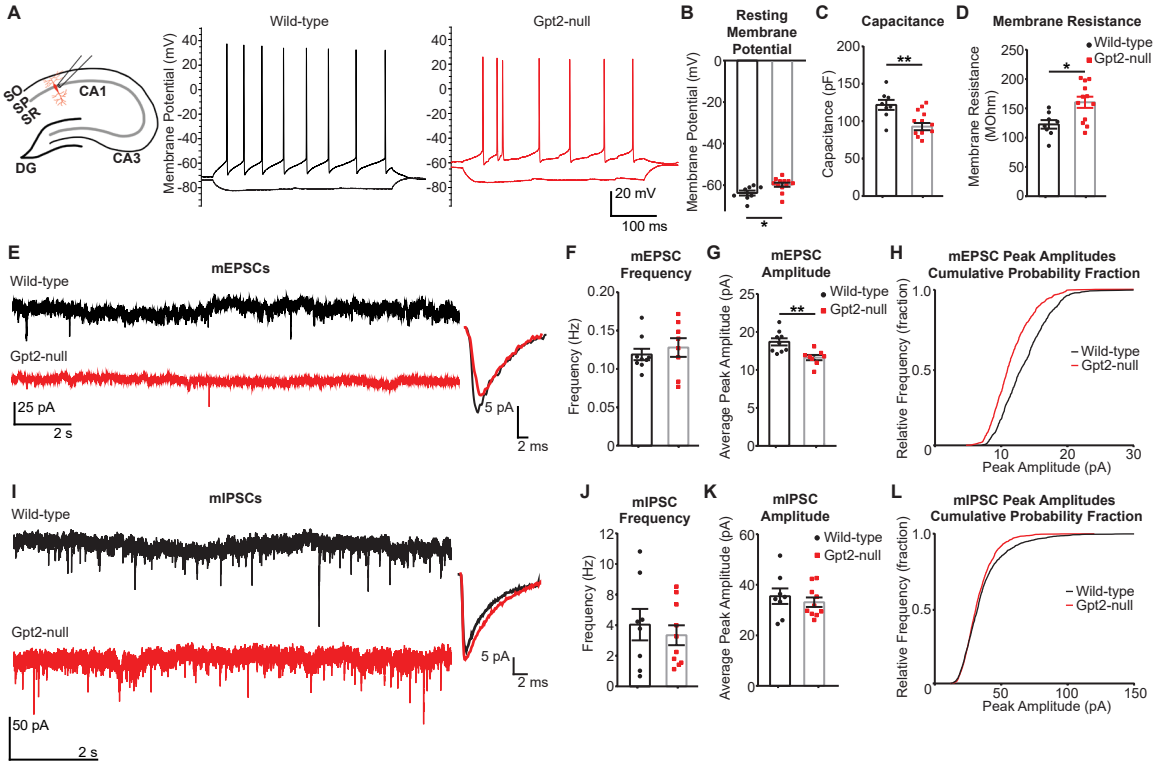
A
SO
SP
SR
CA1
DG
CA3
Wild-type
Gpt2-null
Membrane Potential (mV)
20 mV
100 ms
B
Resting Membrane Potential
Membrane Potential (mV)
C
Capacitance
Capacitance (pF)
D
Membrane Resistance
Membrane Resistance (MOhm)
Wild-type
Gpt2-null
E
mEPSCs
Wild-type
Gpt2-null
25 pA
2 s
5 pA
2 ms
F
mEPSC Frequency
Frequency (Hz)
G
mEPSC Amplitude
Average Peak Amplitude (pA)
H
mEPSC Peak Amplitudes Cumulative Probability Fraction
Relative Frequency (fraction)
Peak Amplitude (pA)
I
mIPSCs
Wild-type
Gpt2-null
50 pA
2 s
5 pA
2 ms
J
mIPSC Frequency
Frequency (Hz)
K
mIPSC Amplitude
Average Peak Amplitude (pA)
L
mIPSC Peak Amplitudes Cumulative Probability Fraction
Relative Frequency (fraction)
Peak Amplitude (pA)

FIGURE 3

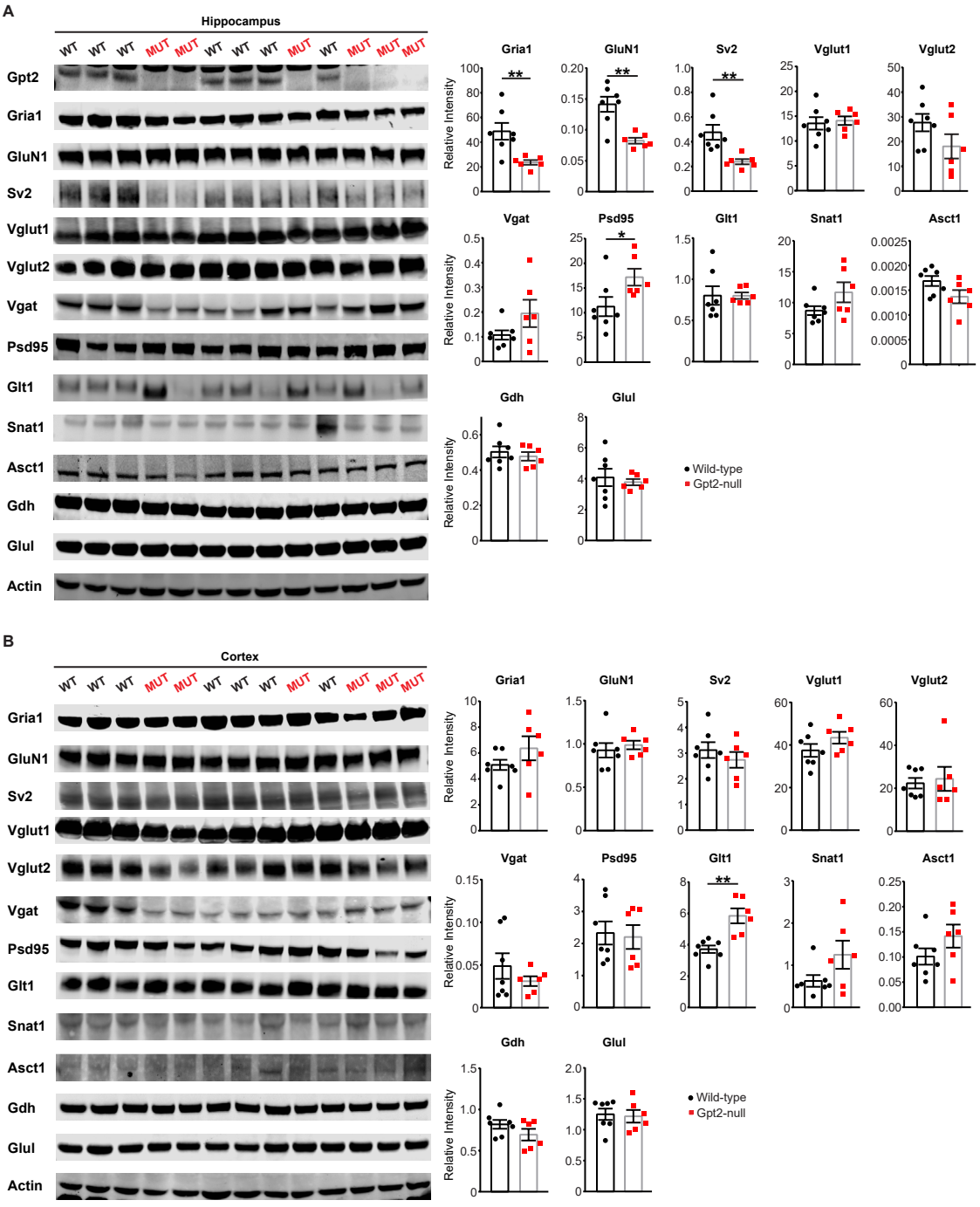
A
Hippocampus
WT WT WT MUT MUT WT WT WT MUT WT MUT MUT MUT
Gpt2
Gria1
GluN1
Sv2
Vglut1
Vglut2
Vgat
Psd95
Glt1
Snat1
Asct1
Gdh
Glul
Actin
Relative Intensity
Wild-type
Gpt2-null
B
Cortex
WT WT WT MUT MUT WT WT WT MUT WT MUT MUT MUT
Gria1
GluN1
Sv2
Vglut1
Vglut2
Vgat
Psd95
Glt1
Snat1
Asct1
Gdh
Glul
Actin
Relative Intensity
Wild-type
Gpt2-null

FIGURE 4

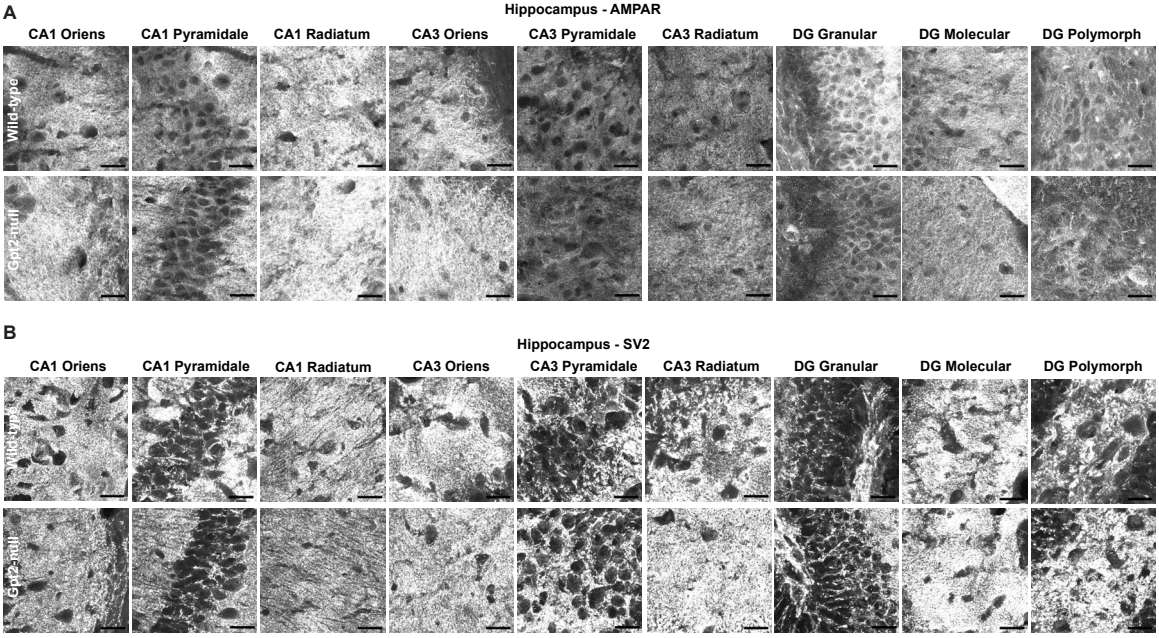
A
Hippocampus - AMPAR
CA1 Oriens
CA1 Pyramidale
CA1 Radiatum
CA3 Oriens
CA3 Pyramidale
CA3 Radiatum
DG Granular
DG Molecular
DG Polymorph
Wild-type
Gpr2-null
B
Hippocampus - SV2
CA1 Oriens
CA1 Pyramidale
CA1 Radiatum
CA3 Oriens
CA3 Pyramidale
CA3 Radiatum
DG Granular
DG Molecular
DG Polymorph
Wild-type
Gpr2-null

FIGURE 5

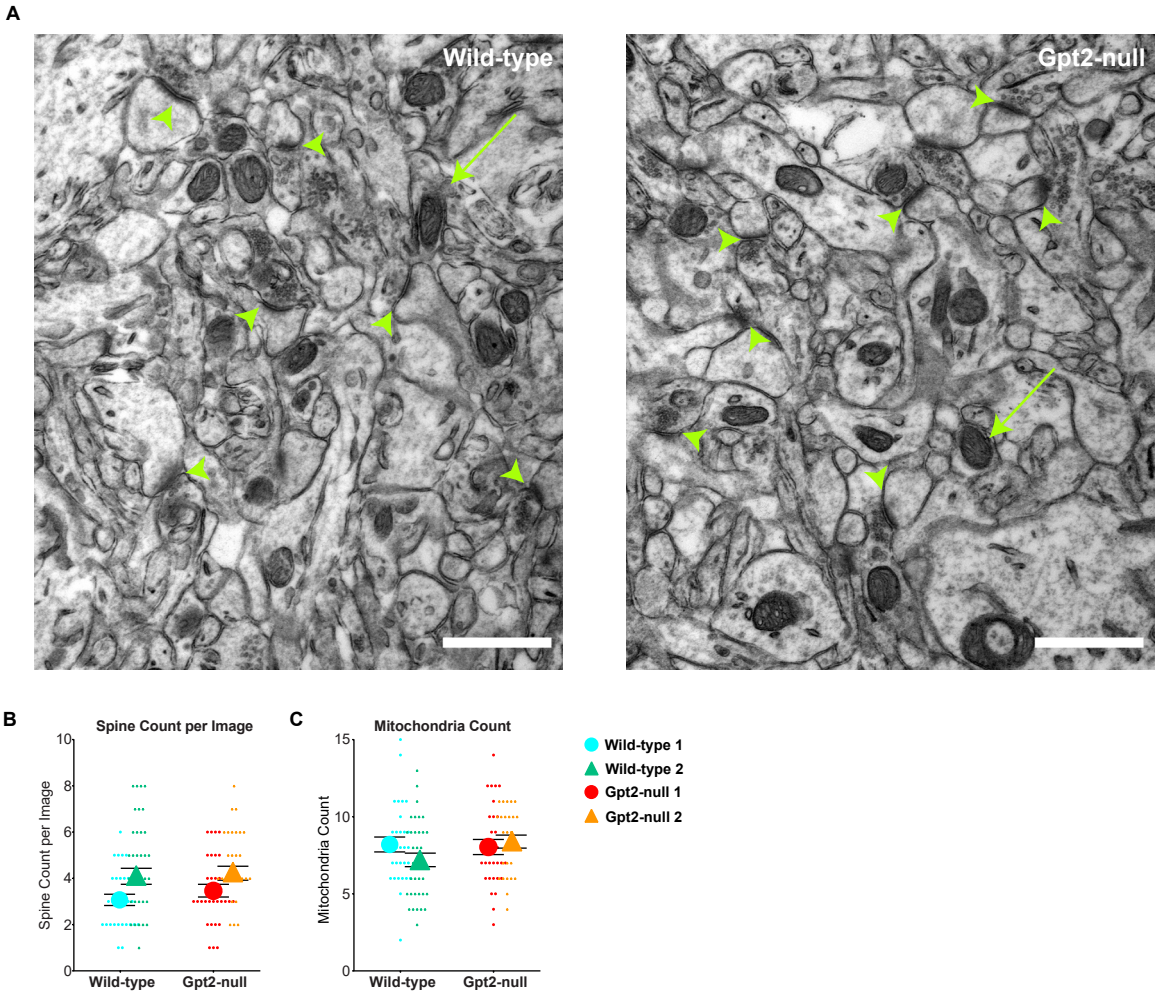
A
Wild-type
Gpt2-null
B
Spine Count per Image
Spine Count per Image
0
2
4
6
8
10
Wild-type
Gpt2-null
C
Mitochondria Count
Mitochondria Count
0
5
10
15
Wild-type
Gpt2-null
Wild-type 1
Wild-type 2
Gpt2-null 1
Gpt2-null 2

FIGURE 6

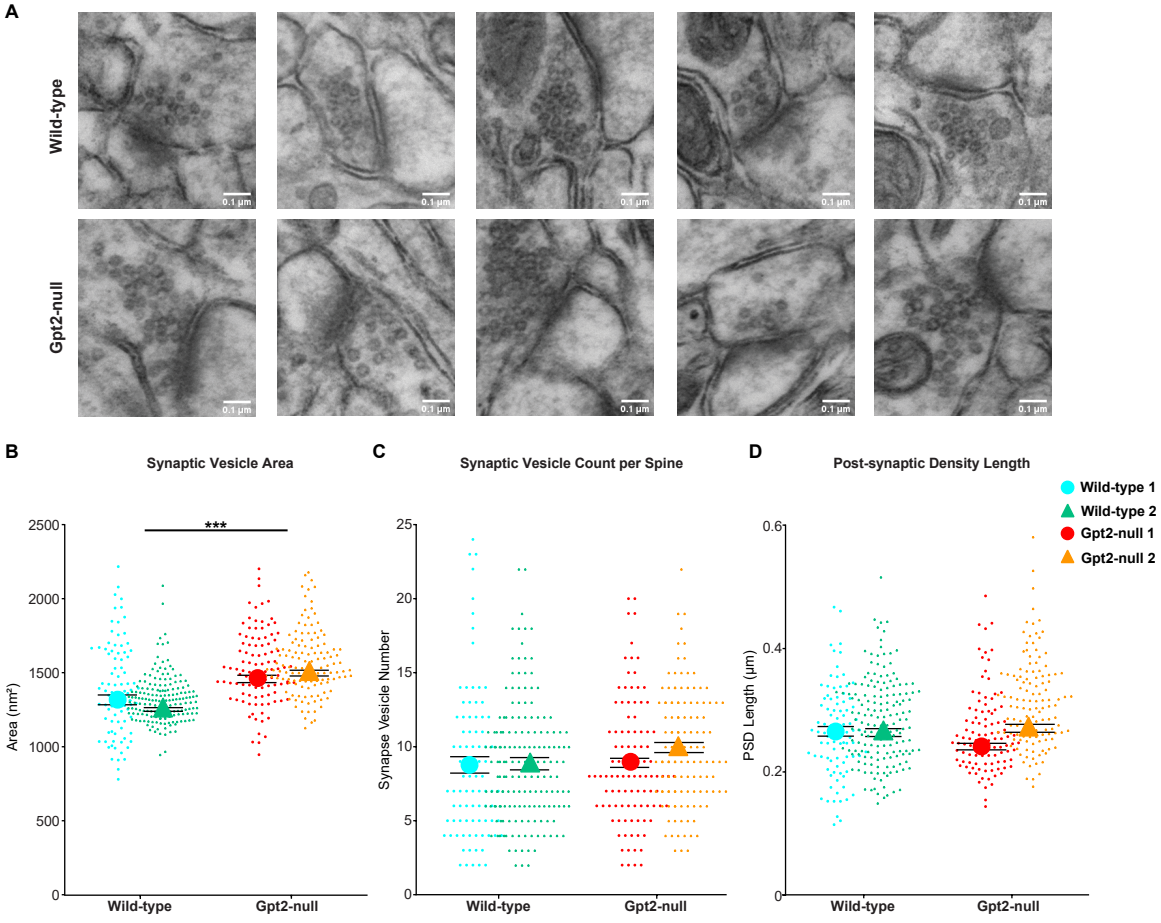
A
Wild-type
Gpt2-null
0.1 µm
B
Synaptic Vesicle Area
***
Area (nm²)
2500
2000
1500
1000
500
0
Wild-type
Gpt2-null
C
Synaptic Vesicle Count per Spine
Synapse Vesicle Number
25
20
15
10
5
0
Wild-type
Gpt2-null
D
Post-synaptic Density Length
PSD Length (µm)
0.6
0.4
0.2
0
Wild-type
Gpt2-null
Wild-type 1
Wild-type 2
Gpt2-null 1
Gpt2-null 2

FIGURE 7

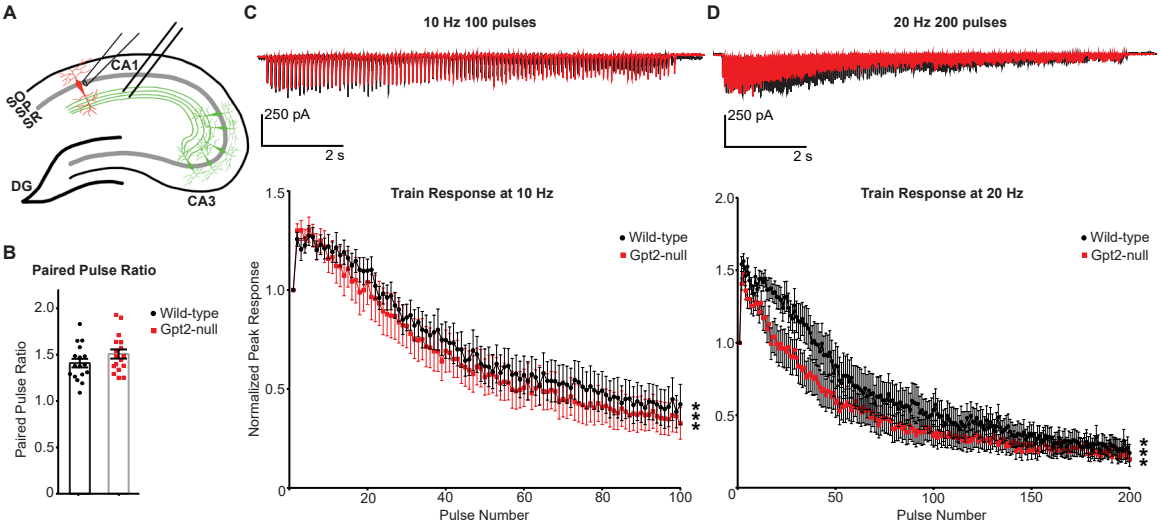
A
CA1
SO SR SLM
DG
CA3
B
Paired Pulse Ratio
Paired Pulse Ratio
2.0
1.5
1.0
0.5
0
Wild-type
Gpt2-null
C
10 Hz 100 pulses
250 pA
2 s
Train Response at 10 Hz
Normalized Peak Response
1.5
1.0
0.5
0
20
40
60
80
100
Pulse Number
Wild-type
Gpt2-null
***
D
20 Hz 200 pulses
250 pA
2 s
Train Response at 20 Hz
2.0
1.5
1.0
0.5
0
50
100
150
200
Pulse Number
Wild-type
Gpt2-null
***

FIGURE 8

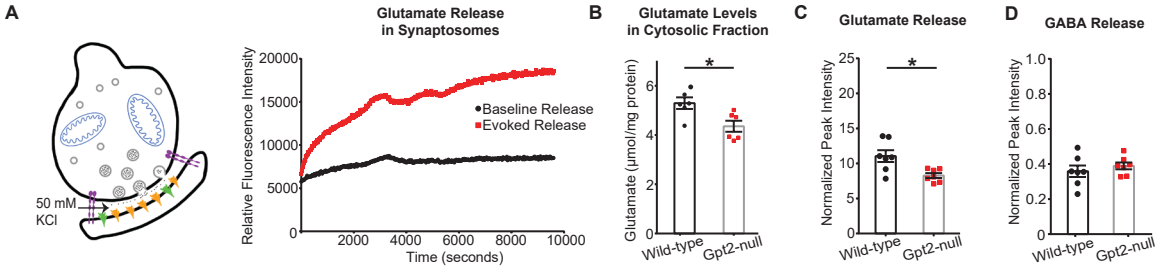
A
50 mM
KCl
Glutamate Release
in Synaptosomes
Relative Fluorescence Intensity
20000
15000
10000
5000
0
2000
4000
6000
8000
10000
Time (seconds)
Baseline Release
Evoked Release
B
Glutamate Levels
in Cytosolic Fraction
Glutamate (µmol/mg protein)
6
4
2
0
*
Wild-type
Gpt2-null
C
Glutamate Release
Normalized Peak Intensity
25
20
15
10
5
0
*
Wild-type
Gpt2-null
D
GABA Release
Normalized Peak Intensity
1.0
0.8
0.6
0.4
0.2
0
Wild-type
Gpt2-null

FIGURE 9

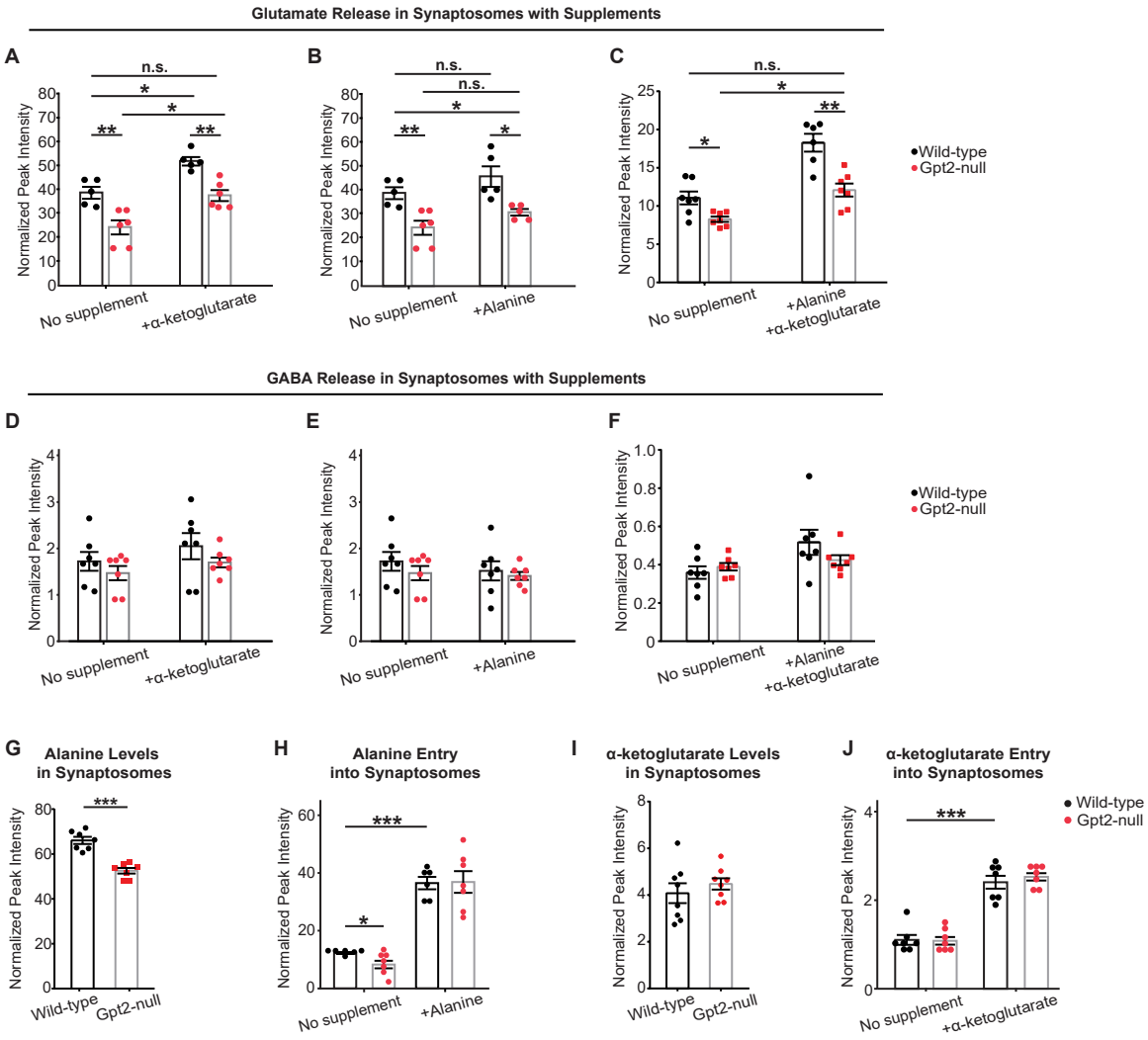
Glutamate Release in Synaptosomes with Supplements
A
B
C
n.s.
*
**
Normalized Peak Intensity
No supplement
+α-ketoglutarate
+Alanine
+Alanine
+α-ketoglutarate
Wild-type
Gpt2-null
GABA Release in Synaptosomes with Supplements
D
E
F
G
Alanine Levels in Synaptosomes
H
Alanine Entry into Synaptosomes
I
α-ketoglutarate Levels in Synaptosomes
J
α-ketoglutarate Entry into Synaptosomes
***

FIGURE 10

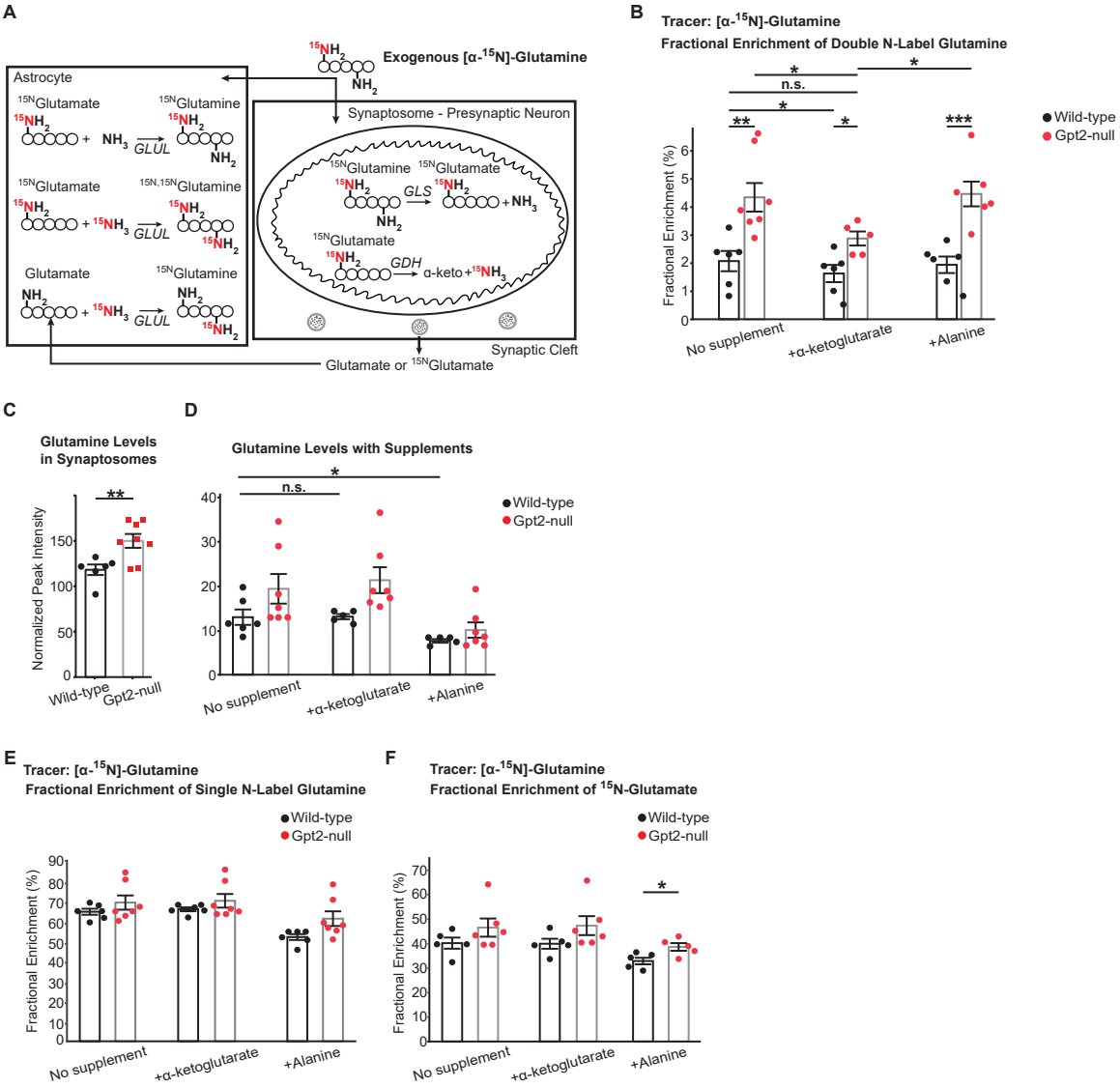
A
Astrocyte
Exogenous [α-15N]-Glutamine
Synaptosome - Presynaptic Neuron
GLUL
GLS
GDH
Synaptic Cleft
Glutamate or 15NGlutamate
B
Tracer: [α-15N]-Glutamine
Fractional Enrichment of Double N-Label Glutamine
Fractional Enrichment (%)
n.s.
Wild-type
Gpt2-null
No supplement
+α-ketoglutarate
+Alanine
C
Glutamine Levels in Synaptosomes
Normalized Peak Intensity
Wild-type
Gpt2-null
D
Glutamine Levels with Supplements
n.s.
Wild-type
Gpt2-null
No supplement
+α-ketoglutarate
+Alanine
E
Tracer: [α-15N]-Glutamine
Fractional Enrichment of Single N-Label Glutamine
Fractional Enrichment (%)
Wild-type
Gpt2-null
No supplement
+α-ketoglutarate
+Alanine
F
Tracer: [α-15N]-Glutamine
Fractional Enrichment of 15N-Glutamate
Fractional Enrichment (%)
Wild-type
Gpt2-null
No supplement
+α-ketoglutarate
+Alanine

FIGURE 11

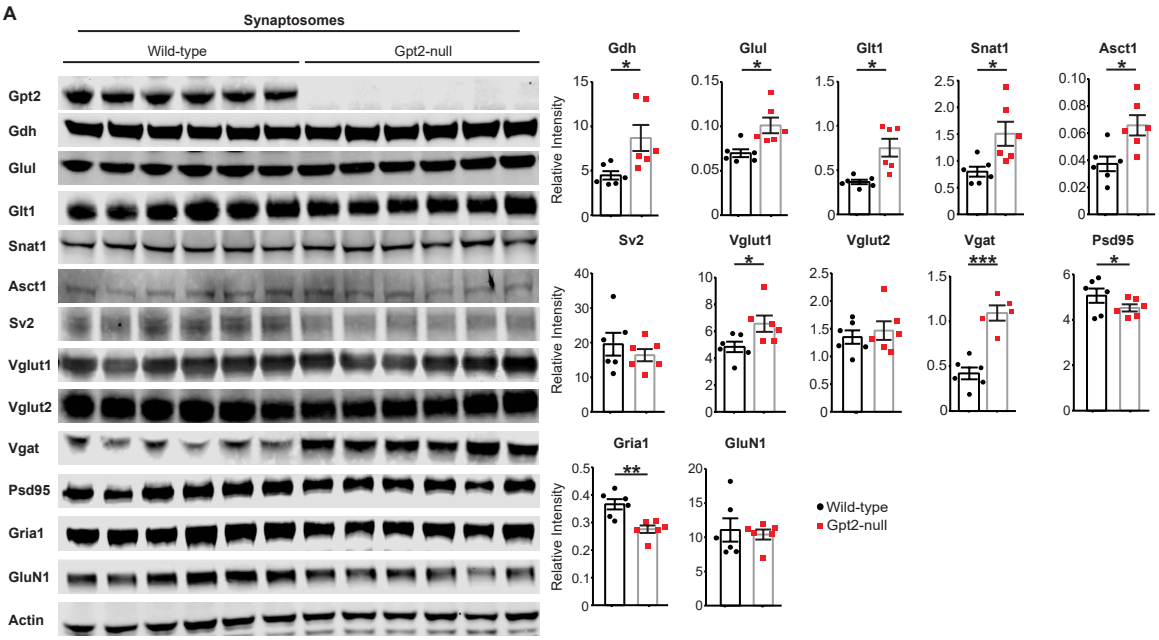
A
Synaptosomes
Wild-type
Gpt2-null
Gpt2
Gdh
Glul
Glt1
Snat1
Asct1
Sv2
Vglut1
Vglut2
Vgat
Psd95
Gria1
GluN1
Actin
Gdh
Glul
Glt1
Snat1
Asct1
Sv2
Vglut1
Vglut2
Vgat
Psd95
Gria1
GluN1
Relative Intensity
Wild-type
Gpt2-null

FIGURE 12

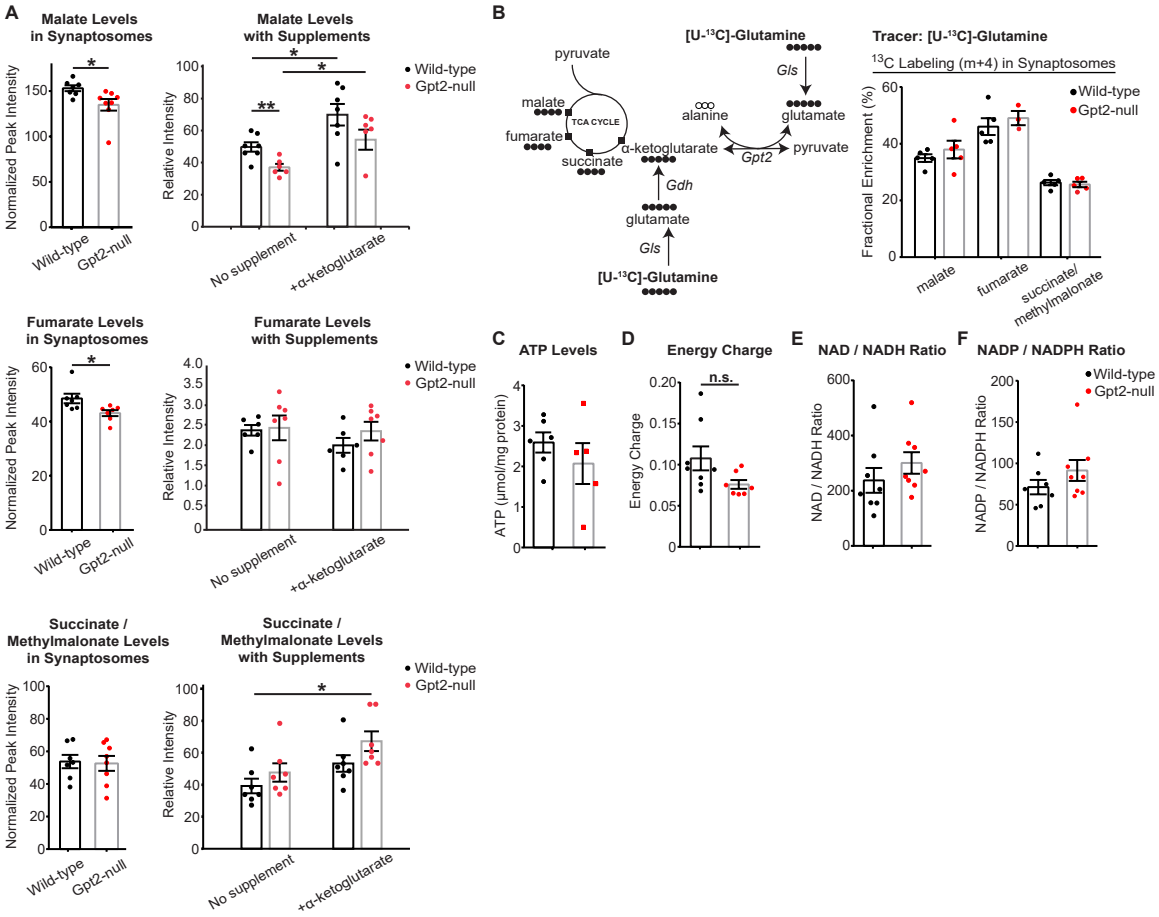
A
Malate Levels in Synaptosomes
Normalized Peak Intensity
Wild-type
Gpt2-null
Malate Levels with Supplements
Relative Intensity
No supplement
+α-ketoglutarate
Wild-type
Gpt2-null
Fumarate Levels in Synaptosomes
Fumarate Levels with Supplements
Succinate / Methylmalonate Levels in Synaptosomes
Succinate / Methylmalonate Levels with Supplements
B
[U-13C]-Glutamine
pyruvate
malate
fumarate
succinate
TCA CYCLE
α-ketoglutarate
Gls
alanine
glutamate
Gpt2
pyruvate
Gdh
glutamate
Gls
[U-13C]-Glutamine
Tracer: [U-13C]-Glutamine
13C Labeling (m+4) in Synaptosomes
Fractional Enrichment (%)
malate
fumarate
succinate/ methylmalonate
C
ATP Levels
ATP (μmol/mg protein)
D
Energy Charge
n.s.
E
NAD / NADH Ratio
F
NADP / NADPH Ratio

Figure Legends

Figure 1. Gpt2 is the primary glutamate pyruvate transaminase in synaptic terminals.

A. Fractionation of the mouse brain into fractions containing myelin and other membranes, synaptosomes (isolated nerve terminals) and mitochondria. Note that the synaptosomes are extracted from brain tissue containing only the forebrain, excluding olfactory bulb, midbrain and the brain stem.

B. Metabolic pathways relevant to Gpt2 and glutamate metabolism in synaptosomes including pre-synaptic neuron, post-synaptic neuron and astrocytic components. Ala: alanine, a-keto: alpha-ketoglutarate, Glu: glutamate, Gln: glutamine, Pyr: pyruvate, *GDH*: glutamate dehydrogenase, *GLS*: glutaminase, *GLUL*: glutamine synthetase.

C. Gpt2 is enriched in synaptosomes and mitochondria. Western blotting of the homogenate, cytosolic, myelin and membranes, synaptosomes and mitochondria fractions obtained from a wild-type mouse at postnatal day 18 (P18) for Gpt2, Gpt1, Mtco1 (mitochondrial marker, subunit 1 of complex IV cytochrome c oxidase), Gdh (glutamate dehydrogenase), Glul (glutamine synthetase), Lsd1 (nuclear marker, lysine-specific demethylase 1), Syn1 (synapsin I) and Gapdh (cytosolic marker, glyceraldehyde 3-phosphate dehydrogenase).

D. Gpt2 is enriched in mitochondria of synaptosomes. Western blotting of synaptosomes that were fractionated further into synaptic membrane, synaptic cytosol and synaptic vesicles obtained from a wild-type mouse at P18 for Gpt2, Sv2 (synaptic vesicle protein 2), Vglut1 (vesicular glutamate transporter 1), Vgat (vesicular GABA transporter), Glt1 (glutamate transporter 1, astrocytic), Gria1 (AMPA receptor subunit 1), Actin, Gapdh.

E. Overall Gpt enzyme activity in Gpt2-null is greatly reduced in Gpt2-null synaptosomes at P18. Each dot represents the total enzymatic activities of Gpt2 and Gpt1 in synaptosome

samples obtained from different wild-type (black) or Gpt2-null (red) mice. The enzymatic activities are expressed as mU/mg per protein. P <0.0001.

F. Glutamine can not be used as a precursor for alanine in Gpt2-null synaptosomes at P18. Isotope tracing in wild-type (black) and Gpt2-null (red) synaptosomes at P18 using glutamine labeled with heavy nitrogen at the amine position. Each dot represents fractional enrichment of labeled pool of alanine in synaptosome from a different animal, expressed as percentage of total alanine pool. For pellet, $^{**}P$ = 0.006 and for medium, $^{***}P$ = 0.00016.

G. Alanine and alpha-ketoglutarate can be used as precursors for glutamate in wild-type but not in Gpt2-null synaptosomes at P18. Isotope tracing in wild-type (black) and Gpt2-null (red) synaptosomes at P18 using heavy nitrogen labeled alanine. Each dot represents fractional enrichment of labeled pool of glutamate in synaptosome from a different animal, expressed as percentage of total glutamate pool. For pellet and medium, $^{***}P$ <0.0001.

Figure 2. Glutamatergic transmission is diminished in Gpt2-null CA1 hippocampus pyramidal neurons.

A. Schematic of the hippocampal slice preparation and a CA1 pyramidal neuron (red) and recording pipette. The representative whole-cell recordings of wild-type (left, black) and Gpt2-null (right, red) CA1 pyramidal neurons in current clamp mode at postnatal day 18 (P18). Current steps of 20 pA were used to depolarize or hyperpolarize the neuron.

B. Resting membrane potentials of Gpt2-null CA1 pyramidal neurons are slightly depolarized. The resting membrane potential of CA1 neurons from wild-type (black) and

Gpt2-null (red) mice at P18 was obtained immediately after breaking into the cell in current clamp mode. n = 4-5 mice/4-5 slices/8-12 cells. *P = 0.019.

C. Gpt2-null pyramidal neurons have lower capacitance. Each dot represents a different cell recording from wild-type (black) and Gpt2-null (red) mice at P18. **P = 0.002.

D. Gpt2-null CA1 pyramidal neurons have greater membrane input resistance. Each dot represents a different cell recording from wild-type (black) and Gpt2-null (red) mice at P18. n = 4-5 mice/4-5 slices/8-12 cells. *P = 0.01.

E. Representative traces of miniature excitatory synaptic currents (mEPSC) from whole-cell recordings in CA1 pyramidal neurons of wild-type (top, black) and Gpt2-null (bottom, red) mice at P18. Averaged mEPSCs from one representative cell from wild-type (black) and Gpt2-null (red) cells at P18 are shown on the right.

F. mEPSC frequency is not changed in Gpt2-null CA1 pyramidal neurons. Each dot represents a different cell recording from wild-type (black) and Gpt2-null (red) mice at P18. n = 4-6 mice/4-6 slices/8-9 cells. P = 0.52.

G. mEPSC peak amplitude is reduced in Gpt2-null CA1 pyramidal neurons. Each dot represents a different cell recording from wild-type (black) and Gpt2-null (red) mice at P18. n = 4-5 mice/4-5 slices/8-12 cells. **P = 0.0035.

H. Cumulative probability histogram of mEPSC peak amplitudes from representative wild-type (black) and Gpt2-null (red) CA1 pyramidal neurons at P18. Kolmogorov-Smirnov test was conducted, 4 neurons from each genotype were used to construct the curves; total mEPSC events, wild-type: 799 and Gpt2-null: 793. ***P <0.0001; d = 0.2386.

I. Representative traces of miniature inhibitory synaptic currents (mIPSC) from whole-cell recordings in CA1 pyramidal neurons of wild-type (top, black) and Gpt2-null (bottom, red) mice at P18. Averaged mIPSCs from one representative cell from wild-type (black) and Gpt2-null (red) CA1 pyramidal neurons at P18 are shown on the right.

J. mIPSC frequency is not changed in Gpt2-null CA1 pyramidal neurons. Each dot represents a different cell recording from wild-type (black) and Gpt2-null (red) mice at P18. n = 4-6 mice/4-6 slices/8-9 cells. $P = 0.5614$.

K. mIPSC peak amplitude is not changed in Gpt2-null CA1 pyramidal neurons. Each dot represents a different cell recording from wild-type (black) and Gpt2-null (red) mice at P18. n = 4-6 mice/4-6 slices/8-9 cells. $P = 0.4999$

L. Cumulative probability histogram of mIPSC peak amplitudes from representative wild-type (black) and Gpt2-null (red) CA1 pyramidal neurons at P18. Kolmogorov-Smirnov test was conducted, 4 neurons from each genotype were used to construct the curves; total mEPSC events, wild-type: 800 and Gpt2-null: 800. $P = 0.1960$; D = 0.0539.

Figure 3. AMPAR, NMDAR and SV2 protein levels are reduced in Gpt2-null hippocampus.

A. Western blotting of wild-type and Gpt2-null hippocampus protein lysates collected at P18. Note that Gpt2 is absent in Gpt2-null (MUT) but present in wild-type (WT) protein lysates. Each dot represents a different protein lysate sample from wild-type (black) or Gpt2-null (red) mice. $^{**}P$ (Gria1, AMPAR, AMPA receptor subunit 1) = 0.0068; $^{**}P$ (GluN1, NMDA receptor, subunit 1) = 0.0014; $^{**}P$ (Sv2, synaptic vesicle protein 2) = 0.0052; P (Vglut1, vesicular glutamate transporter 1) = 0.7385; P (Vglut2, vesicular

glutamate transporter 2) = 0.1329; *P* (Vgat, vesicular GABA transporter) = 0.1388; **P* (Psd95, post-synaptic density protein 95) = 0.0454; *P* (Glt1, glutamate transporter 1, astrocytic) = 0.9902; *P* (Snat1, sodium-coupled neutral amino acid transporter 1) = 0.1065; *P* (Asct1, alanine/serine/cysteine transporter 1) = 0.0809; *P* (Gdh, glutamate dehydrogenase) = 0.5524; *P* (Glul, glutamine synthetase) = 0.646. Each protein band is normalized to its corresponding intensity of the actin band.

B. Western blotting of wild-type and Gpt2-null cortex protein lysates collected at P18. Each dot represents a different protein lysate sample from wild-type (black) or Gpt2-null (red) mice. *P* (Gria1) = 0.2058; *P* (GluN1) = 0.5595; *P* (Sv2) = 0.4032; *P* (Vglut1) = 0.1789; *P* (Vglut2) = 0.7331; *P* (Vgat) = 0.3243; *P* (Psd95) = 0.8146; ***P* (Glt1) = 0.0015; *P* (Snat1) = 0.0963; *P* (Asct1) = 0.1671; *P* (Gdh) = 0.1784; *P* (Glul) = 0.8154. Each protein band is normalized to its corresponding intensity of the actin band.

Figure 4. AMPAR and SV2 staining patterns appear unchanged in the Gpt2-null CA1 hippocampus.

A. Representative images of AMPA receptor (AMPAR) staining in wild-type (top) and Gpt2-null (bottom) hippocampus at P18. Various regions of the CA1, CA3 and dentate gyrus (DG) are shown. Scale bar: 20 μm.

B. Representative images of SV2 staining in wild-type (top) and Gpt2-null (bottom) hippocampus at P18. Various regions of the CA1, CA3 and dentate gyrus (DG) are shown. Scale bar: 20 μm.

Figure 5. Spine and mitochondria counts are unchanged in electron micrographs of CA1 stratum radiatum of Gpt2-null hippocampus.

A. Representative electron micrographs of wild-type (left) and Gpt2-null (right) CA1 stratum radiatum of the hippocampus at P18. Green arrowheads point to the spines, arrows point to the mitochondria. Scale bar: 1 μm.

B. Quantification of spines per image (21000X magnification). More than 25 micrographs from each animal were analyzed. Spine count: *P* (1^{st} pair: 0.2833, 2^{nd} pair: 0.9177).

C. Quantification of mitochondria per image (21000X magnification). More than 25 micrographs from each animal were analyzed. Mitochondria count: *P* (1^{st} pair: 0.8094, 2^{nd} pair: 0.0629).

Figure 6. Number of synaptic vesicles per spine remains unchanged and synaptic vesicle area is increased in Gpt2-null CA1 stratum radiatum.

A. Representative images of spines in wild-type (top) and Gpt2-null (bottom) CA1 stratum radiatum at P18. Scale bar: 0.1 μm.

B. Quantification of the area of synaptic vesicles. Each dot represents the area of synaptic vesicles averaged for each spine. *P* (1^{st} pair: 0.0006, 2^{nd} pair: <0.0001).

C. Quantification of the number of synaptic vesicles per spine. *P* (1^{st} pair: 0.9051, 2^{nd} pair: 0.0257).

D. Quantification of the post-synaptic density length. Each dot represents a spine. *P* (1^{st} pair: 0.8426, 2^{nd} pair: 0.0004).

*** denotes statistical significance in differences between both animal pairs.

Figure 7. More rapid decline of glutamatergic synaptic transmission with electrical stimulation of Schaffer collaterals to CA1 in Gpt2-null hippocampus.

A. Schematic of the hippocampal slice, a CA1 pyramidal neuron (red) and recording pipette, CA3 pyramidal neurons and Schaffer collaterals are shown in green. The stimulating electrode was placed approximately 200 microns away from each recorded CA1 pyramidal neuron.

B. Paired pulse ratios were unchanged as recorded in Gpt2-null CA1 pyramidal neurons at P18. Each dot represents a different cell recording from wild-type (black) and Gpt2-null (red) mice at P18. n = 7-9 mice/17 slices/17 cells. $P = 0.157$

C. A modest reduction in half-life of the fitted curve in the Gpt2-null pyramidal neurons during a 10 Hz stimulus train. Representative wild-type (black) and Gpt2-null (red) traces are shown on the top. The averaged peak amplitudes normalized to the first peak amplitude plotted by pulse number are shown on the bottom. Nonlinear regression with one-phase decay fit was performed; F = 8.126 (3,2594); wild-type half-life = 39.79 with 95% confidence interval of 31.07 to 55.31 vs Gpt2-null half-life = 31.63 with 95% confidence interval of 25.45 to 41.78. n = 7-9 mice/11-15 slices/11-15 cells. ***P <0.0001.

D. A greater reduction is seen in the half-life of the fitted curve in the Gpt2-null pyramidal neurons during a 20 Hz stimulus train. Representative wild-type (black) and Gpt2-null (red) traces are shown on the top. The averaged peak amplitudes normalized to the first peak amplitude plotted by pulse number are shown on the bottom. Nonlinear regression with one-phase decay fit was performed; F=95.48 (3,5387); Wild-type half-life

45.34 with 95% confidence interval of 40.51 to 51.47 vs Gpt2-null half-life 31.70 with 95% confidence interval of 28.87 to 35.15. n = 7-9 mice/13-14 slices/13-14 cells. ***P <0.0001.

Figure 8. Glutamate amount released upon depolarization is reduced in Gpt2-null synaptosomes.

A. Schematic of the synaptosomes and evoking glutamate release from synaptic vesicles with 50 mM KCl. Viability of synaptosomes was confirmed by adding 50 mM KCl to synaptosomes and comparing baseline (black) and evoked (red) glutamate levels in wild-type synaptosomes obtained at postnatal day 18 (P18).

B. Overall glutamate levels in the cytosolic fraction are reduced in Gpt2-null mice. Cytosol fraction of the forebrain was obtained by separating the supernatant from the crude synaptosomal pellet. Glutamate was detected by enzymatic method and expressed as μmol per mg of protein. Each dot represents a different synaptosome sample obtained from wild-type (black) or Gpt2-null (red) mice at P18. *P = 0.0161.

C. Glutamate levels released upon depolarization are reduced in Gpt2-null synaptosomes. Each dot represents a different synaptosome sample obtained from wild-type (black) or Gpt2-null (red) mice at P18. *P = 0.0106.

D. Released GABA levels were unchanged in Gpt2-null synaptosomes. Each dot represents a different synaptosome sample obtained from wild-type (black) or Gpt2-null (red) mice at P18. P = 0.4385.

Figure 9. Decreases in released glutamate are restored by alpha-ketoglutarate in Gpt2-null synaptosomes.

A. Glutamate levels are restored by alpha-ketoglutarate in Gpt2-null synaptosomes. Each dot represents a different synaptosome sample obtained from wild-type (black) or Gpt2-null (red) mice at P18. Wild-type vs. Gpt2-null no supplement: $^{**}P = 0.00533$; +alpha-ketoglutarate: $^{**}P = 0.001$. Wild-type no supplement vs. Gpt2-null +alpha-ketoglutarate: $P = 0.7272$. Wild-type no supplement vs. wild-type +alpha-ketoglutarate: $P = 0.002$. Wild-type vs. Gpt2-null +alpha-ketoglutarate: $P = 0.001$. n.s. = statistically non-significant.

B. Glutamate levels are not restored by alanine in Gpt2-null synaptosomes. Each dot represents a different synaptosome sample obtained from wild-type (black) or Gpt2-null (red) mice at P18. Wild-type vs. Gpt2-null no supplement: $^{**}P = 0.00533$; +alanine: $^{*}P = 0.0109$. Wild-type no supplement vs. Gpt2-null +alanine: $^{*}P = 0.0212$. Wild-type no supplement vs. alanine: $P = 0.211$. Gpt2-null no supplement vs. alanine: P = 0.104. n.s. = statistically non-significant.

C. Glutamate levels are restored by alanine and alpha-ketoglutarate combined supplementation in Gpt2-null synaptosomes. Each dot represents a different synaptosome sample obtained from wild-type (black) or Gpt2-null (red) mice at P18. Wild-type vs. Gpt2-null no supplement: $^{*}P = 0.0106$. Wild-type vs. Gpt2-null +alanine +alpha-ketoglutarate: $^{**}P = 0.0011$. Wildtype no supplement vs. Gpt2-null +alanine +alpha-ketoglutarate: $P = 0.4109$. Wild-type no supplement vs. +alanine+alpha-ketoglutarate: $^{***}P = 0.0003$. Gpt2-null no supplement vs. +alanine+alpha-ketoglutarate: $P = 0.001$. n.s. = statistically non-significant.

D. Released GABA levels were unchanged with or without alpha-ketoglutarate in Gpt2-null synaptosomes. Each dot represents a different synaptosome sample obtained from wild-type (black) or Gpt2-null (red) mice at P18. Wild-type vs. Gpt2-null no supplement: $P = 0.4385$. Wild-type vs. Gpt2-null +alpha-ketoglutarate: $P = 0.2652$.

E. Released GABA levels with or without alanine. Each dot represents a different synaptosome sample obtained from wild-type (black) or Gpt2-null (red) mice at P18. Wild-type vs. Gpt2-null no supplement: $P = 0.4385$. Wild-type vs. Gpt2-null +alanine +alpha-ketoglutarate $P = 0.634$.

F. Released GABA levels with or without alanine and alpha-ketoglutarate combined supplementation. Each dot represents a different synaptosome sample obtained from wild-type (black) or Gpt2-null (red) mice at P18. Wild-type vs. Gpt2-null no supplement: 0.3395. Wild-type vs. Gpt2-null +alanine +alpha-ketoglutarate $P = 0.2119$.

G. Alanine levels are reduced in Gpt2-null synaptosomes. Each dot represents a different synaptosome sample obtained from wild-type (black) or Gpt2-null (red) mice at P18. ***$P<0.0001$.

H. Alanine can readily enter the synaptosomes. Each dot represents a different synaptosome sample obtained from wild-type (black) or Gpt2-null (red) mice at P18. No supplement: wild-type vs. Gpt2-null *$P = 0.019$. Wild-type no supplement vs. wild-type +alanine: ***$P < 0.0001$. +alanine: wild-type vs. Gpt2-null $P = 0.9356$.

I. Alpha-ketoglutarate levels are not changed in Gpt2-null synaptosomes. Each dot represents a different synaptosome sample obtained from wild-type (black) or Gpt2-null (red) mice at P18. $P = 0.4291$.

J. Alpha-ketoglutarate can readily enter the synaptosomes. Each dot represents a different synaptosome sample obtained from wild-type (black) or Gpt2-null (red) mice at P18. Wild-type no supplement vs. wild-type +alpha-ketoglutarate: ***P <0.0001.

Figure 10. Glutamine metabolism is altered in Gpt2-null synaptosomes and rescued by alpha-ketoglutarate.

A. Metabolic pathways relevant to glutamate/glutamine metabolism and isotope labeling patterns originating from exogenous amine nitrogen labeled glutamine in synaptosomes. *GLS*: glutaminase, *GDH*: glutamate dehydrogenase. *GLUL*: glutamine synthetase.

B. Fractional enrichment of double-labeled glutamine is increased in Gpt2-null synaptosomes and restored by alpha-ketoglutarate. Each dot represents a different synaptosome sample obtained from wild-type (black) or Gpt2-null (red) mice at P18. Wild-type vs. Gpt2-null no supplement: P = **0.0047; +alpha-ketoglutarate: *P = 0.0135; +alanine: ***P = 0.0008. Gpt2-null no supplement vs. Gpt2-null +alpha-ketoglutarate: *P = 0.0457. Gpt2-null +alanine vs. Gpt2-null +alpha-ketoglutarate: *P = 0.0162. Wild-type no supplement vs. Gpt2-null +alpha-ketoglutarate: P = 0.1135. Wild-type no supplement vs. alpha-ketoglutarate: *P (paired Student's t-test) = 0.0007.

C. Baseline glutamine levels are increased in Gpt2-null synaptosomes. Each dot represents synaptosome samples obtained from different wild-type (black) or Gpt2-null (red) mice at P18. Wild-type vs. Gpt2-null **P = 0.0088.

D. Entry of glutamine is unaffected by alpha-ketoglutarate. Each dot represents synaptosome samples obtained from different wild-type (black) or Gpt2-null (red) mice

at P18. Wild-type no supplement vs. +alanine: *P = 0.0232; Wild-type no supplement vs. +alpha-ketoglutarate: P = 0.953.

E. Exogenous amine labeled glutamine labels the majority of glutamine pool in synaptosome. Each dot represents synaptosome samples obtained from different wild-type (black) or Gpt2-null (red) mice at P18. Wild-type vs. Gpt2-null no supplement: P = 0.287; +alanine: P = 0.0513; +alpha-ketoglutarate: P = 0.2885.

F. Fractional enrichment of labeled glutamate with the amine heavy nitrogen labeled glutamine precursor. Each dot represents synaptosome samples obtained from different wild-type (black) or Gpt2-null (red) mice at P18. Wild-type vs. Gpt2-null no supplement: P = 0.2; +alanine: *P = 0.023; +alpha-ketoglutarate: P = 0.147.

Figure 11. Upregulation of proteins related to glutamate metabolism and transport in Gpt2-null synaptosomes.

A. Western blotting of wild-type and Gpt2-null synaptosome protein lysates collected at P18. Note that Gpt2 is absent in Gpt2-null (MUT) but present in wild-type (WT) protein lysates. Each dot represents a different protein lysate sample from wild-type (black) or Gpt2-null (red) mice. Wild-type vs. Gpt2-null: *P (Gdh, glutamate dehydrogenase) = 0.0211; *P (Glul, glutamine synthetase) = 0.01; *P (Glt1, glutamate transporter 1, astrocytic) = 0.0305; *P (Snat1, sodium-coupled neutral amino acid transporter 1) = 0.0155; *P (Asct1, alanine/serine/cysteine transporter 1) = 0.0177; P (Sv2, synaptic vesicle protein 2) = 0.4176; *P (Vglut1, vesicular glutamate transporter 1) = 0.0378; P (Vglut2, vesicular glutamate transporter 2) = 0.5829; ***P (Vgat, vesicular GABA transporter) = 0.0001; *P (Psd95, post-synaptic density protein 95) = 0.0343; **P (Gria1,

AMPA receptor subunit 1) = 0.0028; *P* (GluN1, NMDA receptor, subunit 1) = 0.7273. Each protein band is normalized to its corresponding intensity of the actin band.

Figure 12. The TCA cycle has deficits but glutamine entry into the TCA cycle is intact in Gpt2-null synaptosomes.

A. Baseline malate and fumarate levels are reduced in Gpt2-null synaptosomes. Each dot represents a different sample from wild-type (black) or Gpt2-null (red) mice at P18. Baseline wild-type vs. Gpt2-null malate: **P* = 0.0298; fumarate: **P* = 0.0298; succinate: *P* = 0.8557. Malate wild-type vs. Gpt2-null no supplement: ***P* = 0.006; +alpha-ketoglutarate: *P* = 0.116. Malate wild-type no supplement vs. +alpha-ketoglutarate: **P* = 0.0178. Malate Gpt2-null no supplement vs. +alpha-ketoglutarate: *P* = 0.033. Fumarate wild-type vs. Gpt2-null no supplement: *P* = 0.868; +alpha-ketoglutarate: *P* = 0.269. Succinate/methylmalonate wild-type vs. Gpt2-null no supplement: *P* = 0.273; +alpha-ketoglutarate: *P* = 0.109. Succinate/methylmalonate Gpt2-null no supplement vs +alpha-ketoglutarate: **P* = 0.038.

B. Fractional enrichments of carbon labeled TCA cycle intermediates with the uniformly carbon labeled [U-^{13}C]-Glutamine precursor is unchanged in Gpt2-null synaptosomes. Each dot represents synaptosome samples obtained from different wild-type (black) or Gpt2-null (red) mice at P18. Wild-type vs. Gpt2-null malate: *P* = 0.402; succinate/methylmalonate: *P* = 0.634; fumarate: *P* = 0.513.

C. ATP levels are unchanged in Gpt2-null synaptosomes. Each dot represents synaptosome samples obtained from different wild-type (black) or Gpt2-null (red) mice at P18. ATP levels were enzymatically determined. Wild-type vs. Gpt2-null: *P* = 0.3533.

D. Energy charge is unchanged in Gpt2-null synaptosomes. Each dot represents synaptosome samples obtained from different wild-type (black) or Gpt2-null (red) mice at P18. Energy charge is calculated as: [(ATP+0.5*ADP) / (ATP + ADP + AMP)]. Wild-type vs. Gpt2-null: $P = 0.0761$.

E. NAD to NADH ratio is unchanged in Gpt2-null synaptosomes. Each dot represents synaptosome samples obtained from different wild-type (black) or Gpt2-null (red) mice at P18. Wild-type vs. Gpt2-null: $P = 0.3071$.

F. NADP to NADPH ratio is unchanged in Gpt2-null synaptosomes. Each dot represents synaptosome samples obtained from different wild-type (black) or Gpt2-null (red) mice at P18. Wild-type vs. Gpt2-null: $P = 0.2254$.

Discussion

Glutamate metabolism is maintained and tightly regulated by a multitude of metabolic enzymes and substrate transporters (Anderson and Swanson, 2000; Erecinska and Silver, 1990b; Haslam and Krebs, 1963; Schousboe et al., 1993; Yudkoff et al., 1993). An imbalance of substrates or proteins involved in glutamate metabolism often leads to a compensatory mechanism that takes advantage of alternative metabolic pathways (Alkan et al., 2018; Chen et al., 2018; Hohnholt et al., 2018; Motori et al., 2020; Yang et al., 2014). This flexibility of the metabolome related to glutamate is realized by 44 distinct enzymes that consume or produce glutamate, as curated in Kyoto Encyclopedia of Genes and Genomes (KEGG) (Kanehisa et al., 2020). Here, we report that loss of glutamate pyruvate transaminase 2 (Gpt2) causes reprogramming of glutamate metabolism which channels the use of glutamate to sustain the tricarboxylic acid (TCA) cycle in synaptic terminals.

The enzymes that produce or consume glutamate are many, but glutaminase and aspartate aminotransferase have been the focus of vast literature on glutamate synthesis (Erecinska and Silver, 1990a; Kovacevic, 1971; Masson et al., 2006; McKenna and Ferreira, 2016). Gpt2 has seen very little attention in the nervous system, particularly within the context of glutamate metabolism. This is most likely due to the observations that enzymatic activity of aspartate aminotransferase (also known as glutamate oxaloacetate transaminase, Got) has been found to be up to 100-fold greater than that of glutamate pyruvate transaminase in brain homogenates (Benuck et al., 1971; Salganicoff and Derobertis, 1965; Wilbur and Patel, 1974). Glutaminase and glutamate dehydrogenase have been shown to have higher enzymatic rates as well. Therefore, it is

unlikely that glutamate production is driven considerably by Gpt2. However, biochemical studies of enzyme activity rates have usually included both cytosolic and mitochondrial isoforms of glutamate pyruvate transaminase. Our study is the first to determine the effects of genetic ablation of Gpt2 on glutamate metabolism. Our results confirm the expectation that glutamate pyruvate transaminase does not produce or regulate glutamate to a great extent, evident in modest changes in our slice electrophysiology and synaptosome studies. However, as others have reported (Erecinska et al., 1994; Peng et al., 1993; Peng et al., 1991; Yudkoff et al., 1990), our studies also show that sufficient quantities of alanine and alpha-ketoglutarate can be used to make glutamate via transamination. Precedence of enzymes such as glutaminase, aspartate aminotransferase or glutamine synthetase in the regulation of glutamate metabolism is also reflected in the observation that genetic ablation of these enzymes lead to embryonic lethality in mice (Dickinson et al., 2016; He et al., 2007; Masson et al., 2006) whereas the loss of Gpt2 causes premature death, but only around weaning age (P21) (Ouyang et al., 2016).

Gpt2 is an equilibrium enzyme, that is it will try to balance the concentrations of both sides of the reaction (Krebs, 1953). Given Km values and relative concentrations of its substrates in neurons, Gpt2 has been predicted to work in the direction of alanine and alpha-ketoglutarate formation *in vivo* (Bak et al., 2006; Erecinska et al., 1994; Lenartowicz and Wojtczak, 1988; Miller et al., 1973; Waagepetersen et al., 2000). Therefore, it might be initially expected that glutamate levels would be increased in Gpt2-null brain tissue; however, we observe decreases both electrophysiologically and biochemically. If we think along the lines of functional implications of the Gpt2 reaction in physiological conditions, that is production of alanine and alpha-ketoglutarate,

reduction of glutamate levels may not be as surprising. Glutamate, the major excitatory neurotransmitter, is an excellent source of carbon for the TCA cycle (therefore energy) in mitochondria (Hertz et al., 2007; Kovacevic, 1971; McKenna, 2007; Westergaard et al., 1995). Gpt2 contributes to glutamate oxidation in mitochondria and loss of Gpt2 may lead to upregulation of other metabolic enzymes that allow for glutamate oxidation into the TCA cycle, a crucial part of anaplerotic processes (replenishment of the TCA cycle). We find increases of glutamate dehydrogenase levels in Gpt2-null synaptic terminals that may be carrying out this task, along with increases in glutamine synthetase that allows for efficient ammonia fixation. Glutamate dehydrogenase catalyzes practically an irreversible reaction that favors glutamate deamination, and thus once glutamate is consumed by this enzyme, it is fixed to its keto acid, alpha-ketoglutarate (Hohnholt et al., 2018; McKenna et al., 2000; Westergaard et al., 1996) and may provide an explanation as to why glutamate levels tend to decrease in Gpt2-null brain tissue.

We find deficits in the TCA cycle of synaptosomes, such as decreases in malate and fumarate levels, but glutamine can still be efficiently used as a precursor to the TCA cycle intermediates. There are anaplerotic pathways, other than glutamate dehydrogenase and Gpt2, that may support the TCA cycle in the absence of Gpt2 such as pyruvate carboxylase and other aminotransferases that yield alpha-ketoglutarate from glutamate including branched-chain amino acid aminotransferases (Hutson, 2001; Morken et al., 2014). All these processes likely contribute to sustain the TCA cycle in Gpt2-null brain as long as they are able; however, each have certain complications. For example, pyruvate carboxylase exists mainly in astrocytes and utilizes ATP to make oxaloacetate (Hertz et al., 2007; Yu et al., 1983). Glutamate dehydrogenase is found both in neurons

and astrocytes but depends on NADP availability (Aoki et al., 1987). Aminotransferases that degrade essential amino acids usually work in the direction of producing glutamate and not alpha-ketoglutarate (Conway and Hutson, 2016). In contrast, Gpt2 depends neither on ATP nor NADP availability, thereby conferring a unique anaplerotic ability to the cell. Levels of Gpt2 and Gpt1 protein have been shown to increase in models of oxidative phosphorylation deficits induced by mitochondrial DNA mutations (Chen et al., 2018) and disrupted mitochondrial fusion dynamics (Motori et al., 2020). Gpt2's unique support of the TCA cycle may enhance both biosynthesis and energetics to sustain cell growth and this is also evident in smaller soma sizes and slightly depolarized CA1 pyramidal neurons (Figure 2) as well as microcephaly seen in both mice and human patients with Gpt2 mutations (Ouyang et al., 2016).

Alpha-ketoglutarate rescues glutamate levels and augments the TCA cycle intermediates. It is yet unclear whether alpha-ketoglutarate exerts its effects through other transaminases or by blocking glutamate dehydrogenase, or both. Nevertheless, by a metabolic intervention, i.e. alpha-ketoglutarate supplementation, it was possible to correct both glutamate levels and alterations in the glutamine metabolism in Gpt2-null synaptic terminals. This puts emphasis on the changes in the metabolome on top of the changes we observed in electrophysiological properties of Gpt2-null CA1 pyramidal neurons (decreased membrane potential, decreased capacitance, increase membrane resistance) or levels of synaptic proteins.

Alanine on the other hand had minimal effect on glutamate levels and glutamine metabolism. It is possible that there was a modest effect of alanine supplementation on glutamate levels in synaptosomes with a modest significance p-value (0.109). This is

possible through the residual Gpt1 in synaptosomes, however alanine failed to increase glutamate levels above wild-type levels and it failed to correct double-labeled glutamine unlike alpha-ketoglutarate. Reduction in fraction of double-labeled glutamine most likely occurs through inhibition of glutamate dehydrogenase by alpha-ketoglutarate as previously demonstrated as substrate inhibition (Engel and Chen, 1975).

Released GABA levels do not change in Gpt2-null synaptosomes and are not elevated by alpha-ketoglutarate. Glutamine has been shown to be a much better precursor than alpha-ketoglutarate which preferentially is converted into glutamate (Peng et al., 1993; Shank and Campbell, 1982, 1984). Our synaptosomes preparations contain not only glutamatergic but GABAergic nerve terminals and presence of glutamate decarboxylase which irreversibly converts glutamate into GABA (Roberts and Eidelberg, 1960) and possibly account for the unchanged GABA levels in Gpt2-null synaptosomes.

Synaptosomes, isolated nerve terminals, are artificial organelles that normally do not exist *in vivo* and, in most preparations, may reflect both neuronal metabolism and astrocytic metabolism (Dunkley et al., 2008). Tripartite synapses (presynaptic terminals, postsynaptic spines and associated astrocyte components) exist only in approximately 50% of all spines in the stratum radiatum of the CA1 hippocampus (Ventura and Harris, 1999). It is yet unclear whether Gpt2 would have more profound effects on glutamatergic synapses that do not rely on astrocytic processes. Given our data, Gpt2 may provide additional contributions to the TCA cycle at non-tripartite synapses *in vivo*.

Gpt2 belongs to the protein family of pyridoxal phosphate (PLP)-dependent aspartate aminotransferase superfamily (Yang et al., 2002). Aspartate aminotransferase 2 has been found to localize in both mitochondria and synaptic vesicles (Takeda and Ueda,

2017). Localization to synaptic vesicles has been proposed as a mechanism to locally synthesize glutamate to be loaded to synaptic vesicles (Takeda et al., 2012). Gpt2 however does not appear in synaptic vesicles and thus modulates glutamate levels from within mitochondria.

Electrophysiological and biochemical interpretations of glutamate levels may have been impacted by decreases in AMPA receptor subunit (Gria1) and SV2 in the hippocampus and increases in astrocytic glutamate transporter (Glt1) in synaptic terminals. While none of our experiments can conclude that the glutamate pool is decreased specifically in neurons, there is a reduction in overall glutamate levels (Figure 4). Gpt2 in mice is expressed in both neurons and astrocytes (Zhang et al., 2016). Further experiments are needed to identify changes in glutamate levels and enzymes in different cell types.

All processes related to glutamate metabolism have major differences across species. Most notably, Gpt1 seems to be absent in the human brain and Gpt2 is the sole alanine aminotransferase detected (Hodge et al., 2019; Kang et al., 2011). Another notable example is glutamate dehydrogenase; the *GDH* gene has seen a recent duplication event in humans and non-human primates, that is absent in rodents (Li et al., 2016). Therefore, caution must be taken when extrapolating interpretations of metabolic changes across species.

In conclusion, here we report the contributions of Gpt2 to glutamate metabolism and the functional consequences of Gpt2 loss. Gpt2 can be used to make vesicular glutamate if alanine and alpha-ketoglutarate are sufficiently supplied. Gpt2 loss results in changes in both synaptic protein composition and metabolism which can partly be

alleviated by alpha-ketoglutarate. Compensatory mechanisms including upregulation of metabolic enzymes and transporters may act in lieu of Gpt2 to sustain energetics and neurotransmitter availability. In sum, we find that Gpt2 is a metabolic enzyme enriched in synaptic terminals linking glutamate metabolism to alanine and TCA cycle metabolism that maintains proper functioning of the glutamatergic synaptic transmission.

Materials and Methods

Ethics Statement

All experiments that involved mice were done in accordance with the National Institutes of Health *Guide for the Care and Use of Laboratory Animals (Council, 2011)* and approved by the Brown University Institutional Animal Care and Use Committee.

Animals

Gpt2-null animals were obtained from Knockout Mouse Project at University of California, Davis (RRID: MMRRC_047980-UCD), genotyped and maintained as described previously (Ouyang et al., 2016). The background of all mice was C57B6/J (Jackson Laboratory Strain No. 664, RRID: IMSR_JAX:000664). The mice were maintained under a 12-hour light/dark cycle (lights on at 7 am and off at 7 pm). The mice had ad libitum access to feed and water. All experiments were conducted on mice at postnatal day 18 (P18).

Synaptosome Preparation

The protocol was adapted from (Sims and Anderson, 2008) and (Dunkley et al., 2008). Immediately after cervical dislocation, the brain was removed at an angle with double-

ended surgical spatula so that the midbrain, pons, medulla, and cerebellum were excluded (Figure 1A). Olfactory bulb was also excluded. The tissue was rinsed in ice-cold 1X brain homogenization buffer (0.32 M sucrose, 1 mM EDTA, 5 mM Tris, pH 7.4). Fresh 1X brain homogenization buffer (10 mL/g) was added, and the brain was cut into small pieces with surgical scissors. A Kimble pestle was used to homogenize the tissue with 12 strokes (each 4 sec). The tube was spun at 1300 x *g* for 3 min at 4ºC. The first supernatant was stored on ice and the pellet was re-suspended in half starting volume with 1X brain homogenization buffer. The pellet was homogenized with a Kimble pestle with 8 strokes (each 4 sec). The tubes were spun at 1300 x *g* for 3 min at 4ºC. The first and second supernatants were combined, and the sample was spun at 10000 x *g* for 10 min at 4ºC with a Sorvall RC6Plus centrifuge using the SS34 rotor. The pellet was re-suspended in 10 mL per gram of original tissue with 15% Percoll (Percoll, Cytiva 17089102, prepared in 1X brain homogenization buffer). The suspension was carefully layered onto a Percoll gradient (23%-40%) and the tube was spun at 22000 x *g* for 10 min at 4ºC. The top layer contains myelin and associated membranes, the middle layer contains synaptosomes and associated membranes and the bottom layer contains the mitochondrial fraction. After carefully removing the upper layer, the synaptosomes were aspirated and re-spun with 4 volumes of 1X brain homogenization buffer, at 16000 x *g* for 10 min at 4ºC. The supernatant was carefully removed, and 4 volumes of Krebs-like buffer (118 mM NaCl, 5 mM KCl, 1 mM $MgCl_2$, 1.2 mM $CaCl_2$, 0.1 mM $Na_2HPO_4.H_2O$, 20 mM HEPES, 10 mM glucose, pH 7.4) was added. The tube was spun at 18000 x *g* for 10 min at 4ºC. The final pellet was flash frozen in liquid nitrogen for experiments in which baseline metabolite levels were determined. For all other experiments, the final

pellet was re-suspended in the Krebs-like buffer with 0.5 mM glutamine (Invitrogen, 25030081).

For isolation of synaptic vesicles, after the synaptosomes were washed with 4 volumes of Krebs-like buffer, the pellet was re-suspended in 450 µl ice-cold ddH_2O. The pellet was homogenized by pipetting. 4.95 µl 1M HEPES (pH7.4, with NaOH) was immediately added and the mixture was incubated on ice for 30 min. The mixture was spun at 43,100 x *g* with SS-34 rotor at 4ºC for 15 min. The supernatant was distributed equally to TLA 120.1 (Beckman Coulter) rotor thick-walled polycarbonate tubes (Beckman Coulter, 343776). The tubes were spun at 165,000 x *g* at 4ºC for 1 hour. The pellet was re-suspended in 30 µl RIPA buffer (50 mM Tris, 0.15 M NaCl, 1 mM EDTA, 1% TritonX-100, 0.5% (w/v) sodium deoxycholate, 0.1% SDS) with 1X PhosStop and 1X PIC for Western blotting.

Western Blotting

Tissues were homogenized in RIPA buffer (50 mM Tris, 0.15 M NaCl, 1 mM EDTA, 1% TritonX-100, 0.5% (w/v) sodium deoxycholate, 0.1% SDS) with 1X PhosStop and 1X PIC. Protein samples (20 µg) were incubated in 1X NuPage Sample buffer (Invitrogen, NP0007) and 1X NuPage reducing agent (Invitrogen, NP0004) at 70ºC for 10 min and immediately placed on ice. The samples were run in NuPage 4-12% Bis-Tris gel (Invitrogen, NP0321) at 170 V until the dye front was at the end of the gel. The gel was transferred to a nitrocellulose membrane (Invitrogen, LC2000) in 1X FisherScientific Pierce Western Blot Transfer Buffer (35040) with 20% methanol at 30 V for 1 hour. The blot was blocked with Li-Cor Blocking Buffer (Li-Cor Biosciences, 927-50000) for 30

min and permeabilized for 5 min in TBST (FisherScientific, BP2411) with 0.05% Tween20 (Sigma-Aldrich, P7949). The blot was incubated with primary antibodies in Li-Cor Intercept Antibody Diluent (Li-cor Biosciences, 927-65001) at 4ºC overnight. The blot was washed 3 x 5 min with TBST, incubated with secondary antibodies diluted in TBST for 1 hour, washed with TBST and finally placed in TBS. The blot was imaged using the Li-Cor Odyssey CLx Imaging System (resolution: 84 μm, background subtraction: median) and analyzed using Image Studio Lite software (RRID:SCR_013715). Protein amount in each sample was determined using the bicinchoninic acid (BCA) assay (ThermoScientific Pierce, PI23227). Primary antibodies used in the study: mouse anti-Actin (Sigma, A3853, RRID:AB_262137, 42 kDa, 1:2000), rabbit anti-Asct1 (Alomone, ANT081, RRID:AB_2756719, 80 kDa, 1:250), mouse anti-Gapdh (Sigma, G8795, RRID:AB_1078991, 37 kDa, 1:40,000), rabbit anti-Gdh (Invitrogen, PA5-29492, RRID:AB_2546968, 55 kDa, 1:2000), mouse anti-Glt1 (Millipore, MAB2262, RRID:AB_10615610, 62 kDa, 1:1000), mouse anti-Glul (BD Biosciences, 610517, RRID:AB_397879, 42 kDa, 1:2000), mouse anti-GluN1 (SynapticSystems, 114001, RRID:AB_887749, 100 kDa, 1:1000), mouse anti-Gpt1 (Sigma, SAB1412234, RRID:AB_2885183, 55 kDa, 1:1000), rabbit anti-Gpt2 (Proteintech, 16757-1-AP, RRID:AB_2112098, 58 kDa, 1:600), rabbit anti-Gria1 (abcam, ab31232, RRID:AB_2113447, 100 kDa, 1:1000), rabbit anti-Lsd1 (CellSignaling, 2184, RRID:AB_2070132, 110 kDa, 1:1000), mouse anti-Mtco1 (abcam, ab14705, RRID:AB_2084810, 40 kDa, 1:2000), mouse anti-Psd95 (Pierce, ma1-046, RRID:AB_2092361, 95 kDa, 1:2000), mouse anti-Snat1 (Millipore, MABN502, RRID:AB_2716561, 50 kDa, 1:500), mouse anti-Sv2 (DSHB, SV2, RRID:AB_2315387,

90 kDa, 1:1000), rabbit anti-SynapsinI (Millipore, AB1543P, RRID:AB_90757, 77&80 kDa, 1:1000), guinea pig anti-Vgat (SynapticSystems, 131004, RRID:AB_887873, 50 kDa, 1:1000), guinea pig anti-Vglut1 (SynapticSystems, 135304, RRID:AB_887878, 50 kDa, 1:1000), guinea pig anti-Vglut2 (SynapticSystems, 135404, RRID:AB_887884, 55 kDa, 1:1000). Secondary antibodies used in the study: goat anti-Rabbit IRDye 680RD (Li-Cor Biosciences, 926-68071, RRID:AB_10956166, 1:20,000), goat anti-Rabbit IRDye 800CW (Li-Cor Biosciences, 925-32211, RRID:AB_2651127, 1:20,000), goat anti-Mouse IRDye 680RD (Li-Cor Biosciences, 925-68070, RRID:AB_2651128, 1:20,000), goat anti-Mouse IRDye 800CW (Li-Cor Biosciences, 926-32210, RRID:AB_621842, 1:20,000), donkey anti-Guinea pig IRDye 680RD (Li-Cor Biosciences, 925-68077, RRID:AB_2814914, 1:20,000), donkey anti-Guinea pig IRDye 800CW (Li-Cor Biosciences, 925-32411, RRID:AB_2814905, 1:20,000).

GPT Enzyme Activity Assay

GPT activity assay was performed using the Alanine Aminotransferase (ALT) Assay Kit (Sigma-Aldrich, MAK052) according to the manufacturer's manual. Synaptosomes were resuspended in 1X ALT Assay buffer. 5 µg protein sample was used. Protein amount in each sample was determined using the BCA assay (ThermoScientific Pierce, PI23227). BioTek Cytation5 plate reader was used to detect fluorescence; Gen5 software was used to analyze the data (RRID:SCR_017317).

Metabolite detection by Liquid Chromatography - Mass Spectrometry (LC-MS)

For all experiments in which metabolites were detected in synaptosomes without any additional supplements, synaptosomes were collected as above and the final pellet was flash frozen in liquid nitrogen. The pellet was homogenized in 400 µL of 80% (vol/vol) methanol cooled to -80ºC with Kimble pestle and motor, then vortexed for 1 min, incubated at -80ºC for 4 hours. The samples were spun at 14000 x *g* for 10 min at 4ºC and the pellet was resuspended in 400 µL of 80% methanol while the supernatant was stored at -80ºC. The suspension was incubated at -80ºC for 30 min and then spun at 14000 x *g* for 10 min at 4ºC. The supernatants were combined and re-spun at 14000 x *g* for 10 min at 4ºC. The supernatants were concentrated using a Savant SpeedVac vacuum concentrator (Thermo Scientific) at ambient temperature in 1.5-mL Eppendorf tubes. Liquid chromatography with tandem mass spectrometry (MS) was done at Beth Israel Deaconess Medical Center Mass Spectrometry Facility. The samples were re-suspended in liquid chromatography (LC) / mass spectrometry (MS)-grade water and run-in tandem LC-MS/MS. Samples were injected into hydrophilic interaction liquid chromatography (HILIC) at high pH using HPLC coupled to a 5500 QTRAP mass spectrometer (AB/SCIEX). Selected Reaction Monitoring (SRM) mode for 300 transitions with positive/negative polarity switching fragmented precursor ions and selected for product ions. Peak areas for each detected metabolite were integrated using MultiQuant software (AB/SCIEX). All data were normalized by median normalization of at least 100 metabolite peaks. Unpaired Student's t-test assuming equal variance was used to generate a p-value.

For all experiments that involve additional supplement with 1.6 mM alanine (Sigma, A7627) and 1.6 mM alpha-ketoglutarate (Sigma, 75890), synaptosomes in all conditions

were incubated in Krebs-like buffer with 0.5 mM glutamine for 15 min at 37ºC. For evoked glutamate release, a final concentration of 50 mM KCl was added, and the suspension was incubated for 1 min at 37ºC. The pellet was spun immediately after at 16000 x *g* at 4ºC for 1 min. LC−MS analysis for soluble metabolites was achieved on the Q Exactive PLUS hybrid quadrupole-orbitrap mass spectrometer (Thermo Scientific) coupled with hydrophilic interaction chromatography (HILIC). To perform the LC separation, an XBridge BEH Amide column (150 mm × 2.1 mm, 2.5 µM particle size, Waters, Milford, MA) was used with a gradient of solvent A (95%:5% H_2O: acetonitrile with 20 mM ammonium acetate, 20 mM ammonium hydroxide, pH 9.4), and solvent B (100% acetonitrile). The gradient was 0 min, 85% B; 2 min, 85% B; 3 min, 80% B; 5 min, 80% B; 6 min, 75% B; 7 min, 75% B; 8 min, 70% B; 9 min, 70% B; 10 min, 50% B; 12 min, 50% B; 13 min, 25% B; 16 min, 25% B; 18 min, 0% B; 23 min, 0% B; 24 min, 85% B; 30 min, 85% B. The flow rate was 150 µL/min; the injection volume was 10 µL; the column temperature was 25ºC. MS full scans were in negative ion mode with a resolution of 140,000 at m/z 200 and scan range of 75-1000 m/z. The automatic gain control (AGC) target was 1×10^6.

Isotope Labeling in Synaptosomes. Synaptosome metabolite pool was labeled with 0.5 mM [α-^{15}N]-glutamine (Sigma-Aldrich, 486809), 0.5 mM [U-^{13}C]-glutamine (Sigma-Aldrich, 605166) or 1.6 mM [α-^{15}N]-alanine (Cambridge Isotope Laboratories, NLM-454) for 15 min at 37ºC. All conditions had labeled or unlabeled 0.5 mM glutamine in Krebs-like buffer.

Brain slice preparation

Coronal slices (250 μm) were prepared from anesthetized mice at postnatal day 18, as described previously (Brown et al., 2013). Briefly, the brain was immediately extracted and placed in a vibratome (Leica, VT1000). Slices were cut in ice-cold oxygenated artificial cerebrospinal fluid (ACSF, in mM): 119 NaCl, 2.5 KCl, 2.5 $CaCl_2.2H_2O$, 1.0 $NaH_2PO_4.H_2O$, 1.3 $MgSO_4.7H_2O$, 26.0 $NaHCO_3$, 11 glucose. Slices were recovered in the same oxygenated ACSF solution at room temperature for 1 hour and then transferred to a recording chamber where they were continuously submerged in ACSF at 28^oC with a flow rate of 1-2 ml/min.

Electrophysiological recordings

Whole cell recordings of CA1 pyramidal neurons were performed using a MultiClamp 700B Amplifier (Molecular Devices). Signals were low-pass filtered at 3 kHz and digitized at 10 kHz via a Digidata 1550 digitizer (Molecular Devices). Patch electrodes were fabricated from borosilicate glass capillaries (Sutter Instruments) using a P-97 micropipette puller (Sutter Instruments). Patch pipettes had a resistance of 3-8 MOhm. For determining intrinsic cell properties, the patch pipette internal solution consisted of (in mM): 125.0 KCl, 2.8 NaCl, 10.0 HEPES, 2.0 $MgCl_2$, 2.37 ATP-Mg, 0.32 GTP-Na, 0.6 EGTA, (pH 7.23-7.28, 270-278 mOsm). Capacitance and membrane resistance were calculated from voltage response during injection of -100 pA.

For measuring miniature synaptic currents, the patch pipette internal solution consisted of (in mM): 125.0 CsCl, 2.8 NaCl, 10.0 HEPES, 2.0 $MgCl_2$, 2.37 ATP-Mg, 0.32 GTP-Na, 0.6 EGTA, (pH 7.23-7.28, 270-278 mOsm). At least 80 events were detected in ASCF with 1 μM TTX (Tocris, 1078) and 33 μM Bicuculline (Tocris, 0130) for miniature

excitatory synaptic currents or with 1 μM TTX and 10 μM DNQX (Sigma, D0540) for miniature inhibitory synaptic currents, while the cell was voltage-clamped at -80mV. The series resistance was monitored throughout the recording and the cell was excluded from analysis if it changed by 20%. Miniature events with multiple consecutive peaks or "shoulders" were counted for frequency but excluded from amplitude calculations. For miniature excitatory currents only: the traces were low-pass (Gaussian) filtered with a -3dB cutoff frequency of 1000 Hz for better visualization of miniature events with smaller amplitudes. The miniature events were detected using a template compiled from each recording individually in Clampfit software (SCR_011323).

For train analysis, the patch pipette internal solution consisted of (in mM): 125.0 KCl, 2.8 NaCl, 10.0 HEPES, 2.0 $MgCl_2$, 2.37 ATP-Mg, 0.32 GTP-Na, 0.6 EGTA, 5 mM QX-314 (Tocris, 2313) (pH 7.23-7.28, 270-278 mOsm). The external solution consisted of ASCF with 50 μM d-APV (Tocris, 0106) and 100 μM picrotoxin (Sigma, P1675). CA3 was surgically removed from the slice to minimize epileptic activity. To stimulate Schaffer collaterals, bipolar stainless steel microelectrodes with 2-5 MOhm impedance (FHC, UESMEGSEKNNM) were gently placed approximately 200 μm away from the recorded pyramidal neuron. Paired pulses, 50 msec apart, were used to achieve a stable current response of approximately 150 - 300 pA. Trains were applied at 10 Hz for 10 seconds. Paired pulses were used to achieve the stable response and the process was repeated a total of 2-3 times. If the current response was able to recover to the original baseline response, then the trains were repeated with 20 Hz stimulation for 10 seconds. Cells with at least two rounds of trains were used for analysis. Paired pulse ratio was calculated by

dividing the peak amplitude of the second response to that of the first. All electrophysiological recordings were analyzed using Clampfit software.

Electron Microscopy

The animals were perfused with 1X PBS and then 2.5% glutaraldehyde, 2% paraformaldehyde, 2 mM calcium chloride in 0.15 M sodium cacodylate buffer. The 100 μm thick tissue sections were obtained using a vibratome and fixed in glutaraldehyde/paraformaldehyde/calcium chloride/sodium cacodylate buffer for 3 hours at 4^{o}C. The sections were washed in cold 0.15 M sodium cacodylate with 2 mM calcium chloride for 3 minutes, 5 times and then in filtered ddH2O for 3 minutes, 5 times. The sections were placed in filtered thiocarbohydrazide (TCH) solution (10 mg/ml in ddH_2O) for 20 minutes. The sections were rinsed with ddH_2O for 3 minutes, 5 times. The sections were treated with 2% osmium oxide for 30 minutes and then washed with ddH_2O for 3 minutes, 5 times. The sections were placed in 1% (w/v) uranyl acetate at 4^{o}C overnight. The tissue was washed with ddH_2O for 3 minutes, 5 times and then placed in lead aspartate solution (6.6 mg/ml, pH 5.5) at 60^{o}C for 30 minutes. The tissues were washed in ddH_2O for 3 minutes, 5 times and then dehydrdated in increasing concentration of ethanol (70%, 90%, 95%, 20 minutes once each and then 100% for 10 minutes, 3 times.). Epon embedding was performed with Embed-812 (Electron Microscopy Sciences, 14120), Araldite 502 (Electron Microscopy Sciences, 13900), DDSA (Electron Microscopy Sciences, 13700), DMP-30 (Electron Microscopy Sciences, 13600) in Chien molds and the tissues were left to polymerase overnight at 60^{o}C overnight. The electron micrographs were obtained using Philips EM 410 transmission electron microscope.

Glutamate Detection by Enzymatic Method

Free glutamate levels in the cytosolic fraction, that is the supernatant obtained along with the pellet that was re-suspended in Percoll, were determined by enzymatic method using glutamate dehydrogenase. Protein concentration was quantified by the bicinchoninic acid (BCA) assay (ThermoScientific Pierce, PI23227). 100 µg of each sample was added to their respective wells in a black clear-bottom 96-well plate (Greiner Bio-One, 655090) and the final volume was completed to 200 µl with Krebs-like buffer. $NADP^+$ (Sigma, N5755) at a final concentration of 1 mM was added to each well. After 6 minutes of equilibration, five units of glutamate dehydrogenase (Sigma, G2626) was added to each well. The excitation and emission filters were 340 and 460 nm, respectively. All readings were taken at 37ºC. Glutamate standard (Sigma, G1251) was used for calibration.
To validate the viability of synaptosomes, 50 mM KCl was added to synaptosomes immediately after the glutamate dehydrogenase epoch reached a plateau. The readings were taken the parameters outlined above.

ATP Assay in Synaptosomes

In addition to LC-MS/MS, ATP levels in wild-type and Gpt2-null synaptosomes at P18 were quantified with ATP Assay Kit (abcam, 83355, lot: GR3299138) according to the manufacturer's instructions. The samples were deproteinized by PCA/KOH method as recommended by the manual. Protein amount in each sample was determined using the BCA assay (ThermoScientific Pierce, PI23227).

Experimental Design and Statistical Analyses

All data in the Figures and the Results section are presented as average ± standard error of the mean, unless otherwise noted. The statistical test for comparisons of two groups was unpaired two-tailed Student t-test unless otherwise noted. All statistical analyses were compiled using GraphPad Prism software (RRID:SCR_002798).

References

Alkan, H.F., Walter, K.E., Luengo, A., Madreiter-Sokolowski, C.T., Stryeck, S., Lau, A.N., Al-Zoughbi, W., Lewis, C.A., Thomas, C.J., Hoefler, G.*, et al.* (2018). Cytosolic Aspartate Availability Determines Cell Survival When Glutamine Is Limiting. Cell Metab *28*, 706-720 e706.

Anderson, C.M., and Swanson, R.A. (2000). Astrocyte glutamate transport: Review of properties, regulation, and physiological functions. Glia *32*, 1-14.

Aoki, C., Milner, T.A., Sheu, K.F., Blass, J.P., and Pickel, V.M. (1987). Regional distribution of astrocytes with intense immunoreactivity for glutamate dehydrogenase in rat brain: implications for neuron-glia interactions in glutamate transmission. The Journal of Neuroscience *7*, 2214-2231.

Bak, L.K., Schousboe, A., and Waagepetersen, H.S. (2006). The glutamate/GABA-glutamine cycle: aspects of transport, neurotransmitter homeostasis and ammonia transfer. J Neurochem *98*, 641-653.

Benuck, M., Stern, F., and Lajtha, A. (1971). Transamination of amino acids in homogenates of rat brzain. J Neurochem *18*, 1555-1567.

Brown, T.E., Chirila, A.M., Schrank, B.R., and Kauer, J.A. (2013). Loss of interneuron LTD and attenuated pyramidal cell LTP in Trpv1 and Trpv3 KO mice. Hippocampus *23*, 662-671.

Chen, Q., Kirk, K., Shurubor, Y.I., Zhao, D., Arreguin, A.J., Shahi, I., Valsecchi, F., Primiano, G., Calder, E.L., Carelli, V.*, et al.* (2018). Rewiring of Glutamine Metabolism Is a Bioenergetic Adaptation of Human Cells with Mitochondrial DNA Mutations. Cell Metab *27*, 1007-1025 e1005.

Conway, M.E., and Hutson, S.M. (2016). BCAA Metabolism and NH3 Homeostasis. Adv Neurobiol *13*, 99-132.

Cooper, A.J., and Jeitner, T.M. (2016). Central Role of Glutamate Metabolism in the Maintenance of Nitrogen Homeostasis in Normal and Hyperammonemic Brain. Biomolecules *6*.

Council, N.R. (2011). Guide for the Care and Use of Laboratory Animals: Eighth Edition (Washington, DC: The National Academies Press).

Dickinson, M.E., Flenniken, A.M., Ji, X., Teboul, L., Wong, M.D., White, J.K., Meehan, T.F., Weninger, W.J., Westerberg, H., Adissu, H.*, et al.* (2016). High-throughput discovery of novel developmental phenotypes. Nature *537*, 508-514.

Dunkley, P.R., Jarvie, P.E., and Robinson, P.J. (2008). A rapid Percoll gradient procedure for preparation of synaptosomes. Nat Protoc *3*, 1718-1728.

Engel, P.C., and Chen, S.S. (1975). A product-inhibition study of bovine liver glutamate dehydrogenase. Biochem J *151*, 305-318.

Erecinska, M., Nelson, D., Nissim, I., Daikhin, Y., and Yudkoff, M. (1994). Cerebral alanine transport and alanine aminotransferase reaction: alanine as a source of neuronal glutamate. J Neurochem *62*, 1953-1964.

Erecinska, M., and Silver, I. (1990a). Metabolism and role of glutamate in mammalian brain. Progress in Neurobiology *35*, 245-296.

Erecinska, M., and Silver, I.A. (1990b). Metabolism and role of glutamate in mammalian brain. Prog Neurobiol *35*, 245-296.

Fatt, P., and Katz, B. (1952). Spontaneous Subthreshold Activity At Motor Nerve Endings. J Physiol.

Fonnum, F. (1984). Glutamate: a neurotransmitter in mammalian brain. J Neurochem *42*, 1-11.

Genda, E.N., Jackson, J.G., Sheldon, A.L., Locke, S.F., Greco, T.M., O'Donnell, J.C., Spruce, L.A., Xiao, R., Guo, W., Putt, M.*, et al.* (2011). Co-compartmentalization of the astroglial glutamate transporter, GLT-1, with glycolytic enzymes and mitochondria. J Neurosci *31*, 18275-18288.

Haslam, R.J., and Krebs, H.A. (1963). The Metabolism of Glutamate in Homogenates and Slices of Brain Cortex. Biochem J *88*, 566-578.

He, Y., Hakvoort, T.B., Vermeulen, J.L., Lamers, W.H., and Van Roon, M.A. (2007). Glutamine synthetase is essential in early mouse embryogenesis. Dev Dyn *236*, 1865-1875.

Hertz, L. (2013). The Glutamate-Glutamine (GABA) Cycle: Importance of Late Postnatal Development and Potential Reciprocal Interactions between Biosynthesis and Degradation. Front Endocrinol (Lausanne) *4*, 59.

Hertz, L., Peng, L., and Dienel, G.A. (2007). Energy metabolism in astrocytes: high rate of oxidative metabolism and spatiotemporal dependence on glycolysis/glycogenolysis. J Cereb Blood Flow Metab *27*, 219-249.

Hodge, R.D., Bakken, T.E., Miller, J.A., Smith, K.A., Barkan, E.R., Graybuck, L.T., Close, J.L., Long, B., Johansen, N., Penn, O.*, et al.* (2019). Conserved cell types with divergent features in human versus mouse cortex. Nature *573*, 61-68.

Hohnholt, M.C., Andersen, V.H., Andersen, J.V., Christensen, S.K., Karaca, M., Maechler, P., and Waagepetersen, H.S. (2018). Glutamate dehydrogenase is essential to sustain neuronal oxidative energy metabolism during stimulation. J Cereb Blood Flow Metab *38*, 1754-1768.

Hutson, S. (2001). Structure and function of branched chain aminotransferases. In, pp. 175-206.

Jin, L., Li, D., Alesi, G.N., Fan, J., Kang, H.B., Lu, Z., Boggon, T.J., Jin, P., Yi, H., Wright, E.R.*, et al.* (2015). Glutamate dehydrogenase 1 signals through antioxidant glutathione peroxidase 1 to regulate redox homeostasis and tumor growth. Cancer Cell *27*, 257-270.

Kanehisa, M., Furumichi, M., Sato, Y., Ishiguro-Watanabe, M., and Tanabe, M. (2020). KEGG: integrating viruses and cellular organisms. Nucleic Acids Res.

Kang, H.J., Kawasawa, Y.I., Cheng, F., Zhu, Y., Xu, X., Li, M., Sousa, A.M., Pletikos, M., Meyer, K.A., Sedmak, G.*, et al.* (2011). Spatio-temporal transcriptome of the human brain. Nature *478*, 483-489.

Kim, M., Gwak, J., Hwang, S., Yang, S., and Jeong, S.M. (2019). Mitochondrial GPT2 plays a pivotal role in metabolic adaptation to the perturbation of mitochondrial glutamine metabolism. Oncogene *38*, 4729-4738.

Kovacevic, Z. (1971). The pathway of glutamine and glutamate oxidation in isolated mitochondria from mammalian cells. Biochem J *125*, 757-763.

Krebs, H.A. (1953). Equilibria in transamination systems. Biochem J *54*, 82-86.
Kurmi, K., and Haigis, M.C. (2020). Nitrogen Metabolism in Cancer and Immunity. Trends Cell Biol *30*, 408-424.

Leke, R., and Schousboe, A. (2016). The Glutamine Transporters and Their Role in the Glutamate/GABA-Glutamine Cycle. Adv Neurobiol *13*, 223-257.

Lenartowicz, E., and Wojtczak, A.B. (1988). Significance of the alanine aminotransferase reaction in the formation of α-ketoglutarate in rat liver mitochondria. Archives of Biochemistry and Biophysics *260*, 309-319.

Li, Q., Guo, S., Jiang, X., Bryk, J., Naumann, R., Enard, W., Tomita, M., Sugimoto, M., Khaitovich, P., and Paabo, S. (2016). Mice carrying a human GLUD2 gene recapitulate aspects of human transcriptome and metabolome development. Proc Natl Acad Sci U S A *113*, 5358-5363.

Lindblom, P., Rafter, I., Copley, C., Andersson, U., Hedberg, J.J., Berg, A.L., Samuelsson, A., Hellmold, H., Cotgreave, I., and Glinghammar, B. (2007). Isoforms of alanine aminotransferases in human tissues and serum--differential tissue expression using novel antibodies. Arch Biochem Biophys *466*, 66-77.

Masson, J., Darmon, M., Conjard, A., Chuhma, N., Ropert, N., Thoby-Brisson, M., Foutz, A.S., Parrot, S., Miller, G.M., Jorisch, R.*, et al.* (2006). Mice lacking brain/kidney phosphate-activated glutaminase have impaired glutamatergic synaptic transmission, altered breathing, disorganized goal-directed behavior and die shortly after birth. J Neurosci *26*, 4660-4671.

McCommis, K.S., Chen, Z., Fu, X., McDonald, W.G., Colca, J.R., Kletzien, R.F., Burgess, S.C., and Finck, B.N. (2015). Loss of Mitochondrial Pyruvate Carrier 2 in the Liver Leads to Defects in Gluconeogenesis and Compensation via Pyruvate-Alanine Cycling. Cell Metab *22*, 682-694.

McKenna, M.C. (2007). The glutamate-glutamine cycle is not stoichiometric: fates of glutamate in brain. J Neurosci Res *85*, 3347-3358.

McKenna, M.C., and Ferreira, G.C. (2016). Enzyme Complexes Important for the Glutamate-Glutamine Cycle. Adv Neurobiol *13*, 59-98.

McKenna, M.C., Stevenson, J.H., Huang, X., and Hopkins, I.B. (2000). Differential distribution of the enzymes glutamate dehydrogenase and aspartate aminotransferase in cortical synaptic mitochondria contributes to metabolic compartmentation in cortical synaptic terminals. Neurochem Int *37*, 229-241.

Miller, A.L., Hawkins, R.A., and Veech, R.L. (1973). The mitochondrial redox state of rat brain. J Neurochem *20*, 1393-1400.

Morken, T.S., Brekke, E., Haberg, A., Wideroe, M., Brubakk, A.M., and Sonnewald, U. (2014). Neuron-astrocyte interactions, pyruvate carboxylation and the pentose phosphate pathway in the neonatal rat brain. Neurochem Res *39*, 556-569.

Motori, E., Atanassov, I., Kochan, S.M.V., Folz-Donahue, K., Sakthivelu, V., Giavalisco, P., Toni, N., Puyal, J., and Larsson, N.G. (2020). Neuronal metabolic rewiring promotes

resilience to neurodegeneration caused by mitochondrial dysfunction. Sci Adv *6*, eaba8271.

Ouyang, Q., Nakayama, T., Baytas, O., Davidson, S.M., Yang, C., Schmidt, M., Lizarraga, S.B., Mishra, S., Ei-Quessny, M., Niaz, S.*, et al.* (2016). Mutations in mitochondrial enzyme GPT2 cause metabolic dysfunction and neurological disease with developmental and progressive features. Proc Natl Acad Sci U S A *113*, E5598-5607.

Owen, O.E., Kalhan, S.C., and Hanson, R.W. (2002). The key role of anaplerosis and cataplerosis for citric acid cycle function. J Biol Chem *277*, 30409-30412.

Peng, L., Hertz, L., Huang, R., Sonnewald, U., Petersen, S.B., Westergaard, N., Larsson, O., and Schousboe, A. (1993). Utilization of glutamine and of TCA cycle constituents as precursors for transmitter glutamate and GABA. Dev Neurosci *15*, 367-377.

Peng, L.A., Schousboe, A., and Hertz, L. (1991). Utilization of alpha-ketoglutarate as a precursor for transmitter glutamate in cultured cerebellar granule cells. Neurochem Res *16*, 29-34.

Roberts, E., and Eidelberg, E. (1960). Metabolic and Neurophysiological Roles of γ-Aminobutyric Acid. In, pp. 279-332.

Ropert, N., Miles, R., and Korn, H. (1990). Characteristics of miniature inhibitory postsynaptic currents in CA1 pyramidal neurones of rat hippocampus. J Physiol *428*, 707-722.

Salganicoff, L., and Derobertis, E. (1965). Subcellular Distribution of the Enzymes of the Glutamic Acid, Glutamine and Gamma-Aminobutyric Acid Cycles in Rat Brain. J Neurochem *12*, 287-309.

Schousboe, A., Westergaard, N., and Hertz, L. (1993). Neuronal-astrocytic interactions in glutamate metabolism. Biochem Soc Trans *21*, 49-53.

Sedlak, T.W., Paul, B.D., Parker, G.M., Hester, L.D., Snowman, A.M., Taniguchi, Y., Kamiya, A., Snyder, S.H., and Sawa, A. (2019). The glutathione cycle shapes synaptic glutamate activity. Proc Natl Acad Sci U S A *116*, 2701-2706.

Shank, R.P., Baldy, W.J., and Ash, C.W. (1989). Glutamine and 2-oxoglutarate as metabolic precursors of the transmitter pools of glutamate and GABA: correlation of regional uptake by rat brain synaptosomes. Neurochem Res *14*, 371-376.

Shank, R.P., and Bennett, D.J. (1993). 2-Oxoglutarate transport: a potential mechanism for regulating glutamate and tricarboxylic acid cycle intermediates in neurons. Neurochem Res *18*, 401-410.

Shank, R.P., and Campbell, G.L. (1982). Glutamine and alpha-ketoglutarate uptake and metabolism by nerve terminal enriched material from mouse cerebellum. Neurochem Res *7*, 601-616.

Shank, R.P., and Campbell, G.L. (1984). Alpha-ketoglutarate and malate uptake and metabolism by synaptosomes: further evidence for an astrocyte-to-neuron metabolic shuttle. J Neurochem *42*, 1153-1161.

Sims, N.R., and Anderson, M.F. (2008). Isolation of mitochondria from rat brain using Percoll density gradient centrifugation. Nat Protoc *3*, 1228-1239.

Smith, B., Schafer, X.L., Ambeskovic, A., Spencer, C.M., Land, H., and Munger, J. (2016). Addiction to Coupling of the Warburg Effect with Glutamine Catabolism in Cancer Cells. Cell Rep *17*, 821-836.

Sonnewald, U., and McKenna, M. (2002). Metabolic compartmentation in cortical synaptosomes: influence of glucose and preferential incorporation of endogenous glutamate into GABA. Neurochem Res *27*, 43-50.

Takeda, K., Ishida, A., Takahashi, K., and Ueda, T. (2012). Synaptic vesicles are capable of synthesizing the VGLUT substrate glutamate from alpha-ketoglutarate for vesicular loading. J Neurochem *121*, 184-196.

Takeda, K., and Ueda, T. (2017). Effective Mechanism for Synthesis of Neurotransmitter Glutamate and its Loading into Synaptic Vesicles. Neurochem Res *42*, 64-76.

Ventura, R., and Harris, K.M. (1999). Three-Dimensional Relationships between Hippocampal Synapses and Astrocytes. The Journal of Neuroscience *19*, 6897-6906.

Villa, K.L., and Nedivi, E. (2016). Excitatory and Inhibitory Synaptic Placement and Functional Implications. In Dendrites, pp. 467-487.

Waagepetersen, H.S., Sonnewald, U., Larsson, O.M., and Schousboe, A. (2000). A possible role of alanine for ammonia transfer between astrocytes and glutamatergic neurons. J Neurochem *75*, 471-479.

Westergaard, N., Drejer, J., Schousboe, A., and Sonnewald, U. (1996). Evaluation of the importance of transamination versus deamination in astrocytic metabolism of [U-13C] glutamate. Glia *17*, 160-168.

Westergaard, N., Sonnewald, U., and Schousboe, A. (1995). Metabolic trafficking between neurons and astrocytes: the glutamate/glutamine cycle revisited. Dev Neurosci *17*, 203-211.

Wilbur, D.O., and Patel, M.S. (1974). Development of mitochondrial pyruvate metabolism in rat brain. J Neurochem *22*, 709-715.

Yang, C., Ko, B., Hensley, C.T., Jiang, L., Wasti, A.T., Kim, J., Sudderth, J., Calvaruso, M.A., Lumata, L., Mitsche, M.*, et al.* (2014). Glutamine oxidation maintains the TCA cycle and cell survival during impaired mitochondrial pyruvate transport. Mol Cell *56*, 414-424.

Yang, R.Z., Blaileanu, G., Hansen, B.C., Shuldiner, A.R., and Gong, D.W. (2002). cDNA cloning, genomic structure, chromosomal mapping, and functional expression of a novel human alanine aminotransferase. Genomics *79*, 445-450.

Young, V.R., and Ajami, A.M. (2000). Glutamate: an amino acid of particular distinction. J Nutr *130*, 892S-900S.

Yu, A.C., Drejer, J., Hertz, L., and Schousboe, A. (1983). Pyruvate carboxylase activity in primary cultures of astrocytes and neurons. J Neurochem *41*, 1484-1487.

Yudkoff, M., Nissim, I., Daikhin, Y., Lin, Z.P., Nelson, D., Pleasure, D., and Erecinska, M. (1993). Brain glutamate metabolism: neuronal-astroglial relationships. Dev Neurosci *15*, 343-350.

Yudkoff, M., Nissim, I., and Hertz, L. (1990). Precursors of glutamic acid nitrogen in primary neuronal cultures: studies with 15N. Neurochem Res *15*, 1191-1196.

Zhang, Y., Sloan, S.A., Clarke, L.E., Caneda, C., Plaza, C.A., Blumenthal, P.D., Vogel, H., Steinberg, G.K., Edwards, M.S., Li, G.*, et al.* (2016). Purification and Characterization of Progenitor and Mature Human Astrocytes Reveals Transcriptional and Functional Differences with Mouse. Neuron *89*, 37-53.

Chapter 6: Loss of GPT2 leads to reduced cellular growth and altered metabolome in near-haploid HAP1 cancerous cell lines.

I conducted all experiments; Tara Srivinas performed experiments in Figures 1E, 2, 3, 4, 5A&B, 6. The project was done under the supervision of Eric M. Morrow. For funding sources, please refer to the Funding information in Chapters 2, 3, 4 and 5.

Loss of GPT2 leads to reduced cellular growth and altered metabolome in HAP1 cells.

Ozan Baytas, Tara Srinivas, Eric M Morrow

ABSTRACT

Glutamate pyruvate transaminase 2 (GPT2) plays a central role in cellular growth and energetics by linking amino acid metabolism to the tricarboxylic acid cycle. Here we model the loss of GPT2 in two clones of near-haploid HAP1 cell lines. The loss of GPT2 is confirmed by Sanger sequencing, Western blotting, enzymatic activity and confocal microscopy. GPT2 loss in HAP1 cells causes decreases in cell size. Various medium conditions are employed including alanine deprivation and glutaminase inhibition to expose metabolic vulnerabilities of GPT2 loss *in vitro*. Proliferation rates of GPT2-null cells are reduced in medium deprived of alanine. We find decreases in cell proliferation rate with glutaminase inhibition only in Clone 2 GPT2-null cells. We do not find increases in apoptosis in either clone with or without alanine deprivation or glutaminase inhibition. We find no differences in mitochondrial membrane potential and reactive oxygen species as measured by confocal microscopy between the wild-type and mutant clones. Only Clone 2 GPT2-null cells displayed abnormal mitochondrial respiration. We discover alterations in the metabolic profiles of both GPT2-null clones particularly in the tricarboxylic cycle, alanine metabolism and overall amino acid metabolism. We conclude that HAP1 cells may be used to model cellular and biochemical alterations that result from loss of GPT2 and reveal fundamental mechanisms of cellular growth.

INTRODUCTION

Glutamate pyruvate transaminase 2 (GPT2), also known as alanine transaminase 2 (ALT2) or alanine aminotransferase 2 (ALAT2), plays a critical role in cellular growth and energetics by catalyzing the reversible transamination between alanine and α-ketoglutarate to produce pyruvate and glutamate (Glinghammar et al., 2009; Ouyang et al., 2016). Previously we had reported that loss-of-function mutations in *GPT2* cause a rare neurodevelopmental disorder that is characterized by microcephaly, intellectual disability, and motor abnormalities in humans (Baytas and Morrow, 2018; Ouyang et al., 2019; Ouyang et al., 2016). The products of the GPT2 reaction can be utilized to support ATP, protein synthesis and neurotransmitter production, all integral to neurodevelopmental processes. GPT2 has been shown to augment the biosynthetic capacity of not only neuronal cells but also of cancerous cells thereby granting them the ability of tumorigenesis (Kim et al., 2019; Smith et al., 2016). Understanding the precise role of the GPT2 protein may elucidate mechanisms for cellular growth that are commonly employed in a variety of biological contexts.

Unlike its cytosolic counterpart, GPT1, GPT2 localizes to the mitochondria and regulates metabolic processes such as alanine metabolism and the tricarboxylic acid (TCA) cycle (DeRosa and Swick, 1975; Lindblom et al., 2007). *GPT2* expression increases during the early postnatal stage in the brain, corresponding to high synaptogenic activity and a period of neural circuit development (Kang et al., 2011; Ouyang et al., 2016). As mitochondria are actively recruited to the presynaptic terminal to provide neurons with the energy required for synaptic growth and signaling (Devine and Kittler, 2018), and mitochondrial transport is tightly regulated during neuronal development (Morris and

Hollenbeck, 1993; Ruthel and Hollenbeck, 2003), dysfunction of mitochondrial processes could lead to substantial cellular impairments with neurological implications.

In mitochondria, glutamine is metabolized to glutamate by glutaminase, where it can be further converted to α-ketoglutarate, a TCA cycle intermediate (McKenna and Ferreira, 2016). The integration of α-ketoglutarate into the TCA cycle through glutamine metabolism is a key anaplerotic step in proliferating cells (DeBerardinis et al., 2007). Specifically, cancer cells exhibit a dependence on glutamine as the primary mitochondrial substrate for maintaining not only proliferation but also mitochondrial membrane potential and integrity, redox control, and macromolecular synthesis essential for cell survival (Wise and Thompson, 2010). GPT2 activity is critical to cancer cell proliferation but otherwise dispensable in non-malignant cells (Smith et al., 2016), pointing to a specific metabolic vulnerability associated with cancer cell progression that is regulated by GPT2.

We had previously generated Gpt2-null mice to assess morphological and metabolic phenotypes *in vivo* (Ouyang et al., 2016). Gpt2-null mice demonstrated significant reductions in brain size, weight and motor activity beginning at P18. Targeted metabolomics using coupled liquid chromatography and mass spectrometry (LC-MS/MS) performed using P18 Gpt2-null mouse brain samples revealed reductions in alanine and TCA cycle intermediates. Gpt2-null mouse embryonic fibroblasts exhibited almost complete loss of alanine secretion and nitrogen transfer from [α-^{15}N]-glutamine to alanine and diminished carbon transfer from [U-^{13}C]-glutamine to TCA cycle intermediates as measured by isotope tracing, confirming the importance of GPT2 in alanine and TCA cycle metabolism.

Here we modeled the loss of GPT2 in two clones of near-haploid HAP1 cell lines achieved with the CRISPR/Cas9 technique, derived from cells of a human patient with malignant chronic myeloid leukemia (Kotecki et al., 1999). As they are derived from a cancer cell lineage, HAP1 cells divide without cell cycle arrest and thus continuously face with profound metabolic needs. With increased metabolic demand and abundant cell counts, the HAP1 cell lines provide robust sampling for experimental design and analysis to assess the role of GPT2 in cellular growth. Given that GPT2 function is critical for cancer progression, we hypothesized that loss-of-function mutations in GPT2 would result in decreased cell proliferation and survival, altered metabolome and dysregulated mitochondrial mechanisms including changes in mitochondrial membrane potential and respiration. We further tested if alanine deprivation or glutaminase inhibition would expose or exacerbate any metabolic vulnerabilities in the absence of GPT2.

The loss of GPT2 in HAP1 cells is confirmed by Sanger sequencing, Western blotting, enzymatic activity and confocal microscopy. GPT2 loss in HAP1 cells causes decreases in cell size. Proliferation rates of GPT2-null cells are reduced in medium deprived of alanine. We find decreases in cell proliferation rate with glutaminase inhibition only in Clone 2 GPT2-null cells. We do not find increases in number of apoptotic cells in either clone with or without alanine deprivation or glutaminase inhibition. Assays measuring mitochondrial membrane potential and reactive oxygen species yield no differences between the wild-type and mutant clones. Seahorse XF Mito Stress Test measuring mitochondrial respiration results in varying findings across the two clones tested and overall only Clone 2 GPT2-null cells display abnormalities in respiration. We discover alterations in the metabolic profiles of both GPT2-null clones particularly in the TCA

cycle, alanine metabolism and overall amino acid metabolism. In addition to elucidating the biosynthetic mechanisms mediated by GPT2 important for cancer cell metabolism and cellular growth, this study provides a resource to study metabolic pathways that may have substantial implications for neurodevelopment.

RESULTS

Confirmation of loss of GPT2 in HAP1 cells

To confirm that the deletions in the *GPT2* gene in HAP1 cell lines were successfully introduced by CRISPR/Cas9 system, we performed Sanger sequencing of two clones. The sequences along exon 6 of the coding region confirmed an 11-base pair deletion starting at position 607 and a 20-base pair deletion starting at position 609 in the NM_133443 transcript in clone 1 (starting at position 183 in the Sanger sequence) and clone 2 (starting at position 184 in the Sanger sequence), respectively (Figure 1A). Both deletions resulted in loss of protein as evidenced by Western blotting (Figure 1B). The overall GPT enzyme activity assay, which would include activities of both GPT2 and GPT1, showed approximately 50% reduction in both clones indicating that the deletion mutations were loss-of-function.

Localization of GPT2 in mitochondria of HAP1 cells

We confirmed the mitochondrial localization of the GPT2 protein to mitochondria by both structural illumination microscopy (SIM) and confocal microscopy. In the SIM images the GPT2 puncta were enclosed by the MitoTracker Red puncta (Figure 1D). In the confocal microscopy, nearly all MitoTracker Red puncta appeared to be overlapped by the GPT2 puncta (Figure 1E). GPT2 fluorescence in the GPT2-null clones was much dimmer

compared to their wild-type clones and not appreciably greater than the background (Figure 1E).

Diminished cell size and proliferation in GPT2-null HAP1 cells.

Given the role of GPT2 in alanine biosynthesis, we hypothesized that alanine may become an essential amino acid in the absence of GPT2 and that alanine deprivation may decrease cell proliferation and survival. To this end, we continuously charted the growth of GPT2-null HAP1 cells in customized alanine-free Iscove's Modified Dulbecco's Medium (IMDM)-based media with dialyzed fetal bovine serum (dFBS) using the IncuCyte live-cell imaging system (Figure 2A). Alanine deprivation did cause a decrease in growth rate in both clones, however Clone 2 already had a decreased growth rate in the regular IMDM medium (Figure 2B). These results were particularly visible when the growth rates in mutant clones were expressed as a percentage of their respective wild-type clones (Figure 2B). Overall in all conditions, the cell areas of the GPT2-null clones were reduced compared to their wild-type clones suggesting a defect in overall growth of the cell (Figure 2C). Alanine deprivation failed to exacerbate this result; the overall cell size was already profoundly affected by the loss of GPT2. Clone 2 GPT2-null cells had smaller cell area compared to the other clones albeit with some variability across medium conditions (Figure 2C).

Given the role of GPT2 in using glutamate as a substrate to replenish the TCA cycle (anaplerosis) and the role of glutamine in cancer progression, we hypothesized that inhibition of the direct conversion of glutamine into glutamate may also cause decreases in cell proliferation and cell size (Figure 2D-E). To achieve this, we inhibited glutaminase, a mitochondrial enzyme that deaminates glutamine and produces glutamate, by a

glutaminase inhibitor bis-2-(5-phenyl acetamido-1,3,4-thiadiazol-2-yl) ethyl sulfide, BPTES. While BPTES caused decreases in growth rate in all wild-type and GPT2-null clones, only Clone 2 GPT2-null cells had a combined effect of genotype and BPTES (Figure 2D). BPTES also caused decreases in cell area in all wild-type and GPT2-null clones but the decrease was more profound in Clone 2 GPT2-null cells (Figure 2E). Glutaminase inhibition did not have the specific effect of alanine deprivation in GPT2-null clones but an overall effect on HAP1 cells. These results suggest that HAP1 cells are very susceptible to glutaminase inhibition but this is not exacerbated by the absence of GPT2.

To determine whether differences in cell proliferation are partly due to increased cell death, we continuously detected apoptotic cells in wild-type and GPT2-null clones using the IncuCyte live-cell imaging system (Figure 3A). Apoptosis was detected by the fluorescent Annexin V Orange Reagent which binds to phosphatidylserine residues that vertically flip to the outer plasma membrane during early apoptosis. There were no differences in number of apoptotic cell counts over time with or without alanine deprivation (Figure 3B) or glutaminase inhibition (Figure 3C). This suggests that decreases in growth rate in GPT2-null cells likely reflect a decrease in proliferative capacity rather than an increase in cell death.

Mitochondrial membrane potential, ROS levels and mitochondrial respiration in GPT2-null HAP1 cells.

As GPT2 localized to mitochondria and replenishes the TCA cycle, we investigated whether defects in growth rate and size in GPT2-null HAP1 cells are due to mitochondrial mechanisms. One of the major roles of the TCA cycle is to produce NADH and FADH2, electron donors for the electron transport chain. With continuous supply of substrates and

co-factors, the electron transport chain produces and utilizes the hyperpolarized membrane potential in order to produce ATP. Mitochondrial membrane potential can be indirectly assessed by the fluorescence emitted by positively charged dyes that locate to the hyperpolarized mitochondrial membrane, such as tetramethylrhodamine, ethyl ester (TMRE). We determined whether absence of GPT2 in HAP1 cells may have an effect on the mitochondrial membrane potential that may underlie the observed growth defects. We could not find any differences between the fluorescence intensities of wild-type and GPT2-null cells with or without alanine deprivation (Figure 4B) or glutaminase inhibition (Figure 4D). We also quantified the mitochondrial footprint per cell as a measure of mitochondrial mass using the TMRE staining through the Mitochondrial Network Analysis toolkit in ImageJ. We failed to find any differences in mitochondrial footprint across all media conditions with or without alanine deprivation (Figure 4C) or glutaminase inhibition (Figure 4E). These results indicate that mitochondrial membrane potential and mass appear to be intact in GPT2-null HAP1 cells.

Mitochondrial superoxide production is a major source of oxidative stress. We evaluated the levels of mitochondrial superoxide by using MitoSOX which locates to mitochondria with its positively charged residues and fluoresces red when oxidized by superoxide (Figure 5A). We failed to find any changes in the fluorescence intensity of MitoSOX in GPT2-null cells with or without alanine deprivation or glutaminase inhibition (Figure 5B). To corroborate this finding, we performed a 2',7'-dichlorodihydrofluorescein diacetate (DCFDA) assay to indirectly quantify overall levels of reactive oxygen species (ROS) in HAP1 cells with tert-butyl hydroperoxide (TBHP) as a control oxidant. Similarly,

there were no changes in the fluorescence intensity of DCFDA in GPT2-null HAP1 cells. We conclude that overall ROS levels are unchanged in GPT2-null HAP1 cells.

Mitochondrial dysfunction may manifest in abnormal mitochondrial respiration. We performed Seahorse XFe96 Mito Stress Test on GPT2-null HAP1 clones (Figure 6). Mito Stress Test sequentially injects compounds to inhibit different complexes of the electron transport chain to assess oxygen consumption associated with each complex. First oligomycin which inhibits ATP synthase (Complex V), then Carbonyl cyanide-p-trifluoromethoxyphenylhydrazone (FCCP), an uncoupling agent, which collapses the proton gradient and allows for a free flow of protons through Complex IV for maximum possible respiration, and finally Rotenone/Antimycin A which inhibit Complexes I and III respectively to shut down mitochondrial respiration. This serves as a way to examine various aspects of mitochondrial respiration, including basal and maximal respiration, proton leak, spare respiratory capacity, ATP production and non-mitochondrial oxygen consumption. Oxygen consumption rate (OCR) normalized by cell count plotted over time revealed no changes between Clone 1 wild-type and GPT2-null HAP1 cells (Figure 6A). However, the overall respiration of the Clone 2 GPT2-null cells was lower compared to all other clones. Extracellular acidification rates (ECAR) plotted over time were similar across all clones with trending decreases in Clone 2 GPT2-null cells (Figure 6A). We also plotted OCR to ECAR ratio to assess whether the cells relied more on either oxidative phosphorylation or glycolysis (Figure 6B). The ratios were unchanged across all clones with trending decreases in Clone 2 GPT2-null cells. In all Mito Stress Test assay parameters, only Clone 2 GPT2-null cells showed decreases in oxygen consumption associated with basal respiration, maximal respiration, spare respiratory capacity, and ATP

production (Figure 6C). Clone 2 GPT2-null also showed trending decreases in spare respiratory capacity expressed as percentage of basal respiration, and respiratory control ratio (maximal respiration divided by proton leak) which represents maximum respiration achievable relative to the respiration spent to balance the proton leak (Brand and Nicholls, 2011).

Mito Stress Test may be performed after glutaminase inhibition with BPTES to expose any mitochondrial vulnerability to blockage of glutamine utilization as a substrate. (Figure 6D). We did not observe any major changes with glutaminase inhibition and Clone 2 GPT2-null cells showed diminished OCR levels throughout the assay. ECAR values were unchanged (Figure 6D) and OCR to ECAR ratios were similar across all clones (Figure 6E). In all Mito Stress Test assay parameters, similar to the test without any previous inhibition, only Clone 2 GPT2-null cells had decreased maximal respiration and a very slight but statistically significant decrease in non-mitochondrial oxygen consumption along with trending decreases in basal respiration, proton leak, spare respiratory capacity and ATP production (Figure 6F). Acute response to BPTES had trending decreases in Clone 1 GPT2-null, Clone 2 wild-type and GPT2-null cells compared to Clone 1 wild-type. Overall, we did not observe major changes in mitochondrial respiration or the associated parameters as measured by Seahorse Extracellular Flux Analyzer in Clone 1 GPT2-null cells but Clone 2 GPT2-null cells displayed abnormal mitochondrial respiration characteristics.

Altered metabolic profiles in GPT2-null HAP1 Cells.

To investigate the metabolic mechanisms behind the decreased proliferative capacity and reduced cell size of GPT2-null clones, we performed targeted metabolomics by liquid chromatography coupled to mass spectrometry (LC-MS/MS) (Figure 7,

Supplementary Table 1). The 2D Score plots of principal component analysis (PCA) showed that the two GPT2-null clones separated well from their respective wild-type clones although Clone 1 mutants overall appeared to separate better than Clone 2 mutants (Figure 7A). We plotted the metabolites with statistically significant fold changes with respect to their wild-type clones in a volcano plot (Figure 7B). Both clones exhibited major decreases in the TCA cycle intermediates, including fumarate, malate and isocitrate. Interestingly, we observed increases in kynurenine and xanthurenic acid related to tryptophan degradation pathway of which alanine is an end product (Phillips, 2014). A decrease in alanine, previously reported to occur in Gpt2-null mouse brain tissues (Ouyang et al., 2016), was found only in Clone 1 GPT2-null HAP1 cells. We also constructed a heat map consisting of top most significantly changed 25 metabolites (by raw p-value) (Figure 7C). To identify significantly changed processes, we performed an over-representation analysis and showed top 25 processes ordered by raw p-value (Figure 7D). Among the most significantly changed processes in the comparison of Clone 1 wild-type and GPT2-null cells were Alanine metabolism, Urea cycle, Glycine, Serine, Purine, Arginine and Proline metabolism, TCA cycle and Aspartate metabolism, all with false discovery rates less than 0.05. Clone 2 GPT2-null significantly changed processes were Urea cycle, Arginine, Proline, Aspartate and Purine Metabolism, Spermidine and Spermine Biosynthesis, TCA cycle and Pantothenate and CoA Biosynthesis although none were with false discovery rates less than 0.05. While the two GPT2-null clones shared similar metabolic signatures, Clone 1 GPT2-null appeared to result in a more robust alteration of the metabolome. The overall altered metabolic profile indicates dysregulation of alanine metabolism, the TCA cycle and amino acid metabolism in GPT2-null HAP1 cells.

FIGURE 1

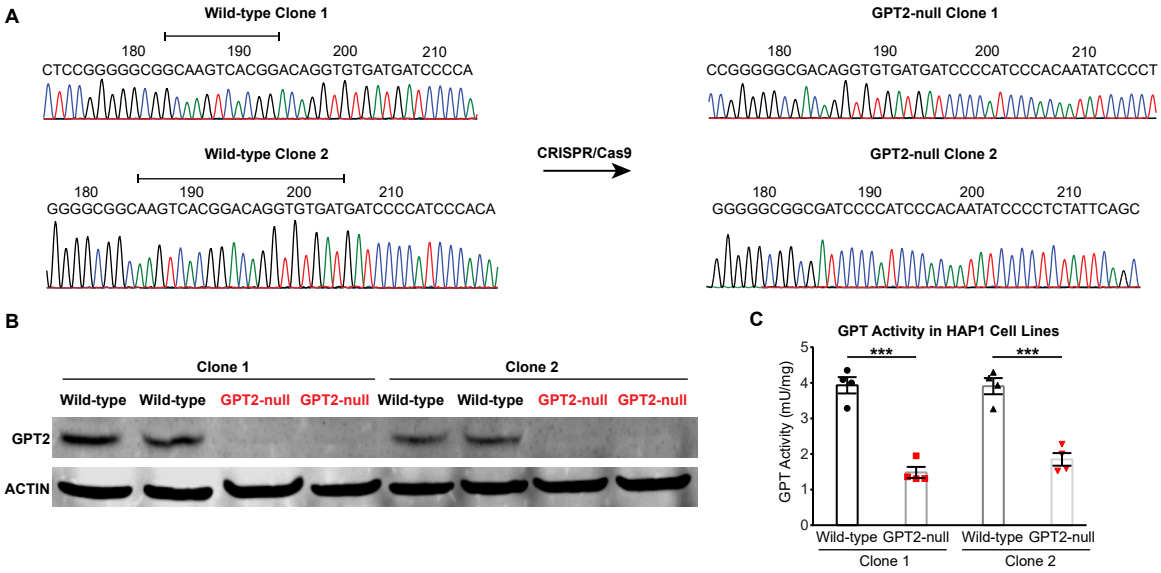

D Structural Illumination Microscopy

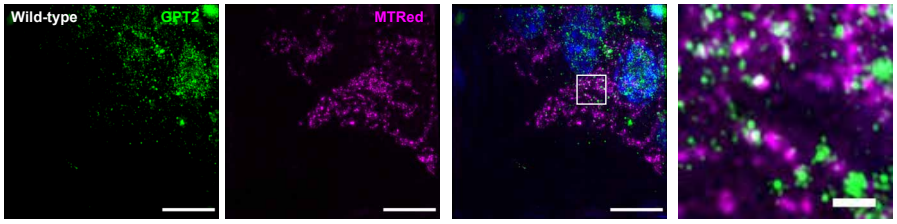

E Confocal Microscopy

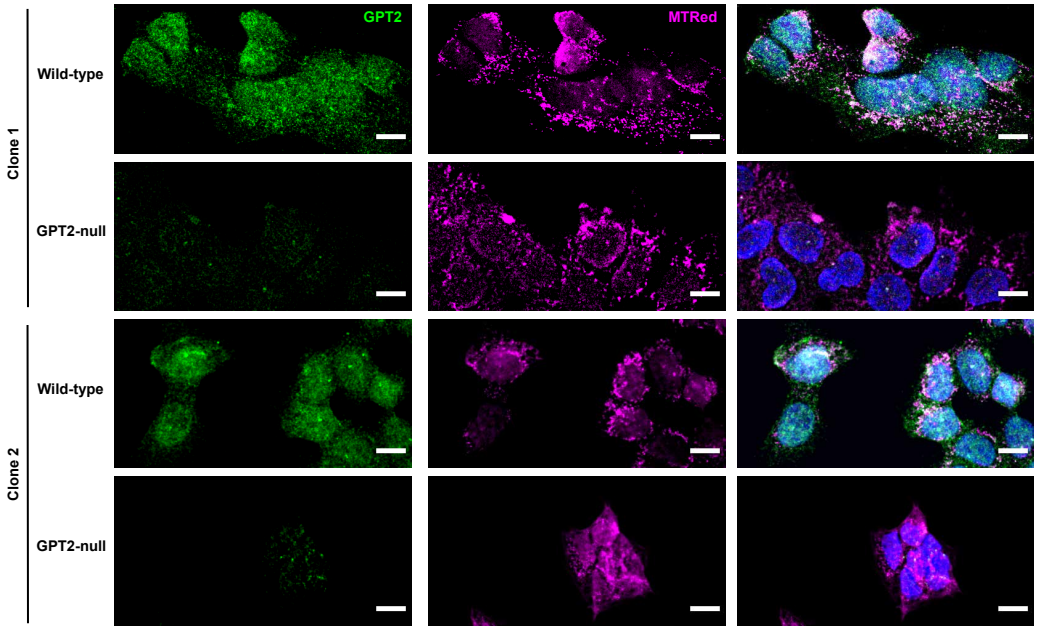

FIGURE 2

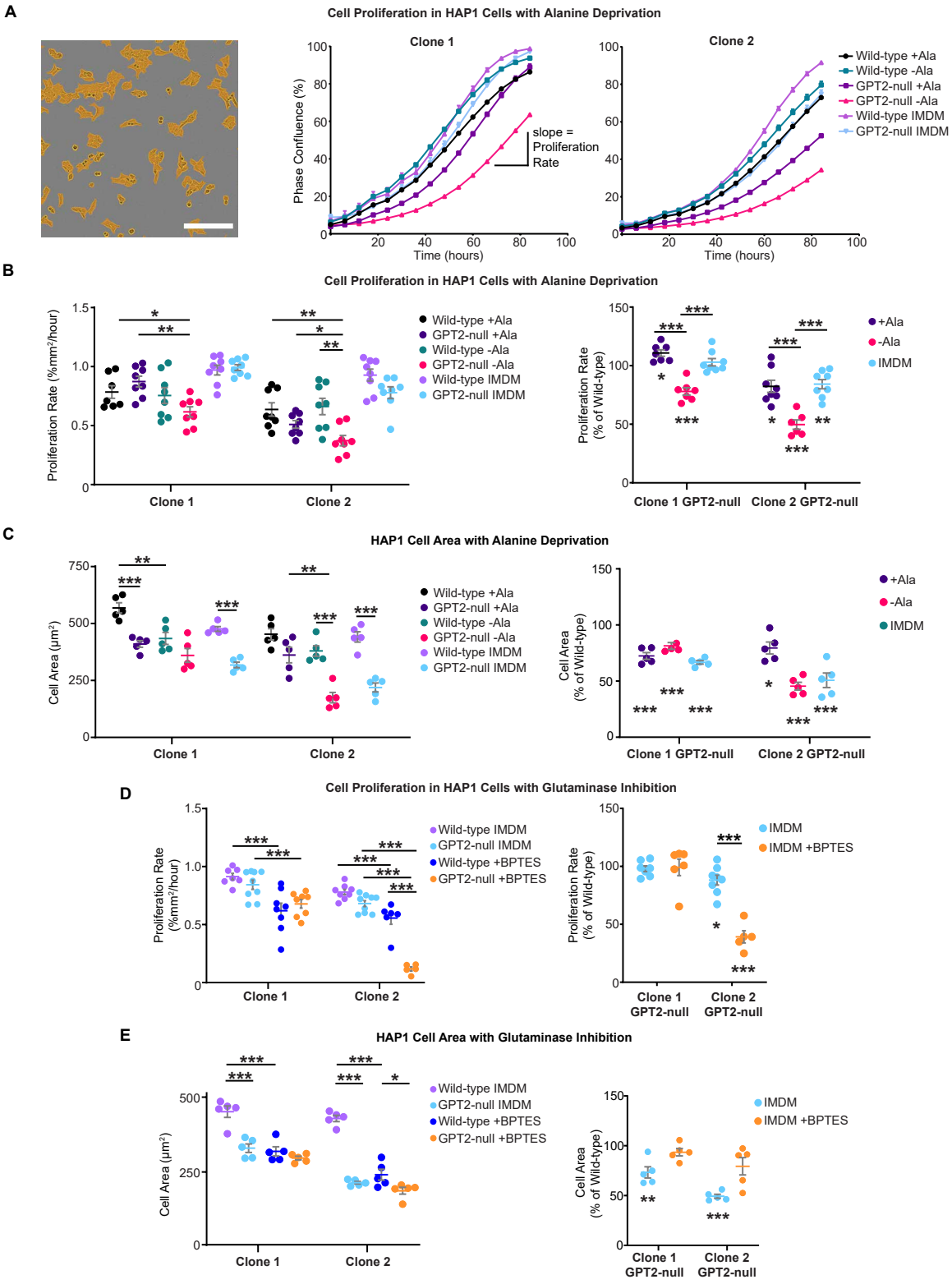
A
Cell Proliferation in HAP1 Cells with Alanine Deprivation
Clone 1
Clone 2
Phase Confluence (%)
Time (hours)
slope = Proliferation Rate
Wild-type +Ala
Wild-type -Ala
GPT2-null +Ala
GPT2-null -Ala
Wild-type IMDM
GPT2-null IMDM
B
Cell Proliferation in HAP1 Cells with Alanine Deprivation
Proliferation Rate (%mm²/hour)
Clone 1
Clone 2
Proliferation Rate (% of Wild-type)
Clone 1 GPT2-null
Clone 2 GPT2-null
+Ala
-Ala
IMDM
C
HAP1 Cell Area with Alanine Deprivation
Cell Area (µm²)
Cell Area (% of Wild-type)
D
Cell Proliferation in HAP1 Cells with Glutaminase Inhibition
GPT2-null IMDM
Wild-type +BPTES
GPT2-null +BPTES
IMDM +BPTES
E
HAP1 Cell Area with Glutaminase Inhibition

FIGURE 3

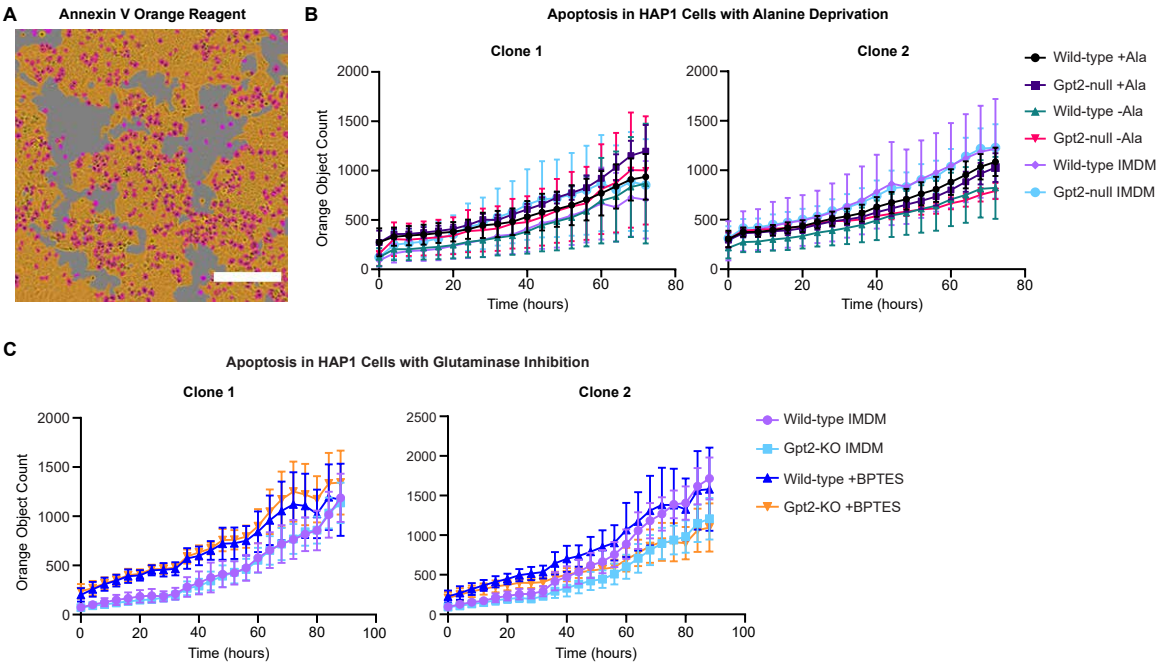
A
Annexin V Orange Reagent
B
Apoptosis in HAP1 Cells with Alanine Deprivation
Clone 1
Clone 2
Orange Object Count
Time (hours)
Wild-type +Ala
Gpt2-null +Ala
Wild-type -Ala
Gpt2-null -Ala
Wild-type IMDM
Gpt2-null IMDM
C
Apoptosis in HAP1 Cells with Glutaminase Inhibition
Clone 1
Clone 2
Orange Object Count
Time (hours)
Wild-type IMDM
Gpt2-KO IMDM
Wild-type +BPTES
Gpt2-KO +BPTES

FIGURE 4

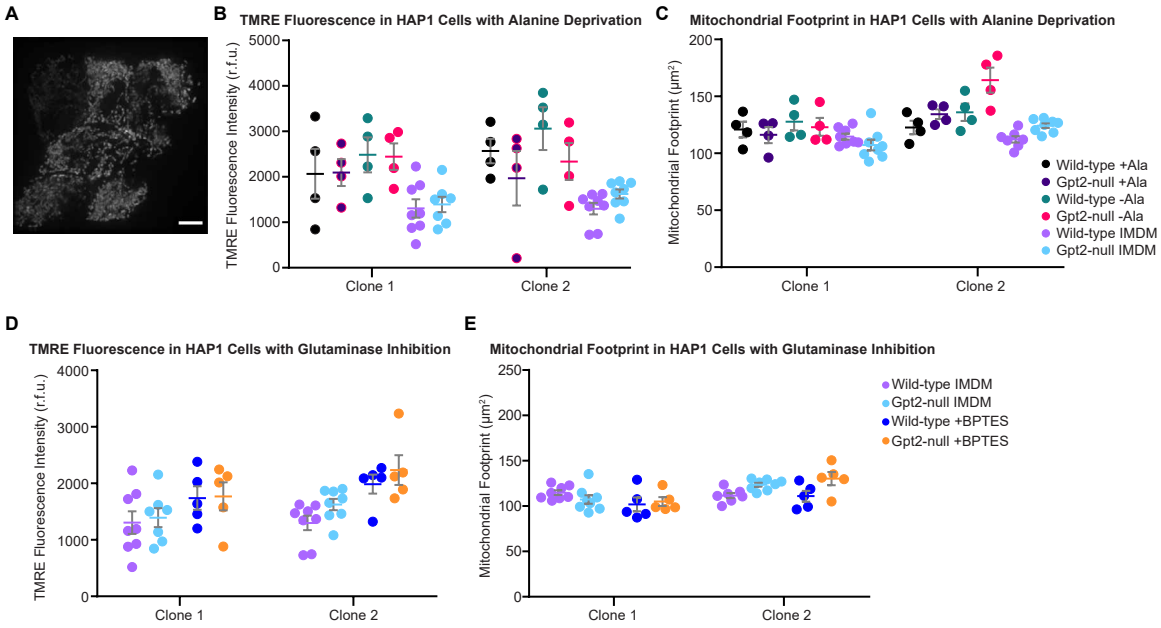
A
B
TMRE Fluorescence in HAP1 Cells with Alanine Deprivation
TMRE Fluorescence Intensity (r.f.u.)
5000
4000
3000
2000
1000
0
Clone 1
Clone 2
C
Mitochondrial Footprint in HAP1 Cells with Alanine Deprivation
Mitochondrial Footprint (µm²)
200
150
100
50
0
Clone 1
Clone 2
Wild-type +Ala
Gpt2-null +Ala
Wild-type -Ala
Gpt2-null -Ala
Wild-type IMDM
Gpt2-null IMDM
D
TMRE Fluorescence in HAP1 Cells with Glutaminase Inhibition
TMRE Fluorescence Intensity (r.f.u.)
4000
3000
2000
1000
0
Clone 1
Clone 2
E
Mitochondrial Footprint in HAP1 Cells with Glutaminase Inhibition
Mitochondrial Footprint (µm²)
250
200
150
100
50
0
Clone 1
Clone 2
Wild-type IMDM
Gpt2-null IMDM
Wild-type +BPTES
Gpt2-null +BPTES

FIGURE 5

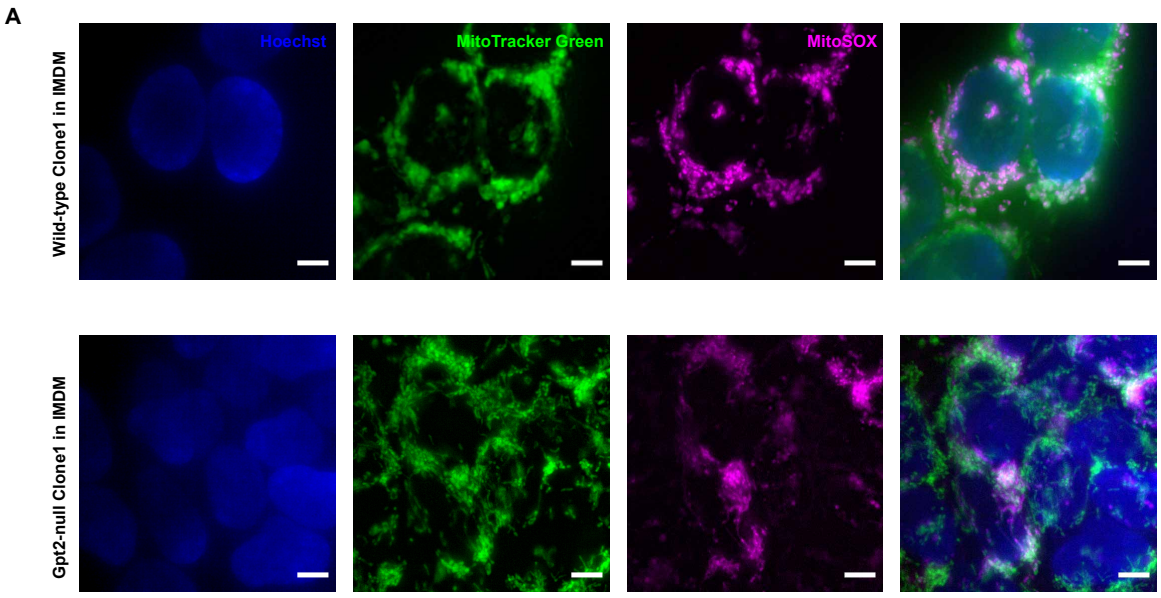
A
Hoechst
MitoTracker Green
MitoSOX
Wild-type Clone1 in IMDM
Gpt2-null Clone1 in IMDM

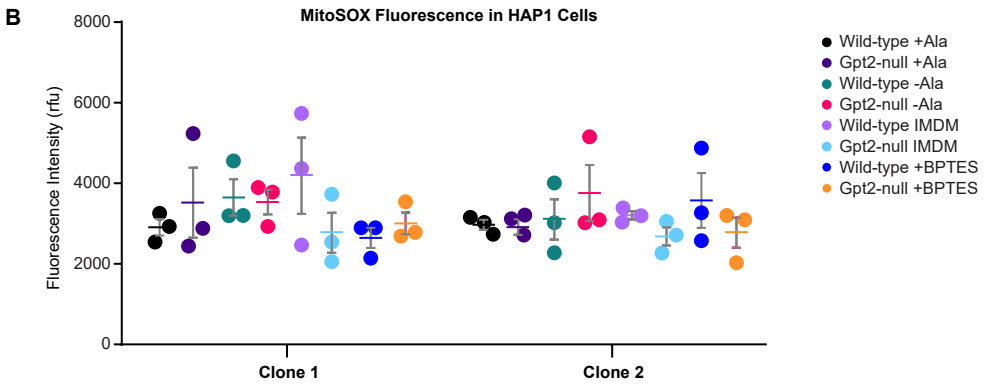
B
MitoSOX Fluorescence in HAP1 Cells
Fluorescence Intensity (rfu)
8000
6000
4000
2000
0
Clone 1
Clone 2
Wild-type +Ala
Gpt2-null +Ala
Wild-type -Ala
Gpt2-null -Ala
Wild-type IMDM
Gpt2-null IMDM
Wild-type +BPTES
Gpt2-null +BPTES

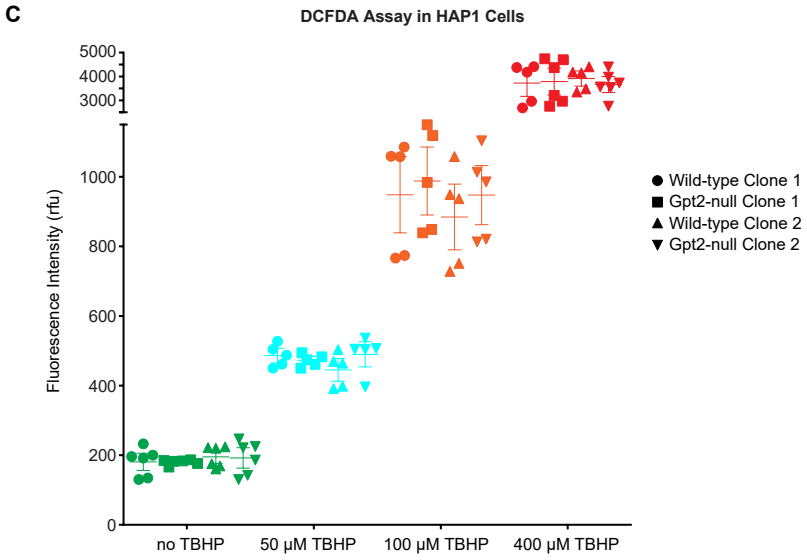
C
DCFDA Assay in HAP1 Cells
Fluorescence Intensity (rfu)
5000
4000
3000
1000
800
600
400
200
0
no TBHP
50 μM TBHP
100 μM TBHP
400 μM TBHP
Wild-type Clone 1
Gpt2-null Clone 1
Wild-type Clone 2
Gpt2-null Clone 2

FIGURE 6

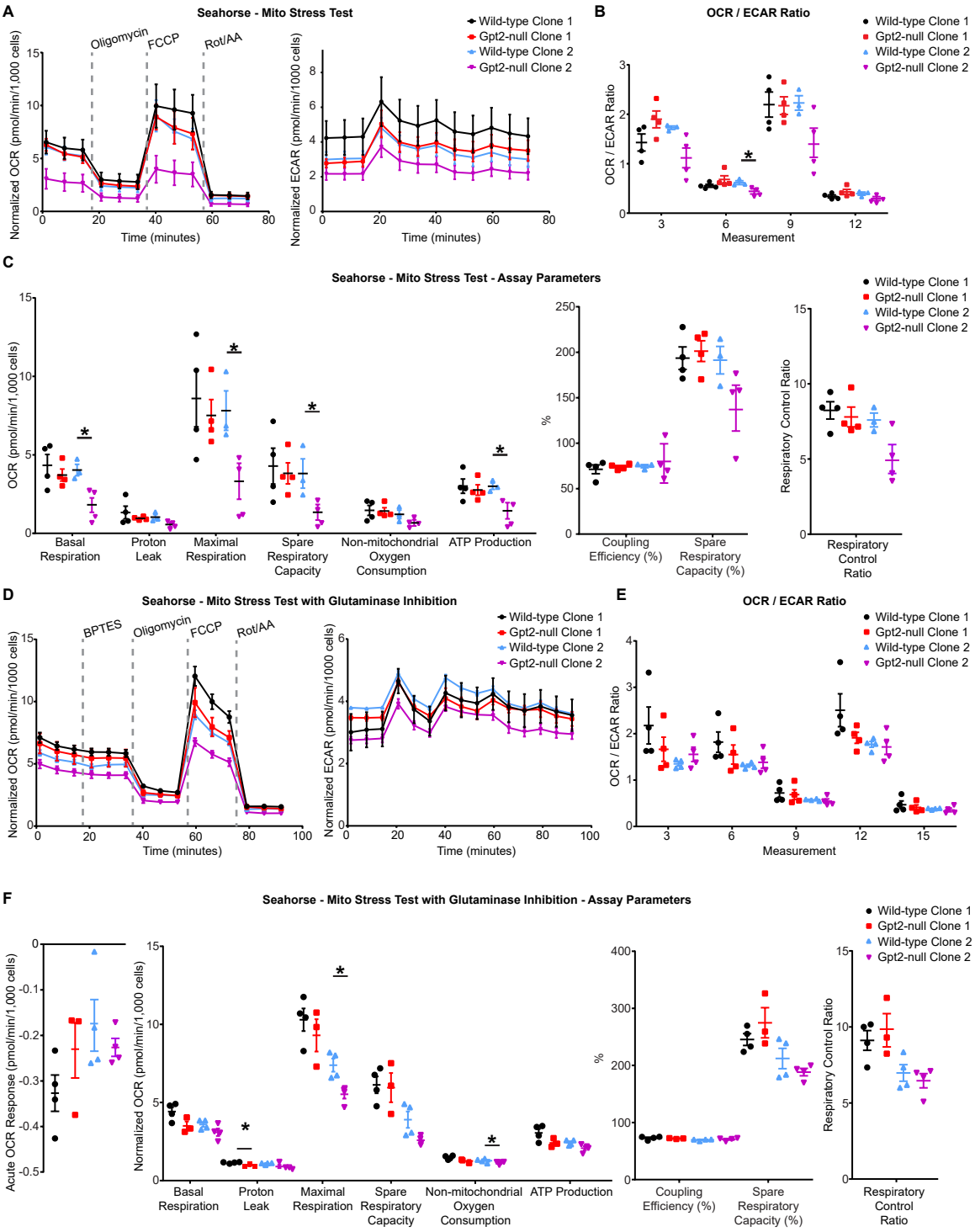
A
Seahorse - Mito Stress Test
Oligomycin
FCCP
Rot/AA
Normalized OCR (pmol/min/1,000 cells)
Normalized ECAR (pmol/min/1000 cells)
Time (minutes)
Wild-type Clone 1
Gpt2-null Clone 1
Wild-type Clone 2
Gpt2-null Clone 2
B
OCR / ECAR Ratio
OCR / ECAR Ratio
Measurement
C
Seahorse - Mito Stress Test - Assay Parameters
OCR (pmol/min/1,000 cells)
Basal Respiration
Proton Leak
Maximal Respiration
Spare Respiratory Capacity
Non-mitochondrial Oxygen Consumption
ATP Production
%
Coupling Efficiency (%)
Spare Respiratory Capacity (%)
Respiratory Control Ratio
Respiratory Control Ratio
D
Seahorse - Mito Stress Test with Glutaminase Inhibition
BPTES
Oligomycin
FCCP
Rot/AA
Normalized OCR (pmol/min/1000 cells)
Normalized ECAR (pmol/min/1000 cells)
Time (minutes)
E
OCR / ECAR Ratio
OCR / ECAR Ratio
Measurement
F
Seahorse - Mito Stress Test with Glutaminase Inhibition - Assay Parameters
Acute OCR Response (pmol/min/1,000 cells)
Normalized OCR (pmol/min/1,000 cells)
Basal Respiration
Proton Leak
Maximal Respiration
Spare Respiratory Capacity
Non-mitochondrial Oxygen Consumption
ATP Production
%
Coupling Efficiency (%)
Spare Respiratory Capacity (%)
Respiratory Control Ratio
Respiratory Control Ratio

FIGURE 7

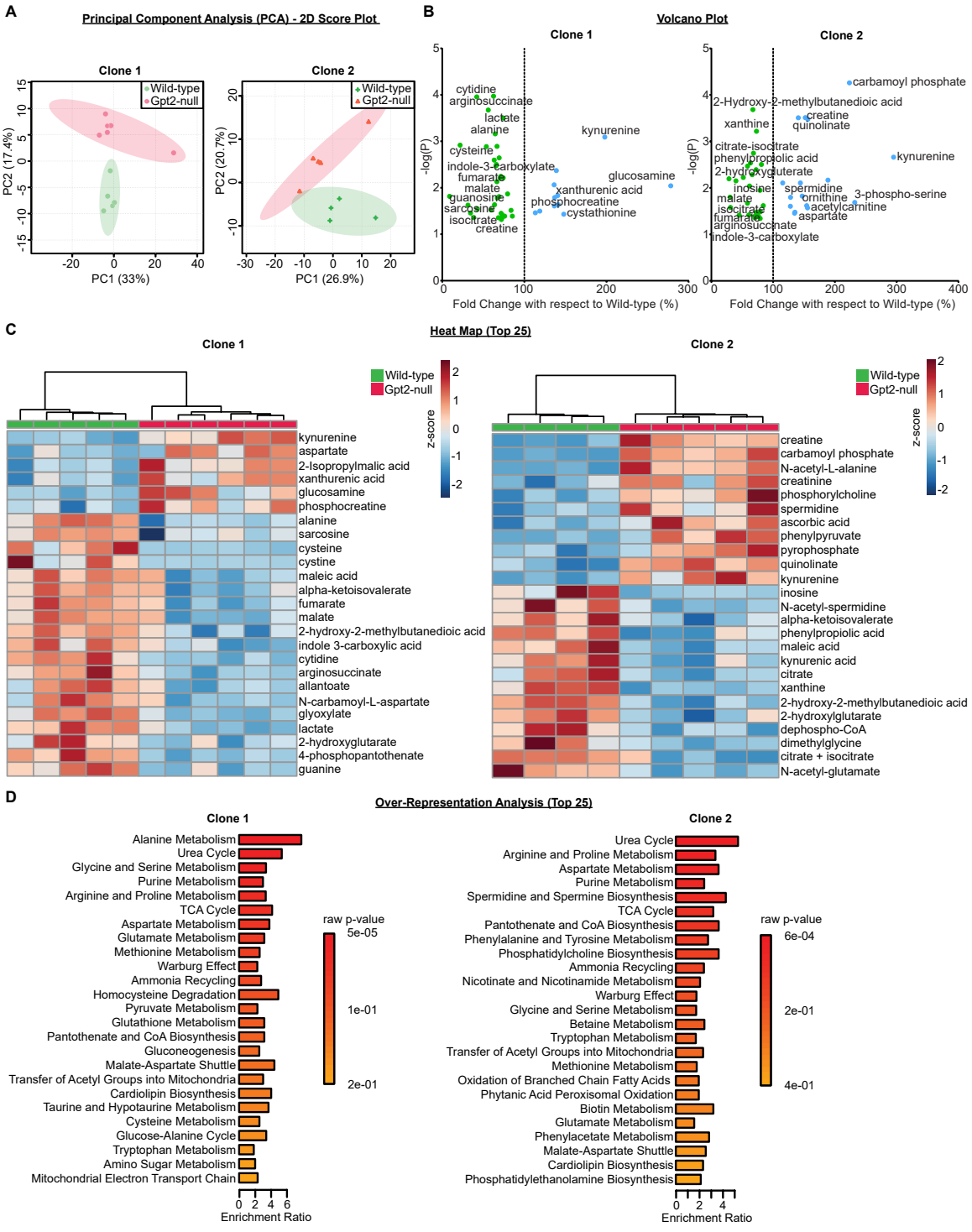
A
Principal Component Analysis (PCA) - 2D Score Plot
Clone 1
Clone 2
Wild-type
Gpt2-null
PC1 (33%)
PC2 (17.4%)
PC1 (26.9%)
PC2 (20.7%)
B
Volcano Plot
Clone 1
Clone 2
-log(P)
Fold Change with respect to Wild-type (%)
cytidine
arginosuccinate
lactate
alanine
cysteine
indole-3-carboxylate
fumarate
malate
guanosine
sarcosine
isocitrate
creatine
kynurenine
glucosamine
xanthurenic acid
phosphocreatine
cystathionine
carbamoyl phosphate
2-Hydroxy-2-methylbutanedioic acid
creatine
xanthine
quinolinate
citrate-isocitrate
phenylpropiolic acid
2-hydroxyglutarate
inosine
spermidine
ornithine
3-phospho-serine
acetylcarnitine
aspartate
C
Heat Map (Top 25)
Clone 1
Clone 2
Wild-type
Gpt2-null
z-score
kynurenine
aspartate
2-Isopropylmalic acid
xanthurenic acid
glucosamine
phosphocreatine
alanine
sarcosine
cysteine
cystine
maleic acid
alpha-ketoisovalerate
fumarate
malate
2-hydroxy-2-methylbutanedioic acid
indole 3-carboxylic acid
cytidine
arginosuccinate
allantoate
N-carbamoyl-L-aspartate
glyoxylate
lactate
2-hydroxyglutarate
4-phosphopantothenate
guanine
creatine
carbamoyl phosphate
N-acetyl-L-alanine
creatinine
phosphorylcholine
spermidine
ascorbic acid
phenylpyruvate
pyrophosphate
quinolinate
kynurenine
inosine
N-acetyl-spermidine
alpha-ketoisovalerate
phenylpropiolic acid
maleic acid
kynurenic acid
citrate
xanthine
2-hydroxy-2-methylbutanedioic acid
2-hydroxylglutarate
dephospho-CoA
dimethylglycine
citrate + isocitrate
N-acetyl-glutamate
D
Over-Representation Analysis (Top 25)
Clone 1
Clone 2
raw p-value
Enrichment Ratio
Alanine Metabolism
Urea Cycle
Glycine and Serine Metabolism
Purine Metabolism
Arginine and Proline Metabolism
TCA Cycle
Aspartate Metabolism
Glutamate Metabolism
Methionine Metabolism
Warburg Effect
Ammonia Recycling
Homocysteine Degradation
Pyruvate Metabolism
Glutathione Metabolism
Pantothenate and CoA Biosynthesis
Gluconeogenesis
Malate-Aspartate Shuttle
Transfer of Acetyl Groups into Mitochondria
Cardiolipin Biosynthesis
Taurine and Hypotaurine Metabolism
Cysteine Metabolism
Glucose-Alanine Cycle
Tryptophan Metabolism
Amino Sugar Metabolism
Mitochondrial Electron Transport Chain
Urea Cycle
Arginine and Proline Metabolism
Aspartate Metabolism
Purine Metabolism
Spermidine and Spermine Biosynthesis
TCA Cycle
Pantothenate and CoA Biosynthesis
Phenylalanine and Tyrosine Metabolism
Phosphatidylcholine Biosynthesis
Ammonia Recycling
Nicotinate and Nicotinamide Metabolism
Warburg Effect
Glycine and Serine Metabolism
Betaine Metabolism
Tryptophan Metabolism
Transfer of Acetyl Groups into Mitochondria
Methionine Metabolism
Oxidation of Branched Chain Fatty Acids
Phytanic Acid Peroxisomal Oxidation
Biotin Metabolism
Glutamate Metabolism
Phenylacetate Metabolism
Malate-Aspartate Shuttle
Cardiolipin Biosynthesis
Phosphatidylethanolamine Biosynthesis

FIGURE LEGENDS

Figure 1. Cellular localization and deletion of GPT2 in HAP1 cell lines.

A. Deletions are successfully introduced to *GPT2* by CRISPR/Cas9 in HAP1 cells. Sanger sequencing around exon 6 of the human *GPT2* transcript NM_133443. The deleted sequences are noted with double-ended lines above the wild-type sequences (left) and the resulting mutant clones are shown on the right.

B. GPT2 protein is absent in both GPT2-null clones. Western blots of the two wild-type and GPT2-null clones with two replicates of each, GPT2 appears at the predicted size of 58 kDa. Actin (42 kDa) is stained for confirming protein loading in each lane.

C. Overall GPT activity is profoundly reduced in GPT2-null clones. This enzyme assay would include both GPT1 and GPT2 enzyme activities. ***$P<0.001$.

D. Structural illumination microscopy shows GPT2 puncta enclosed by mitochondria. The images are taken using Clone 1 wild-type cells. GPT2 is shown in green and mitochondria are labeled with MitoTracker Red (magenta). Scale bar: 10 μm. The white box in the merged image encloses the area of the zoomed-in image on the far right, scale bar: 1 μm.

E. Confocal microscopy confirms the absence of GPT2 protein in GPT2-null clones and localization of GPT2 to mitochondria. GPT2 in green and MitoTracker Red in magenta, with Hoechst 33342 in blue in the merged image on the far right. Scale bar: 10 μm. Inset scale bar: 5 μm.

Figure 2. Cell size and proliferation rate are decreased in GPT2-null HAP1 cells.

A. Masking of HAP1 cells using IncuCyte live-cell imaging system and an example experiment showing the progression of the phase confluence (%) of the culture plotted over time with or without alanine deprivation. The proliferation rate is calculated from the slope of the linear phase. +Ala and -Ala refer to custom-made IMDM-based media (+dialyzed fetal bovine serum, dFBS) with or without alanine, respectively. IMDM refers to the regular medium with normal FBS. Scale bar: 250 μm.

B. Both GPT2-null clones proliferate at a slower rate with alanine deprivation. Proliferation rate is expressed as percent confluence per hour. Proliferation of GPT2-null clones with alanine deprivation expressed as a percentage of their wild-type clones is given on the right. The asterisks above the data refer to the p-value obtained from two-tailed t-test between groups. The asterisks below the data refer to the p-value obtained from two-tailed one-sample t-test.

C. GPT2-null cells in both clones are smaller than their wild-type clones regardless of alanine deprivation. Cell area of GPT2-null clones expressed as a percentage of their wild-type clones in media with or without alanine is given on the right. The asterisks below the data refer to the p-value obtained from two-tailed one-sample t-test.

D. Glutaminase inhibition affects proliferation of all wild-type and GPT2-null clones. The cells were treated with 3 μM BPTES for the entire duration of imaging. Proliferation rate of Clone 2 GPT2-null cells is particularly affected with glutaminase inhibition. The proliferation rate of the mutant clones expressed as a percentage of wild-type clones is given on the right. The asterisks above the data refer to the p-value obtained from two-tailed t-test comparison between media conditions. The asterisks below the data refer to

the p-value obtained from one-sample two-tailed t-test comparison to a hypothetical mean value of 100.

E. Glutaminase inhibition affects cell size of all wild-type and GPT2-null clones. Cell area of GPT2-null clones expressed as a percentage of their wild-type clones in media with or without glutaminase inhibition is given on the right. The asterisks below the data refer to the p-value obtained from one-sample two-tailed t-test comparison to a hypothetical mean value of 100.

*0.01< P <0.05, **0.001< P <0.01, ***P <0.001.

Figure 3. Apoptotic cell counts are unchanged in GPT2-null HAP1 cells.

A. Masking and detection of Annexin V Orange reagent (magenta) in HAP1 cells using IncuCyte live-cell imaging system. Scale bar: 250 μm.

B. Orange object counts plotted over time with or without alanine deprivation. +Ala and -Ala refer to custom-made IMDM-based media (+dFBS) with or without alanine, respectively. IMDM refers to the regular medium with normal FBS. n = 4 vials per group.

C. Orange object counts plotted over time with or without glutaminase inhibition. The cells were treated with 3 μM BPTES for the entire duration of imaging. n = 4 vials per group.

*0.01< P <0.05, **0.001< P <0.01, ***P <0.001.

Figure 4. Mitochondrial membrane potential and footprint are unchanged in GPT2-null HAP1 cells.

A. Example image of TMRE staining in HAP1 cells. Scale bar: 5 μm.

B. Fluorescent intensities of TMRE in HAP1 cells with or without alanine deprivation. +Ala and -Ala refer to custom-made IMDM-based media (+dFBS) with or without alanine, respectively. IMDM refers to the regular medium with normal FBS. r.f.u.: relative fluorescence unit.

C. Mitochondrial footprint per cell measured as area covered by TMRE staining in HAP1 cells with or without alanine deprivation.

D. Fluorescent intensities of TMRE in HAP1 cells with or without glutaminase deprivation. The cells were treated with 3 μM BPTES for the entire duration of imaging.

E. Mitochondrial footprint per cell measured as area covered by TMRE staining in HAP1 cells with or without glutaminase inhibition.

Figure 5. MitoSOX staining and DCFDA assay in HAP1 cells.

A. MitoSOX staining in Clone 1 wild-type (top) and GPT2-null (bottom) cells. Mitochondria were stained with MitoTracker green, MitoSOX shown in magenta and cell nuclei stained with Hoechst 33342 in blue. Scale bar: 5 μm.

B. Fluorescence intensity of MitoSOX in HAP1 cells with or without alanine deprivation or glutaminase inhibition. +Ala and -Ala refer to custom-made IMDM-based media (+dFBS) with or without alanine, respectively. IMDM refers to the regular medium with normal FBS. For glutaminase inhibition, the cells were treated with 3 μM BPTES for the entire duration of imaging. r.f.u: relative fluorescence unit.

C. DCFDA assay with varying concentrations of THBP in HAP1 cells in complete IMDM medium.

Figure 6. Seahorse Mito Stress Test in GPT2-null HAP1 cells.

A. Mitochondrial respiration as measured by Seahorse XFe96 Flux Analyzer in HAP1 cells. Mito Stress Test is shown; oxygen consumption rate per 1,000 cells (OCR, left) and extracellular acidification rate (ECAR, right) plotted over time. The baseline respiration epoch is followed by oligomycin, FCCP and Rotenone/Antimycin A (Rot/AA) epochs each starting after the dashed gray line, each epoch contains three consecutive measurements. n = 3-4 vials per group.

B. OCR to ECAR ratios calculated from the Mito Stress Test. The third, sixth and ninth measurements are immediately taken before oligomycin, FCCP and Rot/AA injections and the twelfth measurement is the last reading of the test.

C. Assay parameters of the Seahorse Mito Stress Test in HAP1 cells. Assay parameters include normalized OCR values associated with basal respiration, proton leak, maximal respiration, spare respiratory capacity, non-mitochondrial oxygen consumption, ATP production, coupling efficiency as a percentage, spare respiratory capacity as a percentage and respiratory control ratio.

D. Mito Stress Test performed with glutaminase inhibition after acute injection of BPTES. Normalized OCR (left) and ECAR (right) values plotted over time are shown. The baseline respiration epoch is followed by BPTES, oligomycin, FCCP and Rot/AA epochs each

starting after the dashed gray line; each epoch contains three consecutive measurements. n = 3-4 vials per group.

E. OCR to ECAR ratios calculated from the Mito Stress Test with glutaminase inhibition. The third, sixth, ninth and twelfth measurements are immediately taken before BPTES, oligomycin, FCCP and Rot/AA injections and the fifteenth measurement is the last reading of the test.

F. Assay parameters of the Seahorse Mito Stress Test with glutaminase inhibition in HAP1 cells. Assay parameters include normalized OCR values associated with acute response to BPTES, basal respiration, proton leak, maximal respiration, spare respiratory capacity, non-mitochondrial oxygen consumption, ATP production, coupling efficiency as a percentage, spare respiratory capacity as a percentage and respiratory control ratio.

*$0.01 < P < 0.05$.

Figure 7. Targeted metabolomics reveals altered metabolic profiles in GPT2-null HAP1 cells.

A. 2D Score plots of principal component analysis (PCA) of targeted metabolomics in HAP1 cells. The peak intensities obtained from liquid chromatography coupled to mass spectrometry (LC-MS/MS) were normalized to the sample median and auto-scaled (mean-centered and divided by the standard deviation of each group). Analyses were performed in MetaboAnalyst 4.0 (https://www.metaboanalyst.ca). Both clones of wild-type (green) and GPT2-null (red) HAP1 cell groups were well separated.

B. Volcano plots of targeted metabolomics in HAP1 cells. The fold changes were plotted on the x-axis, as percentage of the wild-type average peak intensity values. The y-axis is -log (raw p-value) where the higher value indicates more statistically significant difference is between wild-type and GPT2-null clones. The dashed line denotes 100% of the wild-type; any metabolite left side of the line has a decreased value (green dots) and any metabolite right side of the line has an increased value (blue dots) compared to the wild-type. Raw data along with results of all statistical analyses can be found in Supplementary Table 1.

C. Heat map clustering of the most significantly changed metabolites in GPT2-null HAP1 cells. The z-scores color scale is given on the right. The top 25 metabolites with lowest raw p-values are listed. Green samples are wild-type, red are GPT2-null.

D. Alanine, TCA cycle, and amino acid metabolism are altered in GPT2-null HAP1 cells. Over-representation analysis of significantly changed metabolites associated with metabolic pathways. The raw p-value color scale is given on the right. Enrichment ratio is the number of observed hits divided by hits expected by chance in a given metabolite pathway set. Metabolites included in each metabolic pathway set and related statistical analyses can be found in Supplementary Table 1.

DISCUSSION

This study identifies glutamate pyruvate transaminase 2 (GPT2) as a critical metabolic enzyme in determining cell size and proliferation of human cancerous HAP1 cell lines. The loss of GPT2 in HAP1 cells causes decreases in cell size and with alanine deprivation GPT2-null cells divide at a slower rate. We performed various assays investigating possible mitochondrial mechanisms, such as mitochondrial membrane potential, reactive oxygen species, respiration which resulted in varying findings across the two clones tested. We discover alterations in the metabolic profiles of the GPT2-null clones particularly in the TCA cycle, alanine metabolism and overall amino acid metabolism. Our study in HAP1 cell lines provide a tenable biological resource for studying the GPT2 enzyme and its role in mitochondrial mechanisms underlying cellular growth.

We characterize the successful deletion of the GPT2 gene and consequently the protein in HAP1 cells (Figure 1). However, the overall GPT enzyme activity is only halved. Relative contributions of the two proteins to cell size and proliferation have not been studied simultaneously. Although GPT1 and GPT2 catalyze the same reaction in cytosolic and mitochondrial compartments respectively, the two enzymes may act upon different processes. For example, with inhibition of pyruvate entry into the mitochondria, alanine incorporation into lipids depends on GPT2 but not GPT1 in HEK293T cells (Bowman et al., 2016). Future studies are warranted to investigate if loss of GPT1 results in a similar growth defect.

GPT2 has been found to be necessary for survival and proliferation upon glutamine inhibition in HeLa cells (Kim et al., 2019). Our data support this view only for

Clone 2 GPT2-null HAP1 cells. Proliferation rates of Clone 1 wild-type and GPT2-null cells were similarly affected by glutaminase inhibition with BPTES. Clone 2 GPT2-null cells overall behaved abnormally; they did not proliferate or respire at the same rate as the wild-type cells even with complete medium. It is possible that Clone 2 may have acquired genomic changes other than deletion in GPT2 during the CRISPR/Cas9 technique. This discrepancy between our results and those of Kim and co-workers is possibly due to the differences between shRNA and CRISPR/Cas9 techniques. Other inherent differences in cell lines may also be partly responsible; variable expression levels of GPT2 may explain variabilities in resistance to glutaminase inhibition in certain non-small-cell lung cancer cell lines (Caiola et al., 2020).

Decreased cell size and proliferation particularly when alanine is removed from the medium may be linked to autophagy. Transamination is crucial for the mechanistic target of rapamycin (mTOR) activation and cellular growth; alanine and leucine in combination are sufficient to inhibit autophagy (Meijer et al., 2015). Loss of GPT2 has been shown to induce autophagy in a breast cancer cell line (Mitra et al., 2021) and possibly in mouse embryonic fibroblasts (Tan et al., 2017). A comprehensive study into autophagy markers with or without alanine deprivation may reveal mechanisms that underlie defects in cellular growth.

The tricarboxylic acid (TCA) cycle and the replenishment of its intermediates (anaplerosis) are instrumental in cellular growth and energetics as well as tumorigenesis (DeBerardinis et al., 2008). We observe significant decreases in TCA cycle intermediates including fumarate, malate, citrate/isocitrate in both GPT2-null clones, confirming the role of GPT2 as an anaplerotic enzyme in HAP1 cells. GPT2 has been shown to be

upregulated in cell lines with mutations in phosphatidylinositol 3-kinase α (PIK3Cα) associated with colorectal cancer (Hao et al., 2016). With increased GPT2 levels, Hao and co-workers found increased glutamine flux into the TCA cycle with concomitant increases in alanine levels. Maintaining the TCA cycle is fundamental for biosynthesis and energetics and further studies can be performed to test whether exogenously supplied TCA cycle intermediates that readily enter the plasma membrane (e.g. citrate) may correct the decreases cell area or proliferation.

Loss-of-function mutations in GPT2 cause microcephaly, intellectual disability, and motor abnormalities in humans (Ouyang et al., 2016). The results in this study of cancerous HAP1 cell line may have implications for growth of neuronal and glial cells as well. Previously we had reported reduced glutamine entry into the TCA cycle in Gpt2-null mouse embryonic fibroblasts and reduced alanine and TCA cycle metabolism in the Gpt2-null brain. We also found that Gpt2-null mouse brains were smaller than their wild-type controls. These findings suggest parallels between the mechanisms regulated by GPT2 in HAP1 cells and the central nervous system despite the major differences in the two biological contexts. Thus, we conclude that HAP1 cells may be used to model cellular and biochemical alterations that result from loss of GPT2 and reveal fundamental mechanisms of cellular growth.

METHODS

Cell Culture

Human HAP1 wild-type and CRISPR-Cas9 GPT2-deleted cell lines were purchased from Horizon Discovery (Vienna, Austria). Cells were grown in Iscove's Modified Dulbecco's

Medium (IMDM, Thermo Fisher, 12440-053) supplemented with 10% fetal bovine serum (FBS, Thermo Fisher, 16000044) and 1% Penicillin-Streptomycin (P/S, Thermo Fisher, 15140122). Cells were collected using 0.25% Trypsin-EDTA solution (Invitrogen, 25200072) for assays as needed. Unless otherwise noted, cultures were maintained at 37oC in a humidified atmosphere of 5% CO2. Full medium was replaced one day after cell thawing and once every three days thereafter. Cells were allowed to grow to approximately 80% confluency before passaging.

Alanine-free IMDM medium was custom-made according to commercial IMDM formulation (Thermo Fisher, 12440053) with 10% dialyzed fetal bovine serum (dFBS, Thermo Fisher, 26400044) and 1% Penicillin/Streptomycin (P/S, Invitrogen, 15140122).

For glutaminase inhibition, the cells were incubated with 3 μM BPTES both for acute response and continuous administration (Robinson et al., 2007).

PCR and Sanger Sequencing

HAP1 cells were trypsinized at 37oC for 5 min and 15 μL pellet volume was collected. Samples were vortexed for 15 sec in 50 μL Lucigen QuickExtraction buffer (Lucigen, QE09050), then transferred to 65oC heat block for 6 min. Extracts were then vortexed for 15 sec and heat-inactivated at 98oC for 2 min, after which DNA was amplified by touchdown PCR reaction. Primer sequences used to detect the wild-type GPT2 band were as follows: forward primer CSD-GPT2-F (5′-CTA ACT TGT CCT GCA TGG TGT CAG C-3′) and reverse primer CSD-GPT2-R (5′-GGC TTT CTA CCA GGA GGA ACA GAG G-3′) for a wild-type band of 504 bp. The Clone 1 mutant band was 493 bp and the Clone 2 mutant band was 484 bp. DNA amplicons were detected through DNA agarose gel

separation. Amplified products were sent for Sanger sequencing at GENEWIZ facilities (South Plainfield, NJ). Each sample was tested in duplicate. PCR reaction was executed as follows: 5' 95oC, 10 x (30" 95oC, 30" 65oC*, 45" 72oC), 25 x (30" 95oC, 45" 55oC, 45" 72oC), 5' 72oC. *Temperature decreased by 1oC per cycle (touchdown).

Western Blotting

HAP1 cells were lysed using NP40 Cell Lysis Buffer (Thermo Fisher, FNN0021) with 100 μM PMSF (Sigma, 93482), 1X PhosSTOP (Roche, 4986845001), and 1X Protease Inhibitor Cocktail (PIC, Roche, 5892791001). During lysis, cells were kept on ice for 30 min and vortexed at 10 min intervals, then transferred to microcentrifuge tubes and spun at 13,000 rpm for 10 min at 4°C. Total protein was quantified using BCA Protein Assay Kit according to the manufacturer's instructions (Thermo Fisher, 23225) and absorbance was measured using Cytation 5 Plate Reader. Lysates were heated at 90oC for 5 min in 1X NuPage LDS sample buffer (Invitrogen, NP0007) with 1X NuPage sample reducing agent (Invitrogen, NP0009). Protein samples were run on 4–12% Bis-Tris precast polyacrylamide gel (Invitrogen, NP0321) and transferred to nitrocellulose membranes (Invitrogen LC2000) in NuPage Transfer Buffer (Thermo Fisher, NP0006) with 20% methanol (v/v) at 30V for 1 hour. The membrane was then blocked for 30 min at room temperature using TBS blocking buffer (Li-cor Biosciences, 927-50000), washed for 5 min in TBS-Tween (0.05% Tween-20 in 1X TBS), and incubated with primary antibodies overnight at 4oC. The membrane was subsequently washed thrice with TBS-Tween for 5 min per wash and incubated for 1 hour at room temperature in secondary antibody diluted in TBS-Tween. Following three washes with TBS-Tween for 5 min per wash, the

membrane was scanned with the Odyssey CLx Infrared Imaging System (Li-cor Biosciences). The primary antibodies used were rabbit anti-GPT2 (Proteintech, 16757-1-AP, 1:600) and mouse anti-actin (Sigma, A3853, 1:1000). The secondary antibodies used were goat anti-rabbit IRDye680 (Li-cor Biosciences, 926-32221, 1:20,000) and goat anti-mouse IRDye800 (Li-cor Biosciences, 926-32210, 1:20,000).

GPT Enzyme Activity Assay

GPT activity assay was performed using the alanine aminotransferase (ALT) assay kit (Sigma, MAK052) according to the manufacturer's manual. 5 µg protein sample of cell lysates were used. Protein amount in each sample was determined by the bicinchoninic acid (BCA) assay (ThermoScientific Pierce, PI23227). BioTek Cytation5 plate reader was used to detect fluorescence; Gen5 software used to analyze the data.

Immunocytochemistry, Confocal & Structural Illumination Microscopy

HAP1 cells were grown at 20,000 cells/well in Millicell EZ Slide (Thermo Fisher, PEZGS0816) for 48 hours. Cells were then incubated with MitoTracker Red CMXRos (Thermo Fisher, M7512) at a working concentration of 100 nM in IMDM medium for 25 min prior to fixation. Slides were rinsed with 1X PBS and fixed in 4% (w/v) paraformaldehyde for 15 min, after which they were washed thrice with 1X PBS for 5 min each and permeabilized with 0.25% (v/v) Triton X-100 in 1X PBS for 10 min at room temperature. Thereafter, cells were blocked with 10% normal goat serum in 1X PBS + 0.1% Triton X-100 (PBST) for 1 hour at room temperature and incubated

overnight at 4°C with rabbit anti-GPT2 primary antibody (Proteintech, 16757-1-AP, 1:800) in PBST containing 2% normal goat serum. After washing thrice in PBST for 5 min each, cells were incubated for 1 hour at room temperature with AlexaFluor 488 secondary antibody diluted 1:600 in PBST containing 2% normal goat serum. Nuclei were counterstained using 300 nM DAPI (Invitrogen, D1306) for 5 min at room temperature, and cells were subsequently washed thrice with 1X PBS for 5 min per wash. Slides were mounted using Fluoromount-G (SouthernBiotech, 0100-01).

Structured illumination microscopy (SIM) was performed on slides using the DeltaVision OMX SR microscope (GE Healthcare Life Sciences). Z-stack images were obtained using the 60X oil objective (refractive index immersion oil-1.516) and light path-SI under sequential acquisition mode. Z-series images were processed by OMX SI reconstruction, alignment, and maximal projection sequentially using softWoRx software. Slides were also visualized by confocal microscopy using 60X oil objective using FV3000 microscope (Olympus). The laser settings (e.g. laser power, light offset) were kept consistent across conditions and genotypes.

Proliferation and Cell Death Assays

Cell proliferation and death were monitored using the IncuCyte S3 Live-Cell Imaging system (Essen BioScience, v2018B). Cells were seeded at 5,000 cells/well in complete IMDM, custom-made alanine-free medium, custom-made alanine-supplemented IMDM, or complete IMDM treated with 3 μM BPTES (bis-2-(5-phenyl acetamido-1,3,4-thiadiazol-2-yl) ethyl sulfide) (Cayman Technologies, 19284) for glutaminase inhibition.

Proliferation rate was calculated as the slope of the graph plotting phase confluence (%) vs. time (hours).

Apoptosis was measured in real time using IncuCyte Annexin V Orange Reagent (Essen BioScience, 4759), which marks apoptotic cells. The vial containing Annexin V was solubilized in 100 µL 1X PBS and the working dilution of Annexin V in media was 1:200. The total medium volume per well was 200 µl. The cells were treated with Annexin V starting a day after they were seeded in 96-well plates. Cells were seeded in triplicate or quadruplicate wells. Immediately after seeding, cells were incubated in the IncuCyte machine for 30 min to equilibrate. Brightfield and fluorescent images were captured using the 10X objective at 4-hour intervals for 96 hours total. IncuCyte integrated analysis software was employed to measure cell confluence through high-definition phase-contrast imaging, which calculates the density of cells in each imaging field. Artifacts were excluded based on morphological characteristics using cell area thresholding (between 120 and 250 µm2, where needed) and phase mask edge sensitivity (0 to 1) adjustments.

Cell Size

Cells seeded for IncuCyte assays were imaged using brightfield microscopy with the 10X objective. Brightfield images taken 24 hours after IncuCyte initiation were collected and analyzed blindly. 10 cells per image were manually circled using ImageJ. 10 images per experimental sample were analyzed. Each dot in Figures 2C&E represents the cell area

averaged across all cells of the images for each experimental sample. Each sample represents cells that had been thawed from different cryovials.

Mitochondrial Membrane Potential and Morphology

Cells were seeded at 20,000 cells/dish in single 35mm CellVis glass bottom dishes (Fisher Scientific, NC0794151) and allowed to grow for 48 hours until 80% confluent. Cells were subsequently incubated with tetramethylrhodamine, ethyl ester (TMRE) (Sigma, 87917), at working concentration of 500 nM for 20 min and imaged live using the 60X oil objective (refractive index immersion oil 1.526) and conventional light path (568 nm excitation) of the DeltaVision OMX SR microscope (GE Healthcare Life Sciences). Processing of binary-converted images was conducted using Mitochondrial Network Analysis toolkit (MiNA, macro code freely available on Github) (Valente et al., 2017) to ascertain fluorescence intensity of mitochondrial membranes and mitochondrial footprint.

Mitochondrial Respiration Assays

Cells were seeded at 40,000 cells/well in Seahorse XFe96 V3 PS Cell Culture Microplates (Seahorse Biosciences, 101085-004) and allowed to settle for 4 hours at 37oC in a 5% CO2 humidified atmosphere. Cells were subsequently washed with DMEM XF assay medium at pH 7.4 (Seahorse Biosciences, 103575-100) supplemented with 10 mM glucose (Seahorse Biosciences, 103577-100), 2 mM glutamine (Seahorse Biosciences, 103579-100), and 1 mM sodium pyruvate (Seahorse Biosciences, S8636)

and incubated for 1 hour at 37oC in a non-CO2 incubator. Oxygen consumption rate (OCR) and extracellular acidification rate (ECAR) were subsequently measured using Seahorse Extracellular Flux (Seahorse Biosciences, XFe96) analyzer. Working concentrations of 1.5 μM oligomycin, 1 μM FCCP, 0.5 μM rotenone and 0.5 μM antimycin A were loaded into the injection ports in the XFe96 sensor cartridge in sequence and the Mito Stress Test was performed. For Mito Stress Test with glutaminase inhibition, 3 μM BPTES was injected before oligomycin followed by FCCP, rotenone and antimycin A. Mito Stress Test Assay parameters were calculated automatically using Wave software (Seahorse Biosciences).

Following the assay, cells were rinsed gently with 1X PBS and fixed in 4% (w/v) paraformaldehyde for 10 min, after which they were washed twice for 5 min each wash with 1X PBS at room temperature. Nuclei were counterstained using 300 nM DAPI for 5 min at room temperature, and cells were subsequently washed thrice with 1X PBS for 5 min per wash. Cell density per well was measured using the Cytation 5 Plate Reader (Biotek Instruments, Winooski, VT) by imaging wells at 405nm and measures of respiration were normalized to cell density per well.

Mitochondrial ROS Measurements

HAP1 cells were seeded at 20,000 cells/dish in CellVis 35mm glass bottom dishes and incubated for 48 hours at 37oC, 5% CO2. Cells were subsequently treated with 0.2 μM MitoSOX Red (Thermo Fisher, M26008), 0.125 μM MitoTracker Green (Thermo Fisher,

M7514), and 90 μM Hoechst (Thermo Fisher, H3570) at 37oC, 5% CO2 for 10 min. Cells were then imaged live using the 60X oil objective (refractive index immersion oil 1.526) and conventional light path of the DeltaVision OMX SR microscope (GE Healthcare Life Sciences). Mitochondrial superoxide levels were measured by fluorescence intensity of puncta using ImageJ.

DCFDA – Cellular Reactive Oxygen Species Detection Assay

HAP1 cells (25,000 cells per well) were seeded on 96-well black Greiner clear-bottom microplates (Greiner Bio-One, 655090, allowed to settle in complete IMDM medium for 4 hours and stained with 2',7'-dichlorodihydrofluorescein diacetate (DCFDA). The assay performed according to the manufacturer's manual (abcam, ab113851). For a positive control, the cells were treated with varying concentrations of tert-butyl hydroperoxide (TBHP).

Metabolomics

HAP1 cells were grown in complete IMDM until approximately 80% confluence in 10 cm dishes. The cells were quickly washed with 1X PBS at room temperature and then immediately the metabolism was quenched with 500 μl 80% (v/v) methanol (cooled to -80oC). The mixture was vortexed for 1 min and incubated at -80oC for 4 hours. To pellet debris, the sample was spun at 14,000 x g for 10 min at 4oC. While the supernatant was kept at -80oC, 400 μl of 80% methanol (cooled to -80oC) was added to the pellet, which was then vortexed for 1 min, incubated at -80oC for 30 min and then spun at 14,000 x g

for 10 minutes at 4oC. The supernatants were combined and re-spun at 14,000 x g for 10 min 4oC. The supernatants were concentrated in 1.5 ml Eppendorf tubes with SpeedVac at ambient temperature. Tandem mass spectrometry was done at Beth Israel Deaconess Medical Center Mass Spectrometry Facility. The samples were re-suspended in liquid chromatography (LC)/mass spectrometry (MS)-grade water and run in tandem LC-MS/MS. Samples were injected into hydrophilic interaction liquid chromatography (HILIC) at high pH using HPLC coupled to a 5500 QTRAP mass spectrometer (AB/SCIEX). Selected Reaction Monitoring (SRM) mode for 300 transitions with positive/negative polarity switching fragmented precursor ions and select for product ions. Peak areas for each detected metabolite were integrated using MultiQuant software (AB/SCIEX). The statistical analyses and data visualization including PCA plot, volcano plot, heat map and over-representation analysis were done using MetaboAnalyst 4.0 (Chong et al., 2019). If half of data for a metabolite is not available than that metabolite was omitted from analysis. All data was normalized by median normalization and auto-scaled (mean-centered and divided by standard deviation of each variable). For over-representation analysis, we used Small Molecule Pathway Database (SMPDB) metabolite pathway sets (Supplementary Table 1). Unpaired Student's two-tailed t-test assuming equal variance was used to generate a raw p-value.

Statistics

All statistical tests indicated in the text were performed using GraphPad Prism (GraphPad Software, San Diego, CA) unless otherwise noted. Each dot in the graphs represents an average of technical replicates from cell clones that had been thawed from different

cryovials. Two-tailed t-tests were performed to find significant differences between groups unless otherwise noted. One-sample t-test was used to determine statistically significant difference with the hypothetical mean of 100 to compare GPT2-null values when expressed as a percentage of the averaged wild-type value. Raw P values were considered significant below 0.05 and error bars represent standard error of the mean unless otherwise noted.

REFERENCES

Baytas, O., and Morrow, E.M. (2018). The Role of Mitochondrial Glutamate Metabolism in Cognitive Development and Disease. Neuropsychopharmacology 43, 229-230.

Bowman, C.E., Zhao, L., Hartung, T., and Wolfgang, M.J. (2016). Requirement for the Mitochondrial Pyruvate Carrier in Mammalian Development Revealed by a Hypomorphic Allelic Series. Mol Cell Biol 36, 2089-2104.

Brand, M.D., and Nicholls, D.G. (2011). Assessing mitochondrial dysfunction in cells. Biochem J 435, 297-312.

Caiola, E., Colombo, M., Sestito, G., Lupi, M., Marabese, M., Pastorelli, R., Broggini, M., and Brunelli, L. (2020). Glutaminase Inhibition on NSCLC Depends on Extracellular Alanine Exploitation. Cells 9.

Chong, J., Wishart, D.S., and Xia, J. (2019). Using MetaboAnalyst 4.0 for Comprehensive and Integrative Metabolomics Data Analysis. Curr Protoc Bioinformatics 68, e86.

DeBerardinis, R.J., Lum, J.J., Hatzivassiliou, G., and Thompson, C.B. (2008). The biology of cancer: metabolic reprogramming fuels cell growth and proliferation. Cell Metab 7, 11-20.

DeBerardinis, R.J., Mancuso, A., Daikhin, E., Nissim, I., Yudkoff, M., Wehrli, S., and Thompson, C.B. (2007). Beyond aerobic glycolysis: transformed cells can engage in glutamine metabolism that exceeds the requirement for protein and nucleotide synthesis. Proc Natl Acad Sci U S A 104, 19345-19350.

DeRosa, G., and Swick, R.W. (1975). Metabolic implications of the distribution of the alanine aminotransferase isoenzymes. Journal of Biological Chemistry 250, 7961-7967.

Devine, M.J., and Kittler, J.T. (2018). Mitochondria at the neuronal presynapse in health and disease. Nat Rev Neurosci 19, 63-80.

Glinghammar, B., Rafter, I., Lindstrom, A.K., Hedberg, J.J., Andersson, H.B., Lindblom, P., Berg, A.L., and Cotgreave, I. (2009). Detection of the mitochondrial and catalytically active alanine aminotransferase in human tissues and plasma. Int J Mol Med 23, 621-631.

Hao, Y., Samuels, Y., Li, Q., Krokowski, D., Guan, B.J., Wang, C., Jin, Z., Dong, B., Cao, B., Feng, X., et al. (2016). Oncogenic PIK3CA mutations reprogram glutamine metabolism in colorectal cancer. Nat Commun 7, 11971.

Kang, H.J., Kawasawa, Y.I., Cheng, F., Zhu, Y., Xu, X., Li, M., Sousa, A.M., Pletikos, M., Meyer, K.A., Sedmak, G., et al. (2011). Spatio-temporal transcriptome of the human brain. Nature 478, 483-489.

Kim, M., Gwak, J., Hwang, S., Yang, S., and Jeong, S.M. (2019). Mitochondrial GPT2 plays a pivotal role in metabolic adaptation to the perturbation of mitochondrial glutamine metabolism. Oncogene 38, 4729-4738.

Kotecki, M., Reddy, P.S., and Cochran, B.H. (1999). Isolation and characterization of a near-haploid human cell line. Exp Cell Res 252, 273-280.

Lindblom, P., Rafter, I., Copley, C., Andersson, U., Hedberg, J.J., Berg, A.L., Samuelsson, A., Hellmold, H., Cotgreave, I., and Glinghammar, B. (2007). Isoforms of alanine aminotransferases in human tissues and serum--differential tissue expression using novel antibodies. Arch Biochem Biophys 466, 66-77.

McKenna, M.C., and Ferreira, G.C. (2016). Enzyme Complexes Important for the Glutamate-Glutamine Cycle. Adv Neurobiol 13, 59-98.

Meijer, A.J., Lorin, S., Blommaart, E.F., and Codogno, P. (2015). Regulation of autophagy by amino acids and MTOR-dependent signal transduction. Amino Acids 47, 2037-2063.

Mitra, D., Vega-Rubin-de-Celis, S., Royla, N., Bernhardt, S., Wilhelm, H., Tarade, N., Poschet, G., Buettner, M., Binenbaum, I., Borgoni, S., et al. (2021). Abrogating GPT2 in triple-negative breast cancer inhibits tumor growth and promotes autophagy. Int J Cancer 148, 1993-2009.

Morris, R.L., and Hollenbeck, P.J. (1993). The regulation of bidirectional mitochondrial transport is coordinated with axonal outgrowth. Journal of Cell Science 104, 917-927.

Ouyang, Q., Kavanaugh, B.C., Joesch-Cohen, L., Dubois, B., Wu, Q., Schmidt, M., Baytas, O., Pastore, S.F., Harripaul, R., Mishra, S., et al. (2019). GPT2 mutations in autosomal recessive developmental disability: extending the clinical phenotype and population prevalence estimates. Hum Genet 138, 1183-1200.

Ouyang, Q., Nakayama, T., Baytas, O., Davidson, S.M., Yang, C., Schmidt, M., Lizarraga, S.B., Mishra, S., Ei-Quessny, M., Niaz, S., et al. (2016). Mutations in mitochondrial enzyme GPT2 cause metabolic dysfunction and neurological disease with developmental and progressive features. Proc Natl Acad Sci U S A 113, E5598-5607.

Phillips, R.S. (2014). Structure and mechanism of kynureninase. Arch Biochem Biophys 544, 69-74.

Robinson, M.M., McBryant, S.J., Tsukamoto, T., Rojas, C., Ferraris, D.V., Hamilton, S.K., Hansen, J.C., and Curthoys, N.P. (2007). Novel mechanism of inhibition of rat kidney-type glutaminase by bis-2-(5-phenylacetamido-1,2,4-thiadiazol-2-yl)ethyl sulfide (BPTES). Biochem J 406, 407-414.

Ruthel, G., and Hollenbeck, P.J. (2003). Response of Mitochondrial Traffic to Axon Determination and Differential Branch Growth. The Journal of Neuroscience 23, 8618-8624.

Smith, B., Schafer, X.L., Ambeskovic, A., Spencer, C.M., Land, H., and Munger, J. (2016). Addiction to Coupling of the Warburg Effect with Glutamine Catabolism in Cancer Cells. Cell Rep 17, 821-836.

Tan, H.W.S., Sim, A.Y.L., and Long, Y.C. (2017). Glutamine metabolism regulates autophagy-dependent mTORC1 reactivation during amino acid starvation. Nat Commun 8, 338.

Valente, A.J., Maddalena, L.A., Robb, E.L., Moradi, F., and Stuart, J.A. (2017). A simple ImageJ macro tool for analyzing mitochondrial network morphology in mammalian cell culture. Acta Histochem 119, 315-326.

Wise, D.R., and Thompson, C.B. (2010). Glutamine addiction: a new therapeutic target in cancer. Trends Biochem Sci 35, 427-433.

Supplementary Table 1 contains raw data and statistical analysis of targeted metabolomics obtained from Clone 1 and Clone 2 wild-type and GPT2-null HAP1 C

Sheets: RAW DATA, T-TEST, MSEA - ORA (Metabolite Set Enrichment Analysis - Over-representation Analysis

CLONE 1

Genotype	KO	KO	KO	KO	KO	KO	WT	WT	WT	WT	WT	WT
glyoxylate	51561.22814	57208.70333	48869.19418	48090.19989	37171.73472	56492.438	85881.95003	94406.85765	91180.47402	77598.93467	77596.77073	
glycolate	27003.13946	29602.73071	24830.32716	N/A	N/A	N/A	45280.67957	44599.58798	N/A	110868.3584	21683.87822	
pyruvate	38571.13328	57725.02438	49829.81903	39101.19204	27991.27488	50957.546	53936.78472	52698.08361	52852.5716	69848.15267	56963.98886	
lactate	158267.60.13	142928977.74	13663225.09	13907456.5	8943704.583	13503747	21126147.99	16719136.47	17927694.44	17243409.72	13546607.77	
2-oxobutanoate	205131.8742	372448.0964	254504.95	188150.8358	137956.3319	284273.47	341954.981	360725.3149	347041.3991	307651.7693	310424.5175	
acetoacetate	239049.9111	287597.2412	256499.8987	154196.9265	201648.9654	286191.16	339210.168	287272.4711	296489.1888	239992.4375	263131.724	
glycerate	652929.4918	646857.5425	583124.8212	621023.4635	192302.9744	580972.15	629908.1615	593976.4641	599167.145	552364.3917	499029.072	
uracil	51344.33834	55227.97929	56285.96971	54306.11555	11513.95634	38270.807	37144.35495	29370.90135	44146.46779	48919.27329	15130.49053	
fumarate	4058986.71	5021290.125	4743189.797	3921401.924	3289539.611	5238052.6	7135841.302	5976636.406	5865081.816	5559573.123	5993321.121	
Maleic acid	3930212.331	4695542.484	4930172.451	3962953.66	3455585.192	4937782.6	6933701.849	6068870.088	6065560.148	4845052.221	5614168.768	
2-keto-Covalerate	361383.216	490655.829	464006.681	389767.486	355774.325	504543.5	689302.015	589754.784	574184.522	510482.37	556140.007	
Guanidoacetic acid	3150043.931	2817140.747	2784330.184	2839850.182	455893.5048	2937637.3	3150136.604	2308216.281	2245651.154	2010641.836	2063355.355	
succinate	5015051.137	4811372.344	4514163.026	3431515.327	3567470.061	17999952	53193006.663	36097334.705	29275579.372	24378766.099	19005441.908	
Methylmalonic acid	572366.3724	813033.877	544504.95	380543.1274	94964.1	444195.88	1446757.564	1417770.236	1418214.738	1224779.15	1224779.15	
3-S-methylthiopropionate	N/A	5351.515249	N/A	N/A	N/A	N/A	5377.594283	7529.047612	N/A	N/A	4840.821482	
nicotinate	134470.89	69764.6199	113389.6506	142286.2515	139522.95	170622.92	191234.2106	175000.8999	94693.208	79737.88452	69886.17944	
taurine	471052777.72	465223245.97	450411383.21	450377587.58	26317931.29	47387989	41459518.77	36370863.28	35203791.99	31119513.22	35250105.21	
Pyroglutar	1386330.733	1277642.903	1094676.71	1167598.07	136527.0386	1391948.6	1514759.78	1334092.088	1478528.272	1301054.266	1057198.24	
Citraconic acid	936531.1266	1279010.013	1279020.113	1090523.49	880093.9996	1116627.2	1472120.05	1327722.976	1314514.056	1077576.4537	1031987.89	
2-ketohexanoic acid	57062.6996	104065.4599	85745.27874	71263.55775	56211.66557	76747.929	112863.179	106536.0598	95193.39897	58347.99202	86116.79954	
N-Acetyl-L-alanine	3171466.41	3230775.03	28395146.9	29918276.55	7882332.528	26373282	36562953.91	28510499.01	28693220.04	26213671.07	25370875.14	
oxaloacetate	701834.3223	955577.7827	719347.4886	680132.6503	83556.4991	720641.15	1441922.147	1266407.787	823155.2861	700218.1892	907344.4326	
Hydroxyisocaproic acid	29568.8246	35846.01293	39868.03673	26930.08906	18897.09396	66886.343	38727.441	27845.46508	25992.68852	34666.22551	12474.21985	
malate	1943137.8	2250693.2	21455799.54	20884957.26	1840309.78	27040151	36141643.11	31181558.75	32429803.35	30388835.5	31363185.65	
hypoxanthine	5908580.8606	6022183.6228	9486258.2	9486258.2	1499511.31	9191008.384	11859243.27	11499511.31	9191008.384	11859243.27	11859243.27	
anthranilate	329113.4187	401278.1792	3939088.1664	338597.5977	382380.1748	314524.5	414967.8436	427496.2153	430322.7754	389529.4828	378885.5733	
p-aminobenzoate	375670.9876	394440.8928	415791.6019	335233.2375	373123.8515	359765.84	444006.1032	411567.0203	410966.0468	367413.8387	383587.6958	
2-hydroxybenzoate	481940.9079	389458.8813	420669.8438	387564.2995	350.0098	432405.2	481848.2305	470627.1904	439319.3990	380366.4513	405854.7854	
acetylphosphate	946370.388	933214.3477	762536.8693	969073.2329	153289.081	742834.28	888786.7542	928757.4226	1007898.365	462973.8556	709211.798	
Carbamoyl phosphate	1013950.368	1010746.901	1098133.961	1046345.271	381916.4516	782629.73	823570.3496	790762.7887	740196.7192	596625.069	608846.5662	
a-ketoglutarate	58345801.021	61795306.38	60712831.921	6363827.29	1878516.13	62096152	82585341.348	49201101.67	52874611.344	51772426.439	48789889.765	
Phenylpropiolic acid	15950107.38	17134882.68	17501022.15	18091263.38	5177714.029	17393981	16739397.34	13665385.83	14689588.83	13966117.26	14269159.61	
2-oxo-4-methylthiobutanoate	51933.33252	54000.04041	55627.72777	43124.4211	6000.05705	52958.258	59471.6153	49286.49262	49307.85837	42085.47632	42357.25521	
2-Hydroxy-2-methylbutanedioic acid	715521.5055	4083111.605	42001754.55	67575.5436	43479.1227	707932.6	1068021.7	862505.7702	864625.2235	718953.47	817956.34	
3-methylphenylacetic acid	35516.73365	32497.98735	45451.31587	39144.0641	23002.97118	69866.421	101511.7533	153805.2648	31542.48711	42747.37969	81075.2988	
xanthine	620746.6911	631888.1593	612813.6431	615888.2564	87419.66001	582363.6	622836.8	604667.8	617447.7755	535664.8837	499067.8257	
Hydroxyproline	214039.3498	35229.304	500725.42168	279044.1282	285166.5397	184683.75	157448.2974	230180.2775	348064.4665	354100.723	524329.8902	
2,3-dihydroxybenzoic acid	501480.724	484024.3278	534895.1514	762248.7672	7566.914015	973206.93	289112.2049	313668.712	275884.4034	353264.7529	373627.1998	
orotate	129098.5858	135369.3668	135904.7824	125178.2982	28395.5827	176534.38	158428.2271	144067.3861	152416.1194	124273.2121	127901.2213	
dihydroorotate	380812.2641	421609.9576	328243.5176	534555.489	154602.4803	674306.31	314854.015	105600.8513	263872.2115	322276.6395	355031.5798	
allantoin	719053.8599	779575.7999	698655.3343	787184.0388	94387.6749	1009.8	1011523.94	1013597.82	1009318.697	1009318.697	1009318.697	
Aminoadipic acid	559704.8509	567978.5317	432898.4784	330464.5948	356952.9289	4604040.47	8628833.234	6843903.482	556788.2869	5408.66252	632688.5523	
Indole-3-carboxylic acid	553759.3882	61979.4419	423643.9468	370363.5545	339732.7547	434139.08	863610.4735	719956.9648	651040.5769	478136.2232	651028.9766	
phenylacetate	N/A	N/A	N/A	32167.78681	N/A	N/A	28715.2234	N/A	N/A	N/A	4175.446071	
Alloxalic acid	21015.77959	12243.65639	7263.603857	12299.82473	4708.402539	11108.616	18709.02583	9666.878743	14518.97367	4062.422307	7061.058934	
Phenylacetic acid	127468.2452	93332.58145	70453.30918	85114.05947	17750.16567	57041.33	81617.57638	92504.55506	77982.27122	95202.2279	72310.98963	
quinolinate	320786.5316	284545.2913	426023.4977	336838.5029	161741.4705	542063.36	669868.1838	377884.2288	446366.181	346124.6082	371455.4239	
phosphoenolpyruvate	389480.8257	293230.6451	330900.3683	374328.5504	117578.5565	316437.15	419573.2341	290329.5328	333239.2065	364656.0523	167428.5534	
Uric acid	101001.9004	88729.7371	91654.52394	80125.7115	83573.18754	76022.214	84666.88332	88366.19024	74143.70999	95359.73777	81911.32514	
dihydroxy-acetone-phosphate	1003324.492	1089905.049	1263969.535	1007523.3166	638422.2081	6831966.2	13609596.266	9784524.247	8457606.751	7661614.431	5779917163	
D-glyceraldehyde-3-phosphate	808755.9507	798461.0802	1106034.258	580269.1509	464768.9619	284101.85	834044.7195	535490.8631	1499115.359	1500503.011	214546.48418	
sn-glycerol-3-phosphate	182469.1381	182717.032	162057.5921	117940.6021	72797.8819	167168.9	231923.858	178095.1954	191732.1678	135522.559	131956.43	
shikimate	868860.7648	924046.7056	909599.252	856179.1177	90306.67128	1009468.2	1449488.9357	1206068.19	766550.0804	554547.561	464290.7387	
aconitate	290211.2622	295726.1235	323275.8401	269201.292	300724.0307	404195.76	508249.7052	612364.0831	456031.2844	367625.4532	492661.5092	
allantoate	85795.56674	81410.15399	101656.929	91975.56647	13604.72424	89195.5827	176534.38	159258.7799	120478.0936	107353.5403	94118.40377	
Ascorbic acid	121472.8175	67741.7304	88429.94839	74916.94867	57275.26826	129768.58	211218.2665	136905.8731	57293.65866	86525.24727	96695.8553	
2-Isopropylmalic acid	987307.6987	1024014.456	12060124.223	950261.1387	703529.4036	11309117	766050.2617	736796.2106	646030.4374	644491.7015	651987.2006	
N-carbamoyl-L-aspartate-nega	61827.17052	70440.57797	83382.80185	71663.56121	22885.5827	75163.38	97365.67782	110261.6683	91881.12409			
Pyrophosphate	25264940.59	21862321.85	21542846.7	27320824.63	6398198.055	25913241	24546402.7	25606693.32	27077250.3	29661472.53	24806239.44	
glucono-?-lactone	6993.657434	20436.2495	11862.29491	8061.279319	18259.58472	10219.96	13426.95715	14546.97124	7538.016357	9545.555456	8603.817739	
myo-inositol	20388124.5	19548334.7	17495431.08	19355776.55	6268.259	18471.84	13828456.69	13104731.32	13888447.07			
hydroxyphenylpyruvate	85603.03397	66657.46979	53396.19816	82823.36685	22617.9072	57269.081	51080.21711	69734.76477	73361.18786	95921.22962	54974.90656	
homocysteic acid	5924.027668	N/A	6991.662719	N/A	N/A	5912.5413	7529.51579	6867.667363	N/A	3205.386702	4294.73205	
4-Pyridoxic acid	48339.12543	74839.81637	56051.01651	59860.49966	5472.893663	41902.661	92310.48086	43035.10712	67288.16121	63671.25545	59917.74931	
3-phosphoglycerate	920135.948	539618.4881	756885.3573	780171.0827	442181.8564	649151.99	879348.5619	627127.6008	502824.2561	662384.6494	324594.4209	
Indoleacrylic acid	4984.583281	7996.64139	15851.5883	46931.2604	N/A	N/A	16884.62706	10307.50582	N/A	N/A	4980.071357	
Kynurenic acid	1034400.2	1231810.16	1296606.15	1136230.528	627060.8138	1330859.1	1189534.532	1128293.022	1105568.642	1202537.524	1045083.211	
citrate-isocitrate	201995059.31	263248024.23	292980647.43	197052852.8	20065705.55	29113141	39855245	25018759.98	29947391.69	19250654.1	24512134.31	
isocitrate	124350.2393	130933.1	139068.3928	103763.3944	88093.9996	116627.2	154613.165	139722.816	139485.6966	103755.1497	102739.3141	
citrate	8145924.389	10343258.3	11560011.16	7311758.33	1144672.54	10151496	12976468.03	8168207.839	8242166.195	72234501.07	8990021.391	
2-dehydro-D-gluconate	19354.15202	27965.47978	15591.22324	27468.1549	10752.91977	25825.088	29046.46607	23127.69767	17747.2103	11293.78889	23123.14614	
D-gluconate	610750.9621	670360.6978	618416.2524	668284.2574	68081.5257	900663.47	1007153.6	1038685.827	625312.1756	628344.7698	583744.7694	
D-erythrose-4-phosphate	475390.6532	619547.9922	644565.1763	336664.8311	377928.6111	209279.58	575289.2048	456761.6998	353644.8855	313142.4544	157853.1899	
Xanthurenic acid	166860.0279	151688.1159	203445.7898	181055.8898	113145.8731	192076.62	182622.6835	125401.0006	106988.1197	108108.1628	118749.8115	
lipoate	N/A	N/A	N/A	N/A	N/A	N/A	N/A	8852.3782	3764.503446	N/A	N/A	
D-glucarate	13446.13004	20860.53368	8606.806537	11826.61443	9142.353794	18834.696	22022.13996	18288.79435	18567.51121	11841.03371	13981.6326	
deoxyribose-phosphate	206174.3196	240169.5917	259387.53	213595.166	166927.3779	212462.09	256912.0139	183506.7368	267319.3979	215293.6394	245868.1565	
pantothenate	9548673.304	11766703.57	13202765.55	12052356.87	2700231.5	10131116	13291067.29	13114944.06	9731498.885	10874223.5	7778438.039	
prephenate	N/A	N/A	N/A	N/A	7530.715605	2689.9225	N/A	N/A	N/A	N/A	3380.170322	N/A
deoxyuridine	N/A	N/A	N/A	N/A	N/A	N/A	N/A	N/A	N/A	N/A	N/A	N/A
ribose-phosphate	616850.4891	719548.766	699495.5766	594005.0496	415359.1379	366024.44	852611.0591	606519.9274	686256.6016	595350.2083	331814.3745	
thymidine	N/A	12905.74053	N/A	N/A	N/A	N/A	N/A	N/A	43057.21292	N/A	N/A	
uridine	6347.554859	6695.18037	4250.47089	N/A	4363.04674	N/A	12858.0046	4563.019424	N/A	N/A	N/A	
deoxyinosine	28511.64142	40331.40334	36022.28477	25289.64715	28427.49944	19890.814	101993.7919	37060.31904	42140.68769	43029.27266	31754.98174	
shikimate-3-phosphate	43488.01201	72904.99575	56716.56896	32744.6461	27208.61617	23586.239	40300.63466	42931.18572	34189.25173	23790.37579	16548.40348	
D-glucono-?-lactone-6-phosphate	1939384.97	63.1637995	16406.3515	9571260.536	83660.68627	7621631.5	13755554.01	12033835.05	10976668.88	8483240.638	5091579.827	
hexose-phosphate	923974.0204	596640.484	609648.0769	579621.6523	254122.4559	454026.19	439794.1012	408750.0186	430567.2033	397584.2175	317925.3901	
gluconate-6-phosphate	1397305.417	1660.072	1723356.681	1411.421	1260.502506	1625.8298	1941.876	1780.801	1857.662977	1484610.528	1519171.385	
fructose-6-phosphate	172249.2098	1993932.878	2088502.255	1091940.058	885899.3268	674992.83	1776565.556	1332585.503	1140699.696	993902.3912	494591.0654	
1,3-diphosphateglycerate	923193.513	621465.479	761355.2	1003115.1	350147.2	1013116	1293067.29	1311494.06	9731498.885	1087422.5	777438.039	
2,3-Dihydropyridine-2,6-dicarb	129469.565	795575.569	8908094.469	1831621.28	145311.7094	1227305.6	1357998.712	1264735.889	1579519.18	1418291.496	602857.788	
6-thioxyl-L-homocysteine-nega	17743.6961	2291.88081	23130.52569	10540.69966	38958.50872	12878.968	92149.58138	19965.84612	24602.66139	22051.72142	27952.46306	
inosine	1222301.62	1409.6	1025067.79	1025067.79	1025067.79	1025067.79	1025067.79	1025067.79	1025067.79	1025067.79	1025067.79	
6-phospho-D-gluconate	456132.9509	439526.6192	380462.6444	330053.6355	109646.2419	72479.672	329855.4887	349120.1422	271060.6762	230184.4334	56511.87083	
xanthosine	71142.11754	89065.01725	64787.32314	33409.8618	9032.498872	45966.605	105166.2279	59297.94482	53746.29402	55386.04175	39120.42683	
3-sedoheptulose-1-?-phosphate	223624.1	1.86E+08	2851940.241	1.86E+08	1.86E+08	1.86E+08	1.86E+08	1.86E+08	1.86E+08	1.86E+08	1.86E+08	
N-acetyl-glucosamine-1-phosp	546729.1592	521342.091	486085.2661	454910.519	999133.1561	363968.4	410951.2318	403947.6565	352383.8377	375598.9701	385422.7072	
glutathione-nega	8561443.424	10580626.75	10676296.31	11556313.15	1317283.75	10055577	6319918.828	10203897.2	10991646.1	12243006.7	11807863.87	
dUMP-nega	5420.277144	7990.855467	8977.893731	7995.812	1505.247894	6929.6	7608.481	11225.7424	8042.497667	6817.155	3719.625	
Geranyl-PP	109326.0872	111260.375	81484.86596	133320.6956	22508.9017	125044.75	483405.5711	56125.26331	52176.95073	82773.33506	44081.39259	
CMP-O1P	938421.4297	119767.273	956689.7425	892122.5668	62059.692	108405.2	1474232.375	112976.182	82367.3098	98140.0379	114905.1482	
dTMP-nega	18914.49828	19980.09613	16577.33927	16998.29574	4800.81525	19007.6	24257.6444	18223.83894	14007.77098	22857.2887	22127	
cyclic-AMP	46001.87932	54851.7138	54399.39142	36567.70326	101414.784	73075.799	85626.48071	53787.32015	53220.35284	37077.76703	53784.40762	
fructose-1,6-bisphosphate	305412163.5	351062609	293915776.5	3844.136448	3947.521303	3207.393115	7047.038348	N/A	5092.668516	N/A	1234.938068	10757.30788
SBP	1609067.692	1079514.255	1386044.158	934891.4911	654900.5535	897732.81	1787233.225	1096311.889	821716.2907	883051.7395	358731.7052	
trans, trans-farnesyl diphosphate	11834.90635	7133.578621	6970.047301	7831.766832	12396.33987	9081.7828	7069.516812	7479.990233	5372.329488	4867.126077	12323.59194	
S-adenosyl-L-homocysteine-nega	3466468.52	3.04E+08	2.94E+08	2.94E+08	2.94E+08	2.94E+08	2.94E+08	2.94E+08	2.94E+08	2.94E+08	2.94E+08	
dCDP-nega	49452.97642	28184.76022	33295.83054	25996.62884	16691.79521	48942.606	46792.66785	39531.50054	28506.1881	16136.0414	16673.11778	
5-phosphoribosyl-1-pyrophosphate	262624.7004	94470.82419	132455.024	216594.846	50544.64027	28841.89	178089.0867	160922.1616	227145.7874	200735.6102	73272.37821	
Deoxycytidic acid	N/A	N/A	N/A	N/A	N/A	N/A	N/A	N/A	N/A	N/A	N/A	
DBP	104822.7692	100001.3391	111611.6221	88097.57983	42153.07876	68036.372	151090.8406	84991.29966	76248.90866	76506.1466	42888.82383	
dTDP-nega	140921.7064	151859.6452	145252.9791	141226.7991	34256.08175	98581.6	135239.8109	90537.11526	107541.5132	98988.49535	115796.4826	
CDP-nega	175377.7515	75855.50777	80740.31165	90899.83454	159060.6645	120807.6	154128.1918	131275.1848	99495.79494	71281.99043	63253.18953	
UDP-nega	569500.1	2627391.288	2397631.459	3003529.061	4374399.872	4096977.7	4827013.216	4394894.82	2754343.202	2881377.081	2218081.905	
Cholic acid	53564.84634	N/A	2689.660098	N/A	2691.162626	3995.1	4811.7046	3944.770599	4301.972164	N/A	2681.811518	
trehalose-6-Phosphate	846933.7212	746750.3916	779628.4853	537186.198	350282.7211	994509.55	678327.8152	443041.7173	389554.5955	212874.2582	549782.3226	
Thiamine pyrophosphate	229635.2703	275846.85	271197.6669	345434.187	213229.8385	274373.96	284002.2089	214554.6213	238271.8083	207814.5719	243749.4538	
adenosine 5-phosphosulfate	47483.68497	80139.85332	77990.46269	81924.32485	19506.15576	75837.947	109239.2992	94729.6884	67777.97161	38188.92067	48121.91853	
ADP-nega	81404148.599	35737348.006	32111198.668	41031111.835	6950420.097	5847304.8	7490880.927	6195668.548	3610047.451	3109500.544	2895542.721	
dGDP-nega	81404148.599	35737348.006	32111198.668	41031111.835	6950420.097	5847304.8	7490880.927	6195668.548	3610047.451	3109500.544	2895542.721	
IDP-nega	11938668.68	4876754.247	4696495.202	5996.15576	7583.947	7583.947	7583.947	7583.947	7583.947	7583.947	7583.947	
GDP-nega	387529.2573	148409.7953	112231.434	148057.8227	178808.1623	246946.85	321235.6423	227110.0952	113112.4005	111404.5038	80830.42555	
CDP-ethanolamine	70543.25763	58680.40425	55907.29893	29042.50195	24742.40018	27428.025	54317.93526	27960.21459	32279.10302	32791.66199	13987.65038	
FMN	N/A	N/A	N/A	N/A	N/A	N/A	N/A	2689.924814	N/A	N/A	N/A	
cholesteryl sulfate	1607451.237	1474426.877	1745895.992	1995418.965	2920295.908	1583430.4	1905465.639	1890219.648	2159645.18	1837016.574	1209477.094	
dCTP-nega	216304.1042	240958.2248	233566.1	233566.1	233566.1	233566.1	233566.1	233566.1	233566.1	233566.1	233566.1	
dUTP-nega	24210.35978	25280.16628	26895.92092	16665.60659	16100.42181	17786.376	11833.9664	12371.38252	13445.59249	20976.62722	22589.6203	
dTTP-nega	488224.2542	450615.7466	503145.828	566286.7315	346363.5661	494024.69	614562.0108	535869.5387	719010.8039	564669.8249	304041.8385	
GTP-nega	1117016.02	1049.6	1139181.44	1139181.44	1139181.44	1139181.44	1139181.44	1139181.44	1139181.44	1139181.44	1139181.44	
UTP-nega	234694.1348	202340.1121	233764642.57	2306307.39	1186536.01	1964697	1373483.81	1834805.02	2309457.9	2253218.36	1267454.9	
CDP-choline	161222.2182	48945.39269	46258.132	6991.787279	15596.99913	9143.8227	40340.08472	23128.73805	11832.26065	10759.06423	8606.626133	
dATP-nega	106122.4552	111411.0529	89219.7763	133801.6613	33616.33	69312.6878	76726.8444	76726.8444	76726.8444	76726.8444	76726.8444	
Taurodeoxycholic acid	2824.43173	5910.278055	N/A	4844.060703	N/A	N/A	N/A	N/A	N/A	3236.223451	N/A	
ATP-nega	311463555.75	319290995.36	320110039.03	288962131.5	28144047.44	24745583	30257619.78	26669944.35	35070259.34	32270988.21	19868424.31	
dGTP	311463555.75	319290995.36	320110039.03	288962131.5	28144047.44	24745583	30257619.78	26669944.35	35070259.34	32270988.21	19868424.31	
GTP-nega	149675.258	131792.715	113151.9205	205210.956	83418.67108	127466.2	165784.574	103862.8	92171.4526	123412.138	60507.3.256	
UDP-D-glucose	728739.722	1102345.941	1213986.41	1173195.63	1045145.688	1264299.96	721029.8	823179.157	734272.504	581545.688	584437.7987	
UDP-D-glucuronate	1504384.566	976223.1896	1106953.575	1892444.253	285033.318	1224252.1	1297768.372	1337478.604	1759086.973	1485219.472	598655.8515	
ADP-D-glucose	N/A	5379.157229	9144.739361	18288.93861	8605.894241	3764.3346	N/A	N/A	N/A	5378.144756	N/A	
guanosine-5-diphosphate,3-dideoxy	286280.992	272596.8227	302511.093	335298.1951	98595.6987	97240.44	127266.8471	127437.3461	140205.4563	115383.5199	115383.5199	
UDP-N-acetyl-glucosamine	3059602.624	3015080.626	2556453.292	3194908.832	1617322.588	3080713.3	2762956.478	2982324.847	2223959.885	2262219.018	2807938.219	
glutathione disulfide-nega	1767805.2	19682439.6	18404647.39	12411341	3435026.426	17742088	20237607.98	14421033.22	10700181.38	8631227.847	14162298.01	
NAD+-nega	1879895.602	2057677.654	2854902.3	2001477.091	1007046.293	2071441.7	4244283.892	2809257.81	2442746.697	1609982.99	2035154.877	
NADH-nega	28508.34271	29041.36433	25276.98976	21513.28358	23665.99188	16671.64	35499.32292	17749.85114	19364.33128	11295.29919	16136.0661	
dephospho-CoA-nega	38190.49358	16134.37296	8601.973142	5485.518463	1831.03885	9134.5913	24733.42917	3441.26689	7107.078624	17210.34302	6991.629297	
cyclic bis(3'-5') dimeric GMP	N/A	N/A	N/A	N/A	N/A	N/A	N/A	N/A	N/A	N/A	N/A	
NADP+_nega	173638.6759	147931.3076	128562.0808	168910.3278	162063.0998	163479.04	152150.8319	167020.4357	132819.791	130321.2794	105846.8631	
NADPH-nega	16675.02658	12908.19246	16132.61829	5915.477064	3227.213604	9697.0867	18332.51325	17210.79946	19897.73232	9146.024673	10756.12324	
coenzyme A-nega	46581.47731	34917.98686	22584.91482	80124.28156	22051.2597	36561.63788	92727.542	36561.63788	52098.39176	75335.3569	58316.99245	31723.95193
acetyl-CoA-nega	N/A	N/A	N/A	N/A	N/A	N/A	N/A	N/A	N/A	N/A	N/A	
propionyl-CoA-nega	N/A	N/A	N/A	N/A	N/A	N/A	N/A	N/A	N/A	N/A	N/A	
butyryl-CoA	N/A	N/A	N/A	N/A	N/A	N/A	N/A	N/A	N/A	N/A	N/A	
acetoacetyl-CoA-nega	N/A	N/A	N/A	N/A	N/A	N/A	N/A	N/A	N/A	N/A	N/A	
malonyl-CoA-nega	N/A	N/A	N/A	N/A	N/A	N/A	N/A	N/A	N/A	N/A	3227.178518	
3-hydroxybutyryl-CoA	N/A	N/A	N/A	N/A	N/A	2716.4892	N/A	3763.014456	N/A	N/A	N/A	
succinyl-CoA-methylmalonyl-CoA-nega	N/A	N/A	N/A	N/A	7407.6	N/A	N/A	N/A	N/A	N/A	N/A	
3-hydroxy-3-methylglutaryl-CoA-nega	8604.629884	6454.314877	N/A	4840.734072	N/A	N/A	N/A	9845.876626	3227.045102	3227.253151	N/A	
2-hydroxyglutarate	1570253.014	1901608.912	1661964.893	1317614.461	819447.1467	1641750.2	2022283.83	1578743.146	1643664.491	1815642.593	1672174.915	
2-deoxyglucose-6-phosphate	21277207.89	19664942.92	19363441.56	22955219.44	3658383.358	24388081	23224969.57	21074341.31	22319200.66	22069733.16	18289389.31	
4-phosphopantothenate	5922.220766	10191.2666	7244.619187	6995.067177	2470.760975	8343.159	12388.9167	11401.4072	11166.9729	6995.067177	6995.067177	
dehydroascorbic acid	N/A	N/A	N/A	3792.259958	N/A	6452.7185	N/A	N/A	N/A	3807.473136	5379.742434	
3-hydroxybutyrate	321874.1329	239567.86103	42471.56333	39407.37669	22132.74	46345.34384	53474.01412	50269.58881	36867.46648	37115.23927	33515.23927	
Urea	42260.7209	33225.42003	36893.10739	44095.30929	55510.47818	33002.487	32921.02045	32808.0959	41700.44282	41778.1031	13012.75472	
ethanolamine	92776.76222	32732.36699	13377.75005	22269.92565	14131.40367	5523.8419	82368.69633	10117.322	11722.75841	12253.77701	10484.73515	
Imidazole	60746.66160	57670.55653	16361.64765	22116.88076	6211.686078	N/A	N/A	14108.5641	12119.46431	5772.720836	N/A	
glycine	105947.8037	108651.4333	70465.11229	94012.29309	31194.85449	102194.19	122661.3838	108648.5692	97888.11213	78526.0627	107027.865	
alanine	233065215.17	137361.01	20832748.22	21670504.84	7067125.949	22993614	30845338.05	29227838.34	28380062.8	27837019.26	24585051.79	
betaine aldehyde	309191.2464	197116.3044	221745.8792	209342.8964	41135.1987	116575.46	140420.458	169388.7913	165647.8694

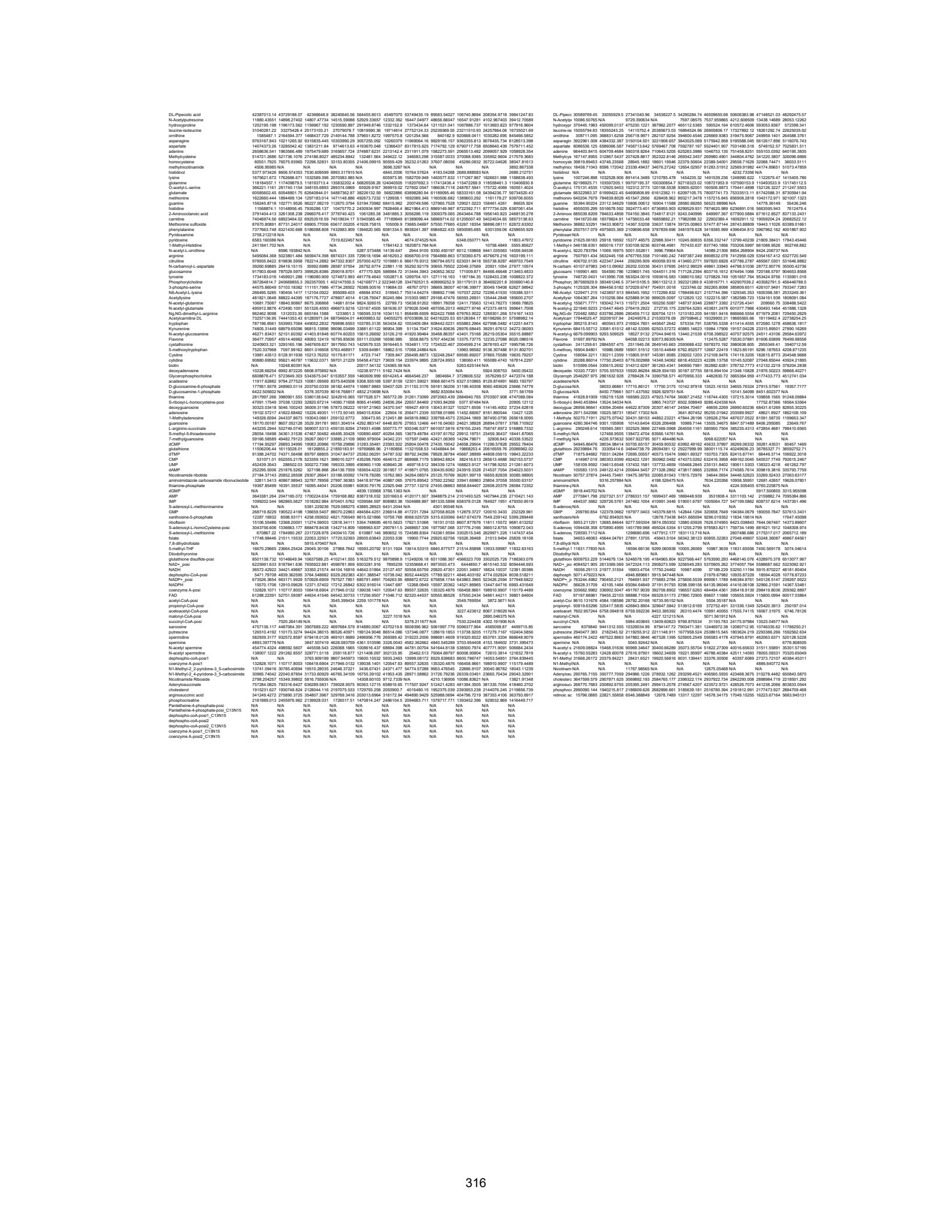

CLONE 1

Metabolite	Fold Change (FC)	log2(FC)	raw P value	-LOG10(P)	False Discovery Rate (FDR)
L-arginino-succinate	0.62497	-0.6781	0.000107	3.9708	0.015944
cytidine	0.4204	-1.2502	0.0001107	3.9558	0.015944
glyoxylate	0.5609	-0.8342	0.0002123	3.6732	0.020376
lactate	0.74233	-0.4299	0.0003154	3.5011	0.022712
alanine	0.64451	-0.6337	0.000692	3.1599	0.039007
Kynurenine	1.9794	0.9851	0.0008127	3.0901	0.039007
cysteine	0.2172	-2.2029	0.0012088	2.9177	0.041576
arginosuccinic acid	0.6673	-0.5836	0.0012851	2.8911	0.041576
4-phosphopantothenate	0.53752	-0.8956	0.0012993	2.8863	0.041576
fumarate	0.69303	-0.529	0.0022765	2.6427	0.065562
2-Hydroxy-2-methylbutanedioic aci	0.63227	-0.6614	0.0025369	2.5957	0.066422
Indole-3-carboxylic acid	0.65921	-0.6012	0.0031587	2.5005	0.07513
malate	0.6541	-0.6124	0.0033913	2.4696	0.07513
2-Isopropylmalic acid	1.3895	0.4746	0.0042681	2.3698	0.087801
Maleic acid	0.71395	-0.4861	0.0056827	2.2454	0.10373
2-keto-isovalerate	0.70481	-0.5047	0.0061166	2.2135	0.10373
allantoate	0.74228	-0.43	0.0061228	2.2131	0.10373
N-carbamoyl-L-aspartate-nega	0.6653	-0.5879	0.0074148	2.1299	0.11864
Xanthurenic acid	1.3625	0.44621	0.0086568	2.0626	0.13074
glucosamine	2.7826	1.4764	0.0090791	2.042	0.13074
2-hydroxygluterate	0.79602	-0.3291	0.013557	1.8678	0.1836
aspartate	1.4066	0.4922	0.014682	1.8332	0.1836
Cystine	0.088847	-3.4925	0.015298	1.8154	0.1836
sarcosine	0.69164	-0.5319	0.015515	1.8093	0.1836
phosphocreatine	1.3694	0.45354	0.016198	1.7905	0.1836
guanine	0.67042	-0.5769	0.016575	1.7805	0.1836
aconitate	0.63699	-0.6507	0.023166	1.6351	0.23479
cystathionine	1.4128	0.49856	0.023175	1.635	0.23479
guanosine	0.31339	-1.6739	0.023642	1.6263	0.23479
betaine aldehyde	1.3653	0.44919	0.024661	1.608	0.23674
inosine	0.4268	-1.2284	0.028432	1.5462	0.26414
deoxyinosine	0.59518	-0.7486	0.030053	1.5221	0.26756
sn-glycerol-3-phosphate	0.83762	-0.2556	0.030658	1.5135	0.26756
glucose-1-phosphate	1.1876	0.24804	0.031831	1.4972	0.26962
taurine	1.1332	0.18043	0.034575	1.4612	0.27637
deoxyguanosine	0.34427	-1.5384	0.034866	1.4576	0.27637
pyruvate	0.71701	-0.4799	0.035506	1.4497	0.27637
trehalose-6-Phosphate	1.4799	0.5655	0.037108	1.4305	0.2802
oxaloacetate	0.73649	-0.4413	0.039607	1.4022	0.2802
quinolinate	0.73953	-0.4353	0.039964	1.3983	0.2802
glycine	0.76011	-0.3957	0.040851	1.3888	0.2802
creatine	0.85385	-0.2279	0.040863	1.3887	0.2802
hypoxanthine	0.38365	-1.3821	0.043716	1.3594	0.28655
isocitrate	0.68391	-0.5481	0.044074	1.3558	0.28655
Pyrophosphate	0.72537	-0.4632	0.044773	1.349	0.28655
Flavone	4.3242	2.1124	0.046807	1.3297	0.29305
Aminoadipic acid	0.72041	-0.4731	0.048205	1.3169	0.29538

CLONE 2

Metabolite	Fold Change (FC)	log2(FC)	raw P value	-LOG10(P)	False Discovery Rate (FDR)
Carbamoyl phosphate	2.235	1.1603	5.52E-05	4.2584	0.015446
2-Hydroxy-2-methylbutanedioic acid	0.67221	-0.573	0.0002076	3.6827	0.018762
N-Acetyl-L-alanine	1.5207	0.60473	0.0003095	3.5094	0.018762
creatine	1.4078	0.49346	0.0003108	3.5075	0.018762
quinolinate	1.5616	0.64303	0.000335	3.4749	0.018762
xanthine	0.73068	-0.4527	0.0006059	3.2176	0.028274
citrate-isocitrate	0.68121	-0.5538	0.0017968	2.7455	0.07187
Kynurenine	2.9505	1.561	0.0021884	2.6599	0.076592
N-acetyl-glutamate	0.63301	-0.6597	0.0029155	2.5353	0.086739
Maleic acid	0.8096	-0.3047	0.0031436	2.5026	0.086739
Phenylpropiolic acid	0.58489	-0.7738	0.0034076	2.4676	0.086739
2-hydroxygluterate	0.72472	-0.4645	0.0040581	2.3917	0.09469
Kynurenic acid	0.66064	-0.5981	0.0051956	2.2844	0.10967
citrate	0.51654	-0.9531	0.0059715	2.2239	0.10967
dephospho-CoA-posi	0.2852	-1.8099	0.0063788	2.1953	0.10967
Ascorbic acid	1.8874	0.91643	0.0068134	2.1666	0.10967
phenylpyruvate	11.29	3.497	0.0068273	2.1658	0.10967
N-acetyl spermidine	0.39769	-1.3303	0.0070572	2.1514	0.10967
Pyrophosphate	1.4415	0.52757	0.0078238	2.1066	0.10967
Phosphorylcholine	1.1552	0.20818	0.0078335	2.106	0.10967
dimethylglycine	0.61831	-0.6936	0.0091233	2.0398	0.12164
2-keto-isovalerate	0.78726	-0.3451	0.011278	1.9478	0.14354
Creatinine	1.4709	0.55669	0.015014	1.8235	0.17876
inosine	0.30357	-1.7199	0.015833	1.8004	0.17876
spermidine	1.2819	0.35833	0.015961	1.797	0.17876
3-phospho-serine	2.321	1.2148	0.020556	1.6871	0.22102
L-arginino-succinate	0.58552	-0.7722	0.021312	1.6714	0.22102
DL-Pipecolic acid	0.83965	-0.2521	0.024121	1.6176	0.23184
ornithine	1.5435	0.62616	0.024122	1.6176	0.23184
2-Isopropylmalic acid	1.2793	0.35531	0.02484	1.6048	0.23184
aminoimidazole carboxamide ribonucleotic	0.30878	-1.6954	0.026326	1.5796	0.23582
Acetylcarnitine DL	1.5567	0.63851	0.026951	1.5694	0.23582
pantothenate	0.79297	-0.3347	0.032581	1.487	0.26245
fumarate	0.75991	-0.3961	0.032982	1.4817	0.26245
cholesterol	1.3521	0.43521	0.033408	1.4762	0.26245
malate	0.72695	-0.4601	0.033744	1.4718	0.26245
aspartate	1.3471	0.42985	0.035094	1.4548	0.26558
arginosuccinic acid	0.60624	-0.722	0.03815	1.4185	0.27704
methylnicotinamide	0.44988	-1.1524	0.038588	1.4135	0.27704
ribose-phosphate	0.70734	-0.4995	0.040395	1.3937	0.27888
Indole-3-carboxylic acid	0.76271	-0.3908	0.040836	1.389	0.27888
isocitrate	0.70599	-0.5023	0.044	1.3565	0.29333
D-gluconate	0.79023	-0.3397	0.045508	1.3419	0.29633

CLONE 1

Metabolic Pathway	Total	Expected	Hits	Raw P value	Holm P value	False Discovery Rate (FDR)	Metabolite Pathway Set	Metabolite Hits
Alanine Metabolism	17	0.764	6	5.04E-05	0.00494	0.00494	Biotin; Adenosine monoph	Glyoxylic acid; Glycine; L-A
Urea Cycle	29	1.3	7	0.000171	0.0166	0.0084	Adenosine monophosphat	Arginosuccinic acid; Fuma
Glycine and Serine Metabolism	59	2.65	9	0.000776	0.0745	0.0253	2-Ketobutyric acid; Betain	Creatine; L-Cystathionine;
Purine Metabolism	74	3.32	10	0.00103	0.098	0.0253	Adenine; Adenosine mono	Deoxyguano Purine Metabo
Arginine and Proline Metabolism	53	2.38	8	0.00171	0.161	0.0335	Tetrahydrobiopterin; Aden	Arginosuccinic acid; Creat
Citric Acid Cycle	32	1.44	6	0.00221	0.205	0.036	Biotin; cis-Aconitic acid; C	cis-Aconitic acid; Fumaric a
Beta-Alanine Metabolism	32	1.44	6	0.00221	0.205	0.036	Biotin; Citric acid; D-Gluco	Citric acid; Fumaric acid; L
Glutamate Metabolism	49	2.2	7	0.00474	0.432	0.0581	Biotin; Adenosine monoph	Glycine; L-Alanine; L-Aspar
Methionine Metabolism	43	1.93	5	0.0391	1	0.391	2-Ketobutyric acid; Betain	L-Cystathionine; Glycine; P
Warburg Effect	58	2.61	6	0.0465	1	0.391	Biotin; Ammonia; Citric ac	Fumaric acid; L-Malic acid;
Ammonia Recycling	32	1.44	4	0.0509	1	0.391	Biotin; Adenosine monoph	Glycine; L-Aspartic acid; Py
Homocysteine Degradation	9	0.404	2	0.0581	1	0.391	2-Ketobutyric acid; Ammo	L-Cystathionine; L-Cysteine
Pyruvate Metabolism	48	2.16	5	0.0588	1	0.391	Biotin; Acetic acid; Acetoa	L-Lactic acid; l-Glycine and
Citrulline-Nitric Oxide Cycle	13	0.584	3	0.0697	1	0.391	Adenosine monophosphat	L-Arginine; L-Aspartic acid;
Pantothenate and CoA Biosynthesis	21	0.943	3	0.064	1	0.391	Adenosine monophosphat	Pyrophosphate; L-Cysteine
Gluconeogenesis	35	1.57	4	0.0672	1	0.391	Biotin; D-Glucose; Fructos	L-Lactic acid; Oxaloacetic ac
Malate-Aspartate Shuttle	10	0.449	2	0.0706	1	0.391	L-Glutamic acid; L-Aspartic	L-Aspartic acid; Oxaloacetic
Transfer of Acetyl Groups into Mitochondri	22	0.988	3	0.0718	1	0.391	Biotin; Citric acid; D-Gluco	L-Malic acid; Oxaloacetic ac
Cardiolipin Biosynthesis	11	0.494	2	0.0839	1	0.433	Cytidine triphosphate; Cyt	Glycerol 3-phosphate; Pyru
Taurine and Hypotaurine Metabolism	12	0.539	2	0.0979	1	0.48	Taurine; L-Cysteine; Fe2+	Taurine; L-Cysteine
Glycolysis	57	2.56	5	0.0981	1	0.48	Biotin; D-Glucose; Fructos	Adenosine monophosphat
Glucose-Alanine Cycle	13	0.584	2	0.112	1	0.501	nmonia; D-Glucose; L-GlutA	Alanine; Pyruvic acid
Tryptophan Metabolism	60	2.7	5	0.126	1	0.536	Tetrahydrobiopterin; Formi	L-Alanine; Quinolinic acid; K
Amino Sugar Metabolism	33	1.48	3	0.181	1	0.74	Acetic acid; Ammonia; Cy	Pyruvic acid; Pyrophosphat
Mitochondrial Electron Transport Chai	19	0.854	2	0.209	1	0.818	Glycerol 3-phosphate; Fur	Cardiolipin Biosynthesis;

CLONE 2

Metabolic Pathway	Total	Expected	Hits	Raw P value	Holm P value	False Discovery Rate (FDR)	Metabolite Pathway Set	Metabolite Hits
Biotin; Adenosine monoph	29	1.13	6	0.000392	0.058	0.058	Adenosine monophospha	Arginosuccinic acid; Fumaric acid; L-Aspartic acid; Ornithine; Pyrophosphate; Carbamoyl phospha
Adenosine monophosphat	53	2.07	7	0.00329	0.319	0.161	Tetrahydrobiopterin; Aden	Arginosuccinic acid; Creatine; Fumaric acid; L-Aspartic acid; Ornithine; Pyrophosphate; Carbamoyl phospha
2-Ketobutyric acid; Betain	35	1.37	5	0.00963	0.924	0.316	Acetic acid; Adenosine m	Arginosuccinic acid; Fumaric acid; L-Aspartic acid; Pyrophosphate; Carbamoyl phosphat
Adenine; Adenosine mono	74	2.89	7	0.0208	1	0.509	Adenine; Adenosine mono	Fumaric acid; L-Aspartic acid; Inosine; Pyrophosphate; Xanthine; Ribose 1-phosphate; AICA
Tetrahydrobiopterin; Aden	18	0.703	3	0.03	1	0.531	Ornithine; Pyrophosphate	Ornithine; Pyrophosphate; Spermidin
Biotin; cis-Aconitic acid; C	32	1.25	4	0.0325	1	0.531	Biotin; cis-Aconitic acid; C	Citric acid; Fumaric acid; L-Malic acid; Isocitric acid
Biotin; Adenosine monoph	58	2.27	6	0.0329	1	0.531	Biotin; Adenosine monoph	Glycine; L-Alanine; L-Aspartic acid; Pyruvic acid; Pyrophosphat
Adenosine monophosphat	28	1.09	3	0.092	1	1	Adenosine monophospha	Fumaric acid; Phenylpyruvic acid; Pyrophosphat
Biotin; Acetic acid; Acetoa	59	2.3	4	0.194	1	1	Cytidine triphosphate; Cyt	Pyrophosphate; Phosphorylcholin
Biotin; Ammonia; Citric ac	32	1.25	3	0.125	1	1	Biotin; Adenosine monopl	L-Aspartic acid; Pyrophosphate; Carbamoyl phosphat
Adenosine monophosphat	60	2.34	4	0.202	1	1	Tetrahydrobiopterin; Form	Quinolinic acid; Pyrophosphate; L-Kynurenine; Kynurenic ac
Biotin; D-Glucose; Fructos	22	0.859	2	0.211	1	1	Biotin; Citric acid; D-Gluco	Citric acid; L-Malic acid
L-Glutamic acid; L-Aspartic	43	1.68	3	0.234	1	1	2-Ketobutyric acid; Betain	Dimethylglycine; Pyrophosphate; Spermidin
Biotin; Citric acid; D-GlucoL	26	1.02	2	0.27	1	1	Ascorbic acid; L-Carnitine	Ascorbic acid; Pyrophosphate
Cytidine triphosphate; Cyt	26	1.02	2	0.27	1	1	Ascorbic acid; Oxoglutaric	Ascorbic acid; Pyrophosphate
Taurine; L-Cysteine; Fe2+	8	0.312	1	0.274	1	1	Biotin; L-Lysine; Pyropho	Pyrophosphate
Adenosine monophosphat	48	1.88	3	0.276	1	1	Biotin; Citric acid; L-Malic	Citric acid; Pyrophosphate; Carbamoyl phosphate
Phenylacetate Metabolism	9	0.352	1	0.302	1	1	Adenosine monophospha	Pyrophosphate
Tetrahydrobiopterin; Formi	10	0.391	1	0.33	1	1	L-Glutamic acid; L-Aspart	L-Aspartic acid
Acetic acid; Ammonia; Cy	11	0.43	1	0.356	1	1	Cytidine triphosphate; Cyt	Pyrophosphate
Glycerol 3-phosphate; FurtG	12	0.469	1	0.382	1	1	Cytidine triphosphate; Cyt	Pyrophosphate

CONCLUSION

Figure 7.1 shows the questions introduced in Chapter 1 (outlined in Figure 1.4) and their summarized answers as obtained in this work. This section summarizes the main findings of the chapters, proposes future directions and extends the discussion that I could not fit in previously.

Does GPT2 confer the ability to synthesize alanine in the cells, i.e. non-essentiality of alanine? Would alanine supplementation alleviate/prevent metabolic or behavioral defects, i.e. may it be a therapeutic target?

We observe decreases in alanine and TCA cycle intermediates followed by increases in amino acid and glycolytic intermediates in the *Gpt2*-null hippocampus over the course of the first three postnatal weeks. By our data mining for the metabolites in the GPT2 reaction in KEGG (Kyoto Encyclopedia of Genes and Genomes) (Kanehisa et al., 2020), pyruvate has 22, glutamate 44, alpha-ketoglutarate 43 and alanine has 14 biochemical reactions that occur in both humans and mice. One may expect that any perturbations in level or function of GPT2 may affect alanine first. This expectation was justified in our previous report where reduction in alanine levels in the *Gpt2*-null whole brain and complete absence of alanine release into the medium by *Gpt2*-null mouse embryonic fibroblasts were observed (Ouyang et al., 2016). Strikingly, in human patients with GPT2 Deficiency, the biochemical panel in the blood plasma was within range of control levels except reduced alanine (Celis et al., 2015).

It may be puzzling to initially find *increases* in *Gpt2*-null brain alanine levels at P0 when at other timepoints there is a prominent decrease. Developmentally, free alanine

levels decrease in the rodent brain from infancy into adulthood while free glutamate levels increase (Levi et al., 1967; Morken et al., 2014). On the other hand, pyruvate and alpha-ketoglutarate concentrations in the brain remain relatively unchanged (Miller et al., 1973). *Gpt2* expression is present at P0 in the mouse brain and it increases during the first three weeks (Ouyang et al., 2016) as does *GPT2* expression in the first nine years of human postnatal brain development (Kang et al., 2011). Whether an increase in alanine levels at P0 is caused by differences in the direction of the GPT2 reaction across development or by a probable influence of the fetal nutrient composition supplied by the *Gpt2*-heterozygous mother is yet unclear. At P0, in addition to alanine, metabolites of the tryptophan-kynurenic acid degradation pathway of which alanine is an end product (Phillips, 2014), are significantly changed in *Gpt2*-null brain, such as kynurenic acid and tryptophan. These metabolites are not changed at other time-points including P7, P14 and P18 supporting the idea of the early fetal effects on *Gpt2*-null pups.

Reduced alanine levels seen in *Gpt2*-null mice brain was also expected given the function of normalizing levels of metabolites in the GPT2 reaction. Glutamate represents a larger pool of the brain metabolome (~10 μmol/gr) (Levi et al., 1967) compared to alanine which is the second most abundant proteinogenic amino acid in the plasma (Cynober, 2002) but is present in much lower concentration in the brain (~0.5 μmol/gr) (Levi et al., 1967). If glutamate and pyruvate constitute a larger pool than alanine and alpha-ketoglutarate, then GPT2, being an equilibrium enzyme (Krebs, 1953), will catalyze the reaction in favor of alanine production. In addition, given higher Km values for alanine in the brain compared to the other primary reaction metabolites, alanine formation has been predicted to be favored *in vivo* (Lysiak et al., 1974) (Miller et al.,

1973). The current study identifies alanine as one of the first metabolites that is altered in the *Gpt2*-null brain, confirming the idea that alanine levels are sustained significantly by GPT2.

Survival and growth of *Gpt2*-null neuronal cultures is severely affected by alanine deprivation in the medium. Conversely, by adding extra alanine in the diet, it was possible to increase chances of survival in *Gpt2*-null mice. These results suggest that alanine became a conditionally essential amino acid; i.e. it has to be supplied exogenously for the organism to function normally. However, not all *Gpt2*-null mice survived under the high alanine diet regimen and this reduced penetrance of alanine supplementation is most likely due to the ad libitum nature of the diet administration. The wild-type mice on high alanine did not show increased alanine levels in the blood, meaning that it is very likely that the *Gpt2*-heterozygous mother on high alanine did not help raise alanine levels in the *Gpt2*-null pup via milk and the Gpt2-null pup that obtained more solid food had better chances of receiving extra alanine. The inability of the mother in passing on the extra alanine to its pup may be due to the first-pass metabolism of alanine in the liver and this is also likely to cause SynapsinI-Cre conditional *Gpt2*-null mice to die even on high alanine diet because there is GPT2 in the liver thereby decreasing free available alanine levels in the blood.

Of course, several follow-up questions are immediately raised. If exogenous alanine is critical to *Gpt2*-null mice, and we assume that alanine decreases are not merely a by-product of the absence of GPT2 reaction, what does alanine deprivation contribute in terms of lethality in mice? What does it mean to have reduced free alanine levels in the brain tissue and serum? What altered process does alanine supplementation reverse in the

body? Naturally, the overarching question would be: why do *Gpt2*-null mice die? The answers to these questions are yet unknown. My thesis work does not provide clear answers to these; however it can provide several lines of thought.

First, we know that SynapsinI-Cre conditional null mice die, and that a critical region in the nervous system is most likely responsible for the premature death. Such a region is likely to localize to the brainstem, possibly controlling autonomous functions such as CO_2, pH regulation on the blood, heart rate, breathing etc. Failure in any of these would lead to eventual death. The fact that the animals are dying close to weaning age (P21) most likely has to do with the increasing *Gpt2* expression pattern in the first two weeks of life and accumulating metabolic damage over time. It is unlikely that any of the motor systems that control gross body movements (fore/hind limbs) are behind the premature death. It is possible that the noradrenergic system, particularly the vagus nerve dysfunction (if any) may be responsible, at least in part, the death of *Gpt2*-null mice. Alanine supplementation may be providing the metabolic support for the brain region in question.

Second, how does extra alanine exert its influence over the system? Does it increase protein synthesis or does it correct gluconeogenesis in the liver thereby helping the body maintain its glucose balance (alanine-glucose cycle)? We do not find major differences in blood glucose (see Appendix for Chapter 3) so this would not work in favor of this hypothesis. However, it would be remiss to dismiss this idea because even if the blood glucose may not be relevant to the pathophysiology, extra alanine in the liver may help with other aspects of hepatic metabolism such as the TCA cycle (McCommis et al., 2015).

Alanine in protein synthesis could be of importance. Two papers have found that extracellular alanine is important for T-cell activation and protein synthesis in cancerous cell lines *in vitro* (Ron-Harel et al., 2019; Rossiter et al., 2021). Alanine is a proteinogenic amino acid and decreases in free alanine levels may slow down translation and in turn other biosynthetic pathways. Decreases in alanine or serine (a precursor for alanine) may also contribute to promiscuity in tRNA synthetases and cause misfolding and degradation in proteins. Mutations in alanyl tRNA-synthetase have been shown to incorporate serine instead of alanine and cause neurodegeneration in the cerebellar Purkinje cells (Vo et al., 2018). It might prove useful to perform stable isotope labeling by amino acids *in vitro* (SILAC) or *in vivo* (SILAM); the rate with which amino acids are incorporated into proteins may tell us the rate of nascent protein synthesis. Other techniques can be done including labeling nascent polypeptides with O-propargyl-puromycin (Forester et al., 2018) or other labels (Dieterich et al., 2010; Iwasaki and Ingolia, 2017).

Slowed down protein synthesis may be coupled to protein or cellular degradation. Alanine and leucine in combination at near-physiological concentrations have been shown to inhibit autophagy *in vitro* and alanine's contribution is transaminase dependent; i.e. autophagy continues in the presence of a transaminase inhibitor, aminooxyacetate (Meijer et al., 2015). Furthermore, inhibition of GPT2 impairs glutamine-mediated mTORC1 reactivation during amino acid starvation (Tan et al., 2017). Autophagy or other proteolytic pathways (ubiquitin-proteasome pathway) may also explain the increase in essential amino acids in *Gpt2*-null brain.

Our data suggest that dietary modifications may involve alanine as a potential therapeutic supplement for human patients with GPT2 Deficiency. Supplemental alanine has been shown to be well tolerated in humans (Bodamer et al., 2000; Carlin et al., 1987; Genuth and Castro, 1974). To date, the only biochemical finding in human patients with GPT2 Deficiency is decreased alanine levels in the plasma (Celis et al., 2015), a result which is supported by our data here in the *Gpt2*-null mouse. This data is very hopeful for a clinical trial involving alanine in people with GPT2 Deficiency.

Is the TCA cycle affected after the loss of GPT2? If so, does it occur in neurons or astrocytes or both? Would TCA cycle supplementation alleviate/prevent metabolic or behavioral defects, may it be a therapeutic target?

In our studies of the metabolome, we also observe prominent increases in glycolytic intermediates, preceded by an undermined TCA cycle in *Gpt2*-null brain. Is glycolysis being used more as ATP source given the deficits in the TCA cycle? While it has yet to be demonstrated, it is highly probable. The increased glycolytic intermediates may also be a result of reduced pyruvate levels which may cause decreased substrate inhibition of glycolytic enzymes. Indeed, glycolysis is regulated not only by pyruvate at the substrate level but also by alanine, which is an allosteric inhibitor of pyruvate kinase (Carbonell et al., 1973). We find no changes in glucose uptake in hippocampal neurons and astrocytes *in vitro* or in glycolytic enzyme protein levels that could have reflected changes in metabolite levels. Glucose uptake and flux analysis *in vivo* may further dissect out the mechanisms behind the increase in glycolytic metabolites.

Amino acids and the TCA cycle are closely linked. We observe increased levels in an intriguingly high number of amino acids in *Gpt2*-null brain. Increased amino acid profile (particularly essential amino acids) in the *Gpt2*-null brain may stem from increased transporter expression driven by the transcription factor ATF4, one of whose targets is GPT2, as the system is predicted to be in need of alanine (Hao et al., 2016; Salgado et al., 2014). However, this was not the case. More studies *in vivo* are warranted to determine the possibilities of changes in specific transporter levels or increased protein breakdown to support both alanine supply and the TCA cycle as free amino acids can readily be converted into TCA cycle intermediates.

The TCA cycle metabolism was profoundly affected in the absence of GPT2. We find decreases in glutamine-dependent anaplerosis (replenishment of the TCA cycle intermediates) in both neurons and astrocytes *in vitro*. Please refer to the Appendix for Chapter 3 for the data on astrocytes; as we had only the data for 13C labeling in alpha-ketoglutarate, I left it for the Appendix. Glutamine entry into the TCA cycle is affected in both cell types, and this is also evident in concomitant decreases in alanine release in both cell types. However, given all the data on survival *in vitro*, astrocytes may be able to utilize other metabolic pathways to support their TCA cycle such as pyruvate carboxylation which is exclusive to astrocytes. This is evident in metabolomics performed in wild-type and *Gpt2*-null astrocytes *in vitro*; no tangible differences in any of the metabolites were found (Appendix for Chapter 3).

We also find deficits in the TCA cycle in *Gpt2*-null synaptosomes (isolated nerve terminals), such as decreases in malate and fumarate levels, but glutamine can still be efficiently used as a precursor to the TCA cycle intermediates. There are anaplerotic

pathways, other than glutamate dehydrogenase and GPT2, that may support the TCA cycle in the absence of GPT2 such as pyruvate carboxylase and other aminotransferases that yield alpha-ketoglutarate from glutamate including branched-chain amino acid aminotransferases (Hutson, 2001; Morken et al., 2014). All these processes likely contribute to sustain the TCA cycle in *Gpt2*-null brain as long as they are able; however, each have certain complications. For example, pyruvate carboxylase exists mainly in astrocytes and consumes ATP to make oxaloacetate (Hertz et al., 2007; Yu et al., 1983). Glutamate dehydrogenase is found both in neurons and astrocytes but depends on NADP availability (Aoki et al., 1987). Aminotransferases that degrade essential amino acids usually work in the direction of producing glutamate and not alpha-ketoglutarate (Conway and Hutson, 2016). In contrast, GPT2 depends neither on ATP nor NADP availability, thereby conferring a unique anaplerotic ability to the cell. Levels of GPT2 and GPT1 protein have been shown to increase in models of oxidative phosphorylation deficits induced by mitochondrial DNA mutations (Chen et al., 2018) and disrupted mitochondrial fusion dynamics (Motori et al., 2020). GPT2's unique support of the TCA cycle may enhance both energetics and biosynthesis to sustain cell growth and this is also evident in smaller neuron soma sizes (e.g. CA1 pyramidal neurons, motor neurons in the spinal cord and motor cortex, noradrenergic neurons) as well as microcephaly seen in both mice and human patients with *GPT2* mutations (Ouyang et al., 2016).

Alpha-ketoglutarate was able to reverse the glutamate deficits in *Gpt2*-null synaptosomes and raise glutamate levels back to that of the wild-type. While it may prove useful to try alpha-ketoglutarate in hippocampal slices to see if glutamate transmission in electrophysiology is rescued, the entry and metabolism of alpha-

ketoglutarate are presumed to be different compared to synaptosomes. Other TCA cycle constituents, such as citrate may be tried as it is readily taken up by neurons and astrocytes (Yodoya et al., 2006).

TCA cycle supplementation *in vivo* is one of the future directions both in terms of rescuing glutamate deficits and also other metabolic derangements. So far, Triheptanoin, the triglyceride of heptanoic acid that can be fed into the TCA cycle via propionyl-CoA, has been tried but failed to rescue survival *in vivo*, however this was most likely due to unpalatability of the diet as it led to decreases in weight in the parents, smaller litter size and smaller stature of the pups. Alpha-ketoglutarate is an option and has been shown to increase lifespan of mice (Asadi Shahmirzadi et al., 2020). As always, first-pass metabolism in the liver is a key complicating problem and the *Gpt2*-null pups have to receive the supplementation early and continuously as the metabolic defects are already apparent at postnatal day 7. Forced feeding is not a practical option, osmotic pumps may be tried but the pups are very young and the procedure may lead to maternal negligence.

Is GPT2 metabolism redundant or essential in neurons?

Given that alanine deprivation leads to death of hippocampal *Gpt2*-null neurons *in vitro* and that SynapsinI-cre conditional *Gpt2*-null mice die the same way as the germline *Gpt2*-null mice, we can safely conclude that GPT2 function in neurons is essential. Astrocytes do not share this dependency on GPT2 as their growth and survival are not impaired in the absence of GPT2 *in vitro* and GFAP-cre conditional astrocyte-specific deletion of *Gpt2*-null mice does not lead to premature death *in vivo*.

Most likely, the functions of GPT2 and GPT1 are not redundant and their individual importance arise from differential expression in various cell types and not so much from compartmentation within different subcellular locations in the same cell. While such compartmentation is crucial for metabolic enzymes such as cytosolic and mitochondrial aspartate aminotransferases within the malate-aspartate shuttle (Berkich et al., 2007; Borst, 2020), no such shuttling has been reported for alanine within the cell, nor any emphasis on presence of the two GPT isoforms in the same cell. This joining of forces of GPT2 and GPT1 may exist in astrocytes (Figure 3) and recently, a candidate gene for a mitochondrial serine/alanine transporter has been published (Kory et al., 2018).

How is the animal behavior affected after GPT2 loss? Are there specific regions in the central nervous system with selective vulnerability to GPT2 loss?

As most humans with *GPT2* mutations suffer from progressive spastic paraplegia, wide gait, and hyperreflexia, we were expecting that *Gpt2*-null mice would re-capitulate the motor abnormalities. Indeed, *Gpt2*-null mice display wide gait and clasping reflex in the hind limbs, however, studies of any progressive nature in motor dysfunction would not be possible because all *Gpt2*-null mice die before post-natal day 30. High Alanine diet allows us to observe progression of the motor dysfunction in *Gpt2*-null mice as they age. At around two to three months, they almost completely lose their ability to walk on all four paws. Motor defects also manifest in neuropathology as reduced number and soma size of motor neurons in the spinal cord, along with a prominent astrogliosis in the gray matter. The observation that extra alanine in the diet improved survival but not the

motor function points at a possible need of extra TCA cycle support in the lower motor neurons, given prominent defects in the TCA cycle found both *in vivo* and *in vitro* experiments (Ouyang et al., 2016). The underlying causes of specific vulnerability of motor neurons in the spinal cord to the metabolic damage caused by absence of GPT2 are yet unknown. It is interesting that only a few mutations in mitochondrial proteins have been reported to cause spastic paraplegia (Blackstone, 2018). This study identifies GPT2 as a key metabolic mitochondrial protein in a mouse model of spastic paraplegia with motor abnormalities.

Smaller soma sizes and loss of spinal cord motor neurons have been observed in other neurological diseases including amyotrophic lateral sclerosis (ALS) (Taylor et al., 2016). Indeed, genetic mutations in SPG11, or Spatacsin, a spastic paraplegia gene, also cause spinal cord motor neuron death (Stevanin et al., 2008). Hereditary spastic paraplegia has been attributed to upper motor neuron degeneration due to greater energetic and biosynthetic demand of long-ranging axons (Blackstone, 2018). While we do not observe any degeneration or cell loss in primary motor cortex of *Gpt2*-null mice, the soma sizes of the layer 5 neurons are reduced, suggesting that GPT2 acts on similar mechanisms of neuronal growth in both upper and lower motor neurons. More in-depth analysis of upper motor neurons is warranted. Whether the loss of lower motor neurons in *Gpt2*-null mice occurs cell-autonomously or whether any other circuitry in the brain is as affected in the *Gpt2*-null mice remain to be explored. Importantly, a majority of mouse models of spastic paraplegia show motor disability without death of upper motor neurons (Blackstone, 2018; Salinas et al., 2008). Interestingly, one recent case report of a patient

with GPT2 Deficiency has demonstrated motor neuropathy consistent with our findings of loss of lower motor neurons in the mouse model (Ruaud et al., 2021).

We see damage in another area of the nervous system in *Gpt2*-null mice, locus coeruleus (LC). Since LC is implicated in Alzheimer's and Parkinson's Disease, much work has been done in humans and disease models; however the exact mechanisms by which this locus degenerates are unknown. This should not be said lightly; there is no consensus on how the LC neurons die, whether it be regarding the neuromelanin levels, oxidative stress or relative metal compositions. GPT2 Deficiency may provide a mechanistic venue for studying metabolic damage in LC and in doing so may help with therapeutics in Alzheimer's and Parkinson's Disease.

Since GPT2 is closely linked to motor function, one might ask whether there is any causality between LC damage in *Gpt2*-null mice and the motor abnormalities. Locus coeruleus projects to virtually the entire central nervous system and descending noradrenergic tracts have been shown to influence motor function (Amaral and Sinnamon, 1977; Foote et al., 1983; Harro et al., 2008; Kwasniewska et al., 2020; Loughlin et al., 1986; Rekling et al., 2000). Examples of motor abnormalities have been correlated with LC. Norepinephrine loss has been found to cause stronger motor deficits than MPTP treatment (resulting in almost complete loss of substantia nigra dopaminergic neurons) on its own (Rommelfanger et al., 2007). KIF5a deficiency, a type of spastic paraplegia (SPG10), presents with decreases in cerebrospinal fluid levels of 3-methoxyl-4-hydroxyphenylglycol, a noradrenergic metabolite (Andreasson et al., 2019). More mechanistic studies are warranted to determine whether motor deficits seen in GPT2 Deficiency are linked primarily to defects of noradrenergic transmission.

One intriguing possibility for the selective vulnerability of LC is the distinct metabolic enzyme and metabolome profile of LC. An intriguing connection between GPT2 Deficiency in human patients and LC metabolism has recently emerged, where Ruaud and co-workers found reduced amount of pterins and homovanilic acid in the cerebrospinal fluid (Ruaud et al., 2021). A decreased level of homovanilic acid, a metabolite of tyrosine metabolism in dopaminergic and noradrenergic neurons, may reflect a secondary consequence of LC dysfunction. A pterin derivative, tetrahydrobiopterin (BH4) acts as a co-enzyme for tyrosine hydroxylase, which is essential for catecholamine synthesis (Ichinose et al., 2013). BH4 is made from dihydrobiopterin by dihydrobiopterin reductase consuming NADPH which is mainly synthesized via the pentose phosphate pathway. NADPH is readily made from glucose 6-phosphate dehydrogenase which is shown to have strong activity in LC of the rat (Amaral and Sinnamon, 1977). The vulnerability in LC may also originate from defective cellular energetics. Biosynthesis of macromolecules using NADPH as co-enzymes depend on a functioning tricarboxylic acid (TCA) cycle (Martinez-Reyes and Chandel, 2020). We have shown previously that TCA cycle intermediates are profoundly diminished in *Gpt2*-null brain. Metabolic studies in LC may allow us to explore the extent of metabolic mechanisms implicated by loss of GPT2.

BH4 is also used as a co-enzyme for nitric oxide synthase, the activity of which has been shown to modulate oxidative stress in LC (Higgins and Gross, 2010; Sanchez-Padilla et al., 2014). In the absence of BH4, electron transport from NADPH to heme, normally facilitated by BH4 in nitric oxide synthase, may be uncoupled leading to an increase in leakage to molecular oxygen causing an increase in superoxide anion.

Increased pacemaking activity may also lead to increases in Ca^{2+} levels leading to more oxidative stress and possibly apoptosis. Oxidative stress has been studied in LC vulnerability particularly in the context of neuromelanin and heavy metals (Zecca et al., 2004a; Zecca et al., 2004b). Detailed studies of metabolic pathways involved in oxidative stress in LC are warranted.

There have been other studies in animal models of Alzheimer's, Parkinson's, Rett syndrome and Down syndrome in addition to a study that involves genetic ablation of the mitochondrial sirtuin T3 that have been shown to cause degeneration, cell loss or gliosis in LC, however, these studies do not give a clearly defined degeneration of LC. To our knowledge, our study is the first to provide strong microgliosis and degeneration in LC in an animal model of a metabolic disease. Studies of GPT2 Deficiency and the link to deficits in LC may provide us clues as to why this locus is vulnerable and eventually lead to a therapeutic target that may be beneficial to a wide range of neurological diseases.

Does GPT2 have major contributions to synaptic glutamate availability?

Overall, our data suggests that GPT2 does not have a major influence on synaptic glutamate availability as evidenced by slight decreases in glutamate levels which may be explained by compensatory upregulation of other enzymes involved in glutamate metabolism. We report that GPT2 is enriched in the mitochondria of isolated synaptic terminals (synaptosomes) and the loss of GPT2 leads to a re-wiring of glutamate metabolism. GPT2 can be used to produce glutamate with alanine and alpha-ketoglutarate as precursors and to control conversion of glutamine into alanine. According to our data, approximately 40% of the glutamate pool released upon depolarization may come from

alanine in isolated synaptic terminals. It should be noted that "can" is not the same as "does" in a physiological setting. It is possible that GPT2 may reverse the reaction in favor of glutamate formation when enough substrates are available, however given that there are modest decrease in glutamate, GPT2 is unlikely to play a major rate-determining enzyme for synaptic glutamate synthesis.

The impaired glutamatergic transmission in mouse brain slices is evident in miniature excitatory current amplitude and faster decline of amplitude response in CA1 pyramidal neurons to repeated stimulation of CA3 Schaffer collaterals. The rest of Chapter 4 provides evidence that reprogramming of glutamate metabolism to support the TCA cycle is most likely the culprit behind decreases in glutamate. It is crucial to keep in mind that different types of synapses may rely on GPT2 differently (e.g. tripartite synapses).

Do any of the findings with GPT2 Deficiency in mice correlate with any phenotype in a cancerous cell line? i.e. is there a ubiquitous mechanism of cellular growth?

Gpt2-null HAP1 cells have smaller cell sizes and their rate of division is reduced with alanine deprivation. Their metabolomic profile contains similarities with those of *Gpt2*-null whole brain and hippocampus tissues, particularly in alanine, TCA cycle intermediates, and several of the amino acids. Therefore, HAP1 cell line may provide a useful and fast way for biochemical assays *in vitro*. Overall, it appears that GPT2 has a ubiquitous function across different cell types in controlling cellular growth and maintenance.

In summary

Recessive loss-of-function mutations in the mitochondrial enzyme glutamate pyruvate transaminase 2 (*GPT2*) in humans cause reduced postnatal brain growth, and cognitive and motor disability. GPT2 catalyzes the reversible addition of an amino group from glutamate to pyruvate, yielding alanine and alpha-ketoglutarate. We demonstrate that GPT2 governs critical metabolic mechanisms in neurons required for neuronal growth and survival in a mouse model of GPT2 Deficiency. These metabolic processes include neuronal alanine synthesis and anaplerosis, the replenishment of tricarboxylic acid (TCA) cycle intermediates. By targeted metabolomics, we find alterations in alanine levels to occur earliest, followed by reduced TCA cycle intermediates and reduced pyruvate. Neuron-specific deletion of *Gpt2* in mice is sufficient to cause motor abnormalities and death pre-weaning, a phenotype identical to the germ-line *Gpt2*-null mouse. Alanine biosynthesis is profoundly impeded in *Gpt2*-null neurons. Exogenous alanine is necessary for *Gpt2*-null neuronal survival *in vitro* but is not needed for *Gpt2*-null astrocytes. Dietary alanine supplementation in *Gpt2*-null mice enhances animal survival. In surviving *Gpt2*-null animals, we observe smaller upper and lower motor neurons in vivo. We observe selective death of lower motor neurons *in vivo* with worsening motor behavior with age. GPT2 Deficiency also involves a novel mechanism of degeneration, gliosis, and neuron loss in locus coeruleus with reduced noradrenergic projections to and norepinephrine levels in hippocampus and spinal cord in *Gpt2*-null mice. We report that GPT2 is enriched in isolated synaptic terminals and GPT2 loss leads to reprogramming of glutamate metabolism. Glutamatergic transmission in *Gpt2*-null CA1 hippocampal slices is impaired. Glutamate levels released from *Gpt2*-null isolated nerve terminals are reduced but restored to wild-type levels by alpha-ketoglutarate. These

studies of the pathophysiology of GPT2 Deficiency have identified metabolic mechanisms that are required for neuronal growth and that may underlie selective vulnerabilities in specific neuronal circuits. Alanine or TCA cycle supplementation may also prove useful as therapeutic targets in patients with GPT2 Deficiency.

REFERENCES

Amaral, D., and Sinnamon, H. (1977). The locus coeruleus: neurobiology of a central noradrenergic nucleus. Progress in Neurobiology *9*, 147-196.

Andreasson, M., Lagerstedt-Robinson, K., Samuelsson, K., Solders, G., Blennow, K., Paucar, M., and Svenningsson, P. (2019). Altered CSF levels of monoamines in hereditary spastic paraparesis 10: A case series. Neurol Genet *5*, e344.

Aoki, C., Milner, T.A., Sheu, K.F., Blass, J.P., and Pickel, V.M. (1987). Regional distribution of astrocytes with intense immunoreactivity for glutamate dehydrogenase in rat brain: implications for neuron-glia interactions in glutamate transmission. The Journal of Neuroscience *7*, 2214-2231.

Asadi Shahmirzadi, A., Edgar, D., Liao, C.Y., Hsu, Y.M., Lucanic, M., Asadi Shahmirzadi, A., Wiley, C.D., Gan, G., Kim, D.E., Kasler, H.G.*, et al.* (2020). Alpha-Ketoglutarate, an Endogenous Metabolite, Extends Lifespan and Compresses Morbidity in Aging Mice. Cell Metab *32*, 447-456 e446.

Berkich, D.A., Ola, M.S., Cole, J., Sweatt, A.J., Hutson, S.M., and LaNoue, K.F. (2007). Mitochondrial transport proteins of the brain. J Neurosci Res *85*, 3367-3377.

Blackstone, C. (2018). Hereditary spastic paraplegia. Handb Clin Neurol *148*, 633-652.

Bodamer, O.A., Halliday, D., and Leonard, J.V. (2000). The effects of l-alanine supplementation in late-onset glycogen storage disease type II. Neurology *55*, 710-712.

Borst, P. (2020). The malate-aspartate shuttle (Borst cycle): How it started and developed into a major metabolic pathway. IUBMB Life.

Carbonell, J., Feliu, J.E., Marco, R., and Sols, A. (1973). Pyruvate kinase. Classes of regulatory isoenzymes in mammalian tissues. Eur J Biochem *37*, 148-156.

Carlin, J.I., Olson, E.B., Jr., Peters, H.A., and Reddan, W.G. (1987). The effects of post-exercise glucose and alanine ingestion on plasma carnitine and ketosis in humans. J Physiol *390*, 295-303.

Celis, K., Shuldiner, S., Haverfield, E.V., Cappell, J., Yang, R., Gong, D.W., and Chung, W.K. (2015). Loss of function mutation in glutamic pyruvate transaminase 2 (GPT2) causes developmental encephalopathy. J Inherit Metab Dis *38*, 941-948.

Chen, Q., Kirk, K., Shurubor, Y.I., Zhao, D., Arreguin, A.J., Shahi, I., Valsecchi, F., Primiano, G., Calder, E.L., Carelli, V.*, et al.* (2018). Rewiring of Glutamine Metabolism Is a Bioenergetic Adaptation of Human Cells with Mitochondrial DNA Mutations. Cell Metab *27*, 1007-1025 e1005.

Conway, M.E., and Hutson, S.M. (2016). BCAA Metabolism and NH3 Homeostasis. Adv Neurobiol *13*, 99-132.

Cynober, L.A. (2002). Plasma amino acid levels with a note on membrane transport: characteristics, regulation, and metabolic significance. Nutrition *18*, 761-766.
Dieterich, D.C., Hodas, J.J., Gouzer, G., Shadrin, I.Y., Ngo, J.T., Triller, A., Tirrell, D.A., and Schuman, E.M. (2010). In situ visualization and dynamics of newly synthesized proteins in rat hippocampal neurons. Nat Neurosci *13*, 897-905.
Foote, S.L., Bloom, F.E., and Aston-Jones, G. (1983). Nucleus locus ceruleus: new evidence of anatomical and physiological specificity. Physiol Rev *63*, 844-914.
Forester, C.M., Zhao, Q., Phillips, N.J., Urisman, A., Chalkley, R.J., Oses-Prieto, J.A., Zhang, L., Ruggero, D., and Burlingame, A.L. (2018). Revealing nascent proteomics in signaling pathways and cell differentiation. Proc Natl Acad Sci U S A *115*, 2353-2358.
Genuth, S.M., and Castro, J. (1974). Effect of oral alanine on blood beta-hydroxybutyrate and plasma glucose, insulin, free fatty acids, and growth hormone in normal and diabetic subjects. Metabolism *23*, 375-386.
Hao, Y., Samuels, Y., Li, Q., Krokowski, D., Guan, B.J., Wang, C., Jin, Z., Dong, B., Cao, B., Feng, X.*, et al.* (2016). Oncogenic PIK3CA mutations reprogram glutamine metabolism in colorectal cancer. Nat Commun *7*, 11971.
Harro, J., Meriküla, A., Lepiku, M., Modiri, A.-R., Rinken, A., and Oreland, L. (2008). Lesioning of Locus coeruleus Projections by DSP-4 Neurotoxin Treatment: Effect on Amphetamine-Induced Hyperlocomotion and Dopamine D2 Receptor Binding in Rats. Pharmacology & Toxicology *86*, 197-202.
Hertz, L., Peng, L., and Dienel, G.A. (2007). Energy metabolism in astrocytes: high rate of oxidative metabolism and spatiotemporal dependence on glycolysis/glycogenolysis. J Cereb Blood Flow Metab *27*, 219-249.
Higgins, C.E., and Gross, S.S. (2010). Tetrahydrobiopterin. In Nitric Oxide, pp. 169-209.
Hutson, S. (2001). Structure and function of branched chain aminotransferases. In, pp. 175-206.
Ichinose, H., Homma, D., Sumi-Ichinose, C., Nomura, T., and Kondo, K. (2013). GTP cyclohydrolase regulation: implications for brain development and function. Adv Pharmacol *68*, 23-35.
Iwasaki, S., and Ingolia, N.T. (2017). The Growing Toolbox for Protein Synthesis Studies. Trends Biochem Sci *42*, 612-624.
Kanehisa, M., Furumichi, M., Sato, Y., Ishiguro-Watanabe, M., and Tanabe, M. (2020). KEGG: integrating viruses and cellular organisms. Nucleic Acids Res.
Kang, H.J., Kawasawa, Y.I., Cheng, F., Zhu, Y., Xu, X., Li, M., Sousa, A.M., Pletikos, M., Meyer, K.A., Sedmak, G.*, et al.* (2011). Spatio-temporal transcriptome of the human brain. Nature *478*, 483-489.
Kory, N., Wyant, G.A., Prakash, G., Uit de Bos, J., Bottanelli, F., Pacold, M.E., Chan, S.H., Lewis, C.A., Wang, T., Keys, H.R.*, et al.* (2018). SFXN1 is a mitochondrial serine transporter required for one-carbon metabolism. Science *362*.
Krebs, H.A. (1953). Equilibria in transamination systems. Biochem J *54*, 82-86.
Kwasniewska, A., Miazga, K., Majczynski, H., Jordan, L.M., Zawadzka, M., and Slawinska, U. (2020). Noradrenergic Components of Locomotor Recovery Induced by Intraspinal Grafting of the Embryonic Brainstem in Adult Paraplegic Rats. Int J Mol Sci *21*.
Levi, G., Kandera, J., and Lajtha, A. (1967). Control of cerebral metabolite levels. Archives of Biochemistry and Biophysics *119*, 303-311.

Loughlin, S.E., Foote, S.L., and Grzanna, R. (1986). Efferent projections of nucleus locus coeruleus: Morphologic subpopulations have different efferent targets. Neuroscience *18*, 307-319.
Lysiak, W., Pienkowska-Vogel, M., Szutowicz, A., and Angielski, S.A. (1974). Inhibition of alanine and aspartate aminotransferases by alpha-oxoderivatives of the branched-chain amino acids. J Neurochem *22*, 77-83.
Martinez-Reyes, I., and Chandel, N.S. (2020). Mitochondrial TCA cycle metabolites control physiology and disease. Nat Commun *11*, 102.
McCommis, K.S., Chen, Z., Fu, X., McDonald, W.G., Colca, J.R., Kletzien, R.F., Burgess, S.C., and Finck, B.N. (2015). Loss of Mitochondrial Pyruvate Carrier 2 in the Liver Leads to Defects in Gluconeogenesis and Compensation via Pyruvate-Alanine Cycling. Cell Metab *22*, 682-694.
Meijer, A.J., Lorin, S., Blommaart, E.F., and Codogno, P. (2015). Regulation of autophagy by amino acids and MTOR-dependent signal transduction. Amino Acids *47*, 2037-2063.
Miller, A.L., Hawkins, R.A., and Veech, R.L. (1973). The mitochondrial redox state of rat brain. J Neurochem *20*, 1393-1400.
Morken, T.S., Brekke, E., Haberg, A., Wideroe, M., Brubakk, A.M., and Sonnewald, U. (2014). Neuron-astrocyte interactions, pyruvate carboxylation and the pentose phosphate pathway in the neonatal rat brain. Neurochem Res *39*, 556-569.
Motori, E., Atanassov, I., Kochan, S.M.V., Folz-Donahue, K., Sakthivelu, V., Giavalisco, P., Toni, N., Puyal, J., and Larsson, N.G. (2020). Neuronal metabolic rewiring promotes resilience to neurodegeneration caused by mitochondrial dysfunction. Sci Adv *6*, eaba8271.
Ouyang, Q., Nakayama, T., Baytas, O., Davidson, S.M., Yang, C., Schmidt, M., Lizarraga, S.B., Mishra, S., Ei-Quessny, M., Niaz, S.*, et al.* (2016). Mutations in mitochondrial enzyme GPT2 cause metabolic dysfunction and neurological disease with developmental and progressive features. Proc Natl Acad Sci U S A *113*, E5598-5607.
Phillips, R.S. (2014). Structure and mechanism of kynureninase. Arch Biochem Biophys *544*, 69-74.
Rekling, J.C., Funk, G.D., Bayliss, D.A., Dong, X.W., and Feldman, J.L. (2000). Synaptic control of motoneuronal excitability. Physiol Rev *80*, 767-852.
Rommelfanger, K.S., Edwards, G.L., Freeman, K.G., Liles, L.C., Miller, G.W., and Weinshenker, D. (2007). Norepinephrine loss produces more profound motor deficits than MPTP treatment in mice. Proc Natl Acad Sci U S A *104*, 13804-13809.
Ron-Harel, N., Ghergurovich, J.M., Notarangelo, G., LaFleur, M.W., Tsubosaka, Y., Sharpe, A.H., Rabinowitz, J.D., and Haigis, M.C. (2019). T Cell Activation Depends on Extracellular Alanine. Cell Rep *28*, 3011-3021 e3014.
Rossiter, N.J., Huggler, K.S., Adelmann, C.H., Keys, H.R., Soens, R.W., Sabatini, D.M., and Cantor, J.R. (2021). CRISPR screens in physiologic medium reveal conditionally essential genes in human cells. Cell Metab *33*, 1248-1263 e1249.
Ruaud, L., Keren, B., Debs, R., Mignot, C., and Mochel, F. (2021). Demyelinating motor neuropathy associated with a homozygous GPT2 pathogenic variant. Muscle Nerve.
Salgado, M.C., Meton, I., Anemaet, I.G., and Baanante, I.V. (2014). Activating transcription factor 4 mediates up-regulation of alanine aminotransferase 2 gene expression under metabolic stress. Biochim Biophys Acta *1839*, 288-296.

Salinas, S., Proukakis, C., Crosby, A., and Warner, T.T. (2008). Hereditary spastic paraplegia: clinical features and pathogenetic mechanisms. The Lancet Neurology *7*, 1127-1138.
Sanchez-Padilla, J., Guzman, J.N., Ilijic, E., Kondapalli, J., Galtieri, D.J., Yang, B., Schieber, S., Oertel, W., Wokosin, D., Schumacker, P.T.*, et al.* (2014). Mitochondrial oxidant stress in locus coeruleus is regulated by activity and nitric oxide synthase. Nat Neurosci *17*, 832-840.
Stevanin, G., Azzedine, H., Denora, P., Boukhris, A., Tazir, M., Lossos, A., Rosa, A.L., Lerer, I., Hamri, A., Alegria, P.*, et al.* (2008). Mutations in SPG11 are frequent in autosomal recessive spastic paraplegia with thin corpus callosum, cognitive decline and lower motor neuron degeneration. Brain *131*, 772-784.
Tan, H.W.S., Sim, A.Y.L., and Long, Y.C. (2017). Glutamine metabolism regulates autophagy-dependent mTORC1 reactivation during amino acid starvation. Nat Commun *8*, 338.
Taylor, J.P., Brown, R.H., Jr., and Cleveland, D.W. (2016). Decoding ALS: from genes to mechanism. Nature *539*, 197-206.
Vo, M.N., Terrey, M., Lee, J.W., Roy, B., Moresco, J.J., Sun, L., Fu, H., Liu, Q., Weber, T.G., Yates, J.R., 3rd*, et al.* (2018). ANKRD16 prevents neuron loss caused by an editing-defective tRNA synthetase. Nature *557*, 510-515.
Yodoya, E., Wada, M., Shimada, A., Katsukawa, H., Okada, N., Yamamoto, A., Ganapathy, V., and Fujita, T. (2006). Functional and molecular identification of sodium-coupled dicarboxylate transporters in rat primary cultured cerebrocortical astrocytes and neurons. J Neurochem *97*, 162-173.
Yu, A.C., Drejer, J., Hertz, L., and Schousboe, A. (1983). Pyruvate carboxylase activity in primary cultures of astrocytes and neurons. J Neurochem *41*, 1484-1487.
Zecca, L., Stroppolo, A., Gatti, A., Tampellini, D., Toscani, M., Gallorini, M., Giaveri, G., Arosio, P., Santambrogio, P., Fariello, R.G.*, et al.* (2004a). The role of iron and copper molecules in the neuronal vulnerability of locus coeruleus and substantia nigra during aging. Proc Natl Acad Sci U S A *101*, 9843-9848.
Zecca, L., Youdim, M.B., Riederer, P., Connor, J.R., and Crichton, R.R. (2004b). Iron, brain ageing and neurodegenerative disorders. Nat Rev Neurosci *5*, 863-873.

ROLE OF GPT2 in NEUROMETABOLISM

GPT2 DEFICIENCY

How does the pathogenic metabolome progress over time?

- Alanine & TCA cycle metabolism defects followed by increases in amino acids metabolism and glycolytic intermediates

How is the animal behavior affected after Gpt2 loss?

- Premature death by weaning, failure to thrive, wide hind-limb gait, hinb-limb clasping reflexes.

Does Gpt2 confer the ability to synthesize alanine in the cells, i.e. non-essentiality of alanine?

- In neurons yes; alanine deprivation causes neuronal death in vitro.
- In astrocytes, alanine deprivation does not cause death in vitro.
- In vivo supplementation increases chances of animal survival.

Is Gpt2 metabolism redundant or essential in neurons?

- Essential.
Animal behavioral and motor phenotype are present in Synapsinl-cre conditional Gpt2-null mouse.
- In vitro assays shows increased neuronal death a fter alanine deprivation.

Is the TCA cycle affected after the loss of Gpt2? If so, does it occur in neurons or astrocytes or both?

- Glutamine-dependent anaplerosis in Gpt2-null neurons and astrocytes is diminished.

Are there specific regions in the central nervous system with selective vulnerability to Gpt2 loss?

- Death of motor neurons in the spinal cord at P90
- Death of locus coeruleus neurons at P18

Would either alanine or TCA cycle supplementation alleviate/prevent metabolic or behavioral defects, i.e. may they be rescue strategies?

- In vivo alanine supplementation increases chances of animal survival.
- Alpha-ketoglutarate rescues glutamate defects in synaptosomes.

Does Gpt2 have major contributions to synaptic glutamate availability?

- Modest decreases in synaptic glutamate.
- Reprogramming of glutamate metabolism.

Chapter 2&3 | Chapter 4

Chapter 5 | Chapter 6

Do any of the findings with Gpt2 deficiency in mice correlate with any phenotype in a cancerous cell line? i.e. is there a ubiquitous mechanism of cellular growth?

- Smaller cell size.
- Similar metabolic profile.
- Reduced division rate with alanine deprivation.

TABLE OF CONTENTS FOR APPENDICES

Appendix for Chapter 5:

1. Additional data on 15N-glutamine labeling in Gpt2-null synaptosomes.
2. Additional data on metabolomics in Gpt2-null synaptosomes.
3. Network firing of cortical Gpt2-null neurons using Microelectrode Arrays (MEA).

Appendix 3.1. Chemical panel of Gpt2-null serum at P18.

Introduction

We performed a chemical panel on the serum of Gpt2-null mice at postnatal day 18 (P18) to identify any pathological biomarkers present in the blood. The serum chemical panel included:

a) aspartate aminotransferase (AST) and alanine aminotransferase (ALT), both have been used as indicator of liver damage.

b) total protein

c) creatine kinase, as an indicator of muscle damage

d) blood nitrogen urea (BUN)

e) cholesterol

f) glucose

g) bicarbonate (Total CO2)

h) triglycerides

Results/Key Points

- No major differences in any metric, except for a decrease in cholesterol levels in Gpt2-null serum at P18. There is also a modest decrease in triglycerides though statistically non-significant ($P = 0.188$).

Discussion

The difference in cholesterol is slight but could reflect decreases in lipid synthesis in Gpt2-null mice. The origin of this deficit is yet unclear.

Method

The serum was collected terminally by cardiac puncture after injection of sodium pentobarbital. The blood was collected in mini-SST gold tubes (IDEXX) with clot activator and gel barrier. The blood was inverted 10 times, incubated for 20 minutes, and spun at 2500 x *g* for 12 minutes. The serum was collected in a separate tube and stored at -80^{o}C until day of shipment. The chemical panel was performed at IDEXX BioResearch (North Grafton, MA).

Figure Legends

Figure – Serum chemical panel in Gpt2-null mice at postnatal day 18.

A. Different measures in the chemical panel in wild-type (black) and Gpt2-null (red) mice at P18. AST: aspartate aminotransferase, ALT: alanine aminotransferase, BUN: blood nitrogen urea. n=4 wild-type (3 females, 1 male), n=6 Gpt2-null (4 females, 2 males).

A

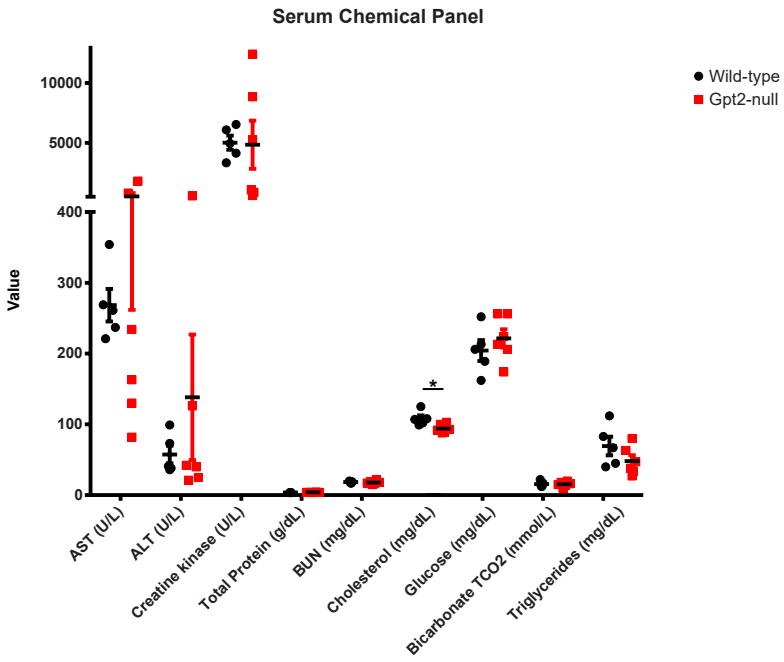

Figure A3.1 – Serum chemical panel in Gpt2-null mice at postnatal day 18.

Appendix 3.2. H&E stains in Gpt2-null muscle tissue at P18.

Introduction

Gpt2 is expressed in brain tissue as well as in skeletal muscle (Lindblom et al., 2007). Gpt2-null mice display motor abnormalities with abnormal wide hind-limb gait and smaller stature. It is possible that there is muscle wasting. The H&E stains in gastrocnemius and soleus muscle of the hind-limb of wild-type and Gpt2-null at postnatal day 18 (P18) are presented here.

Results/Key Points

- No major differences in the staining in either gastrocnemius or soleus muscle of the hind-limb in Gpt2-null mice at P18.

Discussion

It is still possible that there is decreased innervation on the muscle originating from the spinal cord, investigation of the neuromuscular junction may address this possibility.

Method

The mice were transcardially perfused with 1X PBS and then 4% paraformaldehyde. Paraffin sections were obtained of the muscle tissue and standard H&E staining was performed by Charles River Laboratories (Shrewsbury, MA).

Figure Legends

Figure A3.2. – H&E stains in gastrocnemius and soleus muscle of the hind-limb in wild-type and Gpt2-null mice at P18.

A. H&E stains in gastrocnemius (top) and soleus (bottom) muscle of the hind-limb in wild-type

(left) and Gpt2-null (right) mice at P18.

References

Lindblom, P., Rafter, I., Copley, C., Andersson, U., Hedberg, J.J., Berg, A.L., Samuelsson, A., Hellmold, H., Cotgreave, I., and Glinghammar, B. (2007). Isoforms of alanine aminotransferases in human tissues and serum--differential tissue expression using novel antibodies. Arch Biochem Biophys *466*, 66-77.

A

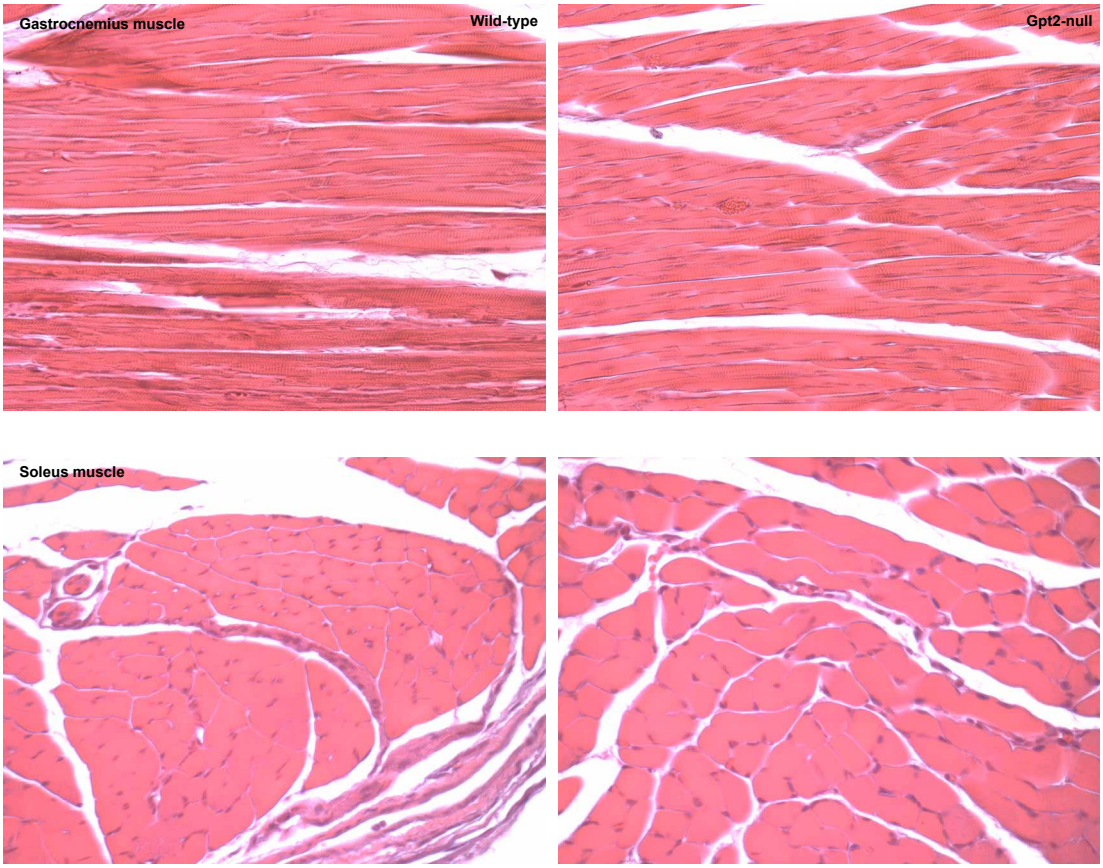

Figure A3.2 – H&E stains in gastrocnemius and soleus muscle of the hind-limb in wild-type and Gpt2-null mice at P18.

Appendix A3.3. Survival and behavior data on additional conditional deletion lines.

Introduction

I tested for phenotypic effects of other conditional deletion (cko) of Gpt2 in specific cell types in vivo. The aims of trying different Cre driver lines to delete Gpt2 in specific cells are to determine if Gpt2-cko mice survive past weaning age and to identify circuits that are most vulnerable to Gpt2 deficiency. As Gpt2-null and SynapsinI-Cre cko mice die just before weaning (postnatal day 21), it would be pertinent to pinpoint exactly in which neuron circuit the Gpt2 deletion leads to premature death. The selective vulnerabilities of different circuits may underlie the pathophysiology of Gpt2 deficiency.

The following Cre driver lines are used:

1) **CamKII-Cre** (Jax Strain No.: 005359): Allows for deletion of Gpt2 in excitatory pyramidal neurons mostly in the forebrain. As SynapsinI-Cre was pan-neuronal, CamKII-Cre can answer the question of whether the excitatory neurons in the forebrain are responsible for the premature death phenotype.

2) **Rbp4-Cre** (MMRRC Strain No.: 037128): Allows for deletion of Gpt2 in layer 5 pyramidal neurons. This is particularly useful in investigating whether Gpt2 deficiency specifically in motor neurons in the cortex would lead to motor abnormalities.

3) **Gfap-Cre** (Jax Strain No.: 024098): Allows for deletion of Gpt2 in astrocytes. This may provide contrast between the necessities for Gpt2 function in neurons versus astrocytes within the context of animal survival and motor behavior.

4) **Rosa26-CreERT2** (Jax Strain No.: 008463): Allows for tamoxifen-inducible time-controlled deletion of Gpt2 in the body. This may answer the question of whether Gpt2 is needed only developmentally or in the adult body as well.

Results/Key Points

- All tested strains of conditional Gpt2-null mice survived past weaning age with no overt abnormalities (motor, gross body anatomy). All mice have been observed until 6 months of age.

Available Data (not shown):

1. CamKII-Cre: Agarose gel electrophoresis showing genomic excision in the cortex, hippocampus (to a lesser degree, spinal cord tissues) and absence of excision in hind-limb muscle, liver, kidney and tail; Open Field Tests; Videos showing absence of Hind-limb clasping reflex; Number of mice that survived.
2. Rbp4-Cre: Agarose gel electrophoresis showing genomic excision in the cortex, hippocampus and liver and absence of excision in spinal cord, hind-limb and fore-limb muscle, tail; Open Field Tests; Number of mice that survived.
3. Gfap-Cre: Number of mice that survived.
4. Rosa26-CreERT2: Agarose gel electrophoresis showing genomic excision in the cortex, hippocampus, liver, kidney and tail. Western Blotting for Hippocampus and Cortex

Discussion

Interpretation of the results from each of the strains (with the associated complications):

1. CamKII-Cre: The expression starts around P4 and later increases to adult levels within first three weeks of life [1] whereas Synapsin-I Cre expression starts at embryonic day 12.5 [2]. Therefore one cannot rule out the possibility of the influence of the developmental timeframe on the effects of the Gpt2 deletion in excitatory neurons. More likely is the interpretation that the Gpt2 deletion in excitatory pyramidal neurons is not sufficient to cause premature death or motor abnormalities.
2. Rbp4-Cre: The expression starts around embryonic day 16.5. However, Rbp4 promoter is present in the brain and the liver (as evident in the PCR results showing genomic excision). Gpt2 is expressed in the liver and most likely this would have contributed to the phenotype. However, the conditional Gpt2-null mice had no phenotype, suggesting Gpt2 deletion in neither the liver nor layer 5 pyramidal neurons is sufficient to cause premature death or motor abnormalities.
3. Gfap-Cre: The expression has not been observed embryonically and only postnatally [3] so the possibility of the influence of the developmental timeframe cannot be ruled out. More likely is the interpretation that the Gpt2 deletion in astrocytes is not sufficient to cause premature death or motor abnormalities.
4. Rosa26-CreERT2: While all tested tissued had genomic excision, it was not 100% (i.e. the floxed allele was still detected. It is not feasible to determine to what extent the excision occurred, in which cell types or brains regions.

One technical complication for all conditional null models is that we lack the antibody for Gpt2 that works in mouse brain tissues. This prevents us from detecting absence of the protein in specific cell types.

Method

Genomic excision – PCR.

The excision of Exon 4 by Cre recombinase was tested by PCR with the following primers: ExcF (5'-CTAACTTGTCCTGCATGGTGTCAGC-3') and ExcR (5'-GGCTTTCTACCAGGAGGAACAGAGG-3') detecting the floxed allele (1479bp), the wild-type allele (1347bp) or the excised allele (687bp).

References

1. Tsien, J.Z., D.F. Chen, D. Gerber, C. Tom, E.H. Mercer, D.J. Anderson, M. Mayford, E.R. Kandel, and S. Tonegawa, *Subregion- and Cell Type–Restricted Gene Knockout in Mouse Brain.* Cell, 1996. **87**(7): p. 1317-1326.
2. Zhu, Y., M.I. Romero, P. Ghosh, Z. Ye, P. Charnay, E.J. Rushing, J.D. Marth, and L.F. Parada, *Ablation of NF1 function in neurons induces abnormal development of cerebral cortex and reactive gliosis in the brain.* Genes Dev, 2001. **15**(7): p. 859-76.
3. Gregorian, C., J. Nakashima, J. Le Belle, J. Ohab, R. Kim, A. Liu, K.B. Smith, M. Groszer, A.D. Garcia, M.V. Sofroniew, et al., *Pten deletion in adult neural stem/progenitor cells enhances constitutive neurogenesis.* J Neurosci, 2009. **29**(6): p. 1874-86.

Appendix 3.4. Data on additional diets and survival of SynapsinI-Cre conditional mice on high alanine diet.

I have tested other diets to improve the phenotype in Gpt2-null mice:

1. **High Fat & High Alanine Diet (w/w 19% Lard, 5% Alanine TD.200002)**: High fat diet may allow the pups to gain weight more easily (the diet induces obesity). While the Gpt2-null mice can survive past P30, they still failed to thrive and had motor abnormalities. I observed ten mice, only three survived up to two months, a fraction that is similar to that obtained from High Alanine diet (TD.190381). TD.200002 is a modified version of TD.06415. I terminated this experiment as it yielded unsatisfactory results and the breeding pair would get fatter and the progeny yield would decrease over time.
2. **Triheptanoin Diet (w/w 23%Triheptanoin, TD.190870)**: Triheptanoin is a triglyceride of heptanoic acid. Triheptanoin is metabolized in the liver and results in heptanoic acid (odd-carbon chain fatty acid that is converted into propionic acid) which may be used to replenish the TCA cycle (i.e. an anaplerotic supplement). It has been used in treatment of fatty acid oxidation disorders, glucose transporter 1 deficiency and pyruvate carboxylase deficiency. However, the mice did not tolerate this diet well. Their litter sizes were very low (2-4 pups per litter) and even the wild-type pups looked skinnier than the pups on the Regular diet. There were 5 Gpt2-null mice observed and none survived past weaning age. I terminated this experiment thereafter. TD.190870 is a modified version of TD.99366.
3. **Triheptanoin with High Alanine (w/w 23%Triheptanoin, 5% Alanine, TD.190871)**: I tested the combination of the two supplements. The results were similar to those of TD.190870.

4. **High Alanine (w/w 5 %) diet on SynapsinI-Cre mouse (TD.190381)**: SynapsinI-Cre conditional Gpt2-null mouse would have absence of Gpt2 protein in neuronal cells and nowhere else. I tested whether this would improve survival fraction along with High Alanine diet. This was not the case. 12 out of 12 conditional Gpt2-null mice did not survive past weaning age. This is most likely due to metabolism of alanine in the liver as Gpt2 is present in the liver.

   The breeding pairs on the special diets were started when the mice were two months old and the diet was given ad libitum. The strain background is C57B6/J (Jax Strain No 664).

Appendix 3.5. Immunohistochemistry in Spinal cord for various stains in Gpt2-null mice at P90 (high alanine diet): Cleaved Caspase3 (CC3), myelin basic protein (MBP), protein kinase C g (PKCg), neurofilament H (NFH), NG2, Olig2, SV2, VGLUT1, VGLUT2, VGAT, MTCO1, glutamate dehydrogenase (GDH), glutamine synthetase (GLUL), glucose transporter 1 (GLUT1).

Introduction

Immunohistochemical analysis in Gpt2-null spinal cord at postnatal day 90 (fed High Alanine diet, 5% w/w). The following proteins are tested, and the corresponding processes or hypotheses are listed:

Cleaved Caspase 3 (CC3): Cell death by apoptosis; death of motor neurons may explain dysfunction in the motor behavior seen in Gpt2-null mice.

Myelin Basic Protein (MBP): deficits in myelination or ascending/descending tracts.

Protein Kinase C γ (PKCγ): Specifically expressed in descending corticospinal tracts and the dorsal horn. Long projections of corticospinal tracts may be more vulnerable to damage.

Neurofilament H (NFH): General assessment of neuronal processes, particularly axons.

NG2: A marker for oligodendrocyte precursor cells. Oligodendrocyte precursor cells appear to have the highest number of fragments per kilobase pf transcript per million

mapped reads (FPKM) as per the RNA-sequencing data done by (Zhang et al., 2014). It is possible that these cells may be particularly vulnerable to Gpt2 loss.

Olig2: A marker for oligodendrocytes. This would exclude the possible involvement of any problems in the number of oligodendrocytes.

SV2: A general marker for synaptic vesicles. We see reductions in SV2 puncta in Gpt2-null hippocampal neurons in vitro.

VGLUT1: An isoform of vesicular glutamate transporter on synaptic vesicles. We observe a slight upregulation of VGLUT1 in Gpt2-null synaptosomes; this may occur in spinal cord tissue as well. Both ascending and descending tracts in the spinal cord contain VGLUT1, any major absences of VGLUT1 puncta may indicate damage to those tracts or neurons that give rise thereto.

VGLUT2: An isoform of vesicular glutamate transporter on synaptic vesicles. Similar to VGLUT1, both ascending and descending tracts in the spinal cord contain VGLUT2, however differences in staining patterns with VGLUT1, may localize any potential abnormalities to a specific tract or nucleus in the spinal cord.

VGAT: A marker for synaptic vesicles containing 4-aminobutyric acid (GABA). We observe three-fold increases in protein levels in Gpt2-null synaptosomes. While we do

not know how this increase occurs, it may uniformly occur across the central nervous system in Gpt2-null mice.

MTCO1: Cytochrome c oxidase subunit 1, a marker of mitochondria. This may reveal problems of mitochondrial biogenesis. As Gpt2 loss results in deficits in the TCA cycle, mitochondrial biogenesis or shape (fission/fusion) may be altered and this may partly contribute to the pathological phenotype.

Glutamate dehydrogenase (GDH): A mitochondrial enzyme that converts glutamate into alpha-ketoglutarate and ammonia. GDH is an anaplerotic enzyme, meaning that it catalyzes a reaction that results in a net production of a TCA cycle intermediate. In the absence of Gpt2, GDH may be upregulated as a compensatory mechanism to support the TCA cycle, this is seen in Gpt2-null synaptosomes.

Glutamine Synthetase (GLUL): A cytosolic enzyme located mainly in astrocytes, that converts glutamate into glutamine. Up-regulation of this enzyme has been seen in animal models of epilepsy and in our data, in Gpt2-null synaptosomes.

Glucose Transporter 1 (GLUT1): A glucose transporter located mainly in endothelial cells that constitute the blood brain barrier. TCA cycle deficits in the Gpt2-null tissue can lead to upregulation of glucose uptake to support cellular energetics, through increased levels of GLUT1.

Results/Key Points

Table. Proteins stained via immunohistochemistry in Gpt2-null spinal cords at P90. "QL": qualitatively assessed. "-": no difference.

Marker	Gpt2-null with respect to Wild-type
CC3 (QL)	Positivity in Ventral Horn of Cervical&Lumbar
MBP (QL)	-
NFH	-
PKCγ	Decrease Total Area in Cervical&Lumbar. Worsened phenotype compared to P18 RegDiet.
SV2	Trending decrease in Cervical and Lumbar Dorsal horn, Lumbar Ventral Horn
VGLUT1	-
VGLUT2	Increases in Lumbar Dorsal&Lateral Horn
VGAT	Decrease in Cervical Dorsal Horn. Trending decreases in Lumbar Dorsal Horn
MTCO1	-
NG2 (QL)	-
GLUT1 (QL)	-
GLUL (QL)	-
GLUD	Trending Increase in Lumbar Lateral Horn.
Olig2	Increase in Lumbar Lateral Horn.

Discussion

The most prominent result here is the decreases in PKCg staining that was also seen in Gpt2-null mice at postnatal day 18 on Regular Diet. This adds credibility to the result. While it is hard to tease the rescuing effects of High Alanine diet, since Gpt2-null mice at P90 have worsened motor abnormalities, a worsened phenotype in all the measures is expected. The reduction in percent area covered by PKCg is worsened at P90 as a measure of percentage of wild-type. There was no difference between percent areas covered in Gpt2-null P18 and P90, suggesting that most likely the tracts were already severely affected and were not rescued by the diet. However we do not have data on spinal cord taken at an earlier timepoint such as P7 or P14 to deduce whether the tracts formed and then degenerated or did not form properly. It is interesting that the wild-type

cervical PKCg area grew in size at P90 compared to P18 whereas the lumbar PKCg area remained the same. While the two wild-types are at a different age, this suggests that the corticospinal tracts continues to develop during that period (most likely primarily in its myelin sheath).

Cleaved Caspase3 staining did show some positivity in the ventral horn at both cervical and lumbar spinal cord levels in Gpt2-null mice at P90; however the Cleaved Caspase3 signal did not localize with any DAPI signal therefore we are unable to categorize this as a true signal. While almost all animals tested showed similar patterns, we cannot verify the staining completely. We also failed to find any good CC3 staining in the literature for comparison. Furthermore, Fluoro-Jade C staining (another marker for neurodegeneration) failed to show any positivity.

While there are similarities in the results of SV2, VGAT and VGLUT2 staining at P90 compared to Gpt2-null mice at P18 on Regular diet, the results obtained with High alanine diet are relatively less striking or simply not statistically significant. The differences found at P18 on Regular diet were very slight and not as compelling as PKCg so the unremarkable results found in Gpt2-null mice fed High Alanine at P90 are not surprising.

Method

The animals received High Alanine diet (5% w/w) (Diet no. 190381) ad libitum.

Immunofluorescence – Tissue. The tissues from mice were dissected out after transcardial perfusion with 1X PBS – 4% PFA. The tissues were cryoprotected serially with 10%, 20% and 30% sucrose, each incubating overnight at 4ºC. The solution was then changed to half by volume sucrose/OCT (Optimal Cutting Temperature, FisherScientific 23-730-571) and gently shaken for 1 hour at 4ºC. The tissues were frozen in dry ice/methanol bath and stored at -80ºC until day of sectioning at the cryostat. The sections were cut at 30µm thickness. The immunofluorescence protocol was as follows, in order: 3-minute fixing with 4% PFA, 3 5-minute 1X PBS washes, 2-hour blocking in Normal Goat or Donkey Serum (NDS, JacksonImmunoResearch, 017-000-121) with 1% (w/v) Bovine Serum Albumin (FisherScientific BP1600), 0.4% TritonX-100 (Sigma-Aldrich T8787), (if mouse-raised antibody is used: 1-hour incubation with 20 µg/ml AffiniPure Fab Fragment Goat Anti-Mouse IgG (H+L) (AB_2338476) or AffiniPure Fab Fragment Donkey Anti-Mouse IgG (H+L) (AB_2307338) in blocking solution), primary antibody in blocking solution incubation overnight at 4ºC, 2 4-minute washes with blocking solution, 3 4-minute washes with 0.4% TritonX-100 in PBS, 2-hour secondary antibody in blocking solution incubation, 2 4-minute washes with blocking solution, 3 4-minute washes with 0.4% TritonX-100 in PBS, 5-minute incubation in DAPI (Invitrogen D1306), 3 5-minute washes with PBS and mounted with Fluoromount G (SouthernBiotech 0100-01). Images were processed and analyzed with ImageJ.

Confocal Microscopy. Olympus FV3000 confocal laser scanning microscope and FluoView software were used (RRID:SCR_017015). Maximum intensity projection of the images was used for the final analysis.

The following macro was used to detect puncta:
“
```
run("Z Project...", "projection=[Max Intensity]");
run("Subtract Background...", "rolling=1 disable stack");
run("Enhance Contrast...", "saturated=0.3");
//run("Threshold...");
setAutoThreshold("Moments dark");
run("Convert to Mask", "method=Moments background=dark calculate");
run("Analyze Particles...", "size=0.15-150 circularity=0.50-1.00 display exclude
summarize add stack");
dir = getDirectory("image");
name = getTitle;
index = lastIndexOf(name, ".");
if (index!=-1) name = substring(name, 0, index);
name = name + ".xls";
saveAs("Results", dir+name);
saveAs("Measurements", dir+name);
print(dir+name);
```
“

Table. Primary antibodies used in this study.

Antibody	Host Species	Company	Catalog No	Dilution
Neurofilament H	Ch	Millipore	AB5539	1:3200
SV2	Ms	DSHB	SV2-c	1:500
VGAT	Gp	SynapticSystems	131004	1:400
VGLUT1	Gp	Millipore	AB5905	1:1000
Olig2	Rb	abcam	ab109186	1:200
VGLUT2	Gp	SynapticSystems	135404	1:1600
GLUT1	Rb	abcam	ab652	1:250
CCas3	Rb	CellSignaling	9661	1:200
MTCO1	Ms	abcam	ab14705	1:400
GLUD	Rb	Invitrogen	PA5-29492	1:1600
NG2	Rb	Millipore	AB5320	1:200
Glutamine Synthetase	Rb	abcam	ab73593	1:800
MBP	Rat	Novus Biologicals	nb600-717	1:50
ChaT	Gt	Phosphosolutions	315-CHAT	1:400

PKCg	Rb	abcam	109539	1:400

Figure Legends

Figure A3.4. Cleaved Caspase 3 staining in spinal cord of Gpt2-null mice at P90 on high alanine diet.

A. Images of cleaved caspase 3 staining in wild-type (left) and Gpt2-null (right) cervical (top) and lumbar (bottom) spinal cords. Scale bar: 100 μm.

B. Images of cleaved caspase 3 (green), DAPI (cyan), ChaT (choline acetyltransferase, red), NeuN (blue) in Gpt2-null lumbar spinal cord at P90. Scale bar: 50 μm.

Figure A3.5. Myelin Basic Protein and Protein Kinase C γ staining in spinal cord of Gpt2-null mice at P90 on high alanine diet.

A. Images of myelin basic protein (MBP) staining in wild-type (left) and Gpt2-null (right) cervical (top) and lumbar (bottom) spinal cords. Scale bar: 100 μm.

B. Images of protein kinase c γ (PKCγ) staining in wild-type (left) and Gpt2-null (right) cervical (top) and lumbar (bottom) spinal cords. Scale bar: 100 μm. Quantification is given at the bottom. **$0.001<P<0.01$.

Figure A3.6. MTCO1 staining in spinal cord of Gpt2-null mice at P90 on high alanine diet..

A. Images of MTCO1 staining in wild-type (left) and Gpt2-null (right) cervical and lumbar spinal cords. Dorsal, lateral and ventral horns are shown. Scale bar: 100 μm. The quantification is given on the right.

Figure A3.7. Neurofilament H staining in spinal cord of Gpt2-null mice at P90 on high alanine diet.

A. Images of neurofilament H (NFH) staining in wild-type (left) and Gpt2-null (right) cervical (top) and lumbar (bottom) spinal cords. Scale bar: 100 μm.

B. White boxes placed over to identify different areas of the spinal cord. Box 1: Corticospinal tract 2: laminae 1,2,3 of spinal gray 3: ventral funiculus 4: rubrospinal tract 5: lateral funiculus 6: laminae 10 of spinal gray. Quantification of NFH is given below.

C. Images of the different areas outlined in B.

Figure A3.8. NG2 and Olig2 staining in spinal cord of Gpt2-null mice at P90 on high alanine diet.

A. Images of NG2 staining in wild-type (left) and Gpt2-null (right) cervical and lumbar spinal cords. Dorsal, lateral and ventral horns are shown. Scale bar: 100 μm.

B. Images of Olig2 staining in wild-type (left) and Gpt2-null (right) cervical and lumbar spinal cords. Scale bar: 100 μm. The quantification of Olig+ cell counts is given at the bottom. *$0.01<P<0.05$.

Figure A3.9. SV2 staining in spinal cord of Gpt2-null mice at P90 on high alanine diet.

A. Images of SV2 staining in wild-type (left) and Gpt2-null (right) cervical and lumbar spinal cords. Dorsal, lateral and ventral horns are shown. Scale bar: 100 μm. The quantification is given on the right.

Figure A3.10. VGAT staining in spinal cord of Gpt2-null mice at P90 on high alanine diet.

A. Images of VGAT staining in wild-type (left) and Gpt2-null (right) cervical and lumbar spinal cords. Dorsal, lateral and ventral horns are shown. Scale bar: 100 μm. The quantification is given on the right. *$0.01<P<0.05$.

Figure A3.11. VGLUT1 staining in spinal cord of Gpt2-null mice at P90 on high alanine diet.

A. Images of VGLUT1 staining in wild-type (left) and Gpt2-null (right) cervical and lumbar spinal cords. Scale bar: 100 μm.

Figure A3.12. VGLUT2 staining in spinal cord of Gpt2-null mice at P90 on high alanine diet.

A. Images of VGLUT2 staining in wild-type (left) and Gpt2-null (right) cervical and lumbar spinal cords. Scale bar: 100 μm. The quantification is given on the right. *$0.01<P<0.05$.

Figure A3.13. Glutamate dehydrogenase and Glutamine synthetase staining in spinal cord of Gpt2-null mice at P90 on high alanine diet.

A. Images of glutamate dehydrogenase (GLUD) staining in wild-type (left) and Gpt2-null (right) cervical and lumbar spinal cords. Dorsal, lateral and ventral horns are shown. Scale bar: 100 μm. The quantification is given on the right.

B. Images of glutamine synthetase (GLUL) staining in wild-type (left) and Gpt2-null (right) cervical (top) and lumbar (bottom) spinal cords. Scale bar: 100 μm.

Figure A3.14. Glucose transporter 1 staining in spinal cord of Gpt2-null mice at P90 on high alanine diet.

A. Images of glucose transporter (GLUT1) staining in wild-type (left) and Gpt2-null (right) cervical (top) and lumbar (bottom) spinal cords. Scale bar: 100 μm.

References

Zhang, Y., Chen, K., Sloan, S.A., Bennett, M.L., Scholze, A.R., O'Keeffe, S., Phatnani, H.P., Guarnieri, P., Caneda, C., Ruderisch, N.*, et al.* (2014). An RNA-sequencing transcriptome and splicing database of glia, neurons, and vascular cells of the cerebral cortex. J Neurosci *34*, 11929-11947.

A

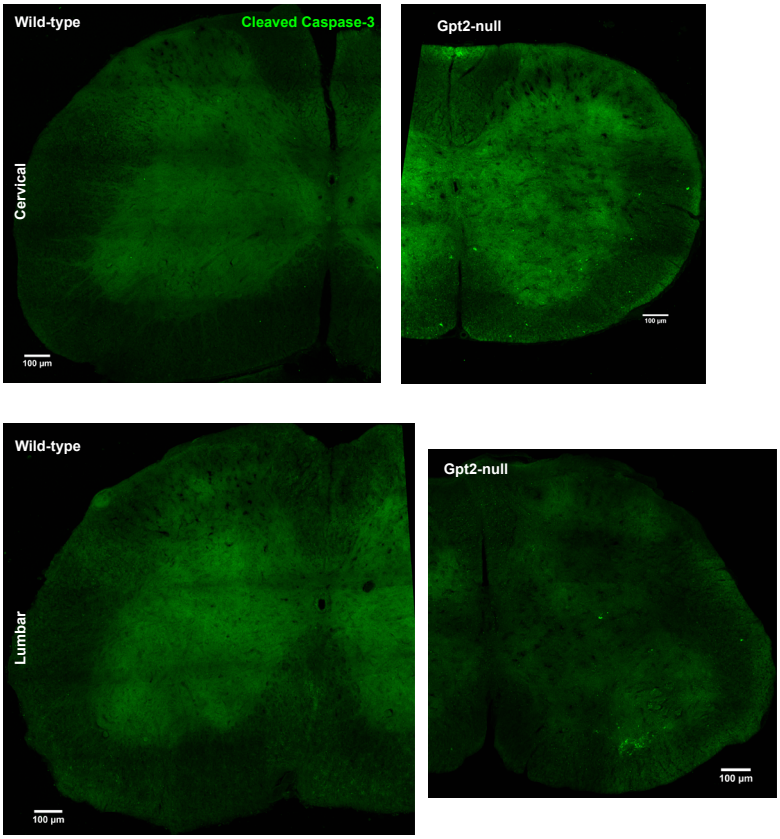

B

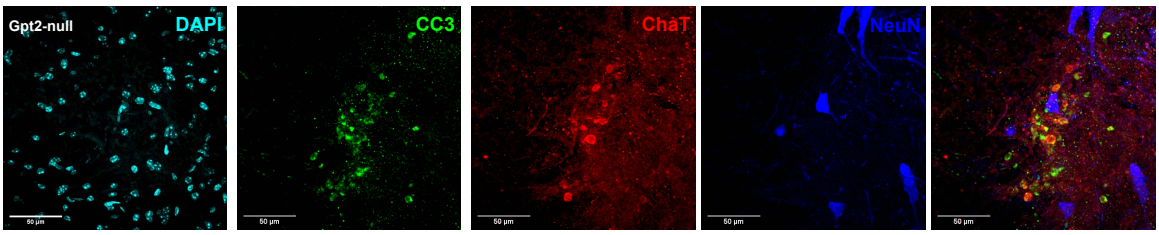

Figure A3.4. Cleaved Caspase 3 staining in spinal cord of Gpt2-null mice at P90 on high alanine diet. A. Images of cleaved caspase 3 staining in wild-type (left) and Gpt2-null (right) cervical (top) and lumbar (bottom) spinal cords. Scale bar: 100 µm. B. Images of cleaved caspase 3 (green), DAPI (cyan), ChaT (choline acetyltransferase, red), NeuN (blue) in Gpt2-null lumbar spinal cord at P90. Scale bar: 50 µm.

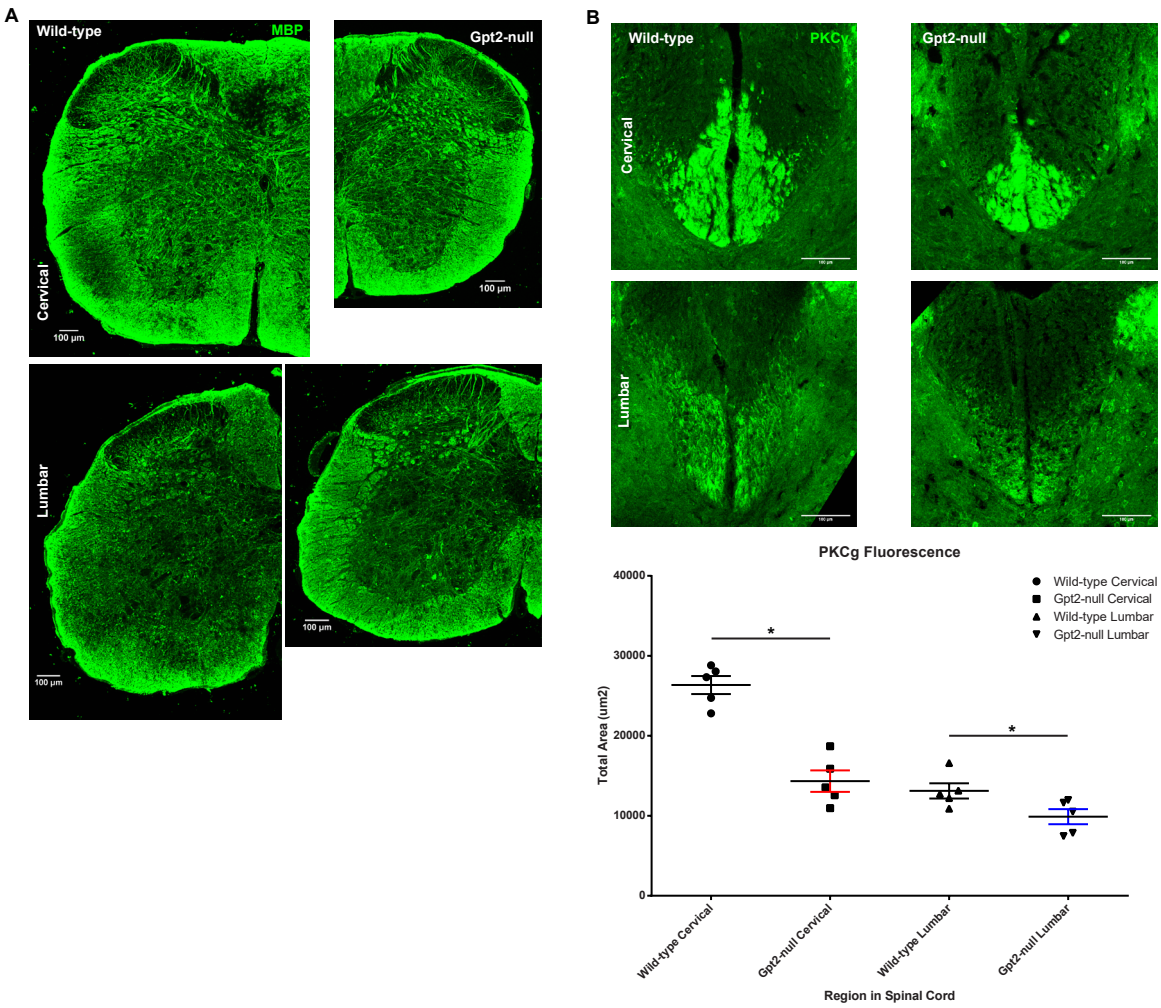

Figure A3.5. Myelin Basic Protein and Protein Kinase C γ staining in spinal cord of Gpt2-null mice at P90 on high alanine diet. A. Images of myelin basic protein (MBP) staining in wild-type (left) and Gpt2-null (right) cervical (top) and lumbar (bottom) spinal cords. Scale bar: 100 µm. B. Images of protein kinase c γ (PKCγ) staining in wild-type (left) and Gpt2-null (right) cervical (top) and lumbar (bottom) spinal cords.
Scale bar: 100 µm. Quantification is given at the bottom. **0.001<P<0.01.

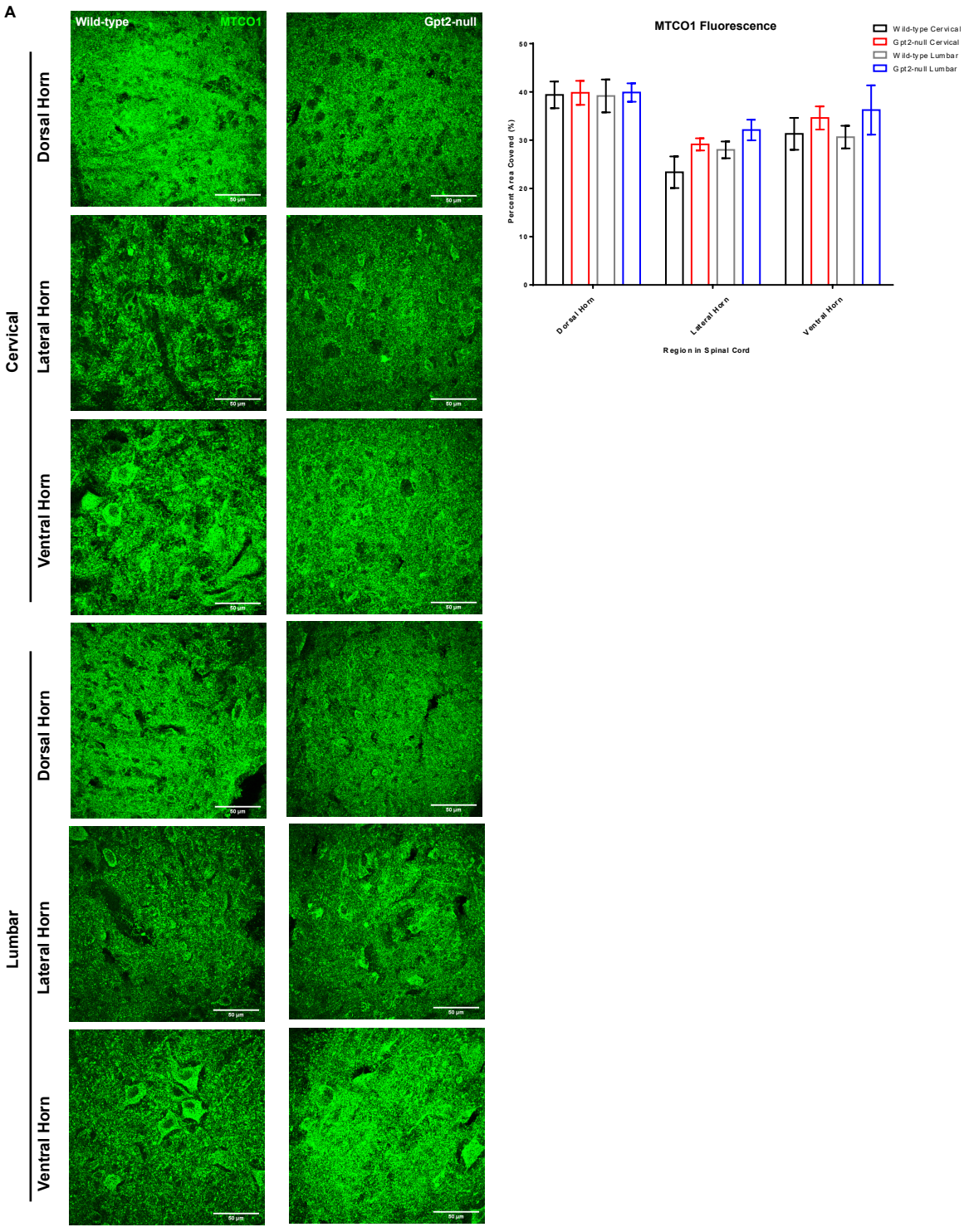

Figure A3.6. MTCO1 staining in spinal cord of Gpt2-null mice at P90 on high alanine diet. A. Images of MTCO1 staining in wild-type (left) and Gpt2-null (right) cervical and lumbar spinal cords. Dorsal, lateral and ventral horns are shown.
Scale bar: 100 μm. The quantification is given on the right.

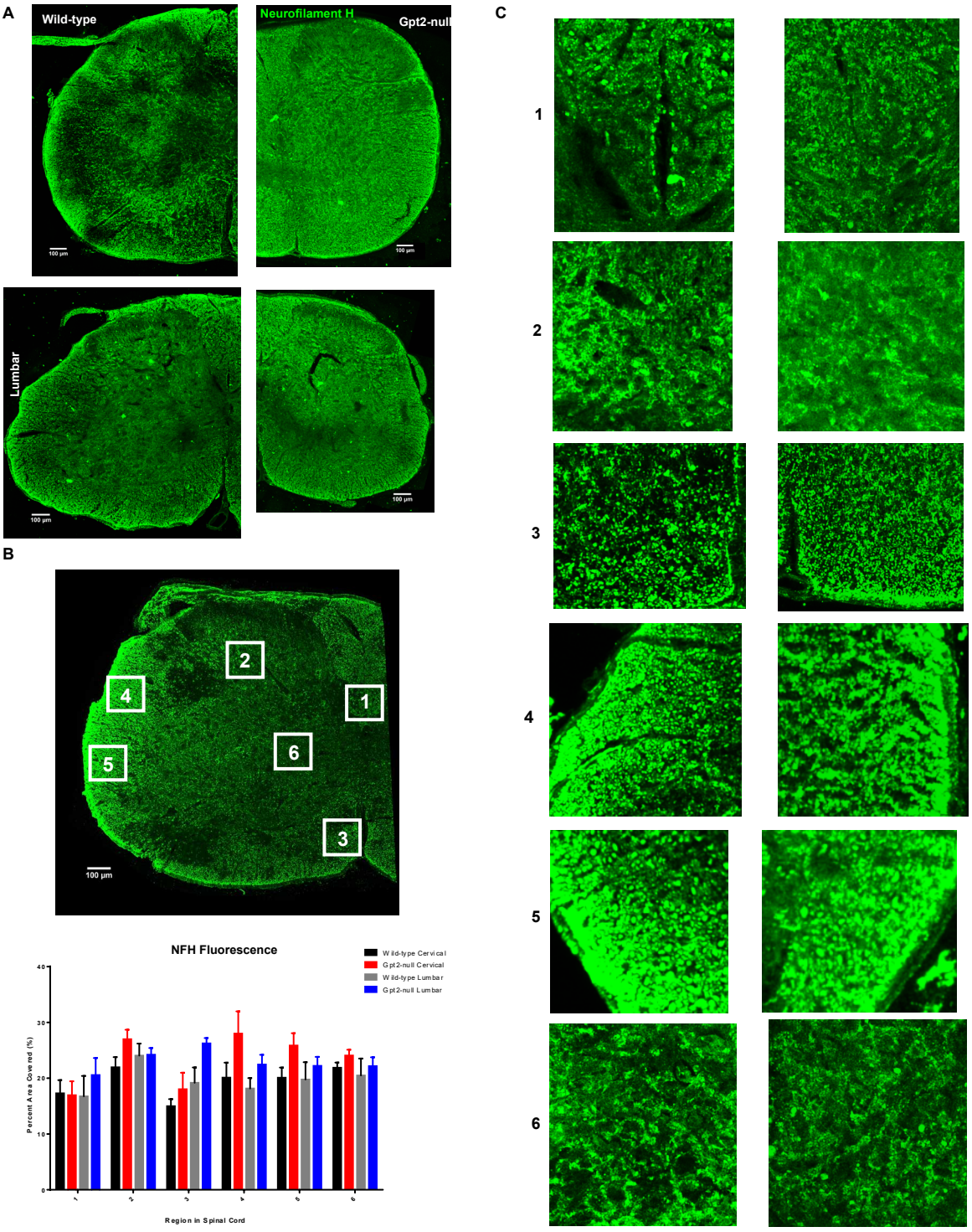

Figure A3.7. Neurofilament H staining in spinal cord of Gpt2-null mice at P90 on high alanine diet.
A. Images of neurofilament H (NFH) staining in wild-type (left) and Gpt2-null (right) cervical (top) and lumbar (bottom) spinal cords. Scale bar: 100 µm.
B. White boxes placed over to identify different areas of the spinal cord. Box 1: Corticospinal tract 2: laminae 1,2,3 of spinal gray 3: ventral funiculus 4: rubrospinal tract 5: lateral funiculus 6: laminae 10 of spinal gray. Quantification of NFH is given below.
C. Images of the different areas outlined in B.

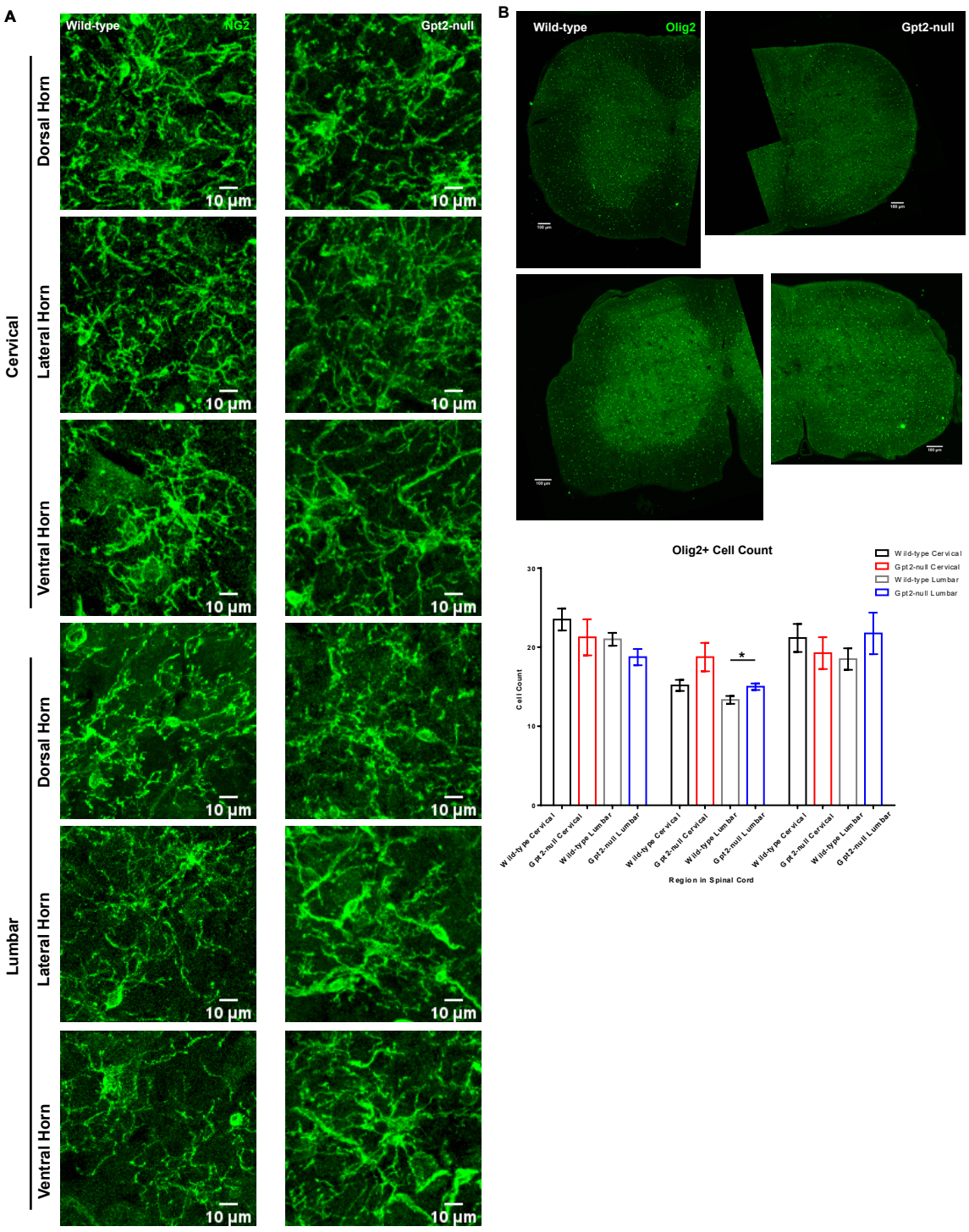

Figure A3.8. NG2 and Olig2 staining in spinal cord of Gpt2-null mice at P90 on high alanine diet.

A. Images of NG2 staining in wild-type (left) and Gpt2-null (right) cervical and lumbar spinal cords. Dorsal, lateral and ventral horns are shown. Scale bar: 100 µm. B. Images of Olig2 staining in wild-type (left) and Gpt2-null (right) cervical and lumbar spinal cords. Scale bar: 100 µm. The quantification of Olig+ cell counts is given at the bottom. *0.01<P<0.05.

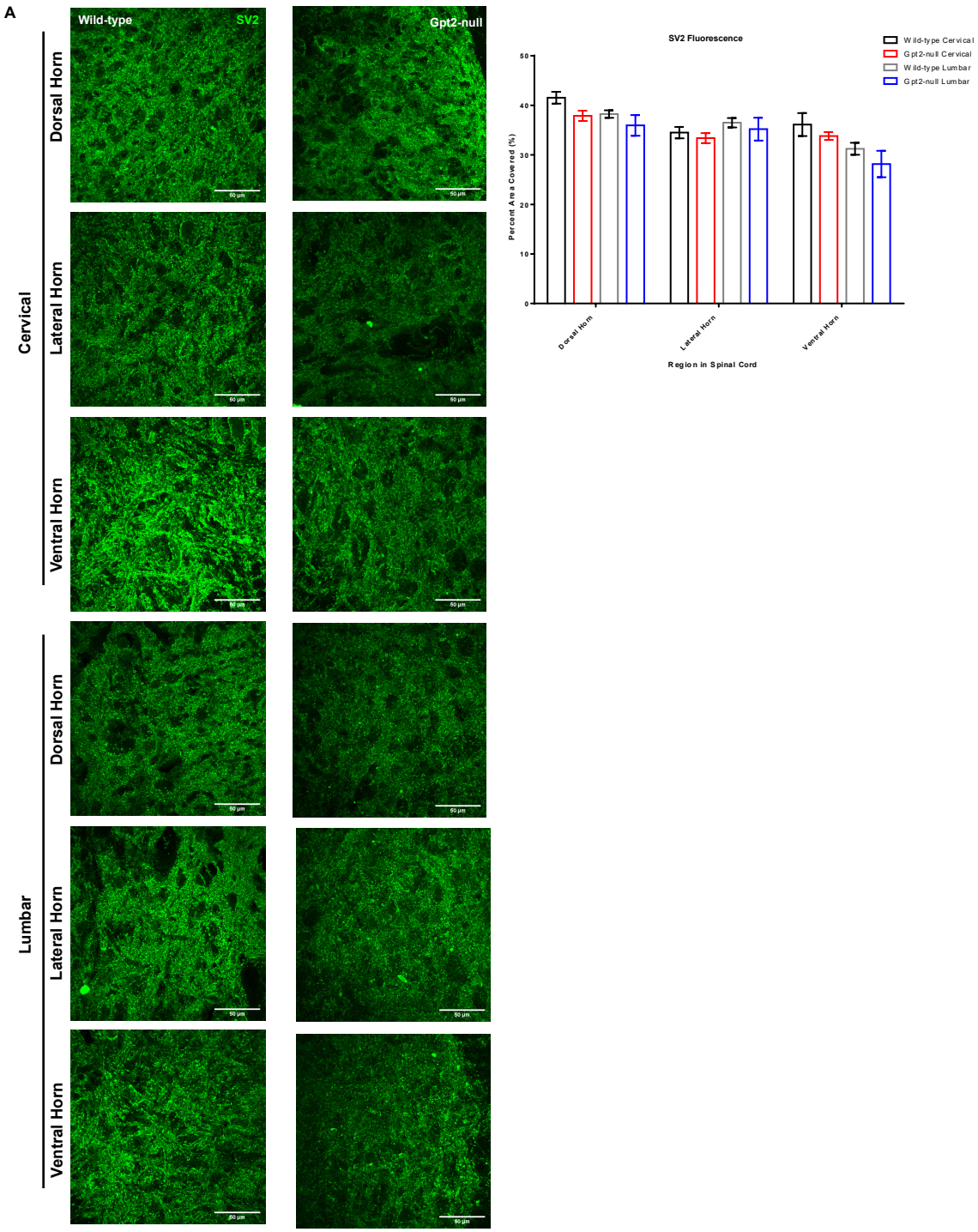

Figure A3.9. SV2 staining in spinal cord of Gpt2-null mice at P90 on high alanine diet. A. Images of SV2 staining in wild-type (left) and Gpt2-null (right) cervical and lumbar spinal cords. Dorsal, lateral and ventral horns are shown. Scale bar: 100 μm.
The quantification is given on the right.

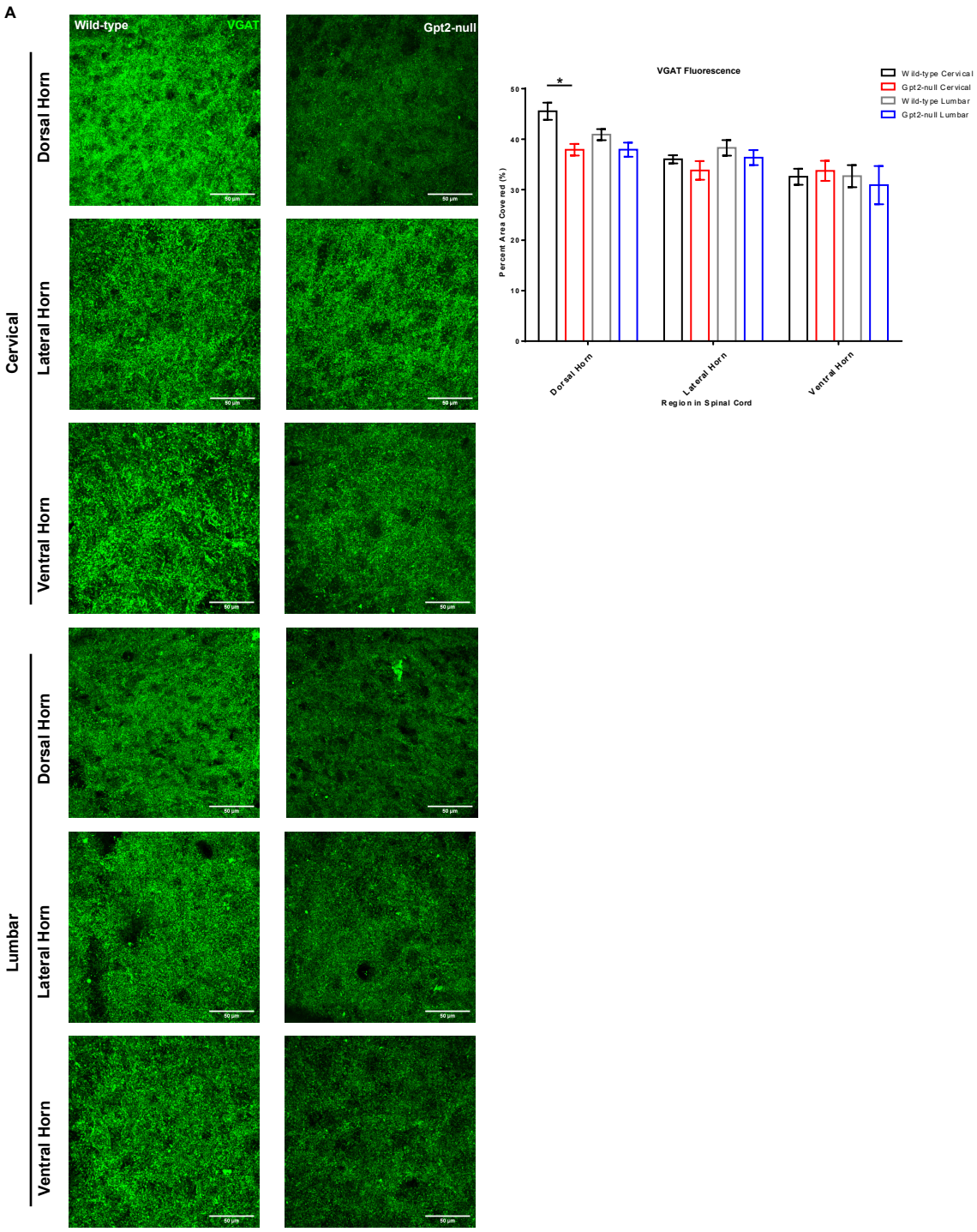

Figure A3.10. VGAT staining in spinal cord of Gpt2-null mice at P90 on high alanine diet.

A. Images of VGAT staining in wild-type (left) and Gpt2-null (right) cervical and lumbar spinal cords. Dorsal, lateral and ventral horns are shown. Scale bar: 100 µm. The quantification is given on the right. *0.01<P<0.05.

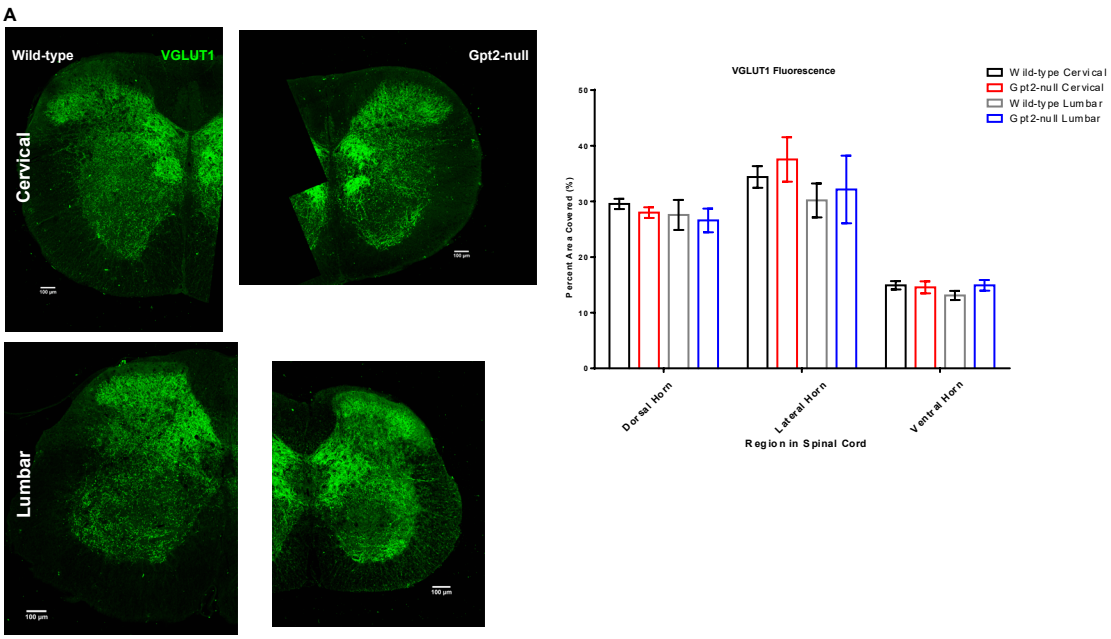

Figure A3.11. VGLUT1 staining in spinal cord of Gpt2-null mice at P90 on high alanine diet.

A. Images of VGLUT1 staining in wild-type (left) and Gpt2-null (right) cervical and lumbar spinal cords. Scale bar: 100 µm.

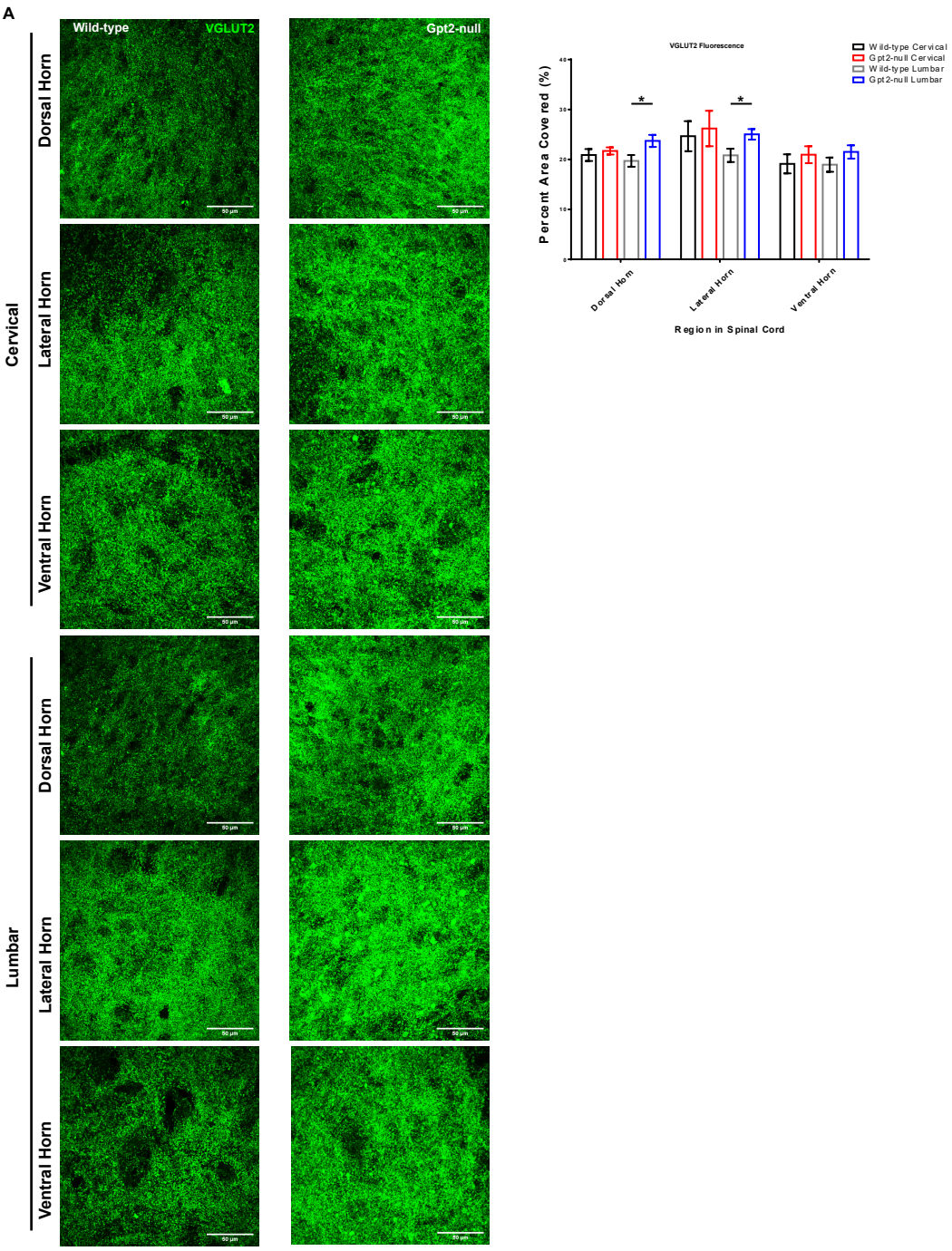

Figure A3.12. VGLUT2 staining in spinal cord of Gpt2-null mice at P90 on high alanine diet.

A. Images of VGLUT2 staining in wild-type (left) and Gpt2-null (right) cervical and lumbar spinal cords.
Scale bar: 100 μm. The quantification is given on the right.
*0.01<P<0.05.

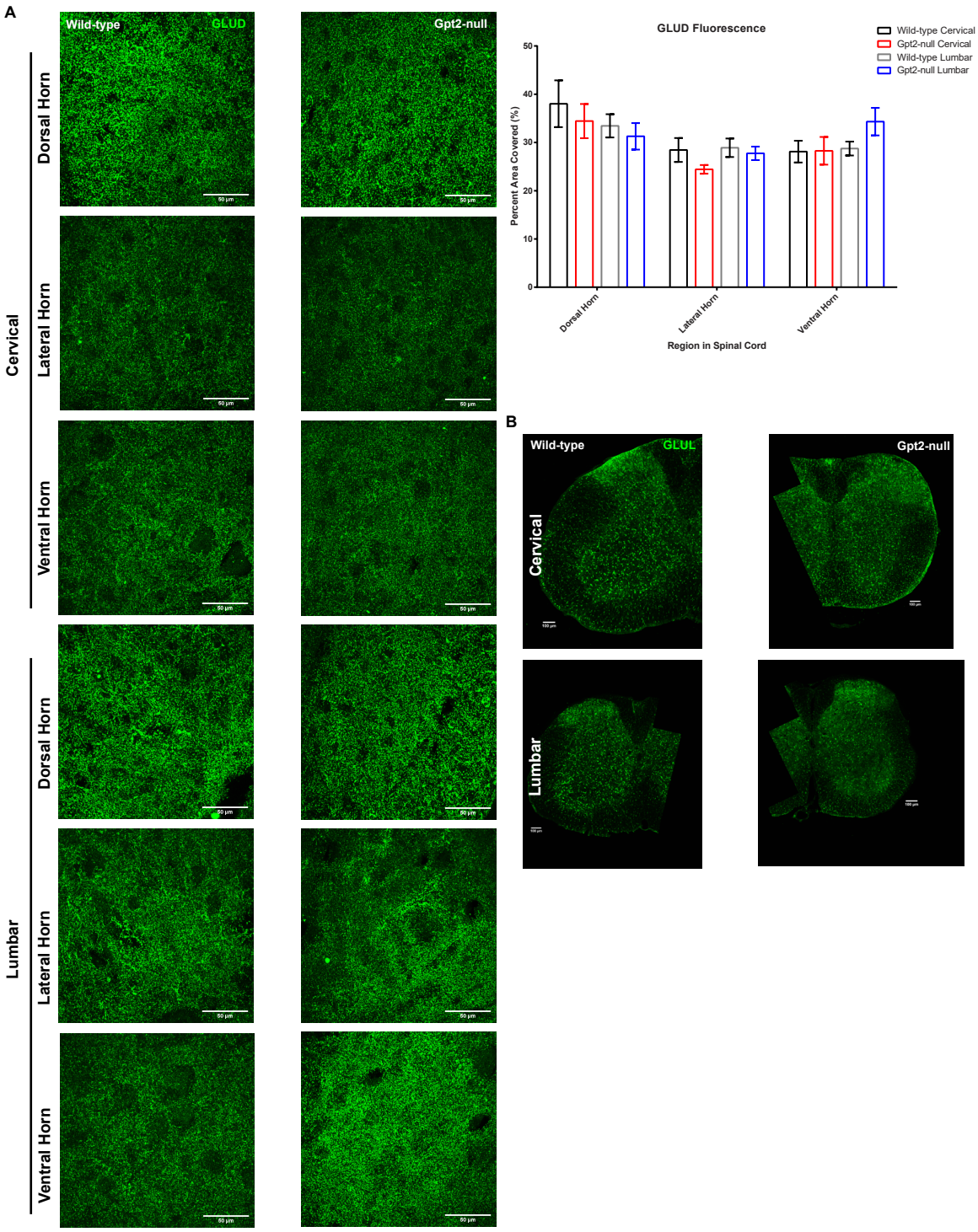

Figure A3.13. Glutamate dehydrogenase and Glutamine synthetase staining in spinal cord of Gpt2-null mice at P90 on high alanine diet.

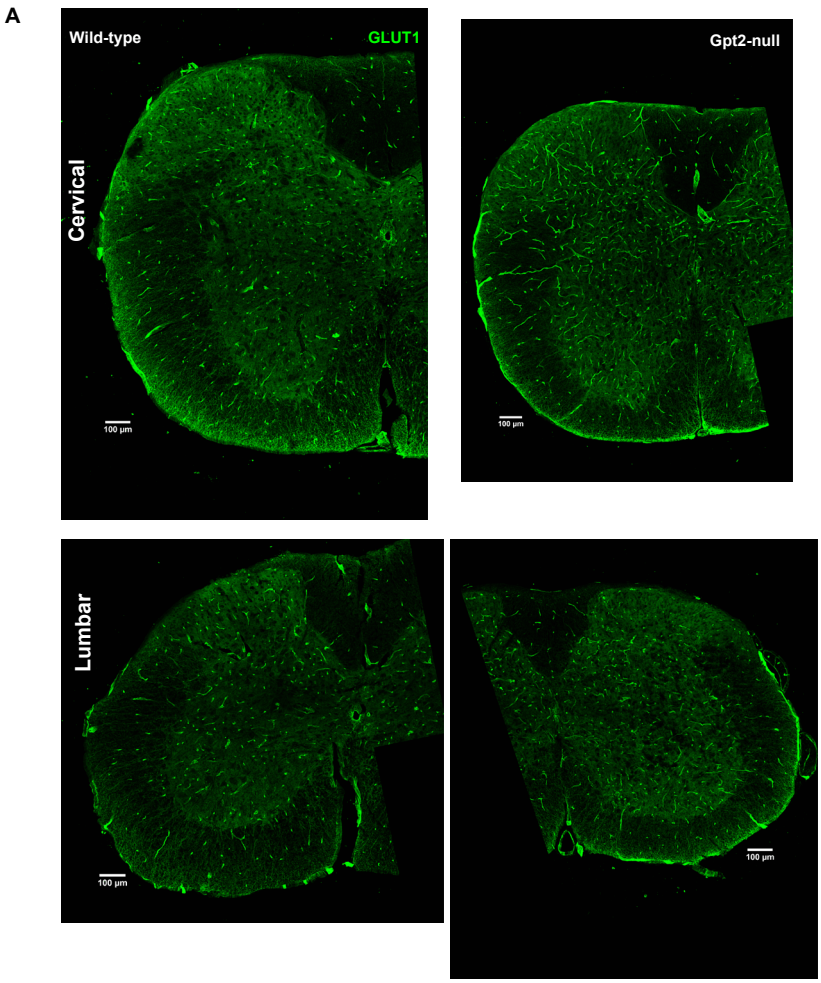

Figure A3.14. Glucose transporter 1 staining in spinal cord of Gpt2-null mice at P90 on high alanine diet. A. Images of glucose transporter (GLUT1) staining in wild-type (left) and Gpt2-null (right) cervical (top) and lumbar (bottom) spinal cords. Scale bar: 100 µm.

Appendix 3.6. Immunohistochemistry in Spinal cord for various stains in Gpt2-null mice at P18 (regular diet): Cleaved Caspase3 (CC3), myelin basic protein (MBP), protein kinase C g (PKCg), neurofilament H (NFH), NG2, Olig2, SV2, VGLUT1, VGLUT2, VGAT, MTCO1, glutamate dehydrogenase (GDH), glutamine synthetase (GLUL), glucose transporter 1 (GLUT1).

Introduction

Immunohistochemical analysis in Gpt2-null spinal cord at postnatal day 18 (fed Regular Diet). The following proteins are tested, and the corresponding processes or hypotheses are listed:

Cleaved Caspase 3 (CC3): Cell death by apoptosis; death of motor neurons may explain dysfunction in the motor behavior seen in Gpt2-null mice.

Myelin Basic Protein (MBP): deficits in myelination or ascending/descending tracts.

Protein Kinase C γ (PKCγ): Specifically expressed in descending corticospinal tracts and the dorsal horn. Long projections of corticospinal tracts may be more vulnerable to damage.

Neurofilament H (NFH): General assessment of neuronal processes, particularly axons.

NG2: A marker for oligodendrocyte precursor cells. Oligodendrocyte precursor cells appear to have the highest number of fragments per kilobase pf transcript per million

mapped reads (FPKM) as per the RNA-sequencing data done by (Zhang et al., 2014). It is possible that these cells may be particularly vulnerable to Gpt2 loss.

Olig2: A marker for oligodendrocytes. This would exclude the possible involvement of any problems in the number of oligodendrocytes.

SV2: A general marker for synaptic vesicles. We see reductions in SV2 puncta in Gpt2-null hippocampal neurons in vitro.

VGLUT1: An isoform of vesicular glutamate transporter on synaptic vesicles. We observe a slight upregulation of VGLUT1 in Gpt2-null synaptosomes; this may occur in spinal cord tissue as well. Both ascending and descending tracts in the spinal cord contain VGLUT1, any major absences of VGLUT1 puncta may indicate damage to those tracts or neurons that give rise thereto.

VGLUT2: An isoform of vesicular glutamate transporter on synaptic vesicles. Similar to VGLUT1, both ascending and descending tracts in the spinal cord contain VGLUT2, however differences in staining patterns with VGLUT1, may localize any potential abnormalities to a specific tract or nucleus in the spinal cord.

VGAT: A marker for synaptic vesicles containing 4-aminobutyric acid (GABA). We observe three-fold increases in protein levels in Gpt2-null synaptosomes. While we do

not know how this increase occurs, it may uniformly occur across the central nervous system in Gpt2-null mice.

MTCO1: Cytochrome c oxidase subunit 1, a marker of mitochondria. This may reveal problems of mitochondrial biogenesis. As Gpt2 loss results in deficits in the TCA cycle, mitochondrial biogenesis or shape (fission/fusion) may be altered and this may partly contribute to the pathological phenotype.

Glutamate dehydrogenase (GDH): A mitochondrial enzyme that converts glutamate into alpha-ketoglutarate and ammonia. GDH is an anaplerotic enzyme, meaning that it catalyzes a reaction that results in a net production of a TCA cycle intermediate. In the absence of Gpt2, GDH may be upregulated as a compensatory mechanism to support the TCA cycle, this is seen in Gpt2-null synaptosomes.

Glutamine Synthetase (GLUL): A cytosolic enzyme located mainly in astrocytes, that converts glutamate into glutamine. Up-regulation of this enzyme has been seen in animal models of epilepsy and in our data, in Gpt2-null synaptosomes.

Glucose Transporter 1 (GLUT1): A glucose transporter located mainly in endothelial cells that constitute the blood brain barrier. TCA cycle deficits in the Gpt2-null tissue can lead to upregulation of glucose uptake to support cellular energetics, through increased levels of GLUT1.

Results/Key Points

Table. Proteins stained via immunohistochemistry in Gpt2-null spinal cords at P18. "QL": qualitatively assessed. "-": no difference.

Marker	Gpt2-null with respect to Wild-type
CC3 (QL)	
MBP (QL)	-
NFH	-
PKCγ	Decrease Total Area in Cervical&Lumbar.
SV2	Decrease in Lumbar Dorsal Horn. Trending Decrease in Lumbar Ventral Horn
VGLUT1	-
VGLUT2	Decrease in Lumbar Lateral Horn. Trending Decrease in Cervical&Lumbar Dorsal Horn
VGAT	Decrease in Cervical&Lumbar Dorsal Horn
MTCO1	Trending Decreases in Cervical Ventral Horn.
NG2 (QL)	-
GLUT1 (QL)	-
GLUL (QL)	-
GLUD	Decrease in Cervical Lateral&Ventral Horn. Trending Decrease in Lumbar Lateral Horn.
Olig2	-

Discussion

There were no major differences in cell death or structural differences in MBP or NFH suggesting that the tracts overall have developmentally formed. However, there was a significant decrease in the area covered by PKCg, indicating a possible decrease in corticospinal tract projections. The total area covered by the staining may not be a very reliable measure because the animal and the spinal cord itself as a whole are smaller than the wild-type. We do not exactly know why this occurs or whether the tissues are uniformly smaller or parts of it are smaller. From the general overview of MBP or NFH staining, it appears that the Gpt2-null spinal cord sections are uniformly smaller. It is possible to prevent the confound of general smaller tissue size by dividing the area of the PKCg staining by the total area of dorsal column assuming the "shrinkage" of the tissue

happens uniformly. The result of PKCg has to be considered as preliminary and needs to be validated by other methodologies. It would be more prudent to trace individual tracts to address the question of whether the corticospinal tract is degenerating. This may be achieved be with either viral injection to the cortex (most pertinently motor cortex – although in mice, fine motor behavior may be coordinated mostly at the cervical level by the corticospinal tract (Moreno-Lopez et al., 2020)) or mice that encodes GFP in sparse neuronal populations (e.g. THY1-YFP). Electron microscopy may also identify individual axons and detect other morphological changes (e.g. myelin thickness, mitochondria number and shape).

SV2 seems to be significantly reduced in dorsal horn of the Gpt2-null lumbar spinal cord although there are trending decreases in the rest of the areas. This may reflect either reduced projections to the spinal cord, reduced SV2 production or reduced synaptic vesicle counts. Only VGAT and VGLUT2 seem to be affected in the same direction as SV2 particularly in the dorsal horn. NeuN+ or Calbindin+ cell counts were not changed so the reductions in VGAT/SV2/VGLUT2 are not due to dorsal horn neuron loss. While the differences are slight, these may point to emerging deficits in the afferent projections. This would not be surprising since if we hypothesize that neurons with long-projections are vulnerable primarily due to the long length of their processes, then this category of neurons includes afferent sensory neurons as well as motor neurons.

GLUD levels were significantly reduced however the background for these staining seems to be slightly different as the images did not show major qualitative differences.

This technical consideration is valid for the other stainings as well. Despite that the image analysis included background correction, this does not work perfectly and the manual counting of puncta was not preferred to prevent experimenter bias.

Another technical consideration could be that although there were at least 5 animals and 2 sections per staining, the sections from all animals were stained for the same protein on the same day to exclude variation within groups. It is possible to repeat the experiment once more for the some of the proteins to validate the first experiment's results.

Method

Immunofluorescence – Tissue. The tissues from mice were dissected out after transcardial perfusion with 1X PBS – 4% PFA. The tissues were cryoprotected serially with 10%, 20% and 30% sucrose, each incubating overnight at 4ºC. The solution was then changed to half by volume sucrose/OCT (Optimal Cutting Temperature, FisherScientific 23-730-571) and gently shaken for 1 hour at 4ºC. The tissues were frozen in dry ice/methanol bath and stored at -80ºC until day of sectioning at the cryostat. The sections were cut at 30µm thickness. The immunofluorescence protocol was as follows, in order: 3-minute fixing with 4% PFA, 3 5-minute 1X PBS washes, 2-hour blocking in Normal Goat or Donkey Serum (NDS, JacksonImmunoResearch, 017-000-121) with 1% (w/v) Bovine Serum Albumin (FisherScientific BP1600), 0.4% TritonX-100 (Sigma-Aldrich T8787), (if mouse-raised antibody is used: 1-hour incubation with 20 µg/ml AffiniPure Fab Fragment Goat Anti-Mouse IgG (H+L) (AB_2338476) or AffiniPure Fab Fragment

Donkey Anti-Mouse IgG (H+L) (AB_2307338) in blocking solution), primary antibody in blocking solution incubation overnight at 4ºC, 2 4-minute washes with blocking solution, 3 4-minute washes with 0.4% TritonX-100 in PBS, 2-hour secondary antibody in blocking solution incubation, 2 4-minute washes with blocking solution, 3 4-minute washes with 0.4% TritonX-100 in PBS, 5-minute incubation in DAPI (Invitrogen D1306), 3 5-minute washes with PBS and mounted with Fluoromount G (SouthernBiotech 0100-01). Images were processed and analyzed with ImageJ.

Confocal Microscopy. Olympus FV3000 confocal laser scanning microscope and FluoView software were used (RRID:SCR_017015). Maximum intensity projection of the images was used for the final analysis.

The following macro was used to detect puncta:
“
```
run("Z Project...", "projection=[Max Intensity]");
run("Subtract Background...", "rolling=1 disable stack");
run("Enhance Contrast...", "saturated=0.3");
//run("Threshold...");
setAutoThreshold("Moments dark");
run("Convert to Mask", "method=Moments background=dark calculate");
run("Analyze Particles...", "size=0.15-150 circularity=0.50-1.00 display exclude
summarize add stack");
dir = getDirectory("image");
name = getTitle;
index = lastIndexOf(name, ".");
if (index!=-1) name = substring(name, 0, index);
name = name + ".xls";
saveAs("Results", dir+name);
saveAs("Measurements", dir+name);
print(dir+name);
```
“

Table. Primary antibodies used in this study.

Antibody	Host Species	Company	Catalog No	Dilution
Neurofilament H	Ch	Millipore	AB5539	1:3200
SV2	Ms	DSHB	SV2-c	1:500

VGAT	Gp	SynapticSystems	131004	1:400
VGLUT1	Gp	Millipore	AB5905	1:1000
Olig2	Rb	abcam	ab109186	1:200
VGLUT2	Gp	SynapticSystems	135404	1:1600
GLUT1	Rb	abcam	ab652	1:250
CCas3	Rb	CellSignaling	9661	1:200
MTCO1	Ms	abcam	ab14705	1:400
GLUD	Rb	Invitrogen	PA5-29492	1:1600
NG2	Rb	Millipore	AB5320	1:200
Glutamine Synthetase	Rb	abcam	ab73593	1:800
MBP	Rat	Novus Biologicals	nb600-717	1:50
PKCg	Rb	abcam	109539	1:400

Figure Legends

Figure A3.15. Cleaved Caspase 3 staining in spinal cord of Gpt2-null mice at P18 on regular alanine diet.

A. Images of cleaved caspase 3 staining in wild-type (left) and Gpt2-null (right) cervical (top) and lumbar (bottom) spinal cords. Scale bar: 100 μm.

Figure A3.16. Myelin Basic Protein and Protein Kinase C γ staining in spinal cord of Gpt2-null mice at P18 on regular alanine diet.

A. Images of myelin basic protein (MBP) staining in wild-type (left) and Gpt2-null (right) cervical (top) and lumbar (bottom) spinal cords. Scale bar: 100 μm.

B. Images of protein kinase c γ (PKCγ) staining in wild-type (left) and Gpt2-null (right) cervical (top) and lumbar (bottom) spinal cords. Scale bar: 100 μm. Quantification is given at the bottom. **0.001<*P*<0.01.

Figure A3.17. MTCO1 staining in spinal cord of Gpt2-null mice at P18 on regular alanine diet.

A. Images of MTCO1 staining in wild-type (left) and Gpt2-null (right) cervical and lumbar spinal cords. Dorsal, lateral and ventral horns are shown. Scale bar: 100 μm. The quantification is given on the right.

Figure A3.18. Neurofilament H staining in spinal cord of Gpt2-null mice at P18 on regular alanine diet.

A. Images of neurofilament H (NFH) staining in wild-type (left) and Gpt2-null (right) cervical (top) and lumbar (bottom) spinal cords. Scale bar: 100 μm.

B. White boxes placed over to identify different areas of the spinal cord. Box 1: Corticospinal tract 2: laminae 1,2,3 of spinal gray 3: ventral funiculus 4: rubrospinal tract 5: lateral funiculus 6: laminae 10 of spinal gray. Quantification of NFH is given below.

C. Images of the different areas outlined in B.

Figure A3.19. NG2 and Olig2 staining in spinal cord of Gpt2-null mice at P18 on regular alanine diet.

A. Images of NG2 staining in wild-type (left) and Gpt2-null (right) cervical and lumbar spinal cords. Dorsal, lateral and ventral horns are shown. Scale bar: 100 μm.

B. Images of Olig2 staining in wild-type (left) and Gpt2-null (right) cervical and lumbar spinal cords. Scale bar: 100 μm. The quantification of Olig+ cell counts is given at the bottom.

Figure A3.20. SV2 staining in spinal cord of Gpt2-null mice at P18 on regular alanine diet.

A. Images of SV2 staining in wild-type (left) and Gpt2-null (right) cervical and lumbar spinal cords. Dorsal, lateral and ventral horns are shown. Scale bar: 100 μm. The quantification is given on the right. *0.01<*P*<0.05.

Figure A3.21. VGAT staining in spinal cord of Gpt2-null mice at P18 on regular alanine diet.

A. Images of VGAT staining in wild-type (left) and Gpt2-null (right) cervical and lumbar spinal cords. Dorsal, lateral and ventral horns are shown. Scale bar: 100 μm. The quantification is given on the right. *0.01<*P*<0.05.

Figure A3.22. VGLUT1 staining in spinal cord of Gpt2-null mice at P18 on regular alanine diet.

A. Images of VGLUT1 staining in wild-type (left) and Gpt2-null (right) cervical and lumbar spinal cords. Scale bar: 100 μm.

Figure A3.23. VGLUT2 staining in spinal cord of Gpt2-null mice at P18 on regular alanine diet.

A. Images of VGLUT2 staining in wild-type (left) and Gpt2-null (right) cervical and lumbar spinal cords. Scale bar: 100 μm. The quantification is given on the right.

Figure A3.24. Glutamate dehydrogenase and Glutamine synthetase staining in spinal cord of Gpt2-null mice at P18 on regular alanine diet.

A. Images of glutamate dehydrogenase (GLUD) staining in wild-type (left) and Gpt2-null (right) cervical and lumbar spinal cords. Dorsal, lateral and ventral horns are shown. Scale bar: 100 µm. The quantification is given on the right. *$0.01<P<0.05$.

B. Images of glutamine synthetase (GLUL) staining in wild-type (left) and Gpt2-null (right) cervical (top) and lumbar (bottom) spinal cords. Scale bar: 100 µm.

Figure A3.24. Glucose transporter 1 staining in spinal cord of Gpt2-null mice at P18 on regular alanine diet.

A. Images of glucose transporter (GLUT1) staining in wild-type (left) and Gpt2-null (right) cervical (top) and lumbar (bottom) spinal cords. Scale bar: 100 µm.

Moreno-Lopez, Y., Bichara, C., Isope, P., and Cordero-Erausquin, M. (2020). Lumbar corticospinal tract in rodents modulates sensory inputs but does not convey motor command.

Zhang, Y., Chen, K., Sloan, S.A., Bennett, M.L., Scholze, A.R., O'Keeffe, S., Phatnani, H.P., Guarnieri, P., Caneda, C., Ruderisch, N.*, et al.* (2014). An RNA-sequencing transcriptome and splicing database of glia, neurons, and vascular cells of the cerebral cortex. J Neurosci *34*, 11929-11947.

A

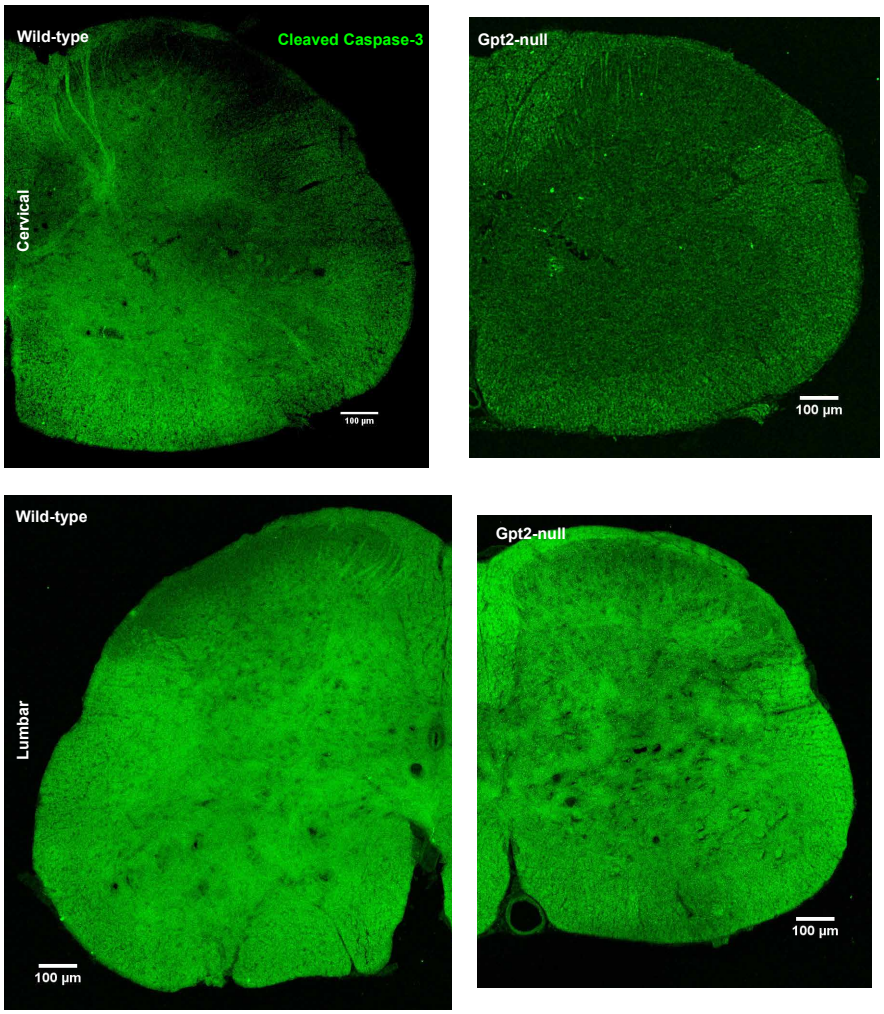

Figure A3.15. Cleaved Caspase 3 staining in spinal cord of Gpt2-null mice at P18 on regular alanine diet. A. Images of cleaved caspase 3 staining in wild-type (left) and Gpt2-null (right) cervical (top) and lumbar (bottom) spinal cords. Scale bar: 100 µm.

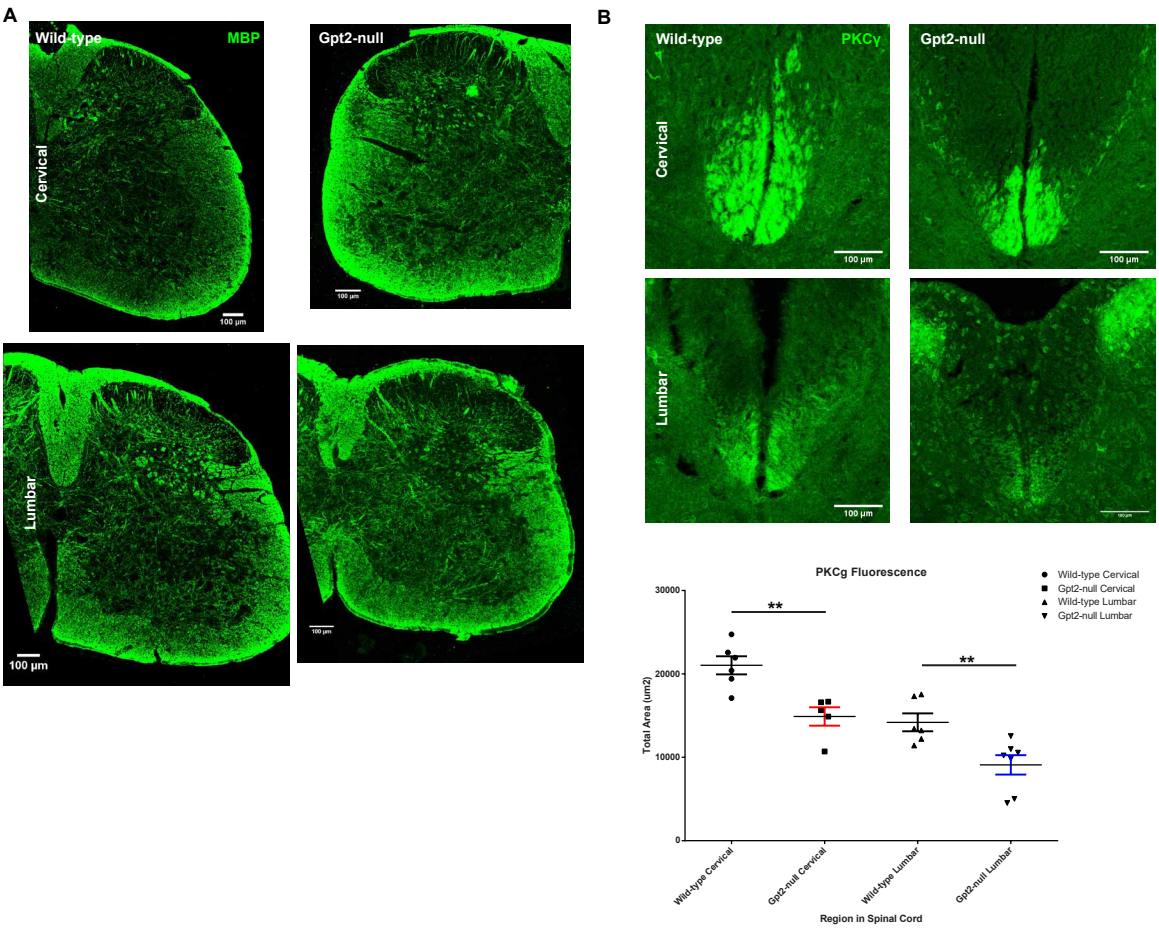

Figure A3.16. Myelin Basic Protein and Protein Kinase C γ staining in spinal cord of Gpt2-null mice at P18 on regular alanine diet.
A. Images of myelin basic protein (MBP) staining in wild-type (left) and Gpt2-null (right) cervical (top) and lumbar (bottom) spinal cords. Scale bar: 100 µm.
B. Images of protein kinase c γ (PKCγ) staining in wild-type (left) and Gpt2-null (right) cervical (top) and lumbar (bottom) spinal cords.
Scale bar: 100 µm. Quantification is given at the bottom. **0.001<P<0.01.

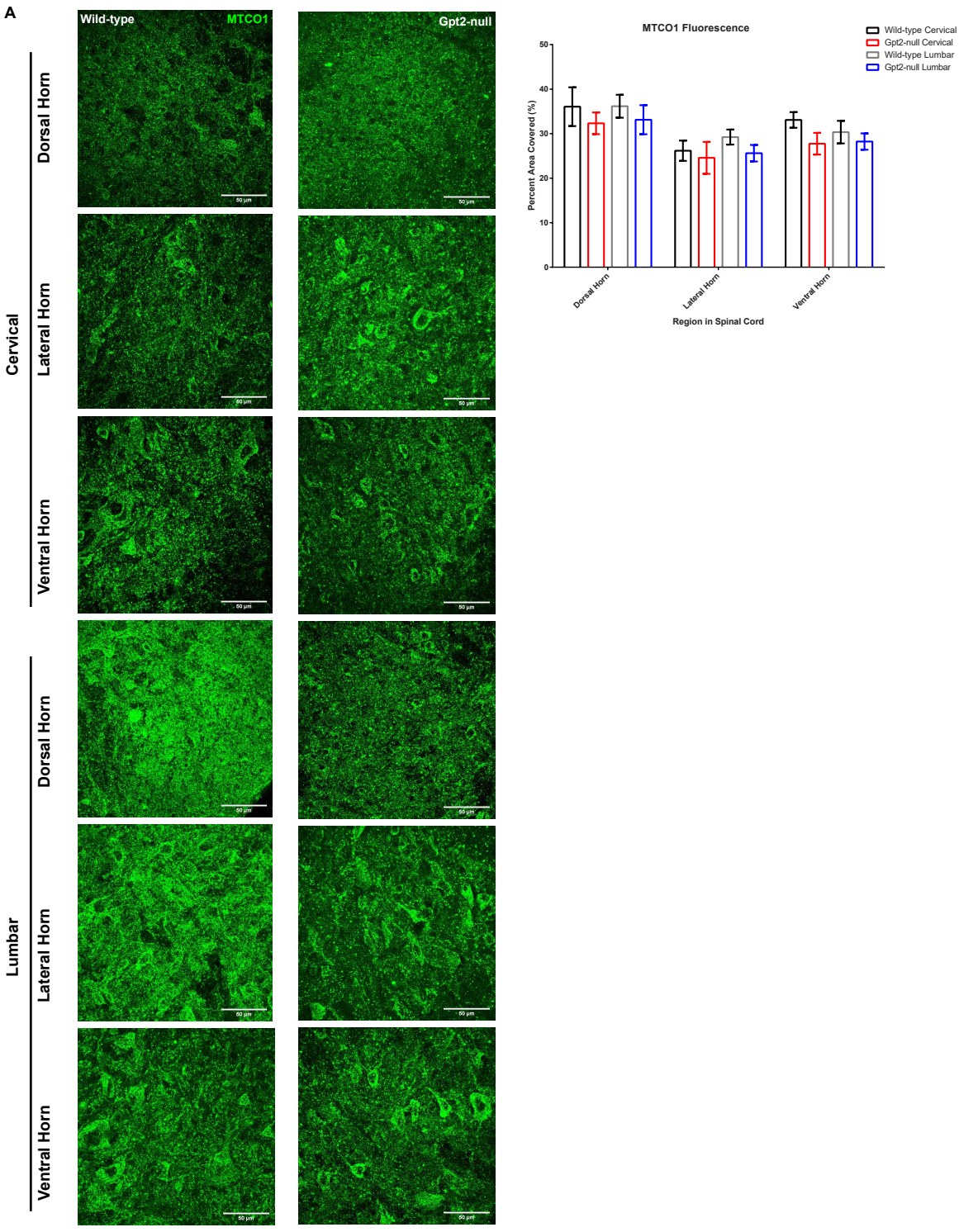

Figure A3.17. MTCO1 staining in spinal cord of Gpt2-null mice at P18 on regular alanine diet.
A. Images of MTCO1 staining in wild-type (left) and Gpt2-null (right) cervical and lumbar spinal cords. Dorsal, lateral and ventral horns are shown. Scale bar: 100 μm.
The quantification is given on the right.

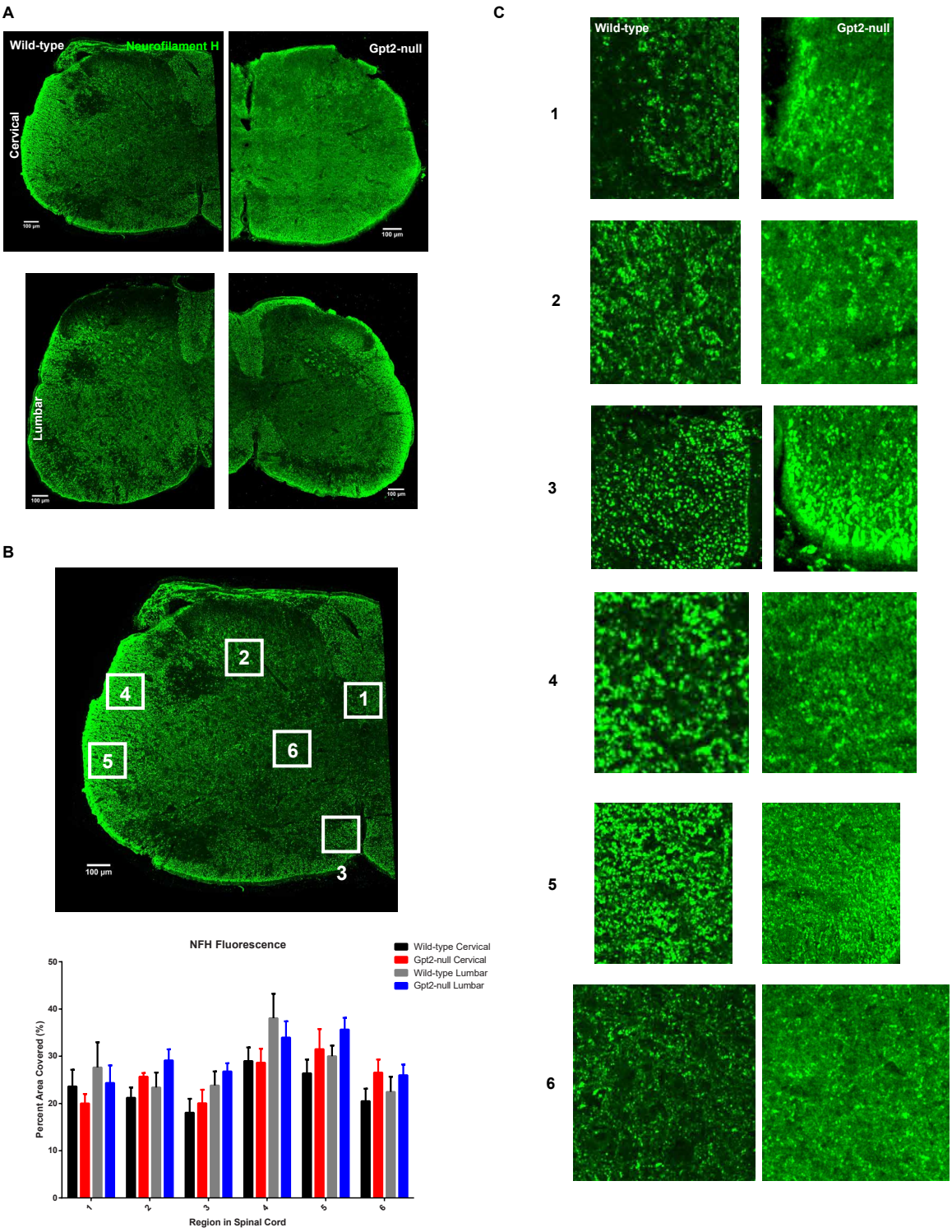

Figure A3.18. Neurofilament H staining in spinal cord of Gpt2-null mice at P18 on regular alanine diet. A. Images of neurofilament H (NFH) staining in wild-type (left) and Gpt2-null (right) cervical (top) and lumbar (bottom) spinal cords. Scale bar: 100 µm. B. White boxes placed over to identify different areas of the spinal cord. Box 1: Corticospinal tract 2: laminae 1,2,3 of spinal gray 3: ventral funiculus 4: rubrospinal tract 5: lateral funiculus 6: laminae 10 of spinal gray. Quantification of NFH is given below.
C. Images of the different areas outlined in B.

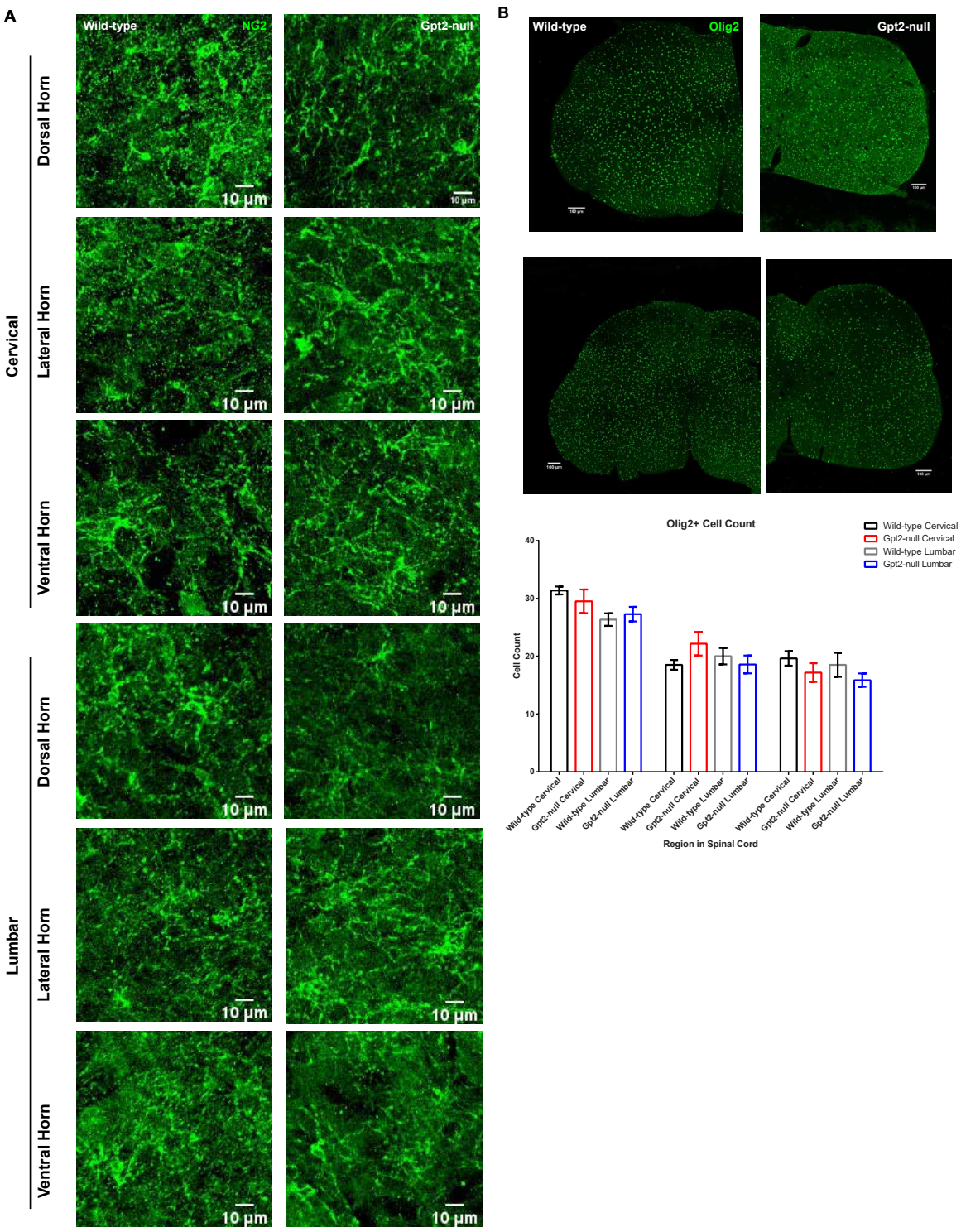

Figure A3.19. NG2 and Olig2 staining in spinal cord of Gpt2-null mice at P18 on regular alanine diet. A. Images of NG2 staining in wild-type (left) and Gpt2-null (right) cervical and lumbar spinal cords. Dorsal, lateral and ventral horns are shown. Scale bar: 100 µm.B. Images of Olig2 staining in wild-type (left) and Gpt2-null (right) cervical and lumbar spinal cords. Scale bar: 100 µm.
The quantification of Olig+ cell counts is given at the bottom.

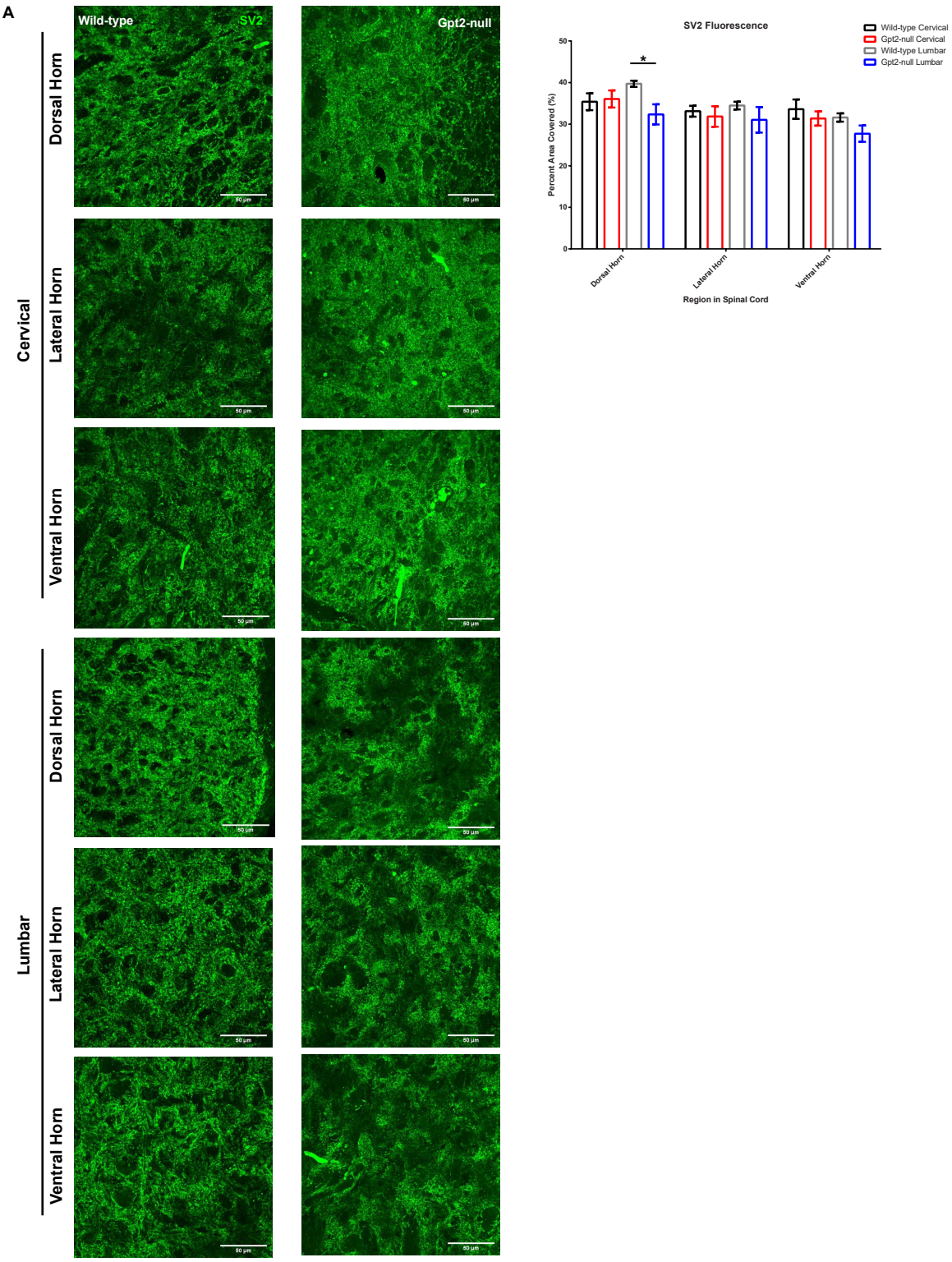

Figure A3.20. SV2 staining in spinal cord of Gpt2-null mice at P18 on regular alanine diet.
A. Images of SV2 staining in wild-type (left) and Gpt2-null (right) cervical and lumbar spinal cords. Dorsal, lateral and ventral horns are shown. Scale bar: 100 µm.
The quantification is given on the right. *0.01<P<0.05.

A

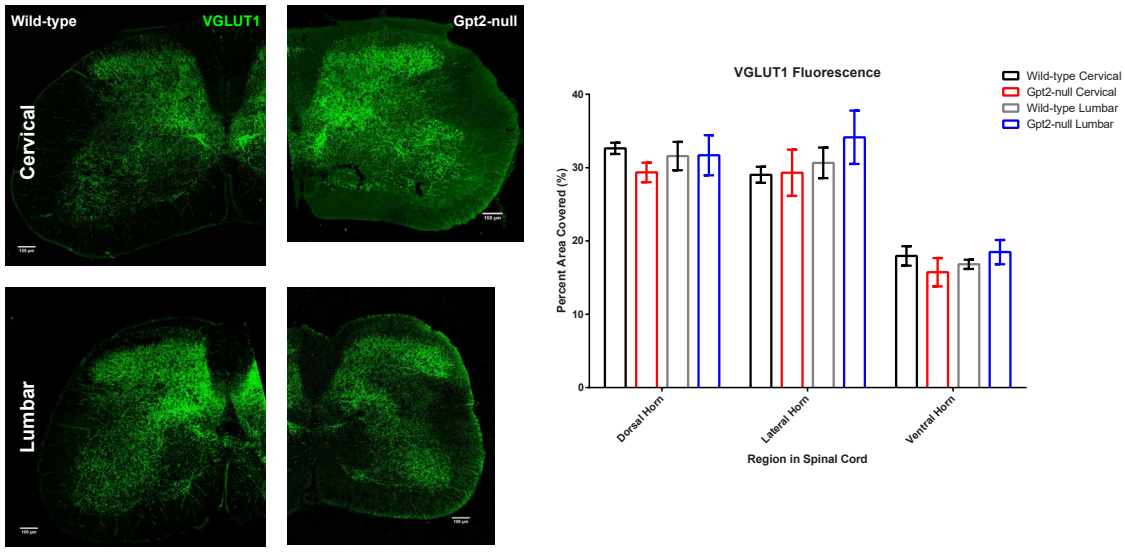

Figure A3.22. VGLUT1 staining in spinal cord of Gpt2-null mice at P18 on regular alanine diet. A. Images of VGLUT1 staining in wild-type (left) and Gpt2-null (right) cervical and lumbar spinal cords. Scale bar: 100 μm.

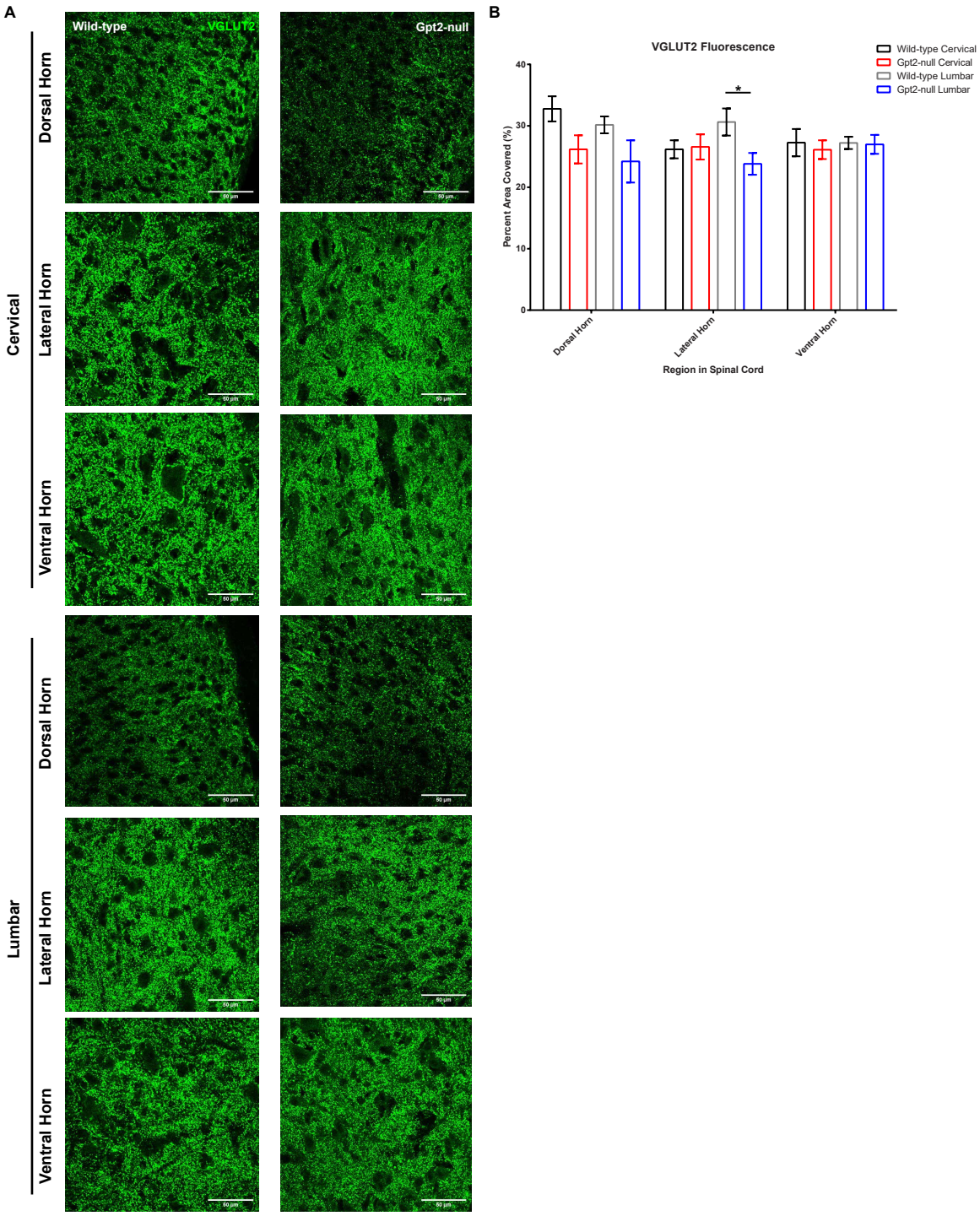

Figure A3.23. VGLUT2 staining in spinal cord of Gpt2-null mice at P18 on regular alanine diet. A. Images of VGLUT2 staining in wild-type (left) and Gpt2-null (right) cervical and lumbar spinal cords. Scale bar: 100 μm. The quantification is given on the right.

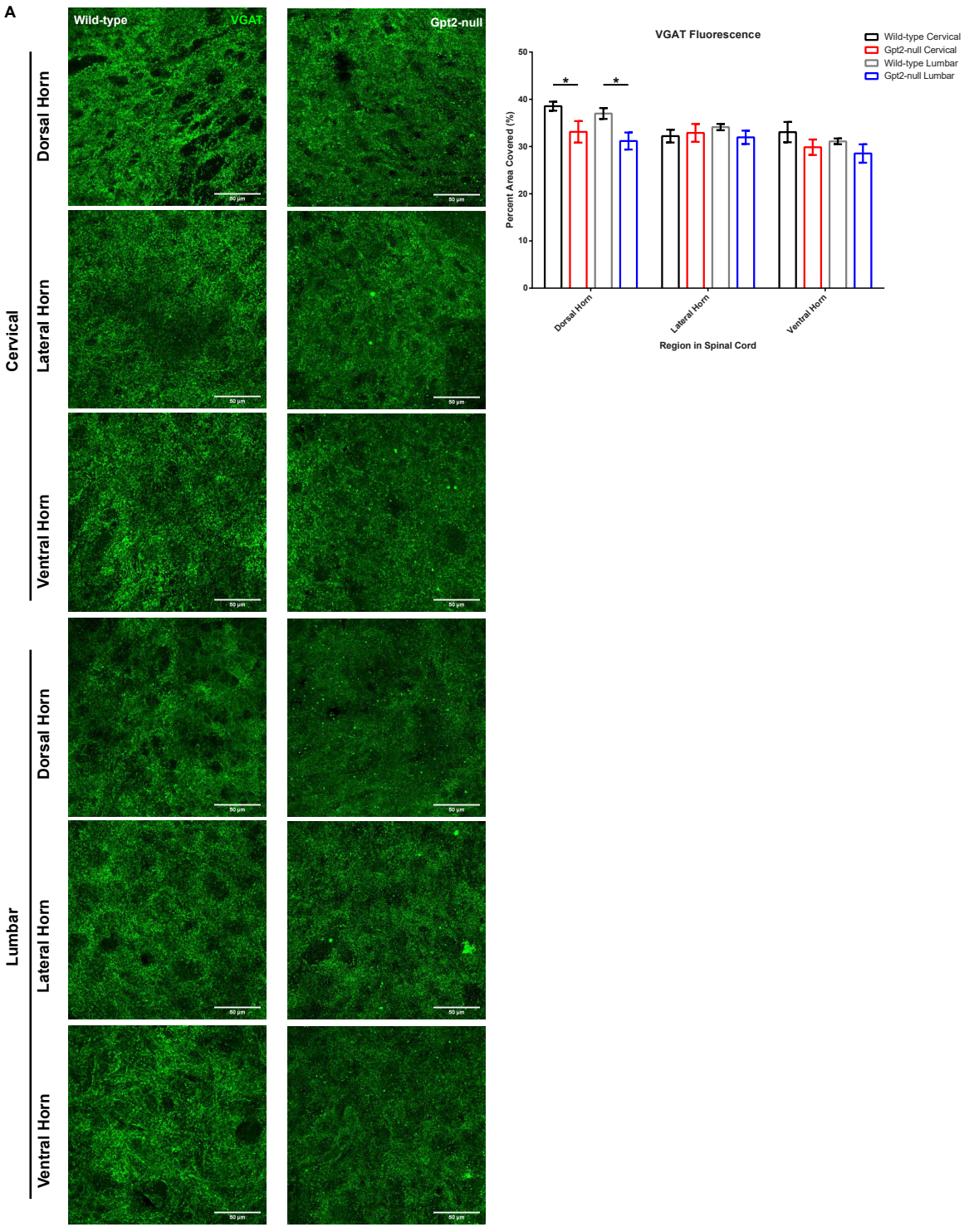

Figure A3.21. VGAT staining in spinal cord of Gpt2-null mice at P18 on regular alanine diet. A. Images of VGAT staining in wild-type (left) and Gpt2-null (right) cervical and lumbar spinal cords. Dorsal, lateral and ventral horns are shown. Scale bar: 100 µm. The quantification is given on the right. *0.01<P<0.05.

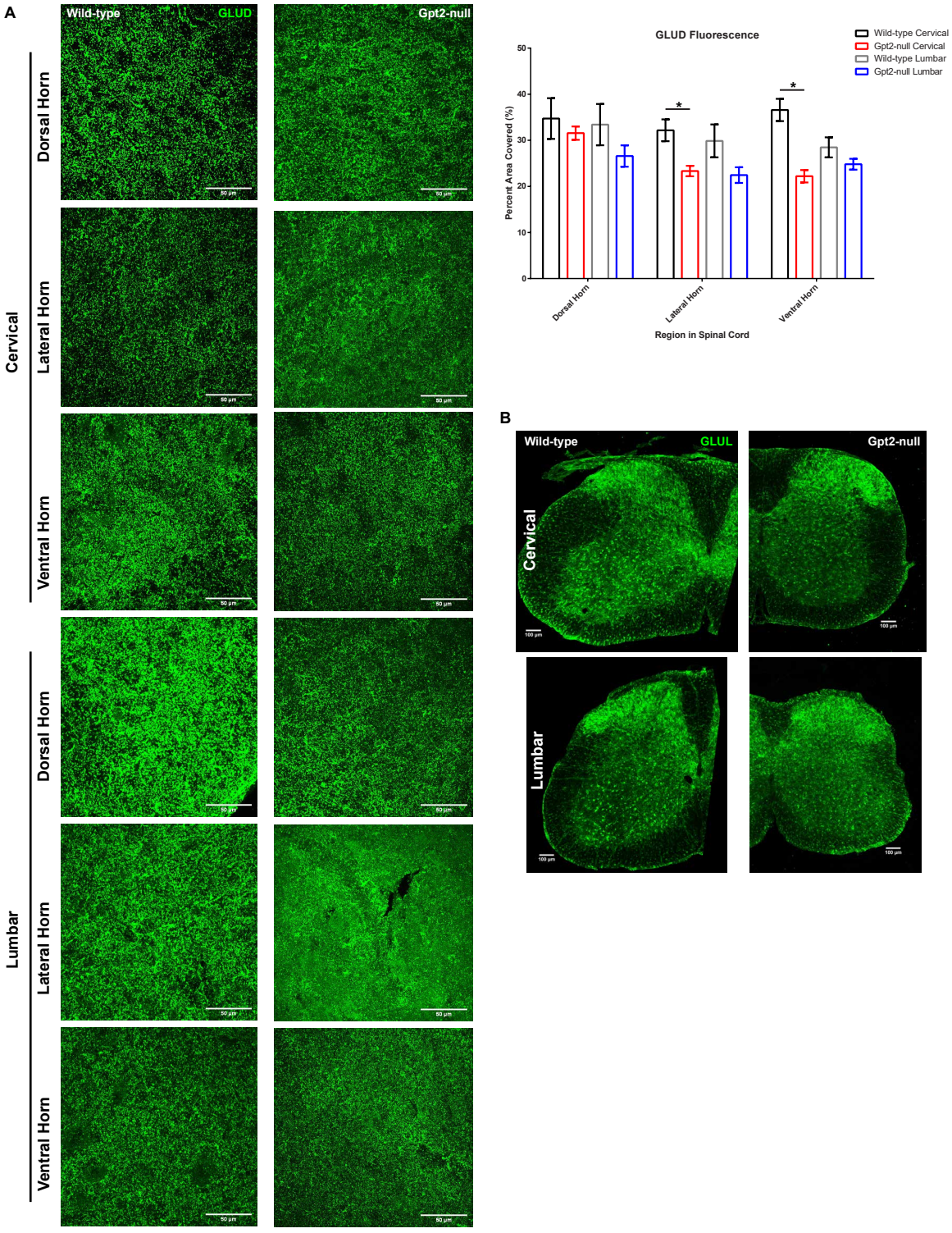

Figure A3.24. Glutamate dehydrogenase and Glutamine synthetase staining in spinal cord of Gpt2-null mice at P18 on regular alanine diet. A. Images of glutamate dehydrogenase (GLUD) staining in wild-type (left) and Gpt2-null (right) cervical and lumbar spinal cords. Dorsal, lateral and ventral horns are shown. Scale bar: 100 μm. The quantification is given on the right. *0.01<P<0.05. B. Images of glutamine synthetase (GLUL) staining in wild-type (left) and Gpt2-null (right) cervical (top) and lumbar (bottom) spinal cords. Scale bar: 100 μm.

A

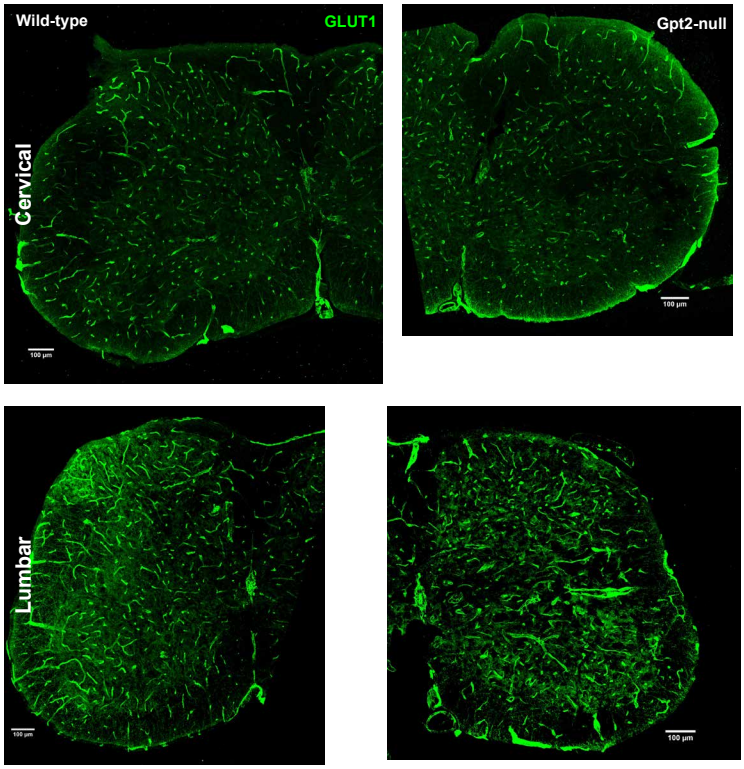

Figure A3.24. Glucose transporter 1 staining in spinal cord of Gpt2-null mice at P18 on regular alanine diet. A. Images of glucose transporter (GLUT1) staining in wild-type (left) and Gpt2-null (right) cervical (top) and lumbar (bottom) spinal cords. Scale bar: 100 µm.

Appendix A3.7. Oligodendrocyte specific protein in staining density in Gpt2-null mouse brains at P18 on regular diet.

Introduction

We investigated whether there are any global changes in the white matter of the Gpt2-null brain. We performed oligodendrocyte specific protein (Claudin-11) staining in coronal Gpt2-null brain sections (age postnatal day 18).

Key Points / Results

- No major differences in corpus callosum, striatum, cingulum bundle in Gpt2-null brains.

Discussion

Naturally the experiment could be expanded to other areas, however there were no major structural abnormalities in the areas tested. There can be subtle differences such as in the striatum, on the background near the nerve bundles, the wild-type seems to have more staining compared to the Gpt2-null image.

Method

Immunofluorescence – Tissue. The tissues from mice were dissected out after transcardial perfusion with 1X PBS – 4% PFA. The tissues were cryoprotected serially with 10%, 20% and 30% sucrose, each incubating overnight at 4ºC. The solution was then changed to half by volume sucrose/OCT (Optimal Cutting Temperature, FisherScientific 23-730-571) and gently shaken for 1 hour at 4ºC. The tissues were frozen in dry ice/methanol bath and stored at -80ºC until day of sectioning at the cryostat. The sections were cut at 30µm thickness. The immunofluorescence protocol was as follows, in order: 3-minute fixing with 4% PFA, 3 5-minute 1X PBS washes, 2-hour blocking in Normal Goat or Donkey Serum (NDS, JacksonImmunoResearch, 017-000-121) with 1% (w/v) Bovine Serum Albumin (FisherScientific BP1600), 0.4% TritonX-100 (Sigma-Aldrich T8787), (if mouse-raised antibody is used: 1-hour incubation with 20 µg/ml AffiniPure Fab Fragment Goat Anti-Mouse IgG (H+L) (AB_2338476) or AffiniPure Fab Fragment Donkey Anti-Mouse IgG (H+L) (AB_2307338) in blocking solution), primary antibody in blocking solution incubation overnight at 4ºC, 2 4-minute washes with blocking solution, 3 4-minute washes with 0.4% TritonX-100 in PBS, 2-hour secondary antibody in blocking solution incubation, 2 4-minute washes with blocking solution, 3 4-minute washes with 0.4% TritonX-100 in PBS, 5-minute incubation in DAPI (Invitrogen D1306), 3 5-minute washes with PBS and mounted with Fluoromount G (SouthernBiotech 0100-01). Images were processed and analyzed with ImageJ.

Confocal Microscopy. Imaging and quantification of cell death, cell count, synapse count, arborization were done with Opera Phenix High-Content Quantification System and Harmony software (PerkinElmer, RRID:SCR_018809). The hippocampal neuronal, astrocyte-enriched cultures or co-cultures were seeded on an OperaPhenix Ultra

CellCarrier 96-well plate (PerkinElmer, 6055302) and at indicated times, different media conditions were tested. Immunofluorescence as described above was done at 14 days in vitro (DIV14) for all plates. The wells were filled with 1X PBS and imaged immediately after. For confocal microscopy on tissues, Olympus FV3000 confocal laser scanning microscope and FluoView software were used (RRID:SCR_017015).
Primary antibody: Oligodendrocyte Specific Protein (abcam, ab53041) 1:200 dilution.

Figure Legends

Figure A.3.25. Oligodendrocyte Specific Protein staining in Gpt2-null coronal brain section at postnatal day 18.

A. Images of oligodendrocyte specific protein (green) in wild-type (left) and Gpt2-null (right) sections containing anterior forceps of corpus callosum, corpus callosum, striatum and cingulum bundle. Quantification of the percent area covered by the staining is given at the bottom. Scale bar: 50 μm.

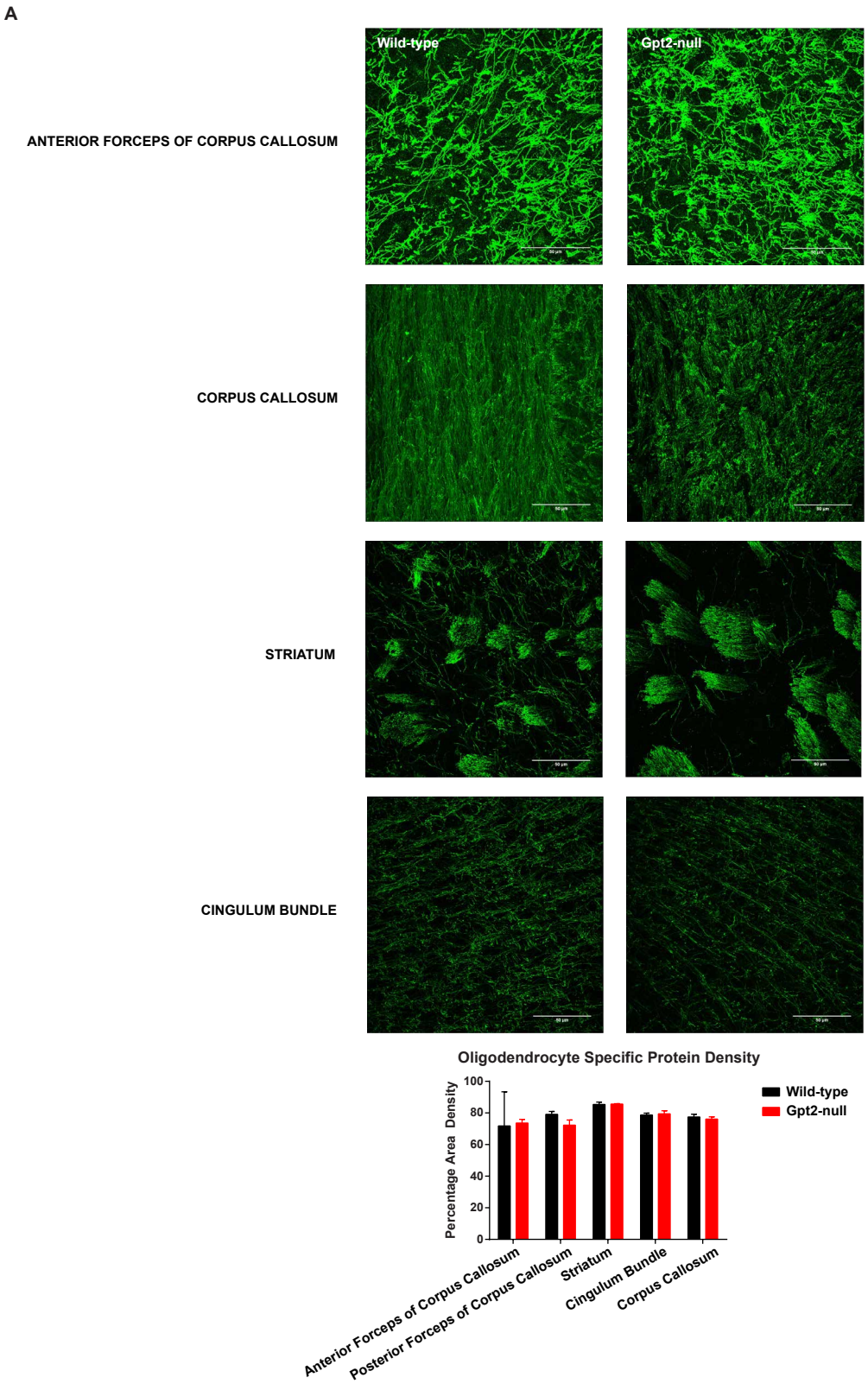

Figure A.3.25. Oligodendrocyte Specific Protein staining in Gpt2-null coronal brain section at postnatal day 18.

Appendix A.3.8. Ng2 & Gpt2 & MitotrackerRed staining in oligodendrocyte precursor cell culture.

Introduction

I characterized GPT2 staining in mouse microglia and oligodendrocyte precursor cells in vitro. GPT2 expression in these cell types has not been studied previously except in some RNA sequencing studies [1, 2].

Results/Key Points

GPT2 is expressed in microglia and oligodendrocyte precursor cells.

Discussion

GPT2 seems to be expressed in multiple cell types in the nervous system, including neurons, astrocytes, microglia and oligodendrocyte precursor cells. It seems to be a ubiquitously expressed protein. This may also be important in the pathophysiology of GPT2 deficiency.

Available data (not analyzed):

- CD68 staining in microglia is available. NG2 staining is also available however I am not sure if it worked.

Method

Cell Culture

A. Mouse Brain Dissection and Primary Mixed Glial Culturing

1. Spray the pup head with 70% ethanol and clean away with Kimwipe. Decapitate P0-P2 mouse. Make a midline incision to the scalp to expose the cranium and incise the cranium from neck to nose. Using forceps, the cranial flaps are gently pulled to the sides and the brain is removed using the flat side of the forceps. Place it in a dissecting dish containing ice-cold HBSS.
2. With the brain dorsal side up, make a shallow incision mid-sagittally. The incision should only pass through the meningeal layer.
3. Peel off the meninges using forceps in a lateral fashion. Make sure the meninges are removed and the brain is undamaged.
4. Gently pry the cortices away from the diencephalon in a lateral fashion. Remove hippocampus and cut the remaining connections with the diencephalon.
5. Dice each cortex into 6 pieces using sharp blade and gently transfer to a 15ml conical tube. Add HBSS to a total volume of 5.625 ml.
6. Add 625 ul of 2.5% Trypsin-EDTA. Mix by inverting and incubate the tissue in the water bath at 37ºC for 30 min. Mix by occasional shaking by hand in a circling motion every 10 min.
7. Centrifuge for 5 min at 300g to pellet cortex tissue pieces.
8. Carefully remove supernatant by decantation into an empty dissecting dish[1]. To avoid losing the tissue pellet you may mechanically retain it using a pipette. Dissociate the tissue into a single cell suspension by adding 3 ml astrocyte plating medium (APM) and vigorous pipetting using a 10ml plastic pipette until tissue pieces are dissociated into single cells (~30 times). Triturate slowly at first, and

[1] And not the liquid trash container as it may lead to contamination.

gradually increase speed as pieces dissociate. Don't introduce bubbles. Adjust volume to 6 ml using APM.

9. Use a 70um nylon mesh to separate chunks of tissue.
10. You can prove the dissociation of the cortex tissue into single cells by counting using a hematocytometer. Transfer 10 ul of cell suspension to 40ul Trypan Blue. One preparation of 1 mouse pup cortices should yield 2.5-3.745x10^6 dissociated single cells.
11. Transfer the cell suspension to the PDL-coated T25 flask.

B. Plating Astrocyte-enriched Culture

1. Do not disturb the culture for 2 days. After 2 days, gently remove the flask from the incubator, stand upright and change the medium completely. At later feedings, you don't need to be this careful. Change 2/3 of the media every 3 days thereafter (aspirate 4 ml and add 4 ml fresh medium). Neurons will wither and die without the proper supplements in media after DIV1.
2. On late day 5, add APM supplemented with insulin such that final concentration in the flask will be 5ug/ml. (aspirate 3 ml and add 3 ml of APM + 10ug/ml Insulin)
3. By day 6, an astrocyte monolayer should clearly be visible.
4. Astrocytes grown to confluency are identifiable as a monolayer of large, flat cells in a "brick wall" arrangement. After 7 to 8 days, when astrocytes are confluent and overlaying microglia sit exposed on the astrocyte layer or are already detached from the astrocyte layer, shake the T25 flask at 50 rpm for 45 min on an orbital shaker to remove loosely attached microglia. Don't disturb the astrocyte

layer, stand the flask upright. Discard the supernatant containing microglia or if you wish to culture and examine microglia, spin it down and plate for culture. This will yield highly enriched microglial population. Put APM+Insulin (5ug/ml) in 5%CO2 incubator for 6 hours.

5. Add 6 ml fresh APM+Insulin (5ug/ml) and continue by shaking the flask at 220 rpm for 18-21 hr to remove oligodendrocyte precursor cells (OPC). Discard the supernatant or spin it down and plate, if you wish to culture OPCs…
6. Add 120 ul of 1 mM Cytosine Arabinofuranoside to 6 ml astrocyte plating medium. (working concentration of Ara-C : 20uM)
7. Incubate in 8.5%CO2 for 48 hours.
8. Refresh medium and allow cells to recover for 24 hours.
9. Repeat steps 6,7,8 (2^{nd} cytosine arabinoside treatment).
10. Rinse the remaining confluent astrocyte layer twice with PBS, aspirate the PBS, add warm 3 ml 0.25% trypsin-EDTA and incubate in the CO2 incubator at 37 °C. Check detachment of astrocytes every 5 min and enforce detachment of astrocytes by hitting the flask on the sides (2-3 times).
11. After astrocytes are detached from the culture flask, add 4 ml of astrocyte culture medium, spin cells at 180 x g for 5 min, aspirate supernatant and add 12 ml fresh astrocyte plating medium. One T25 tissue culture flask should yield around $2.5x10^5$ cells after the first cell split. Plate cells in two T25 culture flasks and incubate at 37 °C in the CO_2 incubator. Change the medium every 2 to 3 days. Alternatively seed directly on coverslips for ICC.
12. You can passage a couple more times.

C. Plating Microglia-enriched Culture

Population 1

1. After obtaining microglial suspension, filter it with 70um nylon mesh, then transfer it to a 15 ml Falcon tube and spin at 300g, 5min.
2. Careful! The pellet is very loose, aspirate supernatant carefully. Re-suspend pellet with 500 ul microglia plating medium (DMEM + 10% FES + 1% Penicillin/Streptomycin).
3. Count cell density by hemocytometer and bring it to $2x10^5$ cells/ml with microglia plating medium.
4. Plate appropriate amount to the PDL-coated coverslips or wells/dishes. Allow microglia to adhere overnight. Use microglia in experiments after 2 days.

Population 2

1. After the overnight shake (step A5) and differential adhesion step (D2), add 1 ml 0.25% Trypsin-EDTA and add 4 ml of microglial plating medium as soon as you observe the cells detach.
2. Pellet cells at 300g, 5min.
3. Count and plate as in Population1. There might be residual astrocytes in this population.

D. Plating Oligodendrocyte Precursor Cells-enriched Culture

1. Equilibrate empty untreated Petri dishes in 5% CO2 incubator for 30 min.
2. Transfer cell suspension with OPCs to the untreated Petri dishes (OPCs tend to attach to dishes treated for tissue culture) for 45 minutes at 37ºC in 5% CO2 incubator. Differential adhesion of microglia and astrocytes will separate them from OPCs.
3. Once the incubation is complete, examine the dishes under bright field. OPCs are identified as small cell clumps, typically of 3-5 cells but sometimes form large aggregates resembling neurospheres. Gently swirl the plates to detach any loosely adhered OPCs, and transfer the cell suspension from each plate into a 15mL conical tube.
4. Spin down cells at 300g, 5min.
5. Resuspend the pellet in 500ul of OPC medium with a P1000 pipette tip, followed by resuspension with a P200 pipette tip. (OPCs tend to grow in clumps).
6. Count the cells with a hemocytometer. Add appropriate amount of OPC medium so that the density is 2-5 x 10^4 cells/ml. Change half of the medium every other day.
7. Plate the cell suspension on poly-ornithine-coated plates for OPC proliferation with OPC medium.
8. For differentiation of OPCs into oligodendrocytes, change the medium to Oligodendrocyte differentiation medium. After 48 hours, oligodendrocyte-specific markers will appear.
9. Co-cultures of oligodendrocytes and neurons can also be achieved.

Immunofluorescence

To visualize mitochondria *in vitro*, the cells were incubated with 100 nM MitoTracker Red CMXRos (Invitrogen M7512) for 25 minutes at 37ºC, 5% CO_2, then proceeded with the Immunofluorescence protocol. The cells were washed with 1X PBS (FisherScientific BP3994) and fixed with 4% paraformaldehyde (PFA) at room temperature for 10 minutes. Following steps were done in order: 3 5-minute 1X PBS washes, 10-minute permeabilization in PBS with 0.25% TritonX-100 (T8787, Sigma); 1-hour blocking with 10% Normal Goat Serum (NGS, JacksonImmunoResearch, 005-000-121) in PBS with 0.1% TritonX-100 (PBST); overnight incubation with primary antibody in 2% NGS-PBST; three washes with PBST; 1-hour incubation with secondary antibody; three washes with PBST; counterstaining with DAPI. Zeiss LSM800 confocal microscope was used. Images were processed and analyzed with ImageJ (RRID:SCR_003070).

Figure Legends

Figure A3.26. GPT2 staining in oligodendrocyte precursor cells and microglia in vitro.

A. GPT2 staining in microglia. DAPI (cyan), GPT2 (green), MitoTracker Red (magenta) and the merged imaged on the far right. Scale bar: 10 μm.

B. GPT2 staining in oligodendrocyte precursor cells (OPCs). DAPI (cyan), GPT2 (green), MitoTracker Red (magenta) and the merged imaged on the far right. Scale bar: 10 μm.

1. Zhang, Y., K. Chen, S.A. Sloan, M.L. Bennett, A.R. Scholze, S. O'Keeffe, H.P. Phatnani, P. Guarnieri, C. Caneda, N. Ruderisch, et al., *An RNA-sequencing transcriptome and splicing database of glia, neurons, and vascular cells of the cerebral cortex.* J Neurosci, 2014. **34**(36): p. 11929-47.
2. Marques, S., D. van Bruggen, D.P. Vanichkina, E.M. Floriddia, H. Munguba, L. Varemo, S. Giacomello, A.M. Falcao, M. Meijer, A.K. Bjorklund, et al., *Transcriptional Convergence of Oligodendrocyte Lineage Progenitors during Development.* Dev Cell, 2018. **46**(4): p. 504-517 e7.

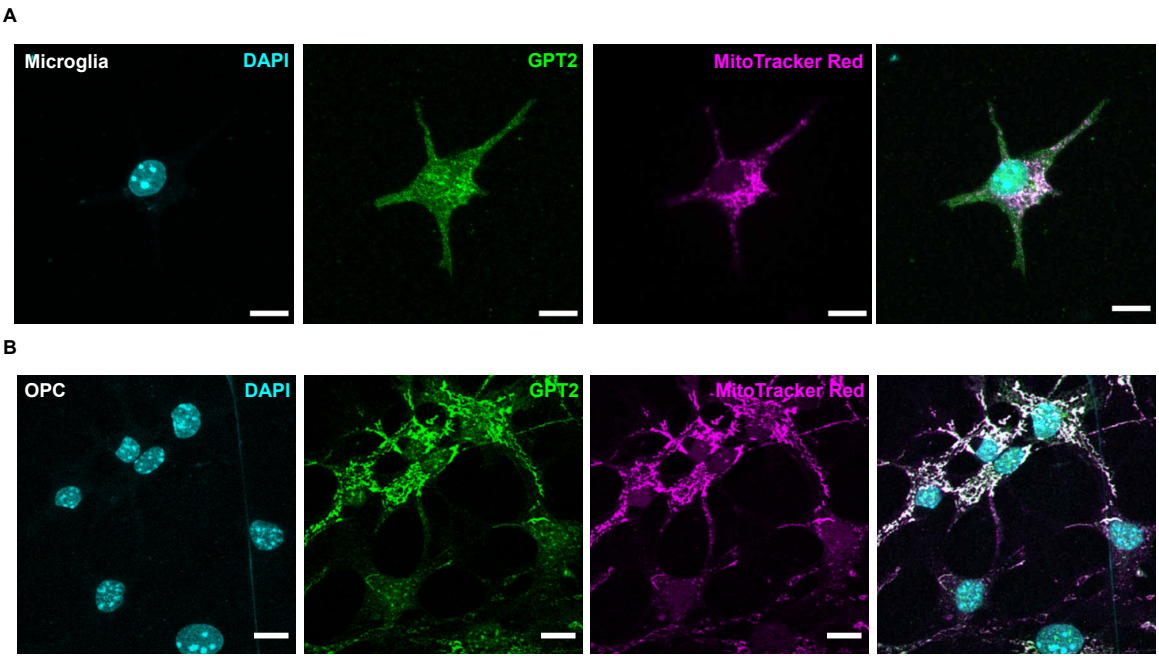

Figure A3.26. GPT2 staining in oligodendrocyte precursor cells and microglia in vitro.

Appendix A.3.9. Metabolomics in isolated mitochondria and cytosol fractions of Gpt2-null forebrains at P19.

Introduction

I performed metabolomics on cytosolic and mitochondrial fractions obtained from homogenization of wild-type and Gpt2-null whole mouse brains at postnatal day 18. This would allow us to observe differences in changes of metabolite pools in different cellular compartments. For example, glutamate concentration in neurons is much greater than that of alanine, pyruvate or alpha-ketoglutarate and this may the reason why the predicted direction of the Gpt2 reaction is alanine production. Therefore, with the absence of Gpt2, glutamate levels in the mitochondria may increase and the cytosolic glutamate levels may not change. This prediction is not supported by the metabolomics data obtained from the whole hippocampus tissue where the Gpt2-null samples had a decreased glutamate level.

Results / Key Points

- Mitochondrial data has similar trends in phosphoenolpyruvate, 2-hydroxyglutarate, glutathione, fumarate, proline, malate, maleic acid, 2-keto-isovalerate as in whole brain and hippocampus tissue data.
- Cytosol data has similar trends in lysine, glucose-6-phosphate, glucose-1-phosphate, fructose-6-phosphate, maleic acid, SBP, threonine, glutathione, proline, fumarate, fructose-1,6-bisphosphate, sn-glycerol-3-phosphate, carnitine, 2-hydroxyglutarate, glutamine, ornithine, succinate as in whole brain and hippocampus tissue data.
- Alanine was decreased though with considerably more variability.

- Glutamate levels were trending toward a decrease in both cytosolic and mitochondrial fractions but no statistical significance was reached.

Discussion

It was very surprising to find that data for alanine had so much variability; in the whole tissue metabolomics data alanine significance had the one of the lowest raw p-values, if not the lowest, of all the data. This may be a variability inherent to fractionation of the whole brain or simply variation within this particular experiment. The inherent variability of fractionation consists of heterogeneity of the whole brain, the time taken to obtain the different fractions (1.5 hours for mitochondria, 0.5 hours for the cytosol fraction). The time spent in sucrose-based homogenization solution may cause washing away or decay of metabolites. Another important consideration is that mitochondria used for metabolomics originate from extra-synaptosomal mitochondria, i.e. the soma. Synaptosomes, isolated synaptic terminals, form during homogenization of brain tissue in sucrose-based solutions and contain copious amount of mitochondria. There are ways to extract the mitochondria (e.g. with digitonin) but it would further introduce chemical intervention and change the metabolome even further.

There are novel and fast ways to extract mitochondria in vivo under 12 minutes [1]. Mito-tag mice allow for conditional expression of the tag which allows for mitochondrial extraction from specific cell types. It would be very interesting to try extracting mitochondria belonging to different cell types (glutamatergic neurons vs. GABAergic

neurons) in Gpt2-null mice; this may pinpoint the differential mechanisms in the pathophysiology of Gpt2 deficiency.

Available Data (not shown): a) all heat maps and tables associated with the metabolomics data.

Method

Subcellular Fractionation of the mouse brain

The protocol was adapted from [2]. The whole brain including cerebellum was immediately removed after cervical dislocation and rinsed in ice-cold 1X Brain homogenization buffer (0.320 M Sucrose, EDTA 1mM, Tris base 5 mM, pH 7.4). After decanting, fresh 10ml/gr 1X Brain homogenization buffer was added, and the brain was cut into small chunks with surgical scissors. A Kimble pestle and motor were used to homogenize the tissue with 12 strokes each lasting 4 seconds. The tube was spun at 1300g for 3 minutes at 4^{o}C. The 1st supernatant was put aside on ice and the pellet was re-suspended in half starting volume with 1X Brain homogenization buffer. The pellet was homogenized with a Kimble pestle and motor with 8 strokes each lasting 4 seconds. The tubes were spun at 1300g for 3 minutes at 4^{o}C. This 2nd supernatant was combined with the first and the sample was spun at 10000g for 10 minutes at 4^{o}C with Sorvall RC6Plus using the SS34 rotor. The supernatant is the cytosolic fraction. The pellet was re-suspended in 10m/gr original tissue of 15% Percoll (Percoll, Cytiva 17089102 prepared in 1X Brain homogenization buffer). The suspension was carefully layered onto a Percoll gradient (23% - 40%) and the tube was spun at 22000g for 10 minutes at 4^{o}C.

The bottom layer is the mitochondria. After carefully removing the upper layers, the mitochondria were aspirated and re-spun with 4 volumes of 1X Brain homogenization buffer, at 11600rpm for 10 minutes at 4ºC. The supernatant was removed, and 4 volumes of Tyrode-like buffer (118mM NaCl, 5mM KCl, 1mM $MgCl_2$, 1.2mM $CaCl_2$, 0.1 mM $Na_2HPO_4.H_2O$, 20mM HEPES, 10mM Glucose, pH7.4) was added. The tube was spun at 18000g for 10 minutes at 4ºC. After carefully removing the supernatant, the mitochondria were resuspended in 0.5 ml/gr (of original tissue) fatty-acid free bovine serum albumin (BSA) (10mg/ml in 1X Brain homogenization buffer). The final volume was brought to 3ml/gr (of original tissue) and tube was spun at 6900g for 10 minutes at 4ºC with a tabletop centrifuge. The final pellet was re-suspended in 80% (v/v) methanol (cooled to -80ºC).

Metabolomics. Done as described with minor modifications [3]. The mitochondria fraction was immersed in 500µL of 80% (v/v) high-performance liquid chromatography (HPLC)-grade methanol (cooled to -80ºC), vortexed for 1 minute and incubated at -80ºC for 4 hours. To pellet debris, the sample was centrifuged at 14000g for 10 min at 4ºC. While the supernatant was kept at -80ºC, 400 ul of 80% (vol/vol) methanol (cooled to -80ºC) was added to the pellet, which was then vortexed for 1 minute, incubated at -80ºC for 30 minutes and then centrifuged at 14000g for 10 minutes at 4ºC. The supernatants were combined and re-spun at 14000g for 10 minutes 4ºC. The supernatants were concentrated with SpeedVac at ambient temperature. The cytosolic fraction was centrifuged at 14,000 g for 10 minutes at 4ºC. Methanol (cooled to -80ºC) was added to the supernatant so that the final solution is 80% (v/v) methanol and incubated at -80ºC for 7 hours. The mixture was centridued at 14000 g for 10 minutes at 4ºC. The supernatants

were concentrated with SpeedVac at ambient temperature. The dried pellets were kept at -80ºC until the day of mass spectrometry.

Tandem mass spectrometry was done at Beth Israel Deaconess Medical Center Mass Spectrometry Facility. The samples were re-suspended in liquid chromatography (LC)/mass spectrometry (MS)-grade water and run in tandem LC-MS/MS. Samples were injected into hydrophilic interaction liquid chromatography (HILIC) at high pH using HPLC coupled to a 5500 QTRAP mass spectrometer (AB/SCIEX). Selected Reaction Monitoring (SRM) mode for 300 transitions with positive/negative polarity switching fragmented precursor ions and select for product ions. Peak areas for each detected metabolite were integrated using MultiQuant software (AB/SCIEX). The statistical analyses and data visualization were done using MetaboAnalyst 4.0 [4] (RRID:SCR_015539). If half of data for a metabolite is not available than that metabolite was omitted from analysis. All data was normalized by median normalization and auto-scaled (mean-centered and divided by standard deviation of each variable). Unpaired Student's t-test assuming equal variance was used to generate a p-value.

1. Bayraktar, E.C., L. Baudrier, C. Ozerdem, C.A. Lewis, S.H. Chan, T. Kunchok, M. Abu-Remaileh, A.L. Cangelosi, D.M. Sabatini, K. Birsoy, et al., *MITO-Tag Mice enable rapid isolation and multimodal profiling of mitochondria from specific cell types in vivo.* Proc Natl Acad Sci U S A, 2019. **116**(1): p. 303-312.
2. Sims, N.R. and M.F. Anderson, *Isolation of mitochondria from rat brain using Percoll density gradient centrifugation.* Nat Protoc, 2008. **3**(7): p. 1228-39.
3. Yuan, M., S.B. Breitkopf, X. Yang, and J.M. Asara, *A positive/negative ion-switching, targeted mass spectrometry-based metabolomics platform for bodily fluids, cells, and fresh and fixed tissue.* Nat Protoc, 2012. **7**(5): p. 872-81.
4. Chong, J., D.S. Wishart, and J. Xia, *Using MetaboAnalyst 4.0 for Comprehensive and Integrative Metabolomics Data Analysis.* Curr Protoc Bioinformatics, 2019. **68**(1): p. e86.

Appendix A.3.10. Metabolomics in Gpt2-null hippocampus on zero alanine diet P18.

Introduction

We investigated changes of the metabolome in the hippocampus obtained from Gpt2-null mice fed with No Alanine diet (0% w/w) ad libitum at P18. It is possible that decreased alanine levels in the diet may exacerbate or quicken the phenotype in Gpt2-null mice.

Key Points

- The metabolic profile of the Gpt2-null hippocampus on No Alanine (0% w/w) at P18 very closely resembles the profile obtained from mice on Regular Diet P18.

Results

The principal component analysis shows that the metabolic profiles of wild-type and Gpt2-null groups were well separated. The list of metabolites that were significantly changed along with the fold changes resemble very closely with the results obtained from mice on Regular Diet at P18.

Discussion

Total alanine that is received by the pups cannot be empirically controlled as the mother gives alanine in the milk, however no alanine in the diet could have worsen the phenotype. To my knowledge, there is no specific way of blocking alanine entry into the brain either, the transporters that carry alanine also carry other neutral amino acids such as serine and glutamine. While it is not possible to eliminate alanine altogether, it is possible to deliver nutrients intraperitoneally or intracranially using an osmotic pump, however this is technically challenging. Other methods such as oral gavage or i.p. injections would have to be done

continuously throughout the day (and night) to ensure high levels of the nutrient in the circulation and this is both stressful to the mice and technically challenging.

Method

As performed in Chapter 3 – Metabolomics.

Figure A.3.27. Metabolomics in Gpt2-null hippocampus at P14 from mice on High Alanine diet.

A. 2D-score plot of Principal Component Analysis. Wild-type (green), Gpt2-null (red).

B. List of significantly changed metabolites in Gpt2-null hippocampus on High Alanine diet at P14.

The metabolites were ordered according to their raw P value. FDR: False discovery rate. Fold changes are given as fraction of the averaged wild-type peak intensity value. The "trend" column refers to the comparison of results obtained from Regular diet and High Alanine diet; if there was a significant change in the same direction for that metabolite in both diets, it is named as "Same"; if there was an opposite trend, then "Opposite". For example, alanine was significantly decreased in the Gpt2-null hippocampus compared to wild-type on High Alanine diet and similarly alanine was significantly decreased in the Gpt2-null hippocampus compared to wild-type on Regular Diet (hence "Same").

A

Principal Component Analysis

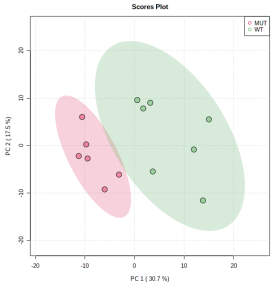

B

	Fold Change	raw p value	FDR	Trend		Fold Change	raw p value	FDR	Trend		Fold Change	raw p value	FDR	Trend
fructose-1,6-bisphosphate	2.1107	1.71E-08	4.90E-06	Same	S-adenosyl-L-methionine	2.7405	0.003315	0.02495		cystathionine	1.2778	0.019097	0.07282	Same
serine	0.51333	4.94E-08	7.06E-06	Same	creatine	0.7761	0.003581	0.02626	Same	adenine	0.81393	0.020479	0.07707	
proline	1.6873	3.99E-06	0.00029	Same	xanthosine	0.64211	0.00397	0.02838	Opposite	L-arginino-succinate	1.5159	0.02084	0.07741	
dTMP	1.9196	4.01E-06	0.00029	Same	aconitate	0.48629	0.004448	0.03028		Methionine sulfoxide	0.51161	0.021432	0.07858	
homoserine	0.38865	9.03E-06	0.00052		1-Methyladenosine	0.7384	0.004521	0.03028		GDP	0.693	0.022244	0.08053	
D-glyceraldehdye-3-phosphate	1.7966	2.23E-05	0.00107	Same	D-glucosamine-6-phosphate	1.7257	0.004552	0.03028	Same	purine	1.4078	0.02391	0.08548	
glycerate	0.44716	5.08E-05	0.00208		dAMP	0.74125	0.005031	0.0327		betaine aldehyde	0.81006	0.026007	0.09183	
glutathione disulfide	0.67554	0.000133	0.00477		taurine	0.76611	0.005238	0.03329	Same	D-glucono--lactone-6-phosphate	1.7122	0.026534	0.09254	Same
glucose-6-phosphate	2.4204	0.000212	0.00674	Same	sarcosine	0.77451	0.005466	0.03392		dGMP	0.80711	0.029148	0.10044	
1-Methyl-Histidine	2.4413	0.000326	0.00933		dGDP	0.69491	0.005864	0.03392		Glycerophosphocholine	0.71607	0.030432	0.10266	
fructose-6-phosphate	2.4874	0.000377	0.00955	Same	succinate	0.68891	0.005948	0.03392	Same	acetoacetyl-CoA	1.9568	0.030511	0.10266	
malate	0.65137	0.000401	0.00955	Same	Carbamoyl phosphate	0.78131	0.006079	0.03392		deoxyadenosine	0.12209	0.031165	0.10279	
valine	1.5929	0.00053	0.01083	Same	acetylphosphate	1.2148	0.006168	0.03392	Same	methionine	0.52598	0.03142	0.10279	
dephospho-CoA	1.7114	0.000571	0.01089	Same	ADP	0.6598	0.006607	0.03515		glyoxylate	0.51123	0.032054	0.10279	Same
myo-inositol	0.68088	0.00062	0.01109		4-aminobutyrate	0.8103	0.006787	0.03515		Pyrophosphate	0.80408	0.032347	0.10279	Opposite
D-gluconate	0.76556	0.000888	0.01423		acadesine	0.50094	0.006856	0.03515	Opposite	hydroxyproline	0.70783	0.033901	0.10526	Same
CMP	0.80244	0.000914	0.01423		arginosuccinic acid	1.5429	0.006882	0.03515		N-acetyl-L-ornithine	0.38954	0.034158	0.10526	
alanine	0.76443	0.001051	0.01423	Same	IDP	0.69676	0.007717	0.03872		glycolate	0.67437	0.034404	0.10526	
AMP	0.80963	0.001058	0.01423	Same	glutathione	0.76442	0.008054	0.03971	Same	phosphocreatine	1.5958	0.034668	0.10526	
O-acetyl-L-serine	0.41926	0.001071	0.01423		hydroxyphenylpyruvate	0.65941	0.00885	0.0429		Urea	0.67147	0.035249	0.10526	
leucine-isoleucine	1.494	0.001094	0.01423	Same	S-adenosyl-L-homocysteine	0.74101	0.009558	0.04487		a-ketoglutarate	1.1701	0.035331	0.10526	Same
4-Pyridoxic acid	0.59833	0.001433	0.01665		D-erythrose-4-phosphate	1.5329	0.00957	0.04487	Same	xanthosine-5-phosphate	0.54002	0.049203	0.13327	
IMP	0.75453	0.001455	0.01665		Methylmalonic acid	0.72966	0.009756	0.04501	Same	thymine	0.77027	0.04942	0.13327	
N-acetyl-L-alanine	0.75971	0.001544	0.01699		Ng,NG-dimethyl-L-arginine	1.3425	0.011563	0.05249	Same	S-ribosyl-L-homocysteine	0.72185	0.0373	0.10998	Same
D-sedoheptulose-1-7-phosphate	1.4856	0.001721	0.01823	Same	fumarate	0.81983	0.013426	0.06	Same	dTTP	2.2683	0.03934	0.1133	
citrulline	1.7379	0.001896	0.01937	Same	Kynurenine	1.7308	0.015494	0.06724		N-acetyl-glutamine	0.77846	0.039425	0.1133	
cysteine	0.42511	0.002034	0.01985	Same	adenosine 5-phosphosulfate	0.70695	0.015773	0.06724		thymidine	0.68615	0.039819	0.1133	
arginine	1.7545	0.002082	0.01985	Same	dihydroxy-acetone-phosphate	1.4361	0.015907	0.06724	Same	3-hydroxybuterate	0.68684	0.040011	0.1133	
2-keto-isovalerate	0.79313	0.002168	0.02	Same	N-acetyl-aspartylglutamic acid	0.77936	0.015986	0.06724		O8P-O1P	1.25	0.043703	0.12254	Same
trehalose-6-Phosphate	0.71357	0.002444	0.02164		phosphoenolpyruvate	1.5227	0.016634	0.06895	Same	NADH	0.61834	0.047177	0.131	
Maleic acid	0.8044	0.002497	0.02164	Same	aminoimidazole carboxamide ribonucleotide	0.64278	0.017352	0.07089		uridine	0.73572	0.049114	0.13327	
indole	1.6595	0.002916	0.02396		Citraconic acid	0.53767	0.01801	0.07157						
tryptophan	1.6235	0.002932	0.02396		Methylcysteine	0.80616	0.018106	0.07157						
dCMP	0.75774	0.003234	0.02495		N-acetyl-glucosamine-1-phosphate	0.72423	0.018269	0.07157						
N-acetyl-glutamate	0.8066	0.003261	0.02495		dimethylglycine	0.65552	0.019088	0.07282	Opposite					

Figure A.3.27. Metabolomics in Gpt2-null hippocampus at P14 from mice on High Alanine diet.
A. 2D-score plot of Principal Component Analysis. Wild-type (green), Gpt2-null (red).
B. List of significantly changed metabolites in Gpt2-null hippocampus on High Alanine diet at P14.
The metabolites were ordered according to their raw P value. FDR: False discovery rate.
Fold changes are given as fraction of the averaged wild-type peak intensity value.
The “trend” column refers to the comparison of results obtained from Regular diet and
High Alanine diet; if there was a significant change in the same direction for that metabolite in both diets, it is named as “Same”; if there was an opposite trend, then “Opposite”. For example, alanine was significantly decreased in the Gpt2-null hippocampus compared to wild-type on High Alanine diet and similarly alanine was significantly decreased in the Gpt2-null hippocampus compared to wild-type on Regular Diet (hence “Same”).

Appendix A3.11. Metabolomics in Gpt2-null hippocampus on high alanine diet P14.

Introduction

We investigated changes of the metabolome in the hippocampus obtained from Gpt2-null mice fed with High Alanine diet (5% w/w) ad libitum at P14. Differences with the results obtained from mice on Regular Diet (1% w/w) may lead to different interpretations. If at P14, the metabolic profile of the Gpt2-null hippocampus is better than the profile obtained from mice fed with Regular Diet, most likely Gpt2-null pups benefit from the mother, despite the first-pass metabolism (particularly in the liver) as at P14 the main source of nourishment for the pups is still the mother's milk. If at P14, the results are the same as Regular Diet, then we can conclude that the pups do not majorly benefit from the mother's milk at this time and the changes seen at P18 can be attributable to the pup's newly acquired ability to feed on solid chow. This is particularly important for alanine, if alanine levels do not improve at P14 then we are safe to assume that the pups do not benefit from the milk at this time.

Key Points

- The metabolic profile of the Gpt2-null hippocampus on High Alanine (5% w/w) at P14 very closely resembles the profile obtained from mice on Regular Diet P14.

Results

The principal component analysis shows that the metabolic profiles of wild-type and Gpt2-null groups were well separated. The list of metabolites that were significantly changed along with the fold changes resemble very closely with the results obtained from

mice on Regular Diet at P14. The most notable difference was that glutamate levels were not significantly changed in Gpt2-null hippocampus on High Alanine diet at P14 whereas there was a slight decrease (~10%) in mice on Regular Diet.

Discussion

Most likely the mother metabolizes the extra alanine and does not pass on supplementary alanine to the pup. Currently, we do not know if serum alanine levels in Gpt2-heterozygous mice are increased after ingestion of High Alanine diet, as serum alanine levels most likely have the biggest influence on the mother's milk composition.

Method

Metabolomics was performed as in Chapter 3.

Figure Legends

Figure A.3.28. Metabolomics in Gpt2-null hippocampus at P14 from mice on High Alanine diet.

A. 2D-score plot of Principal Component Analysis. Wild-type (green), Gpt2-null (red).

B. List of significantly changed metabolites in Gpt2-null hippocampus on High Alanine diet at P14. The metabolites were ordered according to their raw P value. FDR: False discovery rate. Fold changes are given as fraction of the averaged wild-type peak intensity value. The "trend" column refers to the comparison of results obtained from Regular diet and High Alanine diet; if there was a significant change in the same direction for that metabolite in both diets, it is named as "Same"; if there was an opposite trend, then "Opposite". For example, alanine was significantly decreased in the Gpt2-null

hippocampus compared to wild-type on High Alanine diet and similarly alanine was significantly decreased in the Gpt2-null hippocampus compared to wild-type on Regular Diet (hence “Same”).

A

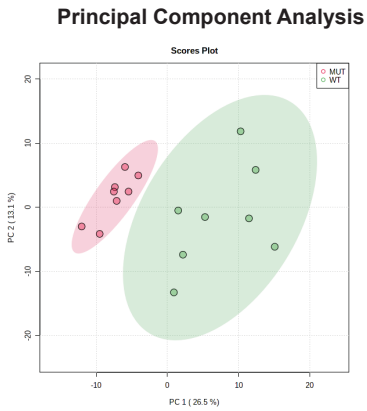

B

	Fold Change	raw p-valu	FDR	Trend		FC	p-value	FDR	Trend
cystathionine	2.0344	3.73E-09	1.07E-06	Same	CMP	0.8745	0.00299	0.01636	Same
glutathione disulfide	0.66257	2.58E-06	0.00026	Same	lactate	0.8577	0.00303	0.01636	
serine	0.66979	2.71E-06	0.00026	Same	4-aminobutyrate	0.8611	0.00318	0.01685	Same
glutathione	0.69301	5.66E-06	0.00035	Same	2-Aminooctanoic acid	0.6394	0.00338	0.01758	
myo-inositol	0.74261	6.41E-06	0.00035	Same	2-keto-isovalerate	0.8542	0.00493	0.02519	Same
valine	1.4053	7.73E-06	0.00035	Same	Creatinine	0.8592	0.00667	0.03348	Same
proline	1.4856	8.55E-06	0.00035	Same	Nicotinamide Riboside	0.7069	0.00707	0.03485	
sarcosine	0.79492	1.27E-05	0.00039	Same	2-ketohaxanoic acid	0.8062	0.00729	0.03534	Same
lysine	1.6335	1.39E-05	0.00039	Same	thymidine	0.7072	0.01068	0.05068	
glycerate	0.55017	1.47E-05	0.00039	Same	D-erythrose-4-phosphate	1.218	0.01081	0.05068	
N-acetyl-glutamate	0.76016	1.51E-05	0.00039		2-Isopropylmalic acid	0.5886	0.01177	0.05363	Same
Glycerophosphocholine	0.68235	2.72E-05	0.00063	Same	Ascorbic acid	0.5739	0.01195	0.05363	Same
glutathione disulfide	0.68381	2.87E-05	0.00063	Same	cytidine	0.6965	0.012	0.05363	
Pyrophosphate	0.82546	5.95E-05	0.0012	Same	Acetylcarnitine DL	0.8831	0.01219	0.05365	Same
fructose-1,6-bisphosphate	1.4465	6.31E-05	0.0012	Same	Hydroxyphenylacetic acid	0.7049	0.01265	0.0548	
N-acetyl-L-alanine	0.83936	9.18E-05	0.00164	Same	CDP	0.7367	0.01304	0.05566	
alanine	0.811	0.00015	0.00255	Same	ribose-phosphate	0.6987	0.01347	0.05664	
hydroxyphenylpyruvate	0.75995	0.00016	0.00255		asparagine	1.1528	0.01388	0.05683	Same
fructose-6-phosphate	1.6959	0.00018	0.00275	Same	Thiamine pyrophosphate	0.3253	0.01391	0.05683	
succinate	0.71283	0.00023	0.00327	Same	dCDP	1.6918	0.01427	0.05746	Opposite
hydroxyproline	0.53947	0.00028	0.00385	Same	Kynurenine	2.063	0.01446	0.05746	
histidinol	0.65753	0.00051	0.00638		xanthine	0.8172	0.01534	0.06012	Same
Methylmalonic acid	0.70086	0.00054	0.00638	Same	AMP	0.8592	0.01609	0.0622	Same
GDP	0.61099	0.00062	0.00684		N-acetyl-L-aspartic acid	0.877	0.01662	0.06337	
D-sedoheptulose-1-7-phosphate	1.3631	0.00064	0.00684	Same	spermidine	1.6078	0.01984	0.07397	
glucose-6-phosphate	1.8325	0.00068	0.00684	Same	cytosine	0.8041	0.01991	0.07397	
ornithine	1.4066	0.00068	0.00684		putrescine	0.3749	0.02023	0.07416	
Carbamoyl phosphate	0.7976	0.00069	0.00684		uracil	0.4962	0.02198	0.07871	Opposite
Pyroglutamic acid	1.2792	0.00081	0.00747	Opposite	leucine-isoleucine	1.2821	0.02217	0.07871	Same
allantoin	0.74271	0.00081	0.00747	Same	dihydroxy-acetone-phosphate	1.7505	0.02229	0.07871	
CDP-ethanolamine	0.77771	0.00096	0.00851		S-adenosyl-L-homocysteine	0.8304	0.02274	0.0793	Same
homoserine	0.66922	0.00099	0.00851	Same	uridine	0.7321	0.02502	0.08562	
citrulline	1.2604	0.00101	0.00851		diphosphate	0.733	0.02515	0.08562	
dTMP	1.5429	0.0011	0.009		adenine	0.8537	0.02617	0.08806	Opposite
arginine	1.2814	0.00125	0.0099	Same	deoxyadenosine	0.5936	0.0283	0.09413	Same
glucosamine	0.5482	0.00142	0.01086	Same	4-phosphopantothenate	0.7898	0.029	0.09534	Same
S-adenosyl-L-homocysteine	0.74829	0.00147	0.01086	Same	inosine	0.7415	0.03056	0.09931	
dephospho-CoA	1.4808	0.00148	0.01086		2,3-dihydroxybenzoic acid	0.607	0.0319	0.10252	
glutathione	0.71577	0.00167	0.01165	Same	S-adenosyl-L-methionine	1.2343	0.03353	0.10655	Opposite
betaine	0.66677	0.00167	0.01165	Same	methionine	1.1835	0.03425	0.10764	Same
creatine	0.8568	0.0018	0.01228	Same	Taurodeoxycholic acid	0.5925	0.03545	0.10923	
2-hydroxygluterate	0.85984	0.00185	0.01231	Same	Phosphorylcholine	0.8632	0.03552	0.10923	
threonine	1.2374	0.00196	0.01245	Same	S-methyl-5-thioadenosine	2.0477	0.03789	0.11529	
UMP	0.86347	0.002	0.01245	Same	N-carbamoyl-L-aspartate	0.8519	0.03938	0.11854	
Maleic acid	0.85285	0.002	0.01245	Same	dTDP	0.6649	0.04012	0.11952	Same
cyclic-AMP	0.69201	0.00217	0.01321		D-glyceraldehdye-3-phosphate	2.0442	0.0409	0.1206	Same
citrate-isocitrate	0.64446	0.00244	0.01454	Same	N-acetyl-glucosamine	0.7894	0.04444	0.1297	
fumarate	0.87589	0.0027	0.01527	Same	IMP	0.8419	0.04731	0.13581	Same
citrate	0.65362	0.0027	0.01527	Same	1-Methyladenosine	0.7249	0.04749	0.13581	
N-acetyl-glucosamine-1-phosphate	0.80588	0.00272	0.01527	Same	isocitrate	0.7028	0.0494	0.13987	

Figure A.3.28. Metabolomics in Gpt2-null hippocampus at P14 from mice on High Alanine diet. A. 2D-score plot of Principal Component Analysis. Wild-type (green), Gpt2-null (red). B. List of significantly changed metabolites in Gpt2-null hippocampus on High Alanine diet at P14. The metabolites were ordered according to their raw P value. FDR: False discovery rate. Fold changes are given as fraction of the averaged wild-type peak intensity value. The “trend” column refers to the comparison of results obtained from Regular diet and High Alanine diet; if there was a significant change in the same direction for that metabolite in both diets, it is named as “Same”; if there was an opposite trend, then “Opposite”. For example, alanine was significantly decreased in the Gpt2-null hippocampus compared to wild-type on High Alanine diet and similarly alanine was significantly decreased in the Gpt2-null hippocampus compared to wild-type on Regular Diet (hence “Same”).

Appendix 3.12. 13C labeling in alpha-ketoglutarate using U-13C-glutamine precursor in Gpt2-null astrocytes in vitro.

Introduction

This section contains data for U-13C-Glutamine labeling of alpha-ketoglutarate in astrocytic cultures.

Results/Key Points

- Reduced fractional enrichment of 13C labeled alpha-ketoglutarate in Gpt2-null astrocytes in vitro.

Discussion

There is decrease in glutamine-fueled anaplerosis (replenishment of the TCA cycle). We currently lack the labeling data for other TCA cycle intermediates malate, fumarate and succinate but they would be reinforcing the observed result with alpha-ketoglutarate.

Method

See Chapter 3 Methods for Isotope Tracing.

Figure Legends

Figure A.3.29. Decreased 13C labeling in alpha-ketoglutarate using U-13C-glutamine in Gpt2-null astrocytes.

A. Fractional enrichment of 13C labeling in alpha-ketoglutarate in wild-type (blue) and Gpt2-null (red) astrocytes in vitro. The raw p-value of the Student's t-test wild-type vs. Gpt2-null comparison are given on the figure. n (wild-type) = 6, n (Gpt2-null) = 5.

A

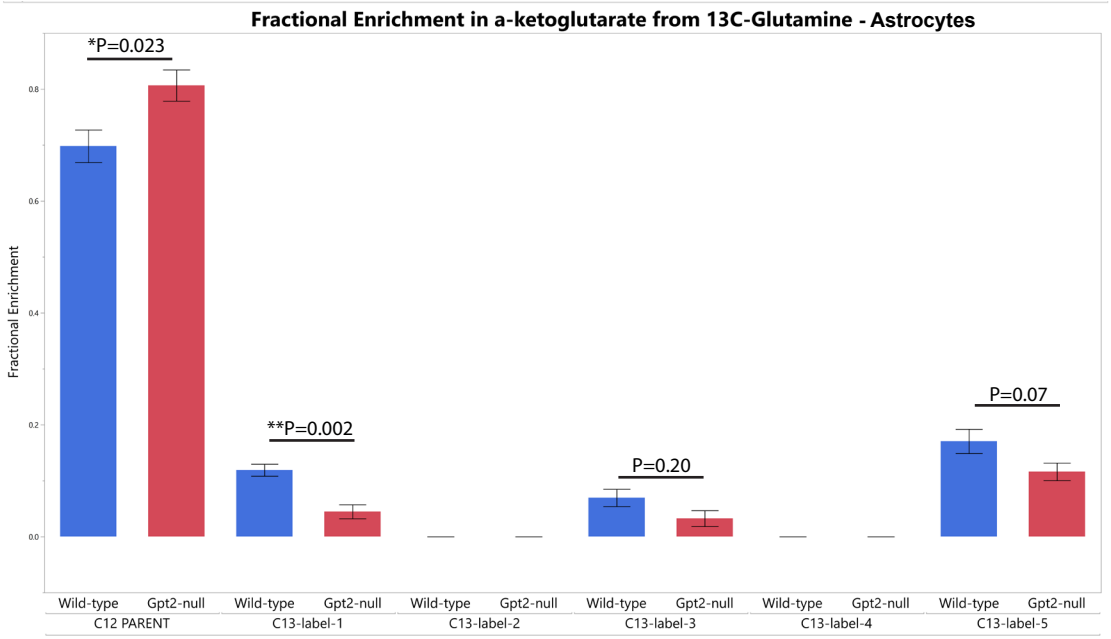

Figure A.3.29. Decreased 13C labeling in alpha-ketoglutarate using U-13C-glutamine in Gpt2-null astrocytes. A. Fractional enrichment of 13C labeling in alpha-ketoglutarate in wild-type (blue) and Gpt2-null (red) astrocytes in vitro. The raw p-value of the Student's t-test wild-type vs. Gpt2-null comparison are given on the figure. n (wild-type) = 6, n (Gpt2-null) = 5.

Appendix A.3.13. TMRE & DHE (dihydroethidium) & MitoSOX in Gpt2-null hippocampal neurons and astrocytes in vitro.

Introduction

Here we investigated changes in the mitochondrial membrane potential and oxidative stress in Gpt2-null hippocampal neurons and astrocytes in vitro. Mitochondrial membrane potential is formed by the electron transport chain that uses electrons resulting from substrate oxidation forming the proton gradient that constitutes the potential between the intermembrane space and the mitochondrial matrix. Gpt2 catalyzes a reaction that feeds into the TCA cycle thereby contributing to the substrate availability. Any deficits in this supply chain may result in deficits in mitochondrial membrane potential which may underlie the pathological phenotype seen in both mice and humans with Gpt2 deficiency. The mitochondrial membrane potential can be indirectly measured by tetramethylrhodamine, ethyl ester (TMRE), a cationic dye that locates to hyperpolarized mitochondria. TMRE staining in vitro also allows for indirect quantification of mitochondrial mass or mitochondrial footprint, the area covered by the TMRE signal per cell.

Oxidative stress may also partly underlie the neurodegeneration seen in vivo thereby contributing to the phenotype seen in mice and humans. Gpt2 modulates glutamate levels and the loss of Gpt2 may have an influence on the glutamate pool that is used to make glutathione, one of the cell's main antioxidant defenses. Glutathione levels were reduced in Gpt2-null mouse brain and we found trending increases in non-mitochondrial oxygen consumption in Gpt2-null hippocampal neurons and astrocytes in vitro by using Seahorse

Extracellular Flux Analyzer, which may indicate increased levels of reactive oxygen species (ROS). To investigate oxidative stress, we stained the cells with MitoSOX, a mitochondrial superoxide anion indicator and dihydroethidium, which reacts with ROS in the cytoplasm and locates to the nucleus.

Key Points

- No differences in TMRE fluorescence intensity or mitochondrial footprint in Gpt2-null hippocampal neurons and astrocytes in vitro.
- No differences in DHE in Gpt2-null hippocampal neurons or astrocytes in vitro.
- Increased MitoSOX intensity in Gpt2-null hippocampal neurons but no differences in astrocytes in vitro.

Results

We first validated the correlation between the TMRE signal and mitochondrial membrane potential by observing the fluorescence intensity of the TMRE signal with 2 μM FCCP, an uncoupler of the mitochondrial membrane potential. Within twenty minutes the TMRE fluorescence intensity dimmed whereas MitoTracker Green, which fluoresces independently of the mitochondrial membrane potential (Pendergrass et al., 2004) remained the same throughout. This indicates that TMRE is a valid method to indirectly measure mitochondrial membrane potential.

The TMRE fluorescence intensity did not change in either Gpt2-null hippocampal neurons grown to 14 days in vitro or astrocytes. The mitochondrial footprint, the area occupied by the TMRE staining per cell remained the same as the wild-type controls as well.

We tested for oxidative stress in Gpt2-null hippocampal neurons and astrocytes by using MitoSOX and DHE. We observe increased fluorescence intensity of MitoSOX in Gpt2-null hippocampal neurons in vitro. This increase was not apparent in the DHE staining. Gpt2-null astrocytes did not show any differences in either MitoSOX or DHE. These results indicate that there may be an increase of ROS specifically localized in the mitochondria of Gpt2-null hippocampal neurons in vitro.

Discussion

We fail to see any changes in mitochondrial membrane potential as measured by TMRE in Gpt2-null hippocampal neurons or astrocytes. These results seem to align with the Seahorse Extracellular Flux Analyzer data where there were no major differences in basal or maximal respiration. Two cautionary notes: fluorescence intensity of TMRE alone is not a direct way of assessing the absolute potential (Gerencser et al., 2016) and these values belong to mitochondria confined to the neuron soma, the mitochondria in the processes might be affected differently. It is also possible to assess the shape and connectivity of the mitochondria in these cells by the TMRE staining; however the results can be unclear. Unless there is a more obvious abnormality in the image, it is difficult to conclude whether there is a pathological shape in mitochondria in these cells. Severe fragmentation may indicate damage, while fusion of mitochondria may also indicate damage and indicate a way in which mitochondria try to share the restricted amount of metabolites. Electron microscopy in vitro or in vivo may help address these questions more quantitatively.

There was a trending increase in non-mitochondrial oxygen consumption in the Gpt2-null hippocampal neurons and astrocytes as measured by Seahorse Extracellular Flux

Analyzer (Refer to Appendix to Chapter 3). This may result from oxidases or ROS that may or may not be in the mitochondria. The increased MitoSOX signal in Gpt2-null hippocampal neurons may be in agreement with the Seahorse findings, even though we fail to see an increase in astrocytes. It must be noted that both MitoSOX and DHE are poor indicators of superoxide anion specifically (Zielonka and Kalyanaraman, 2010) and must be regarded as indirect ways to look at ROS in culture.

Method

Cell Culture

Mouse primary hippocampal neuron culture. Hippocampal neurons were cultured as described previously (Ouyang et al., 2013): Hippocampi from P0-1 pup were dissected in Hank's Balanced Salt Solution (HBSS) (Gibco 14170-112) and placed in 500µl of 20U/ml papain (Worthington LK003176, in Earle's Balanced Salt Solution (EBSS), Worthington, LK003188). The tube with hippocampi/papain was incubated at 37ºC for 15 minutes. The tissue was triturated with 1ml pipette tip for 12 strokes. The tissue was further incubated at 37ºC for 15 minutes and triturated. The remaining bits of tissue sunk and the solution with dissociated cells was spun in a separate tube at 300g, 5 minutes, at RT. The cell pellet was dissolved gently in Inhibitor Solution (540µl EBSS, 60µl Ovomucoid Protease Inhibitor (Worthington Biochemical, LK003182), 30µl DNase (Worthington Biochemical, LK003170) per hippocampi) and filtered through a 70µm nylon mesh (FisherScientific, 22363548). The filtered cell suspension was layered on top of 1ml Ovomucoid Protease Inhibitor and spun at 70g, 10 minutes, at RT. The supernatant was discarded, and the cell pellet was resuspended in Neurobasal A+ (NeuroBasal A (10888022), 1X B27 Supplement (ThermoFisher Scientific, 17504044), 2

mM GlutaMAX (ThermoFisher Scientific, 35050061). The full media was changed the next day and then half media every 3 days.

Mouse primary astrocyte-enriched cultures. The culturing protocol was adapted from (Albuquerque et al., 2009; Schildge et al., 2013): Cortices from P0-1 pup were dissected in HBSS, diced into 6 pieces and transferred to a 15ml conical tube. The tissue is incubated in 0.25% Trypsin-EDTA in HBSS at 37ºC for 30 minutes. The solution is removed carefully to leave the tissue pieces at the bottom, 6ml Astrocyte Plating Medium (APM: DMEM (10569-010), 10% FBS (Invitrogen 16000044), 1% P/S (Invitrogen 15140122)) was added. The tissue is triturated for 15 strokes with 10ml pipette and then 5 strokes more with 1ml pipette. The cell suspension was filtered through 70 µm nylon mesh and seeded in a 25 cm^2-flask (Corning 3289). After 2 days, the full medium was changed, then every 3 days. When the astrocyte layer was confluent (~7 days), the flask was shaken at 225 rpm overnight at 37ºC. The full medium was changed to APM with 20 µM cytosine arabinoside (Ara-C) to remove any other contaminated proliferative cell types. After two days, the full medium was changed to APM. The Ara-C treatment was repeated the next day. Mild trypsin (0.0675%) treatment was used to lift off the astrocyte layer as a whole and leave the remaining microglia at the bottom of the flask. The layer was incubated in 1ml of Accutase (StemCellTechnologies, 07920) in a fresh tube at 37ºC for 10 minutes. The layer was dissociated with 1ml pipette tip with 5 strokes. 2 ml APM was added; the solution was mixed and filtered through a 70 µm nylon mesh.

Mitochondrial Membrane Potential and Footprint

Hippocampal neurons were seeded at a density of 90,000 cells/dish in single 35mm CellVis glass bottom dishes (Fisher Scientific, NC0794151) and allowed to grow for 14 days in

vitro. Astrocytes were seeded at a density of 30,000 cells/dish. Cells were incubated with tetramethylrhodamine, ethyl ester (TMRE) (Sigma, 87917), at working concentration of 500 nM along with 0.125 µM MitoTracker Green (Thermo Fisher, M7514) and 90 µM Hoechst (Thermo Fisher, H3570) for 20 min and live imaged using the 60x oil objective (refractive index immersion oil 1.526) and conventional light path (568 nm excitation) of the DeltaVision OMX SR microscope (GE Healthcare Life Sciences). Processing of binary-converted images was conducted using Mitochondrial Network Analysis toolkit (MiNA, macro code freely available on Github) (Valente et al., 2017) to ascertain fluorescence intensity of mitochondrial membranes and mitochondrial footprint (area covered by the staining per cell). The brightest plane was imaged.

Mitochondrial ROS Measurements

Hippocampal neurons and astrocytes were seeded as above. Cells were treated with 0.2 µM MitoSOX Red (Thermo Fisher, M26008), 0.125 µM MitoTracker Green, and 90 µM Hoechst at 37ºC, 5% CO_2 for 10 min. Cells were then live imaged using the 60X oil objective (refractive index immersion oil 1.526) and conventional light path of the DeltaVision OMX SR microscope (GE Healthcare Life Sciences). Mitochondrial superoxide levels were measured by fluorescence intensity of puncta using ImageJ. Staining and quantification of DHE (working concentration: 10 µM) was performed the same way as MitoSOX.

Figure Legends

Figure A.3.30 – Mitochondrial Membrane Potential as determined by TMRE Fluorescence in Gpt2-null hippocampal neurons and astrocytes in vitro.

A. TMRE (magenta) and MitoTracker Green staining in wild-type (top) and Gpt2-null (bottom) hippocampal neurons at 14 days in vitro. Mitochondrial footprint is measured as area covered by MitoTracker Green fluorescence per cell. Each dot on the graph represents an average of at least 10 cells of a primary culture obtained from a different mouse pup. Scale bar: 10 μm.

B. TMRE (magenta) and MitoTracker Green staining in wild-type (top) and Gpt2-null (bottom) astrocytes at 14 days in vitro. Mitochondrial footprint is measured as area covered by MitoTracker Green fluorescence per cell. Each dot on the graph represents an average of at least 10 cells of a primary culture obtained from a different mouse pup. Scale bar: 10 μm.

Figure A.3.31. MitoSOX and DHE staining in Gpt2-null hippocampal neurons and astrocytes in vitro.

A. MitoSOX (magenta) and MitoTracker Green staining in wild-type (top) and Gpt2-null (bottom) hippocampal neurons at 14 days in vitro. MitoSOX intensities were measured from circling puncta that overlapped with MitoTracker Green staining. Each dot on the graph represents an average of at least 10 cells of a primary culture obtained from a different mouse pup. Scale bar: 10 μm. *$P = 0.0346$.

B. MitoSOX (magenta) and MitoTracker Green staining in wild-type (top) and Gpt2-null (bottom) astrocytes. MitoSOX intensities were measured from circling puncta that overlapped with MitoTracker Green staining. Each dot on the graph represents an average of at least 10 cells of a primary culture obtained from a different mouse pup. Scale bar: 10 μm.

C. DHE staining in the nuclei of wild-type (left) and Gpt2-null (right) hippocampal neurons at 14 days in vitro. Each dot on the graph represents an average of at least 10 cells of a primary culture obtained from a different mouse pup. Scale bar: 10 μm.

D. DHE staining in the nuclei of wild-type (left) and Gpt2-null (right) astrocytes. Each dot on the graph represents an average of at least 10 cells of a primary culture obtained from a different mouse pup. Scale bar: 10 μm.

Figure A.3.32. TMRE fluorescence over time in astrocytes with FCCP in vitro.

A. Images of TMRE (top) and MitoTracker Green (bottom) fluorescence in wild-type astrocytes treated with 2 μM FCCP. Images are taken at 0, 20, 30, 40, 50, 60 minutes. Scale bar: 10 μm.

Albuquerque, C., Joseph, D.J., Choudhury, P., and MacDermott, A.B. (2009). Dissection, plating, and maintenance of cortical astrocyte cultures. Cold Spring Harb Protoc *2009*, pdb prot5273.
Gerencser, A.A., Mookerjee, S.A., Jastroch, M., and Brand, M.D. (2016). Measurement of the Absolute Magnitude and Time Courses of Mitochondrial Membrane Potential in Primary and Clonal Pancreatic Beta-Cells. PLoS One *11*, e0159199.
Ouyang, Q., Lizarraga, S.B., Schmidt, M., Yang, U., Gong, J., Ellisor, D., Kauer, J.A., and Morrow, E.M. (2013). Christianson syndrome protein NHE6 modulates TrkB endosomal signaling required for neuronal circuit development. Neuron *80*, 97-112.
Pendergrass, W., Wolf, N., and Poot, M. (2004). Efficacy of MitoTracker Green and CMXrosamine to measure changes in mitochondrial membrane potentials in living cells and tissues. Cytometry A *61*, 162-169.
Schildge, S., Bohrer, C., Beck, K., and Schachtrup, C. (2013). Isolation and culture of mouse cortical astrocytes. J Vis Exp.
Valente, A.J., Maddalena, L.A., Robb, E.L., Moradi, F., and Stuart, J.A. (2017). A simple ImageJ macro tool for analyzing mitochondrial network morphology in mammalian cell culture. Acta Histochem *119*, 315-326.
Zielonka, J., and Kalyanaraman, B. (2010). Hydroethidine- and MitoSOX-derived red fluorescence is not a reliable indicator of intracellular superoxide formation: another inconvenient truth. Free Radic Biol Med *48*, 983-1001.

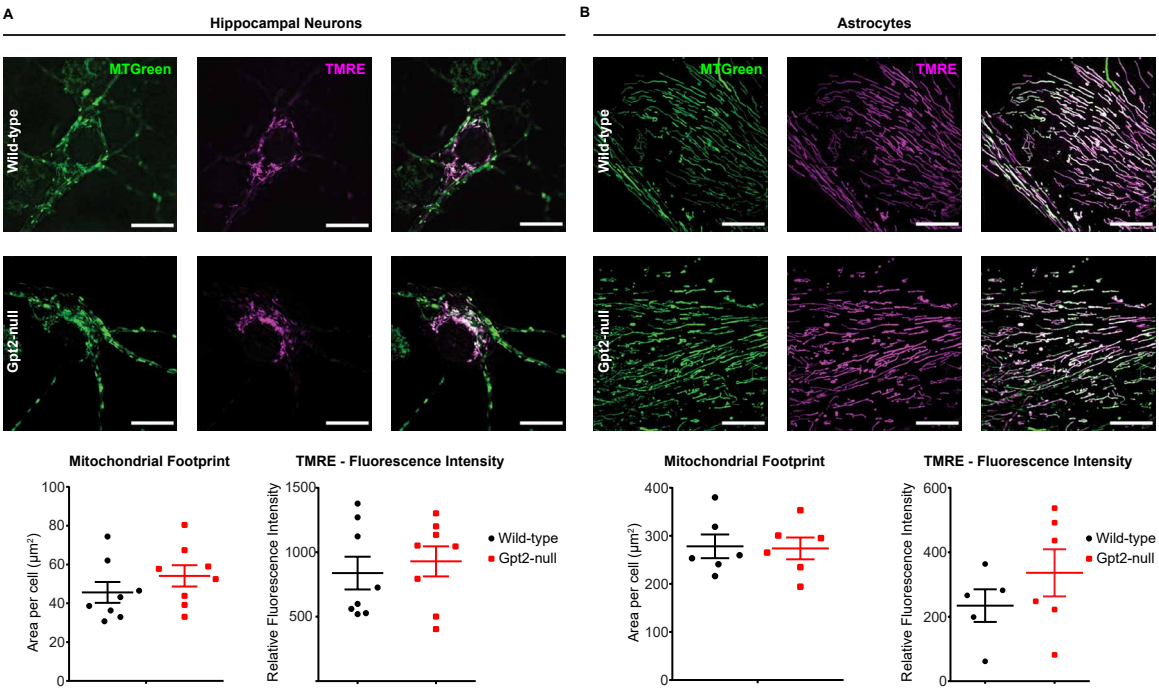

Figure A.3.30 – Mitochondrial Membrane Potential as determined by TMRE Fluorescence in Gpt2-null hippocampal neurons and astrocytes in vitro. A. TMRE (magenta) and MitoTracker Green staining in wild-type (top) and Gpt2-null (bottom) hippocampal neurons at 14 days in vitro. Mitochondrial footprint is measured as area covered by MitoTracker Green fluorescence per cell. Each dot on the graph represents an average of at least 10 cells of a primary culture obtained from a different mouse pup. Scale bar: 10 µm. B. TMRE (magenta) and MitoTracker Green staining in wild-type (top) and Gpt2-null (bottom) astrocytes at 14 days in vitro. Mitochondrial footprint is measured as area covered by MitoTracker Green fluorescence per cell. Each dot on the graph represents an average of at least 10 cells of a primary culture obtained from a different mouse pup. Scale bar: 10 µm.

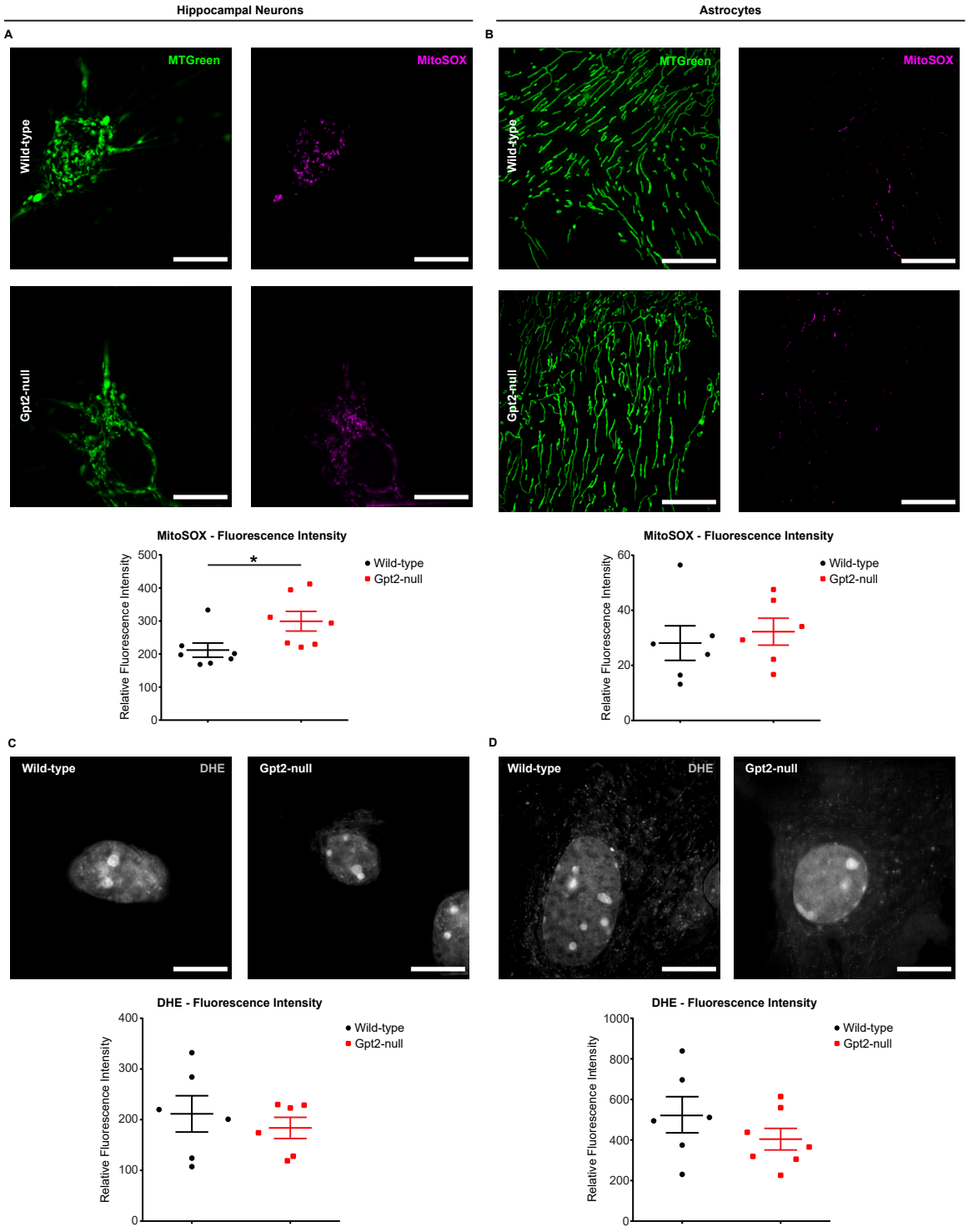

Figure A.3.31. MitoSOX and DHE staining in Gpt2-null hippocampal neurons and astrocytes in vitro.
A. MitoSOX (magenta) and MitoTracker Green staining in wild-type (top) and Gpt2-null (bottom) hippocampal neurons at 14 days in vitro. MitoSOX intensities were measured from circling puncta that overlapped with MitoTracker Green staining. Each dot on the graph represents an average of at least 10 cells of a primary culture obtained from a different mouse pup. Scale bar: 10 µm. *P = 0.0346. B. MitoSOX (magenta) and MitoTracker Green staining in wild-type (top) and Gpt2-null (bottom) astrocytes. MitoSOX intensities were measured from circling puncta that overlapped with MitoTracker Green staining. Each dot on the graph represents an average of at least 10 cells of a primary culture obtained from a different mouse pup. Scale bar: 10 µm. C. DHE staining in the nuclei of wild-type (left) and Gpt2-null (right) hippocampal neurons at 14 days in vitro. Each dot on the graph represents an average of at least 10 cells of a primary culture obtained from a different mouse pup. Scale bar: 10 µm. D. DHE staining in the nuclei of wild-type (left) and Gpt2-null (right) astrocytes. Each dot on the graph represents an average of at least 10 cells of a primary culture obtained from a different mouse pup. Scale bar: 10 µm.

A

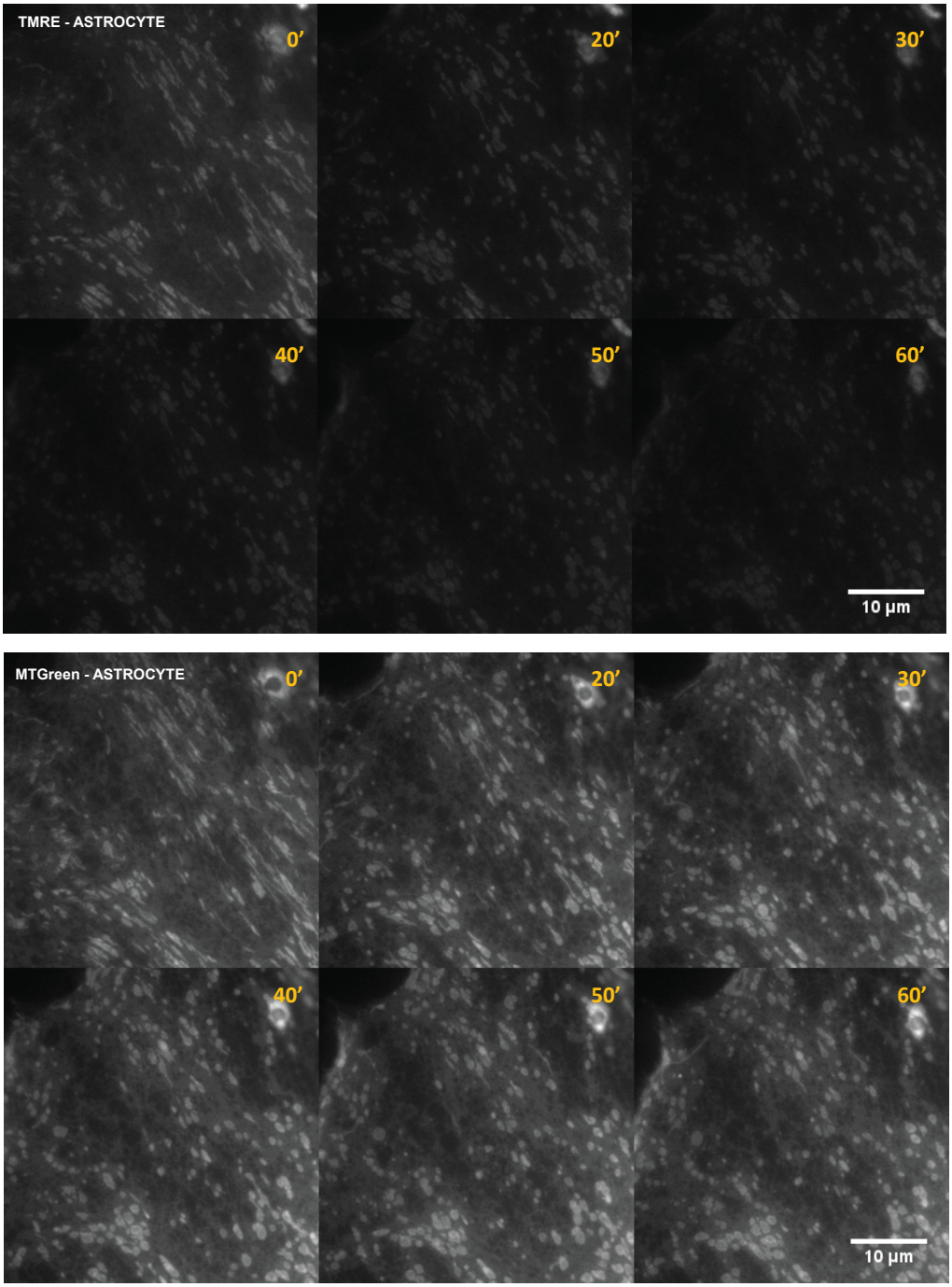

Figure A.3.32. TMRE fluorescence over time in astrocytes with FCCP in vitro. A. Images of TMRE (top) and MitoTracker Green (bottom) fluorescence in wild-type astrocytes treated with 2 µM FCCP. Images are taken at 0, 20, 30, 40, 50, 60 minutes. Scale bar: 10 µm.

Appendix 3.14. Mitochondrial respiration using Seahorse Extracellular Flux Analyzer in Gpt2-null hippocampal neurons and astrocytes.

Introduction

Gpt2 links metabolism of pyruvate, the end product of glycolysis to the TCA cycle and amino acid metabolism. Gpt2 is an anaplerotic enzyme meaning that the reaction Gpt2 catalyzes will result in a net production of a TCA cycle intermediate. Given the influence of Gpt2 on the TCA cycle, we set out to test whether there are any alterations in mitochondrial respiration or glycolysis in Gpt2-null hippocampal neurons and astrocytes in vitro, which may partly contribute to the neurodevelopmental phenotype in Gpt2-null mice and humans. We addressed this question by using the Seahorse Extracellular Flux Analyzer that employs a real-time fluorescence-based detection of oxygen and proton levels. Oxygen consumption rate (OCR) and extracellular acidification rate (ECAR) can be sued to assess oxidative phosphorylation and glycolysis, respectively. We hypothesized that there would be defects in respiration or glycolytic activity at baseline or with additional metabolic stress in Gpt2-null hippocampal neurons and astrocytes in vitro. Metabolic assays tested in this study include Mito Stress Test, Mito Stress Test with inhibition of glutaminase, mitochondrial pyruvate carrier or carnitine palmitoyltransferase, KCl depolarization, Flex Fuel Test and Glycolysis Stress Test.

Key Points

- Respiratory Control Ratio (maximal respiration divided by proton leak) is increased in the Gpt2-null hippocampal neurons in vitro.

- Spare respiratory capacity after glutaminase inhibition is decreased in Gpt2-null hippocampal neurons in vitro.
- Increase in extracellular acidification rate is delayed in response to UK5099 in Gpt2-null hippocampal neurons in vitro.
- Glycolytic reserve is increased in Gpt2-null hippocampal neurons in vitro.
- Gpt2-null astrocytes do not show abnormalities in any of the metrics obtained expect for a slightly increased non-mitochondrial oxygen consumption in vitro.

Results

To determine the extent to which mitochondrial respiration and extracellular acidification rely on Gpt2, we performed various respiration assays in cultured hippocampal neurons and astrocytes using Seahorse Extracellular Flux Analyzer. Mito Stress Test inhibits components of the electron transport chain to expose various metrics of mitochondrial respiration by sequentially injecting inhibitory compounds. Overall oxygen consumption rates (OCR) in Gpt2-null hippocampal neurons grown to 14 days in vitro were unchanged over the course of the assay. The extracellular acidification rates (ECAR) in Gpt2-null neurons were slightly elevated at baseline and when oligomycin was added. Various parameters of the Mito Stress Test including basal respiration, maximal respiration, spare respiratory capacity, ATP production, coupling efficiency, proton leak and non-mitochondrial oxygen consumption were unchanged in Gp2-null hippocampal neurons. There were slight trending increases in maximal respiration and in non-mitochondrial oxygen consumption as well as trending decreases in proton leak although these did not

reach statistical significance. However, there was a significant increase in respiratory control ratio (maximal respiration divided by proton leak) in Gpt2-null hippocampal neurons. In astrocytes, no changes were observed expect an increased non-mitochondrial oxygen consumption. In both cell types, OCR to ECAR ratios were unchanged.

Gpt2 confers to the cell a pathway to replenish as the TCA cycle intermediates with the loss of Gpt2 the cell may not be able to sustain itself at times of high ATP demand. We tested if depolarization of neurons by KCl, a process that increases respiration to produce the ATP needed, would expose any vulnerabilities of Gpt2-null hippocampal neurons. We do not find any differences in either percent increase of OCR or ECAR following depolarization suggesting that Gpt2-null hippocampal neurons respire the same amount as wild-type controls after induction of neuronal firing.

Gpt2 provides one of the ways in which glutamate oxidation fuels the TCA cycle and therefore provides substrates for oxidative phosphorylation. We hypothesized that if various fuel sources are prevented from contributing to substrate pool for oxidative phosphorylation. Gpt2-null cells would present with reduced mitochondrial respiration and possible other defects associated thereof. When we inhibited pyruvate entry into mitochondria using UK5099, a potent inhibitor of mitochondrial pyruvate carrier (MPC), we did not observe any changes in the various metrics of mitochondrial respiration in Gpt2-null hippocampal neurons or astrocytes. It is of note that both wild-type and Gpt2-null maximal respiration in hippocampal neurons is severely affected in UK5099 compared to astrocytes. The acute response to UK5099 in neurons was also greater compared to astrocytes suggesting a general susceptibility to alterations of pyruvate entry into mitochondria in neurons.

When we inhibited glutaminase which converts glutamine into glutamate in the mitochondria, Gpt2-null hippocampal neurons displayed decreased spare respiratory capacity and spare respiratory capacity expressed as percentage of basal respiration. Even though it is a slight decrease (~10%), this change in Gpt2-null hipoocampal neurons may suggest that glutamine may not be able to contribute to the maximal respiration that mitochondria can attain. Gpt2-null astrocytes did not display and differences compared to their wild-type controls.

We were also able to perform Mito Stress Test in the presence of etomoxir, an inhibitor of mitochondrial carnitine palmitoyltransferase in wild-type and Gpt2-null astrocytes. We do not observe any changes in any of the mitochondrial respiration in Gpt2-null astrocytes. Overall the results suggest that Gp2-null hippocampal neurons ay have mitochondrial respiration deficits with glutaminase inhibition but Gpt2-null astrocytes do not show major abnormalities in any of the metrics of the Mito Stress Test with or without inhibition of the glucose, glutamine or fatty acid pathways.

We also performed Flex Fuel Test where the extent to which the cells depend on or can utilize the three metabolic pathways of glucose, glutamine and fatty acids is tested. We do not observe any differences in fuel dependency or capacity of the three metabolic pathways between wild-type and Gpt2-null hippocampal neurons or astrocytes. However, we observed a delayed increase of ECAR in response to UK5099 in Gpt2-null hippocampal neurons but not astrocytes. This trend was observed regardless of whether UK5099 was administered alone or in combination with Etomoxir or BPTES. These results suggest that Gpt2-null neurons did not respond to blockage of pyruvate entry into the mitochondria as fast their wild-type controls.

Given the slow response to UK5099 in neurons, we performed Glycolysis Stress Test on Gpt2-null hippocampal neurons and astrocytes. Glycolysis Stress Test measures how well the cells can respire without glucose and how much they can increase glycolytic activity to meet high ATP demand. The glycolytic reserve in Gpt2-null hippocampal neurons was profoundly increased compared to their wild-type controls. While there were trending decreases in glycolysis and trending increases in glycolytic capacity in Gpt2-null hippocampal neurons, they did not reach statistical significance. Accordingly, the OCR to ECAR ratio had trending decreases in Gpt2-null neurons, particularly after oligomycin injection. Astrocytes, however, did not show any differences in any of the Glycolysis Stress Test metrics. These results suggest that Gpt2-null hippocampal neurons have altered regulation of glycolysis. This is in agreement with profound increases of glycolytic intermediates in Gpt2-null hippocampus at P18 in vivo.

An increased glycolytic reserve may result from increased glycolytic enzyme content or increased glucose uptake. We tested for uptake of 2-NBDG (a fluorescent analog of glucose) in Gpt2-null hippocampal neurons and astrocytes in vitro and did not find any differences. There were no increased glycolytic enzyme content n Gpt2-null hippocampus in vivo. These results suggest that the altered regulation of glycolysis in Gpt2-null neurons is not caused by changes in glycolytic enzyme content or glucose uptake.

Discussion

Gpt2 loss did not lead to major respiration deficits in either hippocampal neurons or astrocytes in vitro. This is likely due to other metabolic enzymes present in the cell supporting the TCA cycle such as pyruvate dehydrogenase, glutamate dehydrogenase and

pyruvate carboxylase (expressed mainly in astrocytes). Given the TCA cycle deficits seen in multiple contexts including mouse embryonic fibroblasts, hippocampal neurons in vitro and brain tissues, we expected altered mitochondrial respiration and glycolytic activity. Paradoxically, however, Gpt2-null neurons exhibited higher respiratory control ratio in which decreases may indicate mitochondrial dysfunction. The nature of the dysfunction may include multiple factors such as deficits in electron transport chain enzymes, substrate oxidation and transporters, substrate availability and dysregulated mechanisms that act on proton leak. It is of importance that the OCR response to FCCP decline immediately after maximal OCR response which may mean either FCCP concentration was too high or our culture system in the media tested are respiring at an already high rate so that the spare capacity is reduced promptly. There were trending increases in maximal respiration (and in spare respiratory capacity) and trending decreases in proton leak in Gpt2-null hippocampal neurons and the resulting increase in respiratory control ratio was statistically significant. While it is unclear which factor is more prominently affecting this result, Gpt2-null neurons clearly showed normal respiration if not apparently better maximal respiration.

Gpt2-null neurons also displayed higher glycolytic reserve and a slow ECAR response to UK5099. We do not see changes in glucose uptake in Gpt2-null hippocampal neurons or greater glycolytic enzyme content in Gpt2-null hippocampus in vivo. Along with these data, the observation that the delayed ECAR response to acute application of UK5099 occurs within ten minutes and the response eventually catches up to the wild-type levels suggest that this altered regulation is at the substrate level. While the reasons are unclear, it is possible that pyruvate levels in Gpt2-null mitochondria may be elevated and may

allow keeping the glycolytic activity in the reserve and delay the increases in ECAR. This may happen particularly because Gpt2 is predicted to catalyze in the direction of alanine and alpha-ketoglutarate production. More studies are warranted to determine changes in the mitochondrial metabolome of Gpt2-null cells.

There was a slight, albeit statistically significant, decrease in spare respiratory capacity in Gpt2-null hippocampal neurons when glutaminase is inhibited. While the effect is not great, glutaminase inhibition may rob the Gpt2-null cells of the glutamate pool that may otherwise enter the TCA cycle. In the Flex Fuel Test, however, glutaminase inhibition affects mitochondrial respiration only slightly, if at all, whereas UK5099 has a profound effect on both wild-type and Gpt2-null hippocampal neurons meaning that glutamine may not play as a big role as glucose in mitochondrial respiration in neurons in the conditions tested.

It is noteworthy that Gpt2-null astrocytes do not show any differences in mitochondrial respiration or glycolytic activity. This is possibly due to the fact that Gpt1, the cytosolic paralog of Gpt2, is more abundantly expressed in mouse astrocytes than in neurons. There was a significant increase in non-mitochondrial oxygen consumption in Gpt2-null astrocytes. Non-mitochondrial oxygen consumption has been attributed to oxidative stress and plasma membrane oxidases such as NAPDH oxidase. While none of the other respiration metrics showed any differences, increased non-mitochondrial oxygen consumption could be due to changes in a metabolic pathway related to Gpt2 that is unexplored in astrocytes.

Method

Cell Culture

Mouse primary hippocampal neuron culture. Hippocampal neurons were cultured as described previously (Ouyang et al., 2013): Hippocampi from P0-1 pup were dissected in Hank's Balanced Salt Solution (HBSS) (Gibco 14170-112) and placed in 500µl of 20U/ml papain (Worthington LK003176, in Earle's Balanced Salt Solution (EBSS), Worthington, LK003188). The tube with hippocampi/papain was incubated at 37ºC for 15 minutes. The tissue was triturated with 1ml pipette tip for 12 strokes. The tissue was further incubated at 37ºC for 15 minutes and triturated. The remaining bits of tissue sunk and the solution with dissociated cells was spun in a separate tube at 300g, 5 minutes, at RT. The cell pellet was dissolved gently in Inhibitor Solution (540µl EBSS, 60µl Ovomucoid Protease Inhibitor (Worthington Biochemical, LK003182), 30µl DNase (Worthington Biochemical, LK003170) per hippocampi) and filtered through a 70µm nylon mesh (FisherScientific, 22363548). The filtered cell suspension was layered on top of 1ml Ovomucoid Protease Inhibitor and spun at 70g, 10 minutes, at RT. The supernatant was discarded, and the cell pellet was resuspended in Neurobasal A+ (NeuroBasal A (10888022), 1X B27 Supplement (ThermoFisher Scientific, 17504044), 2mM GlutaMAX (ThermoFisher Scientific, 35050061). The full media was changed the next day and then half media every 3 days.

Mouse primary astrocyte-enriched cultures. The culturing protocol was adapted from (Schildge et al., 2013, Albuquerque et al., 2009): Cortices from P0-1 pup were dissected in HBSS, diced into 6 pieces and transferred to a 15ml conical tube. The tissue is incubated in 0.25% Trypsin-EDTA in HBSS at 37ºC for 30 minutes. The solution is removed carefully to leave the tissue pieces at the bottom, 6ml Astrocyte Plating Medium

(APM: DMEM (10569-010), 10% FBS (Invitrogen 16000044), 1% P/S (Invitrogen 15140122)) was added. The tissue is triturated for 15 strokes with 10ml pipette and then 5 strokes more with 1ml pipette. The cell suspension was filtered through 70µm nylon mesh and seeded in a 25cm^2-flask (Corning 3289). After 2 days, the full medium was changed, then every 3 days. When the astrocyte layer was confluent (~7 days), the flask was shaken at 225 rpm overnight at 37ºC. The full medium was changed to APM with 20µM cytosine arabinoside (Ara-C) to remove any other contaminated proliferative cell types. After two days, the full medium was changed to APM. The Ara-C treatment was repeated the next day. Mild trypsin (0.0675%) treatment was used to lift off the astrocyte layer as a whole and leave the remaining microglia at the bottom of the flask. The layer was incubated in 1ml of Accutase (StemCellTechnologies, 07920) in a fresh tube at 37ºC for 10 minutes. The layer was dissociated with 1ml pipette tip with 5 strokes. 2ml APM was added; the solution was mixed and filtered through a 70µm nylon mesh.

Mitochondrial Respiration Assays

Mouse hippocampal neurons were seeded at a density of 90,000 cells/well in Seahorse XF24 V7 PS Cell Culture Microplates (Seahorse Biosciences, 100777-004) and allowed to grow in Neurobasal A+ medium for 14 days at 37ºC in a 5% CO_2 humidified atmosphere. Astrocytes were seeded at a density of 25,000 cells/well before the day of the assay. On the day of the assay, cells were subsequently washed with DMEM XF assay medium at pH 7.4 (Seahorse Biosciences, 103575-100) supplemented with 10 mM glucose (Seahorse Biosciences, 103577-100), 2 mM glutamine (Seahorse Biosciences, 103579-100), and 1 mM sodium pyruvate (Seahorse Biosciences, S8636) and incubated for 1 hour at 37ºC in a

non-CO_2 incubator for all assays except Glycolysis Stress Test which excludes glucose and pyruvate from the medium. Oxygen consumption rate (OCR) and extracellular acidification rate (ECAR) were subsequently measured using Seahorse Extracellular Flux (Seahorse Biosciences, XFe24) analyzer. For Mito Stress test, final concentrations of 1 μM oligomycin (Sigma, 75351), 2 μM FCCP (Sigma, C2920), 0.5 μM antimycin A (Sigma, A8674), and 0.5 μM rotenone (Sigma, R8875) were loaded into the injection ports in the XFe24 sensor cartridge in sequence. For Mito Stress Test with blocked pyruvate entry into mitochondria, 2 μM UK5099 (Cayman, 16980) was injected before oligomycin followed by FCCP, rotenone and antimycin A. For Mito Stress Test with glutaminase inhibition, 3 μM BPTES (Cayman, 19284) was injected before oligomycin followed by FCCP, rotenone and antimycin A. For Mito Stress Test with blocked palmitate entry into mitochondria, 4 μM Etomoxir (Cayman, 11969-5) was injected before oligomycin followed by FCCP, rotenone and antimycin A. For Glycolysis Stress Test, 10 mM glucose was injected followed by oligomycin and 50 mM 2-deoxy-glucose (Cayman, 14325). For Flex Fuel Test for the glucose pathway (dependency), UK5099 injection was followed by Etomoxir/BPTES. Glucose pathway (capacity): Etomoxir/BPTES + UK5099. Glutamine pathway (dependency): BPTES + Etomoxir/UK5099. Glutamine pathway (capacity): Etomoxir/UK5099 + BPTES. Fatty acid pathway (dependency): Etomoxir + BPTES/UK5099. Fatty acid pathway (capacity): BPTES/UK5099 + Etomoxir. For depolarization, a final concentration of 50 mM KCl was added to the wells and the percent increase in OCR was calculated by dividing the last measurement before injection to the one immediately after KCl injection.

Mito Stress Test Assay parameters were calculated automatically using Wave software (Seahorse Biosciences). The parameters are calculated as follows: Non-mitochondrial oxygen consumption: Minimum rate measurement after Rot/AA injection. Basal respiration: (last rate measurement before first injection) – (non-mitochondrial oxygen consumption). Maximal Respiration: (Maximum rate measurement after FCCP injection) – (non-mitochondrial oxygen consumption). Proton leak: (Minimum rate measurement after oligomycin injection) – (non-mitochondrial oxygen consumption). ATP Production: (Last rate measurement after oligomycin injection) – (minimum rate measurement after oligomycin injection). Spare Respiratory Capacity: (Maximal respiration) – (Basal respiration). Spare Respiratory Capacity as a %: (Maximal Respiration) / (Basal Respiration) x 100. Acute Response to BPTES, UK5099 or Etomoxir: (Last rate measurement before oligomycin injection) – (Last rate measurement before acute injection). Coupling efficiency: ATP Production / Basal respiration x 100.

Glycolysis Stress Test Assay parameters were calculated automatically using Wave software (Seahorse Biosciences). The parameters are calculated as follows: Glycolysis: (Maximum rate measurement before oligomycin injection) – (Last rate measurement before glucose injection). Glycolytic capacity: (Maximum rate measurement after oligomycin injection) – (last rate measurement before glucose injection). Glycolytic Reserve: Glycolytic capacity – glycolysis. Glycolytic Reserve as a %: Glycolytic Capacity / Glycolysis x 100. Non-glycolytic acidification: last rate measurement before glucose injection.

Following the assay, cells were rinsed gently with 1X PBS and fixed in 4% (w/v) paraformaldehyde for 10 min, after which they were washed twice for 5 min each wash

with 1X PBS at room temperature. Nuclei were counterstained using 300 nM DAPI for 5 min at room temperature, and cells were subsequently washed thrice with 1X PBS for 5 min per wash. Cell density per well was measured using the Cytation 5 Plate Reader (Biotek Instruments, Winooski, VT) by imaging wells at 405nm and measures of respiration were normalized to cell density per well.

Figure Legends

Figure A 3.33. Seahorse Mito Stress Test in Gpt2-null hippocampal neurons and astrocytes.

A. Oxygen consumption (OCR) and extracellular acidification rates (ECAR) measured at baseline and after sequential injections of oligomycin (Oligo), FCCP, rotenone and antimycin A (Rot/AA) in wild-type (black) and Gpt2-null (red) hippocampal neurons at 14 days in vitro. OCR and ECAR values were normalized to cell count and expressed as pmol per minute per 1,000 cells. n=6 litters. **$0.001<P<0.01$, *$0.01<P<0.05$.

B. Mitochondrial respiration parameters obtained from Mito Stress Test in wild-type (black) and Gpt2-null (red) hippocampal neurons at 14 days in vitro. Baseline OCR/ECAR ratio was calculated using the last baseline measurement. *$0.01<P<0.05$.

C. Oxygen consumption (OCR) and extracellular acidification rates (ECAR) measured at baseline and after sequential injections of oligomycin (Oligo), FCCP, rotenone and antimycin A (Rot/AA) in wild-type (black) and Gpt2-null (red) astrocytes in vitro. OCR and ECAR values were normalized to cell count and expressed as pmol per minute per 1,000 cells. n=5 litters.

D. Mitochondrial respiration parameters obtained from Mito Stress Test in wild-type (black) and Gpt2-null (red) astrocytes. Baseline OCR/ECAR ratio was calculated using the last baseline measurement. *$0.01<P<0.05$.

Figure A 3.34. Seahorse Glyco Stress Test in Gpt2-null hippocampal neurons and astrocytes.

A. Oxygen consumption (OCR) and extracellular acidification rates (ECAR) measured at baseline and after sequential injections of glucose, oligomycin (Oligo), 2-deoxyglucose (2-DG) in wild-type (black) and Gpt2-null (red) hippocampal neurons at 14 days in vitro. OCR and ECAR values were normalized to cell count and expressed as pmol per minute per 1,000 cells. n=6-7 litters.

B. Mitochondrial respiration parameters obtained from Glyco Stress Test in wild-type (black) and Gpt2-null (red) hippocampal neurons at 14 days in vitro. Baseline OCR/ECAR ratio was calculated using the last measurement of each epoch.**$0.001<P<0.01$, *$0.01<P<0.05$.

C. Oxygen consumption (OCR) and extracellular acidification rates (ECAR) measured at baseline and after sequential injections of glucose, oligomycin (Oligo), 2-deoxyglucose (2-DG) in wild-type (black) and Gpt2-null (red) astrocytes in vitro. OCR and ECAR values were normalized to cell count and expressed as pmol per minute per 1,000 cells. n=5 litters.

D. Mitochondrial respiration parameters obtained from Mito Stress Test in wild-type (black) and Gpt2-null (red) astrocytes. Baseline OCR/ECAR ratio was calculated using the last measurement of each epoch. *$0.01<P<0.05$.

Figure 3 A 3.35. Seahorse Mito Stress Test with UK5099 in Gpt2-null hippocampal neurons and astrocytes.

A. Oxygen consumption (OCR) and extracellular acidification rates (ECAR) measured at baseline and after sequential injections of UK5099, oligomycin (Oligo), FCCP, rotenone and antimycin A (Rot/AA) in wild-type (black) and Gpt2-null (red) hippocampal neurons at 14 days in vitro. OCR and ECAR values were normalized to cell count and expressed as pmol per minute per 1,000 cells. n=3 litters.

B. Mitochondrial respiration parameters obtained from Mito Stress Test with UK5099 in wild-type (black) and Gpt2-null (red) hippocampal neurons at 14 days in vitro.

C. Oxygen consumption (OCR) and extracellular acidification rates (ECAR) measured at baseline and after sequential injections of UK5099, oligomycin (Oligo), FCCP, rotenone and antimycin A (Rot/AA) in wild-type (black) and Gpt2-null (red) astrocytes in vitro. OCR and ECAR values were normalized to cell count and expressed as pmol per minute per 1,000 cells. n=5 litters.

D. Mitochondrial respiration parameters obtained from Mito Stress Test with UK5099 in wild-type (black) and Gpt2-null (red) astrocytes.

Figure A 3.36. Seahorse Mito Stress Test with BPTES in Gpt2-null hippocampal neurons and astrocytes.

A. Oxygen consumption (OCR) and extracellular acidification rates (ECAR) measured at baseline and after sequential injections of BPTES, oligomycin (Oligo), FCCP, rotenone and antimycin A (Rot/AA) in wild-type (black) and Gpt2-null (red) hippocampal neurons

at 14 days in vitro. OCR and ECAR values were normalized to cell count and expressed as pmol per minute per 1,000 cells. n=4 litters.

B. Mitochondrial respiration parameters obtained from Mito Stress Test with BPTES in wild-type (black) and Gpt2-null (red) hippocampal neurons at 14 days in vitro. *0.01<*P*<0.05.

C. Oxygen consumption (OCR) and extracellular acidification rates (ECAR) measured at baseline and after sequential injections of BPTES, oligomycin (Oligo), FCCP, rotenone and antimycin A (Rot/AA) in wild-type (black) and Gpt2-null (red) astrocytes in vitro. OCR and ECAR values were normalized to cell count and expressed as pmol per minute per 1,000 cells. n=4 litters.

D. Mitochondrial respiration parameters obtained from Mito Stress Test with BPTES in wild-type (black) and Gpt2-null (red) astrocytes.

Figure A 3.37. Seahorse Mito Stress Test with Etomoxir in Gpt2-null astrocytes.

A. Oxygen consumption (OCR) and extracellular acidification rates (ECAR) measured at baseline and after sequential injections of Etomoxir (Eto), oligomycin (Oligo), FCCP, rotenone and antimycin A (Rot/AA) in wild-type (black) and Gpt2-null (red) astrocytes in vitro. OCR and ECAR values were normalized to cell count and expressed as pmol per minute per 1,000 cells. n=3 litters.

B. Mitochondrial respiration parameters obtained from Mito Stress Test with Etomoxir in wild-type (black) and Gpt2-null (red) astrocytes.

Figure A 3.38. Seahorse Flex Fuel Test in Gpt2-null hippocampal neurons and astrocytes.

A. Dependency (top) and capacity (bottom) of the Glucose pathway in wild-type (black, green) and Gpt2-null (red, magenta) hippocampal neurons at 14 days in vitro (left) and astrocytes (right) *in vitro*. To determine dependency on the glucose pathway, UK5099 was injected alone, followed by ETO and BPTES. To determine capacity of the glucose pathway, first ETO and BPTES were injected, followed by UK5099. OCR and ECAR values were expressed as percentage of the last baseline measurement n=6-8 litters. *0.01<*P*<0.05.

B. Dependency (top) and capacity (bottom) of the Glutamine pathway in wild-type (black, green) and Gpt2-null (red, magenta) hippocampal neurons at 14 days in vitro (left) and astrocytes (right) *in vitro*. To determine dependency on the glutamine pathway, BPTES was injected alone, followed by ETO and UK5099. To determine capacity of the glutamine pathway, ETO and UK5099 were injected, followed by BPTES. OCR and ECAR values were expressed as percentage of the last baseline measurement n=6-8 litters. *0.01<*P*<0.05.

C. Dependency (top) and capacity (bottom) of the Fatty Acid pathway in wild-type (black, green) and Gpt2-null (red, magenta) hippocampal neurons at 14 days in vitro (left) and astrocytes (right) *in vitro*. To determine dependency on the glucose pathway, ETO was injected alone, followed by UK5099 and BPTES. To determine capacity of the glucose pathway, UK5099 and BPTES were injected, followed by ETO. OCR and ECAR values were expressed as percentage of the last baseline measurement n=5-8 litters. *0.01<*P*<0.05.

Figure A 3.39. Aggregate dependency and capacity values of Seahorse Flex Fuel Test in Gpt2-null hippocampal neurons and astrocytes.

A. The three metabolic pathways tested in the Seahorse Flex Fuel Test. The glucose pathway is probed by preventing pyruvate entry into mitochondria with the inhibition of the mitochondrial pyruvate carrier (MPC) by UK5099. The glutamine pathway is probed by preventing the conversion of glutamine into glutamate (glu) with the inhibition of glutaminase (GLS) by BPTES. The fatty acid pathway is probed by preventing the palmitate entry into mitochondria with the inhibition of carnitine palmitoyltransferase 1 (CPT1) by Etomoxir (ETO). The GPT2 reaction is shown next to the tricarboxylic acid (TCA) cycle with the primary reaction metabolites, alpha-ketoglutarate, alanine (ala), glutamate (glu) and pyruvate (pyr).

B. Dependency and capacity of the three metabolic pathways in wild-type (black) and Gpt2-null (red) hippocampal neurons (top) at 14 days in vitro and astrocytes (bottom) *in vitro*. For detailed calculations, refer to Methods. n=6-8 litters.

Figure A 3.40. Oxygen consumption after depolarization with KCl in Gpt2-null hippocampal neurons.

A. Oxygen consumption (OCR, left) and extracellular acidification (ECAR, right) rates after KCL depolarization in wild-type (black) and Gpt2-null (red) hippocampal neurons at 14 days in vitro. OCR and ECAR values measured immediately after the addition of 50 mM KCl were divided by the last baseline measurement and expressed as a percentage.

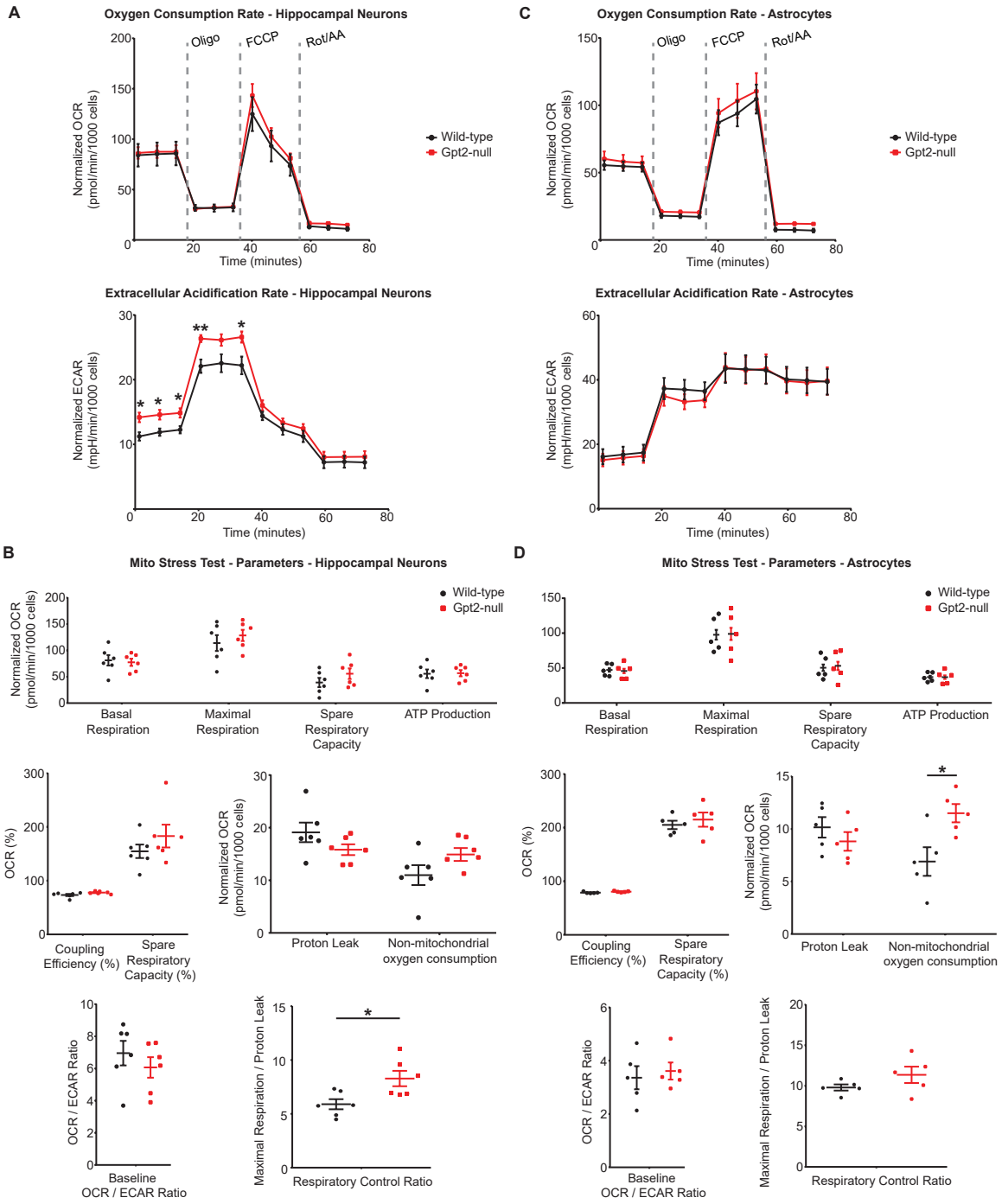

Figure A 3.33. Seahorse Mito Stress Test in Gpt2-null hippocampal neurons and astrocytes.
A. Oxygen consumption (OCR) and extracellular acidification rates (ECAR) measured at baseline and after sequential injections of oligomycin (Oligo), FCCP, rotenone and antimycin A (Rot/AA) in wild-type (black) and Gpt2-null (red) hippocampal neurons at 14 days in vitro. OCR and ECAR values were normalized to cell count and expressed as pmol per minute per 1,000 cells. n=6 litters. **0.001<P<0.01, *0.01<P<0.05. B. Mitochondrial respiration parameters obtained from Mito Stress Test in wild-type (black) and Gpt2-null (red) hippocampal neurons at 14 days in vitro. Baseline OCR/ECAR ratio was calculated using the last baseline measurement. *0.01<P<0.05. C. Oxygen consumption (OCR) and extracellular acidification rates (ECAR) measured at baseline and after sequential injections of oligomycin (Oligo), FCCP, rotenone and antimycin A (Rot/AA) in wild-type (black) and Gpt2-null (red) astrocytes in vitro. OCR and ECAR values were normalized to cell count and expressed as pmol per minute per 1,000 cells. n=5 litters. D. Mitochondrial respiration parameters obtained from Mito Stress Test in wild-type (black) and Gpt2-null (red) astrocytes. Baseline OCR/ECAR ratio was calculated using the last baseline measurement. *0.01<P<0.05.

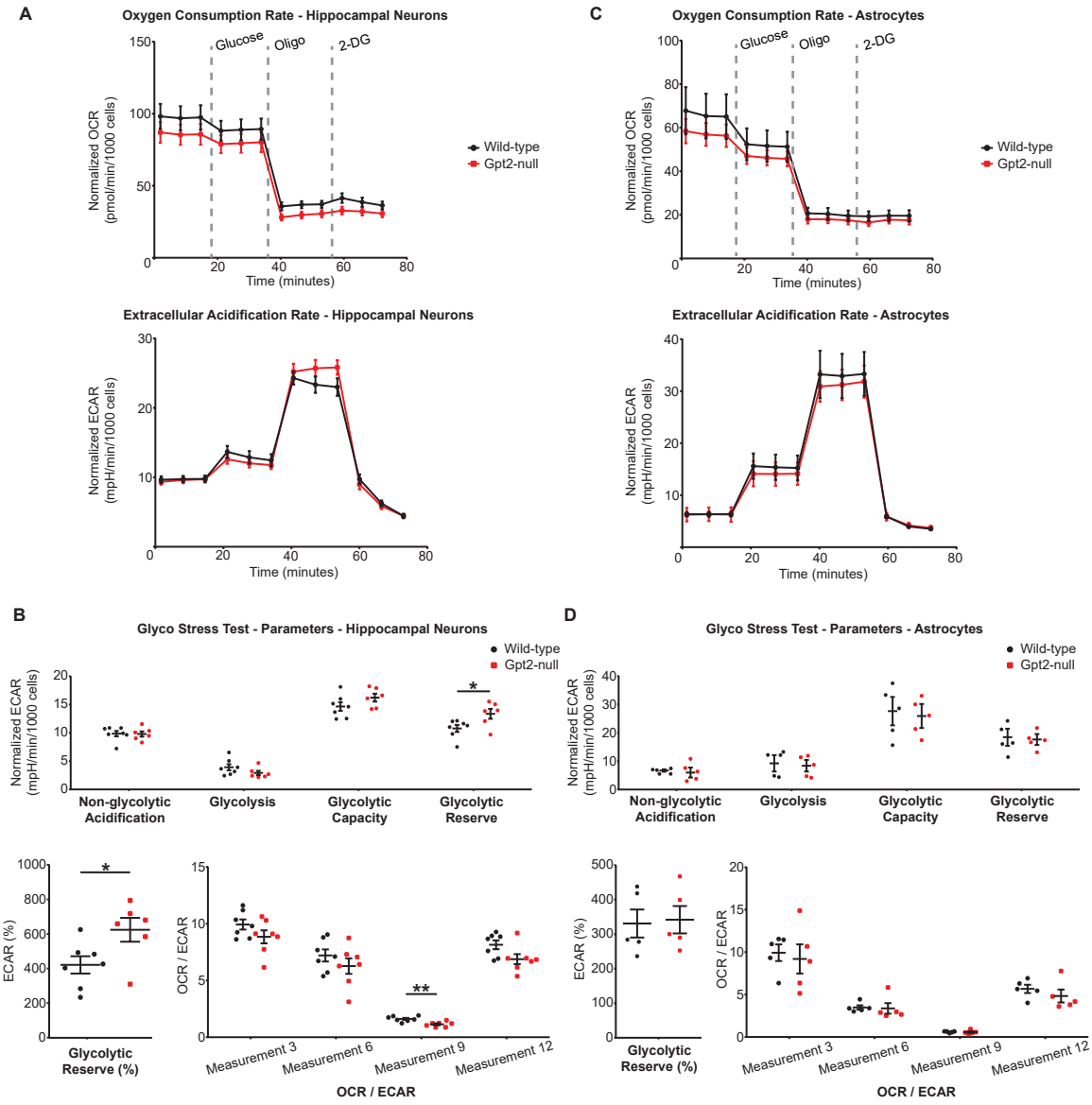

Figure A 3.34. Seahorse Glyco Stress Test in Gpt2-null hippocampal neurons and astrocytes. A. Oxygen consumption (OCR) and extracellular acidification rates (ECAR) measured at baseline and after sequential injections of glucose, oligomycin (Oligo), 2-deoxyglucose (2-DG) in wild-type (black) and Gpt2-null (red) hippocampal neurons at 14 days in vitro. OCR and ECAR values were normalized to cell count and expressed as pmol per minute per 1,000 cells. n=6-7 litters. B. Mitochondrial respiration parameters obtained from Glyco Stress Test in wild-type (black) and Gpt2-null (red) hippocampal neurons at 14 days in vitro. Baseline OCR/ECAR ratio was calculated using the last measurement of each epoch.**0.001<P<0.01, *0.01<P<0.05. C. Oxygen consumption (OCR) and extracellular acidification rates (ECAR) measured at baseline and after sequential injections of glucose, oligomycin (Oligo), 2-deoxyglucose (2-DG) in wild-type (black) and Gpt2-null (red) astrocytes in vitro. OCR and ECAR values were normalized to cell count and expressed as pmol per minute per 1,000 cells. n=5 litters. D. Mitochondrial respiration parameters obtained from Mito Stress Test in wild-type (black) and Gpt2-null (red) astrocytes. Baseline OCR/ECAR ratio was calculated using the last measurement of each epoch. *0.01<P<0.05.

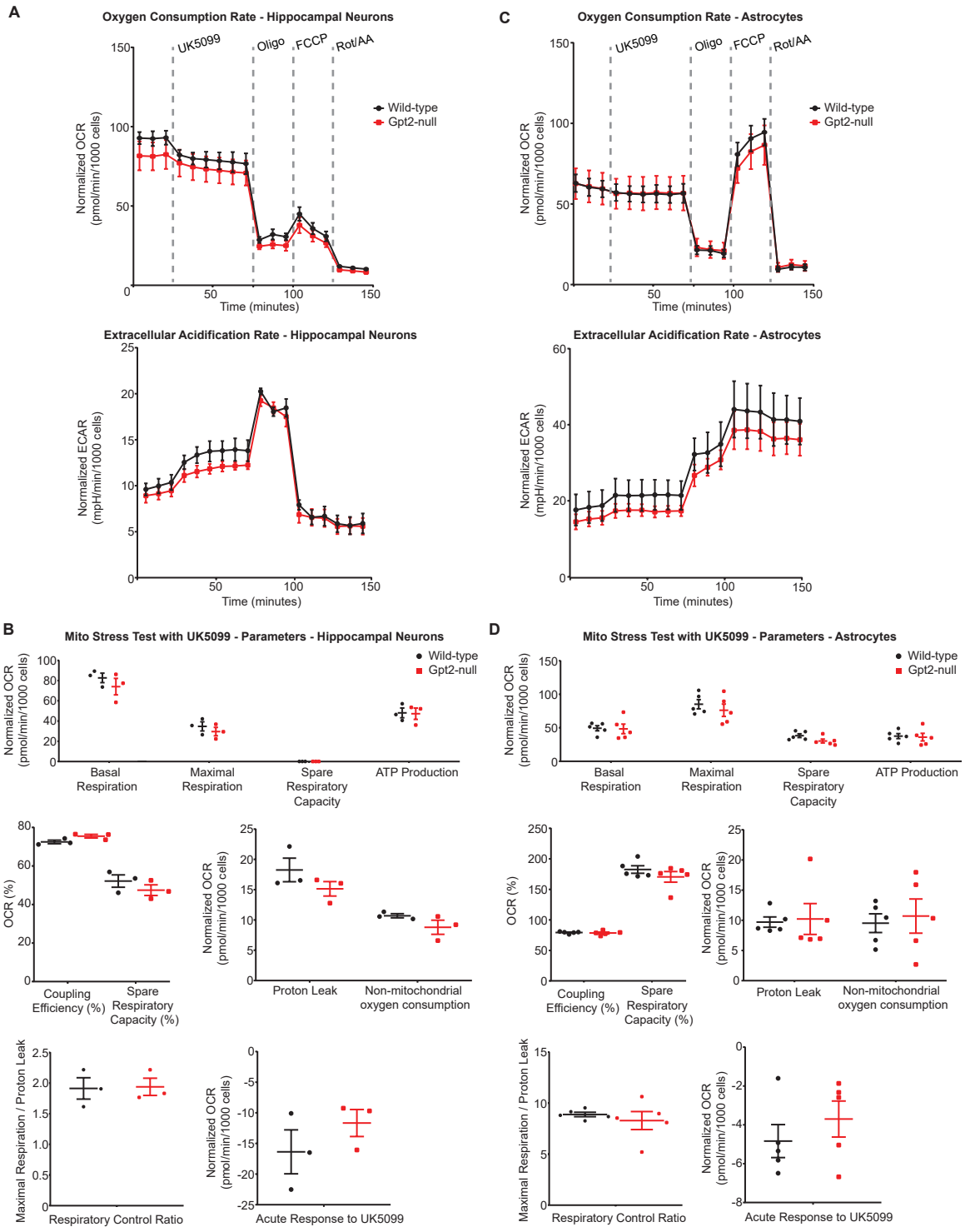

Figure 3 A 3.35. Seahorse Mito Stress Test with UK5099 in Gpt2-null hippocampal neurons and astrocytes. A. Oxygen consumption (OCR) and extracellular acidification rates (ECAR) measured at baseline and after sequential injections of UK5099, oligomycin (Oligo), FCCP, rotenone and antimycin A (Rot/AA) in wild-type (black) and Gpt2-null (red) hippocampal neurons at 14 days in vitro. OCR and ECAR values were normalized to cell count and expressed as pmol per minute per 1,000 cells. n=3 litters. B. Mitochondrial respiration parameters obtained from Mito Stress Test with UK5099 in wild-type (black) and Gpt2-null (red) hippocampal neurons at 14 days in vitro. C. Oxygen consumption (OCR) and extracellular acidification rates (ECAR) measured at baseline and after sequential injections of UK5099, oligomycin (Oligo), FCCP, rotenone and antimycin A (Rot/AA) in wild-type (black) and Gpt2-null (red) astrocytes in vitro. OCR and ECAR values were normalized to cell count and expressed as pmol per minute per 1,000 cells. n=5 litters. D. Mitochondrial respiration parameters obtained from Mito Stress Test with UK5099 in wild-type (black) and Gpt2-null (red) astrocytes.

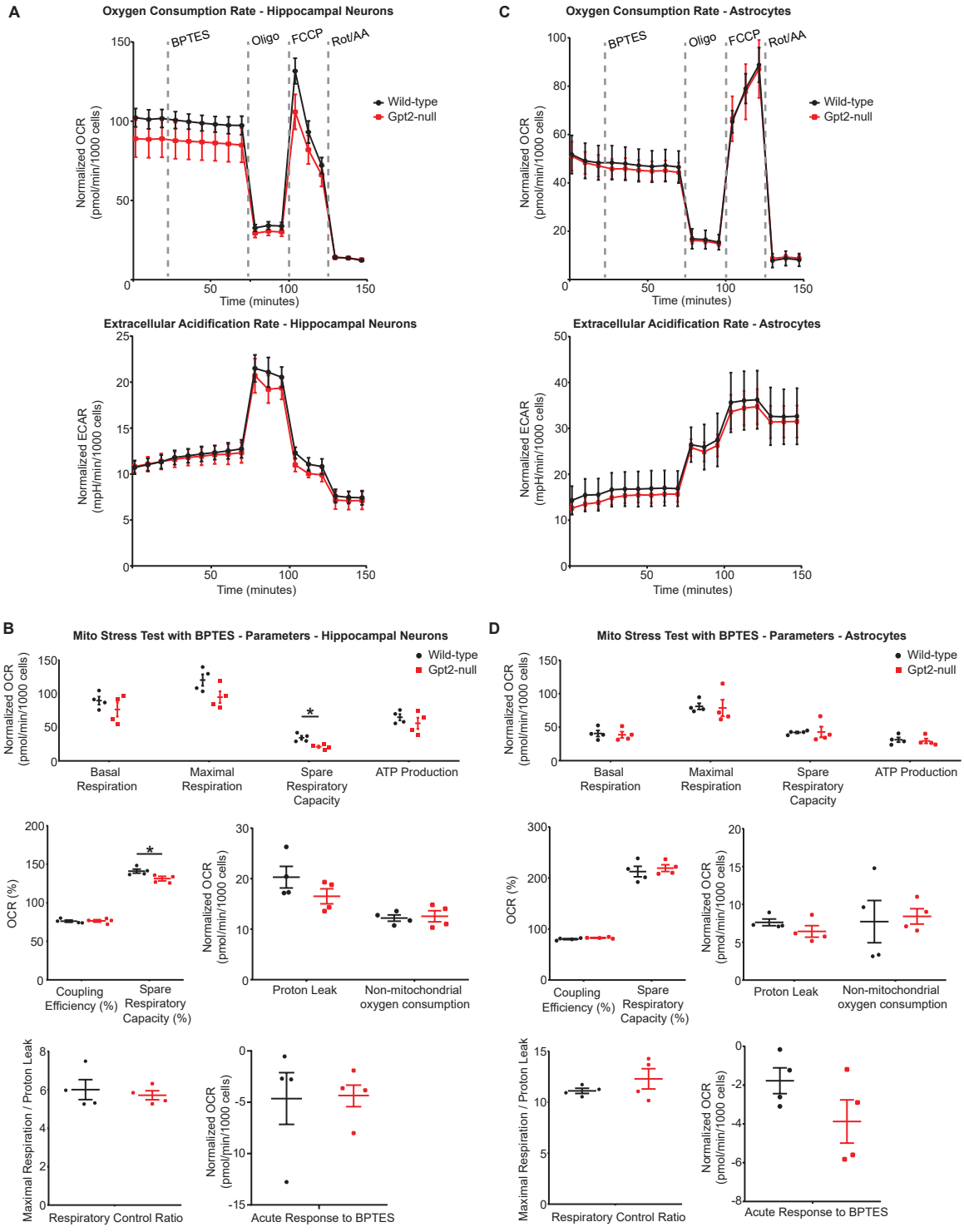

Figure A 3.36. Seahorse Mito Stress Test with BPTES in Gpt2-null hippocampal neurons and astrocytes.
A. Oxygen consumption (OCR) and extracellular acidification rates (ECAR) measured at baseline and after sequential injections of BPTES, oligomycin (Oligo), FCCP, rotenone and antimycin A (Rot/AA) in wild-type (black) and Gpt2-null (red) hippocampal neurons at 14 days in vitro. OCR and ECAR values were normalized to cell count and expressed as pmol per minute per 1,000 cells. n=4 litters.
B. Mitochondrial respiration parameters obtained from Mito Stress Test with BPTES in wild-type (black) and Gpt2-null (red) hippocampal neurons at 14 days in vitro. *0.01<P<0.05. C. Oxygen consumption (OCR) and extracellular acidification rates (ECAR) measured at baseline and after sequential injections of BPTES, oligomycin (Oligo), FCCP, rotenone and antimycin A (Rot/AA) in wild-type (black) and Gpt2-null (red) astrocytes in vitro. OCR and ECAR values were normalized to cell count and expressed as pmol per minute per 1,000 cells. n=4 litters. D. Mitochondrial respiration parameters obtained from Mito Stress Test with BPTES in wild-type (black) and Gpt2-null (red) astrocytes.

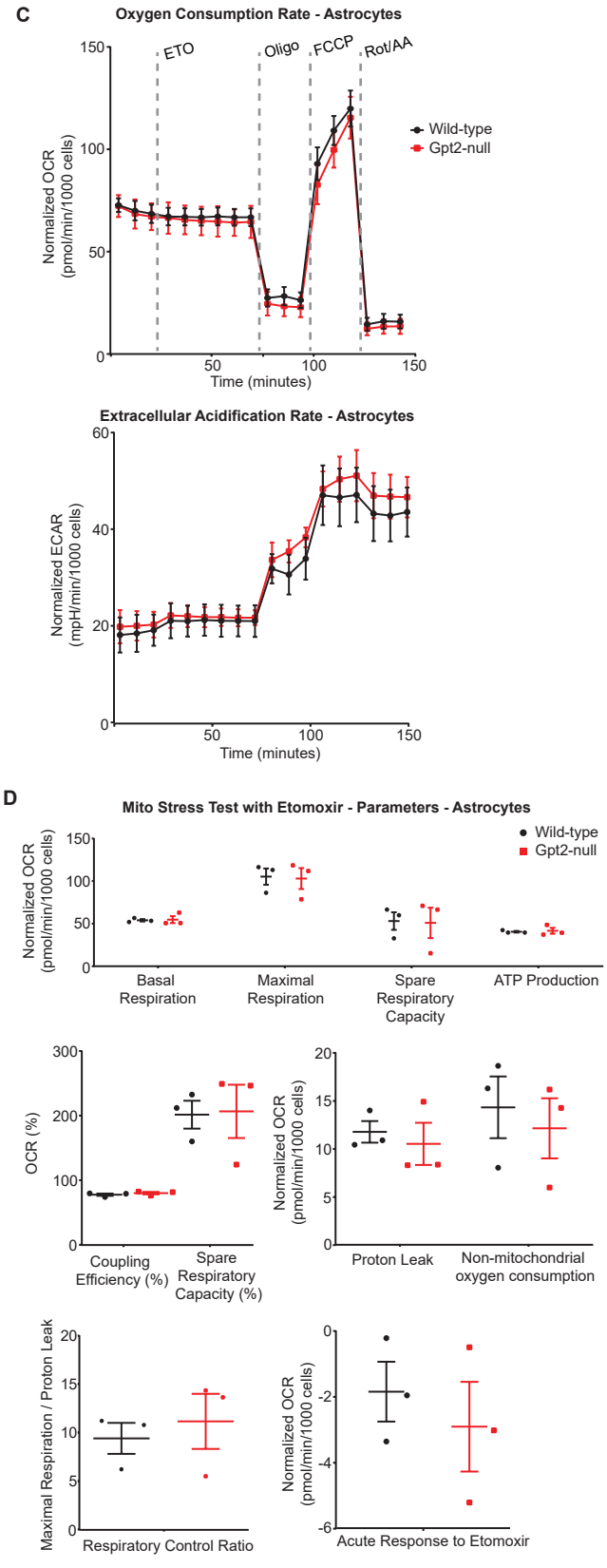

Figure A 3.37. Seahorse Mito Stress Test with Etomoxir in Gpt2-null astrocytes. A. Oxygen consumption (OCR) and extracellular acidification rates (ECAR) measured at baseline and after sequential injections of Etomoxir (Eto), oligomycin (Oligo), FCCP, rotenone and antimycin A (Rot/AA) in wild-type (black) and Gpt2-null (red) astrocytes in vitro. OCR and ECAR values were normalized to cell count and expressed as pmol per minute per 1,000 cells. n=3 litters. B. Mitochondrial respiration parameters obtained from Mito Stress Test with Etomoxir in wild-type (black) and Gpt2-null (red) astrocytes.

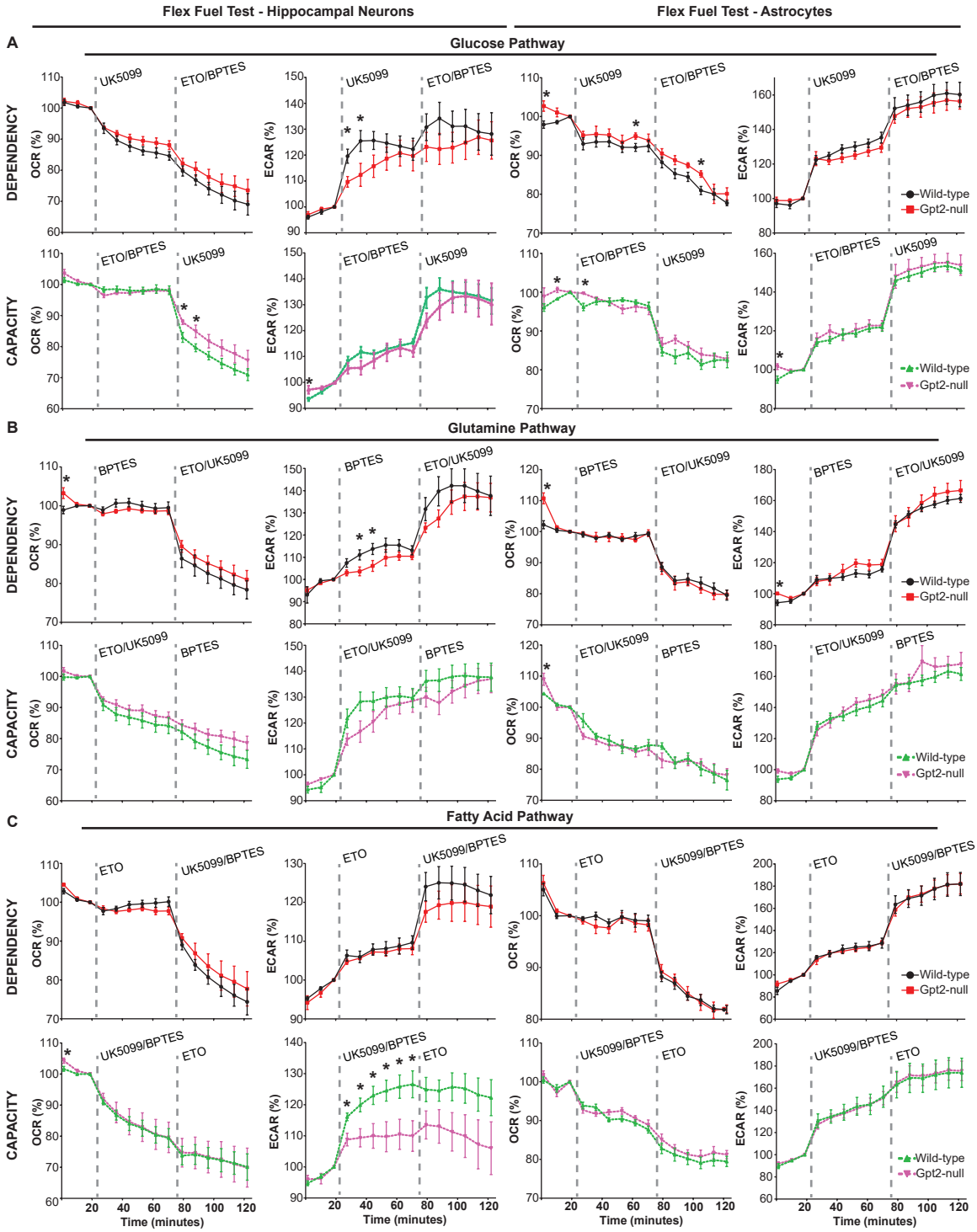

Figure A 3.38. Seahorse Flex Fuel Test in Gpt2-null hippocampal neurons and astrocytes.
A. Dependency (top) and capacity (bottom) of the Glucose pathway in wild-type (black, green) and Gpt2-null (red, magenta) hippocampal neurons at 14 days in vitro (left) and astrocytes (right) in vitro. To determine dependency on the glucose pathway, UK5099 was injected alone, followed by ETO and BPTES. To determine capacity of the glucose pathway, first ETO and BPTES were injected, followed by UK5099. OCR and ECAR values were expressed as percentage of the last baseline measurement n=6-8 litters. *0.01<P<0.05. B. Dependency (top) and capacity (bottom) of the Glutamine pathway in wild-type (black, green) and Gpt2-null (red, magenta) hippocampal neurons at 14 days in vitro (left) and astrocytes (right) in vitro. To determine dependency on the glutamine pathway, BPTES was injected alone, followed by ETO and UK5099. To determine capacity of the glutamine pathway, ETO and UK5099 were injected, followed by BPTES. OCR and ECAR values were expressed as percentage of the last baseline measurement n=6-8 litters. *0.01<P<0.05. C. Dependency (top) and capacity (bottom) of the Fatty Acid pathway in wild-type (black, green) and Gpt2-null (red, magenta) hippocampal neurons at 14 days in vitro (left) and astrocytes (right) in vitro. To determine dependency on the glucose pathway, ETO was injected alone, followed by UK5099 and BPTES. To determine capacity of the glucose pathway, UK5099 and BPTES were injected, followed by ETO. OCR and ECAR values were expressed as percentage of the last baseline measurement n=5-8 litters. *0.01<P<0.05.

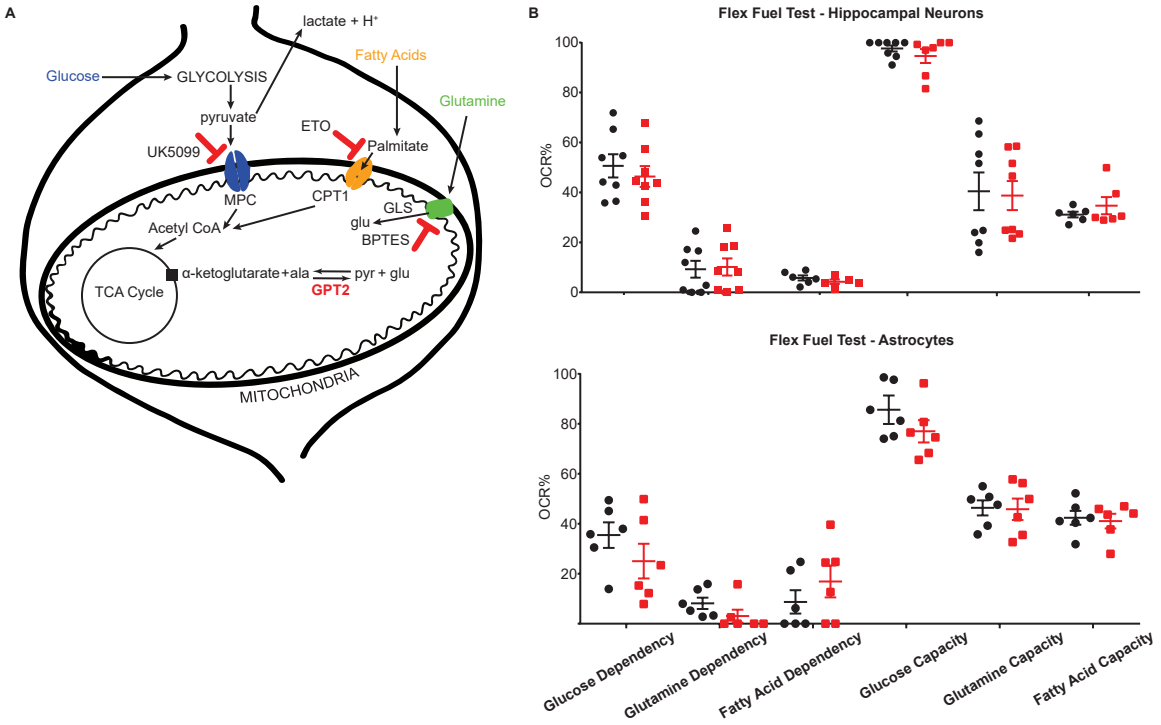

Figure A 3.39. Aggregate dependency and capacity values of Seahorse Flex Fuel Test in Gpt2-null hippocampal neurons and astrocytes. A. The three metabolic pathways tested in the Seahorse Flex Fuel Test. The glucose pathway is probed by preventing pyruvate entry into mitochondria with the inhibition of the mitochondrial pyruvate carrier (MPC) by UK5099. The glutamine pathway is probed by preventing the conversion of glutamine into glutamate (glu) with the inhibition of glutaminase (GLS) by BPTES. The fatty acid pathway is probed by preventing the palmitate entry into mitochondria with the inhibition of carnitine palmitoyltransferase 1 (CPT1) by Etomoxir (ETO). The GPT2 reaction is shown next to the tricarboxylic acid (TCA) cycle with the primary reaction metabolites, alpha-ketoglutarate, alanine (ala), glutamate (glu) and pyruvate (pyr). B. Dependency and capacity of the three metabolic pathways in wild-type (black) and Gpt2-null (red) hippocampal neurons (top) at 14 days in vitro and astrocytes (bottom) in vitro. For detailed calculations, refer to Methods. n=6-8 litters.

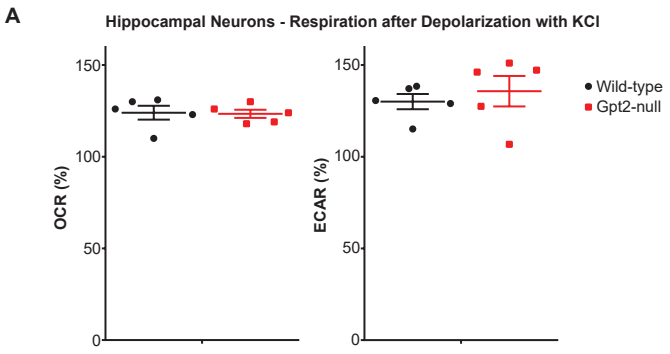

Figure A 3.40. Oxygen consumption after depolarization with KCl in Gpt2-null hippocampal neurons. A. Oxygen consumption (OCR, left) and extracellular acidification (ECAR, right) rates after KCL depolarization in wild-type (black) and Gpt2-null (red) hippocampal neurons at 14 days in vitro. OCR and ECAR values measured immediately after the addition of 50 mM KCl were divided by the last baseline measurement and expressed as a percentage.

Appendix 3.15. Determination of glycogen levels in Gpt2-null whole cortex and hippocampus at P18.

Introduction

We observe increased levels of almost all glycolytic intermediates in Gpt2-null hippocampus by targeted metabolomics at postnatal day 18 (P18). It is possible that the Gpt2-null cells are trying to upregulate glycolysis in order to support their energy supply. I hypothesized that glycogen in astrocytes may be mobilized, i.e. broken down to glucose for metabolic support of the neurons. I quantified glycogen levels in the Gpt2-null cortex and hippocampus.

Results/Key Points

- No changes in glycogen concentration in gpt2-null hippocampus or cortex at P18.

Discussion

The increase of the glycolytic intermediates is unlikely to be caused by glycogen mobilization. Pyruvate, the end product of glycolysis, is the only glycolytic intermediate that has decreased levels in Gpt2-null hippocampus. It is likely that there is decreased substrate inhibition by pyruvate on the upstream glycolytic enzymes. It is also possible that decreased levels of alanine, an allosteric inhibitor of pyruvate kinase, leads to disinhibition of pyruvate kinase thereby increased glycolytic flux into pyruvate (Carbonell et al., 1973). Experiments involving isotope tracing experiments using labeled glucose and glucose uptake in vivo may pinpoint the origin of the increase in glycolytic intermediates.

Method

The hippocampus and cortex tissues of wild-type and Gpt2-null mice were acutely dissected at P18 and weighed. The glycogen assay (Cayman Chemical, 700480) was performed according to the manufacturer's instructions.

Figure Legends

Figure A.3.41. Glycogen concentrations in hippocampus and cortex of wild-type and Gpt2-null mice at P18.

A. Glycogen concentrations normalized to protein content of hippocampus (left) and cortex (right) tissues in wild-type (black) and Gpt2-null (red) mice at P18.

Carbonell, J., Feliu, J.E., Marco, R., and Sols, A. (1973). Pyruvate kinase. Classes of regulatory isoenzymes in mammalian tissues. Eur J Biochem *37*, 148-156.

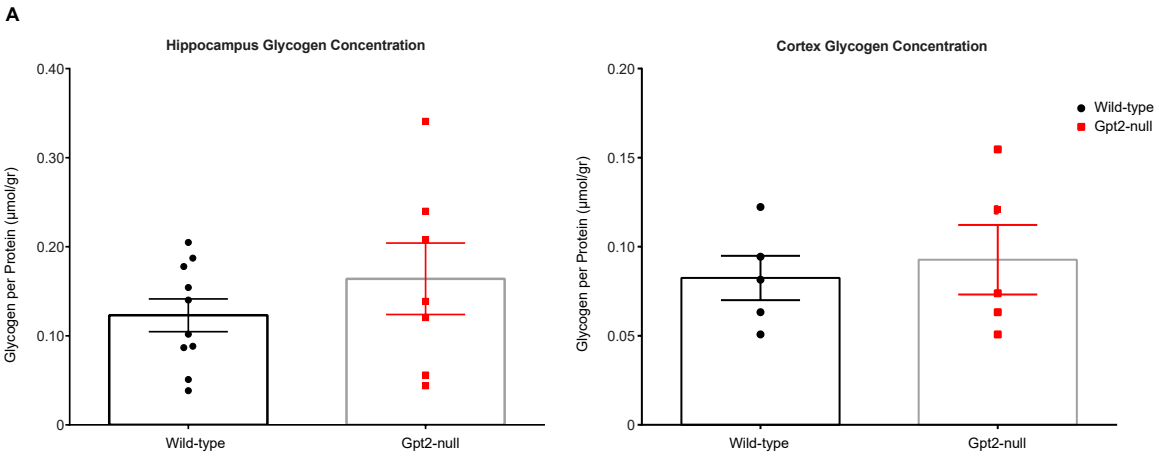

Figure A.3.41. Glycogen concentrations in hippocampus and cortex of wild-type and Gpt2-null mice at P18. A. Glycogen concentrations normalized to protein content of hippocampus (left) and cortex (right) tissues in wild-type (black) and Gpt2-null (red) mice at P18.

Appendix 3.16. Troubleshooting with antibodies for Gpt2.

Introduction

I tried various antibodies for Gpt2 on mouse brain sections. Immunohistochemistry for Gpt2 would be instrumental in:

1) determining differential expression of Gpt2 across different cell types and regions in the central nervous system

2) confirming conditional Gpt2-null mice models (absence of the protein in specific cell types)

3) confirming mitochondrial localization in mouse tissues.

Key methodological parameters tried were as follows:

1) Heat-induced epitope retrieval (HIER) in citrate buffer

2) Incubation of antibodies with Gpt2-null cortical protein (preadsorption that would precipitate) or Mouse GPT protein (Prospec, ENZ-1030) with different weight ratios (10:1, 20:1 or 40:1 ratio of cortical protein or GPT protein to GPT2 antibody)

3) Paraffin (6 μm) or frozen sections (10 μm)

4) Primary antibody concentrations (1:10, 1:20, 1:50, 1:100, 1:200, 1:400, 1:800, 1:1600)

5) Primary antibodies: a) Novus Biologicals NBP2-14072 Rabbit (immunogen: human C-terminus) b) Abcepta AP18028a Rabbit (immunogen: human N-terminus, 15-44 amino acids) c) ProteinTech 16757-1-AP Rabbit (immunogen: human full protein) d) elabscience E-AB-19961 Rabbit (immunogen: human C-terminus: 396-408).

6) Secondary antibodies: anti-rabbit 488 (Invitrogen, A11034) or anti-rabbit 594 (Invitrogen, A11037) AlexaFluor.

7) Negative control without primary antibody

Results / Key Points

1) None of the antibodies in any of the conditions tested worked. All primary antibodies had distinctive puncta in both wild-type and Gpt2-null brain tissue (hippocampus/cortex). Negative control shows no staining.

Discussion

There are homology differences between the immunogen sequences and mouse Gpt2 or Gpt1 sequences. For example, the immunogen for Novus Biological NBP2-14072, "PVSGQAAMDIVVNPPVAGEESFEQFSREKESVLGNLA" has 92% homology with mouse Gpt2 and 76% homology with mouse Gpt1. Any homology greater than 50% is considered to have enough similarities for possible antibody binding. That is why the preadsorption was tried. However, it did not work. It is possible that the Gpt2 protein is still expressed in the Gpt2-null tissue. In the gene trap mouse with the Gpt2 null allele, there is a frameshift after Exon 4 leading to a premature stop codon. This would allow the C-terminus antibodies to not detect the protein made in Gpt2-null if it is made at all. However, both antibodies that tareted the C-terminus detected the protein.

In Western blotting, the protein is not detected at 58kDa in Gpt2-null brain samples by the Proteintech antibody and this is inferred by comparing the samples with their wild-type counterparts. However the antibody detects many different bands, some much higher in intensity compared to the Gpt2 band and these may either non-specific bands, Gpt2

proteins that result from different transcripts, polymerization, post-translation modification or proteins that are bound to Gpt2. In the matter of transcripts, humans have 2 transcripts for Gpt2. In humans, the truncated transcript has been shown to have no catalytic activity [1]. In mice, there appear to be 1 RefSeq RNA transcript (NM.173866) and 6 transcripts (those that cover almost the entire RefSeq transcript region) from GenBank. It is not known how the gene trap cassette affected those other transcripts or whether they have any catalytic activity.

A protein that is tagged with V5 or GFP may be made with genomic insertion. While this may itself affect the GPT2 function, it would have the potential to address the three aims listed in the Introduction.

Available Data (not shown):

- Images for Novus Biological and Proteintech antibodies.

Method

Heat-induced epitope retrieval was achieved by immersing the slides in 10 mM sodium citrate buffer (pH6 with 0.05% Tween 20) at 98ºC for 10 minutes. After the slides cooled down, the immunohistochemistry proceeded as previously described in Chapter 3.

The preadsorption was done for 2 hours at room temperature in blocking solution.

1. Glinghammar, B., I. Rafter, A.K. Lindstrom, J.J. Hedberg, H.B. Andersson, P. Lindblom, A.L. Berg, and I. Cotgreave, *Detection of the mitochondrial and catalytically active alanine aminotransferase in human tissues and plasma.* Int J Mol Med, 2009. **23**(5): p. 621-31.

For Appendices 3.17, .18, .19, .20, .21, I will list my brief observations and more data is available upon request.

Appendix 3.17. Homing/righting reflex and open field test data on Gpt2-null mice at P18.

Homing reflex (the time it takes for the neonate pups to reach the cage bedding from a distance) and right reflexes (the time it takes for the neonate pup to right itself after it has been turned on its back) were normal in Gpt2-null mice. Open Field Test data shows that Gpt2-null mice at P18 tended to move around the open arena less. At around weaning age, they appeared lethargic and eventually died.

Appendix 3.18. Gpt2 expression in SynapsinI-Cre conditional Gpt2-null liver at P18.

The SynapsinI-Cre conditional Gpt2-null shows increased Gpt2 expression in the liver; presumable as a compensatory mechanism to upregulate the TCA cycle in the liver.

Appendix 3.19. Metabolomics in Gpt2-null serum on regular diet at P18.

In the serum taken from Gpt2-null mice by cardial puncture (as in the serum chemical panel), we performed metabolomics and found decreases in glutathione, serine, alanine, citrate/isocitrate. Almost all metabolites with a significant raw p-value had decreased levels. However, PCA plots were unable to distinguish the wild-type and Gpt2-null groups suggesting that overall the serum metabolites are similar.

Appendix 3.20. Metabolomics in Gpt2-null astrocytes in vitro.

We performed metabolomics in Gpt2-null astrocytes in vitro and found no appreciable differences. This is most likely due to their growth medium which had all the metabolites necessary for their functioning metabolome.

Appendix 3.21. Lipidomics in Gpt2-null brain/spinal cord at P18.

We performed lipidomics on brain/spinal cords of Gpt2-null mice at P18 to determine if their lipid profiles had alterations. The most consistent results was increases in Cholesteryl ester in Gpt2-null brain and spinal cord. Increases have been associated with Huntington disease, Multiple sclerosis, Alzheimer's disease. I was expecting an overall decrease in levels given potential problem in macromolecule synthesis but relative quantification of lipidomics failed to reveal decreases in a particular lipid class. Absolute quantification of lipids may reveal further derangements in lipid synthesis or better still isotope tracing involving metabolite incorporation into lipids (e.g. citrate, acetate)

Appendix 4.1. Labeling of locus coeruleus with the NAT-EGFP-Rpl10a line and Western blotting in Gpt2-null locus coeruleus protein samples.

Introduction

In order to investigate the mechanisms behind the degeneration in Locus coeruleus (LC), it is imperative to extract the tissue specifically for metabolic, biochemical and transcriptomic assays. LC is a small nucleus only spanning approximately 400 μm in the anterior/posterior axis and in the dorsal/caudal axis. It is bordered by the motor nuclei of the trigeminal nerve laterally and Barrington's nucleus medially. By specifically labeling LC neurons, it is possible to pinpoint LC exactly and minimize the contamination from the surrounding nuclei. To this end, I crossed the Gpt2 line (Knockout Mouse Project-KOMP 4363039) with the EGFP/Rpl10a line (Jax Strain no.: 031150). EGFP/Rpl10a protein is a ribosomal fusion protein expressed under the control of Slc6a2 (norepinephrine transporter) promoter. It is possible to identify LC neurons by the presence of EGFP and the line also allows for isolation of polysomes and translating mRNAs from LC neurons.

I validated and characterized this line via my LC tissue collection technique by Western blotting. I compared tyrosine hydroxylase (TH), p62, ubiquitin, pmTOR levels.

b) decreases in overall TH levels indicating TH+ neuron loss

c) changes in overall levels of ubiquitinated proteins

d) changes in pmTOR levels that may indicate autophagy

Results/Key Points

Increases in p62 & decreases in TH levels in Gpt2-null LC.

No apparent changes in levels of overall ubiquitanted protein (75-150 kDa) or pmTOR.

Discussion

It is imperative to assess Iba1 or CD68 levels in western blotting to ensure that the method has more validity. However, so far, my western blotting failed to detect a band. It may have to with reductive conditions in the western blotting. Other antibodies may be tried.

Other markers of degeneration or autophagy may be tried in the Western blotting to pinpoint a possible mechanism of neurodegeneration.

Transcriptomics or metabolomics experiments may be helpful to generate hypotheses as to how Gpt2-null LC neurons degenerate. Particularly transcriptomics may be achieved by pulling down the samples probed to GFP and detect mRNA from LC neurons specifically. Currently, the Western blotting described here includes neurons and glia present in the LC.

Available data (not shown)

Data for pS6: The levels of phosprylated ribosomal protein S6 has been corrletaed to protein translation and neuronal activity and we see decreases in LC. since pS6 is prominently expressed in neurons, the decreased levels may reflect decreases of neuron count in of Gpt2-null LC.

Method

The Gpt2 line was crossed to NAT-EGFP/Rpl10a (Jax Strain no. 031150). The brains were flash frozen and stored at -80ºC until sectioning. 150 µm thick cryosections were mounted on slides and LC was visualized with 488 nm LED of an inverted microscope. The LC was dissected with an insulin syringe and forceps and placed in RIPA buffer (0.05 M Tris pH7.4, 0.15 M NaCl, 1 mM EDTA, 1% Triton X-100, 0.01 g/ml sodium deoxycholate, 0.1% SDS, 1X Protease Inhibitor Cocktail (Roche, 11697498001), 1X PhosSTOP (Roche, 4906845001)). Protein concentration was determined by bicinchoninic acid (BCA) Assay (Thermo Scientific, 23225).

Primary antibodies used in Western blotting: GFP Rb CellSignaling 2956 (1:1000), Tubulin Ms Sigma T6074 (1:1000), TH Ms MAB318 MilliporeSigma (1:1000), pmTOR Rb Cellsignaling 5536S (1:1000), Ubiquitin Ms Invitrogen 13-1600 (1:500).

Figure Legends

Figure A4.1. Characterization of NAT-EGFP/Rpl10a line and Western blotting for TH, p62, ubiquitin, pmTOR in Gpt2-null LC.

A. Image of GFP signal in LC (left, scale bar:250 um) and Western blotting characterization of the NAT-EGFP/Rpl10a line (right). EGFP/Rpl10a was detected with an antibody for GFP. The hippocampus (HPC) samples obtained from the same mice as NAT-GFP do not show a major band for EGFP/Rpl10a. Tyrosine hydroxylase (TH) is enriched in locus coeruleus samples. For comparison, the LC was also extracted from mice without GFP expression based on the anatomical hallmarks (LC is lateral to the fourth ventricle). Note that the enrichment of TH is less than the GFP-LC samples indicating the GFP line increased the enrichment of LC in sample collection. The

EGFP/Rpl10a and TH appear at the 50 and 60 kDa bands, respectively. D:dorsal, V:ventral, M:medial, L:lateral.

B. Western blotting for p62, TH, pmTOR, ubiquitin (75-150 kDa) in wildtype and Gpt2-null mice at postnatal day 18. Quantification is given below. For p62 **P*=0.0273, for TH ***P*=0.0062.

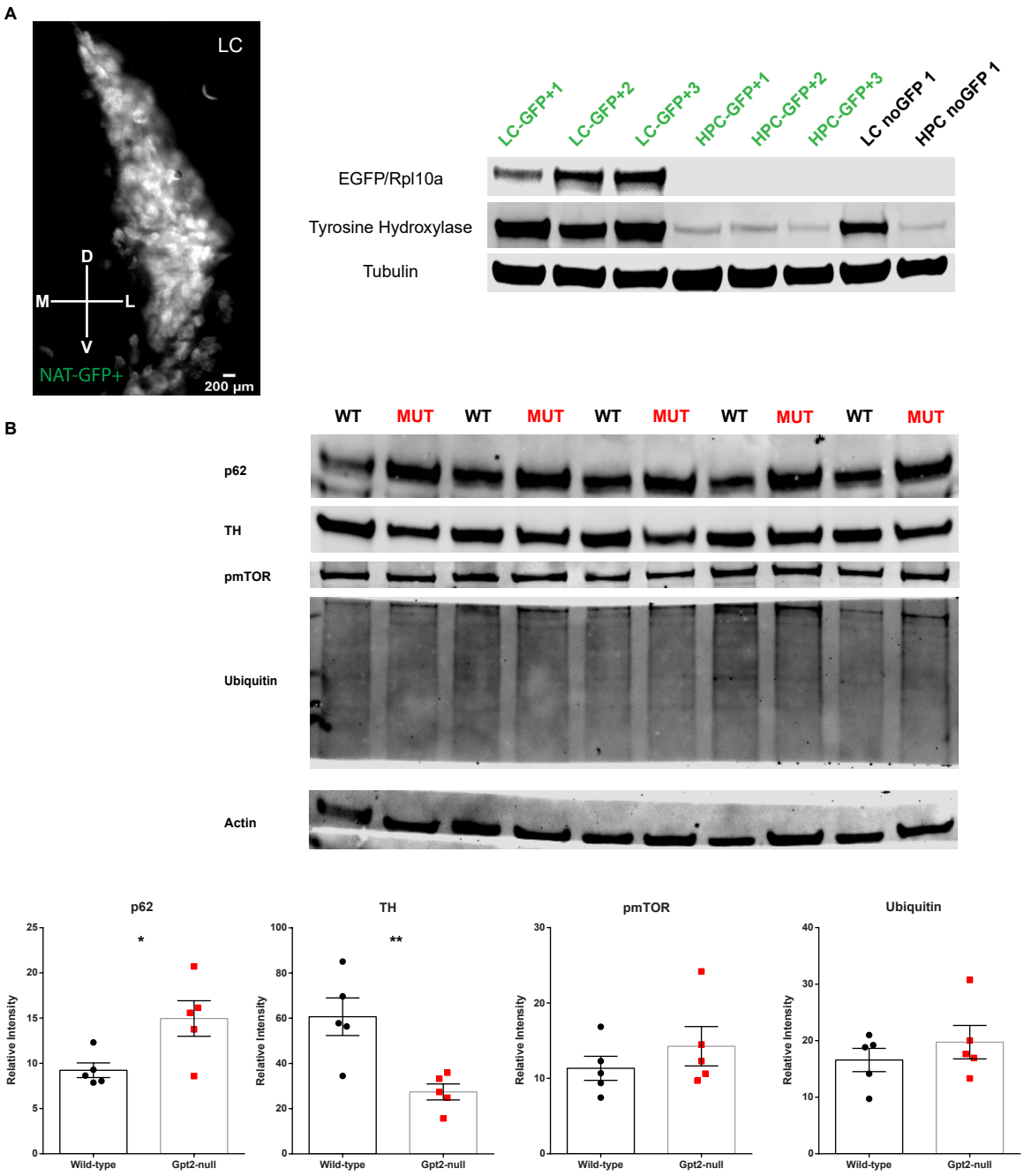

Figure A4.1. Characterization of NAT-EGFP/Rpl10a line and Western blotting for TH, p62, ubiquitin, pmTOR in Gpt2-null LC.

A. Image of GFP signal in LC (left, scale bar:250 um) and Western blotting characterization of the NAT-EGFP/Rpl10a line (right). EGFP/Rpl10a was detected with an antibody for GFP. The hippocampus (HPC) samples obtained from the same mice as NAT-GFP do not show a major band for EGFP/Rpl10a. Tyrosine hydroxylase (TH) is enriched in locus coeruleus samples. For comparison, the LC was also extracted from mice without GFP expression based on the anatomical hallmarks (LC is lateral to the fourth ventricle). Note that the enrichment of TH is less than the GFP-LC samples indicating the GFP line increased the enrichment of LC in sample collection. The EGFP/Rpl10a and TH appear at the 50 and 60 kDa bands, respectively. D:dorsal, V:ventral, M:medial, L:lateral. B. Western blotting for p62, TH, pmTOR, ubiquitin (75-150 kDa) in wildtype and Gpt2-null mice at postnatal day 18. Quantification is given below. For p62 *P=0.0273, for TH **P=0.0062.

Appendix 4.2. Tyrosine hydroxylase and Iba1 staining in locus coeruleus of Slc25a12-null and Acc1-het mice.

Introduction

I tested whether there is a degeneration or gliosis in locus coeruleus in other models of metabolism that were available in Dr. Morrow's laboratory. I used two models: a) Slc25a12 deficiency, Slc25a12 is a glutamate/aspartate exchanger in the mitochondria and deficiencies in this protein lead to developmental delay, seizures in humans as wells as motor abnormalities and death pre-weaning in mutant mice. b) Acc1 deficiency, acetyl-CoA carboxylase 1 catalyzes the irreversible carboxylation of acetyl-CoA into malonyl-CoA, the initial step in de novo synthesis of fatty acids and homozygous deletion of Acc1 causes embryonic lethality in mice. I stained for tyrosine hydroxylase (TH) that stains for noradrenergic neurons in locus coeruleus and Iba1, a marker for microglia.

Results / Key Points

There is no apparent neuron loss or gliosis in locus coeruleus of Slc25a12-null (postnatal day 18, P18) and Acc1-heterozygous (P60) mice.

Discussion

The most relevant finding that can come out of this study is that locus coeruleus degeneration in Gpt2-null mice seem to be specific to Gpt2 deficiency and do not occur in the other two models of metabolic deficiencies. It is not entirely inconceivable that Slc25a12 deficiency would show degeneration in locus coeruleus since the protein is

involved in glutamate metabolism as well as malate-aspartate shuttle which is responsible for NADH transport into the mitochondria. If there had been a positive result, it would have been an interesting line of inquiry.

Method

Immunohistochemistry (Refer to Chapter) done as previously described. Primary antibodies: rabbit anti-Iba1 Wako Chemicals 019-19741 (1:500), mouse anti-tyrosine hydroxylase Millipore MAB318 (1:300). Secondary antibodies: Goat anti-Rabbit IgG (H+L) AlexaFluor488 Invitrogen A11034 (1:600); Goat anti-Mouse IgG (H+L) AlexaFluor594 Invitrogen A11032 (1:600).

Figure Legends

Figure A4.2. Iba1 and Th staining in locus coeruleus of Slc25a12-null and Acc1-heterozygous mice.

A. Images of Iba1 (green) and TH (red) in wild-type (left) and Slc25a12-null (right) mice at postnatal day 18. Scale bar: 100 µm.

B. Images of Iba1 (green) and TH (red) in wild-type (left) and Acc1-heterozygous (right) mice at postnatal day 60. Scale bar: 100 µm.

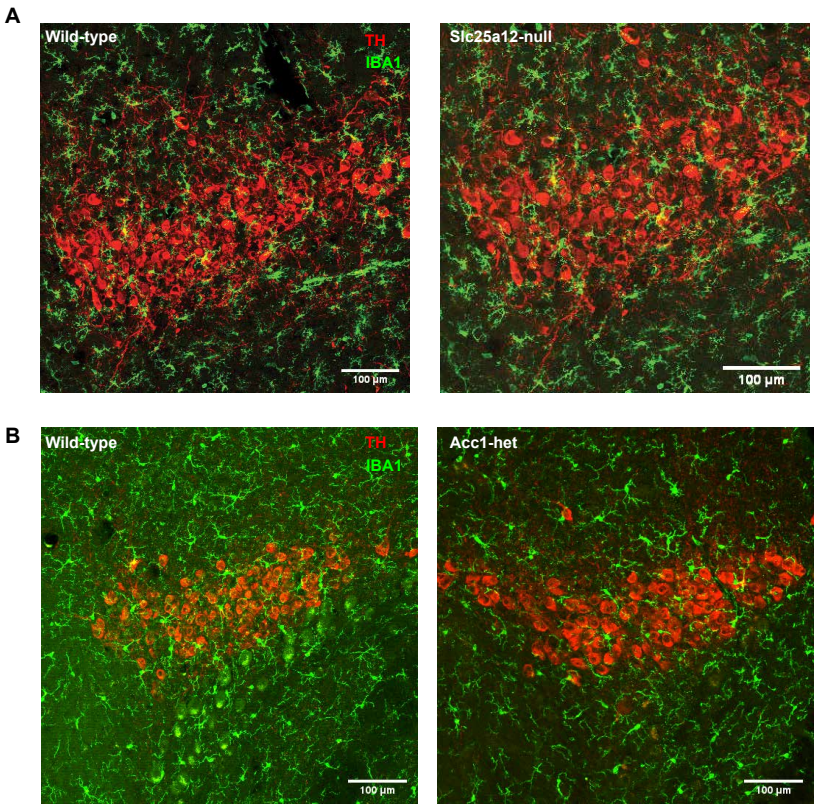

Figure A4.2. Iba1 and Th staining in locus coeruleus of Slc25a12-null and Acc1-heterozygous mice. A. Images of Iba1 (green) and TH (red) in wild-type (left) and Slc25a12-null (right) mice at postnatal day 18. Scale bar: 100 µm. B. Images of Iba1 (green) and TH (red) in wild-type (left) and Acc1-heterozygous (right) mice at postnatal day 60. Scale bar: 100 µm.

Appendix 4.3. Effects of sleep deprivation in locus coeruleus of Gpt2-heterozgous mice at P56.

This experiment was performed by Jimin Shin (Brown Neuroscience undergraduate, 2020).

Introduction

Locus coeruleus (LC) neurons have been shown to degenerate and die after three days of sleep deprivation in mice [1]. We hypothesized that Gpt2-heterozygous animals would show increased metabolic vulnerability in LC to sleep deprivation compared to their wild-type littermates thereby increasing the severity of neuron death.

Results/Key Points

- Confirmed validity of the 3-day sleep deprivation paradigm in wild-type mice at 8 weeks: there is decreased number of tyrosine hydroxylase (TH)+ neurons after sleep deprivation.
- Gpt2-heterozygous mice have more neuron death compared to wild-type mice after sleep deprivation.

Discussion

Although the reasons for why sleep deprivation causes rapid neuron loss in LC are unclear, it appears that even loss of one copy of Gpt2 allele is enough to cause worsening of neuron loss. It is best if the experiment is validated by another trial with increased number of animals and/or better still, by another laboratory.

Available Data (not shown):

- Images of LC for each group/condition.

- TH+ neuron counts for individual animal.
- Videos of animals using the toys that sleep deprivation paradigm is based on.

Method

The sleep deprivation paradigm was performed as described by Zhang and co-workers [1]. Control animals were left undisturbed, “short” sleep deprivation involved 3 hours in an enriched environment and “extended” sleep deprivation involved 8 hours in an enriched environment. Wild-type and Gpt2-heterozygous mice were subjected to sleep deprivation at 8 weeks of age. The toys involved, wheels, ladders, wooden maze and a paper hut. If the mouse were not moving for more than a minute, a gentle nudge was administered or one of the toys was moved to always keep the mouse vigilant. At the end of the experiment, the mice were transcardially perfused with 4% paraformaldehyde. 30 μm thick cryosections of the LC were mounted on slides.

Figure Legends

Figure A4.3. Worsened LC neuron loss after sleep deprivation in Gpt2-heterozygous mice at 8 weeks of age.

A. Tyrosine hydroxylase+ neuron counts in Trial 1 involving only wild-type mice at postnatal day 56 (P56). n(control)=3, n(short)=4, n(extended)=2 mice. ***P<0.001.

B. Tyrosine hydroxylase+ neuron counts in Trial 2 involving only wild-type mice at P56. n(control)=2, n(short)=2, n(extended)=3 mice. ***P<0.001.

C. Tyrosine hydroxylase+ neuron count data from Trial 1&2 combined. ***P<0.001.

D. Tyrosine hydroxylase+ neuron counts of wild-type and Gpt2-heterozygous mice after extended sleep deprivation. n(wild-type)=5 , n(Gpt2-het)=3 mice.

E. Representative images of LC from wild-type and Gpt2-heterozygous mice after normal sleep or extended sleep deprivation. TH is shown in magenta. Scale bar: 50 μm.

1. Zhang, J., Y. Zhu, G. Zhan, P. Fenik, L. Panossian, M.M. Wang, S. Reid, D. Lai, J.G. Davis, J.A. Baur, et al., *Extended wakefulness: compromised metabolics in and degeneration of locus ceruleus neurons.* J Neurosci, 2014. **34**(12): p. 4418-31.

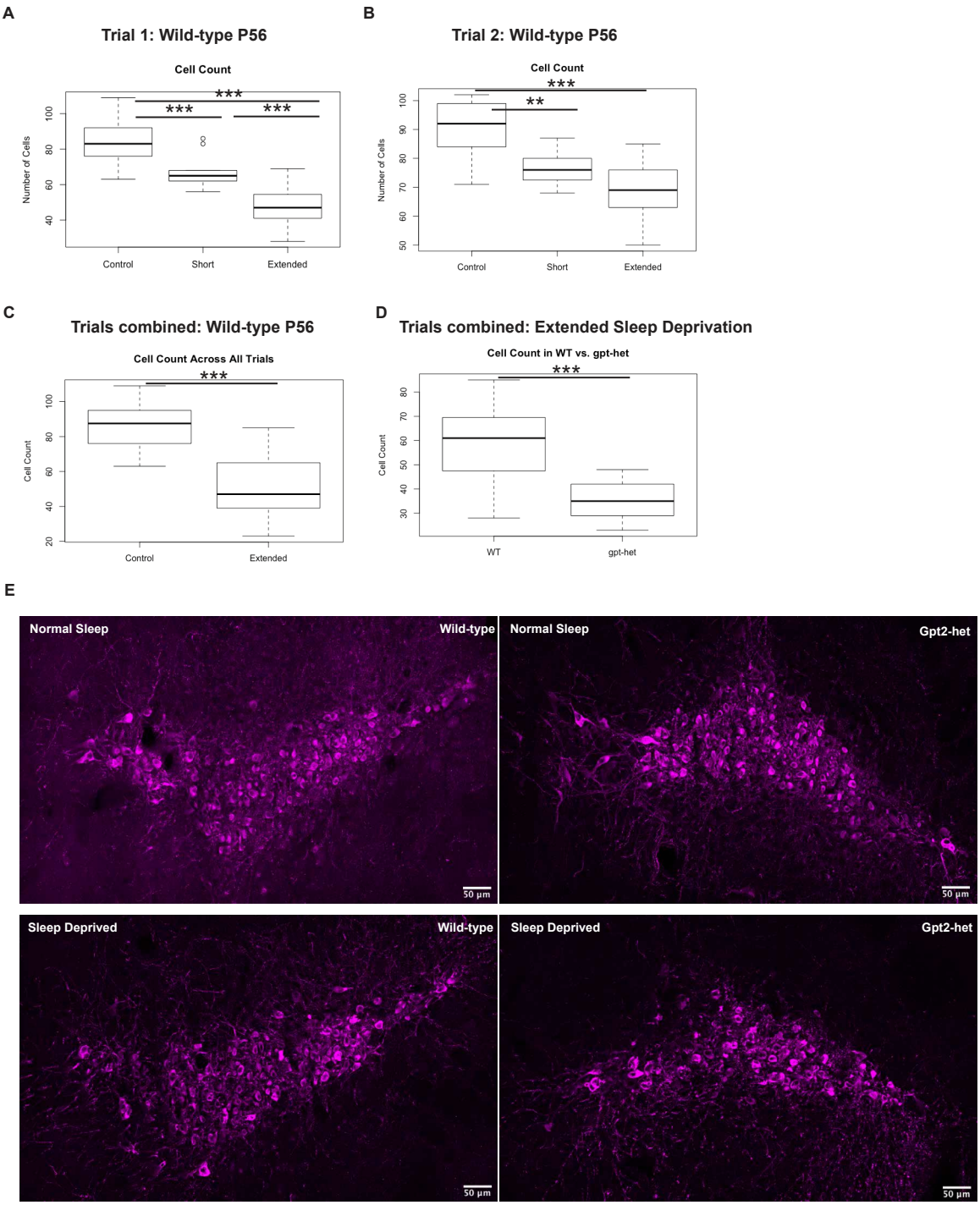

Figure A4.3. Worsened LC neuron loss after sleep deprivation in Gpt2-heterozygous mice at 8 weeks of age. A. Tyrosine hydroxylase+ neuron counts in Trial 1 involving only wild-type mice at postnatal day 56 (P56). n(control)=3, n(short)=4, n(extended)=2 mice. ***P<0.001. B. Tyrosine hydroxylase+ neuron counts in Trial 2 involving only wild-type mice at P56. n(control)=2, n(short)=2, n(extended)=3 mice. ***P<0.001. C. Tyrosine hydroxylase+ neuron count data from Trial 1&2 combined. ***P<0.001. D. Tyrosine hydroxylase+ neuron counts of wild-type and Gpt2-heterozygous mice after extended sleep deprivation. n(wild-type)=5 , n(Gpt2-het)=3 mice. E. Representative images of LC from wild-type and Gpt2-heterozygous mice after normal sleep or extended sleep deprivation. TH is shown in magenta. Scale bar: 50 µm.

For Appendices 5.1, .2, I will list my brief observations and more data is available upon request.

Appendix 5.1. Additional data on 15N-glutamine and 15N-alanine labeling in Gpt2-null synaptosomes.

Fractional enrichments of N-labeling in aspartate and GABA from 15N-glutamine precursor were slightly increased in the Gpt2-null synaptosomes. Glutathione & serine levels showed major decreases. No major changes in levels of phenylalanine, fumarate, succinate, threonine, tryptophan, tyrosine, valine, leucine/isoleucine, NAD, phosphoenolpyruvate.

No N labeling in aspartate or GABA was observed using 15N-alanine as precursor in Gpt2-null synaptosomes.

Appendix 5.2. Additional data on metabolomics in Gpt2-null synaptosomes.

Metabolomics with Gpt2-null synaptosomes at P18 showed increases in cystathionine, proline, lysine, fructose 6-P and decreases in glutathione and serine (in agreement with metabolomics in whole brain and hippocampus tissues – Chapter 2&3). Compared to the whole brain and hippocampus tissue data, the PCA plots did not resolve the wild-type and Gpt2-null as well, this is most likely due alteration of the metabolome during the chemical procedure of obtaining synaptosomes.

Appendix 5.3. Network firing of cortical Gpt2-null neurons using Microelectrode Arrays (MEA).

Introduction

To investigate whether glutamatergic transmission is impacted in Gpt2-null neurons and whether there are developmental deficits in network firing properties in vitro, I used a multi-well microelectrode array (MEA) system, Axion Maestro Edge. It is an in vitro system and fails to capture the in vivo physiology; for example short periods of network firing followed by long periods of pause as seen in the MEAs does not occur in vivo cortical networks [1]. However, MEA system allows for a continuous monitoring of development of network firing in a controlled environment over time in the same wells and gives high-throughout put data with multiple relevant firing parameters such as firing rate, network burst frequency and duration, and coefficient of variation of inter-burst intervals (a measure of firing regularity). The multi-well arrangement also allows for use of multiple drug interventions on cells cultured from the same pup decreasing between pup variability.

Several experiments involved medium composition changes and interfering with the glutamine entry or metabolism to reveal possible vulnerabilities in Gpt2-null cortical neurons in vitro. The experiments and corresponding hypotheses are as follows:

1. Culture development over time in regular Neurobasal Medium: The continuous monitoring (day 4-15 in Neurobasal A medium (NBA)) may reveal delays in network firing in Gpt2-null cells.

2. Firing in Tyrode Medium (artificial cerebrospinal fluid): Medium deprivation in Gpt2-null cells (at day 14, for 24 hours) may cause further/faster decline of firing over time.

3. Firing in Glutaminase inhibition or Glutamine deprivation: Further decreases in glutamate by inhibiting glutaminase (converts glutamine into glutamate) with N,N'-[thiobis(2,1-ethanediyl-1,3,4-thiadiazole-5,2-diyl)]bis-benzeneacetamide (BPTES) or depriving the cultures of glutamine may reveal inability to compensate for glutamate availability in Gpt2-null cells (at day 14, for 24 hours in NBA).

4. Firing in Tyrode Medium with MeAIB: N-methyl-aminoisobutryic acid (MeAIB) inhibits Na-dependent amino acid transport system A transporters (ATA1 and ATA2). By blocking glutamine entry into neurons, we may block glutamine flux into glutamate that may otherwise occur via other metabolic enzymes such as glutamine fructose 6-phosphate aminotransferase (at day 14, for 24 hours in Tyrode).

5. Firing in Co-cultures: I tried four combinations, wild-type neuron&wild-type astrocyte, wild-type neuron&Gpt2-null astrocyte, Gpt2-null neuron & wild-type astrocyte and Gpt2-null neuron & Gpt2-null astrocyte. Contrary to the primary function of normal astrocytes, Gpt2-null astrocytes may dampen the resources available for neurons thereby causing deficits in the development of the neuronal culture (days 4-16 in NBA, then at day 16, for 24 hours in Tyrode).

Parameters of the MEA include: a) Mean Firing Rate b) Burst Frequency c) Burst Duration d) Inter-Burst Interval Coefficient of Variation e) Network Burst Frequency f) Network Burst Duration g) Network Inter-Burst Interval Coefficient of Variation.

Results / Key Points

1. No major differences in the development of firing patterns in Gpt2-null cortical neuronal cultures.
2. Slight decreases in electrode burst and network burst frequency in Gpt2-null neurons in the Tyrode medium toward the end of the 24-hour period.
3. No differences in firing after glutaminase inhibition or glutamine deprivation.
4. Glutamine deprivation allowed for a higher increase in firing compared to glutaminase inhibition in both wild-type and Gpt2-null neurons.
5. Blocking of glutamine entry into the cells by MeAIB did not cause any changes in firing pattern.
6. All four combinations of co-cultures developed in NBA and responded to Tyrode medium similarly.

Discussion

The experiments with multielectrode arrays using Gpt2-null neuronal cultures did not yield any significant results. Electrophysiology in Gpt2-null hippocampal slices showed slight decreases in glutamatergic transmission and upregulation of various proteins related to glutamate metabolism may account for that decrease. Altogether, Gpt2 does not appear to be a primary enzyme that chiefly contributes to glutamatergic transmission. Additional metabolic stresses such as nutrient deprivation (Tyrode medium), glutamine deprivation, glutaminase inhibition, blocking entry of glutamine into the cell did not reveal any vulnerabilities in Gpt2-null cortical neuronal cultures. While expressing the data as the percentage of the value obtained at the first time point may reduce within well and within culture variability, it would capture small significant changes if at all.

There were slight decreases in electrode burst and network burst frequencies in Gpt2-null cortical neurons in the Tyrode medium toward the end of the 24-hour period. The conditions were later repeated when MeAIB was introduced with reduced sample size, and the slight differences were not statistically significant.

The cortical neuronal cultures also contain an appreciable number of astrocytes (10%) and the neuronal firing is most likely supported by astrocytes. The starting astrocytes in the co-cultures would still override the astrocytes that accompany the neuronal culture as the starting astrocytes cover the entire well and the neurons are plated on top. There was no difference among the four co-culture combinations, suggesting that Gpt2-null astrocytes do not confer an additional metabolic burden on the neurons. This is perhaps not surprising since mouse Gpt2 astrocytes express Gpt1 and therefore may be able to adequately contribute to the glutamate metabolism in vitro. Human neurons or astrocytes do not express Gpt1 [2] and induced pluripotent stem cell derived neurons may be able to capture any deficiencies in network connectivity and activity in vitro.

It is possible that mouse hippocampal neurons can be used instead of cortical neurons but their cell yield is lower and does not always allow for using all the available wells. It is unlikely that hippocampal neurons have firing deficits given the absence of phenotype in cortical neurons though the raw data for hippocampal neurons grown in NBA from day 4 to day 16 is available.

It is worth considering if the different medium interventions properly worked. Medium deprivation as performed by using Tyrode medium or NBA without glutamine likely worked as intended even though the cells still contained glutamine and other substrates prior to the deprivation. 24 hours is likely to be enough to capture differences between

the wild-type and Gpt2-null cultures. On the other hand, the drug application is complicated by their efficiency and mechanism of action. MeAIB acts on sodium-dependent glutamine transporters but not on sodium-independent glutamine transporters which have been shown to be expressed in neurons or astrocytes [3]. BPTES is a specific inhibitor of glutaminase and likely inhibited the enzyme fully in our preparation but we did not specifically test for this. However experiments involving both MeIAB and BPTES are complemented by glutamine deprivation, and none of them showed any significant changes suggesting that Gpt2-null neurons are able to fire similarly to the wild-type cultures without depending on glutamine at all.

Another pathway worth investigating is glucose, as it is a major precursor for glutamate. While I have not conducted any experiments with either glucose deprivation or blocking pyruvate entry into the mitochondria, my expectation is that it will not reveal any deficits. The in vitro system does not seem to constitute the developmental and compensatory changes seen in vivo and these processes are likely the reason for why we observe decreases in glutamate levels and glutamatergic transmission in vivo. This idea is reinforced by the observation that Gpt2 normally catalyzes the reaction in the favor of alanine and alpha-ketoglutarate production not glutamate, likely to be the result of differences in concentration and Km values for each substrate in neuronal cells. The expectation that would follow from these observations is an increase of glutamate at least in the mitochondria, contrary to what we observe in vivo. Refer to Chapter 2 for evidence that may suggest why a decrease in glutamate in Gpt2-null brain is observed.

Available data (not analyzed):

- Raw data for wild-type and Gpt2-null hippocampal neurons (75,000 per well) grown in NBA from day 4 to day 16.
- Other metrics from the MEA system (e.g. Inter-quartile range of normalized burst durations, measure of synchrony)

Method

Cell Culture

Mouse primary hippocampal neuron culture. Hippocampal neurons were cultured as described previously [4]: Hippocampi from P0-1 pup were dissected in Hank's Balanced Salt Solution (HBSS) (Gibco 14170-112) and placed in 500µl of 20U/ml papain (Worthington LK003176, in Earle's Balanced Salt Solution (EBSS), Worthington, LK003188). The tube with hippocampi/papain was incubated at 37ºC for 15 minutes. The tissue was triturated with 1ml pipette tip for 12 strokes. The tissue was further incubated at 37ºC for 15 minutes and triturated. The remaining bits of tissue sunk and the solution with dissociated cells was spun in a separate tube at 300g, 5 minutes, at RT. The cell pellet was dissolved gently in Inhibitor Solution (540µl EBSS, 60µl Ovomucoid Protease Inhibitor (Worthington Biochemical, LK003182), 30µl DNase (Worthington Biochemical, LK003170) per hippocampi) and filtered through a 70µm nylon mesh (FisherScientific, 22363548). The filtered cell suspension was layered on top of 1ml Ovomucoid Protease Inhibitor and spun at 70g, 10 minutes, at RT. The supernatant was discarded, and the cell pellet was resuspended in Neurobasal A+ (NeuroBasal A (10888022), 1X B27 Supplement (ThermoFisher Scientific, 17504044), 2mM GlutaMAX (ThermoFisher Scientific, 35050061). The full media was changed the next day and then half media every 3 days. Tyrode medium consisted of 140mM NaCl, 4mM KCl, 2mM

$CaCl_2$, 2mM $MgCl_2$, 10mM HEPES. The concentrations of BPTES and MeAIB were 3 μM and 10 μM respectively.

Mouse primary astrocyte-enriched cultures. The culturing protocol was adapted from [5, 6]: Cortices from P0-1 pup were dissected in HBSS, diced into 6 pieces and transferred to a 15ml conical tube. The tissue is incubated in 0.25% Trypsin-EDTA in HBSS at 37ºC for 30 minutes. The solution is removed carefully to leave the tissue pieces at the bottom, 6ml Astrocyte Plating Medium (APM: DMEM (10569-010), 10% FBS (Invitrogen 16000044), 1% P/S (Invitrogen 15140122)) was added. The tissue is triturated for 15 strokes with 10ml pipette and then 5 strokes more with 1ml pipette. The cell suspension was filtered through 70μm nylon mesh and seeded in a $25cm^2$-flask (Corning 3289). After 2 days, the full medium was changed, then every 3 days. When the astrocyte layer was confluent (~7 days), the flask was shaken at 225 rpm overnight at 37ºC. The full medium was changed to APM with 20μM cytosine arabinoside (Ara-C) to remove any other contaminated proliferative cell types. After two days, the full medium was changed to APM. The Ara-C treatment was repeated the next day. Mild trypsin (0.0675%) treatment was used to lift off the astrocyte layer as a whole and leave the remaining microglia at the bottom of the flask. The layer was incubated in 1ml of Accutase (StemCellTechnologies, 07920) in a fresh tube at 37ºC for 10 minutes. The layer was dissociated with 1ml pipette tip with 5 strokes. 2ml APM was added; the solution was mixed and filtered through a 70 μm nylon mesh. 25,000 cells per well were seeded and maintained until seeding of neurons.

Microelectrode Array (MEA) Recordings

The microelectrode array plate used in the study was M384-tMEA-24W (Axion Biosystems) with 16 poly(3,4-ethylenedioxythiophene) (PEDOT) microelectrodes in each well. The electrodes were coated with 20 µg/ml laminin (10 µl per well) for 2 hours prior to cell seeding. The neurons were seeded in a dotting method at a density of 150,000 cells per well in 10 µl and kept in the incubator for 1 hour before filling the well with medium (400 µl each). Six wells were designated for each experimental group.

The electrical activity was measured by Maestro Edge (Axion Biosystems). Any wells that had less than or equal to 13 active electrodes were excluded (minimum spike rate for active electrode selection criteria: 5 spikes / minute). Single electrode bursts are detected using Inter-Spike Interval (ISI) Threshold parameters, including a maximum of 100 ms inter-spike interval and a minimum of 5 of spikes. Network burst criteria included a maximum of 100 ms inter-spike interval, a minimum of 50 number of spikes and a minimum of 35% participating electrodes. Mean Firing Rate estimation detection window was 10 seconds.

Figure Legends

Figure A 5.1. MEA cortical neuronal culture firing in Neurobasal Medium

A. Images of Spike Amplitude seen in 24 wells of the MEA plate (left) and waveforms of 16 electrodes in a given well during a network burst activity.

B. MEA parameters of mean firing rate, burst frequency, burst duration, inter-burst interval coefficient of variation, network burst frequency, network burst duration and network inter-burst interval coefficient of variation. Wild-type (black), Gpt2-null (red), n=8 cultures. NBA: Neurobasal A medium.

Figure A 5.2 MEA cortical neuronal culture firing Tyrode Medium

A. MEA parameters of mean firing rate, burst frequency, burst duration, inter-burst interval coefficient of variation, network burst frequency, network burst duration and network inter-burst interval coefficient of variation. Wild-type (black), Gpt2-null (red), n=5 cultures. NBA: Neurobasal A medium. The linear regression was performed for the data of the linear phase in the plot (readings 7-26). Slope were compared. *$0.01<P<0.05$, **$0.001<P<0.01$, ***$P<0.001$.

Figure A 5.3. MEA cortical neuronal culture firing after glutamine deprivation or glutaminase inhibition.

A. MEA parameters of mean firing rate, burst frequency, burst duration, inter-burst interval coefficient of variation, network burst frequency, network burst duration and network inter-burst interval coefficient of variation. Wild-type with 3 μM BPTES (black), Gpt2-null with 3 μM BPTES (red), Wild-type without Glutamine (green), Gpt2-null without Glutamine (blue) n=5 cultures. NBA: Neurobasal A medium; NBA – Gln: Neurobasal A medium without Glutamine.

Figure A 5.4. MEA cortical neuronal culture firing after glutamine transport inhibition

A. MEA parameters of mean firing rate, burst frequency, burst duration, inter-burst interval coefficient of variation, network burst frequency, network burst duration and network inter-burst interval coefficient of variation. Wild-type with Tyrode (black),

Gpt2-null with Tyrode (red), Wild-type with 10 μM MeAIB (green), Gpt2-null with 10 μM MeAIB (blue) n=5 cultures. NBA: Neurobasal A medium.

Figure A 5.5. MEA cortical neuronal firing in co-cultures with astrocytes

A. MEA parameters of mean firing rate, burst frequency, burst duration, inter-burst interval coefficient of variation, network burst frequency, network burst duration and network inter-burst interval coefficient of variation. Wild-type neuron & wild-type astrocyte (black), wild-type neuron & Gpt2-null astrocytes (red), Gpt2-null neuron & wild-type astrocytes (green), Gpt2-null neuron & Gpt2-null astrocyte (blue), n=4 cultures. NBA: Neurobasal A medium.

References

1. Zierenberg, J., J. Wilting, and V. Priesemann, *Homeostatic Plasticity and External Input Shape Neural Network Dynamics.* Physical Review X, 2018. **8**(3).
2. Zhang, Y., K. Chen, S.A. Sloan, M.L. Bennett, A.R. Scholze, S. O'Keeffe, H.P. Phatnani, P. Guarnieri, C. Caneda, N. Ruderisch, et al., *An RNA-sequencing transcriptome and splicing database of glia, neurons, and vascular cells of the cerebral cortex.* J Neurosci, 2014. **34**(36): p. 11929-47.
3. Leke, R. and A. Schousboe, *The Glutamine Transporters and Their Role in the Glutamate/GABA-Glutamine Cycle.* Adv Neurobiol, 2016. **13**: p. 223-257.
4. Ouyang, Q., S.B. Lizarraga, M. Schmidt, U. Yang, J. Gong, D. Ellisor, J.A. Kauer, and E.M. Morrow, *Christianson syndrome protein NHE6 modulates TrkB endosomal signaling required for neuronal circuit development.* Neuron, 2013. **80**(1): p. 97-112.
5. Schildge, S., C. Bohrer, K. Beck, and C. Schachtrup, *Isolation and culture of mouse cortical astrocytes.* J Vis Exp, 2013(71).
6. Albuquerque, C., D.J. Joseph, P. Choudhury, and A.B. MacDermott, *Dissection, plating, and maintenance of cortical astrocyte cultures.* Cold Spring Harb Protoc, 2009. **2009**(8): p. pdb prot5273.

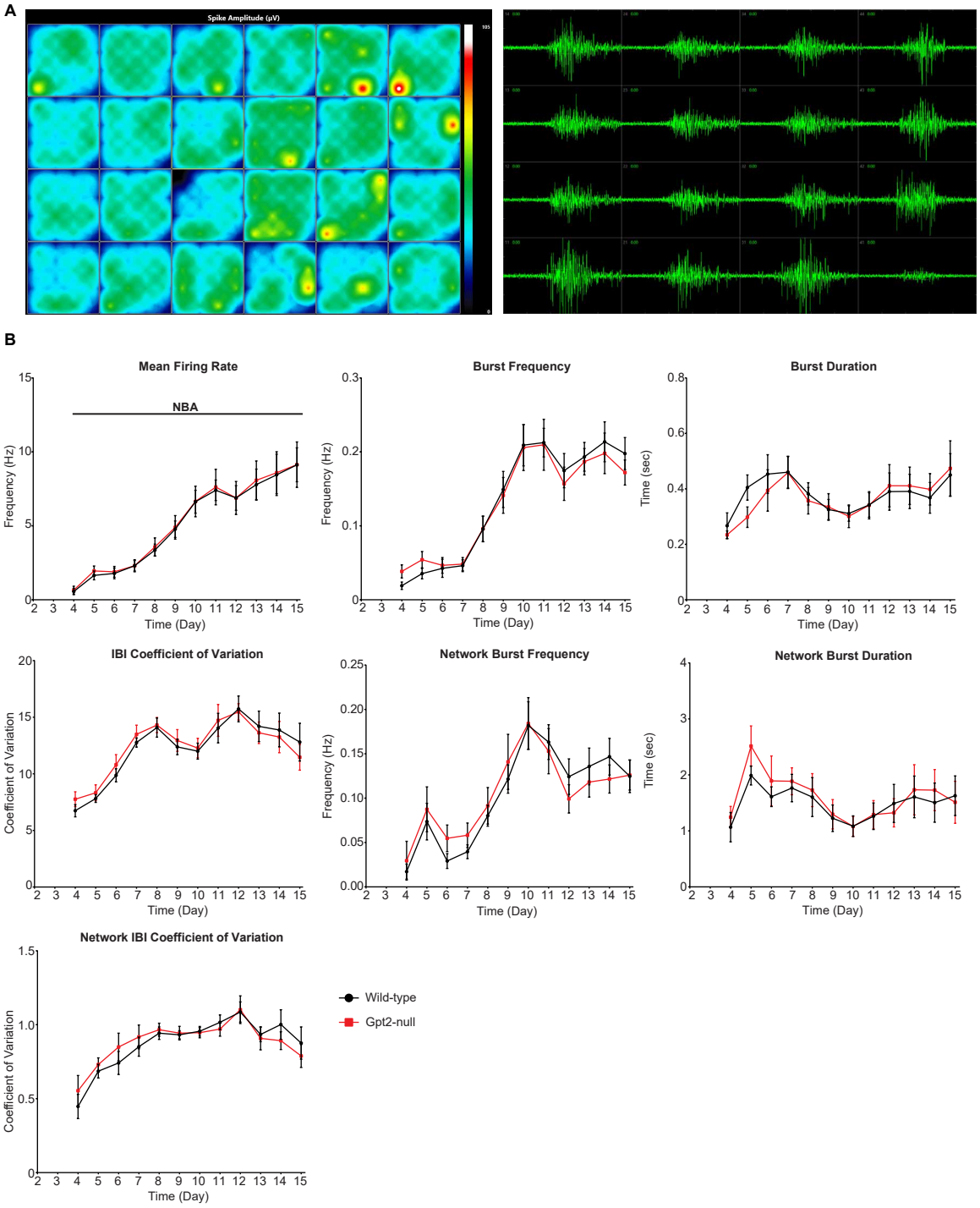

Figure A 5.1. MEA cortical neuronal culture firing in Neurobasal Medium
A. Images of Spike Amplitude seen in 24 wells of the MEA plate (left) and waveforms of 16 electrodes in a given well during a network burst activity. B. MEA parameters of mean firing rate, burst frequency, burst duration, inter-burst interval coefficient of variation, network burst frequency, network burst duration and network inter-burst interval coefficient of variation. Wild-type (black), Gpt2-null (red), n=8 cultures. NBA: Neurobasal A medium.

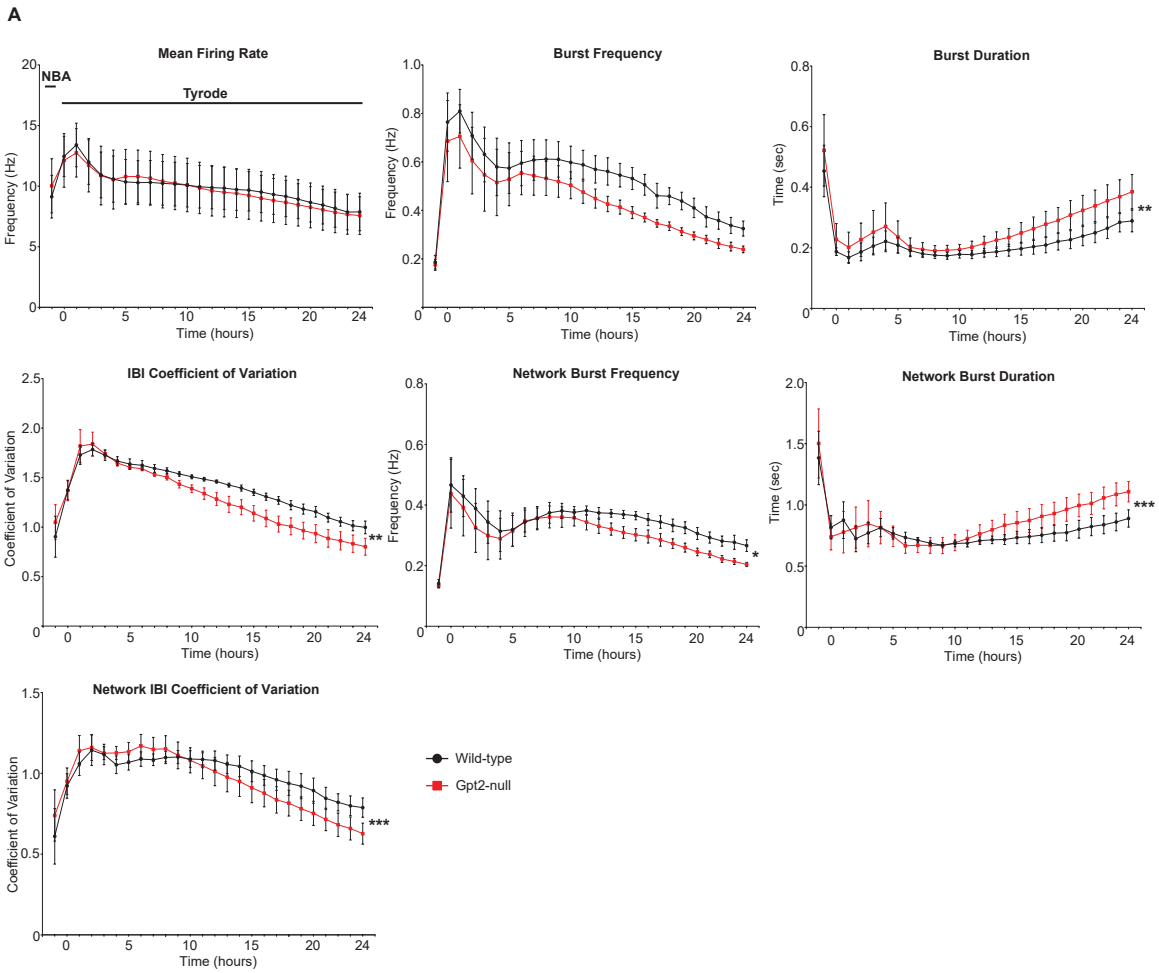

Figure A 5.2 MEA cortical neuronal culture firing Tyrode Medium
A. MEA parameters of mean firing rate, burst frequency, burst duration, inter-burst interval coefficient of variation, network burst frequency, network burst duration and network inter-burst interval coefficient of variation. Wild-type (black), Gpt2-null (red), n=5 cultures. NBA: Neurobasal A medium. The linear regression was performed for the data of the linear phase in the plot (readings 7-26). Slope were compared. *0.01<P<0.05, **0.001<P<0.01, ***P<0.001.

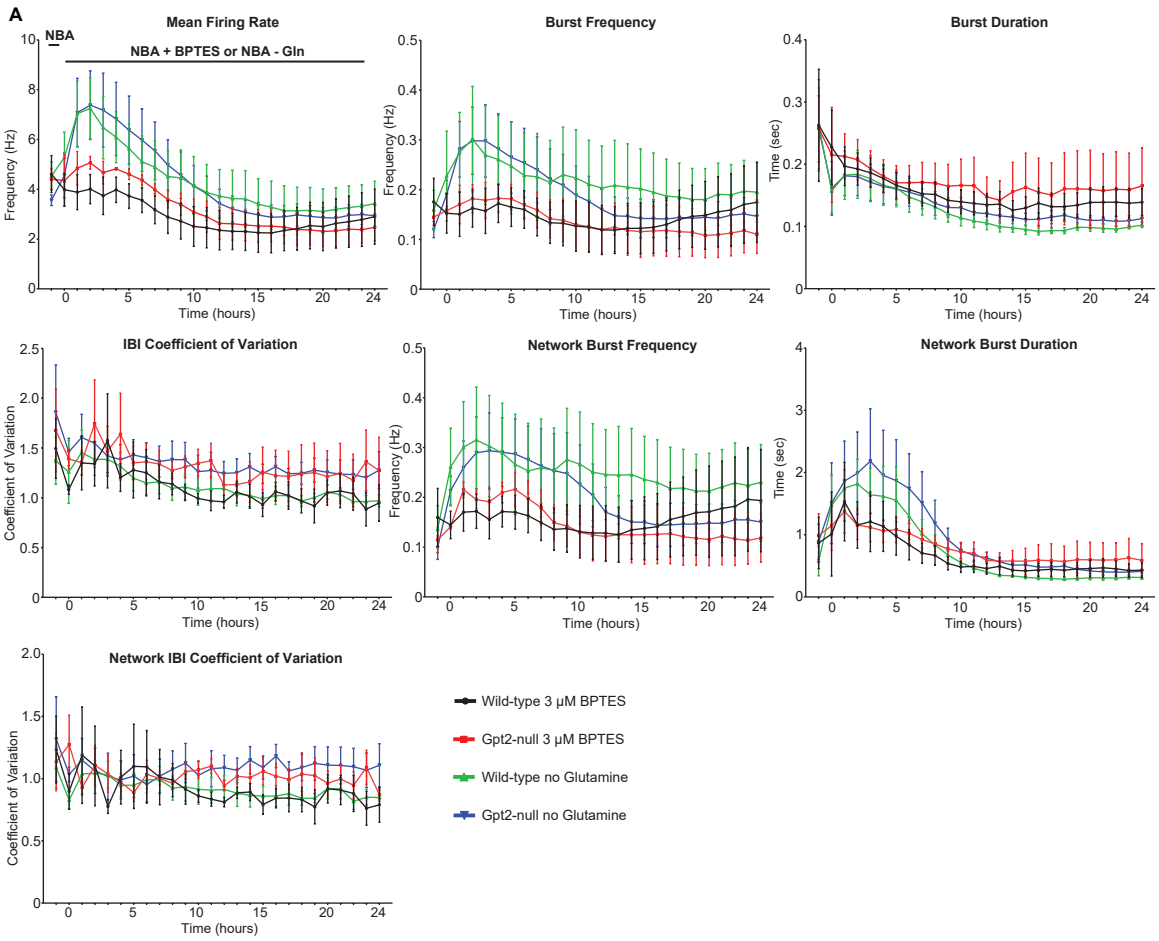

Figure A 5.3. MEA cortical neuronal culture firing after glutamine deprivation or glutaminase inhibition. A. MEA parameters of mean firing rate, burst frequency, burst duration, inter-burst interval coefficient of variation, network burst frequency, network burst duration and network inter-burst interval coefficient of variation. Wild-type with 3 μM BPTES (black), Gpt2-null with 3 μM BPTES (red), Wild-type without Glutamine (green), Gpt2-null without Glutamine (blue) n=5 cultures. NBA: Neurobasal A medium; NBA – Gln: Neurobasal A medium without Glutamine.

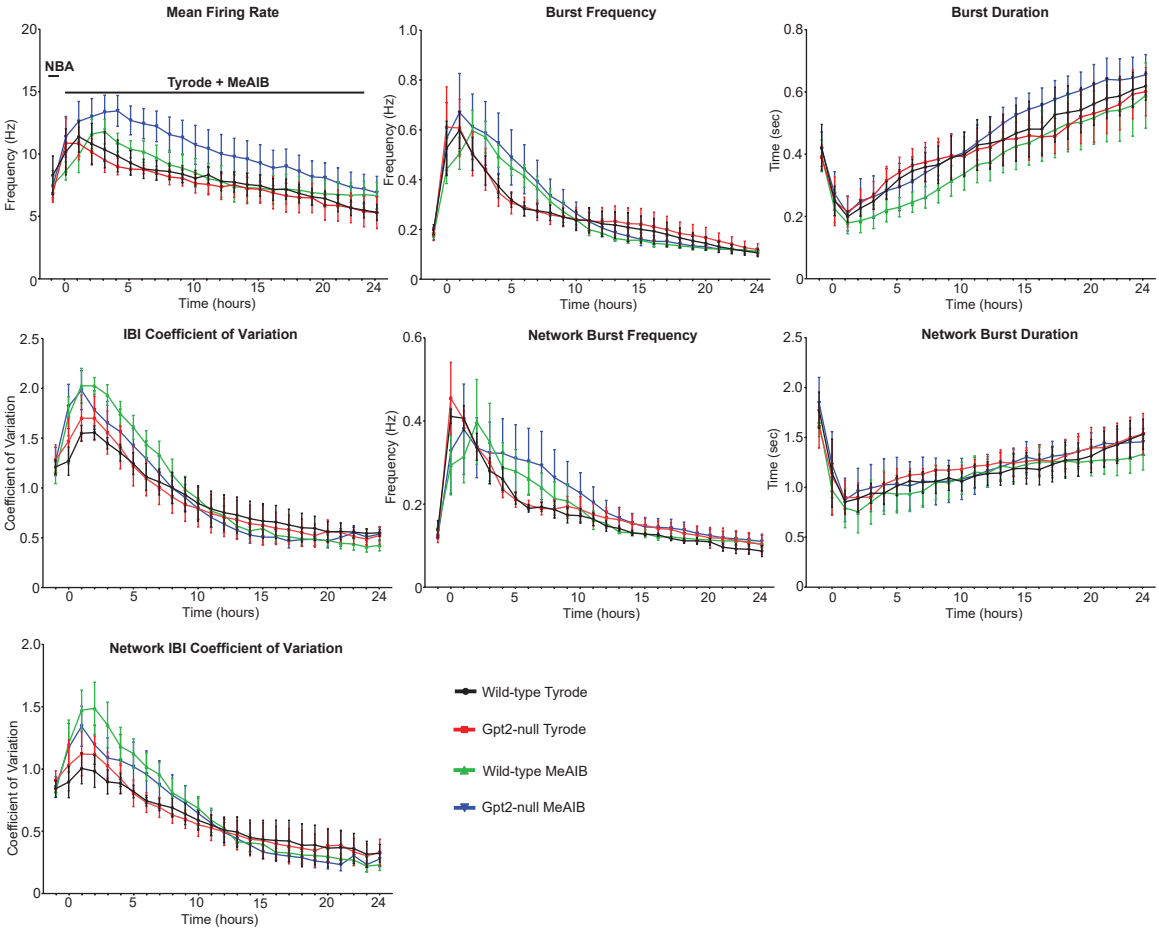

Figure A 5.4. MEA cortical neuronal culture firing after glutamine transport inhibition A. MEA parameters of mean firing rate, burst frequency, burst duration, inter-burst interval coefficient of variation, network burst frequency, network burst duration and network inter-burst interval coefficient of variation. Wild-type with Tyrode (black), Gpt2-null with Tyrode (red), Wild-type with 10 μM MeAIB (green), Gpt2-null with 10 μM MeAIB (blue) n=5 cultures. NBA: Neurobasal A medium.

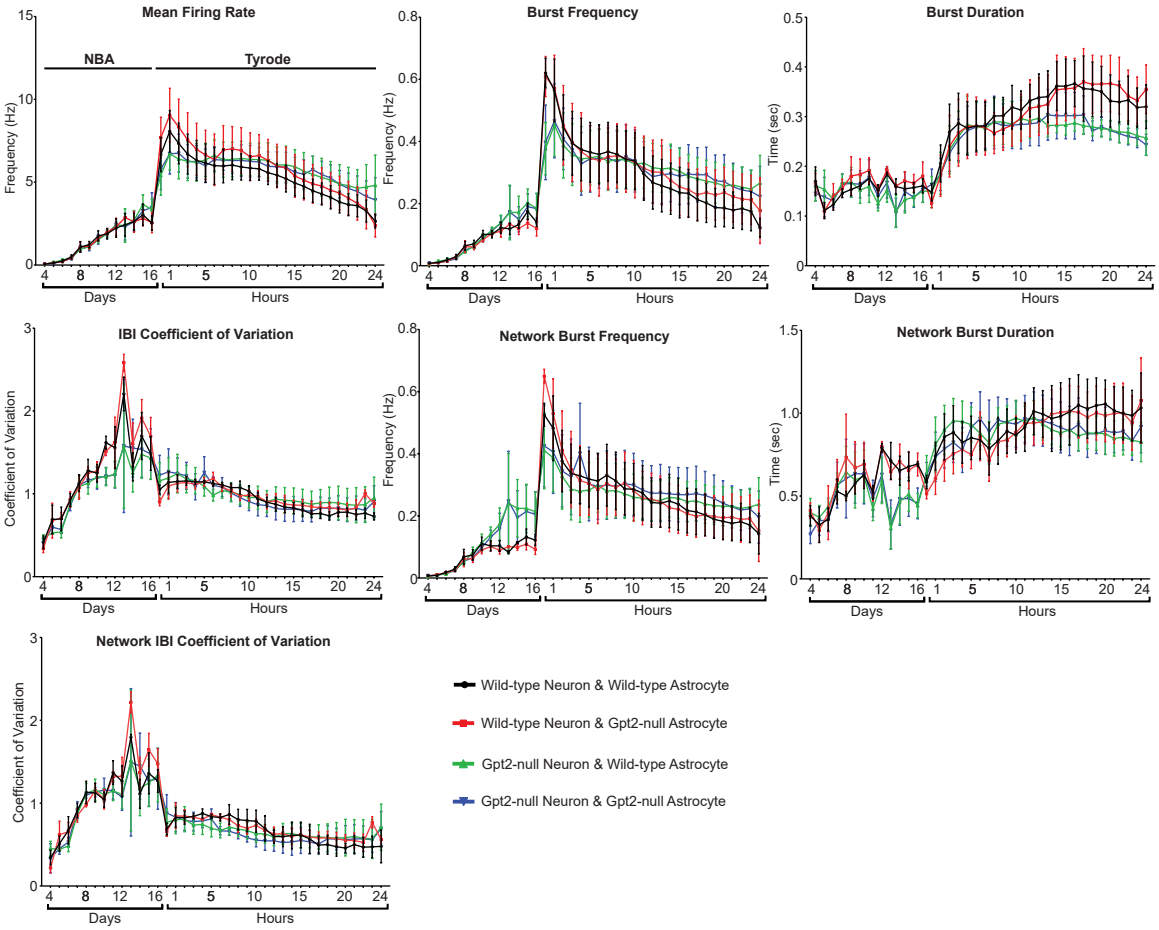

Figure A 5.5. MEA cortical neuronal firing in co-cultures with astrocytes
A. MEA parameters of mean firing rate, burst frequency, burst duration, inter-burst interval coefficient of variation, network burst frequency, network burst duration and network inter-burst interval coefficient of variation. Wild-type neuron & wild-type astrocyte (black), wild-type neuron & Gpt2-null astrocytes (red), Gpt2-null neuron & wild-type astrocytes (green), Gpt2-null neuron & Gpt2-null astrocyte (blue), n=4 cultures.
NBA: Neurobasal A medium.